VOLUME 28 / NUMBER 12
JUNE 23, 1990
ACC. NOS. N90-19190 TO N90-20043

STAR

AN ABSTRACT JOURNAL

Scientific and Technical Aerospace Reports

PRODUCED BY THE
SCIENTIFIC AND TECHNICAL
INFORMATION
DIVISION

NASA

NATIONAL AERONAUTICS AND SPACE ADMINISTRATION

WHAT YOU CAN DO FOR *STAR*

All users of this abstract service are urged to forward reports to be considered for announcement in *STAR*. This will aid NASA in its efforts to provide the fullest possible coverage of all scientific and technical publications that might support aeronautics and space research and development. If you have prepared relevant reports (other than those that you will transmit to NASA, DOD, or DOE through the usual contract- or grant-reporting channels), please send them for consideration to the NASA Scientific and Technical Information Facility, P.O. Box 8757, BWI Airport, MD 21240.

Reprints of journal articles, book chapters, and conference papers are also welcome. These will be considered for announcement in *STAR's* companion journal, *International Aerospace Abstracts*.

You may specify a particular source to be included in a report announcement if you wish; otherwise the report will be placed on public sale at the National Technical Information Service. Copyrighted publications will be announced but not distributed or sold.

PURCHASE OF *STAR*

The semimonthly issues are available to registered users on annual subscription from the NASA Scientific and Technical Information Facility, ATTN: Registration Services, P.O. Box 8757, BWI Airport, MD 21240. *STAR* is publicly available on annual subscription from the Superintendent of Documents, U.S. Government Printing Office, Washington, DC 20402.

PUBLISHED BY:

UNITED STATES GOVERNMENT
NATIONAL AERONAUTICS AND SPACE ADMINISTRATION
SCIENTIFIC AND TECHNICAL INFORMATION DIVISION
Scientific and Technical Aerospace Reports, Volume 28, is prepared by the NASA Scientific and Technical Information Facility operated for the National Aeronautics and Space Administration by RMS Associates.

The Administrator of the National Aeronautics and Space Administration has determined that the publication of this periodical is necessary in the transaction of the public business required by law of this agency. Use of funds for printing this periodical has been approved by the Director of the Office of Management and Budget through March 22, 1991.

US ISSN 0036-8741

Scientific and Technical Aerospace Reports (STAR) is issued twice a month and contains abstracts and indexes of meeting papers, conference proceedings, and unlimited distribution reports that have been added to the NASA Scientific and Technical Information Database during the preceding period. These citations may also be accessed online via NASA/RECON or via AIAA's Aerospace Database (File 108) through Dialog Information Services, Inc.

STAR subject coverage includes all aerospace-related areas that will help NASA achieve its mission. Material is gathered from all over the world and includes significant input from many countries under exchange and access agreements.

Consult the indexes at the back of this volume to help zero in on what you are looking for. These include:

Subject Index
Personal Author Index
Corporate Source Index
Contract Number Index
Report/Accession Number Index

STAR's companion abstract journal *International Aerospace Abstracts* should be used if you are looking for references to periodicals, books, and published meeting papers or conference proceedings.

Questions and comments should be addressed to:

NASA Scientific and Technical Information Facility
User Services
P.O. Box 8757
BWI Airport, MD 21240
301-621-0150

VOLUME 28 NUMBER 12 / JUNE 23, 1990

TABLE OF CONTENTS

AERONAUTICS

Includes aeronautics (general); aerodynamics; air transportation and safety; aircraft communications and navigation; aircraft design, testing and performance; aircraft instrumentation; aircraft propulsion and power; aircraft stability and control; and research and support facilities (air).

For related information see also *Astronautics.*

01 AERONAUTICS (GENERAL) 1597

02 AERODYNAMICS 1597

Includes aerodynamics of bodies, combinations, wings, rotors, and control surfaces; and internal flow in ducts and turbomachinery.

For related information see also *34 Fluid Mechanics and Heat Transfer.*

03 AIR TRANSPORTATION AND SAFETY 1601

Includes passenger and cargo air transport operations; and aircraft accidents.

For related information see also *16 Space Transportation* and *85 Urban Technology and Transportation.*

04 AIRCRAFT COMMUNICATIONS AND NAVIGATION 1601

Includes digital and voice communication with aircraft; air navigation systems (satellite and ground based); and air traffic control.

For related information see also *17 Space Communications, Spacecraft Communications, Command and Tracking* and *32 Communications and Radar.*

05 AIRCRAFT DESIGN, TESTING AND PERFORMANCE 1603

Includes aircraft simulation technology.

For related information see also *18 Spacecraft Design, Testing and Performance* and *39 Structural Mechanics.* For land transportation vehicles see *85 Urban Technology and Transportation.*

06 AIRCRAFT INSTRUMENTATION 1604

Includes cockpit and cabin display devices; and flight instruments.

For related information see also *19 Spacecraft Instrumentation* and *35 Instrumentation and Photography.*

07 AIRCRAFT PROPULSION AND POWER 1604

Includes prime propulsion systems and systems components, e.g., gas turbine engines and compressors; and onboard auxiliary power plants for aircraft.

For related information see also *20 Spacecraft Propulsion and Power, 28 Propellants and Fuels,* and *44 Energy Production and Conversion.*

08 AIRCRAFT STABILITY AND CONTROL 1605

Includes aircraft handling qualities; piloting; flight controls; and autopilots.

For related information see also *05 Aircraft Design, Testing and Performance.*

09 RESEARCH AND SUPPORT FACILITIES (AIR) 1606

Includes airports, hangars and runways; aircraft repair and overhaul facilities; wind tunnels; shock tubes; and aircraft engine test stands.

For related information see also *14 Ground Support Systems and Facilities (Space).*

ASTRONAUTICS

Includes astronautics (general); astrodynamics; ground support systems and facilities (space); launch vehicles and space vehicles; space transportation; space communications, spacecraft communications, command and tracking; spacecraft design, testing and performance; spacecraft instrumentation; and spacecraft propulsion and power.

For related information see also *Aeronautics.*

12 ASTRONAUTICS (GENERAL) 1607

For extraterrestrial exploration see *91 Lunar and Planetary Exploration.*

13 ASTRODYNAMICS 1607

Includes powered and free-flight trajectories; and orbital and launching dynamics.

14 GROUND SUPPORT SYSTEMS AND FACILITIES (SPACE) 1607

Includes launch complexes, research and production facilities; ground support equipment, e.g., mobile transporters; and simulators.

For related information see also *09 Research and Support Facilities (Air).*

15 LAUNCH VEHICLES AND SPACE VEHICLES 1608

Includes boosters; operating problems of launch/space vehicle systems; and reusable vehicles.

For related information see also *20 Spacecraft Propulsion and Power.*

16 SPACE TRANSPORTATION N.A.

Includes passenger and cargo space transportation, e.g., shuttle operations; and space rescue techniques.

For related information see also *03 Air Transportation and Safety* and *18 Spacecraft Design, Testing and Performance.* For space suits see *54 Man/System Technology and Life Support.*

17 SPACE COMMUNICATIONS, SPACECRAFT COMMUNICATIONS, COMMAND AND TRACKING 1612

Includes telemetry; space communications networks; astronavigation and guidance; and radio blackout.

For related information see also *04 Aircraft Communications and Navigation* and *32 Communications and Radar.*

18 SPACECRAFT DESIGN, TESTING AND PERFORMANCE **1612**

Includes satellites; space platforms; space stations; spacecraft systems and components such as thermal and environmental controls; and attitude controls.

For life support systems see *54 Man/System Technology and Life Support.* For related information see also *05 Aircraft Design, Testing and Performance, 39 Structural Mechanics,* and *16 Space Transportation.*

19 SPACECRAFT INSTRUMENTATION **1616**

For related information see also *06 Aircraft Instrumentation* and *35 Instrumentation and Photography.*

20 SPACECRAFT PROPULSION AND POWER **1617**

Includes main propulsion systems and components, e.g. rocket engines; and spacecraft auxiliary power sources.

For related information see also *07 Aircraft Propulsion and Power, 28 Propellants and Fuels, 44 Energy Production and Conversion,* and *15 Launch Vehicles and Space Vehicles.*

CHEMISTRY AND MATERIALS

Includes chemistry and materials (general); composite materials; inorganic and physical chemistry; metallic materials; nonmetallic materials; propellants and fuels; and materials processing.

23 CHEMISTRY AND MATERIALS (GENERAL) **1618**

24 COMPOSITE MATERIALS **1618**

Includes physical, chemical, and mechanical properties of laminates and other composite materials.

For ceramic materials see *27 Nonmetallic Materials.*

25 INORGANIC AND PHYSICAL CHEMISTRY **1621**

Includes chemical analysis, e.g., chromatography; combustion theory; electrochemistry; and photochemistry.

For related information see also *77 Thermodynamics and Statistical Physics.*

26 METALLIC MATERIALS **1625**

Includes physical, chemical, and mechanical properties of metals, e.g., corrosion; and metallurgy.

27 NONMETALLIC MATERIALS **1629**

Includes physical, chemical, and mechanical properties of plastics, elastomers, lubricants, polymers, textiles, adhesives, and ceramic materials.

For composite materials see *24 Composite Materials.*

28 PROPELLANTS AND FUELS **1633**

Includes rocket propellants, igniters and oxidizers; their storage and handling procedures; and aircraft fuels.

For related information see also *07 Aircraft Propulsion and Power, 20 Spacecraft Propulsion and Power,* and *44 Energy Production and Conversion.*

29 MATERIALS PROCESSING **N.A.**

Includes space-based development of products and processes for commercial application.

For biological materials see *55 Space Biology.*

ENGINEERING

Includes engineering (general); communications and radar; electronics and electrical engineering; fluid mechanics and heat transfer; instrumentation and photography; lasers and masers; mechanical engineering; quality assurance and reliability; and structural mechanics.

For related information see also *Physics.*

31 ENGINEERING (GENERAL) **1634**

Includes vacuum technology; control engineering; display engineering; cryogenics; and fire prevention.

32 COMMUNICATIONS AND RADAR **1641**

Includes radar; land and global communications; communications theory; and optical communications.

For related information see also *04 Aircraft Communications and Navigation* and *17 Space Communications, Spacecraft Communications, Command and Tracking.* For search and rescue see *03 Air Transportation and Safety,* and *16 Space Transportation.*

33 ELECTRONICS AND ELECTRICAL ENGINEERING **1650**

Includes test equipment and maintainability; components, e.g., tunnel diodes and transistors; microminiaturization; and integrated circuitry.

For related information see also *60 Computer Operations and Hardware* and *76 Solid-State Physics.*

34 FLUID MECHANICS AND HEAT TRANSFER **1657**

Includes boundary layers; hydrodynamics; fluidics; mass transfer and ablation cooling.

For related information see also *02 Aerodynamics* and *77 Thermodynamics and Statistical Physics.*

35 INSTRUMENTATION AND PHOTOGRAPHY **1662**

Includes remote sensors; measuring instruments and gauges; detectors; cameras and photographic supplies; and holography.

For aerial photography see *43 Earth Resources and Remote Sensing.* For related information see also *06 Aircraft Instrumentation* and *19 Spacecraft Instrumentation.*

36 LASERS AND MASERS **1665**

Includes parametric amplifiers.

For related information see also *76 Solid-State Physics.*

37 MECHANICAL ENGINEERING **1670**

Includes auxiliary systems (nonpower); machine elements and processes; and mechanical equipment.

38 QUALITY ASSURANCE AND RELIABILITY **1673**

Includes product sampling procedures and techniques; and quality control.

39 STRUCTURAL MECHANICS **1673**

Includes structural element design and weight analysis; fatigue; and thermal stress.

For applications see *05 Aircraft Design, Testing and Performance* and *18 Spacecraft Design, Testing and Performance.*

GEOSCIENCES

Includes geosciences (general); earth resources and remote sensing; energy production and conversion; environment pollution; geophysics; meteorology and climatology; and oceanography.

For related information see also *Space Sciences.*

42 GEOSCIENCES (GENERAL) **N.A.**

43 EARTH RESOURCES AND REMOTE SENSING **1677**

Includes remote sensing of earth resources by aircraft and spacecraft; photogrammetry; and aerial photography.

For instrumentation see *35 Instrumentation and Photography.*

44 ENERGY PRODUCTION AND CONVERSION **1680**

Includes specific energy conversion systems, e.g., fuel cells; global sources of energy; geophysical conversion; and windpower.

For related information see also *07 Aircraft Propulsion and Power, 20 Spacecraft Propulsion and Power,* and *28 Propellants and Fuels.*

45 ENVIRONMENT POLLUTION **1684**

Includes atmospheric, noise, thermal, and water pollution.

46 GEOPHYSICS **1690**

Includes aeronomy; upper and lower atmosphere studies; ionospheric and magnetospheric physics; and geomagnetism.

For space radiation see *93 Space Radiation.*

47 METEOROLOGY AND CLIMATOLOGY **1692**

Includes weather forecasting and modification.

48 OCEANOGRAPHY **1695**

Includes biological, dynamic, and physical oceanography; and marine resources.

For related information see also *43 Earth Resources and Remote Sensing.*

LIFE SCIENCES

Includes life sciences (general); aerospace medicine; behavioral sciences; man/system technology and life support; and space biology.

51 LIFE SCIENCES (GENERAL) **1695**

52 AEROSPACE MEDICINE **1696**

Includes physiological factors; biological effects of radiation; and effects of weightlessness on man and animals.

53 BEHAVIORAL SCIENCES **1696**

Includes psychological factors; individual and group behavior; crew training and evaluation; and psychiatric research.

54 MAN/SYSTEM TECHNOLOGY AND LIFE SUPPORT **1697**

Includes human engineering; biotechnology; and space suits and protective clothing.

For related information see also *16 Space Transportation.*

55 SPACE BIOLOGY **1698**

Includes exobiology; planetary biology; and extraterrestrial life.

MATHEMATICAL AND COMPUTER SCIENCES

Includes mathematical and computer sciences (general); computer operations and hardware; computer programming and software; computer systems; cybernetics; numerical analysis; statistics and probability; systems analysis; and theoretical mathematics.

59 MATHEMATICAL AND COMPUTER SCIENCES (GENERAL) **N.A.**

60 COMPUTER OPERATIONS AND HARDWARE **1698**

Includes hardware for computer graphics, firmware, and data processing.

For components see *33 Electronics and Electrical Engineering.*

61 COMPUTER PROGRAMMING AND SOFTWARE **1699**

Includes computer programs, routines, algorithms, and specific applications, e.g., CAD/CAM.

62 COMPUTER SYSTEMS **1703**

Includes computer networks and special application computer systems.

63 CYBERNETICS **1703**

Includes feedback and control theory, artificial intelligence, robotics and expert systems.

For related information see also *54 Man/System Technology and Life Support.*

64 NUMERICAL ANALYSIS **1704**

Includes iteration, difference equations, and numerical approximation.

65 STATISTICS AND PROBABILITY **1708**

Includes data sampling and smoothing; Monte Carlo method; and stochastic processes.

66 SYSTEMS ANALYSIS **N.A.**

Includes mathematical modeling; network analysis; and operations research.

67 THEORETICAL MATHEMATICS **1708**

Includes topology and number theory.

PHYSICS

Includes physics (general); acoustics; atomic and molecular physics; nuclear and high-energy physics; optics; plasma physics; solid-state physics; and thermodynamics and statistical physics.

For related information see also *Engineering.*

70 PHYSICS (GENERAL) **1709**

For precision time and time interval (PTTI) see *35 Instrumentation and Photography;* for geophysics, astrophysics or solar physics see *46 Geophysics, 90 Astrophysics,* or *92 Solar Physics.*

71 ACOUSTICS 1709
Includes sound generation, transmission, and attenuation.
For noise pollution see *45 Environment Pollution.*

72 ATOMIC AND MOLECULAR PHYSICS 1710
Includes atomic structure, electron properties, and molecular spectra.

73 NUCLEAR AND HIGH-ENERGY PHYSICS 1712
Includes elementary and nuclear particles; and reactor theory.
For space radiation see *93 Space Radiation.*

74 OPTICS 1713
Includes light phenomena and optical devices.
For lasers see *36 Lasers and Masers.*

75 PLASMA PHYSICS 1715
Includes magnetohydrodynamics and plasma fusion.
For ionospheric plasmas see *46 Geophysics.* For space plasmas see *90 Astrophysics.*

76 SOLID-STATE PHYSICS 1718
Includes superconductivity.
For related information see also *33 Electronics and Electrical Engineering* and *36 Lasers and Masers.*

77 THERMODYNAMICS AND STATISTICAL PHYSICS 1724
Includes quantum mechanics; theoretical physics; and Bose and Fermi statistics.
For related information see also *25 Inorganic and Physical Chemistry* and *34 Fluid Mechanics and Heat Transfer.*

SOCIAL SCIENCES

Includes social sciences (general); administration and management; documentation and information science; economics and cost analysis; law, political science, and space policy; and urban technology and transportation.

80 SOCIAL SCIENCES (GENERAL) N.A.
Includes educational matters.

81 ADMINISTRATION AND MANAGEMENT N.A.
Includes management planning and research.

82 DOCUMENTATION AND INFORMATION SCIENCE 1725
Includes information management; information storage and retrieval technology; technical writing; graphic arts; and micrography.
For computer documentation see *61 Computer Programming and Software.*

83 ECONOMICS AND COST ANALYSIS N.A.
Includes cost effectiveness studies.

84 LAW, POLITICAL SCIENCE AND SPACE POLICY N.A.
Includes NASA appropriation hearings; aviation law; space law and policy; international law; international cooperation; and patent policy.

85 URBAN TECHNOLOGY AND TRANSPORTATION 1727
Includes applications of space technology to urban problems; technology transfer; technology assessment; and surface and mass transportation.
For related information see *03 Air Transportation and Safety, 16 Space Transportation,* and *44 Energy Production and Conversion.*

SPACE SCIENCES

Includes space sciences (general); astronomy; astrophysics; lunar and planetary exploration; solar physics; and space radiation.
For related information see also *Geosciences.*

88 SPACE SCIENCES (GENERAL) N.A.

89 ASTRONOMY 1728
Includes radio, gamma-ray, and infrared astronomy; and astrometry.

90 ASTROPHYSICS 1730
Includes cosmology; celestial mechanics; space plasmas; and interstellar and interplanetary gases and dust.
For related information see also *75 Plasma Physics.*

91 LUNAR AND PLANETARY EXPLORATION 1744
Includes planetology; and manned and unmanned flights.
For spacecraft design or space stations see *18 Spacecraft Design, Testing and Performance.*

92 SOLAR PHYSICS 1745
Includes solar activity, solar flares, solar radiation and sunspots.
For related information see *93 Space Radiation.*

93 SPACE RADIATION 1745
Includes cosmic radiation; and inner and outer earth's radiation belts.
For biological effects of radiation see *52 Aerospace Medicine.* For theory see *73 Nuclear and High-Energy Physics.*

GENERAL

Includes aeronautical, astronautical, and space science related histories, biographies, and pertinent reports too broad for categorization; histories or broad overviews of NASA programs.

99 GENERAL 1747

Note: N.A. means that no abstracts were assigned to this category for this issue.

SUBJECT INDEX I-1
PERSONAL AUTHOR INDEX I-55
CORPORATE SOURCE INDEX I-63
CONTRACT NUMBER INDEX I-75
REPORT/ACCESSION NUMBER INDEX .. I-77
APPENDIX—ABOUT STAR A-1

TYPICAL CITATION AND ABSTRACT

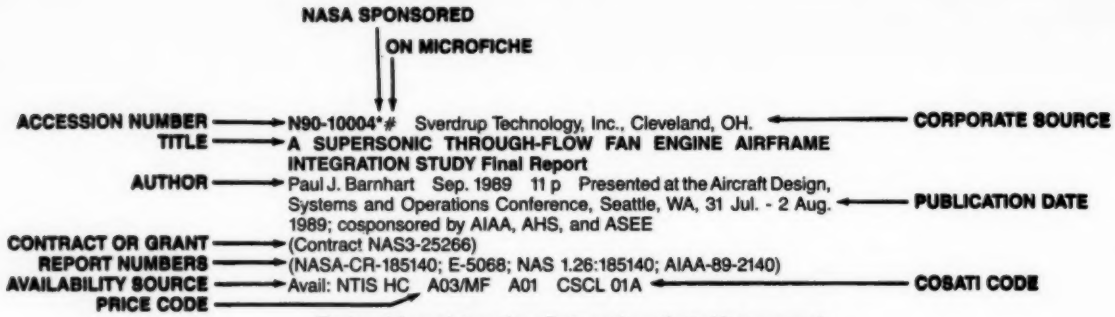
NASA SPONSORED
ON MICROFICHE
ACCESSION NUMBER
N90-10004*# Sverdrup Technology, Inc., Cleveland, OH.
CORPORATE SOURCE
TITLE
A SUPERSONIC THROUGH-FLOW FAN ENGINE AIRFRAME INTEGRATION STUDY Final Report
AUTHOR
Paul J. Barnhart Sep. 1989 11 p Presented at the Aircraft Design, Systems and Operations Conference, Seattle, WA, 31 Jul. - 2 Aug. 1989; cosponsored by AIAA, AHS, and ASEE
PUBLICATION DATE
CONTRACT OR GRANT
(Contract NAS3-25266)
REPORT NUMBERS
(NASA-CR-185140; E-5068; NAS 1.26:185140; AIAA-89-2140)
AVAILABILITY SOURCE
Avail: NTIS HC A03/MF A01 CSCL 01A
COSATI CODE
PRICE CODE

Engine airframe integration effects are investigated for superonsic through-flow fan engines installed on a Mach 3.20 supersonic cruise vehicle. Six different supersonic through-flow fan engine installations covering the effects of engine size, nacelle contour, nacelle placement, and approximate bypass plume effects are presented. The different supersonic through-flow fan installations are compared with a conventional turbine bypass engine configuration on the same basic airframe. The supersonic through-flow fan engine integrations are shown to be comparable to the turbine bypass engine configuration on the basis of installed nacelle wave drag. The supersonic through-flow fan engine airframe integrated vehicles have superior aerodynamic performance on the basis of maximum lift-to-drag ratio than the turbine bypass engine installation over the entire operating Mach number range from 1.10 to 3.20. When approximate bypass plume modeling is included, the supersonic through-flow fan engine configuration shows even larger improvements over the turbine bypass engine configuration. Author

VOLUME 28 NUMBER 12 / JUNE 23, 1990

Scientific and Technical Aerospace Reports

A Semimonthly Publication of the National Aeronautics and Space Administration

01 AERONAUTICS (GENERAL)

N90-19190* National Aeronautics and Space Administration, Washington, DC.
AERONAUTICAL ENGINEERING: A CONTINUING BIBLIOGRAPHY WITH INDEXES (SUPPLEMENT 249)
Feb. 1990 148 p
(NASA-SP-7037(249); NAS 1.21:7037(249)) Avail: NTIS HC A07; NTIS standing order as PB89-914100, $10.50 domestic, $21.00 foreign CSCL 01B

This bibliography lists 637 reports, articles, and other documents introduced into the NASA scientific and technical information system in November, 1988. Subject coverage includes: design, construction and testing of aircraft and aircraft engines; aircraft components, equipment and systems; ground support systems; and theoretical and applied aspects of aerodynamics and general fluid dynamics. Author

02 AERODYNAMICS

Includes aerodynamics of bodies, combinations, wings, rotors, and control surfaces; and internal flow in ducts and turbomachinery.

For related information see also *34 Fluid Mechanics and Heat Transfer.*

N90-19191# National Aerospace Lab., Amsterdam (Netherlands). Informatics Div.
ON THE EVALUATION OF AERODYNAMIC INFLUENCE COEFFICIENTS
H. Schippers 11 Mar. 1987 14 p Presented at the 3rd GAMM-Seminar Kiel on Panel Methods in Mechanics, Kiel, Federal Rep. of Germany, 16-18 Jan. 1987 Previously announced in IAA as A89-11496
(NLR-MP-87019-U; ETN-89-94032) Avail: NTIS HC A03/MF A01

Numerical schemes to reduce the computational work involved in the evaluation of the aerodynamic influence coefficients of panel methods are discussed. The applicability of these schemes is investigated for the calculation of potential flow around an airfoil. The decomposition of the boundary integral operator by splitting the contour integration such that the singular behavior of the kernel function near the trailing edge is taken into account is considered. The decomposition results in a compact operator and a contractive operator. The compact operator contains a smooth kernel function, which is approximated by piecewise linear interpolation. The interpolation provides error terms of the same order as the panel method. For a fixed number of panels the accuracy, however, is decreased significantly. ESA

N90-19192# Institut Franco-Allemand de Recherches, Saint-Louis (France).
A STUDY ON UPSTREAM MOVING PRESSURE WAVES INDUCED BY VORTEX SEPARATION
J. Srulijes and F. Seiler 26 Jan. 1988 12 p Presented at the 16th International Symposium on Shock Tubes and Waves, Aachen, Federal Rep. of Germany, 26-30 Jul. 1987 Previously announced in IAA as A89-12915
(ISL-CO-203/88; ETN-89-94113) Avail: NTIS HC A03/MF A01

Shock tube experiments were performed to investigate subsonic flows around flat plates, cylinders, and wing profiles with blunt trailing edges. Differential interferometry shows that the trailing edge vortex separation induces pressure waves moving upstream along the surfaces of the bodies under investigation. Path-time photographs indicate that each vortex separation is related to the formation of a pressure wave. These pressure waves move upstream at a velocity which is slightly higher than the difference between the speed of sound and the flow velocity. Flow measurements show a relative density variation across the pressure waves of the order of 0.1, increasing slightly with increasing flow Mach number. Particularly in the wing profile investigations, a local supersonic region with a recompression shock formation develops at the upper side of the wing. The pressure waves in the subsonic flow behind the recompression shock can only move up to the local supersonic flow region limited by the recompression shock. Path-time records show that the position of the recompression shock oscillates slightly when it is periodically attacked by the upstream moving pressure waves. At the lower side the pressure waves can reach the wing leading edge. ESA

N90-19193*# National Aeronautics and Space Administration. Langley Research Center, Hampton, VA.
STATIC INVESTIGATION OF A TWO-DIMENSIONAL CONVERGENT-DIVERGENT EXHAUST NOZZLE WITH MULTIAXIS THRUST-VECTORING CAPABILITY
John G. Taylor Washington Apr. 1990 104 p
(NASA-TP-2973; L-16632; NAS 1.60:2973) Avail: NTIS HC A06/MF A01 CSCL 01A

An investigation was conducted in the Static Test Facility of the NASA Langley 16-Foot Transonic Tunnel to determine the internal performance of two-dimensional convergent-divergent nozzles designed to have simultaneous pitch and yaw thrust vectoring capability. This concept utilized divergent flap rotation of thrust vectoring in the pitch plane and deflection of flat yaw flaps hinged at the end of the sidewalls for yaw thrust vectoring. The hinge location of the yaw flaps was varied at four positions from the nozzle exit plane to the throat plane. The yaw flaps were designed to contain the flow laterally independent of power setting. In order to eliminate any physical interference between the yaw flap deflected into the exhaust stream and the divergent flaps, the downstream corners of both upper and lower divergent flaps were cut off to allow for up to 30 deg of yaw flap deflection. The impact of varying the nozzle pitch vector angle, throat area, yaw flap hinge location, yaw flap length, and yaw flap deflection angle on nozzle internal performance characteristics, was studied. High-pressure air was used to simulate jet exhaust at nozzle pressure ratios up to 7.0. Static results indicate that configurations with the yaw flap hinge located upstream of the exit plane provide relatively high levels of thrust vectoring efficiency without causing large losses in resultant thrust ratio. Therefore, these configurations represent a viable concept for providing simultaneous pitch and yaw thrust vectoring. Author

N90-19194 Maryland Univ., College Park.
COMPUTATION OF HYPERSONIC UNSTEADY VISCOUS FLOW

OVER A CYLINDER Ph.D. Thesis
Yunghwan Byun 1988 176 p
Avail: Univ. Microfilms Order No. DA8912269

The purpose was to assess the time required to obtain the steady state and to study the physical nature of the transients during the unsteady approach to the steady state of the flow over an aerodynamic model in the impulsive hypersonic ground test facilities. Numerical simulation of the hypersonic viscous flow over a two dimensional circular cylinder in a shock tunnel has been attempted by using MacCormack's explicit time dependent predictor-corrector finite-difference method. The problem consists of two parts which are a quasi-one-dimensional nozzle flow for a convergent-divergent nozzle section and a flow over a circular cylinder for an aerodynamic model. The time dependent solution of the former has been used as the inflow boundary condition for the latter problem whose governing equations are two dimensional full Navier-Stokes equations. The flow is assumed as a calorically perfect gas and a laminar flow. For a nozzle flow, the start-up process of the shock tunnel and the time required to the steady state have been studied. For a flow over a cylinder, the transients at early time and the effects of the artificial damping terms and the outer boundary have been studied. Dissert. Abstr.

N90-19195 ESDU International Ltd., London (England).
CALCULATION OF EXCRESCENCE DRAG MAGNIFICATION DUE TO PRESSURE GRADIENT AT HIGH SUBSONIC SPEEDS
Aug. 1987 31 p
(ESDU-87004; ISBN-0-85679-597-6; ISSN-0141-4356) Avail: ESDU

This data item gives methods for estimating the factor by which the drag due to an isolated excrescence on a flat plate (for which ESDU 74036, 75031, 76008, 79015 and 84035 provide data) must be multiplied to obtain the drag implement when it is in a pressure gradient. The methods were developed theoretically by computing the change in drag of the aerofoil at constant lift when an increment of momentum thickness is introduced in the boundary layer calculation to represent the excrescence. The factor therefore includes the change in drag due to the incidence change made to keep the lift constant. Calculations were made for two airfoils, designed for high subsonic speeds, over a range of Mach number and incidence, and graphs show the dependence of the factor on lift and excrescence chordwise position, together with the corresponding pressure distributions on upper and lower surfaces. Since the magnification factor depends primarily on pressure gradient, estimating the factor for any other aerofoil requires only that a similar pressure gradient to that at the excrescence location be located on these graphs, and the corresponding magnification factor read. A second method of calculating the magnification factor is also given that depends on the flow properties at the excrescence location and at the trailing-edge. ESDU

N90-19196 Stanford Univ., CA.
UNSTEADY AERODYNAMICS OF DELTA WINGS PERFORMING MANEUVERS TO HIGH ANGLE OF ATTACK Ph.D. Thesis
Mohammad-Ameen Mahmo Jarrah 1989 295 p
Avail: Univ. Microfilms Order No. DA8912910

An experimental program of unsteady aerodynamic measurements motivated by maneuvers which have been proposed for agile fighter aircraft, was carried out. These tests were conducted in one of the 7 ft x 10 ft low speed wind tunnel at NASA on a series of flat delta wing models with sharp leading edges. By means of hydraulic actuation, rapid pitching motions were produced involving angle-of-attack excursions as great as 0 to 90 deg and back. These excursions involved sinusoidal or ramp variations in the angle of attack. Six-component airload histories were obtained for models of aspect ratios 1, 1.5, and 2. Flow visualization results were recorded using high speed cinematography for a model of aspect ratio one. Description of the apparatus and test procedures is presented. Over a range of reduced frequency parameter from 0.01 to 0.08, which is typical of these maneuvers, examples are given and discussed from the large body of data obtained. They include the unsteady response of the leading vortices, as evidenced both by the time dependent airloads and by motion pictures of smoke released from the leading edge and illuminated by a thin sheet of laser light. Unsteady vortex breakdown and reestablishment are emphasized. Dissert. Abstr.

N90-19197 California Univ., Berkeley.
INTERACTION OF AN OBLIQUE SHOCK WAVE WITH SUPERSONIC FLOW OVER A BLUNT BODY Ph.D. Thesis
Young June Moon 1988 139 p
Avail: Univ. Microfilms Order No. DA8916803

A numerical study of shock-on-shock interactions near a cylindrical body representative of the engine inlet cowl of the National AeroSpace Plane (NASP) is presented. Among the six principal interference patterns depending upon the intersection point, noted by Edney, the most critical cases, of types III and IV, were considered. In these cases, anomalous amplifications of peak pressure and heat flux occur at the shear layer and supersonic jet impingement points, respectively. The primary goal was to calculate the entire flow field numerically, capturing all the interacting shocks and complicated shock layer flows. Computational simulation of such flow with shocks and contact surfaces requires the use of a numerical scheme with monotonic properties in the Godunov sense, so as to avoid spurious oscillations near discontinuities. The finite volume formulation of Van Leer's flux vector splitting MUSCL (Monotonic Upstream-centered Scheme for Conservation Laws) scheme, in generalized coordinates, was used to solve the full or thin layer Navier-Stokes equations in strong conservative form. The backward Euler implicit scheme with the approximate factorization method was used for time integration, since only the steady state solution is of interest. The present method was applied to the cases of supersonic blunt body flow, type III, III(+), and IV shock interference patterns. Here type III(+) is defined as a transitional stage of interference pattern changing from the type III to IV. For all cases, the present method captures complicated interacting shocks with monotonic properties and the anomalous pressures and heat fluxes compare reasonably well with experiments. Better agreement would be obtained if proper grid adaptations (grid enrichment algorithm) were employed. Dissert. Abstr.

N90-19198*# Notre Dame Univ., IN. Dept. of Aerospace and Mechanical Engineering.
LEADING EDGE VORTEX DYNAMICS ON A PITCHING DELTA WING M.S. Thesis
Scott P. LeMay Apr. 1988 175 p
(Grant NAG1-727)
(NASA-CR-186327; NAS 1.26:186327) Avail: NTIS HC A08/MF A01 CSCL 01A

The leading edge flow structure was investigated on a 70 deg flat plate delta wing which was pitched about its 1/2 chord position, to increase understanding of the high angle of attack aerodynamics on an unsteady delta wing. The wing was sinusoidally pitched at reduced frequencies ranging from k being identical with 2pi fc/u = 0.05 to 0.30 at chord Reynolds numbers between 90,000 and 350,000, for angle of attack ranges of alpha = 29 to 39 deg and alpha = 0 to 45 deg. The wing was also impulsively pitched at an approximate rate of 0.7 rad/s. During these dynamic motions, visualization of the leading edge vorticies was obtained by entraining titanium tetrachloride into the flow at the model apex. The location of vortex breakdown was recorded using 16mm high speed motion picture photography. When the wing was sinusoidally pitched, a hysteresis was observed in the location of breakdown position. This hysteresis increased with reduced frequency. The velocity of breakdown propagation along the wing, and the phase lag between model motion and breakdown location were also determined. When the wing was impulsively pitched, several convective times were required for the vortex flow to reach a steady state. Detailed information was also obtained on the oscillation of breakdown position in both static and dynamic cases. Author

N90-19199*# National Aeronautics and Space Administration. Langley Research Center, Hampton, VA.
WATER-TUNNEL INVESTIGATION OF CONCEPTS FOR ALLEVIATION OF ADVERSE INLET SPILLAGE INTERACTIONS WITH EXTERNAL STORES
Dan H. Neuhart (Lockheed Engineering and Sciences Co., Hampton, VA.) and Matthew N. Rhode Washington Apr. 1990 36 p
(NASA-TM-4181; L-16710; NAS 1.15:4181) Avail: NTIS HC A03/MF A01 CSCL 01A

A test was conducted in the NASA Langley 16- by 24-Inch Water Tunnel to study alleviation of the adverse interactions of inlet spillage flow on the external stores of a fighter aircraft. A 1/48-scale model of a fighter aircraft was used to simulate the flow environment around the aircraft inlets and on the downstream underside of the fuselage. A controlled inlet mass flow was simulated by drawing water into the inlets. Various flow control devices were used on the underside of the aircraft model to manipulate the vortical inlet spillage flow. Author

N90-19200*# National Aeronautics and Space Administration. Langley Research Center, Hampton, VA.
INTERNAL PERFORMANCE OF TWO NOZZLES UTILIZING GIMBAL CONCEPTS FOR THRUST VECTORING
Bobby L. Berrier and John G. Taylor Washington Apr. 1990 128 p
(NASA-TP-2991; L-16722; NAS 1.60:2991) Avail: NTIS HC A07/MF A01 CSCL 01A

The internal performance of an axisymmetric convergent-divergent nozzle and a nonaxisymmetric convergent-divergent nozzle, both of which utilized a gimbal type mechanism for thrust vectoring was evaluated in the Static Test Facility of the Langley 16-Foot Transonic Tunnel. The nonaxisymmetric nozzle used the gimbal concept for yaw thrust vectoring only; pitch thrust vectoring was accomplished by simultaneous deflection of the upper and lower divergent flaps. The model geometric parameters investigated were pitch vector angle for the axisymmetric nozzle and pitch vector angle, yaw vector angle, nozzle throat aspect ratio, and nozzle expansion ratio for the nonaxisymmetric nozzle. All tests were conducted with no external flow, and nozzle pressure ratio was varied from 2.0 to approximately 12.0. Author

N90-19201*# National Aeronautics and Space Administration. Ames Research Center, Moffett Field, CA.
A STREAMWISE UPWIND ALGORITHM APPLIED TO VORTICAL FLOW OVER A DELTA WING
Peter M. Goorjian and Shigeru Obayashi Oct. 1989 13 p Presented at the 8th GAMM Conference on Numerical Methods in Fluid Mechanics, Delft, Netherlands, 27-29 Sep. 1989
(NASA-TM-102225; A-89230; NAS 1.15:102225) Avail: NTIS HC A03/MF A01 CSCL 01A

Improvements were made to a streamwise upwind algorithm so that it can be used for calculating flows with vortices. A calculation is shown of flow over a delta wing at an angle of attack. The laminar, thin layer, Navier-Stokes equations are used for the calculation. The results are compared with another upwind method, a central differencing method, and experimental data. The present method shows improvements in accuracy and convergence properties. Author

N90-19202# Royal Aerospace Establishment, Farnborough (England).
A STUDY OF FLOWS OVER HIGHLY-SWEPT WINGS DESIGNED FOR MANEUVER AT SUPERSONIC SPEEDS
P. R. Ashill, J. L. Fulker, and M. J. Simmons Oct. 1988 43 p
(AD-A216837; RAE-TM-AERO-2147; DRIC-BR-112012) Avail: NTIS HC A03/MF A01 CSCL 01/1

A wind tunnel investigation into supersonic free stream flows over two wing-body configurations, having wings of different design, suitable for combat aircraft, is described. Both wings have the same quasi-delta planform of 60 deg inboard leading edge sweep and the same 4 pct thickness distribution but have differing camber distributions. Following a description of the design of the wings, the test procedures are discussed and the general features of the flows at conditions close to those for sustained maneuver are identified and constrasted. Comparisons between calculations by CFD methods and measurement are presented, and it is shown that a multiblock method for solving the Euler equations is suitable for designing wings for efficient maneuver at supersonic speeds. Author

N90-19203*# Toledo Univ., OH. Dept. of Chemical Engineering.
HEAT TRANSFER MEASUREMENTS FROM A NACA 0012 AIRFOIL IN FLIGHT AND IN THE NASA LEWIS ICING RESEARCH TUNNEL M.S. Thesis Final Report
Philip E. Poinsatte Washington NASA Mar. 1990 194 p (Grant NAG3-72)
(NASA-CR-4278; E-5228; NAS 1.26:4278) Avail: NTIS HC A09/MF A01 CSCL 01A

Local heat transfer coefficients from a smooth and roughened NACA 0012 airfoil were measured using a steady state heat flux method. Heat transfer measurements on the specially constructed 0.533 meter chord airfoil were made both in flight on the NASA Lewis Twin Otter Research Aircraft and in the NASA Lewis Icing Research Tunnel (IRT). Roughness was obtained by the attachment of small, 2 mm diameter, hemispheres of uniform size to the airfoil surface in four distinct patterns. The flight data was taken for the smooth and roughened airfoil at various Reynolds numbers based on chord in the range of 1.24x10(exp 6) to 2.50x10(exp 6) and at various angles of attack up to 4 degrees. During these flight tests the free stream velocity turbulence intensity was found to be very low (less than 0.1 percent). The wind tunnel data was taken in the Reynolds number range of 1.20x10(exp 6) to 4.52x10(exp 6) and at angles of attack from -4 degrees to +8 degrees. The turbulence intensity in the IRT was 0.5 to 0.7 percent with the cloud making spray off. Results for both the flight and tunnel tests are presented as Frossling number based on chord versus position on the airfoil surface for various roughnesses and angle of attack. A table of power law curve fits of Nusselt number as a function of Reynolds number is also provided. The higher level of turbulence in the IRT versus flight had little effect on heat transfer for the lower Reynolds numbers but caused a moderate increase in heat transfer at the higher Reynolds numbers. Turning on the cloud making spray air in the IRT did not alter the heat transfer. Roughness generally increased the heat transfer by locally disturbing the boundary layer flow. Finally, the present data was not only compared with previous airfoil data where applicable, but also with leading edge cylinder and flat plate heat transfer values which are often used to estimate airfoil heat transfer in computer codes. Author

N90-19204*# National Aeronautics and Space Administration. Ames Research Center, Moffett Field, CA.
THREE-DIMENSIONAL VISCOUS ROTOR FLOW CALCULATIONS USING A VISCOUS-INVISCID INTERACTION APPROACH
Ching S. Chen and John O. Bridgeman (Woodside Summit Group, Inc., Mountain View, CA.) Feb. 1990 24 p Presented at the 15th European Rotorcraft Forum, Amsterdam, Netherlands, Sep. 1989 Submitted for publication
(NASA-TM-102235; A-89246; NAS 1.15:102235) Avail: NTIS HC A03/MF A01 CSCL 01A

A three-dimensional viscous-inviscid interaction analysis was developed to predict the performance of rotors in hover and in forward flight at subsonic and transonic tip speeds. The analysis solves the full-potential and boundary-layer equations by finite-difference numerical procedures. Calculations were made for several different model rotor configurations. The results were compared with predictions from a two-dimensional integral method and with experimental data. The comparisons show good agreement between predictions and test data. Author

N90-19205*# National Aeronautics and Space Administration. Langley Research Center, Hampton, VA.
NUMERICAL SOLUTION OF 3D NAVIER-STOKES EQUATIONS WITH UPWIND IMPLICIT SCHEMES
Yves P. Marx Jan. 1990 65 p
(NASA-TM-101656; NAS 1.15:101656) Avail: NTIS HC A04/MF A01 CSCL 01A

An upwind MUSCL type implicit scheme for the three-dimensional Navier-Stokes equations is presented. Comparison between different approximate Riemann solvers (Roe and Osher) are performed and the influence of the reconstructions schemes on the accuracy of the solution as well as on the convergence of the method is studied. A new limiter is introduced in order to remove the problems usually associated with non-linear upwind schemes. The implementation of a diagonal upwind implicit operator for the three-dimensional Navier-Stokes equations is also discussed. Finally the turbulence modeling is assessed. Good prediction of separated flows are demonstrated if a non-equilibrium turbulence model is used. Author

N90-19206*# National Aeronautics and Space Administration. Langley Research Center, Hampton, VA.
DEVELOPMENT OF A PRELIMINARY HIGH-ANGLE-OF-ATTACK NOSE-DOWN PITCH CONTROL REQUIREMENT FOR HIGH-PERFORMANCE AIRCRAFT
Luat T. Nguyen and John V. Foster (Lockheed Engineering and Sciences Co., Hampton, VA.) Feb. 1990 28 p
(NASA-TM-101684; NAS 1.15:101684) Avail: NTIS HC A03/MF A01 CSCL 01A

The requirements for high-angle-of-attack nose-down pitch control for advanced high-performance aircraft are discussed. Background information on fundamental factors that influence and, to a large extent, determine the high angle-of-attack nose-down control requirement is briefly reviewed. Guidelines currently proposed by other sources which attempt to define these requirements are discussed. A requirement based on NASA analysis of the characteristics of existing relaxed static stability (RSS) aircraft is presented. This analysis could provide the basis for a preliminary design guide. Author

N90-19207# Technische Hochschule, Aachen (Germany, F.R.). Mathematisch-Naturwissenschaftlichen Fakultaet.
A PANEL PROCESS FOR THE CALCULATION OF THE FLOW AROUND A WING WITH FRONT ANGLE DAMPING Ph.D. Thesis [EIN PANELVERFAHREN ZUR BERECHNUNG DER STROEMUNG UM FLUEGEL MIT VORDERKANTENABLOESUNG: ZUR STETIGEN APPROXIMATION VON WIRBELSCHICHTEN]
Karlheinz Haag 1988 93 p In GERMAN
(ETN-90-95367) Avail: NTIS HC A05/MF A01

The influence of free eddy layers, that appear in subsonic flows at the acute angles of the delta wings, on the aerodynamic values and the pressure distribution on the wing, is studied by means of a potential theoretical method. For the digital simulation, a panel process is used, with a total dipole distribution on the discontinuity layers. The nonlinear problem is dicretized and iteratively resolved by a collocation process; the Jacobi matrix is totally analytically calculated in the iteration process. The model is successfully tested for triangular wings, gothic wings, delta wings with vortex valves. By comparison with experiments and other calculation processes, good accordance with pressure distribution and aerodynamic values is obtained. In most described examples, there is no problem of convergence. ESA

N90-19208# Technische Hochschule, Aachen (Germany, F.R.). Fakultaet fuer Maschinenwesen.
CARRIER WING PROFILE IN NONSTATIONARY CURRENT Ph.D. Thesis [TRAGFLUEGELPROFILE IN INSTATIONAERER ANSTROEMUNG]
Willi-Bert Schweitzer 1988 145 p In GERMAN
(ETN-90-95368) Avail: NTIS HC A07/MF A01

The nonstationary current profile is examined in the case of a constant angle of incidence and a time-dependent current velocity, in a water channel and a water gate and in an Eiffel wind channel, with laminar flows. To obtain a periodic, sinusoidal current, this channel is equipped with a rotating retaining valve of variable size, which produces variations of the flow velocity for a mean Reynolds number of 200,000. The turbulence degree of the current is very minimal and the higher harmonics cannot be avoided by any configuration. The measurement of nonstationary pressure distribution was made by means of a moving sonde in the water channel and the examination of the profile current in wind canal was realized by means of a helium wind generator. Both of the experiments showed some similar phenomena in the current processes, despite very different test conditions. ESA

N90-19209# Max-Planck-Inst. fuer Stroemungsforschung, Goettingen (Germany, F.R.).
TOMOGRAPHIC INVESTIGATIONS OF WEAKLY PERTURBED SUPERSONIC FREE JETS
Rupert Wenskus 1988 90 p In GERMAN; ENGLISH summary
(MPIS-Mitt-91; ISSN-0374-1257; ETN-90-95851) Avail: NTIS HC A05/MF A01

A tomographic algorithm is developed for the investigation of three dimensional compressible flow fields by means of interferometric methods. This algorithm is based on the principle which underlies algebraic reconstruction techniques. Reconstruction is combined with averaging over the input data to reduce the influence of measurement errors. Preliminary comparative tests showed an improved quality of reconstruction as compared to the results of other algorithms. The method was applied to the reconstruction of the distribution of density in weakly perturbed super sonic free jets. Small even deviation of the nozzle shape from rotational symmetry result in significant three dimensional effects. ESA

N90-19210# Max-Planck-Inst. fuer Stroemungsforschung, Goettingen (Germany, F.R.).
DRAG REDUCTION BY LONGITUDINAL RIBLETS ON THE SURFACE OF A STREAMWISE ALIGNED BODY OF REVOLUTION
Dieter Neumann 1989 69 p In GERMAN; ENGLISH summary
(MPIS-Mitt-92; ISSN-0374-1257; ETN-90-95852) Avail: NTIS HC A04/MF A01

In flowing water with velocities of up to 9 m/s the friction drag of a streamwise oriented body of revolution was investigated independently to the surface structure. This was done for different types of riblet film fixed on the surface with the riblet direction aligned parallel to the flow. The spacing between two triangular riblets varied between 0.152 mm and 0.033 mm. For all types of film the riblet spacing was equal to the riblet height. For comparison, a smooth reference film was used. Depending on the Reynolds number and the nondimensional riblet spacing, a drag reduction of up to 9 percent could be achieved with riblets, in comparison to the flow over a smooth surface. In the transition region of the turbulent flow and for some values of nondimensional riblet spacing, drag reductions of up to 13 percent were obtained. It is assumed that, in addition to the hampering of the near wall momentum exchange, the riblets delay the development of initial turbulent structures by time and space. ESA

N90-19211*# National Aeronautics and Space Administration. Langley Research Center, Hampton, VA.
CONICAL EULER SOLUTION FOR A HIGHLY-SWEPT DELTA WING UNDERGOING WING-ROCK MOTION
Elizabeth M. Lee and John T. Batina Mar. 1990 18 p
(NASA-TM-102609; NAS 1.15:102609) Avail: NTIS HC A03/MF A01 CSCL 01A

Modifications to an unsteady conical Euler code for the free-to-roll analysis of highly-swept delta wings are described. The modifications involve the addition of the rolling rigid-body equation of motion for its simultaneous time-integration with the governing flow equations. The flow solver utilized in the Euler code includes a multistage Runge-Kutta time-stepping scheme which uses a

finite-volume spatial discretization on an unstructured mesh made up of triangles. Steady and unsteady results are presented for a 75 deg swept delta wing at a freestream Mach number of 1.2 and an angle of attack of 30 deg. The unsteady results consist of forced harmonic and free-to-roll calculations. The free-to-roll case exhibits a wing rock response produced by unsteady aerodynamics consistent with the aerodynamics of the forced harmonic results. Similarities are shown with a wing-rock time history from a low-speed wind tunnel test. Author

N90-19212# National Aeronautical Lab., Bangalore (India). Experimental Aerodynamics Div.
STUDY OF THE TURBULENT BOUNDARY LAYER ON AN AFTERBODY
V. Krishnan Apr. 1989 55 p
(TM-EA-8901) Avail: NTIS HC A04/MF A01

Experiments were conducted to study the turbulent boundary layer on a circular arc boat-tailed afterbody model of 80 mm maximum diameter (D). Tests were conducted at free stream velocities up to 28 m/sec and without jet. There is a favorable pressure gradient (FPG) on the afterbody before strong adverse pressure gradient (APG) close to the base. The boundary layer thickness increases from 0.25 to 0.67 times local radius which may be considered thick especially close to the base. The parameters of the boundary layer remain fairly constant in FPG and change rapidly in APG. The mass flow shape factor is slightly greather than the predictions made using Green's relationship in APG. Mean velocity profiles have considerable portion of the logarithmic region when plotted in the two-dimensional wall law coordinates. The log law constants have universal values and the wake component decreases in FPG. In APG, slope of the velocity profile when plotted in wall law coordinates increases. The intercept of the defect law is smaller compared to the two-dimensional case in FPG. Normal static pressure measurements in the boundary layer show linear variations and it is such that the longitudinal pressure gradient is less at the edge of the boundary layer than at the model surface. Author

N90-19213# National Aeronautical Lab., Bangalore (India). Computational and Theoretical Fluid Dynamics Div.
ANALYSIS AND DESIGN OF SYMMETRICAL AIRFOILS
P. Ramamoorthy and S. K. Prasad Dec. 1989 21 p
(PD-CF-8943) Avail: NTIS HC A03/MF A01

A new theory is developed for the analysis and design of symmetrical airfoils. It is based on Lanczos polynomial interpolation and Goldsteins approximations to thick airfoil theory. The theory gave velocity, agreeing with the exact method of Theodorsen correct to three decimals. The inverse design part gave back the known airfoil coordinates again correct to three decimals. Author

03 AIR TRANSPORTATION AND SAFETY

Includes passenger and cargo air transport operations; and aircraft accidents.

For related information see also *16 Space Transportation* and *85 Urban Technology and Transportation.*

N90-19214# Federal Aviation Administration, Washington, DC. Office of Aviation Medicine.
EVALUATION OF THE SCOTT AVIATION PORTABLE PROTECTIVE BREATHING DEVICE FOR CONTAMINANT LEAKAGE AS PRESCRIBED BY FAA ACTION NOTICE A-8150.2. PHASE 1: ORIGINAL TESTS OF THE PORTABLE PROTECTIVE BREATHING DEVICE. PHASE 2: TESTS OF THE REDESIGNED PORTABLE PROTECTIVE BREATHING DEVICE
E. A. Higgins, Garnet A. McLean, Peggy J. Lyne, Gordon E. Funkhouser, and Joseph W. Young Nov. 1989 34 p
(AD-A216799; DOT/FAA/AM-89/11) Avail: NTIS HC A03/MF A01 CSCL 01/5

At the request of Scott Aviation, performance tests of the crew portable protective breathing (CPBE) device (PN-802300-11) were conducted at ground level and 8,000 ft. altitude. The first tests at ground level measured contaminant leakage, oxygen and carbon dioxide levels, inhalation and/or exhalation pressures and internal and/or external dry bulb temperatures; replications at 8,000 ft. were performed for all the variables except contaminant leakage. For ten male subjects, the device proved satisfactory for all measures tested; compliance with A-8150.2 could be established for internal CPBE temperature since no wet bulb values were obtained. Devices were also tested on nine female subjects; the findings were successful for all measures except contaminant leakage. A new set of tests, approved by the FAA Certification Office in New York, was conducted after changes in neck seal material and opening size were made by Scott Aviation, using only 1 male and 5 females with small neck circumferences (11.81 to 13.07 ins.) and 1 male with a large neck size (16.62 ins.). These tests proved successful for all but two devices on subjects with unusually protruding larynxes, for which a further reduction in neck seal opening size afforded adequate protection for these individuals, as well as an acceptable comfort level for a large individual. It is concluded that the Scott CPBE device with a 1/16 in thick neoprene foam neck seal, having a 2.5 in. diameter opening, performs as required by FAA Action Notice A-8150.2. GRA

N90-19215# Sandia National Labs., Albuquerque, NM. Experimental Mechanics Dept.
HELICOPTER FLIGHT VIBRATION OF LARGE TRANSPORTATION CONTAINERS: A CASE FOR TESTING TAILORING
J. D. Rogers, D. B. Beightol, and J. W. Doggett 1989 7 p Presented at the 36th Institute of Environmental Science Annual Technology Meeting, New Orleans, LA, 23-27 Apr. 1990
(Contract DE-AC04-76DP-00789)
(DE90-007429; SAND-89-2140C; CONF-900479-4) Avail: NTIS HC A02/MF A01

A testing situation is described in which the test specification was derived from MIL-STD-810D for helicopter flight vibration of some test items. The items were to be inside two very large transportation containers (masses on the order of 2000 to 4000 pounds). Severe testing difficulties were anticipated in achieving the desired levels from the test specification. It was then decided to obtain appropriate field data to modify the test specification. The data were obtained during flights of CH-47D helicopters containing the transportation containers. The vibration levels experienced by the test items were significantly below those specified in the original test plan. DOE

04 AIRCRAFT COMMUNICATIONS AND NAVIGATION

Includes digital and voice communication with aircraft; air navigation systems (satellite and ground based); and air traffic control.

For related information see also *17 Space Communications, Spacecraft Communications, Command and Tracking* and *Communications and Radar.*

N90-19216# Federal Aviation Administration, Washington, DC.
SYMPOSIUM ON AIR TRAFFIC CONTROL TRAINING FOR TOMORROW'S TECHNOLOGY
1989 268 p Symposium held in Oklahoma City, OK, 6-8 Dec. 1988
(PB90-127325) Avail: NTIS HC A12/MF A02 CSCL 17G

The symposium focused on recent research findings and technologies related to FAA training requirements. Specific objectives of the symposium were: to identify strategies and structures for changing FAA training procedures and processes, as required to meet future air traffic control needs; to discuss, review, and demonstrate the latest innovation in simulation, interactive instruction techniques (including part-task simulation), and other technologies applicable to present and future air traffic control training requirements; and to discuss and review

contemporary learning theory and its relevant application to the air traffic control training environment. Author

N90-19217# Sandia National Labs., Albuquerque, NM.
HELI/SITAN: A TERRAIN REFERENCED NAVIGATION ALGORITHM FOR HELICOPTERS
Jeff Hollowell 1990 10 p Presented at PLANS 90, Las Vegas, NV, 20-23 Mar. 1990
(Contract DE-AC04-76DP-00789; AVRADA Proj. 5620112DA)
(DE90-005193; SAND-89-1972C; CONF-900372-1) Avail: NTIS HC A02/MF A01

Heli/SITAN is a Terrain Referenced Navigation (TRN) algorithm that utilizes radar altimeter ground clearance measurements in combination with a conventional navigation system and a stored digital terrain elevation map to accurately estimate a helicopter's position. Multiple Model Adaptive Estimation (MMAE) techniques are employed using a bank of single state Kalman filters to ensure that reliable position estimates are obtained even in the face of large initial position errors. A real-time implementation of the algorithm was tested aboard a U.S. Army UH-1 helicopter equipped with a Singer-Kearfott Doppler Velocity Sensor (DVS) and a Litton LR-80 strapdown Attitude and Heading Reference System (AHRS). The median radial error of the position fixes provided in real-time by this implementation was less than 50 m for a variety of mission profiles. DOE

N90-19218# National Geodetic Survey, Rockville, MD.
ACCURACY OF GLOBAL POSITIONING SYSTEM BROADCAST ORBITS FOR RELATIVE SURVEYS
B. W. Remondi and B. Hofmann-Wellenhof Oct. 1989 37 p
(PB90-125428; NGS-45; NOAA-TR-NOS-132) Avail: NTIS HC A03/MF A01 CSCL 17G

The accuracy of the Global Positioning System (GPS) broadcast orbits is important to the GPS community for both military and civilian applications. Surveyors, for examples, would like to know if field processing of GPS baselines can be considered final. There is widespread belief that for accurate surveys, post processing with precise ephemerides is required. Precise versus broadcast comparisons are given in terms of along track, cross track, and radial plots and statistics based on hundreds of actual broadcast orbit comparisons. The proper use of the broadcast orbits is discussed. A strong measure of orbital accuracy is the effect of orbit errors on baseline vector computations. Numerous baseline vector solutions, using both precise orbits and broadcast orbits, are given. Author

N90-19219# Technische Univ., Delft (Netherlands). Vakgroep Mathematische en Fysische Geodaesie.
CALCULATION OF IONOSPHERIC CORRECTIONS FOR SINGLE FREQUENCY GPS OBSERVATIONS: INVESTIGATION OF TWO MODELS Thesis [DE BEREKENING VAN IONOSFEERCORRECTIES VOOR ENKEL-FREQUENTIE GPS WAARNEMINGEN: EEN ONDERZOEK NAAR TWEE MODELLEN]
J. J. Melgers May 1989 70 p In DUTCH; ENGLISH summary
(ETN-90-95450) Avail: NTIS HC A04/MF A01

The correction of the ionospheric effect on the propagation velocity of radiowaves using ionosphere and the GPS (global positioning system) are introduced, and the two models are described. The first model is based on observations of the maxiumum electron density in the ionospheric F2-layer from several stations. The second model uses one double frequency receiver and can be applied if, during a GPS measurement, one double frequency receiver is used besides one or more single frequency receivers. The comparison of the results from both models with double frequency results shows that the first model fails, while the second model gives reasonably good results. ESA

N90-19220# Technische Univ., Delft (Netherlands). Vakgroep Mathematische en Fysische Geodesie.
CARIN AND GPS: THE COMBINATION OF DEAD RECKONING, MAP MATCHING AND SATELLITE NAVIGATION IN A HYBRID AUTOMOBILE NAVIGATION SYSTEM Thesis [CARIN EN GPS: DE COMBINATIE VAN DEAD-RECKONING, MAP-MATCHING EN SATELLIETPLAATSBEPALING IN EEN HYBRIDE AUTONAVIGATIESYSTEEM]
Rob L. G. Lemmens 1989 173 p In DUTCH
(ETN-90-95451) Avail: NTIS HC A08/MF A01

The possible coupling between the Philips Carin (car information and navigation system) automobile navigation system and the Global Positioning System (GPS)/Navstar satellite positioning system was investigated. The Carin system is based on a combination of dead reckoning and map matching. Since the system can drift, a correction by an absolute position sensor such as GPS, is desirable. The possibilities and feasibility of a coupling between Carin and GPS were examined using test ride simulations and a dynamic model that determines a weighted solution between the GPS and the Carin position, based on error models. It is shown that GPS does not function well in urban areas, in contrast with Carin. Outside urban areas the situation is reversed, demonstrating the complementary character of both systems. The hybrid system provides in any situation a better accuracy than that of each system separately. ESA

N90-19221# Stuttgart Univ. (Germany, F.R.). Sonderforschungsbereich 228.
HIGHLY ACCURATE NAVIGATION: INTEGRATION OF NAVIGATION AND GEODESIC METHODS Studies and Summary Reports, 1987 - 1989 [HOCHGENAUE NAVIGATION INTEGRATION NAVIGATORISCHER UND GEODATISCHER METHODEN. ARBEITS- UND ERGEBNISBERICHT 1987-1989]
1989 169 p In GERMAN
(SFB-228; ETN-90-95866) Avail: NTIS HC A08/MF A01

The following topics are studied: highly accurate integrated navigation by positioning with navigation satellites, microwaves and laser ranging process, altimetry; geodesic utilization of highly accurate navigation sensors by utilization of global satellite navigation systems for local deformation surveillance, nuclear resonance gyroscope, implementation of navigation data in the photogrammetry; images processing by digital ground models and microwaves, digital image correlation, transmission chain of the optic image recording process for flight and satellite recording, digital processing of radar images; and geodesic inertial process by intertial geodesic position and testing and utilization of geodesic inertia navigation systems. ESA

N90-19222# Air War Coll., Maxwell AFB, AL.
THE GLOBAL POSITIONING SYSTEM
Mark J. Fischer May 1989 28 p
(AD-A217266) Avail: NTIS HC A03/MF A01 CSCL 17/7

A description of the Global Positioning System (GPS) and current program status are provided. The importance of timing and position data are highlighted, using several historical examples. Potential uses for GPS by all the military services are explored. The author examines the role of the current GPS program office. The major drawback to the program, in the author's view, is that GPS requirements are not addressed from a joint Department of Defense perspective. A solution to this deficiency is suggested. GRA

N90-19223# Air War Coll., Maxwell AFB, AL.
INTEROPERABILITY ISSUES IN THE USE OF SATELLITE-BASED NAVIGATION SYSTEMS FOR CIVIL AVIATION PURPOSES
Marcos Costilla May 1989 88 p
(AD-A217279) Avail: NTIS HC A05/MF A01 CSCL 17/7

This study analyzes that compatibility and interoperability issues related to the use of the USAF NAVSTAR Global Positioning System for civil aviation purposes. It also compares the USSR GLONASS navigation system to GPS to provide similar services worldwide. The GPS is primarily a military asset with significant

civil applications especially as it applies to air traffic control (ATC). It is recognized by the civil sector as a system which will revolutionize the present day navigation methodology and indeed make way for new ATC concepts and procedures. Several compatibility and interoperability issues are described wherein the system integrity issue remains outstanding and must be resolved prior to using GPS for civil aviation. It appears the USAF and FAA intend to utilize GPS to meet their air navigation system requirements of the future. However, the USAF GPS program implementation is years ahead of the FAA. It is recommended the programs be compared and evaluated to ensure maximum compatibility and to expedite the use of GPS for civil applications. FAA is presently working with the USSR and the International Civil Aviation Organization (ICAO) in an effort to develop international standards for satellite-based navigation systems such as GPS and GLONASS. This effort appears to be progressing well in spite of limited data regarding the GLONASS system.

GRA

05 AIRCRAFT DESIGN, TESTING AND PERFORMANCE

Includes aircraft simulation technology.

For related information see also *18 Spacecraft Design, Testing and Performance* and *39 Structural Mechanics*.For land transportation vehicles see *85 Urban Technology and Transportation.*

N90-19224*# National Aeronautics and Space Administration. Hugh L. Dryden Flight Research Facility, Edwards, CA.

COMPENSATING FOR PNEUMATIC DISTORTION IN PRESSURE SENSING DEVICES

Stephen A. Whitmore and Cornelius T. Leondes (California Univ., Los Angeles.) Jan. 1990 21 p Presented at the AIAA 28th Aerospace Sciences Meeting, Reno, NV, 8-11 Jan. 1990 Previously announced in IAA as A90-19956

(NASA-TM-101716; H-1586; NAS 1.15:101716) Avail: NTIS HC A03/MF A01 CSCL 01C

A technique of compensating for pneumatic distortion in pressure sensing devices was developed and verified. This compensation allows conventional pressure sensing technology to obtain improved unsteady pressure measurements. Pressure distortion caused by frictional attenuation and pneumatic resonance within the sensing system makes obtaining unsteady pressure measurements by conventional sensors difficult. Most distortion occurs within the pneumatic tubing which transmits pressure impulses from the aircraft's surface to the measurement transducer. To avoid pneumatic distortion, experiment designers mount the pressure sensor at the surface of the aircraft, (called in-situ mounting). In-situ transducers cannot always fit in the available space and sometimes pneumatic tubing must be run from the aircraft's surface to the pressure transducer. A technique to measure unsteady pressure data using conventional pressure sensing technology was developed. A pneumatic distortion model is reduced to a low-order, state-variable model retaining most of the dynamic characteristics of the full model. The reduced-order model is coupled with results from minimum variance estimation theory to develop an algorithm to compensate for the effects of pneumatic distortion. Both postflight and real-time algorithms are developed and evaluated using simulated and flight data. Author

N90-19225*# National Aeronautics and Space Administration. Hugh L. Dryden Flight Research Facility, Edwards, CA.

X-29A AIRCRAFT STRUCTURAL LOADS FLIGHT TESTING

Robert Sims, Paul McCrosson, Robert Ryan, and Joe Rivera (Grumman Aerospace Corp., Edwards, CA.) Dec. 1989 37 p Presented at the 20th Annual Society of Flight Test Engineers Symposium, Reno, NV, 18-21 Sep. 1989

(NASA-TM-101715; H-1574; NAS 1.15:101715) Avail: NTIS HC A03/MF A01 CSCL 01C

The X-29A research and technology demonstrator aircraft has completed a highly successful multiphase flight test program. The primary research objective was to safely explore, evaluate, and validate a number of aerodynamic, structural, and flight control technologies, all highly integrated into the vehicle design. Most of these advanced technologies, particularly the forward-swept-wing platform, had a major impact on the structural design. Throughout the flight test program, structural loads clearance was an ongoing activity to provide a safe maneuvering envelope sufficient to accomplish the research objectives. An overview is presented of the technologies, flight test approach, key results, and lessons learned from the structural flight loads perspective. The overall design methodology was considered validated, but a number of structural load characteristics were either not adequately predicted or totally unanticipated prior to flight test. While conventional flight testing techniques were adequate to insure flight safety, advanced analysis tools played a key role in understanding some of the structural load characteristics, and in maximizing flight test productivity. Author

N90-19226*# Analytical Services and Materials, Inc., Hampton, VA.

PERFORMANCE OF AN OPTIMIZED ROTOR BLADE AT OFF-DESIGN FLIGHT CONDITIONS

Aditi Chattopadhyay Washington NASA Mar. 1990 17 p Presented at the AHS Vertical Lift Aircraft Design Conference, San Francisco, CA, 17-19 Jan. 1990

(Contract NAS1-18599)

(NASA-CR-4288; NAS 1.26:4288) Avail: NTIS HC A03/MF A01 CSCL 01C

An investigation is made of the dynamic and aerodynamic performance of a helicopter rotor previously optimized for minimum 4/rev vertical shear and blade weight subject to certain dynamic and structural constraints. The program CAMRAD which was used in designing the optimized blade is used for both dynamic and aerodynamic analaysis. The behavior of the optimized rotor is analyzed over a wide range of operating conditions and for a larger number of rotor characteristics than those considered in designing the blade. To assess the dynamic behavior, the blade root vibratory shears and moments that are transmitted to the rotor hub are calculated. The aerodynamic performance assessments are made based on the power required by the rotor for a given rotor task, the rotor lifting efficiencies, maximum rotor thrust envelopes and the control margins. Results are presented for the optimized blade and the control margins. Results are presented for the optimized blade and the reference blade, which was used as the baseline for the optimized blade, for two rotor tasks. Author

N90-19227*# National Aeronautics and Space Administration. Langley Research Center, Hampton, VA.

AEROSERVOELASTICITY

Thomas E. Noll Mar. 1990 13 p Presented at the AIAA 31st Structures, Structural Dynamics, and Materials Conference, Long Beach, CA, 2-4 Apr. 1990

(NASA-TM-102620; NAS 1.15:102620) Avail: NTIS HC A03/MF A01 CSCL 01C

Accomplishments and current research projects along four main thrusts in aeroservoelasticity at the NASA Langley Research Center are described. One activity focuses on enhancing the modelling and the analysis procedures to accurately predict aeroservoelastic interactions. In the area of modelling, improvements to the minimum-state method of approximating unsteady aerodynamics are shown to provide precise, low-order models for design and simulation tasks. Recent extensions in aerodynamic correction factor methodology are also described. With respect to analysis procedures, the paper reviews novel enhancements to Matched Filter Theory and Random Process Theory for predicting the critical gust profile and the associated time-correlated gust loads for structural design considerations. In another activity, two research projects leading towards improved design capability are summarized. The first program involves the development of an integrated structure/control design capability; the second provides procedures for obtaining low-order, robust digital control laws for aeroelastic applications. Experimental

validation of new theoretical developments is the third activity. As such, a short description of the Active Flexible Wing Project is presented, and recent wind-tunnel test accomplishments are summarized. Finally within the area of application, a study performed to assess the state-of-the-art of aeroelastic and aeroservoelastic analysis and design technology with respect to hot, hypersonic flight vehicles is reviewed. Author

N90-19228# National Aerospace Lab., Amsterdam (Netherlands). Materials and Structures Div.
STATIC STRENGTH AND DAMAGE TOLERANCE TESTS ON THE FOKKER 100 AIRFRAME
H. Vlieger Mar. 1988 16 p In DUTCH; ENGLISH summary Presented at the NVvL-VSV Symposium Certificatie van Vliegtuigen, Delft, Netherlands, 29 Apr. 1988
(Contract NIVR-06501N)
(NLR-MP-88023-U; ETN-90-95419) Avail: NTIS HC A03/MF A01

A full scale static and flight simulation fatigue test program was performed on the airframe of the Fokker 100 to show compliance with the requirements of the airworthiness authorities regarding static strength and damage tolerance of a new design. The aircraft was split up into a number of specimens, each constituting a major assembly of the total airframe. The tests carried out on one of the specimen (the horizontal stabilizer) are described. The design of the test rig and the load introduction system, the loading program for static and flight simulation testing, the load control during testing, and the various measurements are discussed. The preliminary testing results are presented. ESA

N90-19229# Technische Univ., Brunswick (Germany, F.R.). Fakultaet fuer Maschinenbau und Elektrotechnik.
CALCULATION AND OPTIMIZATION OF ROTOR START PROCESS Ph.D. Thesis [EIN BEITRAG ZUR BERECHNUNG UND OPTIMIERUNG VON HUBSCHRAUBER-STARTVERFAHREN]
Thomas Cerbe 1989 138 p In GERMAN
(ETN-90-95894) Avail: NTIS HC A07/MF A01

Appropriate simulation models are developed for the calculation and the optimization of rotor start process and the checkout by flight tests. The quasi stationary model needs a calculation time ten times lower than the simulated real time. For the ground effect in forward flight a half-empirical model is integrated into the rotor calculation. The dynamic ground effect is taken into account in the slow flight area by a filter of first order. The comparison of the different simulations shows a very good estimation of the power needs. The total simulation of the longitudinal motion and the characteristic field show negligible differences of power. Several decisive points for the start of a rotor are obtained, that are dependent on the plane mass, the start power, and the atmospheric conditions. A critical decisive velocity is established that is similar to the flight velocity for minimal ascent. ESA

N90-19230# Air War Coll., Maxwell AFB, AL.
LIMITATIONS OF THE CONVENTIONAL ROLE OF THE B-1B IN THE EUROPEAN THEATER
Paul J. Frichtl May 1989 36 p
(AD-A217285) Avail: NTIS HC A03/MF A01 CSCL 15/6

This report outlines the capabilities of the Soviet defenses the B-1B would encounter on a European conventional mission and the characteristics of the B-1B that make it suited for this mission. A description of the conventional limitations of the weapon system follows with discussion of technological fixes. The lack of planning on how the B-1B could best be exploited in a conventional role has led to developing an extremely limited conventional capability that is based on two weapons; the Mk 82,500 pound gravity bomb, and the Mk 36,500 pound mine. These are the only conventional munitions planned for the B-1B. The author suggests a long range perspective is lacking and for the B-1B to be viable in a conventional role new munitions must be developed. GRA

06 AIRCRAFT INSTRUMENTATION

Includes cockpit and cabin display devices; and flight instruments.

For related information see also *19 Spacecraft Instrumentation* and *35 Instrumentation and Photography.*

N90-19231# LITEF, Freiburg (Germany, F.R.).
DEVELOPMENT OF A STANDARDIZED THREE AXIS SENSOR FOR INERTIAL DATA ACHIEVEMENT FOR FUTURE FLIGHT RULE SYSTEMS [ENTWICKLUNG EINES STANDARDISIERTEN DREIACHSIGEN STRAPDOWNSENSORS ZUR INERTIALEN MESSWERTERFASSUNG FUER ZUKUENFTIGE FLUGREGELSYSTEME]
Michael Kleinschmidt, ed., Glynn Everett, Kurt Keller, Uwe Kirchhoff, and Demir Ozdes Jul. 1989 192 p In GERMAN
(Contract BMFT-LFL-7974)
(ETN-90-96075) Avail: NTIS HC A09/MF A01

The use of strapdown technology allows the production of an integrated board-autonomous sensor system for the achievement of flight state magnitudes. The system output values are continuously and immediately available. The coordinate transformations and the velocities are calculated by means of quaternions. By considering the earth as a sphere, a radius and gravity model is created. The system satisfies the essential requirements of a strapdown attitude and heading reference system. The use of Kalman filters for the system support generates time varying reaction amplification. The employed subroutines are detailed. ESA

N90-19417*# Mississippi State Univ., Mississippi State. Dept. of Computer Science.
MARSHALL AVIONICS TESTBED SYSTEM (MAST)
Wayne D. Smith *In* Alabama Univ., Research Reports: 1989 NASA/ASEE Summer Faculty Fellowship Program Dec. 1989 39 p (For primary document see N90-19390 12-31)
(Grant NGT-01-008-021)
Avail: NTIS HC A99/MF E06 CSCL 01D

07 AIRCRAFT PROPULSION AND POWER

Includes prime propulsion systems and systems components, e.g., gas turbine engines and compressors; and onboard auxilliary power plants for aircraft.

For related information see also *20 Spacecraft Propulsion and Power, 28 Propellants and Fuels,* and *44 Energy Production and Conversion.*

N90-19232# Advisory Group for Aerospace Research and Development, Neuilly-Sur-Seine (France). Propulsion and Energetics Panel.
THE UNIFORM ENGINE TEST PROGRAMME
Peter F. Ashwood and James J. Mitchell, ed. Feb. 1990 147 p
(AGARD-AR-248; ISBN-92-835-0501-8) Copyright Avail: NTIS HC A07/MF A01; Non-NATO Nationals requests available only from AGARD/Scientific Publications Executive

The results of the Propulsion and Energetics Panel Working Group 15 are summarized. The Group was in operation 1980 to 1987 and performed test runs of two J57 turbojet engines at eight different facilities for ground-level and altitude tests, in five different nations. At two facilities the tests were repeated in order to review a possible deterioration of the engines. The test rig accompanied the engines to the test facilities. The tests were performed observing a carefully composed General Test Plan, being the same for all facilities. Each facility used its own data asquisition and processing system. Author

N90-19233# Ballistic Research Labs., Aberdeen Proving Ground, MD.
EXTERNAL FLOW COMPUTATIONS FOR A FINNED 60mm RAMJET IN STEADY SUPERSONIC FLIGHT Memorandum Report
Bernard J. Guidos Dec. 1989 50 p
(DA Proj. 1L1-62618-AH-80)
(AD-A216998; BRL-MR-3801) Avail: NTIS HC A03/MF A01 CSCL 16/2

The U.S. Army Ballistic Research Laboratory (BRL) has participated in the development of the launch and flight technologies for a family of solid fuel ramjet (SFRU) projectiles. The ramjet is a tubular projectile which utilizes air ingested through the inlet to burn the solid fuel. When the combustion process ceases, the projectile becomes a high drag configuration. Several designs have been developed as potential tank gun training rounds (TGTR) for kinetic energy (KE) penetrators. This report documents a computational fluid dynamics study of the external aerodynamics of a finned 60mm solid-fuel ramjet in steady, supersonic, atmospheric flight. The main objective is to compute the external contribution to the pitch-plane aerodynamics using established in-house capabilities. Two space-marching finite-difference procedures are used to compute the external flow fields. Viscous flow results are generated using a thin-layer, parabolized Navier-Stokes technique; inviscid results are generated using an Euler solver. Results are shown for three configurations: body-alone, body with original fins, and body with extended fins. The influence of initial marching conditions on the modeling of an inlet configuration is examined. A generalized scaling law is introduced which may improve the accuracy of future external space-marching flow computations for ramjets. GRA

N90-19234*# National Aeronautics and Space Administration. Lewis Research Center, Cleveland, OH.
INDUCTION MOTOR CONTROL
Irving G. Hansen 1990 5 p Prepared for presentation at the National Aerospace and Electronics Conference, Dayton, Ohio, 21-25 May 1990; sponsored in part by the IEEE
(NASA-TM-102533; E-5342; NAS 1.15:102533) Avail: NTIS HC A01/MF A01 CSCL 21E

Electromechanical actuators developed to date have commonly utilized permanent magnet (PM) synchronous motors. More recently switched reluctance (SR) motors have been advocated due to their robust characteristics. Implications of work which utilizes induction motors and advanced control techniques are discussed. When induction motors are operated from an energy source capable of controlling voltages and frequencies independently, drive characteristics are obtained which are superior to either PM or SR motors. By synthesizing the machine frequency from a high frequency carrier (nominally 20 kHz), high efficiencies, low distortion, and rapid torque response are available. At this time multiple horsepower machine drives were demonstrated, and work is on-going to develop a 20 hp average, 40 hp peak class of aerospace actuators. This effort is based upon high frequency power distribution and management techniques developed by NASA for Space Station Freedom. Author

N90-19235# Technische Hochschule, Aachen (Germany, F.R.). Inst. fuer Strahlantriebe und Turboarbeitsmaschinen.
INFLUENCE OF FRICTION AND SEPARATION PHENOMENA ON THE DYNAMIC BLADE LOADING OF TRANSONIC TURBINE CASCADES [EINFLUSS VON REIBUNGS- UND ABLOESEVORGAENGEN AUF DIE DYNAMISCHE SCHAUFELBELASTUNG VON TRANSSONISCHEN TURBINENGITTERN]
H. E. Gallus and J. Henne Nov. 1988 163 p In GERMAN Sponsored by Wissenschaftsminister des Landes Nordrhein-Westfalen
(Mitt-88-04; ETN-90-95324) Avail: NTIS HC A08/MF A01

The steady and unsteady flow in a transonic, plane turbine cascade with rigid blades as well as blades capable of vibration were investigated. The emphasis was on the behavior of the boundary layers and their interaction with compressional shocks with a view to an aerodynamic vibrational excitation of the blades. The experiments show that a careful shielding of the flow against unsteady perturbations is required for the measurement of unsteady cascade flow effects. The steady, transonic flow was calculated using a time marching method. The measurements of the unsteady flow show a largely stable shock-boundary-layer configuration. The amplitude variations of the compressional shocks is not substantially affected by the vibration capability of the blades. ESA

N90-19236# Stuttgart Univ. (Germany, F.R.). Inst. fuer Thermische Stroemungsmaschinen und Maschinenlab.
DIGITAL DETERMINATION OF THE THREE DIMENSIONAL FLOW IN TURBOMACHINES WITH THE S1-S2 CURRENT FUNCTION PROCESS [DIE NUMERISCHE ERFASSUNG DER DREIDIMENSIONALEN STROEMUNG IN TURBOMASCHINEN MIT DEM S1-S2-STROMFUNKTIONVERFAHREN]
Michael Sollinger Nov. 1988 120 p In GERMAN
(ITSM-Mitt-30; ETN-90-95865) Avail: NTIS HC A06/MF A01

A flow model of Wu is presented, based on the assumption that the flow can be described by two current surface perpendicular masses. It is presumed that the flow is stationary in the arrested or rotating blade files. The current function process is limited to the subsonic velocity area for the calculation of the stationary turbomachine flow and is based on Euler equations. The friction effects in the viscosity layers are studied. The equations are transformed with the flow area in an equidistant calculation grid and are solved by the finite difference method. ESA

N90-19237# Massachusetts Inst. of Tech., Cambridge. Gas Turbine Lab.
EXPERIMENTAL AND THEORETICAL INVESTIGATIONS OF FLOWFIELDS AND HEAT TRANSFER IN MODERN GAS TURBINES Final Summary Report, 1 Jan. 1981 - 31 Mar. 1987
A. H. Epstein, M. B. Giles, G. R. Guenette, and W. T. Thompkins, Jr. Jan. 1990 35 p
(Contract N00014-81-K-0024)
(AD-A217663) Avail: NTIS HC A03/MF A01 CSCL 20/4

Aerodynamics and heat transfer of high pressure turbines were studied computationally and experimentally. Two- and three-dimensional steady, and two-dimensional unsteady viscous codes were written. An 0.3 second duration, full rotating stage, test rig was built and instrumented to yield both steady state and time-resolved data. The computational fluid dynamic (CFD) solution and experimental data were in good agreement. The rotating rig data resembled that from cascades rather than full scale engines. GRA

N90-19421*# Alabama Univ., Huntsville. Dept. of Aerospace Engineering.
THE INFLUENCE OF A WALL FUNCTION ON TURBINE BLADE HEAT TRANSFER PREDICTION
Kevin W. Whitaker *In its* Research Reports: 1989 NASA/ASEE Summer Faculty Fellowship Program Dec. 1989 21 p (For primary document see N90-19390 12-31)
(Grant NGT-01-008-021)
Avail: NTIS HC A99/MF E06 CSCL 21E

08 AIRCRAFT STABILITY AND CONTROL

Includes aircraft handling qualities; piloting; flight controls; and autopilots.

For related information see also *05 Aircraft Design, Testing and Performance.*

N90-19238 Princeton Univ., NJ.
A RULE-BASED PARADIGM FOR INTELLIGENT ADAPTIVE FLIGHT CONTROL Ph.D. Thesis
David Andrew Handelman 1989 339 p
Avail: Univ. Microfilms Order No. DA8918852

Investigated here is the use of highly integrated symbolic and

numeric processing in real-time knowledge-based system for enhanced automatic aircraft failure accommodation. A rule-based control technique is proposed whereby procedural activity is attained through the manipulation of declarative expressions. Rules are used to encode common-sense dependencies, expert knowledge on specific situations, and to invoke algorithmic mathematical procedures. Task execution occurs as a by-product of search through these knowledge base rules. Also proposed is a rule-based controller development system that utilizes a high-level symbolic LISP environment for preliminary system design. Automatic LISP-to-Pascal knowledge base translation is then used to provide dramatically increased execution speed and an environment for highly integrated symbolic and numeric computation. The utility of the control technique is demonstrated through the construction of a multi-microprocessor Rule-Based Flight Control System (RBFCS). Integrating methods of statistical hypothesis testing and rule-based automatic emergency procedure execution, the RBFCS is shown to accommodate multiple simulated failures affecting the electrical, hydraulic, and stability augment subsystems of a CH-47 helicopter. It is found that in addition to enabling significant control system capabilities, the rule-based control technique enhances designer productivity. Dissert. Abstr.

N90-19239*# National Aeronautics and Space Administration. Langley Research Center, Hampton, VA.
LOW-SPEED WIND-TUNNEL INVESTIGATION OF THE FLIGHT DYNAMIC CHARACTERISTICS OF AN ADVANCED TURBOPROP BUSINESS/COMMUTER AIRCRAFT CONFIGURATION
Paul L. Coe, Jr., Steven G. Turner, and D. Bruce Owens Washington Apr. 1990 50 p
(NASA-TP-2982; L-16664; NAS 1.60:2982) Avail: NTIS HC A03/MF A01 CSCL 01C

An investigation was conducted to determine the low-speed flight dynamic behavior of a representative advanced turboprop business/commuter aircraft concept. Free-flight tests were conducted in the NASA Langley Research Center's 30- by 60-Foot Tunnel. In support of the free-flight tests, conventional static, dynamic, and free-to-roll oscillation tests were performed. Tests were intended to explore normal operating and post stall flight conditions, and conditions simulating the loss of power in one engine. Author

N90-19240 Colorado Univ., Boulder.
NEUROCONTROL SYSTEMS AND WING-FLUID INTERACTIONS UNDERLYING DRAGONFLY FLIGHT Ph.D. Thesis
Mark Holcombe Kliss 1989 173 p
Avail: Univ. Microfilms Order No. DA8923505

Studies were performed on the dragonfly, which exhibits a variety of flight modes from hovering to high speed escape. The experiments conducted focus on the neurocontrol strategies and wing-fluid interactions which underlie these flight modes. It appears that an understanding of the dragonfly flight control mechanisms can provide a more comprehensive picture of the control strategies utilized by insects during flight. A simplified model of wing-fluid interactions likely to support particular flight modes was investigated in order to determine the crucial kinematic variables to be controlled. The constraints imposed on dragonfly flight performance by the biomechanics of the flight hardware, and the composition and structure of the nervous system were identified. Specific experiments were then performed to provide insight into the fundamental neurocontrol strategies inherent to the dragonfly nervous system. These studies focused on the cellular, synaptic, and network properties of the ganglia, and the extent to which these properties shape the motor pattern output. Based on the aerodynamic, electrophysiological, histological, and neurophysiological results obtained, a model of dragonfly flight control mechanisms was proposed. Dissert. Abstr.

N90-19241*# National Aeronautics and Space Administration. Hugh L. Dryden Flight Research Center, Edwards, CA.
OUTPUT MODEL-FOLLOWING CONTROL SYNTHESIS FOR AN OBLIQUE-WING AIRCRAFT
Joseph W. Pahle Apr. 1990 30 p
(NASA-TM-100454; H-1522; NAS 1.15:100454) Avail: NTIS HC A03/MF A01 CSCL 01C

Recent interest in oblique-wing aircraft has focused on the potential aerodynamic performance advantage of a variable-skew oblique wing over a conventional or symmetric sweep wing. Unfortunately, the resulting asymmetric configuration has significant aerodynamic and inertial cross-coupling between the aircraft longitudinal and lateral-directional axes. Presented here is a decoupling control law synthesis technique that integrates stability augmentation, decoupling, and the direct incorporation of desired handling qualities into an output feedback controller. The proposed design technique uses linear quadratic regulator concepts in the framework of explicit model following. The output feedback strategy used is a suboptimal projection from the state space to the output space. Dynamics are then introduced into the controller to improve steady-state performance and increase system robustness. Closed-loop performance is shown by application of the control laws to the linearized equations of motion and nonlinear simulation of an oblique-wing aircraft. Author

N90-19420*# Kentucky Univ., Lexington. Dept. of Electrical Engineering.
YAW RATE CONTROL OF AN AIR BEARING VEHICLE
Bruce L. Walcott *In* Alabama Univ., Research Reports: 1989 NASA/ASEE Summer Faculty Fellowship Program Dec. 1989 46 p (For primary document see N90-19390 12-31)
(Grant NGT-01-008-021)
Avail: NTIS HC A99/MF E06 CSCL 01C

09 RESEARCH AND SUPPORT FACILITIES (AIR)

Includes airports, hangars and runways; aircraft repair and overhaul facilities; wind tunnels; shock tubes; and aircraft engine test stands.

For related information see also *14 Ground Support Systems and Facilities (Space).*

N90-19242*# National Aeronautics and Space Administration. Lewis Research Center, Cleveland, OH.
COMPARISON BETWEEN DESIGN AND INSTALLED ACOUSTIC CHARACTERISTICS OF NASA LEWIS 9- BY 15-FOOT LOW-SPEED WIND TUNNEL ACOUSTIC TREATMENT
Milo D. Dahl and Richard P. Woodward Washington Apr. 1990 28 p Presented at the 115th Meeting of the Acoustical Society of America, Seattle, WA, 16-20 May 1988
(NASA-TP-2996; E-4981; NAS 1.60:2996) Avail: NTIS HC A03/MF A01 CSCL 14B

The test section of the NASA Lewis 9- by 15-Foot Low-Speed Wind Tunnel was acoustically treated to allow the measurement of sound under simulated free-field conditions. The treatment was designed for high sound absorption at frequencies above 250 Hz and for withstanding the environmental conditions in the test section. In order to achieve the design requirements, a fibrous, bulk-absorber material was packed into removable panel sections. Each section was divided into two equal-depth layers packed with material to different bulk densities. The lower density was next to the facing of the treatment. The facing consisted of a perforated plate and screening material layered together. Sample tests for normal-incidence acoustic absorption were also conducted in an impedance tube to provide data to aid in the treatment design. Tests with no airflow, involving the measurement of the absorptive properties of the treatment installed in the 9- by 15-foot wind tunnel test section, combined the use of time-delay spectrometry with a previously established free-field measurement method. This new application of time-delay spectrometry enabled these free-field

measurements to be made in nonanechoic conditions. The results showed that the installed acoustic treatment had absorption coefficients greater than 0.95 over the frequency range 250 Hz to 4 kHz. The measurements in the wind tunnel were in good agreement with both the analytical prediction and the impedance tube test data. Author

12 ASTRONAUTICS (GENERAL)

For extraterrestrial exploration see *91 Lunar and Planetary Exploration.*

N90-19243*# National Aeronautics and Space Administration. Goddard Space Flight Center, Greenbelt, MD.
COMPENDIUM OF METEOROLOGICAL SPACE PROGRAMS, SATELLITES, AND EXPERIMENTS
Leland L. Dubach and Carolyn Ng (Science Applications Research, Lanham, MD.) Mar. 1988 285 p
(NASA-TM-102924; NSSDC/WDC-A-R/S-88-03; NAS 1.15:102924) Avail: NTIS HC A13/MF A02 CSCL 22A

This compendium includes plans and events known to the authors through January 1987. Compilation of the information began in 1967. This document is intended: (1) as a historical record of all satellites and instrumentation that has been useful for meteorological research or operational uses; and (2) as a working document to be used to assist meteorologists in identifying meteorological satellites, locating data from these satellites, and understanding experiment operation which is related to satellite data that may be of interest to them. A summary of all known launched satellites for all countries and their experiments, which were concerned with meteorological operations or research, are included. Programs covered include AEM, Apollo, ATS, Bhaskara, Cosmos, Discoverer, DMSP, DOD, DODGE, EOLE, ERBE, ESSA, Explorer, Gemini, GMS, GOES/SMS, INSAT, IRS, LANDSAT, Mercury, Meteor 1 and 2, Meteosat, Molniya, MOS, Nimbus, NOAA (1-5)/ITOS, NOAA (6,7,D)/TIROS-N, NOAA (8-10, H-J)/ATN, Salyut, Seasat, Shuttle 1, Shuttle 2: Spacelab, Skylab, Soyuz, TIROS, TOPEX, Vanguard, Voskhod, Vostok, and Zond. K.C.D.

N90-19244# OHB-System G.m.b.H., Bremen (Germany, F.R.).
TOPAS PREPARATION STUDY: SUMMARY REPRESENTATION OF THE STUDY RESULTS [TOPAS VORBEREITUNGSSTUDIE. ZUSAMMENFASSENDE DARSTELLUNG DER STUDIENERGEBNISSE]
6 Nov. 1987 26 p In GERMAN
(OHB-TN-TOP-011/87; ETN-90-95874) Avail: NTIS HC A03/MF A01

TOPAS is a German-Italian program particularly aimed at gravity research. TOPAS is exclusively based on existing and tested hardware and can be implemented by 1990 with relatively low program costs. With a live load weight of 80 to 100 kg and a mission time up to 3 weeks, TOPAS is an interesting and flexible mission possibility, which complements the programs Texus and Mikroba. TOPAS allows integration initialization, working and safeguard of live loads autonomously, so that experiments can be carried out with regular intervals. TOPAS may be in 1987 the bond between the rare flight opportunities EURECA and Spacelab and the Columbus program which must be operational by 1996. ESA

13 ASTRODYNAMICS

Includes powered and free-flight trajectories; and orbital and launching dynamics.

N90-19245# Air Force Inst. of Tech., Wright-Patterson AFB, OH. School of Engineering.
SERIES REVERSION/INVERSION OF LAMBERT'S TIME FUNCTION M.S. Thesis
James Dana Thorne Dec. 1989 50 p
(AD-A216243; AFIT/GA/ENY/89D-6) Avail: NTIS HC A03/MF A01 CSCL 03/3

The time of flight of a two-body orbit may be determined by integrating the radial velocity equation for a conic section. The resulting expression is sometimes called Lambert's Time Function, which depends on the gravitational constant, two position vectors, and the semi-major axis of the conic flight path. For mission planning purposes, it is often desirable to know the semi-major axis as a function of time, rather than the reverse. Normally, a root finding technique such as Newton-Raphson is employed to find the value of a characteristic orbital parameter which matches a given time of flight. Alternatively, Lambert's Time Function may be expanded as a power series involving the inverse semi-major axis. The expression for semi-major axis is then determined through series reversion and inversion of the resulting series. A simplified method of obtaining the series coefficients is given, as well as a numerical study of convergence properties. GRA

N90-19246# Stuttgart Univ. (Germany, F.R.). Inst. fuer Raumfahrtsysteme.
FLIGHT AND DRIVING OPTIMIZATION OF AIR BREATHING AERODYNAMIC SPACE VEHICLE Ph.D. Thesis [FLUG- UND ANTRIEBSOPTIMIERUNG LUFTATMENDER AERODYNAMISCHER RAUMFAHRTTRAEGER]
Ulrich Michael Schoettle 1988 236 p In GERMAN Sponsored by Deutsche Forschungsgemeinschaft
(ETN-90-95379) Avail: NTIS HC A11/MF A02

A digital analysis process is developed for flight performance predictions of vehicle transfer in the near earth orbit. The parameter optimization problem is resolved by a gradient projection algorithm and a sequential quadratic optimization method. Sensitivity studies show the influences of some launching parameters and plane position limitations, the advantages and the disadvantages of the utilization of flood piloting mechanisms towards the rockets. Unlike the boosters, the horizontal takeoff is superior to the vertical takeoff for the air breathing space transporters, which are particularly adapted to atmospheric piloting. ESA

14 GROUND SUPPORT SYSTEMS AND FACILITIES (SPACE)

Includes launch complexes, research and production facilities; ground support equipment, e.g., mobile transporters; and simulators.

For related information see also *09 Research and Support Facilities (Air).*

N90-19247# Sandia National Labs., Albuquerque, NM. Applied Mechanics Div.
COMPUTATIONAL AND EXPERIMENTAL OF RAILGUN STRUCTURAL PERFORMANCE
G. W. Wellman Dec. 1989 55 p
(Contract DE-AC04-76DP-00789)
(DE90-006418; SAND-89-2535) Avail: NTIS HC A04/MF A01

The structural response of plasma armature railguns to the electromagnetic load imposed during operation has a significant effect on performance. The railgun support structure must minimize bore deformation; thus stiffness and strength are important design parameters. The step by step evolution of the design toward a structure which will tolerate operation with 500 to 700 kA rail currents is presented. The design effort started with the traditional rail/insulator core structure contained within a V-block which provides a preload. Nonlinear dynamic analyses together with model tests were used to assess the effects of changes in geometry, materials, and preload on the railgun structural performance. DOE

N90-19248# Los Alamos National Lab., NM. Physics Div.
MUZZLE SHUNT AUGMENTATION OF CONVENTIONAL RAILGUNS
Jerald V. Parker 1990 6 p Presented at the 5th IEEE Symposium on Electromagnetic Launch Technology, Destin, FL,

1-5 Apr. 1990
(Contract W-7405-eng-36)
(DE90-007505; LA-UR-90-668; CONF-9004136-3) Avail: NTIS HC A02/MF A01

Augmentation is a well-known technique for reducing the armature current and hence the armature power dissipation in a plasma armature railgun. In spite of the advantages, no large augmented railguns have been built, primarily due to the mechanical and electrical complexity introduced by the extra conductors required. It is possible to achieve some of the benefits of augmentation in conventional railgun by diverting a fraction (phi) of the input current through a shunt path at the muzzle of the railgun. In particular, the relation between force and armature current is the same as that obtained in an n-turn, series connected augmented railgun with n = 1/(1-(phi)). The price of this simplification is a reduction in electrical efficiency and some additional complexity in the external electrical system. Additions to the electrical system are required to establish the shunt current and to control its magnitude during projectile acceleration. The relationship between muzzle shunt augmentation and conventional series augmentation is developed and various techniques for establishing and controlling the shunt current are illustrated with a practical example. DOE

15 LAUNCH VEHICLES AND SPACE VEHICLES

Includes boosters; operating problems of launch/space vehicle systems; and reusable vehicles.

For related information see also *20 Spacecraft Propulsion and Power.*

N90-19249*# National Aeronautics and Space Administration. Langley Research Center, Hampton, VA.
EARTH SCIENCE GEOSTATIONARY PLATFORM TECHNOLOGY
Robert L. Wright, ed. and Thomas G. Campbell, ed. Washington Jul. 1989 386 p Workshop held in Hampton, VA, 21-22 Sep. 1988
(NASA-CP-3040; L-16612; NAS 1.55:3040) Avail: NTIS HC A17/MF A03 CSCL 22B

The objective of the workshop was to address problems in science and in four technology areas (large space antenna technology, microwave sensor technology, electromagnetics-phased array adaptive systems technology, and optical metrology technology) related to Earth Science Geostationary Platform missions. For individual titles, see N90-19250 through N90-19272.

N90-19250*# National Oceanic and Atmospheric Administration, Washington, DC. Office of Systems Development.
OPERATIONAL REQUIREMENTS AND THE GEOSTATIONARY PLATFORM **c18**
James K. Sparkman, Jr. *In* NASA, Langley Research Center, Earth Science Geostationary Platform Technology Jul. 1989 p 29-33 (For primary document see N90-19249 12-15)
Avail: NTIS HC A17/MF A03 CSCL 22B

For 22 years (from ATS-1 to GOES-H) a single technology has dominated imaging from geosynchronous altitudes. In 1990, with the scheduled launch of GOES-I, a major change will occur which will in turn open the way for the Geostationary Platform. The need for improved observations of severe storms has led NOAA to a decision to replace spinning geostationary spacecraft with a three-axis-stabilized type (non-spinning) vehicle already common among communications spacecraft and demonstrated by INSAT. Also, the current spin-scan imager with sounder channels will be replaced by separate instruments capable of independent aiming. The advantages and challenges of the changes are discussed. Author

N90-19251*# Massachusetts Inst. of Tech., Cambridge. Research Lab. of Electronics.
SCIENCE REQUIREMENTS FOR PASSIVE MICROWAVE SENSORS ON EARTH SCIENCE GEOSTATIONARY PLATFORMS **c19**
A. J. Gasiewski and D. H. Staelin *In* NASA, Langley Research Center, Earth Science Geostationary Platform Technology Jul. 1989 p 37-53 (For primary document see N90-19249 12-15)
Avail: NTIS HC A17/MF A03 CSCL 22B

It is suggested that the science requirements for passive geostationary microwave observations be met by near- and far-term sensors for each of two overlapping bands, with each band covering no more than a decade in frequency. The low-frequency band includes channels near 6, 10, 18, 22, 31 to 37, and possibly 50 to 60 GHz. The high-frequency band includes channels near 220 to 230, 183, 166, 118, 90 to 110, and possibly 50 to 60 and 31 to 37 GHz. The precise channel specifications will have to comply with international frequency allocations. The near-term goal is a high-frequency sensor based on a filled-aperture solid reflector antenna, which should rely on currently existing technology. The most critical issues for the near-term sensor are momentum compensation and the design of the feed assembly; these issues are coupled through the desired scan rate. The successful demonstration of the near-term (high-frequency) sensor will be essential for the continued development of far-term sensors satisfying the ideal science requirements. The far-term goal includes both a high-frequency sensor which meets the ideal science requirements, and a low-frequency sensor whose design will depend on advances in large antenna technology. The low-frequency (far-term) sensor might be based on one of several concepts: a deployable mesh reflector antenna of diameter at least 20 m, which shows promise for use at frequencies up to 30-GHz, a synthetic aperture interferometer of maximum baseline from 100 to 300 m, or a deployable phased-array bootlace lens, of diameter from 100 to 300 m. The first of these, a deployable mesh reflector antenna, will satisfy only the adequate spatial resolution requirements. The last two concepts meet the ideal spatial resolution science requirements, although they present significant structural and meteorological challenges. Author

N90-19252*# Lockheed Missiles and Space Co., Sunnyvale, CA.
GEOSTATIONARY EARTH SCIENCE PLATFORM CONCEPTS **c18**
M. M. Herardian *In* NASA, Langley Research Center, Earth Science Geostationary Platform Technology Jul. 1989 p 55-62 (For primary document see N90-19249 12-15)
Avail: NTIS HC A17/MF A03 CSCL 22B

The new concepts are presented for the Geostationary Earth Science Platform. Bus and payload arrangements, with instrument locations on the payload module and basic payload dimensions, are depicted and compared for each concept. The Titan 4 SRMU (with solid rocket motor upgrage) launch vehicle is described and compared to the standard Titan 4. The upgraded Titan 4 is capable of launching a 13,500 lb payload to GEO. The launch configuration showing each concept packaged within the 16 ft diameter payload envelope is presented. This presentation is represented by viewgraph only. Author

N90-19253*# Rockwell International Corp., Seal Beach, CA. Satellite and Space Electronics Div.
LARGE SPACE ANTENNA CONCEPTS FOR ESGP **c32**
Allan W. Love *In* NASA, Langley Research Center, Earth Science Geostationary Platform Technology Jul. 1989 p 65-68 (For primary document see N90-19249 12-15)
Avail: NTIS HC A17/MF A03 CSCL 20N

It is appropriate to note that 1988 marks the 100th anniversary of the birth of the reflector antenna. It was in 1888 that Heinrich Hertz constructed the first one, a parabolic cylinder made of sheet zinc bent to shape and supported by a wooden frame. Hertz demonstrated the existence of the electromagnetic waves that had been predicted theoretically by James Clerk Maxwell some 22 years earlier. In the 100 years since Hertz's pioneering work

the field of electromagnetics has grown explosively: one of the technologies is that of remote sensing of planet Earth by means of electromagnetic waves, using both passive and active sensors located on an Earth Science Geostationary Platform (ESEP). For these purposes some exquisitely sensitive instruments were developed, capable of reaching to the fringes of the known universe, and relying on large reflector antennas to collect the minute signals and direct them to appropriate receiving devices. These antennas are electrically large, with diameters of 3000 to 10,000 wavelengths and with gains approaching 80 to 90 dB. Some of the reflector antennas proposed for ESGP are also electrically large. For example, at 220 GHz a 4-meter reflector is nearly 3000 wavelengths in diameter, and is electrically quite comparable with a number of the millimeter wave radiotelescopes that are being built around the world. Its surface must meet stringent requirements on rms smoothness, and ability to resist deformation. Here, however, the environmental forces at work are different. There are no varying forces due to wind and gravity, but inertial forces due to mechanical scanning must be reckoned with. With this form of beam scanning, minimizing momentum transfer to the space platform is a problem that demands an answer. Finally, reflector surface distortion due to thermal gradients caused by the solar flux probably represents the most challenging problem to be solved if these Large Space Antennas are to achieve the gain and resolution required of them. Author

N90-19254*# Lockheed Missiles and Space Co., Sunnyvale, CA.
LARGE-DIAMETER GEOSTATIONARY MILLIMETER WAVELENGTH ANTENNA CONCEPT **c18**
W. S. Gregorwich, H. A. Malliot, and A. K. Sinha *In* NASA, Langley Research Center, Earth Science Geostationary Platform Technology Jul. 1989 p 69-81 (For primary document see N90-19249 12-15)
Avail: NTIS HC A17/MF A03 CSCL 22B

The concept of a curved reflecting surface by means of an electrostatic membrane appeared as early as 1932 in the British patent by Muller. The use of the electrostatic membrane in space applications as large-reflector antennas was proposed. A schematic of the concept is provided. Advantages of wrap-rib; wrap-radial-rib command surface; electromembrane applied to laser mirrors; membrane control concept; dual band elements; millimeter wavelength reflector; and the proof of concept and demonstration model are briefly presented. B.G.

N90-19255*# Lockheed Missiles and Space Co., Sunnyvale, CA.
DESIGN OF A LOW-FREQUENCY (5-20 GHz), 15-METER-DIAMETER PASSIVE RADIOMETER FOR GEOSTATIONARY EARTH SCIENCE PLATFORMS **c19**
A. K. Sinha *In* NASA, Langley Research Center, Earth Science Geostationary Platform Technology Jul. 1989 p 83-108 (For primary document see N90-19249 12-15)
Avail: NTIS HC A17/MF A03 CSCL 14B

The Wrap-Rib Antenna is a deployable lightweight shaped reflector. It consists of a central hub, parabolic ribs, and an rf reflector mesh. The wrap-rib reflector approximates the desired surface by means of pie-shaped segments of parabolic cylinders. The elements of the total system and the feasibility of the system are discussed. B.G.

N90-19256*# Astro Aerospace Corp., Carpinteria, CA.
STRUCTURES FOR REMOTELY DEPLOYABLE PRECISION ANTENNAS **c32**
J. M. Hedgepeth *In* NASA, Langley Research Center, Earth Science Geostationary Platform Technology Jul. 1989 p 109-128 (For primary document see N90-19249 12-15)
Avail: NTIS HC A17/MF A03 CSCL 20N

Future space missions such as the Earth Science Geostationary Platform (ESGP) will require highly accurate antennas with apertures that cannot be launched fully formed. The operational orbits are often inaccessible to manned flight and will involve expendable launch vehicles such as the Delta or Titan. There is therefore a need for completely deployable antenna reflectors of large size capable of efficiently handling millimeter wave electromagnetic radiation. The parameters for the type of mission are illustrated. The logarithmic plot of frequency versus aperture diameter shows the regions of interest for a large variety of space antenna applications, ranging from a 1500-meter-diameter radio telescope for low frequencies to a 20-meter-diameter infrared telescope. For the ESGP, a major application is the microwave radiometry at high frequencies for atmospheric sounding. Almost all existing large antenna reflectors for space employ a mesh-type reflecting surface. Examples are shown and discussed which deal with the various structural concepts for mesh antennas. Fortunately, those concepts are appropriate for creating the very large apertures required at the lower frequencies for good resolution. The emphasis is on the structural concepts and technologies that are appropriate to fully automated deployment of dish-type antennas with solid reflector surfaces. First the structural requirements are discussed. Existing concepts for fully deployable antennas are then described and assessed relative to the requirements. Finally, several analyses are presented that evaluate the effects of beam steering and segmented reflector design on the accuracy of the antenna. Author

N90-19257*# Composite Optics, Inc., San Diego, CA.
UNFURLABLE, CONTINUOUS-SURFACE REFLECTOR CONCEPT **c32**
J. E. Stumm and S. Kulick *In* NASA, Langley Research Center, Earth Science Geostationary Platform Technology Jul. 1989 p 129-136 (For primary document see N90-19249 12-15)
Avail: NTIS HC A17/MF A03 CSCL 20N

Various concepts for large, deployable reflectors were developed and some have flown. In each case the surface material was either a continuous mesh of some sort or an assembly of rigid, continuous-surface facets or petals. Performance issues arise in each case. For mesh, reflectance diminishes with increasing frequency. For rigid sections, seams and relative positioning of the segments have to be dealt with. These two issues prompted the evolution of the concept of an unfurlable, continuous-surface reflector. The concept is described and what is learnt is presented, what is suspected will be learned, and also questions raised yet to be addressed. Author

N90-19258*# L'Garde, Inc., Tustin, CA.
ADVANCES IN LARGE INFLATABLE REFLECTORS **c32**
M. Thomas and G. Williams *In* NASA, Langley Research Center, Earth Science Geostationary Platform Technology Jul. 1989 p 137-151 (For primary document see N90-19249 12-15)
Avail: NTIS HC A17/MF A03 CSCL 20N

For most applications in space for which they were tried, inflatable structures show a significant weight reduction when compared to mechanical structures. Inflatables are unmatched when compared to mechanical structures when packaged volume is considered. The reliability of deployment of inflatable structures was known for years. When properly designed, such a system is inherently more reliable because it has very few points of failure. Fully inflatable vs. rigidized inflatable structures are discussed. The L'Garde solar concentrator experience is described. Reflector surface and cylinder rigidization, improvement in gore design tools, and expected advances in rigidization schemes with near future are examined. B.G.

N90-19259*# Massachusetts Univ., Amherst. Dept. of Electrical and Computer Engineering.
COHERENT RADAR MEASUREMENT OF OCEAN CURRENTS FROM GEOSTATIONARY ORBIT **c43**
R. E. McIntosh *In* NASA, Langley Research Center, Earth Science Geostatonary Platform Technology Jul. 1989 p 155-165 (For primary document see N90-19249 12-15)
Avail: NTIS HC A17/MF A03 CSCL 08C

A coherent HF radar system developed by Barrick has successfully measured ocean surface currents near shore. This innovative system, called CODAR, can map the current vector for coastal areas as large as 10,000 sq km. CODAR's range is limited

owing to the strong attenuation suffered by HF ground waves. An alternate technique was proposed by Schuler, in which the cross-product power spectrum of two (different frequency) microwave signals is processed. The frequency of the resonant peak corresponds close by to the Doppler shift of an ocean gravity wave traveling toward the radar at the phase velocity, v(sub p). The slight difference between the frequency of the measured resonant delta K peak and the Doppler frequency shift caused by the motion of the gravity wave is attributed to be the current velocity in the pointing direction of the radar. The Microwave Remote Sensing Laboratory (MIRSL) has considered the feasibility of using this technique to measure ocean surface currents from geostationary satellite platforms. Problems are discussed that must be overcome if a satellite current measurement system is to be realized. MIRSL research activities that address some of these problem areas are discussed. Current measurements are presented that were made using a specially-designed C-Band, step-frequency delta K radar. These measurements suggest that progress is being achieved in detecting ocean surface current motion for a wide variety of ocean surface conditions. Author

N90-19260*# Jet Propulsion Lab., California Inst. of Tech., Pasadena.

MILLIMETER RADIOMETER SYSTEM TECHNOLOGY **c19**

W. J. Wilson and P. N. Swanson *In* NASA, Langley Research Center, Earth Science Geostationary Platform Technology Jul. 1989 p 167-177 (For primary document see N90-19249 12-15)

Avail: NTIS HC A17/MF A03 CSCL 14B

JPL has had a large amount of experience with spaceborne microwave/millimeter wave radiometers for remote sensing. All of the instruments use filled aperture antenna systems from 5 cm diameter for the microwave Sounder Units (MSU), 16 m for the microwave limb sounder (MLS) to 20 m for the large deployable reflector (LDR). The advantages of filled aperture antenna systems are presented. The requirements of the 10 m Geoplat antenna system, 10 m multified antenna, and the MLS are briefly discussed. B.G.

N90-19261*# Jet Propulsion Lab., California Inst. of Tech., Pasadena.

SYNTHETIC APERTURE INTERFEROMETRIC RADIOMETER (SAIR) **c19**

C. S. Ruf *In* NASA, Langley Research Center, Earth Science Geostationary Platform Technology Jul. 1989 p 179-189 (For primary document see N90-19249 12-15)

Avail: NTIS HC A17/MF A03 CSCL 14B

The aperture size requirements of imaging microwave radiometers in geosynchronous orbit ruled out filled aperture antenna systems below 10 GHz. In the regions 10 to 30 GHz, filled apertures are only marginally practical. The size requirements in turn aggravate the problems with a mechanically steered antenna beam. Both the aperture size and steering problems are resolved with a synthetic aperture interferometric radiometer (SAIR). The SAIR imaging is discussed, along with the requirements of the two-dimensional antenna elements. B.G.

N90-19262*# Kansas Univ. Center for Research, Inc., Lawrence. Radar Systems and Remote Sensing Lab.

RAIN RADARS FOR EARTH SCIENCE GEOSTATIONARY PLATFORMS: SOME POSSIBILITIES **c43**

S. P. Gogineni and R. K. Moore *In* NASA, Langley Research Center, Earth Science Geostationary Platform Technology Jul. 1989 p 191-200 (For primary document see N90-19249 12-15)

Avail: NTIS HC A17/MF A03 CSCL 04B

Results of a feasibility study for a geostationary rain radar are presented. A 2-cm wavelength radar with a 15 to 20 mm antenna will be useful for general scale meteorology. The transmitter power of 500 W with a pulse compression ratio of 200 will provide adequate signal-to-noise ratio for a rain rate of 1 mm/hour. Various problems associated with a geostationary radar and solutions are also discussed. Author

N90-19263*# Jet Propulsion Lab., California Inst. of Tech., Pasadena.

LARGE ANTENNA MEASUREMENT AND COMPENSATION TECHNIQUES **c33**

Y. RahmatSamii *In* NASA, Langley Research Center, Earth Science Geostationary Platform Technology Jul. 1989 p 203-215 Presented at the 11th ESTEC Antenna Workshop on Antenna Measurements, Gothenburg, Sweden, 20-22 Jun. 1988 (For primary document see N90-19249 12-15)

Avail: NTIS HC A17/MF A03 CSCL 20N

Antennas in the range of 20 meters or larger will be an integral part of future satellite communication and scientific payloads. In order to commercially use these large, low sidelobe and multiple-beam antennas, a high level of confidence must be established as to their performance in the 0-g and space environment. It is also desirable to compensate for slowly varying surface distortions which could results from thermal effects. An overview of recent advances in performing rf measurements on large antennas is presented with emphasis given to the application of a space-based far-field range utilizing the Space Shuttle. The concept of surface distortion compensation is discussed by providing numerical and measurement results. Author

N90-19264*# National Aeronautics and Space Administration. Lewis Research Center, Cleveland, OH.

A COMPARISON OF REFLECTOR ANTENNA DESIGNS FOR WIDE-ANGLE SCANNING **c32**

M. Zimmerman, S. W. Lee, B. Houshmand, Y. RahmatSamii (Jet Propulsion Lab., California Inst. of Tech., Pasadena.), and R. J. Acosta *In* NASA, Langley Research Center, Earth Science Geostationary Platform Technology Jul. 1989 p 217-240 Previously announced as N89-21138 (For primary document see N90-19249 12-15)

Avail: NTIS HC A17/MF A03 CSCL 20N

Conventional reflector antennas are typically designed for up to + or - 20 beamwidths scan. An attempt was made to stretch this scan range to some + or - 300 beamwidths. Six single and dual reflector antennas were compared. It is found that a symmetrical parabolic reflector with f/D = 2 and a single circular waveguide feed has the minimum scan loss (only 0.6 dB at Theta sub 0 = 8 deg, or a 114 beamwidths scan). The scan is achieved by tilting the parabolic reflector by an angle equal to the half-scan angle. The f/D may be shortened if a cluster 7 to 19 elements instead of one element is used for the feed. The cluster excitation is adjusted for each new beam scan direction to compensate for the imperfect field distribution over the reflector aperture. The antenna can be folded into a Cassegrain configuration except that, due to spillover and blockage considerations, the amount of folding achievable is small. Author

N90-19265*# Atlantic Research Corp., Rome, NY.

ARRAYS FOR SPACE APPLICATIONS **c32**

Harvey K. Schuman, Paul Antonik, and Carmen Malagisi *In* NASA, Langley Research Center, Earth Science Geostationary Platform Technology Jul. 1989 p 241-263 (For primary document see N90-19249 12-15)

Avail: NTIS HC A17/MF A03 CSCL 20N

Concepts that were studied for application in space based radar (SBR) systems are presented. These antenna systems were for low earth orbit and require large fields of view (FOV). The systems included both space-fed and corporate-fed arrays. B.G.

N90-19266*# National Aeronautics and Space Administration. Lewis Research Center, Cleveland, OH.

CONJUGATE FIELD APPROACHES FOR ACTIVE ARRAY COMPENSATION **c32**

R. J. Acosta *In* NASA, Langley Research Center, Earth Science Geostationary Platform Technology Jul. 1989 p 265-271 (For primary document see N90-19249 12-15)

Avail: NTIS HC A17/MF A03 CSCL 20N

Two approaches for calculating the compensating feed array complex excitations are namely, the indirect conjugate field matching (ICFM) and the direct conjugate field matching (DCFM)

approach. In the ICFM approach the compensating feed array excitations are determined by considering the transmitting mode and the reciprocity principle. The DCF, in contrast calculates the array excitations by integrating directly the induced surface currents on the reflector under a receiving mode. DCFM allows the reflector to be illuminated by an incident plane wave with a tapered amplitude. The level of taper can effectively control the sidelobe level of the compensated antenna pattern. Both approaches are examined briefly. Author

N90-19267*# National Aeronautics and Space Administration. Lewis Research Center, Cleveland, OH.
REFLECTOR SURFACE DISTORTION ANALYSIS TECHNIQUES (THERMAL DISTORTION ANALYSIS OF ANTENNAS IN SPACE) **c32**
R. Sharp, M. Liao, J. Giriunas, J. Heighway, A. Lagin, and R. Steinbach *In* NASA, Langley Research Center, Earth Science Geostationary Platform Technology Jul. 1989 p 273293 (For primary document see N90-19249 12-15)
Avail: NTIS HC A17/MF A03 CSCL 20N

A group of large computer programs are used to predict the farfield antenna pattern of reflector antennas in the thermal environment of space. Thermal Radiation Analysis Systems (TRASYS) is a thermal radiation analyzer that interfaces with Systems Improved Numerical Differencing Analyzer (SINDA), a finite difference thermal analysis program. The programs linked together for this analysis can now be used to predict antenna performance in the constantly changing space environment. They can be used for very complex spacecraft and antenna geometries. Performance degradation caused by methods of antenna reflector construction and materials selection are also taken into consideration. However, the principal advantage of using this program linkage is to account for distortions caused by the thermal environment of space and the hygroscopic effects of the dry-out of graphite/epoxy materials after the antenna is placed into orbit. The results of this type of analysis could ultimately be used to predict antenna reflector shape versus orbital position. A phased array antenna distortion compensation system could then use this data to make RF phase front corrections. That is, the phase front could be adjusted to account for the distortions in the antenna feed and reflector geometry for a particular orbital position. Author

N90-19268*# North Carolina State Univ., Raleigh. Dept. of Electrical and Computer Engineering.
MESH SURFACES FOR REFLECTOR APPLICATIONS **c32**
Frank Kauffman *In* NASA, Langley Research Center, Earth Science Geostationary Platform Technology Jul. 1989 p 295-311 (For primary document see N90-19249 12-15)
Avail: NTIS HC A17/MF A03 CSCL 20N

The topics of mesh reflectors, methods of analysis, measurements, problems of current interest, and future research, are those which should be addressed in assessing the current state of metallic mesh technology for spaceborne reflector antennas. The study of the properties of the conducting mesh material is discussed. To calculate the radiation patterns of antennas with conducting mesh reflectors, the electromagnetic properties of the mesh material must be integrated into an appropriate reflector antenna computer code. Such a code would take into account such factors as the curvature of the reflector surface, the radiation pattern(s) of the feed(s), etc. Many organizations have developed their own codes for these calculations. An excellent example of such a code is the one developed by Rahmat-Samii and Lee. Author

N90-19269*# TRW Electronic Systems Group, Redondo Beach, CA. Antenna Systems Lab.
ANTENNAS FOR 20/30 GHz AND BEYOND **c32**
C. Harry Chen, William C. Wong, and S. Jim Hamada *In* NASA, Langley Research Center, Earth Science Geostationary Platform Technology Jul. 1989 p 313-327 (For primary document see N90-19249 12-15)
Avail: NTIS HC A17/MF A03 CSCL 20N

Antennas of 20/30 GHz and higher frequency, due to the small wavelength, offer capabilities for many space applications. With the government-sponsored space programs (such as ACTS) in recent years, the industry has gone through the learning curve of designing and developing high-performance, multi-function antennas in this frequency range. Design and analysis tools (such as the computer modelling used in feedhorn design and reflector surface and thermal distortion analysis) are available. The components/devices (such as BFN's, weight modules, feedhorns and etc.) are space-qualified. The manufacturing procedures (such as reflector surface control) are refined to meet the stringent tolerance accompanying high frequencies. The integration and testing facilities (such as Near-Field range) also advance to facilitate precision assembling and performance verification. These capabilities, essential to the successful design and development of high-frequency spaceborne antennas, shall find more space applications (such as ESGP) than just communications. Author

N90-19270*# Digital Signal Corp., Springfield, VA.
APPLICATIONS OF FM-CW LASER RADAR TO ANTENNA CONTOUR MAPPING **c19**
A. R. Slotwinski *In* NASA, Langley Research Center, Earth Science Geostationary Platform Technology Jul. 1989 p 331-337 (For primary document see N90-19249 12-15)
Avail: NTIS HC A17/MF A03 CSCL 14B

The FM-CW coherent laser radar concept, based on the FM radar principle which makes use of the coherence and lunability of injection laser diodes, is discussed. Laser radar precision/time tradeoffs, block diagrams, system performance, fiber optic system implantation, and receiver improvements are briefly described. B.G.

N90-19271*# Ball Aerospace Systems Div., Boulder, CO.
REMOTE ATTITUDE MEASUREMENT SENSOR (RAMS) **c19**
H. W. Davis *In* NASA, Langley Research Center, Earth Science Geostationary Platform Technology Jul. 1989 p 339-368 (For primary document see N90-19249 12-15)
Avail: NTIS HC A17/MF A03 CSCL 14B

Remote attitude measurement sensor (RAMS) offers a low-cost, low-risk, proven design concept that is based on mature, demonstrated space sensor technology. The electronic design concepts and interpolation algorithms were tested and proven in space hardware like th Retroreflector Field Tracker and various star trackers. The RAMS concept is versatile and has broad applicability to both ground testing and spacecraft needs. It is ideal for use as a precision laboratory sensor for structural dynamics testing. It requires very little set-up or preparation time and the output data is immediately usable without integration or extensive analysis efforts. For on-orbit use, RAMS rivals any other type of dynamic structural sensor (accelerometer, lidar, photogrammetric techniques, etc.) for overall performance, reliability, suitability, and cost. Widespread acceptance and extensive usage of RAMS will occur only after some interested agency, such as OAST, adopts the RAMS concept and provides the funding support necessary for further development and implementation of RAMS for a specific program. Author

N90-19272*# Jet Propulsion Lab., California Inst. of Tech., Pasadena. Optical Sciences and Application Section 385.
PRECISION SEGMENTED REFLECTOR, FIGURE VERIFICATION SENSOR **c19**
Paul K. Manhart and Steve A. Macenka *In* NASA, Langley Research Center, Earth Science Geostationary Platform Technology Jul. 1989 p 369-374 (For primary document see N90-19249 12-15)
Avail: NTIS HC A17/MF A03 CSCL 14B

The Precision Segmented Reflector (PSR) program currently under way at the Jet Propulsion Laboratory is a test bed and technology demonstration program designed to develop and study the structural and material technologies required for lightweight, precision segmented reflectors. A Figure Verification Sensor (FVS) which is designed to monitor the active control system of the segments is described, a best fit surface is defined, and an image

or wavefront quality of the assembled array of reflecting panels is assessed
Author

16 SPACE TRANSPORTATION

Includes passenger and cargo space transportation, e.g., shuttle operations; and space rescue techniques.

For related information see also *03 Air Transportation and Safety* and *18 Spacecraft Design, Testing and Performance.* For space suits see *54 Man/System Technology and Life Support.*

No abstracts in this category.

17 SPACE COMM., SPACECRAFT COMM., COMMAND & TRACKING

Includes telemetry; space communications networks; astronavigation and guidance; and radio blackout.

For related information see also *04 Aircraft Communications and Navigation* and *32 Communications and Radar.*

N90-19273# Midwest Research Inst., Golden, CO. Solar Energy Research Inst.
PC-BASED PCM (PULSE CODE MODULATION) TELEMETRY DATA REDUCTION SYSTEM HARDWARE
Feb. 1990 11 p
(Contract DE-AC02-83CH-10093)
(DE90-000316; SERI/TP-257-3662) Avail: NTIS HC A03/MF A01

The Solar Energy Research Institute's (SERI) Wind Research Program is using pulse code modulation (PCM) telemetry systems to study horizontal-axis wind turbines. SERI has developed a low-cost PC-based PCM data acquisition system to facilitate quick PCM data analysis in the field. The SERI PC-PCM system consists of AT-compatible hardware boards for decoding and combining PCM data streams and DOS software for control and management of data acquisition. Up to four boards can be installed in a single PC, providing the capability to combine data from four PCM streams direct to disk or memory. The SERI PC-PCM system hardware is described focusing on the practicality of PC-based PCM data reduction. A related paper highlights the comprehensive PCM data management software program which can be used in conjunction with this hardware to provide full quick-look data processing and display. The PC-PCM hardware boards support a subset of the Inter-Range Instrumentation Group (IRIG) PCM standard, designed to synchronize and decommutate NRZ or Bi-Phase L PCM streams in the range of 1 to 800 Kbits/sec at 8 to 12 bits per word and 2 to 64 words per frame. Multiple PCM streams (at various rates) can be combined and interleaved into a contiguous digital time series. Maximum data throughput depends on characteristics of the PC hardware, such as CPU rate and disk access speed.
DOE

N90-19444*# Jet Propulsion Lab., California Inst. of Tech., Pasadena.
SOME EASILY ANALYZABLE CONVOLUTIONAL CODES
R. McEliece, S. Dolinar, F. Pollara, and H. VanTilborg (Technische Univ., Eindhoven, Netherlands) *In its* The Telecommunications and Data Acquisition Report 15 Nov. 1989 p 105-114 (For primary document see N90-19434 12-32)
Avail: NTIS HC A10/MF A02 CSCL 09F

18 SPACECRAFT DESIGN, TESTING AND PERFORMANCE

Includes satellites; space platforms; space stations; spacecraft systems and components such as thermal and environmental controls; and attitude controls.

For life support systems see *54 Man/System Technology and Life Support.* For related information see also *05 Aircraft Design, Testing and Performance, 39 Structural Mechanics,* and *16 Space Transportation.*

N90-19274 North Carolina State Univ., Raleigh.
ADVANCED TOPICS IN STRUCTURAL DYNAMICS: THE MANEUVER OF FLEXIBLE SPACECRAFT, AND ON-OFF DECENTRALIZED CONTROL OF FLEXIBLE STRUCTURES Ph.D. Thesis
Lester Anderson Foster 1989 100 p
Avail: Univ. Microfilms Order No. DA8918091

Two approaches to maneuver flexible spacecraft and an approach to suppress vibration of flexible structures using decentralized feedback on-off control are described. The first maneuver method suppresses spacecraft motion relative to the motion of a fictitious shadow spacecraft using a decentralized feedback control. The second maneuver method is equivalent to the first method but it applies open-loop control with a decentralized feedback control suppressing motion relative to the open-loop path. First, the dynamics of maneuvering flexible spacecraft are reviewed in general and then specifically for a non-dimensional free-free beam with well separated dimensions. For the first maneuver method, several in-plane rest-to-spin maneuvers are investigated for different choices of shadow coordinates including the maneuver corresponding to minimum fuel. In order to prescribe actual spacecraft motion, lag compensation of the shadow coordinates is introduced to account for feedback lag between the shadow and actual spacecraft coordinates. Also in-plane and out-of-plane maneuvers are investigated. Next, on-off decentralized control is presented. Fuel minimization is achieved by turning on actuators when local kinetic energy is at a maximum and local potential energy is at a minimum.
Dissert. Abstr.

N90-19275*# Georgia Inst. of Tech., Atlanta. School of Aerospace Engineering.
RAPID NEAR-OPTIMAL TRAJECTORY GENERATION AND GUIDANCE LAW DEVELOPMENT FOR SINGLE-STAGE-TO-ORBIT AIRBREATHING VEHICLES Final Technical Report, 1 Jan. - 31 Dec. 1989
A. J. Calise, G. A. Flandro, and J. E. Corban Jan. 1990 69 p
(Grant NAG1-922)
(NASA-CR-186299; NAS 1.26:186299) Avail: NTIS HC A04/MF A01 CSCL 22B

General problems associated with on-board trajectory optimization, propulsion system cycle selection, and with the synthesis of guidance laws were addressed for an ascent to low-earth-orbit of an air-breathing single-stage-to-orbit vehicle. The NASA Generic Hypersonic Aerodynamic Model Example and the Langley Accelerator aerodynamic sets were acquired and implemented. Work related to the development of purely analytic aerodynamic models was also performed at a low level. A generic model of a multi-mode propulsion system was developed that includes turbojet, ramjet, scramjet, and rocket engine cycles. Provisions were made in the dynamic model for a component of thrust normal to the flight path. Computational results, which characterize the nonlinear sensitivity of scramjet performance to changes in vehicle angle of attack, were obtained and incorporated into the engine model. Additional trajectory constraints were introduced: maximum dynamic pressure; maximum aerodynamic heating rate per unit area; angle of attack and lift limits; and limits on acceleration both along and normal to the flight path. The remainder of the effort focused on required modifications to a previously derived algorithm when the model complexity cited above was added. In particular, analytic switching conditions were derived which, under appropriate assumptions, govern optimal transition from one propulsion mode to another for two cases: the case in

which engine cycle operations can overlap, and the case in which engine cycle operations are mutually exclusive. The resulting guidance algorithm was implemented in software and exercised extensively. It was found that the approximations associated with the assumed time scale separation employed in this work are reasonable except over the Mach range from roughly 5 to 8. This phenomenon is due to the very large thrust capability of scramjets in this Mach regime when sized to meet the requirement for ascent to orbit. By accounting for flight path angle and flight path angle rate in construction of the flight path over this Mach range, the resulting algorithm provides the means for rapid near-optimal trajectory generation and propulsion cycle selection over the entire Mach range from take-off to orbit. Author

N90-19276# Instituto de Pesquisas Espaciais, Sao Jose dos Campos (Brazil).
SELF-TUNING CONTROL TECHNIQUES, IMPLICIT AND EXPLICIT, WITH PARAMETER ESTIMATION IN KALMAN FILTERS, APPLIED TO ARTIFICIAL SATELLITE ATTITUDE M.S. Thesis [TECNICAS DE CONTROLE AUTO-SINTONIZAVEL IMPLICITA E EXPLICITA, COM ESTIMACAO DE PARAMETROS VIA FILTRO DE KALMAN, APLICADAS A ATITUDE DE SATELITES ARTIFICIAIS]
Orlando SanchesPadilha Aug. 1989 176 p In PORTUGUESE; ENGLISH summary
(INPE-4857-TDL/368) Avail: NTIS HC A09/MF A01

An application in three axis remote sensing satellite attitude control of the self-tuning technique in both explicit and implicit forms, using parameter estimation with the Kalman filter is presented. The satellite attitude dynamics is represented by a vetorial difference equation relating applied torques to the satellite attitude outputs. The coefficients of this equation, named parameters in the work, are estimated in real time. The mathematical model for the parameters adopted in the filter uses a constant noise level in order to achieve an adequate weighting for the present observations, so entailing a better performance for the implemented algorithm. Through the analysis of tests performed by numerical simulation in digital computers the performance of these procedures is evaluated in comparison with the self-tuning algorithms that use least square parameter estimation. In these tests one considers nominal operational conditions and conditions in which dynamical factors are changed during the process; these last cases are used to evaluate the estimator adaptive capacity. This analysis has shown a good performance in the algorithms performed in both versions.
Author

N90-19277# Instituto de Pesquisas Espaciais, Sao Jose dos Campos (Brazil).
ATTITUDE AND SPIN RATE CONTROL OF A SPINNING SATELLITE USING GEOMAGNETIC FIELD
Luiz Danilo DamascenoFerreira and Jose Jaime daCruz Jun. 1989 17 p Submitted for publication
(INPE-4818-NTE/289) Avail: NTIS HC A03/MF A01

The attitude and spin rate control of spinning satellites is examined. It is shown that this can be performed by conveniently switching two coils with axes respectively parallel and orthogonal to the spin axis. The interaction between the coils' magnetic moments and the geomagnetic field provides the control torques.
Author

N90-19278* National Aeronautics and Space Administration. Lyndon B. Johnson Space Center, Houston, TX.
HATCH COVER Patent
Charles S. Allton, inventor (to NASA) and James H. OKane, inventor (to NASA) 27 Jun. 1989 8 p Filed 9 Mar. 1988
(NASA-Case-MSC-21356-1; US-Patent-4,842,223; US-Patent-Appl-SN-165956; US-Patent-Class-244-158R; US-Patent-Class-49-253; US-Patent-Class-114-112; US-Patent-Class-114-201R; US-Patent-Class-244-129.5) Avail: US Patent and Trademark Office CSCL 22B

This invention relates to a hatch and more particularly to a hatch for a space vehicle where the hatch has a low volume sweep and can be easily manipulated from either side of the hatch. The hatch system includes an elliptical opening in a bulkhead and an elliptical hatch member. The hatch cover system includes an elliptical port opening in a housing and an elliptical cover member supported centrally by a rotational bearing for rotation about a rotational axis normal to the cover member and by pivot pins in a gimbal member for pivotal movement about axes perpendicular to the rotational axis. Arm members support the gimbal member pivotally by pivot members so that upon rotation and manipulation the cover member can be articulatedly moved from a closed position to the port opening to an out of the way position with a minimum of volume sweep by the cover member.
Official Gazette of the U.S. Patent and Trademark Office

N90-19279*# National Aeronautics and Space Administration. Langley Research Center, Hampton, VA.
ADVANCING AUTOMATION AND ROBOTICS TECHNOLOGY FOR THE SPACE STATION FREEDOM AND FOR THE US ECONOMY: SUBMITTED TO THE UNITED STATES CONGRESS Progress Report No. 9, Mar. - Jul. 1989
Mar. 1990 39 p
(NASA-TM-101647; NAS 1.15:101647) Avail: NTIS HC A03/MF A01 CSCL 22B

In April 1985, as required by Public Law 98-371, the NASA Advanced Technology Advisory Committee (ATAC) reported to Congress the results of its studies on advanced automation and robotics technology for use on the Space Station Freedom. This material was documented in the initial report (NASA Technical Memorandum 87566). A further requirement of the law was that ATAC follow NASA's progress in this area and report to Congress semiannually. This report is the ninth in a series of progress updates and covers the period between February 24, 1989, and July 12, 1989. NASA has accepted the basic recommendation of ATAC for its Space Station Freedom efforts. ATAC and NASA agree that the thrust of Congress is to build an advanced automation and robotics technology base that will support an evolutionary Space Station program and serve as a highly visible stimulator, affecting the U.S. long-term economy. The work of NASA and the Freedom contractors, e.g., Work Packages, as well as the Flight Telerobotic Servicer is identified. Research in progress is also described and assessments of the advancement of automation and robotics technology on the Space Station Freedom are given. Author

N90-19280*# Texas Univ., Austin. Center for Aeronautical Research.
APPLICATION OF ATTACHMENT MODES IN THE CONTROL OF LARGE SPACE STRUCTURES
Roy R. Craig, Jr. Sep. 1989 56 p
(Contract NAS9-17254)
(NASA-CR-185604; NAS 1.26:185604; CAR-89-3) Avail: NTIS HC A04/MF A01 CSCL 22B

Various ways are examined to obtain reduced order mathematical models of structures for use in dynamic response analyses and in controller design studies. Attachment modes are deflection shapes of a structure subjected to specified unit load distributions. Attachment modes are frequently employed to supplement free-interface normal modes to improve the modeling of components (structures) employed in component mode synthesis analyses. Deflection shapes of structures subjected to generalized loads of some specified distribution and of unit magnitude can also be considered to be attachment modes. Several papers which were written under this contract are summarized herein. Author

N90-19281*# National Aeronautics and Space Administration. Langley Research Center, Hampton, VA.
INTEGRATED CONTROL/STRUCTURE OPTIMIZATION BY MULTILEVEL DECOMPOSITION
Thomas A. Zeiler (Lockheed Engineering and Sciences Co., Hampton, VA.) and Michael G. Gilbert Mar. 1990 13 p Presented at the 31st AIAA Structures, Structural Dynamics, and Materials Conference, Long Beach, CA, 2-4 Apr. 1990

(NASA-TM-102619; NAS 1.15:102619) Avail: NTIS HC A03/MF A01 CSCL 22B

A method for integrated control/structure optimization by multilevel decomposition is presented. It is shown that several previously reported methods were actually partial decompositions wherein only the control was decomposed into a subsystem design. One of these partially decomposed problems was selected as a benchmark example for comparison. The system is fully decomposed into structural and control subsystem designs and an improved design is produced. Theory, implementation, and results for the method are presented and compared with the benchmark example. Author

N90-19282# Nuclear Utility Services, Inc., Gaithersburg, MD.
SAFETY STATUS REPORT FOR THE ULYSSES MISSION. BOOK 1: RISK ANALYSIS. GENERAL PURPOSE HEAT SOURCE RADIOSOTOPE THERMOELECTRIC GENERATOR PROGRAM
31 Jan. 1990 28 p
(Contract DE-AC01-87NE-32134)
(DE90-006826; NUS-5235-Bk-1) Avail: NTIS HC A03/MF A01

The purpose of this report is to provide the most recent results of the analysis of the range of potential consequences of accidents which have been identified during the launching and deployment of the Ulysses mission spacecraft. The specific consequences analyzed are those associated with the possible release of radioactive material (fuel) of the radioisotope thermoelectric generator (RTG). They are in terms of radiation doses to people and areas of deposition of radioactive material. These consequence analyses can be used in several ways. One way is to identify the potential range of consequences which might have to be dealt with if there were to be an accident with a release of fuel to assure that, given such an accident, the health and safety of the public will be reasonably protected. Another use of the information, along with accident and release probabilities, is to estimate the risks associated with the mission. That is, most space launches occur without incident. Given an accident, the most probable result relative to the RTGs is complete containment of the radioactive material. Only a small fraction of accidents might result in a release of fuel and subsequent radiological consequences. The combination of probability with consequence is risk, which can be compared to other human and societal risks to assure that no undue risks are implied by undertaking the mission. DOE

N90-19283# Nuclear Utility Services, Inc., Gaithersburg, MD.
SAFETY STATUS REPORT FOR THE ULYSSES MISSION. BOOK 2: RISK ANALYSIS. GENERAL PURPOSE HEAT SOURCE RADIOSOTOPE THERMOELECTRIC GENERATOR PROGRAM
31 Jan. 1990 177 p
(Contract DE-AC01-87NE-32134)
(DE90-006827; NUS-5235-Bk-2) Avail: NTIS HC A09/MF A01

This appendix describes the methods used in evaluating the radiological consequences and the integrated mission risks presented in the Safety Status Report (SSR): Risk Analysis (Book 1) for the Ulysses mission. DOE

N90-19284# Nuclear Utility Services, Inc., Gaithersburg, MD.
SAFETY STATUS REPORT FOR THE ULYSSES MISSION: SUMMARY. GENERAL PURPOSE HEAT SOURCE RADIOSOTOPE THERMOELECTRIC GENERATOR PROGRAM
31 Jan. 1990 25 p
(Contract DE-AC01-87NE-32134)
(DE90-006828; NUS-5238) Avail: NTIS HC A03/MF A01

This document is a condensation of the important features of the Ulysses mission Safety Status Report (SSR). The SSR reports the best information available at this time on the accident and risk analysis for the Ulysses mission. These are ongoing analyses of SRB failure accidents which could alter the results. These updated analyses will be documented in the Final Safety Analysis Report, scheduled for completion in March 1990. Meanwhile NASA requires information on mission risks to support its Environmental Impact Statement and the Interagency Nuclear Safety Review Panel can use the SSR as initial input to its review process. The central estimate (base case) results of this interim risk assessment indicate that none of the postulated accidents of the mission would be expected to result in a health effect (fatal cancer). Calculated maximum radiation doses to individuals for the base case releases are low (in the millirem to tens of millirem range). Probabilities of an accident with a release in the launch area are below one in ten million. Therefore launch area risk to individuals is effectively zero. However, there is a potential, in the event of an accident release, of up to 26 sq. km of land area to require evaluation for the necessity of remedial action because of land contamination exceeding an EPA screening level. DOE

N90-19285# General Electric Co., Philadelphia, PA. Astro Space Div.
SAFETY STATUS REPORT FOR THE ULYSSES MISSION. BOOK 1: ACCIDENT ANALYSIS. GENERAL PURPOSE HEAT SOURCE RADIOSOTOPE THERMOELECTRIC GENERATOR PROGRAM
Jan. 1990 127 p
(Contract DE-AC01-79ET-32043)
(DE90-006829; DOE/ET-32043/T29-Bk-1) Avail: NTIS HC A07/MF A01

The status of the accident analysis for the Ulysses outer planetary space science mission is presented in this Safety Status Report (SSR). This mission employs a Radioisotope Thermoelectric Generator (RTG) as the prime electrical power source for the spacecraft. Ulysses will be launched into earth orbit using the Space Shuttle and will use the Inertial Upper Stage (IUS)/Payload Assist Module-Special (PAM-S) boosters to place the spacecraft into an earth escape trajectory. The RTG employs silicon-germanium thermoelectric couples to produce electricity from the heat energy that results from the decay of the radioisotope fuel, Plutonium-238, used in the RTG heat source. The heat source configuration used in the RTG is termed General Purpose Heat Source (GPHS), and the RTG is designated GPHS-RTG. The use of radioactive material in these missions necessitates evaluations of the radiological risks that may be encountered by launch complex personnel as well as by the earth's general population resulting from postulated malfunctions or failures occurring in the mission operations. The SSR presents the results of a rigorous safety assessment, including substantial analyses and testing, of the launch and deployment of the RTG for the Ulysses mission. DOE

N90-19286# General Electric Co., Philadelphia, PA. Astro Space Div.
SAFETY STATUS REPORT FOR THE ULYSSES MISSION. BOOK 2: ACCIDENT ANALYSIS-APPENDICES. GENERAL PURPOSE HEAT SOURCE RADIOISOTOPE THERMOELECTRIC GENERATOR PROGRAM
Jan. 1990 625 p
(Contract DE-AC01-79ET-32043)
(DE90-006830; DOE/ET-32043/T29-Bk-2) Avail: NTIS HC A99/MF A04

This section of the Accident Analysis presents the appendices which describe the various analyses that have been conducted for use in the Ulysses Safety Status Report. Included in these appendices are the approaches, techniques, conditions and assumptions used in the development of the analytical models plus the detailed results of the analyses. Also included in these appendices are summaries of the accidents and their associated probabilities and environment models taken from the Shuttle Data Book (NSTS-08116), plus summaries of the several segments of the recent GPHS safety test program. The information presented in these appendices is used in Section 3 of Book 1 to develop the Failure/Abort Sequence Trees (FASTs) and to determine the fuel releases (source terms) resulting from the potential Space Shuttle/IUS accidents throughout the missions. DOE

N90-19287# Technische Univ., Brunswick (Germany, F.R.). Abteilung fuer Raumflugtechnik.
PRESENT AND FUTURE RISK OF SATELLITE AND MANNED PLATFORMS COLLISIONS WITH OTHER SPACE OBJECTS AND PARTICLES ON EARTH ORBITS [KURZBERICHT UEBER KONSEQUENZEN UND ERFORDERLICHE MASSNAHMEN DER STUDIE: DAS GEGENWAERTIGE UND ZUKUENFTIGE RISIKO DER KOLLISION VON SATELLITEN UND BEMANNTEN PLATTFORMEN MIT ANDEREN RAUMFLUGOBJEKTEN UND SCHROTTEILEN AUF ERDNAHEN UMLAUFBAHNEN]
P. Eichler and D. Rex 1988 11 p In GERMAN
(Contract BMFT-01QV86810)
(R-8841; ETN-90-95896) Avail: NTIS HC A02/MF A01

The collision probability can reach a certain percentage for big structures and long missions. In view of the Hermes and Columbus projects, the Europeans examined the American approach to this problem, such as the foundation of the U.S. intergovernmental Working Group on Space Debris. The manned modules of the future International Space Station will be protected with enclosures, whose weight represents 25 percent of the total structure mass. Another problem arises with the extravehicular activities, for which NASA calculated a risk of collision for 700,000 hours. It is essential to produce new mathematic models of the simulation of production of debris by explosions and collisions in space, and of the dynamics of debris clouds. A better cooperation with NASA is advisable. Future explosions in space must be avoided, and objects must be moved away from the terrestrial orbit as quickly as possible in order to limit the creation of new debris. ESA

N90-19288# Technische Univ., Brunswick (Germany, F.R.). Abteilung fuer Raumflugtechnik.
PRESENT AND FUTURE RISK OF COLLISION OF SATELLITES AND MANNED PLATFORMS WITH OTHER SPACE OBJECTS AND PARTICLES IN TERRESTRIAL ORBIT Final Report [DAS GEGENWAERTIGE UND ZUKUENFTIGE RISIKO DER KOLLISION VON SATELLITEN UND BEMANNTEN PLATTFORMEN MIT ANDEREN RAUMFLUGOBJEKTEN UND SCHROTTEILEN AUF ERDNAHEN UMLAUFBAHNEN]
P. Eichler and D. Rex 1988 172 p In GERMAN
(Contract BMFT-01QV86810)
(R-8840; ETN-90-95897) Avail: NTIS HC A08/MF A01

For nonprotected satellites, an object with a diameter of 1 mm is dangerous. Others are jeopardized by objects with a diameter of 1 cm. There are few direct measurement data for objects between 1 to 10 cm. A simulation of the most important explosion facts can give information about debris number and orbit distribution. Since a lot of data about Russian or military satellites is missing, a second method is employed to estimate the surface charge using an iteration process. A broad dispersion is found, with a reducing frequency at the higher surface charges. The explosion intensity is evaluated by the mass of the exploding object, the typically produced mass spectrum, and the number of measurable debris. Another program allows calculation of the long term development of a debris cloud. All these methods give a representative set of data about 35,000 objects greater than 1 cm in earth orbit. To calculate the collision probability, a model based on the shock process that appear by the gas diffusion, according to the kinetic gas theory, is used. ESA

N90-19289# Technische Univ., Brunswick (Germany, F.R.). Abteilung fuer Raumflugtechnik.
SATELLITES AND DEBRIS IN EARTH REVOLUTION ORBITS AND FIRST ESTIMATION OF THE COLLISION PROBABILITY [BESETZUNG VON ERDUMLAUFBAHNEN MIT SATELLITEN UND TRUEMMERN UND ERSTE ABSCHAETZUNG DER KOLLISIONSWAHRSCHEINLICHKEIT]
P. Eichler and D. Rex 1987 92 p In GERMAN
(Contract BMFT-01-OO-8604)
(R-8709; ETN-90-95898) Avail: NTIS HC A05/MF A01

A model of the collision probability based on the shock processes of the gas diffusion is given. The special orbit mechanics of objects in the earth gravitational field is thereby disregarded. The debris distribution is examined. The maximal object flux and the maximal congestion ratio is between 600 and 1100 km orbit height. In this critical area, the object flux-particle size curve is proposed. The objects of a diameter lower than 1 cm are principally meteorites, but for greater diameters, artificial satellites are the most numerous. The evolution of the number of objects in orbit for the last thirty years is described. A data base was produced, that contained the orbit parameters for every considered object, such as incline, apogee and perigee height, eccentricity and great half axis. ESA

N90-19290# Bundesministerium fuer Forschung und Technologie, Bonn (Germany, F.R.).
PROJECT FOR THE EUROPEAN SPACE ORGANIZATION IN THE AREA OF SPACE DEBRIS [RAUMFAHRTRUECKSTAENDE]
25 Jul. 1989 44 p In GERMAN
(Rept-29/89; ETN-90-95903) Avail: NTIS HC A03/MF A01

A strong angle dependence of the object flow in terrestrial space is established by a deterministic calculation process, that takes into account the trajectory mechanics of every object in earth orbit. The object flow that is equivalent to the collision risk, seems to be in a plane vertical to the trajectory plane. A good orientation can then reduce the object flow and the necessary protection costs; for a cylinder, that corresponds to the free flyer of Columbus, the transverse position in the debris plane is the best. Another position can increase the object flow by 31 percent. The ultimate development of the space station might be as far as possible, inside the debris plane. Critical manned modules might be put inside towards the back, uncritical modules might be ouside towards the front. The uncritical parts would screen the critical parts, whose collision risk could be practically nil, without additional protection costs. To limit debris production, which will be greater than those of meteorites, the engineers decided to address unnecessary explosions. ESA

N90-19291# Sandia National Labs., Albuquerque, NM. Engineering Analysis Dept.
THREE-DIMENSIONAL STRUCTURAL ANALYSES OF REENTRY VEHICLES
Kenneth W. Gwinn 1990 15 p Presented at the AIAA/ASME SDM Conference, Long Beach, CA, 2-4 Apr. 1990
(Contract DE-AC04-76DP-00789)
(DE90-006278; SAND-90-0092C; CONF-9004116-1) Avail: NTIS HC A03/MF A01

The three-dimensional structural analysis of reentry vehicles presents a considerable challenge to the analyst. This is due to the mechanics of the problem as well as the incorporation of results from several disciplines into the environmental description of the problem. Separate results from aero-analyses, frequently computed in one-dimensional form, must be combined into a three-dimensional format suitable for a structural finite element analysis. Features required for the analysis include the ablated thickness of the heatshield structure, as well as pressure on the vehicle and the temperature distribution through the heatshield. By combining these environments, a complete description of all factors which affect the structural performance of reentry vehicles are included into one analysis. This paper presents a method of analyzing the structural response of reentry vehicles using the complete three-dimensional environmental load description. In addition, this method permits the timely completion of such analyses on a production basis without making assumptions or simplifying the loading environments involved. Results from an analysis are presented which illustrate this method. The analysis uses a composite material description of the aeroshell along with temperature dependent properties. DOE

N90-19292# Volunteers in Technical Assistance, Inc., Arlington, VA.
LOW EARTH ORBITING SATELLITE FOR INTERNATIONAL INFORMATION EXCHANGE SYSTEM
Gary L. Garriott 21 Nov. 1989 32 p
(Contract DE-FG01-87CE-33007)

(DE90-007186; DOE/CE-33007/T2) Avail: NTIS HC A03/MF A01

VITA exceeded the goals outlined in the grant, especially in the development of networks of ground stations which can ultimately uplink to PACSAT. The University of Surrey (UK) designed and constructed the store and forward payloads. VITA demonstrated and helped install terrestrial networks in several countries for various agencies. This document is the second deliverable item under the VITA PACSAT Payload Contract (SST 88/157). It describes the design and construction of the Prototype PACSAT payload, which will be used for in-orbit tests on UoSAT satellite. It also notes how the goals set forth in the Preliminary System Specification have been met in the Prototype Payload design. The most recent formal report was the Preliminary System Specification of 25 March 1988. After that report, the in-orbit test opportunity for the VITA PACSAT Payload was re-scheduled. A review of the new test mission is presented in Section 2. DOE

N90-19293# Los Alamos National Lab., NM. Space Science Div.

LOW-COST SMALL SATELLITES FOR ASTROPHYSICAL MISSIONS

William C. Priedhorsky 1989 6 p Presented at the NASA Workshop on High Energy Astrophysics, Taos, NM, 10-14 Dec. 1989

(Contract W-7405-eng-36)

(DE90-007625; LA-UR-90-443; CONF-891276-4) Avail: NTIS HC A02/MF A01

A miniature satellite is a low-cost platform to support a small space experiment. Space astrophysics has been hindered by decades-long delays in important experiments. With miniature satellites, one hopes to reduce both experiment cost and lead time to an affordable level. Miniature satellites are not a new idea. The first scientific satellites, including Explorer I, were small and developed on a timescale of months. Important science was done by these pioneer missions. Though the easy discoveries have been made, important missions in exploration and follow-up can still be carried out from small platforms. Successful small satellite programs continue to this day. These include the OSCAR amateur radio satellite program, in which 12 small satellites, built by amateurs, have been flown over 25 years with no satellite failures (Fleeter, 1988). Two small free-flyers, GLOMAR and NUSAT, were ejected from the Shuttle in 1985. GLOMAR, a radio-relay experiment, was built in less than a year for under $1 million, and operated over a year in orbit. Small satellite projects continue to this day. NASA has started a small explorer program, beginning with SAMPEX, a solar and magnetospheric particle explorer; FAST, a fast auroral snapshot experiment; and SWAS, a submillimeter astronomy experiment. DOE

N90-19294# Pacific Northwest Lab., Richland, WA.

TECHNOLOGY EVALUATION FOR SPACE STATION ATMOSPHERIC LEAKAGE

D. K. Lemon, M. A. Friesel, J. W. Griffin, J. R. Skorpik, C. L. Shepard, Z. I. Antoniak, and R. J. Kurtz Feb. 1990 110 p

(Contract DE-AC06-76RL-01830)

(DE90-007844; PNL-7269) Avail: NTIS HC A06/MF A01

A concern in operation of a space station is leakage of atmosphere through seal points and through the walls as a result of damage from particle (space debris and micrometeoroid) impacts. This report describes a concept for a monitoring system to detect atmosphere leakage and locate the leak point. The concept is based on analysis and testing of two basic methods selected from an initial technology survey of potential approaches. DOE

N90-19295# Air War Coll., Maxwell AFB, AL.

ORBITAL SERVICING: ISSUE OR ANSWER

Douglas P. Hotard May 1989 58 p

(AD-A217284) Avail: NTIS HC A04/MF A01 CSCL 22/1

On-orbit satellite servicing as a forward-based logistic concept through an examination of its potential military benefits to endurance and survivability of space systems is reviewed. Reasons for opposition to implementation of the program within the military space environment are analyzed by focusing on the orbital refueling subfunction. The potential of orbital servicing to increase system capability and survivability while reducing system costs is assessed. GRA

N90-19250*# National Oceanic and Atmospheric Administration, Washington, DC. Office of Systems Development.

OPERATIONAL REQUIREMENTS AND THE GEOSTATIONARY PLATFORM

James K. Sparkman, Jr. *In* NASA, Langley Research Center, Earth Science Geostationary Platform Technology Jul. 1989 p 29-33 (For primary document see N90-19249 12-15)

Avail: NTIS HC A17/MF A03 CSCL 22B

N90-19252*# Lockheed Missiles and Space Co., Sunnyvale, CA.

GEOSTATIONARY EARTH SCIENCE PLATFORM CONCEPTS

M. M. Herardian *In* NASA, Langley Research Center, Earth Science Geostationary Platform Technology Jul. 1989 p 55-62 (For primary document see N90-19249 12-15)

Avail: NTIS HC A17/MF A03 CSCL 22B

N90-19254*# Lockheed Missiles and Space Co., Sunnyvale, CA.

LARGE-DIAMETER GEOSTATIONARY MILLIMETER WAVELENGTH ANTENNA CONCEPT

W. S. Gregorwich, H. A. Malliot, and A. K. Sinha *In* NASA, Langley Research Center, Earth Science Geostationary Platform Technology Jul. 1989 p 69-81 (For primary document see N90-19249 12-15)

Avail: NTIS HC A17/MF A03 CSCL 22B

N90-19393*# South Carolina Univ., Columbia. Dept. of Mechanical Engineering.

KALMAN ESTIMATION FOR SEDS MEASUREMENTS

Connie K. Carrington *In* Alabama Univ., Research Reports: 1989 NASA/ASEE Summer Faculty Fellowship Program Dec. 1989 20 p (For primary document see N90-19390 12-31)

(Grant NGT-01-008-021)

Avail: NTIS HC A99/MF E06 CSCL 22B

N90-19423*# Alabama Univ., Tuscaloosa. Dept. of Engineering Mechanics.

A VECTORIZED ALGORITHM FOR 3D DYNAMICS OF A TETHERED SATELLITE

Howard B. Wilson *In* Alabama Univ., Research Reports: 1989 NASA/ASEE Summer Faculty Fellowship Program Dec. 1989 30 p (For primary document see N90-19390 12-31)

(Grant NGT-01-008-021)

Avail: NTIS HC A99/MF E06 CSCL 22B

N90-19974*# Stanford Univ., CA.

DRAG-FREE SATELLITE CONTROL

Daniel B. DeBra *In* NASA, Relativistic Gravitational Experiments in Space Aug. 1989 p 206-210 (For primary document see N90-19940 12-90)

Avail: NTIS HC A11/MF A02 CSCL 22B

19 SPACECRAFT INSTRUMENTATION

For related information see also *06 Aircraft Instrumentation* and *35 Instrumentation and Photography.*

N90-19296# Los Alamos National Lab., NM.

IDENTIFICATION AND SOLUTION OF A CHARGING PROBLEM IN A HIGH-ALTITUDE DETECTOR

George J. Berzins, John E. Valencia, Harry E. Felthauser, Joseph E. Nanevicz, and Jeffrey S. Thayer (SRI International Corp., Menlo Park, CA.) 1989 9 p Presented at the Spacecraft Charging Technology Conference, Monterey, CA, 31 Oct. - 3 Nov. 1989

(Contract W-7405-eng-36)

(DE90-008637; LA-UR-90-170; CONF-8910358-2) Avail: NTIS HC A02/MF A01

The unwanted response of spacecraft borne instruments to electrons and other charged particles in orbit has long been at least a nuisance. In the benign case these particles generate background signals that require processing on orbit, increasing the instrument dead time, and sometimes interfere with the measurement of small effects. In the severe extreme, electrons can charge dielectrics in or near the instrument. Such charging can be followed by a breakdown discharge that can either generate false data, or, in rare cases, cause malfunction of the instrument. In recounting how we identified and solved the problem, we would like do so from the viewpoint of experimenters who were unfamiliar with the phenomenology of spacecraft charging and unaware of the considerable work that had been done already on the subject. Such a perspective is not only descriptive, but may be potentially useful to others in similar situations. A preliminary report was presented as a poster paper at the 1986 Hardened Electronics And Radiation Technology (HEART) conference. DOE

N90-19251*# Massachusetts Inst. of Tech., Cambridge. Research Lab. of Electronics.
SCIENCE REQUIREMENTS FOR PASSIVE MICROWAVE SENSORS ON EARTH SCIENCE GEOSTATIONARY PLATFORMS
A. J. Gasiewski and D. H. Staelin *In* NASA, Langley Research Center, Earth Science Geostationary Platform Technology Jul. 1989 p 37-53 (For primary document see N90-19249 12-15)
Avail: NTIS HC A17/MF A03 CSCL 22B

N90-19255*# Lockheed Missiles and Space Co., Sunnyvale, CA.
DESIGN OF A LOW-FREQUENCY (5-20 GHz), 15-METER-DIAMETER PASSIVE RADIOMETER FOR GEOSTATIONARY EARTH SCIENCE PLATFORMS
A. K. Sinha *In* NASA, Langley Research Center, Earth Science Geostationary Platform Technology Jul. 1989 p 83-108 (For primary document see N90-19249 12-15)
Avail: NTIS HC A17/MF A03 CSCL 14B

N90-19260*# Jet Propulsion Lab., California Inst. of Tech., Pasadena.
MILLIMETER RADIOMETER SYSTEM TECHNOLOGY
W. J. Wilson and P. N. Swanson *In* NASA, Langley Research Center, Earth Science Geostationary Platform Technology Jul. 1989 p 167-177 (For primary document see N90-19249 12-15)
Avail: NTIS HC A17/MF A03 CSCL 14B

N90-19261*# Jet Propulsion Lab., California Inst. of Tech., Pasadena.
SYNTHETIC APERTURE INTERFEROMETRIC RADIOMETER (SAIR)
C. S. Ruf *In* NASA, Langley Research Center, Earth Science Geostationary Platform Technology Jul. 1989 p 179-189 (For primary document see N90-19249 12-15)
Avail: NTIS HC A17/MF A03 CSCL 14B

N90-19270*# Digital Signal Corp., Springfield, VA.
APPLICATIONS OF FM-CW LASER RADAR TO ANTENNA CONTOUR MAPPING
A. R. Slotwinski *In* NASA, Langley Research Center, Earth Science Geostationary Platform Technology Jul. 1989 p 331-337 (For primary document see N90-19249 12-15)
Avail: NTIS HC A17/MF A03 CSCL 14B

N90-19271*# Ball Aerospace Systems Div., Boulder, CO.
REMOTE ATTITUDE MEASUREMENT SENSOR (RAMS)
H. W. Davis *In* NASA, Langley Research Center, Earth Science Geostationary Platform Technology Jul. 1989 p 339-368 (For primary document see N90-19249 12-15)
Avail: NTIS HC A17/MF A03 CSCL 14B

N90-19272*# Jet Propulsion Lab., California Inst. of Tech., Pasadena. Optical Sciences and Application Section 385.
PRECISION SEGMENTED REFLECTOR, FIGURE VERIFICATION SENSOR
Paul K. Manhart and Steve A. Macenka *In* NASA, Langley Research Center, Earth Science Geostationary Platform Technology Jul. 1989 p 369-374 (For primary document see N90-19249 12-15)
Avail: NTIS HC A17/MF A03 CSCL 14B

20 SPACECRAFT PROPULSION AND POWER

Includes main propulsion systems and components, e.g., rocket engines; and spacecraft auxilliary power sources.

For related information see also *07 Aircraft Propulsion and Power, 28 Propellants and Fuels, 44 Energy Production and Conversion,* and *15 Launch Vehicles and Space Vehicles.*

N90-19297# California Inst. of Tech., Pasadena. Div. of Engineering and Applied Science.
PROCEEDINGS OF A CONTRACTORS MEETING ON COMBUSTION ROCKET PROPULSION DIAGNOSTICS OF REACTING FLOW
J. M. Tishkoff, M. A. Birkan, G. S. Roy, and S. G. Lekoudis 13 Jun. 1988 349 p Meeting held in Monrovia, CA, 13-17 Jun. 1988 Sponsored in part by Navy
(Grant AF-AFOSR-0337-86; AF Proj. 2308)
(AD-A216445; AFOSR-89-1710TR) Avail: NTIS HC A15/MF A02 CSCL 21/8

Abstracts are given for research efforts on airbreathing combustion, rocket propulsion, and diagnostics of reacting flows. Author

N90-19298* National Aeronautics and Space Administration. Langley Research Center, Hampton, VA.
DUAL-FUEL, DUAL-MODE ROCKET ENGINE Patent
James A. Martin, inventor (to NASA) 23 May 1989 9 p Filed 9 Mar. 1988
(NASA-Case-LAR-13773-1; US-Patent-4,831,818; US-Patent-Appl-SN-165946; US-Patent-Class-60-204; US-Patent-Class-60-259; US-Patent-Class-60-260) Avail: US Patent and Trademark Office CSCL 21H

The invention relates to a dual fuel, dual mode rocket engine designed to improve the performance of earth-to-orbit vehicles. For any vehicle that operates from the earth's surface to earth orbit, it is advantageous to use two different fuels during its ascent. A high density impulse fuel, such as kerosene, is most efficient during the first half of the trajectory. A high specific impulse fuel, such as hydrogen, is most efficient during the second half of the trajectory. The invention allows both fuels to be used with a single rocket engine. It does so by adding a minimum number of state-of-the-art components to baseline single made rocket engines, and is therefore relatively easy to develop for near term applications. The novelty of this invention resides in the mixing of fuels before exhaust nozzle cooling. This allows all of the engine fuel to cool the exhaust nozzle, and allows the ratio of fuels used throughout the flight depend solely on performance requirements, not cooling requirements.

Official Gazette of the U.S. Patent and Trademark Office

N90-19299*# National Aeronautics and Space Administration. Lewis Research Center, Cleveland, OH.
AEOLIAN REMOVAL OF DUST FROM PHOTOVOLTAIC SURFACES ON MARS
James R. Gaier, Marla E. Perez-Davis, and Mark Marabito (Cleveland State Univ., OH.) Feb. 1990 19 p
(NASA-TM-102507; E-5309; NAS 1.15:102507) Avail: NTIS HC A03/MF A01 CSCL 10A

It is well documented that Mars is totally engulfed in huge dust storms nearly each Martian year. Dust elevated in these global

dust storms, or in any of the numerous local dust storms could settle on photovoltaic surfaces and seriously hamper photovoltaic power system performance. Using a recently developed technique to uniformly dust simulated photovoltaic surfaces, samples were subjected to Martian-like winds in an attempt to determine whether natural aeolian processes on Mars would sweep off the settled dust. The effects of wind velocity, angle of attack, height off the Martian surface, and surface coating material were investigated. Principles which can help to guide the design of photovoltaic arrays bound for the Martian surface were uncovered. Most importantly, arrays mounted with an angle of attack approaching 45 deg show the most efficient clearing. Although the angular dependence is not sharp, horizontally mounted arrays required significantly higher wind velocities to clear off the dust. From the perspective of dust-clearing it appears that the arrays may be erected quite near the ground, but previous studies have suggested that saltation effects can be expected to cause such arrays to be covered by sand if they are set up less than about a meter from the ground. Providing that the surface chemistry of Martian dusts is comparable to our test dust, the materials used for protective coating may be optimized for other considerations such as transparency, and chemical or abrasion resistance. The static threshold velocity is low enough that there are regions on Mars which experience winds strong enough to clear off a photovoltaic array if it is properly oriented. Turbulence fences proved to be an ineffective strategy to keep dust cleared from the photovoltaic surfaces. Author

N90-19415*# Alabama Univ., Tuscaloosa. Dept. of Engineering Mechanics.
ROCOPT: A USER FRIENDLY INTERACTIVE CODE TO OPTIMIZE ROCKET STRUCTURAL COMPONENTS
William K. Rule *In* Alabama Univ., Research Reports: 1989 NASA/ASEE Summer Faculty Fellowship Program Dec. 1989 28 p (For primary document see N90-19390 12-31)
(Grant NGT-01-008-021)
Avail: NTIS HC A99/MF E06 CSCL 21H

N90-19416*# Memphis State Univ., TN. Dept. of Mechanical Engineering.
ITERATIVE PROCEDURES FOR SPACE SHUTTLE MAIN ENGINE PERFORMANCE MODELS
L. Michael Santi *In* Alabama Univ., Research Reports: 1989 NASA/ASEE Summer Faculty Fellowship Program Dec. 1989 29 p (For primary document see N90-19390 12-31)
(Grant NGT-01-008-021)
Avail: NTIS HC A99/MF E06 CSCL 21H

23 CHEMISTRY AND MATERIALS (GENERAL)

N90-19300* National Aeronautics and Space Administration. Lewis Research Center, Cleveland, OH.
NEW CONDENSATION POLYIMIDES CONTAINING 1,1,1-TRIARYL-2,2,2-TRIFLUOROETHANE STRUCTURES
Patent
William B. Alston, inventor (to NASA) and Roy F. Gratz, inventor (to NASA) 4 Jul. 1989 18 p Filed 29 Oct. 1986
(NASA-Case-LEW-14346-1; US-Patent-4,845,167; US-Patent-Appl-SN-924470; US-Patent-Class-528-353; US-Patent-Class-528-352; US-Patent-Class-528-229; US-Patent-Class-528-188) Avail: US Patent and Trademark Office CSCL 07A

The invention relates to a condensation polyimide containing a 1,1,1-triaryl 2,2,2-trifluoroethane structure and other related condensation polyimides. The process for their preparation, which comprises polymerization of a cyclic dianhydride with a diamine is also covered.
Official Gazette of the U.S. Patent and Trademark Office

N90-19301*# National Aeronautics and Space Administration. Lewis Research Center, Cleveland, OH.
FLUORINATED GRAPHITE FIBERS AS A NEW ENGINEERING MATERIAL: PROMISES AND CHALLENGES
Ching-cheh Hung and Martin Long (Cleveland State Univ., OH.) 1989 23 p Presented at the 19th Biennial Conference on Carbon, University Park, PA, 25-30 Jun. 1989; sponsored by American Carbon Society
(NASA-TM-102511; E-5313; NAS 1.15:102511) Avail: NTIS HC A03/MF A01 CSCL 07A

Pitch based graphitized carbon fibers with electrical resistivity of 300 micro-Ohm/cm were brominated and partially debrominated to 18 percent bromine at room temperature, and then fluorinated at 300 to 450 C, either continuously or intermittently for several cycles. In addition, on fluorine and titanium fluoride intercalated fiber sample was fluorinated at 270 C from the same fiber source. The mass and conductivity of the brominated-debrominated then fluorinated fibers (with fluorine-to-carbon atom ratio of 0.54 or higher) stabilized at room temperature air in a few days. However, at 200 C, these values decreased rapidly and then more slowly, throughout a 2-week test period. The electrically insulative or semiconductive fibers were found to be compatible with epoxy and have the fluorine-to-carbon atom ratio of 0.65 to 0.68, thermal conductivity of 5 to 24 W/m-K, electrical resistivity of 10(exp 4) to 10(exp 11) Ohm/cm, tensile strength of 70 to 150 ksi, Young's modulus of 20 to 30 msi, and CTE (coefficient of thermal expansion) values of 7 ppm/deg C. Data of these physical property values are preliminary. However, it is concluded that these physical properties can be tailor-made. They depend largely on the fluorine content of the final products and the intercalant in the fibers before fluorination, and, to a smaller extent, on the fluorination temperature histogram. Author

24 COMPOSITE MATERIALS

Includes physical, chemical, and mechanical properties of laminates and other composite materials.
For ceramic materials see *27 Nonmetallic Materials*.

N90-19302*# National Aeronautics and Space Administration. Lewis Research Center, Cleveland, OH.
HEAT TREATMENT STUDY OF THE SiC/Ti-15-3 COMPOSITE SYSTEM Final Report
Bradley A. Lerch, Timothy P. Gabb, and Rebecca A. MacKay Washington Jan. 1990 31 p
(NASA-TP-2970; E-4985; NAS 1.60:2970) Avail: NTIS HC A03/MF A01 CSCL 11D

The oxidation and aging behaviors of a continuous fiber SiC/Ti-15V-3Cr-3Sn-3Al composite (SiC/Ti-15-3) were investigated. The aging characteristic of the composite were compared with those of the unreinforced Ti-15-3 matrix material, which was processed in the same manner as the composite. Various age hardened conditions of both the unreinforced matrix and the composite were evaluated by using optical microscopy, hardness measurements, and room temperature tensile tests (unreinforced matrix only). The Ti-15-3 material formed a thick surface oxide at temperature at or above 550 C when heat treated in air. The in situ composite matrix was softer than the unreinforced matrix for equivalent aging conditions. Both materials hardened to a maximum, then softened during overaging. The temperature at which peak aging occurred was approx. 450 C for both the in situ composite matrix and the unreinforced matrix. The room temperature elastic modulus and ultimate tensile strength of the unreinforced matrix varied as a function of aging treatment and paralleled the hardness behavior. The modulus and tensile strength showed little response to aging up to temperatures of 300 C; however, these properties increased after aging at 550 C. Aging at temperatures above 550 C resulted in a decrease in the modulus and tensile strength. The failure strain was a function of the precipitation state and of the amount of oxidation resulting from the heat treatment. Aging in air at the higher temperatures (greater than 550 C) caused the formation of a thick oxide layer and

reduced the ductility. Aging in vacuum at these temperatures resulted in significantly higher ductilities. Long term exposures at 700 C caused the formation of a large grain boundary alpha-phase which reduced the ductility, even though the specimens were heat treated in vacuum. Author

N90-19303 Council for National Academic Awards (England).
EVALUATION OF REPEATED IMPACT DAMAGE IN COMPOSITE STRUCTURES Ph.D. Thesis
Fadhil A. Habib 1988 313 p
Avail: Univ. Microfilms Order No. BRDX86532

The research program reported considers the effects of repeated low velocity impact damage on Chopped Strand Mat (CSM) laminates. The residual strength and stiffness (modulus) of CSM laminates subjected to repeated concurrent impacts was experimentally and theoretically evaluated. A special purpose test rig was used to accurately measure the energy absorbed by the composite plates. A maximum of 30 impacts was considered. The damaged areas for the impacted and opposite sides of the specimens were related to the number of impacts and the impacting energy. The significance of the damage was determined by subjecting the specimens to tensile testing and measuring the difference in strength and stiffness (modulus) between the damaged and undamaged specimens. The impact force-time was also experimentally measured. In addition to mechanical testing, the damage caused by repeated impact was evaluated by employing four NonDestructive Evaluation (NDE) methods: radiography, ultrasonics (A-scan, B-scan, and C-scan), thermography, and liquid penetrant. The first three methods were used to study the internal damage caused by repeated impact and the fourth used to study the surface damage. It is shown that the present theory realistically predicts the loss in ultimate tensile strength and modulus of CSM specimens subjected to the aforementioned impact loading. In addition, the maximum extent of damage is theoretically modelled with reasonable accuracy. Dissert. Abstr.

N90-19304# Battelle Memorial Inst., Columbus, OH.
AC LOSS MEASUREMENTS OF TWO MULTIFILAMENTARY NbTi COMPOSITE STRANDS
E. W. Collings, K. R. Marken, M. D. Sumption, R. B. Goldfarb, and R. J. Loughran (National Inst. of Standards and Technology, Boulder, CO.) 1989 9 p Presented at the International Cryogenic Materials Conference, Los Angeles, CA, 24-28 Jul. 1989
(Contract DE-AC02-86ER-40296)
(DE90-005388; CONF-890701-23) Avail: NTIS HC A02/MF A01

As part of an interlaboratory comparative testing program conducted in support of the Versailles Agreement on Advanced Materials and Standards (VAMAS), transverse-field dc hysteresis loss measurements were made at liquid-helium temperatures at fields of up to 3 T (30 kG) on two samples of multifilamentary NbTi composite. The strands differed widely in filament number, were comparable in filament diameter, and one of them was provided with a Cu-Ni barrier between the filaments. The results have been analyzed, and magnetically deduced critical current density values obtained (for comparison with directly measured transport data) using various standard techniques. Based on these studies, a figure-of-merit for ac loss is recommended. The Cu-matrix strand, with its interfilamentary spacing of less than 1 micron, exhibited pronounced proximity-effect-induced coupling losses; this was not observed in the mixed-matrix strand which possessed not only a Cu-Ni barrier but also an interfilamentary spacing of typically 4 microns. DOE

N90-19305# Department of the Army, Washington, DC.
FAST OPTICAL SWITCH AND LIMITER USING QUANTUM SIZE EFFECT IN METAL GRAIN COMPOSITES Patent Application
Joseph W. Haus, inventor (to Army), Nauser Kalyaniwalla, inventor (to Army), Ramarao Inguva, inventor (to Army), and Charles M. Rowden, inventor (to Army) 7 Aug. 1989 10 p
(AD-D014332; US-Patent-Appl-SN-392866) Avail: NTIS HC A02/MF A01 CSCL 09/5

A block of composite material includes a dielectric material with a dielectric constant of epsilon sub d = 4.66 and which is at least 4 micrometers thick and has electrically conductive microparticles randomly distributed throughout. The composite material exhibits an optical bistability without cavity feedback. The microparticles must be nearly uniform in size and of spherical diameter much smaller than the wavelength of light in the particle. The composite, when illuminated by laser light in the range of 500 nm and of varying intensity, becomes opaque at a critical input intensity and stays opaque until the input intensity reaches a certain level both below and above the intensity at which it initially became opaque. Thus the material behaves as an optical switch and a limiter. GRA

N90-19306# Department of the Army, Washington, DC.
HETEROGENEOUS COMPOSITE AND METHOD OF MAKING Patent Application
William L. Wade, Jr., inventor (to Army), Robert J. Mammone, inventor (to Army), and Michael Binder, inventor (to Army) 3 Nov. 1989 9 p
(AD-D014337; US-Patent-Appl-SN-431277) Avail: NTIS HC A02/MF A01 CSCL 11/4

The invention described herein may be manufactured, used, and licensed by or for the Government for governmental purposes without the payment to us of any royalty thereon. This invention relates in general to heterogeneous composites and to their method of making and in particular to a free-standing, flexible heterogeneous composite of insulating polymeric film containing relatively small percentages of electrically conductive polymer wherein the conductive polymer exists as the dispersed phase and to their method of making. Polymers designed with high dielectric constants, low dissipation factors and high electric field breakdown strengths have application as dielectrics in capacitors for communication equipment, computers, and space power systems. GRA

N90-19307# Pennsylvania State Univ., University Park.
CARBON BLACK/POLYETHYLENE COMPOSITES FOR PTC (POSITIVE TEMPERATURE COEFFICIENT) THERMISTOR APPLICATIONS M.S. Thesis
Lori Louise Rohlfing Dec. 1987 110 p Sponsored in part by NSF
(Contract N00014-86-C-2028)
(AD-A215988) Avail: NTIS HC A06/MF A01 CSCL 11/4

A new class of composite Positive Temperature Coefficient (PTC) thermistors are commercially available. These composite thermistors exhibit a PTC measuring 6 to 8 orders of magnitude and have several advantages over conventional Barium Titanate 3 thermistors, including lower room temperature resistivity, better thermal shock resistance, and high temperature stability. Composite PTC thermistors are produced from a carbon black/polyethylene composition that exhibited a PTC of resistance measuring 6 to 8 orders of magnitude at 125 C. The composites are irradiated (gamma source) to induce polymer crosslinking. Crosslinking imparts mechanical integrity and prevents the onset of an NTC effect above the transition temperature. Crosslinking stabilizes the high temperature resistivity to 200 C. The electrical properties of these crosslinked composites are examined as functions of temperature, frequency, and thermal cycling. To eliminate the crosslinking procedure, an insulating mullite phase was incorporated into the diphasic mixture to form a triphasic composite. Addition of the third filler yielded two effects. First, the filler provided sufficient mechanical stabilization of the composite structure to maintain high post-PTC resistance without an NTC effect. Second, the addition of an insulating filler resulted in a shift of the room temperature resistivity caused by a shift in the percolation curve. Author

N90-19308*# Maryland Univ., College Park. Dept. of Mechanical Engineering.
INNOVATIVE DESIGN OF COMPOSITE STRUCTURES: THE USE OF CURVILINEAR FIBER FORMAT IN STRUCTURAL DESIGN OF COMPOSITES Final Report
R. F. Charette and M. W. Hyer Mar. 1990 158 p
(Grant NAG1-665)
(NASA-CR-186406; NAS 1.26:186406) Avail: NTIS HC A08/MF A01 CSCL 11D

The influence is investigated of a curvilinear fiber format on load carrying capacity of a layered fiber reinforced plate with a centrally located hole. A curvilinear fiber format is descriptive of layers in a laminate having fibers which are aligned with the principal stress directions in those layers. Laminates of five curvilinear fiber format designs and four straightline fiber format designs are considered. A quasi-isotropic laminate having a straightline fiber format is used to define a baseline design for comparison with the other laminate designs. Four different plate geometries are considered and differentiated by two values of hole diameter/plate width equal to 1/6 and 1/3, and two values of plate length/plate width equal to 2 and 1. With the plates under uniaxial tensile loading on two opposing edges, alignment of fibers in the curvilinear layers with the principal stress directions is determined analytically by an iteration procedure. In-plane tensile load capacity is computed for all of the laminate designs using a finite element analysis method. A maximum strain failure criterion and the Tsai-Wu failure criterion are applied to determine failure loads and failure modes. Resistance to buckling of the laminate designs to uniaxial compressive loading is analyzed using the commercial code Engineering Analysis Language. Results indicate that the curvilinear fiber format laminates have higher in-plane tensile load capacity and comparable buckling resistance relative to the straightline fiber format laminates. Author

N90-19309*# Michigan Univ., Ann Arbor. Radiation Lab.
A COMBINED FINITE ELEMENT-BOUNDARY ELEMENT FORMULATION FOR SOLUTION OF TWO-DIMENSIONAL PROBLEMS VIA CGFFT Technical Report, Sep. 1989 - Feb. 1990
Jeffrey D. Collins, Jian-Ming Jin, and John L. Volakis 1990 54 p
(Grant NAG2-541)
(NASA-CR-186464; NAS 1.26:186464; UM-025921-11-T) Avail: NTIS HC A04/MF A01 CSCL 11D

A method for the computation of electromagnetic scattering from arbitrary two-dimensional bodies is presented. The method combines the finite element and boundary element methods leading to a system for solution via the conjugate gradient Fast Fourier Transform (FFT) algorithm. Two forms of boundaries aimed at reducing the storage requirement of the boundary integral are investigated. It is shown that the boundary integral becomes convolutional when a circular enclosure is chosen, resulting in reduced storage requirement when the system is solved via the conjugate gradient FFT method. The same holds for the ogival enclosure, except that some of the boundary integrals are not convolutional and must be carefully treated to maintain O(N) memory requirement. Results for several circular and ogival structures are presented and shown to be in excellent agreement with those obtained by traditional methods. Author

N90-19310*# National Aeronautics and Space Administration. Lewis Research Center, Cleveland, OH.
THERMO-OXIDATIVE STABILITY STUDIES OF PMR-15 POLYMER MATRIX COMPOSITES REINFORCED WITH VARIOUS FIBERS
Kenneth J. Bowles 1990 16 p Presented at the 35th International SAMPE Symposium and Exhibition, Anaheim, CA, 2-5 Apr. 1990
(NASA-TM-102439; E-5208; NAS 1.15:102439) Avail: NTIS HC A03/MF A01 CSCL 11D

An experimental study was conducted to measure the thermo-oxidative stability of PMR-15 polymer matrix composites reinforced with various fibers and to observe differences in the way they degrade in air. The fibers that were studied included graphite and the thermally stable Nicalon and Nextel ceramic fibers. Weight loss rates for the different composites were assessed as a function of mechanical properties, specimen geometry, fiber sizing, and interfacial bond strength. Differences were observed in rates of weight loss, matrix cracking, geometry dependency, and fiber-sizing effects. It was shown that Celion 6000 fiber-reinforced composites do not exhibit a straight-line Arrhenius relationship at temperatures above 316 C. Author

N90-19311# Stuttgart Univ. (Germany, F.R.). Fakultaet fuer Luft- und Raumfahrttechnik.
PRACTICAL CALCULATION OF THE LIVELOAD OF CARBON FIBER REINFORCED PLASTICS BY THE FINITE ELEMENT METHOD Ph.D. Thesis [UEBER DIE PRAXISORIENTIERTE BERECHNUNG DER TRAGFAEHIGKEIT VON KOHLEFASERVERSTAERKTEN KUNSTSTOFFBAUTEILEN MIT DER METHODE DER FINITEN ELEMENTE]
Klaus Ickert 1988 122 p In GERMAN
(ETN-90-95867) Avail: NTIS HC A06/MF A01

The model is based on the formulation of layered sheet elements, to which the laminate theory is applied. The nonlinear charge-deformation behavior is determined. A tension criterium was used with bending parameters (a generalized hardness assumption), as a constitutent additional condition. The possible response of the binder was examined. The necessary edge values of the interlaminar tensions were calculated under static equilibrium conditions (as an approximation solution) from the layer strength tensions. ESA

N90-19312# Technische Univ., Delft (Netherlands). Faculteit der Luchtvaart- en Ruimtevaarttechniek.
THE CREEP BEHAVIOR OF AN ARAMIDE FIBER REINFORCED WOUND TOW-STRAP [HET KRUIPGEDRAG VAN EEN ARAMIDEVEZELVERSTERKTE NYLON GEWIKKELDE TREKLUS]
L. G. Meijers Sep. 1987 12 p In DUTCH
(LR-546; ETN-90-95989) Avail: NTIS HC A03/MF A01

Creep experiments were performed on a tow-strap, made of aramide fiber reinforced nylon (PA-12) and fabricated using a numerically controlled winding bench. The deformation due to creep is about 0.1 percent of the total length of the strap and 5.8 percent of the total deformation during a 10T test loading. The creeping seems to stop after 48 hours. Climatic effects (temperature and relative humidity) lead to deviations of about 20 percent of the total creep deformation. A prestretching process affects favorably the behavior of the strap. The friction between the strap and the adjacent parts of the construction have a negative effect in case of fast loading. ESA

N90-19313# Technische Univ., Brunswick (Germany, F.R.). Fakultaet fuer Maschinenbau und Elektrotechnik.
EVALUATION AND CHOICE ALGORITHMS OF COST OPTIMAL PREPREG-APPLICATION PROCESSES: PRODUCTION OF STRONGLY CHARGED PLANE PARTS MADE OF FIBER REINFORCED PLASTICS Ph.D. Thesis [BEWERTUNGS- UND AUSWAHLALGORITHMEN KOSTENOPTIMALER PREPREG-APPLIKATIONSVERFAHREN IM RAHMEN DER FERTIGUNG HOCHBELASTETER FLUGZEUBAUTEILE AUS FASERVERSTAERKTEM KUNSTSTOFF]
Juergen Klenner 1989 193 p In GERMAN
(ETN-90-95895) Avail: NTIS HC A09/MF A01

In the near future, carbon reinforced plastics in Prepreg form with a hard duromer-matrix will be the main FRP (fiber reinforced plastic) of flight materials. Using the simulation program the optimal production directions for every type of construction element can be determined and the power and utilization costs and the working degree can be calculated. The parameters of the description of construction elements were chosen so that the algorithms and the calculation programs are universally useful. ESA

N90-19314# Essen Univ. (Germany, F.R.). Fachbereich Maschinentechnik.
UTILIZATION OF THERMOMETRIC METHODS FOR THE TESTING OF CARBON REINFORCED PLASTICS Ph.D. Thesis [ANWENDUNG THERMOMETRISCHER METHODEN BEI DER PRUEFUNG KOHLENSTOFFASERVERSTAERKTER KUNSTSTOFFE]
Harald Neubert 1989 152 p In GERMAN Sponsored by Wissenschaftsminister des Landes Nordrhein-Westfalen
(ETN-90-96076) Avail: NTIS HC A08/MF A01

The distinction can be made between temperature changes due to thermoelastic effects and temperature variations caused by dissipative processes. Temperature measurements with a sensitivity of a mK are made with thermoelements, for a matrix made of an epoxy-resin mixture and a bismaleimide. Elastic deformations and voltage changes define, by means of their magnitude and sign, the temperature variations due to the thermoelastic effect. The sensitivity of the method allows examination of the changes of the laminate state for montone and cyclic charges. With a one-step charge, the slopes of the temperature curves point out the formation velocities of the fatigue damages (tears or delaminations). ESA

N90-19315# Oak Ridge National Lab., TN.
IDENTIFICATION AND DEVELOPMENT OF OPTIMUM SiC WHISKERS FOR SILICON NITRIDE MATRIX COMPOSITES
T. Tiegs, L. F. Allard, P. F. Becher, and M. F. Ferber 1989 27 p Presented at the Annual Automotive Technology Development Contractors Coordination Meeting, Dearborn, MI, 23-26 Oct. 1989
(Contract DE-AC05-84OR-21400)
(DE90-006888; CONF-8910248-2) Avail: NTIS HC A03/MF A01

Using micromechanics modeling and observed increases in fracture toughness for whisker-reinforced alumina and silicon nitride, SiC whisker strengths were calculated. Based on those results, flaw sizes were estimated and compared to scanning and transmission electron microscopy observations of the structure in typical whiskers. The sizes of the strength-limiting flaws were calculated to be in the range of 0.1 and 0.4 microns, which corresponds to the size of defects observed in many of the current commercial whiskers. Defects identified in this size range include the core regions, which are accumulations of smaller inclusions as well as voids located within some whisker types. Another defect that decreases whisker strength is excessive surface roughness (usually associated with crystallographic phase changes) that results in stress concentrations. Calculations indicate that if high-strength SiC whiskers were made available by eliminating strength-limiting flaws, silicon nitride composites with toughnesses (K(sub IC)) (gt)15 MPa(m)(sup 1/2) may be realized. DOE

N90-19405*# New Orleans Univ., LA. Dept. of Mechanical Engineering.
LOW-ENERGY IMPACT RESISTANCE OF GRAPHITE-EPOXY PLATES AND ALS HONEYCOMB SANDWICH PANELS
David Hui *In* Alabama Univ., Research Reports: 1989 NASA/ASEE Summer Faculty Fellowship Program Dec. 1989 46 p (For primary document see N90-19390 12-31)
(Grant NGT-01-008-021)
Avail: NTIS HC A99/MF E06 CSCL 11D

25 INORGANIC AND PHYSICAL CHEMISTRY

Includes chemical analysis, e.g., chromatography; combustion theory; electrochemistry; and photochemistry.

For related information see also *77 Thermodynamics and Statistical Physics.*.

N90-19316 Carnegie-Mellon Univ., Pittsburgh, PA.
NUMERICAL STUDY OF DIFFUSION JET FLAMES Ph.D. Thesis
Kenneth Jerry Laskey 1989 386 p
Avail: Univ. Microfilms Order No. DA8920046

The focus is on the numerical study of diffusion jet flames. In particular, chemical reaction with heat release is studied to determine its effect on the reacting fuel jet and a coflowing air stream. The fuel jet consists of a hydrogen-nitrogen mixture, and the fuel composition, jet and coflow velocities, and nozzle geometry are chosen to model flame experiments performed at the Air Force Wright Aeronautical Laboratory. Two fuel jet velocities, 3.26 and 20 m/s, are studied, and the computational results for the lower velocity jet are compared with available experimental data. Both the experimental and numerical results show the formation and shedding of vortex structures in the coflow region outside the flame. In addition, for the 20 m/s jet, a higher frequency structure is seen at the shear layer formed by the fuel jet and the product generated at the flame surface. Good agreement is seen between calculated velocity and temperature profiles and their experimental counterparts. Calculations of the 3.26 and 20 m/s fuel jets were also performed without gravity to examine the effect of buoyancy on diffusion jet flames. There are major differences between these and the bouyant flames, and the results are discussed in the context of the Lewis drop-tower experiments for much smaller nozzles and flowrates. A major effort was the development of the Axisymmetric, Low-speed Jet Flame (ALJF) code to perform the jet diffusion flame simulations. A detailed description of the models for convection, buoyancy, thermal conduction, molecular diffusion, and chemical reaction are included. In addition, a viscous dissipation model which is implemented in the code is also described. Dissert. Abstr.

N90-19317# Clarkson Univ., Potsdam, NY.
SIMULATION OF THERMAL DYNAMICS OF A VAPORIZING COAL-WATER DROPLET IN A COMBUSTOR
Marek A. Sitarski 1988 10 p Presented at the 13th International Conference on Coal and Slurry Technology, Denver, CO, 12-15 Apr. 1988
(Contract DE-AC21-85MC-22073)
(DE90-005356; CONF-880418-2) Avail: NTIS HC A02/MF A01

The fate of the slurry droplet in a combustor of a heat engine depends strongly on the vaporization dynamics of the slurry liquid during the first few milliseconds after injection of the droplet into the combustor. To predict the fate of the slurry droplets in combustors and to find the most advantageous conditions for secondary atomization of the droplets, a complex model of the thermal dynamics of a vaporizing coal-water droplet in a combustor is being developed. This novel two-dimensional transient approach includes such elements as: (1) time dependent absorption patterns of the incident radiation inside the slurry droplets during the vaporization, (2) description of the coupled mass and energy transfer in the gas phase surrounding the droplet based on a solution of the Boltzmann equation which takes into account gas-surface accommodation coefficients and Knudsen effects, (3) shrinking droplet dynamics, and (4) nonlinear boundary conditions. The transient heat dissipation inside the heterogeneous droplet is simulated by the Monte Carlo method. The effect of a surfactant on the droplet dynamics is studied by changing values of the evaporation coefficient. DOE

N90-19318# Department of the Navy, Washington, DC.
A HIGH OPTICAL DENSITY MEASURING SPECTROMETER Patent Application
Jeanne A. Welch, inventor (to Navy) 29 Sep. 1989 13 p
(AD-D014331; US-Patent-Appl-SN-415740) Avail: NTIS HC A03/MF A01 CSCL 20/5

An apparatus is disclosed for measuring the spectra of a high optical density sample having substantially known optical properties. In a preferred embodiment, the apparatus comprises: a laser for producing a light beam; a Raman cell responsive to the light beam for generating a first containing a plurality of preselected wavelength components; an optical system for directing the first light through the sample; a dispersion device for spatially

separating the first light passed through the sample into its plurality of preselected wavelength components. GRA

N90-19319# Mound Lab., Miamisburg, OH.
INVESTIGATION OF A SIMULATED TRITIUM PLASMA USING COHERENT ANTI-STOKES RAMAN SPECTROSCOPY (CARS)
Stephen A. Siwecki and Larry R. Dosser 30 Nov. 1989 18 p
(Contract DE-AC04-88DP-43495)
(DE90-005696; MLM-3613) Avail: NTIS HC A03/MF A01

The production of T(sup minus) in a tritium beta plasma occurs when a thermal electron and a tritium molecule undergo a dissociative attachment reaction. A measurement of the T(sup minus) concentration in tritium indicated that it was high, but further analysis showed this result to be inconclusive. It was then suggested that a high T(sup minus) concentration could arise if tritium molecules undergoing dissociative attachment were vibrationally excited. The reaction rate for such a process is orders of magnitude higher when vibrationally excited molecules are involved. Both the thermal electron and the vibrationally excited molecules are a result of the energy supplied by the beta decay of tritium. A search for the presence of vibrationally excited molecules in a simulated tritium plasma was undertaken using Coherent Anti-Stokes Raman Spectroscopy. The results show no presence of vibrationally excited molecules and therefore did not support the foregoing hypothesis. DOE

N90-19320# California Univ., Los Angeles. Dept. of Chemical Engineering.
SYNTHESIS AND PROPERTIES OF A NOVEL CATALYST FOR THE COMBUSTION OF METHANE Annual Report, Jul. 1988 - Jul. 1989
Robert F. Hicks Jul. 1989 74 p
(Contract GRI-5086-260-1247)
(PB90-127499; GRI-89/0209) Avail: NTIS HC A04/MF A01 CSCL 21B

The objective of the research was to develop criteria for the combustion of methane. Methane oxidation over supported platinum and palladium catalysts has been found to be a structure-sensitive reaction. On alumina, platinum and palladium can form either a dispersed phase or a crystalline phase, depending on the amount of metal deposited and the preparation conditions. All of the metal atoms of the dispersed phase are exposed to the gas. Under reaction conditions, the dispersed phase is completely oxidized to the corresponding metal oxide. Conversely, the crystalline phases of platinum and palladium are not oxidized under reaction conditions. Instead, the surface of the crystals are covered with a layer of oxygen. The turnover rates for methane oxidation are higher on palladium than on platinum and are higher on the crystallites than on the dispersed phase. GRA

N90-19321# California Univ., San Diego, La Jolla. Dept. of Chemistry.
SYNTHESIS AND CHEMISTRY OF UNSATURATED METAL NITROGEN COMPOUNDS Final Report, May 1986 - Nov. 1989
William C. Trogler 13 Dec. 1989 10 p
(Grant AF-AFOSR-0027-86; AF Proj. 2303)
(AD-A216550; AFOSR-89-1867TR) Avail: NTIS HC A02/MF A01 CSCL 07/2

The synthesis of the reactive highly unsaturated dianionic reagent, LiN(Ph)N=NN(Ph)Li=1, has provided us with a general synthetic route to main group and early transition metal tetraazabutadiene complexes. The synthetic scheme is outlined in figure 1. For main group elements, such as silicon or Germanium, both linear and cyclic tetrazenes can be prepared. For transition metals, the cyclic tetrazene is generally isolated. In certain instances the intermediate complex formed by addition of 1 to a dihalocomplex precursor fragments to generate metal nitrene intermediates. This reactivity is illustrated by the reaction between 1 and PdCl2(PEt3)2, which produced the first example of a palladium cluster containing imido ligands. When 1 is added to CuCl2(phen) an extremely reactive Cu nitrene species CuNPh(phen) is generated which dimerizes by insertion of the coordinated nitrene fragment into and ortho C-H bond of the phenanthroline ligand. The resulting complex exhibits an extremely short Cu-Cu bond length of 2.600(2) A. Thus, a new reagent was developed, 1, that permits the synthesis of a wide range of unsaturated metal nitrogen complexes. The method of synthesis used for 1 also provides a new method for N-N bond formation, by addition of a deprotonated amine to an organic azide. The latter chemistry is relevant to the synthesis of new energetic materials that contain unsaturated nitrogen linkages and the transition metal complexes generated are of current interest as precursors for new elemental nitrides. GRA

N90-19322# George Washington Univ., Washington, DC. Dept. of Chemistry.
ELECTRON STIMULATED O(-) DESORPTION FROM O2 CONDENSED ON A RARE-GAS FILM: EVIDENCE FOR AN INDIRECT BOUNCE TRAJECTORY Interim Technical Report
H. Sambe and David E. Ramaker Dec. 1989 4 p
(Contract N00014-89-J-1103)
(AD-A216725; TR-54) Avail: NTIS HC A01/MF A01 CSCL 07/4

The electron-stimulated O(-) dissociation of O2 gas is well understood. In the energy range from 4 to 10 eV, O(-) ions are produced by dissociative attachment (DA) via the transient O2(-)(2Pi(u)) state. This same DA process was identified in electron-stimulated desorption (ESD) or O(-) ions from O2. However, electron-energy-dependence curve of the O(-) yield is quite different from that for gaseous O2. The gas phase curve rises slowly at the threshold and has a symmetric bell shape, while the condensed phase curve rises sharply at the threshold and has an asymmetric triangular shape. Furthermore, the threshold energy of the condensed-phase curve depends on the rare gas substrate. In this note, an explanation is offered for the threshold changes and a trajectory is suggested for the O(-) ion desorption via the O2(-)(2 Pi(u)) intermediate state. GRA

N90-19323# Birmingham Univ. (England). School of Physics and Space Research.
ION AND ELECTRON INTERACTIONS AT THERMAL AND SUPRATHERMAL ENERGIES
David Smith, Nigel G. Adams, and Charles R. Hers 30 Sep. 1989 120 p Sponsored in part by Science Research Council
(Grant AF-AFOSR-0355-87; AF Proj. 2303)
(AD-A216905; GL-TR-89-0266; SR-2) Avail: NTIS HC A06/MF A01 CSCL 07/4

The flowing afterglow/Langmuir probe (FALP) apparatus was used to study: (1) dissociative electron attachment reactions of several haloethanes; (2) the neutral products of the dissociative recombination reactions of several ground state polyatomic ions (using the FALP together with LIF and VUV spectroscopic techniques). The selected ion flow tube (SIFT) apparatus was used to study (3) the reactions of ions in the series (PH sub n) + (n=0 to 4) and the reactions of Kr+, Xe+, Kr2(+) and Xe2(+) with several molecular gases. Details of these studies are given in seven appendices. GRA

N90-19324# California Univ., Berkeley. Dept. of Chemical Engineering.
VAPOR-LIQUID EQUILIBRIA FOR COMPLEX MIXTURES WITH SPECIAL EMPHASIS ON THE CRITICAL REGION Final Report, 1 Sep. 1984 - 30 Sep. 1988
G. F. Chou and J. M. Prausnitz Oct. 1988 107 p
(Contract GRI-5083-260-0953)
(PB90-130345; GRI-88/0301) Avail: NTIS HC A06/MF A01 CSCL 07D

This work consists of three parts. The first part presents a thermodynamic framework for performing adiabatic flash calculations using continuous thermodynamics and an equation of state. The equation of state parameters and ideal gas heat capabilities are correlated to molecular weight for five hydrocarbon homologous series. Examples which illustrate are given for both single stage and multistage calculations. The second part reports new measurements of high pressure vapor-liquid equilibria for binary and ternary systems containing CO2, decane and tetralin at 71

and 104 C. The third section presents a phenomenological correction to a classical equation of state to improve representation in the vapor-liquid critical region. The correction uses volume translation to locate the critical point and a nonclassical residual Helmholtz energy to account for density fluctuations near the critical point. Calculated phase equilibria and coexistent densities for pure components and binary mixtures are compared with experimental results. Author

N90-19325# California Univ., Berkeley. Lawrence Berkeley Lab. Materials and Chemical Sciences Div.
EFFECTS OF NONUNIFORM POTENTIAL AND CURRENT DISTRIBUTIONS IN ELECTROCHEMICAL SYSTEMS Ph.D. Thesis
A. C. West Dec. 1989 216 p Prepared in cooperation with California Univ., Berkeley
(Contract DE-AC03-76SF-00098)
(DE90-007349; LBL-28076) Avail: NTIS HC A10/MF A02

The effects that nonuniform current and potential distributions have on electrochemical systems are examined. Chapter 1 provides definitions used by researchers studying these phenomena. In chapter 2, boundary integral techniques are discussed, which are powerful numerical methods used in such studies. In chapters 3 and 4, an asymptotic solution is developed that shows explicitly how the extreme characteristics of a primary current distribution are approached when the ohmic resistance of the cell becomes large compared to the resistance of the faradaic reaction. It is shown how these results can be used to complement and verify more common numerical analyses. Chapters 5 and 6 show how to determine exchange current densities and transfer coefficients when the reaction rate along the electrode is nonuniform. The results can be used to design experiments that provide for a more straightforward interpretation of data. The ohmic resistance and current distribution for a recessed disk electrode are given in chapter 7. Chapter 8 discusses briefly experimental work intended to elucidate whether the dissolution kinetics of ferrous-sulfate films must be included in mathematical descriptions of the complicated dynamic behavior of iron dissolution in sulfuric acid. DOE

N90-19326*# Alabama Univ., Huntsville. Dept. of Mechanical Engineering.
EFFECTS OF TURBULENCE MIXING, VARIABLE PROPERTIES, AND VAPORIZATION ON SPRAY DROPLET COMBUSTION
Y. M. Kim and T. J. Chung [1990] 22 p
(Grant NAG8-095)
(NASA-CR-186463; NAS 1.26:186463) Avail: NTIS HC A03/MF A01 CSCL 07D

Combustion of liquid fuels in the form of spray droplets is simulated numerically. Various vaporization models are examined as to their performance in finite element calculations involving a turbulent flow field. The Eulerian coordinate for the gas and Lagrangian coordinate for the liquid spray droplets are coupled through source terms being updated in the equations of continuity, momentum, and energy. The k-epsilon and modified eddy breakup models are used for simulating turbulent spray combustion flow field. Numerical results for the droplet trajectories, droplet heating, recirculation characteristics, and effects of evaporation models are evaluated. It is also shown that the finite element method is advantageous in dealing with complex geometries, complex boundary conditions, adaptive unstructured grids. Author

N90-19327# Technische Univ., Berlin (Germany, F.R.). Fachbereich Physik.
OPTOGALVANIC LASER SPECTROSCOPIC AND INTERFERENCE SPECTROSCOPIC EXPERIMENTS OF ISOTOPE GAP AND HYPERFINE STRUCTURE FOR SPECTRUM OF EUROPIUM 1 AND ERBIUM 2 Ph.D. Thesis [OPTOGALVANISCH-LASERSPEKTROSKOPISCHE SOWIE INTERFERENZSPEKTROSKOPISCHE UNTERSUCHUNGEN VON ISOTOPIEVERSCHIEBUNG UND HYPERFEINSTRUKTUR AM SPEKTRUM DES EUROPIUM 1 UND ERBIUM 2]
Pedro Seifert 1989 185 p In GERMAN
(ETN-90-95358) Avail: NTIS HC A09/MF A01

Core physics data of average quadratic core charge radius variation between different isotopes or the core quadrupole momenta are investigated. The experiments are made in optic spectral area by measurements of light emission of excited atoms or by measurements of absorption by the selective excitation with appropriate light sources (color lasers). Properties of the change of polarization direction of the exciting light or the variation of the service voltage are examined. With this laser system and the optogalvanic technique the multiplet b 8 D of the Europium 1 configuration 4f75d6s could be observed. The parameters which describe the multiplet dependence on the isotope gap are obtained in the cases of Erbium 2 and Europium 1. The great number of hyperfine components and the weak resolution disturbed the examination of the hyperfine structure of the isotope Er-167. ESA

N90-19328# Stuttgart Univ. (Germany, F.R.). Inst. fuer Thermomdynamik der Luft- und Raumfahrt.
SPATIALLY HIGH-RESOLUTION FLAME DIAGNOSIS BY MEANS OF SPONTANEOUS RAMAN SPECTROSCOPY Ph.D. Thesis [RAEUMLICH HOCHAUFLOESENDE FLAMMENDIAGNOSTIK MIT HILFE DER SPONTANEN RAMANSPEKTROSKOPIE]
Peter Kasal 1988 94 p In GERMAN Sponsored by Deutsche Forschungsanstalt
(ETN-90-95870) Avail: NTIS HC A05/MF A01

Numerous contactless stationary measurements are carried out for laminar turbulent subsonic and supersonic flames in atmospheric pressure. The measurement equipment was improved for examination of the most luminous flames. The excitation source was an argon-ion laser, pulsed by an acousto-optic coupling. The frequency selection from the Raman diffuse radiation was made by means of a narrow band interference filter and the recording of the selected diffuse radiation was made with photomultipliers. These methods multiplied the signal to noise ratio by 150 from the usual Raman measurement equipment, and allowed the study of flames with carbonaceous fuels. For several flames the temperature and particle concentration are obtained. The measured values for a laminar methane/air diffusion flame are compared successfully with those of a theoretic calculation. ESA

N90-19329# Technische Univ., Delft (Netherlands). Faculteit der Luchtvaart- en Ruimtevaarttechniek.
THE USE OF THE GAS FEED SYSTEM AND THE VITIATOR FOR THE SOLID FUEL COMBUSTION CHAMBER [GERBRUIK VAN HET GASTOEVOERSYSTEEM EN DE VITIATOR VOOR DE VASTE BRANDSTOF VERBRANDINGSKANER]
P. A. O. G. Korting Aug. 1987 97 p In DUTCH Prepared in cooperation with Prins Maurits Lab. TNO, Rijswijk, Netherlands
(Contract DLR-15.0120)
(LR-528; SFCC-47; PML-1987-C103; ETN-90-95756) Avail: NTIS HC A05/MF A01

The gas feed system of the solid fuel combustion chamber testing installation is presented. The components of the installation and the important mass flow control are described, with emphasis on the vitiator and the ignition of the combustion chamber. The servicing aspects and the most important gas properties are discussed. ESA

N90-19330# Sandia National Labs., Albuquerque, NM. Solar Thermal Collector Technology Div.
ENHANCEMENT OF PROCESSES FOR SOLAR PHOTOCATALYTIC DETOXIFICATION OF WATER
James E. Pacheco and Craig E. Tyner 1990 5 p Presented at the ASME International Solar Energy Conference, Miami, FL, 1-4 Apr. 1990
(Contract DE-AC04-76DP-00789)
(DE90-003949; SAND-89-1506C; CONF-900449-5) Avail: NTIS HC A01/MF A01

A solar-driven photocatalytic process is being developed to destroy low levels of toxic organics in water. Parabolic troughs

with a glass pipe reactor and heliostats (large tracking mirrors) with a falling-film reactor were used to conduct engineering-scale solar detoxification of water experiments. We have assessed the effect of catalyst (titanium dioxide) loading and hydrogen peroxide concentration on the destruction of a model organic compound, salicylic acid. We found the optimal catalyst loading to be 0.1 percent for the conditions of 30 ppM salicylic acid and 300 ppM hydrogen peroxide. Hydrogen peroxide affected the reaction rates significantly, increasing the reaction rate over 4 times for stoichiometric amounts and more than 19 times for 10 times the stoichiometric amount. Destruction rates appear to be linearly proportional to the ultraviolet light intensity, though more data are needed to fully establish the relation. Initial tests with an actual water pollutant, trichloroethylene, demonstrated destruction from 1.2 ppM to less than 50 ppB in less than 5 minutes of exposure with a trough system. DOE

N90-19331# Argonne National Lab., IL.
ACTIVATION OF METHANE BY TRANSITION METAL-SUBSTITUTED ALUMINOPHOSPHATE MOLECULAR SIEVES
V. A. Maroni, K. A. Willms, Hiephoa Nguyen, and L. E. Iton Dec. 1989 9 p Presented at the 199th National Meeting of the American Chemical Society, Boston, MA, 22-27 Apr. 1990 Submitted for publication
(Contract W-31-109-eng-38)
(DE90-005663; CONF-900402-4) Avail: NTIS HC A02/MF A01

Recent experiments in the laboratory have demonstrated that aluminophosphate molecular sieves substituted with cobalt and cobalt/silicon combinations and having the AlPO(4)-34 or AlPO(4)-5 structure activate methane starting at approx. 350 C. Between 400 and 500 C the rate of methane conversion increases steadily with typical conversion efficiencies at 500 C ranging from 15 to 60 percent. The cobalt and silicon substituted AlPO(4)-34 structure (CoAPSO-34) produces ethylene, ethane, propylene, and propane in varying proportions, depending on reactions conditions. The cobalt-substituted AlPO(4)-5 (CoAPSO-5) produces propylene in very high yield with ethane, ethylene, and propane also seen. Analogous aluminophosphate molecular sieves substituted with magnesium or silicon, but containing no transition metal (e.g., SAPO-34, MAPO-5), do not activate methane under the conditions described above. The activation mechanism is based on reduction of the cobalt(III) form of the molecular sieve to the cobalt(II) form with accompanying oxidative dehydrogenation of the methane. Reoxidation of the cobalt(II) for to the cobalt(III) form can be done either chemically (e.g., using O2) or electrochemically. DOE

N90-19332# Idaho National Engineering Lab., Idaho Falls.
HYDROGEN ASSAY FOIL COUNTING SYSTEM
J. W. Rogers 1989 7 p Presented at the Seminar on the Measurements and Analyses Performed by the Hydrogen Assay Foil Counting System, Columbia, MO, 17 Oct. 1989
(Contract DE-AC07-76ID-01570)
(DE90-007415; EGG-M-89447) Avail: NTIS HC A02/MF A01

The purpose of this seminar is to describe the measurements and analyses performed by the Hydrogen Assay Foil Counting System (HAFCS) in use at the Idaho National Engineering Laboratory. These measurements and analyses are related to the non-destructive assay of the hydrogen content of materials specimens using a notched neutron spectrum technique. The notched spectrum technique employs the way in which hydrogen atoms moderate neutrons in scattering collisions where the neutrons are thermalized or slowed down. A beam of neutrons from a thermal reactor is tailored by filtering the neutrons with cadmium and indium to produce a notched spectrum. This notched spectrum neutron beam is then used to activate a pair neutron detecting indium foils sandwiching a test material specimen containing hydrogen. The neutron moderation by the hydrogen causes differential activation in the foils which can be interpreted as a signal-to-noise (S/N) ratio that varies with the hydrogen content of the specimen. The 54.15 minute (116)In radioactivities of the foils are measured by NaI(Tl) scintillation counting equipment. DOE

N90-19333# Johns Hopkins Univ., Baltimore, MD.
INVESTIGATION OF THE PROCESSES CONTROLLING THE FLAME GENERATION OF REFRACTORY MATERIALS Progress Report, 1 Jul. 1989 - 30 Jun. 1990
Joseph L. Katz Jan. 1990 8 p
(Contract DE-FG02-88ER-45356)
(DE90-007564; DOE/ER-45356/3) Avail: NTIS HC A02/MF A01

The processes involved in the formation of refractory material powders were studied using the counterflow diffusion flame burner. Understanding refractory particle generation processes requires measurement of the concentrations of the reactive species, the temperature, and particle nucleation, growth, and agglomeration, all as a function of their spatial distributions. Optical techniques are valuable for obtaining this information since they are species specific, provide good spatial and temporal resolution, and are essentially non-intrusive. During the past year several significant improvements in our optical measurement techniques have been made. DOE

N90-19334# EG and G Mound Applied Technologies, Miamisburg, OH.
IGNITION OF HMX (CYCLOTETRAMETHYLENETETRANITRAMINE) USING LOW ENERGY LASER DIODES
D. W. Ewick, T. M. Beckman, J. A. Holy, and R. Thorpe 1990 14 p Presented at the 14th Symposium on Explosives and Pyrotechnics, Burlingame, CA, 13-15 Feb. 1990
(Contract DE-AC04-88DP-43495)
(DE90-007637; MLM-3628-OP; CONF-900254-2) Avail: NTIS HC A03/MF A01

The sensitivity of blends of cyclotetramethylenetetranitramine (HMX) with carbon black and graphite to laser diode ignition was investigated. Using a 100-micron optical fiber, a blend of 15,700 sq cm/g HMX with 3 percent carbon black by weight was the most sensitive material tested, with a threshold of 72 mW. Pure, or undoped, HMX could not be ignited using 10 ms laser diode pulses with power levels up to 880 mW. In general, the HMX/carbon black blends were more sensitive than the HMX/graphite blends. HMX specific surface area also had a significant effect on sensitivity. Doubling the spot size increased the ignition threshold by a factor of approx. 2.7. Increasing the pulse width from 10 to 100 ms did not significantly reduce the laser diode power required for ignition. Photoacoustic spectrometer was used to compare the absorption characteristics of the HMX blends. The absorption spectra obtained correlated well with the sensitivity test data. DOE

N90-19335# Texas Univ., Austin. Dept. of Chemistry.
STUDIES OF PHOTOCHEMICALLY AND ELECTROCHEMICALLY DRIVEN ELECTRON TRANSPORT IN ZEOLITES Progress Report, Sep. 1987 - Feb. 1990
Thomas E. Mallouk Feb. 1990 22 p
(Contract DE-FG05-87ER-13789)
(DE90-007659; DOE/ER-13789/3) Avail: NTIS HC A03/MF A01

The basic thrust of our DOE-funded research program involves the use of microporous aluminosilicates (zeolites and clays) as organizing media for molecular electron transport chains. In these studies the aluminosilicates cause self-assembly, by virtue of size exclusion effects, ion exchange equilibria, and specific adsorption, of photosensitizers, electron donors, and electron acceptors at the solid/solution interface. Spectroscopic and electrochemical methods are used to study the kinetics of photochemically and electrochemically driven vectorial electron transfer reactions in these assemblies. DOE

N90-19336# Sandia National Labs., Albuquerque, NM. Fuel Science Div.
HYDROUS METAL OXIDE-SUPPORTED CATALYSTS. PART 2: CATALYTIC PROPERTIES AND APPLICATIONS
R. G. Dosch, H. P. Stephens, and F. V. Stohl Feb. 1990 149 p
(Contract DE-AC04-76DP-00789)
(DE90-008098; SAND-89-2400-Pt-2) Avail: NTIS HC A07/MF A01

Research leading to the development of new catalytic materials based on hydrous metal oxide (HMO) ion exchangers is presented. Present in this part are results of catalyst-related research and application of the materials to catalytic reactions for direct coal liquefaction processes. HMO materials are inorganic ion exchangers, derived from the alkoxides of Ti, Zr, Nb, or Ta, that exhibit a number of properties applicable to the preparation of catalysts. Research on the catalytic properties of HMO's has focused on the hydrous titanium oxide (HTO) system. However, exploratory coal liquefaction experiments with hydrous niobium oxides (HNO's) and hydrous zirconium oxides (HZO's) have demonstrated that these HMO's also exhibit potential as coal liquefaction catalysts. Studies performed during the course of this research include: (1) preliminary coal liquefaction and hydrotreating tests, (2) test of hydrogenation, hydrodesulfurization, hydrodeoxygenation and hydrodenitrogenation activity using model compounds, (3) development of catalyst pretreatment and activation procedures, (4) modification of HTO supports with silicon, (5) preparation and testing of thin film HTO catalysts, (6) synthesis, characterization and evaluation of base and noble metal catalyst deactivation tests, and (7) exploratory tests of applications other than direct liquefaction. The versatility of the HTO system for synthesis of catalysts allows great potential for further improvements in activity and selectivity as well as tailoring of catalysts for specific processes. Research is continuing in these areas. DOE

N90-19337# Brookhaven National Lab., Upton, NY.
IEA (INTERNATIONAL ENERGY AGENCY) IMPLEMENTING AGREEMENT FOR A PROGRAM OF RESEARCH AND DEVELOPMENT ON THE PRODUCTION OF HYDROGEN FROM WATER. TASK 9: HYDROGEN PRODUCTION
Alessio Mezzina, ed. and Bernd Dieter Struck (Kernforschungsanlage, Juelich, Germany, F.R.) Jan. 1989 109 p
(Contract DE-AC02-76CH-00016)
(DE90-007354; BNL-43428; TR-1988; HUF-2) Avail: NTIS HC A06/MF A01

Research programs on hydrogen production from USA, Canada, Japan, and the Federal Republic of Germany, are described. The programs are in the areas of electrolyte hydrogen production, thermochemical hydrogen production, and photocatalytic hydrogen production. Author

N90-19338# Naval Research Lab., Washington, DC.
ELASTIC SOLUTIONS IN A SEMI-INFINITE SOLID WITH AN ELLIPSOIDAL INCLUSION Final Report, Jan. - Oct. 1989
H. Y. Yu (Geo-Centers, Inc., Fort Washington, MD.) and S. C. Sanday 25 Jan. 1990 18 p
(AD-A217063; NRL-MR-6583) Avail: NTIS HC A03/MF A01 CSCL 07/4

The elastic field caused by an ellipsoidal inclusion in a semi-infinite solid is investigated. The solutions for the inclusion with misfit stress-free strain components (e sup T) sub ij with (e sup T) sub 11 = (e sup T) sub 22 and (e sup T) sub 12 = 0 are solved by the application of the Hankel transformation method for the solution of axisymmetric problems together with Mindlin's solution for the nuclei of strain in the semi-infinite solid and Eshelby's solution for ellipsoidal inclusions. The resultant stresses have the property that the traction vanishes across the plane boundary of the solid. GRA

N90-19339# Brown Univ., Providence, RI. Dept. of Chemistry.
PREPARATION AND CHARACTERIZATION OF ALUMINA FILMS PREPARED BY A NOVEL SPRAY PYROLYSIS METHOD
W. J. DeSisto, Y.-T. Qian, C. Hannigan, J. O. Edwards, R. Kershaw, K. Dwight, and A. Wold 15 Jan. 1990 9 p
(Contract N00014-89-J-1849)
(AD-A217570; TR-3) Avail: NTIS HC A02/MF A01 CSCL 07/2

Alumina thin films of 2000 A were deposited on n-type silicon wafers by a novel spray pyrolysis method. The spray solution contained an aluminum acetylacetonato complex which was characterized by NMR techniques. The deposited films of Al2O3 were homogeneous, uniform, dense and had breakdown potentials of greater than 10 V. Aluminum oxide is an attractive candidate for thin insulating layers in electronic devices because of its high dielectric constant, low sensitivity to Na+ diffusion and high radiation resistance. These films would be useful for numerous applications including surface protection and selective masking during diffusion in device isolation masking against impurities, junction passivation, and insulation between metal layers. GRA

N90-19340*# North Carolina State Univ., Raleigh. Dept. of Chemical Engineering.
CHARACTERIZATION OF REACTION KINETICS IN A POROUS ELECTRODE Final Report
Peter S. Fedkiw 23 Apr. 1990 128 p
(Grant NAG3-649)
(NASA-CR-186504; NAS 1.26:186504) Avail: NTIS HC A07/MF A01 CSCL 07D

A continuum-model approach, analogous to porous electrode theory, was applied to a thin-layer cell of rectangular and cylindrical geometry. A reversible redox couple is assumed, and the local reaction current density is related to the potential through the formula of Hubbard and Anson for a uniformily accessible thin-layer cell. The placement of the reference electrode is also accounted for in the analysis. Primary emphasis is placed on the effect of the solution-phase ohmic potential drop on the voltammogram characteristics. Correlation equations for the peak-potential displacement from E(sup 0 prime) and the peak current are presented in terms of two dimensionless parameters. Author

26 METALLIC MATERIALS

Includes physical, chemical, and mechanical properties of metals, e.g., corrosion; and metallurgy.

N90-19341# Argonne National Lab., IL. Materials Science Div.
IRRADIATION-INDUCED AMORPHIZATION AND ELASTIC SHEAR INSTABILITY IN INTERMETALLIC COMPOUNDS
J. Koike, P. R. Okamoto, L. E. Rehn, R. Bhadra, M. H. Grimsditch, and M. Meshii (Northwestern Univ., Evanston, IL.) 1989 6 p Presented at the Materials Research Society Fall Meeting, Boston., MA, 27 Nov. - 2 Dec. 1989
(Contracts W-7405-eng-36; W-31-109-eng-38)
(DE90-004845; LA-UR-89-4160; CONF-891119-47) Avail: NTIS HC A02/MF A01

Previously we reported a substantial (approximately 50 pct) decrease in shear modulus prior to amorphization in Kr irradiated Zr3 Al, and proposed that amorphization is triggered when the crystalline lattice becomes unstable against shear stress. In the present work, the relation between amorphization and shear elastic instability has been investigated in two additional compounds (FeTi and NiAl) during room temperature irradiation with 1.7 MeV Kr(+). A shear modulus was measured using Brillouin scattering; structural information was obtained in situ in a high voltage electron microscope interfaced to a tandem accelerator. During irradiation of FeTi, chemical disordering and a large (approximately 40 pct) decrease of shear modulus were observed, and an amorphous phase developed subsequently. In contrast, NiAl remained crystalline and chemically ordered during irradiation, and exhibited only an approximately 10 pct decrease in shear modulus. Hence, these two results provide further support that a shear instability

triggers irradiation-induced amorphization. The shear instability mechanism may also apply to other solid-state amorphization techniques, e.g., hydrogen charging and mechanical deformation. DOE

N90-19342# Brookhaven National Lab., Upton, NY. Div. of Materials Science.
NANOLAYER REACTIONS IN ALUMINUM-METAL INTERFACES
Enrique V. Barrera, M. W. Ruckman, and S. M. Heald 1989 6 p Presented at the Materials Research Society Fall Meeting, Boston, MA, 27 Nov. - 2 Dec. 1989
(Contracts DE-AC02-76CH-00016; DE-AS05-80ER-10742)
(DE90-004955; BNL-43235; CONF-891119-58) Avail: NTIS HC A02/MF A01

Surface extended x ray absorption fine structure (SEXAFS) measurements on the nanometer level were made for aluminum/metal (Al/M) interfaces where M was Cu or Ni. The samples were studied immediately after deposition and after heat treatments. Significant differences in interface reactions were observed depending on deposition direction (Cu on Al or Al on Cu) and the amount of mixing was also related to whether M was Cu or Ni. The SEXAFS measurements revealed that there were no detectable amounts of C or O present. One percent Zn was observed to be in the Al layers. The results obtained from the as-deposited interfaces correlate well with data obtained from buried interfaces of like element combinations. DOE

N90-19343# American Society of Mechanical Engineers, Naperville, IL. Gear Research Inst.
AUSTEMPERED DUCTILE IRON DATA BASE: A COOPERATIVE PROGRAM BETWEEN INDUSTRY AND THE TRADE ADJUSTMENT ASSISTANCE PROGRAM OF THE DEPARTMENT OF COMMERCE Final Report, 1984 - 1989
Dale H. Breen and Douglas V. Doane Jun. 1989 139 p
(Grant ITA-99-26-07220-30)
(PB90-115569; ITA-90-26-001) Avail: NTIS HC A07/MF A01 CSCL 11F

The activities and findings resulting from a cooperatively funded program to enhance the technical base of Austempered Ductile Iron (ADI) are outlined. The program was started in Jan. 1984 and addressed many direct and indirect technical areas associated with ADI. Author

N90-19344# Japan Atomic Energy Research Inst., Tokyo. Dept. of Physics.
EFFECT OF ELECTRON-EXCITATION ON RADIATION DAMAGE IN ION-IRRADIATED FCC METALS
Akihiro Iwase Jun. 1989 90 p In JAPANESE; ENGLISH summary
(DE90-719537; JAERI-M-89-071) Avail: NTIS (US Sales Only) HC A05/MF A01

FCC metals (Al, Cu, Ag, Ni) were irradiated with 0.5 to 1.8 MeV H, He, N and Ar ions, and 84 to 126 MeV C, F, Si, Cl, Br and I ions at liquid helium temperatures. After the irradiations, thermal annealing experiments were performed up to 300 K. Anomalous reduction of Stage-I recovery was observed in Al and Ni irradiated with high-energy heavy ions. Radiation annealing by 100 MeV I ions was studied in predoped Ni and Cu. The experimental results were analyzed by using a new model which describes the production and radiation annealing of two or more types of defects. The extraordinarily large cross sections for subthreshold recombination of Stage-I defects were obtained in Ni. These results show that in Al and Ni, the energies transferred from the excited electrons to lattice through the electron-lattice interaction contribute to the annihilations of defects during irradiation. DOE

N90-19345# Trento Univ. (Italy).
INTERNATIONAL CONFERENCE ON SURFACE MODIFICATION OF METALS BY ION BEAMS
16 Sep. 1988 161 p Conference held in Riva del Garda, Italy, 12-16 Sep. 1988
(Contract DAJA45-88-M-0134)
(AD-A215872; R/D-6003-EE-02) Avail: NTIS HC A08/MF A01

The proceedings from this conference are presented. The conference has oral and poster presentations. Some session titles were: Fundamentals of surface modification by ion beams; Ion induced surface phases; Modification of mechanical properties; Mechanisms and applications of ion beam assisted deposition; Modification of chemical, electrochemical, and oxidation properties; Thin film metallurgy for microelectronic application; and Industrial applications of ion beam techniques. E.R.

N90-19346# Naval Postgraduate School, Monterey, CA.
OPTIMIZING SUPERPLASTIC RESPONSE IN NAVALITE, A LITHIUM CONTAINING ALUMINUM-MAGNESIUM ALLOY M.S. Thesis
Alden P. Chester, III Jun. 1989 72 p
(AD-A216552) Avail: NTIS HC A04/MF A01 CSCL 11/6

Superplastic ductilities up to 428 percent have been attained during research into thermomechanical processing of Al(2.70) Mg(2.04) Li(0.50) Cu(0.13) Zr (composites in wt. pct.; alloy composition corresponding to NAVALITE). Variation in dislocation density induced by means of warm rolling at a series of temperatures below the discontinuous recrystallization temperature were expected to significantly affect the superplastic response by further grain size refinement. Experimental results indicate no beneficial enhancement in ductilities associated with rolling below 250 C. Consistent elongations in the 400 percent range during this initial evaluation of the NAVALITE alloy indicates further investigation of superplastic response is warranted. GRA

N90-19347# Army Materials Technology Lab., Watertown, MA. Materials Productibility Branch.
A NEW MODEL FOR HYDROGEN ABSORPTION IN WELDS Final Report
Steven A. Gedeon and Thomas W. Egar (Massachusetts Inst. of Tech., Cambridge.) May 1989 23 p
(DA Proj. 1L1-62105-AH-84)
(AD-A216951; MTL-TR-89-46) Avail: NTIS HC A02/MF A01 CSCL 07/4

A systematic review of previous research has shown that the use of Sievert's law to calculate the hydrogen absorption reaction temperature in the weld pool is invalid. A new model of hydrogen absorption is proposed which can explain both previously measured data and the data obtained in this study. The hydrogen content measured in a diffusible hydrogen test will be governed by three distinctly different phenomena: (1) hydrogen absorption into the molten pool, (2) hydrogen trapping or rejection from the solidification front, and (3) hydrogen diffusion away from the solidified weld. These are separate occurrences which must be separately modelled in order to obtain a complete understanding of the hydrogen remaining in the weld. This study has separated out these effects in order to determine the amount of hydrogen initially absorbed. Once this value is known, a new model can be developed in order to gain a greater understanding of the basic gas metal reaction occurring in the weld pool, and how it is affected by the welding arc. GRA

N90-19348# Lawrence Livermore National Lab., CA.
HIGH-PURITY BERYLLIUM FOILS
J. E. Hanafee, R. G. Musket, and M. S. Stratman 22 Dec. 1989 21 p
(Contract W-7405-eng-48)
(DE90-006408; UCID-21847) Avail: NTIS HC A03/MF A01

Thin, high-purity beryllium sheet was obtained and made into foils with thicknesses ranging from 8 to 25 microns. The characterization of the foil included transmission electron microscopy (TEM) for the microstructure and a novel x ray fluorescence method for quantitatively determining the amount of oxygen on and in the foils. The foil preparation techniques and results of the characterizations are described. DOE

N90-19349# International Centre for Theoretical Physics, Trieste (Italy).
EXCHANGE AND CORRELATION EFFECTS IN THE VISSCHER-FALICOV MODEL FOR METAL INTERCALATED GRAPHITE
H. M. Miesenboeck and M. P. Tosi Sep. 1989 27 p Submitted for publication
(DE90-610553; IC-89/241) Avail: NTIS (US Sales Only) HC A03/MF A01

A simple model for metal intercalated graphite as a layered electron gas treated in the random phase approximation, which was proposed in early work of Visscher and Falicov, is extended to include exchange and short-range intraplane correlations between the electrons. Main attention is focussed on the static screening function of the model system, in relation to effective pair potentials in metal intercalants. The local field factor accounting for exchange and correlation is related to the intraplane electron structure factor and the latter is evaluated in a simple pseudoclassical approach, which is tested against known results for a quantal 2D electron gas. Screening of an external point charge is shown to be appreciably modified by exchange and correlation in the case when it lies in an electron plane, leading to a deeper main attractive well between two external charges lying in the same electron plane. On the other hand, exchange and correlation have only minor effects when the charges lie at mid distance between two electron planes, at least if reasonable physical requirements are made on acceptable values for the electron screening length in the relevant range of model parameters. DOE

N90-19350# Japan Atomic Energy Research Inst., Tokai. Dept. of Fuels and Material Research.
AN ATTEMPT OF IMPROVING HIGH-TEMPERATURE FATIGUE PROPERTIES OF Ni-Cr-W SUPERALLOYS IN HTGR HELIUM
Hirokazu Tsuji and Hajime Nakajima Aug. 1989 19 p In JAPANESE; ENGLISH summary
(DE90-741482; JAERI-M-89-108) Avail: NTIS (US Sales Only) HC A03/MF A01

A series of strain controlled low cycle fatigue tests were conducted in simulated HTGR helium on two heats of Ni-Cr-W superalloy, i.e., SSS-113M and its modified version containing Mn and Si. Materials were tested in the conventional single solid solution treated condition as well as in the double heat treated one, which aimed alpha(sub 2)-W phase to precipitate along the grain boundaries. In those tests a possibility of improving the high temperature fatigue resistance of Ni-Cr-W superalloys in simulated HTGR helium was studied. The obtained results are as follows: The double heat treatment was effective in improving the intergranular fracture resistance in some degree. But the degree of the beneficial effect was inadquate for the modified version containing Mn and Si; and the addition of Mn and Si showed no advantage in the high temperature fatigue strength in HTGR helium. Based on the above mentioned results it was concluded that another type of alloy modification than the addition of Mn and Si is required in order to improve corrosion and fatigue resistance of Ni-Cr-W superalloys in HTGR helium simultaneously. DOE

N90-19351# Technische Univ., Munich (Germany, F.R.). Fakultaet fuer Maschinenwesen.
OSCILLATION AND DAMPING BEHAVIOR OF FINE STEEL TEST TUBES, WITH PARTICULAR CONSIDERATION TO DESTRUCTION FREE PROOFS FROM HYDROGEN FRAGILIZATION Ph.D. Thesis [SCHWINGUNGS- UND DAEMPFUNGSVERHALTEN VON PROBEN AUS VERGUETUNGSSTAEHLEN UNTER BESONDERER BERUECKSICHTIGUNG DES ZERSTOERUNGSFREIEN NACHWEISES VON VERSPROEDENDEM WASSERSTOFF]
Alfred Bauberger 1987 117 p In GERMAN
(ETN-90-95371) Avail: NTIS HC A06/MF A01

By means of the oscillation analysis, hydrogen absorption of a steel material is studied to avoid material damages. For the experiments the steels 50 CrV4 and 34 CrMo4 are used. The hydrogen loading produces selenium acid by cathodic polarization in an electrolyte (1nH2SO4) with a catalyst. Several hydrogen concentrations are produced by variation of loading time and current density. A good correlation appears between hydrogen concentration and hydrogen fragilization, that is no longer reversible after a loading time longer than 5 mn, because of the formation of cracks during the loading. The damages are less important with 34 CrMo4 than 50 CrV4. Experiments with forced oscillations give reproducible results which do not depend on temperature variations in the area 0 to 50 C. The application of an external voltage causes a resonance peak drop in the oscillation spectrum, but charges in the elastic area do not produce irreversible changes of the oscillation spectrum. ESA

N90-19352# Oak Ridge National Lab., TN.
EVALUATION OF RADIATION-INDUCED SENSITIZATION USING ELECTROCHEMICAL POTENTIOKINETIC REACTIVATION TECHNIQUE FOR AUSTENITIC STAINLESS STEELS
T. Inazumi, G. E. C. Bell, and A. Hishinuma (Japan Atomic Energy Research Inst., Tokai.) 1990 11 p Presented at the Corrosion '90, Las Vegas, NV, 23-27 Apr. 1990
(Contract DE-AC05-84OR-21400)
(DE90-002708; CONF-900403-1) Avail: NTIS HC A03/MF A01

The electrochemical potentiokinetic reactivation (EPR) test technique was applied to the determination of sensitization in a neutron-irradiated (420 C, 10 dpa) titanium-modified austenitic stainless steel. Miniaturized specimens (3 mm diam by 0.25 mm thick) in solution-annealed and 25 pct cold-worked conditions were tested. The degree of sensitization (DOS) was calculated in terms of the reactivation charge (Pa). Results indicated the occurrence of radiation-induced sensitization when compared to control specimens thermally aged at the irradiation temperature. Post-EPR examination of the specimen surfaces showed etching across the face of each grain as well as at grain boundaries. This indicates that the Pa value normalized by the total grain boundary area, which is an accepted EPR-DOS criterion, cannot be directly used as an indicator of the DOS to determine the susceptibility of this irradiated material to intergranular stress corrosion cracking (IGSCC). Further investigations are necessary to correlate the results in this study to the IGSCC susceptibility of the irradiated stainless steel. DOE

N90-19353# Brookhaven National Lab., Upton, NY.
GLANCING ANGLE XAFS (X RAY ABSORPTION FINE STRUCTURE) AND X RAY REFLECTIVITY STUDIES OF TRANSITION-METAL/ALUMINUM INTERFACES
Steve M. Heald, Enrique V. Barrera, and Huaiyu Chen 1990 20 p Presented at the Structure of Surfaces and Interfaces As Studied By Synchrotron Radiation: Foraday Disc. 89, Manchester, NH, 4-6 Apr. 1990
(Contracts DE-AC02-76CH-00016; DE-AS05-80ER-10742)
(DE90-005575; BNL-43662; CONF-900497-1) Avail: NTIS HC A03/MF A01

The combination of glancing angle x ray absorption fine structure (XAFS) and x ray reflectivity measurements provide detailed structural information about interfaces. Results from transition metal/Al interfaces are used to illustrate the capabilities of the techniques. Reflectivity measurements are used to determine the thickness and density profile of the films, along with the amount of interfacial or surface roughness. The XAFS measurements provide information about the local bonding at the interface, and are well suited for studying the interfacial chemistry. Of interest is the role of impurities such as oxygen in modifying interface structure and thermal stability. For Cu/Al, Ni/Al, and Cr/Al a small amount of interfacial oxygen is found to strongly affect both the initial interface structure, and the response of the interface to thermal annealing. For Ni/Al it is also found that interfacial oxygen affects primarily the interface reaction, while oxygen within the Al layer suppresses the grain boundary reaction channel. DOE

N90-19354# Argonne National Lab., IL. Materials and Components Technology Div.

MITIGATION OF STRESS CORROSION CRACKING OF AISI 304 STAINLESS STEEL IN OXYGENATED WATER AT 289 C BY ORGANIC SPECIES AT LOW CONCENTRATION

F. Kassner, W. E. Ruther, and W. K. Soppet Oct. 1989 28 p Presented at the Corrosion '90, Las Vegas, NV, 23-27 Apr. 1990
(Contract W-31-109-eng-38)
(DE90-005631; CONF-900403-7) Avail: NTIS HC A03/MF A01

In constant-extension-rate tests on sensitized AISI 304 stainless steel (SS) at 289 C, some organic substances (oxygen scavengers) in feedwater containing approx. 0.2 ppm dissolved oxygen decrease effluent oxygen concentration, electrochemical potential (ECP) of the steel, and stress corrosion cracking (SCC) susceptibility to very low levels. Other organic substances neither decrease oxygen concentration nor ECP of the steel significantly, but also mitigate SCC susceptibility relative to that in high purity oxygenated water. The latter species apparently block active sites where cathodic reduction of oxygen occurs and thereby limit anodic dissolution of metal at the crack tip in a slip-dissolution mechanism of crack advance. In SCC tests on fracture-mechanics-type specimens under high load ratio, low frequency cyclic loading conditions at 289 C, the organic inhibitors at a concentration of approx. 1.0 ppm stop crack growth in the sensitized steel, but are not effective in oxygenated water containing ionic impurities such as sulfate or chloride at the 0.1-ppm level. These results are consistent with the site blockage mechanism for different species that undergo cathodic reduction and control the rate of crack growth of the steel in the SCC tests. DOE

N90-19355# Los Alamos National Lab., NM.

CREEP BEHAVIOR OF ALLOYS BASED ON TiAl CONTAINING TiB2 AND TiN PARTICULATES

Patrick L. Martin, David H. Carter, Robert M. Aikin, Sr., Robert M. Aikin, Jr., and Leo Christodoulou (Martin Marietta Corp., Baltimore, MD.) 1990 12 p Presented at the 4th International Conference on Creep and Fracture of Engineering Materials and Structures, Swansea (England), 1-6 Apr. 1990
(Contract W-7405-eng-36)
(DE90-006489; LA-UR-90-24; CONF-900425-3) Avail: NTIS HC A03/MF A01

Ordered alloys based on the L1 sub 0 crystal structure compound TiAl were tested in constant stress creep. The alloys ranged from 45 to 47 at. percent Al with and without V substitutions. The ingot processing, utilizing the XD(trademark) technique, incorporated 1 to 5 micron diameter particles of boride or nitride compounds. Emphasis was placed on characterizing the initial stages of creep using digital data acquisition and analysis in the range 70 to 280 MPa stress and 760 to 850 C temperature. When TiN converting to Ti2 AlN in processing and TiB2 are both added to the matrix, the creep properties are significantly improved. Fine particles were observed to decorate dislocations and to have nucleated homogeneously within the TiAl grains. DOE

N90-19356# Los Alamos National Lab., NM. Materials Science and Technology Div.

DEFORMATION AND FRACTURE OF TiAl + W AT ELEVATED TEMPERATURES

Patrick L. Martin and Harry A. Lipsitt (Wright State Univ., Dayton, OH.) 1990 10 p Presented at the 4th International Conference on Creep and Fracture of Engineering Materials and Structures, Swansea (England), 1-6 Apr. 1990
(Contract W-7405-eng-36)
(DE90-006490; LA-UR-90-25; CONF-900425-1) Avail: NTIS HC A02/MF A01

The ternary alloy, Ti - 49 at. percent Al -2 at. percent W, was produced using Rotating Electrode Powder (REP) compacted by hot extrusion. The tensile properties of this alloy (strength, ductility and fracture mode) were studied from room temperature to 900 C. Constant load creep properties were measured from 700 to 900 C and analyzed using conventional power law equations to calculate the stress exponent and activation energy. These parameters were approximately 4 and 400 KJ/mole respectively. TEM examination showed that the W was held in solid solution during the tensile and creep deformation when the material was tested in the as-extruded condition. These results are interpreted as evidence for solid solution strengthening of the TiAl matrix by the W solute. DOE

N90-19357# Lawrence Livermore National Lab., CA.

TIME-DEPENDENT FAILURE OF SILVER-INTERLAYER DIFFUSION BONDS BETWEEN NON-DEFORMING BASE-METALS

M. E. Kassner, R. S. Rosen, G. A. Henshall, and K. D. Challenger (Cincinnati Univ., OH.) 22 Nov. 1989 10 p Presented at the 4th International Conference on Creep and Fracture of Engineering Materials and Structures, Swansea, England, 1-6 Apr. 1990
(Contract W-7405-eng-48)
(DE90-006925; UCRL-102284; CONF-900425-4) Avail: NTIS HC A03/MF A01

Silver interlayer diffusion bonds, fabricated at low temperatures using planar-magnetron sputtering, exhibit very high tensile strengths. Earlier work has shown that these joints undergo delayed failure at relatively low tensile stresses at ambient temperature for the case in which plasticity occurs in the base materials. Failure apparently occurs by a microvoid coalescence mechanism at the bond interfaces. Delayed tensile failures were investigated for the case in which the applied stress does not produce any plastic deformation in the base metal. Failure occurs and appears to be controlled by time dependent plasticity within the silver interlayer, which is governed by the effective stress in the interlayer. The plasticity causes cavity nucleation and, eventually, interlinkage and failure. These findings are believed to be generally applicable to any thin interlayer bond, including those prepared by processes different than physical vapor deposition. DOE

N90-19358# Los Alamos National Lab., NM. Materials Science and Technology Div.

MODIFICATION OF SURFACE MECHANICAL PROPERTIES OF HIGH-CHROMIUM TOOL STEEL BY CARBON-IMPLANTED CODEPOSITED Fe-Ti FILMS

J.-P. Hirvonen, M. Nastasi, T. R. Jervis, and T. Zocco 1990 23 p Presented at the 8th International Triennial Conference on Thin Films and the 17th International Conference on Metallurgical Coatings, San Diego, CA, 1-6 Apr. 1990
(Contract W-7405-eng-36)
(DE90-007502; LA-UR-90-654; CONF-900419-1) Avail: NTIS HC A03/MF A01

An iron-titanium film 300 nm thick was deposited on a tool steel (1.55 percent C, 0.3 percent Si, 0.3 percent Mn, 12 percent Cr, 0.8 percent Mo, and 0.8 percent V) by coevaporation of Fe and Ti. Subsequently this surface film was implanted with carbon at energies of 55, 120, and 200 keV to a total fluence of 1.24 x 10(exp 18) C(+)/sq cm. This treatment produced a surface hardness of 15 GPa. The effect of this coating on unlubricated wear and friction was tested in air at a relative humidity of 10 percent in a pin-on-disc tester using a 440 C pin as a counterface. The sliding mechanism of the untreated substrate was found to be based on the transfer of pin material and subsequent growth of uneven oxide hillocks on the wear track. Oxide scales were observed also on a wear scar of the pin, presumably as a result of back-deposition. In contrast, the sliding mechanism on the coated sample was drastically different. A more uniform transfer film originating in the coating was found on the pin, resulting in sliding between identical materials. No wearthrough of the coating occurred during the test of 5000 cycles at a Hertzian pressure of 835 MPa, and the surface of the wear track showed extreme smoothness to the very end of the test. The friction coefficient was decreased from 0.7 for the uncoated to 0.2 for the coated surface. The wear track on the coated surface was also found to be slightly oxidized, as determined by a nuclear reaction. The reduction of friction was mainly attributed to the increased hardness of the counterfaces and an adequate but controlled oxidation. DOE

N90-19359# Los Alamos National Lab., NM.
DEFECT STRUCTURES IN COPPER AND GOLD IRRADIATED WITH FAST NEUTRONS, 14 MeV NEUTRONS AND 600 TO 800 MeV PROTONS
A. Horsewell, B. N. Singh, S. Proennecke, W. F. Sommer, and H. L. Heinisch (Pacific Northwest Lab., Richland, WA.) 1989 8 p Presented at the 4th International Conference on Fusion Reactor Materials, Kyoto, Japan, 4-8 Dec. 1989
(Contract W-7405-eng-36)
(DE90-007529; LA-UR-90-452; CONF-891204-20) Avail: NTIS HC A02/MF A01

Copper and Gold were irradiated with fast neutrons (mixed spectrum thermal reactor), 14 MeV neutrons (RTNS-II) and 600 to 800 MeV protons (PIREX II and LAMPF) at 300 to 373 K over a dose range of 10(exp 21) to 10(exp 24) particles x m(exp -2). Defect cluster concentrations and sizes were obtained by transmission electron microscopy. The variation in cascade damage structures resulting from a change in average recoil energy from 10(exp 4) to 10(exp 6) eV is shown. DOE

N90-19398*# Southern Univ., Baton Rouge, LA. Dept. of Mechanical Engineering.
LIQUID OXYGEN LOX COMPATIBILITY EVALUATIONS OF ALUMINUM LITHIUM (Al-Li) ALLOYS: INVESTIGATION OF THE ALCOA 2090 AND MMC WELDALITE 049 ALLOYS
Ravinder M. Diwan *In* Alabama Univ., Research Reports: 1989 NASA/ASEE Summer Faculty Fellowship Program Dec. 1989 31 p (For primary document see N90-19390 12-31)
(Grant NGT-01-008-021)
Avail: NTIS HC A99/MF E06 CSCL 11F

27 NONMETALLIC MATERIALS

Includes physical, chemical, and mechanical properties of plastics, elastomers, lubricants, polymers, textiles, adhesives, and ceramic materials.

For composite materials see *24 Composite Materials.*

N90-19360 Department of the Navy, Washington, DC.
CONDUCTIVE POLYMERS OF TRANSITION-METAL COMPLEXES COORDINATED BY A DIAMINO-DICHALCOGEN-BENZENE COMPOUND Patent
Oh-Kil Kim, inventor (to Navy) 29 Aug. 1989 9 p Filed 28 Mar. 1988 Supersedes AD-D013814
(AD-D014326; US-Patent-4,861,859; US-Patent-Appl-SN-174261; US-Patent-Class-528-210) Avail: US Patent and Trademark Office CSCL 07/6

Polymeric metal complexes were prepared by coordination reactions of 2,5-diamino 1,4-benzenedithiol (DADT) with divalent metal halides (cobalt chloride, iron chloride, copper chloride, and nickel chloride) in an aqueous alkaline solution at reflux temperatures. A black precipitate which conducted electricity was formed. Resistivity of the material increased upon exposure to air but decreased when oxygen was removed from the material. GRA

N90-19361# Lawrence Livermore National Lab., CA.
ELIMINATION OF PLATINUM INCLUSIONS IN PHOSPHATE LASER GLASSES
J. H. Campbell, E. P. Wallerstein, J. S. Hayden, D. L. Sapak, D. E. Warrington, A. J. Marker, Jr., H. Toratani, H. Meissner, S. Nakajima, and T. Izumitani (Hoya Optics USA, Inc., Fremont, CA.) 26 May 1989 62 p
(Contract W-7405-eng-48)
(DE90-004479; UCRL-53932) Avail: NTIS HC A04/MF A01

Results from small-scale glass melting experiments aimed at reducing the density of platinum particles in phosphate laser glasses are discussed. The platinum particles originate from the crucibles used to melt the laser glass and can cause optical damage in glasses used in high peak power lasers; this problem was particularly acute in the LLNL 120 kJ, 100 TW Nova laser. The melting experiments examine the effects of: (1) N2, O2, and Cl2 gas atmospheres; (2) temperature and temperature gradients; (3) processing time; and (4) platinum alloys on the formation and dissolution of platinum inclusions in LHG-8 and LG-750 phosphate laser glasses. Results show that most platinum inclusions originate early in the melt cycle, with thermal gradients within the melter being one of the major causes. By using oxidizing gas conditions (O2, Cl2, or O2 + Cl2), the platinum inclusions can be dissolved into the glass during the course of the melt cycle. The dissolution rate of platinum under oxidizing conditions has been measured, and a model is used to quantify the description of the dissolution process. The effect of ionic platinum on the transmission spectra of the laser glasses produced under various oxidizing conditions was also measured. Results from the above laboratory-scale melting experiments were incorporated into proprietary laser-glass melting processes. The laser glasses prepared under these conditions have an average of less than 0.1 platinum inclusions/liter, which represents a 1000-fold reduction over the previously available phosphate laser glasses. DOE

N90-19362# Instituto de Pesquisas Energeticas e Nucleares, Sao Paulo (Brazil).
PROCESSING OF ADVANCED CERAMICS USING MICROWAVES THERMAL TREATMENTS [PROCESSAMENTO DE CERAMICAS AVANCADAS UTILZANDO TRATAMENTOS TERMICOS POR MICROONDAS]
Clauer deFreitas Trench 1989 1 p In PORTUGESE
(DE90-606349; INIS-BR-1640) Avail: NTIS (US Sales Only) HC A01/MF A01

A one page summary of the processing of advanced ceramics using microwave thermal treatments is given. DOE

N90-19363# Central Research Inst. of Electric Power Industry, Tokyo (Japan).
DEVELOPMENT OF CERAMIC COMBUSTOR FOR LOW BTU GASES. DESIGN AND BASIC COMBUSTION CHARACTERISTICS
Toru Hisamatsu, Toshio Abe, Noriyuki Mori, and Toshiaki Hasegawa Jun. 1988 31 p In JAPANESE; ENGLISH summary
(DE89-782287; CRIE-W-87047) Avail: NTIS (US Sales Only) HC A03/MF A01

Because of characteristics of gasified coal fuels which have lower calorific value and contain ammonia, it is an important subject to develop a high temperature combustor, which is able to burn constantly gasified coal with low NOx, for a high temperature gas turbine of the integrated coal gasification combined cycle power plant. The ceramic combustor that has a root flame from a subcombustor was studied to improve the stability of low BTU gas combustion at the first stage of development of a ceramic combustor using low BTU gas. The features of this combustor were as follows: a subcombustor which aid to burn primarily by high BTU gas was applied for improvement of the combustion stability; low BTU gases were injected at two sections to axis of the combustor for improvement of combustion at partial loads. The combustor was designed on the basis of experimental results of the water flow model test which was performed in order to grasp mixing and flow characteristics and to examine appropriate construction such as a swirler. As a combustion test result, it was showed that the combustion was stable. DOE

N90-19364# Materials Research Labs., Ascot Vale (Australia).
EFFECT OF TEMPERATURE ON THE STORAGE LIFE OF POLYSULFIDE AIRCRAFT SEALANTS
John W. Barber, Peter J. Hanhela, Robert H. E. Huang, and D. Brenton Paul Aug. 1989 44 p
(MRL-TR-89-31; AR-005-730) Avail: NTIS HC A03/MF A01

The storage performances of a range of PR-1422, PR-1436G and PR-1750 two-part polysulfide aircraft sealants of A and B classes, packaged both in cans and Semkit form, were surveyed. The sealants were separately maintained at temperatures of -16 , 2, 13, and 25 C and changes in viscosity of the polymer base compound, cure rate, peel strength and application life were monitored over 26 months. Concurrent changes in thiol content

of the liquid polymer in the base compound and concentrations of Mn(IV) or CR(VI) in the cure pastes were also determined. Variations in activity of cure pastes with time were assessed using LP-32 as a standard polymer and changes in polymer base compounds were monitored by measuring cure rate with laboratory prepared reference cure pastes. Low temperature storage extended storage life significantly. After maintenance at temperatures of 2 C and below, the canned sealants still performed satisfactorily after two to three years storage. Most materials were procured several months after manufacture and with reduction of acquisition time further extension of the low temperature storage life could be expected. No significant storage differences between PT-1750 and PR-1422 sealants or the A or B classes were noted. Author

N90-19365# SRI International Corp., Menlo Park, CA.
SECOND-GENERATION ORDERED POLYMERS Final Report, 1 Nov. 1987 - 31 Oct. 1988
Steven P. Bitler, Andrea W. Chow, and James F. Wolfe Mar. 1989 122 p
(Contracts F49620-88-K-0001; F49620-85-K-0015; AF Proj. 2307; SRI Proj. PYU-4621)
(AD-A216126; AFOSR-89-0397TR) Avail: NTIS HC A06/MF A01 CSCL 07/6

The goals of this research were: (1) to understand the structure-property relationships that lead to organic materials with high figures of merit for nonlinear optical (NLO) applications and to develop the processibility and optical utility of such materials, (2) to investigate the effects of temperature and shear on the polymerization kinetics of lyotropic polymers, and (3) to examine the dilute and concentrated solution properties of rigid rod and extended chain poly(benzazoles). A homologous series of benzazole-containing donor-acceptor compounds was synthesized that should exhibit high figures of merit in NLO applications. These compounds, called ALHD compounds, are composed of an electron-accepting group, an unsaturated linking group, a conjugated heterocyclic segment, and an electron-donating group E.G., 2-(4-N,N dimethylaminophenyl 6- (N-nitrophenylmine) benzoxazole). The reaction kinetics and solution properties of lyotropic poly(benzazoles) were also investigated. The study of dilute and concentrated solutions of poly (2,6-benzothiazole), or ABPBT, and poly(2,5-benzoxazole), or ABPBO, involved the use of viscometry and low angle light scattering. These polymers can be classified as intrinsically semirigid, with persistence lengths of 130 A for ABPBT and 90 A for ABPBO. GRA

N90-19366# Rutgers - The State Univ., New Brunswick, NJ. Dept. of Ceramics.
ELASTIC PROPERTIES OF SILICA XEROGELS
Bennet Abramoff and Lisa C. Klein 3 Jan. 1990 19 p Submitted for publication
(Contract N00014-87-K-0529)
(AD-A216528; TR-2) Avail: NTIS HC A03/MF A01 CSCL 11/2

Longitudinal and transverse acoustic wave velocities have been measured for silica xerogels as a function of relative humidity in order to calculate elastic constants. The silica zerogels studied are microporous with open porosity of 53 vol percent. The longitudinal wave velocity exhibits a minimum at about 35 percent RH (relative humidity). The transverse wave velocity decreases to a constant value for 35 percent and greater relative humidity. Consequently, Young's modulus is a minimum at 35 percent RH while the shear modulus decreases to a constant value at 35 percent RH. The bulk modulus and Poissons' ratio exhibit minimum values at about 15 percent RH. Young's modulus decreases from 4.91 GPa to 3.42 GPa at 35 percent RH and then increases to 3.60 GPa at 55 percent RH. Poisson's ratio decreases from 0.184 to 0.164 at 15 percent RH and then increases to 0.272 at 55 percent RH. Below 35 percent RH, silica xerogels adsorb a monolayer of hydroxyls while above 35 percent RH silica xerogels show pore filling. GRA

N90-19367# Massachusetts Inst. of Tech., Cambridge. Dept. of Chemical Engineering.
SYNTHESIS OF POLY(DIMETHYLSILOXANE) - NYLON 6 DIBLOCK COPOLYMERS
C. A. Veith (North Carolina Univ., Chapel Hill.) and R. E. Cohen 1 Dec. 1989 15 p
(Contract N00014-87-K-0517)
(AD-A216850; TR-8) Avail: NTIS HC A02/MF A01 CSCL 07/6

Two diblock copolymers of polydimethylsiloxane and nylon 6 were synthesized using a macromonomer approach. PDMS was synthesized anionically in THF and terminated with 11-(dimethyl chlorosilyl) N-undecanoyl 1-caprolactam, yielding a macromonomer capable of participating in the ring opening polymerization of caprolactam. This second step was carried out with LiAlH2(OtBu)2 catalyst to activate the caprolactam monomer. Good yields and high molecular weight PDMS and Nylon 6 blocks were achieved. GRA

N90-19368# Oak Ridge National Lab., TN. High Temperature Materials Lab.
FRACTURE STRENGTH ANALYSIS OF SILICON NITRIDE AND SILICON CARBIDE CERAMICS FROM AN INTERNATIONAL COOPERATIVE RESEARCH PROGRAM
V. J. Tennery and M. K. Ferber 1989 9 p Presented at the Annual Automotive Technology Development Contractors Coordination Meeting, Dearborn, MI, 23-26 Oct. 1989
(Contract DE-AC05-84OR-21400)
(DE90-005319; CONF-8910248-3) Avail: NTIS HC A02/MF A01

Statistical analyses of the flexure strength of one silicon carbide and two silicon nitride ceramics obtained in an international research program between the United States, the Federal Republic of Germany, and Sweden are reported. The work represents the results from 2597 specimens measured in 21 laboratories. This International Energy Agency (IEA) project was motivated by a desire to develop international standards for determining the mechanical properties of structural ceramic materials. The strength of all specimen sets (N = 60 to 80) were measured in the same type of fixtures and at the same stressing rate. The strength was best described by a Weibull probability distribution; and the two parameters, (alpha) and (beta), which describe this distribution were best determined using Maximum Likelihood (ML) estimators. The maximum variation observed for the parameter (alpha) was 39, 48, and 69 percent for the ESK silicon carbide, ASEA silicon nitride, and GTE/WESGO silicon nitride, respectively. The variation in the values for (beta) were much smaller, ranging from 15 to 18 percent. DOE

N90-19369# Language Services, Knoxville, TN.
HEAT-RESISTANT AND ANTICORROSIVE PAINT
Kunion Katsuma (Hitachi Metals Ltd., Chiba, Japan) 1989 8 p Transl. into ENGLISH of Japanese Patent no. 62-227968 (6 Oct. 1987) 3 p Prepared for Oak Ridge Gaseous Diffusion Plant, TN
(Contract DE-AC05-84OR-21400)
(DE90-006077; K/TR-89/7) Avail: NTIS HC A02/MF A01

The invention, consisting of a paint formed from an alkali metal silicate compound mixed within a specified range and specified quantities of zinc powder, water, and ethylene glycol, is a single-liquid type with a long service life as well as an appropriate curing time. It can be used effectively with general paint application methods, and the heat resistant and anticorrosive properties of the solidified paint film obtained by painting and then processing with heat treatment are excellent. Furthermore, the addition of zinc powder makes this paint excellent for use with steel materials. DOE

N90-19370# Secretaria Estadual de Ciencia e Tecnologia, Rio de Janeiro (Brazil).
ADVANCED CERAMICS
Waldimir PirroeLongo, Sergio NevesMonteiro, and Jamil DuailibiFilho 1989 356 p In PORTUGUESE and ENGLISH Proceedings of the 2nd State Meeting of New Materials and 1st

Florida-Brazil Seminar on Materials, Rio de Janeiro, Brazil, 2-4 Aug. 1989
(DE90-608004; INIS-BR-1752; CONF-8908187) Avail: NTIS (US Sales Only) HC A16/MF A02

The First Florida-Brazil Seminar on Materials and the Second State Meeting about new materials in Rio de Janeiro State show the specific technical contribution in advanced ceramic sector. The others main topics discussed for the development of the country are the advanced ceramic programs the market, the national technic-scientific capacitation, the advanced ceramic patents, etc. DOE

N90-19371# Utah Univ., Salt Lake City. Dept. of Materials Science and Engineering.
FABRICATION, PHASE TRANSFORMATION STUDIES, AND CHARACTERIZATION OF SiC-AlN-Al2OC CERAMICS
Anil V. Virkar 3 Jan. 1990 15 p
(Contract DE-FG02-87ER-45286)
(DE90-006591; DOE/ER-45286/3) Avail: NTIS HC A03/MF A01

The research effort conducted to date had two specific objectives: to determine phase relations and phase transformations in SiC-AlN, AlN-Al2OC, and SiC-Al2OC pseudobinary systems and in SiC-AlN-Al2OC pseudoternary system, and to determine the effects of composition and microstructure on high temperature creep deformation properties. Published literature in this field shows that SiC, AlN, and Al2OC exhibit extensive solid solubility. Subsequently, the work showed that the solid solution undergoes phase separation upon annealing. In particular, phase separation in the SiC-AlN and AlN-Al2OC systems by the formation of modulations (by spinodal decomposition) as well as by cellular precipitation was documented. The demonstration of diffusional phase transformations in these covalently bonded refractory structural ceramics in itself is interesting. More importantly, however, is the potential for establishing property/microstructure relationships in this system. DOE

N90-19372# Georgia Univ., Athens. Dept. of Physics and Astronomy.
OPTICAL STUDIES OF DYNAMICAL PROCESSES IN DISORDERED MATERIALS
William N. Yen Dec. 1989 11 p
(Contract DE-FG09-87ER-45291)
(DE90-007080; DOE/ER-45291/3) Avail: NTIS HC A03/MF A01

A brief narrative is presented of the progress attained in relaxation and transfer studies, in the identification and determination of the nature of the sites of Cr ions in the disordered phases of ceramics and in the study of the optical properties of fibers, inclusive of attempts to localize a single atom in a glass. A number of continuing studies will be pursued in the second period: (1) attempts to stimulate energy transfer process, (2) continued attempts to isolate a single ion in a fiber, and (3) exploitation of the fiber configuration for spectroscopic purposes. DOE

N90-19373*# National Aeronautics and Space Administration. Lewis Research Center, Cleveland, OH.
HOT FILAMENT TECHNIQUE FOR MEASURING THE THERMAL CONDUCTIVITY OF MOLTEN LITHIUM FLUORIDE
Donald A. Jaworske and William D. Perry (Auburn Univ., AL.) 1990 13 p Proposed for presentation at the AIChE Summer National Meeting Session on Space Power Systems Technology, San Diego, CA, 19-22 Aug. 1990; sponsored by American Institute of Chemical Engineers
(NASA-TM-102506; E-5308; NAS 1.15:102506) Avail: NTIS HC A03/MF A01 CSCL 11C

Molten salts, such as lithium fluoride, are attractive candidates for thermal energy storage in solar dynamic space power systems because of their high latent heat of fusion. However, these same salts have poor thermal conductivities which inhibit the transfer of heat into the solid phase and out of the liquid phase. One concept for improving the thermal conductivity of the thermal energy storage system is to add a conductive filler material to the molten salt. High thermal conductivity pitch-based graphite fibers are being considered for this application. Although there is some information available on the thermal conductivity of lithium fluoride solid, there is very little information on lithium fluoride liquid, and no information on molten salt graphite fiber composites. This paper describes a hot filament technique for determining the thermal conductivity of molten salts. The hot filament technique was used to find the thermal conductivity of molten lithium fluoride at 930 C, and the thermal conductivity values ranged from 1.2 to 1.6 W/mK. These values are comparable to the slightly larger value of 5.0 W/mK for lithium fluoride solid. In addition, two molten salt graphite fiber composites were characterized with the hot filament technique and these results are also presented. Author

N90-19374*# Ohio State Univ., Columbus. Dept. of Materials Science and Engineering.
CRYSTALLIZATION BEHAVIOR AND PROPERTIES OF BaO-Al2O3-2SiO2 GLASS MATRICES Final Report
Charles H. Drummond, III and Narottam P. Bansal (Case Western Reserve Univ., Cleveland, OH.) Feb. 1990 23 p Presented at the 14th Annual Conference on Composite and Advanced Ceramics, Cocoa Beach, FL, 14-17 Jan. 1990; sponsored by American Ceramic Society
(Contract NCC3-133)
(NASA-CR-185209; E-5314; NAS 1.26:185209) Avail: NTIS HC A03/MF A01 CSCL 11C

Glass of stoichiometric celsian composition, BaO-Al2O3-2SiO2, is a potential glass-ceramic matrix for high-temperature composites. The glass has a density of 3.39 g/cu cm, thermal expansion coefficient of 6.6 x 10(exp -6)/deg C glass transition temperature of 910 C, and dilatometric softening point of 925 C. On heat treatment, only hexacelsian crystallized out on the surface, but both celsian and hexacelsian were present in the bulk. Effects of cold isostatic pressing (CIP), sintering, and hot pressing, in the presence and absence of an additive, on the formation of the celsian phase in the glass were studied. CIP'ed samples, after appropriate heat treatments, always crystallized out as celsian whereas the presence of 5 to 10 weight percent of an additive was necessary for formation of celsian in sintered as well as hot pressed specimens. Green density increased with CIP'ing pressure but had no effect on sintered density. Hot pressing resulted in fully dense samples. Author

N90-19375# Deutsche Gesellschaft fuer Chemisches Apparatewesen (Dechema), Frankfurt am Main (Germany, F.R.).
INFLUENCE OF HEAT TREATING ON THE MECHANICAL VALUES AND THE STABILITY OF HEAT BARRIER COATINGS Final Report [EINFLUSS DER WAERMEBEHANDLUNG AUF DIE MECHANISCHEN KENNWERTE UND DIE STABILITAET VON WAERMEDAEMMSCHICHTEN]
Kh. G. Schmitt-Thomas (Technische Univ., Munich, German, F.R.) 25 Nov. 1989 82 p In GERMAN
(ETN-90-95902) Avail: NTIS HC A05/MF A01

A sample of 7 percent yttrium stabilized heat barrier coating on a ZrO2 base is studied. The original powder was made of the tetragonal phase of ZrO2. Under the influence of the temperature and the time, a lattice modification by yttrium diffusion appears and produces a monocline or cubic phase, the porosity increases significantly and the hardness drops. Since the erosion ratio is proportional to the porosity, a ductile behavior of the zirconium oxide is assumed. The corrosion tests were carried out with deposits of NaCl, Na2SO4, NaVO3 on the ceramic barrier coatings. No corrosion attack appear with NaCl and Na2SO4; NaVO3 reacts with Y2O3 to form YVO4, the resulting impoverishment of the stabilization oxide favors a phase transformation. ESA

N90-19376# Bayreuth Univ. (Germany, F.R.).
TRANSIENT PHOTOCONDUCTION IN DOPED POLYMERS: SPATIAL AND ENERGETIC DISORDER Ph.D. Thesis [TRANSIENTE PHOTOLEITUNG IN DOTIERTEN POLYMEREN: ASPEKTE RAEUMLICHER UND ENERGETISCHER UNORDNUNG]

Helmut Domes 1988 105 p In GERMAN Sponsored by DFG Bonn, Federal Rep. of Germany
(ETN-90-95917) Avail: NTIS HC A06/MF A01

The charge transport in noncrystalline, organic photoconductors is different from normal Gaussian transport because of the energy structure and the irregular molecule organization. This disorder was treated with a BTAPC (benztriasol derived as a binder, bisphenol-A-polycarbonate as a matrix) system because of the good reproducibility of the measurements and the sufficiently short transit time. The photoconductivity was examined by the time of flight method, with variation of the temperature and the field intensity. The results show the influence of the transport molecule concentration on the current intensity and the transit time. The system doping was done with rhodamine B and astrazonorange. For very high coloring concentrations the transit time evaluation is no longer possible. ESA

N90-19377# Sandia National Labs., Albuquerque, NM.
THEORY OF POLYMER BLENDS
John G. Curro and Kenneth S. Schweizer 1989 7 p Presented at the 199th National Meeting of the American Chemical Society, Boston, MA, 22-27 Apr. 1990
(Contract DE-AC04-76DP-00789)
(DE90-002532; SAND-89-2512C; CONF-900402-1) Avail: NTIS HC A02/MF A01

We have recently developed a new theoretical approach to the study of polymer liquids. The theory is based on the reference interaction site model (RISM theory) of Chandler and Andersen, which has been successful in describing the structure of small molecule liquids. We have recently extended our polymer RISM theory to the case of polymer blends. In the present investigation we have applied this theory to two special binary blends: (1) the athermal mixture where we isolate structural effects, and (2) the isotopic mixture in which structurally identical polymer chains interact with dissimilar attractive interactions. By studying these two special cases we are able to obtain insights into the molecular factors which control the miscibility in polymer mixtures. DOE

N90-19378# Sandia National Labs., Albuquerque, NM. Passive Components Div.
ALTERNATE FILM DIELECTRIC MATERIALS
James C. Foster (General Electric Co., Largo, FL.), James O. Harris, and Jesus I. Martinez 1990 7 p Presented at the 1990 Capacitor and Resistor Technology Symposium, San Francisco, CA, 26-29 Mar. 1990
(Contract DE-AC04-76DP-00789)
(DE90-007213; SAND-89-3135C; CONF-900371-2) Avail: NTIS HC A02/MF A01

Data is presented on polymeric dielectric films evaluated to support the design of high-energy-density capacitors. Evaluated materials include polycarbonate, polyphenylene sulfide, polyvinylidene fluoride, polyethermide, polyimide, polyethersulfone, and polyetherether ketone. A polyester was evaluated as the control material since many of the prior designs utilized this dielectric. The film evaluations were based on dielectric constant and dissipation factor variation as a function of temperature from -55 to 300 C, as well as dielectric breakdown strength. Additionally, film/foil capacitors in a dry, wrap-and-fill configuration were fabricated and tested to determine insulation resistance, breakdown voltage, and radiation hardness. Results are presented for all the evaluations based on the several criteria. DOE

N90-19379# Oak Ridge National Lab., TN.
MICROSTRUCTURAL CHARACTERIZATION OF MULTIPHASE COATINGS PRODUCED BY CHEMICAL VAPOR DEPOSITION
Richard A. Lowden, Karren L. More, T. M. Besmann, and R. D. James 1989 7 p Presented at the Materials Research Society Fall Meeting, Boston, MA, 27 Nov. - 2 Dec. 1989
(Contract DE-AC05-84OR-21400)
(DE90-007573; CONF-891119-99) Avail: NTIS HC A02/MF A01

Chemical vapor deposition has been utilized to produce ternary, multiphase coatings of various compositions of silicon carbide (SiC) with Ti, Cr, and Mo. Thermodynamic calculations have been performed for a variety of experimental conditions in each system. Scanning, transmission and analytical electron microscopy, and x ray diffraction techniques have been used to characterize the microstructures and to determine compositions. DOE

N90-19380# Oak Ridge National Lab., TN.
THE EFFECT OF FIBER COATINGS ON INTERFACIAL SHEAR STRENGTH AND THE MECHANICAL BEHAVIOR OF CERAMIC COMPOSITES
Richard A. Lowden and Karren L. More 1989 10 p Presented at the Materials Research Society Fall Meeting, Boston, MA, 27 Nov. - 2 Dec. 1989
(Contract DE-AC05-84OR-21400)
(DE90-007574; CONF-891119-100) Avail: NTIS HC A02/MF A01

Thin coatings (boron nitride and carbon) deposited on ceramic fibers prior to densification employing chemical vapor infiltration techniques have been used to limit fiber-matrix bonding. This has resulted in improvements in strength and toughness at room and elevated temperatures in Nicalon (trademark) fiber-reinforced/SiC matrix composites. The properties of the fiber-matrix interface in fiber-reinforced ceramic composites have been examined utilizing an indentation method in which a standard microhardness indentor is used to push on fibers embedded in the ceramic matrix. Compositions and microstructures at the interface have been characterized employing analytical electron microscopy. Correlations between interfacial phenomena and observed mechanical behavior have been made. DOE

N90-19381# Houston Univ., TX. Dept. of Physics.
DIFFRACTION STUDIES OF THE STRUCTURE OF GLASSES AND LIQUIDS Technical Progress Report
S. C. Moss 1989 31 p
(Contract DE-FG05-87ER-45325)
(DE90-007662; DOE/ER-45325/3) Avail: NTIS HC A03/MF A01

At the University of Houston, our program on glasses and liquids has continued with emphasis on melanin; vitreous TiO2; metallic glasses/quasicrystals, including the computer modelling of quasicrystals via icosahedral glass models; and the structure of C(+) ion beam deposited carbon films. The development of a dedicated glass and liquid diffractometer (GLAD) at the Argonne IPNS has entered the prototype stage. A fully operating facility is quite close and commissioning should take place in the Spring 1990 with beam time available for participating scientists, on state-of-the-art experiments, shortly thereafter. DOE

N90-19382# Oak Ridge National Lab., TN.
LIGHT-SCATTERING MEASUREMENTS OF CVD (CHEMICAL VAPOR DEPOSITION) SILICON CARBIDE
B. W. Sheldon and T. M. Besmann 1989 8 p Presented at the Materials Research Society Fall Meeting, Boston, MA, 27 Nov. - 2 Dec. 1989
(Contract DE-AC05-84OR-21400)
(DE90-007885; CONF-891119-101) Avail: NTIS HC A02/MF A01

Surface morphologies created by the chemical vapor deposition (CVD) of silicon carbide were examined with light scattering. Silicon carbide was deposited from methyltrichlorosilane under various conditions to create different surfaces. A helium neon laser was used, and the scattered light was measured over a range of scattering angles. These measurements are compared with scanning electron microscopy (SEM) observations and profilometer measurements of the same surfaces. In theory that scattered light contains all of the information needed to provide a statistical description of a given surface; however, a complete vector theory for the scattering phenomena is too complex to provide any simple basis for experimental analysis. The application and limits of existing descriptions of scattering from a rough surface are discussed. DOE

N90-19383# Sandia National Labs., Albuquerque, NM. Theoretical Div.
RADIATION-INDUCED DENSITY CHANGES AND CREEP IN SURFACE LAYERS OF GLASS
W. G. Wolfer and A. J. Antolak Jan. 1990 31 p
(Contract DE-AC04-76DP-00789)
(DE90-008112; SAND-90-8200) Avail: NTIS HC A03/MF A01

When glass surfaces are bombarded by energetic charged particles, radiation induced density changes happen within the damaged surface layer. As a result of the lateral constraints imposed by the undamaged substrate material, stresses are also generated within the damaged layer. A detailed analysis of the stress evolution is given together with an analysis of the surface displacement and the bending of plate-like specimens bombarded from one side. The damaged material is assumed to deform as a viscoelastic material with a power law stress dependence. The results of this analysis are applied to earlier experimental results in order to extract creep parameters which describe this viscoelastic and radiation induced deformation in hydrogen-free vitreous silica. DOE

N90-19384# Wisconsin Univ., Madison. Engine Research Center.
ELASTIC RECOVERY AND POLYMER-POLYMER INTERACTIONS
Arthur S. Lodge 1989 13 p Repr. from Rheologica Acta, 1989 p 351-362
(Contract DAAL03-86-K-0174)
(AD-A217085; ARO-24623.44-EG-UIR) Avail: NTIS HC A03/MF A01 CSCL 07/6

Elastic recovery in polymeric liquids is a cooperative phenomenon in the sense that individual polymer molecules undergoing retraction must interact with one another in order to generate recovery. Stress generated by polymer molecules under an externally imposed flow field may or may not be a cooperative phenomenon. It is suggested that the ability to describe the large elastic recovery exhibited by many polymeric liquids furnishes a crucial test of the validity of methods used to model the interaction of a given polymer molecule with its neighbors. Temporary-junction network models appear to be capable of explaining observed recoveries. Elastic recovery cannot be explained by single molecule-in-a-mean-filed theories which involve no calculation of the effect of the single molecule on the field. A Gaussian network theory equation for the change of volume with elongation for a cross linked elastomer is generalized in order to allow the bulk compliance to depend on elongation. It is proved that two classes of flow history, namely shear-free and shear, are constitutively independent in the sense that, for a given viscoelastic liquid of unknown constitutive equation, the behavior in one class cannot be predicted from rheological measurements (however extensive) made solely in the other class. GRA

28 PROPELLANTS AND FUELS

Includes rocket propellants, igniters, and oxidizers; their storage and handling procedures; and aircraft fuels.

For related information see also *07 Aircraft Propulsion and Power, 20 Spacecraft Propulsion and Power,* and *44 Energy Production and Conversion.*

N90-19385# Materials Research Labs., Ascot Vale (Australia).
AN EVALUATION OF ETHYLENE-VINYL ACETATE COPOLYMERS AS DESENSITIZERS FOR RDX IN INSENSITIVE BOOSTER COMPOSITIONS PREPARED BY SLURRY COATING TECHNOLOGY
I. J. Dagley, H. J. Spencer, C. N. Louey, and R. P. Parker Aug. 1989 48 p
(MRL-TR-89-33; AR-005-735) Avail: NTIS HC A03/MF A01

Twelve ethylene-vinyl acetate (EVA) copolymers with vinyl acetate contents ranging from 12 to 51 percent have been evaluated as desensitizers for RDX, for production of insensitive booster compositions. The RDX/EVA compositions were prepared by a solvent-slurry coating process, in which a solution of the EVA copolymer in a suitable solvent is added to an aqueous suspension of RDX, the solvent then being removed by distillation to effect coating of the polymer on the RDX. The efficiency with which the EVA copolymers coat the RDX crystal surfaces increases with increasing vinyl acetate content, and can be altered by the use of surfactants. The RDX/EVA compositions all have excellent thermal stability, as assessed by the vacuum thermal stability test. The shock sensitivities of compositions prepared with copolymers containing 28 to 51 percent vinyl acetate were found to be between those of tetryl and PBXW-7, with the shock sensitivity generally decreasing with increasing vinyl acetate content. In general, the EVA coatings gave little desensitization to impact or cookoff; only one composition had a figure of insensitiveness (F of I) which meets current impact sensitiveness requirements for booster explosives for fuzes, and only two compositions gave mild reactions in small-scale cookoff tests. Author

N90-19386*# Battelle Columbus Labs., OH. Metals and Ceramics Information Center.
THE MEASUREMENT, MODELING, AND PREDICTION OF TRACTION FOR ROCKET PROPELLANT 1 Final Report
J. L. Tevaarwerk Oct. 1989 72 p
(Contract NASA Order C-30012-M; DLA900-83-C-1744)
(NASA-CR-185186; NAS 1.26:185186; G8558-8701) Avail: NTIS HC A04/MF A01 CSCL 21I

Traction tests were performed on RP-1, a common kerosene based rocket propellant. Traction data on this fluid are required for purposes of turbopump bearing design, using codes such as SHABERTH. To obtain the traction data, an existing twin disc machine was used, operating under the side slip mode and using elliptical contacts. The range of test variables were: contact peak Hertz stress from 1.0 to 2.0 GPa, disc surface speed from 10 to 50 m/s, fluid inlet temperature from 30 to 70 C, and with a contact aspect ratio of 1.7. The resulting traction curves were reduced to fundamental fluid property parameters using the Johnson and Tevaarwerk traction model. Theoretical traction predictions were performed by back substitution of the fundamental properties into the traction model. Comparison of the predicted with the measured curves gives a high degree of confidence in the correctness of the traction model. For purposes of input to the NASA SHABERTH program, the traction model was next used to predict the expected traction of RP-1 under line contact conditions. Author

N90-19387# Federal Aviation Administration, Atlantic City, NJ.
IN-FLIGHT EVALUATIONS OF TURBINE FUEL EXTENDERS Final Report
Augusto M. Ferrara and Carol Rea Feb. 1990 37 p
(DOT/FAA/CT-89/33) Avail: NTIS HC A03/MF A01

Flight tests were conducted which evaluated the use of ethanol as a blending agent for aircraft turbine fuels. As part of this study, a Beech King Air 200 was modified to incorporate a cabin tank which contained ethanol, and the fuel system was modified to deliver the ethanol to the starboard engine. Ten percent ethanol was mixed with JP-4 in the project fuel line, just before entering the engine. The test was performed over a broad range of operating conditions, and key performance parameters were measured. The use of ethanol as a blending agent reduced the power available and resulted in an increase in fuel consumption. The increase in fuel consumption was greater than the decrease in energy density. When operating on the ethanol/JP-4 mixtures, the test pilots noted the test engine required more throttle (throttle stagger). No other operational problems were uncovered during the course of the flight tests. A pre- and post-test engine inspection revealed no fuel related damage. Author

N90-19388# SRI International Corp., Menlo Park, CA.
DETERMINATION OF THE MECHANISM OF DECOMPOSITION OF ENERGETIC MOLECULES Final Technical Report, 1 Feb. 1986 - 31 Jan. 1989
Donald F. McMillien, Jay B. Jeffries, Paul H. Stewart, Jean-Michel Zellweger, Alan B. McEwen, and David M. Golden Dec. 1989 56 p

(Contract DAAL03-86-K-0030)
(AD-A217061; ARO-23338.5-CH) Avail: NTIS HC A04/MF A01 CSCL 07/4

As a prototype for more complex nitramines, the gas-phase decomposition of dimethylnitramine was studied in three laser-pyrolysis systems. Results in two of these systems, unlike those reported in the literature, indicate that a nitro-nitrite rearrangement pathway is competitive with the expected (and previously invoked) NNO2 bond scission. This rearrangement pathway has been obscure because it can lead to some of the same products that are yielded by the bond scission route. The principal evidence for nitro-nitrite rearrangement includes: (1) Arrhenius parameters for decomposition that are two orders of magnitude too low to be consistent with simple N-NO2 bond scission as the sole rate-determining step, (2) molecular-beam, mass-spectro-metrically sampled laser pyrolysis studies that show direct detection of NO and the nitroxyl radical (CH3)2NO on a time scale too short to allow for the production of these substances in secondary bimolecular reactions, and (3) ab initio calculations (in concurrent AFOSR-funded work) that find a rearrangement pathway at slightly lower energy than that of simple bond scission. These results suggest that such rearrangement pathways may be a common feature of nitramine decomposition, as other studies have recently shown them to be for C-NO2 compounds. GRA

29 MATERIALS PROCESSING

Includes space-based development of products and processes for commercial applications.
For biological materials see *55 Space Biology*.

N90-19424*# Alabama Univ., Huntsville. Dept. of Biological Sciences.
TECHNIQUES FOR STUDYING THE EFFECTS OF MICROGRAVITY ON MODEL PARTICLE/CELL SYSTEMS
Ronald B. Young *In its* Research Reports: 1989 NASA/ASEE Summer Faculty Fellowship Program Dec. 1989 18 p (For primary document see N90-19390 12-31)
(Grant NGT-01-008-021)
Avail: NTIS HC A99/MF E06 CSCL 22A

31 ENGINEERING (GENERAL)

Includes vacuum technology; control engineering; display engineering; cryogenics; and fire prevention.

N90-19389*# National Aeronautics and Space Administration, Washington, DC.
AEROSPACE SAFETY ADVISORY PANEL Annual Report
Mar. 1989 105 p
(NASA-TM-101748; NAS 1.15:101748) Avail: NTIS HC A06/MF A01 CSCL 13B

This report provides findings, conclusions and recommendations regarding the National Space Transportation System (NSTS), the Space Station Freedom Program (SSFP), aeronautical projects and other areas of NASA activities. The main focus of the Aerospace Safety Advisory Panel (ASAP) during 1988 has been monitoring and advising NASA and its contractors on the Space Transportation System (STS) recovery program. NASA efforts have restored the flight program with a much better management organization, safety and quality assurance organizations, and management communication system. The NASA National Space Transportation System (NSTS) organization in conjunction with its prime contractors should be encouraged to continue development and incorporation of appropriate design and operational improvements which will further reduce risk. The data from each Shuttle flight should be used to determine if affordable design and/or operational improvements could further increase safety. The review of Critical Items (CILs), Failure Mode Effects and Analyses (FMEAs) and Hazard Analyses (HAs) after the Challenger accident has given the program a massive data base with which to establish a formal program with prioritized changes. K.C.D.

N90-19390*# Alabama Univ., Huntsville.
RESEARCH REPORTS: 1989 NASA/ASEE SUMMER FACULTY FELLOWSHIP PROGRAM Final Report
Gerald R. Karr, ed., Frank Six, ed. (National Aeronautics and Space Administration. Marshall Space Flight Center, Huntsville, AL.), and L. Michael Freeman, ed. Dec. 1989 888 p Fellowship program held in Huntsville, AL, 5 Jun. - 11 Aug. 1989 Prepared in cooperation with Alabama Univ., Tuscaloosa
(Grant NGT-01-008-021)
(NASA-CR-183837; NAS 1.26:183837) Avail: NTIS HC A99/MF E06 CSCL 13B

For the twenty-fifth consecutive year, a NASA/ASEE Summer Faculty Fellowship Program was conducted at the Marshall Space Flight Center (MSFC). The basic objectives of the programs are: (1) to further the professional knowledge of qualified engineering and science faculty members; (2) to stimulate an exchange of ideas between participants and NASA; (3) to enrich and refresh the research and teaching activities of the participants' institutions; and (4) to contribute to the research objectives of the NASA Centers. The Faculty Fellows spent ten weeks at MSFC engaged in a research project compatible with their interests and background and worked in collaboration with a NASA/MSFC colleague. For individual titles, see N90-19391 through N90-19424.

N90-19391*# Auburn Univ., AL. Dept. of Electrical Engineering.
CHARACTERIZATION OF THUNDERSTORM INDUCED MAXWELL CURRENT DENSITIES IN THE MIDDLE ATMOSPHERE **c46**
Michael Edward Baginski *In* Alabama Univ., Research Reports: 1989 NASA/ASEE Summer Faculty Fellowship Program Dec. 1989 p 1-21 (For primary document see N90-19390 12-31)
(Grant NGT-01-008-021)
Avail: NTIS HC A99/MF E06 CSCL 04A

Middle atmospheric transient Maxwell current densities generated by lightning induced charge perturbations are investigated via a simulation of Maxwell's equations. A time domain finite element analysis is employed for the simulations. The atmosphere is modeled as a region contained within a right circular cylinder with a height of 110 km and radius of 80 km. A composite conductivity profile based on measured data is used when charge perturbations are centered about the vertical axis at altitudes of 6 and 10 km. The simulations indicate that the temporal structure of the Maxwell current density is relatively insensitive to altitude variation within the region considered. It is also shown that the electric field and Maxwell current density are not generally aligned. Author

N90-19392*# Alabama A & M Univ., Huntsville. Mathematics.
AUGMENTING AND UPDATING NASA SPACELINK ELECTRONIC INFORMATION SYSTEM **c32**
Jean A. Blake *In* Alabama Univ., Research Reports: 1989 NASA/ASEE Summer Faculty Fellowship Program Dec. 1989 8 p (For primary document see N90-19390 12-31)
(Grant NGT-01-008-021)
Avail: NTIS HC A99/MF E06 CSCL 17B

The development of Spacelink during its gestation, birth, infancy, and childhood are described. In addition to compiling and developing more material for implementation in Spacelink, Summer 1989 was spent scanning the insignias of the various manned missions into Spacelink. Material for the above was extracted from existing NASA publications, documents and photographs. Author

N90-19393*# South Carolina Univ., Columbia. Dept. of Mechanical Engineering.
KALMAN ESTIMATION FOR SEDS MEASUREMENTS **c18**
Connie K. Carrington *In* Alabama Univ., Research Reports: 1989 NASA/ASEE Summer Faculty Fellowship Program Dec. 1989 20 p (For primary document see N90-19390 12-31)
(Grant NGT-01-008-021)
Avail: NTIS HC A99/MF E06 CSCL 22B

The first on-orbit experiment of the Small Expendable Deployer System (SEDS) for tethered satellites will collect telemetry data for tethered length, rate of deployment, and tether tension. The post-flight analysis will use this data to reconstruct the deployment history and determine payload position and tether shape. Two Kalman estimator algorithms were written, and output using simulated measurement data was compared. Both estimators exhibited the same estimated state histories, indicating that numerical instability in the traditional algorithm was not the cause of filter divergence. Estimation of acceleration biases was added, which reduced the error but did not correct the divergence. An add-a-bead estimator that adds lumped masses as the tether is deployed was written, which provides a state model that matches the BEADSIM simulation providing the true measurements and states. This twenty-one bead estimator produced state histories similar to those of the two-bead estimator, indicating that the filter divergence was not caused by a reduced-order model. The noise models used to date are relatively simple and may be the source of estimator divergence. The investigation of colored noise models, cross-correlated measurement and process covariances, and noise-adaptive filter techniques is recommended. Author

N90-19394*# Texas Technological Univ., Lubbock. Atmospheric Science Group.

A PBL-RADIATION MODEL FOR APPLICATION TO REGIONAL NUMERICAL WEATHER PREDICTION **c47**

Chia-Bo Chang *In* Alabama Univ., Research Reports: 1989 NASA/ASEE Summer Faculty Fellowship Program Dec. 1989 21 p (For primary document see N90-19390 12-31)
(Grant NGT-01-008-021)
Avail: NTIS HC A99/MF E06 CSCL 04B

Often in the short-range limited-area numerical weather prediction (NWP) of extratropical weather systems the effects of planetary boundary layer (PBL) processes are considered secondarily important. However, it may not be the case for the regional NWP of mesoscale convective systems over the arid and semi-arid highlands of the southwestern and south-central United States in late spring and summer. Over these dry regions, the PBL can grow quite high up into the lower middle troposphere (600 mb) due to very effective solar heating and hence a vigorous air-land thermal interaction can occur. The interaction representing a major heat source for regional dynamical systems can not be ignored. A one-dimensional PBL-radiation model was developed. The model PBL consists of a constant-flux surface layer superposed with a well-mixed (Ekman) layer. The vertical eddy mixing coefficients for heat and momentum in the surface layer are determined according to the surface similarity theory, while their vertical profiles in the Ekman layer are specified with a cubic polynomial. Prognostic equations are used for predicting the height of the nonneutral PBL. The atmospheric radiation is parameterized to define the surface heat source/sink for the growth and decay of the PBL. A series of real-data numerical experiments has been carried out to obtain a physical understanding how the model performs under various atmospheric and surface conditions. This one-dimensional model will eventually be incorporated into a mesoscale prediction system. The ultimate goal of this research is to improve the NWP of mesoscale convective storms over land. Author

N90-19395*# Illinois Univ., Chicago. Dept. of Mechanical Engineering.

POTENTIAL THEORY OF RADIATION **c34**

Huei-Huang Chiu *In* Alabama Univ., Research Reports: 1989 NASA/ASEE Summer Faculty Fellowship Program Dec. 1989 20 p (For primary document see N90-19390 12-31)
(Grant NGT-01-008-021)
Avail: NTIS HC A99/MF E06 CSCL 20D

A theoretical method is being developed by which the structure of a radiation field can be predicted by a radiation potential theory, similar to a classical potential theory. The introduction of a scalar potential is justified on the grounds that the spectral intensity vector is irrotational. The vector is also solenoidal in the limits of a radiation field in complete radiative equilibrium or in a vacuum. This method provides an exact, elliptic type equation that will upgrade the accuracy and the efficiency of the current CFD programs required for the prediction of radiation and flow fields. A number of interesting results emerge from the present study. First, a steady state radiation field exhibits an optically modulated inverse square law distribution character. Secondly, the unsteady radiation field is structured with two conjugate scalar potentials. Each is governed by a Klein-Gordon equation with a frictional force and a restoring force. This steady potential field structure and the propagation of radiation potentials are consistent with the well known results of classical electromagnetic theory. The extension of the radiation potential theory for spray combustion and hypersonic flow is also recommended. Author

N90-19396*# Middle Tennessee State Univ., Murfreesboro. Dept. of Mathematics and Statistics.

METHODS FOR TREND ANALYSIS: EXAMPLES WITH PROBLEM/FAILURE DATA **c38**

Curtis K. Church *In* Alabama Univ., Research Reports: 1989 NASA/ASEE Summer Faculty Fellowship Program Dec. 1989 29 p (For primary document see N90-19390 12-31)
(Grant NGT-01-008-021)
Avail: NTIS HC A99/MF E06 CSCL 14D

Statistics are emphasized as an important role in quality control and reliability. Consequently, Trend Analysis Techniques recommended a variety of statistical methodologies that could be applied to time series data. The major goal of the working handbook, using data from the MSFC Problem Assessment System, is to illustrate some of the techniques in the NASA standard, some different techniques, and to notice patterns of data. Techniques for trend estimation used are: regression (exponential, power, reciprocal, straight line) and Kendall's rank correlation coefficient. The important details of a statistical strategy for estimating a trend component are covered in the examples. However, careful analysis and interpretation is necessary because of small samples and frequent zero problem reports in a given time period. Further investigations to deal with these issues are being conducted. Author

N90-19397*# Carnegie-Mellon Univ., Pittsburgh, PA. Dept. of Mechanical Engineering.

A PARAMETRIC HEAT TRANSFER STUDY FOR CRYOGENIC BALL BEARINGS IN SSME HPOTP **c37**

Mingking K. Chyu *In* Alabama Univ., Research Reports: 1989 NASA/ASEE Summer Faculty Fellowship Program Dec. 1989 24 p (For primary document see N90-19390 12-31)
(Grant NGT-01-008-021)
Avail: NTIS HC A99/MF E06 CSCL 13I

A numerical modeling is to examine the effects of coolant convective heat transfer coefficient and frictional heating on the local temperature characteristics of a ball element in Space Shuttle Main Engine (SSME) High Pressure Oxidizer Turbopump (HPOTP) bearing. The present modeling uses a control-volume based, finite-difference method to solve the non-dimensionalized heat conduction equation in spherical coordinate system. The dimensionless temperature is found as a function of Biot number, heat flux ratio between the two race contacts, and location in the ball. The current results show that, for a given cooling capability, the ball temperature generally increases almost linearly with the heat input from the race-contacts. This increase is always very high at one of the two contacts. An increase in heat transfer coefficient generally reduces the ball temperature and alleviates the temperature gradient, except for the regions very close to the race contacts. For a 10-fold increase of heat transfer coefficient, temperature decrease is 35 percent for the average over entire ball, and 10 percent at the inner-race contact. The corresponding change of temperature gradient displays opposing trends between the regions immediately adjacent to the contacts and the remaining portion of the ball. The average temperature gradient in the vicinity of both contacts increases approximately 70 to 100 percent. A higher temperature gradient produces excessive thermal stress locally which may be detrimental to the material integrity. This,

however, is the only unfavorable issue for an increase of heat transfer coefficient. Author

N90-19398*# Southern Univ., Baton Rouge, LA. Dept. of Mechanical Engineering.
LIQUID OXYGEN LOX COMPATIBILITY EVALUATIONS OF ALUMINUM LITHIUM (Al-Li) ALLOYS: INVESTIGATION OF THE ALCOA 2090 AND MMC WELDALITE 049 ALLOYS c26
Ravinder M. Diwan *In* Alabama Univ., Research Reports: 1989 NASA/ASEE Summer Faculty Fellowship Program Dec. 1989 31 p (For primary document see N90-19390 12-31)
(Grant NGT-01-008-021)
Avail: NTIS HC A99/MF E06 CSCL 11F

The behavior of liquid oxygen (LOX) compatibility of aluminum lithium (Al-Li) alloys is investigated. Alloy systems of Alcoa 2090, vintages 1 to 3, and of Martin Marietta Corporation (MMC) Weldalite 049 were evaluated for their behavior related to the LOX compatibility employing liquid oxygen impact test conditions under ambient pressures and up to 1000 psi. The developments of these aluminum lithium alloys are of critical and significant interest because of their lower densities and higher specific strengths and improved mechanical properties at cryogenic temperatures. Of the different LOX impact tests carried out at the Marshall Space Flight Center (MSFC), it is seen that in certain test conditions at higher pressures, not all Al-Li alloys are LOX compatible. In case of any reactivity, it appears that lithium makes the material more sensitive at grain boundaries due to microstructural inhomogeneities and associated precipitate free zones (PFZ). The objectives were to identify and rationalize the microstructural mechanisms that could be relaxed to LOX compatibility behavior of the alloy system in consideration. The LOX compatibility behavior of Al-Li 2090 and Weldalite 049 is analyzed in detail using microstructural characterization techniques with light optical metallography, scanning electron microscopy (SEM), electron microprobe analysis, and surface studies using secondary ion mass spectrometry (SIMS), electron spectroscopy in chemical analysis (ESCA) and Auger electron spectroscopy (AES). Differences in the behavior of these aluminum lithium alloys are assessed and related to their chemistry, heat treatment conditions, and microstructural effects. Author

N90-19399*# University of Central Arkansas, Conway. Dept. of Physics.
BACKGROUND STUDIES IN GAS IONIZING X RAY DETECTORS c35
Hudson B. Eldridge *In* Alabama Univ., Research Reports: 1989 NASA/ASEE Summer Faculty Fellowship Program Dec. 1989 31 p (For primary document see N90-19390 12-31)
(Grant NGT-01-008-021)
Avail: NTIS HC A99/MF E06 CSCL 14B

The background response of a gas ionizing proportional x ray detector is estimated by solving the one dimensional photon transport equation for two regions using Monte Carlo techniques. The solution was effected using the SSL VAX 780 and the CRAY XMP computers at Marshall Space Flight Center. The isotropic photon energy spectrum encompassing the range from 1 to 1000 KeV incident onto the first region, the shield, is taken so as to represent the measured spectrum at an altitude of 3 mb over Palastine, Texas. The differential energy spectrum deposited in the gas region, xenon, over the range of 0 to 100 KeV is written to an output file. In addition, the photon flux emerging from the shield region, tin, over the range of 1 to 1000 KeV is also tabulated and written to a separate file. Published tabular cross sections for photoelectric, elastic and inelastic Compton scattering as well as the total absorption coefficient are used. Histories of each incident photon as well as secondary photons from Compton and photoelectric interactions are followed until the photon either is absorbed or exits from the regions under consideration. The effect of shielding thickness upon the energy spectrum deposited in the xenon region for this background spectrum incident upon the tin shield was studied. Author

N90-19400*# Virginia Polytechnic Inst. and State Univ., Blacksburg. Dept. of Mechanical Engineering.
INVESTIGATION OF SSME ALTERNATE HIGH PRESSURE FUEL TURBOPUMP LIFT-OFF SEAL FLUID AND STRUCTURAL DYNAMIC INTERACTION c37
David A. Elrod *In* Alabama Univ., Research Reports: 1989 NASA/ASEE Summer Faculty Fellowship Program Dec. 1989 15 p (For primary document see N90-19390 12-31)
(Grant NGT-01-008-021)
Avail: NTIS HC A99/MF E06 CSCL 11A

The Space Shuttle main engine (SSME) alternate turbopump development program (ATD) high pressure fuel turbopump (HPFTP) design utilizes an innovative lift-off seal (LOS) design that is located in close proximity to the turbine end bearing. Cooling flow exiting the bearing passes through the lift-off seal during steady state operation. The potential for fluid excitation of lift-off seal structural resonances is investigated. No fluid excitation of LOS resonances is predicted. However, if predicted LOS natural frequencies are significantly lowered by the presence of the coolant, pressure oscillations caused by synchronous whirl of the HPFTP rotor may excite a resonance. Author

N90-19401*# University of Central Florida, Orlando. Dept. of Mechanical Engineering.
A STUDY OF THE EFFECTS OF DISK FLEXIBILITY ON THE ROTORDYNAMICS OF THE SPACE SHUTTLE MAIN ENGINE TURBO-PUMPS c37
George T. Flowers *In* Alabama Univ., Research Reports: 1989 NASA/ASEE Summer Faculty Fellowship Program Dec. 1989 28 p (For primary document see N90-19390 12-31)
(Grant NGT-01-008-021)
Avail: NTIS HC A99/MF E06 CSCL 13I

Rotor dynamical analyses are typically performed using rigid disk models. Studies of rotor models in which the effects of disk flexibility were included indicate that is may be an important effect for many systems. This issue is addressed with respect to the Space Shuttle Main Engine high pressure turbo-pumps. Finite element analyses have been performed for a simplified free-free flexible disk rotor model and the modes and frequencies compared to those of a rigid disk model. The simple model was then extended to a more sophisticated HPTOP rotor model and similar results were observed. Equations were developed that are suitable for modifying the current rotordynamical analysis program to account for disk flexibility. Some conclusions are drawn from the results of this work as to the importance of disk flexibility on the HPTOP rotordynamics and some recommendations are given for follow-up research in this area. Author

N90-19402*# Memphis State Univ., TN. Dept. of Physics.
A COMPUTER CONTROL SYSTEM FOR THE ALTERNATING GRADIENT MAGNETOMETER c33
Michael M. Garland *In* Alabama Univ., Research Reports: 1989 NASA/ASEE Summer Faculty Fellowship Program Dec. 1989 32 p (For primary document see N90-19390 12-31)
(Grant NGT-01-008-021)
Avail: NTIS HC A99/MF E06 CSCL 09A

An alternating gradient magnetometer was interfaced to a computer for the automation of data taking. Using a fast Fourier transform analysis system data can be acquired and processed in real time. Data are stored on disk and can be recalled for plotting and further analysis. With the addition of a simple liquid nitrogen cryostat, magnetization measurements can be performed in the range from 300 to 77 K. Results are reported on three different types of piezoelectric transducers. Author

N90-19403*# Mankato State Coll., MN. Dept. of Mathematics, Astronomy, and Statistics.
MONTE CARLO MODELS AND ANALYSIS OF GALACTIC DISK GAMMA-RAY BURST DISTRIBUTIONS c93
Jon Hakkila *In* Alabama Univ., Research Reports: 1989 NASA/ASEE Summer Faculty Fellowship Program Dec. 1989 22 p (For primary document see N90-19390 12-31)

(Grant NGT-01-008-021)
Avail: NTIS HC A99/MF E06 CSCL 03B

Gamma-ray bursts are transient astronomical phenomena which have no quiescent counterparts in any region of the electromagnetic spectrum. Although temporal and spectral properties indicate that these events are likely energetic, their unknown spatial distribution complicates astrophysical interpretation. Monte Carlo samples of gamma-ray burst sources are created which belong to Galactic disk populations. Spatial analysis techniques are used to compare these samples to the observed distribution. From this, both quantitative and qualitative conclusions are drawn concerning allowed luminosity and spatial distributions of the actual sample. Although the Burst and Transient Source Experiment (BATSE) experiment on Gamma Ray Observatory (GRO) will significantly improve knowledge of the gamma-ray burst source spatial characteristics within only a few months of launch, the analysis techniques described herein will not be superceded. Rather, they may be used with BATSE results to obtain detailed information about both the luminosity and spatial distributions of the sources. Author

N90-19404*# Lafayette Coll., Easton, PA. Dept. of Electrical Engineering.
ARTIFICIAL INTELLIGENCE ISSUES RELATED TO AUTOMATED COMPUTING OPERATIONS **c63**
William A. Hornfeck *In* Alabama Univ., Research Reports: 1989 NASA/ASEE Summer Faculty Fellowship Program Dec. 1989 17 p (For primary document see N90-19390 12-31)
(Grant NGT-01-008-021)
Avail: NTIS HC A99/MF E06 CSCL 09B

Large data processing installations represent target systems for effective applications of artificial intelligence (AI) constructs. The system organization of a large data processing facility at the NASA Marshall Space Flight Center is presented. The methodology and the issues which are related to AI application to automated operations within a large-scale computing facility are described. Problems to be addressed and initial goals are outlined. Author

N90-19405*# New Orleans Univ., LA. Dept. of Mechanical Engineering.
LOW-ENERGY IMPACT RESISTANCE OF GRAPHITE-EPOXY PLATES AND ALS HONEYCOMB SANDWICH PANELS **c24**
David Hui *In* Alabama Univ., Research Reports: 1989 NASA/ASEE Summer Faculty Fellowship Program Dec. 1989 46 p (For primary document see N90-19390 12-31)
(Grant NGT-01-008-021)
Avail: NTIS HC A99/MF E06 CSCL 11D

Low energy impact may be potentially dangerous for many highly optimized stiff structures. Impact by foreign objects such as birds, ice, and runways stones or dropping of tools occur frequently and the resulting damage and stress concentrations may be unacceptable from a designer's standpoint. The barely visible, yet potentially dangerous dents due to impact of foreign objects on the Advanced Launch System (ALS) structure are studied. Of particular interest is the computation of the maximum peak impact force for a given impactor mass and initial velocity. The theoretical impact forces will be compared with the experimental dropweight results for the ALS face sheets alone as well as the ALS honeycomb sandwich panels. Author

N90-19406*# Ohio Univ., Athens. Dept. of Electrical and Computer Engineering.
INVESTIGATIONS INTO A NEW ALGORITHM FOR CALCULATING H INFINITY OPTIMAL CONTROLLERS **c61**
R. Dennis Irwin *In* Alabama Univ., Research Reports: 1989 NASA/ASEE Summer Faculty Fellowship Program Dec. 1989 28 p (For primary document see N90-19390 12-31)
(Grant NGT-01-008-021)
Avail: NTIS HC A99/MF E06 CSCL 09B

A new algorithm for calculating H (sup infinity) optimal controllers is investigated. The algorithm is significantly simpler than existing approaches and yields much simpler controllers. The design equations are first presented. Special system transformations required to apply the algorithm are then presented. The use of the algorithm with sampled-data systems is outlined in detail. Several constraints on the characteristics of the problem formulation are required for the application of the design equations. The consequences of these constraints are investigated by applying the algorithm to a simplified design for a subsystem of a large space structure ground test facility. The investigation of these constraints is continued by application of the design equations and constraints to an extremely simple tracking problem. The result of these investigations is the development of a frequency dependent weighting strategy that allows realistic control problems to be cast in a form compatible with the new algorithm. Further work is indicated in the area of developing strategies for choosing frequency-dependent weights to achieve specific design goals. The use of the freedom in problem formulation to achieve robustness/performance tradeoffs should also be investigated. It is not clear that the algorithm always leads to simpler controllers. The more restrictive formulation may dictate that frequency-dependent weighting adds to the controller order disproportionately. This effect must also be investigated. Author

N90-19407*# Tennessee Univ., Knoxville. Dept. of Mechanical and Aerospace Engineering.
EVALUATION OF THE HEAT TRANSFER MODULE (FAHT) OF FAILURE ANALYSIS NONLINEAR THERMAL AND STRUCTURAL INTEGRATED CODE (FANTASTIC) **c34**
Majid Keyhani *In* Alabama Univ., Research Reports: 1989 NASA/ASEE Summer Faculty Fellowship Program Dec. 1989 33 p (For primary document see N90-19390 12-31)
(Grant NGT-01-008-021)
Avail: NTIS HC A99/MF E06 CSCL 20D

The heat transfer module of FANTASTIC Code (FAHT) is studied and evaluated to the extend possible during the ten weeks duration of this project. A brief background of the previous studies is given and the governing equations as modeled in FAHT are discussed. FAHT's capabilities and limitations based on these equations and its coding methodology are explained in detail. It is established that with improper choice of element size and time step FAHT's temperature field prediction at some nodes will be below the initial condition. The source of this unrealistic temperature prediction is identified and a procedure is proposed for avoiding this phenomenon. It is further shown that the proposed procedure will converge to an accurate prediction upon mesh refinement. Unfortunately due to lack of time FAHT's ability to accurately account for pyrolysis and surface ablation has not been verified. Therefore, at the present time it can be stated with confidence that FAHT can accurately predict the temperature field for a transient multi-dimensional, orthotropic material with directional dependence, variable property, with nonlinear boundary condition. Such a prediction will provide an upper limit for the temperature field in an ablating decomposing nozzle liner. The pore pressure field, however, will not be known. Author

N90-19408*# Mississippi State Univ., Mississippi State. Dept. of Physics and Astronomy.
RADIAL RESPONSE OF THE BURST AND TRANSIENT SOURCE EXPERIMENT **c93**
John Patrick Lestrade *In* Alabama Univ., Research Reports: 1989 NASA/ASEE Summer Faculty Fellowship Program Dec. 1989 29 p (For primary document see N90-19390 12-31)
(Grant NGT-01-008-021)
Avail: NTIS HC A99/MF E06 CSCL 03B

The Gamma Ray Observatory (GRO) includes four experiments designed for observe the gamma-ray universe, one of which is the Burst And Transient Source Experiment (BATSE). During the first summer with the BATSE team in 1988, laboratory measurements were completed which test the response of the BATSE modules to gamma-ray sources that are non-axial. The results of these observations are necessary for the correct interpretation of BATSE data obtained after it is put in earth orbit. Subsequent analysis of the data revealed a shift in the centroids of the full-energy photopeaks for angles of incidence between about 70 and 110 degrees. This effect was diagnosed as being

due to a radial dependence of the light collecting efficiency of the large-area detector (LAD). Energy-depositing events that occur near the perimeter of the 10-inch radius NaI disc are not as efficiently collected as those events that occur near the disc's center. This radial response is analyzed and in so doing the non-Gaussian shape of the photopeaks seen in the spectra taken at all angles is explained. Author

N90-19409*# Alabama Univ., Tuscaloosa. Dept. of Electrical Engineering.
DETERMINATION OF THE IMPLEMENTATION OF THE 3-AXIS ATTITUDE MOTION SIMULATOR DIGITAL POSITION CONTROLLER **c63**
Mario E. Magana *In* Alabama Univ., Research Reports: 1989 NASA/ASEE Summer Faculty Fellowship Program Dec. 1989 15 p (For primary document see N90-19390 12-31)
(Grant NGT-01-008-021)
Avail: NTIS HC A99/MF E06 CSCL 09B

The digital position controller implemented in the control computer of the 3-axis attitude motion simulator is mathematically reconstructed and documented, since the information supplied with the executable code of this controller was insufficient to make substantial modifications to it. Also developed were methodologies to introduce changes in the controller which do not require rewriting the software. Finally, recommendations are made on possible improvement to the control system performance. Author

N90-19410*# Tulane Univ., New Orleans, LA. Dept. of Mechanical Engineering.
MECHANICS OF AEOLIAN PROCESSES: SOIL EROSION AND DUST PRODUCTION **c45**
M. M. Mehrabadi *In* Alabama Univ., Research Reports: 1989 NASA/ASEE Summer Faculty Fellowship Program Dec. 1989 25 p (For primary document see N90-19390 12-31)
(Grant NGT-01-008-021)
Avail: NTIS HC A99/MF E06 CSCL 13B

Aeolian (wind) processes occur as a result of atmosphere/land-surface system interactions. A thorough understanding of these processes and their physical/mechanical characterization on a global scale is essential to monitoring global change and, hence, is imperative to the fundamental goal of the Earth observing system (Eos) program. Soil erosion and dust production by wind are of consequence mainly in arid and semi arid regions which cover 36 percent of the Earth's land surface. Some recent models of dust production due to wind erosion of agricultural soils and the mechanics of wind erosion in deserts are reviewed and the difficulties of modeling the aeolian transport are discussed. Author

N90-19411*# Mississippi State Univ., Mississippi State. Dept. of Electrical Engineering.
EVALUATION AND ANALYSIS OF THE ORBITAL MANEUVERING VEHICLE VIDEO SYSTEM **c32**
Robert J. Moorhead, II *In* Alabama Univ., Research Reports: 1989 NASA/ASEE Summer Faculty Fellowship Program Dec. 1989 27 p (For primary document see N90-19390 12-31)
(Grant NGT-01-008-021)
Avail: NTIS HC A99/MF E06 CSCL 17B

The work accomplished in the summer of 1989 in association with the NASA/ASEE Summer Faculty Research Fellowship Program at Marshall Space Flight Center is summarized. The task involved study of the Orbital Maneuvering Vehicle (OMV) Video Compression Scheme. This included such activities as reviewing the expected scenes to be compressed by the flight vehicle, learning the error characteristics of the communication channel, monitoring the CLASS tests, and assisting in development of test procedures and interface hardware for the bit error rate lab being developed at MSFC to test the VCU/VRU. Numerous comments and suggestions were made during the course of the fellowship period regarding the design and testing of the OMV Video System. Unfortunately from a technical point of view, the program appears at this point in time to be trouble from an expense prospective and is in fact in danger of being scaled back, if not cancelled altogether. This makes technical improvements prohibitive and cost-reduction measures necessary. Fortunately some cost-reduction possibilities and some significant technical improvements that should cost very little were identified. Author

N90-19412*# Florida Univ., Gainesville. Dept. of Physics.
TRANSMISSION AND REFLECTION STUDIES OF THIN FILMS IN THE VACUUM ULTRAVIOLET **c74**
Lennart R. Peterson *In* Alabama Univ., Research Reports: 1989 NASA/ASEE Summer Faculty Fellowship Program Dec. 1989 12 p (For primary document see N90-19390 12-31)
(Grant NGT-01-008-021)
Avail: NTIS HC A99/MF E06 CSCL 20F

Both the transmittance and reflectance of 2 mm thick MgF2 substrates and of thin films of BaF2, CaF2, LaF3, MgF2, Al2O3, HfO2, and SiO2 deposited on these substrates were measured for the wavelength range 120 nm to 230 nm. Results for BaF2, LaF2 and MgF2 show promise as being good materials from which interference filters can be made. The software and related hardware needed to take large amounts of data automatically in future measurements of the transmittance and reflectance was developed. Author

N90-19413*# Alabama Univ., Huntsville. Dept. of Mathematical Sciences.
ANALYTICAL OPTICAL SCATTERING IN CLOUDS **c74**
Dieudonne D. Phanord *In its* Research Reports: 1989 NASA/ASEE Summer Faculty Fellowship Program Dec. 1989 16 p (For primary document see N90-19390 12-31)
(Grant NGT-01-008-021)
Avail: NTIS HC A99/MF E06 CSCL 20F

An analytical optical model for scattering of light due to lightning by clouds of different geometry is being developed. The self-consistent approach and the equivalent medium concept of Twersky was used to treat the case corresponding to outside illumination. Thus, the resulting multiple scattering problem is transformed with the knowledge of the bulk parameters, into scattering by a single obstacle in isolation. Based on the size parameter of a typical water droplet as compared to the incident wave length, the problem for the single scatterer equivalent to the distribution of cloud particles can be solved either by Mie or Rayleigh scattering theory. The super computing code of Wiscombe can be used immediately to produce results that can be compared to the Monte Carlo computer simulation for outside incidence. A fairly reasonable inverse approach using the solution of the outside illumination case was proposed to model analytically the situation for point sources located inside the thick optical cloud. Its mathematical details are still being investigated. When finished, it will provide scientists an enhanced capability to study more realistic clouds. For testing purposes, the direct approach to the inside illumination of clouds by lightning is under consideration. Presently, an analytical solution for the cubic cloud will soon be obtained. For cylindrical or spherical clouds, preliminary results are needed for scattering by bounded obstacles above or below a penetrable surface interface. Author

N90-19414*# Ohio Univ., Athens. Dept. of Electrical and Computer Engineering.
RADAR TRANSPONDER ANTENNA PATTERN ANALYSIS FOR THE SPACE SHUTTLE **c32**
Roger Radcliff *In* Alabama Univ., Research Reports: 1989 NASA/ASEE Summer Faculty Fellowship Program Dec. 1989 25 p (For primary document see N90-19390 12-31)
Avail: NTIS HC A99/MF E06 CSCL 17I

In order to improve tracking capability, radar transponder antennas will soon be mounted on the Shuttle solid rocket boosters (SRB). These four antennas, each being identical cavity-backed helices operating at 5.765 GHz, will be mounted near the top of the SRB's, adjacent to the intertank portion of the external tank. The purpose is to calculate the roll-plane pattern (the plane perpendicular to the SRB axes and containing the antennas) in the presence of this complex electromagnetic environment. The large electrical size of this problem mandates an optical

(asymptotic) approach. Development of a specific code for this application is beyond the scope of a summer fellowship; thus a general purpose code, the Numerical Electromagnetics Code - Basic Scattering Code, was chosen as the computational tool. This code is based on the modern Geometrical Theory of Diffraction, and allows computation of scattering of bodies composed of canonical problems such as plates and elliptic cylinders. Apertures mounted on a curved surface (the SRB) cannot be accomplished by the code, so an antenna model consisting of wires excited by a method of moments current input was devised that approximated the actual performance of the antennas. The improvised antenna model matched well with measurements taken at the MSFC range. The SRB's, the external tank, and the shuttle nose were modeled as circular cylinders, and the code was able to produce what is thought to be a reasonable roll-plane pattern.
Author

N90-19415*# Alabama Univ., Tuscaloosa. Dept. of Engineering Mechanics.
ROCOPT: A USER FRIENDLY INTERACTIVE CODE TO OPTIMIZE ROCKET STRUCTURAL COMPONENTS **c20**
William K. Rule *In* Alabama Univ., Research Reports: 1989 NASA/ASEE Summer Faculty Fellowship Program Dec. 1989 28 p (For primary document see N90-19390 12-31)
(Grant NGT-01-008-021)
Avail: NTIS HC A99/MF E06 CSCL 21H

ROCOPT is a user-friendly, graphically-interfaced, micro-computer-based computer program (IBM compatible) that optimizes rocket components by minimizing the structural weight. The rocket components considered are ring stiffened truncated cones and cylinders. The applied loading is static, and can consist of any combination of internal or external pressure, axial force, bending moment, and torque. Stress margins are calculated by means of simple closed form strength of material type equations. Stability margins are determined by approximate, orthotropic-shell, closed-form equations. A modified form of Powell's method, in conjunction with a modified form of the external penalty method, is used to determine the minimum weight of the structure subject to stress and stability margin constraints, as well as user input constraints on the structural dimensions. The graphical interface guides the user through the required data prompts, explains program options and graphically displays results for easy interpretation.
Author

N90-19416*# Memphis State Univ., TN. Dept. of Mechanical Engineering.
ITERATIVE PROCEDURES FOR SPACE SHUTTLE MAIN ENGINE PERFORMANCE MODELS **c20**
L. Michael Santi *In* Alabama Univ., Research Reports: 1989 NASA/ASEE Summer Faculty Fellowship Program Dec. 1989 29 p (For primary document see N90-19390 12-31)
(Grant NGT-01-008-021)
Avail: NTIS HC A99/MF E06 CSCL 21H

Performance models of the Space Shuttle Main Engine (SSME) contain iterative strategies for determining approximate solutions to nonlinear equations reflecting fundamental mass, energy, and pressure balances within engine flow systems. Both univariate and multivariate Newton-Raphson algorithms are employed in the current version of the engine Test Information Program (TIP). Computational efficiency and reliability of these procedures is examined. A modified trust region form of the multivariate Newton-Raphson method is implemented and shown to be superior for off nominal engine performance predictions. A heuristic form of Broyden's Rank One method is also tested and favorable results based on this algorithm are presented.
Author

N90-19417*# Mississippi State Univ., Mississippi State. Dept. of Computer Science.
MARSHALL AVIONICS TESTBED SYSTEM (MAST) **c06**
Wayne D. Smith *In* Alabama Univ., Research Reports: 1989 NASA/ASEE Summer Faculty Fellowship Program Dec. 1989 39 p (For primary document see N90-19390 12-31)
(Grant NGT-01-008-021)
Avail: NTIS HC A99/MF E06 CSCL 01D

Work accomplished in the summer of 1989 in association with the NASA/ASEE Summer Faculty Research Fellowship Program at Marshall Space Flight Center is summarized. The project was aimed at developing detailed specifications for the Marshall Avionics System Testbed (MAST). This activity was to include the definition of the testbed requirements and the development of specifications for a set of standard network nodes for connecting the testbed to a variety of networks. The project was also to include developing a timetable for the design, implementation, programming and testing of the testbed. Specifications of both hardware and software components for the system were to be included.
Author

N90-19418*# Wichita State Univ., KS. Dept. of Mechanical Engineering.
HEAT SINK EFFECTS ON WELD BEAD: VPPA PROCESS **c37**
Paul O. Steranka, Jr. *In* Alabama Univ., Research Reports: 1989 NASA/ASEE Summer Faculty Fellowship Program Dec. 1989 27 p (For primary document see N90-19390 12-31)
(Grant NGT-01-008-021)
Avail: NTIS HC A99/MF E06 CSCL 11F

An investigation into the heat sink effects due to weldment irregularities and fixtures used in the variable polarity plasma arc (VPPA) process was conducted. A basic two-dimensional model was created to represent the net heat sink effect of surplus material using Duhamel's theorem to superpose the effects of an infinite number of line heat sinks of variable strength. Parameters were identified that influence the importance of heat sink effects. A characteristic length, proportional to the thermal diffusivity of the weldment material divided by the weld torch travel rate, correlated with heat sinking observations. Four tests were performed on 2219-T87 aluminum plates to which blocks of excess material were mounted in order to demonstrate heat sink effects. Although the basic model overpredicted these effects, it correctly indicated the trends shown in the experimental study and is judged worth further refinement.
Author

N90-19419*# Alabama Univ., Huntsville. Dept. of Mechanical Engineering.
FREQUENCY RESPONSE OF ELECTROCHEMICAL CELLS **c44**
Daniel L. Thomas *In its* Research Reports: 1989 NASA/ASEE Summer Faculty Fellowship Program Dec. 1989 23 p (For primary document see N90-19390 12-31)
(Grant NGT-01-008-021)
Avail: NTIS HC A99/MF E06 CSCL 10A

Impedance concepts can be applied to the analysis of battery electrodes, yielding information about the structure of the electrode and the processes occurring in the electrode. Structural parameters such as the specific area (surface area per gram of electrode) can be estimated. Electrode variables such as surface overpotential, ohmic losses, and diffusion limitations may be studied. Nickel and cadmium electrodes were studied by measuring the ac impedance as a function of frequency, and the specific areas that were determined were well within the range of specific areas determined from BET measurements. Impedance spectra were measured for the nickel and cadmium electrodes, and for a 20 A-hr NiCd battery as functions of the state of charge. More work is needed to determine the feasibility of using frequency response as a nondestructive testing technique for batteries.
Author

N90-19420*# Kentucky Univ., Lexington. Dept. of Electrical Engineering.
YAW RATE CONTROL OF AN AIR BEARING VEHICLE **c08**
Bruce L. Walcott *In* Alabama Univ., Research Reports: 1989 NASA/ASEE Summer Faculty Fellowship Program Dec. 1989 46 p (For primary document see N90-19390 12-31)
(Grant NGT-01-008-021)
Avail: NTIS HC A99/MF E06 CSCL 01C

The results of a 6 week project which focused on the problem

of controlling the yaw (rotational) rate the air bearing vehicle used on NASA's flat floor facility are summarized. Contained within is a listing of the equipment available for task completion and an evaluation of the suitability of this equipment. The identification (modeling) process of the air bearing vehicle is detailed as well as the subsequent closed-loop control strategy. The effectiveness of the solution is discussed and further recommendations are included. Author

N90-19421*# Alabama Univ., Huntsville. Dept. of Aerospace Engineering.
THE INFLUENCE OF A WALL FUNCTION ON TURBINE BLADE HEAT TRANSFER PREDICTION **c07**
Kevin W. Whitaker *In its* Research Reports: 1989 NASA/ASEE Summer Faculty Fellowship Program Dec. 1989 21 p (For primary document see N90-19390 12-31)
(Grant NGT-01-008-021)
Avail: NTIS HC A99/MF E06 CSCL 21E

The second phase of a continuing investigation to improve the prediction of turbine blade heat transfer coefficients was completed. The present study specifically investigated how a numeric wall function in the turbulence model of a two-dimensional boundary layer code, STAN5, affected heat transfer prediction capabilities. Several sources of inaccuracy in the wall function were identified and then corrected or improved. Heat transfer coefficient predictions were then obtained using each one of the modifications to determine its effect. Results indicated that the modifications made to the wall function can significantly affect the prediction of heat transfer coefficients on turbine blades. The improvement in accuracy due the modifications is still inconclusive and is still being investigated. Author

N90-19422*# Auburn Univ., AL. Dept. of Mechanical Engineering.
MULTIBODY MODELING AND VERIFICATION
Gloria J. Wiens *In* Alabama Univ., Research Reports: 1989 NASA/ASEE Summer Faculty Fellowship Program Dec. 1989 42 p (For primary document see N90-19390 12-31)
(Grant NGT-01-008-021)
Avail: NTIS HC A99/MF E06 CSCL 13B

A summary of a ten week project on flexible multibody modeling, verification and control is presented. Emphasis was on the need for experimental verification. A literature survey was conducted for gathering information on the existence of experimental work related to flexible multibody systems. The first portion of the assigned task encompassed the modeling aspects of flexible multibodies that can undergo large angular displacements. Research in the area of modeling aspects were also surveyed, with special attention given to the component mode approach. Resulting from this is a research plan on various modeling aspects to be investigated over the next year. The relationship between the large angular displacements, boundary conditions, mode selection, and system modes is of particular interest. The other portion of the assigned task was the generation of a test plan for experimental verification of analytical and/or computer analysis techniques used for flexible multibody systems. Based on current and expected frequency ranges of flexible multibody systems to be used in space applications, an initial test article was selected and designed. A preliminary TREETOPS computer analysis was run to ensure frequency content in the low frequency range, 0.1 to 50 Hz. The initial specifications of experimental measurement and instrumentation components were also generated. Resulting from this effort is the initial multi-phase plan for a Ground Test Facility of Flexible Multibody Systems for Modeling Verification and Control. The plan focusses on the Multibody Modeling and Verification (MMV) Laboratory. General requirements of the Unobtrusive Sensor and Effector (USE) and the Robot Enhancement (RE) laboratories were considered during the laboratory development. Author

N90-19423*# Alabama Univ., Tuscaloosa. Dept. of Engineering Mechanics.
A VECTORIZED ALGORITHM FOR 3D DYNAMICS OF A TETHERED SATELLITE **c18**
Howard B. Wilson *In* Alabama Univ., Research Reports: 1989 NASA/ASEE Summer Faculty Fellowship Program Dec. 1989 30 p (For primary document see N90-19390 12-31)
(Grant NGT-01-008-021)
Avail: NTIS HC A99/MF E06 CSCL 22B

Equations of motion characterizing the three dimensional motion of a tethered satellite during the retrieval phase are studied. The mathematical model involves an arbitrary number of point masses connected by weightless cords. Motion occurs in a gravity gradient field. The formulation presented accounts for general functions describing support point motion, rate of tether retrieval, and arbitrary forces applied to the point masses. The matrix oriented program language MATLAB is used to produce an efficient vectorized formulation for computing natural frequencies and mode shapes for small oscillations about the static equilibrium configuration; and for integrating the nonlinear differential equations governing large amplitude motions. An example of time response pertaining to the skip rope effect is investigated. Author

N90-19424*# Alabama Univ., Huntsville. Dept. of Biological Sciences.
TECHNIQUES FOR STUDYING THE EFFECTS OF MICROGRAVITY ON MODEL PARTICLE/CELL SYSTEMS **c29**
Ronald B. Young *In its* Research Reports: 1989 NASA/ASEE Summer Faculty Fellowship Program Dec. 1989 18 p (For primary document see N90-19390 12-31)
(Grant NGT-01-008-021)
Avail: NTIS HC A99/MF E06 CSCL 22A

In an effort to learn more about the effects of a simulated low gravity environment on skeletal muscle, skeletal muscle cell cultures were grown within the lumen of XM-80 hollow fibers (i.d. = 0.5 mm) in a Clinostat rotating at 100 rpm. Cells were isolated from the thigh muscle tissue of 12 day embryos and were cultured for up to 14 days in the hollow fiber environment. Cells proliferated to confluency within several days, and fusion into multinucleated myotubes was then apparent. Fibers were stretched by a built-in spring mechanism to hold the fiber tightly at the center of rotation, and sections of the fiber were removed at 3, 7 and 14 days for electron microscopic analysis. When the Clinostat is rotated in the horizontal position, the gravity vector approaches zero and the cells are in an environment that simulates microgravity. Control experiments consist of one fiber rotated in the vertical position in the clinostat and another fiber that is held in a horizontal configuration in a comparable sized tube that is not rotated at all. Examination of skeletal muscle cells by electron microscopy revealed that myoblast fusion and myofibril accumulation were extensive. Two general conclusions were apparent. First, muscle cells undergo the normal progression of proliferation, fusion, and myofibril assembly in the presence of simulated microgravity for the first week in culture. After 14 days, however, many muscle fibers undergo degeneration such that myofibrillar structures are not extensive or well organized. Second, although no major abnormalities in myofibril assembly were detected in Clinostat-rotated cultures in comparison to controls that were not rotated in a Clinostat, the myofibrils in non-rotated controls tend to be more highly organized than those in either horizontally or vertically rotated Clinostat samples. Author

N90-19425* National Aeronautics and Space Administration. Pasadena Office, CA.
HIGH DENSITY TAPE CASTING SYSTEM Patent
Earl R. Collins, Jr., inventor (to NASA) 13 Jun. 1989 61 p Filed 21 Oct. 1986
(NASA-Case-NPO-16901-1-CU; US-Patent-4,839,121; US-Patent-Appl-SN-921574; US-Patent-Class-264-114; US-Patent-Class-264-311; US-Patent-Class-425-75; US-Patent-Class-425-425; US-Patent-Class-425-435; US-Patent-Class-425-73) Avail: US Patent and Trademark Office CSCL 13H

A system is provided for casting thin sheets (or tapes) of particles bound together, that are used for oxygen membranes and other applications, which enables the particles to be cast at a high packing density in a tape of uniform thickness. A slurry contains the particles, a binder, and a solvent, and is cast against the inside walls of a rotating chamber. Prior to spraying the slurry against the chamber walls, a solvent is applied to a container. The solvent evaporates to saturate the chamber with solvent vapor. Only then is the slurry cast. As a result, the slurry remains fluid long enough to spread evenly over the casting surface formed by the chamber, and for the slurry particles to become densely packed. Only then is the chamber vented to remove solvent, so the slurry can dry. The major novel feature is applying solvent vapor to a rotating chamber before casting slurry against the chamber walls.
Official Gazette of the U.S. Patent and Trademark Office

N90-19426# Center for Night Vision and Electro-Optics, Fort Belvoir, VA.
RELIABILITY TESTING OF THE HUGHES TEMPERATURE CONTROLLED 1/4 WATT SPLIT CYCLE CRYOGENIC COOLER (HD-1045 (V)/UA) Final Report, 7 Jun. 1988 - 6 Mar. 1989
James Shaffer, Howard Dunmire, Raemon Samuels, and Martin Trively Dec. 1989 31 p
(AD-A216696; AMSEL-NV-TR-0089) Avail: NTIS HC A03/MF A01 CSCL 13/1

The U.S. Army CECOM Center for Night Vision and Electro-Optics (C2NVEO) is responsible for developing cryogenic coolers for all infrared imaging systems for the Army. C2NVEO also maintains configuration management control of the forward-looking infrared (FLIR) Common Module coolers used in thermal imagers in fielded Army weapon systems such as: M60A3 and M1 Tanks, Bradley Fighting Vehicle (BFV) System, tube-launched, optically tracked, wire-guided (TOW) Missile System, and Army Attack Helicopters. Currently, there are over 30,000 coolers in fielded systems and several thousand more are added each year. C2NVEO conducts development programs and monitors contractor internal research and development efforts to improve cooler performance such as reliability, audio noise, power consumption, and output vibration. The HD-1045 1/4-Watt Split Stirling Cooler was originally designed and developed by the C2NVEO in the early 1970s as a replacement for the gas bottle/cryostat used on the Manportable Common Thermal Night Sights. To date, however, the HD-1045 cooler has been used in the field in the Integrated Sight Unit (ISU) of the BFV System and is currently being used in the Driver Thermal Viewer (DTV) full scale development program. This document describes and reports the results of reliability testing done on Hughes Temperature Controlled 1/4 Watt split Cycle Cryogenic Coolers (HD-1045 (V)/UA), referred to herein as the coolers. GRA

N90-19427* National Aeronautics and Space Administration. Langley Research Center, Hampton, VA.
METHOD FOR MAINTAINING PRECISE SUCTION STRIP POROSITIES Patent
Frank H. Gallimore, inventor (to NASA) (McDonnell-Douglas Corp., Huntington Beach, CA.) 25 Jul. 1989 10 p Filed 22 Jul. 1988
(NASA-Case-LAR-13638-1; US-Patent-4,851,071;
US-Patent-Appl-SN-223124; US-Patent-Class-156-344;
US-Patent-Class-244-133; US-Patent-Class-427-272) Avail: US Patent and Trademark Office CSCL 13H

This invention relates to a masking method generally and, more particularly to a method of masking perforated titanium sheets having laminar control suction strips. As illustrated in the drawings, a nonaerodynamic surface of a perforated sheet has alternating suction strip areas and bonding land areas. Suction strip tapes overlie the bonding land areas during application of a masking material to an upper surface of the suction strip tapes. Prior to bonding the perforated sheet to a composite structure, the bonding land tapes are removed. The entire opposite aerodynamic surface is masked with tape before bonding. This invention provides a precise control of suction strip porosities by ensuring that no chemicals penetrate the suction strip areas during bonding.
Official Gazette of the U.S. Patent and Trademark Office

N90-19428# Oak Ridge National Lab., TN. Building Equipment Research Program.
ADVANCED ABSORPTION TECHNOLOGY DEVELOPMENT IN THE UNITED STATES
R. C. DeVault 1990 13 p Presented at the 3rd International Energy Agency Heat Pump Conference, Tokyo, Japan, 12-15 Mar. 1990
(Contract DE-AC05-84OR-21400)
(DE90-001336; CONF-900334-1) Avail: NTIS HC A03/MF A01

Advanced technologies for gas-fired absorption heat pumps, air-conditioners, and chillers for building space conditioning are being developed in the United States with support from a number of organizations and manufacturers. Single-effect cycle absorption heat pumps were developed in the 1970's, but proved to be too costly to manufacture. Several advanced cycle heat pump projects were started in 1982 and 1983 and have demonstrated substantially improved efficiency with simultaneously reduced manufacturing cost. Development of advanced cycle residential heat pumps continues with a goal of product introduction by 1992 or 1993. Because of the importance of air-conditioning, projects have also been underway since the mid 1980's to substantially improve the cooling performance of absorption equipment. Air-cooled LiBr/H2O air-conditioning technology is being developed to increase the potential markets for double-effect equipment, and triple-effect cycles are being developed to dramatically improve cooling efficiency compared to existing absorption chillers. DOE

N90-20002# Army Cold Regions Research and Engineering Lab., Hanover, NH.
INTRODUCTION TO DRILLING TECHNOLOGY
Malcom Mellor *In* ESA, Physics and Mechanics of Cometary Materials Dec. 1989 p 95-114 (For primary document see N90-19989 12-90)
Copyright Avail: NTIS HC A10/MF A02; ESA Publications Div., ESTEC, Noordwijk, Netherlands, 60 Dutch guilders

32 COMMUNICATIONS AND RADAR

Includes radar; land and global communications; communications theory; and optical communications.

For related information see also *04 Aircraft Communications and Navigation* and *17 Space Communications, Spacecraft Communications, Command and Tracking.* For search and rescue see *03 Air Transportation and Safety,* and *16 Space Transportation.*

N90-19429*# Hawaii Univ., Honolulu. Dept. of Electrical Engineering.
ON LINEAR STRUCTURE AND PHASE ROTATION INVARIANT PROPERTIES OF BLOCK 2(SUP I)-PSK MODULATION CODES
Shu Lin 31 Jan. 1990 14 p
(Grant NAG5-931)
(NASA-CR-186308; NAS 1.26:186308) Avail: NTIS HC A03/MF A01 CSCL 20N

Two important structural properties of block 2(l)-ary PSK (phase shift keying) modulation codes, linear structure and phase symmetry, are investigated. For an additive white Gaussian noise (AWGN) channel, the error performance of a modulation code depends on its squared Euclidean distance distribution. Linear structure of a code makes the error performance analysis much easier. Phase symmetry of a code is important in resolving carrier phase ambiguity and ensuring rapid carrier phase resynchronization after temporary loss of synchronization. It is desirable for a code to have as many phase symmetries as possible. A 2(l)-ary modulation code is represented here as a code with symbols from the integer group. S sub 2(l) PSK = (0,1,2,...,2(l)-1), under the modulo-2(l) addition. The linear structure of block 2(l)-ary PSK modulation codes over S sub 2(l)-ary PSK with respect to the modulo-2(l) vector addition is defined, and conditions under which

a block 2(l)-ary PSK modulation code is linear are derived. Once the linear structure is developed, phase symmetry of a block 2(l)-ary PSK modulation code is studied. It is a necessary and sufficient condition for a block 2(l)-PSK modulation code, which is linear as a binary code, to be invariant under 180 deg/2(l-h) phase rotation, for 1 is less than or equal to h is less than or equal to l. A list of short 8-PSK and 16-PSK modulation codes is given, together with their linear structure and the smallest phase rotation for which a code is invariant. Author

N90-19430# Department of the Navy, Washington, DC.
APPARATUS AND METHOD FOR MINIMIZING POLARIZATION-INDUCED SIGNAL FADING IN AN INTERFEROMETRIC FIBER-OPTIC SENSOR USING INPUT-POLARIZATION MODULATION Patent Application
Alan A. Kersey, inventor (to Navy) and Michael J. Marrone, inventor (to Navy) 21 Jul. 1989 35 p LIMITED REPRODUCIBILITY: Availability: Document partially illegible
(AD-D014315; US-Patent-Appl-SN-838390) Avail: NTIS HC A03/MF A01 CSCL 20/6

An apparatus for minimizing polarization-induced signal fading in an interferometric fiber optic sensor is disclosed. The apparatus includes an optical source for providing an input light beam, a polarization modulator for modulating the state of polarization of the input beam into at least three states represented by mutually perpendicular polarization vectors on a Poincare Sphere. The apparatus further includes means for conveying the input light beam with the at least three mutually perpendicular modulated states of polarization to the fiber optic sensor, the interferometric fiber optic sensor being responsive to the input light beam with modulated polarization states for developing an interference pattern output, wherein the interference pattern output has at least three visibilities corresponding to the input states of polarization. A photodetector is responsive to the interference pattern output for developing an electrical signal having at least three amplitudes corresponding to the at least three states of polarization. An output circuit is responsive to the electrical photodetector signal for time-sampling the photodetector signal having three amplitudes corresponding to the at least three mutually perpendicular input states of polarization and selecting the one having maximum visibility. A method for minimizing polarization-induced signal fading is also disclosed. GRA

N90-19431 Department of the Navy, Washington, DC.
AUTOMATIC THRESHOLDING MULTICHANNEL DIGITAL RADAR EARLY WARNING SYSTEM Patent
William P. Huntley, inventor (to Navy) 22 Aug. 1989 6 p Filed 4 Apr. 1988
(AD-D014323; US-Patent-4,860,013; US-Patent-Appl-SN-176958)
Avail: US Patent and Trademark Office CSCL 17/9

An RF multiplexer divides an incoming signal from an RF antenna into discrete frequency bands. Each frequency band has its own separate circuit on separate lines to operate on the frequency band and determine if a radar signal is present or if only noise is present on the line. This is done by comparing the incoming signal for magnitude with a DC signal that is generated within the circuit and is proportional to the noise within the frequency band. An indication that any of the signals within the discrete frequency bands exceed the DC signal generated within the same band results in an alarm indication. GRA

N90-19432 Department of the Navy, Washington, DC.
HIGH THROUGHPUT DATA COMMUNICATION SYSTEM Patent
Paul J. Giorgio, inventor (to Navy) 4 May 1988 15 p Filed 4 May 1988
(AD-D014342; US-Patent-4,864,567; US-Patent-Appl-SN-195992)
Avail: US Patent and Trademark Office

A multiline modem system provides to a computer connect ion a plurality of telephone lines for transmitting and receiving digital computer data at throughput rates that exceed those of single line modem systems. The system determines the number of available telephone lines, sequences through a series of telephone re-dials, and acknowledges all connections. When the last connection is verified, the system is on-line and data transfer can begin. The system described uses state-of-the-art components and meets FCC Part 68 requirements for connection to the switched telephone network. GRA

N90-19433# Naval Postgraduate School, Monterey, CA. Dept. of Computer Science.
DYNAMIC RECONFIGURATION AND LINK FAULT TOLERANCE IN A TRANSPUTER NETWORK M.S. Thesis
Winfred Prescott Pikelis Jun. 1989 161 p
(AD-A215105) Avail: NTIS HC A08/MF A01 CSCL 12/7

This thesis explores dynamic reconfiguration and link fault tolerance in a transputer network using software controlled crossbars. A message exchange system was designed, implemented and evaluated to facilitate various aspects of dynamic interconnectivity between processing nodes, as well as detection and recovery from failed network links without loss of data. As implemented, the message exchange can be embedded with application code which can direct network topology to facilitate code execution. GRA

N90-19434*# Jet Propulsion Lab., California Inst. of Tech., Pasadena.
THE TELECOMMUNICATIONS AND DATA ACQUISITION REPORT Quarterly Report, Jul. - Sep. 1989
E. C. Posner, ed. 15 Nov. 1989 225 p
(NASA-CR-185033; JPL-TDA-PR-42-99; NAS 1.26:185033) Avail: NTIS HC A10/MF A02 CSCL 17B

Developments in programs managed by JPL's Office of Telecommunications and Data Acquisition (TDA) are provided. Activities of the Deep Space Network and its associated Ground Communications Facility in planning, in supporting research and technology, in implementation, and in operations are reported in space communications, radio navigation, radio science, and ground-based radio and radar astronomy. For individual titles, see N90-19435 through N90-19452.

N90-19435*# Jet Propulsion Lab., California Inst. of Tech., Pasadena.
DETERMINATION OF EARTH ORIENTATION USING THE GLOBAL POSITIONING SYSTEM **c43**
A. P. Freedman *In its* The Telecommunications and Data Acquisition Report 15 Nov. 1989 p 1-11 (For primary document see N90-19434 12-32)
Avail: NTIS HC A10/MF A02 CSCL 08E

Modern spacecraft tracking and navigation require highly accurate Earth-orientation parameters. For near-real-time applications, errors in these quantities and their extrapolated values are a significant error source. A globally distributed network of high-precision receivers observing the full Global Positioning System (GPS) configuration of 18 or more satellites may be an efficient and economical method for the rapid determination of short-term variations in Earth orientation. A covariance analysis using the JPL Orbit Analysis and Simulation Software (OASIS) was performed to evaluate the errors associated with GPS measurements of Earth orientation. These GPS measurements appear to be highly competitive with those from other techniques and can potentially yield frequent and reliable centimeter-level Earth-orientation information while simultaneously allowing the oversubscribed Deep Space Network (DSN) antennas to be used more for direct project support. Author

N90-19436*# Jet Propulsion Lab., California Inst. of Tech., Pasadena.
SIMPLE ANALYTIC POTENTIALS FOR LINEAR ION TRAPS
G. R. Janik, J. D. Prestage, and L. Maleki *In its* The Telecommunications and Data Acquisition Report 15 Nov. 1989 p 12-19 (For primary document see N90-19434 12-32)
Avail: NTIS HC A10/MF A02 CSCL 17B

A simple analytical model was developed for the electric and ponderomotive (trapping) potentials in linear ion traps. This model was used to calculate the required voltage drive to a mercury trap, and the result compares well with experiments. The model

gives a detailed picture of the geometric shape of the trapping potenital and allows an accurate calculation of the well depth. The simplicity of the model allowed an investigation of related, more exotic trap designs which may have advantages in light-collection efficiency. Author

N90-19437*# Jet Propulsion Lab., California Inst. of Tech., Pasadena.
MICROWAVE OSCILLATOR WITH REDUCED PHASE NOISE BY NEGATIVE FEEDBACK INCORPORATING MICROWAVE SIGNALS WITH SUPPRESSED CARRIER **c33**
G. J. Dick and J. Saunders *In its* The Telecommunications and Data Acquisition Report 15 Nov. 1989 p 20-33 (For primary document see N90-19434 12-32)
Avail: NTIS HC A10/MF A02 CSCL 09A

Oscillator configurations which reduce the effect of 1/f noise sources for both direct feedback and stabilized local oscillator (STALO) circuits are developed and analyzed. By appropriate use of carrier suppression, a small signal is generated which suffers no loss of loop phase information or signal-to-noise ratio. This small signal can be amplified without degradation by multiplicative amplifier noise, and can be detected without saturation of the detector. Together with recent advances in microwave resonator Qs, these circuit improvements will make possible lower phase noise than can be presently achieved without the use of cryogenic devices. Author

N90-19438*# Jet Propulsion Lab., California Inst. of Tech., Pasadena.
EFFECT OF LASER FREQUENCY NOISE ON FIBER-OPTIC FREQUENCY REFERENCE DISTRIBUTION **c36**
R. T. Logan, Jr., G. F. Lutes, and L. Maleki *In its* The Telecommunications and Data Acquisition Report 15 Nov. 1989 p 34-42 (For primary document see N90-19434 12-32)
Avail: NTIS HC A10/MF A02 CSCL 20E

The effect of the linewidth of a single longitude-mode laser on the frequency stability of a frequency reference transmitted over a single-mode optical fiber is analyzed. The interaction of the random laser frequency deviations with the dispersion of the optical fiber is considered to determine theoretically the effect on the Allan deviation (square root of the Allan variance) of the transmitted frequency reference. It is shown that the magnitude of this effect may determine the limit of the ultimate stability possible for frequency reference transmission on optical fiber, but is not a serious limitation to present system performance. Author

N90-19439*# Jet Propulsion Lab., California Inst. of Tech., Pasadena.
THERMAL COEFFICIENT OF DELAY FOR VARIOUS COAXIAL AND FIBER-OPTIC CABLES
G. F. Lutes and W. Diener *In its* The Telecommunications and Data Acquisition Report 15 Nov. 1989 p 43-59 (For primary document see N90-19434 12-32)
Avail: NTIS HC A10/MF A02 CSCL 17B

Data are presented on the thermal coefficient of delay for various coaxial and fiber optic cables, as measured by the Frequency and Timing Systems Engineering Group and the Time and Frequency Systems Research Group. The measured pressure coefficient of delay is also given for the air-dielectric coaxial cables. A description of the measurement method and a description of each of the cables and its use at JPL and in the DSN are included. An improvement in frequency and phase stability by a factor of ten is possible with the use of fiber optics. Author

N90-19440*# Jet Propulsion Lab., California Inst. of Tech., Pasadena.
PERFORMANCE OF THE ALL-DIGITAL DATA-TRANSITION TRACKING LOOP IN THE ADVANCED RECEIVER
U. Cheng and S. Hinedi *In its* The Telecommunications and Data Acquisition Report 15 Nov. 1989 p 60-71 (For primary document see N90-19434 12-32)
Avail: NTIS HC A10/MF A02 CSCL 17B

The performance of the all-digital data-transition tracking loop (DTTL) with coherent or noncoherent sampling is described. The effects of few samples per symbol and of noncommensurate sampling rates and symbol rates are addressed and analyzed. Their impacts on the loop phase-error variance and the mean time to lose lock (MTLL) are quantified through computer simulations. The analysis and preliminary simulations indicate that with three to four samples per symbol, the DTTL can track with negligible jitter because of the presence of earth Doppler rate. Furthermore, the MTLL is also expected to be large engough to maintain lock over a Deep Space Network track. Author

N90-19441*# Jet Propulsion Lab., California Inst. of Tech., Pasadena.
COSTAS LOOP LOCK DETECTION IN THE ADVANCED RECEIVER
A. Mileant and S. Hinedi *In its* The Telecommunications and Data Acquisition Report 15 Nov. 1989 p 72-89 (For primary document see N90-19434 12-32)
Avail: NTIS HC A10/MF A02 CSCL 17B

The advanced receiver currently being developed uses a Costas digital loop to demodulate the subcarrier. Previous analyses of lock detector algorithms for Costas loops have ignored the effects of the inherent correlation between the samples of the phase-error process. Accounting for this correlation is necessary to achieve the desired lock-detection probability for a given false-alarm rate. Both analysis and simulations are used to quantify the effects of phase correlation on lock detection for the square-law and the absolute-value type detectors. Results are obtained which depict the lock-detection probability as a function of loop signal-to-noise ratio for a given false-alarm rate. The mathematical model and computer simulation show that the square-law detector experiences less degradation due to phase jitter than the absolute-value detector and that the degradation in detector signal-to-noise ratio is more pronounced for square-wave than for sine-wave signals. Author

N90-19442*# Jet Propulsion Lab., California Inst. of Tech., Pasadena.
PHOTON STATISTICAL LIMITATIONS FOR DAYTIME OPTICAL TRACKING **c74**
W. M. Folkner and M. H. Finger *In its* The Telecommunications and Data Acquisition Report 15 Nov. 1989 p 90-97 (For primary document see N90-19434 12-32)
Avail: NTIS HC A10/MF A02 CSCL 20F

Tracking of interplanetary spacecraft equipped with optical communication systems by using astrometric instruments is being investigated by JPL. Existing instruments are designed to work at night and, for bright sources, are limited by tropospheric errors. To provide full coverage of the solar system, astrometric tracking instruments must either be capable of daytime operation or be space-based. The integration times necessary for the ground-based daytime photon statistical errors to reach a given accuracy level (5 to 50 nanoradians) were computed for an ideal astrometric instrument. The required photon statistical integration times are found to be shorter than the tropospheric integrations times for the ideal detector. Since the astrometric need not be limited by photon statistics even under daytime conditions, it may be fruitful to investigate instruments for daytime optical tracking. Author

N90-19443*# Jet Propulsion Lab., California Inst. of Tech., Pasadena.
MEMORY MANAGEMENT IN TRACEBACK VITERBI DECODERS **c60**
O. Collins (Johns Hopkins Univ., Baltimore, MD.) and F. Pollara *In its* The Telecommunications and Data Acquisition Report 15 Nov. 1989 p 98-104 (For primary document see N90-19434 12-32)
Avail: NTIS HC A10/MF A02 CSCL 09B

The new Viterbi decoder for long constraint length codes, under development for the Deep Space Network, stores path information according to an algorithm called traceback. The details of a particular implementation of this algorithm, based on three memory buffers, are described. The penalties in increased storage

requirement and longer decoding delay are offset by the reduced amount of data that needs to be exchanged between processors, in a parallel architecture decoder. Author

N90-19444*# Jet Propulsion Lab., California Inst. of Tech., Pasadena.
SOME EASILY ANALYZABLE CONVOLUTIONAL CODES c17
R. McEliece, S. Dolinar, F. Pollara, and H. VanTilborg (Technische Univ., Eindhoven, Netherlands) *In its* The Telecommunications and Data Acquisition Report 15 Nov. 1989 p 105-114 (For primary document see N90-19434 12-32)
Avail: NTIS HC A10/MF A02 CSCL 09F

Convolutional codes have played and will play a key role in the downlink telemetry systems on many NASA deep-space probes, including Voyager, Magellan, and Galileo. One of the chief difficulties associated with the use of convolutional codes, however, is the notorious difficulty of analyzing them. Given a convolutional code as specified, say, by its generator polynomials, it is no easy matter to say how well that code will perform on a given noisy channel. The usual first step in such an analysis is to computer the code's free distance; this can be done with an algorithm whose complexity is exponential in the code's constraint length. The second step is often to calculate the transfer function in one, two, or three variables, or at least a few terms in its power series expansion. This step is quite hard, and for many codes of relatively short constraint lengths, it can be intractable. However, a large class of convolutional codes were discovered for which the free distance can be computed by inspection, and for which there is a closed-form expression for the three-variable transfer function. Although for large constraint lengths, these codes have relatively low rates, they are nevertheless interesting and potentially useful. Furthermore, the ideas developed here to analyze these specialized codes may well extend to a much larger class. Author

N90-19445*# Jet Propulsion Lab., California Inst. of Tech., Pasadena.
QUANTIZATION EFFECTS IN VITERBI DECODING RATE 1/n CONVOLUTIONAL CODES c61
I. M. Onyszchuk, K.-M. Cheung, and O. Collins *In its* The Telecommunications and Data Acquisition Report 15 Nov. 1989 p 115-121 (For primary document see N90-19434 12-32)
Avail: NTIS HC A10/MF A02 CSCL 09B

A Viterbi decoder's performance loss due to quantizing data from the additive white Gaussian noise (AWGN) channel is studied. An optimal quantization scheme and branch metric calculation method are presented. The uniformly quantized channel capacity C(sub u)(q) is used to determine the smallest number of quantization bits q that does not cause a significant loss. The quantizer stepsize which maximizes C(sub u)(q) almost minimizes the decoder bit error rate (BER). However, a slightly larger stepsize is better, like the value that minimizes the Bhattacharyya bound. The range and renormalization of state metrics is analyzed, in particular for K = 15 decoders such as the Big Viterbi Decoder (BVD) for the Galileo mission. These results are required to design reduced hardware complexity Viterbi decoders with a negligible quantization loss. Author

N90-19446*# Jet Propulsion Lab., California Inst. of Tech., Pasadena.
BIG VITERBI DECODER (BVD) RESULTS FOR (7,1/2) CONVOLUTIONAL CODE c61
J. Statman, J. Rabkin, and B. Siev *In its* The Telecommunications and Data Acquisition Report 15 Nov. 1989 p 122-129 (For primary document see N90-19434 12-32)
Avail: NTIS HC A10/MF A02 CSCL 09B

The Big Viterbi Decoder (BVD), capable of decoding convolutional codes with constraint lengths of up to 15, is under development for the Deep Space Network (DSN). As part of the development, a commercial single-chip (7,1/2) Viterbi decoder is used to enable early start of system integration. Tests of the integrated partial system (including simulator, input systems, output interfaces, and computer controls) were recently completed at the DSN Compatibility Test Area (CTA-21) at JPL. The system elements used for the demonstration and test results are described. Author

N90-19447*# Jet Propulsion Lab., California Inst. of Tech., Pasadena.
FAST TRANSFORM DECODING OF NONSYSTEMATIC REED-SOLOMON CODES c61
T. K. Truong, K.-M. Cheung, I. S. Reed, and A. Shiozaki (Osaka Electro-Communication Univ., Japan) *In its* The Telecommunications and Data Acquisition Report 15 Nov. 1989 p 130-140 (For primary document see N90-19434 12-32)
Avail: NTIS HC A10/MF A02 CSCL 09B

A Reed-Solomon (RS) code is considered to be a special case of a redundant residue polynomial (RRP) code, and a fast transform decoding algorithm to correct both errors and erasures is presented. This decoding scheme is an improvement of the decoding algorithm for the RRP code suggested by Shiozaki and Nishida, and can be realized readily on very large scale integration chips. Author

N90-19448*# Jet Propulsion Lab., California Inst. of Tech., Pasadena.
APPLICATION OF ADAPTIVE LEAST-SQUARES ALGORITHM TO MULTI-ELEMENT ARRAY SIGNAL RECONSTRUCTION c61
R. Kumar *In its* The Telecommunications and Data Acquisition Report 15 Nov. 1989 p 141-160 (For primary document see N90-19434 12-32)
Avail: NTIS HC A10/MF A02 CSCL 09B

Results are presented in terms of the performance improvement of a multi-feed array configuration over the usual single feed system when an adaptive least-squares algorithm is applied for the signal reconstruction. Two versions of the least-squares algorithm are presented, one of which is based on the maximization of the signal-to-noise ratio while the other is based on the deconvolution of received signal field. These algorithms were developed for the purpose of minimizing degradations arising from various sources, which can severely limit the performance (gain) of a single-feed system. Author

N90-19449*# Jet Propulsion Lab., California Inst. of Tech., Pasadena.
THE EFFECTS OF SINUSOIDAL INTERFERENCE ON THE SECOND-ORDER CARRIER TRACKING LOOP PRECEDED BY A BANDPASS LIMITER IN THE BLOCK 4 RECEIVER
C. J. Ruggier *In its* The Telecommunications and Data Acquisition Report 15 Nov. 1989 p 161-169 (For primary document see N90-19434 12-32)
Avail: NTIS HC A10/MF A02 CSCL 17B

Drop-lock relationships for the second-order phase-locked loop are derived when the carrier and a sinusoidal signal lie within the predetection filter bandwidth of the Block 4 receiver. Limiter suppression factors are calculated when a bandpass hard limiter is used to maintain constant total power at the loop. The parameters of interest are the interference-to-signal power ratio (ISR), the input signal-to-noise power ratio (NSR), and the interference signal frequency offset from carrier delta f. Limiter suppression caused by the combined effects of the noise and the interference signal accounts for the variability in the drop-lock threshold for given values of the input SNR and ISR parameters. Going beyond earlier published work that focused on the limiter's effect on the drop-lock threshold; an account is made for the limiter action in the interference mode and an overall imporvement is provided in the prediction accuracy of the drop-lock model. Author

N90-19450*# Jet Propulsion Lab., California Inst. of Tech., Pasadena.
DISTURBANCE TORQUE REJECTION PROPERTIES OF THE NASA/JPL 70-METER ANTENNA AXIS SERVOS c33
R. E. Hill *In its* The Telecommunications and Data Acquisition Report 15 Nov. 1989 p 170-188 (For primary document see N90-19434 12-32)
Avail: NTIS HC A10/MF A02 CSCL 09A

Analytic methods for evaluating pointing errors caused by external disturbance torques are developed and applied to determine the effects of representative values of wind and friction torque. The expressions relating pointing errors to disturbance torques are shown to be strongly dependent upon the state estimator parameters, as well as upon the state feedback gain and the flow versus pressure characteristics of the hydraulic system. Under certain conditions, when control is derived from an uncorrected estimate of integral position error, the desired type 2 servo properties are not realized and finite steady-state position errors result. Methods for reducing these errors to negligible proportions through the proper selection of control gain and estimator correction parameters are demonstrated. The steady-state error produced by a disturbance torque is found to be directly proportional to the hydraulic internal leakage. This property can be exploited to provide a convenient method of determining system leakage from field measurements of estimator error, axis rate, and hydraulic differential pressure. Author

N90-19451*# Jet Propulsion Lab., California Inst. of Tech., Pasadena.
PARKES RADIO SCIENCE SYSTEM DESIGN AND TESTING FOR VOYAGER NEPTUNE ENCOUNTER
T. A. Rebold and J. F. Weese *In its* The Telecommunications and Data Acquisition Report 15 Nov. 1989 p 189-205 (For primary document see N90-19434 12-32)
Avail: NTIS HC A10/MF A02 CSCL 17B

The Radio Science System installed at Parkes, Australia for the Voyager Neptune encounter was specified to meet the same stringent requirements that were imposed upon the Deep Space Network Radio Science System. The system design and test methodology employed to meet these requirements at Parkes are described, and data showing the measured performance of the system are presented. The results indicate that the system operates with a comfortable margin on the requirements. There was a minor problem with frequency-dependent spurious signals which could not be fixed before the encounter. Test results characterizing these spurious signals are included. Author

N90-19452*# Jet Propulsion Lab., California Inst. of Tech., Pasadena.
THE 32-GHz PERFORMANCE OF THE DSS-14 70-METER ANTENNA: 1989 CONFIGURATION
M. S. Gatti, M. J. Klein, and T. B. H. Kuiper *In its* The Telecommunications and Data Acquisition Report 15 Nov. 1989 p 206-219 (For primary document see N90-19434 12-32)
Avail: NTIS HC A10/MF A02 CSCL 17B

The results of preliminary 32 GHz calibrations of the 70 meter antenna at Goldstone are presented. Measurements were done between March and July 1989 using Virgo A and Venus as the primary efficiency calibrators. The flux densites of theses radio sources at 32 GHz are not known with high accuracy, but were extrapolated from calibrated data at lower frequencies. The measured value of efficiency (0.35) agreed closely with the predicted value (0.32), and the results are very repeatable. Flux densities of secondary sources used in the observations were subsequently derived. These measurements were performed using a beamswitching radiometer that employed an uncooled high-electron mobility transistor (HEMT) low-noise amplifier. This system was installed primarily to determine the performance of the antenna in its 1989 configuration, but the experience will also aid in successful future calibration of the Deep Space Network (DSN) at this frequency. Author

N90-19453*# National Aeronautics and Space Administration. Langley Research Center, Hampton, VA.
CAUSALITY OF PLASMA PERMITTIVITY WITH LOSS AND RESTORING TERMS
C. R. Cockrell Dec. 1989 15 p
(NASA-TM-101671; NAS 1.15:101671) Avail: NTIS HC A03/MF A01 CSCL 20I

The causality of the complex permittivity for a plasma model in which both loss and restoring terms are included is shown. Discussions as to what occurs in this causality property when the loss and restoring terms vanish are presented. Results are shown to agree with earlier work. Author

N90-19454*# National Aeronautics and Space Administration. Lewis Research Center, Cleveland, OH.
EFFECTS OF AMPLITUDE DISTORTIONS AND IF EQUALIZATION ON SATELLITE COMMUNICATION SYSTEM BIT-ERROR RATE PERFORMANCE
Robert J. Kerczewski, Gene Fujikawa, James S. Svoboda, and Paul J. Lizanich (Analex Corp., Cleveland, OH.) 1990 13 p Presented at the 13th International Communication Satellite Systems Conference, Los Angeles, CA, 11-15 Mar. 1990; sponsored by AIAA
(Contracts NAS3-25266; NAS3-24564)
(NASA-TM-102415; E-5180; NAS 1.15:102415; AIAA-90-0878)
Avail: NTIS HC A03/MF A01 CSCL 17B

Satellite communications links are subject to distortions which result in an amplitude versus frequency response which deviates from the ideal flat response. Such distortions result from propagation effects such as multipath fading and scintillation and from transponder and ground terminal hardware imperfections. Bit-error rate (BER) degradation resulting from several types of amplitude response distortions were measured. Additional tests measured the amount of BER improvement obtained by flattening the amplitude response of a distorted laboratory simulated satellite channel. The results of these experiments are presented. Author

N90-19455# Air Force Inst. of Tech., Wright-Patterson AFB, OH. School of Engineering.
GREEN'S FUNCTIONS FOR A THEORETICAL MODEL OF AN APERTURE FED STACKED-PATCH MICROSTRIP ANTENNA M.S. Thesis
James B. Nazar Dec. 1989 157 p
(AD-A216280; AFIT/GE/ENG/89D-37) Avail: NTIS HC A08/MF A01 CSCL 09/1

A theoretical model for the analysis of an aperture fed stacked-patch microstrip antenna is presented. The mixed potential integral equation approach (MPIE) is used. The aperture is closed by using opposing magnetic currents on each side of the ground plane. The necessary Green's functions associated with the vector and scalar potentials are evaluated in the spatial domain using stratified media theory. The Green's functions are expressed as Sommerfeld integrals. A method of moments technique to solve for the currents of the antenna is outlined. Basis and test functions are found for use with the Green's functions in the MPIEs to form a solution matrix. No actual solutions for the currents are calculated. The Sommerfeld integrals in the Green's functions are analyzed to determine their characteristics. These characteristics include complex, oscillatory integrands; singularities; surface waves and semi-infinite integration intervals. Several numerical integration techniques to deal with these characteristics are developed. Both FORTRAN code and Mathematical packages written to implement these techniques are discussed. Example calculations for several of the Green's functions are accomplished. The cut-off frequencies for the surface waves are evaluated and it is shown that with a proper choice of material parameters only one surface wave mode will propagate. The Green's functions are then evaluated accurately and efficiently with sample results provided. GRA

N90-19456# Department of the Navy, Washington, DC.
DUAL FREQUENCY LAUNCHER FOR CIRCULARLY POLARIZED ANTENNA Patent
Ming H. Chen, inventor (to Navy) 3 Oct. 1989 4 p Filed 10 Aug. 1988
(AD-D014361; US-Patent-4,872,211; US-Patent-Appl-SN-242001; US-Patent-Class-343-778) Avail: US Patent and Trademark Office CSCL 09/1

A dual frequency antenna feed is formed from a central, circular waveguide connected to the flat boundry of circular, disk-shaped resonant cavity. A second circular waveguide is connected one end of a disk-shaped resonant cavity. Energy of one frequency enters and exits the cavity along the common axis of the

waveguides. Energy of the second frequency is introduced to the same resonant cavity by way of a plurality of bandpass filters, also connected to the cavity. This energy enters by way of slots in the cylindrical walls of the cavity. The central circular waveguide is propagating at one frequency but cut off at the second frequency. These bandpass filters are at this pass band for the second frequency, but at the rejection band for the first frequency. Therefore, the isolation between these two input ports are obtained. GRA

N90-19457# Defence Research Establishment, Ottawa (Ontario). Radar Countermeasure Section.
AN INVESTIGATION OF THE TRANSFER OF MONOPULSE TRACKING BETWEEN TWO COHERENT POINT SOURCES Technical Note
Shawn Charland Aug. 1989 33 p
(AD-A217007; DREO-TN-89-15) Avail: NTIS HC A03/MF A01 CSCL 17/9

This investigation deals with the effects of phase and amplitude differences between two coherent point source radiators on the tracking behavior of a monopulse radar. The tracking function of the radar is modelled in a single plane containing two point sources located at a finite distance from the radar antenna. The complex illumination of the antenna aperture by the point sources and the resulting monopulse sum and difference antenna responses are derived, including the effects of finite range. The monopulse discriminator characteristic is formed using the antenna responses. A set of calibration curves are presented which show the transfer of the tracking point of the radar from one source to the other as the phase and amplitude differences between the sources vary. The application of this investigation is in specifying the excitation of two point sources to move the tracking point of a radar smoothly and continuously from one source to the other, in order to simulate continuous target motion using discrete positioned radiating elements. GRA

N90-19458# BDM Corp., Albuquerque, NM.
NEAR-FIELD BISTATIC RCS (RADAR CROSS-SECTION) MEASUREMENTS Final Technical Report, 30 Sep. 1986 - 20 Mar. 1989
Everett G. Farr, Robert B. Rogers, Glen R. Salo, and Theodore N. Truske Oct. 1989 168 p
(Contract F19628-86-C-0208; AF Proj. 2305)
(AD-A217011; BDM/ABQ-88-0996-TR; RADC-TR-89-198) Avail: NTIS HC A08/MF A01 CSCL 17/9

This Final Technical Report presents the results of a feasibility investigation of a technique for calculating the far-field radar cross section of an object based upon measurements made in the near-field of the object. This technique is an extension of existing planar near-field antenna measurement technology, and is capable of measuring monostatic radar cross section and bistatic radar cross section at both narrow and wide angles. Included are the detailed formulation of the theory of near-field planar bistatic radar cross section measurement, and discussion of details of the mechanical scanner and software implementation. The comparison of measurement with predictions is presented; the agreement is excellent, and suggests that a larger-scale demonstration would be appropriate. Also included are concepts for reducing the amount of data required for reconstructing radar cross section, and a discussion of limitations of this method of radar cross-section measurement. Specific recommendations are presented for technology development areas that should be pursued to mature this measurement technique into a viable, operational technology. Among those areas are calibration, data handling, computational optimization, data analysis, operational considerations, and additional theoretical development. GRA

N90-19459# Lawrence Livermore National Lab., CA.
TWO-DIMENSIONAL, LONG-PULSE COMPUTER CALCULATION OF MICROWAVE-INDUCED ELECTRON LAYER FORMATION IN LOW-PRESSURE AIR
D. J. Mayhall, J. H. Yee, G. E. Sieger, and R. A. Alvarez 1989 24 p Presented at the Workshop on Artificial Ionized Layers in the Atmosphere, Kiev, USSR, 9-12 Oct. 1989
(Contract W-7405-eng-48)
(DE90-005994; UCRL-101952; CONF-8910342-1) Avail: NTIS HC A03/MF A01

Laboratory chamber experiments in low-pressure (0.1 to 10 Torr) air with long-pulse (150 to 600 ns), 2.856 GHz crossed microwave beams, created by the reflection of an incident beam from a metal plate inclined at 45 degrees, have shown that multiple, luminous electron density layers form toward the source of the incident beam. Previous two-dimensional calculations of microwave air breakdown in a rectangular waveguide with full resolution of each radio frequency cycle of the driving electric field Cray I computer computation times of about 0.5 hr/ns for runs of up to 20 ns of simulation time. Since we desire to simulate chamber experiments with pulses at 150 to 600 ns duration, computation times with full-cycle resolution must be expected to be 75 to 300 hours per run. Because these are prohibitive amounts of computer time, a computer code, which follows only the driving pulse envelope, has been developed to reduce the required computation time. This envelope approximation is an extension of the one-dimensional envelope technique for atmospheric microwave propagation reported previously. DOE

N90-19460*# Johns Hopkins Univ., Baltimore, MD. Dept. of Electrical and Computer Engineering.
DIRECT DETECTION OPTICAL INTERSATELLITE LINK AT 220 Mbps USING AlGaAs LASER DIODE AND SILICON APD WITH 4-ary PPM SIGNALING Interim Progress Report, Sep. 1989 - Feb. 1990
Xiaoli Sun and Frederic M. Davidson Mar. 1990 26 p
(Grant NAG5-356)
(NASA-CR-186380; NAS 1.26:186380) Avail: NTIS HC A03/MF A01 CSCL 17B

A newly developed 220 Mbps free-space 4-ary pulse position modulation (PPM) direct detection optical communication system is described. High speed GaAs integrated circuits were used to construct the PPM encoder and receiver electronic circuits. Both PPM slot and word timing recovery were provided in the PPM receiver. The optical transmitter consisted of an AlGaAs laser diode (Mitsubishi ML5702A, lambda=821nm) and a high speed driver unit. The photodetector consisted of a silicon avalanche photodiode (APD) (RCA30902S) preceded by an optical interference filter (delta lambda = 10nm). Preliminary tests showed that the self-synchronized PPM receiver could achieve a receiver bit error rate of less than 10(exp -6) at 25 nW average received optical signal power or 360 photons per transmitted information bit. The relatively poor receiver sensitivity was believed to be caused by the insufficient electronic bandwidth of the APD preamplifier and the poor linearity of the preamplifier high frequency response. Author

N90-19461# International Centre for Theoretical Physics, Trieste (Italy).
RADIATION OF ELECTROMAGNETIC WAVES BY AN ACCELERATED CHARGED PARTICLE IN MEDIUM
A. A. Risbud and N. L. Tsintsadze Jun. 1989 10 p Submitted for publication
(DE90-610458; IC-89/151) Avail: NTIS (US Sales Only) HC A02/MF A01

The effect was investigated of acceleration of a charged particle on its Cerenkov emission and ionization losses. The accelerated motion of a charged particle in an infinite medium was considered with acceleration along with the direction of its motion. The Maxwell equations, with appropriate current and charge densities, are solved to obtain electromagnetic fields. Hence the force arising from the interaction of the accelerated charged particle with the medium (dielectric or plasma) is calculated. Part 1 is more general and its results are applicable to any acceleration. Part 2 deals with small acceleration and small interaction time. It is found that the acceleration of charged particle strongly changes both its Cerenkov emission and ionization-losses. The results obtained are analyzed and discussed in both parts. DOE

N90-19462# International Centre for Theoretical Physics, Trieste (Italy).
PROPAGATION OF ELECTROMAGNETIC WAVES IN MULTIDIMENSIONAL HOMOGENEOUS COSMOLOGIES
Leszek M. Sokolowski, Marco Litterio, and Franco Occhionero (Osservatorio Astronomico, Rome, Italy) Aug. 1989 15 p Submitted for publication
(DE90-610474; IC-89/199) Avail: NTIS (US Sales Only) HC A03/MF A01

It is shown that electromagnetic waves initially emitted towards the higher dimensions cannot emerge in the physical external space-time as ordinary photons. Two frequencies can be assigned to an ordinary photon: one associated with the physical 4-space and the other with the total space-time. It is a general property of known multidimensional cosmological solutions that the latter decreases in time (redshift) while the former increases (blueshift). DOE

N90-19463# National Telecommunications and Information Administration, Boulder, CO. Inst. for Telecommunication Sciences.
POWER SPECTRAL DENSITIES FOR SELECTED DIGITAL PHASE-CONTINUOUS MFSK (M-ary FREQUENCY SHIFT KEYING) EMISSIONS
M. Nesenbergs, D. L. Smith, and L. T. Jones Oct. 1989 70 p
(PB90-129990; NTIA-89-250) Avail: NTIS HC A04/MF A01 CSCL 17B

A brief outline and catalog of 11 power spectral densities for certain M-ary frequency shift keying waveforms is presented. Spectral equations are displayed in graphical form for easy visualization. The spectra pertain to real signals centered on their carrier frequencies. Specific waveform shapes include square (or rectangular) pulses, sine-pulses, raised cosine pulses, and squared raised-cosine pulses. The concluding sections cover two special systems of recent practical interest. They are the M=4 and k=2, alternating frequency, format of Rockwell/Collins and the M=8, k=2, scheme developed by MITRE and Harris Corps. Author

N90-19464# Rochester Inst. of Tech., NY. Center for Imaging Science.
SIGNAL PROCESSING Final Report
Roger L. Easton, Jr. Jan. 1990 11 p
(Contract DE-FG01-88DP-20153)
(DE90-006904; DOE/DP-20153/T4; RIT/DIRS-89/90-50-135)
Avail: NTIS HC A03/MF A01

Space-variant coordinate transformations may be profitably applied to many signal processing problems; for example, image convolutions are often computed by multiplying the Fourier transforms of the images rather than by direct methods (i.e., shift, multiply, and add). Some signal processing algorithms are presently under study that operate on projection-based representations of the function. The best known projection representation is the Radon transform (Radon, 1917) (Easton, 1986), which is the mathematical basis for several medical imaging techniques, e.g., medical computed tomography (CT or CAT) and nuclear magnetic resonance imaging (MRI). The Radon transform reduces the 2-D data set to a series of 1-D line integral projections at each azimuth. DOE

N90-19465# National Lab. for High Energy Physics, Tsukuba (Japan).
A SIMPLE METHOD USING MAFIA TO CALCULATE EXTERNAL Q VALUES OF WAVEGUIDE-LOADED CAVITIES
Tatsuya Kageyama Jun. 1989 13 p
(DE90-741487; KEK-89-4) Avail: NTIS (US Sales Only) HC A03/MF A01

A fundamental theory on waveguide-loaded cavities in the book of Microwave Electronics by Slater was applied to numerical calculation with MAFIA of the external Q value of a klystron output cavity. This method is also applicable to accelerating structures with slots for damping out higher modes as proposed for future linear colliders. DOE

N90-19466*# Ohio State Univ., Columbus. ElectroScience Lab.
ELECTROMAGNETIC PROPERTIES OF MATERIAL COATED SURFACES Annual Report
L. Beard, J. Berrie, R. Burkholder, A. Dominek, E. Walton, and N. Wang Oct. 1989 48 p
(Grant NAG3-913)
(NASA-CR-186466; NAS 1.26:186466; OSU-TR-720964-5) Avail: NTIS HC A03/MF A01 CSCL 20N

The electromagnetic properties of material coated conducting surfaces were investigated. The coating geometries consist of uniform layers over a planar surface, irregularly shaped formations near edges and randomly positioned, electrically small, irregularly shaped formations over a surface. Techniques to measure the scattered field and constitutive parameters from these geometries were studied. The significance of the scattered field from these geometries warrants further study. Author

N90-19467 Physics and Electronics Lab. TNO, The Hague (Netherlands).
TRACKING PERFORMANCE OF THE AN/GPN-22 PRECISION APPROACH RADAR
J. Hordijk Jun. 1988 51 p In DUTCH; ENGLISH summary
(Contract A85/KLu/113)
(FEL-1988-34; TD-88-3861; ETN-90-95076) Copyright Avail: Physics and Electronics Lab. TNO, P.O. 96864, 2509 JG 's-Gravenhage, Netherlands

The performance of the software developed for the AN/GPN-22 precision approach radar (PAR) was evaluated. The PAR sometimes gives a bad tracking performance (loss of track) when an aircraft deviates from the ideal glide path. A simulation, containing the geometry and control loops for range, azimuth and elevation, was used to analyze the performance of the tracker component of the software. The bad tracking turns out to be caused by faults or imperfections in the tracker component of the software. It is shown that the tracking performance can be improved by the introduction of some changes in the software. ESA

N90-19468 Forschungsinstitut fuer Hochfrequenzphysik, Werthhoven (Germany, F.R.).
ASPECTS OF VHF RADARS ILLUSTRATED BY THE EXAMPLE OF AN EXPERIMENTAL SYSTEM
H. Kuschel Jan. 1989 60 p In GERMAN; ENGLISH summary
(Contract BMVg-T/RF31/I0003/I1303)
(Rept-1-89; Lfd-282; ETN-90-95347) Copyright Avail: Forschungsinstitut fuer Hochfrequenzphysik, Wachtberg-Werthhoven, Fed. Republic of Germany

The advantages and disadvantages of the long wavelength radar concept are illustrated taking as an example the detection of low flying targets such as helicopters and cruise missiles. The choice of the optimum frequency is always a tradeoff between the task related capabilities and deficiences of the chosen frequency range. Antenna configurations, wave propagation effects such as diffraction, target radar cross section in the resonance region and echo signature of a hovering helicopter are considered for VHF radar system concepts. The experimental system Lara (large wavelength radar) is introduced as a demonstration model. ESA

N90-19469# Technische Univ., Berlin (Germany, F.R.). Fachbereich Elektrotechnik.
FIELD THEORETICAL ANALYSIS AND SYNTHESIS OF BROADBAND WAVEGUIDE: HEIGHT, PLANE SHUNT CIRCULATORS WITH MULTIPLE LAYER MATERIAL INSERTIONS Ph.D. Thesis [FELDTHEORETISCHE ANALYSE UND SYNTHESE BREITBANDIGER HOHLLEITER-H-EBENEN-VERZWEIGUNGSZIRKULATOREN MIT MEHRFACH GESCHICHTETEN STOFFEINSAETZEN]
Dietrich Hahn 1989 126 p In GERMAN
(ETN-90-95360) Avail: NTIS HC A07/MF A01

The partial-height circulation is calculated by means of a relatively low cost method, adapted to the logical optimization of this method. The influence magnitudes, as geometric and material parameters, are calculated with the eigen values of the structure.

The critical parameters are formulated from the ferrite dimensions. The material parameters of the ferrite and the dimensioning of the transformer, particularly of the transformer radius in relation to the resonant cavity radius, are established. The strong field concentration in the ferrite is weakened by a greater than 1 permittivity. The calculation of the field distribution showed the principal fashion of the circulation and the existence of three types of field that determine the broadband behavior of the structure. ESA

N90-19470# Technische Univ., Berlin (Germany, F.R.). Fachbereichsrat.
GENERAL MULTIDIMENSIONAL SCANNING RATIO TRANSFORMATION AND ITS UTILIZATION FOR NORM TRANSFORMATION OF TELEVISION SIGNALS Ph.D. Thesis [ALLGEMEINE MEHRDIMENSIONALE ABTASTRATENUMSETZUNG UND IHRE ANWENDUNG ZUR NORMUMSETZUNG VON FERNSEHSIGNALEN]
Thomas Reuter 1989 130 p In GERMAN
(ETN-90-96058) Avail: NTIS HC A07/MF A01

The calculation of the spectrum of the analyzed signal is carried out for some periodic scanning samples, also nonregular. The ideal scanning was in the first place described in the frequency area. The frequency response of conventional norm-change processes was calculated as a time and space varying system and compared with the ideal frequency response. By this method, a systematic classification of apparent errors was possible, and opportunities of improving the transformation were clearly envisaged. Some remarked errors result from the insufficient approximation of the ideal frequency response: for example, the ideal band limitation of the input signal is an erroneous assumption. Therefore the interpolation filter must be fitted to the spectrum of the signal. In the case of a moving object, a nonlinear study of the movement vectors is essential to use the nonhomogeneous vector field for an adaptive interpolation. ESA

N90-19471# Technische Univ., Brunswick (Germany, F.R.).
EXPERIMENTAL MEASUREMENTS IN SECONDARY RADAR FIELD: CONCEPTION AND FIRST RESULTS [EXPERIMENTELLE MESSUNGEN IM SEKUNDAERRADARFUNKFELD: MESSAUFBAU UND ERSTE ERGEBNISSE]
Roland Mallwitz Jun. 1988 60 p In GERMAN
(ETN-90-96074) Avail: NTIS HC A04/MF A01

A measurement installation for the estimation of the main radio field charge in secondary surveillance radar channels is described. First measurements give information about the conditions in the listening channel for a supposed minimally charged air space above Germany, F.R. For this area it is shown that the formation of mean values testifies little to the transmission security and the transmissibility of the mode S-transactions. Furthermore the probability of the appearance of interferences depends on the surrounding field in the air and on the ground. The measurements are influenced by geographic time variations. ESA

N90-19472# Federal Aviation Administration, Atlantic City, NJ. Technical Center.
OPERATIONAL EVALUATION OF INITIAL DATA LINK AIR TRAFFIC CONTROL SERVICES, VOLUME 1 Final Report
Nicholas J. Talotta, Clark Shingledecker, and Michael Reynolds (Midwest Systems Research, Inc., Dayton, OH.) Feb. 1990 67 p
(DOT/FAA/CT-90/1-Vol-1) Avail: NTIS HC A04/MF A01

The results are detailed of an operational evaluation of initial data link air traffic control (ATC) services. The operational evaluation was conducted at the Federal Aviation Administration (FAA) Technical Center utilizing the data link test bed. Initial data link services were evaluated in order to identify service delivery methods which optimize controller acceptance, performance, and workload. Author

N90-19473# Lawrence Livermore National Lab., CA.
SPARSE BREAKDOWN AND STATISTICAL SNEAKTHROUGH EFFECTS IN LOW-ALTITUDE MICROWAVE PROPAGATION
R. A. Alvarez, P. R. Bolton, G. E. Sieger, and D. N. Fittinghoff Jan. 1990 8 p Presented at the High Powered Microwave and Broadband Radio Frequency Propagation/Phenomenology/ Methodology Workshop, Livermore, CA, 23-26 Oct. 1989
(Contract W-7405-eng-48)
(DE90-007252; UCRL-101807; CONF-891097-4) Avail: NTIS HC A02/MF A01

It is generally assumed that the beam intensity that can be transmitted through the atmosphere by a high-power microwave pulse will be limited by the air-breakdown threshold. Air breakdown by microwave has been studied extensively, both theoretically and experimentally. It is a cascade process in which free electrons, driven by the microwave electric field, generate further ionization through collisions with air molecules. The process can disrupt the propagation of a microwave pulse if the electron plasma density grows to within an appreciable fraction of critical density. In a pulsed beam this can happen if, and only if, the field strength is sufficiently large and the beam encounters one or more initiating free 'seed' electrons sufficiently early in the pulse. This paper discusses this sparse breakdown in low-altitude wave propagation. DOE

N90-19474# Lawrence Livermore National Lab., CA.
SINGLE ANTENNA INTERFEROMETRY
J. P. Fitch 16 Dec. 1989 10 p
(Contract W-7405-eng-48)
(DE90-008120; UCID-21835) Avail: NTIS HC A02/MF A01

Interferometry from air and space borne platforms which require synthetic aperture radar image synthesis has been demonstrated in earlier experiments by using either two physical antennas mounted on one airframe or two passes of the same antenna over the same scene. In this paper, one pass of a single antenna radar system with a high pulse repetition frequency is used to form an interferometric image which, under initial investigation, appears to be sensitive to ocean surface effects due to ship-generated internal waves. DOE

N90-19475# Axiomatix, Los Angeles, CA.
PACKET RADIO NETWORKS UNDER DYNAMIC JAMMING Interim Report
Andreas Polydoros 15 Dec. 1989 20 p
(Contract DAAL03-87-C-0007)
(AD-A217094; R8912-1; ARO-24649.8-EL-S) Avail: NTIS HC A03/MF A01 CSCL 25/2

The purpose of this report is: (1) to briefly review and classify the various research efforts developed so far in the broad area of Spread Spectrum (S2) Random-Access Packet Radio Networks (sometimes referred to as Code-Division Random-Access or CRDA), and (2) to point out certain directions that we perceive as being important to the Army, particularly in relation to the intelligent jamming of such networks. GRA

N90-19476 British Broadcasting Corp., Kingswood (England). Engineering Div.
DIGITAL VIDEO: STUDIO SIGNAL PROCESSING
C. K. P. Clarke 1989 26 p
(BBC-RD-1989/14) Copyright Avail: BBC, Kingswood Warren, Tadworth, Surrey, England

Several features of the digital component standard for television studios are described with a view to explaining the principles on which they are based and the modes of operation which were intended. For example, the sampling and filtering techniques were chosen to support multiple signal conversions with minimal loss of quality and the multiplexing techniques used were selected to simplify interconnections. The implications of the coding parameters for signal processing and studio synchronization are discussed and some simple test waveforms are suggested. Author

N90-19477 British Broadcasting Corp., Kingswood (England). Engineering Div.
A DIGITAL HDTV RECORDER USING A CLUSTER OF FOUR D1 DVTRS
P. R. Burfield 1989 11 p
(BBC-RD-1989/13) Copyright Avail: BBC, Kingswood Warren, Tadworth, Surrey, England

The design philosophy of a digital high definition TV (HDTV) video recording system that was constructed from four conventional D1 digital video component records is outlined. Technical specifications of the recorder are given with explanations of how the system can be used to edit source material into good quality programs. At present, the HDTV recorder is housed in a mobile laboratory together with other HDTV equipment, and has been used by the BBC to make programs for both itself and other members of the Eureka 95 consortium. Author

N90-19478 British Broadcasting Corp., Kingswood (England). Engineering Div.
A WAVEFORM CAPTURE AND STORAGE UNIT AND ITS USE FOR INVESTIGATING DISTURBANCES ON DIGITAL TRANSMISSION LINKS
A. Oliphant, R. E. Vialls, and R. M. Inman 1989 12 p
(BBC-RD-1989/17) Copyright Avail: BBC, Kingswood Warren, Tadworth, Surrey, England

A unit to capture analogue waveforms and store tham digitally is described. It was designed for investigation of bitstream disturbances in the BBC's pulse code modulation (PCM) audio distribution network which uses an 8448 kbit/s multiplex of digital audio signals carried on analogue video circuits. The unit was successfully used in the diagnosis and subsequent elimination of bitstream disturbances that had given rise to complaints from listeners; several examples of its use so far are given and other applications are suggested. Author

N90-19253*# Rockwell International Corp., Seal Beach, CA. Satellite and Space Electronics Div.
LARGE SPACE ANTENNA CONCEPTS FOR ESGP
Allan W. Love *In* NASA, Langley Research Center, Earth Science Geostationary Platform Technology Jul. 1989 p 65-68 (For primary document see N90-19249 12-15)
Avail: NTIS HC A17/MF A03 CSCL 20N

N90-19256*# Astro Aerospace Corp., Carpinteria, CA.
STRUCTURES FOR REMOTELY DEPLOYABLE PRECISION ANTENNAS
J. M. Hedgepeth *In* NASA, Langley Research Center, Earth Science Geostationary Platform Technology Jul. 1989 p 109-128 (For primary document see N90-19249 12-15)
Avail: NTIS HC A17/MF A03 CSCL 20N

N90-19257*# Composite Optics, Inc., San Diego, CA.
UNFURLABLE, CONTINUOUS-SURFACE REFLECTOR CONCEPT
J. E. Stumm and S. Kulick *In* NASA, Langley Research Center, Earth Science Geostationary Platform Technology Jul. 1989 p 129-136 (For primary document see N90-19249 12-15)
Avail: NTIS HC A17/MF A03 CSCL 20N

N90-19258*# L'Garde, Inc., Tustin, CA.
ADVANCES IN LARGE INFLATABLE REFLECTORS
M. Thomas and G. Williams *In* NASA, Langley Research Center, Earth Science Geostationary Platform Technology Jul. 1989 p 137-151 (For primary document see N90-19249 12-15)
Avail: NTIS HC A17/MF A03 CSCL 20N

N90-19264*# National Aeronautics and Space Administration. Lewis Research Center, Cleveland, OH.
A COMPARISON OF REFLECTOR ANTENNA DESIGNS FOR WIDE-ANGLE SCANNING
M. Zimmerman, S. W. Lee, B. Houshmand, Y. RahmatSamii (Jet Propulsion Lab., California Inst. of Tech., Pasadena.), and R. J. Acosta *In* NASA, Langley Research Center, Earth Science Geostationary Platform Technology Jul. 1989 p 217-240 Previously announced as N89-21138 (For primary document see N90-19249 12-15)
Avail: NTIS HC A17/MF A03 CSCL 20N

N90-19265*# Atlantic Research Corp., Rome, NY.
ARRAYS FOR SPACE APPLICATIONS
Harvey K. Schuman, Paul Antonik, and Carmen Malagisi *In* NASA, Langley Research Center, Earth Science Geostationary Platform Technology Jul. 1989 p 241-263 (For primary document see N90-19249 12-15)
Avail: NTIS HC A17/MF A03 CSCL 20N

N90-19266*# National Aeronautics and Space Administration. Lewis Research Center, Cleveland, OH.
CONJUGATE FIELD APPROACHES FOR ACTIVE ARRAY COMPENSATION
R. J. Acosta *In* NASA, Langley Research Center, Earth Science Geostationary Platform Technology Jul. 1989 p 265-271 (For primary document see N90-19249 12-15)
Avail: NTIS HC A17/MF A03 CSCL 20N

N90-19267*# National Aeronautics and Space Administration. Lewis Research Center, Cleveland, OH.
REFLECTOR SURFACE DISTORTION ANALYSIS TECHNIQUES (THERMAL DISTORTION ANALYSIS OF ANTENNAS IN SPACE)
R. Sharp, M. Liao, J. Giriunas, J. Heighway, A. Lagin, and R. Steinbach *In* NASA, Langley Research Center, Earth Science Geostationary Platform Technology Jul. 1989 p 273293 (For primary document see N90-19249 12-15)
Avail: NTIS HC A17/MF A03 CSCL 20N

N90-19268*# North Carolina State Univ., Raleigh. Dept. of Electrical and Computer Engineering.
MESH SURFACES FOR REFLECTOR APPLICATIONS
Frank Kauffman *In* NASA, Langley Research Center, Earth Science Geostationary Platform Technology Jul. 1989 p 295-311 (For primary document see N90-19249 12-15)
Avail: NTIS HC A17/MF A03 CSCL 20N

N90-19269*# TRW Electronic Systems Group, Redondo Beach, CA. Antenna Systems Lab.
ANTENNAS FOR 20/30 GHz AND BEYOND
C. Harry Chen, William C. Wong, and S. Jim Hamada *In* NASA, Langley Research Center, Earth Science Geostationary Platform Technology Jul. 1989 p 313-327 (For primary document see N90-19249 12-15)
Avail: NTIS HC A17/MF A03 CSCL 20N

N90-19392*# Alabama A & M Univ., Huntsville. Mathematics.
AUGMENTING AND UPDATING NASA SPACELINK ELECTRONIC INFORMATION SYSTEM
Jean A. Blake *In* Alabama Univ., Research Reports: 1989 NASA/ASEE Summer Faculty Fellowship Program Dec. 1989 8 p (For primary document see N90-19390 12-31)
(Grant NGT-01-008-021)
Avail: NTIS HC A99/MF E06 CSCL 17B

N90-19411*# Mississippi State Univ., Mississippi State. Dept. of Electrical Engineering.
EVALUATION AND ANALYSIS OF THE ORBITAL MANEUVERING VEHICLE VIDEO SYSTEM
Robert J. Moorhead, II *In* Alabama Univ., Research Reports: 1989 NASA/ASEE Summer Faculty Fellowship Program Dec. 1989 27 p (For primary document see N90-19390 12-31)
(Grant NGT-01-008-021)
Avail: NTIS HC A99/MF E06 CSCL 17B

N90-19414*# Ohio Univ., Athens. Dept. of Electrical and Computer Engineering.
RADAR TRANSPONDER ANTENNA PATTERN ANALYSIS FOR THE SPACE SHUTTLE
Roger Radcliff *In* Alabama Univ., Research Reports: 1989

NASA/ASEE Summer Faculty Fellowship Program Dec. 1989 25 p (For primary document see N90-19390 12-31)
Avail: NTIS HC A99/MF E06 CSCL 17I

N90-19970*# Jet Propulsion Lab., California Inst. of Tech., Pasadena.
HIGH STABILITY RADIO LINKS
E. Robert Kursinski *In* NASA, Relativistic Gravitational Experiments in Space Aug. 1989 p 171-178 (For primary document see N90-19940 12-90)
Avail: NTIS HC A11/MF A02 CSCL 17B

33 ELECTRONICS AND ELECTRICAL ENGINEERING

Includes test equipment and maintainability; components, e.g., tunnel diodes and transistors; microminiaturization; and integrated circuitry.

For related information see also *60 Computer Operations and Hardware* and *76 Solid-State Physics*.

N90-19479 Virginia Polytechnic Inst. and State Univ., Blacksburg.
SUBOPTIMAL PERIOD DESIGN FOR A MANEUVERING MISSILE TO EVADE TRACKING FILTERS Ph.D. Thesis
Lin-Ying Lai 1988 170 p
Avail: Univ. Microfilms Order No. DA8913749

The engagement between an antiship missile and a ship's defence system is investigated. The missile is equipped with proportional navigation guidance for homing in on its ship target. The ship's defense system consists of a radar, an estimation system (the extended Kalman filter and the jump filter are used), and a gun system. The performance index is defined as the estimated number of hits (EHITS) of projectiles on the missile. The main objective is to determine maneuvering periods for the missile which minimize the EHITS to evade the ship's gunfire under different engagement conditions. The maneuvering periods are design parameters in the missile's controls of both the vertical and the horizontal planes. The engagement conditions are as follows: the maximum amplitude of the maneuvering functions, the homing in position of the missile on the ship, the measurement noise condition of the ship's radar, and the missile's model assumed in the ship's filters. The missile's control functions considered are periodic and of specific types (sinusoidal, square and sawtooth waveforms); therefore, the periods which minimize the EHITS in this study are suboptimal for the general engagement problem. Two methods are used to obtain the suboptimal periods: one is the brute force method of computing the EHITS for certain equally spaced periods, the other uses an optimization software to search for the minimum point. Dissert. Abstr.

N90-19480 Department of the Navy, Washington, DC.
ACTIVE PHASE AND AMPLITUDE MODULATOR Patent
Terence E. Olver, inventor (to Navy) 29 Aug. 1989 6 p Filed 17 Oct. 1988
(AD-D014318; US-Patent-4,862,116; US-Patent-Appl-SN-262380)
Avail: US Patent and Trademark Office CSCL 20/15

An active phase and amplitude modulator separates an input carrier into four phases. The phases are amplified and modulated separately. Summing circuits combine the phases into a single resultant output. Modulators are an essential part of adaptive signal cancellers. The function of a modulator is to provide a signal exactly in amplitude but 180 degrees out of phase with an unwanted signal existing in the canceller circuit. The result is that the unwanted signal is nulled out and cancelled. Unwanted signals may be, for example, signals from a nearby transmitter coupled into the input circuits of a receiver, or distortion causing signals in transmitter circuits. GRA

N90-19481 Department of the Navy, Washington, DC.
DISCONTINUOUS-TAPER DIRECTIONAL COUPLER Patent
George L. Millican, inventor (to Navy) and Joseph A. Mosko, inventor (to Navy) 12 Apr. 1988 9 p Filed 26 May 1983
(AD-D014324; US-Patent-4,737,740; US-Patent-Appl-SN-498338; US-Patent-Class-333-116) Avail: US Patent and Trademark Office

A stripline coupler exhibiting higher coupling coefficients and improved scattering properties in the plus 10 GHz range, utilizes a section of discrete areal dimension in each of two tapered striplines, such that the said sections form a discontinuity in the taper, in conjunction with perforations of the bilateral ground planes coincident with each section. The dielectric separating each stripline from the ground plane is modified in the region of the perforations to reduce the dielectric constant in the region. GRA

N90-19482# Department of the Army, Washington, DC.
TEMPERATURE COMPENSATED CRYSTAL OSCILLATOR (TCXO) WITH IMPROVED TEMPERATURE COMPENSATION Patent Application
John A. Kosinski, inventor (to Army) 4 Oct. 1989 11 p
(AD-D014334; US-Patent-Appl-SN-417132) Avail: NTIS HC A03/MF A01 CSCL 09/1

A TCXO including a series capacitance is improved by having the temperature sensitivity of the series load capacitance be chosen in accordance with the formula T(sub CL) = T sub Co + 2(T sub K)/(1 - alpha(sub 0)) wherein TCL is the temperature coefficient of the series load capacitor, T(sub Co) is the temperature coefficient of the resonator static capacitance, TK is the temperature coefficient of the piezoelectric coupling for the resonator, and alpha(sub 0) is the center value of load factor alpha wherein the load factor, alpha, is defined as alpha = sub Co sub Co + sub CL wherein sub Co is the resonator static capacitance and sub CL is the series load capacitance. GRA

N90-19483# Department of the Army, Washington, DC.
LIGHTNING PROTECTION APPARATUS FOR RF EQUIPMENT AND THE LIKE Patent Application
Nathan W. Feldman, inventor (to Army) and Malvin L. Shar, inventor (to Army) 30 Oct. 1989 24 p
(AD-D014336; US-Patent-Appl-SN-428792) Avail: NTIS HC A03/MF A01 CSCL 09/7

Lightning protection apparatus for antenna coupled RF equipment is provided. A one quarter wavelength shorting stub bandpass filter shunts the RF equipment and a distributed capacitance, high voltage coaxial capacitor is serially coupled between the equipment and antenna. The shorting stub is tuned to one quarter wavelength of the RF equipment operating frequency. The series capacitor passes frequencies at or above the operating frequency of the RF equipment. GRA

N90-19484*# National Aeronautics and Space Administration. Lewis Research Center, Cleveland, OH.
HIGH POWER, HIGH FREQUENCY COMPONENT TEST FACILITY
Mary Ellen Roth and Walter Krawczonek (Sverdrup Technology, Inc., Cleveland, OH.) Feb. 1990 12 p
(NASA-TM-102500; E-5297; NAS 1.15:102500) Avail: NTIS HC A03/MF A01 CSCL 09A

The NASA Lewis Research Center has available a high frequency, high power laboratory facility for testing various components of aerospace and/or terrestrial power systems. This facility is described here. All of its capabilities and potential applications are detailed. Author

N90-19485# Central Research Inst. of Electric Power Industry, Tokyo (Japan).
PROPOSAL OF ARC DRIVING TYPE FAULT CURRENT LIMITER
Masayuki Okazaki and Tsuginori Inaba Jul. 1988 34 p In JAPANESE; ENGLISH summary
(DE89-782290; CRIE-W-87040) Avail: NTIS (US Sales Only) HC A03/MF A01

In order to develop a repeat type of fault current limiter (FCL) for power distribution lines, a new type of FCL adopting arc driving type adjustable resistor was proposed and its arc running velocity

between parallel resistible electrodes was experimentally prepared. This new type of FCL, using conductive ceramics, is for a kind of arc driving method which increases at high speed the resistance between terminals of parallel resistible electrodes by rapidly running the arc generated at terminal of the electrode to the other. Iron electrodes and resistant electrodes were tested under the condition of the amp range from 1 to 3 kA and the electrode distance range from 5 to 30 mm. Main test results were as follows: arc running velocity increased nearly in proportion to arc current; arc running velocity between resistance electrodes became slower when internal resistance increase and was as same as between iron electrodes for the resistance electrodes of 1 mill-ohm/cm; using auxiliary driving devices in combinations with a self excited coil and a reaction type arc driving method, arc running velocity were able to be fastened more than 3 times for the running velocity of parallel electrodes only. DOE

N90-19486# Instituto de Pesquisas Espaciais, Sao Jose dos Campos (Brazil).
CONSTRUCTION AND CHARACTERIZATION OF A VALVE FOR RAPID GAS INJECTION
M. Uedo, J. O. Rossi, Y. Aso, L. S. Mangueira, and C. A. Pereira Jan. 1989 25 p In PORTUGUESE; ENGLISH summary
(INPE-4789-RPE/583) Avail: NTIS HC A03/MF A01

An electromagnetic valve for fast gas injection was built and characterized. This type of gas injection valve is routinely applied to various plasma experiments: in magnetic confinement devices as TOKAMAK, FRP, and Compact Toroids as well as intense ion beam and neutral particle generators. The valve is capable of injecting gas pulses with up to 80 m Torr peak pressure, rising time less than 400 microsec and duration time of 40 ms, in the present experimental set-up. It is easy to build and its components can be totally acquired in the country. Author

N90-19487# Instituto de Pesquisas Espaciais, Sao Jose dos Campos (Brazil).
MONOSTABLE ELECTROVALVE
Evaldo Jose Corat, Vladimir Jesus Trava Airoldi, Ismael Emilio deOliveira, Jr., and Jose Nivaldo Hinckel Nov. 1989 32 p In PORTUGUESE; ENGLISH summary
(INPE-4928-RPE/595) Avail: NTIS HC A03/MF A01

The fundamental calculus, the design, the complete development of a laboratory model, and all necessities of tests to certify the complete and reliable functioning of a monostable electrovalve are presented. An analysis of the results, that made possible the knowledge of the necessary parameters for the design of a qualification model, is presented too. Author

N90-19488# United Technologies Research Center, East Hartford, CT.
CdTe BUFFERED GaAs THIN-SLAB IR WAVEGUIDE MODULATORS AND T/R FILTER
P. K. Cheo, R. T. Brown, G. Carrier, W. Glueck, R. Wagner, and M. Gilden Jul. 1989 31 p Prepared for Massachusetts Inst. of Technology, Lexington, MA
(Contract F19628-85-C-0002)
(AD-A215999; ESD-TR-89-222) Avail: NTIS HC A03/MF A01 CSCL 09/5

Broadband electrooptic modulation and frequency shifting of CO2 lasers using GaAs thin-slab waveguides have been described previously. The performance of an unbuffered GaAs waveguide traveling-wave modulator has been found to yield a sideband power conversion efficiency of 4.5 + or - .0000045 or -43.6 dB for one watt of microwave drive power. This paper presents the performance of CdTe buffered GaAs waveguide modulator and describes the structural parameters that have been modified to gain 5 dB improvement from that provided by unbuffered IR waveguide modulators. CdTe buffered GaAs thin-slab waveguide modulators with very low optical and microwave insertion losses, have been fabricated. The measured single sideband power that can be converted from the CO2 laser input power is -39 dB for one watt microwave driver power, as compared to a measured value of -44 dB from an unbuffered modulator. The output beam quality has also been improved significantly. A transmission/reflection filter designed to separate the sidebands from the carrier has been fabricated and tested. The rejection ratio of carrier power to sideband power is -19 dB. GRA

N90-19489 Department of the Navy, Washington, DC.
INTERNAL TRANSMISSION LINE FILTER ELEMENT Patent
Alfred R. Hislop, inventor (to Navy) 10 Oct. 1989 6 p Filed 27 Jun. 1986
(AD-D014353; US-Patent-4,873,501; US-Patent-Appl-SN-881419; US-Patent-Class-333-204) Avail: US Patent and Trademark Office CSCL 09/1

An improved transmission line filter element allows a higher difference between even and odd mode impedances than previously obtainable from planar structures. The filter element comprises a U-shaped gap formed in the strip conductor of a strip line transmission line, a microstrip structure or a suspended strip line structure. The internal transmission line filters can be cascaded to produce electromagnetic energy filters with deeper notches and steeper skirts than previously obtainable from other planar structures with the same number of elements. GRA

N90-19490 Department of the Navy, Washington, DC.
ELASTOMERIC ELECTRICAL ISOLATION MEMBRANE Patent
Victor J. Marolda, Jr., inventor (to Navy) 17 Oct. 1989 5 p Filed 20 Sep. 1988
(AD-D014365; US-Patent-4,874,326; US-Patent-Appl-SN-246703; US-Patent-Class-439-273) Avail: US Patent and Trademark Office CSCL 11/10

A plug-receptacle type electrical connector is described in combination with a thin, circular, elastomeric membrane joining a plurality of cylindrical elastomeric embossment formed as an integral part thereof. Each embossment further has conical ends at each extremity and an outside diameter slightly larger than the receptacle socket cavity it will contact. Each embossment also has a longitudinal through-hole of inside diameter (ID) slightly smaller than the electrical connector plug pin it is intended to fit over. The membrane is coated with a dielectric grease and slipped over the plug pins. Connector clamping force produce hydrostatic forces, first on each embossment which causes water remaining between the pin and the embossment ID and then pin-to-pin to be broken into a discontinuous series of microspheres. The resulting discontinuity produces full electrical isolation for the assembled pins and sockets and pin-to-pin for the mated connector. Total refurbishment of a connector may thus be accomplished in situ. GRA

N90-19491# Massachusetts Inst. of Tech., Cambridge. Research Lab. of Electronics.
PARALLEL DISTRIBUTED NETWORKS FOR IMAGE SMOOTHING AND SEGMENTATION IN ANALOG VSLI Memorandum Report
A. Lumsdaine, J. Wyatt, and I. Elfadel Sep. 1989 10 p Presented at the 28th IEEE Conference on Decision and Control, Tampa, FL, 13-15 Dec. 1989 Submitted for publication Sponsored in part by Du Pont de Nemours (E. I.) and Co. and Dynatech Corp.
(Contract N00014-87-K-0825; NSF MIP-88-14612)
(AD-A216780; VLSI-MEMO-89-562) Avail: NTIS HC A02/MF A01 CSCL 09/1

Image smoothing and segmentation algorithms are frequently formulated as optimization problems. Linear and nonlinear (reciprocal) resistive networks have solutions characterized by an extremum principle. Thus, appropriately designed networks can automatically solve certain smoothing and segmentation problems in robot vision. This paper considers switched linear resistive networks and nonlinear resistive networks for such tasks. A new derivation of the latter network type from the former is given via an intermediate stochastic formulation, and a new result relating the solution sets of the two is given for the zero temperature limit. We then present simulation studies of several continuation methods that can be gracefully implemented in analog VLSI and that seem to give good results for these non-convex optimization problems. GRA

N90-19492* National Aeronautics and Space Administration. Marshall Space Flight Center, Huntsville, AL.
A DIGITALLY CONTROLLED SYSTEM FOR EFFECTING AND PRESENTING A SELECTED ELECTRICAL RESISTANCE Patent
James C. Fletcher, inventor (to NASA) and Walter L. Ross, inventor (to NASA) (Rockwell International Corp., Pittsburgh, PA.) 18 Jul. 1989 8 p Filed 15 Jul. 1987
(NASA-Case-MFS-29149-1; US-Patent-4,849,903; US-Patent-Appl-SN-073541; US-Patent-Class-364-482; US-Patent-Class-364-481; US-Patent-Class-324-62; US-Patent-Class-323-354) Avail: US Patent and Trademark Office CSCL 09A

A digitally controlled resistance generator is described, in which resistors having values selected according to an expression 2(sup N-1)(R), where N is equal to the number of terms in the expression, and R is equal to the lowest value of resistance, are electrically inserted into a resistive circuit in accordance with a parallel binary signal provided by an analog-to-digital converter or a programmable computer. This binary signal is coupled via optical isolators which, when activated by a logical 1, provides a negative potential to some or all of the gate inputs of the normally on field effect transistors which, when on, shorts out the associated resistor. This applied negative potential turns the field effect transistors off and electrically inserts the resistor coupled between the source terminal and the drain terminal of that field effect transistor into the resistive circuit between the terminals.
Official Gazette of the U.S. Patent and Trademark Office

N90-19493# Oak Ridge National Lab., TN.
VLSI IMPLEMENTATION OF MOMENT INVARIANTS FOR AUTOMATED INSPECTION
G. A. Armstrong, M. L. Simpson, and D. W. Bouldin (Tennessee Univ., Knoxville.) 1990 6 p Presented at the 22nd IEEE Southeastern Symposium on System Theory, Cookville, TN, 11-13 Mar. 1990
(Contract DE-AC05-84OR-21400)
(DE90-005318; CONF-900378-1) Avail: NTIS HC A02/MF A01

This paper describes the design of a very large scale integration (VLSI) application specific integrated circuit (ASIC) for use in automated inspection. The inspection scheme uses Hu and Maitra's algorithms for moment invariants. A prototype design was generated that resolved the long delay time of the multiplier by custom designing adder cells based on the Manchester carry chain. The prototype ASIC is currently being fabricated in 2.0-micron CMOS technology and has been simulated at 20 MHz. The final ASICs will be used in parallel at the board level to achieve the 230 MOPs necessary to perform the moment invariant algorithms in real time on 512 by 512 pixel images with 256 grey scales.
DOE

N90-19494# Sandia National Labs., Albuquerque, NM.
IMPEDANCE CHARACTERISTICS OF TERAWATT ION DIODES
C. W. Mendel, Jr., M. P. Desjarlais, T. D. Pointon, J. P. Quintenz, S. E. Rosenthal, D. B. Seidel, and S. A. Slutz 1990 16 p Presented at the Topical Conference on Research Trends in Nonlinear and Relativistic Effects in Plasmas, San Diego, CA, 5-8 Feb. 1990
(Contract DE-AC04-76DP-00789)
(DE90-006276; SAND-90-0258C; CONF-900264-1) Avail: NTIS HC A03/MF A01

Light ion fusion research has developed ion diodes that have unique properties when compared to other ion diodes. These diodes involve relativistic electrons, ion beam stagnation pressures that compress the magnetic field to the order of 10 Tesla, and large space charge and particle current effects throughout the accelerating region. These diodes have required new theories and models to account for effects that previously were unimportant. One of the most important effects of the magnetic field compression and large space charge has been impedance collapse. The impedance collapse can lead to poor energy transfer efficiency, beam debunching, and rapid change of the beam focus. The current understanding of these effects is discussed including some of the methods used to ameliorate them, and the future directions the theory and modeling will take.
DOE

N90-19495# Helsinki Univ. of Technology, Espoo (Finland). Electromagnetics Lab.
VECTOR CIRCUIT THEORY FOR MULTILAYERED ISOTROPIC AND CHIRAL STRUCTURES: REFLECTION AND TRANSMISSION
Sergei A. Tretyakov and Markku I. Oksanen Aug. 1989 38 p
(PB90-122474; ISBN-951-754-981-4; Rept-50) Avail: NTIS HC A03/MF A01 CSCL 09A

A third part of this author's study on vector circuit modelling of achiral and chiral isotropic slabs is presented. Here, the emphasis is on evaluating reflection and transmission dyadic coefficients for multilayered structures. As examples, reflection and transmission properties of a chiral slab in free space or on an ideally conducting surface as well as of a four layered chiral structure are studied. The new approach allows one to calculate the reflection and transmission for arbitrary angle of incidence and for arbitrary polarization. As it is seen, chiral layers can be used in antenna technology for changing polarization of waves.
Author

N90-19496# Stanford Linear Accelerator Center, CA.
NUMERICAL SIMULATION OF CROSS FIELD AMPLIFIERS
Kenneth Eppley Jan. 1990 16 p Presented at the Accelerator Computer Code Meeting, Los Alamos, NM, 22-25 Jan. 1990
(Contract DE-AC03-76SF-00515)
(DE90-006459; SU-SLAC-PUB-5183; CONF-900163-2) Avail: NTIS HC A03/MF A01

Cross field amplifiers (CFA) have been used in many applications where high power, high frequency microwaves are needed. Although these tubes have been manufactured for decades, theoretical analysis of their properties is not as highly developed as for other microwave devices such as klystrons. One feature distinguishing cross field amplifiers is that the operating current is produced by secondary emission from a cold cathode. This removes the need for a heater and enables the device to act as a switch tube, drawing no power until the RF drive is applied. However, this method of generating the current does complicate the simulation. We are developing a simulation model of cross field amplifiers using the PIC code CONDOR. We simulate an interaction region, one traveling wavelength long, with periodic boundary conditions. An electric field with the appropriate phase velocity is imposed on the upper boundary of the problem. Evaluation of the integral of E(center dot)J gives the power interchanged between the wave and the beam. Given the impedance of the structure, we then calculate the change in the traveling wave field. Thus we simulate the growth of the wave through the device. The main advance of our model over previous CFA simulations is the realistic tracking of absorption and secondary emission.
DOE

N90-19497 Physics and Electronics Lab. TNO, The Hague (Netherlands).
DUAL-MODE LATCHING RECIPROCAL FERRITE PHASE SHIFTER [DUAL-MODE LATCHING RECIPROKE FERRIET FASEDRAAIER]
P. J. Koomen Aug. 1988 37 p In DUTCH
(Contract A83/KLu/055)
(FEL-1988-55; TD-88-3881; ETN-90-95078) Copyright Avail: Physics and Electronics Lab. TNO, P.O. Box 96864, 2509 JG 's-Gravenhage, Netherlands

The operation and construction of a dual-mode latching reciprocal ferrite phase shifter are discussed, taking as an example the Raytheon model Mp XM5 ferrite phase shifter. This phase shifter is equipped with an omnidirectional radiator and is used in a phased array radar. Faraday rotator, polarizers, quartz lens, and complete phase shifter are described. The effects of polarizer magnets are discussed. A method to adjust the polarizer such that it fulfills the specifications is described.
ESA

N90-19498 Physics and Electronics Lab. TNO, The Hague (Netherlands).
SINA: A TEST SYSTEM FOR PROXIMITY FUSES
M. G. A. Ruizenaar Apr. 1989 37 p In DUTCH; ENGLISH summary
(Contract A85/KM/119)
(FEL-1989-101; TD-89-1656; ETN-90-95088) Copyright Avail: Physics and Electronics Lab. TNO, P.O. Box 96864, 2509 JG 's-Gravenhage, Netherlands

SINA, a signal generator that can be used for testing proximity fuses, is described. The circuitry of proximity fuses is presented; the output signal of the RF circuit results from a mixing of the emitted signal and received signal that is Doppler shifted in frequency by the relative motion of the fuse with respect to the reflecting target of surface. With SINA, digitized and stored target and clutter signals (previously measured) can be transformed to Doppler signals, for example during a real flight. SINA can be used for testing fuse circuitry, for example in the verification of results of computer simulations of the low frequency Doppler signal processing. The software of SINA and its use are explained. ESA

N90-19499 Max-Planck-Inst. fuer Physik und Astrophysik, Garching (Germany, F.R.). Inst. fuer Extraterrestrische Physik.
INVESTIGATIONS OF X RAY SENSITIVE PN-CCD'S Thesis - Tech. Univ., Munich [UNTERSUCHUNGEN AN ROENTGENEMPFINDLICHEN PN-CCDS]
Martin Meier Mar. 1989 59 p In GERMAN Original contains color illustrations
(MPE-213; ISSN-0178-0719; ETN-90-95338) Copyright Avail: Max-Plank-Inst. fuer Physik und Astrophysik, Inst. fuer Extraterrestrische Physik, 8046 Garching bei Munich, Fed. Republic of Germany

The modus operandi of PN-CCD's (charge coupled devices) with high detection probability for soft x rays is presented with a view to x ray astronomy. The transfer efficiency of a two dimensional CCD was determined for standard conditions as well as in vacuum at a detector temperature of 135 K using laser flashes. In both cases the efficiency is higher than 0.995 per image cell at a timing pulse rate of 1 MHz and a transported charge of about 80,000 electrons. The separation between the image columns is so effective that a charge loss to neighboring columns was not found. The energy resolution is limited to 3.6 keV by the noise of the applied hybrid preamplifier. ESA

N90-19500# Technische Univ., Berlin (Germany, F.R.). Fachbereich Elektrotechnik.
UTILIZATION CRITERIA FOR TRANSISTORS OF DIVERSE TECHNOLOGY IN PULSE INVERTERS WITH HIGH SWITCHING FREQUENCY Ph.D. Thesis [EINSATZKRITERIEN FUER TRANSISTOREN UNTERSCHIEDLICHER TECHNOLOGIE IN PULSWECHSELRICHTERN MIT HOHER SCHALTFREQUENZ]
Helmut Schroeder 1988 114 p In GERMAN
(ETN-90-95359) Avail: NTIS HC A06/MF A01

Inverter supplied asynchronous machines are well adapted to stationary driving problems and to traction. The squirrel-cage motor is cheaper and smaller than a comparable direct-current motor and shows very minimal maintenance costs because of the missing brushes. The development of new connectable power semiconductors permits the manufacturing of inverters, whose properties and costs make alternating current motors competitive. In the area of low and mean power, transistors of diverse technology are currently available. The obtained high pulse frequencies weaken the noises in the inverter and the machine, give good modulation and rule properties and reduce the necessary filters. Field effect transistor technology reduces the switching time by a factor of 10. By means of a simulation program, the effects of the latent period and the command time on the pulse prototype are examined. The results suggest a good estimation of the possibilities of this technology. ESA

N90-19501# Technische Univ., Berlin (Germany, F.R.). Fachbereich Elektrotechnik.
POWER DIODE SWITCHING BEHAVIOR Ph.D. Thesis [DAS ABSCHALTVERHALTEN VON LEISTUNGSDIODEN]
Paul Christiaan Mourick 1988 219 p In GERMAN
(ETN-90-95363) Avail: NTIS HC A10/MF A02

The objective is the analysis of the relations between the return current behavior and the diode configuration and the waking conditions. In case of rupture, very high overvoltages due to inductivities appear because of the high values of di/dt, which can delete the diode or other components. In the case of soft recovery, a great dissipation arises by switching and the diode is not useful for the high frequencies. Five types of net diode are studied: p+n n+ diode with thick middle zone, charge carrier life expectancy is high and returns currents; p+n n+ diode with thin middle zone, an homogeneous distribution of recombination centers makes the zone n available for the dynamic inverse voltage and a good choice of concentration limits return currents; p+n n+ diode with extremely thin middle zone, because of the weak inductivity, and the high value of du/dt, return current peak and work losses are minimal; p+n n+ diode with a doping which limits the room charge zone, the result is analog to the second diode; p+n n+p+n+, if the p-base is well dimensioned, there is no blocking voltage and the conduction voltage is very low. ESA

N90-19502# Technische Univ., Berlin (Germany, F.R.). Fachbereich Elektrotechnik.
A GATE ARRAY STRUCTURE FOR THE EFFICIENT PROJECT OF DIGITAL CIRCUITS: THE UNIT CELL ARRAY Ph.D. Thesis [DAS UNITCELL-ARRAY EINE GATE-ARRAY-STRUKTUR FUER DEN EFFIZIENTEN ENTWURF DIGITALER SCHALTUNGEN]
Olaf Geisler 1989 152 p In GERMAN
(ETN-90-95364) Avail: NTIS HC A08/MF A01

In this study the principles for the development of a unit-cell-array-master, which shows all the advantages of gate-arrays, are presented. By taking the cabling influence on the chip surface into account, a stochastic model of cabling for sea-of-gates-structures is used, which allows establishment of the minimal dimensions of the master-components for the cabling. As regards the cell architecture, the gate isolation technique and smaller asymmetric p-n channel transistor pairs are employed. With logical structures such as Ram, Rom or PLA (programmed logic array), the Gt density increases. The analysis of gate-array cabling capacity shows that transistors with commercial gate-arrays are often of too great dimension. A greater transistor density and a lower dissipation without any performance decrease are possible by using smaller transistors and a parallel connection in circuit paths with higher cabling capacity. Apart from its initial high cost, unit cell array is interesting from an economical point of view. ESA

N90-19503# Stuttgart Univ. (Germany, F.R.). Inst. fuer Computer-Anwendungen.
INFLUENCE OF THE PARAMETERS: CHARGE ORDER, SEQUENCE CLASSIFICATION, PARTIAL SEQUENTIAL CIRCUIT, AND PROCESS REGULARITY OF A WORKING CHARGE (GAUSSIAN PROCESS) ON THE LIFETIME OF A COMPONENT MADE OF 3.1354 T3 AND 3.4377 T761 Ph.D. Thesis [EINFLUSS DER PARAMETER LASTABFOLGE, SEQUENZKLASSIFIZIERUNG, TEILFOLGENUMFANG UND PROZESSIRREGULARITAT EINER BETRIEBSBELASTUNG (GAUSSPROZESS) AUF DIE LEBENSDAUER EINES BAUELEMENTES AUS 3.1354 T3 UND 3.4377 T761]
Hans-Juergen Ertelt 1988 290 p In GERMAN
(ETN-90-95378) Avail: NTIS HC A13/MF A02

The influence of several parameters of a working charge, by systematic change of the control sequence (stationary Gaussian process), is explained and represented by experiments. Some variations of an irregularly oscillating charge sequence have nearly no effect on the charge interactions. The influence of the classification on the component lifetime is principally dependent on the voltage ratio and the irregularity of the charge sequence;

a smaller irregularity factor increases the lifetime; a least level reduction does not compensate totally for the influence of the process classification. But the principal effect on the component lifetime is the crest factor. ESA

N90-19504# Technische Univ., Berlin (Germany, F.R.). Fachbereich Elektrotechnik.
CHARGE PUMPING AS A MEASUREMENT METHOD FOR THE CHARACTERIZATION OF SHORT CHANNEL MOSFETS: REVIEW, DEVELOPMENT, AND COMPARISON OF MEASUREMENT PROCESS Ph.D. Thesis [DAS LADUNGSPUMPEN ALS MESSMETHODE ZUR CHARAKTERISIERUNG VON KURZKANAL-MOSFET'S UEBERSICHT, ERWEITERUNG UND VERGLEICHENDE DARSTELLUNG DES MESSVERFAHRENS]
Georges Przyrembel 1989 93 p In GERMAN
(ETN-90-95726) Avail: NTIS HC A05/MF A01

MOS transistors with channel length in submicron area play an important part in the developing of highly integrated switching devices. The change pumping method has a high resolution power and allows measurement of all technologically realized interface state densities. It has a signal to noise ratio that is one or two decades higher than that of the conductance process or the surface recombination velocity. For measurements with varying temperatures a cryostat was developed which allows experiments in the temperature area 77 to 300 K. A capacity measurement and the charge pumping give an evaluation of the spatial distribution of the damages and the interface, which are generated by hot charge carriers. ESA

N90-19505# Tuebingen Univ. (Germany, F.R.). Astronomisches Inst.
QUANTUM YIELD OF PHOTOCATHODES IN FAR AND EXTREME ULTRAVIOLET WAVELENGTH AREA Thesis [QUANTENAUSBEUTE VON PHOTOKATHODEN IM FERNEN UND EXTREMEN ULTRAVIOLETTEN WELLENLAENGENBEREICH]
Christoph Haas 1989 87 p In GERMAN
(ETN-90-95731) Avail: NTIS HC A05/MF A01

A microchannel plate detector is developed for a spectrograph working in far ultraviolet light. The choice of the photocathode materials is investigated. In this wavelength area, alkali halides are employed because they are generally hygroscopic. A model for the quantum yield is developed which takes into account the angle of incidence of the radiation, the layer reflectivity, the linear absorption coefficient and the number of emitted photoelectrons and their output probability. For the photocathode, hydrogen was chosen, because of the three lines of the Lyman spectrum. The tests show a good reproductibility of the photocathode and a weak increase of the quantum yield under vacuum conditions. This study forms a part of the Orpheus telescope project. ESA

N90-19506# Nationaal Inst. voor Kernfysica en Hoge Energiefysica, Amsterdam (Netherlands).
COMPTON AMPLIFIER [COMPTON VERSTERKER]
J. T. vanEs and J. C. Verkooijen 1989 15 p In DUTCH
(DIGEL-1985-5; ETN-90-95802) Avail: NTIS HC A03/MF A01

An amplifier was developed for Compton detectors signals, used for the positioning of the electron beam of the linear accelerator MEA (Medium Energy Accelerator). The wire between detector and amplifier have to be about 30 m long due to radioactive radiation. The amplifier is broadband (60Hz to 2.3MHz), low noise (equivalent to 1 microA input current), and has a high common mode rejection (more than 80 dB); the inputs are galvanically separated with an input sensitivity of 1 microA. The signal to be detected is gated. Signals can be amplified to an output voltage of 5 V on 50 ohms with a 150 ms rise time. ESA

N90-19507# Technische Univ., Berlin (Germany, F.R.). Fachbereich Elektrotechnik.
DEVELOPMENT OF DYNAMIC EQUIVALENT NETWORK STRUCTURES WITH A UNIVERSAL IDENTIFICATION AND OPTIMIZATION PROCESS Ph.D. Thesis [BILDUNG DYNAMISCHER ERSATZNETZSTRUKTUREN MIT EINEM UNIVERSELLEN IDENTIFIKATIONS- UND OPTIMIERUNGSVERFAHREN]
Hans-Juergen Hinrichs 1989 134 p In GERMAN
(ETN-90-95822) Avail: NTIS HC A07/MF A01

A network reduction process is developed for stability experiences in energy distribution networks. The differential equation systems of linear and nonlinear networks can then be easily reduced. In any of the branches, limit network areas can be separated from a network core and described by dynamic equivalent circuits. The process is integrated in a program system and all schemes are easily realizable. Only the voltage (modules and phase), active and reactive power must be known. A dynamic equivalent scheme of a machine in connection with a passive charge is more suitable in short circuit weak networks for the development of dynamic processes than a frequency-stable supply and gives good description, for examples of reactive and active power compensating oscillations. ESA

N90-19508# Nationaal Inst. voor Kernfysica en Hoge Energiefysica, Amsterdam (Netherlands).
DIGITAL INTEGRATOR Thesis - Amsterdam Univ. [DIGITALE INTEGRATOR]
M. vanBeuzekom 1989 65 p
(DIGEL-1989-2; ETN-90-95977) Avail: NTIS HC A04/MF A01

A traveling digital integrator was developed and built for hadron detectors used on an MEA (Medium Energy Accelerator). The integral of the input signal of the integrator is continuously determined using digital signal processing. This integrator is a prototype of a faster digital integrator which has to be developed. The prototype has a maximum sampling frequency of 40 MHz, which could be extended to 70 MHz. The tests with the prototype show that the integrator functions well in principle, but does not allow conclusions about the exact accuracy of the integrator. ESA

N90-19509# Nationaal Inst. voor Kernfysica en Hoge Energiefysica, Amsterdam (Netherlands).
DIGITAL TO POSITION CONVERTER
J. T. vanEs and A. H. Kruijer 1989 19 p In DUTCH
(DIGEL-1984-4; ETN-90-95978) Avail: NTIS HC A03/MF A01

A digitally controllable servosystem for mechanical displacements was developed. The circuitry of this prototype is explained. The control and power supply are performed from a Camac module, Borer type 1084A. The system was applied in the phase shifter of a klystron control and in the attenuator at the output of this klystron. ESA

N90-19510# Nationaal Inst. voor Kernfysica en Hoge Energiefysica, Amsterdam (Netherlands).
HIGH VOLTAGE PICKUP PLATE
Tom Sluijk and Nils Dobbe 2 Mar. 1989 21 p In DUTCH
(LINO-1989-3; ETN-90-95406) Avail: NTIS HC A03/MF A01

A High Voltage Pickup Plate (HVPP) and the accompanying electronics were developed for the electron gun of the electron accelerator in order to investigate the stability of the voltage on the electron gun. The system is based on the capacitive divider voltage. Special attention was paid to the shielding of the high voltage (fail safe provisions). The HVPP allows the measurement of the absolute quantities of the instabilities due to rectification and pulsed loading, in contrast with existing systems. ESA

N90-19511# Hochschule der Bundeswehr, Hamburg (Germany, F.R.). Fachbereich Elektrotechnik.
A CONTRIBUTION TO THE THEORY OF TRANSIENT CONDUCTOR SIMULATIONS Ph.D. Thesis [EIN BEITRAG ZUR THEORIE TRANSIENTER LEITUNGSNACHBILDUNGEN]

Dieter Heidorn 1988 237 p In GERMAN
(ETN-90-95891) Avail: NTIS HC A11/MF A02

A frequency dependent model for connection cables is presented, which can be used for several network types. It is based on an analytic resolution of the current penetration problems in parallel nonpermeable conductors of cylindrical cutting, or high constant permeability conductors. Another model is developed for alternating current air line, which can calculate the frequency response of the impedance and admittance matrices and can be used for the transient programs. An analytic description of the cable impedance and the utilization of some expressions such as the Dubanton formula give the poles of the dipole matrix. No discretization fault occurs. ESA

N90-19512# Technische Univ., Berlin (Germany, F.R.). Fachbereich Elektrotechnik.

THEORETICAL AND EXPERIMENTAL STUDIES OF A BRUSHLESS DISK ROTOR MOTOR WITH PERMANENT MAGNETIC EXCITATION AND GAP WINDINGS Ph.D. Thesis [THEORETISCHE UND EXPERIMENTELLE UNTERSUCHUNGEN AN EINEM PERMANENTMAGNETERREGTEN BUERSTENLOSEN SCHEIBENLAEUFERMOTOR MIT LUFTSPALTWICKLUNGEN]

Lutz-Ruediger Walkhoff 1989 197 p In GERMAN
(ETN-90-96056) Avail: NTIS HC A09/MF A02

With the utilization of high value magnets with stiff magnetization, it is possible to establish a 3-D, analytic field calculation process in which the influence of the permeability is taken into account. The process is based on the reflection laws for the scalar magnetic potential and allows examination of the influence of the permeability on the profile of the induction in gap. The inductivity of the windings is approximately obtained with the magnetic field of the stator windings, that is found three dimensionally in the winding area. Since the permanent magnet material used is a good electrical conductor, eddy current losses can appear in the magnet with phase currents. For the first losses estimation, the stationary stator field in the magnet area was calculated. The induction in the rotor is relatively low for maximal currents so that only very minimal losses occur. The dissipation was calculated with the Paynting vector from the vector potential. ESA

N90-19513# Pennsylvania Univ., Philadelphia. Dept. of Materials Science and Engineering.

ZIRCONIA-BASED ELECTRODES FOR SOLID OXIDE FUEL CELLS Final Report

Wayne L. Worrell Dec. 1989 9 p
(Contract DE-FG21-86MC-23139)
(DE90-000462; DOE/MC-23139/2794) Avail: NTIS HC A02/MF A01

The objective of this contract is the syntheses and electrical characterization of new mixed-conducting yttria-stabilized zirconia-titania solutions. The results will provide the fundamental data necessary for the quantitative evaluation of the potential electrode applications of these new mixed conducting oxides in solid oxide fuel cells (SOFC). DOE

N90-19514# Oak Ridge National Lab., TN. Applied Technology Div.

DESIGN OF A HIGH POWER DENSITY, PERMANENT MAGNET, AXIAL GAP dc MOTOR

R. A. Hawsey, D. S. Daniel, R. J. Thomas, and J. M. Bailey (Tennessee Univ., Knoxville.) 1990 19 p Presented at the IEEE Southeastcon, New Orleans, LA, 1-4 Apr. 1990
(Contract DE-AC05-84OR-21400)
(DE90-005449; CONF-900464-2) Avail: NTIS HC A03/MF A01

In the design of drive motors for undersea vehicles, the premium placed on noise suppression suggests the use of a brush-commutated dc motor. The additional constraints of weight and volume, as well as unusual configuration, presents the axial air-gap configuration, with a permanent magnet field, as a viable candidate. In such a configuration the design of the brushes and commutator and the resulting structure becomes critical. A novel solution to this problem is described. The basic motor consists of two discs containing permanent magnets on either side of a magnetic structure containing the copper windings. An advantage of this motor concept is that copper cooling may easily be accomplished through the use of liquid circulating through the stator windings. The role of field and armature in a conventional disc motor configuration are reversed. The two discs containing the permanent magnets are rotating. The brushes are on the discs. The magnetic structure with the coils is stationary. The commutator bars are imbedded in the stationary member. Input power is supplied to the brushes through a brush-and-slip ring assembly. An electromagnetic design analysis for a 92 ft-lb, 700 rpm motor was performed. A finite element analysis was conducted and the results show that magnetic saturation is not a limiting factor in this design. The motor torque is achievable within weight and volume constraints. DOE

N90-19515# Lawrence Livermore National Lab., CA.

FIELD EFFECT TRANSISTOR STRUCTURES BASED ON STRAIN INDUCED POLARIZATION CHARGES

D. L. Smith, R. T. Collins, T. F. Kuech (IBM Watson Research Center, Yorktown Heights, NY.), and C. Mailhiot Dec. 1989 8 p Presented at the Materials Research Society Fall Meeting, Boston, MA, 27 Nov. - 2 Dec. 1989
(Contract W-7405-eng-48)
(DE90-007247; UCRL-102757; CONF-891119-96) Avail: NTIS HC A02/MF A01

A new field effect transistor based on strain induced polarization charges is suggested. The structure utilizes the pseudomorphic growth of a strained barrier layer on a substrate oriented in a polar direction such as (111) or (211). Polarization charges in the barrier layer are generated by the piezoelectric effect. A 2-D electron gas, whose density can be modulated by an external bias, forms at the hetero-interface and it screens the polarization charge. Zero bias densities of several 10(exp 11) e/sq cm and threshold voltages of 0.5 V can be achieved. Both normally-on and normally-off structures are possible. DOE

N90-19516# Los Alamos National Lab., NM.

ANODE PLASMA FORMATION AS A POSSIBLE MECHANISM FOR AN ELECTRICAL STRESS LIMIT IN COLD CATHODE DIODES

Louis A. Rosocha 1990 7 p Presented at the Large Area Electron Beam Diode Workshop, Monterey, CA, 7 Jun. 1989
(Contract W-7405-eng-36)
(DE90-007503; LA-UR-90-655; CONF-8906200-4) Avail: NTIS HC A02/MF A01

Recent interest in scaling electron beam pumped KrF fusion lasers to the energy levels thought necessary for ignition (MJ-class) has stimulated the development of technology related to broad-area electron beam generators. At this conference, McGeoch has proposed, based upon an examination of widespread electron beam pumped KrF laser data, that a fundamental limit for electrical stress within the electron gun diode exists. McGeoch and others have attributed the mechanism for the limit to gas evolution at the anode due to heating by the e-beam, and a consequent breakdown in the diode due to this gas. DOE

N90-19517# Los Alamos National Lab., NM.

TIME RESOLVED GAIN/LOSS STUDIES UNDER LOW AND HIGH POWER LOADING FOR THE XeF C-A TRANSITION

Robert C. Sze, Marc Sentis, and Matteo Vannini (Consiglio Nazionale delle Ricerche, Florence, Italy) 1990 9 p Presented at the International Conference on Optical Science and Engineering, Hague, Netherlands, 12-16 Mar. 1990
(Contract W-7405-eng-36)
(DE90-007506; LA-UR-89-669; CONF-900368-2) Avail: NTIS HC A02/MF A01

The behavior of gain versus peak power deposition and the gain-length product versus total energy deposited are measured for devices with power deposition levels from 1 to 13 MW/cu cm under a variety of gas mixtures. The temporal correlation between the power deposition and gain shows that both the fluorescence

and the gain occur after the power deposition has concluded for excitation pulses in the range of 10 to 30 ns. It was found that both B-X and C-A fluorescence takes place in the afterglow and their temporal shapes are similar. This indicates that the C and B states are tightly coupled. This tight coupling has two detrimental consequences for C-state lasing. First is that the population of the B and C states are approximately equal rather than 90 percent in the C state believed to exist for short pulse electron beam excitation. It is believed that this close coupling is due to the presence of electric fields in the afterglow which keep the electron temperature relatively hot. The relative populations of the B and C states are determined by a Boltzman distribution governed by the electron temperature and their relative energy separation. Second is that with the C state lifetime approximately the same as the B state lifetime the C-A saturation intensity is very high and efficient energy extraction is substantially more difficult.
DOE

N90-19518# Giner, Inc., Waltham, MA.
ADVANCED DOUBLE LAYER CAPACITOR Quarterly Interim Technical Report No. 6, 1 Aug. - 31 Oct. 1989
Anthony B. LaConti, Philip Lessner, and S. Sarangapani Jan. 1990 17 p
(Contract N00014-88-C-0391; ARPA Order 9526)
(AD-A217110; C87A-25) Avail: NTIS HC A03/MF A01 CSCL 09/1

The overall goal of this project is to develop electrochemical capacitors utilizing a solid ionomer electrolyte. An advantage of these devices over conventional double layer capacitors would be the absence of free liquid electrolyte and thus greater safety and reliability. In the sixth quarter, we concentrated our efforts in three areas: (1) preparation and characterization of electrode materials, (2) preparation of membrane and electrode (M and E) assemblies that have high capacitance and minimum internal resistance, and (3) development of cell hardware that can contain the M and E for extended periods of time without loss of water and contributes negligibly to the total internal resistance. GRA

N90-19519# Massachusetts Inst. of Tech., Cambridge. Lab. for Computer Science.
MODELING A CIRCUIT SWITCHED MULTIPROCESSOR INTERCONNECT
Daniel Nussbaum, Ingmar Vuong-Adlerberg, and Anant Agarwal Oct. 1989 23 p Sponsored in part by Sloan Foundation and IBM Corp.
(Contract N00014-87-K-0825)
(AD-A217122; VLSI-MEMO-89-567) Avail: NTIS HC A03/MF A01 CSCL 12/6

This study began as an attempt to understand discrepancies between Patel's classic model of a circuit-switched interconnection network and simulations as part of the MIT ALEWIFE Multiprocessor project. After a careful analysis of Patel's model, we developed a model with fewer approximations that produced results generally closer to detailed simulation. The major source of inaccuracy in Patel's model is the unit-request approximation, which treats a t-cycle request as t 1-cycle requests producing significant inaccuracies for networks with many switching levels and for small packet sizes. Our model followed the behavior of the network more closely, explicitly modeling the effects of switch size, network depth, packet size and memory latency, thereby alleviating some inaccuracies in Patel's model. However, despite the slightly lower accuracy of Patel's model, we believe that its simplicity makes it the practical choice for most applications. Thus, our main contribution was to understand the causes of inaccuracies in both models, allowing us to predict the quality of the estimations they yielded. Another research result is validating a complicated simulator using relatively simple models, not a common use for a model. We found that some of the original discrepancies between Patel's model and the simulator were due to hidden inconsistancies between parameters used by the model and those used by the simulator, and that others were due to bugs in the simulator code. GRA

N90-19520# Texas Univ., Austin. Microwave Lab.
PLANAR INTEGRATED CIRCUITS FOR MICROWAVE TRANSMISSION AND RECEPTION
Joel Birkeland and Tatsuo Itoh Aug. 1989 123 p
(Contract DAAL03-88-K-0005)
(AD-A217676; MW-89-P-4; ARO-25045.31-EL) Avail: NTIS HC A06/MF A01 CSCL 09/1

The design and test of planar integrated circuits for the transmission and reception of microwave power are described. The circuits consist of MESFET transistor oscillators incorporating periodic microstrip antennas to form transmitters and transceivers. The nature of the periodic antennas allows their use as both resonant and radiating elements in the oscillator design, resulting in a simple and inexpensive circuit. The transmitter and transceiver circuits described here may be divided into two types; single device and dual device. The single device circuits use a single MESFET oscillating into a periodic microstrip patch antenna. The dual device circuits use two MESFETS which oscillate into a couple rampart line microstrip antenna. In the dual device circuit, the FETs may oscillate out of phase for power combining or in phase for frequency doubling. The transmitter circuits generate a beam of RF energy which radiates normal to the planar circuit surface. The transceiver circuits operate in a similar fashion, except that in this case, the antenna also acts to receive RF energy and direct it back to the oscillating MESFET. The MESFET then functions as a self-oscillating mixer for down-conversion of the received signal to the IF frequency. GRA

N90-19263*# Jet Propulsion Lab., California Inst. of Tech., Pasadena.
LARGE ANTENNA MEASUREMENT AND COMPENSATION TECHNIQUES
Y. RahmatSamii *In* NASA, Langley Research Center, Earth Science Geostationary Platform Technology Jul. 1989 p 203-215 Presented at the 11th ESTEC Antenna Workshop on Antenna Measurements, Gothenburg, Sweden, 20-22 Jun. 1988 (For primary document see N90-19249 12-15)
Avail: NTIS HC A17/MF A03 CSCL 20N

N90-19402*# Memphis State Univ., TN. Dept. of Physics.
A COMPUTER CONTROL SYSTEM FOR THE ALTERNATING GRADIENT MAGNETOMETER
Michael M. Garland *In* Alabama Univ., Research Reports: 1989 NASA/ASEE Summer Faculty Fellowship Program Dec. 1989 32 p (For primary document see N90-19390 12-31)
(Grant NGT-01-008-021)
Avail: NTIS HC A99/MF E06 CSCL 09A

N90-19437*# Jet Propulsion Lab., California Inst. of Tech., Pasadena.
MICROWAVE OSCILLATOR WITH REDUCED PHASE NOISE BY NEGATIVE FEEDBACK INCORPORATING MICROWAVE SIGNALS WITH SUPPRESSED CARRIER
G. J. Dick and J. Saunders *In its* The Telecommunications and Data Acquisition Report 15 Nov. 1989 p 20-33 (For primary document see N90-19434 12-32)
Avail: NTIS HC A10/MF A02 CSCL 09A

N90-19450*# Jet Propulsion Lab., California Inst. of Tech., Pasadena.
DISTURBANCE TORQUE REJECTION PROPERTIES OF THE NASA/JPL 70-METER ANTENNA AXIS SERVOS
R. E. Hill *In its* The Telecommunications and Data Acquisition Report 15 Nov. 1989 p 170-188 (For primary document see N90-19434 12-32)
Avail: NTIS HC A10/MF A02 CSCL 09A

34 FLUID MECHANICS AND HEAT TRANSFER

Includes boundary layers; hydrodynamics; fluidics; mass transfer; and ablation cooling.

For related information see also *02 Aerodynamics* and *77 Thermodynamics and Statistical Physics.*

N90-19521 Arizona Univ., Tucson.
ANALYSIS OF UNSTEADY HEAT TRANSFER BY NATURAL CONVECTION IN A TWO-DIMENSIONAL SQUARE CAVITY USING A HIGH ORDER FINITE-VOLUME METHOD Ph.D. Thesis
Hashim Salman Mahdi 1989 265 p
Avail: Univ. Microfilms Order No. DA8919042

Unsteady heat transfer by natural convection in a closed square cavity is investigated numerically. A new finite-volume approach is developed and applied to the two-dimensional continuity, vorticity, and energy equations. The variation of the field variables is approximated by bi-quadratic interpolation formulas over the space occupied by the finite volume and the region surrounding it. These are used in the integral conservation laws for energy, vorticity, and mass. The convective transport is modelled using a new upstream-weighting approach which uses volume averages for the vorticity and the energy transported across the boundaries of the finite volume. The weighting is dependent on the skewness of the velocity field to the surfaces of the finite volume as well as its strength. It is adaptive to local flow conditions. The velocities are obtained from the application of the velocity induction law. Use is made of an image system for the free vorticity of fluid. In this way, the no-penetration condition is enforced at the cavity boundaries, but at the same time it may allow a slip condition to exist. This is not permitted in a viscous flow analysis, and the slip velocity is reduced to zero by the production of free vorticity at the boundaries. Two test cases are treated which have exact solutions. Dissert. Abstr.

N90-19522 ESDU International Ltd., London (England).
HEAT TRANSFER DEFINITIONS AND EQUATIONS
Aug. 1989 5 p Supersedes ESDU-Struct-H.00.00.02
(ESDU-89022; ESDU-Struct-H.00.00.02; ISBN-0-85679-693-X; ISSN-0141-4097) Avail: ESDU

This data item defines quantities and gives equations required in estimating the temperature of a structure due to aerodynamic heating. The terms are specific heat capacity, thermal conductivity, thermal diffusivity, emissivity, absorptivity, heat transfer coefficient, Biot number, stagnation temperature, and recovery temperature and factor. The equation is given for the equilibrium skin temperature under aerodynamic heating allowing for radiation heating both to and from the structure, and its applicability to thin skins in which no temperature gradient exists is considered. The case of thick skins is also considered, and methods of determining the temperature distribution under various simplifying assumptions are discussed. ESDU

N90-19523*# National Aeronautics and Space Administration. Goddard Space Flight Center, Greenbelt, MD.
NUMERICAL AND EXPERIMENTAL ANALYSIS OF A THIN LIQUID FILM ON A ROTATING DISK RELATED TO DEVELOPMENT OF A SPACECRAFT ABSORPTION COOLING SYSTEM
Amir Faghri (Wright State Univ., Dayton, OH.) and Theodore D. Swanson Sep. 1989 335 p Presented at the National Heat Transfer Conference, Philadelphia, PA, Aug. 1989
(Grant NAG5-956)
(NASA-CR-183457; NAS 1.26:183457) Avail: NTIS HC A15/MF A02 CSCL 20D

The numerical and experimental analysis of a thin liquid film on a rotating and a stationary disk related to the development of an absorber unit for a high capacity spacecraft absorption cooling system, is described. The creation of artificial gravity by the use of a centrifugal field was focused upon in this report. Areas covered include: (1) One-dimensional computation of thin liquid film flows; (2) Experimental measurement of film height and visualization of flow; (3) Two-dimensional computation of the free surface flow of a thin liquid film using a pressure optimization method; (4) Computation of heat transfer in two-dimensional thin film flow; (5) Development of a new computational methodology for the free surface flows using a permeable wall; (6) Analysis of fluid flow and heat transfer in a thin film in the presence and absence of gravity; and (7) Comparison of theoretical prediction and experimental data. The basic phenomena related to fluid flow and heat transfer on rotating systems reported here can also be applied to other areas of space systems. K.C.D.

N90-19524*# National Aeronautics and Space Administration. Ames Research Center, Moffett Field, CA.
DYNAMICS OF A CLASS OF VORTEX RINGS Ph.D. Thesis - Stanford Univ.
Karim Shariff, Anthony Leonard, and Joel H. Ferziger (Stanford Univ., CA.) Dec. 1989 291 p
(NASA-TM-102257; A-90016; NAS 1.15:102257) Avail: NTIS HC A13/MF A02 CSCL 20D

The contour dynamics method is extended to vortex rings with vorticity varying linearly from the symmetry axis. An elliptic core model is also developed to explain some of the basic physics. Passage and collisions of two identical rings are studied focusing on core deformation, sound generation and stirring of fluid elements. With respect to core deformation, not only the strain rate but how rapidly it varies is important and accounts for greater susceptibility to vortex tearing than in two dimensions. For slow strain, as a passage interaction is completed and the strain relaxes, the cores return to their original shape while permanent deformations remain for rapidly varying strain. For collisions, if the strain changes slowly the core shapes migrate through a known family of two-dimensional steady vortex pairs up to the limiting member of the family. Thereafter energy conservation does not allow the cores to maintain a constant shape. For rapidly varying strain, core deformation is severe and a head-tail structure in good agreement with experiments is formed. With respect to sound generation, good agreement with the measured acoustic signal for colliding rings is obtained and a feature previously thought to be due to viscous effects is shown to be an effect of inviscid core deformation alone. For passage interactions, a component of high frequency is present. Evidence for the importance of this noise source in jet noise spectra is provided. Finally, processes of fluid engulfment and rejection for an unsteady vortex ring are studied using the stable and unstable manifolds. The unstable manifold shows excellent agreement with flow visualization experiments for leapfrogging rings suggesting that it may be a good tool for numerical flow visualization in other time periodic flows. Author

N90-19525# Cambridge Univ. (England). Dept. of Engineering.
SEPARATION BUBBLES AT HIGH REYNOLDS NUMBER: MEASUREMENT AND COMPUTATION Ph.D. Thesis
William John Devenport Jun. 1985 259 p Sponsored in part by Jersey Education Committee and RAE
(CUED/A-AERO/15; ISSN-0309-7293) Avail: NTIS HC A12/MF A02

Two flows through a sudden expansion in a pipe (an axisymmetric backward facing step) of area ratio 3.56, were studied experimentally. Both flows separated at the step, where the boundary layer was turbulent, and reattached to the pipe wall downstream enclosing a separation bubble. For one of the flows, a centerbody was mounted downstream of the step to provide an annular flow contraction and to impose a strong negative streamwise pressure gradient on the flow in the reattachment region. Both flows were effectively incompressible and of Reynolds number 1.5 x 10(exp 5). Pulsed-wire techniques were used to measure velocity and skin friction. A new pulsed-wire probe was developed to make detailed measurements of velocity in turbulent reversing flow between 0.15 mm and 0.55 mm from a wall. Without the centerbody, the bubble length was 10.7 step heights. For some distance downstream of the step the flow was in some

ways similar to a free jet, though the shear layer grew at a slower rate and turbulence intensities were higher than in a jet. With the centerbody, the bubble length was 3.1 step heights. The separated shear layer was strongly curved towards its low-speed side by the centerbody. This had a stabilizing effect on turbulence in the layer. The shear layer approached the wall at a larger angle and was thinner in the reattachment region than it was without the centerbody. In both cases, the near-wall flow upstream of reattachment and in the attachment region was very different to that in a normal attached turbulent boundary layer. An inviscid empirically based computation method for flows with separation bubbles was developed. The flow is computed only on the high-speed side of the time-mean dividing streamline, the position of which is computed by specifying a static-pressure distribution along it. The effects of turbulence in the shear layer are modelled by specifying a distribution of stagnation pressure here, similar to that found in a fully-developed plane mixing layer. Several axisymmetric flows with separation bubbles were computed. The level of agreement with measurements is encouraging. Author

N90-19526# Heat Pump Technology Center of Japan, Tokyo.
SURVEY ON THE SOCIAL AND ECONOMIC INFLUENCES OF WIDE-SPREADING HEAT-PUMP TECHNOLOGY
Kozo Katayama Jul. 1988 127 p
(DE89-782294; HPTC-05) Avail: NTIS (US Sales Only) HC A07/MF A01

A survey was conducted on the current status of utilization, trends in technical development for future and policy of heat pumps (HP). Heat pumps exceeded 65 pct of shipment of air conditioners for home and 70 pct for business. Proportion of installation was 20 pct per household and a 4.8 pct per room in 1984. It was already applied to industrial processes. Technological developments are in progress on HP for cold regions, multisystem for air conditioning/hot water supply, and absorption-type HP in order to widen its application. In political aspects, its proliferation is promoted by the financial aids and favorable charging system. The use of HP in 2000 is estimated as 26 to 51 pct per room for air conditioning, 40 to 64 pct of total heat demands for air conditioning, and 7 to 17 pct in heat demands for hot water supply. Share of HP in business application will be 39 to 68 pct for air conditioning, and 3 to 9 pct for hot water supply. About 2.3 to 5.0 pct of demands for industrial process will be filled with HP. HP will have a significant influence on energy conservation and environmental improvement. DOE

N90-19527# Heat Pump Technology Center of Japan, Tokyo.
OPERATIONAL FACT-FINDING REPORT ON HEAT PUMP SYSTEMS FOR INDUSTRIAL USE
Jun Kamisawa Mar. 1988 188 p
(DE89-782295; HPTC-8801) Avail: NTIS (US Sales Only) HC A09/MF A01

Operational circumstances of heat pump systems for industrial use were widely investigated to open their successful cases in practical applications to the public and to widely spread them throughout the industrial sector. As a summary of questionaire totaled 144 cases, 79 cases were motor-operated heat pumps, 37 cases absorption heat pumps and 28 cases engine-driven heat pumps, and, in application, 65 cases were manufacturing process use, 46 cases for factory air conditioning and 5 cases for others (such as snow melting and pool water heating). Most of them were motor-operated heat pumps in application of heat sources for manufacturing process and air conditioning, however, it was recognized a trend toward spreading uses for primary industries and increasing absorption heat pumps and engine-driven heat pumps. As for successful examples, outlines of a motor-operated heat pump system for distilling alcohol at Osaka Plant of Suntory Ltd. and an absorption heat pump system for refining alcohol at Ishioka Alcohol Factory of NEDO (New Energy and Industrial Technology Development Organization) and others were illustrated. Their operational circumstances and energy conservation results were investigated. DOE

N90-19528# Materials Research Labs., Ascot Vale (Australia).
NUMERICAL MODELLING OF SHOCKS IN GASES AND METALS
M. B. Tyndall Sep. 1989 47 p
(MRL-RR-8-89; AR-005-742) Avail: NTIS HC A03/MF A01

Results are presented for a range of one-dimensional shock wave problems in gaseous and metallic materials. These problems were solved numerically using Flux-Corrected Transport (FCT). FCT is a numerical technique which achieves high resolution without non-physical oscillations, especially in regions of steep gradients such as shock fronts. These types of problem involve solving the Eulerian inviscid fluid flow equations, namely the continuity equation, conservation of momentum and conservation of energy, with an appropriate equation of state. For gaseous materials the ideal gas equation of state was used and for metallic materials the stiffened-gas or the Mie-Grueneisen equation of state. Shock wave problems in gases included the one-dimensional shock tube problem, a shock wave hitting a density discontinuity and shocks of equal magnitude colliding. Using the stiffened-gas equation of state and the Mie-Grueneisen equation of state similar types of problems were solved for metallic materials, for example, a shock propagating through a piece of metal. A discussion of the performance of FCT to accurately model these problems is given. Currently work is being done on adding elastic-plastic (or viscous) terms and heat conduction terms to the fluid flow equations, to improve the description of flow in a solid material. Author

N90-19529# Notre Dame Univ., IN. Dept. of Aerospace and Mechanical Engineering.
AN EXPERIMENTAL INVESTIGATION OF THE FLOW FIELD AROUND YAWED STRANDED CABLES Contractor Report, Jul. 1987 - Nov. 1988
Stephen M. Batill, Robert C. Nelson, and Jose V. Nebres Nov. 1989 164 p
(Contract N00014-83-K-0239)
(AD-A215782; NCSC-CR-2210-89-1) Avail: NTIS HC A08/MF A01 CSCL 20/4

An experimental study was conducted to investigate the flow field about stranded cables. The objective was to gain insight into the flow mechanisms associated with the generation of fluid forces on cables. Five rigid cable models and a circular cylinder were tested in a wind tunnel. The models represented full-scale cable geometries and were yawed at four different cable angles (90, 60, 40, and 20 degrees) for Reynolds numbers in a range from 5,800 to 13,800 based on cable diameter and freestream velocity. Smoke flow visualization and hot wire anemometry were used to collect qualitative and quantitative data, consisting of pictures of the vortex wake, vortex shedding angles and wake widths, shedding frequency and spanwise coherence of the vortex wake. Results show that the cable geometry influences the flow field about the cable. GRA

N90-19530# Texas Univ., Austin. Dept. of Electrical and Computer Engineering.
APPLICATIONS OF FREQUENCY AND WAVENUMBER NONLINEAR DIGITAL SIGNAL PROCESSING TO NONLINEAR HYDRODYNAMICS RESEARCH Final Report
Edward J. Powers and Richard W. Miksad 18 Dec. 1989 16 p
(Contract N00167-88-K-0049)
(AD-A216259) Avail: NTIS HC A02/MF A01 CSCL 20/4

Recent progress is summarized in applying higher-order statistical techniques (such as higher-order spectra) and associated nonlinear system identification techniques to nonlinear hydrodynamic phenomena. In particular, it is estimated, given model-test data of wave excitation and vessel/structure response, either frequency-domain or time-domain Volterra kernels. Knowledge of the Volterra Kernels is important because the nonlinear physics is imbedded in them. Also such experimental knowledge is necessary to compare with theory, and to quantify the nonlinear mechanisms whereby energy is extracted from the wave excitation and downconverted or up-converted in the response frequency spectrum. Of fundamental practical importance

is the fact that the approach is valid for Gaussian as well as nonGaussian excitation. GRA

N90-19531# Ballistic Research Labs., Aberdeen Proving Ground, MD.
COMPUTATIONAL FLUID DYNAMICS METHOD FOR LOW REYNOLDS NUMBER FLOW IN A PRECESSING/SPINNING, LIQUID FILLED CYLINDER WITH ROUNDED ENDCAPS Memorandum Report
Michael J. Nusca Dec. 1989 36 p
(DA Proj. 1L1-62618-AH-80)
(AD-A216997; BRL-MR-3792) Avail: NTIS HC A03/MF A01 CSCL 19/10

The flight stability of liquid-filled, spin-stabilized projectiles has been considered for a wide variety of conditions. The three-dimensional, steady, laminar, Navier-Stokes equations are solved using an implicit finite-difference scheme based on successive-over-relaxation. These numerical simulations are used to predict the behavior of incompressible liquids undergoing steady spin and steady precession at a fixed precession angle. The liquid is contained in a fully-filled cylinder with flat or rounded endcaps. These numerical simulations can predict steady viscous and pressure moments due to the liquid fill at low Reynolds number. These moments tend to increase the precession angle and reduce the spin rate of the container. Liquid-induced roll and side (yaw) moments are computed as functions of endcap height to cylinder radius, cylinder half-height to radius, Reynolds number, ratio of precession to spin rate, and precession angle. For a given cylinder, rounded endcaps can decrease the resonant liquid-induced moment by about 25 percent and shift the resonance to a smaller Reynolds number. GRA

N90-19532# Notre Dame Univ., IN. Dept. of Chemical Engineering.
STUDY OF INTERFACIAL BEHAVIOR IN COCURRENT GAS-LIQUID FLOWS Progress Report, 1 May 1989 - 30 Apr. 1990
Mark J. McCready Jan. 1990 23 p
(Contract DE-FG02-88ER-13913)
(DE90-005988; DOE/ER-13913/2) Avail: NTIS HC A03/MF A01

The machanism was examined of formation of solitary waves on gas-liquid flows and found, that these form from existing periodic waves which have sufficiently large (approx. 1.5 to 2 depending upon fluid properties) amplitude to liquid layer thickness ratios. The exact process for the wave shape change is not understood but it does not seem to be related to the wave steepness (amplitude/wavelength) or to separation of gas flow over the waves. The observed confinement of solitary waves to low liquid Reynolds numbers results because the necessary large precursor waves do not form if the wave speed dispersion is too large or if the wavelength of the dominant waves is too short, as occurs for higher Re(sub L). Measurements of interface tracings and calculations of power spectra and bispectra as a function of flow distance for conditions close to neutral stability reveal that the initially, linearly unstable mode is stabilized by formation of overtones which are linearly stable and can dissipate energy. As a result, a stable wave field can occur. Mode equations, which include quadratic nonlinearities, can model this process to the extent of producing some degree of quantitative predictions for the amplitudes of the wave modes. However, a complete picture of the wave field must include sidebands as well because these are observed for some flow conditions. DOE

N90-19533# Laboratorio de Computacao Cientifica, Rio de Janeiro (Brazil).
FINITE ELEMENT APPROXIMATIONS OF THE STOKES FLOW PROBLEM BASED UPON VARIOUS VARIATIONAL PRINCIPLES
Leopoldo P. Franca, Thomas J. R. Hughes, and Rolf Stenberg May 1989 17 p
(DE90-608612; LNCC-010/89) Avail: NTIS (US Sales Only) HC A03/MF A01

Finite element methods are constructed by adding to the usual Galerkin method terms that are mesh-dependent least squares forms of the Euler-Lagrange equations. The methods are consistent and possess additional stability compared to the Galerkin method. Finite element interpolations, which are unstable in the Galerkin approach, are now convergent. The methodology is applied to the velocity-pressure formulation, a.k.a., Herrmann's formulation, to the stress-velocity formulation, a.k.a., Hellinger-Reissner's formulation and to a new formulation based on augmented stress, pressure and velocity. DOE

N90-19534* National Aeronautics and Space Administration. Langley Research Center, Hampton, VA.
METHOD AND APPARATUS FOR DETECTING LAMINAR FLOW SEPARATION AND REATTACHMENT Patent
John P. Stack, inventor (to NASA) and Sivaramakrishnan M. Mangalam, inventor (to NASA) (Analytical Services and Materials, Inc., Hampton, VA.) 18 Jul. 1989 13 p Filed 7 Jun. 1988
(NASA-Case-LAR-13952-1-SB; US-Patent-4,848,153; US-Patent-Appl-SN-203178; US-Patent-Class-73-432.1) Avail: US Patent and Trademark Office CSCL 20D

The invention is a method and apparatus for detecting laminar flow separation and flow reattachment of a fluid stream by simultaneously sensing and comparing a plurality of output signals, each representing the dynamic shear stress at one of an equal number of sensors spaced along a straight line on the surface of an airfoil or the like that extends parallel to the fluid stream. The output signals are concurrently compared to detect the sensors across which a reversal in phase of said output signal occurs, said detected sensors being in the region of laminar separation or reattachment. The novelty in this invention is the discovery and use of the phase reversal phenomena to detect laminar separation and attachment of a fluid stream from any surface such as an airfoil supported therein.
Official Gazette of the U.S. Patent and Trademark Office

N90-19535*# Pennsylvania State Univ., University Park. Gas Dynamics Lab.
SWEPT SHOCK/BOUNDARY LAYER INTERACTION EXPERIMENTS IN SUPPORT OF CFD CODE VALIDATION Interim Technical Report, 15 Jan. 1989 - 14 Jan. 1990
G. S. Settles and Y. Lee Mar. 1990 9 p
(Grant NAG2-592)
(NASA-CR-186397; NAS 1.26:186397; PSU-ME-R-89/90-0011)
Avail: NTIS HC A02/MF A01 CSCL 20D

Research on the topic of shock wave/turbulent boundary layer interaction was carried out. Skin friction and surface pressure measurements in fin-induced, swept interactions were conducted, and heat transfer measurements in the same flows are planned. The skin friction data for a strong interaction case (Mach 4, fin-angles equal 16 and 20 degrees) were obtained, and their comparison with computational results was published. Surface pressure data for weak-to-strong fin interactions were also obtained. Author

N90-19536# Cornell Univ., Ithaca, NY.
DEVELOPMENT AND UTILIZATION OF NEW DIAGNOSTICS FOR DENSE-PHASE PNEUMATIC TRANSPORT Quarterly Technical Progress Report, 1 Oct. - 31 Dec. 1989
Michel Y. Louge and James T. Jenkins 1989 6 p
(Contract DE-AC22-88PC-88947)
(DE90-006787; DOE/PC-88947/T5) Avail: NTIS HC A02/MF A01

The main objective is to develop probes for local measurements of solid velocity and holdup in dense gas-solid flows. In particular, capacitance probes are designed to measure local, time dependent particle concentrations. In addition, a new optical fiber probe based on laser-induced-phosphorescence is developed to measure particle velocities. The principles for the capacitance and optical diagnostics were given in the first and second quarterly reports. The feasibility of the optical fiber probe was demonstrated with success. Another objective of this work is to develop a model of dense-phase conveying and to test this model in a setup that

incorporates diagnostics. In this period, as a prelude to these modeling efforts scheduled for the third year of the contract, additional computer simulations of rapid granular flows were performed to verify the theories of Jenkins and Richman (1988) on the anisotropy of the second moment in simple shear. DOE

N90-19537*# Institute for Computer Applications in Science and Engineering, Hampton, VA.
APPLICATION OF A REYNOLDS STRESS TURBULENCE MODEL TO THE COMPRESSIBLE SHEAR LAYER Final Report
S. Sarkar and L. Balakrishnan Feb. 1990 30 p Submitted for publication
(Contract NAS1-18605)
(NASA-CR-182002; NAS 1.26:182002; ICASE-90-18) Avail: NTIS HC A03/MF A01 CSCL 20D

Theoretically based turbulence models have had success in predicting many features of incompressible, free shear layers. However, attempts to extend these models to the high-speed, compressible shear layer have been less effective. In the present work, the compressible shear layer was studied with a second-order turbulence closure, which initially used only variable density extensions of incompressible models for the Reynolds stress transport equation and the dissipation rate transport equation. The quasi-incompressible closure was unsuccessful; the predicted effect of the convective Mach number on the shear layer growth rate was significantly smaller than that observed in experiments. Having thus confirmed that compressibility effects have to be explicitly considered, a new model for the compressible dissipation was introduced into the closure. This model is based on a low Mach number, asymptotic analysis of the Navier-Stokes equations, and on direct numerical simulation of compressible, isotropic turbulence. The use of the new model for the compressible dissipation led to good agreement of the computed growth rates with the experimental data. Both the computations and the experiments indicate a dramatic reduction in the growth rate when the convective Mach number is increased. Experimental data on the normalized maximum turbulence intensities and shear stress also show a reduction with increasing Mach number. Author

N90-19538*# Institute for Computer Applications in Science and Engineering, Hampton, VA.
ANALYTICAL METHODS FOR THE DEVELOPMENT OF REYNOLDS STRESS CLOSURES IN TURBULENCE Final Report
Charles G. Speziale Mar. 1990 60 p Submitted for publication
(Contract NAS1-18605)
(NASA-CR-182017; NAS 1.26:182017; ICASE-90-26) Avail: NTIS HC A04/MF A01 CSCL 20D

Analytical methods for the development of Reynolds stress models in turbulence are reviewed in detail. Zero, one and two equation models are discussed along with second-order closures. A strong case is made for the superior predictive capabilities of second-order closure models in comparison to the simpler models. The central points are illustrated by examples from both homogeneous and inhomogeneous turbulence. A discussion of the author's views concerning the progress made in Reynolds stress modeling is also provided along with a brief history of the subject. Author

N90-19539*# Institute for Computer Applications in Science and Engineering, Hampton, VA.
CONFORMING CHEBYSHEV SPECTRAL COLLOCATION METHODS FOR THE SOLUTION OF LAMINAR FLOW IN A CONSTRICTED CHANNEL Final Report
Andreas Karageorghis and Timothy N. Phillips (University Coll. of Wales, Aberystwyth.) Mar. 1990 46 p Submitted for publication
(Contract NAS1-18605)
(NASA-CR-182011; NAS 1.26:182011; ICASE-90-22) Avail: NTIS HC A03/MF A01 CSCL 20D

The numerical simulation of steady planar two-dimensional, laminar flow of an incompressible fluid through an abruptly contracting channel using spectral domain decomposition methods is described. The key features of the method are the decomposition of the flow region into a number of rectangular subregions and spectral approximations which are pointwise C(1) continuous across subregion interfaces. Spectral approximations to the solution are obtained for Reynolds numbers in the range 0 to 500. The size of the salient corner vortex decreases as the Reynolds number increases from 0 to around 45. As the Reynolds number is increased further the vortex grows slowly. A vortex is detected downstream of the contraction at a Reynolds number of around 175 that continues to grow as the Reynolds number is increased further. Author

N90-19540# Technische Univ., Munich (Germany, F.R.). Lehrstuhl C fuer Thermodynamik.
EXPERIMENTAL AND ANALYTICAL INVESTIGATION OF ADIABATIC CRITICAL WATER AIR TWO PHASE FLOW IN SMALL DIAMETER TUBES Final Report [EXPERIMENTELLE UND ANALYTISCHE UNTERSUCHUNG ADIABATER KRITISCHER WASSER/LUFT-ZWEIPHASENSTROEMUNGEN IN ROHREN KLEINER DURCHMESSER]
Edgar R. F. Winter and Michael Deichsel Jun. 1988 235 p In GERMAN
(Contract DFG-Wi-364/26)
(TB-88/1; ETN-90-95318) Avail: NTIS HC A11/MF A02

The hydromechanical nonequilibrium (slip) between the phases of water-air critical two phase flow was determined in end cross sections of tubes with different length to diameter ratios. A test stand was designed and built in which two phase flows with different composition were investigated as a function of the orientation in the field of gravity and of the pressure level. The results of the measurements were used for a two dimensional modeling of the critical flow states, and the radial distribution of the phases and their velocities. It is shown that the local slip between the phases becomes unity, so that there is locally an homogeneous two phase fluid. Hence, the radial distribution of the velocities can be substituted by that of the sound speeds. The prediction capability of models in the literature was checked and suitable model relations for the prediction of several quantities are given. ESA

N90-19541# Technische Hochschule, Darmstadt (Germany, F.R.). Fachbereich Maschinenbau.
THEORETICAL AND EXPERIMENTAL EXAMINATION OF THE BEGINNING OF TURBULENCE IN A HEATED LAMINAR CONDUIT FLOW Ph.D. Thesis [THEORETISCHE UND EXPERIMENTELLE UNTERSUCHUNG ZUM TURBULENZBEGINN IN EINER BEHEIZTEN LAMINAREN ROHRSTROEMUNG]
Wolfgang Kottnik 1988 142 p In GERMAN
(ETN-90-95369) Avail: NTIS HC A07/MF A01

By heat transfer measurements of a conduit wall of constant temperature in the medium of oil and water, the influence of the materials on the heat transfer, the pressure losses and the turbulence beginning is tested for a laminar flow with Reynolds numbers greater than 1,000. For the turbulence beginning, it is possible to define a critical Reynolds number, if the corresponding viscosity is established with the mean calorific liquid temperature at the location of the turbulence beginning. A calculation program gives the Nusselt numbers, the heat transfer variations, the geometric, thermal and hydraulic parameters of the flow, and the gaps between the measured and calculated values of the pressure by means of a finite difference method. ESA

N90-19542# Karlsruhe Univ. (Germany, F.R.). Inst. fuer Hydrologie und Wasserwirtschaft.
WIND TUNNEL DESIGN OF HEAT ISLAND TURBULENT BOUNDARY LAYER Ph.D. Thesis [WINDKANALMODELLIERUNG VON WAERMEINSELN IN TURBULENTER GRENZSCHICHT]
Bernhard Bloechl 1988 159 p In GERMAN
(IHW-ET/50; ETN-90-95372) Avail: NTIS HC A08/MF A01

The design and physical and mechanical properties of a wind tunnel for the examination of heat islands are presented. City

climatology elements, where heat adsorption and radiation and carbon dioxide emission are too high and dangerous are considered. Measurements and calculations are based principally on Reynolds number variations. The heat transfer is described by Stantom number. The Navier-Stokes equations for a compressible gas of constant viscosity in steady state are employed. After comparison to some city meteorology data, it is established that such a model of an atmospheric turbulent boundary layer is, predictably, impossible in water. Modified Nusselt number and temperature diagrams are easy to use with the proposed parameterization for all experimental conditions. ESA

N90-19543# National Aerospace Lab., Amsterdam (Netherlands). Informatics Div.
FLOW SIMULATION FOR AIRCRAFT
W. Loeve and J. vanderVooren 22 Dec. 1987 44 p In DUTCH; ENGLISH summary
(NLR-MP-87082-U; ETN-90-95413) Avail: NTIS HC A03/MF A01

The various aspects of computer simulation of flow about aircrafts, and their role in aircraft design are discussed. The general tendency in the industrial development process to accelerate product innovation by an integrated approach to the design is explained. Experimental wind tunnel investigations and mathematical modeling are discussed as the two available methods for the analysis of flow about aircrafts. The various flow models used in flow simulation are discussed in successive order of decreasing complexity, and their applicability is outlined. The successive steps in flow simulation are presented. The state of the art in relation to computer technology is described. Information aspects of simulation are discussed in general terms. ESA

N90-19544# Max-Planck-Inst. fuer Stroemungsforschung, Goettingen (Germany, F.R.).
EXPERIMENTS OF THERMOCONVECTION IN A CUBIC CELL Thesis [EXPERIMENTE ZUR THERMOKONVEKTION IN EINER KUBISCHEN ZELLE]
Stefan Koch Mar. 1989 58 p In GERMAN Original contains color illustrations
(MPIS-6/1989; ISSN-0436-1199; ETN-90-95853) Avail: NTIS HC A04/MF A01

By photographs of the tracks of temperature sensitive liquid crystal tracers in vertical and horizontal light layers, the topology of the flow and the vortex in some vertical planes can be evaluated for a cubic cell with two different temperature lateral walls with several Rayleigh numbers. Asymmetric current lines in the lateral walls, ground, and cover are noticed but not explained, such as the influence of the strongly temperature dependent viscosity. These phenomena can only be solved by digital three dimensional calculations, because of the difficulties in creating appropriate test conditions. ESA

N90-19545# Heidelberg Univ. (Germany, F.R.). Sonderforschungsbereich 123.
IMPLEMENTATION OF A FINITE ELEMENT PROCESS FOR THE EULER EQUATIONS OF THE GAS DYNAMICS [IMPLEMENTIERUNG EINES FINITE-ELEMENTE-VERFAHRENS FUER DIE EULER-GLEICHUNGEN DER GASDYNAMIK]
A. Walter Jan. 1989 18 p In GERMAN Sponsored by Deutsche Forschungsgemeinschaft
(Preprint-500; ETN-90-95880) Avail: NTIS HC A03/MF A01

Aerodynamic line diffusion is studied by discretization of hyperbolic conservation equations with the Petrov-Galerkin process. The Euler equations are studied and the entropy and the internal energy are calculated. Several cases were solved, such as a subsonic flow and a flow without limit conditions. The velocity vectors are calculated. A comparison between the numerical results on the symmetry axis of the nozzle and theory shows a good agreement. ESA

N90-19546# Essen Univ. (Germany, F.R.). Fachbereichs Maschinentechnik.
AN OPTICAL WHITE LIGHT SPECKLE PROCESS IN FORWARD DISPERSION FOR MEASUREMENT OF THE VELOCITY FIELD IN FREE CONVECTIVE CURRENTS Ph.D. Thesis [EIN OPTISCHES WEISSLICHT-SPECKLE-VERFAHREN IN VORWAERTSSTREUUNG ZUR MESSUNG DES GESCHWINDIGKEITSFELDES IN FREIEN KONVEKTIONSSTROEMUNGEN]
Michael Grobel 1988 43 p In GERMAN
(ETN-90-95913) Avail: NTIS HC A03/MF A01

The utilization of Particle Image Velocimetry (PIV) in a natural convection current is studied. The currents of three different contours (plane wall, exponential contour, half cylindrical contour) were experimentally examined in a water reservoir. Since the classical boundary layer equations of first order cannot describe the current damping, a more extensive theory was established by means of equations of higher order or a double-decker theory. The advantages and drawbacks if different optical structures and the properties of different light sources were discussed, which are responsible for the PIV, based on a photographic double exposure of particles. For the evaluation of the snaps the point-by point method was used, with which the velocity is obtained by Young Analysis. The experiments show a good agreement with the theory for the plane wall and also with other measurements. The PIV can estimate very weak velocities with strong velocity gradients. The image preparation resolution influences essentially the accuracy of the results. ESA

N90-19547# Goettingen Univ. (Germany, F.R.).
EXPERIMENTAL STUDY OF VALIDITY OF THE UNSTATIONARY KUTTA CONDITION, WITH HIGH STROUHAL NUMBERS Ph.D. Thesis [EXPERIMENTELLE UNTERSUCHUNG ZUR GUELTIGKEIT DER INSTATIONAEREN KUTTA-BEDINGUNG BEI HOHEN STROUHALZAHLEN]
Klaus Schaaf 1988 153 p In GERMAN Sponsored by Deutsche Forschungsgemeinschaft
(ETN-90-95914) Avail: NTIS HC A08/MF A01

By means of an external nonstationary, the output condition at a wing back edge was studied with different Strouhal numbers. The total flow fields were carefully and accurately measured for two continuous flow configurations in the surroundings of a sheet back edge. The highest Strouhal number is slightly lower than the one for which the maximum of the local blast of the shear layer instability appears. From the measured data, the vortex is calculated. It can be remarked, that the Kutta condition for high Strouhal numbers is no longer valid. A strong transverse motion is proved, by a higher vertical field component at the edge with high Strouhal number than with low Strouhal number. ESA

N90-19548# Technische Univ., Delft (Netherlands). Fakulteit der Luchtvaart- en Ruimtevaarttechniek.
CALIBRATION OF THE SONIC MEASURING AND CONTROL CROSS SECTION IN THE GAS FEED INSTALLATION OF THE SOLID FUEL COMBUSTION CHAMBER [CALIBRATIE VAN SONISCHE MEET- EN REGELDOORSNEDE IN DE GASTOEVOERINSTALLATIE VOOR DE VASTE BRANDSTOF VERBRANDINGSKAMER]
G. Heppe and R. P. vandenBerg Mar. 1988 38 p In DUTCH Prepared in cooperation with Prins Maurits Lab. TNO, Rijswijk, Netherlands
(LR-552; PML-1988-C27; SFCC-51; ETN-90-95999) Avail: NTIS HC A03/MF A01

A calibration method was developed for the SMCC (sonic measuring and control cross section) which provides a fast and accurate control and measurement of gas mass flows. The method gives the relation between the pen position and the throughflow surface using a second degree polynomial. The static error of this calibration is lower than 35 percent. Three SMCC's were calibrated by this method: in the methane, air, and oxygen pipe. ESA

N90-19549# Universitaet der Bundeswehr Muenchen, Neubiberg (Germany, F.R.). Fakulataet fuer Luft- und Raumfahrttechnik.
EXPERIMENTAL EXAMINATION OF THE DEVELOPMENT BEHAVIOR OF A GASEOUS BODY IN A STEADY STATE AND NEUTRAL LAYER TURBULENT SHEET BOUNDARY LAYER WITH GROUND ASPERITY Ph.D. Thesis [EXPERIMENTELLE UNTERSUCHUNG DES AUSBREITUNGSVERHALTENS EINES GASFOERMIGEN STOFFES IN NEUTRAL- UND STABIL-GESCHICHTETEN TURBULENTEN PLATTENGRENZSCHICHTEN BEI UNTERSCHIEDLICHER BODENRAUHIGKEIT]
Michael Kerruth 1988 112 p In GERMAN
(ETN-90-96067) Avail: NTIS HC A06/MF A01

The influence of the stability and the ground bumps on the development of a gaseous body in turbulent isobaric boundary layers is studied. Data from a simulation of atmospheric boundary layers is compared to wind tunnel data and atmospheric data. The velocity, temperature and turbulence diagrams are obtained by a thermic measure process. To measure the behavior of a gaseous body, CO2 was used as tracer gas. The lateral and vertical concentration curves were evaluated with a Gaussian model. The vertical concentrations were approximated by an exponential profile from the solution of the diffusion equation. The variation of the vertical concentration with the horizontal coordinate and the stability is in good agreement with the gradient theory and the Lagrange similarity. ESA

N90-19550# Science Applications International Corp., Torrance, CA.
A REVIEW OF MODELS FOR THE ANALYSIS OF THE INJECTION OF DENSELY LOADED FLOWS INTO ENTRAINED FLOW GASIFIERS Final Report
R. Edelman and M. A. Rizk Nov. 1989 47 p
(Contract DE-AC21-85MC-22064)
(DE90-000453; DOE/MC-22064/2796) Avail: NTIS HC A03/MF A01

An analysis of turbulent gas-particle flow has been conducted for which dilute and dense flows were considered. This study showed that, although, there are a variety of models postulated for the analysis of dilute-phase particulate transport, there exists limited information on dense-phase flow. Several derivations of multi-phase flow equations have appeared in the literature. The differences between these equations are in the momentum source terms, the pressure gradient terms and in the convection terms of the dispersed phase momentum equation. In most of the studies on dilute two-phase flow, the effects of the dispersed phase on fluid turbulence have not been considered at all or considered only in an ad hoc fashion. In the few studies where such effects have been incorporated properly, many simplifying assumptions and various empirical constants were introduced. Evaluation of the constants was made via a comparison between model predictions and experimental data. Among these studies the work of Elghobashi and his co-workers, in general, and of Rizk (1985), in particular, provides a foundation for the extension to densely loaded gas/solid flows. Based on this approach, a new mathematical model has been formulated to analyze densely loaded gas/solid flows taking into account particle-particle interactions and gas-particle interactions. DOE

N90-19551# Sandia National Labs., Albuquerque, NM. Experimental Mechanics Dept.
TEST COMPONENT ATTACHMENT EFFECTS ON RESONANT PLATE PYROTECHNIC SHOCK SIMULATION
R. Glenn Bell and Roger M. Zimmerman 1989 12 p Presented at the 36th Inst. of Environmental Science Annual Technology Meeting, New Orleans, LA, 23-27 Apr. 1990
(Contract DE-AC04-76DP-00789)
(DE90-006478; SAND-89-1658C; CONF-900479-3) Avail: NTIS HC A03/MF A01

An accepted technique for simulating pyrotechnic shock inputs has been the resonant plate test. The plate is designed so that its predominant modes generate the desired frequency content of a given shock test specification. The success of the test is dependent on the engineer's ability to effectively design and control the response of the resonant plate. In designing a test to simulate a pyrotechnic environment, the location and mass of the test item become very important considerations since they have a profound impact on the dynamic response of the resonant plate. A relatively massive test item can change the plates's resonant frequency. Differences in the relative frequencies of the test item's fixture and the resonant plate may also effect the input to the test items. In this study, a simple mock test assembly is used to study test item and resonant plate interactions during a test. The implications of this interaction regarding the deviations of the shock test specification are also discussed. Data from shock tests performed with the test assembly mounted to a rigid mounting surface and a flexible resonant plate are compared. Frequency response functions and shock response spectra are generated from the test data and compared to show the significance of: (1) the relative stiffness of the mounting surface; and (2) the location of the input control point during a resonant plate test. DOE

N90-19395*# Illinois Univ., Chicago. Dept. of Mechanical Engineering.
POTENTIAL THEORY OF RADIATION
Huei-Huang Chiu *In* Alabama Univ., Research Reports: 1989 NASA/ASEE Summer Faculty Fellowship Program Dec. 1989 20 p (For primary document see N90-19390 12-31)
(Grant NGT-01-008-021)
Avail: NTIS HC A99/MF E06 CSCL 20D

N90-19407*# Tennessee Univ., Knoxville. Dept. of Mechanical and Aerospace Engineering.
EVALUATION OF THE HEAT TRANSFER MODULE (FAHT) OF FAILURE ANALYSIS NONLINEAR THERMAL AND STRUCTURAL INTEGRATED CODE (FANTASTIC)
Majid Keyhani *In* Alabama Univ., Research Reports: 1989 NASA/ASEE Summer Faculty Fellowship Program Dec. 1989 33 p (For primary document see N90-19390 12-31)
(Grant NGT-01-008-021)
Avail: NTIS HC A99/MF E06 CSCL 20D

35 INSTRUMENTATION AND PHOTOGRAPHY

Includes remote sensors; measuring instruments and gages; detectors; cameras and photographic supplies; and holography.

For aerial photography see *43 Earth Resources and Remote Sensing.* For related information see also *06 Aircraft Instrumentation,* and *19 Spacecraft Instrumentation.*

N90-19552*# California Univ., Los Angeles. Dept. of Chemical Engineering.
MECHANO-CALORIC COOLING DEVICE Final Report
T. H. K. Frederking, Jack Luna, P. Abbassi, and R. M. Carandang 1989 72 p
(Grant NAG2-516)
(NASA-CR-186316; NAS 1.26:186316; UCLA-ENG-90-05) Avail: NTIS HC A04/MF A01 CSCL 14B

The mechano-caloric effect is potentially useful in the He II temperature range. Aside from demonstration work, little quantification effort appears to have been known since other refrigeration possibilities have been available for some time. Successful He II use-related system examples are as follows: in space, the utilization of the latent heat of vaporization has been quite successful in vapor-liquid phase separation (VLPS) in conjunction with thermomechanical force application in plugs. In magnet cooling systems, the possibility of using the mechano-caloric cooling effect in conjunction with thermo-mechanical circulation pump schemes, has been assessed (but not quantified yet to the extent desirable). A third example is quoted in conjunction with superfluid wind tunnel studies and liquid helium tow tank for surface vessels respectively. In all of these (partially future) R and D areas, the question of refrigerator

effectiveness using the mechano-caloric effect appears to be relevant, possibly in conjunction with questions of reliability and simplicity. The present work is concerned with quantification of phenomena including simplified thermodynamic cycle calculations. Author

N90-19553# Central Research Inst. of Electric Power Industry, Tokyo (Japan).
DEVELOPMENT OF THE BLACKBODY PROBE TYPE PYROMETER, PART 1. EXPERIMENTAL STUDY ON THE FUNDAMENTAL CHARACTERISTICS
Toru Hisamatsu, Noriyuki Mori, Teruhide Hamamatsu, and Toshio Abe Jun. 1988 19 p In JAPANESE; ENGLISH summary
(DE89-782288; CRIE-W-87046) Avail: NTIS (US Sales Only)
HC A03/MF A01

For the benefit of the monitoring and controlling high temperature equipment, such as a coal gasification furnace or a gas turbine, measuring the internal temperature of equipment is very important. The black body probe type pyrometer using cavity radiation was designed and studied to develop a pyrometer with high accuracy of measurement in very high temperature of nearly 2000 C or in the corrosive ambient atmosphere. This pyrometer has a small spherical cavity as a pseudo-blackbody at the tip of its probe. Temperature measurement with this pyrometer is carried out by measuring infrared radiation from the cavity. It was shown that the ceramic probe with microcavity can be manufactured by sintering an assembly of powder mouldings to one body. As a calibration result of this pyrometer using an electric furnace, the infrared radiation output of the probe conformed with one measured by a blackbody furnace for calibration with an error of + or - 1 percent or less. The accuracy of temperature measurement was as high as that of the thermocouple. DOE

N90-19554 Department of the Navy, Washington, DC.
OPTICAL PARAMAGNETIC/DIAMAGNETIC GAS SENSOR Patent
Thomas G. Giallorenzi, inventor (to Navy) 24 Oct. 1989 11 p Filed 10 Feb. 1988
(AD-D014368; US-Patent-4,875,357; US-Patent-Appl-SN-154565)
Avail: US Patent and Trademark Office CSCL 20/3

An improved gas sensor which optically senses a signal indication proportional to the concentration of a paramagnetic/diamagnetic gas in a gaseous mixture. In a preferred embodiment of the invention a chamber is adapted to contain a gaseous mixture to be measured for the concentration of a para magnetic/diamagnetic gas in the mixture. An optical source provides light to a movable element to be displaced by a distance proportional to the concentration of the paramagnetic/diamagnetic gas in the gaseous mixture. A photodetector circuit receives light from the movable element having a characteristic indicative of the distance that the movable element was displaced. In response to such received light, the photodetector provides a signal output proportional to the concentration of the paramagnetic/diamagnetic gas in the gaseous mixture. GRA

N90-19555*# National Aeronautics and Space Administration. Langley Research Center, Hampton, VA.
THE UTILIZATION OF AN INFRARED IMAGING SYSTEM AS A COOLING SLOT BLOCKAGE DETECTOR IN THE INSPECTION OF A TRANSPIRATION COOLED NOZZLE
Stephen E. Borg, Robert E. Wright, Jr., David W. Alderfer, and Janet C. Whipple Jan. 1990 23 p
(NASA-TM-102608; NAS 1.15:102608) Avail: NTIS HC
A03/MF A01 CSCL 14B

A comprehensive examination of the 8 foot temperature tunnel's transpiration cooled nozzle was completed using an infrared imaging radiometer to locate regions of cooling flow irregularities caused by obstruction of three or more adjacent cooling slots. Restrictions in the cooling flow were found and cataloged. Blockages found were due primarily to the presence of residual phosphoric acid being discharged from some of the cooling slots. This acid was used during construction of the nozzle components and was to have been purged prior to its delivery to the NASA Langley Research Center (LaRC). In addition, a radial displacement of one selection of discs located in the spool piece was inspected and cataloged for future reference. There did not seem to be a serious restriction of flow in this defect, but evidence from the infrared images indicated reduced slot activity within the gouge. The radiometer survey uncovered regions where closer inspection is recommended but did not cover the entire surface area of the three nozzle subsections due to equipment limitations. A list of areas with suspected problems is included in Appendix A. Author

N90-19556*# National Aeronautics and Space Administration. Marshall Space Flight Center, Huntsville, AL.
FEASIBILITY OF USING EXTREME ULTRAVIOLET EXPLORER (EUVE) REACTION WHEELS TO SATISFY SPACE INFRARED TELESCOPE FACILITY (SIRTF) MANEUVER REQUIREMENTS
W. D. Lightsey Feb. 1990 22 p
(NASA-TM-100389; NAS 1.15:100389) Avail: NTIS HC
A03/MF A01 CSCL 14B

A digital computer simulation is used to determine if the extreme ultraviolet explorer (EUVE) reaction wheels can provide sufficient torque and momentum storage capability to meet the space infrared telescope facility (SIRTF) maneuver requirements. A brief description of the pointing control system (PCS) and the sensor and actuator dynamic models used in the simulation is presented. A model to represent a disturbance such as fluid sloshing is developed. Results developed with the simulation, and a discussion of these results are presented. Author

N90-19557# Lawrence Livermore National Lab., CA.
DESIGN CONSIDERATIONS IN ACHIEVING 1 MW CW OPERATION WITH A WHISPERING-GALLERY-MODE GYROTRON
K. Felch, E. Jongewaard, H. Jory, C. Hess, H. Huey, J. Neilson, R. Pendleton, and D. Pirkle Sep. 1989 7 p Presented at the IEEE International Electron Devices Meeting, Washington, DC, 3-6 Dec. 1989 Prepared in cooperation with Varian Associates, Inc., Palo Alto, CA
(Contract W-7405-eng-48)
(DE90-007283; UCRL-101784; CONF-891205-3) Avail: NTIS
HC A02/MF A01

Varian is developing high-power, CW gyrotrons at frequencies in the range 100 GHz to 150 GHz, for use in electron cyclotron heating applications. Early test vehicles have utilized a TE(sub 15,2,1) interaction cavity, have achieved short-pulse power levels of 820 kW and average power levels of 80 kW at 140 GHz. Present tests are aimed at reaching 400 kW under CW operating conditions and up to 1 MW for short pulse durations. Work is also underway on modifications to the present design that will enable power levels of up to 1 MW CW to be achieved. DOE

N90-19558# Lawrence Livermore National Lab., CA.
PROGRESS IN THE CW OPERATION OF A 140 GHz GYROTRON
K. Felch, E. Jongewaard, H. Jory, C. Hess, H. Huey, J. Neilson, R. Pendleton, and D. Pirkle Sep. 1989 3 p Presented at the 14th International Conference on Infrared and Millimeter Waves, Wuerzburg, Federal Rep. of Germany, 2 Oct. 1989 Prepared in cooperation with Varian Associates, Inc., Palo Alto, CA
(Contract W-7405-eng-48)
(DE90-007382; UCRL-21231; CONF-8910353-2) Avail: NTIS
HC A01/MF A01

Tests on a 140 GHz, whispering-gallery-mode gyrotron have resulted in short-pulse power levels of 820 kW and average power levels of 81 kW. Tests are currently underway on a new tube with the goal of achieving an ouput power of 400 kW CW. DOE

N90-19559# Technische Univ., Hanover (Germany, F.R.). Fachbereich Bauingenieur- und Vermessungswesen.
A HIGH RESOLUTION AUTOMATIC IMAGE MEASURING SYSTEM Ph.D. Thesis [EIN HOCHAUFLOESENDES AUTOMATISCHES BILDMESSSYSTEM]

Thomas Luhmann 1988 109 p In GERMAN
(Wiss-Arb-Vermessungswesen-154; ISSN-0174-1454;
ETN-90-95351) Avail: NTIS HC A06/MF A01

A high resolution automatic image measuring system was developed for the single image measurement of signalized points in scanned and digitized photogrammetric images. The digital image data acquisition is performed with charge coupled device junction sensors. An algorithm was developed for the reliable detection and measurement of taster point with high accuracy (better than 1 micron). The components of the automatic image measurement are presented. The efficiency of the automatic measurement is illustrated by two examples of application. In spite of the necessary interactive interventions of the operator a high degree of automation with high accuracy is reached. ESA

N90-19560# Tuebingen Univ. (Germany, F.R.). Astronomisches Inst.

THE MICROCHANNEL PLATE CAMERA AS A DETECTOR AT HIGH RESOLUTION SPECTROGRAPHS: EXPERIMENTS FOR VELOCITY DISTRIBUTION IN PLANETARY NEBULAE Thesis [DIE MIKROKANALPLATTENKAMERA ALS DETEKTOR AN HOCHAUFLOESENDEN SPEKTROGRAPHEN: UNTERSUCHUNGEN UEBER GESCHWINDIGKEITSVERTEILUNGEN IN PLANETARISCHEN NEBELN]

Christoph Diesch Apr. 1988 91 p In GERMAN
(ETN-90-95733) Avail: NTIS HC A05/MF A01

The factors influencing the spatial homogeneity of the sensitivity and the detector resolution, particularly relating to the spectroscopic recording evaluation, are investigated. A light source is developed that gives flat field images under reproductible conditions; with these the relative sensitivity of the detector can be estimated according to the recorded impact point of the photon. Measurements were carried out to determine the influence of the differential nonlinearities in the characteristic curves of the analog to digital converter. Good results are obtained for the evaluation of high resolution spectra of planetary nebulae obtained with a telescope at the European station in La Silla (Chile). ESA

N90-19561# Technische Univ., Delft (Netherlands). Facultaeit der Luchtvaart- en Ruimtevaarttechniek.

DESIGN OF A PYROMETER FOR TEMPERATURE MEASUREMENTS ON THE SOLID FUEL COMBUSTION CHAMBER [ONTWERP VAN EEN PYROMETER TEN BEHOEVE VAN TEMPERATUURMETINGEN AAN DE VASTE BRANDSTOF VERBRANDINGSKAMER]

W. J. A. M. Aarts and T. Wijchers Oct. 1987 32 p In DUTCH
Sponsored by Stichting Technische Wetenschappen Prepared in cooperation with Prins Maurits Lab. TNO, Rijkswijk, Netherlands
(LR-530; PML-1987-C123; SFCC-48; ETN-90-95997) Avail: NTIS HC A03/MF A01

A pyrometer was developed for the measurement of the flame temperature of the solid fuel combustion chamber. The principle of the design is based on the measurement of the spectral intensity at two wavelengths, 577 and 830 nm, emitted by the soot in the flame. The ratio of the intensities is a univocal measure of the color temperature at these wavelengths. The apparatus is small, robust and user friendly. Calibration currents which imitate the output of the detectors are used to control the electronic circuits. The preliminary measuring accuracy between 1400 and 2800 K is about 20 K if the pyrometer is calibrated every 4 months using a qualified tungsten ribbon lamp. ESA

N90-19562# Sandia National Labs., Albuquerque, NM.

FINITE ELEMENT ANALYSIS OF A QUARTZ ROTATION SENSOR

D. W. Lobitz, E. L. Marek, and G. M. Reese 1989 16 p Presented at the AIAA/ASME SDM Conference, Long Beach, CA, 2-4 Apr. 1990
(Contract DE-AC04-76DP-00789)
(DE90-006959; SAND-89-1980C; CONF-9004116-2) Avail: NTIS HC A03/MF A01

A finite element study in support of the design of a quartz crystal resonator for use as a rotation sensor is presented. This work is the first 3-D analysis of such a resonator. Rotation is sensed by measuring the coupling induced by Coriolis forces between two orthogonal shear modes. These shear modes are measured and excited through the piezoelectric effect. They consist of low-order shear motions coupled to high-order flexure. A highly refined mesh is required to accurately capture this behavior. The design is driven by the need to geometrically tune the sensor such that the two shear modes coincide in frequency. Finite element modeling proved to be indispensible in achieving this design goal. Experimental results from parts fabricated in accordance with the final design indicate that the measured and predicted modal frequencies agree with less than 1 percent error. The desired shear modes, which are greater than the 200th mode in the spectrum, are carefully classified using a straight-forward procedure which gives the effective piezoelectric coupling to specific electrode geometries. A description of the evolution of the finite element model is given along with various obstacles that were overcome during the course of the analysis. DOE

N90-19563# Environmental Research Inst. of Michigan, Ann Arbor.

ARGUS/LLNL IR CAMERA CALIBRATION AND CHARACTERIZATION Final Report, Oct. - Nov. 1989

David J. Witte Nov. 1989 73 p
(AD-A217076; ERIM-222300-1-F) Avail: NTIS HC A04/MF A01 CSCL 17/5

The results and description are presented of a laboratory characterization and calibration performed on the ARGUS Infrared Imaging System (IRI). ARGUS is a USAF aircraft (modified NC-135) that serves as a platform for a variety of optical imaging sensors. These sensors collect data on a variety of targets, including reentry vehicles, objects in low earth orbit, missile plumes, and other aircraft. The IRI is a mid-wave infrared (MWIR) sensor used to collect radiometrically calibratable image data on targets. Recently, some questions have arisen regarding the instrument's performance characteristics and calibration. Consequently, the characterization effort described was undertaken. The specific objectives of this effort were the following: (1) Define calibration curves/equations that relate sensor output signal level to received irradiance; (2) Determine the system radiometric sensitivity, specifically, the Noise Equivalent Spectral Radiance (NESR) in each of the sensor's four spectral bands; (3) Determine the sensor's spatial resolution and assess whether or not the fixed-focus telescope is focussed at infinity. During the course of the laboratory tests, an additional objective was defined; and (4) Assess the change in sensor performance due to cooling the entire camera assembly. GRA

N90-19399*# University of Central Arkansas, Conway. Dept. of Physics.

BACKGROUND STUDIES IN GAS IONIZING X RAY DETECTORS

Hudson B. Eldridge *In* Alabama Univ., Research Reports: 1989 NASA/ASEE Summer Faculty Fellowship Program Dec. 1989 31 p (For primary document see N90-19390 12-31)
(Grant NGT-01-008-021)
Avail: NTIS HC A99/MF E06 CSCL 14B

N90-19972*# Smithsonian Astrophysical Observatory, Cambridge, MA.

A REVIEW OF ATOMIC CLOCK TECHNOLOGY, THE PERFORMANCE CAPABILITY OF PRESENT SPACEBORNE AND TERRESTRIAL ATOMIC CLOCKS, AND A LOOK TOWARD THE FUTURE

Robert F. C. Vessot *In* NASA, Relativistic Gravitational Experiments in Space Aug. 1989 p 186-201 (For primary document see N90-19940 12-90)
Avail: NTIS HC A11/MF A02 CSCL 14B

N90-19973*# Jet Propulsion Lab., California Inst. of Tech., Pasadena.

IMPROVED RANGING SYSTEMS

Larry E. Young *In* NASA, Relativistic Gravitational Experiments in Space Aug. 1989 p 203-205 (For primary document see N90-19940 12-90)
Avail: NTIS HC A11/MF A02 CSCL 14B

N90-19975*# Maryland Univ., College Park. Dept. of Physics and Astronomy.
SUPERCONDUCTING GRAVITY GRADIOMETER AND A TEST OF INVERSE SQUARE LAW
M. V. Moody and Ho Jung Paik *In* NASA, Relativistic Gravitational Experiments in Space Aug. 1989 p 211-212 (For primary document see N90-19940 12-90)
Avail: NTIS HC A11/MF A02 CSCL 14B

N90-19976*# Jet Propulsion Lab., California Inst. of Tech., Pasadena.
INERTIAL CORRECTIONS BY DYNAMIC ESTIMATION
David Sonnabend *In* NASA, Relativistic Gravitational Experiments in Space Aug. 1989 p 213-214 (For primary document see N90-19940 12-90)
Avail: NTIS HC A11/MF A02 CSCL 14B

N90-19977*# Clauser (J. F.) and Associates, Livermore, CA. Custom Sensor Development.
ULTRA-SENSITIVE INERTIAL SENSORS VIA NEUTRAL-ATOM INTERFEROMETRY
John F. Clauser *In* NASA, Relativistic Gravitational Experiments in Space Aug. 1989 p 215-221 (For primary document see N90-19940 12-90)
Avail: NTIS HC A11/MF A02 CSCL 14B

36 LASERS AND MASERS

Includes parametric amplifiers.
For related information see also *76 Solid-State Physics.*

N90-19564# Laser Technology Center, Knoxville, TN. Center for Research and Development.
LASER TECHNOLOGY CENTER Final Report
James E. Parks 11 Jul. 1989 125 p
(Contract ARC-87-154/CO-9901)
(PB90-115387) Avail: NTIS HC A06/MF A01 CSCL 20E

A survey of industries established a need for training laser technicians at Pellissippi State Technical Community College in Knoxville, Tennessee. The four courses that were set up by the Laser Technology Center, the implementation of a laser research laboratory, and progress on defining long term research and methods of industrial collaboration are all described. Author

N90-19565 Department of the Navy, Washington, DC.
CO2 LASER PLUS OPTIMIZATION FOR HARMONIC GENERATION Patent
Barry J. Feldman, inventor (to Navy) 10 Mar. 1987 5 p Filed 10 Mar. 1987
(AD-D014341; US-Patent-4,864,580; US-Patent-Appl-SN-024202; US-Patent-Class-372-25) Avail: US Patent and Trademark Office

This patent discloses a pulsed carbon dioxide laser that eliminates the nitrogen tail on the pulse by placing a Brewster angle absorption cell inside the optical cavity of the laser. This Brewster angle absorption cell contains a gas which exhibits a preferential absorption in the 10 micron spectral regime. This preferential absorption causes the laser to lase in the 9.6 micron regime which allows for easier harmonic generation and elimination of the nitrogen tail. GRA

N90-19566# Westinghouse Electric Corp., Pittsburgh, PA. Science and Technology Center.
DEVELOPMENT OF A RECEIVER FOR A SPACE-BASED LASER RADAR SYSTEM Final Technical Report, 1 Sep. 1988 - 30 Sep. 1989
P. J. Chantry, D. Bhasavanich, and I. Liberman 15 Oct. 1989 52 p
(Contract N00014-88-C-0600)
(AD-A215079) Avail: NTIS HC A04/MF A01 CSCL 17/9

The objective of the contract was to perform basic measurements of quantities relevant to determining the engineering viability of a Tl-Cs atomic line filter (ALF) for use as a receiver to predict the performance of such cells, by improving the theoretical model. A space-based laser radar system must be capable of operating in the presence of intense broadband background from the sun and other bright sources likely to be present in the field of view. Background immunity can be greatly enhanced by exploiting the narrow band feature of the laser transmitter, provided a matched narrow band receiver is available. An additional requirement is that the receiver have a sufficiently fast response for the system bandwidth not to be compromised. These requirements are similar in many respects to those applicable to satellite-based laser communication systems, and previous work on the system of present interest was performed with a view toward using it for communicating through sea water from a satellite to a submarine at operational depths. GRA

N90-19567# Systems Science and Software, La Jolla, CA.
TWO-METER LASER MATERIAL RESPONSE IMPULSE MEASUREMENTS Technical Report, 19 Apr. 1985 - 1 Apr. 1987
Karin Robertson and Michael C. Cates 11 Feb. 1988 45 p
(Contract DNA001-85-C-0186)
(AD-A215834; DNA-TR-87-144) Avail: NTIS HC A03/MF A01 CSCL 20/5

Impulse generated by Excimer Laser Target interactions has been extensively studied at Maxwell Labs. Inc. Results are presented of impulse measurements on aluminum targets using the SDIO/MLI Two Meter Laser operating with KrF as the lasing media. The results of previous MLI impulse measurements using XeF laser media are summarized. The work presented was motivated by earlier impulse measurements also taken on the Two Meter Laser. The data showed much higher impulse to energy ratios than predicted. Additionally, work done elsewhere gave lower I/E values than those found at MLI. The initial MLI impulse studies used a Fotonic gauge as a velocity sensor. As a check on its accuracy, impulse was measured using a simple pendulum; the results agreed with the Fotonic gauge data. A careful investigation of the pendulum experimental technique followed; no problem were found. The S-Cubed ZOOS code was also examined. It is a 1 and 1/2-D code, and only accounts for impulse delivered under the Laser footprint. Additional momentum, however, is provided outside the laser spot via the plasma cloud that results from the laser target interaction. Author

N90-19568 Department of the Navy, Washington, DC.
NARROW-BANDWIDTH UNSTABLE LASER RESONATOR Patent
John F. Reintjes, inventor (to Navy) and David G. Cooper, inventor (to Navy) 19 Sep. 1989 16 p Filed 21 Oct. 1988
(AD-D014362; US-Patent-4,868,515; US-Patent-Appl-SN-260847; US-Patent-Class-330-4.3) Avail: US Patent and Trademark Office CSCL 09/3

This abstract discloses narrow-bandwidth, unstable laser resonator comprising: an output section including a laser gain medium for generating and amplifying light, a first reflective element for reflecting and collimating light from the gain medium back through the gain medium, and a second reflective element having a hole therein. The second reflective element is responsive to the collimated light passed through the gain medium for reflecting most of the collimated light out of the unstable laser resonator as an output beam and for passing the remaining portion of the collimated light through the hole therein as a residual beam. A feedback ring includes an optical path, a beam splitter for passing a first portion of the residual beam into the optical path in a first direction, and a frequency-narrowing element disposed at a position in the optical path where the first portion of the residual beam is collimated. The frequency-narrowing element is operative to narrow the frequency bandwidth of the first portion of the residual beam to produce a narrow-bandwidth collimated beam. A lens is disposed

in the optical path for focusing the narrow-bandwidth collimated beam to cause light from that beam to be reflected from the beam splitter and passed through the hole in the second reflective element as a narrow-bandwidth convergent beam is amplified by the gain medium. GRA

N90-19569# Air Force Office of Scientific Research, Bolling AFB, Washington, DC.
PROCEEDINGS OF AIR FORCE OFFICE OF SCIENTIFIC RESEARCH WORKSHOP ON LASER PROPULSION
Mitat A. Birkan 10 Feb. 1988 282 p Workshop held in Urbana-Champaign, IL, 8-10 Feb. 1988
(AF Proj. 2308)
(AD-A216563; AFOSR-88-1340TR) Avail: NTIS HC A13/MF A02

Laser propulsion consists of using energy from a remotely located laser to heat a low molecular weight gas to extremely high temperatures then expand the gas through a nozzle to provide thrust. Because of the potential for significantly higher specific impulse than chemical propulsion and adequate thrust to provide reasonable transit times, laser propulsion can be considered for a wide range of mission applications. An overview is presented of the status of continuous laser propulsion and is based on the AFOSR Laser Propulsion Workshop. Author

N90-19570# Illinois Univ., Urbana. Dept. of Electrical and Computer Engineering.
THE III-V SEMICONDUCTOR QUANTUM WELL LASERS AND RELATED OPTOELECTRONIC DEVICES ON SILICON
N. Holonyak, Jr., K. C. Hsieh, and G. E. Stillman Dec. 1989 31 p
(Contract DAAL03-89-K-0008)
(AD-A216980; TR-2; ARO-26434.2-EL) Avail: NTIS HC A03/MF A01 CSCL 09/3

The research goal is to further develop quantum well heterostructure (QWH) lasers and to realize reliable Al(x)-Ga(1-x)As-GaAs QWH lasers on Si. In spite of the significant lattice and thermal expansion mismatch between GaAs and Si, the idea of splicing III-V semiconductor technology, i.e., optoelectronics and photonics, onto Si has obvious appeal. Adding to this is the fact, as shown earlier in this work, that CW 300 K Al(x)Ga(1-x)As-GaAs QWH lasers can be grown on Si, and that the Si substrate serves as a better heat sink than GaAs. This makes possible the right-side-up heat sinking needed for electronic-photonic integrated circuits. This report contains research results on quantum well heterostructures on Si, impurity-induced layer disordering, phonon-assisted laser operations and other laser studies. GRA

N90-19571# Lawrence Livermore National Lab., CA.
NOISE FLOORS OF SUBNANOSECOND TRANSIENT RECORDING SYSTEMS
Karla G. Hagans 11 Oct. 1989 6 p Presented at the Department of Defense Fiber Optics Conference, McLean, VA, 20-23 Mar. 1990
(Contract W-7405-eng-48)
(DE90-002339; UCRL-102151; CONF-900333-2) Avail: NTIS HC A02/MF A01

The laser diode relative intensity noise, the detector shot noise and the amplification system noise is compared for three different approaches to high bandwidth transient recording. The first approach is a 1300nm direct modulation oscilloscope based link. The second approach is an 810nm indirect modulation streak camera based system. The third approach is an attempt to provide the 1300nm direct modulation link with multichannel streak camera capability by replacing the oscilloscope with a second 810nm laser diode and a streak camera. By comparing the noise floors of these systems, the system trade-offs in dynamic range, bandwidth and number of channels can be identified. DOE

N90-19572# Sandia National Labs., Albuquerque, NM.
LOW THRESHOLD CURRENT IMPLANTED-PLANAR-BURIED-HETEROSTRUCTURE, GRADED-INDEX, SEPARATE-CONFINEMENT-HETEROSTRUCTURE GaAs-AlGaAs LASER
G. A. Vawter, D. R. Myers, T. M. Brennan, and B. E. Hammons 1990 6 p Presented at the IEEE/LEOS/OSA Topical Meeting on Integrated Photonics Research, Hilton Head Island, NC, 26-28 Mar. 1990
(Contract DE-AC04-76DP-00789)
(DE90-002579; SAND-89-2631C; CONF-900328-1) Avail: NTIS HC A02/MF A01

We report low threshold current, CW operation of an Implanted-Planar-Buried-Heterostructure, Graded-Index, Separate-Confinement-Heterostructure laser. Implantation forms the p-n-p-n current-blocking layers and a buried-heterostructure waveguide resulting in high-quality, index-guided laser diodes for photonic circuit applications. DOE

N90-19573# Sandia National Labs., Albuquerque, NM.
EXPERIMENTAL RESULTS OF AGING AND THERMAL EFFECTS IN HIGH-POWER LASER DIODES
J. Rupert, M. J. Landry (Scot, Inc., Downers Grove, IL.), A. Mittas, and T. L. Woolston 1989 10 p Presented at the International Conference on Lasers '89, New Orleans, LA, 3-8 Dec. 1989
(Contract DE-AC04-76DP-00789)
(DE90-005955; SAND-1350C; CONF-891261-3) Avail: NTIS HC A02/MF A01

This paper describes the aging and thermal effects of high-power GaAlAs laser diodes constructed by Spectra Diode Laboratory (SDL) with multiple stripes, containing single- and multiple-quantum wells. Thermal effects are described for laser diodes constructed by McDonnell Douglas Astronautics Company/Optoelectronics Center (MDAC/OEC) with a single broad stripe containing a single-quantum well. The laser diodes are grown using metalorganic chemical vapor deposition (MOCVD). Experimental data are given showing the aging and thermal effects of these laser diodes while operating CW for different on-times and operating up to 2.0 W for an overdriven SDL commercial laser diode, 4.0 W for a SDL engineering prototype and 5.0 W for a MDAC/OEC prototype. Thermal effects are observed by operating at different intervals between shots and power levels when cooled by a fin heat-sink or thermoelectric cooler. Aging is caused by operating the laser diodes at elevated optical power levels. The characteristics used to describe these effects include: (1) optical power versus current, (2) efficiency versus optical power, (3) beam intensity distribution and (4) divergence. Laser diode output powers decreased by 2.5 percent to 22 percent because of aging. The different cooling methods resulted in a difference in output power of 7 percent. DOE

N90-19574# Washington Univ., Seattle. Dept. of Applied Mathematics.
TRANSIENT AND SUSTAINED RESONANCE IN VERY SLOWLY VARYING OSCILLATORY HAMILTONIAN SYSTEMS WITH APPLICATION TO FREE-ELECTRON LASERS Ph.D. Thesis
David Lee Bosley Nov. 1989 211 p
(Contract DE-FG06-86ER-25019)
(DE90-005984; DOE/ER-25019/14; TR-89-7) Avail: NTIS HC A10/MF A02

Slowly varying oscillatory systems occur frequently in both natural and man made applications, including the free electron laser. The long time solutions to these systems often prove difficult as numerical integration becomes too time consuming and inaccurate, and standard asymptotic techniques require large expansions not easily calculable by hand. This is especially true for the very slow time considered, which requires higher order expansions than the usual slow time. By formulating these systems into Hamiltonian standard form, the technique of averaging through a series of canonical transformations can be performed automatically by symbolic manipulation programs. When resonance

is exhibited in these systems, the averaging technique results in N - 1 adiabatic invariants which are constants of the motion, and reduces the original system of 2N first order differential equations to two differential equations which embody the resonance behavior. For the very slow time considered, transient resonance (where the system makes a slow passage through the resonance) is characterized by an O(1) transfer in energy, which is extremely sensitive to initial conditions. Sustained resonance, also referred to as phase locking, is a strictly nonlinear phenomenon. A frequently occurring class of reduced problems is examined and a highly accurate asymptotic solution is found. The free electron laser is a device which operates in the resonance state; therefore the results for sustained resonance can be directly applied. A solution is found for the energy and phase of the relativistic electrons in the electron beam, which indicates significant design advantages for this case of very slow variation of the parameters. DOE

N90-19575# Los Alamos National Lab., NM.
POTENTIAL BIOMEDICAL APPLICATION OF THE LOS ALAMOS INFRARED FREE-ELECTRON LASER: DNA SPECTROSCOPY
A. H. Lumpkin, J. Trewhella, and A. E. Garcia 1989 15 p Presented at the 11th International Free Electron Laser Conference, Naples, FL, 28 Aug. - 1 Sep. 1989
(Contract W-7405-eng-36)
(DE90-006505; LA-UR-90-223; CONF-8908134-26) Avail: NTIS HC A03/MF A01

Recently, the Los Alamos Free-Electron Laser has demonstrated optical output at wavelengths from 9 to 45 microns. Potential application of such a laser are proposed for the study of vibrational modes predicted in different conformations of DNA and in DNA complexed with drugs and/or proteins that regulate replication and/or transcription. DOE

N90-19576# Lawrence Livermore National Lab., CA.
ON 140 GHz MICROWAVE FEL EXPERIMENTS USING ELF-2
A. L. Throop, R. A. Jong, S. L. Allen, D. P. Atkinson, J. C. Clark, B. Felker, S. W. Ferguson, M. A. Makowski, W. E. Nexsen, and B. W. Rice et al Sep. 1989 21 p Presented at the 11th International Free Electron Laser Conference, Naples, Italy, 28 Aug. - 1 Sep. 1989
(Contract W-7405-eng-48)
(DE90-006764; UCRL-101946; CONF-8908134-28) Avail: NTIS HC A03/MF A01

We describe the modeling, the experimental facility, and the initial operating results for ELF-II, an induction-linac based free-electron laser designed to produce up to 2 GW of peak power at 140 GHz. ELF-II is the initial configuration of a free electron laser (FEL) system which will eventually produce up to 2 MW of average power at a frequency of 250 GHz, for use in plasma heating experiments in the Microwave Tokamak Experiment. DOE

N90-19577# Rochester Univ., NY. Lab. for Laser Energetics.
EFFECT OF BARRIER LAYERS IN BURN-THROUGH EXPERIMENTS WITH 351-nm LASER ILLUMINATION
J. Delettrez, D. K. Bradley, P. A. Jaanimagi, and C. P. Verdon Feb. 1990 42 p Sponsored in part by Empire State Electric Energy Research Corp., New York, NY; New York State Energy Research and Development Authority; and Ontario Hydro
(Contract DE-FC03-85DP-40200)
(DE90-006806; DOE/DP-40200/113) Avail: NTIS HC A03/MF A01

The time-resolved x ray emission is measured from spherical targets consisting of glass shells overcoated with plastic in which thin signature layers are embedded. These targets are illuminated at 351 nm by the 24-beam OMEGA laser system at the Laboratory for Laser Energetics of the University of Rochester. We measure a large burn-through rate for bare plastic targets, which can only be replicated in 1-D hydrodynamic simulations with laser intensities in excess of ten times the nominal intensity. We observe that the burn-through times are affected by the presence of a thin outer coating (barrier layer). The burn-through times depend strongly on the barrier-layer material and thickness, whereas one-dimensional simulation results predict only a small effect. Several processes are considered to explain these results: illumination nonuniformity, early shine-through of the laser light through the plastic, prepulses, filamentation, self-focussing of hot spots, and the Rayleigh-Taylor instability. We conclude that mixing due to the Rayleigh-Taylor instability, enhanced by early shine-through, is the most probable cause of the observed large burn-through rates. DOE

N90-19578# Lawrence Livermore National Lab., CA.
RESULTS OF THE PALADIN EXPERIMENT
J. T. Weir, T. J. Orzechowski, J. L. Miller, Y. P. Chong, F. Chambers, G. A. Deis, C. Paul, D. Prosnitz, E. T. Scharlemann, and K. Halbach (California Univ., Berkeley. Lawrence Berkeley Lab.) Mar. 1989 8 p Presented at the International Congress on Optical Science and Engineering, Paris, France, 24-28 Apr. 1989 Prepared in cooperation with TRW, Inc., Livermore , CA
(Contracts W-7405-eng-48; DE-AC03-76SF-00098)
(DE90-006776; UCRL-100367; CONF-8904242-4) Avail: NTIS HC A02/MF A01

PALADIN is a single pass, free laser amplifier located at the Lawrence Livermore National Laboratory. This free electron laser (FEL) is designed to run at 10.6 micrometers. The 1-kA, 45-MeV electron beam is provided by the Advanced Test Accelerator. The wiggler is 25 m long with an 8 cm period. The input optical signal to the amplifier is provided by a conventional CO2 laser, which can produce a peak input power of either 18 kW or 3.6 MW. We have demonstrated 31 dB of gain with the 18-kW input and 12.9 dB of gain for the 3.6-MW input, producing over 70 MW of optical power. Using the 18-kW input, the gain saturated at about 12 m into the wiggler; with the 3.6-MW input, the gain saturated at about 8 m. Modeling results are shown. DOE

N90-19579# Lawrence Livermore National Lab., CA.
LINEAR THEORY OF THERMAL BLOOMING IN TURBULENCE
D. H. Chambers, T. J. Karr, J. R. Morris, P. Cramer, J. A. Viecelli, and A. K. Gautesen (Iowa State Univ. of Science and Technology, Ames.) 16 Jan. 1990 10 p Presented at the SPIE Optics, Electro-Optics and Laser Applications in Science and Engineering Conference and Exhibition, Los Angeles, CA, 14-19 Jan. 1990
(Contracts W-7405-eng-48; MIPR-W31-RPD-7-D4041)
(DE90-007243; UCRL-102673; CONF-900140-9) Avail: NTIS HC A02/MF A01

It is shown how the electric field spectrum for a high energy laser beam propagating through a uniform atmosphere can be calculated using the linear theory of small fluctuations. The beam is modeled analytically as an infinite plane wave which propagates through a medium with constant absorption and no transverse wind. Return-wave phase compensation is modeled as a filter in the transverse wind. Return-wave phase compensation is modeled as a filter in the transverse Fourier domain. The linear theory describes the growth of small fluctuations on the beam and accurately predicts the evolution of the electric field spectrum until the magnitude of the fluctuations approach the original beam irradiance. The accuracy is tested by comparing with the spectrum calculated using ORACLE, a full wave optics thermal blooming code. DOE

N90-19580# Lawrence Livermore National Lab., CA.
TURBULENT MIXING EFFECTS IN MODELS OF THERMAL BLOOMING
D. H. Chambers, J. A. Viecelli, and T. J. Karr 16 Jan. 1990 9 p Presented at the SPIE Optics, Electro-Optics and Laser Applications in Science and Engineering Conference and Exhibition, Los Angeles, CA, 14-19 Jan. 1990
(Contracts W-7405-eng-48; MIPR-W31-RPD-7-D4041)
(DE90-007245; UCRL-102674; CONF-900140-6) Avail: NTIS HC A03/MF A01

A 2-D hydrodynamic model incorporating turbulent mixing is derived by averaging the 3-D hydrodynamics equations over slabs of thickness L in the direction of propagation. The resulting equations are identical with those for 2-D, incompressible flow with additional terms representing the average effect of velocity

fluctuations within each slab. These equations depend only parametrically on the coordinate in the direction of propagation. The extra terms have a simple physical interpretation but must be modeled in order to close the equations. Correlation times of scintillations are computed from a numerical simulation of plane wave blooming using this model. A comparison with the correlation times from simulations with only wind shear indicate that the effect of turbulent mixing is relatively small for typical values of the Kolmogorov inner scale. DOE

N90-19581# Technische Univ., Berlin (Germany, F.R.). Fachbereich Physik.
GENERATION OF INTENSIVE UV LASER RADIATION AND UTILIZATION IN HIGH RESOLUTION SPECTROSCOPY OF SO2 Ph.D. Thesis [ERZEUGUNG VON INTENSIVER UV-LASERSTRAHLUNG UND ANWENDUNG IN DER HOCHAUFLOESENDEN SPEKTROSKOPIE AM SO2]
Falk vonMoers 1989 135 p In GERMAN
(ETN-90-95361) Avail: NTIS HC A07/MF A01

The development of a narrowband, continuous, adjustable light source for UV spectroscopy is described. A system made of an external resonator with eigen laser medium is considered; a theory of this system is formulated that depicts the internal power and the output power as a function of laser parameters such as small signal strengthening and saturation power. High resonator internal power and high output power can be observed. A UV spectroscopy of sulfur dioxide is described. The SO2 molecules are prepared in a cool nozzle jet, made of a mixture of SO2/Ar, and excited by diagonalization of the energy matrix. ESA

N90-19582# Beleidscommissie Remote Sensing, Delft (Netherlands).
DEFINITION STUDY OF LASER EXPERIMENTAL ACTIVE FLUORSENSOR (LEAF) Final Report [DEFINITIE STUDIE VAN LASER EXPERIMENTAL ACTIVE FLUOROSENSOR (LEAF)]
C. Smorenburg (Technische Physische Dienst TNO-TH, Delft, Netherlands) Dec. 1988 30 p In DUTCH
(Contract BCRS-Proj-4551/TE-1.14)
(BCRS-88-18; TPD-733.806; ETN-90-95479) Avail: NTIS HC A03/MF A01

A study was performed to define the measuring instrument LEAF with a view to remote sensing of vegetation. LEAF is an active measuring instrument that illuminates the vegetation with a laser pulse and measures the induced fluorescence in a number of spectral bands. A conceptual design was made which fulfills the wishes and requirements of the users. A preliminary calculation of the expected amplitude of the fluorescence signal shows that measurements are very possible under all specified circumstances. No optical, mechanical and electronic technical problems are expected to occur. The most important open question is the definitive choice of the laser. ESA

N90-19583# Technische Univ., Berlin (Germany, F.R.). Fachbereich fuer Elektrotechnik.
NOISE BEHAVIOR OF SEMICONDUCTOR LASERS BY OPTIC FEEDBACK Ph.D. Thesis [RAUSCHVERHALTEN VON HALBLEITERLASERN BEI OPTISCHER RUECKWIRKUNG]
Nikolaus Schunk 1989 171 p In GERMAN
(ETN-90-95728) Avail: NTIS HC A08/MF A01

The stability behavior of a monomodal semiconductor laser is determined by digital simulation of the coupled nonlinear differential equation system with external reflection. A first differentiation criterium is found regarding the length of the external resonator. Semiconductor lasers with a long external resonator are not appropriate as emitters in coherent optic interference systems despite a great line width shrinkage. Because of the strong noise rises due to multiplicity of the external resonator resonance frequency, no remarkable reduction of the minimal transmissible bit ratio appears. With a reduction of the line broadening factor, an extension of the short external resonator length is possible, without the formation of an instability area. A quantum wave distributed feedback laser diode with monolithicly integrated short external resonator is a promising emission element in future coherent optic transmission systems. ESA

N90-19584# Los Alamos National Lab., NM.
BLUE UPCONVERSION THULIUM LASER
Dinh C. Nguyen, George E. Faulkner, Michael E. Weber, and Michael Dulick 1990 10 p Presented at the Technical Symposium on Laser Spectroscopy, Los Angeles, CA, 15-18 Jan. 1990
(Contract W-7405-eng-36)
(DE90-006517; LA-UR-90-161; CONF-900162-2) Avail: NTIS HC A03/MF A01

Upconversion has been an active area of research for at least two decades, mainly because of its wide ranging applications from infrared quantum counters, visible-emitting phosphors, to upconversion lasers. The upconversion lasers have recently become attractive with the advent of semiconductor laser diodes as the pump source. In an upconversion laser, the laser active ion is excited by internal upconversion of near-IR or red light via multiphoton excitation or cooperative processes and emits anti-Stokes visible light. Since the laser diode output wavelength can be composition turned to match the upconversion laser ion absorption lines, a substantial fraction of the ions can be driven into higher energy levels, thus enhancing the upconversion process. These upconversion solid-state lasers offer a potentially simple and compact source of visible coherent light with semiconductor laser diode excitation. We recently reported a novel upconversion thulium laser that emits blue light at 77 K. In this paper additional data on this 77 K upconversion laser as well as preliminary results on the room temperature upconversion laser are presented. In these demonstrations, dye lasers were used instead of diode lasers because they were more readily available than high power semiconductor laser diodes and their wavelengths could be adjusted easily. DOE

N90-19585# Los Alamos National Lab., NM. Chemical and Laser Sciences Div.
LASER MASS SPECTROMETRIC STUDIES OF HIGH TEMPERATURE SUPERCONDUCTOR ABLATION
Ron C. Estler and Nicholas S. Nogar 1990 8 p Presented at the SPIE Optics, Electro-Optics and Laser Applications in Science and Engineering Conference and Exhibition, Los Angeles, CA, 20-25 Jan. 1990
(Contract W-7405-eng-36)
(DE90-006518; LA-UR-90-165; CONF-900140-10) Avail: NTIS HC A02/MF A01

Laser ablation of bulk High Temperature Superconductor (HTS) material promises to provide a useful means of producing high quality HTS thin films. Mass spectrometric probes of the ablation plume provide a microscopic understanding of the ablation event and plume development as well as providing a process monitor for the thin film production. Detection of the nascent ions in the plume provides real time analytical information, e.g., identification of impurities, major and minor ablation species, etc. The common contaminants sodium and strontium were easily detected by this technique in a variety of different HTS bulk materials. In contrast, detection of the ablated neutral species by Resonance Ionization Mass Spectrometry (RIMS) provides physical information about the ablation process. Time-of-flight/RIMS detection of Cu, Y, and BaO ablated from YBa2Cu3O(x) indicates the ablation involves post-desorption gas phase collisions, thereby influencing the ablation chemistry and dynamics (e.g., angular and velocity distributions). Approximately equal velocities are observed for all neutral species at constant ablation laser fluence. DOE

N90-19586# Lawrence Livermore National Lab., CA.
A GROUND STATE DEPLETED LASER IN NEODYMIUM DOPED YTTRIUM ORTHOSILICATE
R. Beach, G. Albrecht, R. Solarz, W. Krupke, B. Comaskey, S. Mitchell, C. Brandle, and G. Berkstresser (Bell Telephone Labs., Inc., Murray Hill, NJ.) 16 Jan. 1990 23 p Presented at the SPIE Optics, Electro-Optics and Laser Applications in Science and Engineering Conference and Exhibition, Los Angeles, CA, 20-25

Jan. 1990
(Contract W-7405-eng-48)
(DE90-006773; UCRL-101650; CONF-900140-11) Avail: NTIS HC A03/MF A01

A ground state depleted (GSD) laser was demonstrated in the form of a Q-switched oscillator operating at 912 nm. Using Nd(3+) as the active ion and Y2SiO5 as the host material, the laser transition is from the lowest lying stark level of the Nd(3t)F(sub 3/2) level to a stark level 355 cm(exp -1) above the lowest lying one in the (4)I(sub 9/2) manifold. The necessity of depleting the ground (4)I(sub 9/2) manifold is evident for this level scheme as transparency requires a 10 percent inversion. To achieve the high excitation levels required for the efficient operation of this laser, bleach wave pumping using an alexandrite laser at 745 nm was employed. The existence of a large absorption feature at 810 nm also allows for the possibility of AlGaAs laser diode pumping. Using KNbO3, noncritical phase matching is possible at 140 C using d(sub 32) and was demonstrated. The results of Q-switched laser performance and harmonic generation in KNbO3 is presented. Orthosilicate can be grown in large boules of excellent optical quality using a Czochralski technique. Because of the relatively small 912 nm emission cross section of 2 to 3 x 10(exp -20) sq cm (orientation dependent) fluences of 10 to 20 J/sq cm must be circulated in the laser cavity for the efficient extraction of stored energy. This necessitates very aggressive laser damage thresholds. Results from the Reptile laser damage facility at Lawrence Livermore National Laboratory (LLNL) is presented showing Y2SiO5 bulk and AR sol-gel coated surface damage thresholds of greater than 40 J/sq cm for 10 nsec, 10 Hz, 1.06 micropulses. DOE

N90-19587# Oak Ridge National Lab., TN. Chemical Physics Section.
LASER SURFACE INTERACTIONS OF HIGH-(Tc) SUPERCONDUCTORS
C. H. Chen, M. P. McCann, and R. C. Phillips Jan. 1990 8 p Presented at the Advances in Material Science and Applications of High Temperature Superconductors, Greenbelt, MD, 2-6 Apr. 1990
(Contract DE-AC05-84OR-21400)
(DE90-006894; CONF-900414-1) Avail: NTIS HC A02/MF A01

During the past two years, one of the most exciting research fields in science has been the study of the newly discovered high-(Tc) metal oxide superconductors. Although many theoretical models were proposed, there has been no general agreement on any theory to explain these materials. One of the peculiar features of these high-(Tc) materials is the noninteger number of oxygen atoms. The oxygen content is extremely critical to the superconductive properties. Our results from mass spectroscopy of laser desorbed species indicate that significant quantities of oxygen molecules are trapped in the bulk of these superconductors. It appears that these trapped oxygen molecules may play key roles in superconductive properties. DOE

N90-19588# Consultec Scientific, Inc., Knoxville, TN.
ASSESSMENT OF RESEARCH NEEDS FOR LASER TECHNOLOGIES APPLIED TO ADVANCED SPECTROSCOPIC METHODS
Jan. 1990 73 p
(Contract DE-AC01-88ER-30131)
(DE90-007402; DOE/ER-30131/T9) Avail: NTIS HC A05/MF A01

The Department of Energy (DOE) recognizes that new developments in laser technology and laser spectroscopy can substantially improve the ability to carry out the mission of its Office of Health and Environmental Research (OHER). In brief, the mission of OHER is to support programs of research which allow DOE to understand and anticipate long term effects upon human health and the environment from the production and utilization of alternate forms of energy, and to apply the department's unique capabilities to solve numerous problems in biology and medicine. A DOE study was managed by Consultec Scientific, Inc. who furnished from its staff the Principal Investigator who, in turn, coordinated the enthusiastic efforts of a group of consultants consisting of some of the world's best scientists. The panel made six specific recommendations which dealt with three important areas. First the panel recommends that OHER closely monitor and be prepared to use the advances now being made in solid-state laser technology. These advances, comparable in nature to the revolution which began during the 1950's in solid-state electronics, will radically improve present-day laser technology. Secondly, the panel addressed the use of this advanced technology to maintain the preeminent position which OHER has already created for itself in the development of selective and sensitive instruments for the analysis of atomic and molecular substances and to extend the use of these to measure chemical pollutants in air, soil, and water. Finally, another area of the recommendations dealt with the use of lasers to determine structural and dynamical features of macromolecules and especially to develop x ray lasers and other imaging techniques, including holographic ones, for sequencing DNA and the human genome. DOE

N90-19589# Los Alamos National Lab., NM.
FIRST DIRECT OBSERVATION OF FEL (FREE-ELECTRON LASER) FROM LAMBDA=20 TO 45 MICRONS
A. H. Lumpkin, D. W. Feldman, R. W. Warren, W. E. Stein, W. J. Johnson, J. M. Watson, J. E. Sollid, B. E. Newnam, and J. C. Goldstein 1989 14 p Presented at the 11th International Free Electron Laser Conference, Naples, Italy, 28 Aug. - 1 Sep. 1989
(Contract W-7405-eng-36)
(DE90-007508; LA-UR-90-696; CONF-8908134-30) Avail: NTIS HC A03/MF A01

In recent experiments at Los Alamos, free electron laser (FEL) fundamental wavelengths were directly observed for the first time from 20 to 45 micron. The 1988 facility's demonstrated wavelength span now extends from 9 to 45 micron. Upgrades are in progress to increase this span. This wavelength region uniquely complements existing FEL applications facilities. DOE

N90-19590# Los Alamos National Lab., NM.
LASER-MATTER INTERACTION AT INTENSITIES OF 10(SUP 12) W/CM(SUP 2) AND BELOW
S. Robert Goldman, Ronald S. Dingus, Ronald C. Kirkpatrick, Roger A. Kopp, Elmer K. Stover, and Robert G. Watt 1990 9 p Presented at the International Conference on Optical Science and Engineering, Hague, Netherlands, 12-16 Mar. 1990
(Contract W-7405-eng-36)
(DE90-007536; LA-UR-90-496; CONF-900368-1) Avail: NTIS HC A02/MF A01

For single pulsed laser-matter interactions at sufficiently high intensity, the electron density in the ablated vapor is large enough to absorb the laser radiation before it can reach the dense target material. The resulting interaction can be described in terms of energy flows: laser energy is absorbed in the plasma in front of the target and reappears as thermal electron energy and secondary radiation, part of which impinges upon and heats the dense target material at the dense material-vapor interface. This heating in turn drives ablation, thereby providing a self-consistent mass source for the laser absorption, energy conversion, and transmission. Under typical conditions of laser intensity, pulse width and spot size, the flow patterns can be strongly two-dimensional. We have modified the inertial confinement fusion code LASNEX to simulate gaseous and some dense material aspects for the relatively low intensity, long-pulse-length conditions of interest in many laser-related applications. The unique aspect of our treatment consists of an ablation model which defines a dense material vapor interface and then calculates the mass flow across this interface. The model, at present, treats the dense material as a rigid, two-dimensional simulational mass and heat reservoir, suppressing all hydrodynamical motion in the dense material. DOE

N90-19591# Rochester Univ., NY.
CORRELATION-INDUCED CHANGES OF SPECTRA
Emil Wolf Dec. 1989 78 p

(Contract DAAL03-86-K-0173)
(AD-A217087; ARO-24626.119-PH-UIR) Avail: NTIS HC A05/MF A01 CSCL 20/5

It is generally taken for granted that the spectrum of light does not change on propagation. This belief is implicit in all spectroscopy. In the last few years it was discovered that while such spectral invariance holds for radiation from commonly used sources it does not hold, in general, because the spectrum of emitted radiation depends not only on the source spectrum but also on the coherence properties of the source. It was found that in some cases the induced changes may be appreciable, possibly resulting in frequency shifts of spectral lines. It has also been demonstrated that similar spectral changes may be produced by scattering on random media whose dielectric susceptibility fluctuations are appropriately correlated. Very recently it was shown that under certain circumstances the frequency shifts generated by dynamic scattering may imitate the Doppler effect, even though the source, the scatterer and the observer are all at rest relative to each other. GRA

N90-19438*# Jet Propulsion Lab., California Inst. of Tech., Pasadena.
EFFECT OF LASER FREQUENCY NOISE ON FIBER-OPTIC FREQUENCY REFERENCE DISTRIBUTION
R. T. Logan, Jr., G. F. Lutes, and L. Maleki *In its* The Telecommunications and Data Acquisition Report 15 Nov. 1989 p 34-42 (For primary document see N90-19434 12-32)
Avail: NTIS HC A10/MF A02 CSCL 20E

N90-19969*# Stanford Univ., CA. Dept. of Applied Physics.
FREQUENCY STABLE HIGH POWER LASERS IN SPACE
Robert L. Byer *In* NASA, Relativistic Gravitational Experiments in Space Aug. 1989 p 166-170 (For primary document see N90-19940 12-90)
Avail: NTIS HC A11/MF A02 CSCL 20E

37 MECHANICAL ENGINEERING

Includes auxiliary systems (nonpower); machine elements and processes; and mechanical equipment.

N90-19592 Rochester Univ., NY.
KINEMATIC CONTROL OF ROBOTIC MANIPULATORS WITH MULTIPLE INTERCHANGEABLE WRISTS Ph.D. Thesis
Marcelo Huibonhoa Ang, Jr. 1988 238 p
Avail: Univ. Microfilms Order No. DA8907452

The objective is threefold, namely: to advance the state-of-the art in the kinematic analysis, design, and control of robotic manipulators; to introduce the interchangeable wrist concept; and to provide design guidelines for modular robots. A general-purpose and computationally efficient kinematic framework is founded upon simple applied geometric notions and basic principles of rigid-body motion. General-purpose algorithms for performing efficient position, velocity, acceleration, and force/torque transformations are formulated. Comparative evaluations demonstrate the efficacy and computational efficiency of these algorithms. The limitations of robot motion at singular points in the robot workspace are then discussed. The interactions between the arm, the wrist, and the manipulator singularities are then quantified through a set of singularity decoupling theorems. The concept of multiple interchangeable wrist mechanisms is introduced as a cost effective and practical method to improve the flexibility of a robotic system without increasing the complexity of the wrist design. A mathematically robust modular algorithm for general-purpose inverse kinematics that naturally accommodates interchangeable wrists was developed. An array of simulation experiments demonstrates the robustness, accuracy, and computational efficiency of the modular algorithm. Finally, manipulator design guidelines are formulated to ensure proper arm-wrist coordination, and to safeguard the interchangeable wrist concept. The interplay between the arm and wrists is formally defined and a quantitative measure for it is developed. The impact of the manipulator geometry and configuration on effective arm-wrist coordination is then highlighted through a series of numerical simulations which demonstrate the utility of the design guidelines. Dissert. Abstr.

N90-19593*# Illinois Univ., Chicago. Dept. of Mechanical Engineering.
THEORY OF GEARING
Faydor L. Litvin 1989 479 p Prepared in cooperation with Army Aviation System s Command, Cleveland, OH
(Grants NAG3-783; NAG3-655; DA Proj. 1L1-62209-AH-76)
(NASA-RP-1212; E-2641; NAS 1.61:1212; AVSCOM-TR-88-C-035; L-89-600204) Avail: NTIS HC A21/MF A03; Also Avail: SOD HC $40.00 as 033-000-01068-1 CSCL 13I

Basic mathematical problems on the theory of gearing are covered in this book, such as the necessary and sufficient conditions of envelope existence, relations between principal curvatures and directions for surfaces of mating gears. Also included are singularities of surfaces accompanied by undercutting the process of generation, the phenomena of envelope of lines of contact, and the principles for generation of conjugate surfaces. Special attention is given to the algorithms for computer aided simulation of meshing and tooth contact. This edition was complemented with the results of research recently performed by the author and his doctoral students. The book contains sample problems and also problems for the reader to solve. K.C.D.

N90-19594 Texas A&M Univ., College Station.
VISCOELASTIC ADHEREND EFFECTS IN ADHESIVELY BONDED COMPOSITE-TO-COMPOSITE JOINTS Ph.D. Thesis
Lezza Ann Mignery 1988 305 p
Avail: Univ. Microfilms Order No. DA8913416

A complex state of stress is present in adhesive joints. With composite adherends, this can cause a considerable amount of creep even in the absence of an extreme operational environment. The present research is centered around characterizing a composite polymeric adherend material and studying, experimentally and theoretically, its reaction in one adhesive joint configuration. The particular material investigated is a fibrous graphite/epoxy composite material with a rubber-toughened matrix. The objective is to develop a constitutive equation to account for this behavior and to use it in a finite element analysis of an adhesive joint. Experimental verifications of the constitutive model and adhesive joint are made. The graphite/epoxy composite is characterized using a viscoelastic model and a work-potential model. Unlike the viscoelastic model, the work-potential model accounts for changes in the microstructure, or damage, as well as viscoelasticity. The quasi-elastic method, in which the actual deformation behavior is approximated by a time-dependent elastic behavior, is used in the second characterization to account for the time dependence of the material. Parameters necessary for each model are determined from creep/recovery and constant load rate data. Single-lap joints made of the same material and a brittle adhesive are then tested at two different load rates to failure. Dissert. Abstr.

N90-19595*# National Aeronautics and Space Administration. Langley Research Center, Hampton, VA.
MODELING AND ANALYSIS OF THE SPACE SHUTTLE NOSE-GEAR TIRE WITH SEMIANALYTIC FINITE ELEMENTS
Kyun O. Kim, Ahmed K. Noor (Joint Inst. for Advancement of Flight Sciences, Hampton, VA.), and John A. Tanner Washington Apr. 1990 36 p
(NASA-TP-2977; L-16639; NAS 1.60:2977) Avail: NTIS HC A03/MF A01 CSCL 22B

A computational procedure is presented for the geometrically nonlinear analysis of aircraft tires. The Space Shuttle Orbiter nose gear tire was modeled by using a two-dimensional laminated anisotropic shell theory with the effects of variation in material and geometric parameters included. The four key elements of the procedure are: (1) semianalytic finite elements in which the shell variables are represented by Fourier series in the circumferential direction and piecewise polynominals in the meridional direction; (2) a mixed formulation with the fundamental unknowns consisting

of strain parameters, stress-resultant parameters, and generalized displacements; (3) multilevel operator splitting to effect successive simplifications, and to uncouple the equations associated with different Fourier harmonics; and (4) multilevel iterative procedures and reduction techniques to generate the response of the shell. Numerical results of the Space Shuttle Orbiter nose gear tire model are compared with experimental measurements of the tire subjected to inflation loading. Author

N90-19596 Stanford Univ., CA.
EXPERIMENTS IN END-POINT CONTROL OF A FLEXIBLE ROBOT WITH A MINI-MANIPULATOR Ph.D. Thesis
Raymond H. Kraft 1989 217 p
Avail: Univ. Microfilms Order No. DA8925900

The speed and precision of present day robots is limited by both manipulator size and flexibility. Robots that are required to operate over a large workspace are naturally large in size, precisely controlling the end-point of such a large manipulator is complicated by mechanical amplification of joint motions. Direct end-point position and force control of a large flexible manipulator equipped with a quick, lightweight, rigid mini-manipulator is examined. By directly measuring the end-point position and force, errors due to flexibility are eliminated, and much faster performance is possible. Through the use of a mini-manipulator, the problem of mechanical amplification is also solved; the mini-manipulator is a five link, closed kinematic chain. A method is developed for mapping the highly nonlinear, Multi-Input-Multi-Output mini-manipulator into a set of multiple, approximately linear, Single-Input-Single-Output systems, and the resulting linear systems are identified. Next, a LQG controller is developed to control the set of linear systems. Finally, the linear control law outputs are then mapped back into the set of control torques that are meaningful, and therefore effective, for control of the actual nonlinear system itself.
Dissert. Abstr.

N90-19597 Catholic Univ. of America, Washington, DC.
MODIFIED INDEPENDENT MODAL SPACE CONTROL OF FLEXIBLE STRUCTURES Ph.D. Thesis
Soon-Neo Poh 1989 89 p
Avail: Univ. Microfilms Order No. DA8925990

A Modified Independent Modal Space Control (MIMSC) method is developed for designing active vibration control systems for large flexible structures. The method modified the well known Independent Modal Space Control (IMSC) method by accounts for the interaction between the controlled and residual modes. It incorporates also optimal placement procedures for selecting the optimal locations of the actuators in the structure in order to minimize the structural vibrations as well as the actuation effort. The MIMSC method relies on an important feature which is based on time sharing of a small number of actuators, in the modal space, to control effectively a large number of modes. Numerical examples as well as an experiment employing flexible cantilever beams were presented to demonstrate the effectiveness of MIMSC method. The results obtained indicate that the MIMSC with maximum modal energy ranking is more effective in damping the vibration than the IMSC, the PI (pseudo-inverse), and the MIMSC with sequential time sharing. The MIMSC requires, however, higher control energy than the IMSC and PI method. Dissert. Abstr.

N90-19598 Catholic Univ. of America, Washington, DC.
DYNAMICS AND CONTROL OF ROBOT MANIPULATORS WITH CLOSED-KINEMATIC CHAIN MECHANISM Ph.D. Thesis
Farhad Jabbari Pooran 1989 238 p
Avail: Univ. Microfilms Order No. DA8925999

Kinematic and dynamic equations were developed for a class of closed-kinematic chain mechanism robot manipulators with parallel actuators. Advanced control schemes were investigated and suitable schemes were developed for controlling position/force of the above type of manipulators. The kinematic analysis of the CKCM manipulators is performed and a closed-form solution for inverse kinematic problem of the manipulator is obtained. Since the forward kinematic problem does not possess a closed-form solution, it is solved iteratively. An algorithm is developed to facilitate the solution. The investigation of workspace results in the development of an algorithm which determines the reachable workspace of CKCM manipulators. Using Lagrangian approach closed-form dynamic equations of CKCM manipulators are developed. The developed dynamic model can be used to derive equations of motion for manipulators having up to six degrees of freedom and six actuators. In addition, this model is suitable to nonlinear control schemes since the individual interaction and coupling forces in the model can be easily identified. Utilizing computer simulation the effect of system parameters on the manipulator dynamics are investigated and a general guideline is provided to minimize the power requirement, weights, and sizes of the manipulator actuators. Since robotic assembly often occurs in a slow motion mode, the dynamics of manipulators performing slow motion is also studied through computer simulation.
Dissert. Abstr.

N90-19599*# Catholic Univ. of America, Washington, DC. Dept. of Electrical Engineering.
ADVANCED CONTROL SCHEMES AND KINEMATIC ANALYSIS FOR A KINEMATICALLY REDUNDANT 7 DOF MANIPULATOR
Charles C. Nguyen and Zhen-Lei Zhou Feb. 1990 19 p
(Grant NAG5-1124)
(NASA-CR-186175; NAS 1.26:186175) Avail: NTIS HC A03/MF A01 CSCL 13I

The kinematic analysis and control of a kinematically redundant manipulator is addressed. The manipulator is the slave arm of a telerobot system recently built at Goddard Space Flight Center (GSFC) to serve as a testbed for investigating research issues in telerobotics. A forward kinematic transformation is developed in its most simplified form, suitable for real-time control applications, and the manipulator Jacobian is derived using the vector cross product method. Using the developed forward kinematic transformation and quaternion representation of orientation matrices, we perform computer simulation to evaluate the efficiency of the Jacobian in converting joint velocities into Cartesian velocities and to investigate the accuracy of Jacobian pseudo-inverse for various sampling times. The equivalence between Cartesian velocities and quaternion is also verified using computer simulation. Three control schemes are proposed and discussed for controlling the motion of the slave arm end-effector. Author

N90-19600# Department of the Navy, Washington, DC.
JAM RESISTANT FLUID POWER ACTUATOR FOR BALLISTIC-DAMAGE TOLERANT REDUNDANT CYLINDER ASSEMBLIES Patent
John W. Holtrop, inventor (to Navy) 19 Sep. 1989 7 p Filed 26 Nov. 1984
(AD-D014360; US-Patent-4,867,044; US-Patent-Appl-SN-674901; US-Patent-Class-92-169.1) Avail: US Patent and Trademark Office CSCL 13/7

This patent discloses a hydraulic actuator having redundant cylinder assemblies, each assembly being of lightweight and economical construction in having a relatively thin tubular wall reinforced to withstand hydraulic pressure by a layer of resin reinforced filament, the thickness and the material of the wall being such that petals formed from the wall by projectile penetration are sheared by engagement with a piston of the assembly as this piston is moved, together with an actual element, by the piston of the other assembly. GRA

N90-19601# Massachusetts Inst. of Tech., Cambridge. Artificial Intelligence Lab.
DESIGN AND IMPLEMENTATION OF A FLEXIBLE ROBOT
Andrew D. Christian Aug. 1989 166 p
(Contract N00014-86-K-0685)
(AD-A216453; AI-TR-1153) Avail: NTIS HC A08/MF A01 CSCL 23/3

The design, implementation, and control of a robot that has low natural frequencies of vibration is reported. Insights into the problems of designing joint and link flexibility are discussed. The deflection of the robot under gravity is correlated with the fundamental frequency of vibration. Different link geometries and

materials are evaluated. The robot has three rotary actuators and two links, with two actuators at the base and the third as an elbow joint between the links. The links are interchangeable and the joints have a variable flexibility built in. The robot is controlled by three separate processors running on a VMEbus. A Sun 3/180 workstation provides the development environment. A collection of operator controls were built including a panel to control the amplifiers and brakes, and a joystick for teleoperation. A PD servo loop runs the robot in either joint or cartesian space. Results from experiments on the control of residual vibration are presented. Three different motions of the arm were studied: a constant vibrational frequency move, a changing vibrational frequency move, and a cartesian move. Impulse prefiltering and slowly accelerating moves are compared and shown to be effective at reducing residual vibration. GRA

N90-19602* National Aeronautics and Space Administration. Marshall Space Flight Center, Huntsville, AL.
TRAILER SHIELD ASSEMBLY FOR A WELDING TORCH Patent
Gerald E. Dyer, inventor (to NASA) (Rockwell International Corp., Huntsville, AL.) 13 Jun. 1989 8 p Filed 16 Feb. 1988
(NASA-Case-MFS-29260-1; US-Patent-4,839,489; US-Patent-Appl-SN-156059; US-Patent-Class-219-74; US-Patent-Class-219-72) Avail: US Patent and Trademark Office CSCL 13I

This invention relates generally to trailer shields for gas shielded arc welding torches, and more particularly to a trailer shield assembly provided with a shield gas manifold for providing an even dispersion of shield gas to the interior of the shield assembly, which generally encloses a joint being welded and a welding trailing portion of hot welded metal. The novelty of the invention lies in providing trailer shield with a manifold tube having a plurality of openings from which shield gas is distributed. A gas manifold region ahead of the torch is also provided with shield gas from a tube to protect metal preheated by the torch. Further novelty lies in constructing portions of sides and housing and portions of side walls of the guide of stainless steel screen having a tight mesh.
Official Gazette of the U.S. Patent and Trademark Office

N90-19603# Japan Atomic Energy Research Inst., Tokyo. Dept. of Reactor Engineering.
A COMPLETE DESCRIPTION OF ROBOT MANIPULATOR DYNAMICS BASED ON LAGRANGIAN MECHANICS
Shinobu Sasaki Sep. 1989 83 p In JAPANESE; ENGLISH summary
(DE90-741467; JAERI-M-89-121) Avail: NTIS (US Sales Only) HC A05/MF A01

Manipulator dynamics is one of the most important research topics in the field of robotics. Many different approaches were taken to obtain a good understanding of what the kinetic equations exactly are. Their complete descriptions for a full six-jointed arm, however, have hardly been reported due to extremely laborious and complicated processes of derivation. With the aid of computer code REDUCE, which has a capability to carry out algebraic operations accurately, a new attempt was made in this paper to derive dynamics equations in a systematic manner based on Lagrange mechanics. The full description shown will give useful information in designing the control algorithms for robot manipulators. DOE

N90-19604# Technische Univ., Berlin (Germany, F.R.). Fachbereich Informatik.
IMPROVED PROCESSES FOR ULTRASONIC OBJECT RECOGNITION IN ROBOTICS Ph.D. Thesis [FORTGESCHRITTENE VERFAHREN ZUR ULTRASCHALLBASIERTEN OBJEKTERKENNUNG IN DER ROBOTIK]
Alois Knoll 1988 145 p In GERMAN
(ETN-90-95362) Avail: NTIS HC A07/MF A01

The experiments are based on the theory of soundwave propagation in the air, and particularly on monofrequency acoustic holography, discrete multi-frequency-holography or pulse holography. It is shown that the local resolution, as a decisive parameter of an ultrasonic sensor, depends directly on the bandwidth of the used signal. With holography processes the measurements velocity is very high. The process of acoustic stereo gives information about the incline on the object surface but not about the object distance. It is particularly appropriate for the manufacturing of autonomous sensors for simple utilization cases or as a support of other sensors such as cameras. To have a very good precision, these sensors can be combined with optic sensors in the future integration of artificial intelligence methods. ESA

N90-19605# Technische Univ., Berlin (Germany, F.R.). Fachbereich Verkehrswesen.
ANALYSIS OF ALTERNATIVE CONCEPTS FOR TRANSPORT SYSTEMS ON THE MOON SURFACE Ph.D. Thesis [ANALYSE ALTERNATIVER KONZEPTE FUER TRANSPORTSYSTEME AUF DER MONDOBERFLAECHE]
Uwe Apel 1989 149 p In GERMAN
(ETN-90-95727) Avail: NTIS HC A07/MF A01

A life cycle simulation of possible lunar surface transport systems is proposed which contains a transport model, a working model, a life cycle cost model and a use model. The transport need must be initially limited to small traffic unities and small distant ones to other colonies. The infrastructure must be cheap and flexible. Transport means such as band conveyors and pipelines could be good substitutes for the Moon. ESA

N90-19606# Sandia National Labs., Albuquerque, NM.
EXTENDING TERRESTRIAL MOBILE ROBOTICS TO A PROPOSED LUNAR BASE
Paul R. Klarer 1989 7 p Presented at the Engineering, Construction and Operations for Space, Albuquerque, NM, Apr. 1990
(Contract DE-AC04-76DP-00789)
(DE89-016179; SAND-89-0753C; CONF-900442-1) Avail: NTIS HC A02/MF A01

The National Aeronautics and Space Administration (NASA) has recently been conducting studies regarding missions to establish permanent manned facilities either on Earth's moon or on Mars sometime in the next few decades. This paper addresses issues associated with the operation of manned, teleoperated and autonomous land vehicles to be used in the lunar environment. Current capabilities in teleoperation and autonomous navigation for land vehicles in the terrestrial environment are discussed, as are the technology issues and new capabilities required to extend the current capabilities to a lunar operating environment. DOE

N90-19607# Texas A&M Univ., College Station. Dept. of Mechanical Engineering.
DEVELOPMENT AND USE OF AN ADVANCED COAL-FUELED DIESEL ENGINE CYCLE SIMULATION WITH GROUP EFFECTS Final Report
J. A. Caton and K. Annamalai Dec. 1989 96 p
(Contract DE-AC21-86MC-23256)
(DE90-000450; DOE/MC-23256/2787-Vol-2) Avail: NTIS HC A05/MF A01

This report contains the listing for an engine cycle simulation computer program for modeling conventional medium-speed engines with overall equivalence ratios of less than .8 and with low or no swirl. DOE

N90-19397*# Carnegie-Mellon Univ., Pittsburgh, PA. Dept. of Mechanical Engineering.
A PARAMETRIC HEAT TRANSFER STUDY FOR CRYOGENIC BALL BEARINGS IN SSME HPOTP
Mingking K. Chyu *In* Alabama Univ., Research Reports: 1989 NASA/ASEE Summer Faculty Fellowship Program Dec. 1989 24 p (For primary document see N90-19390 12-31)
(Grant NGT-01-008-021)
Avail: NTIS HC A99/MF E06 CSCL 13I

N90-19400*# Virginia Polytechnic Inst. and State Univ., Blacksburg. Dept. of Mechanical Engineering.
INVESTIGATION OF SSME ALTERNATE HIGH PRESSURE FUEL TURBOPUMP LIFT-OFF SEAL FLUID AND STRUCTURAL DYNAMIC INTERACTION
David A. Elrod *In* Alabama Univ., Research Reports: 1989 NASA/ASEE Summer Faculty Fellowship Program Dec. 1989 15 p (For primary document see N90-19390 12-31)
(Grant NGT-01-008-021)
Avail: NTIS HC A99/MF E06 CSCL 11A

N90-19401*# University of Central Florida, Orlando. Dept. of Mechanical Engineering.
A STUDY OF THE EFFECTS OF DISK FLEXIBILITY ON THE ROTORDYNAMICS OF THE SPACE SHUTTLE MAIN ENGINE TURBO-PUMPS
George T. Flowers *In* Alabama Univ., Research Reports: 1989 NASA/ASEE Summer Faculty Fellowship Program Dec. 1989 28 p (For primary document see N90-19390 12-31)
(Grant NGT-01-008-021)
Avail: NTIS HC A99/MF E06 CSCL 13I

N90-19418*# Wichita State Univ., KS. Dept. of Mechanical Engineering.
HEAT SINK EFFECTS ON WELD BEAD: VPPA PROCESS
Paul O. Steranka, Jr. *In* Alabama Univ., Research Reports: 1989 NASA/ASEE Summer Faculty Fellowship Program Dec. 1989 27 p (For primary document see N90-19390 12-31)
(Grant NGT-01-008-021)
Avail: NTIS HC A99/MF E06 CSCL 11F

38 QUALITY ASSURANCE AND RELIABILITY

Includes product sampling procedures and techniques; and quality control.

N90-19608*# Morton Thiokol, Brigham City, UT. Space Operations.
DEVELOPMENT OF INSPECTION TECHNIQUES FOR QUANTITATIVELY MEASURING SURFACE CONTAMINATION ON SRM HARDWARE Interim Report
R. D. Law 13 Oct. 1989 247 p
(Contract NAS8-30490)
(NASA-CR-183902; NAS 1.26:183902; TWR-50087; LSDI-90-08)
Avail: NTIS HC A11/MF A02 CSCL 14D

A contaminant is any material or substance which is potentially undesirable or which may adversely affect any part, component, or assembly. Contamination control of SRM hardware surfaces is a serious concern, for both Thiokol and NASA, with particular concern for contaminants which may adversely affect bonding surfaces. The purpose of this study is to develop laboratory analytical techniques which will make it possible to certify the cleanliness of any designated surface, with special focus on particulates (dust, dirt, lint, etc.), oils (hydrocarbons, silicones, plasticizers, etc.), and greases (HD-2, fluorocarbon grease, etc.). The hardware surfaces of concern will include D6AC steel, aluminum alloys, anodized aluminum alloys, glass/phenolic, carbon/phenolic, NBR/asbestos-silica, and EPDM rubber.
Author

N90-19396*# Middle Tennessee State Univ., Murfreesboro. Dept. of Mathematics and Statistics.
METHODS FOR TREND ANALYSIS: EXAMPLES WITH PROBLEM/FAILURE DATA
Curtis K. Church *In* Alabama Univ., Research Reports: 1989 NASA/ASEE Summer Faculty Fellowship Program Dec. 1989 29 p (For primary document see N90-19390 12-31)
(Grant NGT-01-008-021)
Avail: NTIS HC A99/MF E06 CSCL 14D

39 STRUCTURAL MECHANICS

Includes structural element design and weight analysis; fatigue; and thermal stress.

For applications see *05 Aircraft Design, Testing and Performance* and *18 Spacecraft Design, Testing and Performance.*

N90-19609 Salford Univ. (England).
AN EXPERIMENTAL STUDY OF THE AEROELASTIC BEHAVIOUR OF TWO PARALLEL INTERFERING CIRCULAR CYLINDERS Ph.D. Thesis
Eduardo Bauzer Medeiros 1988 316 p
Avail: Univ. Microfilms Order No. BRD-84966

Considered here is an experimental study of the flow-induced oscillations of two parallel interfering circular cylinders, the associated flow-induced excitations and the suppression of the resulting oscillations by increasing the damping. All three arrangements are discussed, namely: tandem, side-by-side and staggered with respect to the approaching fluid flow. The ratio-of-diameters of the two cylinders employed is 1:1, 1:2 and 2:1. The study describes the observed excitations for a wide range of reduced velocities Vr, relative transverse and streamwise spacings between the cylinders, L/D and T/D, and the damping expressed by the Scruton number Sc. The latter is varied by means of an eddy-current damping system, which stimulates the variation of structural damping of a structure. The main objective of the experiments is to relate the Scruton number, the reduced velocity and the relative spacings to the response of the two cylinders. Particular emphasis is put on the determination of the critical reduced velocity Vrc on the threshold of instability and the associated Scruton number Sc. The experimental program and the experimental apparatus are described in detail, including a discussion of the philosophy used when designing the test rig.
Dissert. Abstr.

N90-19610*# National Aeronautics and Space Administration. Langley Research Center, Hampton, VA.
COMPUTATIONAL ASPECTS OF SENSITIVITY CALCULATIONS IN LINEAR TRANSIENT STRUCTURAL ANALYSIS Ph.D. Thesis - Virginia Polytechnic Inst. and State Univ.
William H. Greene Washington Apr. 1990 107 p
(NASA-TM-4156; L-16643; NAS 1.15:4156) Avail: NTIS HC A06/MF A01 CSCL 20K

A study was performed focusing on the calculation of sensitivities of displacements, velocities, accelerations, and stresses in linear, structural, transient response problems. One significant goal of the study was to develop and evaluate sensitivity calculation techniques suitable for large-order finite element analyses. Accordingly, approximation vectors such as vibration mode shapes are used to reduce the dimensionality of the finite element model. Much of the research focused on the accuracy of both response quantities and sensitivities as a function of number of vectors used. Two types of sensitivity calculation techniques were developed and evaluated. The first type of technique is an overall finite difference method where the analysis is repeated for perturbed designs. The second type of technique is termed semi-analytical because it involves direct, analytical differentiation of the equations of motion with finite difference approximation of the coefficient matrices. To be computationally practical in large-order problems, the overall finite difference methods must use the approximation vectors from the original design in the analyses of the perturbed models. In several cases this fixed mode approach resulted in very poor approximations of the stress sensitivities. Almost all of the original modes were required for an accurate sensitivity and for small numbers of modes, the accuracy was extremely poor. To overcome this poor accuracy, two semi-analytical techniques were developed. The first technique accounts for the change in eigenvectors through approximate eigenvector derivatives. The second technique applies the mode acceleration method of transient analysis to the sensitivity calculations. Both result in accurate values of the stress sensitivities

with a small number of modes and much lower computational costs than if the vibration modes were recalculated and then used in an overall finite difference method. Author

N90-19611 ESDU International Ltd., London (England).
INFORMATION ON THE USE OF DATA ITEMS ON HOT STRUCTURES
Aug. 1989 3 p Supersedes ESDU-Struct-H.02.00.00
(ESDU-89021; ESDU-Struct-H.02.00.00; ISBN-0-85679-694-8; ISSN-0141-4097) Avail: ESDU

This data item sets out the basic equations used in ESDU 89023 to 89027 which present temperature distributions, and stresses and moments, in various structural elements due to aerodynamic heating on the exposed faces. The equation is given for the temperature distribution through a thick sheet heated by forced convection on one side and insulated on the other. Then the equations are given for the stresses and moments on a plate with completely restrained edges; the effects on those equations of relaxing the constraints are considered, first to completely free edges and then to edges either free only to expand in the plane of the plate or free to expand in the plane of the plate and to rotate. ESDU

N90-19612 ESDU International Ltd., London (England).
STEADY STATE TEMPERATURES AND THERMAL STRESSES IN A SPHERICAL OR CYLINDRICAL LAMINATED SHELL
Aug. 1989 6 p Supersedes ESDU-Struct-H.04.00.01
(ESDU-89027; ESDU-Struct-H.04.00.01; ISBN-0-85679-699-9; ISSN-0141-4097) Avail: ESDU

This data item gives equations for calculating the temperature and stresses at any point when the inner and outer surfaces are at different constant temperatures. They require a knowledge of the temperature at which there is no thermal stress and the thickness should not exceed 10 percent of the radius. The analysis is elastic and assumes that the material properties are temperature independent. The layers can be of different materials, and the thermal resistance of a bond can be allowed for as another layer. The expressions given determine the temperature at any point and, for a sphere, the circumferential stress or, for a cylinder, the circumferential and axial stresses. In addition, expressions are given for the pressure exerted on the bonds between the layers. A worked example illustrates the calculation procedure. ESDU

N90-19613# Sydney Univ. (Australia). School of Civil and Mining Engineering.
PLASTIC BENDING TESTS OF COLD-FORMED RECTANGULAR HOLLOW SECTIONS
S. W. Hasan and G. J. Hancock Dec. 1988 83 p Sponsored in part by Tubemakers of Australia Ltd.
(PB90-124611; R-586) Avail: NTIS HC A05/MF A01 CSCL 20K

An experimental investigation of the plastic flexural behavior of Australian-produced cold-formed RHS (rectangular hollow sections) is described. Simple beam tests were performed on 19 specimens comprising 10 different rectangular and square hollow sections. The primary aim of the investigation was to evaluate the plastic hinge rotation capacities of RHS beams having various flange slendernesses, and to compare these measured capacities with the value considered to be the minimum requirement for plastic design. The results of the beam tests are tabulated and graphs detailing the behavior of each specimen are also presented. Based on the test results, a flange slenderness limit for the plastic analysis and design of the cold-formed RHS is proposed. The limiting value is compared with corresponding values in American, British and Canadian specifications and is recommended for adoption by the Australian Steel Structures Code. GRA

N90-19614# Army Armament Research, Development and Engineering Center, Watervliet, NY. Close Combat Armaments Center.
MODAL ANALYSIS OF NONPRISMATIC BEAMS: UNIFORM SEGMENT METHOD Final Report
Ronald G. Gast and H. J. Sneck Dec. 1989 35 p Submitted for publication Sponsored by Army Armament, Research, and Development Center, Picatinny Arsenal, NJ
(AD-A216952; ARCCB-TR-89033) Avail: NTIS HC A03/MF A01 CSCL 13/13

A method to determine the free vibration frequencies and mode shapes of nonprismatic beams that are end-mounted on various supports is described. The term Uniform Segment Method (USM) is used to distinguish this method from finite element (FEM) techniques. The analytical details are presented along with a description of the implementing computer routines. The results are compared with finite element models. Directions for continued research using this modelling technique are also outlined. GRA

N90-19615# International Centre for Theoretical Physics, Trieste (Italy).
DISLOCATION ANNIHILATION MECHANISM FOR THE FORMATION OF DISLOCATION FREE ZONE AT A CRACK TIP
C. W. Lung Aug. 1989 14 p Submitted for publication
(DE90-610552; IC-89/240) Avail: NTIS (US Sales Only) HC A03/MF A01

A dislocation annihilation model is proposed for the formation of dislocation free zone at a crack tip which may be appropriate to explain more results on DFZ investigations. DOE

N90-19616*# National Aeronautics and Space Administration. Marshall Space Flight Center, Huntsville, AL.
PATRAN-STAGS TRANSLATOR (PATSTAGS)
Neil Otte Feb. 1990 22 p
(NASA-TM-100388; NAS 1.15:100388) Avail: NTIS HC A03/MF A01 CSCL 20K

A a computer program used to translate PATRAN finite element model data into Structural Analysis of General Shells (STAGS) input data is presented. The program supports translation of nodal, nodal constraints, element, force, and pressure data. The subroutine UPRESS required for the readings of live pressure data into STAGS is also presented. Author

N90-19617*# National Aeronautics and Space Administration. Lewis Research Center, Cleveland, OH.
A TRANSIENT PLASTICITY STUDY AND LOW CYCLE FATIGUE ANALYSIS OF THE SPACE STATION FREEDOM PHOTOVOLTAIC SOLAR ARRAY BLANKET
Sasan C. Armand, Mei-Hwa Liao, and Ronald W. Morris (Sverdrup Technology, Inc., Cleveland, OH.) 1990 16 p Presented at the 1990 MSC World Users Conference, Los Angeles, CA, 26-30 Mar. 1990; sponsored by Macneal-Schwendler Corporation
(NASA-TM-102516; E-5321; NAS 1.15:102516) Avail: NTIS HC A03/MF A01 CSCL 20K

The Space Station Freedom photovoltaic solar array blanket assembly is comprised of several layers of materials having dissimilar elastic, thermal, and mechanical properties. The operating temperature of the solar array, which ranges from -75 to +60 C, along with the material incompatibility of the blanket assembly components combine to cause an elastic-plastic stress in the weld points of the assembly. The weld points are secondary structures in nature, merely serving as electrical junctions for gathering the current. The thermal mechanical loading of the blanket assembly operating in low earth orbit continually changes throughout each 90 min orbit, which raises the possibility of fatigue induced failure. A series of structural analyses were performed in an attempt to predict the fatigue life of the solar cell in the Space Station Freedom photovoltaic array blanket. A nonlinear elastic-plastic MSC/NASTRAN analysis followed by a fatigue calculation indicated a fatigue life of 92,000 to 160,000 cycles for the solar cell weld tabs. Additional analyses predict a permanent buckling phenomenon in the copper interconnect after the first loading cycle. This should reduce or eliminate the pulling of the copper interconnect on the joint where it is welded to the silicon solar cell. It is concluded that the actual fatigue life of the solar array blanket assembly should be significantly higher than the calculated 92,000 cycles, and thus the program requirement of 87,500 cycles (orbits) will be met. Another important conclusion that can be drawn from the overall analysis is that, the strain results obtained

from the MSC/NASTRAN nonlinear module are accurate to use for low-cycle fatigue analysis, since both thermal cycle testing of solar cells and analysis have shown higher fatigue life than the minimum program requirement of 87,500 cycles. Author

N90-19618# Technische Univ., Berlin (Germany, F.R.). Inst. fuer Luft- und Raumfahrt.
TENSILE BEHAVIOR OF CYLINDRICAL PRESSURE TANKS IN FIBER ASSEMBLING + METAL HYBRID STRUCTURE [ZUM TRAGVERHALTEN VON ZYLINDRISCHEN DRUCKBEHAELTERN IN FASERVERBUND + METALL-HYBRIDBAUWEISE]
Holger Voelzke 1988 114 p In GERMAN
(Contract DFG-Wi-32/35-1)
(ILR-Mitt-213; ETN-90-95353) Avail: NTIS HC A06/MF A01

High pressure tanks, whose fibers are located in the cylindrical part only, are examined between the pure metal structure with high weight and the pure fiber structure, of a minimal weight. They are used as pressure gas bottles, in solar hydrogen technology. It is intended to minimize the weight and the cost, as regards the cylindrical tank section with the variables of metal and fiber section thickness. From an elastic point of view, metal hybrid structures present few advantages towards pure metal structures, and there is no cost reduction. To estimate the tractive capacity of hybrid tanks, the busting behavior must to be tested. As the multiaxis elastoplastic behavior of the metal component plays an important part in it, the global charge-deformation-behavior will be described, as the resistance of the metal component can be totally used. Experiments with a cylindrical metal object (AlMgSiO5) are made to examine elongation behavior. ESA

N90-19619# Stuttgart Univ. (Germany, F.R.). Inst. fuer Computer-Anwendungen.
DEVELOPMENT OF FINISHED BEAM AND SHELL ELEMENTS FROM ENGINEERING MODELS FOR STRUCTURES UNDER HIGH INELASTIC DEFORMATIONS Ph.D. Thesis [ENTWICKLUNG FINITER BALKEN- UND SCHALENELEMENTE AUS INGENIEURMODELLEN FUER STRUKTUREN UNTER GROSSEN (INELASTISCHEN) VERFORMUNGEN]
Ulrich Gerhard Wilhe Hindenlang 1988 136 p In GERMAN
(ETN-90-95377) Avail: NTIS HC A07/MF A01

Some special beam and shell elements from a finite element system are described. This system is a nonlinear finite element pack fitted to elastoplastic problems, and particularly to elastic and nonelastic stability and to the nonelastic material behavior of metals and concrete. A widening of this method develops elastic cylindrical beam elements on an elastoplastic layer hardening element, as an inelastic formulation of this beam with articulations. Some calculations show the utilization possibilities of the method. The nonlinear strength-deformation behavior of the developed beam elements is shown by some examples (calculation of the inelastic breakdown of a roof span). ESA

N90-19620# Metaalinstitut TNO, Apeldoorn (Netherlands).
ORIGIN AND EFFECT OF PORES IN ALUMINUM WELDED JOINTS Literature Survey [ONTSTAAN EN EFFECT VAN PORIEEN IN ALUMINIUMLASVERBINDINGEN (LITERATUUROVERZICHT)]
C. P. Scheepens 22 May 1987 93 p Partly in DUTCH and ENGLISH
(Contract A83/KM/017)
(Rept-87M/43/05720/SCP/GRF; ETN-90-95470) Avail: NTIS HC A05/MF A01

The data available in the literature on the creation of pores and their effects on aluminum welded joints are surveyed. Some general information about possible creation of pores and other welding defects is given. The factors which affect the formation of pores in aluminum welds are discussed. The influence of pore formation on the mechanical properties of aluminum welded joints is outlined. ESA

N90-19621# Technische Univ., Berlin (Germany, F.R.). Fachbereich Physikalische Ingenieurwissenschaft.
DIGITAL TREATMENT OF ELASTIC-PLASTIC STRUCTURES BY MEANS OF QUADRATIC OPTIMIZATION PROCESSES FROM THE FINITE ELEMENT METHOD Ph.D. Thesis [ZUR NUMERISCHEN BEHANDLUNG ELASTISCH-PLASTISCHER STRUKTUREN MIT HILFE QUADRATISCHER OPTIMIERUNGSVERFAHREN AUF DER GRUNDLAGE DER FINITE-ELEMENT-METHODE]
Bernd Kost 1989 265 p In GERMAN; ENGLISH summary
(ETN-90-95823) Avail: NTIS HC A12/MF A02

Quadratic programming problems (in finite or incremental formulation) are stated for several applications in the field of elastic plastic structures (beams, torsion of bars, bending of plates). Such programming problems are developed from the minimum principles of plasticity, using the finite element method as a basis and approximating the nonlinear yield condition by a polyhedron in the stress space. Solutions are computed by various algorithms. With special regard to the conjugate gradient method of De Donato and Franchi for the treatment of sign-constrained quadratic problems, a modification is suggested, which results in an altered rule for the subspace enlargment. Both procedures are then used to develop a gradient method, which is based on preconditioning. Numerical comparisons for some incremental programming problems show a reduction in computation time between 42 and 78 percent for the modified method versus the original version of De Donato and Franchi. By using the preconditioning, computation time is further reduced. ESA

N90-19622# Stuttgart Univ. (Germany, F.R.). Inst. fuer Computer-Anwendungen.
CALCULATION OF NONLINEAR VISCOELASTIC PROCESSES FOR PLASTIC LAYER TEXTILE MEMBRANES Ph.D. Thesis [ZUR BERECHNUNG NICHTLINEARER VISKOELASTISCHER VORGAENGE AM BEISPIEL KUNSTSTOFFBESCHICHTETER TEXTILMEMBRANEN]
Vitor DiasdaSilva 1989 155 p In GERMAN Sponsored by Deutsches Akademischen Austauschdienstes
(ETN-90-95868) Avail: NTIS HC A08/MF A01

A time-integration process is developed, based on the interpolation of the tension or the total elongation by exponential or polynomial functions. The differential matter equation with time depending coefficients was solved on the material plane and was used to produce an interpolation function for the inelastic elongation. This process allows the removal of the stability limit by the explicit algorithm and the bypass of the convergence limit of the Jacobi iteration by the implicit process. These limits are similar for materials, whose viscoelastic deformations are bigger than the elastic response. The stability, convergence and oscillation properties of the developed process are investigated, as well as the rheology properties of textile membranes. The threads are shown to play the principal part in the membrane behavior. ESA

N90-19623# Stuttgart Univ. (Germany, F.R.). Inst. fuer Computer-Anwendungen.
DEVELOPMENT OF FINITE BEAM AND SHELL ELEMENTS FOR STRUCTURES UNDER GREAT INELASTIC DEFORMATIONS Ph.D. Thesis [ENTWICKLUNG FINITER BALKEN- UND SCHALENELEMENTE AUS INGENIEURMODELLEN FUER STRUKTUREN UNTER GROSSEN (INELASTISCHEN) VERFORMUNGEN]
Ulrich Gerhard Wilhe Hindenlang 1988 136 p In GERMAN
(ETN-90-95869) Avail: NTIS HC A07/MF A01

An elasto-plastic layer sheet element is developed to solve elastic and inelastic stability problems, particularly for the behavior of metals and concrete. A cylindrical elastic beam element is used to study an elastoplastic reinforcement element by an inelastic formulation. The nonlinear strength-deformation behavior of the beam elements are explained by simple examples with a lateral charge. The calculation of the inelastic response of a loft brace, for which experimental data were known, is presented. ESA

N90-19624# Hochschule der Bundeswehr, Hamburg (Germany, F.R.). Fachbereich Elektrotechnik.
SECURITY CALCULATIONS OF RIP REACHED CONSTRUCTION ELEMENTS BY MEANS OF PROBABILISTIC BREAKING MECHANICS AND A MARKOV PROCESS Ph.D. Thesis [ZUVERLAESSIGKEITSBERECHNUNG RISSBEHAFTETER-BAUTEILE MITTELS PROBABILISTISCHER BRUCHMECHANIK UND EINES MARKOVSCHEN ANSATZES]
Thomas Schmidt 1989 186 p In GERMAN
(ETN-90-95890) Avail: NTIS HC A09/MF A01

The numerical reliability calculation of ripped construction elements under cyclic fatigue stresses is shown to be possible by Monte Carlo simulation, despite the high calculation times and the necessity of using variance-reducing processes. An alternative to this method is proposed with a stochastic Markov-process, which allows validation of the results and takes into account the effects of maintenance and inspections. Accident probability and breakdown frequency can be calculated as functions to time, with the transition and state probabilities of the original Markov process. ESA

N90-19625# Fraunhofer Inst. fuer Werkstoffmechanik, Freiburg (Germany, F.R.).
THREE-DIMENSIONAL Fe ANALYSIS OF THE SURFACE DISTRIBUTION IN NOTCHED COMPACT SAMPLES OF 20 MnMoNI 55 [DREIDIMENSIONALE FE-ANALYSEN DER SVERTEILUNG IN SEITENGEKERBTEN KOMP AUS 20 MN MO NI 55]
H. Stoeckl Jan. 1989 52 p In GERMAN
(Contract DFG-AZ-Schm-522/6-1)
(W-1/89; ETN-90-96072) Avail: NTIS HC A04/MF A01

The influence of the test thickness on the fault of laterally notched compact samples made of 20 Mn Mo Ni 55 is studied by finite elements in the temperature area of the transition from fragile to ductile fault-charge-broadening curves and the surface energy; broadening curves are in good agreement with measurement results. The local energy values along the rip front increase in the vicinity of the lateral curve in the elastic area. With increasing plastic deformations a nearly constant energy distribution is obtained at first, but then the energy drops, particularly by thin samples in the proximity of the lateral notches. The same tendency is observed for the vertical tension component on the ligament and for the factor h (h equals hydrostatic tension/reference tension). For thin samples these quantities become higher with the distance of the rip front. ESA

N90-19626# Oak Ridge National Lab., TN.
EVALUATION OF THE RESPONSE OF ALUMINUM ALLOYS TO SINGLE AND MULTIPLE PARTICLE IMPACTS
James R. Keiser and Mukund Rao 1989 17 p Presented at the Corrosion '90, Las Vegas, NV, 23-27 Apr. 1990
(Contract DE-AC05-84OR-21400)
(DE90-003689; CONF-900403-2) Avail: NTIS HC A03/MF A01

Samples of annealed 1100 aluminum and 7075-T6 aluminum were eroded to steady-state conditions in a multiple particle erosion system. The samples were sectioned through the eroded areas, and a mechanical properties microprobe was used to measure the hardness of the material. The oblique multiple particle impacts produced a rippled surface with the hardness at the top of the wave crests approximately equal to that in the valleys. However, the total depth of hardening was significantly greater in material below the wave crests and was a function of the material for both wave crests and valleys. The depth of hardened material below the wave crest was about equal to the height of the wave plus the depth of hardening below the valley. DOE

N90-19627# Sandia National Labs., Albuquerque, NM. Experimental Mechanics Dept.
USE OF CHAOTIC AND RANDOM VIBRATIONS TO GENERATE HIGH FREQUENCY TEST INPUTS. PART 2: CHAOTIC VIBRATIONS
Thomas L. Paez and Dan L. Gregory 1990 9 p Presented at the 36th Institute of Environmental Science Annual Technology Meeting, New Orleans, LA, 23-27 Apr. 1990
(Contract DE-AC04-76DP-00789)
(DE90-007153; SAND-90-0335C-Pt-2; CONF-900479-2) Avail: NTIS HC A02/MF A01

It is shown that the traditional limits on amplitude and frequency that can be generated in a laboratory test on a vibration exciter can be substantially extended. This is accomplished by attaching a device to the shaker that permits controlled metal to metal impacts that generate a high acceleration, high frequency environment on a test surface. A companion paper derives some of the mechanical relations for the system. This paper shows that a sinusoidal shaker input can be used to excite deterministic chaotic dynamics of the system yielding a random vibration environment on the test surface, or a random motion of the shaker can be used to generate a random vibration environment on the test surface. Numerical examples are presented to show the kind of environments that can be generated in this system. DOE

N90-19628# Sandia National Labs., Albuquerque, NM. Experimental Mechanics Dept.
USE OF CHAOTIC AND RANDOM VIBRATIONS TO GENERATE HIGH FREQUENCY TEST INPUTS
Dan L. Gregory and Thomas L. Paez 1990 7 p Presented at the 36th Institute of Environmental Science Annual Technology Meeting, New Orleans, LA, 23-27 Apr. 1990
(Contract DE-AC04-76DP-00789)
(DE90-007412; SAND-90-0334C; CONF-900479-5) Avail: NTIS HC A02/MF A01

It is shown that the traditional limits on amplitude and frequency that can be generated in a laboratory test on a vibration exciter can be substantially extended. This is accomplished by attaching a device to the shaker that permits controlled metal to metal impacts that generate high frequency, high acceleration environment on a test surface. A companion paper (Reference 1) shows that a sinusoidal or random shaker input can be used to generate a random vibration environment on the test surface. This paper derives the three response components that occur on the test surface due to an impact on the bottom surface and the base driven response from the shaker input. These response components are used to generate impulse response functions and frequency response functions which are used in the companion paper to derive power spectral density functions for the overall response. DOE

N90-19629*# National Aeronautics and Space Administration. Lewis Research Center, Cleveland, OH.
DEMONSTRATION OF CAPABILITIES OF HIGH TEMPERATURE COMPOSITES ANALYZER CODE HITCAN
Surendra N. Singhal, Joseph J. Lackney (Sverdrup Technology, Inc., Cleveland, OH.), Christos C. Chamis, and Pappu L. N. Murthy Mar. 1990 56 p
(NASA-TM-102560; E-5380; NAS 1.15:102560) Avail: NTIS HC A04/MF A01 CSCL 20K

The capabilities a high temperature composites analyzer code, HITCAN which predicts global structural and local stress-strain response of multilayered metal matrix composite structures, are demonstrated. The response can be determined both at the constituent (fiber, matrix, and interphase) and the structure level and includes the fabrication process effects. The thermo-mechanical properties of the constituents are considered to be nonlinearly dependent on several parameters including temperature, stress, and stress rate. The computational procedure employs an incremental iterative nonlinear approach utilizing a multifactor-interactive constituent material behavior model. Various features of the code are demonstrated through example problems for typical structures. Author

N90-19630*# National Aeronautics and Space Administration. Langley Research Center, Hampton, VA.
INTERLAMINAR SHEAR STRESS EFFECTS ON THE POSTBUCKLING RESPONSE OF GRAPHITE-EPOXY PANELS
S. P. Engelstad, N. F. Knight, Jr., and J. N. Reddy (Virginia Polytechnic Inst. and State Univ., Blacksburg.) Mar. 1990 8 p

Proposed for presentation at the International Conference on Structural Testing, Analysis and Design, Bangalore, India, 29 Jul. - 3 Aug. 1990
(NASA-TM-102626; NAS 1.15:102626) Avail: NTIS HC A02/MF A01 CSCL 20K

The influence of shear flexibility on overall postbuckling response was assessed, and transverse shear stress distributions in relation to panel failure were examined. Nonlinear postbuckling results are obtained for finite element models based on classical laminated plate theory and first-order shear deformation theory. Good correlation between test and analysis is obtained. The results presented analytically substantiate the experimentally observed failure mode. Author

42 GEOSCIENCES (GENERAL)

No abstracts in this category.

43 EARTH RESOURCES AND REMOTE SENSING

Includes remote sensing of earth resources by aircraft and spacecraft; photogrammetry; and aerial photography.

For instrumentation see *35 Instrumentation and Photography.*

N90-19631# European Space Agency. European Space Research and Technology Center, ESTEC, Noordwijk (Netherlands).
ESRIN
Valerie David, comp. and Norman Longdon, comp. Mar. 1989 17 p Original contains color illustrations
(ESA-BR-58; ISSN-0250-1589) Avail: NTIS HC A03/MF A01

The European Space Agency (ESA) information link, ESRIN, is described. Located in Frascati, Italy, ESRIN is the Center in which data from numerous sources is acquired, processed, and archived, for use throughout ESA member states. Much of the information handled by ESRIN is in written form, except for data of the Earthnet program. Earthnet receives data from Earth observation satellites through its network of ground stations stretching form the North of Sweden to the Canary Islands. Besides Earthnet, two other sectors of activity are found on the ESRIN site: (1) the ESA information Retrieval Service (ESA-IRS) which is Europe's largest on-line information service; and (2) the Information Systems Division (ISD) which was set up in 1988 to harmonize information handling systems within ESA's programs, and with the Agency's contractors and its scientific communities. K.C.D.

N90-19632# Instituto de Pesquisas Espaciais, Sao Jose dos Campos (Brazil).
A METHOD FOR DETERMINATION OF CONTROL PIXELS FOR LANSAT USING A REFLECTOR [UM METODO PARA DETERMINACAO DE PIXELS DE CONTROLE PARA O LANDSAT USANDO UM REFLETOR]
Roberto PereiradaCunha, Luiz Danilo DamascenoFerreira, and Paul Cesar GurgeldeAlbuquerque Apr. 1989 18 p In PORTUGUESE; ENGLISH summary Presented at the 3rd Brazilian Symposium on Remote Sensing, Rio de Janeiro, Brazil, 28-30 Nov. 1984
(INPE-4884-PRE/1491) Avail: NTIS HC A03/MF A01

A method to determine ground control points on satellite imageries is described. The method consists in achieving a radiometrically contrasted area in a chosen point on the ground. The ground radiometrical level is obtained by using a small, pointable mirror, which is correctly positioned in the terrain for the sun-satellite (sensor) geometry, yields an area with a high radiometric contrast. As a result of this a conspicuous pixel is obtained on satellite imagery. Pixels determined in this way can be used for geometric corrections, radiometric studies, imagery coregistration, or cartographic purposes. Author

N90-19633# Instituto de Pesquisas Espaciais, Sao Jose dos Campos (Brazil).
AREAS OF AQUATIC MACROPHYTES CLASSIFIED THROUGH VEGETATIVE INDEXES EXTRACTED FROM LANDSAT/TM IMAGERY [AREAS DE MACROFITAS AQUATICAS CLASSIFICADAS ATRAVES DE INDICES DE VEGETACAO EXTRAIDOS DE IMAGENS LANDSAT/TM]
Myrian deMAbdon and Divino C. Figueiredo Aug. 1989 6 p In PORTUGUESE; ENGLISH summary Presented at the 14th Brazilian Conference on Cartography in Gramado-RS, 21-26 May 1989
(INPE-4880-PRE/1489) Avail: NTIS HC A02/MF A01

LANDSAT/TM data were used to identify the occurrence of aquatic macrophytes within the Tucurui Reservoir, Para State, Brazil. A Vegetative Index Imagery (VII) was derived by applying the normalized ratio between bands 3 and 4. The VII histogram was sliced into 4 vegetation classes, from which 2 displayed macrophyte populations. Those classes were then used as training sites to implement a maximum likelihood classification on the remaining study area. The method proven to be efficient as shown by the statistical results. Author

N90-19634# Instituto de Pesquisas Espaciais, Sao Jose dos Campos (Brazil).
AVAILABILITY OF MULTITEMPORAL LANDSAT DATA ACCOMPANYING THE VARIATION OF WATER SURFACES IN THE PROGRAM AREA OF CAREIRO PDRI/AM
Madalene NieroPereira, Sergio dosAnjosFerreiraPinto, Paulo Roberto Martini, and Glenio BruckdeAndrade (Centro de Desenvolvimento Pesquisas e Tecnologia do Estado do Amazonas, Manaus, Brazil) Jul. 1989 15 p Presented at the 3rd Brazilian Sumposium on Remote Sensing, Rio de Janeiro-RJ, 28-30 Nov. 1984
(INPE-4896-PRE/1496) Avail: NTIS HC A03/MF A01

The objective is to analyze the variation of the flooded areas during high water situations (July 1977, July 1979, and July 1982) and low water situations (December 1981), through the analysis of multitemporal LANDSAT data. By means of digital processing the spectral separability of the classes was verified, which were characterized by the presence of water surfaces with different intensities of participation in the integrating response of a pixel in the near infrared band. A density slicing algorithm, implemented at the Image-100 systems, was applied for this purpose. The multitemporal analysis of the data was accomplished through the registration of the images corresponding to dry and wet periods. Mutlitemporal color composites were generated utilizing the color filters available at the Image-100 system (blue, green, and red). The area of Careiro Program, in the region adjacent to the Careiro Island (AM), was selected because it is an important crop land periodically affected by flood. The following classes were analyzed: water areas, shallow water areas, areas presenting water plus vegetation and humid areas. The density slicing technique showed efficiency in the classification process of flooded areas. The multitemporal analysis of the data allowed the detection of areas affected by the flooding in the analyzed periods. Author

N90-19635# Instituto de Pesquisas Espaciais, Sao Jose dos Campos (Brazil).
ANALYSIS OF PHOTOGEOLOGIC LINEAMENTS IN THE ITHACARE (BA) REGION: A PROPOSED METHODOLOGY [ANALISE DOS LINEAMENTOS FOTOGEOLOGICOS NA REGIAO DE ITACARE (BA): UMA PROPOSTA METODOLOGICA]
Chan Chiang Liu and Jose Eduardo Rodrigues Aug. 1989 13 p In PORTUGUESE; ENGLISH summary Presented at the 3rd Brazilian Symposium on Remote Sensing, Rio de Janeiro, Brazil, 28-30 Nov. 1984
(INPE-4855-PRE/1478) Avail: NTIS HC A03/MF A01

Examination of LANDSAT and SLAR images in Southern Bahia

reveals numerous linear features, which can be grouped into five sets, based on their trends: N65 deg E, N70 deg W, N45 deg W, N40 deg E and NS/N15 deg E. Owing to their topographic expressions, distributive patterns and mutual relationships, the lineament sets of N65 deg E and N70 deg W directions, as well as the sets of N40 deg E and N45 deg W, can be considered as two pairs of conjugate-shear fractures and the former is older and is always cut by the latter. Their conjugate-shear angles are 45 deg and 85 deg and their bissector lines are approximately in east-west and north-south directions, respectively. According to the theory on the conjugate-shear angles, the former conjugate-shear fractures would be caused by an east-west compression, under a condition of low confining pressure and temperature. The other conjugate pair (N45 deg W and N40 deg E) would be caused by a strong compression in north-south direction. The lineaments with NS/N15 deg E trend are concordant with the regional structures represented by foliations and axis of folding. Author

N90-19636# Instituto de Pesquisas Espaciais, Sao Jose dos Campos (Brazil).

SATELLITE IMAGERY FOR WATER QUALITY ASSESSMENT IN COASTAL REGIONS

Claudia ZuccariFernandesBraga and Luiz DrudedeLacerda (Universidade Federal Fluminense, Niteroi, Brazil) Aug. 1989 10 p In PORTUGUESE; ENGLISH summary Presented at the 3rd Congresso Brasileiro de Defesa do Meio Ambiente, Rio de Janeiro, Brazil, 24-28 Jul. 1989

(INPE-4891-PRE/1492) Avail: NTIS HC A02/MF A01

In the region of the Guanabara Bay, RJ, the water quality parameters responsible for the TM/LANDSAT image spectral response were identified. Simultaneously to the LANDSAT passage over the study area, the temperature salinity; Secchi depth, the total suspended solids (TSS) and the TSS concentrations of iron and manganese were measured in the water. Simple and multiple regression analysis were applied to these ground truth data and to the spectral data of the TM bands 1, 2, 3, 4, and 6. The results, in two dates, showed differences that are explained by tidal and wind conditions observed in each case. In high tidal conditions, the parameters that correlated with the multispectral data are the ones related to the sea water, such as temperature, salinity, and Secchi depth; in low tidal conditions the parameters that correlated with multispectral data are the ones related to continental water, such as iron and manganese contents of TSS, with no relation between temperature, salinity, and Secchi depth. Author

N90-19637# Army Cold Regions Research and Engineering Lab., Hanover, NH.

DATA REDUCTION OF GOES (GEOSTATIONARY OPERATIONAL ENVIRONMENTAL SATELLITE) INFORMATION FROM DCP (DATA COLLECTION PLATFORM) NETWORKS

Gary W. DeCoff, Steven F. Daly, Timothy Pangburn, and Clay Thomson Sep. 1989 18 p

(AD-A215844; CRREL-SR-89-29) Avail: NTIS HC A03/MF A01 CSCL 04/2

A software system, DCP.FOR, was developed to provide a convenient and efficient method of decoding, reducing, and storing data from the Data Collection Platform (DCP) networks transmitted through the Geostationary Operational Environmental Satellite (GOES) data collection system. The software system includes a simple means of defining the arrangement of sensors at a DCP site that can be easily updated if the sensor arrangement is changed or the sensors are modified. Any linear data reduction procedure can be processed. Precise temperature measurements using individually calibrated thermistors can be processed through the use of voltage divider circuits, nonlinear resistance to temperature calibration, and impedance mismatch detection and correction. The system can process data from DCPs manufactured by four companies. User-defined maximum and minimum limits determine the acceptability of the processed data. Data values not within these limits or missing data are flagged with a missing value marker. The database created by the system is independent of the particular sensor arrangement at any DCP site. The data can be easily transferred to other database systems. GRA

N90-19638# Rochester Inst. of Tech., NY. Center for Imaging Science.

SELECTION OF OPTIMAL TEXTURAL FEATURES FOR MAXIMUM LIKELIHOOD IMAGE CLASSIFICATION

Wendy I. Rosenblum, Carl Salvaggio, and John R. Schott Jan. 1990 59 p

(Contract DE-FG01-88DP-20153)

(DE90-006901; DOE/DP-20153/T7; RIT/DIRS-89/90-66-131)

Avail: NTIS HC A04/MF A01

The classification or segmentation of images into land cover or object class is one of the fundamental remote sensing/image processing tasks. The classification techniques have reached a high level of maturity in the forms of statistical pattern recognition techniques applied to multispectral images. According to this approach each pixel has a spectral vector associated with it and pixels are segmented into the class they most closely resemble spectrally. While these techniques are reasonably successful they do not take advantage of the brightness patterns within a class or at object boundaries nor are they readily applicable to monochrome images or highly correlated multispectral images (e.g., true color images). To overcome these limitations several investigators have suggested the use of image derived features as additional factors for use in image classification. Robert (1989) has identified over forty textural features that have been suggested by various authors as useful for scene classification. Regrettably it is very compute intensive to generate all these features for every pixel in an image and to then use them in a classifier. Schott et al. (1988) developed a technique for selecting a small subset of spectral bands from a large set based on criteria intended to optimize maximum likelihood classification. Salvaggio et al. (1990) have implemented code to generate 46 image derived textural features and applied a two-step feature reduction and optimization process based largely on the band selection process of Schott et al. (1988). The current effort drew on this proof-of-concept work mentioned above and improved on several limitations noted in the earlier work. Specifically, the initial feature set reduction algorithm of Robert (1989) is shown to be deficient and an improved method implemented. DOE

N90-19639# National Aerospace Lab., Amsterdam (Netherlands). Space Div.

THE POTENTIAL OF COMBINED USE OF SATELLITE DATA WITH TOPOGRAPHIC TM INFORMATION FOR MANUAL/VISUAL AND DIGITAL UPDATING OF LAND USE

F. B. vanderLaan 23 Mar. 1988 60 p In DUTCH; ENGLISH summary Submitted for publication Sponsored by Beleids Commissie Remote Sensing, Delft, Netherlands Original contains color illustrations

(NLR-MP-88021-U; ETN-90-95418) Avail: NTIS HC A03/MF A01

The potential of regular updating of land use information on topographic maps using LANDSAT Thematic Mapper, SPOT panchromatic and SPOT multispectral imagery was investigated. Information from topographic maps was digitally combined with satellite imagery using raster based techniques. In a first phase a product was developed that is mainly suited to obtain a quick overview of changes in the landscape; the resulting image map allows manual updating of land use changes down to details of 4 to 8 m, and mapping of land use types not indicated on a topographic map. In a second phase all nonlinear land use information indicated on a topographic map was digitized. The regular availability of satellite imagery in principle permits continuous updating of land use data. A large variety of land use types can be discriminated. ESA

N90-19640# Technische Univ., Delft (Netherlands). Faculteit der Geodaesie.
DEVELOPMENT OF SOFTWARE ROUTINES FOR REMOTE SENSING DIGITAL IMAGE PROCESSING Thesis [ONTWIKKELING VAN ENKELE SOFTWARE ROUTINES VOOR DIGITALE BEELDVERWERKING IN DE REMOTE SENSING]
P. J. M. Meijers Mar. 1989 107 p In DUTCH
(ETN-90-95452) Avail: NTIS HC A06/MF A01

Software was developed and modified to support research in the field of digital image processing for photogrammetry and remote sensing purposes. Two digital images were created, one with line segment, and one with a circular surface. The theory of preprocessing and image improvement is outlined. Programs were developed for image analysis with a view to the plotting of image edges and gray value histogram. For further analysis a binary digitation can also be performed using threshold segmentation. A procedure that processes the image by a median filter and substracts the result from the original image gives surprisingly good results in tracing single-pixel-thick lines in the image. The images are presented by plotting the gray value of each pixel with the program DRAW. Numerical results can be graphically represented through the plotter. ESA

N90-19641# Beleidscommissie Remote Sensing, Delft (Netherlands).
POSSIBLE APPLICATIONS OF REMOTE SENSING SATELLITE PICTURES FOR THE WATER QUALITY MANAGEMENT OF THE FRISIAN LAKES, NETHERLANDS Final Report [DE TOEPASSINGSMOGELIJKHEDEN VAN REMOTE SENSING SATELLIETOPNAMEN VOOR HET WATERKWALITEITSBEHEER VAN DE FRIESE MEREN]
Dec. 1988 51 p In DUTCH Prepared in cooperation with DHV Raadgevend Ingenieursbureau B.V., Amersfoort, Netherlands Original contains color illustrations
(BCRS-88-17; ETN-90-95478) Avail: NTIS HC A04/MF A01

Applications of digital remote sensing satellite pictures for the water quality management of surface water in general and that of the Frisian lakes (Netherlands) in particular are described. Two LANDSAT Thematic Mapper satellite pictures were analyzed using digital image processing and multiple regression techniques, resulting in quantitative maps of chlorophyll-a, suspended substances, and transparency. The digital satellite pictures allow the calculation of the concentration of a number of water quality parameters for each location in the lakes. The spreading of the concentrations in the lakes with respect to the measuring points is found to be considerable, indicating the inferior representativeness of the measuring point for a lake as a whole. Suggestions for improvements are given. The remote sensing satellite pictures can be used to follow the evolution of a number of water quality characteristics. ESA

N90-19642# Beleidscommissie Remote Sensing, Delft (Netherlands).
POSSIBLE APPLICATIONS OF REMOTE SENSING IN THE PREPARATORY PHASE OF A LAND MANAGEMENT PROJECT Final Report [TOEPASSINGSMOGELIJKHEDEN VAN REMOTE SENSING IN DE VOORBEREIDINGSFASE VAN EEN LANDINRICHTINGSPROJECT]
Wim J. Droesen and Arno M. vanLieshout (Instituut voor Culturrtechniek en Waterhuishouding, Wageningen, Netherlands) Dec. 1988 95 p In DUTCH
(BCRS-88-19; ICW-1832; ETN-90-95480) Avail: NTIS HC A05/MF A01

The applicability of remote sensing techniques in the preparatory phase of land management projects was examined. The theoretical fundamentals are outlined. Three flights provided false color pictures and scanner pictures in the green, red, heat IR and thermal IR wavelength regions. On the false color pictures the land use can almost unequivocally be determined. The scanner pictures were treated with a supervised automatic classification procedure. The false color and scanner pictures are sufficiently detailed for an inventory of grassland vegetation. The correlations between soil moisture and radiation intensity and temperature have to be improved. The soil science information in remote sensing pictures is limited, and pattern recognition is impossible on a large part of the pictures. ESA

N90-19643# Beleidscommissie Remote Sensing, Delft (Netherlands).
TECHNICAL AND ADMINISTRATIVE FEASIBILITY OF MICROLIGHT REMOTE SENSING APPLICATIONS FOR RIVER BOARDS [TECHNISCHE- EN BESTUURLIJKE HAALBAARHEID VAN MICROLIGHT REMOTE SENSING TOEPASSINGEN BIJ WATERSCHAPPEN]
Jan. 1989 16 p In DUTCH Prepared in cooperation with Environmental Analysis and Remote Sensing, Delft, Netherlands
(BCRS-89-01; ETN-90-95483) Avail: NTIS HC A02/MF A01

The utilization of aerial photography (remote sensing) with a view to an efficient management of dams was studied. A photo reportage with stereo pictures could be a functional aid for inventories of plantation and cultivation on dams, for the evaluation of concession applications, for a well structured evaluation of quantitative and qualitative aspects of dams, and for the completion of obsolete maps. The photo reportage could also be part of a data base with a view to the future dam law. The photos have a good quality and lend themselves well to optical orientation and to the intended applications. ESA

N90-19644# Beleidscommissie Remote Sensing, Delft (Netherlands).
SEGMENTATION OF SIDE-LOOKING AIRBORNE RADAR (SLAR) IMAGES USING A PRIORI KNOWLEDGE [SEGMENTATIE VAN SLAR-BEELDEN MET GEBRUIKMAKING VAN A-PRIORI KENNIS]
Jan C. M. Kleijweg Feb. 1989 93 p In DUTCH; ENGLISH summary
(BCRS-89-03; ETN-90-95485) Avail: NTIS HC A05/MF A01

A method to segment SLAR images was developed, with a view to the use of microwave remote sensing as a tool in agriculture and forestry for vegetation mapping, crop classification, yield forecasting, etc. The method, based on a split-and-merge algorithm, was developed to perform the grouping of quad-tree blocks into regions where the grouping is applied iteratively until a predefined quality criterion is met. The segmentation results are very satisfactory, but the complete procedure is rather time-consuming. A method was designed for the utilization of a priori information about the agricultural region in the automatic processing of the SLAR imagery, leading to a dramatic decrease in computation time. ESA

N90-19645# Technische Univ., Delft (Netherlands). Faculteit der Geodesie.
COMPARISON OF ARTIFICIAL MATRICES AND COVARIANCE FUNCTIONS Thesis [EEN VERGELIJKING VAN KUNSTMATRICES EN COVARIANTIEFUNCTIES]
R. C. P. vanderSchoot Feb. 1989 118 p In DUTCH; ENGLISH summary
(ETN-90-95722) Avail: NTIS HC A06/MF A01

An investigation into whether artificial (or subsitute) matrices, deduced from other covariance functions, give a better description of the precision of a plane geodetic network was carried out. The parameters of the artificial matrix were estimated from the equations of the elements of the artificial matrix and the covariance functions were applied in order to get the optimal artificial matrix. The applied method of estimation depends strongly on the computation method and on the choice of observation quantities. The Baarda function seems to give a better result than the Gauss function, and can be used as a good covariance function. ESA

N90-19646# Technische Univ., Delft (Netherlands). Werkeenheid der Fotogrammetrie en Remote Sensing.
THEMATIC COUPLING BETWEEN DIGITAL IMAGES AND GEOGRAPHIC INFORMATION SYSTEMS Thesis [THEMATISCHE KOPPELING TUSSEN DIGITALE BEELDEN EN GEOGRAFISCHE INFORMATIE SYSTEMEN]

C. S. Han Feb. 1989 117 p In DUTCH; ENGLISH summary
(ETN-90-95723) Avail: NTIS HC A06/MF A01

A procedure that accomplishes a fast update of a Geographic Information System (GIS) was developed. It is based on a numerical interface between digital images and a GIS, based on thematic information. The GIS is first used to analyze a labeled image obtained by a multispectral classification method. Changes in the land use since the last update are determined with a type of histogram check. The segments in which changes are found are further investigated. The image is enhanced by eliminating bad classifications and new borders are detected. The starting point and the chain codes of every digital arc are determined. The resulting nodes can be seen as a temporary vectorization. A minimax polygon approximation leads to the final vectorization. The GIS can be updated with the new polygon nodes. ESA

N90-19647# Beleidscommissie Remote Sensing, Delft (Netherlands).
[ACTIVITIES REPORT IN REMOTE SENSING] Annual Report, 1987
1987 112 p In DUTCH; ENGLISH summary Original contains color illustrations
(ETN-90-95472) Avail: NTIS HC A06/MF A01

The activities carried out in the Netherlands Remote Sensing Program are overviewed and the organizational structure of the Netherlands Remote Sensing Board (BCRS) is displayed. Remote sensing techniques were used for monitoring tidal waters. Satellite imagery was used for water quality research. Meteorological and oceanographic interactions were investigated. Progress was made in the field of operationalization of geometric and atmospheric corrections. Crop identification and classification experiments were performed. Developments were made for the numerical processing of satellite data. Radar and 'seatruth' data were analyzed for agricultural purposes. The BCRS participated in the ERS-1 project. Technology development in the field of IR sensors was performed. ESA

N90-19648# Technische Univ., Delft (Netherlands). Werkeenheid Fotogrammetrie en Remote Sensing.
APPLICATIONS OF THE GPS IN PHOTOGRAMMETRY Thesis [TOEPASSING VAN GPS IN DE FOTOGRAMMETRIE]
Richard Witmer Mar. 1988 83 p In DUTCH; ENGLISH summary
(ETN-90-96004) Avail: NTIS HC A05/MF A01

Block adjustment was combined with GPS (global positioning system) to reduce the amount of ground control in photogrammetry. The coordinates of the projection centers were measured with GPs in a photoflight. The GPS coordinates are found to be accurate enough to have effect in block adjustments. The GPS determined projection center positions in block adjustments can be used as control points or in a supermodel. The results of the block adjustments were used to investigate the precision of terrain points. One of the main conclusions is that the use of control points in a block adjustment of a block of 4 strips with 8 ground control points gives good results; the precision of the terrain points meets defined demands. The use of the supermodel does not give good results. ESA

N90-19649# IIT Research Inst., Bartlesville, OK. National Inst. for Petroleum and Energy Research.
USING IMAGE ANALYSIS TO DETERMINE PETROPHYSICAL PROPERTIES OF RESERVOIR ROCKS
Livin Tomutsa and Alan Brinkmeyer Mar. 1990 18 p
(Contract DE-FC22-83FE-60149)
(DE90-000222; NIPER-444) Avail: NTIS HC A03/MF A01

The objective of this work is to apply computer image analysis methods to measurements of pore and grain parameters in reservoir rocks and to use the measured values of these parameters to predict petrophysical properties such as porosity, permeability, and capillary pressure. By computer image analysis, rapid measurements of pore and grain diameters, areas, and perimeters can be performed, and from these measurements various other parameters, such as shape factor, form factor, and specific surface can be derived. A commercially available PC-based image analysis system previously adapted for computations of petrophysical properties has been improved. Based on pore and pore throat measurements, rapid and reliable predictions of porosity, permeability, grain size distribution, and capillary pressure can be made from thin sections fabricated from rock samples as small as drill cuttings. DOE

N90-19259*# Massachusetts Univ., Amherst. Dept. of Electrical and Computer Engineering.
COHERENT RADAR MEASUREMENT OF OCEAN CURRENTS FROM GEOSTATIONARY ORBIT
R. E. McIntosh *In* NASA, Langley Research Center, Earth Science Geostatonary Platform Technology Jul. 1989 p 155-165 (For primary document see N90-19249 12-15)
Avail: NTIS HC A17/MF A03 CSCL 08C

N90-19262*# Kansas Univ. Center for Research, Inc., Lawrence. Radar Systems and Remote Sensing Lab.
RAIN RADARS FOR EARTH SCIENCE GEOSTATIONARY PLATFORMS: SOME POSSIBILITIES
S. P. Gogineni and R. K. Moore *In* NASA, Langley Research Center, Earth Science Geostationary Platform Technology Jul. 1989 p 191-200 (For primary document see N90-19249 12-15)
Avail: NTIS HC A17/MF A03 CSCL 04B

N90-19435*# Jet Propulsion Lab., California Inst. of Tech., Pasadena.
DETERMINATION OF EARTH ORIENTATION USING THE GLOBAL POSITIONING SYSTEM
A. P. Freedman *In its* The Telecommunications and Data Acquisition Report 15 Nov. 1989 p 1-11 (For primary document see N90-19434 12-32)
Avail: NTIS HC A10/MF A02 CSCL 08E

44 ENERGY PRODUCTION AND CONVERSION

Includes specific energy conversion systems, e.g., fuel cells; global sources of energy; geophysical conversion; and windpower.

For related information see also *07 Aircraft Propulsion and Power, 20 Spacecraft Propulsion and Power,* and *28 Propellants and Fuels.*

N90-19650# Institute of Energy Economics of Japan.
ANALYSIS OF COMPETITION AMONG KINDS OF ENERGY AT THE ERA OF COMPLEXED ENERGY. (REPORT ON OVERSEAS STUDY)
31 Dec. 1988 178 p In JAPANESE
(DE89-910213; IEE-SR-207) Avail: NTIS (US Sales Only) HC A09/MF A01

Transition features of competition among kinds of energy in America, England, France are explained along with a study on movement by each country. As for the characteristic point for each country, revival of coal energy in America, policy for accepting atomic energy as main source in France, and utilization of cheap petroleum gas from North Sea in England, were explained and transition feature of which were given by figures. Energy industries were classified into electricity, town gas, coal, and petroleum, and competitive situation in each country were explained. Energy policy in each country was explained by taking taxation of each country as primary index. DOE

N90-19651# Institute of Energy Economics of Japan.
VISION FOR THE INTRODUCTION OF THE WIND POWER GENERATION SYSTEM. SURVEY ON THE PROSPECTIVE MARKET, PART 2
Toshiaki Senda, Koichi Nagata, Yasuharu Nakazawa, Hideto Miyachika, and Eiko Matsuda Mar. 1988 244 p In

JAPANESE
(DE89-910386; NEDOJ-P-8731) Avail: NTIS (US Sales Only) HC A11/MF A02

Fifty points were selected, each having a potential for wind power generation considering the wind conditions, out of the total AMeDAS point (838 sites) by screening the annual average wind velocity; simulation analyses were made on the operating conditions of the power generation system in the case of a 100 kW class wind power generation plants and were installed at the respective sites by utilizing WPES-AMeDAS. Based on the results, 15 prospective sites were selected and assessment as plant locations was made by actual field observation. Then a comprehensive assessment was made by the analysis of the economical aspects of the wind power plant. Finally, as a result, 14 prospective sites were proposed. Major items of study are as follows: (1) selection of sites with prospective wind conditions; (2) analysis and assessment of prospective sites; and (3) economic aspects of a wind power generation system. DOE

N90-19652# Stanford Univ., CA. Dept. of Chemistry.
ENERGY TRANSFER AND PHOTOCHEMISTRY IN BIOMIMETIC SOLAR CONVERSION Final Report, Aug. 1983 - Jul. 1989
Steven G. Boxer Sep. 1989 13 p
(Contract GRI-5083-260-0824)
(PB90-114562; GRI-89/0223) Avail: NTIS HC A03/MF A01 CSCL 10A

The research program developed methods for studying electron transfer reactions and electron transfer in biomimetic solar energy systems. Over the course of the project results were obtained in several areas. The distance and orientation dependence of energy transfer were measured quantitatively in a completely defined 3-D array of chromophores. Synthetic methods were developed for covalently modifying DNA bases with electron donors and acceptors. Electric field effects were measured on the absorption and emission of photosynthetic systems. This led to the development of a general method for modulating electron transfer reactions in electric fields. Applications of this method to transition metal complexes were developed for the first time. Author

N90-19653# Westinghouse Electric Corp., Pittsburgh, PA. Advanced Energy Conversion Dept.
SOLID OXIDE FUEL CELL COGENERATION SYSTEM CONCEPTUAL DESIGN, PROGRAM 2 Final Report, 30 Apr. 1987 - 31 Jul. 1989
W. L. Lundberg Jul. 1989 119 p
(Contract GRI-5086-294-1273)
(PB90-114968; Rept-1273-15; GRI-89/0162) Avail: NTIS HC A06/MF A01 CSCL 10A

Results of a solid oxide fuel cell cogeneration system conceptual design study are presented. The baseline system, rated at 200 kWe net power and fueled by natural gas, is applied in a baseloaded electric mode at a commercial site. The system satisfies part of the site's needs for ac power and supplies exhaust heat to generate 170 C (338 F) saturated steam for site use. In evaluating cogeneration system economics, it is assumed that this steam is supplied directly to an existing steam-driven chiller. Solid oxide fuel cell cogeneration systems rated at 50, 500, and 2000 kWe are also evaluated. The 2000 kWe system is assumed to be sited in a small industrial application. GRA

N90-19654# New Energy Development Organization, Tokyo (Japan).
SURVEY ON THE POSSIBILITY OF INTRODUCING NEW ENERGY TO REGIONAL DEVELOPMENT PLANS
Mar. 1988 129 p In JAPANESE; ENGLISH summary
(DE89-782627; NEDOJ-P-8717) Avail: NTIS (US Sales Only) HC A07/MF A01

This report covers nationwide large-scale resort plans and at the same time studies the possibility of introducing new energy systems, mainly cogeneration, and their effects. Japanese industrial structure is rapidly moving toward information and service areas, and the development of resorts has become very active. With the increase of resort demands, much is expected of resort development as a means of regional promotion. Special features of energy consumption in resort facilities are that annual demand is large, that energy consumption fluctuates greatly, and that energy supply cost is high. These features are especially conspicuous in smaller facilities. Most suited for resort lodging facilities is a co-generation system, especially a diesel engine system. This system is expected to conserve energy; but to promote this system, it is necessary to revise the preferential tax treatment and Fire Service Act to meet the actual circumstances, and to develop a highly reliable system that can be operated unattended. An economical system in view of overall costs is also essential. DOE

N90-19655# Sanders Nuclear Corp., Nashua, NH. Energy Systems Center.
LOW COST BRAYTON ENGINE FOR GAS-FIRED COGENERATION SYSTEM, PHASE 1 Final Report, Apr. - Dec. 1988
James Kesseli and Roger Saunders Aug. 1989 82 p
(Contract GRI-5087-293-1514)
(PB90-127457; GRI-89/0134-Phase-1) Avail: NTIS HC A05/MF A01 CSCL 10B

The turbo generator portion of a 30 kW recuperated Brayton (gas turbine) cycle has been tested. The intended application for this assembly is for a 20 to 40 kWe cogeneration system. Electrical power is generated by a two shaft gas turbine which drives an induction generator through a single stage gearbox. To minimize capital costs required for production and its initial cost, this innovative engine concept utilizes turbocharger components for both the gasifier and power turbine sections. The design and successful test results achieved with the prototype unit are described. When state point measurements are adjusted for the eventual addition of the recuperator, a thermal to electric efficiency of 34 percent (30 percent at HHV) was attained. GRA

N90-19656# Instituto de Pesquisas Espaciais, Sao Jose dos Campos (Brazil).
STUDY OF THE OPTIMIZATION OF REFERENCE PARAMETERS TO THE DYNAMIC CONSTRAINTS OF SOLAR PANELS M.S. Thesis - 1988 [ESTUDO DE OPTIMIZACAO DE PARAMETROS REFERENTES AO COMPORTAMENTO DINAMICO DE PAINEIS SOLARES]
Cassia deAssis Fleury Jan. 1989 94 p
(INPE-4793-TDL/355) Avail: NTIS HC A05/MF A01

A new approach is presented for mass minimization of solar panels used in artificial satellites, considering mechanical strength and dynamical behavioral constraints. The structural dynamics is represented by the first mode vibration frequency of interconnected beam elements linked by torsional springs. The finite element and mass lumped methods are used to discretize the structural model, considering variable configuration during the mission. For a given panel, the optimization problem is reduced to the achievement of the minimal cross-section area along the structure to maintain an imposed frequency, considering geometric and strength constraints. A gradient projection method is used for numerical solution in a digital computer. The procedure is applied to a medium size satellite solar panel. Numerical results are presented and discussed. Author

N90-19657# Department of the Navy, Washington, DC.
PHASE CONTROL MECHANISM FOR WAVE ENERGY CONVERSION Patent
Paul N. Jaenichen, Sr., inventor (to Navy) 10 Oct. 1989 7 p Filed 7 Dec. 1988
(AD-D014354; US-Patent-4,872,309; US-Patent-Appl-SN-280869; US-Patent-Class-60-497) Avail: US Patent and Trademark Office CSCL 10/1

A phase control mechanism for a wave energy conversion apparatus is provided by means of a cam brake locking mechanism. Frictionally contacting locking cams retain a reciprocable drive shaft alternately in upper lower positions with minimal expenditure of electrical power. When the wave crests and troughs have reached

predetermined levels, the cams are released allowing the drive shaft of the mechanism to translate to the opposite position. GRA

N90-19658# JAYCOR, Fremont, CA.
TOPICS IN HPM (HIGH-POWER MICROWAVE) GENERATION, COUPLING, AND INTERACTION Technical Report, 1 Sep. 1983 - 1 Feb. 1986
Kendall F. Casey 1 Jan. 1990 184 p
(Contract DNA001-86-C-0003)
(AD-A216882; DNA-TR-89-108) Avail: NTIS HC A09/MF A01 CSCL 20/14

A collection is presented of technical notes on various aspects of high power microwave (HPM) generation, coupling, and interaction. Time and resources did not permit either as detailed an editing job would have been desirable, or recalculation and plotting of the numerical results in a more elegant form. It is to be hoped, however, that this integrated document will prove useful to the community. The selection of topics addressed in the Microwave Notes was influenced by questions which arose at various stages of the author's involvement in HPM-related activities. The subject of pulse radiation from aperture antennas subject to turn-on time errors, for example, arose in the context of a proposed HPM generation scheme. Consideration of the scattering cross-section of a simple dipole and of its dual problem, the effective area of a thin slot, was motivated by the need to understand the penetration of such slot apertures by HPM pulses. GRA

N90-19659# Argonne National Lab., IL. Energy Systems Div.
EXPERIMENTAL INVESTIGATION OF CONDENSATION OF STEAM IN THE PRESENCE OF NONCONDENSABLE GASES USING PLATE HEAT EXCHANGERS
C. B. Panchal 1990 15 p Presented at the 2nd International Symposium on Condensers and Condensation, Bath, England, 28-30 Mar. 1990
(Contract W-31-109-eng-38)
(DE90-002251; CONF-900339-1) Avail: NTIS HC A03/MF A01

An experimental investigation was carried out to determine the overall performance of a parallel-plate condenser for the Open-Cycle Ocean Thermal Energy Conversion power system. In this paper, the experimental results are analyzed and compared with theoretical predictions. In the experimental study, the warm surface seawater was flash evaporated, and the resulting steam was condensed in a plate-and-shell heat exchanger with deep-ocean cold water used as coolant. The theoretical analysis includes the local calculation of mass and heat fluxes and a two-dimensional integration of heat- and mass-balance equations. Appropriate boundary conditions are applied for determination of the inlet steam distribution in the direction of water flow. The predicted rate of condensation is compared with the experimentally measured values; total condensation and from three individual sections along the condenser length. DOE

N90-19660# Midwest Research Inst., Golden, CO. Solar Energy Research Inst.
SOLID STATE PHOTOVOLTAIC RESEARCH BRANCH Annual Report, FY 1988
Jul. 1989 265 p
(Contract DE-AC02-83CH-10093)
(DE89-009463; SERI/PR-212-3494) Avail: NTIS HC A12/MF A02

This report summarizes the progress of the Solid State Photovoltaic Research Branch of the Solar Energy Research Institute (SERI) from October 1, 1987, through September 30, 1988. Six technical sections cover the main areas of SERI's in-house solid state photovoltaic research: Semiconductor Crystal Growth, Amorphous Silicon Research, Polycrystalline Thin Films, III-V High-Efficiency Photovoltaic Cells, Solid State Theory, and Laser Raman and Photoluminescence Spectroscopy. Principal achievements and experimental details of current work are covered in each section. Each section was written by the group leader principally in charge of the work. The task in each case was to explain the purpose and major accomplishments of the branch's work in the context of the U.S. Department of Energy's National Photovoltaic Research Program plans. DOE

N90-19661 Deutscher Wetterdienst, Offenbach am Main (Germany, F.R.).
PYRANOMETRY [PYRANOMETRIE]
Klaus Dehne and Reinhard Trapp 1987 27 p In GERMAN
(Contract BMFT-03E8543A/4)
(DWD-14; ETN-90-94422) Avail: Deutscher Wetterdienst, Meteorologisches Observatorium Hamburg, Frahmredder 95, 2000 Hamburg 65. Fed. Republic of Germany

Pyranometric investigations were performed in the framework of the International Energy Agency, Solar Radiation and Pyranometry Studies. For several pyranometer types the dependence of the measurement sensitivity on the angle of incidence, the so-called cosinus and azimuth error, was determined. Using black body radiation the influence of thermal radiation and thermal shocks on the measurement sensitivity of pyranometers with and without ventilation was determined and represented as a zero shift. Aging tests were conducted using UV radiation. Using pyroheliometers the influence of the circumsolar radiation on the measurement sensitivity was calculated as a function of the angle of view and the angle of slope, in order to estimate the accuracy of the pyranometer calibration. ESA

N90-19662# Technische Univ., Berlin (Germany, F.R.). Inst. fuer Luft- und Raumfahrt.
CONSTRUCTIBILITY LIMITS OF MULTIFLOW WIND TURBINES WITH PIVOTS Final Report [GRENZEN DER BAUBARKEIT VON MEHRFLUEGLIGEN WINDTURBINEN MIT INDIVIDUELLEM SCHLAGGELENK]
Joerg Maurer 1988 203 p In GERMAN
(Contract ERP-2565)
(ILR-Mitt-215; ETN-90-95354) Avail: NTIS HC A10/MF A02

If windmill wings are rigidly fixed to the hub, strong torques due to the windforce appear. The wing is bent by a conic angle, that requires much lighter wings. Tests in laboratory prove that for a rotor diameter of 3.5 to 7 m, it is possible to use wings of a five or three times lower weight. In this study, the feasibility of suitable wings for the higher than 15 m real diameters is discussed from a theoretical and economic point of a view. The maximum strength on the rotors appear on stopping and braking with extreme wind velocity. Wing mass increases very quickly with the rotor diameter. The first eigenfrequency increases almost linearly with the turn number. Higher eigen frequencies are very rarely dependent on turn number. With very high wind velocities, negative air force damping brings about oscillations where amplitudes does not depend on wing size. ESA

N90-19663# Deutsche Forschungs- und Versuchsanstalt fuer Luft- und Raumfahrt, Stuttgart (Germany, F.R.). Inst. fuer Technische Thermodynamik.
SOLAR AND THERMIC UTILIZATION IN HIGH TEMPERATURE AREA: RESEARCH AND DEVELOPMENT Ph.D. Thesis [FORSCHUNGS- UND ENTWICKLUNGSPROGRAMM ZUR SOLARTHERMISCHEN NUTZUNG IM HOCHTEMPERATURBEREICH]
Rainer Koehne Mar. 1988 42 p In GERMAN
(Contract DFVLR-FV-0328617-A)
(ETN-90-96062) Avail: NTIS HC A03/MF A01

The physical problems of the direct coupling of highly concentrated solar radiation in the matter are investigated, without taking into account the heat exchanger walls. Some chemical processes for the longterm stocking of solar energy are examined as well as the necessary receiver technologies for high temperature utilizations. A Sun simulator with a radiation power of around 1.1 kW was built with a membrane parabolised mirror of varying radiation power in the interval 25 to 120 kW. Alkaline Earth hydroxides in ceramic radial structures seem to be appropriate as accumulators for mean temperature areas around 500 C. First simulation calculations show that the catalytic gas reaction of the methane reform seems to be a good example reaction for a solar

chemical long term accumulation. According to the simulation calculations, the mechanical stresses, that appear because of the high temperature gradients, seem tolerable for the tested Si-C fiber receiver. ESA

N90-19664# Sandia National Labs., Albuquerque, NM.
MEASURING FLOW PROPERTIES OF WICKS FOR HEAT PIPE SOLAR RECEIVERS
Douglas R. Adkins and Timothy Moss 1990 12 p Presented at the ASME International Solar Energy Conference, Miami, FL, 1-4 Apr. 1990
(Contract DE-AC04-76DP-00789)
(DE89-016537; SAND-89-1582C; CONF-900449-1) Avail: NTIS HC A03/MF A01

A program is currently under way to develop liquid-metal heat pipes that can transfer energy from the focal point of a parabolic solar concentrator to the heater tubes of one or more Stirling engines. To design high performance wicks for heat-pipe solar receivers, it is necessary to have an accurate assessment of the wick's properties. Procedures for measuring the flow properties of wicks before and after fabrication processes take place are presented in this paper. These testing procedures provide a useful method of determining the validity of a wick design before full-scale testing is attempted. DOE

N90-19665# Midwest Research Inst., Golden, CO. Solar Energy Research Inst.
RADIATIVE TRANSPORT MODELS FOR SOLAR THERMAL RECEIVER/REACTORS
Mark S. Bohn and Mark S. Mehos Dec. 1989 8 p Presented at the ASME International Solar Energy Conference, Miami, FL, 1-4 Apr. 1990
(Contract DE-AC02-83CH-10093)
(DE90-000303; SERI/TP-253-3614; CONF-900449-7) Avail: NTIS HC A02/MF A01

Modeling the behavior of solar-driven chemical reactors requires detailed knowledge of the absorbed solar flux throughout the calculation domain. Radiative transport models, which determine the radiative intensity field and absorbed solar flux, are discussed in this paper with special attention given to particular needs for the application of solar thermal receiver/reactors. The geometry of interest is an axisymmetric cylinder with a specified intensity field at one end, diffuse reflection at boundaries, and containing a participating medium. Participating media are of interest because receiver/reactors are expected to have one or more zones containing small particles or monoliths acting as absorbers or catalyst supports, either of which will absorb, emit, and scatter radiation. A general discussion of modeling techniques is given, followed by a more complete discussion of three models -- the two-flux, discrete ordinate, and the Monte Carlo methods. The methods are compared with published benchmark solutions for simplified geometries -- the infinite cylinder and plane slab -- and for geometries more closely related to receiver/reactors. Conclusions are drawn regarding the applicability of the techniques to general receiver/reactor models considering accuracy, ease of implementation, ease of interfacing with solution techniques for the other conservation equations, and numerical efficiency. DOE

N90-19666# Midwest Research Inst., Golden, CO. Solar Energy Research Inst.
EXPERIMENTS ON OXYGEN DESORPTION FROM SURFACE WARM SEAWATER UNDER OPEN-CYCLE OCEAN THERMAL ENERGY CONVERSION (OC-OTEC) CONDITIONS
Ahmad A. Pesaran Dec. 1989 8 p Presented at the ASME International Solar Energy Conference, Miami, FL, 1-4 Apr. 1990
(Contract DE-AC02-83CH-10093)
(DE90-000308; SERI/TP-254-3619; CONF-900449-8) Avail: NTIS HC A02/MF A01

This paper reports the results of scoping deaeration experiments conducted with warm surface seawater under open-cycle ocean thermal energy conversion (OC-OTEC). Concentrations of dissolved oxygen in seawater at three locations (in the supply water, water leaving a predeaerator, and discharge water from an evaporator) were measured and used to estimate oxygen desorption levels. The results suggest that 7 pct to 60 pct of dissolved oxygen in the supply water was desorbed from seawater in the predeaerator for pressures ranging from 9 to 35 kPa. Bubble injection in the upcomer increased the oxygen desorption rate by 20 pct to 60 pct. The dependence of oxygen desorption with flow rate could not be determined. The data also indicated that at typical OC-OTEC evaporator pressures when flashing occurred, 75 pct to 95 pct of dissolved oxygen was desorbed overall from the warm seawater. The uncertainty in results is larger than one would desire. These uncertainties are attributed to the uncertainties and difficulties in the dissolved oxygen measurements. Methods to improve the measurements for future gas desorption studies for warm surface and cold deep seawater under OC-OTEC conditions are recommended. DOE

N90-19667# Midwest Research Inst., Golden, CO. Solar Energy Research Inst.
DIRECT ABSORPTION RECEIVER
Mark S. Bohn and Meir Carasso Dec. 1989 124 p
(Contract DE-AC02-83CH-10093)
(DE90-000311; SERI/TR-253-3438) Avail: NTIS HC A06/MF A01

This report describes research on several technical issues associated with the molten-salt direct absorption receiver concept. In particular, we consider the hydrodynamic stability of a long, liquid film, the ejection of droplets from the film, the convective and radiative heat-transfer mechanisms within the film and between the film and the support surface, and the stability of the liquid film with respect to thermocapillary breakdown in the presence of high flux and temperature gradients. The research showed that very small droplets originate from the bursting of turbulent eddies on the liquid surface and larger droplets begin to be ejected where the wave growth begins. The rate of droplet ejection increases exponentially along the flow length. Measuring the convective heat transfer between the nitrate salt film and the support surface showed that very high convective heat-transfer coefficients result, indicating that adding a dopant to darken the salt film may not be needed. These coefficients can be predicted reliably with existing heat-transfer correlations. Using a dimensionless scaling law, we found that the film should not be susceptible to thermocapillary breakdown; however, additional data at high Reynold numbers are needed to verify this. DOE

N90-19668# Westinghouse Electric Corp., Pittsburgh, PA. Advanced Energy Systems Div.
GAS COOLED FUEL CELL SYSTEMS TECHNOLOGY DEVELOPMENT PROGRAM Quarterly Report, Sep. - Nov. 1989
J. M. Feret Dec. 1989 37 p
(Contract DE-AC21-82MC-24223)
(DE90-000446; DOE/MC-24223/2792) Avail: NTIS HC A03/MF A01

This report addresses the fourth logical unit of work of a multiyear program whose overall objective is the development of a gas-cooled phosphoric acid fuel cell (PAFC) for electric utility power plant application. This PAFC Technology Development Program continuation is structured to build upon the current cell technology baseline so as to advance critical component technologies to meet the performance, endurance, reliability and cost goals associated with successful energy service. Progress is described. DOE

N90-19669# Sandia National Labs., Albuquerque, NM.
STATUS OF STRETCHED-MEMBRANE HELIOSTATS
D. J. Alpert, R. M. Houser, and A. A. Heckes 1990 13 p Presented at the ASME International Solar Energy Conference, Miami, FL, 1-4 Apr. 1990
(Contract DE-AC04-76DP-00789)
(DE90-000801; SAND-89-1500C; CONF-900449-2) Avail: NTIS HC A03/MF A01

Since the early 1980s, Sandia National Laboratories has been developing stretched-membrane heliostats for solar central receiver

power plants. They differ from conventional glass-mirror heliostats in that the optical surface is a stretched membrane -- a thin metal foil stretched over both sides of a large diameter ring. The reflective surface is provided by either a silvered-acrylic film or thin glass mirrors attached to the front membrane. Heliostats with single 14 m diameter (150 sq meter) stretched-membrane reflectors have been designed. Because of their simplicity and light weight, stretched-membrane heliostats are expected to cost up to one-third less than conventional glass-mirror designs. Two generations of 50 sq meter prototype stretched-membrane mirror modules have been built and evaluated at Sandia's Central Receiver Test Facility in Albuquerque, NM. They demonstrated that the optical performance of membrane heliostats rivals that of glass-mirror heliostats. The durability of the silvered-acrylic reflective film has improved so that a lifetime of at least 5 years is likely; methods of replacing the film in the field are being investigated. Sandia recently initiated the final phase of development: the design of fully integrated, market-ready heliostats. Field tests of these heliostats are planned to begin in FY90. DOE

N90-19670# Sandia National Labs., Albuquerque, NM.
EVALUATION OF THERMAL CYCLING CREEP-FATIGUE DAMAGE FOR A MOLTEN SALT RECEIVER
James W. Grossman, Wendell B. Jones, and Paul S. Veers 1990 13 p Presented at the ASME International Solar Energy Conference, Miami, FL, 1-4 Apr. 1990
(Contract DE-AC04-76DP-00789)
(DE90-002907; SAND-89-2360C; CONF-900449-3) Avail: NTIS HC A03/MF A01

A molten salt cavity receiver was solar tested at Sandia National Laboratories during a year-long test program. Upon completion of testing, an analysis was performed to determine the effect of thermal cycling on the receiver. The results indicate a substantial fatigue damage accumulation for the receiver when the relatively short test time is considered. This paper describes the methodology used to analyze the cycling, the results as they pertain to this receiver, and how they affect future receiver design. DOE

N90-19671# Sandia National Labs., Albuquerque, NM.
TEST RESULTS FROM A FULL-SCALE SODIUM REFLUX POOL-BOILER SOLAR RECEIVER
J. B. Moreno, C. E. Andraka, R. B. Diver, W. C. Ginn, V. Dudley, and K. S. Rawlinson 1990 8 p Presented at the ASME International Solar Energy Conference, Miami, FL, 1-4 Apr. 1990
(Contract DE-AC04-76DP-00789)
(DE90-003577; SAND-89-2772C; CONF-900449-4) Avail: NTIS HC A02/MF A01

A sodium reflux pool-boiler solar receiver has been tested on a nominal 75 kW sub t parabolic-dish concentrator. The purpose was to demonstrate the feasibility of reflux-receiver technology for application to Stirling-engine dish-electric systems. In this application, pool boilers (and more generally liquid-metal reflux receivers) have a number of advantages over directly-illuminated tube receivers. The advantages, to be discussed, include more uniform temperature, which results in longer lifetime and higher temperature available to the engine. DOE

N90-19419*# Alabama Univ., Huntsville. Dept. of Mechanical Engineering.
FREQUENCY RESPONSE OF ELECTROCHEMICAL CELLS
Daniel L. Thomas *In its* Research Reports: 1989 NASA/ASEE Summer Faculty Fellowship Program Dec. 1989 23 p (For primary document see N90-19390 12-31)
(Grant NGT-01-008-021)
Avail: NTIS HC A99/MF E06 CSCL 10A

45 ENVIRONMENT POLLUTION

Includes atmospheric, noise, thermal, and water pollution.

N90-19672# National Aerospace Lab., Amsterdam (Netherlands). Informatics Div.
REAL TIME ENVIRONMENT MONITORING USING DATA FROM METEOSAT AND NOAA IMAGING SATELLITES
H. A. vanIngenSchenau and J. C. Venema 5 Oct. 1987 9 p Presented at the SPIE Symposium on Digital Image Processing and Visual Communications Technologies in Meteorology, Cambridge, MA, 27-28 Oct. 1987 Previously announced in IAA as A89-11730 Sponsored by the Food and Agriculture Organization of the United Nations, Rome, Italy and The Netherlands Ministry of Foreign Affairs/International Development Cooperation
(NLR-MP-87070-U; ETN-89-94044) Avail: NTIS HC A02/MF A01

An operational remote sensing system which supports environment monitoring using the multi sensor - multi temporal data acquired by the geostationary and polar orbiting weather satellites is described. The information derived from the satellite images are maps on a continental scale with data on the estimated rainfall, the vegetation index (NDVI), and for experimental use, with data on the soil water available for crops. The operational system, called ARTEMIS, meets the information requirements of the FAO monitoring programs in the areas of food and feed security and plant protection. ESA

N90-19673# Pacific Northwest Lab., Richland, WA.
A PRELIMINARY ANALYSIS OF US CO2 EMISSIONS REDUCTION POTENTIAL FROM ENERGY CONSERVATION AND THE SUBSTITUTION OF NATURAL GAS FOR COAL IN THE PERIOD TO 2010
J. A. Edmonds, W. B. Ashton, H. C. Cheng, and M. Steinberg (Brookhaven National Lab., Upton, NY.) Feb. 1989 63 p
(Contract DE-AC06-76RL-01830)
(DOE/NBB-0085; TR045) Avail: NTIS HC A04/MF A01

The U.S. Department of Energy (DOE) Carbon Dioxide Research Division (CDRD) sponsored research to do a preliminary assessment of the technical feasibility and consequences of reducing U.S. CO2 emissions from 1985 levels by 10, 25 or 50 percent by either the year 1995 or 2010. In addition, DOE/CDRD sponsored a day-long roundtable attended by nine experts in the field to discuss this issue. Two methods of CO2 emissions reduction were considered: energy intensity reductions (conservation), and substitution of natural gas for coal. The study did not address the contribution of other energy supply options or the feasibility of pre- or post-combustion CO2 removal. Furthermore, the study made no attempt to explore specific policies that might be employed to achieve technically feasible CO2 emissions reductions. Six assessment tasks were performed. After a reference forecast was developed from NEPP, CO2 emissions reduction targets were established based on 1985 emissions rates. Conservation potential studies were then examined to see what energy and conservation efficiency improvements are feasible at current and anticipated energy technologies and prices. The potential for CO2 emissions reductions through the substitution of natural gas for coal was studied by examining potential natural gas availability, new natural gas electric power generation technologies, and the cost of coal and natural gas as industrial fuels. Author

N90-19674# Oregon State Univ., Corvallis. Global Climate Change Research Team.
SENSITIVITY OF ECOLOGICAL LANDSCAPES AND REGIONS TO GLOBAL CLIMATIC CHANGE
Ronald P. Neilson, George A. King, Robert L. DeVelice, James Lenihan, Danny Marks, Jayne Dolph, Bill Campbell, and Gail Glick (NSI Technology Services Corp., Corvallis, OR.) Sep. 1989 193 p
(Contract EPA-68-C8-0006)
(PB90-120072; EPA/600/3-89/073) Avail: NTIS HC A09/MF A01 CSCL 13B

Increasing awareness of the potential impacts from global climatic change has elicited a storm of research planning among all the major federal agencies. One of the primary difficulties confronted in the planning effort is the need to objectively define clear priorities for research dollars. The report is an attempt to contribute to the process of defining those priorities by scientifically defining specific regions, ecological systems and attributes of those systems that might be particularly sensitive to climate change. Two approaches to addressing sensitivity have been defined, intrinsic sensitivity and sensitivity relative to a particular stressor. Intrinsic sensitivity is gauged by past variations in different ecosystems. Extrinsic or stressor relative sensitivity addressed the same question, but from the perspective of a particular stress.
GRA

N90-19675# California Univ., Davis. Dept. of Land, Air, and Water Resources.
TRANSPORT OF ATMOSPHERIC AEROSOLS ABOVE THE SIERRA NEVADA SLOPES Final Report, 1985 - 1986
L. O. Myrup, R. G. Flocchini, and Diane Ewell 15 Jan. 1989 324 p
(Contract ARB-A4-127-32)
(PB90-120288; ARB-R-89/417) Avail: NTIS HC A14/MF A02 CSCL 13B

This program documented the boundary-layer transport of aerosol pollution into Sequoia National Park. Four measurement programs were carried out: (1) tethersonde profiles of temperature, humidity, and wind velocity; (2) tethered balloon measurements of aerosol concentrations; (3) pibal wind measurements at three sites in the park; and (4) measurement of surface meteorological parameters at the pibal wind sites. Data was collected during July and August 1985 at Emerald Lake, Wolverton Meadow, and Ash Mountain. Conclusions are: (1) when averaged over the entire measurement period the concentration of all fine particles is higher in upslope flows than otherwise; (2) the fluxes of most elements also exhibit similar behavior; (3) the concentrations of certain course particle elements show a strong tendency to increase with height in the lower 200 m during the nighttime hours; (4) the potential for smog front phenomena seems to exist in the lower regions of the park, due to convergence in the mesoscale wind field; and (5) the upslope/downslope boundary layer, mesoscale, and large scale winds seem to interact in a complex fashion to produce the observed transport.
GRA

N90-19676# Central Research Inst. of Electric Power Industry, Tokyo (Japan). Energy and Environment Lab.
DEVELOPMENT OF AN ATMOSPHERIC DIFFUSION MODEL IN FOG (1). LITERATURE REVIEW OF SCAVENGING PROCESS BY PRECIPITATION
Hisayuki Kato, Shinichi Fujita, and Sakae Nishinomiya Aug. 1988 40 p In JAPANESE; ENGLISH summary
(DE89-782318; CRIE-T-87104) Avail: NTIS (US Sales Only) HC A03/MF A01

In prediction of diffusion/deposition of pollutants, it is necessary to evaluate the degree of effect of fog besides precipitation, snowfall. In order to clarify the fog effects on diffusion/deposition of pollutants quantitatively, a literature survey was taken about precipitation scavenging. General ideas, theories, and experimental and observational data required for the diffusion/deposition model in fog were collected through the review and discussed. Results of the work are: Fog effects, on diffusion/deposition of pollutants required in the model, were clarified qualitatively; Removed mechanism of pollutants by precipitation elements, which is a skeleton of the diffusion model in fog, are shown in flow charts. (It was clarified that five scavenging coefficients, which determine the quantities of gaseous material/particulate matters collected by fog droplets and rain droplets, were required in the model); and The order of these scavenging coefficients were determined based on the theories and the observational data.
DOE

N90-19677# Central Research Inst. of Electric Power Industry, Tokyo (Japan). Energy and Environment Lab.
CHEMICAL COMPOSITION OF PRECIPITATION AND WET/DRY DEPOSITION OF SULFUR COMPOUNDS AROUND THE COASTAL AREA
Shinichi Fujita Sep. 1988 21 p In JAPANESE; ENGLISH summary
(DE89-782324; CRIE-T-87103) Avail: NTIS (US Sales Only) HC A03/MF A01

Precipitation, gas and particles were observed at coastal region of Western Kyushu district from June 1986 to May 1987. These compositions were analyzed for sulfur compounds. Mean concentration of ex SO4(-2) (excess nonmaritine sulfate) in precipitation was 32 micro eq/L. Although precipitation amount in the cold season is only 29 percent of annual amount, wet deposition of SO4(2-) (precipitation amount* concentration) was 54 percent of annual amount. Dry and wet deposition rate was larger than emission rate in this area, indicating that inflow amount from outside cannot be neglected. Strong northern wind component is excellent in upper air. Washout ratio of SO4(2-) (concentration in precipitation/concentration in air) indicates higher value in the cold season and was inversely proportional to the 1/3 power of precipitation amount. Supposing that washout mechanism of sulfur compounds is combined with the cloud process, higher concentration of SO4(2-) in the cold season is related to two mechanisms of the increase of washout rate in cloud and transport by northwesterly wind.
DOE

N90-19678# Northeastern Forest Experiment Station, Broomall, PA. Publications Group.
PROCEEDINGS OF THE 2ND UNITED STATES/USSR SYMPOSIUM ON AIR POLLUTION EFFECTS ON VEGETATION INCLUDING FOREST ECOSYSTEMS Final Report
Reginald D. Noble, ed., Juri L. Martin, ed., and Keith F. Jensen, ed. (Forest Service, Delaware, OH.) 1989 319 p Symposium held in Raleigh, NC; Corvallis, OR; and Gatlinburg, TN, 13-25 Sep. 1988 Sponsored by EPA; Forest Service; ORNL; Bowling Green State Univ.; Oregon State Univ.; National Council of the Paper Industry for Air and Stream Improvement; Edward Lamb Foundation; Electric Power Research Inst.; National Park Service and BP America
(PB90-127119; NEFES/89-18) Avail: NTIS HC A14/MF A02 CSCL 13B

To commemorate the 10th year of cooperation between the US-USSR in the field of environmental protection, a symposium was organized, the major objectives of which were to acquaint US-USSR scientists with project accomplishments; to promote understanding of the nature of environmental problems that relate to air pollution effect on vegetation on a more global scale; to share research priorities, interests, and methodologies; and to plan future research cooperation.
GRA

N90-19679# Alliance Technologies Corp., Bedford, MA.
NAPAP (NATIONAL ACID PRECIPITATION ASSESSMENT PROGRAM) EMISSIONS INVENTORY: OVERVIEW OF ALLOCATION FACTORS, 1985 Final Report, Nov. 1988 - Jun. 1989
Robert A. Walters, Lysa G. Modica, and David B. Fratt Oct. 1989 111 p Sponsored in part by Energy Engineering Research Lab. and National Acid Precipitation Assessment Program, Washington, DC
(Contracts EPA-68-02-4274; EPA-68-02-4396)
(PB90-126012; EPA/600/7-89/010A) Avail: NTIS HC A06/MF A01 CSCL 13B

The development of temporal, spatial, and species allocation factors for the 1985 National Acid Precipitation Assessment Program (NAPAP) anthropogenic point and area source emissions inventories is discussed. These allocation factors are used to apportion annual emissions totals into gridded, hourly, speciated emissions estimates suitable for use as input to atmospheric transport models such as the Regional Acid Deposition Model. The temporal, spatial, and species allocation factors are discussed in detail in separate report sections. Each section contains a

description of the methodology for application of the factors, a discussion of data sources, and documentation of the activities undertaken to create the allocation factor data sets used in the 1985 NAPAP resolved modeling inventories. GRA

N90-19680# Cologne Univ. (Germany, F.R.). Inst. fuer Geophysik und Meteorologie.
THE EURAD MODEL: STRUCTURE AND FIRST RESULTS [DAS EURAD-MODELL: AUFBAU UND ERSTE ERGEBNISSE]
A. Ebel, ed., F. M. Neubauer, ed., E. Raschke, ed., and P. Speth, ed. 1989 168 p In ENGLISH and GERMAN Conference held in Cologne, Fed. Republic of Germany, 20-21 Feb. 1989
(Rept-61; ISSN-0069-5882; ETN-90-95335) Avail: NTIS HC A08/MF A01

Several aspects of the development and the use of the European Acid Deposition (EURAD) model for the simulation of the far transfer of atmosphere tracers are investigated: development and status of the EURAD project concerning the gas phase chemical mechanism; simulation of the radioactive substances of Chernobyl (USSR) diffusion for spray effects; cloud parameterization in EURAD; the role of the clouds in the photochemistry of the background troposphere; estimation of the SO2 and NOX emission distribution in Europe; modelization of the dry deposition in the chemistry transfer model of EURAD; implementation of the regional acid deposition model of EURAD on the Juelich calculation system; and simulation of a weather situation with high ozone concentrations. For individual titles, see N90-19681 through N90-19701.

N90-19681# Cologne Univ. (Germany, F.R.).
DEVELOPMENT AND STATUS OF THE EURAD PROJECT [ENTWICKLUNG UND STAND DES EURAD-VORHABENS]
A. Ebel *In its* The EURAD Model: Structure and First Results 1989 p 1-5 In GERMAN (For primary document see N90-19680 12-45)
Avail: NTIS HC A08/MF A01

In the addressing of industrial and chemical emissions which jeopardize air environment, European acid deposition (EURAD) is a model for a realistic digital representation of the far transfer of the polluting agents in the troposphere above Europe. The boundary layer parameterization and the digital processing of the transfer terms in the continuity equations are planned. ESA

N90-19682# Cologne Univ. (Germany, F.R.).
THE MESOSCALE METEOROLOGICAL MODEL MM4 AND ITS MODIFICATIONS FOR EURAD [DAS MESOSKALIGE METEOROLOGISCHE MODELL MM4 UND SEINE MODIFIKATION FUER EURAD]
Hermann J. Jakobs *In its* The EURAD Model: Structure and First Results 1989 p 6-13 In GERMAN (For primary document see N90-19680 12-45)
Avail: NTIS HC A08/MF A01

The universal adaptability of the mesoscale model 4 (MM4) system allows the examination of a number of meteorological situations over all continents. Three different geographic projections can be chosen (Mercator, Lambert, polar stereographic). The different processes are described. The meteorological data of the model can be used for the European acid deposition (EURAD) chemical transport model. ESA

N90-19683# Cologne Univ. (Germany, F.R.).
THE CHEMICAL TRANSFER MODEL (CTM) OF EURAD: DEVELOPMENT STATUS [DAS CHEMIE-TRANSPORT-MODELL (CTM) VON EURAD: STAND DER ENTWICKLUNG]
Heinz Hass *In its* The EURAD Model: Structure and First Results 1989 p 14-24 In GERMAN (For primary document see N90-19680 12-45)
Avail: NTIS HC A08/MF A01

It is a three dimensional mesoscale Euler-model, that includes the physical and chemical processes of formation, transfer and deposition of the tropospheric air pollution. The concentrations of sulfur dioxide, nitrogen oxide, several radicals such as HO and HO2, hydrogen peroxides, and organic peroxides can be obtained. The pyrolysis coefficients are calculated with a radiation transfer model for a clear sky. The integration technique of the continuity equation for the chemical components is presented. ESA

N90-19684# State Univ. of New York, Albany. Atmospheric Sciences Research Center.
THE RADM 2 GAS-PHASE CHEMICAL MECHANISM
William R. Stockwell, Julius S. Chang, and Xiao-Yan Tang *In* Cologne Univ., The EURAD Model: Structure and First Results 1989 p 25-32 (For primary document see N90-19680 12-45)
Avail: NTIS HC A08/MF A01

The regional acid deposition model (RADM) 2 gas phase mechanism includes 63 species in 158 reactions, 14 stable inorganic species, 4 reactive intermediates and 3 meteorological species. The reaction of HO with HO2 was added to the mechanism which is an important termination channel for HOX radicals. Treatment of NO3 chemistry is relatively extensive because of its importance for night time chemistry. Five species of alkanes are included; because the photo-oxidation of alkanes is a very important source of radicals (one quarter of the NO to NO2 conversions result from the oxidation of alkanes). Changes of the concentration of alkanes in an atmospheric mixture can lead to large changes in the HO reactivity on the mixture, alkanes can also react with ozone to produce aldehydes and other very reactive intermediates. They are represented by three surrogate species. Since almost one third of NO-to-NO2 conversions are due to the photo-oxidation of aromatic species from highly polluted regions, the RADM 2 mechanism includes two primary aromatic groups. The chemistry of aldehydes, ketones, dicarbonyl species, and peroxy radicals is included in the mechanism. ESA

N90-19685# Cologne Univ. (Germany, F.R.).
SIMULATION OF THE PROPAGATION OF RADIACTIVE SUBSTANCES FROM THE EXAMPLE OF CHERNOBYL (USSR) [SIMULATION DER AUSBREITUNG RADIOAKTIVER SUBSTANZEN AM BEISPIEL TSCHERNOBYL]
M. Memmesheimer, Heinz Hass, Hermann J. Jakobs, H. Geiss, and Manfred Laube *In its* The EURAD Model: Structure and First Results 1989 p 33-44 In GERMAN (For primary document see N90-19680 12-45)
Avail: NTIS HC A08/MF A01

The radioactive Chernobyl (USSR) contaminants allowed testing of the European acid decomposition (EURAD) model, since they spread above North Europe. The data, as wind, temperature, precipitation and humidity are assumed to be known. As tracer substances Cs-137 and I-131 are chosen, because they are the most responsible for the measured activity. Wet and dry deposition processes are parameterized. The results are in good accordance with the Chernobyl data. ESA

N90-19686# Cologne Univ. (Germany, F.R.).
SIMULATION OF A WEATHER SITUATION WITH HIGH OZONE CONCENTRATIONS DURING ALPEX [SIMULATION EINER WETTERLAGE MIT HOHEN OZONKONZENTRATIONEN WAEHREND ALPEX]
Hermann J. Jakobs *In its* The EURAD Model: Structure and First Results 1989 p 45-50 In GERMAN (For primary document see N90-19680 12-45)
Avail: NTIS HC A08/MF A01

During the Alpex (Alpine experiment), the first calculations with mesoscale model 4 (MM4) on the European integration area were realized in the case of a cyclogenesis in the Gulf of Genoa (Italy). Measurements of ozone concentrations, from a plane or on Earth, are made. The results show that the intrusion of stratospheric air plays a part in the ozone concentration. The representation of the potential vorticity, and the dryness of the air confirm this prognosis. The weak influence of the orography is also established. ESA

N90-19687# Kernforschungsanlage, Juelich (Germany, F.R.). Inst. fuer Chemie 2.
IMPLEMENTATION OF THE RADM/EURAD MODELS ON THE GREAT CALCULATION SYSTEM OF THE JUELICH KFA [IMPLEMENTIERUNG DES RADM/EURAD-MODELLS AUF DEM GROSSRECHNERSYSTEM DER KFA JUELICH]
H. Geiss and Heinz Hass *In* Cologne Univ., The EURAD Model: Structure and First Results 1989 p 51-58 In GERMAN (For primary document see N90-19680 12-45)
Avail: NTIS HC A08/MF A01

Model simulations with complex meteorological prediction models, such as European acid decomposition (EURAD) must be implemented on great calculations systems because of the memory capacity and the calculation times. The computers used and the other machines are described. For regional acid decomposition model (RADM) the emission data must be suited to the model structure; the results of mesoscale model 4 (MM4) must be vertically interpolated and the deposition velocities must be calculated. The difficulties of this implementation are minimal.
ESA

N90-19688# Cologne Univ. (Germany, F.R.).
GEONET 88: CALCULATION CONNECTION SYSTEM CONCEPT FOR THE EURAD PROJECT [GEONET 88: KONZEPT EINES RECHNERVERBUNDSYSTEMS FUER DAS EURAD VORHABEN]
M. Liebchen, A. Oberreuter, and N. Drees *In its* The EURAD Model: Structure and First Results 1989 p 59-66 In GERMAN (For primary document see N90-19680 12-45)
Avail: NTIS HC A08/MF A01

The calculations made for European acid decomposition (EURAD) for the simulation of the atmosphere transfer and the air chemical processes exceed the power limits of the regional calculus center in Cologne, (Germany, F.R.) considering the peripheric memory space, the central memory and the performance. An implementation on a Cray computer was unavoidable. The data for processing is treated. The different materials used are described. Particularly, a file server can make the data available on Ethernet for all users, without prejudice to the performance of a work station.
ESA

N90-19689# Kernforschungsanlage, Juelich (Germany, F.R.). Inst. fuer Chemie 2.
COMPARISON OF A 6-LAYER AND A 15-LAYER VERSION OF THE CHEMICAL TRANSFER MODEL (CTM) [VERGLEICH EINER 6-SCHICHTEN UND EINER 15-SCHICHTEN VERSION DES CHEMIE- UND TRANSPORT-MODELLS (CTM)]
H. Geiss and Heinz Hass *In* Cologne Univ., The EURAD Model: Structure and First Results 1989 p 67-84 In GERMAN (For primary document see N90-19680 12-45)
Avail: NTIS HC A08/MF A01

The calculation velocity is not high enough for the model calculation with high vertical and horizontal resolution to obtain results in justifiable time scales. A reduction of the number of the vertical grid is considered. For experiments of dry and wet deposition of SO2, nitrate or sulfate, a 6-layer version seems to give enough exact results. But if more solid results of photooxidation are required, particularly as regards the measured values interpretation, the utilization of higher resolution model versions seems absolutely necessary.
ESA

N90-19690# Cologne Univ. (Germany, F.R.).
CONTROL OF THE RADM CHEMISTRY MECHANISM OF THE GAS PHASE [ZUR VERIFIKATION DES RADM-CHEMIEMECHANISMUS DER GASPHASE]
Dirk Poppe *In its* The EURAD Model: Structure and First Results 1989 p 85-90 In GERMAN (For primary document see N90-19680 12-45)
Avail: NTIS HC A08/MF A01

An essential part of the chemical transformation of atmospheric pollutants is realized by reactions in the gas phase, because a lot of species are emitted in gaseous form in the atmosphere, by photolysis for example. To explain the properties of such a mechanism, the case of the radical HO is examined, because it is only produced by chemical reaction in the atmosphere, and little dependent on the transfer. All calculations were made for regional acid deposition model (RADM) in a steady-state approximation for the short-life substances, by fixed concentrations for the long-life species. OH is principally produced from the reaction of O(D-1) with H2O and from the ozonoxidation of alkenes; HNO3 is produced by a reaction with NO2; OH initiates the oxidation of a lot of organic and unorganic compounds.
ESA

N90-19691# Cologne Univ. (Germany, F.R.).
ON THE QUESTION OF SPRAY EFFECTS [ZUR FRAGE VON AEROSOLEFFEKTEN]
Andreas Koetz *In its* The EURAD Model: Structure and First Results 1989 p 91-97 In GERMAN (For primary document see N90-19680 12-45)
Avail: NTIS HC A08/MF A01

The Chemistry Transport Model describes the chemical transformation and the transfer of the most important gases of sprays such as NH3, HNO3, H2SO4 and allows examination of the part of the sprays produced by gas reaction in such phenomena as acid rain and smog. The dependence of the number, the surface and the volume of the particles on the diameter is studied. Great particles deposit near the source; the life time of small particles is limited by coagulation; the other particles are moved away from the atmosphere by wet deposition processes. Sprays influence the radiation of the atmosphere directly and indirectly: a direct effect is shown by the turbidity of the atmosphere, an indirect effect is the change of the radiation properties of the clouds.
ESA

N90-19692# Cologne Univ. (Germany, F.R.).
CLOUD PARAMETERIZATION IN EURAD AND ITS FUTURE DEVELOPMENT [WOLKENPARAMETRISIERUNG IN EURAD UND IHRE WEITERENTWICKLUNG]
Manfred Laube *In its* The EURAD Model: Structure and First Results 1989 p 98-107 In GERMAN (For primary document see N90-19680 12-45)
Avail: NTIS HC A08/MF A01

In meteorological prediction models such as EURopean Acid Deposition the role of the latent heat in the total energy is not negligible; for the modelization of the radiation transfer and the chemical transformations, a description of the microphysical state of the clouds is essential. The problem of the cumulus convection must be taken into consideration. In MM4 (mesoscale model 4), the latent heat and the phase transformation of water vapor were considered and the ice fraction of the condensed phase was calculated as a linear function of temperature under 0 C; (under -18 C, the entire cloudwater is frozen). The model gives good results for the SO2 concentration in the air and the vertical layer description of the atmosphere. But the parameterization of the ice in convective clouds is too simplified.
ESA

N90-19693# Cologne Univ. (Germany, F.R.).
VALIDATION OF THE EURAD CLOUD MODULES [ZUR VALIDATION DES EURAD-WOLKEN-MODULS]
Nicole Moelders *In its* The EURAD Model: Structure and First Results 1989 p 108-116 In GERMAN (For primary document see N90-19680 12-45)
Avail: NTIS HC A08/MF A01

The EURAD Model has three clouds modules, the capabilities of which were tested by three simulation experiments, in the case of the Chernobyl (USSR) accident. The maps of the clouded cover and the precipitation predictions are compared. The NOAA module uses a radiometer that measures the solar and terrestrial radiation. The different spectral properties allow a multispectral representation of the clouds and therefore the possibility to distinguish ice and water clouds. These comparisons show the exactness of the parameterization of convective processes and the cloud water distribution but underline the bad results for the humidity. The satellite data and the precipitation observation must be taken into account for a better parameterization of the clouds.
ESA

N90-19694# Max-Planck-Inst. fuer Chemie, Mainz (Germany, F.R.).
THE ROLE OF CLOUDS IN THE PHOTOCHEMISTRY OF THE BACKGROUND TROPOSPHERE
J. Lelieveld *In* Cologne Univ., The EURAD Model: Structure and First Results 1989 p 117-120 (For primary document see N90-19680 12-45)
Avail: NTIS HC A08/MF A01

Photochemical processes in air parcel are drastically altered once the air parcel is in a cloud. After dissolution in a drop, CH2O immediately forms CH2(OH)2 which reacts rapidly with aqueous-phase OH radicals. This reaction is a source of formic acid in the atmosphere, whose concentration is however limited by the oxidation by OH in the droplets. These reactions produce HO2, dissociated into H(+) and O2(-). This ion can react with dissolved O3, which produces OH again, which is recycled through aqueous-phase chemistry and reacts with the hydrated form of formaldehyde again. The global scale effect of cloud chemistry on the concentration of CH2O may be a reduction by several tens of percent. The global average production rate of CO through oxidation of CH2O in the lower atmosphere is decreased also by several tens of percent. Similar results are obtained regarding the production of H2. An important reaction in the cloudless atmosphere is the reaction of HO2 with NO, which leads to the formation of NO2 and O3. In clouds, HO2 is largely dissolved in the aqueous-phase and can form H2O2. ESA

N90-19695# Cologne Univ. (Germany, F.R.).
INITIALIZATION OF EURAD. PART 1: UTILIZATION OF ECMWF ANALYSIS DATA [ZUR INITIALISIERUNG VON EURAD. TEIL 1: VERWENDUNG VON ECMWF-ANALYSEDATEN]
M. Stendel *In its* The EURAD Model: Structure and First Results 1989 p 121-128 In GERMAN (For primary document see N90-19680 12-45)
Avail: NTIS HC A08/MF A01

The utilization of European Center for Medium Range Weather Forecast analysis data for the initialization of EURopean Acid Decomposition is discussed. For the interpolation of the irregularity distributed observations, several digital analysis processes exist and give a good approximation of the data, but if an initial value is necessary for prognostic variables in a prediction model, unrealistic oscillations of high frequency and great magnitude appear for short periods. To control these waves, the analyses must be initialized, by means of the model equations linearization; but the better results are obtained with a nonlinear initialization, that allows a realistic representation of orographic induced vertical moves. But the process of a nonlinear initialization does not always converge, for instance in the case of nonadiabatic, convective processes. ESA

N90-19696# Cologne Univ. (Germany, F.R.).
INITIALIZATION OF EURAD, PART 2 [ZUR INITIALISIERUNG VON EURAD, TEIL 2]
Heribert Petry *In its* The EURAD Model: Structure and First Results 1989 p 129-133 In GERMAN (For primary document see N90-19680 12-45)
Avail: NTIS HC A08/MF A01

For the initialization of the EURopean Acid Decomposition model, an objective analysis and an assimilation of the data remain real problems. A weighting function is chosen to take into account the mesoscale properties of the wind and the relative humidity. A vertical profile for every tracer gas in pure air is proposed. The model uncertainty, principally caused by errors in the input data, is estimated. The error margin stays lower than 25 percent. ESA

N90-19697# Cologne Univ. (Germany, F.R.).
BOUNDARY LAYER PARAMETERIZATION IN CTM AND MM4 [GRENZSCHICHTPARAMETRISIERUNG IN CTM UND MM4]
Annette Muenzenberg *In its* The EURAD Model: Structure and First Results 1989 p 134-141 In GERMAN (For primary document see N90-19680 12-45)
Avail: NTIS HC A08/MF A01

For boundary layer parameterization in Chemical Transfer Model and Mesoscale Model 4, underscale turbulent exchange processes are studied from the point of view of the covariance terms that appear in the hydrodynamic fundamental equations. The specific heat by constant pressure, the latent heat, the turbulence and the free or forced convection are considered. The parameters are the Richardson number and the altitudes. Description of a particle-flux by a gradient is addressed. Some results were obtained in the case of the Chernobyl (USSR) accident, for CS-137; a map of the contaminant concentration was realized. ESA

N90-19698# Cologne Univ. (Germany, F.R.).
MODELIZATION OF DRY DEPOSITION IN THE CHEMICAL TRANSPORT MODEL (CTM) OF EURAD [DIE MODELLIERUNG DER TROCKENEN DEPOSITION IM CHEMIE-TRANSPORT-MODELL (CTM) VON EURAD]
Heinz Hass *In its* The EURAD Model: Structure and First Results 1989 p 142-146 In GERMAN (For primary document see N90-19680 12-45)
Avail: NTIS HC A08/MF A01

The dry deposition of particles is investigated in the EURopean Acid Decomposition model. The deposition velocity describes the transfer process efficiency and is a function of the aerodynamic drag and of the resistance in the contact surface between air and ground, estimated by molecular diffusion. Deposition velocities of SO2, SO4, HNO3, O3 are calculated. Above water, a strong dependence on the wind velocity is observed, with weak time variations. HNO3 deposition velocity is influenced by the meteorological situations. In the case of SO4 there is a correlation with the thermic stratification. The values calculated for CTM remain in the area of the measured values. ESA

N90-19699# Kernforschungsanlage, Juelich (Germany, F.R.).
ESTIMATION OF THE DISTRIBUTION OF SO2 AND NOX EMISSION IN EUROPE [ABSCHAETZUNG DER VERTEILUNG DER SO2- UND NOX-EMISSION IN EUROPA]
Christian Holzapfel *In* Cologne Univ., The EURAD Model: Structure and First Results 1989 p 147-152 In GERMAN (For primary document see N90-19680 12-45)
Avail: NTIS HC A08/MF A01

To calculate acid precipitations and ozone concentrations it is necessary to know the hourly emission of SO2, NOX, NH3 and CO. The emission is assumed to be proportional to the population, and the people density is constant in a given state. The towns are first taken into account and their geographic coordinates must be calculated and integrated into the model grid. The comparison with the known data and the calculated values shows an underestimation of NO2 emission and an overevaluation of SO2 emission. ESA

N90-19700# Cologne Univ. (Germany, F.R.).
EMISSION DATA FOR THE EURAD PROJECT [EMISSIONSDATEI FUER DAS EURAD-VORHABEN]
M. Memmesheimer and M. Liebchen *In its* The EURAD Model: Structure and First Results 1989 p 153-158 In GERMAN (For primary document see N90-19680 12-45)
Avail: NTIS HC A08/MF A01

The EURopean Acid Decomposition model resolves the pronostic equations for the chemical elements on a spatial grid to time with an horizontal breadth of 80 km. Vertically it is worked with 15 layers. Emission from surface and line sources go to the lower layer. By point sources an effective emission height is calculated, that depends on the source parameters (temperature of the gas for instance) and the meteorological conditions (wind velocity, stability) and of the season. The species (SO2, SO4, CO, NO, NO2, NH3, CO) are taken into account, just as volatile organic compounds, that are classified in ethane, alkanes, ethene, propene, butene, toluol, xycol, formaldehyde, acetaldehyde and high aldehydes. The observations show the necessity of a European emission chart. ESA

N90-19701# Cologne Univ. (Germany, F.R.).
THE EURAD MODEL IN EUROTRAC [DAS EURAD-MODELL IN EUROTRAC]
A. Ebel *In its* The EURAD Model: Structure and First Results 1989 p 159-161 In GERMAN (For primary document see N90-19680 12-45)
Avail: NTIS HC A08/MF A01

European experiment on Transport and Transformation of Environmentally Relevant Trace Constituents in the Troposphere over Europe (EUROTRAC) is a EUREKA project, whose aim is to examine the tropospheric ozone and its evolution by human activities, the acid rain and some multiphase processes in the atmosphere, and the biospheric-atmospheric effects of emitted pollutants. EURAD (European acid decomposition) is a contribution to EUROTRAC; which is divided into several modules, such as EUMAC (European modeling of atmospheric constituents), whose purpose is the simulation of transport, chemical transformation and deposition of air contaminants in the atmosphere above Europe, the development of the model and its validation. ESA

N90-19702# Heidelberg Univ. (Germany, F.R.). Naturwissenschaftlich-Mathematischen Gesamtfakultaet.
SIMULATION OF GLOBAL Kr-85 AND (14)CO2 DISTRIBUTION BY MEANS OF A TIME-DEPENDENT, TWO DIMENSIONAL MODEL OF THE ATMOSPHERE Ph.D. Thesis [SIMULATION DER GLOBALEN KR 85 UND 14CO2 VERTEILUNG MIT HILFE EINES ZEITABHAENGIGEN, ZWEIDIMENSIONALEN MODELLS DER ATMOSPHAERE]
Hans-Karl Rath 1988 125 p In GERMAN
(ETN-90-95376) Avail: NTIS HC A06/MF A01

Quantification of atmospheric transfer and mixture processes could be explained by the worldwide distribution of the radioactive gas Kr-85 in air, produced by the nuclear industry, despite the small annual Kr-85 emission data. But the gage process is perhaps a weak point, although the Kr-85 confirms the adaptability of the results; the atmospheric transport at the South Pole could also be improved: it causes weak increase of the model results for Kr-85 and overestimates the vertical exchange for C-14. The calculated interhemisphere concentration differences and the gradients between troposphere and stratosphere coincide with the experiments values when the measurement errors are taken into account. With the C-14 simulations, the contributions of the fossil CO2 source, the biosphere and the ocean to the atmospheric C-14 contents can be estimated and their seasonal influences can be established. ESA

N90-19703# IIT Research Inst., Bartlesville, OK. National Inst. for Petroleum and Energy Research.
APPLICATION OF NATURAL ISOTOPES IN GROUNDWATER FOR SOLVING ENVIRONMENTAL PROBLEMS Final Report
Michael Szpakiewicz Mar. 1990 70 p
(Contract DE-FC22-83FE-60149)
(DE90-000223; NIPER-450) Avail: NTIS HC A04/MF A01

An aim of this project is to review a diverse body of information presently scattered throughout the international groundwater literature and demonstrate the usefulness of natural isotopes in environmental research. Identification of isotopic composition of water molecules, dissolved compounds, and undissociated gases in a protected groundwater system provides valuable and sometimes unique information for quantification of critical parameters in groundwater modeling. The most applicable isotopes in the environmental area are such natural isotopes as oxygen-18, deuterium, tritium, radiocarbon, carbon-13, sulfur-34, chlorine-36, and bomb-chlorine-36. A considerable potential is in application of strontium-87, nitrogen-15, chlorine-37, and silicon-32. Some other isotopes may find application for solving specific environmental problems; for example, beryllium-10, krypton-85, argon-39, helium-3, and uranium-234. Yet few such applications have been reported in the United States. This work provides an evaluation of the potential and suggests areas where applications of natural isotope measurements can be most helpful to solving environmental problems. DOE

N90-19704# Oak Ridge National Lab., TN.
PREDICTING EFFECTS OF GLOBAL CLIMATE CHANGE ON RESERVOIR WATER QUALITY AND FISH HABITAT
Lisa H. Chang and Steven F. Railsback 1989 6 p Presented at the 1990 American Society of Civil Engineers Water Resources Planning and Management Division Specialty Conference, Fort Worth, TX, 17-20 Apr. 1990
(Contract DE-AC05-84OR-21400)
(DE90-003674; CONF-900483-1) Avail: NTIS HC A02/MF A01

This paper demonstrates the use of general circulation models (GCMs) for assessing global climate change effects on reservoir water quality and illustrates that general conclusions about the effects of increased carbon dioxide (CO2) concentrations on water resources can be made by using GCMs. These conclusions are based on GCM predictions of the climatic effects of doubling CO2 concentrations. We also point out inadequacies in using information from GCM output alone to simulate reservoir water quality effects of climate change. Our investigation used Douglas Lake, a large multipurpose reservoir in eastern Tennessee, as an example. We studied water temperature and dissolved oxygen (DO), important water quality parameters that are expected to respond to a changed climate. Finally, we used the temperature and DO requirements of striped bass as an indicator of biological effects of combined changes in temperature and DO. DOE

N90-19705# Department of Energy, Washington, DC. Atmospheric and Climate Research Div.
ATMOSPHERIC RADIATION MEASUREMENT PROGRAM PLAN
Feb. 1990 19 p
(DE90-006349; DOE/ER-0442) Avail: NTIS HC A03/MF A01

In order to understand energy's role in anthropogenic global climate change, significant reliance is being placed on General Circulation Models (GCMs). A major goal is to foster the development of GCMs capable of predicting the timing and magnitude of greenhouse gas-induced global warming and the regional effects of such warming. The Atmospheric Radiation Measurement (ARM) Program will contribute to the Department of Energy goal by improving the treatment of cloud radiative forcing and feedbacks in GCMs. Two issues will be addressed: the radiation budget and its spectral dependence and the radiative and other properties of clouds. The experimental objective of the ARM Program is to characterize empirically the radiative processes in the earth's atmosphere with improved resolution and accuracy. A key to this characterization is the effective treatment of cloud formation and cloud properties in GCMs. Through this characterization of radiative properties, it will be possible to understand both the forcing and feedback effects. DOE

N90-19706# Army Biomedical Research and Development Lab., Fort Detrick, MD.
THE POLLUTION HAZARD ASSESSMENT SYSTEM: DOCUMENTATION AND USERS MANUAL Final Report, Jan. 1988 - Sep. 1989
Mitchell J. Small 1 Oct. 1989 10 p
(AD-A217108; USABRDL-TR-9003) Avail: NTIS HC A02/MF A01 CSCL 13/2

The preliminary pollutant limit value approach has been used to assess soil and water contamination at several U.S. Army installations. This report documents the adaptation of this approach into a software computer package, the Pollution Hazard Assessment System (PHAS). PHAS, programmed in BASIC code, is capable of being handled on many personal computer configurations and can be supported with a system with 640K memory, two-disk drives, a monochrome monitor, and a line printer. PHAS has been prepared in modular form. The user is guided through the system with menu displays in user-friendly format. The user can prepare information for immediate analysis, or store information in off-line files for recall. Files can be recalled for analysis or modification. Three set of user files are employed: files which store information about scenario pathways of human exposure; files which store data about human intake, livestock characteristics (for human consumption of beef or milk), and site-specific factors; and files which store information about

chemical-specific properties. The user can select up to 8 exposure pathways for water-based contamination problems. A chemical estimation module is provided to assist in developing data for chemicals. This module can be used in conjunction with the rest of the system or as a stand-alone routine. The main test provides the user with system instructions. GRA

N90-19410*# Tulane Univ., New Orleans, LA. Dept. of Mechanical Engineering.
MECHANICS OF AEOLIAN PROCESSES: SOIL EROSION AND DUST PRODUCTION
M. M. Mehrabadi *In* Alabama Univ., Research Reports: 1989 NASA/ASEE Summer Faculty Fellowship Program Dec. 1989 25 p (For primary document see N90-19390 12-31)
(Grant NGT-01-008-021)
Avail: NTIS HC A99/MF E06 CSCL 13B

46 GEOPHYSICS

Includes aeronomy; upper and lower atmosphere studies; ionospheric and magnetospheric physics; and geomagnetism.

For space radiation see *93 Space Radiation.*

N90-19707# Central Research Inst. of Electric Power Industry, Tokyo (Japan).
GEOCHEMICAL SURVEY ON FAULTS OVERLAND WITH ALLUVIAL DEPOSITS, PART 1. APPLICATION FOR THE NEODANI AND THE ATERA FAULTS SURVEY
Kenzo Kiho and Yuji Kanaori Aug. 1988 37 p In JAPANESE; ENGLISH summary
(DE89-782326; CRIE-U-88004) Avail: NTIS (US Sales Only) HC A03/MF A01

The effectiveness of the geochemical survey was evaluated as a technique for investigating the fault which is overlaid with alluvial deposits. This was done, using underground gas as the indicator, at the Neodani Fault (NF) and Atera Fault (AF) where the location of faults has been known by the trenches. Five measuring lines were established normally crossing with the NF. Measuring points at AF were selected at crossing points of 15 to 30 m grids in an area of 90 m in the south to north direction and 150 m in east to west direction. Several zones with commonly high ratios of He/Ar and Ne/Ar and Rn concentration were found, and zones that coincide with the faults were observed in both areas. At zones with high concentrations and those corresponding to the faults, high values of He/Ar and Ne/Ar ratios distributed immediately above faults and high Rn concentations were found at the hanging wall side. Some zones other than those with confirmed faults have shown high values of concentrations, suggesting other faults overlaid under the alluvial deposits. DOE

N90-19708# Instituto de Pesquisas Espaciais, Sao Jose dos Campos (Brazil).
ANALYSIS OF TECTONIC MOVEMENTS UTILIZING REMOTE SENSOR PRODUCTS IN THE SOUTHERN ESPINHACO (SE) REGION [ANALISE DE MOVIMENTOS TECTONICOS UTILIZANDO PRODUTOS DE SENSORES REMOTOS NA REGIAO DO ESPINHACO MERIDIONAL (MG)]
Paulo Veneziani, Juercio TavaresdeMattos, and Tomoyuki Ohara Jun. 1989 15 p In PORTUGUESE; ENGLISH summary Presented at the 5th Brazilian Symposium on Remote Sensing, Natal, Brazil, 11-15 Oct. 1988
(INPE-4830-PRE/1451) Avail: NTIS HC A03/MF A01

The area under study, the Southern Espinhaco Region, Minas Gerais State, Brazil, comprises metasedimentary sequences of Proterozoic, a typical granite-greenstone belt of Archaean age, gneiss, mignatites, granulites, and metasedimentary, and mafic to felsic units attributed to undifferentiated Precambrian. The region suffered a complex geologic evolution, including polycyclic and polymetamorphic events. Deformations occurred during the deposition of sediments (synsedimentary) due to compressive forces acting repeatedly during the geologic history of the region, resulting in superimposed orogenesis. The ruptile, ruptile-ductile tectonics that were part of different events registered in the petrographic and structural record were analyzed by LANDSAT (MSS, RBV, and TM) and radar images, aeromagnetic data, and field work. The main results of this research are: identification of 7 sets of joint zones which are controlled along N-S, EW and NW-SE directions during the Archaean to Late Proterozoic events; identification of sinistral transcurrent movements along N50-60W lineaments during the compressive phase of Late Proterozoic; occurrence of different tectonic movements (compression and tension) along the main directions of fracturing; finally the analysis of lithostratigraphic and fracturing data permits to envisage the geologic history of Proterozoic evolution of the region characterized by mechanism compatible to intraplate tectonic movements (ensialic environment). Author

N90-19709# Pacific-Sierra Research Corp., Los Angeles, CA.
IONOSPHERIC HEATING WITH OBLIQUE WAVES. VOLUME 1: ELECTRON DENSITY PERTURBATIONS Scientific Report No. 1, 13 Feb. 1987 - 31 Aug. 1988
E. C. Field, Jr., R. M. Bloom, and K. E. Heikes Sep. 1988 63 p
(Contract F19628-87-C-0028; AF Proj. 2310)
(AD-A216260; PSR-1864-Vol-1; AFGL-TR-88-0336-Vol-1; SR-1-Vol-1) Avail: NTIS HC A04/MF A01 CSCL 04/1

The transport and chemical equations that described electron density and temperature changes produced by electric fields in the ionosphere are derived and cast into a form suitable for numerical integration. By using those equations in conjunction with previously developed methods for calculating electric fields near caustics, the density and temperature changes produced by an oblique ionospheric high frequency heater can be computed straightforwardly. The necessary inputs are: (1) heater power, (2) heater radiation pattern, (3) heat frequency, and (4) model ionosphere. Analytical solutions for idealized heater beamshapes indicate that heat conduction and diffusion are also presented. Author

N90-19710*# Maryland Univ., College Park. Dept. of Geology.
P-T CONDITION FO DEFORMATION FROM FLUID INCLUSIONS IN MYLONITES
Eileen McLellan 1990 31 p
(Grant NAG5-968)
(NASA-CR-186377; NAS 1.26:186377) Avail: NTIS HC A03/MF A01 CSCL 08G

Structural petrology of fluid inclusions in deformed rocks can be used to identify inclusions entrapped during various stages of deformation. Standard thermobarometry on these inclusions can then provide estimates of the P-T (pressure-temperature) conditions of deformation. The application of this technique is illustrated using fluid inclusions in mylonites from the Quetico Fault Zone, Canada. The inferred P-T conditions fall with the P-T field of mylonitisation derived from isotopic, microstructural and phase equilibrium studies. Author

N90-19711# Non-Linear Systems, Inc., Cambridge, MA.
ATMOSPHERIC THERMAL BLOOMING AND BEAM CLEARING BY AEROSOL VAPORIZATION
Vladimir B. Krapchev 1990 24 p Presented at the Conference on Propagation of High Energy Laser Beams Through the Earth's Atmosphere, Los Angeles, CA, 14-19 Jan. 1990 Prepared in cooperation with Lawrence Livermore Lab., CA
(Contracts W-7405-eng-48; MIPR-W43-GBL-0-5007)
(DE90-006271; UCRL-21272; CONF-900164-1) Avail: NTIS HC A03

The propagation of ground based (GB), high energy laser (HEL) beams in the atmosphere is limited by a number of physical processes. Those include stimulated Raman scattering, which drives the system design toward higher duty factors, and cloud cover, which leads to an increase in the number of sites. The most important considerations come from atmospheric absorption and the resulting thermal blooming because they affect all ground based HELs. DOE

N90-19712# International Centre for Theoretical Physics, Trieste (Italy).
UNIQUENESS OF CLOSURE OF THE CONSTRAINT ALGEBRA FOR QUANTUM GRAVITY
T. Christodoulakis and E. Korfiatis (Athens Univ., Greece) Aug. 1989 21 p Submitted for publication
(DE90-610476; IC-89/248) Avail: NTIS (US Sales Only) HC A03/MF A01

We investigate the closure of the quantum algebra for the constraints of pure gravity considering a wide class of regularization assumptions. We thus establish that the only regularization assumption, within this class, that closes the algebra is the one introduced by one of the authors (T.C. with Jorge Zanelli) in earlier publications and that the closure is a result of both the regularization and the introduction of a tensor distribution. DOE

N90-19713*# Arizona Univ., Tucson. Dept. of Geosciences.
EVOLUTION OF MIDPLATE HOTSPOT SWELLS: NUMERICAL SOLUTIONS
Mian Liu and Clement G. Chase [1990] 36 p
(Grant NAG5-444)
(NASA-CR-186462; NAS 1.26:186462) Avail: NTIS HC A03/MF A01 CSCL 08G

The evolution of midplate hotspot swells on an oceanic plate moving over a hot, upwelling mantle plume is numerically simulated. The plume supplies a Gaussian-shaped thermal perturbation and thermally-induced dynamic support. The lithosphere is treated as a thermal boundary layer with a strongly temperature-dependent viscosity. The two fundamental mechanisms of transferring heat, conduction and convection, during the interaction of the lithosphere with the mantle plume are considered. The transient heat transfer equations, with boundary conditions varying in both time and space, are solved in cylindrical coordinates using the finite difference ADI (alternating direction implicit) method on a 100 x 100 grid. The topography, geoid anomaly, and heat flow anomaly of the Hawaiian swell and the Bermuda rise are used to constrain the models. Results confirm the conclusion of previous works that the Hawaiian swell can not be explained by conductive heating alone, even if extremely high thermal perturbation is allowed. On the other hand, the model of convective thinning predicts successfully the topography, geoid anomaly, and the heat flow anomaly around the Hawaiian islands, as well as the changes in the topography and anomalous heat flow along the Hawaiian volcanic chain. Author

N90-19714*# Arizona Univ., Tucson. Dept. of Geosciences.
AN ANALYTIC MODEL OF AXISYMMETRIC MANTLE PLUME DUE TO THERMAL AND CHEMICAL DIFFUSION
Mian Liu and Clement G. Chase [1990] 30 p
(Grant NAG5-444)
(NASA-CR-186461; NAS 1.26:186461) Avail: NTIS HC A03/MF A01 CSCL 08G

An analytic model of axisymmetric mantle plumes driven by either thermal diffusion or combined diffusion of both heat and chemical species from a point source is presented. The governing equations are solved numerically in cylindrical coordinates for a Newtonian fluid with constant viscosity. Instead of starting from an assumed plume source, constraints on the source parameters, such as the depth of the source regions and the total heat input from the plume sources, are deduced using the geophysical characteristics of mantle plumes inferred from modelling of hotspot swells. The Hawaiian hotspot and the Bermuda hotspot are used as examples. Narrow mantle plumes are expected for likely mantle viscosities. The temperature anomaly and the size of thermal plumes underneath the lithosphere can be sensitive indicators of plume depth. The Hawaiian plume is likely to originate at a much greater depth than the Bermuda plume. One suggestive result puts the Hawaiian plume source at a depth near the core-mantle boundary and the source of the Bermuda plume in the upper mantle, close to the 700 km discontinuity. The total thermal energy input by the source region to the Hawaiian plume is about 5 x 10(10) watts. The corresponding diameter of the source region is about 100 to 150 km. Chemical diffusion from the same source does not affect the thermal structure of the plume. Author

N90-19715*# Arizona Univ., Tucson. Dept. of Geosciences.
STORED MAFIC/ULTRAMAFIC CRUST AND EARLY ARCHEAN MANTLE DEPLETION
Clement G. Chase and P. J. Patchett [1990] 17 p
(Grants NAG5-444; NSF EAR-86-15844)
(NASA-CR-186460; NAS 1.26:186460) Avail: NTIS HC A03/MF A01 CSCL 08G

Both early and late Archean rocks from greenstone belts and felsic gneiss complexes exhibit positive epsilon(Nd) values of +1 to +5 by 3.5 Ga, demonstrating that a depleted mantle reservoir existed very early. The amount of preserved pre-3.0 Ga continental crust cannot explain such high epsilon values in the depleted residue unless the volume of residual mantle was very small: a layer less than 70 km thick by 3.0 Ga. Repeated and exclusive sampling of such a thin layer, especially in forming the felsic gneiss complexes, is implausible. Extraction of enough continental crust to deplete the early mantle and its destructive recycling before 3.0 Ga ago requires another implausibility, that the sites of crustal generation of recycling were substantially distinct. In contrast, formation of mafic or ultramafic crust analogous to present-day oceanic crust was continuous from very early times. Recycled subducted oceanic lithosphere is a likely contributor to present-day hotspot magmas, and forms a reservoir at least comparable in volume to continental crust. Subduction of an early mafic/ultramafic oceanic crust and temporary storage rather than immediate mixing back into undifferentiated mantle may be responsible for the depletion and high epsilon(Nd) values of the Archean upper mantle. Author

N90-19716 Deutsche Geodaetische Kommission, Munich (Germany, F.R.).
DEVELOPMENT AND TESTING OF A UNIVERSALLY IMPLEMENTABLE RECORDING ALIGNING SYSTEM Ph.D. Thesis - Bonn Univ. [ENTWICKLUNG UND ERPROBUNG EINES UNIVERSELL EINSETZBAREN, REGISTRIERENDEN ALIGNEMENTSYSTEMS]
Martin Drude 1989 119 p In GERMAN
(Ser-C-349; ISBN-3-7696-9397-3; ISSN-0065-5325; ETN-90-95885) Copyright Avail: Fachinformationszentrum Karlsruhe, 7514 Eggenstein-Leopoldshafen 2, Federal Republic of Germany

A quasi-continuum working automatic aligning system is described, which estimates the components of the relative motion in appropriately arranged point fields, especially for tectonically active areas. Some long term variations of the atmospheric state, thermic instabilities in the measurement assembly on sensor deviations can provoke a few frequent and regular variations of the position signal. The estimation of the refraction error is difficult because the real conditions must be strongly idealized to obtain quantitative results with a reasonable cost. It is possible to calculate the variations of the curvature properties of the light trajectory, by variations in the refractive index field. Despite these inaccuracies, this process is adapted to engineering measurements or earthquake surveillance, since it allows virtually continuous observations. ESA

N90-19391*# Auburn Univ., AL. Dept. of Electrical Engineering.
CHARACTERIZATION OF THUNDERSTORM INDUCED MAXWELL CURRENT DENSITIES IN THE MIDDLE ATMOSPHERE
Michael Edward Baginski *In* Alabama Univ., Research Reports: 1989 NASA/ASEE Summer Faculty Fellowship Program Dec. 1989 p 1-21 (For primary document see N90-19390 12-31)
(Grant NGT-01-008-021)
Avail: NTIS HC A99/MF E06 CSCL 04A

N90-20007# Eidgenoessisches Inst. fuer Schnee- und Lawinenforschung, Weissfluhjoch/Davos (Switzerland).
LABORATORY TECHNIQUES FOR THE CHARACTERISATION OF SNOW STRUCTURES

W. Good *In* ESA, Physics and Mechanics of Cometary Materials Dec. 1989 p 147-151 (For primary document see N90-19989 12-90)
Copyright Avail: NTIS HC A10/MF A02; ESA Publications Div., ESTEC, Noordwijk, Netherlands, 60 Dutch guilders

47 METEOROLOGY AND CLIMATOLOGY

Includes weather forecasting and modification.

N90-19717 Texas A&M Univ., College Station.
SYNOPTIC-SCALE FORCING OF THE LOW-LEVEL JET IN DEVELOPING BAROCLINIC WAVES Ph.D. Thesis
Michael Kent Walters 1988 145 p
Avail: Univ. Microfilms Order No. DA8903417

A series of numerical simulations of low-level jet (LLJ) formation in a developing baroclinic wave is presented. The simulations were performed using the Limited Area Mesoscale Prediction System (LAMPS) model. The LAMPS model is a 15 layer primitive equation model with a terrain following vertical coordinate. The numerical simulations were initiated with a schematic baroclinic wave which includes a sloping polar front and a realistically shaped tropopause. The location of the tropopause was diagnosed from derived equations which constrain the geostrophic wind at the top of the model atmosphere to vanish. The initial conditions were altered selectively to study the effect of low-level stable layers on the subsequent development of the LLJ. In each simulation synoptically-forced LLJ develops in the absence of surface terrain. A low-level stable layer is not necessary to confine the LLJ to low-levels. Each LLJ develops with a highly ageostrophic component which in turn has a large tendency wind component as described by Brill et al. (1985). The horizontal configuration of the LLJ is similar to the warm-conveyor belt described by Carlson (1980) and the schematic LLJ model of Djuric and Ladwig (1983). Areas of mass convergence and mass divergence at low-levels are not strongly related to the position and strength of the upper-level jet streak or the location and magnitude of the upper-level mass divergence pattern. Dissert. Abstr.

N90-19718*# National Aeronautics and Space Administration. Langley Research Center, Hampton, VA.
SPANWISE MEASUREMENTS OF VERTICAL COMPONENTS OF ATMOSPHERIC TURBULENCE
Robert K. Sleeper Washington Apr. 1990 67 p
(NASA-TP-2963; L-16550; NAS 1.60:2963) Avail: NTIS HC A04/MF A01 CSCL 04B

Correlation and spectrum magnitude estimates are computed for vertical gust velocity measurements at the nose and wing tips of a NASA B-57B aircraft for six level flight, low speed and low altitude runs and are compared with those of the von Karman atmospheric turbulence model extended for spanwise relationships. The distance between the wing tips was 62.6 ft. Airspeeds ranged from about 330 to 400 ft/sec, heights above the ground ranged from near ground level to about 5250 ft. and gust velocity standard deviations ranged from 4.10 to 8.86 ft/sec. Integral scale lengths, determined by matching measured autocorrelation estimates with those of the model, ranged from 410 to 2050 ft. Digital signals derived from piezoelectric sensors provided continuous pressure and airspeed measurements. Some directional acceleration sensitivity of the sensors was eliminated by sensor orientation, and their performance was spectrally verified for the higher frequencies with supplemental onboard piezoresistive sensors. The model appeared to satisfactorily predict the trends of the measured cross-correlations and cross-spectrum magnitudes, particularly between the nose and wing tips. However, the measured magnitude estimates of the cross-spectra between the wing tips exceeded the predicted levels at the higher frequencies. Causes for the additional power across the wing tips were investigated. Vertical gust velocity components evaluated along and lateral to the flight path implied that the frozen-turbulence-field assumption is a suitable approximation. Author

N90-19719 Liverpool Univ. (England).
EXPLOITING SURFACE OBSERVATIONS OF CLOUDINESS FOR GLOBALSCALE NEPHANALYSES Ph.D. Thesis
Frances Drake 1987 499 p
Avail: Univ. Microfilms Order No. BRDX86173

The need for an accurate global cloud climatology with which to validate climate model results and to use as input into climate models has resulted in the initiation of the International Satellite Cloud Climatology Project (ISCCP). A comparison of surface observed and satellite retrieved cloudiness over southern Britain, France and West Germany highlighted several areas where surface observations could supplement a satellite retrieved cloud climatology such as ISCCP. Thin cirrus, small gaps in cloud and subresolution clouds were all detected by surface observers but missed by the satellite retrieval. Surface observers were not confused by near coastal locations whereas the satellite retrieval often produced erroneous results. Pixel sampling in order to reduce the volume of satellite data processed was found to have an adverse effect on the satellite retrieval and thus the intercomparison. Studies of the relationship between surface incident radiation and surface observed cloud amount were carried out under two very different climatological regimes: Amazon, Brazil and Wallingford, U.K. Both studies illustrated the point specific nature of incident surface radiation. Incident surface radiation was found to be dependent not only on cloud amount and cloud optical thickness but also on the distribution of the clouds in the sky. Dissert. Abstr.

N90-19720# National Center for Atmospheric Research, Boulder, CO. Climate and Global Dynamics Div.
COLLOQUIUM ON SYNOPTIC METEOROLOGY
Stephen J. Colucci, Frederick H. Carr, and David P. Baumhefner Aug. 1989 449 p Colloquium held in Boulder, CO, 5-22 Jul. 1988
(Grant NSF ATM-87-09659)
(PB90-121112) Avail: NTIS HC A19/MF A03 CSCL 04B

Partial contents on synoptic phenomena include: (1) Synoptic scale-planetary scale interaction (a comparison of wintertime climatological flows and blocking flows); (2) Historical review of cyclones and related phenomena; (3) Persistent large-scale flow Anomalies and Blocking; (4) Extreme cold air outbreaks over eastern North America; (5) Anticyclones; and (6) A 500 mb closed circulation center. Partial contents on weather prediction include: (1) Mesoscale atmospheric modeling (challenges for the 90s); (2) Studies of polar air stream cyclogenesis; (3) Forecasting cold-core severe weather outbreaks; (4) Recent progress and future plans for numerical weather prediction at the National Meteorological Center; and (5) Extended-range forecasting and forecasting forecast skill. Partial contents on observational techniques include: (1) New observing systems; (2) Radar applications; (3) Observations of gravity waves in a midlatitude squall line; (4) Satellites and applications; and (5) Principles of operation and meteorological applications of ground-based atmospheric profilters. GRA

N90-19721# Central Research Inst. of Electric Power Industry, Tokyo (Japan). Energy and Environment Lab.
LIGHTNING SURGE CHARACTERISTICS OF TRANSMISSION TOWERS. LIGHTNING SURGE CHARACTERISTICS OF 15-METER-HIGH SCALE MODEL TOWER
Atsuyuki Inoue, Hideki Motoyama, and Yoshihide Aoshima Sep. 1988 47 p In JAPANESE; ENGLISH summary
(DE89-782322; CRIE-T-87088) Avail: NTIS (US Sales Only) HC A03/MF A01

Experiments were conducted to establish the lightning surge characteristics using simulated power transmission line with a reduced size 15 meter tower model. Surge characteristics were determined by vertically injecting steep and large impulse current with a rise time of 30 ns and current of 3 kA from the top of the tower. Rise of arm made the potential 10 to 20 pct higher than predicted values. This is a response to currents vertically injected from top and equivalent to cases where the return strokes of actual lightning develops from the storm clouds to the tower instead of development from the tower top. This direction of current is

possible with the winter lightning, suggesting the generation of an arm potential higher than the prediction and occurrence of many faults. About 50 pct of the incident current flows out to the overhead grounding wire. Its value rapidly decreased along time and the waveform was greatly different from computed ones. Highest velocity of surge propagation in tower was 82 pct of the light velocity and the most frequently observed velocity was 60 pct of the light velocity. At the top of the tower, 60 pct of the current flowed in the main member but not in oblique members. DOE

N90-19722# Instituto de Pesquisas Espaciais, Sao Jose dos Campos (Brazil).
CYCLOGENESES AND EXTRATROPICAL CYCLONES IN THE SOUTH-SOUTHEAST REGION OF BRAZIL AND ITS INFLUENCE IN TIME M.S. Thesis - Nov. 1986
[CICLOGENESES E CICLONE EXTRATROPICAIS NA REGIAO SUL-SUDESTE DO BRASIL E SUAS INFLUENCIA NO TEMPO]
Celeste daConceicaoFerreira Jun. 1989 109 p In PORTUGUESE; ENGLISH summary
(INPE-4812-TDL/359) Avail: NTIS HC A06/MF A01

A climatology of cyclogeneses and the cylconic vortex passages in the South American region south 15 S between 30 to 70 W for the seven-year period 1980 to 1986 was obtained based on satellite imagery. It is observed that in the years 1980 and 1983 there were, 20 percent more occurrences of cyclogeneses than the average. The geographic distribution showed that the South Brazil and Uruguay region and along the east coast are favored by cyclogeneses. The season of frequency cyclogeneses is summer and winter has minimum frequency. This agrees very well with the seasonal distribution of precipitation. Two cases of cyclogeneses, one in summer and the other in winter were presented. The winter cyclogeneses is essentially caused by baroclinic instability as could be seen from the thermal contrast. Although baroclinity is an indispensable factor in the development of summer cyclones, other agents such as water vapor convergence and sensible heating are more active in this season which helps cyclogeneses. Author

N90-19723# Instituto de Pesquisas Espaciais, Sao Jose dos Campos (Brazil).
AN OBSERVATIONAL STUDY OF SQUALL LINES IN THE AMAZON M.S. Thesis
Julia Clarinda Paiva Cohen May 1989 162 p In PORTUGUESE; ENGLISH summary
(INPE-4865-TDL/376) Avail: NTIS HC A08/MF A01

Bands of convective clouds are originated at the northern coast of South America. Some of bands move inland as Squall Lines (SL). The non-propagating lines are denominated Coastal Squall Lines (CSL) and the propagating SL are identified by PSL. There are two categories of PSL: Horizontal displacement between 170 and 400 km from the coast (PSL1) and horizontal penetration beyond 400 km (PSL2). The greatest frequency of SL occurs between April and August. The average speed of propagation of PSL1 and PSL2 are 12 and 16 m/s, respectively. Most of the SL are observed to the South of the Atlantic ITCZ. The PSL2 is more frequent when ITCZ is established and PSL1 is not dependent on the ITCZ condition. The mean dimensions of the SL are 1400 km in length and 170 km in width. A lower level easterly jet is a dominant element in the propagation of the SL. The SLP is associated with a deep layer of almost constant speed of the easterly jet. The thermodynamical and dynamics characteristics before and after the passage of the SL are similar to the observed structure of SL in other regions. Author

N90-19724# Scripps Institution of Oceanography, La Jolla, CA. Marine Physical Lab.
AUTOMATED VISIBILITY AND CLOUD COVER MEASUREMENTS WITH A SOLID-STATE IMAGING SYSTEM Final Report, 26 Sep. 1984 - 25 Sep. 1988
Richard W. Johnson, Wayne S. Hering, and Janet E. Shields Mar. 1989 128 p
(Contract F19628-84-K-0047; AF Proj. 317J)
(AD-A216906; MPL-U-26/89; SIO-REF-89-7; GL-TR-89-0061)
Avail: NTIS HC A07/MF A01 CSCL 04/2

The development status is summarized of two computer-controlled, video-based imaging systems, their initial deployment and the preliminary application of their output data for the objective determination of cloud free paths of sight, total cloud cover, and sector visibilities. The effort was directed toward the development of two related systems, one for the automatic assessment of total cloud cover and its related distributional statistics, and the other for the automatic determination of local sector visibilities. Both systems involve the use of similar hardware for image acquisition and manipulation, but quite different analytics and control algorithms, thus they are discussed separately. The development status at the conclusion of this contract interval is such that two prototype systems, the Whole Sky Imager which is used for cloud cover assessments and the Automatic Horizon Scanner which is used for visibility determinations, are built, operational in several locations, and are producing image oriented data bases appropriate for computer analysis. Preliminary analytic algorithms for the use of these data in automated processes were developed and are undergoing refinement. GRA

N90-19725*# Pennsylvania State Univ., University Park. Dept. of Geography.
REGIONAL CLIMATE CHANGE PREDICTIONS FROM THE GODDARD INSTITUTE FOR SPACE STUDIES HIGH RESOLUTION GCM Progress Report, 15 May 1989 - 15 Feb. 1990
Robert G. Crane and Bruce Hewitson Mar. 1990 28 p
(Grant NAG5-1133)
(NASA-CR-186375; NAS 1.26:186375) Avail: NTIS HC A03/MF A01 CSCL 04B

Model simulations of global climate change are seen as an essential component of any program aimed at understanding human impact on the global environment. A major weakness of current general circulation models (GCMs), however, is their inability to predict reliably the regional consequences of a global scale change, and it is these regional scale predictions that are necessary for studies of human/environmental response. This research is directed toward the development of a methodology for the validation of the synoptic scale climatology of GCMs. This is developed with regard to the Goddard Institute for Space Studies (GISS) GCM Model 2, with the specific objective of using the synoptic circulation form a doubles CO2 simulation to estimate regional climate change over North America, south of Hudson Bay. This progress report is specifically concerned with validating the synoptic climatology of the GISS GCM, and developing the transfer function to derive grid-point temperatures from the synoptic circulation. Principal Components Analysis is used to characterize the primary modes of the spatial and temporal variability in the observed and simulated climate, and the model validation is based on correlations between component loadings, and power spectral analysis of the component scores. The results show that the high resolution GISS model does an excellent job of simulating the synoptic circulation over the U.S., and that grid-point temperatures can be predicted with reasonable accuracy from the circulation patterns. Author

N90-19726# Johann-Wolfgang-Goethe-Univ., Frankfurt am Main (Germany, F.R.). Zentrum fuer Umweltforschung.
NUMERICAL MODELING OF ATMOSPHERIC GROWTH PROCESSES [NUMERISCHE MODELLIERUNG VON ATMOSPHAERISCHEN AUSWASCHPROZESSEN]
D. Bayer, K. D. Beheng, and F. Herbert Sep. 1987 82 p In GERMAN
(Rept-70; ETN-90-95336) Avail: NTIS HC A05/MF A01

The removal of aerosol particles from the atmosphere into cloud and raindrops was numerically modeled. The first type of collection processes occur essentially in the first phase of the cloud formation and are called Nucleation Aerosol Scavenging (NAS). The second type of processes occur essentially in the later phase of the cloud formation and are called Collision Aerosol Scavenging (CAS) with in-cloud as well as below-cloud effects.

The growth process equations for NAS and CAS are derived. The computer program for the description of the time evolution of particle spectra by CAS for steady and unsteady droplet spectra is presented, and the most important computer programs are enclosed. ESA

N90-19727 Deutscher Wetterdienst, Offenbach am Main (Germany, F.R.).
WIND CONDITIONS NEAR THE GROUND IN FEDERAL REPUBLIC OF GERMANY [DIE BODENNAHEN WINDVERHAELTNISSE IN DER BUNDESREPUBLIK DEUTSCHLAND. 2. VOLLSTAENDIG NEU BEARBEITETE AUFLAGE]
Juergen Christoffer and Monika Ulbricht-Eissing 1989 190 p In GERMAN; ENGLISH summary
(ISBN-3-88148-248-2; ISSN-0072-4130; ETN-90-95729)
Copyright Avail: Deutscher Wetterdienst, Zentralamt, Frankfurter Str. 135, D-6050 Offenbach am Main, Fed. Republic of Germany

On the basis of measurements of the wind speed during a period of 10 years, the wind conditions near the ground are extensively represented. A description of the parameters exerting an influence on the wind is proposed, and problems arising in the measurement of wind speed are reviewed. The usual statistical methods, such as the Weibull distribution are presented. Detailed evaluations of wind speed data of selected stations are made. The wind speed is measured 10 m above ground in conformity with the international convention. The wind speed profile up to 150 m above the ground, the low level jet, the use of wind energy and some special storm events are investigated. ESA

N90-19728# Cologne Univ. (Germany, F.R.). Inst. fuer Geophysik und Meteorologie.
THE ATMOSPHERIC ENERGY CYCLE OF STATIONARY AND TRANSIENT WAVES [DER ATMOSPHAERISCHE ENERGIEZYKLUS DER STATIONAREN UND DER TRANSIENTEN WELLEN]
Uwe Ulbrich 1989 99 p In GERMAN
(Contract BF-07KF212)
(ISSN-0069-5882; ETN-90-96069) Avail: NTIS HC A05/MF A01

For the years 1980 to 1987 the energy cycle of the atmosphere for January and July is compared with the results of a climate model by means of analysis data. The results show that the stationary waves play an important part in the energy reservoir and transformations of the total energy cycle in January, essentially in the Northern Hemisphere. However, this influence is significantly weaker in July and equally distributed in both hemispheres. Transient and stationary waves are linked to the baroclinic transformations. ESA

N90-19729# Cologne Univ. (Germany, F.R.). Inst. fuer Geophysik und Meteorologie.
DIGITAL SIMULATION OF A BOENLINE [NUMERISCHE SIMULATION EINER BOEENLINIE]
Peter Scheidgen 1989 138 p In GERMAN
(ISSN-0069-5882; ETN-90-96070) Avail: NTIS HC A07/MF A01

A digital cloud model for the mesoscale area of the atmosphere is presented. The ice phase and the liquid phase are taken into account. It is also a compressible, nonhydrostatic, bidimensional cloud model, that defines the partial components water and ice. The parametrization of the rain phase is based on the Kessler model of the condensed ice phase. Therefore the coexistance of both phases can be simulated. A comparison of the calculations of radar reflectivity factors and the qualitative curve of the simulated wind fields show a very good agreement with the experimentally observed fields. The Boenline system is in a quasi-steady state after three or four hours. The ice phase plays an important part in the development of the convective circulation. The results show that the appearance of new thunderstorm cells slows down and that the system expansion, particularly for the Cirrus layer, increases. ESA

N90-19730# Brookhaven National Lab., Upton, NY. Environmental Chemistry Div.
LABORATORY STUDIES OF FREE RADICAL REACTIONS IN CLOUDWATER
Stephan E. Schwartz and Judith Weinstein-Lloyd (State Univ. of New York, Old Westbury.) Nov. 1989 7 p Presented at the 199th National Meeting of the American Chemical Society, Boston, MA, 22-27 Apr. 1990
(Contract DE-AC02-76CH-00016)
(DE90-003961; BNL-43551; CONF-900402-2) Avail: NTIS HC A02/MF A01

Reactions in cloudwater can be important pathways for chemical transformation of atmospheric trace gases because of high solubility of reagent gases, rapid aqueous-phase kinetics, and large thermodynamic driving force. A key cloudwater reaction is oxidized of dissolved SO2 and H2O2. It is thus important to understand processes controlling H2O2 formation in the atmosphere by gas- and aqueous-phase reactions of HO2 free radicals. A concern with models of free radical chemistry in cloudwater is that of the applicability of present chemical kinetic schemes to such complex milieus. This concern arises because, at the low free radical concentrations expected for cloudwater, reactions of radicals with trace impurities are favored over radical-radical reactions, which dominate at high radical concentrations commonly employed in laboratory investigations. Initial results are reported of a study in which the rate of change in H2O2 concentration is monitored in synthetic and authentic cloudwater in which HO2 radicals are produced by (60)Co-gamma radiolysis at rates comparable to those expected upon transfer of HO2 from interstitial cloud air to cloudwater. These results indicate that micromolar concentrations of Fe(III) decrease H2O2 yields and can even lead to H2O2 loss rather than formation. Implications on cloud chemistry are discussed. DOE

N90-19731# Sandia National Labs., Albuquerque, NM. Electromagnetic Testing.
SIMULATION FIDELITY IN LIGHTNING PENETRATION STUDIES
R. J. Fisher and M. A. Uman (Florida Univ., Gainesville.) Feb. 1990 33 p
(Contract DE-AC04-76DP-00789)
(DE90-006367; SAND-89-3051) Avail: NTIS HC A03/MF A01

An extensive literature review has been conducted as part of an effort to quantify the fidelity of Sandia's lightning burn-through simulation technique. The dominant parameters affecting damage have been identified and are discussed. Two alternative techniques for qualitatively improving the Sandia simulation have been identified, but quantification of the correlation of the results of each with those of natural lightning awaits completion of further experimental work. A systematic set of laboratory experiments is proposed to assess the sensitivity of each technique to key simulation parameters. An available calibration linkage to natural lightning is the reproduction of damage spots that were created by lightning on a set of copper disks mounted on TV towers, and an attempt to do this is included in the proposed experiments. In order to reduce the uncertainties of this approach, more lightning-spot data are required, along with records of the flash currents that produced them. It is recommended that such data be acquired in conjunction with the Rocket-Triggered Lightning Program being conducted each summer at the Kennedy Space Center. DOE

N90-19394*# Texas Technological Univ., Lubbock. Atmospheric Science Group.
A PBL-RADIATION MODEL FOR APPLICATION TO REGIONAL NUMERICAL WEATHER PREDICTION
Chia-Bo Chang *In* Alabama Univ., Research Reports: 1989 NASA/ASEE Summer Faculty Fellowship Program Dec. 1989 21 p (For primary document see N90-19390 12-31)
(Grant NGT-01-008-021)
Avail: NTIS HC A99/MF E06 CSCL 04B

48 OCEANOGRAPHY

Includes biological, dynamic, and physical oceanography; and marine resources.

For related information see also *43 Earth Resources and Remote Sensing.*

N90-19732# National Oceanic and Atmospheric Administration, Miami, FL. Oceanography and Meteorological Lab.
DRIFTING BUOY DATA FROM WESTERN TROPICAL PACIFIC FOR THE PERIOD FEBRUARY 1, 1986 THROUGH FEBRUARY 28, 1989
Liao Qiyu (National Bureau of Oceanography, Qingdao, China) and Mayra C. Pazos Jul. 1989 131 p
(PB90-113978; NOAA-DR-ERL-AOML-14) Avail: NTIS HC A07/MF A01 CSCL 08C

Satellite-tracked drifting buoy data is presented which was collected in the Western Tropical Pacific Ocean as part of The People's Republic of China and U.S. cooperative study air-sea interaction in the Western Tropical Pacific program. The data covers the deployed drifting buoy from cruise 1 to cruise 4. One of the tables details deployment time and locations and end time and locations of each buoy. Author

N90-19733# Instituto de Pesquisas Espaciais, Sao Jose dos Campos (Brazil).
EVOLUTION OF FINITE AMPLITUDE BAROCLINIC WAVES IN THE ATMOSPHERE AND OCEAN Ph.D. Thesis [EVOLUCAO PARA AMPLITUDE FINITA DAS ONDAS BAROCLINICAS NA ATMOSFERA E NO OCEANO]
Jose Paulo Bonatti Dec. 1988 300 p In PORTUGUESE; ENGLISH summary
(INPE-4752-TDL/346) Avail: NTIS HC A13/MF A02

Two multi-level models are developed: a linear quasi-geostrophic and a balance nonlinear model with Rayleigh frinction and Newtonian cooling. Both models take into account the latent release, parameterized with Mak's wave-CISK scheme and are used to study the proprieties of baroclinic disturbances in the atmosphere. The models are applied with some modifications to the baroclinic waves in the ocean. From a linear point of view, the atmospheric intermediate-scale (1000 - 2000 km) perturbations, with assoicated comma clouds observed over North Pacific and South Central South America, and the oceanic mesoscale (200 - 400 km) disturbances found near the Brazilian and Falkland currents confluence zone, seem to be generated by baroclinic instability. In the atmospheric case the baroclinic instability is modified by humidity effects. Nongeostrophic, nonlinear effects due to a single original wave are superimposed on the linear fields given by the most unstable wave for both amotpheric and oceanic cases. Characteristics very similar to observations are obtained in the evolution to finite amplitude. In the atmospheric case, the latent heat release is found to be a fundamental factor to obtain realistic horizontal and vertical cloud structures. The evolution of the thermal rings in the oceanic case is very well reproduced by the nonlinear model. In both the atmospheric and oceanic cases, the stages of saturation are not reached since the feedback to thermal basic states is not included. Another atmospheric case, starting from an initial linear dry frontal configurations, is also studied. Again the inclusion of latent heat of condensation is found to be crucial in determining not only the cloud structures, but also the upper level flow structure. It is also found that dissipation is important for the structure of potential temperature, principally in the lower levels. Author

N90-19734# Technische Univ., Delft (Netherlands). Faculteit der Geodesie.
EARTH TIDAL ANALYSIS BASED ON GRAVIMETER OBSERVATIONS AND THE INFLUENCE OF OCEAN TIDES Thesis [EEN AARDGETIJDENANALYSE UIT ZWAARTEKRACHTSWAARNEMINGEN EN DE INVLOED VAN ZEEGETIJDEN]
W. T. deVries Oct. 1988 89 p In DUTCH
(ETN-90-95721) Avail: NTIS HC A05/MF A01

An Earth tidal analysis based on gravimeter observations was performed, and the effects of ocean tides on Earth tides were investigated. The theory of tides in general and that of Earth tides in particular is outlined. The tidal analysis method for gravimeter observations is presented. The effects of ocean tides on the gravity on Earth are calculated using loading numbers and Green function of quality factors and energy dissipation. It is concluded that a more extensive analysis is required, with more attention to software and observation dependent effects, and that ellipsoidal and rotational effects have to be taken into account in the theoretical determination of tidal factors. ESA

N90-19735 Royal Netherlands Meteorological Inst., De Bilt. Afdeling Dynamische Meteorologie.
STATUS OF A NONLINEAR WATER SURGE MODEL IN FEBRUARY 1988 [NAAR EEN NIET-LINEAIR WATEROPZETMODEL; STAND VAN ZAKEN FEBRUARI 1988]
C. J. Kok 1988 114 p In DUTCH
(KNMI-WR-88-03; ISSN-0169-1651; ETN-90-95599) Copyright Avail: Royal Netherlands Meteorological Institute, P.O. Box 201, 3730 AE de Bilt, Wilhelminalaan 10, Netherlands

The status after one year's experience with the IOS (Institute of Oceanographic Sciences, Bidston, England) water surge model is evaluated. The modifications performed in the model are described; nonlinear interactions were introduced because the model did not fulfill the Waddenzee-Eensmand correction. The simulation of the nonlinear interaction is largely determined by the quality of the model tide description. A correction of the wind speed in coastal areas was made. The results of the present model are presented, and the possible origins of errors are discussed. Developments with a view to improvements in the model are suggested. ESA

51 LIFE SCIENCES (GENERAL)

N90-19736# London Univ. (England). Toxicology Unit.
STUDY OF HYDRAZINE METABOLISM AND TOXICITY Annual Report No. 1, 15 Sep. 1988 - 14 Sep. 1989
J. A. Timbrell 13 Nov. 1989 36 p
(Grant AF-AFOSR-0313-88; AF Proj. 2301)
(AD-A217103; EOARD-TR-90-013) Avail: NTIS HC A03/MF A01 CSCL 02/5

The research project studying hydrazine in rats has revealed the following: (1) The uptake of hydrazine into the liver may be a saturable process; (2) After a hepatotoxic dose of hydrazine the concentration in the liver is about 0.2mM; (3) Some hydrazine remains in the liver 24 hours after a single dose at a level higher than the plasma level; (4) At the highest dose level (81mg/kg) rats lost weight over the following 4 days and liver weight was decreased. At a dose of 27mg/kg, the liver weight was elevated 4 days after the single dose; (5) The rats given the highest dose still showed fatty liver 4 days after dosing. Rats given lower doses also showed some vacuolation in hepatocytes; (6) Determination of hydrazine and acetylhydrazine in urine after various single doses showed a dose dependent decrease in acetylation; (7) NMR revealed a number of metabolites: unchanged hydrazine, acetyl and diacetylhydrazine, hydrazones with pyruvate and 2-oxoglarate, urea and ammonia; (8) Studies in hepatocytes have shown that hydrazine is cytotoxic at concentrations of 16mM and above; (9) Hepatocyte studies have also shown that 8mM hydrazine depletes ATP and glutathione; and (10) Preliminary studies in microsomes have shown that hydrazine is metabolised by a cytochrome P450 dependent system. Chemical breakdown and other enzymic breakdown are also involved however. GRA

52 AEROSPACE MEDICINE

Includes physiological factors; biological effects of radiation; and effects of weightlessness on man and animals.

N90-19737# Oregon Univ., Eugene. Dept. of Psychology.
VISUAL PROCESSING IN TEXTURE SEGREGATION Annual Report, 1 Sep. 1988 - 30 Sep. 1989
Jacob Beck 29 Nov. 1989 64 p
(Grant AF-AFOSR-0323-88; AF Proj. 2313)
(AD-A216539; AFOSR-89-1780TR) Avail: NTIS HC A04/MF A01 CSCL 12/9

Beck (1988) reported that the outputs of 2-D Gabor filters can account for much of the segregation of a periodic visual display (tripartite pattern) into regions. We have conducted a series of experiments showing that grouping processes, as well as the outputs of spatial-frequency/orientation channels, yield automatic spontaneous segregation. In our tripartite patterns, the arrangement of local properties is different in different regions so that if the display is suitably filtered by convolving the appropriate property at each point, or by performing some equivalent filtering process in the Fourier domain, the regions in the filtered display differ in different regions. We have shown that this type of computation is not able to account for the spontaneous segregation of a line in a display of disconnected shapes. A striking finding reported by Beck (1988) was that squares differing by a large lightness difference sometimes failed to give region segregation in a tripartite pattern while the same pattern of squares differing by a smaller lightness differences yielded strong region segregation. GRA

N90-19738 Institute for Perception RVO-TNO, Soesterberg (Netherlands). Afdeling Audiologie.
VESTIBULAR EXAMINATION OF MOTION SICK STUDENT PILOTS
W. Bles Dec. 1988 19 p In DUTCH; ENGLISH summary
(Contract A83/KLu/115)
(IZF-1988-22; TD-89-0531; ETN-90-95091) Copyright Avail: Institute for Perception RVO-TNO, P.O. Box 23, 3769 ZG Soesterberg, Netherlands

Seventeen student pilots of the Royal Dutch Air Force who experience severe motion sickness problems were examined on their equilibrium function. The results were evaluated with a view to selection tests of motion sickness susceptibility. Although presently there is no appropriate control group of experienced pilots, comparison with normal individuals indicates that Coriolis tests with congruent and incongruent sensory information can be useful. ESA

N90-19739# National Aerospace Medical Centre, Soesterberg (Netherlands).
[ACTIVITIES IN AEROSPACE MEDICINE] Annual Report, 1987 [JAARVERSLAG 1987]
1987 41 p In DUTCH
(ETN-90-95468) Avail: NTIS HC A03/MF A01

The medical examinations of the personnel are tabulated and discussed. Research and development activities were performed in fields of psychodiagnostic examination and selection, ophthalmology, general medical examination, flight physiology, and the mental stress of helicopter pilots. ESA

N90-19740# Minnesota Univ., Duluth. Dept. of Biochemistry.
METABOLISM, SEIZURES, AND BLOOD FLOW IN BRAIN FOLLOWING ORGANOPHOSPHATE EXPOSURE: MECHANISMS OF ACTION AND POSSIBLE THERAPEUTIC AGENTS Annual Summary Report, 21 Oct. 1986 - 20 Oct. 1987
Lester R. Drewes and Padala V. Reddy 25 Aug. 1989 42 p
(Contract DAMD17-86-C-6036; DA Proj. 3M1-61102-BS-10)
(AD-A217098) Avail: NTIS HC A03/MF A01 CSCL 15/6

The acute neurotoxicity of the organophosphorus (OP) compounds soman and sarin was investigated using the isolated, perfused canine brain preparation. Intracarotid injection of soman (100 ug) or sarin (400 ug) produced immediate vasodilation and seizure within 4 to 6 min. Rapid, large increases in cerebral metabolic rates for glucose, oxygen, lactate, and carbon dioxide were observed during seizure. To investigate the cholinergic mechanisms of OP-induced seizure and vasodilation, oxotremorine (10 uM), a muscarinic agonist, and arecoline (1 uM and 20 uM), a muscarinic and nicotinic agonist, were used. Both agonists quickly induced vasodilation but not seizure. When soman was injected, additional vasodilation occurred in brains pretreated with arecoline but not with oxotremorine; however, soman-induced seizure and hypermetabolism occurred in brains pretreated with arecoline. Oxotremorine treatment caused a substantially greater increase in glucose than in oxygen metabolism. Based on our results with cholinergic agonists and antagonists, the development of seizure and the vasodilation induced by OP agents are separate and independent responses. Consequently, independent mechanism(s) must exist for OP-induced cerebral vasodilation. GRA

53 BEHAVIORAL SCIENCES

Includes psychological factors; individual and group behavior; crew training and evaluation; and psychiatric research.

N90-19741*# BBN Systems and Technologies Corp., Cambridge, MA.
FLIGHT CREW AIDING FOR RECOVERY FROM SUBSYSTEM FAILURES Final Report
E. Hudlicka, K. Corker, R. Schudy, and Sheldon Baron Jan. 1990 97 p
(Contract NAS1-17335)
(NASA-CR-181905; NAS 1.26:181905; Rept-6990) Avail: NTIS HC A05/MF A01 CSCL 05I

Some of the conceptual issues associated with pilot aiding systems are discussed and an implementation of one component of such an aiding system is described. It is essential that the format and content of the information the aiding system presents to the crew be compatible with the crew's mental models of the task. It is proposed that in order to cooperate effectively, both the aiding system and the flight crew should have consistent information processing models, especially at the point of interface. A general information processing strategy, developed by Rasmussen, was selected to serve as the bridge between the human and aiding system's information processes. The development and implementation of a model-based situation assessment and response generation system for commercial transport aircraft are described. The current implementation is a prototype which concentrates on engine and control surface failure situations and consequent flight emergencies. The aiding system, termed Recovery Recommendation System (RECORS), uses a causal model of the relevant subset of the flight domain to simulate the effects of these failures and to generate appropriate responses, given the current aircraft state and the constraints of the current flight phase. Since detailed information about the aircraft state may not always be available, the model represents the domain at varying levels of abstraction and uses the less detailed abstraction levels to make inferences when exact information is not available. The structure of this model is described in detail. Author

N90-19742# Air War Coll., Maxwell AFB, AL.
PILOT CANDIDATE SELECTION
Robert M. Negley, Jr. and Gerald V. Boesche May 1989 121 p
(AD-A217296) Avail: NTIS HC A06/MF A01 CSCL 05/9

With the demand for pilots, there is a need to produce a better finished product from Undergraduate Pilot Training. The answer would seem to be Specialized Undergraduate Pilot Training, which is what the U.S. Air Force and Air Training Command are advocating and have been for years. Much research and development has been done, especially in the last 10 years, to come up with a better selection system for pilot candidates. An improved selection system would help decrease attrition and could be used for earlier track selection for Specialized Undergraduate Pilot Training. This paper evaluates the current selection system

and the selection methods and tools that are available and could be used in the future. The main focus is on what selection criteria is the best predictor of success and should be used in the future to select candidates for pilot training. GRA

54 MAN/SYSTEM TECHNOLOGY AND LIFE SUPPORT

Includes human engineering; biotechnology; and space suits and protective clothing.

For related information see also *16 Space Transportation.*

N90-19743# Army Test and Evaluation Command, Aberdeen Proving Ground, MD.
HUMAN FACTORS ENGINEERING TESTING OF AIRCRAFT COCKPIT LIGHTING SYSTEMS Final Report
2 Aug. 1989 28 p
(AD-A216853; TOP-7-2-513) Avail: NTIS HC A03/MF A01 CSCL 01/3

The procedures, test equipment and facilities are specified to perform tests and evaluations of aircraft cockpit lighting systems. The topics include display luminance, illuminance, contrast, balance, uniformity, sunlight readability, display color, night vision goggle compatibility, crewstation reflections and mockup evaluations. These procedures are closely tied to U.S. Army lighting requirements. GRA

N90-19744# Los Alamos National Lab., NM. Dept. of Earth and Environmental Sciences.
WORKING ON THE MOON: THE APOLLO EXPERIENCE
Eric M. Jones 1989 11 p Presented at the Engineering, Construction and Operations for Space, Albuquerque, NM, Apr. 1990
(Contract W-7405-eng-36)
(DE90-003662; LA-UR-89-3858; CONF-900442-3) Avail: NTIS HC A03/MF A01

The successful completion of any scientific or engineering project on the moon will depend, in part, on human ability to do useful work under lunar conditions. In making informed decisions about such things as the use of humans rather than robots for specific tasks, the scheduling of valuable human time, and the design and selection of equipment and tools, good use can be made of the existing experience base. During the six completed landing missions, Apollo lunar surface crews conducted 160 astronaut-hours of extra-vehicular activities (EVAs) and also spent a similar sum of waking hours working in the cramped confines of the Lunar Module. The first three missions were primarily proof-tests of flight hardware and procedures. The ability to land equipment and consumables was very modest but, despite stay times of no more than 32 hours, the crews of Apollos 11, 12, and 14 were able to test their mobility and their capability of doing useful work outside the spacecraft. For the last three missions, thanks to LM modifications which enabled landings with significant amounts of cargo, stay times more than doubled to three days. The crews were able to use Lunar Rovers to conduct extensive local exploration and to travel up to 10 kilometers away from their immediate landing sites. DOE

N90-19745# Oak Ridge National Lab., TN. Center for Engineering Systems Advanced Research.
AN APPROACH TO ELEMENTAL TASK LEARNING
Philippe Belmans 1990 11 p Presented at the 8th SPIE Applications of Artificial Intelligence Conference, Orlando, FL, 17-19 Apr. 1990
(Contract DE-AC05-84OR-21400)
(DE90-006614; CONF-9004125-1) Avail: NTIS HC A03/MF A01

In this article we deal with the automated learning of tasks by a robotic system through observation of a human operator. Particularly, we explain what is meant by a learning ability in autonomous robots and in teleoperation systems, where several operators and several machines may work in cooperation to perform tasks. We discuss different approaches to learning in these systems and outline the features of the models they are based upon. This leads us to choose an analytical model suited for tasks analysis. We then present the software architecture for our proposed approach and show the first results obtained on sample tests. DOE

N90-19746# Oak Ridge National Lab., TN.
A HUMAN FACTORS TESTBED FOR GROUND-VEHICLE TELEROBOTICS RESEARCH
G. K. Corbett, S. M. Killough, B. S. Richardson, and M. Herman (National Inst. of Standards and Technology, Gaithersburg, MD.) 1990 4 p Presented at the IEEE Southeastcon, New Orleans, LA, 1-4 Apr. 1990
(Contract DE-AC05-84OR-21400)
(DE90-006618; CONF-900464-4) Avail: NTIS HC A01/MF A01

A human factors testbed has been designed for the U.S. Army Human Engineering Laboratory to experiment in the area of remote control of wheeled vehicles. The testbed's capabilities have been demonstrated by remotely driving a high maneuverability and mobility wheeled vehicle (HMMWV). Details of testbed design and experiments are presented. DOE

N90-19747# Oak Ridge Gaseous Diffusion Plant, TN.
REPORT OF THE FIRST ANNUAL AIRBORNE WEAPONS TRAINING TECHNOLOGY REVIEW
Cathrine E. Snyder, ed., Gail B. Payne, ed., and Inga E. Treitler, ed. (Tennessee Univ., Knoxville.) Jan. 1990 56 p Review held in Oak Ridge, TN, 29-31 Mar. 1989
(Contract DE-AC05-84OT-21400)
(DE90-007189; K/DSRD-119) Avail: NTIS HC A04/MF A01

The First Annual Airborne Weapons Training Technology Review is documented. It was an exchange of ideas and information among the members of the network supporting the Naval Air Systems Command's (NAVAIR's) PMA205-11, Program Manager for Ordnance Training. The briefings and demonstrations presented at the Review are described, and the discussion at the informal caucus where significant issues were raised from the first two days' presentations are summarized. The meeting agenda, a participant list with addresses and telephone numbers, a list of the Department of Defense activities represented, NAVAIR's follow-up communication, and a brief description of Martin Marietta Energy Systems, Inc.'s training technology project support are presented. A broad range of topics related to training systems and training support was covered during the Review. Synopses of the presentations and demonstrations included here cover computer-based and interactive systems, portability of software, reuse of training systems for different weapons, standardization of trainers, instructional systems design, cognitive task analysis, tracking of training resources, and the application of Computer-aided Acquisition and Logistic Support. DOE

N90-19748# Douglas Aircraft Co., Inc., Long Beach, CA.
ASSESSMENT OF CREW WORKLOAD MEASUREMENT METHODS, TECHNIQUES AND PROCEDURES. VOLUME 2: GUIDELINES FOR THE USE OF WORKLOAD ASSESSMENT TECHNIQUES IN AIRCRAFT CERTIFICATION Final Report, Jul. 1986 - Feb. 1989
William H. Corwin, Diane L. Sandry-Garza, Michael A. Biferno, and George P. Boucek, Jr. 12 Sep. 1989 51 p Prepared in cooperation with Boeing Commercial Airplanes, Seattle, WA Sponsored in part by FAA
(Contract F33615-86-C-3600; AF Proj. 2403)
(AD-A217067; WRDC-TR-89-7006-Vol-2) Avail: NTIS HC A04/MF A01 CSCL 05/9

The purpose of Volume 2 is to present specific guidelines and recommendations for evaluating workload certification plans. No attempt is being made to provide a list of simple-to-follow directions for the generation of an aircraft workload certification plan, as this is the responsibility of the manufacturer. The workload assessment techniques are discussed by domain area: Subjective, Physiological, Performance, and Analytic techniques. The distinction

by domain is convenient because of the methods and equipment in common among techniques within a domain. Evaluation criteria for assessing a workload certification plan includes treatment of the validity, reliability, and applicability of candidate workload measures. For a workload measure to demonstrate validity, it must be able to discriminate among varying task demands imposed upon the flightcrew. In order for a measure to demonstrate reliability, it should provide the same results with repeated applications. Applicability is simply the ability for workload to be assessed in an aircraft flightdeck environment. GRA

55 SPACE BIOLOGY

Includes exobiology; planetary biology; and extraterrestrial life.

N90-19749 Maharishi International Univ., Fairfield, IA.
THE EFFECTS OF COLD DARK MATTER ON BIG BANG NUCLEOSYNTHESIS Ph.D. Thesis
Ronald John David Parker 1989 134 p
Avail: Univ. Microfilms Order No. DA8918486

The annihilation of cold, weakly-interacting dark matter candidates (chi) subsequent to chi chi freeze-out can significantly affect the primordial abundance of light elements. The largest effects are between the n/p freeze-out temperature and the onset of nucleosynthesis at T is approximate or equal to 0.1 MeV, chi chi annihilations increase the n/p ratio, leading to increased He-4 production; following He-4 synthesis, baryonic products of n, n(-), and p(-) of chi chi annihilations dissociate some of the He-4 into D and He-3, leading to increased D + He-3 abundances; toward the end of nucleosynthesis, neutrons from chi chi annihilation lead to n + Be-7 yields p + Li-7, resulting in increased Li-7 + Be-7 production for low values of eta is equivalent to n(sub b)/n(sub gamma) and decreased Li-7 + Be-7 production for large eta; and long after nucleosynthesis, once the universe cools below T approximatly equal to 1 keV, the electromagnetic shower produced by electrons, positrons, and photons from residual chi chi annihilations cause further dissociation of He-4, leading to increased CD + He-3 abundances. The most important result is that for Direc and Majorna neutrinos, the Li-7 constraints on eta from the Standard Big Band Nucleosynthesis (SBBN) are noticeably affected, with larger values of eta being favored. A summary of scattering rates for processes in the electromagnetic shower, containing corrections to numerous misprints in other sources is presented. A listing of FORTRAN code used in the shower calculations is also included. Dissert. Abstr.

59 MATHEMATICAL AND COMPUTER SCIENCES (GENERAL)

No abstracts in this category.

60 COMPUTER OPERATIONS AND HARDWARE

Includes hardware for computer graphics, firmware, and data processing.

For components see *33 Electronics and Electrical Engineering.*

N90-19750 Department of the Navy, Washington, DC.
HIGH SPEED MODEM Patent
Paul J. Giorgio, inventor (to Navy) 29 Aug. 1989 14 p Filed 4 May 1988
(AD-D014319; US-Patent-4,862,456; US-Patent-Appl-SN-195991)
Avail: US Patent and Trademark Office CSCL 12/6

A multiline modem system provides to a computer connection a plurality of telephone lines for transmitting and receiving digital computer data at throughput rates that exceed those of single line modem systems. The system determines the number of available telephone lines, sequences through a series of telephone re-dials, and acknowledges all connections. When the last connection is verified, the system is on-line and data transfer can begin. The system described uses state-of-the-art components and meets FCC Part 68 requirements for connection to the switched telephone network. GRA

N90-19751# Ohio State Univ., Columbus. Dept. of Computer and Information Science.
HIGH-LEVEL CONNECTIONIST MODELS Semiannual Report
Jordan B. Pollack Aug. 1989 87 p
(Contract N00014-89-J-1200)
(AD-A216581) Avail: NTIS HC A05/MF A01 CSCL 12/9

The significant revision and extension of the Recursive Auto-Associative Memory (RAAM) work for publication in the journal Artificial Intelligence was achieved. Included as an appendix to this report, the article includes several new elements: (1) Background - The work was more clearly set into the area of recursive distributed representations, machine learning, and the adequacy of the connectionist approach for high level cognitive modeling; (2) New Experiment - RAAM was applied to finding compact representations for sequences of letters; (3) Analysis - The developed representations were analyzed as features which range from categorical to distinctive. Categorical features distinguish between conceptual categories while distinctive features vary within categories and discriminate or label the members. The representations were also analyzed geometrically; and (4) Applications - Feasibility studies were performed and described on inference by association, and on using RAAM-generated patterns along with cascaded networks for natural language parsing. Both of these remain long term goals of the project. GRA

N90-19752# Technische Univ., Berlin (Germany, F.R.). Fachbereich Informatik.
DESIGN AND ARCHITECTURE OF FOURTH AND FIFTH GENERATION SOFTWARE ENGINEERING ENVIRONMENTS Ph.D. Thesis [KONZEPTE UND ARCHITEKTUREN VON SOFTWARE-ENTWICKLUNGS-UMGEBUNGEN DER VIERTEN UND FUENFTEN GENERATION]
Joerg Richter 1989 269 p In GERMAN
(ETN-90-95365) Avail: NTIS HC A12/MF A02

A system is presented whose principal aspects are: closing of the gap between user and software engineer, integration of software development tools, software development in large projects and knowledge based software development. The proposed system consists of a data base manager suited to the language C, data base administration and business graph, another data base manager with a programming language unity for COBOL, FORTRAN and PASCAL, a terminology control applied to indexation of data and texts, a controlled information exchange used for pictures and graphics, exchange of documents in text, direct communication, information retrieval and diffusion and so on and a diagnostic, classifying expert system shell. ESA

N90-19753# Oak Ridge National Lab., TN.
A VIRTUAL ZERO-TIME, MONOLITHIC SYSTOLIC SORTING ARRAY
C. L. Britton, Jr., M. N. Ericson, and D. W. Bouldin (Tennessee Univ., Knoxville.) 1990 12 p Presented at the IEEE Southeastcon, New Orleans, LA, 1-4 Apr. 1990
(Contract DE-AC05-84OR-21400)
(DE90-001000; CONF-900464-1) Avail: NTIS HC A03/MF A01

A virtual zero-time monolithic sorting chip is described. The chip has a systolic array architecture and implements the sinking sort algorithm. The basic functional module of the systolic array is detailed and development techniques employed as well as

functional simulation and results are presented. Lessons learned and educational significance of the development of this chip at a university are discussed. DOE

N90-19754# Universitaet der Bundeswehr Muenchen, Neubiberg (Germany, F.R.). Fakulaet fuer Elektrotechnik.
MARGINAL TEST AND ANALYSIS OF DRAM WITH MASKED ALPHA RADIATION Ph.D. Thesis [MARGINALTEST UND ANALYSE VON DRAM'S MIT MASKIERTER ALPHA-BESTRAHLUNG]
Dieter Gleis 1988 89 p In GERMAN
(RB-4180; ETN-90-96068) Avail: NTIS HC A05/MF A01

A measure process is developed, with which the alpha sensitivity of individual parts of the Direct Random Access Memory (DRAM) can be measured. Only the examined parts are radiated; this allows separate measuring of the soft error rates of the bit conductors, reference bit conductors and values for every supply voltage, timing, and all rythyms. A test measures the change reserves qualitatively for all working conditions. The DRAM design failures and technology oscillations can also be analyzed, such as asymmetric values or word conductor low voltages. For a 1 m DRAM, the surface values are only a small part of the memory, but they are nearly exclusively responsible for the soft error rate of the memory. ESA

N90-19755# National Aeronautical Lab., Bangalore (India). Computational and Theoretical Fluid Dynamics Div.
FLOSOLVER Mk1B: AN EIGHT PROCESSOR PARALLEL MACHINE
C. R. Sreenivasan, Rajalakshmy Sivaramakrishnan, and V. R. Sarasamma Dec. 1989 25 p
(PD-CF-8941) Avail: NTIS HC A03/MF A01

Flosolver Mk1B has been operational since November 1987. The Flosolver Mk1B has two nodes, each having four processing elements based on Intel's 8086/8087 chips. In each node one of the processors acts as the host. The internode communication is done through the parallel ports available on the hosts. Within a node the synchronization and inter-processor communication is done through the global memory. As a sample case the flow past NACA 0012 aerofoil at zero incidence using Transonic Small Perturbation equation is computed and an efficiency of 90 percent is obtained. Author

N90-19443*# Jet Propulsion Lab., California Inst. of Tech., Pasadena.
MEMORY MANAGEMENT IN TRACEBACK VITERBI DECODERS
O. Collins (Johns Hopkins Univ., Baltimore, MD.) and F. Pollara *In its* The Telecommunications and Data Acquisition Report 15 Nov. 1989 p 98-104 (For primary document see N90-19434 12-32)
Avail: NTIS HC A10/MF A02 CSCL 09B

61 COMPUTER PROGRAMMING AND SOFTWARE

Includes computer programs, routines, alogorithms, and specific applications, e.g., CAD/CAM.

N90-19756# National Aerospace Lab., Amsterdam (Netherlands). Structures and Materials/Informatics Div.
COCOMAT: A COMPUTER AIDED ENGINEERING (CAE) SYSTEM FOR COMPOSITE STRUCTURES DESIGN
H. J. W. M. Koelman and H. W. Veerbeek 26 Nov. 1987 18 p Presented at the Computer Aided Design in Composite Material Technology CADCOMP 1988, Southampton, England, 13-15 Apr. 1988 Previously announced in IAA as A89-19981
(Contract NIVR-03506N)
(NLR-MP-87078-U; ETN-89-94047) Avail: NTIS HC A03/MF A01

Capabilities of a system called COCOMAT are given as an example of a CAE system for assistance during the preliminary design phase of a structure. The features of the system are illustrated with an example of the design of a post-buckled, hat stiffened, composite wing panel. ESA

N90-19757*# Houston Univ., Clear Lake, TX. Research Inst. for Computing and Information Systems.
DEVELOPMENT OF AN Ada PROGRAMMING SUPPORT ENVIRONMENT DATABASE SEAD (SOFTWARE ENGINEERING AND Ada DATABASE) ADMINISTRATION MANUAL
Morris Liaw and Donna Evesson (GHG Corp., Houston, TX.) Dec. 1988 161 p
(Contract NCC9-16)
(NASA-CR-186064; NAS 1.26:186064) Avail: NTIS HC A08/MF A01 CSCL 09B

Software Engineering and Ada Database (SEAD) was developed to provide an information resource to NASA and NASA contractors with respect to Ada-based resources and activities which are available or underway either in NASA or elsewhere in the worldwide Ada community. The sharing of such information will reduce duplication of effort while improving quality in the development of future software systems. SEAD data is organized into five major areas: information regarding education and training resources which are relevant to the life cycle of Ada-based software engineering projects such as those in the Space Station program; research publications relevant to NASA projects such as the Space Station Program and conferences relating to Ada technology; the latest progress reports on Ada projects completed or in progress both within NASA and throughout the free world; Ada compilers and other commercial products that support Ada software development; and reusable Ada components generated both within NASA and from elsewhere in the free world. This classified listing of reusable components shall include descriptions of tools, libraries, and other components of interest to NASA. Sources for the data include technical newletters and periodicals, conference proceedings, the Ada Information Clearinghouse, product vendors, and project sponsors and contractors. Author

N90-19758*# Houston Univ., Clear Lake, TX. Research Inst. for Computing and Information Systems.
OBJECT ORIENTED PROGRAMMING SYSTEMS (OOPS) AND FRAME REPRESENTATIONS: AN INVESTIGATION OF PROGRAMMING PARADIGMS Final Report
David Auty (Softech, Inc., Houston, TX.) 31 Jul. 1988 21 p
(Contract NCC9-16)
(NASA-CR-186084; NAS 1.26:186084) Avail: NTIS HC A03/MF A01 CSCL 09B

The project was initiated to research Object Oriented Programming Systems (OOPS) and frame representation systems, their significance and applicability, and their implementation in or relationship to Ada. Object orientated is currently a very popular conceptual adjective. Object oriented programming, in particular, is promoted as a particularly productive approach to programming; an approach which maximizes opportunities for code reuse and lends itself to the definition of convenient and well-developed units. Such units are thus expected to be usable in a variety of situations, beyond the typical highly specific unit development of other approaches. Frame represenation systems share a common heritage and similar conceptual foundations. Together they represent a quickly emerging alternative approach to programming. The approach is to first define the terms, starting with relevant concepts and using these to put bounds on what is meant by OOPS and Frames. From this the possibilities were pursued to merge OOPS with Ada which will further elucidate the significant characteristics which make up this programming approach. Finally, some of the merits and demerits of OOPS were briefly considered as a way of addressing the applicability of OOPS to various programming tasks. Author

N90-19759# Massachusetts Inst. of Tech., Cambridge. Artificial Intelligence Lab.
ON THE VERIFICATION OF HYPOTHESIZED MATCHES IN MODEL-BASED RECOGNITION

W. Eric L. Grimson and Daniel P. Huttenlocher (Cornell Univ., Ithaca, NY.) May 1989 22 p
(Contracts N00014-86-K-0685; N00014-85-K-0124)
(AD-A214718; AI-M-1110) Avail: NTIS HC A03/MF A01 CSCL 12/9

In model-based recognition a number of ad hoc techniques are used to decide whether or not a match of data to a model is correct. Generally an empirically determined threshold is placed on the fraction of model features that must be matched. In this paper we present a more rigorous approach in which the conditions under which to accept a match are derived based on fundamental grounds. We obtain an expression that relates the probability of a match occurring at random to the reaction of a model features that are accounted for by the match. This expression is a function of the number of model features, the number of image features, and a bound on the degree on the degree of sensor noise. One implication of our analysis is that a proper threshold for matching must vary with the number of model and data features. Thus, it is important to be able to set the threshold as a function of a particular matching problem, rather than setting a single threshold based on experimentation. We analyze some existing recognition systems and find that our method yields thresholds similiar to the ones determined empirically for these systems, providing evidence of the validity of the technique. GRA

N90-19760# National Telecommunications and Information Administration, Boulder, CO. Inst. for Telecommunication Sciences.
USER-FRIENDLY SOFTWARE FOR THE DESIGN OF DIGITAL LINE-OF-SIGHT RADIO LINKS
J. E. Farrow and S. L. Rothschild Aug. 1989 66 p Sponsored by Army Information Systems Engineering Command, Fort Huachuca, AZ
(PB90-118472; NTIA-89-246) Avail: NTIS HC A04/MF A01 CSCL 09B

Digital Line-of-Sight (DLOS) computer programs and the operating instructions for them are presented. These programs, which run on a desk-top computer, automate the calculations involved in design of line-of-sight microwave radio relay paths. The programs manipulate information about earth geometry, terrain profiles, ray paths, median basic transmission loss, variability of loss, equipment effects, and path performance. The computer hardware and software configurations are designed to be convenient to operate and to give the design engineer immediate access to calculated results corresponding to changes in design parameters. The programs are intended to be used interactively by persons having no experience in programming. The algorithms may be applied over a wide range of path parameters. The frequency range is from 1 GHz to 10 GHz; the path length may be up to 200 km; and the path must have adequate terrain clearance. GRA

N90-19761# PK Corp., Storrs, CT.
RANDOM ACCESS TRANSMISSION ALGORITHMS FOR DATA LOCAL AREA NETWORKS Final Report, 15 Sep. 1987 - 15 Sep. 1989
P. Papantoni-Kazakos 24 Oct. 1989 11 p
(Contract F49620-87-C-0107; AF Proj. D822)
(AD-A216443; PKC-TR-89-3; AFOSR-89-1718TR) Avail: NTIS HC A02/MF A01 CSCL 12/7

The objective of this research is to address some of the fundamental issues that arise in the modeling, analysis and design of interconnected wire and radio Local Area Networks (LANs). In the case of wire LANs, the individual LANs are interconnected through store-and-forward devices, which relay packets between adjacent LANs and route them to their final destination. In radio networks, multi-hop packet radio networks that consist of a collection of interconnected local clusters are studied; a local cluster is a single-hop network in which the (possibly mobile) users are within transmission range of each other. The local cluster interconnection is provided by relay nodes that belong to the intersection of two or more local clusters, or by special bridge nodes if local clusters are disjoint. The focus of the research is on the mutual impact of interconnection and access protocols, possible network architectures for interconnecting devices and backbone networks, routing policies, and flow and network-access control for congestion prevention and performance optimization. GRA

N90-19762# Oak Ridge National Lab., TN. Engineering Physics and Mathematics Div.
AN OPTIMIZED ALGORITHM FOR SOLVING THE NODAL DIFFUSION METHOD ON SHARED MEMORY MULTIPROCESSORS
Bernadette L. Kirk and Yousry Y. Azmy 1990 3 p Presented at the Supercomputing in Nuclear Applications, Mito City, Japan, 12-16 Mar. 1990
(Contract DE-AC05-84OR-21400)
(DE90-002703; CONF-900343-1) Avail: NTIS HC A01/MF A01

Nodal methods play a special role in reactor physics calculations. In recent papers the high computational efficiency of nodal methods has been established and the development of more efficient algorithms tailored to the advanced architectures of modern day computers proposed. The rapidly changing architectures of today's computer influence the way codes have to be programmed so that reasonable speed up and efficiency are attained. These concepts were applied in solving the one-group neutron diffusion equation in 2-D geometry on parallel computers like the Intel iPSC/2 hypercube and the Sequent Balance 8000. The efficiency of the hypercube for the neutron diffusion equation is highly determined by the message passing scheme; on the other hand, on a shared memory processor like the Sequent, it is dependent on the manipulation of variables in shared memory. A scheme is presented on shared memory processors which produces very high computing efficiencies in agreement with Amdahl's law. DOE

N90-19763*# City Univ., London (England). Centre for Software Reliability.
RECALIBRATING SOFTWARE RELIABILITY MODELS
Sarah Brocklehurst, P. Y. Chan, Bev Littlewood, and John Snell [1989] 36 p Sponsored in part by Science Research Council; Alvey Directorate; and ICL
(Grant NAG1-771)
(NASA-CR-186407; NAS 1.26:186407) Avail: NTIS HC A03/MF A01 CSCL 09B

In spite of much research effort, there is no universally applicable software reliability growth model which can be trusted to give accurate predictions of reliability in all circumstances. Further, it is not even possible to decide a priori which of the many models is most suitable in a particular context. In an attempt to resolve this problem, techniques were developed whereby, for each program, the accuracy of various models can be analyzed. A user is thus enabled to select that model which is giving the most accurate reliability predictions for the particular program under examination. One of these ways of analyzing predictive accuracy, called the u-plot, in fact allows a user to estimate the relationship between the predicted reliability and the true reliability. It is shown how this can be used to improve reliability predictions in a completely general way by a process of recalibration. Simulation results show that the technique gives improved reliability predictions in a large proportion of cases. However, a user does not need to trust the efficacy of recalibration, since the new reliability estimates produced by the technique are truly predictive and so their accuracy in a particular application can be judged using the earlier methods. The generality of this approach would therefore suggest that it be applied as a matter of course whenever a software reliability model is used. Author

N90-19764*# George Washington Univ., Washington, DC.
A NONPARAMETRIC SOFTWARE RELIABILITY GROWTH MODEL
Douglas R. Miller and Ariela Sofer (George Mason Univ., Fairfax, VA.) Aug. 1988 12 p
(Grant NAG1-771)

(NASA-CR-186438; NAS 1.26:186438) Avail: NTIS HC A03/MF A01 CSCL 09B

Miller and Sofer have presented a nonparametric method for estimating the failure rate of a software program. The method is based on the complete monotonicity property of the failure rate function, and uses a regression approach to obtain estimates of the current software failure rate. This completely monotone software model is extended. It is shown how it can also provide long-range predictions of future reliability growth. Preliminary testing indicates that the method is competitive with parametric approaches, while being more robust. Author

N90-19765*# Maryland Univ., College Park. Dept. of Computer Science.

LESSONS LEARNED IN THE TRANSITION TO ADA FROM FORTRAN AT NASA/GODDARD M.S. Thesis

Carolyn Elizabeth Brophy Aug. 1989 98 p

(Grants NsG-5172; NsG-5123)

(NASA-CR-186458; NAS 1.26:186458; UMIACS-TR-89-84; CS-TR-2305) Avail: NTIS HC A05/MF A01 CSCL 09B

A case study was done at Goddard Space Flight Center, in which two dynamics satellite simulators are developed from the same requirements, one in Ada and the other in FORTRAN. The purpose of the research was to find out how well the prescriptive Ada development model worked to develop the Ada simulator. The FORTRAN simulator development, as well as past FORTRAN developments, provided a baseline for comparison. Since this was the first simulator developed here, the prescriptive Ada development model had many similarities to the usual FORTRAN development model. However, it was modified to include longer design and shorter testing phases, which is generally expected with Ada development. One surprising result was that the percentage of time the Ada project spent in the various development activities was very similar to the percentage of time spent in these activities when doing a FORTRAN project. Another surprising finding was the difficulty the Ada team had with unit testing as well as with integration. In retrospect it is realized that adding additional steps to the design phase, such as an abstract data type analysis, and certain guidelines to the implementation phase, such as to use primarily library units and nest sparingly, would have made development much easier. Author

N90-19766*# Maryland Univ., College Park. Inst. for Advanced Computer Studies.

SOFTWARE DEVELOPMENT: A PARADIGM FOR THE FUTURE

Victor R. Basili Jun. 1989 30 p Sponsored in part by ITALSIEL

(Contract NsG-5123; N00014-87-K-0307; AF-AFOSR-0130-87)

(NASA-CR-186456; NAS 1.26:186456; UMIACS-TR-89-57; CS-TR-2263) Avail: NTIS HC A03/MF A01 CSCL 09B

A new paradigm for software development that treats software development as an experimental activity is presented. It provides built-in mechanisms for learning how to develop software better and reusing previous experience in the forms of knowledge, processes, and products. It uses models and measures to aid in the tasks of characterization, evaluation and motivation. An organization scheme is proposed for separating the project-specific focus from the organization's learning and reuse focuses of software development. The implications of this approach for corporations, research and education are discussed and some research activities currently underway at the University of Maryland that support this approach are presented. Author

N90-19767# Technische Univ., Munich (Germany, F.R.). Lehrstuhl fuer Datenverarbeitung.

ERROR DETECTION IN DATA PROCESSING DEVICES BY MEANS OF RESIDUE CODES Ph.D. Thesis [FEHLERERKENNUNG IN DATENVERARBEITUNGSANLAGEN MITTELS RESIDUEN-CODES]

Markus Bayer 1987 135 p In GERMAN

(ETN-90-95370) Avail: NTIS HC A07/MF A01

The widening of data processing installations by microelectronics requires measures to protect them against hazardous errors. By means of residue codes, data transfer, data processing and memory units are continually examined. Two new codes classes are presented: a multidimensional residue code, with which by an appropriate choice of the parameters unidirectional distortions of data can be corrected in a precise area, and an A-residue-code, that is linear. Based on empirical experiments codes are found which can recognize or correct several errors with a minimal redundancy. Tests show the accuracy of arithmetic and logic operations. Relations between technical realization and code parameter regarding error detection are examined. The process overcost is minimal due to the safety device integrated in the processing system. ESA

N90-19768 Deutsche Geodaetische Kommission, Munich (Germany, F.R.).

DIGITAL PRODUCTION OF PERSPECTIVE IMAGES Ph.D. Thesis - Karlsruhe Univ. [DIGITALE ERZEUGUNG VON PERSPEKTIVBILDERN]

Helmut Kuhn 1989 95 p In GERMAN Original contains color illustrations

(Ser-C-347; ISBN-3-7696-9395-7; ISSN-0065-5325; ETN-90-95884) Copyright Avail: Fachinformationszentrum Karlsruhe, 7514 Eggenstein-Leopoldshafen 2, Federal Republic of Germany

The use of the methods of digital image processing for planning simulations is explained. The production of perspective oblique views from digital produced orthophotographs is given special emphasis. A digital ground model is necessary. The developed process allows the calculation of landscape perspectives from preset viewpoints with any view direction. The circumstances of the monocular deep perception and the aliasing problem are taken into account by a hidden-surface algorithm. Hierarchical images contribute to a realistic landscape representation. The developed program system is modular and can be modified or broadened at any time. The transposition of planning data, such as construction plans or graphs in synthetic perspective images, was also developed. Examples show the combination of planning data from construction and surface exploitation plans with synthetic images. ESA

N90-19769# Technische Univ., Brunswick (Germany, F.R.). Fakultaet fuer Maschinenbau und Elektrotechnik.

POSITIONING CONTROL OF HIGHEST ACCURACY FOR VERY DYNAMIC COUPLED SYSTEM Ph.D. Thesis [STELLANTRIEB HOECHSTER GENAUIGKEIT FUER HOCHDYNAMISCHE, GEKOPPELTE SYSTEME]

Roland Gauggel 1988 169 p In GERMAN

(ETN-90-95893) Avail: NTIS HC A08/MF A01

A tandem positioning control was developed on the basis of simplified mathematic models and justified with a limited degree of confidence by mathematic simulations. The flexible commutation between the digital simulation model and the physical position control seemed unavoidable because of the difficult mathematic description of the motion. The microscopic processes such as friction and plastic and elastic deformations play the principal part in the desired position accuracy. These influences are difficult to represent mathematically. For the validation, HAMIS (hardware as macro in the simulation) was used and gave good results because of its flexibility, speed and easy manageability. It is concluded that the mathematic and digital simulations are both essential. ESA

N90-19770# Los Alamos National Lab., NM.

OBJECT DETECTION AND AMPLITUDE ESTIMATION BASED ON MAXIMUM A POSTERIORI RECONSTRUCTIONS

K. M. Hanson 1990 22 p Presented at the SPIE Technical Conference and Exhibition on Medical Imaging, Newport Beach, CA, 4-9 Feb. 1990

(Contract W-7405-eng-36)

(DE90-007511; LA-UR-90-714; CONF-900238-1) Avail: NTIS HC A03/MF A01

The behavior is reported of the linear maximum a posteriori (MAP) tomographic reconstruction technique as a function of the

assumed rms noise sigma (sub n) in the measurements, which specifies the degree of confidence in the measurement data. The unconstrained MAP reconstructions are evaluated on the basis of the performance of two related tasks; object detection and amplitude estimation. It is found that the detectability of medium-sized discs remains constant up to relatively large sigma (sub n) before slowly diminishing. However, the amplitudes of the discs estimated from the MAP reconstructions increasingly deviate from their actual values as sigma (sub n) increases. DOE

N90-19771# Los Alamos National Lab., NM.
IMAGE MANIPULATION IN THE SIGGRAPH INTERACTIVE PROCEEDINGS
Richard L. Phillips and Richard J. Beach (Xerox Corp., Palo Alto, CA.) 1990 8 p Presented at the SPIE/SPSE Symposium and Exhibition on Electronic Imaging: Science and Technology, Santa Clara, CA, 11-16 Feb. 1990
(Contract W-7405-eng-36)
(DE90-007542; LA-UR-90-540; CONF-900230-1) Avail: NTIS HC A02/MF A01

We built a multimedia document system for the SIGGRAPH Interactive Proceedings to demonstrate the potentials and challenges in using technology to capture better the essence of SIGGRAPH conferences. The prototype system uses the NeXT computer system to present textual, mathematical, illustrative, colorful, audio, video and animated material. Special attention was given to including tools for interactive manipulation of images included in typical SIGGRAPH papers. DOE

N90-19772# Stanford Linear Accelerator Center, CA.
USING REXX TO COORDINATE RELATIONAL COMMANDS
Frank Rothacker Feb. 1990 5 p
(Contract DE-AC03-76SF-00515)
(DE90-007569; SU-SLAC-TN-90-2) Avail: NTIS HC A01/MF A01

Relational technology has drastically reduced, but not eliminated, the need for a procedural language. The main advantage of relational commands is that they can manipulate entire sets of records in complex ways, without the need to loop through files. What remains is coordinating the execution of relational commands. How Rexx may help to fill that void is discussed. DOE

N90-19773# Army Inst. for Research in Management Information and Computer Sciences, Atlanta, GA.
GENERIC DISTRIBUTED SYSTEMS MODEL Final Report
Dharma P. Agrawal Mar. 1989 21 p
(Contract DAAL03-86-D-0001)
(AD-A217078; ASQBG-C-89-024; ARO-TCN-88-048) Avail: NTIS HC A03/MF A01 CSCL 12/7

The term distributed system applies to a very generic class of decentralized systems. It encompasses all systems having geographically distributed multiple processor with some kind of coordination between them. What is expected in a distributed system is an appropriate coordination of data and control among various functional units. (In a networked system, all the computers are autonomous and each one works independently of others, even though messages could be transferred between them.) Various issues associated with the design of distributed systems are identified and an overview is presented of existing modeling efforts. It is felt that the design tools are primarily oriented towards the software design and additional efforts are needed to address the problem in totality. Future directions and recommendations are also included. GRA

N90-19774# Harvard Univ., Cambridge, MA.
THEORY AND APPLICATIONS OF BELIEF FUNCTIONS Final Report, 15 Mar. 1986 - 30 Sep. 1989
Arthur P. Dempster 30 Nov. 1989 5 p
(Contract DAAL03-86-K-0042)
(AD-A217092; ARO-22964.14-MA) Avail: NTIS HC A01/MF A01 CSCL 12/3

Graphical or network belief function models are defined and analyzed. Computational aspects are studied, including description and implementation of fusion and propagation algorithms. Applications to reliability of complex systems and to modelling dynamic systems are described. GRA

N90-19775# Colorado Univ., Boulder. Dept. of Computer Science.
ADAPTIVE, ASYNCHRONOUS STOCHASTIC GLOBAL OPTIMIZATION ALGORITHMS FOR SEQUENTIAL AND PARALLEL COMPUTATION Technical Report, 1 Sep. 1988 - 31 Aug. 1989
Sharon Smith, Elizabeth Eskow, and Robert B. Schnabel 26 Oct. 1989 31 p
(Contract DAAL03-88-K-0086; AF-AFOSR-0251-85)
(AD-A217093; CU-CS-449-89; ARO-24923.6-MA) Avail: NTIS HC A03/MF A01 CSCL 12/7

We discuss new global optimization algorithms that are related to the stochastic methods of Rinnooy Kan and Timmer, and to our previous static, synchronous parallel version of this method. The new algorithms have two main new features. First, they adaptively concentrate the computation in the areas of the domain space that appear most likely to produce the global minimum. Secondly, on parallel computers, they use an asynchronous approach, combined with a central work scheduler, to avoid load balancing problems. We investigate several mechanisms for deciding when and how to make the adaptive adjustments. We also describe both algorithmic and implementation considerations involved in constructing the parallel asynchronous algorithm. Computational tests on sequential and parallel computers show that the adaptive and asynchronous features of our new method can substantially reduce the number of function evaluations, and the execution time, required by previous stochastic methods to solve global optimization problems. GRA

N90-19406*# Ohio Univ., Athens. Dept. of Electrical and Computer Engineering.
INVESTIGATIONS INTO A NEW ALGORITHM FOR CALCULATING H INFINITY OPTIMAL CONTROLLERS
R. Dennis Irwin *In* Alabama Univ., Research Reports: 1989 NASA/ASEE Summer Faculty Fellowship Program Dec. 1989 28 p (For primary document see N90-19390 12-31)
(Grant NGT-01-008-021)
Avail: NTIS HC A99/MF E06 CSCL 09B

N90-19445*# Jet Propulsion Lab., California Inst. of Tech., Pasadena.
QUANTIZATION EFFECTS IN VITERBI DECODING RATE 1/n CONVOLUTIONAL CODES
I. M. Onyszchuk, K.-M. Cheung, and O. Collins *In its* The Telecommunications and Data Acquisition Report 15 Nov. 1989 p 115-121 (For primary document see N90-19434 12-32)
Avail: NTIS HC A10/MF A02 CSCL 09B

N90-19446*# Jet Propulsion Lab., California Inst. of Tech., Pasadena.
BIG VITERBI DECODER (BVD) RESULTS FOR (7,1/2) CONVOLUTIONAL CODE
J. Statman, J. Rabkin, and B. Siev *In its* The Telecommunications and Data Acquisition Report 15 Nov. 1989 p 122-129 (For primary document see N90-19434 12-32)
Avail: NTIS HC A10/MF A02 CSCL 09B

N90-19447*# Jet Propulsion Lab., California Inst. of Tech., Pasadena.
FAST TRANSFORM DECODING OF NONSYSTEMATIC REED-SOLOMON CODES
T. K. Truong, K.-M. Cheung, I. S. Reed, and A. Shiozaki (Osaka Electro-Communication Univ., Japan) *In its* The Telecommunications and Data Acquisition Report 15 Nov. 1989 p 130-140 (For primary document see N90-19434 12-32)
Avail: NTIS HC A10/MF A02 CSCL 09B

N90-19448*# Jet Propulsion Lab., California Inst. of Tech., Pasadena.
APPLICATION OF ADAPTIVE LEAST-SQUARES ALGORITHM TO MULTI-ELEMENT ARRAY SIGNAL RECONSTRUCTION
R. Kumar *In its* The Telecommunications and Data Acquisition Report 15 Nov. 1989 p 141-160 (For primary document see N90-19434 12-32)
Avail: NTIS HC A10/MF A02 CSCL 09B

62 COMPUTER SYSTEMS

Includes computer networks and special application computer systems.

N90-19776* National Aeronautics and Space Administration. Pasadena Office, CA.
LOCAL AREA NETWORK WITH FAULT-CHECKING, PRIORITIES, AND REDUNDANT BACKUP Patent
Sergio Morales, inventor (to NASA) and Gary L. Friedman, inventor (to NASA) (California Inst. of Tech., Pasadena.) 11 Jul. 1989 16 p Filed 8 Sep. 1986
(NASA-Case-NPO-16949-1-CU; US-Patent-4,847,837; US-Patent-Appl-SN-927987; US-Patent-Class-371-8; US-Patent-Class-370-16) Avail: US Patent and Trademark Office CSCL 09B

This invention is a redundant error detecting and correcting local area networked computer system having a plurality of nodes each including a network connector board within the node for connecting to an interfacing transceiver operably attached to a network cable. There is a first network cable disposed along a path to interconnect the nodes. The first network cable includes a plurality of first interfacing transceivers attached thereto. A second network cable is disposed in parallel with the first cable and, in like manner, includes a plurality of second interfacing transceivers attached thereto. There are a plurality of three position switches each having a signal input, three outputs for individual selective connection to the input, and a control input for receiving signals designating which of the outputs is to be connected to the signal input. Each of the switches includes means for designating a response address for responding to addressed signals appearing at the control input and each of the switches further has its signal input connected to a respective one of the input/output lines from the nodes. Also, one of the three outputs is connected to a repective one of the plurality of first interfacing transceivers. There is master switch control means having an output connected to the control inputs of the plurality of three position switches and an input for receiving directive signals for outputting addressed switch position signals to the three position switches as well as monitor and control computer means having a pair of network connector boards therein connected to respective ones of one of the first interfacing transceivers and one of the second interfacing transceivers and an output connected to the input of the master switch means for monitoring the status of the networked computer system by sending messages to the nodes and receiving and verifying messages therefrom and for sending control signals to the master switch to cause the master switch to cause respective ones of the nodes to use a desired one of the first and second cables for transmitting and receiving messages and for disconnecting desired ones of the nodes from both cables.
Official Gazette of the U.S. Patent and Trademark Office

N90-19777# California Inst. of Tech., Pasadena. Concurrent Computation Project.
PARALLEL NEURAL NET PATH-PLANNER ON HYPERCUBE AND TRANSPUTER
Alex W. Ho and Geoffrey C. Fox 8 Dec. 1989 6 p Presented at the International Conference on Parallel Processing in Nervous System and Computers, Dusseldorf, Fed. Republic of Germany, Mar. 1990 Sponsored in part by Joint Tactical Fusion Office
(Contract DE-FG03-85ER-25009)
(DE90-006324; DOE/ER-25009/848; CONF-900392-1) Avail: NTIS HC A02/MF A01

The task of finding a good path is of prime importance to any automated vehicle navigation controller. This task has been formulated as problems in computational geometry, which is commonly reduced to a graph search problem. We report here the preliminary results of a new approach that finds a good, if not optimal, path dynamically and in real-time by casting the task as a classification problem. The path-planner implements a back-propagation model for classification. The multi-scale representational strategy used for mapping the problem domain onto the input space of the back-propagation model ensures the applicability of the trained network to instances of the problem, which differ in the distribution of obstacles and the size of the problem domain. Software simulations based on the parallel computer EXPRESS operating system run, without modification of code, in Transputer-based systems as well as hypercube concurrent processor, with satisfactory efficiency. DOE

63 CYBERNETICS

Includes feedback and control theory, artificial intelligence, robotics and expert systems.

For related information see also *54 Man/System Technology and Life Support.*

N90-19778# Massachusetts Inst. of Tech., Cambridge. Artificial Intelligence Lab.
NETWORKS AND THE BEST APPROXIMATION PROPERTY
Federico Girosi and Tomaso Poggio Oct. 1989 25 p
(Contracts DACA76-85-C-0010; N00014-85-K-0124)
(AD-A216712; AI-M-1164) Avail: NTIS HC A03/MF A01
CSCL 12/2

Networks can be considered as approximation schemes. Multilayer networks of the backpropagation type can approximate arbitrarily well continuous functions (Cybenko, 1989; Funahashi, 1989; Stinchcombe and White, 1989). It is proved that networks derived from regularization theory and including Radial Basis functions (Poggio and Girosi, 1989), have a similar property. From the point of view of approximation theory, however, the property of approximation continuous functions arbitrarily well is not sufficient for characterizing good approximation schemes. More critical is the property of best approximation. The main result is that multilayer networks, of the type used in back propagation, are not best approximation. For regularization networks (in particular Radial Basis Function networks) existence and uniqueness of best approximation is proved. GRA

N90-19779# Oak Ridge National Lab., TN. Engineering Physics and Mathematics Div.
HYBRID NEURAL NETWORK AND RULE-BASED PATTERN RECOGNITION SYSTEM CAPABLE OF SELF-MODIFICATION
Charles W. Glover, Mike Silliman, Mark Walker, and Nageswara S. V. Rao (Old Dominion Univ., Norfolk, VA.) 1990 11 p Presented at the 8th SPIE Applications of Artificial Intelligence Conference, Orlando, FL, 17-19 Apr. 1990
(Contract DE-AC05-84OR-21400)
(DE90-007482; CONF-9004125-2) Avail: NTIS HC A03/MF A01

This paper describes a hybrid neural network and rule-based pattern recognition system architecture which is capable of self-modification or learning. The central research issue to be addressed for a multiclassifier hybrid system is whether such a system can perform better than the two classifiers taken by themselves. The hybrid system employs a hierarchical architecture, and it can be interfaced with one or more sensors. Feature extraction routines operating on raw sensor data produce feature vectors which serve as inputs to neural network classifiers at the next level in the hierarchy. These low-level neural networks are trained to provide further discrimination of the sensor data. A set of feature vectors is formed from a concatenation of information from the feature extraction routines and the low-level neural network results. A rule-based classifier system uses this feature set to determine if certain expected environmental states,

conditions, or objects are present in the sensors' current data stream. The rule-based system has been given an a priori set of models of the expected environmental states, conditions, or objects which it is expected to identify. The rule-based system forms many candidate directed graphs of various combinations of incoming features vectors. DOE

N90-19404*# Lafayette Coll., Easton, PA. Dept. of Electrical Engineering.
ARTIFICIAL INTELLIGENCE ISSUES RELATED TO AUTOMATED COMPUTING OPERATIONS
William A. Hornfeck *In* Alabama Univ., Research Reports: 1989 NASA/ASEE Summer Faculty Fellowship Program Dec. 1989 17 p (For primary document see N90-19390 12-31)
(Grant NGT-01-008-021)
Avail: NTIS HC A99/MF E06 CSCL 09B

N90-19409*# Alabama Univ., Tuscaloosa. Dept. of Electrical Engineering.
DETERMINATION OF THE IMPLEMENTATION OF THE 3-AXIS ATTITUDE MOTION SIMULATOR DIGITAL POSITION CONTROLLER
Mario E. Magana *In* Alabama Univ., Research Reports: 1989 NASA/ASEE Summer Faculty Fellowship Program Dec. 1989 15 p (For primary document see N90-19390 12-31)
(Grant NGT-01-008-021)
Avail: NTIS HC A99/MF E06 CSCL 09B

64 NUMERICAL ANALYSIS

Includes iteration, difference equations, and numerical approximation.

N90-19780# Ohio State Univ., Columbus. Dept. of Industrial and Systems Engineering.
USE OF COXIAN-TYPE DISTRIBUTIONS IN A GENERAL MODEL OF THE MAXIMUM OF BIVARIATE RANDOM VARIABLES
M. V. Kalkunte (Bell Telephone Labs., Inc., Columbus, OH.) and W. E. Wilhelm 1989 37 p
(Grant NSF DMC-85-00898)
(PB90-121229; NSF/ENG-89052) Avail: NTIS HC A03/MF A01 CSCL 12A

An approach is extended that uses trivariate reduction to model the maximum of bivariate random variables. Coxian-type phase distributions are used to define each element in the reduction because they are known to represent general distributions and, therefore, lend a generality to the bivariate cases that can be modeled. Exact expressions of the moments and for the distribution function of the maximum are presented. Numerical examples demonstrate use of the model and provide some insights about the nature of the maximum. Author

N90-19781# Oak Ridge National Lab., TN. Engineering Physics and Mathematics Div.
A COMPARISON BETWEEN THE PROPAGATORS METHOD AND THE DECOMPOSITION METHOD FOR NONLINEAR EQUATIONS
Yousry Y. Azmy, D. G. Cacuci (California Univ., Santa Barbara.), and V. Protopopescu Jan. 1990 19 p
(Contract DE-AC05-84OR-21400)
(DE90-005783; ORNL/TM-11316) Avail: NTIS HC A03/MF A01

Recently, a new formalism for solving nonlinear problems has been formulated. The formalism is based on the construction of advanced and retarded propagators that generalize the customary Green's functions in linear theory. One of the main advantages of this formalism is the possibility of transforming nonlinear differential equations into nonlinear integral equations that are usually easier to handle theoretically and computationally. The aim of this paper is to compare, on an example, the performances of the propagator method with other methods used for nonlinear equations, in particular, the decomposition method. The propagator method is stable, accurate, and efficient for all initial values and time intervals considered, while the decomposition method is unstable at large time intervals, even for very conveniently chosen initial conditions. DOE

N90-19782# Instituto de Pesquisas Espaciais, Sao Jose dos Campos (Brazil).
THE 0-1 MULTIKNAPSACK PROBLEM: HEURISTIC AND REDUCTION METHODS
Luiz Antonio NogueiraLorena Aug. 1989 22 p In PORTUGUESE; ENGLISH summary Presented at the 1st Brazilian School of Optimization, Rio de Janeiro, Brazil, 16-27 Jan. 1989
(INPE-4894-PRE/1495) Avail: NTIS HC A03/MF A01

The 0-1 multiknapsack problem was largely used as a model of resource allocation problems. Like this problem, NP-hard, heuristical methods are used to obtain an approximate solution. For an exact solution two phases are used: the reduction of the problem size by fixing variables to their optimal values and/or eliminating redundant constraints; and the solution of the reduced problem by implicit enumeration. A survey of the main heuristical methods and the reduction phase is made and improving possibilities are reported. Author

N90-19783*# National Aeronautics and Space Administration. Lewis Research Center, Cleveland, OH. Inst. for Computational Mechanics in Propulsion.
PARALLEL ALGORITHMS FOR BOUNDARY VALUE PROBLEMS
Avi Lin (Temple Univ., Philadelphia, PA.) Jan. 1990 21 p
(NASA Order C-99066-G)
(NASA-TM-102498; ICOMP-90-03; E-5292; NAS 1.15:102498)
Avail: NTIS HC A03/MF A01 CSCL 12A

A general approach to solve boundary value problems numerically in a parallel environment is discussed. The basic algorithm consists of two steps: the local step where all the P available processors work in parallel, and the global step where one processor solves a tridiagonal linear system of the order P. The main advantages of this approach are two fold. First, this suggested approach is very flexible, especially in the local step and thus the algorithm can be used with any number of processors and with any of the SIMD or MIMD machines. Secondly, the communication complexity is very small and thus can be used as easily with shared memory machines. Several examples for using this strategy are discussed. Author

N90-19784# Massachusetts Inst. of Tech., Cambridge. Lab. for Computer Science.
PRIORITY ARBITRATION WITH BUSSES
Shlomo Kipnis 16 Oct. 1989 22 p
(Contract N00014-87-K-0825)
(AD-A216392; MIT/LCS/TM-408) Avail: NTIS HC A02/MF A01 CSCL 12/7

Priority arbitation schemes are explored that employ busses to arbitrate among n modules in a digital system. We focus on distributed mechanisms that employ m busses, for lg n = or less than m = or less than n, and use asynchronous combinational arbitration logic. A widely used distributed asynchronous mechanism is the binary arbitration scheme, which with m = lg n busses arbitrates in t = lg n units of time. A new asynchronous scheme, binomial arbitration, is presented that by using m = lg n + 1 busses reduces tha arbitration time to t = 1/2 lg n. Extending this result, the generalized binomial abitration scheme is presented that achieves a bus-time tradeoff of the form m = Theta(tn to the 1 over t power) between the number of arbitration busses m and the arbitration time t (in units of bus-settling delay), for values of 1 = or less than t = or less than lg n and lg n = or less than m = or less than n. The schemes are based on an analysis of data-dependent delays and generalize the two known schemes; linear arbitration, which with m = n busses achieves t = 1 time, and binary arbitration, which with m = lg n busses achieves t = lg n time. Most importantly, the schemes can be adopted with no

changes to existing hardware and protocols; they merely involve selecting a good set of priority arbitration codewords. GRA

N90-19785# West Virginia Univ., Morgantown. Dept. of Mathematics.
MINIMUM CYCLE COVERING AND INTEGER FLOWS Final Technical Report, Nov. 1988 - Oct. 1989
Cun-Quan Zhang 15 Oct. 1989 14 p
(Grant AF-AFOSR-0068-89; AF Proj. 2304)
(AD-A216546; AFOSR-89-1865TR) Avail: NTIS HC A03/MF A01 CSCL 12/2

It was conjectured by Fan that if a graph G = (V,E) has a nowhere-zero 3-flow, then G can be covered by two even subgraphs of total size at most the absolute value of V + the absolute value of E - 3. This conjecture is proved in this paper. It is also proved that the optimum solution of the Chinese Postman problem and the solution of minimum cycle covering problem are equivalent for any graph admitting a nowhere-zero 4-flow. GRA

N90-19786# West Virginia Univ., Morgantown. Dept. of Mathematics.
PANCONNECTIVITY OF LOCALLY CONNECTED K(1,3)-FREE GRAPHS Final Technical Report, Nov. 1988 - Oct. 1989
Cun-Quan Zhang 15 Oct. 1989 29 p
(Grant AF-AFOSR-0068-89; AF Proj. 2304)
(AD-A216548; AFOSR-89-1866TR) Avail: NTIS HC A03/MF A01 CSCL 12/2

A locally connected, K(1,3)-free graph is panconnected if and only if the graph is 3-connected. GRA

N90-19787# Massachusetts Inst. of Tech., Cambridge. Microsystems Technology Labs.
OPTIMAL LAYOUT VIA BOOLEAN SATISFIABILITY Memorandum Report
Srinivas Devadas Sep. 1989 6 p Presented at the International Conference of Computer Aided Design, Nov. 1989
(Contract N00014-87-K-0825)
(AD-A216777; VLSI-MEMO-89-556) Avail: NTIS HC A02/MF A01 CSCL 09/1

Most optimization problems in layout have been shown to be NP-complete, resulting in researchers abandoning the search for optimum solutions even for small scale problem instances. Various NP-complete problems are transformed in layout, namely two-and multi-layer dogleg routing, two-way partitioning, 1-D and 2-D placement, into Boolean satisfiability problems. The transformations are efficient in that the number of inputs to the Boolean function, for which must be found a satisfying assignment, only grows linearly or quasi-linearly with the layout problem size. These transformations also produce a minimal-sized Boolean function, in order to speed up satisfiability check performance. Sophisticated test generation and logic verification strategies that can be used to check for Boolean function satisfiability are applied to these layout problems. Experimental results are presented which indicate that problems of significant size can be solved optimally using this approach. This approach to optimal layout is considerably more efficient than exhaustive search. Further, it is shown that this approach to layout optimization offers an elegant means of representing and searching the entire space of feasible solutions in an attempt to optimize a complex cost function with associated constraints. GRA

N90-19788# Defence and Civil Inst. of Environmental Medicine, Downsview (Ontario).
QUEUING THEORY APPROACH TO MODELLING THE DYNAMICS OF THE HUMAN-COMPUTER INTERFACE
J. M. E. vandeVegte Jul. 1989 40 p
(AD-A216870; DCIEM-89-RR-45) Avail: NTIS HC A03/MF A01 CSCL 23/2

A model is studied of the human-computer interface based on the idea of a message passing from one partner (the human) to the other (the computer) by means of an arbitrary number of layers which represent levels of abstraction of the message. The model uses a queuing theory formulation and assumes Poisson arrival and service characteristics to describe the movement of packets through the interface and to develop a criterion for network stability. Simulations are included to illustrate some of the theoretical results obtained. GRA

N90-19789# Maryland Univ., College Park. Inst. for Physical Science and Technology.
THE p- AND h-p VERSIONS OF THE FINITE ELEMENT METHOD: AN OVERVIEW Final Report
Ivo Babuska and Manil Suri (Maryland Univ. Baltimore County, Catonsville.) May 1989 37 p
(Contract N00014-85-K-0169; AF-AFOSR-0252-89)
(AD-A216902; BN-1101) Avail: NTIS HC A03/MF A01 CSCL 12/1

A survey is presented of the state of the art of the p and h-p versions. The emphasis is on the theoretical aspects related to their use in approximating elliptic equations stemming from structural mechanics. The origins of the finite element method (FEM), like those of the spectral method, may be traced back a long time. If it is understood that the FEM is the application of variational principles and approximation by piecewise smooth functions, then this idea was already used by Leibnitz in 1696 (in one dimension with piecewise linear functions). In two dimensions, Schellbach used triangulation and piecewise linear functions. Nevertheless, the modern FEM era starts with a paper which demonstrated the potential for the use of the computer. Since then, more than 30,000 papers have appeared. These papers are generally based on the h-version of the FEM, where the accuracy of the approximate solution is achieved by refining the mesh while using low order polynomials on the mesh. GRA

N90-19790# Laboratorio de Computacao Cientifica, Rio de Janeiro (Brazil).
ERROR ANALYSIS OF SOME GALERKIN LEAST SQUARES METHODS FOR THE ELASTICITY EQUATIONS
Leopoldo P. Franca and Rolf Stenberg May 1989 28 p
(DE90-608611; LNCC-009/89) Avail: NTIS (US Sales Only) HC A03/MF A01

The recent technique is considered of stabilizing mixed finite element methods by augmenting the Galerkin formulation with least squares terms calculated separately on each element. The error analysis is performed in a unified manner yielding improved results for some methods introduced earlier. In addition, a new formulation is introduced and analyzed. DOE

N90-19791*# Institute for Computer Applications in Science and Engineering, Hampton, VA.
ON THE PARALLEL EFFICIENCY OF THE FREDERICKSON-MCBRYAN MULTIGRID Final Report
Naomi H. Decker Feb. 1990 11 p Submitted for publication
(Contract NAS1-18605)
(NASA-CR-181999; NAS 1.26:181999; ICASE-90-17) Avail: NTIS HC A03/MF A01 CSCL 12A

To take full advantage of the parallelism in a standard multigrid algorithm requires as many processors as points. However, since coarse grids contain fewer points, most processors are idle during the coarse grid iterations. Frederickson and McBryan claim that retaining all points on all grid levels (using all processors) can lead to a superconvergent algorithm. The purpose of this work is to show that the parellel superconvergent multigrid (PSMG) algorithm of Frederickson and McBryan, though it achieves perfect processor utilization, is no more efficient than a parallel implementation of standard multigrid methods. PSMG is simply a new and perhaps simpler way of achieving the same results.
Author

N90-19792# Washington Univ., Seattle. Dept. of Applied Mathematics.
A TENSOR PRODUCT B-SPLINE METHOD FOR NUMERICAL GRID GENERATION Ph.D. Thesis
Joseph W. Manke Oct. 1989 100 p
(Contract DE-FG06-88ER-25061)
(DE90-005979; DOE/ER-25061/4; TR-89-4) Avail: NTIS HC A06/MF A01

A tensor product B-spline method is presented for fast elliptic grid generation. The Cartesian coordinate functions for a block are represented as a sum of tensor product B-spline basis functions defined on the computational domain for the block. The tensor product B-spline basis functions are constructed so that the basis functions and their first partials are continuous on the computational domain for the block. The coordinate functions inherit this smoothness: a grid computed by evaluating the coordinate function along constant parameter lines leads to smooth grid lines with smoothly varying tangents. The expansion coefficients for the coordinates functions are computed by solving the elliptic grid generation equations using collocation. This assures that the computer grid has the smoothness and resolution expected for an elliptic grid with appropriate control. The collocation equations are solved with an ADI solution algorithm analogous to the ADI solution algorithm for the finite difference method. The speed of the method derives from the smoothness of the B-spline basis functions; in effect, a fine grid in the physical domain is obtained by constructing a smooth expansion of the coordinate functions on a coarse grid of knots in the computational domain. Thus, the tensor product B-spline method will be faster than the finite difference method, if a sufficiently smooth fine grid in the physical domain can be obtained for an appropriately coarse grid of knots in the computational domain. DOE

N90-19793# Washington Univ., Seattle. Dept. of Applied Mathematics.
HIERARCHICAL BASIS PRECONDITIONERS FOR SECOND ORDER ELLIPTIC PROBLEMS IN THREE DIMENSIONS Ph.D Thesis
Maria Elizabeth Go Ong Oct. 1989 251 p
(Contract DE-FG06-88ER-25061; NSF ASC-85-19353)
(DE90-005980; DOE/ER-25061/5; TR-89-3) Avail: NTIS HC A12/MF A02

The discretization uses nodal basis functions and the preconditioner arises. Preconditioners are presented for a symmetric, positive definite linear system arising from the finite element discretization of a second order elliptic problem in three dimensions. The discretization uses nodal basis functions and the preconditioner arises from the use of hierarchical basis functions. It is shown that the condition number of the linear hierarchical basis coefficient matrix (cflx A) scaled by a coarse grid operator is O(N(sup 1/3) log N(sup 1/3)) when uniform tetrahedral refinement is used, where N is the number of unknowns. If additional diagonal scaling by levels is applied in the fine grid, a condition number of O(N(sup 1/3)) is obtained. The same result is obtained if (cflx A) is scaled by its block diagonal. Moreover, it is shown that any other block diagonal scaling of (cflx A) will yield a condition number that grows at least as O(N(sup 1/3)). These results compare favorably with the condition number of O(N(sup 2/3)) of the nodal coefficient matrix. Numerical results are provided which confirm this theory. These results are extensions of those obtained by Yserentant for 2-D problems. The analysis of the linear preconditioner is also extended to the case of non-uniform refinement. DOE

N90-19794# Maryland Univ., College Park. Lab. for Plasma Research.
CHAOTIC TRANSIENTS, HIGHER DIMENSIONAL PHENOMENA, AND COUPLED ORDINARY DIFFERENTIAL EQUATIONS Progress Report, Jan. - Dec. 1989
Celso Grebogi and James A. Yorke Jan. 1990 17 p
(Contract DE-FG05-87ER-25036)
(DE90-006641; DOE/ER-25036/3) Avail: NTIS HC A03/MF A01

Some areas of discussion are: crises and chaotic transients; the dimension of chaotic attractors; fractal basin boundaries; and control of chaotic processes. DOE

N90-19795# International Centre for Theoretical Physics, Trieste (Italy).
DIFFERENTIAL OPERATORS ASSOCIATED WITH GEGENBAUER POLYNOMIALS. 3: THE REGULAR CASE
V. P. Onyango-Otieno Jul. 1989 15 p Submitted for publication
(DE90-610422; IC-89/193-3) Avail: NTIS (US Sales Only) HC A03/MF A01

The regular case of the Gegenbauer differential equation was studied in both the right-definite and left-definite cases by using a method based on a classical approach due to E.C. Titchmarsh. Then the Titchmarsh approach was linked with operator theoretical results in the spaces L(sub w)(sup 2)(-1,1) and H(sub p,q)(sup 2)(-1,1). DOE

N90-19796# International Centre for Theoretical Physics, Trieste (Italy).
SUPERCONFORMAL ALGEBRA ON MEROMORPHIC VECTOR FIELDS WITH THREE POLES ON SUPER-RIEMANN SPHERE
Shikun Wang (Academia Sinica, Beijing, China) and Kaiwen Xu Jul. 1989 9 p Submitted for publication
(DE90-610423; IC-89/207) Avail: NTIS (US Sales Only) HC A02/MF A01

Based upon the Riemann-Roch theorem, we construct superconformal algebra of meromorphic vector fields with three poles and the relevant abelian differential of the third kind on super Riemann sphere. The algebra includes two Ramond sectors as subalgebra, and implies a picture of interaction of three superstrings. DOE

N90-19797# International Centre for Theoretical Physics, Trieste (Italy).
A METHOD FOR COMPUTING THE STATIONARY POINTS OF A FUNCTION SUBJECT TO LINEAR EQUALITY CONSTRAINTS
U. L. Uko Sep. 1989 6 p Submitted for publication
(DE90-610427; IC-89/269) Avail: NTIS (US Sales Only) HC A02/MF A01

A new method is given for the numerical calculation of stationary points of a function when it is subject to equality constraints. An application to the solution of linear equations is given, together with a numerical example. DOE

N90-19798# International Centre for Theoretical Physics, Trieste (Italy).
BANACH C*-ALGEBRAS NOT CONTAINING A SUBSPACE ISOMORPHIC TO C(SUB 0)
Bolis Basit Sep. 1989 6 p
(DE90-610428; IC-89/285) Avail: NTIS (US Sales Only) HC A02/MF A01

If X is a locally Hausdorff space and C(sub 0)(X) the Banach algebra of continuous functions defined on X vanishing at infinity, it is shown that a subalgebra A of C(sub 0)(X) is finite dimensional if it does not contain a subspace isomorphic to the Banach space C(sub 0) of convergent to zero complex sequences. This result is extended to noncommutative Banach C*-algebras and Banach* algebras. DOE

N90-19799# International Centre for Theoretical Physics, Trieste (Italy).
ITERATION METHODS FOR SOLVING NONLINEAR EQUATIONS IN FRECHET SPACES
Nguyen Minh Chuong and Khuat vanNinh (Institute of Mathematics, Hanoi, Vietnam) Sep. 1989 11 p Submitted for publication
(DE90-610429; IC-89/300) Avail: NTIS (US Sales Only) HC A03/MF A01

The equation f(epsilon)x + Tx for some classes of operators T is studied. These operators acting in normed spaces or in Frechet spaces, include as special cases the class of monotone operators if the considered spaces are Hilbert ones. The solutions of this equation are obtained by iteration methods with estimates of the rate of convergence. DOE

N90-19800# International Centre for Theoretical Physics, Trieste (Italy).
ON THE APPROXIMATIVE NORMAL VALUES OF MULTIVALUED OPERATORS IN TOPOLOGICAL VECTOR SPACE
Nguyen Minh Chuong and Khuat vanNinh (Institute of Mathematics, Hanoi, Vietnam) Sep. 1989 13 p Submitted for publication
(DE90-610430; IC-89/301) Avail: NTIS (US Sales Only) HC A03/MF A01

The problem of approximation of normal values of multivalued linear closed operators from topological vector Mackey space into E-space is considered. Existence of normal value and convergence of approximative values to normal value are proved. DOE

N90-19801# International Centre for Theoretical Physics, Trieste (Italy).
PROJECTION-ITERATION METHODS FOR SOLVING NONLINEAR OPERATOR EQUATIONS
Nguyen Minh Chuong, Tran thi Lan Anh, and Tran Quoc Binh (Institute of Mathematics, Hanoi, Vietnam) Sep. 1989 24 p Submitted for publication
(DE90-610433; IC-89/305) Avail: NTIS (US Sales Only) HC A03/MF A01

A nonlinear operator equation is investigated in uniformly convex Banach spaces as in metric spaces by using stationary and nonstationary generalized projection-iteration methods. Convergence theorems in the strong and weak sense were established. DOE

N90-19802# Sandia National Labs., Albuquerque, NM. Exploratory Systems Development Div.
A TECHNIQUE FOR CONVOLVING UNEQUALLY SPACED SAMPLES USING FAST FOURIER TRANSFORMS
Thomas D. Sullivan Jan. 1990 32 p
(Contract DE-AC04-76DP-00789)
(DE90-006466; SAND-89-0077) Avail: NTIS HC A03/MF A01

A method is presented that allows one to make use of the fast Fourier transform for convolving unequally spaced samples with a system response function. The technique is a shared-power approach and can be described as a type of reverse interpolation. Application to the formation of simulated radar images is also presented. DOE

N90-19803# Technische Univ., Delft (Netherlands). Faculty of Technical Mathematics and Informatics.
FINITE ELEMENT MESH GENERATION STARTING FROM GENERAL GEOMETRIC MODELS [EINDIGE ELEMENTEN ROOSTERGENERATIE VANUIT ALGEMENE GEOMETRISCHE MODELLEN]
E. Boender 1988 40 p In DUTCH
(Rept-88-93; ISSN-0920-2358; ETN-90-95435) Copyright Avail: NTIS HC A03/MF A01

The present models for automatic finite element mesh generation in two dimensions (2-D) and three dimensions (3-D) are surveyed and evaluated. The most frequently used methods are the interpolation methods; they are not fully automatic and cannot be recommended for 3-D objects with complicated geometry. Methods that are only based on subdivision for mesh generation sometimes provide badly formed elements. The present modified outtree method can lead to badly formed elements at the edge of the object. With some modifications, the Delaunay triangulation leads to a good tetrahedron formation of the object; the problem is the generation of mesh points on boundary curves, on surfaces, and in the interior of the objects. ESA

N90-19804# Oak Ridge National Lab., TN.
CONVERGENCE PROPERTIES OF ITERATIVE ALGORITHMS FOR SOLVING THE NODAL DIFFUSION EQUATIONS
Yousry Y. Azmy and Bernadette L. Kirk 1990 13 p Presented at the International Conference on the Physics of Reactors: Operation, Design and Computation, Marseilles (France), 23-27 Apr. 1990
(Contract DE-AC05-84OR-21400)
(DE89-016859; CONF-900418-1) Avail: NTIS HC A03/MF A01

We drive the five point form of the nodal diffusion equations in two-dimensional Cartesian geometry and develop three iterative schemes to solve the discrete-variable equations: the unaccelerated, partial Successive Over Relaxation (SOR), and the full SOR methods. By decomposing the iteration error into its Fourier modes, we determine the spectral radius of each method for infinite medium, uniform model problems, and for the unaccelerated and partial SOR methods for finite medium, uniform model problems. Also for the two variants of the SOR method we determine the optimal relaxation factor that results in the smallest number of iterations required for convergence. Our results indicate that the number of iterations for the unaccelerated and partial SOR methods is second order in the number of nodes per dimension, while, for the full SOR this behavior is first order, resulting in much faster convergence for very large problems. We successfully verify the results of the spectral analysis against those of numerical experiments, and we show that for the full SOR method the linear dependence of the number of iterations on the number of nodes per dimension is relatively insensitive to the value of the relaxation parameter, and that it remains linear even for heterogenous problems. DOE

N90-19805# Los Alamos National Lab., NM. Center for Nonlinear Studies.
RULE MATRICES, DEGREE VECTORS, AND PREIMAGES FOR CELLULAR AUTOMATA
Erica Jen 1989 15 p Presented at the Santa Fe Institute Summer School on Complex Systems, Santa Fe, NM, 5-30 Jun. 1989
(Contract W-7405-eng-36)
(DE90-007492; LA-UR-90-627; CONF-8906239-3) Avail: NTIS HC A03/MF A01

Cellular automata are mathematical systems characterized by discreteness (in space, time, and state values), determinism, and local interaction. Few analytical techniques exist for such systems. The rule matrix and degree vectors of a cellular automaton (both of which are determined a priori from the function defining the automaton, rather than a posteriori from simulations of its evolution) are introduced here as tools for understanding certain qualitative features of automaton behavior. The rule matrix represents in convenient form the information contained in an automaton's rule table; the degree vectors are computed from the rule matrix, and reflect the extent to which the system is one-to-one versus many-to-one on restricted subspaces of the mapping. The rule matrix and degree vectors determine, for example, several aspects of the enumeration and prediction of preimages for spatial sequences evolving under the rule, where the preimages of a sequence S are defined to be the set of sequences mapped by the automaton rule onto S. DOE

N90-19806# Texas Univ., San Antonio.
PARALLEL METHODS FOR SOLVING NONLINEAR BLOCK BORDERED SYSTEMS OF EQUATIONS Technical Report, 1 Sep. 1988 - 31 Dec. 1989
Xiaodong Zhang, Richard H. Byrd, and Robert B. Schnabel (Colorado Univ., Boulder.) 31 Dec. 1989 39 p
(Contract DAAL03-88-K-0086; AF-AFOSR-0251-85; NSF CDA-84-20944)
(AD-A217062; CU-CS-454-89; ARO-24923.7-MA) Avail: NTIS HC A03/MF A01 CSCL 12/1

A group of parallel algorithms, and their implementation is discussed, for solving a special class of large sparse nonlinear equations. The type of sparsity occurring in these problems, which arise in VLSI design, structural engineering and many other areas, is called a block bordered structure. An explicit method and several implicit methods are described for solving block bordered nonlinear problems, and a mathematical analysis and computational comparisons are made for the two types of methods. Several variations and globally convergent modifications of the implicit method are also presented. Parallel algorithms for solving block bordered nonlinear equations are described and experimental

results presented on the Intel hypercube that show the effectiveness of the parallel implicit algorithms. These experiments include a fairly large circuit simulation that leads to a multi-level block bordered system of nonlinear equations. GRA

65 STATISTICS AND PROBABILITY

Includes data sampling and smoothing; Monte Carlo method; and stochastic processes.

N90-19807# Massachusetts Inst. of Tech., Cambridge. Lab. for Information and Decision Systems.
DISTRIBUTED DETECTION BY A LARGE TEAM OF SENSORS IN TANDEM
Jason D. Papastavrou and Michael Athans 1 Nov. 1989 33 p Submitted for publication
(Contract N00014-84-K-0519; NSF IRI-89-02755)
(AD-A216607; LIDS-P-1929) Avail: NTIS HC A03/MF A01
CSCL 17/8

The problem of decentralized binary hypothesis testing by a team consisting of N decision makers (DMs) in tandem is considered. Each DM receives an observation and transmits a binary message to its successor; the last DM has to decide which hypothesis is true. Necessary and sufficient conditions are derived for the probability of error to asymptotically (as N approaches infinity) go to zero. The result is generalized for multiple hypotheses and multiple messages. An easily implementable suboptimal decision scheme is also considered; necessary and sufficient conditions for the probability of error to asymptotically go to zero are derived for this case as well. The trade off between the complexity of the decision rules and their performance is examined and numerical results are presented. GRA

N90-19808# Ustav Jaderneho Vyzumu, Rez (Czechoslovakia). Information Centre.
NUMERICAL SOLUTION TO THE PROBLEM OF CRITICALITY BY MONTE CARLO METHOD
J. Kyncl Apr. 1989 6 p
(DE90-608886; UJV-8727-R) Avail: NTIS (US Sales Only) HC A02/MF A01

A new method of numerical solution of the criticality problem is proposed. The method is based on the results of the Krein and Rutman theory. Monte Carlo method is used and the random process is chosen in such a way that the differences between results obtained and exact ones would be arbitrarily small. The method can be applied for both analogous and nonanalogous random processes. DOE

N90-19809# Universitaet der Bundeswehr Muenchen, Neubiberg (Germany, F.R.). Forschungsschwerpunkt Simul. und Optimierung Deterministischer und Stochastischer Dynamischer Sys.
OPTIMAL ITERATION STEPS BY STOCHASTIC APPROXIMATION PROCESSES FOR THE SOLUTION OF OPTIMIZATION PROBLEMS WITH TWICE DIFFERENTIABLE FUNCTIONS [OPTIMALE SCHRITTWEITEN BEI STOCHASTISCHEN APPROXIMATIONSVERFAHREN ZUR LOESUNG VON OPTIMIERUNGSPROBLEMEN MIT ZWEIMAL DIFFERENZIERBARER ZIELFUNKTION]
Ernst Ploechinger Jan. 1989 24 p In GERMAN
(ETN-90-95887) Avail: NTIS HC A03/MF A01

In many of practical cases, the gradient of a function with multiple variables is very expensive to calculate. However, a stochastic approximation can frequently evaluate this gradient. The properties of the matrices and vectors used in this optimization are given. A series of optimal iteration steps is found to be monotone with a convergence of type 1/n. ESA

N90-19810# Los Alamos National Lab., NM.
NONLINEAR SYSTEM VIBRATION: THE APPEARANCE OF CHAOS
Norman F. Hunter 1990 8 p Presented at the 36th Institute of Environmental Science Annual Technology Meeting, New Orleans, LA, 23-27 Apr. 1990
(Contract W-7405-eng-36)
(DE90-007546; LA-UR-90-356; CONF-900479-6) Avail: NTIS HC A02/MF A01

This paper begins with an examination of the differential equation for a single degree of freedom force excited oscillator and considers the state space behavior of linear, nonlinear, and chaotic single degree of freedom systems. The fundamental characteristics of classical chaos are reviewed: sensitivity to initial conditions, positive Lyapunov exponents, complex Poincare maps, fractal properties of motion in the state space, and broadening of the power spectrum of the system response. Illustrated examples of chaotic behavior include motion in a two well potential -- the chaos beam described in Moon and a hardening base excited Duffing system. Chaos-like phenomenon which occur with nonperiodic forcing are examined in the context of the two well potential and hardening Duffing systems. The paper concludes with some suggestions for detecting and modelling nonlinear or chaotic behavior. DOE

66 SYSTEMS ANALYSIS

Includes mathematical modeling; network analysis; and operations research.

No abstracts in this category.

67 THEORETICAL MATHEMATICS

Includes topology and number theory.

N90-19811# Los Alamos National Lab., NM. Center for Nonlinear Studies.
COMPUTATION AT THE EDGE OF CHAOS: PHASE TRANSITION AND EMERGENT COMPUTATION
Chris Langton 25 Jan. 1990 75 p Presented at the Conference on Emergent Computation, Los Alamos, NM, 22-26 May 1989
(Contract W-7405-eng-36)
(DE90-007488; LA-UR-90-379; CONF-8905201-5) Avail: NTIS HC A04/MF A01

In order for computation to emerge spontaneously and become an important factor in the dynamics of a system, the material substrate must support the primitive functions required for computation: the transmission, storage, and modification of information. Under what conditions might we expect physical systems to support such computational primitives. Research is presented on Cellular Automata which suggests that the optimal conditions for the support of information transmission, storage, and modification, are achieved in the vicinity of a phase transition. Surprising similarities were observed between the behaviors of computations and systems near phase transitions, finding analogs of computational complexity classes and the Halting problem within the phenomenology of phase transitions. We conclude that there is a fundamental connection between computation and phase transitions, and discuss some of the implications for our understanding of nature if such a connection is borne out. DOE

70 PHYSICS (GENERAL)

For precision time and time interval (PTTI) see *35 Instrumentation and Photography;* for geophysics, astrophysics or solar physics see *46 Geophysics, 90 Astrophysics,* or *92 Solar Physics.*

N90-19812# Maryland Univ., College Park. Dept. of Mathematics.
NONLINEAR CONTINUUM MECHANICS AND APPLIED ANALYSIS Final Report, 1 Jun. 1986 - 31 May 1989
J. H. Maddocks Jun. 1989 5 p
(Grant AF-AFOSR-0097-86; AF Proj. 2304)
(AD-A213629; AFOSR-89-1278TR) Avail: NTIS HC A01/MF A01 CSCL 20/11

Kinetics (maneuvering) of mobile robots, elastic beam theory, remote crystals, and variational principle/stability in continuum mechanics are discussed. Author

N90-19813*# Rochester Univ., NY. Dept. of Mechanical Engineering.
SIPHON FLOWS IN ISOLATED MAGNETIC FLUX TUBES. 3: THE EQUILIBRIUM PATH OF THE FLUX TUBE ARCH Annual Report, 1989
John H. Thomas and Benjamin Montesinis (Oxford Univ., England) 21 Sep. 1989 55 p Submitted for publication
(Grants NAG5-934; NsG-7562)
(NASA-CR-186297; NAS 1.26:186297) Avail: NTIS HC A04/MF A01 CSCL 20C

The arched equilibrium path of a thin magnetic flux tube in a plane-stratified, nonmagnetic atmosphere is calculated for cases in which the flux tube contains a steady siphon flow. The large scale mechanical equilibrium of the flux tube involves a balance among the magnetic buoyancy force, the net magnetic tension force due to the curvature of the flux tube axis, and the inertial (centrifugal) force due to the siphon flow along curved streamlines. The ends of the flux tube are assumed to be pinned down by some other external force. Both isothermal and adiabatic siphon flows are considered for flux tubes in an isothermal external atmosphere. For the isothermal case, in the absence of a siphon flow the equilibrium path reduces to the static arch calculated by Parker (1975, 1979). The presence of a siphon flow causes the flux tube arch to bend more sharply, so that magnetic tension can overcome the additional straightening effect of the inertial force, and reduces the maximum width of the arch. The curvature of the arch increases as the siphon flow speed increases. For a critical siphon flow, with supercritical flow in the downstream leg, the arch is asymmetric, with greater curvature in the downstream leg of the arch. Adiabatic flow have qualitatively similar effects, except that adiabatic cooling reduces the buoyancy of the flux tube and thus leads to significantly wider arches. In some cases the cooling is strong enough to create negative buoyancy along sections of the flux tube, requiring upward curvature of the flux tube path along these sections and sometimes leading to unusual equilibrium paths of periodic, sinusoidal form. Author

N90-19814# Parke Mathematical Labs., Inc., Carlisle, MA.
OPTO-EM AND DEVICES INVESTIGATION Final Technical Report, 29 May 1987 - 31 May 1988
Joseph A. Adamski, Jerome H. Bloom, H. J. Caulfield, Joseph J. Comer, Robert S. Kennedy, John D. Kierstead, and Michael Salour Jun. 1989 131 p
(Contract F19628-87-C-0155; AF Proj. 4600)
(AD-A215033; RADC-TR-89-67) Avail: NTIS HC A07/MF A01 CSCL 09/5

A summary is provided of work accomplished in several diverse areas of optical transmission, materials processing. The areas include: A description of the experimental program on the synthesis and single crystal growth of indium phosphide; Device processing techniques covering the use of ultra high vacuum deposition system for evaporating a dielectric layer of silicon monoxide; Materials evaluation techniques under the general heading of electron microscopy; and a description regarding connecting a two-hidden-layer neural network through an intermediate multiplicative layer showing that it can yield full or partial disambiguities of results from a single traditional neural network. Communication security was achieved in fiber optic communication systems (IROCS) by ensuring that any undetected intrusion will deliver so little power to a potential intruder that no useful information can be extracted from it. Photorefractive and resonant nonlinear optical interactions are being studied, and the requirements of nonlinear optical materials are discussed and fundamental limits are derived. GRA

N90-19815# Colorado State Univ., Fort Collins. Dept. of Chemistry.
LOW TEMPERATURE ELASTIC AND DIELECTRIC PROPERTIES OF INCOMMENSURATE BARIUM SODIUM NIOBATE
W. F. Oliver, J. F. Scott (Colorado Univ., Boulder.), R. Nowak, and E. R. Bernstein 15 Dec. 1989 47 p Submitted for publication
(Contract N00014-79-C-0647; NSF DMR-86-0666)
(AD-A216969; TR-64) Avail: NTIS HC A03/MF A01 CSCL 20/3

Dielectric and Brillouin spectroscopic measurements on incommensurate (IC) Ba2NaNb5O15 from ca. 15 K to room temperature and have related the measurements to earlier studies of birefringence and x ray and neutron crystallography, with special emphasis upon the structural phase transition near 105 and 40 K. The 105 K transition is from Ccm2(1) to a modulated structure, which appears to be a reentrant phase also found at atmospheric pressure from 565 to 582 K. Such a reentrant IC/C/IC sequence is predicted in the phenomenological theory of Ishibashi. The lock-in phase below 40 K is tetragonal and probably of space group P4nc (structural refinements of preliminary neutron scattering data are in progress). GRA

71 ACOUSTICS

Includes sound generation, transmission and attenuation. For noise pollution see *45 Environmental Pollution.*

N90-19816 Stanford Univ., CA.
FOUNDATIONS OF MILLIMETER-WAVE FREQUENCY ACOUSTIC MICROSCOPY Ph.D. Thesis
Lloyd John LaComb, Jr. 1989 259 p
Avail: Univ. Microfilms Order No. DA8925901

Advancements in the field of millimeter-wave superfluid helium acoustic microscopy are discussed. The superfluid helium acoustic microscope operating at a center frequency of eight GHz at temperatures less than 0.2 K has been shown to have a resolution of at least 200 A. In order to increase the operating frequency, and hence the resolution, of the acoustic microscope, nearly all the components of the eight GHz microscope had to be redesigned. Multilayer ZnO transducers were used to generate approximately 28 GHz sound with two-way conversion losses as low as 27 dB. Multilayer transducers were also fabricated for operation at frequencies as high as 100 GHz, where the two-way conversion loss is approximately 50 dB. These ZnO multilayer transducers represent the highest operating frequency of any ZnO transducer and the highest conversion efficiencies for any type of transducer in this frequency range. The theoretical aspects of multilayer transducers are explored along with experimental verification of some theoretical predictions. A piezoelectric mechanical scanning system was designed for operation at temperatures as low as 100 milliKelvin. The resolution, frequency characteristics and heat dissipation properties of the scanner are presented. The possibility of using superconducting bolometers for incoherent signal detection of millimeter-wave frequency acoustic waves is investigated. Several different configurations for using bolometers in conjunction with multilayer acoustic transducers are described. Image processing algorithms for automatically correcting phase delays and single point and single line scan errors which occur in many different types of scanning microscopy are presented. The

usefulness of several types of two-dimensional image interpolation techniques is evaluated using data obtained from the scanning tunneling microscope. Dissert. Abstr.

N90-19817# Naval Postgraduate School, Monterey, CA.
A LINEAR SYSTEMS THEORY APPROACH TO THE RANGE-INDEPENDENT ACOUSTIC CHANNEL M.S. Thesis
Luiz Alberto LopesdeSouza Jun. 1989 105 p
(AD-A216551) Avail: NTIS HC A06/MF A01 CSCL 20/1

Using linear systems theory as a framework, the solution for the acoustic field present in a range-independent acoustic channel excited by a complex-weighted, planar array of point sources with an arbitrary input electrical signal is derived. The ocean medium is characterized by a transfer function, obtainable as the solution to the Helmholtz wave equation. The transfer function for an isospeed, three-layer waveguide is derived. The unbounded homogeneous medium equations are derived as a special case of the waveguide problem. The problem of interference due to the presence of a pressure-release surface is also derived as a special case. The linear systems approach lends itself to a modular computer implementation, in which different ocean medium models are represented by subroutines implementing their transfer functions. The equations for a range-independent medium are implemented as a group of subprograms. Results are presented for the special cases of a homogeneous medium and the surface reflection problem, which can be checked against known, easily interpreted analytical solutions. Finally, an example of waveform prediction for the isospeed, three-layer waveguide is presented. GRA

N90-19818# Technische Univ., Berlin (Germany, F.R.). Fachbereich Elektrotechnik.
MODELING AND REALIZATION OF PLANE ACOUSTO-OPTIC UNILATERAL BAND MODULATORS Ph.D. Thesis [MODELLIERUNG UND REALISIERUNG PLANARER AKUSTOOPTISCHER EINSEITENBANDMODULATOREN]
Christian Schaeffer 1989 134 p In GERMAN Sponsored by Deutsche Forschungsgemeinschaft
(ETN-90-95824) Avail: NTIS HC A07/MF A01

LiNbO3 has particularly good acousto-optic properties, in comparison with other materials such as quartz. A wave guide is manufactured by diffusion of titanium in LiNbO3. A good approximation can be obtained by the Beam Propagation Method (BPM). A digital process is proposed with which the acousto-optic feedback can be simulated. The BPM can solve the scalar equation and simulate the optic field distribution in diffusion waveguides. By means of the effective index method a two dimensional refractivity profile is realized. With the built modulators and a polarization, an integrated optic device is conceived which contains the whole optical signal processing of a fiber gyroscope system. ESA

N90-19819# Universitaet der Bundeswehr Muenchen, Neubiberg (Germany, F.R.). Inst. fuer Mechanik.
THE DRUM: MECHANICAL OSCILLATORS AND ACOUSTIC RAD IATORS [DIE PAUKE: MECHANISCHER SCHWINGER UND AKUSTISCHER STRAHLER]
Helmut Fleischer 1988 59 p In GERMAN
(Rept-FB-01/88; ETN-90-95889) Avail: NTIS HC A04/MF A01

The skin of a kettle drum was mathematically described by means of a model of the membrane. A comparison between theory and practice shows that the calculated and measured oscillation forms were not in good agreement with the corresponding frequencies. It is not possible to exclusively consider the skin as a mechanic oscillator. It is also necessary to calculate its function as an acoustic radiator. The air mass, moving at the front side of the skin, must be taken into account. The eigen frequencies are reduced. With this broadening of the membrane model a good agreement is achieved between the calculated values and the experimental ones, for the real drum skin. An important part of the problem study is the evaluation of the eigen frequency spectrum with a tonal highness calculation process. ESA

N90-19820# Sandia National Labs., Albuquerque, NM.
SANDIA NATIONAL LABORATORIES' NEW HIGH LEVEL ACOUSTIC TEST FACILITY
Jonathan D. Rogers and David M. Hendrick 1989 7 p Presented at the 36th Institute of Environmental Science Annual Technology Meeting, New Orleans, LA, 23-27 Apr. 1990
(Contract DE-AC04-76DP-00789)
(DE90-006810; SAND-89-2867C; CONF-900479-1) Avail: NTIS HC A02/MF A01

A high intensity acoustic test facility has been designed and is under construction at Sandia National Laboratories in Albuquerque, NM. The chamber is designed to provide an acoustic environment of 154dB (re 20 microPa) overall sound pressure level over the bandwidth of 50 Hz to 10,000 Hz. The chamber has a volume of 16,000 cubic feet with interior dimensions of 21.6 ft x 24.6 ft x 30 ft. The construction of the chamber should be complete by the summer of 1990. The design goals and constraints of the facility are discussed. The construction characteristics are discussed in detail, as are the acoustic performance design characteristics. The authors hope that this work will help others in designing acoustic chambers. DOE

N90-19821*# National Aeronautics and Space Administration. Langley Research Center, Hampton, VA.
A NOTE ON AN ACOUSTIC RESPONSE DURING AN ENGINE NACELLE FLIGHT EXPERIMENT
James A. Schoenster Jan. 1990 16 p
(NASA-TM-102585; NAS 1.15:102585) Avail: NTIS HC A03/MF A01 CSCL 20A

During a flight test study of the noise effects on laminar flow on the outside surface of a simulated engine nacelle, an intense acoustic response was observed. The aircraft speed at which this signal occurred and the frequency content of the signal fell within the test conditions of the experiment and had to be eliminated prior to continuing. The signal was identified as an aerodynamic excitation of an acoustic mode in the simulated by-pass duct of the nacelle. By modifying the trailing edges of the support struts of the nacelle, the aerodynamic excitation was changed enough to eliminate the resonant response of the offending duct modes, eliminating the unwanted acoustic problem. Author

N90-19822# Vista Research Corp., Mountain View, CA.
NUMERICAL SIMULATION OF ACOUSTIC SCATTER FROM SUBSURFACE BUBBLE CLOUDS Technical Report, 15 Jun. - 31 Oct. 1989
Charles L. Rino and Hoc D. Ngo 18 Oct. 1989 85 p
(Contract N00014-87-C-0473; ARPA Order 4462)
(AD-A217068) Avail: NTIS HC A05/MF A01 CSCL 20/1

A new technique is described that allows computation of the scattering characteristics of an object near a rough surface in terms of the free-space scattering characteristics of the rough surface and the scattering object. The method is applied to the problem of acoustic scatter from a small bubble cloud below the ocean surface. The results show that under most conditions of interest the backscatter from the bubble cloud is enhanced over its free-spaced level. The ramifications for acoustic reverberation noise are discussed. GRA

72 ATOMIC AND MOLECULAR PHYSICS

Includes atomic structure, electron properties, and molecular spectra.

N90-19823# Northwestern Univ., Evanston, IL. Dept. of Chemistry.
LINEAR FREE ENERGY RELATIONS FOR MULTIELECTRON TRANSFER KINETICS: A BRIEF LOOK AT THE BRONSTED/TAFEL ANALOGY
M. S. Ram and Joseph T. Hupp Nov. 1989 16 p
(Contract N00014-88-K-0369)
(AD-A215078; TR-3) Avail: NTIS HC A02/MF A01 CSCL 07/4

A comparison is made between electrochemical and homogeneous redox reactivity for species involving the transfer of multiple electrons at a single thermodynamic potential. In the electrochemical case the co-reactant is the electrode; in the homogeneous case it is any of several members of a homologous series of one-electron reagents. In the latter case it is shown that the slope of a plot of the observed pseudo first order rate constant (one-electron reagent in excess) versus the thermodynamic driving force rate constant identify the cross reaction's rate-determining step. It is noted that the proposed use of a homogeneous linear free energy relation (Bronsted plot) for mechanistic purpose is closely analogous to the well known Tafel approach (log current vs. potential) in electrochemical kinetics. GRA

N90-19824# Argonne National Lab., IL. High Energy Physics Div.
TRANSVERSE SPIN OBSERVABLES IN CHROMODYNAMICS
Dennis Sivers Dec. 1989 9 p Presented at the 6th Topical Conference on Physics with Polarized Beams on Polarized Targets, Spencer, IN, 16-18 Oct. 1989
(Contract W-31-109-eng-38)
(DE90-005638; ANL-HEP-CP-89-132; CONF-8910121-2) Avail: NTIS HC A02/MF A01

Quantum Chromodynamics confronts a harsh series of tests in the attempt to formulate a comprehensive approach to the calculation of transverse spin observables. The basic obstacles to understanding transverse spin can be illustrated by considering a transverse structure function extracted from deep-inelastic scattering using a polarized lepton and a polarized proton. The inadequacy of the transverse-spin basis for quarks and gluons found there suggests a new approach to the problems of single-spin observables in large-transverse-momentum processes. This approach, presented earlier for single spin production asymmetries, is discussed here. It is shown that the mechanism can also lead to baryon polarization effects at large P(sub T). DOE

N90-19825# Lawrence Livermore National Lab., CA.
ELECTRON ENERGY DISTRIBUTIONS AND VIBRATIONAL POPULATION DISTRIBUTIONS
J. R. Hiskes 1989 20 p Presented at the 5th International Symposium on the Production and Neutralization of negative Ions and Beams, Upton, NY, 30 Oct. - 3 Nov. 1989
(Contract W-7405-eng-48)
(DE90-005550; UCRL-102454; CONF-891055-2) Avail: NTIS HC A03/MF A01

This last year two experimental groups have reported on the vibrational population distributions of hydrogen molecules, H2(v double prime), generated in a hydrogen discharge. These distributions extend up to the v(double prime) = 5 vibrational level corresponding to the threshold excitation for significant H(-) production. A comparison of theoretical modelling distributions with the measured distributions of Stutzin et al., has shown a qualitative agreement taking into account known excitation processes, and fair quantitative agreement when account was taken of the calculated wall relaxation parameters. These comparisons are extended to include the distributions of Eenshuistra et al., and provide further insights into the formation processes. A novel feature of the Eenshuistra distributions is a five-fold enhancement of the high v(double prime) levels with increased discharge current. These data are shown for the 5 Amp and 30 Amp cases summarized. The sources of this enhancement are considered. DOE

N90-19826# Cornell Univ., Ithaca, NY. School of Chemical Engineering.
MOLECULAR THEORY AND COMPUTER SIMULATION STUDIES OF NATURAL AND SYNTHETIC GAS MIXTURES Annual Report, 1 Jan. - 31 Dec. 1988
Keith E. Gubbins 31 Jan. 1989 45 p
(Contract GRI-5087-260-1452)
(PB90-130329; GRI-89/0178) Avail: NTIS HC A03/MF A01 CSCL 20H

The effect of molecular associations on the phase equilibria of fluids with multiple bonding sites is investigated. Initially, the individual molecules are represented by hard sphere repulsive cores with off center, square well attractive sites. Such a system's thermodynamic properties can be calculated by using expressions based on a theory recently proposed by Wertheim. A simple van der Waals mean field term is also added to account for the dispersion forces. Isothermal isobaric Monte Carlo simulations of hard sphere fluids with one and two attractive sites are shown to be in good aggreement with the results of the theory. The critical points and phase equilibria of the associating fluids are determined for various values of the strength and range of the attractive site. Furthermore, results are presented for the degree of association in the gas and liquid phases along the vapor pressure curve. The effect of size is then incorporated by developing an equation of state for chain molecules. The theory can treat fluids with strong hydrogen bonding associations such as the carboxylic acids, the aliphatic alcohols, hydrogen fluoride, water, etc. Author

N90-19827# Technische Univ., Berlin (Germany, F.R.). Fachbereich Physik.
PARTICLE EMISSION BY OBLIQUE ION BOMBARDMENT OF GOLD Ph.D. Thesis [TEILCHENEMISSION BEI SCHIEFWINKLIGEM IONENBESCHUSS VON GOLD]
Martin Sternberg 1989 93 p In GERMAN
(ETN-90-95825) Avail: NTIS HC A05/MF A01

The anisotropic atom emission of Au-111 is examined with 23 keV Ar-ions. The bombardment angle varied from minus 60 to 90 degrees perpendicular to the target. The whole non-bent atom emission distributions were measured. The effects of the grid correlated anisotropic emission and the underground intensity could be distinguished. The emission of secondary electrons shows in transparent directions, a lower bombardment angle dependence than the atom emission. Other experiments were made with a liquid-metal ion radiation equipment. The influence of the space charges is noticeable in the current-voltage and angle-intensity curves. Mass spectroscopy experiments with secondary ions show that only a few particles of a gold-surface are gold ions. Under normal high vacuum conditions this method can be recommended only with reserve for quantitative measurements. ESA

N90-19828# Max-Planck-Inst. fuer Physik und Astrophysik, Munich (Germany, F.R.).
ALGORITHMS FOR CALORIMETER SIMULATION WITH PARAMETERIZED SHOWERS BY EXAMPLE OF H1 DETECTORS Thesis - Hamburg Univ. [ALGORITHMEN ZUR KALORIMETERSIMULATION MIT PARAMETRISIERTEN SCHAUERN AM BEISPIEL DES H1-DETEKTORS]
Matthias Rudowicz 31 Jan. 1989 133 p In GERMAN
(MPI-PAE/Exp.El-200; ETN-90-95859) Avail: NTIS HC A07/MF A01

The simulation of the energy distributions of electromagnetic and hadronic showers was implemented on a proton-antiproton accelerator. The calculation cost for the shower simulation increases linearly with the shower energy but can be reduced by a good parameterization, developed by an algorithm that does not depend on the geometry. The mean values and the fluctuations in the characteristic magnitudes were parameterized as a function of the shower energy in the area 1 to 200GeV. The statistical character of the physical process was described by the Monte Carlo method. The influence of the fluctuation pi-part of the deponent energy on the total energy was taken into account. The influences of the pi-fluctuations of the deponent energy and of different calorimeter structures are well demonstrated by the simulation. ESA

N90-19829# Lawrence Livermore National Lab., CA. Physics Dept.
MEASUREMENT OF CROSS SECTIONS: NEW NEEDS AND POSSIBILITIES
1 Nov. 1989 16 p Presented at the Workshop on Primordial Nucleosynthesis, Chapel Hill, NC, 7-8 Oct. 1989 Prepared in cooperation with Ohio State Univ., Columbus

(Contract W-7405-eng-48)
(DE90-007248; UCRL-102293; CONF-8910320-3) Avail: NTIS HC A03/MF A01

Experimental studies of nuclear cross sections over the past several decades have done much to elucidate the processes of nucleosynthesis and energy generation in a variety of astrophysical sites. Recent studies have begun to focus on reactions which have not previously been studied either because they were experimentally difficult, or because they had been overlooked as being important a proposed study of the (26)Al(sup m)(p, gamma)(27)Si reaction as an example of an experiment which will soon be feasible. It will then present results of some new theoretical work on primordial nucleosynthesis which pinpoints some of the critical reactions for which no cross section measurements were made. These primarily involve (8)Li, a key nucleus in one model of primordial nucleosynthesis. Finally, instrumentation needed for future measurements in nuclear astrophysics will be discussed. DOE

N90-19830# Boston Univ., MA.
RESEARCH ACCOMPLISHMENTS AND FUTURE GOALS IN PARTICLE PHYSICS
Jan. 1990 139 p
(Contract DE-AC02-89ER-40509)
(DE90-007296; DOE/ER-40509/1) Avail: NTIS HC A07/MF A01

Eight projects in high energy physics research are reviewed: study of high energy electron-positron annihilation, using SLD detector at SLAC. Development of integrated transition radiation detection and tracking for an SSC detector; Development of new concepts for particle accelerator components, including design and prototyping of high-precision electrostatic and magnetic elements; Development of a new underground detector facility in the Gran Saso Laboratory in Italy to search for magnetic monopoles and to study astrophysical muons and neutrinos; Search for proton decay and neutrinos from point astrophysical sources, and the study of cosmic ray muons and neutrinos in the IMB detector; Study of theoretical particle physics, including lattice gauge theories, string theories, phenomenology of the Standard Model and its extensions, and application of particle physics concepts to the early universe, cosmology and astrophysics, as well as the extension of these techniques into computational physics; Preparation of an experiment to measure the anomalous magnetic moment of the muon in a new superconducting storage ring and detector system at BNL; Fabrication (with M.I.T. and Princeton) of the BGO endcaps and associated tracking chambers for the L3 detector at LEP. Development of a central tracker for the SSC; and this new tasks requests support for research, development, and beam testing of a prototype SSC calorimeter featuring a tower geometry and composed of lead alloy and scintillating fibers. DOE

N90-19831# Los Alamos National Lab., NM.
FIFTH-ORDER ABERRATIONS IN MAGNETIC QUADRUPOLE-OCTUPOLE SYSTEMS
K. M. Ling 1990 75 p Presented at the Accelerator Computer Code Meeting, Los Alamos, NM, 22-25 Jan. 1990
(Contract W-7405-eng-36)
(DE90-007489; LA-UR-90-383; CONF-900163-3) Avail: NTIS HC A04/MF A01

Explicit integral expressions are given for the fifth-order geometrical aberration coefficients in rectilinear magnetic quadrupole-octupole systems used for the transport of nonrelativistic charged particle beams. The numerical values of the fifth-order geometrical aberration coefficients for a rare earth cobalt (REC) quadrupole doublet are given as an example. DOE

N90-19832# Los Alamos National Lab., NM. Theoretical Div.
BOSE CONDENSATE IN SUPERFLUID (SUP 4)He AND MOMENTUM DISTRIBUTIONS BY DEEP INELASTIC SCATTERING
Richard N. Silver and Paul E. Sokol (Pennsylvania State Univ., University Park.) 1989 30 p Presented at the 6th International Conference on Recent Progress in Many Body Theories, Arad, Israel, 6-10 Nov. 1989
(Contract W-7405-eng-36)
(DE90-007541; LA-UR-90-539; CONF-8911150-2) Avail: NTIS HC A03/MF A01

There are several reasons for the high interest in the recent experimental and theoretical progress in understanding deep inelastic neutron scattering from liquid (sup 4)He: it tests the fundamental London hypothesis of a connection between superfluidity and Bose condensation; it provides a quantitative test of ab initio calculational methods for all systems with strong correlations which are the focus of current quantum many-body research; and it establishes the range of validity of deep inelastic scattering as a method for measuring momentum distributions. In this paper we introduce the concepts of impulse approximation in more detail, we describe recent progress in the theory for final state corrections to the impulse approximation, we present quantitative predictions for neutron scattering experiments, we compare with recent high energy pulsed neutron source experiments on liquid (sup 4)He by P. Sokol and colleagues as well as other attempts to extract the Bose condensate fraction from the neutron scattering data, and we discuss the implications of this progress for future momentum distribution experiments in other systems such as liquid (sup 4)He and quasi-elastic electron nucleus scattering. DOE

N90-19833# Los Alamos National Lab., NM.
THE ELECTRON MOMENTUM-TRANSFER CROSS SECTIONS OF TUNGSTEN, SILICON, AND SILICON DIOXIDE AT ENERGIES FROM 0.1 TO 10,000 eV
Joseph J. Devaney Jan. 1990 19 p
(Contract W-7405-eng-36)
(DE90-009041; LA-11725-MS) Avail: NTIS HC A03/MF A01

For the purpose of estimating effective stopping of low energy electrons in a particular direction, the momentum-transfer cross sections of Tungsten, Silicon, and Silicon Dioxide are furnished. The elastic scattering momentum-transfer cross sections are obtained by integration over the differential elastic scattering cross sections either in the individual references or in this paper numerically. At 10eV and below the elastic scattering momentum-transfer cross sections were also obtained from the total scattering cross section, swarm experiments and the microwave method, as well as theoretical calculations. The inelastic collision momentum-transfer cross sections were calculated from the electron stopping powers by an approximate theory due to Devaney. The total momentum-transfer cross section is then the sum of the elastic scattering and the inelastic collision cross sections. DOE

73 NUCLEAR AND HIGH-ENERGY PHYSICS

Includes elementary and nuclear particles; and reactor theory.

For space radiation see *93 Space Radiation.*

N90-19834# Washington Univ., Seattle. Dept. of Physics.
EXPERIMENTAL AND THEORETICAL HIGH ENERGY PHYSICS
David Boulware 1988 59 p
(Contract DE-AS06-88ER-40423)
(DE90-005974; DOE/ER-40423/26) Avail: NTIS HC A04/MF A01

We are carrying out a research program in high energy experimental particle physics. Studies of high energy hadronic interactions and leptoproduction processes continue using several experimental techniques. Progress has been made on the study of multiparticle production processes in nuclei. Ultra-high energy cosmic ray nucleus-nucleus interactions have been investigated by the Japanese American Cosmic Emulsion Experiment (JACEE) using balloon-borne emulsion chamber detectors. In the area of particle astrophysics, our studies of cosmic ray nuclear interactions have enabled us to make the world's most accurate determination of the composition of the cosmic rays above 10(13) eV. We have

the only detector that can observe interaction vertices and identify particles at energies up to 10 to 15 eV. Our observations are getting close to placing limits on the acceleration mechanisms postulated for pulsars in which the spin and magnetic moment axes are at different angles. In June, 1989 approval was given by NASA for our participation in the Space Station program. The SCINATT experiment will make use of emulsion chamber detectors, similar to the planned JACEE hybrid balloon flight detectors. These detectors will permit precise determination of secondary particle charges, momenta and rapidities, and the accumulation of data will be at least a factor of 10 to 100 greater than in balloon experiments. DOE

N90-19835# Argonne National Lab., IL.
ANALYSIS AND EVALUATION OF ZPPR (ZERO POWER PHYSICS REACTOR) CRITICAL EXPERIMENTS FOR A 100 KILOWATT-ELECTRIC SPACE REACTOR
Harold F. McFarlane, Peter J. Collins, Stuart G. Carpenter, David N. Olsen, Dale M. Smith, Robert W. Schaefer, Richard A. Doncals, Sandra Andre, Charles A. Porter, and Charles L. Cowan (General Electric Co., San Jose, CA.) et al 1990 14 p Presented at the International Conference on the Physics of Reactors: Operation, Design and Computation, Marseilles (France), 23-27 Apr. 1990
(Contracts W-31-109-eng-38; DE-AC03-868S-16006)
(DE90-005634; CONF-900418-4) Avail: NTIS HC A03/MF A01

ZPPR critical experiments were used for physics testing the reactor design of the SP-100, a 100-kW thermoelectric LMR that is being developed to provide electrical power for space applications. These tests validated all key physics characteristics of the design, including the ultimate safety in the event of a launch or re-entry accident. Both the experiments and the analysis required the use of techniques not previously applied to fast reactor designs. A few significant discrepancies between the experimental and calculated results leave opportunities for further optimization. An initial investigation was made into application of the ZPPR-20 results, along with those of other relevant integral data, to the SP-100 design. DOE

N90-19836# Department of Energy, Washington, DC.
THE ULTIMATE STRUCTURE OF MATTER: THE HIGH ENERGY PHYSICS PROGRAM FROM THE 1950S THROUGH THE 1980S
Feb. 1990 43 p
(DE90-005682; DOE/ER-0435) Avail: NTIS HC A03/MF A01

This discusses the following topics in High Energy Physics: The Particle Zoo; The Strong and the Weak; The Particle Explosion; Deep Inside the Nucleon; The Search for Unity; Physics in Collision; The Standard Model; Particles and the Cosmos; and Practical Benefits. DOE

N90-19837# British Columbia Univ., Vancouver. TRIUMF Facility.
THE TISOL FACILITY AT TRIUMF
J. DAuria, M. Dombsky (Simon Fraser Univ., Burnaby, British Columbia), L. Buchmann, H. Sprenger, and J. Vincent Oct. 1989 6 p Presented at the 1st International Conference on Radioactive Nuclear Beams, Berkeley, CA, 16-18 Oct. 1989
(DE90-006882; TRI-PP-89-92; CONF-891044-5) Avail: NTIS (US Sales Only) HC A02/MF A01

The TISOL facility at TRIUMF is now an operational on-line isotope separator, capable of delivering ion beams for over 100 radioisotopes from two different types of ion sources including an Electron Cyclotron Resonance (ECR) source, and is now entering a phase which it can be used productively for basic physics research. A summary progress report is provided on this new facility including observed production yields and details of the new ECR installation. The plans for the future development of the facility to perhaps use proton beams of intensities approaching 5 microamps is also discussed. The status of the proposed ISAC facility is reviewed. DOE

N90-19838# Stanford Linear Accelerator Center, CA.
THE EGS4 CODE SYSTEM: SOLUTION OF GAMMA-RAY AND ELECTRON TRANSPORT PROBLEMS
W. R. Nelson and Yoshihito Namito Feb. 1990 14 p Presented at the International Conference on Supercomputing in Nuclear Applications, Mito City, Japan, 12-16 Mar. 1990
(Contract DE-AC03-76SF-00515)
(DE90-008100; SU-SLAC-PUB-5193; CONF-900343-3) Avail: NTIS HC A03/MF A01

In this paper we present an overview of the EGS4 Code System -- a general purpose package for the Monte Carlo simulation of the transport of electrons and photons. During the last 10 to 15 years EGS has been widely used to design accelerators and detectors for high-energy physics. More recently the code has been found to be of tremendous use in medical radiation physics and dosimetry. The problem-solving capabilities of EGS4 will be demonstrated by means of a variety of practical examples. To facilitate this review, we will take advantage of a new add-on package, called SHOWGRAF, to display particle trajectories in complicated geometries. These are shown as 2-D laser pictures in the written paper and as photographic slides of a 3-D high-resolution color monitor during the oral presentation. DOE

74 OPTICS

Includes light phenomena; and optical devices.
For lasers see *36 Lasers and Masers.*

N90-19839# General Atomic Co., San Diego, CA.
FOMA: A FAST OPTICAL MULTICHANNEL ANALYZER
J. S. Haskovec, G. Bramson, N. H. Brooks, and M. Perry Dec. 1989 3 p Presented at the 13th IEEE Symposium on Fusion Engineering, Knoxville, TN, 2-6 Oct. 1989
(Contract DE-AC03-89ER-51114; GA Proj. 3466)
(DE90-004093; GA-A-19753; CONF-891007-112) Avail: NTIS HC A01/MF A01

A Fast Optical Multichannel Analyzer (FOMA) was built for spectroscopic measurements with fast time resolution on the DIII-D tokamak. The FOMA utilizes a linear photodiode array (RETICON RL 1024 SA) as the detector sensor. An external recharge switch and ultrafast operational amplifiers permit a readout time per pixel of 300 ns. In conjunction with standard CAMAC digitizer and timing modules, a readout time of 500 microns is achieved for the full 1024-element array. Data acquired in bench tests and in actual spectroscopic measurements on the DIII-D tokamak is presented to illustrate the camera's capability. DOE

N90-19840 Department of the Navy, Washington, DC.
THERMAL MODULATION OF LIGHT BEAMS Patent
Lloyd C. Bobb, inventor (to Navy), J. White, inventor (to Navy), and Jon P. Davis, inventor (to Navy) 22 Aug. 1989 4 p Filed 13 Jan. 1988
(AD-D014322; US-Patent-4,859,059; US-Patent-Appl-SN-145020; US-Patent-Class-356-345) Avail: US Patent and Trademark Office CSCL 09/5

The phase of light passing through an optical waveguide is modulated by applying electric current to heat the waveguide and thereby alter the length and refractive index thereof. An application for the thermal phase modulation concept is provided in a Mach-Zehnder interferometer. GRA

N90-19841 Department of the Navy, Washington, DC.
ALL-FIBER SFPM (STIMULATED FOUR PHOTON MIXING) AMPLIFIER Patent
Timothy C. Stamnitz, inventor (to Navy) and Stephen D. Russell, inventor (to Navy) 19 Sep. 1989 7 p Filed 31 Aug. 1988
(AD-D014358; US-Patent-4,867,518; US-Patent-Appl-SN-239156; US-Patent-Class-350-96.15) Avail: US Patent and Trademark Office CSCL 20/6

An integrated fiber device provides optical signal amplification to: provide for increased distances between undersea repeaters and/or optical regeneration nodes in fiber optic transmission

systems, or support an increased number of multiple users on an optical data bus network or multiple parallel signal processing channels in an optical processor/computer. In the latter case a greater number of divisions of the signal can occur before the divided signal amplitude falls below the threshold needed for processing or detection. A combination of fiber components is incorporated that include: 2 optically tapered portions for conditioning of 2 input laser beams to a wavelength selective single-mode coupler used to combine the concentrated information signal and concentrated pump wave, and one of whose output ports is then optically coupled to a predetermined length of single-mode fiber. The fibers optogeometric parameters are especially designed for intrinsic phase-matching to effect pump wave frequency conversion and signal amplification by the nonlinear optical SFPM process. The amplified signal light is coupled out of the especially designed SFPM fiber by a mode-field conditioning device enabling beam expansion, such that the output core diameter of the mode-field conditioner equals the core diameter of the single-mode fiber used in the transmission link. An important aspect of this patent is that it can be configured for field and/or undersea installation. GRA

N90-19842# Aerospace Medical Research Labs., Wright-Patterson AFB, OH.
A NEW METHOD FOR MEASURING THE TRANSMISSIVITY OF AIRCRAFT TRANSPARENCIES Final Report, Oct. 1988 - Sep. 1989
Harry L. Task and Harold S. Merkel Dec. 1989 27 p
(AF Proj. 7184)
(AD-A216953; AAMRL-TR-89-044) Avail: NTIS HC A03/MF A01 CSCL 20/6

Transmissivity is a measurement of the relative amount of light transmitted through a part. It is an important optical parameter for aircraft transparencies, since it determines the apparent brightness of the objects observed outside the cockpit. Because visual parameters such as acuity, contrast threshold, and color perception vary with brightness at low luminance values, transmissivity can have a direct effect on vision. The transmissivity of aircraft transparencies is currently measured following the American Standard for Testing and Materials Test Method D-1003. This method, originally intended for the measurement of small, thin, flat parts, has several shortcomings for measuring aircraft transparencies. A new method for measuring transmissivity, which overcomes the shortcomings of D-1003, is described. The precision of both methods was determined in laboratory tests; the results of these tests are presented. The new test method, in addition to its application advantages, is slightly more precise than ASTM D-1003. GRA

N90-19843# Cornell Univ., Ithaca, NY. Lab. of Atomic and Solid State Physics.
SEARCH FOR FAR INFRARED RADIATION FROM OPTICALLY PUMPED DEFECT MODES Final Report, 15 Jun. 1986 - 30 Sep. 1989
A. J. Sievers 13 Nov. 1989 62 p
(Contract DAAL03-86-K-0103)
(AD-A216976; ARO-23654.28-PH) Avail: NTIS HC A04/MF A01 CSCL 07/5

A comprehensive experimental study of the near millimeter wave dynamics of a variety of solids is being carried out. Since in many cases the investigation involves driving the system far from equilibrium with IR or UV laser radiation, knowledge of the time dependent optical response over a broad frequency region is required. Effects such as persistent IR spectral hole burning and population inversion in internal vibrational modes in solids have been uncovered using this approach. The discovery that persistent IR hole burning can be used to manipulate the near millimeter wave response of defects in crystals, such as NO2(-):KI, and that it also provides a sensitive probe of the optical photodarkening in chalcogenide glasses have opened up new research avenues which require simultaneous probes of very different frequencies in the IR and visible. On going exploration of the far IR response of high temperature superconductors in sintered, thin film, single crystal and even single grain form continue to provide new information about the dynamical response of these unusual materials both in the normal and superconducting states. GRA

N90-19844# Arizona Univ., Tucson. Optical Sciences Center.
OPTICALLY TUNABLE GRATINGS FOR OPTICAL INTERCONNECTS Final Report, 1 Aug. 1986 - 31 Jul. 1989
G. I. Stegeman 30 Oct. 1989 9 p
(Contract DAAL03-86-K-0143)
(AD-A216978; ARO-23845.1-PH) Avail: NTIS HC A02/MF A01 CSCL 20/6

The properties of a nonlinear grating coupler were investigated for application to an all-optical beam scanner for optical interconnects. En route, this program achieved four distinct goals: (1) Bistability was demonstrated for grating coupling into ZnS waveguides utilizing a diffusive nonlinearity (thermal). (2) It was shown theoretically that a diffusive nonlinearity is required to obtain bistability in a nonlinear grating (or prism) coupler. This cleared up a 5-year controversy in the literature. (3) An all-optical beam scanner was demonstrated in which the scan angle of a signal beam is tuned by varying the input power of the control beam. Both smooth and bistable scanning was implemented. (4) This device was analysed theoretically for both non-local and local (Kerr) nonlinearities. It was shown that Kerr nonlinearities lead to a non-unique response. GRA

N90-19845# Rochester Inst. of Tech., NY. Center for Imaging Science.
THERMAL INFRARED SCENE SIMULATION Final Report
James S. Warnick, Eric Shor, and John R. Schott Jan. 1990 93 p
(Contract DE-FG01-88DP-20153)
(DE90-006900; DOE/DP-20153/T8; RIT/DIRS-89/90-51-133)
Avail: NTIS HC A05/MF A01

The complexity and interplay between the thermodynamic and radiometric phenomena associated with longwave infrared (LWIR) images make the analyses of these images quite difficult and the development of algorithms for image analysis quite complex. This image analysis process is further complicated when the algorithms are part of a real time targeting, tracking, or positioning system because the sensor's electro-optical system can have a significant and variable impact on the image. As a result, it is often desirable to perform evaluations of fully packaged thermal infrared imaging systems against dynamic scenes. The high cost of field testing these systems prohibits this approach in all but the research and development and early engineering stages. Even in the research and development stage the scenarios required for full system testing are often difficult to acquire. These factors have led to the search for a capability to produce a synthetically generated, self-emitting thermal infrared scene which can be dynamically updated. Sensors or algorithms exposed to this simulator could then be tested in an end-to-end (buttoned up) configuration to evaluate system performance in as close to a real world scenario as practical. One major goal was to assemble and test the performance characteristics of a system for generating dynamic self-emitting scenes. The system consisted of an argon laser source, a spatial light modulator to generate a brightness image and a 2-D visible-to-infrared transducer to convert the monochromatic laser energy into a broad band self-emitting thermal infrared image. DOE

N90-19846 Physics and Electronics Lab. TNO, The Hague (Netherlands).
THE INFLUENCE OF GAMMA-RADIATION ON THE BANDWIDTH OF OPTICAL FIBRES AND THE REDUCTION OF THE INDUCED ATTENUATION BY BLEACHING AND HARDENING THE FIBRE
A. J. W. M. Backhuijs, A. M. Bosman, and A. J. T. deKrijger Aug. 1988 60 p In DUTCH; ENGLISH summary
(Contract A82/KL/040)
(FEL-1988-62; TD-88-4127; ETN-90-95080) Copyright Avail: Physics and ELectronics Lab. TNO, P.O. Box 96864, 2509 JG 's-Gravenhage, Netherlands

The influence of gamma radiation on the pulse dispersion of a step-index and a graded-index optical fiber was investigated. The measurements were performed at a dose of 3 krad and 10 krad at a wavelength of 820 nm. The step-index fiber shows no changes in the pulse dispersion, while the graded-index fiber shows a reduced dispersion when exposed to gamma radiation. The reduction of the induced attenuation by increasing the optical power level during and after the irradiation or by preirradiating the fiber with gamma radiation is determined. ESA

N90-19847 Institute for Perception RVO-TNO, Soesterberg (Netherlands). Afdeling Visuologie.
PROCESSING INFRARED IMAGES FOR TARGET DETECTION: A LITERATURE STUDY
B. P. Alblas Jul. 1988 46 p In DUTCH; ENGLISH summary
(Contract R87/KL/094)
(IZF-1988-12; TD-88-4124; ETN-90-95089) Copyright Avail: Institute for Perception RVO-TNO, P. O. Box 23, 3769 Soesterberg, Netherlands

Methods of image processing applied to IR images to obtain better detection and/or recognition of military targets, particularly vehicles, are reviewed. The following subjects are dealt with: histogram specification, scanline degradation, correlation, clutter and noise. Only a few studies deal with the effects of image processing on human performance. Most of the literature concerns computer vision. Local adaptive and image dependent techniques appear to be the most promising methods of obtaining higher observation performance. In particular the size-contrast box filter and histogram specification methods seem to be suitable. There is a need for a generally applicable definition of image quality and clutter level to evaluate the utility of a specified algorithm. Proposals for further research are given. ESA

N90-19848# Oak Ridge National Lab., TN. Health and Safety Div.
THE OPTICAL PROPERTIES OF BERYLLIUM
E. T. Arakawa, T. A. Callcott, and Yun-Ching Chang Feb. 1990 29 p
(Contract DE-AC05-84OR-21400)
(DE90-006372; ORNL/OMIS-89/9) Avail: NTIS HC A03/MF A01

We review the published data on the optical properties of beryllium for the spectral region from 0.03 to 300 eV. In the visible and infrared spectral regions, where published data from various authors show very large variations, we have performed experiments that identify the most probable sources of error, and use this information to select the best data from published sources. The effects of surface oxide overlayers have also been studied. In the far infrared spectral region, where only normal incidence reflectance data are available, and in the extreme ultraviolet, where only transmission data are available, there is insufficient information to fully determine the optical properties at each photon energy. Between 0.06 and 26 eV, however, a normal incidence reflectance curve is fully determined. This curve has been used for a Kramers-Kronig analysis to determine the optical properties in this spectral range. DOE

N90-19849# Georgia Inst. of Tech., Atlanta. School of Electrical Engineering.
INTEGRATED OPTICS ANISOTROPIC WAVEGUIDES AND DEVICES Final Report, Aug. 1986 - Apr. 1989
Thomas K. Gaylord 30 Apr. 1989 48 p
(Contract DAAL03-86-K-0157)
(AD-A217064; ARO-23602.2-EL) Avail: NTIS HC A03/MF A01 CSCL 20/6

A simple procedure employing an extension of the general Jacobi method is introduced for determining the properties of the two allowed elliptical eigen-polarizations for an arbitrary direction of propagation as well as the principal indices and axes of a general lossless, electro-optic, and gyrotropic medium. The Jacobi method presented is an iterative procedure used for performing a unitary transformation to diagonalize the Hermitian impermeability tensor. In addition, a complex polarization variable is defined from elements of the unitary transformation matrix to determine the ellipticity, azimuth angle, relative amplitude and phase, and handedness of the two orthogonal elliptical polarizations. Also, the phase velocity indices of refraction are readily calculated with simple derived expressions. This procedure is numerically stable and accurate for any crystal, external field direction, and direction of propagation. GRA

N90-19412*# Florida Univ., Gainesville. Dept. of Physics.
TRANSMISSION AND REFLECTION STUDIES OF THIN FILMS IN THE VACUUM ULTRAVIOLET
Lennart R. Peterson *In* Alabama Univ., Research Reports: 1989 NASA/ASEE Summer Faculty Fellowship Program Dec. 1989 12 p (For primary document see N90-19390 12-31)
(Grant NGT-01-008-021)
Avail: NTIS HC A99/MF E06 CSCL 20F

N90-19413*# Alabama Univ., Huntsville. Dept. of Mathematical Sciences.
ANALYTICAL OPTICAL SCATTERING IN CLOUDS
Dieudonne D. Phanord *In its* Research Reports: 1989 NASA/ASEE Summer Faculty Fellowship Program Dec. 1989 16 p (For primary document see N90-19390 12-31)
(Grant NGT-01-008-021)
Avail: NTIS HC A99/MF E06 CSCL 20F

N90-19442*# Jet Propulsion Lab., California Inst. of Tech., Pasadena.
PHOTON STATISTICAL LIMITATIONS FOR DAYTIME OPTICAL TRACKING
W. M. Folkner and M. H. Finger *In its* The Telecommunications and Data Acquisition Report 15 Nov. 1989 p 90-97 (For primary document see N90-19434 12-32)
Avail: NTIS HC A10/MF A02 CSCL 20F

75 PLASMA PHYSICS

Includes magnetohydrodynamics and plasma fusion.
For ionospheric plasmas see *46 Geophysics*. For space plasmas see *90 Astrophysics*.

N90-19850 Virginia Univ., Charlottesville.
LONGITUDINAL TRAVELING WAVES BIFURCATING FROM VLASOV PLASMA EQUILIBRIA Ph.D. Thesis
James Paul Holloway 1989 171 p
Avail: Univ. Microfilms Order No. DA8919114

The kinetic equations governing longitudinal motion along a straight magnetic field in a multi-species collisionless plasma are investigated. A necessary condition for the existence of small amplitude spatially periodic equilibria and traveling waves near a given spatially uniform background equilibrium is derived, and the wavelengths which such solutions must approach as their amplitude decreases to zero are discussed. A sufficient condition for the existence of these small amplitude waves is also established. This is accomplished by studying the nonlinear ordinary differential equation (ODE) for the potential which arises when the distribution functions are represented in a BGK form; the arbitrary functions of energy that describe the BGK representation are treated as an infinite dimensional set of parameters in a bifurcation theory for the ODE. The positivity and zero current condition in the wave frame of the BGK distribution functions are maintained. The undamped small amplitude nonlinear waves so constructed can be made to satisfy the Vlasov dispersion relation exactly, but in general they need only satisfy it approximately. Numerical calculations reveal that even a thermal equilibrium electron-proton plasma with equal ion and electron temperatures will support undamped traveling waves with phase speeds greater than 1.3 times the electron theritial velocity. Dissert. Abstr.

N90-19851# Minnesota Univ., Minneapolis.
THE 41ST ANNUAL GASEOUS ELECTRONICS CONFERENCE Final Report, 1 Jul. 1988 - 30 Jun. 1989
Douglas W. Ernie Sep. 1989 190 p Conference held in

Minneapolis, MN, 18-21 Oct. 1988 Sponsored in part by NSF; General Electric Co.; and GTE, Inc.
(Grant AF-AFOSR-0207-88; AF Proj. 2301)
(AD-A214540; AFOSR-89-1333TR) Avail: NTIS HC A09/MF A01 CSCL 20/9

Session Topics include: Electron-atom collisions; Charged particle distributions and electric fields; Thermal and high pressure plasma processes; Electron and photon interactions; Workshop on the design, calibration, and modeling of research RF plasma processing systems; Posters -- Gaseous electronics; Models and diagnostics of lighting discharges; Electron collisions, including excited states; Lasers; Plasma-surface phenomena; Silane plasmas; Beam-plasma interactions; Non-equilibrium electron transport; Neutral particle distributions; Heavy particle interactions; RF glow discharge modeling; Breakdown and switching; Physics in a Positron Trap; Low-pressure discharges; Experimental -- Electron-molecule collisions; Follow-up to the Workshop on the Design, Calibration, and Modeling of Research RF Plasma Processing Systems. GRA

N90-19852# Maryland Univ., College Park. Div. of Mathematical and Physical Engineering.
NONLINEAR MECHANICS OF UNSTABLE PLASMAS AS RELATED TO HIGH ALTITUDE AERODYNAMICS Final Report, 30 Sep. 1976 - 31 Dec. 1980
H. Lashinsky, J. Silverman, and R. F. Ellis May 1981 9 p
(Grant AF-AFOSR-3129-76; AF Proj. 2307)
(AD-A215126) Avail: NTIS HC A02/MF A01

In the initial stages, research was concerned with the application and experimental techniques which were well known in lumped-parameter systems. Particular emphasis was given to plasma instabilities, nonlinear effects leading to heating of plasma, and turbulence phenomena which affect hypersonic plasma flow. The work consisted of a theoretical program supported by experimental work in a low-temperature plasma device known as a Q-machine. A van der Pol equation was modified, a new equation (Lashinsky-Cap) was derived to describe various periodic instabilities typical of high-speed flow in fluids and plasmas, and a new form of the Mathieu equation developed which describes nonlinear effects in the degenerate parametric excitation of plasma waves. Author

N90-19853# Oak Ridge National Lab., TN.
OVERVIEW OF RECENT RESULTS FROM THE ADVANCED TOROIDAL FACILITY
M. Murakami, E. Anabitarte, F. S. B. Anderson, G. L. Bell, J. D. Bell, T. S. Bigelow, B. A. Carreras, L. A. Charlton, T. L. Clark (Tennessee Univ., Knoxville.), and R. J. Colchin et al 1989 5 p Presented at the 1st International Toki Conference on Plasma Physics and Controlled Nuclear Fusion, Toki, Japan, 4-8 Dec. 1989 Prepared in cooperation with Georgia Inst. of Tech., Atlanta; Kyoto Univ., Japan; Texas Univ., Austin and National Inst. for Fusion Science, Nagoya, Japan
(Contract DE-AC05-84OR-21400)
(DE90-005673; CONF-891240-5) Avail: NTIS HC A01/MF A01

An overview of recent experimental results from the Advanced Toroidal Facility (ATF) is presented. Beam-heated plasmas with bar n(sub e) of 10(exp 20)/cu m and tau(sub E)* of approximately 20 ms were achieved. Thermal collapse of the plasmas is mitigated by wall conditioning and particle fueling. Confinement time scales positively with density and magnetic field, offsetting deterioration with power. Results fit the LHD scaling and the drift wave turbulence scaling. Bootstrap currents observed during ECH agree with neoclassical theory in magnitude and parameter dependences. Fast reciprocating Langmuir probe measurements show that edge fluctuations in ATF have many similarities to those in the TEXT tokamak. The location of magnetic flux instabilities has shifted outward in radius, consistent with the broader pressure profiles. DOE

N90-19854# Instituto de Pesquisas Espaciais, Sao Jose dos Campos (Brazil).
PLASMA CENTRIFUGE WITH VACUUM ARC DISCHARGE APPLIED TO THE SEPARATION OF STABLE ISOTOPES Ph.D. Thesis
Edson DelBosco Sep. 1989 205 p In PORTUGUESE; ENGLISH summary
(INPE-4925-TDL/385) Avail: NTIS HC A10/MF A02

The results of a vacuum-arc plasma centrifuge experiment are described. A plasma centrifuge is an apparatus where a plasma column is produced due to the interaction of an electric current with an externally applied magnetic field, vector J x vector B. Among the applications of a rotating plasma, this work deals particularly with its utilization in an isotope enrichment device. The main characteristics of the plasma produced in this experiment are presented, with special attention to the plasma column rotation and the isotope enrichment. The analysis of the results is performed using a fluid model for a completely ionized rigid body rotating plasma column in steady state equilibrium. The main results are: (1) rotation frequency of the plasma column in the range 2 x (exp 4) to 3 x 10 (exp 5) rad/s; (2) enrichment of 10 to 30 pct for the magnesium isotopes, and 290 to 490 pct for the carbon-13 isotope; (3) rigid body rotation of the plasma column only for radii smaller than the characteristic radius of the plasma column, r(sub e); (4) linear dependence of the rotation frequency upon the magnetic field strength only for r is less than r(sub e); (5) existence of an optimum value of the magnetic field for maximum enrichment; and (6) dependence of the rotation frequency upon the inverse of the atomic mass. Author

N90-19855# Northeastern Univ., Boston, MA.
ACTIVE PROBING OF SPACE PLASMAS Final Report, 25 Oct. 1985 - 30 Sep. 1989
Chang Chan, Michael B. Silevitch, and Elena Villalon 1 Sep. 1989 110 p
(Contract F19628-85-K-0053)
(AD-A216867; GL-TR-89-0272) Avail: NTIS HC A06/MF A01 CSCL 04/1

During the course of the research period our efforts were focused on the following areas: (1) An examination of stochastic acceleration mechanisms in the ionosphere; (2) A study of nonequilibrium dynamics of the coupled magnetosphere - ionosphere system; and (3) Laboratory studies of active space experiments. Reprints include: Dynamics of charged particles in the near wake of a very negatively charged body -- Laboratory experiment and numerical simulation; Laboratory study of the electron temperature in the near wake of a conducting body; New model for auroral breakup during substorms; Substorm breakup on closed field lines; New model for substorm on sets -- The pre-breakup and triggering regimes; Model of the westward traveling surge and the generation of Pi 2 pulsations; Ionospheric electron acceleration by electromagnetic waves near regions of plasma resonances; Relativistic particle acceleration by obliquely propagating electromagnetic fields; Some consequences of intense electromagnetic wave injection into space plasmas. GRA

N90-19856# Academy of Sciences (USSR), Novosibirsk. Inst. of Nuclear Physics.
NEGATIVE ION SURFACE PLASMA SOURCE DEVELOPMENT FOR PLASMA TRAP INJECTORS IN NOVOSIBIRSK
Yu. I. Belchenko, G. I. Dimov, V. G. Dudnikov, and A. S. Kupriyanov 1989 33 p Prepared for ORNL, TN
(Contract DE-AC05-84OR-21400)
(DE90-006082; ORNL/tr-89/54; Preprint-88-14) Avail: NTIS HC A03/MF A01

Work on high-current ion sources carried out at the Novosibirsk Institute of Nuclear Physics (INP) is presented. The INP investigations on pure plasma planotron and pure surface secondary emission systems of H(-) generation, which preceded the surface-plasma concept developed in Novosibirsk, are described. The physical basis of the surface-plasma method of negative-ion production is considered. The versions and operating characteristics of different surface-plasma sources including the

multi-ampere (is approximately or greater than 10 A) source are discussed. Research on efficient large-area (approximately 10(exp 2)/sq cm) negative ion surface-plasma emitters is described. The INP long-pulse multiaperture surface-plasma generators, with a current of about 1A, are described. DOE

N90-19857# International Centre for Theoretical Physics, Trieste (Italy).
NONLINEAR INTERACTION OF ELECTROSTATIC WAVES AT A NARROW INHOMOGENEOUS LAYER OF A WARM MAGNETOACTIVE PLASMA
A. M. Hussein Jul. 1989 7 p Submitted for publication
(DE90-610624; IC-89/165) Avail: NTIS (US Sales Only) HC A02/MF A01

An investigation is made of nonlinear interaction of electrostatic waves at a narrow inhomogeneous layer of a warm magnetoactive plasma. The amplitudes of the radiated second-harmonic waves are calculated. The effect of the external magnetic field is to increase the amplitudes of the generated waves. DOE

N90-19858# International Centre for Theoretical Physics, Trieste (Italy).
A STORAGE PROCESS OF THE MAGNETIC ENERGY RESULTS FROM THE UNSTEADY PLASMA FLOW FIELD IN THE SPACE ACTIVE REGIONS AND STELLAR ATMOSPHERE
Zhongyuan Li Aug. 1989 5 p Submitted for publication
(DE90-610638; IC-89/200) Avail: NTIS (US Sales Only) HC A01/MF A01

In the discussion about the energy storage by a pure azimuthal motion in the active regions of solar and stellar atmosphere we consider the unsteady poloidal flow field and the unsteady coupling process between the magnetic field and both the toroidal and the poloidal velocity components. DOE

N90-19859# Hampton Univ., VA.
ANOMALOUS TRANSPORT IN TOROIDAL PLASMAS Final Progress Report, 15 Mar. 1988 - 1 Nov. 1989
Alkesh Punjabi Dec. 1989 49 p Sponsored in part by LANL and ORAU
(Contract DE-FG05-88ER-53265)
(DE90-006549; DOE/ER-53265/1) Avail: NTIS HC A03/MF A01

When the magnetic moment of particle is conserved, there are three mechanisms which cause anomalous transport. These are: variation of magnetic field strength in flux surface, variation of electrostatic potential in flux surface, and destruction of flux surface. The anomalous transport of different groups of particles resulting from each of these mechanisms is different. This fact can be exploited to determine the cause of transport operative in an experimental situation. This approach can give far more information on the transport than the standard confinement time measurements. To implement this approach, Monte Carlo codes were developed for toroidal geometries. The equations of motion are developed in a set of non-canonical, practical Boozer co-ordinates by means of Jacobian transformations of the particle drift Hamiltonian equations of motion. Effects of collisions are included by appropriate stochastic changes in the constants of motion. Effects of the loop voltage on particle motions are also included. The method will be applied to study two problems: the problem of the hot electron tail observed in edge region of ZT-40, and the energy confinement time in TOKAPOLE II. For the ZT-40 problem three situations are considered: a single mode in the core, a stochastic region that covers half the minor radius, a stochastic region that covers the entire plasma. A turbulent spectrum of perturbations based on the experimental data of TOKAPOLE II are developed. This is used to simulate electron transport resulting from ideal instabilities and resistive instabilities in TOKAPOLE II. DOE

N90-19860# Spectra Technology, Inc., Bellevue, WA.
THEORY OF FIELD REVERSED CONFIGURATIONS Final Report
Loren C. Steinhauer Jan. 1990 20 p
(Contract DE-AC06-80ER-53098)
(DE90-006702; DOE/ER-53098/T1) Avail: NTIS HC A03/MF A01

This final report surveys the results of work conducted on the theory of field reversed configurations. This project has spanned ten years, beginning in early 1980. During this period, Spectra Technology was one of the leading contributors to the advances in understanding FRC. The report is organized into technical topic areas, FRC formation, equilibrium, stability, and transport. Included as an appendix are papers published in archival journals that were generated in the course of this report. DOE

N90-19861# Lawrence Livermore National Lab., CA.
ELECTRICAL RESISTIVITY OF STRONGLY COUPLED PLASMAS IN INTENSE FIELDS
Aug. 1989 6 p Presented at the 24th Yamada Conference on Strongly Coupled Plasma Physics, Tokyo (Japan), 29 Aug. - 2 Sep. 1989
(Contract W-7405-eng-48)
(DE90-002236; UCRL-102037; CONF-8908133-9) Avail: NTIS HC A02/MF A01

It is now possible to measure the electrical resistivity, or alternatively the electron collision frequency, in strongly coupled plasmas through the use of very fast laser pulses. In such experiments, the effect of the intense laser field needs to be included in the calculation of material transport coefficients. A form was derived for the electrical resistivity which includes the effects of strong correlations, as well as an external electric field. The results are compared with other theories and a recent set of experiments. DOE

N90-19862# Sandia National Labs., Albuquerque, NM.
DYNAMICS OF PLASMA INJECTION ALONG MAGNETIC FIELD LINES IN THE PBFA 2 (PARTICLE BEAM FUSION ACCELERATOR 2) PLASMA OPENING SWITCH
Michael H. Frese (NumerEx, Albuquerque, NM.) Nov. 1989 37 p
(Contract DE-AC04-76DP-00789)
(DE90-006751; SAND-89-7154) Avail: NTIS HC A03/MF A01

In the magnetically injected plasma (MIP) plasma opening switch (POS) presently under study for use on the Particle Beam Fusion Accelerator 2 (PBFA 2), plasma is injected along an imposed poloidal field to control the position of the plasma. The magnetic field and the plasma density combine to make the Alfven velocity very high relative to the injection velocity of the plasma. In fact, the ration of these velocities, the Alfven-Mach number of the flow, ranges from 0.001 to 0.01. Explicit computation at these low Mach numbers is exceedingly tedious, and implicit computation without a very high convergence rate scheme is little better. However, the physical effect is clear: the field lines are effectively very stiff and not subject to displacement by the plasma. The plasma motion may thus be computed by simply restricting the velocity to lie along the field. Simulations in the true experimental geometry using this approach agree qualitatively with microwave interferometry measurements of the plasma density in the experimental test stand. The agreement is quantitative, subject only to the adjustment of the unknown plasma source mass flux rate. DOE

N90-19863# Japan Atomic Energy Research Inst., Tokai.
RECORD OF FORUM ON COLD FUSION
Naomoto Shikazono, Enzo Tachikawa, and Tatsucki Takeda Sep. 1989 43 p
(DE90-749883; JAERI-M-89-132) Avail: NTIS (US Sales Only) HC A03/MF A01

At the forum 10 lectures and comments were given, which were followed by lively discussion. Emphasis of the forum was put on theoretical aspects to clarify the mechanisms of the cold fusion phenomena. This record of the forum is compilation of revised extended abstracts based on the abstracts which were distributed at the forum. DOE

N90-19864# Technische Hochschule, Darmstadt (Germany, F.R.). Mathematisch-Naturwissenschaftlichen Fachbereiche.
INCOHERENT RETRODIFFUSION OF RADIOWAVES IN PLASMA WITH PARTICLE IMPULSE Ph.D. Thesis [INKOHAERENTE RUECKSTREUUNG VON RADIOWELLEN DURCH EIN PLASMA UNTER BERUECKSICHTIGUNG VON TEILCHEN-STOESSEN]
Volker Grassmann 1988 52 p In GERMAN
(ETN-90-95375) Avail: NTIS HC A04/MF A01

The incoherent retrodiffusion with constant momentum and energy is studied. The most important parameter is the relation to the pulse number on the one hand and the particle velocity and the radar frequency on the other hand. Retrodiffusion spectrum is described by the Dougherty-Farley formula and the kinetic and hydrodynamic Fokker-Planck model, developed by Stubbe. Their descriptions of the phenomena are similar but they are different as regards the calculation of absolute values of ionosphere parameters. Isotherm changes of state are difficult to describe by the Fokker-Planck model, which demonstrates the impossibility of correctly depicting a plasma with only the energy, the momentum and the particle density. ESA

N90-19865# Los Alamos National Lab., NM.
PLASMA SIMULATION ON MAGNETOHYDRODYNAMIC TIME SCALES
J. U. Brackbill 1990 7 p Presented at the Supercomputing in Nuclear Applications, Mito City, Japan, 12-16 Mar. 1990
(Contract W-7405-eng-36)
(DE90-007490; LA-UR-90-608; CONF-900343-4) Avail: NTIS HC A02/MF A01

Progress in the development of implicit-moment methods for plasma simulation on magnetohydrodynamic time scales is described. The objective of the development is a method that is applicable not only to transport phenomena on long time scales, but also to plasma interactions with a wall and sheath formation. The implicit field equations for a plasma in a dc magnetic field are given, and a method is described for their solution. An adaptive grid formulation is outlined, and a problem initialization presented to illustrate its application. The issue of nonlinear stability, which is still unresolved, is reviewed. DOE

N90-19866# Los Alamos National Lab., NM. Physics Div.
AN ELECTRICAL MODEL FOR PLASMA ARMATURE VOLTAGE
Jerald V. Parker 1990 7 p Presented at the 5th IEEE Symposium on Electromagnetic Launch Technology, Destin, FL, 1-5 Apr. 1990
(Contract W-7405-eng-36)
(DE90-007530; LA-UR-90-456; CONF-9004136-2) Avail: NTIS HC A02/MF A01

Scaling of armature voltage with bore diameter is an important issue since it affects the predicted efficiency and the predicted velocity performance of proposed large bore EM launchers. In this paper the experimental data for railguns with plastic/composite insulation is shown to fit a scaling relation of the form V(sub m) = V(sub e) + E(j)d, where the electric field dependence on current density is given by E(j) = E(sub 0) + J/sigma. This scaling relation predicts a linear increase in armature voltage with bore diameter for d greater than 0.1 m. The model is in better agreement with the limited data on large bore railguns than earlier models. DOE

N90-19867# Naval Research Lab., Washington, DC. Beam Physics Branch.
THE NONLINEAR INTERACTION OF INTENSE LASER PULSES IN PLASMAS Interim Report
P. Sprangle, E. Esarey, and A. Ting 22 Dec. 1989 38 p
(AD-A217604; NRL-MR-6545) Avail: NTIS HC A03/MF A01
CSCL 09/3

A nonlinear 1D theory is developed which describes some important aspects of intense laser-plasma interactions. The self-consistent laser-plasma analysis included nonlinear plasma wakefield generation, relativistic optical guiding, coherent harmonic radiation production, as well as other related phenomena. Relativistic optical guiding is found to be most effective for long laser pulses having slow rise times. Short laser pulses are shown to be weakly guided. Coherent harmonic generation using a linearly polarized laser is found to be most efficient for short laser pulses and can be enhanced by the presence of large amplitude plasma wakefields. Aspects of particle acceleration by laser pulses as well as possible methods for upshifting the frequency of laser pulses are also discussed. GRA

N90-19868# Naval Research Lab., Washington, DC. Space Sensing and Space Applications Branch.
DISTRIBUTED BOSONIC STATES AND CONDENSED MATTER FUSION Final Report, Apr. - Sep. 1989
S. R. Chubb and T. A. Chubb (Bendix Field Engineering Corp., Columbia, MD.) 1 Feb. 1990 19 p
(AD-A217605; NRL-MR-6600) Avail: NTIS HC A03/MF A01
CSCL 18/1

The article explains how it is possible for deuterons separated by macroscopic distances to interact in a nuclear fashion through the formation of a Bose Bloch Condensate (BBC) within a solid. Under suitable conditions, the formation of a BBC may lead to nuclear fusion and a variety of heretofore unobserved nuclear processes. The application of these ideas is used to explain the anomalous heating of Pd through the electrolysis of D2O and LiOD and conclude that only a small concentration of BBC deutrons is required. Various experiments associated with condensed matter fusion are suggested that may provide a test of our theory. GRA

76 SOLID-STATE PHYSICS

Includes superconductivity.

For related information, see also *33 Electronics and Electrical Engineering* and *36 Lasers and Masers.*

N90-19869# Argonne National Lab., IL. Materials Science Div.
SUPERCONDUCTIVITY IN Ba(1-x)BiO3
Marcos H. Degani (Instituto de Fisica e Quimica, Sao Carlos, Brazil), Rajiv K. Kalia, and Priya Vashishta Oct. 1989 12 p Presented at the 7th International Conference on Solid-State Ionics, Hakone, Japan, 5-9 Nov. 1989
(Contract W-31-109-eng-38)
(DE90-003781; CONF-891124-2) Avail: NTIS HC A03/MF A01

Phonon density-of-states (DOS) of insulating BaBiO3 and superconducting Ba(0.6)K(0.4)BiO3 is studied using effective interaction potentials and molecular dynamics (MD) method. MD results are in good agreement with the inelastic neutron scattering and electron tunneling experiments. Calculated oxygen isotope effect using the Eliashberg gap equations is also in good agreement with the experiments. Cumulative evidence based on the neutron scattering, tunneling, and the isotope effect suggests that this material is a normal BCS electron-phonon superconductor. DOE

N90-19870# Westinghouse Savannah River Co., Aiken, SC. Scientific Computations Section.
SUPERCOMPUTER APPLICATIONS FOR MATERIALS SCIENCE: ORDERING EFFECTS OF HYDROGEN IN PALLADIUM
1989 16 p Presented at the Annual Westinghouse Computer Symposium, Pittsburgh, PA, 6-7 Nov. 1989
(Contracts DE-AC09-76SR-00001; DE-AC09-88SR-18035)
(DE90-004664; WSRC-RP-89-475; CONF-891192-26) Avail: NTIS HC A03/MF A01

Total energy computed with the Ab Initio PSeudoFunction (PSF) energy band method is used to analyze from first principles the electronic structure and relative stability of Hydrogen (H) in a Palladium (Pd) matrix of well separated H atoms. The results indicate the importance of Hydrogen ordering effects in the Palladium matrix. In an expanded lattice (i.e., beta phase, with a lattice constant of 4.025A), total energies were calculated for incremental displacement of the Hydrogen atoms along five distinct paths starting from octahedral sites and terminating at the

tetrahedral sites. Results are reported for these different combinations of seemingly equivalent tetrahedral sites, along with a description of the computational procedures used. DOE

N90-19871# Brookhaven National Lab., Upton, NY. Dept. of Applied Science.
OXYGENATION AND POSSIBLE ETCHING OF HIGH T(SUB c) SUPERCONDUCTING FILMS BY OXYGEN PLASMA
M. W. Ruckman, R. C. Budhani, and S. L. Qiu 1989 8 p Presented at the 36th American Vacuum Society National Vacuum Symposium, Boston, MA, 23-27 Oct. 1989
(Contracts DE-AC02-76CH-00016; DE-AS05-80ER-10742)
(DE90-004956; BNL-43119; CONF-891093-20) Avail: NTIS HC A02/MF A01

The use of a radio frequency (rf) excited oxygen plasma for cleaning and oxygenation of high (Tc) superconducting films at room temperature is studied by photoemission spectroscopy. Plasma oxidation at approximately 10 mT pressure, removes contaminants like carbon and causes the Ba 5p and 4d and the 0 1s corelevels to shift to lower binding energy. Valence band spectra for an epitaxial Y2 Ba4 Cu8 O sub 15+x film on SrTiO3 (001) show a Fermi edge and resemble spectra presented by other groups for YBa2 Cu3 sub 7 single crystals and epitaxial films. These films also show a sharp 0 is corelevel near 528 eV. Possible reactive ion etching of a degraded YBCO film surface is demonstrated in a series of spectra taken after successive oxygen plasma treatments. A surface contaminated with BaCO3 becomes barium deficient after the initial plasma treatment but a second plasma treatment of a substrate biased to minus 200 V to promote sputtering produces photoemission features typical of an YBa2 Cu3 O7 surface. DOE

N90-19872 Department of the Navy, Washington, DC.
PASSIVATING LAYER FOR III-V SEMICONDUCTOR MATERIALS Patent
Berned T. Jonker, inventor (to Navy), Gary A. Prinz, inventor (to Navy), and James J. Krebs, inventor (to Navy) 9 May 1989 5 p Filed 30 Mar. 1988 Supersedes US-Patent-Appl-SN-176115, AD-D013963
(AD-D014321; US-Patent-4,828,935; US-Patent-Appl-SN-176115) Avail: US Patent and Trademark Office CSCL 09/1

This invention relates to a semiconductor structure in which an epitaxial semiconductor layer is used to electrically passivate and insulate the semiconductor on which it is deposited. In today's world, developments in electronic devices demand faster and faster reaction speed. We have found that the Zinc Selenide binary semiconductors and alloys of this invention having the general formula Zn(1-x-y)M(x)Q(y)Se:D provide a suitable passivating layer for III-V semiconductor materials which sufficiently minimizes surface state density, surface charge accumulation or charge carrier recombination to significantly improve practical electronic device operation. GRA

N90-19873*# North Carolina State Univ., Raleigh. College of Engineering.
SILICON CARBIDE SEMICONDUCTOR DEVICE FABRICATION AND CHARACTERIZATION Final Report, 10 Feb. 1987 - 9 Feb. 1990
R. F. Davis and K. Das 8 Feb. 1990 35 p
(Contract NAG3-782; N00014-85-K-0182)
(NASA-CR-186354; NAS 1.26:186354) Avail: NTIS HC A03/MF A01 CSCL 20L

A number of basic building blocks i.e., rectifying and ohmic contacts, implanted junctions, MOS capacitors, pnpn diodes and devices, such as, MESFETs on both alpha and beta SiC films were fabricated and characterized. Gold forms a rectifying contact on beta SiC. Since Au contacts degrade at high temperatures, these are not considered to be suitable for high temperature device applications. However, it was possible to utilize Au contact diodes for electrically characterizing SiC films. Preliminary work indicates that sputtered Pt or Pt/Si contacts on beta SiC films are someways superior to Au contacts. Sputtered Pt layers on alpha SiC films form excellent rectifying contacts, whereas Ni layers following anneal at approximately 1050 C provide an ohmic contact. It has demonstrated that ion implantation of Al in substrates held at 550 C can be successfully employed for the fabrication of rectifying junction diodes. Feasibility of fabricating pnpn diodes and platinum gated MESFETs on alpha SiC films was also demonstrated. Author

N90-19874# State Univ. of New York, Buffalo. Dept. of Chemistry.
BCS (BARDEEN-COOPER-SCHRIEFFER) PRIMER: A GUIDE TO COMPUTATIONAL METHODS IN SUPERCONDUCTIVITY THEORY
Devaraj Sahu, Andreas Langner, and Thomas F. George Dec. 1989 11 p Submitted for publication Sponsored in part by New York State Inst. on Superconductivity and New York State Energy Research and Development Authority, New York
(Contract N00014-90-J-1193)
(AD-A216393; UBUFFALO/DC/89/TR-4) Avail: NTIS HC A02/MF A01 CSCL 20/3

Because of the recent revival of interest in superconductivity, we have felt that a pedagogical, yet concise review of the fundamental ideas of the Bardeen-Cooper-Schrieffer (BCS) theory of superconductivity is timely. We discuss the basic ideas of the BCS theory and list the formulae for the thermodynamic quantities of this theory in the usual real-time representation. We also represent these formulae in the alternate imaginary-time representation, which makes hands-on numerical evaluation of the thermodynamic quantities of interest readily accessible. Finally, we point out the limitations of the BCS theory and describe some of its proposed extensions for describing the behavior of some of the new, unconventional superconductors. GRA

N90-19875# Naval Research Lab., Washington, DC. Materials Physics Branch.
CRITICAL CURRENT DENSITY AND TRANSITION TEMPERATURE MEASUREMENTS OF Y-Ba-Cu-O RODS
T. L. Francavilla, G. A. Candela, and R. J. Soulen, Jr. 19 Dec. 1989 35 p
(AD-A216695; NRL-MR-6534) Avail: NTIS HC A03/MF A01 CSCL 20/13

Measurements were made on the superconducting properties of cylindrical Y-Ba-Cu-O rods prepared by ICI Americas Inc. The transition temperature was determined from measurements of ac susceptibility as a function of temperature. The critical current density at 77 K was determined by measuring the voltage as a function of current using four terminal transport measurements, in magnetic fields of different intensities. GRA

N90-19876# Harvard Univ., Cambridge, MA. Div. of Applied Sciences.
TUNNELING MICROSCOPY OF SUBMONOLAYER ADSORBATES ON Si3
Peter John Bedrossian Oct. 1989 223 p
(Contract N00014-87-K-0511)
(AD-A216985; TR-1) Avail: NTIS HC A10/MF A02 CSCL 20/12

The first real space observation are reported for several new types of ordered surface structures induced by submonolayer gallium or boron adsorption on Si(111). Where surface doping concentrations can be controlled, one can identify distinct electronic characteristics, spatially localized on the atomic scale, that reflect both average and local dopant distributions and binding configurations. The experiments make use of a scanning tunneling microscope constructed for vacuum operation. For each known, ordered phase of gallium adsorption, multiple-phase-domain images are employed to identify the respective adsorbate binding configurations. For boron adsorption, one finds one ordered surface phase, which can accommodate boron concentrations from very low coverage up to 1/3 monolayer. Local tunneling spectroscopy performed over the available range of boron concentration leads to the identification of distinct current-voltage characteristics with the presence or absence of the dopant at individual atomic sites. Under certain systematic conditions, negative differential was

observed conductivity in the microscope's tunnel junction, and spatially localized electronic characteristics were identified that enable single atoms to act as isolated tunnel diodes together with the microscope's tunneling tip. The qualitative corroboration of the results of recent surface energy and stress calculations by the structural and electronic observations suggests that the conceptual approaches behind these computations might eventually offer a substantial predictive capability. GRA

N90-19877# Oak Ridge National Lab., TN. Solid State Div.
HETEROEPITAXIAL GROWTH OF GERMANIUM FILMS BY SUPERSONIC FREE JET CHEMICAL BEAM EPITAXY
Djula Eres, J. W. Sharp (Tennessee Univ., Knoxville.), and D. H. Lowndes Nov. 1989 5 p Presented at the Materials Research Society Fall Meeting, Boston, MA, 27 Nov. - 2 Dec. 1989 Submitted for publication
(Contract DE-AC05-84OR-21400)
(DE90-006621; CONF-891119-87) Avail: NTIS HC A01/MF A01

A supersonic free jet operated in continuous wave and pulsed mode was used to grow Ge films on (100) GaAs and (100) Si substrates. The Ge-bearing source molecule digermane (Ge2 H6) was seeded (at 5 percent concentration) in a helium carrier gas. A free jet expansion of this gas mixture was directed toward the heated substrate surface, where Ge film growth took place by surface-induced thermal decomposition of the ballistically impinging digermane molecules. The thickness distribution across the substrate surface was fitted by a cos (m) theta distribution. The values of m spanned the range 6 to 35. The upper limit on growth resulting from background gas scattered out of the jet was found to be less than 10 percent of the Ge film thickness for growth on (100) GaAs, and around 25 percent for growth on (100) Si. DOE

N90-19878# Oak Ridge National Lab., TN. Solid State Div.
CHARACTERIZATION OF GROUND STATE NEUTRAL AND ION TRANSPORT DURING LASER ABLATION OF 1:2:3 SUPERCONDUCTORS BY TRANSIENT OPTICAL ABSORPTION SPECTROSCOPY
David B. Geohegan and Douglas N. Mashburn Nov. 1989 4 p Presented at the Materials Research Society Fall Meeting, Boston, MA, 27 Nov. - 2 Dec. 1989 Submitted for publication
(Contract DE-AC05-84OR-21400)
(DE90-006623; CONF-891119-86) Avail: NTIS HC A01/MF A01

Optical absorption in the plume produced by excimer laser ablation of YBa2Cu3O(7-x) under film growth conditions has been observed for the first time and used to characterize the transport of ground state Y, Ba, and Cu neutrals as well as Y+ and Ba+ ions. Spatially and temporally resolved absorption measurements (0.6 mm, 20 ns resolution) indicate significant ground state number densities at times following the laser pulse that are up to an order of magnitude longer than the duration of fluorescence from excited states. Time-of-flight absorbance profiles result in velocity distributions that are broadened significantly toward lower velocities and reveal a low velocity component (less than 10(sup 5) cm/s) to the ablation process which is not observed using emission spectroscopy. Electric ion probe measurements of the time dependence of Y+ ions confirm the existence of the new, slow velocity component. Electron densities greater than 10(sup 16)/cu cm in the white plasma close to the pellet have been estimated using spectrally broadened emission lines. The effects of oxygen ambient pressures and the detection of YO, BaO, and CuO also are reported. This technique is applicable as an situ monitor of the kinetic energy of ablated species during low temperature deposition of epitaxial 1:2:3 superconducting thin films. DOE

N90-19879# International Centre for Theoretical Physics, Trieste (Italy).
A SIMPLE MODEL FOR THE DETERMINATION OF L(SUB 0), D AND TAU IN A SEMICONDUCTOR AND THEIR TEMPERATURE DEPENDENCE
Feroz Ahmed Jul. 1989 5 p Submitted for publication
(DE90-610564; IC-89/175) Avail: NTIS (US Sales Only) HC A01/MF A01

It is very important to characterize the quality of a semiconductor material before it is processed into a device. Diffusion length L(sub 0), diffusion constant (D) and carrier lifetime (tau) of minority carriers are some of the parameters which play a vital role in determining the quality of a semiconductor material. It was shown that by measuring the frequency response of a time varying (e(sup iwt)) light (or electron) beam one can determine all the important parameters including the absorption coefficient of light and surface recombination velocity. A simple method is proposed by which one can obtain L(sub 0), D and tau separately from measured phase shift of short circuit photo current at some modulation frequency (omega) and at two different wavelengths of incident light. It is suggested that the above procedure is particularly suitable for inferring the temperature dependence of these parameters. DOE

N90-19880# International Centre for Theoretical Physics, Trieste (Italy).
NUCLEATION OF VORTICES IN SUPERFLUID HELIUM-4
Mubarak Ahmad Dec. 1988 21 p Submitted for publication
(DE90-610675; IC-88/400) Avail: NTIS (US Sales Only) HC A03/MF A01

Nucleation of vortices and strings is studied in superfluid helium in the context of phase transitions in this system. It is shown that the formation of these structures depends on the homotopy groups of the manifold of degenerate condensed states. The subsequent evolution of these structures is investigated and then impact on superfluid nature of this system is analyzed. The cross section for the scattering of quasi particles is estimated. This is exploited to find the effect of scatterings on the dynamics of shrinking vortex. DOE

N90-19881# International Centre for Theoretical Physics, Trieste (Italy).
GOLDSTONE EXCITATION AND SYMMETRY BREAKING MECHANISM IN SUPERFLUID He-4
Mubarak Ahmad, Mikhaeil H. Hanna, S. K. Tikoo, and T. K. Raina (Kashmir Univ., Srinagar, India) Dec. 1988 14 p Submitted for publication
(DE90-610676; IC-88/401) Avail: NTIS (US Sales Only) HC A03/MF A01

The form of Goldstone excitation in superfluid He-4 is envisaged by the formalism of scaling transformation. This is achieved within the framework of symmetry breaking mechanism which is akin to that of the relativistic quantum field theory. DOE

N90-19882# International Centre for Theoretical Physics, Trieste (Italy).
COHERENT STATE IN THE ROTON REGION OF SUPERFLUID HELIUM-4
Mubarak Ahmad, Mikhaeil H. Hanna, S. K. Tikoo, and T. K. Raina (Kashmir Univ., Srinagar, India) Dec. 1988 13 p Submitted for publication
(DE90-610677; IC-88/402) Avail: NTIS (US Sales Only) HC A03/MF A01

Coherent states in the roton region of superfluid He-4 are studied with a view to determine the transition probability from phonon to roton states. These states are formed such that they are found to be identical to those of the angular momentum states. DOE

N90-19883# Executive Office of the President, Washington, DC.
NATIONAL ACTION PLAN ON SUPERCONDUCTIVITY RESEARCH AND DEVELOPMENT
Dec. 1989 79 p
(PB89-138512) Avail: NTIS HC A05/MF A01 CSCL 20L

The Superconductivity Action Plan pursuant to the Superconductivity and Competitiveness Act of 1988 is presented. The plan draws upon contributions from leaders in the technical community of the Federal Government responsible for research and development in superconductivity programs, as well as from

the report of the Committee to Advise the President on Superconductivity. Input from leaders in the private sector was obtained during the formulation and review of the plan. Some contents: Coordination of the plan; Technical areas (high temperature superconductivity materials in general, high temperature superconductivity films for sensors and electronics, magnets, large area high temperature superconductivity films, bulk conductors); and Policy areas. Author

N90-19884* National Aeronautics and Space Administration. Pasadena Office, CA.
ANNEALING GROUP III-V COMPOUND DOPED SILICON-GERMANIUM ALLOY FOR IMPROVED THERMO-ELECTRIC CONVERSION EFFICIENCY Patent
Jan W. Vandersande, inventor (to NASA), Charles Wood, inventor (to NASA), and Susan L. Draper, inventor (to NASA) (California Inst. of Tech., Pasadena.) 18 Jul. 1989 8 p Filed 21 Apr. 1988
(NASA-Case-NPO-17259-1-CU; US-Patent-4,849,033; US-Patent-Appl-SN-184234; US-Patent-Class-148-13.1; US-Patent-Class-148-13; US-Patent-Class-437-903; US-Patent-Class-428-641) Avail: US Patent and Trademark Office CSCL 20L

The thermoelectric conversion efficiency of a GaP doped SiGe alloy is improved about 30 percent by annealing the alloy at a temperature above the melting point of the alloy, preferably stepwise from 1200 C to 1275 C in air to form large grains having a size over 50 microns and to form a GeGaP rich phase and a silicon rich phase containing SiP and SiO2 particles.
Official Gazette of the U.S. Patent and Trademark Office

N90-19885# Oak Ridge National Lab., TN.
NEUTRON SCATTERING MEASUREMENTS OF THE MAGNETIC EXCITATIONS OF HIGH-TEMPERATURE SUPERCONDUCTING MATERIALS
H. A. Mook, G. Aeppli, S. M. Hayden, Z. Fisk, and D. Rytz (Hughes Research Labs., Malibu, CA.) 1989 14 p Presented at the NATO Advanced Research Workshop on Dynamics of Magnetic Fluctuations in High Temperature Superconductors, Crete, Greece, 10-14 Oct. 1989
(Contract DE-AC05-84OR-21400)
(DE90-006567; CONF-8910350-1) Avail: NTIS HC A03/MF A01

Since the discovery of superconductivity in La sub 1-x Ba sub x sub 2 CuO4 by Bednorz and Mueller in 1986, there has been an enormous interest in all aspects of this family of materials. Our measurements have used neutron scattering techniques to study the magnetic properties of these materials. The measurements were made at the Institut Laue-Langevin in Grenoble, France, and at the Risoe National Laboratory at Roskilde, Denmark. A number of studies of these types of materials have previously been made at other laboratories, particularly Brookhaven National Laboratory. Many of our measurements have been made on a different energy scale than the earlier measurements, and different aspects of the problem have been addressed. Where the experiments have overlapped, good agreement has generally been found. We have chosen to address the problem by first using high-energy neutrons so that the fundamental properties of the excitations such as the spin wave velocity and lifetimes can be isolated. We then used lower energy neutrons to cover a wide energy scale. Indeed, particularly for La2 CuO4, we have used incident neutrons varying in energy from 0.3 eV to 4 MeV. This required experiments on a number of different neutron spectrometers. DOE

N90-19886# California Inst. of Tech., Pasadena.
INVESTIGATIONS OF CuInSe2 THIN FILMS AND CONTACTS
Jan. 1990 12 p
(Contract DE-AC02-83CH-10093)
(DE90-000301; SERI/STR-211-3612) Avail: NTIS HC A03/MF A01

Various studies of copper indium diselenide (CuInSe2) thin-film materials and contacts are described. The CuInSe2 films prepared on substrates of glass or Mo-coated glass show the same polycrystalline structure, a Cu-rich composition, and a preferential grain orientation; however, they exhibit different surface morphologies, grain sizes, and shapes. Rutherford backscattering measurements were performed on different samples before and after 600 C annealing. This treatment induced Se evaporation from the CuInSe2 films and interdiffusion between Mo and CuInSe2. DOE

N90-19887# Sandia National Labs., Albuquerque, NM. Compound Semiconductor and Device Research Dept.
CCST (CENTER FOR COMPOUND SEMICONDUCTOR TECHNOLOGY) RESEARCH BRIEFS
Dec. 1989 37 p
(Contract DE-AC04-76DP-00789)
(DE90-006446; SAND-89-2784) Avail: NTIS HC A03/MF A01

This paper discusses the following topics: theoretical predictions of valence and conduction band offsets in III-V semiconductors; reflectance modulation of a semiconductor superlattice optical mirror; magnetoquantum oscillations of the phonon-drag thermoelectric power in quantum wells; correlation between photoluminescence line shape and device performance of p-channel strained-layer materials; control of threading dislocations in heteroepitaxial structures; improved growth of CdTe on GaAs by patterning; role of structure threading dislocations in relaxation of highly strained single-quantum-well structures; InAlAs growth optimization using reflection mass spectrometry; nonvolatile charge storage in III-V heterostructures; optically triggered thyristor switches; InAsSb strained-layer superlattice infrared detectors with high detectivities; resonant periodic gain surface-emitting semiconductor lasers; performance advantages of strained-quantum-well lasers in AlGaAs/InGaAs; optical integrated circuit for phased-array radar antenna control; and deposition and novel device fabrication from Ti2 Ca2 Ba2 Cu3 O sub y thin films. DOE

N90-19888# Bayreuth Univ. (Germany, F.R.).
STRUCTURES INSTABILITIES IN FILAMENT LIQUID CRYSTALS Ph.D. Thesis [STRUKTURBILDENDE INSTABILITAETEN IN NEMATISCHEN FLUESSIGKRISTALLEN]
Walter Zimmermann 1987 187 p In GERMAN Sponsored by Sonderforschungsbereich 213
(ETN-90-95916) Avail: NTIS HC A09/MF A01

For the Rayleigh-Benard convection, a full three dimensional linear stability analysis of the nonstructured state was carried out to derive an analytic expression for the critical voltage. The oblique rolls appear for the low frequencies of the outside voltage. The point of the transition of vertical to oblique rolls is like a Lipschitz point in the equilibrium thermodynamics. The entire study of the time dependence in the equations for the electrohydrodynamics show some new qualitative aspects. It is shown that with a further outside magnetic field, the anisotropic instability mechanism can be eliminated, two further Lipschitz points can be reached experimentally, and convection structures are adaptable to a preferential direction. ESA

N90-19889# Bayreuth Univ. (Germany, F.R.).
ON DISSIPATIVE STATES IN NARROW CURRENT-CARRYING SUPERCONDUCTING FILAMENTS Ph.D. Thesis
Rafael Ernesto RangelCardenas 1988 201 p Sponsored by the Venezuelan National Council for Scientific and Technological Research
(ETN-90-95915) Avail: NTIS HC A10/MF A02

The dynamics of current carrying dissipative states in quasi one dimensional superconductors is studied near the transition temperature. The equations of motion are derived. The time dependence is included via the realtime Keldysh formalism. The linear response to a small amplitude time periodic current, superimposed on to a spatially homogeneous current carrying state, is derived. Analytical expressions for the linear conductivity and the relaxation times are derived in the limit of small currents. Numerical calculations are made for arbitrary currents. The theoretical results are compared with experiments and found to

be in good agreement. The nonlinear dynamics of spatially homogeneous states for time dependent currents is studied and some phenomena such as period-doubling-transition to chaos, intermittency and chaotic attractors are observed. ESA

N90-19890# Technische Univ., Berlin (Germany, F.R.). Fachbereich Physik.
DIGITAL CAPACITY TRANSIENT SPECTROSCOPY OF DEEP STRUCTURE DEFECTS IN III-V-SEMICONDUCTOR STRUCTURES Ph.D. Thesis [DIGITALE KAPAZITAETSTRANSIENTENSPEKTROSKOPIE TIEFER STOERSTELLEN IN III-V-HALBLEITERSTRUKTUREN]
Wolfgang Korb 1989 145 p In GERMAN
(ETN-90-96057) Avail: NTIS HC A07/MF A01

The advantages of Deep Level Transient Spectroscopy (DLTS) methods with digital transients were shown. Different evaluation methods were estimated, such as simulated Boxcar processes with many varied time windows and adaptation of multiexponential theory curves at the measurement data with modulation functions. Measurements were made for n minus and p minus conducting GaAs, n minus and p minus conducting In 0.53 Ga0.47As, N minus In 0.53 Ga0.47As-MOS structures and n minus In P. The samples were doped with vanadium, tungsten, titanium and iron. Measurements with n-Ga-As-Molecular Beam Epitaxy (MBE) layers showed a nickel-impurity by the growth discontinuity. A defect was found in all MBE layers. With Fe-doped and nondoped p+/n minus In GaAs diodes the energetic level of this transient metal in InGaAs can be estimated. InGaAs-MOS structures and contacts with oxide intermediate layers on n minus In P showed a dominating influence of the oxide on the measurements results. ESA

N90-19891# Technische Univ., Berlin (Germany, F.R.). Fachbereich Physik.
SELF-CONSISTANT CALCULATION OF POINT AND PAIR STRUCTURE DEFECTS IN SILICIUM Ph.D. Thesis [SELBSTKONSISTENTE BERECHNUNG VON PUNKT- UND PAARSTOERSTELLEN IN SILICIUM]
Dietmar Weider 1989 178 p In GERMAN
(ETN-90-96059) Avail: NTIS HC A09/MF A01

To calculate structure deep defects in semiconductors, the Green function method was used in the formalism of Hohenberg and Kohn with pseudo potentials. The electronic structure and the charge distribution of the deep defect states in the band holes of point and pair structure defects with sulfur atoms in silicon are investigated. The results for the electronic structure of the sulfur vacancy pairs in silicon correspond to the results obtained for GaAS with a metastable state, that allows assumption of a similar metastable system for the silicon system. The method of the experimental estimation of the distorsion of deep defects is used with pressure-dependent deep-level transient spectroscopy measurement. A theoretical model is proposed, that processes the thermic transfer deep defects with a Green function formalism. ESA

N90-19892# Sandia National Labs., Albuquerque, NM.
NOVEL PROCESSING OF HTS BASED CONDUCTORS
D. S. Ginley, E. L. Venturini, J. F. Kwak, R. J. Baughman, R. J. Bourcier, M. A. Mitchell, B. Morosin, J. W. Halloran, N. J. Neal, and D. W. Capone (Supercon, Inc., Shrewsbury, MA.) 1990 9 p Presented at the Spring Meeting of the Materials Research Society, San Francisco, CA, 16-21 Apr. 1990
(Contract DE-AC04-76DP-00789)
(DE90-005956; SAND-89-2959C; CONF-900466-1) Avail: NTIS HC A02/MF A01

Conductor development is one of the major long term goals in high temperature superconductor research. Two promising processing technologies that were utilized to produce superconducting HTS conductors are reported. First, melt spun YBa2Cu3O7 fibers rapid thermal processed for 1 to 8 sec at 950 to 1075 C have (Tc)'s to 92 K, J(sub c)'s to 1100 A/sq cm and the orthorhombic twinned morphology typical for high quality YBa2Cu3O7. A processing matrix of time, temperature and composition for these fibers shows that slightly CuO-rich starting compositions give the best results. Second, silver tube encapsulated wires of Bi(1.7)Pb(0.3)Sr2Ca2Cu3O10 were made by extrusion, wire drawing and cold rolling. The resulting tapes show orientation of the crystallites, zero resistance up to 100 K and improved magnetic hysteresis above 50 K. The combination of mechanical reprocessing and extended thermal anneals near 850 C appears to significantly improve these materials. DOE

N90-19893# Sandia National Labs., Albuquerque, NM.
FWP EXECUTIVE SUMMARIES: BASIC ENERGY SCIENCES MATERIALS SCIENCES PROGRAMS
F. L. Vook and G. A. Samara Feb. 1990 46 p
(Contract DE-AC04-76DP-00789)
(DE90-006373; SAND-90-0395) Avail: NTIS HC A03/MF A01

The Basic Energy Sciences (BES) Materials Science program at Sandia Albuquerque has the central theme of Scientifically Tailored Materials. The major objective of this program is to combine Sandia's expertise and capabilities in the areas of solid state sciences, advanced atomic-level diagnostics and materials-processing science to produce new classes of tailorable materials for the US energy industry, the electronics industry and for defense needs. Current research in this program includes the physics and chemistry of ceramics, the use of energetic particles for the synthesis and study of materials, high-temperature and organic superconductors, tailored surfaces for materials applications, chemical vapor deposition sciences, strained-layer semiconductors, advanced growth techniques for improved semiconductor structures and boron-rich very high temperature semiconductors. A new start just getting underway deals with the atomic level science of interfacial adhesion. Our interdisciplinary program utilizes a broad array of sophisticated, state-of-the-art experimental capabilities provided by other programs. The major capabilities include several molecular-beam epitaxy and chemical-vapor-deposition facilities, electron- and ion-beam accelerators, laser-based diagnostics, advanced surface spectroscopies, unique combined high-pressure, low-temperature, high-magnetic-field facilities, and the soon to be added scanning tunneling and atomic force microscopies. DOE

N90-19894# Michigan Technological Univ., Houghton. Dept. of Metallurgical Engineering.
THE EFFECTS OF GRADIENTS ON BOUNDARY STABILITY
S. A. Hackney, M. R. Plichta, J. K. Lee, T. M. Lillo, J. L. Trice, and S. H. Yu 1989 20 p
(Contract DE-FG02-87ER-45315)
(DE90-007428; DOE/ER-45315/3) Avail: NTIS HC A03/MF A01

The results are presented from the study of gradient effects on boundary stability. They are tabulated in three categories, designated by the type of boundary being studied: grain boundaries; surfaces; and phase boundaries. DOE

N90-19895# Los Alamos National Lab., NM.
MICROSTRUCTURAL SIMULATIONS OF DYNAMIC RECRYSTALLIZATION
A. D. Rollett, D. J. Srolovitz, and M. J. Luton (Exxon Research and Engineering Co., Annandale, NJ.) 1989 8 p Presented at the TMS Meeting on Simulation and Theory of Evolving Microstructures, Indianapolis, IN, Oct. 1989
(Contract W-7405-eng-36)
(DE90-007504; LA-UR-90-660; CONF-8910304-3) Avail: NTIS HC A02/MF A01

A Monte Carlo model for the simulation of static recrystallization and grain growth has been adapted for dynamic recrystallization by adding recrystallization nuclei and stored energy continuously with time. The results of the simulations have shown that many of the essential features of dynamic recrystallization are reproduced. The stored energy of the system, which may be interpreted as the flow stress, goes through a maximum and then decays, monotonically under some conditions and otherwise in an oscillatory manner. The principal parameters that were varied were the rate of adding stored energy, Delta H, and the rate of adding nuclei, Delta N. As Delta H increases, for fixed Delta N, the

oscillations decay more rapidly and the asymptotic stored energy rises. As Delta N increases, again the oscillations decay more rapidly but the asymptotic stored energy decreases. The mean grain size of the system also oscillates in a similar manner to the stored energy but 90 deg out of phase. Necklacing of the prior grain structure by new grains is observed for low Delta H and high Delta N; it is however, not an invariable feature of grain refinement, i.e., cases where the dynamic grain size is smaller than the initial grain size. All these results were obtained without the addition of special parameters to the model such as a critical strain for the initiation of recrystallization. DOE

N90-19896# Los Alamos National Lab., NM. Material Science and Technology Div.
COMPUTER SIMULATION OF RECRYSTALLIZATION IN THE PRESENCE OF SECOND PHASE PARTICLES
A. D. Rollett, D. J. Srolovitz, R. D. Doherty, M. P. Anderson, and G. S. Grest (Exxon Research and Engineering Co., Annandale, NJ.) 1989 9 p Presented at the TMS Meeting on Simulation and Theory of Evolving Microstructures, Indianapolis, IN, Oct. 1989
(Contract W-7405-eng-36)
(DE90-007531; LA-UR-90-459; CONF-8910304-2) Avail: NTIS HC A02/MF A01

Recrystallization in the presence of inert second-phase particles was simulated with a Monte Carlo technique. The technique is the same one as has been employed successfully to model grain growth, recrystallization and grain growth in the presence of second-phase particles. The results show that at low stored energies, the particles retard the growth of recrystallization nuclei and can prevent the recrystallization process from going to completion. At high enough stored energies, however, growth is not impeded such that the particles do not affect the kinetics of recrystallization. Post-recrystallization is strongly affected by the presence of particles because grain growth is inhibited and the microstructures to be less equiaxed than in grain growth. DOE

N90-19897# California Univ., San Diego. Dept. of Electrical and Computer Engineering.
ION MIXING AND SURFACE MODIFICATION IN METAL-SEMICONDUCTOR SYSTEMS Report, 1 Aug. 1987 - 31 Jan. 1990
S. S. Lau and J. W. Mayer (Cornell Univ., Ithaca, NY.) 1990 15 p
(Contract DE-FG03-84ER-45156)
(DE90-007557; DOE/ER-45156/T3) Avail: NTIS HC A03/MF A01

The phenomenon of ion mixing in metal semiconductor systems was investigated. The primary objectives of this research program were to investigate: the effect of damage distribution to test whether atomic transport was determined by damage concentration. The identity and the control of the moving species are critical factors in forming uniform, ion-mixed layers; and the effect of substrate temperature on the moving species and on the reaction product under ion mixing condition. This part of the research was designed to correlate the interplay between thermodynamical driving forces and kinetic restrictions in ion induced reactions. DOE

N90-19898# North Carolina State Univ., Raleigh. Dept. of Chemistry.
BAND ELECTRONIC STRUCTURES AND CRYSTAL PACKING FORCES Progress Report, Jan. 1989 - Feb. 1990
M.-H. Whangbo 23 Feb. 1990 7 p
(Contract DE-FG05-86ER-45259)
(DE90-007669; DOE/ER-45259/8) Avail: NTIS HC A02/MF A01

The progress was achieved in several areas of the research: organic conducting salts, high temperature copper oxide superconductor, and low dimensional oxides and chalcogenides exhibiting charge density wave phenomena. DOE

N90-19899# Michigan Technological Univ., Houghton. Dept. of Physics.
NMR (NUCLEAR MAGNETIC RESONANCE) IMAGING DEVELOPMENT FOR THE STUDY OF SOLIDS Final Report, 27 Aug. 1986 - 17 Nov. 1989
B. H. Suits 20 Dec. 1989 10 p
(Contract DAAL03-86-G-0065)
(AD-A217073; ARO-23808.3-MS-F) Avail: NTIS HC A02/MF A01 CSCL 20/5

The Techniques of Nuclear Magnetic Resonance imaging are developed for simple inorganic solids and applied to the study of mechanically induced defects in NaCl. The Feasibility of the technique is demonstrated for defect (dislocation) densities greater than 10 million/sq cm with a resolution of better than 1mm. GRA

N90-19900# Martin Marietta Labs., Baltimore, MD.
CONTACT FORMATION ON (Hg,Cd) Te Final Report, Aug. 1985 - Nov. 1989
W. A. Beck and G. D. Davis Dec. 1989 76 p
(Contract DAAG29-85-C-0023)
(AD-A217088; MML-TR-89-117C; ARO-21077.8-MS) Avail: NTIS HC A05/MF A01 CSCL 20/12

Ohmic contacts are an important part of (Hg,Cd) Te infrared detectors. To achieve high sensitivity in staring detectors it is important that the noise be low at frequencies above the video frame rate. Low contact resistance is important both for high-frequency heterodyne detectors, where the resistance may determine the RC time constant of the detector, and for lower-frequency photodiodes because the 1/f noise of the diode junction strongly depends on the junction bias. If the contact resistance is too high, the operating bias on the detector shifts with changing photocurrent, so that even if the junction is optimally biased when looking at one scene, it is improperly biased when looking at a different scene, resulting in excess 1/f noise. Surface-sensitive measurements during overlayer growth on many semiconductors have shown that defects in the semiconductor induced by the metal strongly influence the electron transport between the two materials. These defects can be caused by such processes as chemical reactions, indiffusion of the contact metal, and outdiffusion of the semiconductor components and generally involve decomposition of the semiconductor near the interface. They are especially important during interactions between reactive metals and semiconductors with low thermodynamic stability, such as (Hg,Cd) Te. GRA

N90-19901# Brown Univ., Providence, RI. Dept. of Chemistry.
PREPARATION AND PROPERTIES OF THE SYSTEM Cu(x)Pd(1-x)O (0 LESS THAN OR EQUAL TO x LESS THAN OR EQUAL TO 0.175)
C-M. Niu, P. H. Rieger, K. Dwight, and A. Wold 15 Jan. 1990 19 p
(Contract N00014-89-J-1849)
(AD-A217567; TR-6) Avail: NTIS HC A03/MF A01 CSCL 07/2

Samples of Cu(x)Pd(1-x)O were prepared by code composition of the nitrates. Single phase products were obtained for x less than = 0.15. The presence of Cu(II) in D2h symmetry coordination has been confirmed by magnetic susceptibility and ESR spectra. The results are discussed, compared with those of the system Cu(x)Mg(1-x)O, and interpreted in terms of the Cu(II) coordination symmetry and the electron orbitals. GRA

N90-19902# Brown Univ., Providence, RI. Dept. of Chemistry.
GROWTH AND CHARACTERIZATION OF GALLIUM (III) OXIDE FILMS
P. Wu, Y-M. Gao, R. Kershaw, K. Dwight, and A. Wold 15 Jan. 1990 9 p
(Contract N00014-89-J-1849)
(AD-A217568; TR-5) Avail: NTIS HC A02/MF A01 CSCL 07/2

A simple spray pyrolysis technique has been applied to the formation of dense, homogeneous gallium(III) oxide thin films on

both silicon and silica substrates. The high quality of these films has been established by transmission electron microscopy, x ray diffraction, optical spectra, and current-voltage measurements. GRA

N90-19903# Brown Univ., Providence, RI. Dept. of Chemistry.
THE PREPARATION AND PROPERTIES OF IRON DOPED II-VI CHALCOGENIDES
J. CiCarlo, M. Albert, K. Dwight, and A. Wold 15 Jan. 1990 17 p LIMITED REPRODUCIBILITY: Availability: Document partially illegible
(Contract N00014-89-J-1849)
(AD-A217569; TR-7) Avail: NTIS HC A03/MF A01 CSCL 07/4

Semi-magnetic semiconductors are a class of doped II-VI compounds which are of interest in the study of magnetic interactions. Samples of iron-doped ZnS, ZnSe, and CdS were prepared by the direct combination of the elements. Magnetic measurements indicate that the antiferromagnetic interactions of the iron in the zinc systems were greater than those observed in the cadmium chalcogenides. Single crystals of iron-doped zinc chalcogenides were grown by chemical vapor transport. Their IR transmission was measured and the iron concentration for maximum hardness was determined. GRA

77 THERMODYNAMICS AND STATISTICAL PHYSICS

Includes quantum mechanics; theoretical physics; and Bose and Fermi statistics.

For related information see also *25 Inorganic and Physical Chemistry* and *34 Fluid Mechanics and Heat Transfer.*

N90-19904 ESDU International Ltd., London (England).
TEMPERATURES IN PLATES SUBJECTED TO A SUDDEN INCREASE IN RECOVERY TEMPERATURE
Aug. 1989 5 p Supersedes ESDU-Struct-H.02.00.05
(ESDU-89026; ESDU-Struct-H.02.00.05; ISBN-0-85679-698-0; ISSN-0141-4097) Avail: ESDU

This data item treats the transient situation of the variation of the temperature distribution in a thick plate insulated on one side when the aerodynamic heating temperature on the other side suffers a step change from an initial constant temperature condition. Curves are given that allow the temperatures at both the heated and the insulated surfaces to be obtained at any time, and also to obtain an approximate value for the temperature at any point through the thickness of the plate from a knowledge of those surface values. A fully worked example illustrates the use of the method. ESDU

N90-19905# Los Alamos National Lab., NM. Theoretical Div.
THE RENORMALIZATION GROUP AND LATTICE QCD
Rajan Gupta 1989 46 p Presented at TASI '89: Theoretical Advanced Summer Inst., Boulder, CO, 12-30 Jun. 1989
(Contract W-7405-eng-36)
(DE90-004860; LA-UR-89-4210; CONF-8906267-3) Avail: NTIS HC A03/MF A01

The following topics are discussed: scaling of thermodynamic quantities and critical exponents; scaling relations; block spin idea of Kadanoff; exact RG solution of the 1-d Ising model; Wilson's formulation of the renormalization group; linearized transformation matrix and classification of exponents; derivation of exponents from the eigenvalues of Tau(sub alpha beta); simple field theory: the Gaussian model; linear renormalization group transformations; numerical methods: MCRG; block transformations for 4-d SU(N) LGT; asymptotic freedom makes QCD simple; non-perturbative beta-function and scaling; and the holy grail: the renormalized trajectory. DOE

N90-19906# Gosudarstvennyi Komitet po Ispolzovaniyu Atomnoi Energii, Serpukhov (USSR). Inst. Fiziki Vysokikh Ehnergij.
CLASSICAL MECHANICS ON SUPERSPACE
P. N. Pyatov, A. V. Razumov, and G. N. Rybkin 1988 39 p In RUSSIAN; ENGLISH summary
(DE90-608907; IFVE-OTF-88-212) Avail: NTIS (US Sales Only) HC A03/MF A01

Classical mechanics of systems with states described both by commuting and anticommuting variables is presented. Systems with nonsingular lagrangian functions are considered. The approach based on the concept of superspace where standard functions are determined was used. Grassman algebra with an infinite number of generators was used for constructing analysis. DOE

N90-19907# International Centre for Theoretical Physics, Trieste (Italy).
ON EINSTEINIZATION OF BACKGROUND CURVED SPACE IN THE INDUCED QUANTUM GRAVITY
Yuri V. Novozhilov (Leningrad State Univ., USSR) and D. V. Vassilevich Sep. 1989 7 p Submitted for publication
(DE90-610477; IC-89/280) Avail: NTIS (US Sales Only) HC A02/MF A01

It is shown within the induced quantum gravity approach that approximate invariance of the vacuum (up to topological terms) under rescaling of background tetrads requires that these tetrads should satisfy the Einstein equation with the Newton and cosmological constants defined by low energy parameters. DOE

N90-19908# Los Alamos National Lab., NM. Theoretical Div.
CONSTRUCTION OF FOUR-DIMENSIONAL OPEN SUPERSTRINGS
Zvi Bern and David C. Dunbar (Liverpool Univ., England) 1989 9 p Presented at the 1989 Superstrings Workshop, Tuscaloosa, AL, 8-11 Nov. 1989 Submitted for publication Sponsored in part by Science Research Council
(Contract W-7405-eng-36)
(DE90-006484; LA-UR-90-3; CONF-8911164-1) Avail: NTIS HC A02/MF A01

We present the first examples of space-time supersymmetric one-loop finite four-dimensional open superstrings. DOE

N90-19909# Brigham Young Univ., Provo, UT. Dept. of Chemistry.
THERMODYNAMIC PROPERTIES OF SUPERCRITICAL MIXTURES Final Report, 15 Sep. 1982 - 14 Jun. 1989
R. M. Izatt Jan. 1990 9 p
(Contract DE-FG02-85ER-13443)
(DE90-006720; DOE/ER-13443/3) Avail: NTIS HC A02/MF A01

The focus of the research effort was to gain increased understanding of the energetics associated with chemical and physical interactions involving supercritical fluids. Using a flow calorimetric procedure, heats of mixing (H(sup E)) were determined in temperature and pressure regions spanning critical loci for a large number of binary systems involving combinations of carbon dioxide, Freons, and hydrocarbons. Temperature and pressure ranges covered were 298 to 678 K and 0.1 to 16 MPa, respectively. Use of appropriate models, equations of state, and scaling terms allowed a quantitative understanding of the H(sup E) data to be obtained for the various systems investigated. In those cases where phase splitting occurred, the calorimetric data allowed phase compositions to be determined. These phase compositions were in excellent agreement with literature data obtained by conventional procedures. Advantages of the calorimetric method for phase composition determination are its simplicity, rapidity, avoidance of withdrawing samples from the system, and precise control of the temperature and pressure of measurement. Procedures were developed and tested using carbon dioxide, n-hexane, and toluene for the prediction of H(sup E) values for ternary systems from the H(sup E) values for the component binary systems. The calculated and measured H(sup E) values for the ternary system were in good agreement. DOE

N90-19910# Tokyo Univ., Tanashi (Japan). Inst. for Nuclear Study.
DIMENSIONAL TRANSITION OF THE UNIVERSE

Hidezumi Terazawa Aug. 1989 16 p
(DE90-741461; INS-762) Avail: NTIS (US Sales Only) HC A03/MF A01

In the extended n-dimensional Einstein theory of gravitation, where the spacetime dimension can be taken as a dynamical variable which is determined by the Hamilton principle of minimizing the extended Einstein-Hilbert action, it is suggested that the Universe of four-dimensional spacetime may encounter an astonishing dimensional transition into a new universe of three-dimensional or higher-than-four-dimensional spacetime. DOE

N90-19911# Hiroshima Univ., Takehara (Japan). Research Inst. for Theoretical Physics.
REPARAMETRIZATION BRS COHOMOLOGY IN TWO-DIMENSIONAL GRAVITY AND NON-CRITICAL STRING THEORIES
Kazuo Fujikawa Jul. 1989 30 p Presented at the Spring School of Superstrings, Trieste, Italy, 3-11 Apr. 1989
(DE90-741468; RRK-89-24) Avail: NTIS (US Sales Only) HC A03/MF A01

Various anomalies related to the gravitational BRS current in two-dimensional theories are explained from the view point of the path integral formalism, and the algebraic properties of composite operators are confirmed by the operator product technique. The implications of the reparametrization BRS cohomology on possible non-critical string theory are illustrated by using the string field theoretical technique. The appearance of the Higgs (or Stueckelberg)-like mechanism due to the Liouville freedom is shown. DOE

N90-19912# Hiroshima Univ., Takehara (Japan). Research Inst. for Theoretical Physics.
QUANTUM FIELD THEORY ON HIGHER-GENUS RIEMANN SURFACES
Reijiro Kubo, Hisahiro Yoshu, Shuichi Ojima, Samir K. Paul, and Marg Sachivalaya (Sachivalaya Marg, Bhubaneswar, India) Jul. 1989 20 p Sponsored in part by Grant-in-Aid for Encouragement of Young Scientists
(DE90-741469; RRK-89-25) Avail: NTIS (US Sales Only) HC A03/MF A01

Quantum field theory for b-c systems is formulated on Riemann surfaces with arbitrary genus. We make use of the formalism recently developed by Krichever and Novikov. The Hamiltonian is defined properly, and the Ward-Takahashi identities are derived on higher-genus Riemann surfaces. DOE

N90-19913# Hiroshima Univ., Takehara (Japan). Research Inst. for Theoretical Physics.
LINEARIZED ANALYSIS OF (2+1)-DIMENSIONAL EINSTEIN-MAXWELL THEORY
Jiro Soda Aug. 1989 9 p
(DE90-741470; RRK-89-27) Avail: NTIS (US Sales Only) HC A02/MF A01

On the basis of previous result by Hosoya and Nakao that (2+1)-dimensional gravity reduces the geodesic motion in moduli space, we investigate the effects of matter fields on the geodesic motion using the linearized theory. It is shown that the transverse-traceless parts of energy-momentum tensor make the deviation from the geodesic motion. This result is important for the Einstein-Maxwell theory due to the existence of global modes of Maxwell fields on torus. DOE

N90-19914# Tokyo Univ., Tanashi (Japan). Inst. for Nuclear Study.
ON THE LANGEVIN EQUATION FOR STOCHASTIC QUANTIZATION OF GRAVITY
Nachito Nakazawa Oct. 1989 13 p
(DE90-750024; INS-778) Avail: NTIS (US Sales Only) HC A03/MF A01

The Langevin equation was studied for stochastic quantization of gravity. By introducing two independent variables with a second-class constraint for the gravitational field, a pair of the Langevin equations is formulated for gravity which couples with white noises. After eliminating the multiplier field for the second-class constraint, it is shown that the equations leads to stochastic quantization of gravity including a unique superspace metric. DOE

N90-19915# Technische Univ., Berlin (Germany, F.R.). Fachbereich Mathematik.
CAUSAL BOUNDARY CONSTRUCTION FOR SPACE-TIMES OF THE GENERAL RELATIVITY THEORY Ph.D. Thesis [KAUSALE RANDKONSTRUKTIONEN FUER RAUM-ZEITEN DER ALLGEMEINEN RELATIVITAETSTHEORIE]
Petra Ruebe 1988 142 p In GERMAN
(ETN-90-95357) Avail: NTIS HC A07/MF A01

Several boundaries were examined for general relativistic space-times. A general property of these boundaries is that they can be represented as a quotient of the manifold with preboundary. It is shown that strong causality is not sufficient for the natural inclusion of a space-time in its completeness following Geroch-Kronheimer-Penrose (GKP) to be an embedding. The new causality condition closed strongly causal is shown to be a possibly weakly sufficient requirement; in the hierarchy of the causality conditions it has to be classified between (strongly causal of the second order and steady causal. Some statements on the explicit description of the GKP boundary construction are proved, and some difficulties in the description are explained. Natural mappings between the described boundary constructions and the Budic-Sachs construction for causally continuous space-times were investigated. ESA

80 SOCIAL SCIENCES (GENERAL)

Includes educational matters.

No abstracts in this category.

81 ADMINISTRATION AND MANAGEMENT

Includes management planning and research.

No abstracts in this category.

82 DOCUMENTATION AND INFORMATION SCIENCE

Includes information management; information storage and retrieval technology; technical writing; graphic arts; and micrography.

For computer documentation see *61 Computer Programming and Software.*

N90-19916*# National Aeronautics and Space Administration. Marshall Space Flight Center, Huntsville, AL.
FY 1989 SCIENTIFIC AND TECHNICAL REPORTS, ARTICLES, PAPERS, AND PRESENTATIONS
Joyce E. Turner, comp. Oct. 1989 63 p
(NASA-TM-100384; NAS 1.15:100384) Avail: NTIS HC A04/MF A01 CSCL 05B

A compendium of bibliographic references to papers presented by Marshall Space Flight Center (MSFC) personnel and contractors during FY 1989 is provided. The papers include formal NASA technical reports, memoranda, papers which were published in technical journals, and presentations by MSFC personnel. The

formal NASA technical reports and memoranda have abstracts included. Sources for obtaining these documents are also included. Author

N90-19917 Maryland Univ., College Park.
THE EXPRESSION OF SYNTAGMATIC RELATIONSHIPS IN FRAME-BASED INDEXING Ph.D. Thesis
Rebecca Joyce Green 1989 758 p
Avail: Univ. Microfilms Order No. DA8924157

According to many language models, lower-level units combine to form higher-level composite structures. Within such a model, a distinction can be made between paradigmatic relationships, which pertain to relationships between units/constructs in isolation, and syntagmatic relationships, which pertain to relationships between language units/constructs in combination. After reviewing syntagmatic relator systems used in information retrieval, as well as linguistics and artificial intelligence, the dissertation proposes that the frame, a gestalt structure grounded in conventional situations, be used as the basic syntagmatic indexing unit. Recent research regarding metonymy, prototype and basic-level effects, metaphor, and mental spaces, however, suggests that propositional models operate within restricted bounds; frames may be subject to similar limitations. This study: (1) developed a prototype frame-based indexing language for the New Testament; (2) used this language to index significant portions of the four gospels; and (3) using the case study method, analyzed the indexing to determine whether frame-based indexing is effective and efficient in its expression of syntagmatic relationships. Findings include: (1) frame-based index language development is feasible; (2) frame-based indexing permits retrieval based on syntagmatic structures, thus supporting analogically-based retrieval; (3) through specification of syntagmatic relationships within frames, frame-based indexing facilitates increased precision; (4) frame-based indexing constitutes a stand-alone semantic analysis of a text; (5) additional costs are associated with frame-based indexing and searching; (6) additional mechanisms are required for frame-based index systems to give fully adequate treatment to quantification, profiling, metonymic references, paradigmatic relationships, and mental spaces; (7) frames are a composite of syntagmatic structure and semantic scope; and (8) paradigmatic relationships between syntagmatic structures are highly important. Dissert. Abstr.

N90-19918# Vrije Univ., Amsterdam (Netherlands). Dept. of Mathematics and Computer Science.
AN EQUATIONAL LANGUAGE FOR SPECIFYING, QUERYING, AND UPDATING DATABASE DOMAINS
Roel Wieringa Jun. 1989 92 p
(PB90-124694; IR-192) Avail: NTIS HC A05/MF A01 CSCL 05B

The report draws together the results from earlier research by defining an equational language for the specification of conceptual models (CM's). The specification of a CM consists of four parts, a value specification part to specify unchangeable eternal objects like Booleans, integers, etc., an attribute specification part to specify the attributes applicable to each object identity, an event specification part to specify the possible state changes of each object, and a process specification part to specify how events are composed into processes. All specifications are equational. The specification language can also be used to specify queries, which are equations to be solved in a particular part of the language. The process which the CM executes is the solution of a single process query. Finally, value queries yield information about the unchanging objects, independently of the current state of the CM. It thus gives a formally based and intuitively simple picture of database specification and querying, which integrates traditional programming and database programming in a single equational framework. GRA

N90-19919# Instituto de Pesquisas Espaciais, Sao Jose dos Campos (Brazil).
VISIBILITY PROBLEMS IN NUMERICAL MODELS OF TERRAIN M.S. Thesis
Ewerton SantosSilva Sep. 1989 119 p In PORTUGUESE; ENGLISH summary
(INPE-4921-TDL/382) Avail: NTIS HC A06/MF A01

The use of the Geographic Information System (GIS) developed by Instituto de Pesquisas Espaciais (INPE) to study military problems of visibility and infiltration routes through relief data in Digital Elevation Model (DEM) format is examined. Overviews on terrain military utilization, INPEs GIS and DEM are performed as an introduction to the principal subject. Several kinds of visibility maps are presented and discussed considering a lot of factors such as earth curvature, atmospheric refraction, observation height, and vegetation influence. The infiltration route is researched taking into account only relief variations and distances as a minimum energetic cost path to a walker. Algorithms used to solve the tasks are presented and some problems encountered are discussed. Author

N90-19920# MiTech, Inc., Washington, DC.
EXECUTIVE INFORMATION SYSTEMS FOR PROVIDING NEXT GENERATION STRATEGIC INFORMATION: AN EVALUATION OF EIS (EXECUTIVE INFORMATION SYSTEM) SOFTWARE AND RECOMMENDED APPLICABILITY WITHIN THE FAA COMPUTING ENVIRONMENT Final Report
Jan. 1989 186 p
(Contract DTFA03-88-C-00064)
(AD-A216672; MT/01-89.A1; DOT/FAA/CT-89/8) Avail: NTIS HC A09/MF A01 CSCL 12/5

Commercially-available Executive Information System (EIS) software products are evaluated. Their performance is analyzed against criteria approved by the FAA. Criteria include functionality and ease of use, ease of design and development, hardware and software issues, and maintenance. Data transmission and mainframe storage options within the FAA are identified and evaluated. A recommendation for complete EIS implementation within the FAA is provided. GRA

N90-19921# National Technical Information Service, Springfield, VA.
NATIONAL TECHNICAL INFORMATION SERVICE 1989 USERS CONFERENCE PROCEEDINGS
1989 24 p Conference held in Arlington, VA, 12 Apr. 1989
(PB90-142563) Avail: NTIS HC A03/MF A01 CSCL 05B

This annual event is designed to provide a forum for the exchange of information and ideas between customers and NTIS. The conference was a panel discussion in which CD-ROM users from industry, academia, and the Federal government discussed their experiences with this new technology. NTIS presenters talked about new directions for NTIS, joint ventures, data bases, special products and services, and Federal computer products. Author

N90-19922# National Inst. of Health, Bethesda, MD.
CRISP (COMPUTER RETRIEVAL OF INFORMATION ON SCIENTIFIC PROJECTS) THESAURAS, FISCAL YEAR 1990
1990 754 p
(PB90-138652) Avail: NTIS HC A99/MF A04 CSCL 05B

The CRISP Thesaurus is the controlled vocabulary used to assign indexing terms for the CRISP (Computer Retrieval of Information on Scientific Projects) System, and to subsequently retrieve subject related infomation from it. CRISP is a comprehensive data base which contains records describing research in progress that is supported by the U.S. Public Health Service. It includes extramural programs as well as intramural projects. Two components of the PHS comprise the great majority of records in the System: the National Institutes of Health, and the Alcohol, Drug Abuse, and Mental Health Administration. Author

N90-19923*# Cornell Univ., Ithaca, NY. Dept. of Computer Science.
DECEIT: A FLEXIBLE DISTRIBUTED FILE SYSTEM
Alex Siegel, Kenneth Birman, and Keith Marzullo 7 Dec. 1989 35 p

(Contract NAG2-593; N00014-87-C-8904; ARPA Order 6037) (NASA-CR-186412; NAS 1.26:186412; TR-89-1042) Avail: NTIS HC A03/MF A01 CSCL 05B

Deceit, a distributed file system (DFS) being developed at Cornell, focuses on flexible file semantics in relation to efficiency, scalability, and reliability. Deceit servers are interchangeable and collectively provide the illusion of a single, large server machine to any clients of the Deceit service. Non-volatile replicas of each file are stored on a subset of the file servers. The user is able to set parameters on a file to achieve different levels of availability, performance, and one-copy serializability. Deceit also supports a file version control mechanism. In contrast with many recent DFS efforts, Deceit can behave like a plain Sun Network File System (NFS) server and can be used by any NFS client without modifying any client software. The current Deceit prototype uses the ISIS Distributed Programming Environment for all communication and process group management, an approach that reduces system complexity and increases system robustness. Author

N90-19924# Nationaal Inst. voor Kernfysica en Hoge Energiefysica, Amsterdam (Netherlands).
LITERATURE FILE ON FAST KICKERS AND SEPTA: COMPONENTS FOR DEFLECTION AND SEPARATION OF PARTICLE BEAMS
Ad vanderLinden Nov. 1988 48 p In DUTCH; ENGLISH summary
(LINO-162; ETN-90-95408) Avail: NTIS HC A03/MF A01

A file consisting of classified and numbered articles from the literature was established. It covers the following subjects: kickers, fast switching (electro)magnetic or electrostatic components for small deflection; spectrum magnets, both small and large deflecting components to create or bridge space between the deflected beam and the other, unperturbed beam; electrostatic septa, low loss beam splitting components which give small deflection for the extracted part of the beam without perturbation for the rest of the beam. ESA

N90-19925# Los Alamos National Lab., NM. Physics Div.
SEARCHING FOR EXISTING NUCLEAR DATA
J. R. Tesmer, H. Cokal, and C. J. Maggiore 1989 5 p Presented at the Materials Research Society Materials Analysis Workshop, Albuquerque, NM, 14-17 Jun. 1989
(Contract W-7405-eng-36)
(DE90-007535; LA-UR-90-493; CONF-8906186-7) Avail: NTIS HC A01/MF A01

As an example of finding existing data useful for high energy and heavy ion materials analysis the Nuclear Structure References of Brookhaven National Laboratory's National Nuclear Data Center was searched. The search was limited to incident ions of mass less than or = 7 amu (excluding alphas) with energies under 100 MeV, and the target nuclei were limited to mass less than or = 30 amu. Ease of use, time necessary for retrieval as well as pertinence was explored. Examples of applicable data found during the search are presented. DOE

83 ECONOMICS AND COST ANALYSIS

Includes cost effectiveness studies.

No abstracts in this category.

84 LAW, POLITICAL SCIENCE AND SPACE POLICY

Includes NASA appropriation hearings; aviation law; space law and policy; international law; international cooperation; and patent policy.

No abstracts in this category.

85 URBAN TECHNOLOGY AND TRANSPORTATION

Includes applications of space technology to urban problems; technology transfer; technology assessment; and surface and mass transportation.

For related information see also *03 Air Transportation and Safety, 16 Space Transportation,* and *44 Energy Production and Conversion.*

N90-19926# Office of Science and Technology, Washington, DC.
SCIENCE AND TECHNOLOGY REPORT AND OUTLOOK, 1985-1988
1989 195 p Prepared in cooperation with NSF, Washington, DC
(PB90-115270) Avail: NTIS HC A09/MF A02 CSCL 05A

A comprehensive statement is provided of science and technology policy and priorities for the years 1985 through 1988. Chapter 1 describes the significant decisions and actions in science and technology during the reporting period. Chapter 2 developes the outlook in selected areas of science and development programs, with indications of results or achievements, as appropriate. Finally, Chapter 4 describes the international cooperation aspects of federal research and development programs, with a summary of the associated negotiations. Author

N90-19927# Mohawk Research Corp., Rockville, MD.
FROM INVENTION TO INNOVATION: COMMERCIALIZATION OF NEW TECHNOLOGY BY INDEPENDENT AND SMALL BUSINESS INVENTORS
15 May 1989 91 p Prepared for Argonne National Lab., IL
(Contract W-31-109-eng-38)
(DE90-006944; DOE/NBB-0087) Avail: NTIS HC A05/MF A01

This handbook emerged from the commitment of Energy-Related Inventions Program personnel to supporting the commercialization efforts of independent and small business inventors with new technologies. As you read this document, you will face questions that may seem far removed from technological concerns--questions about the market, your competition, your business structure, and about legal and regulatory requirements. These may seem peripheral to your present and future work. But, make no mistake, you must carefully and honestly consider and answer these if you expect to penetrate the market in sustained way and profit from your work. Over four hundred of your peers--some by success, others by failure--have shown us the lessons incorporated in this volume. By using it, and by commenting on it, you benefit from their collective experience, and make invaluable additions to it. DOE

88 SPACE SCIENCES (GENERAL)

No abstracts in this category.

89 ASTRONOMY

Includes radio, gamma-ray, and infrared astronomy, and astrometry.

N90-19928# Geneva Observatory (Switzerland).
MAGNETIC FIELDS IN LATE-TYPE DWARFS: PRELIMINARY RESULTS FROM A MULTILINE APPROACH
G. Mathys and S. K. Solanki (Saint Andrew's Univ., Scotland) 1988 15 p Previously announced in IAA as A89-27132 Submitted for publication
(Ser-C-Prepub-Fasc-31; ETN-89-93747) Avail: NTIS HC A03/MF A01

Results of a multiline approach to the diagnosis of magnetic fields in late-type dwarfs are presented. The spectra of four stars observed with the Coude echelle spectrometer of the European Southern Observatory are analyzed using the Stenflo-Lindegren technique, which permits empirical relations to be obtained between various parameters characterizing a statistical sample of observed line profiles and the atomic quantities pertaining to the corresponding transitions. These empirical relations are tested on solar and stellar data and interpreted with a simple model of the line formation. Constraints on the magnetic field properties (mean strength, filling factor, thermodynamic properties of the magnetic regions compared to the nonmagnetic parts of the stellar surface) are derived. In spite of the crudeness of approximations, the results are compatible with those obtained with other methods. The advantages of the Stenflo-Lindegren technique over other approaches are sketched. ESA

N90-19929 Johns Hopkins Univ., Baltimore, MD.
ULTRAVIOLET OBSERVATIONS OF THE ATMOSPHERE OF Io AND THE PLASMA TORUS Ph.D. Thesis
Gilda E. Ballester 1989 167 p
Avail: Univ. Microfilms Order No. DA8923657

Observations of Jupiter's satellite Io and the plasma torus encompassing its orbit were made with the International Ultraviolet Explorer (IUE) satellite. The near-ultraviolet sunlight reflected by Io was observed for the first time in high resolution, in an effort to determine the atmospheric abundance of sulfur dioxide, thought to be the main component near the surface. An upper limit was placed on the average column density, implying that a collisionally-thick SO2 atmosphere of intermediate density may be present on Io with sufficiently large densities near the terminator to reproduce the evening ionospheric profile measured by Pioneer 10. Neutral oxygen and sulfur emissions were detected for the first time in the atmosphere of Io. The O I emissions are consistent with torus electrons of temperature approx. 5 eV interacting with the exosphere. Dissert. Abstr.

N90-19930 Edinburgh Univ. (Scotland).
AN OPTICAL AND INFRARED STUDY OF BLAZARS Ph.D. Thesis
Andrew Robert Graham Mead 1988 286 p
Avail: Univ. Microfilms Order No. BRD-86418

Some of the optical and infrared properties of blazars are discussed. The evidence of bulk relativistic flows in quasars and blazars is also discussed. The observational study has two parts. First a series of infrared and optical polarization measurements are presented. Second a study of the cluster environments of blazars is reported. The polarization study consisted of 156 observations of 37 blazars and candidate blazars at infrared and optical frequencies. The observations of the quasar 1253-055 (3C 279) showed a U polarization of 45.5 + or - 0.9 percent. This is the highest ever seen in a blazar. The effect of the proposed blue bump on the observations of 1641+399 (3C 345) is discussed, as are other sources of unpolarized contaminating flux. The interpretation of the observed spectrum is discussed in terms of shock acceleration models and the synchrotron-self-Compton jet pictures. It is shown that frequency dependence is a common feature of the polarization behavior with the polarization generally increasing towards higher frequencies. No evidence is found to support the claim that frequency dependence is related to high levels of polarization. The possible explanations of the observed frequency dependence are discussed. The study of the cluster environments of blazars was formulated as a test of a unified scheme. Deep CCD observations were obtained for a sample of blazars and quasars with extended radio structure. The strength of the cluster environment was parameterized by the amplitude of the quasar-galaxy spatial correlation function B(sub gq). The evaluation of this quantity is subject to large systematic errors as a result of the uncertainty in the galaxy luminosity function. Dissert. Abstr.

N90-19931# Los Alamos National Lab., NM. Theoretical Div.
NEON NOVAE, RECURRENT NOVAE, AND TYPE I SUPERNOVAE
Sumner Starrfield, Warren M. Sparks, James W. Truran, and Giora Shaviv (Israel Inst. of Tech., Haifa.) 1989 5 p Presented at the Colloquium on Supernovae, Santa Cruz, CA, Jul. 1989
(Contract W-7405-eng-36)
(DE90-003188; LA-UR-89-3737; CONF-8907176-1) Avail: NTIS HC A02/MF A01

Over the past few years, we have been investigating the effects of accretion onto massive white dwarfs and its implications for their growth in mass toward the Chandrasekhar limit, in attempts to identify a possible relationship between SN I and novae. In our studies we have considered accretion at various mass accretion rates onto a variety of different white dwarf masses. We have found that there is a critical white dwarf mass above which a significant fraction of the accreted mass can remain on the white dwarf after the outburst. Below this value of the white dwarf mass, all of the accreted mass, plus core material dredged up into the envelope, is ejected as a result of the explosion. Our latest results include accretion and boundary layer heating produced by the infalling material. From these studies, we have identified some members of the class of recurrent novae, those involving a thermonuclear runaway, as the novae that are occurring on very massive white dwarfs and evolving toward an SN I explosion. One of the outgrowths of our UV studies of novae in outburst has been the identification of a class of novae which eject material that is very rich in the elements from oxygen to aluminum. We have shown that these outbursts occur on ONeMg white dwarfs, which are necessarily very massive white dwarfs. DOE

N90-19932*# Johns Hopkins Univ., Baltimore, MD. Dept. of Physics and Astronomy.
NEARLY SIMULTANEOUS OPTICAL, ULTRAVIOLET, AND X RAY OBSERVATIONS OF THREE PG QUASARS Final Technical Report
Gerard A. Kriss 8 Mar. 1990 19 p
(Grant NAG8-562)
(NASA-CR-186355; NAS 1.26:186355) Avail: NTIS HC A03/MF A01 CSCL 03B

Nearly simultaneous optical, ultraviolet, and x ray observations of three low redshift quasars are presented. The EXOSAT x ray spectra span the range of observed spectral indices for quasars from the canonical 0.7 energy index typical of Seyfert galaxies for PG0923+129 (Mrk 705) to the steep spectral indices frequently seen in higher luminosity quasars with an index of 1.58 for PG0844+349 (Ton 951). None of the quasars exhibits any evidence for a soft x ray excess. This is consistent with accretion disk spectra fit to the IR through UV continua of the quasars -- the best fitting disk spectra peak at approximately 6 eV with black hole masses in the range 5 x 10(exp 7) to 1 x 10(exp 9) solar mass and mass accretion rates of approximately 0.1 times the Eddington-limited rate. These rather soft disk spectra are also compatible with the observed optical and ultraviolet line ratios. Author

N90-19933# Technische Univ., Delft (Netherlands). Faculty of Technical Mathematics and Informatics.
THE MOON HAS SET [DEDYKE MEN A SELANNA]
I. S. Herschberg and J. E. Mebius 1989 19 p Submitted for publication
(Rept-89-07; ETN-90-95441) Copyright Avail: NTIS HC A03/MF A01

The Sappho epigram mentioned in the title is shown to contain implicit astronomical information, which must have contributed to the expressiveness of Sappho's short poem to contemporary audiences. Astronomical computations are given to discover the earliest and the latest time of year for which the Pleiads set at midnight while being visible earlier in the evening, taking into account the atmospheric refraction. The time of year for which Sappho's poem is valid is concluded to run from 17 Jan. to 29 Mar. ESA

N90-19934# Tuebingen Univ. (Germany, F.R.). Astronomisches Inst.
SIGNATURE OBJECTS: PRELIMINARIES FOR THE SATELLITE PROJECT HIPPARCOS/TYCHO Thesis [SIGNATURE-OBJEKTE: VORBEREITUNGEN FUER DAS SATELLITENPROJEKT HIPPARCOS/TYCHO]
Harald Jankiewitz Jan. 1989 155 p In GERMAN
(ETN-90-95730) Avail: NTIS HC A08/MF A01

The scientific mission of the Hipparcos/Tycho mission were carried out by means of a special optical telescope in geostationary orbit to measure the position, the eigen motions and the trigonometric parallaxes and the luminosity of a lot of stars. To obtain the position of the stars, the angle between two distant stars is measured. Since around 100,000 stars are listed in the Hipparcos input catalog, a lot of stars can be recorded. ESA

N90-19935# Tuebingen Univ. (Germany, F.R.). Astronomisches Inst.
CONCEPTION OF AN AUTOMATIC MEASUREMENT INSTALLATION FOR SPATIAL RESOLUTION DETECTORS Thesis [AUFBAU EINER AUTOMATISCHEN MESSEINRICHTUNG FUER ORTSAUFLOESENDE DETEKTOREN]
Herbert Schroeder Dec. 1988 87 p In GERMAN
(ETN-90-95732) Avail: NTIS HC A05/MF A01

A program written with TURBO-PASCAL is proposed for the automatization of the measurements of detectors for telescopes in the hard x ray area. It is divided into four sections: control of the photometer table (two procedures for the two direction X-Y), measurements (calibrating, data safeguard, magnitude and time distribution), estimation and safeguard of the detector data and graphic representation of the most important measured magnitudes. The data files are of the type file of records. ESA

N90-19936# Tuebingen Univ. (Germany, F.R.). Fakultaet fuer Physik.
SPECKLE INTERFEROMETRY FOR HIGH RESOLUTION PICTURES OF ASTRONOMICAL OBJECTS Ph.D. Thesis [SPECKLE-INTERFEROMETRIE ALS MITTEL ZUR GEWINNUNG HOCHAUFGELOESTER BILDER ASTRONOMISCHER OBJEKTE]
Roberto Neri 1988 126 p In GERMAN
(ETN-90-95827) Avail: NTIS HC A07/MF A01

The photon counter microchannel plates detector was widened to a speckle camera system for astronomical observations in visible light area. By laboratory experiments, the modular structure of a speckle interferometer was simulated with different atmospheric observation conditions. Dispersion prisms implementation for correction of chromatic aberration of astronomic sources with higher zenith distances could be avoided by a good choice of the objects and the use of narrow band interference filters. Because of a nearly unlimited dynamic, a relatively high sensitivity in visible light area and the low underground noise (lower than 0.001 photon/second), the use of the speckle recording system can be recommended particularly for the observation of lightweak astronomic sources. ESA

N90-19937# Tuebingen Univ. (Germany, F.R.). Fakultaet fuer Physik.
HIGH ENERGY X RAY OBSERVATIONS ON THE CRAB NEBULA AND THE DOUBLE STAR SOURCE GX 1+4 Ph.D. Thesis [HOCHENERGIE-ROENTGENBEOBACHTUNGEN AM CRAB UND AN GX 1+4]
Raffaello Carli 1989 87 p In GERMAN
(ETN-90-95829) Avail: NTIS HC A05/MF A01

With help of the data from the HIBAU 86 experiment and the High Energy X-ray Experiment onboard the Soviet space station MIR, an experiment of the period development of the galactic double star source GX 1+4 was carried out. This source is characterized by its spin-up time scale of 50 years instead of the usual 1,000 years for an x ray pulsar. Because of the long period, it was considered as a sample example for a slow rotator, that was a long way from a theoretically predicted equilibrium state (between accelerating and braking-torques). These new measurements and those that were made with the Japanese x ray satellite GINGA, give the assumption that GX 1+4 is much nearer to an equilibrium state than it was previously believed. By taking the Ghoshand Lamb theory into account, it can be established that the magnetic field of the neutron stars is 100 Teragauss strong. ESA

N90-19938# Bundesministerium fuer Forschung und Technologie, Bonn (Germany, F.R.).
ASTRONOMY AND ASTROPHYSICS [ASTRONOMIE UND ASTROPHYSIK]
11 Aug. 1989 8 p In GERMAN
(Rept-33/89; ETN-90-95904) Avail: NTIS HC A02/MF A01

An historic review of astronomy and astrophysics is presented. Astronomy is principally the observation of stars and the estimation of their position and moving. Fixed stars are distinguishable from the Sun, the Moon and the planets. Before the seventeenth century, the study of astronomy and astrophysics established maps of the sky for navigation. Huyghens and Kepler improved the calculation of the movement of planets; during the nineteenth century, Herschel and Grauenhoffer improved observation instruments. The 1960's saw the advent of space programs. Later, new areas of research appeared: ultrahigh gamma-ray astronomy, neutrino astrophysics and gravity waves. German scientists have started projects in infrared, optical, ultraviolet and x ray areas. ESA is preparing an x ray observatory program for the year 2000. The Max Planck Institute is working with the Spanish on a telescope in Spain. ESA

N90-19939# Erlangen-Nuremberg Univ. (Germany, F.R.). Naturwissenschaptlichen Fakultaeten.
INFORMATION RECONSTRUCTION FROM SPECKLE INTERFEROGRAMS Ph.D. Thesis [INFORMATIONSREKONSTRUKTION AUS SPECKLE-INTERFEROGRAMMEN: OPTISCHE EIGENSCHAFTEN DER ERDATMOSPHAERE UND SPACE-TELESKOP-ROLL-ENTFALTUNG]
Manfred Mueller 1988 85 p In GERMAN
(ETN-90-95918) Avail: NTIS HC A05/MF A01

The resolving power of the conventional recorded astrophotography is limited to 1 arc second, although the theoretical value is 0.03 arc second. This distorsion is caused by the earth atmosphere. The refractive index oscillations in the terrestrial atmosphere distort incident fronts that interfere in the local plane and produce interferences samples; the speckle interferograms, which are achieved with terrestrial telescopes and in coded shape contain very interesting information about the lifted object and the earth atmosphere. For the space telescope, there are speckles caused by the aberration that will provoke a resolution drop of the telescope in ultraviolet light. The optical parameters of the terrestrial atmosphere and the Hubble Space Telescope (HST) are described. The roll deconvolution method can improve the resolution of the HST from 50 arc ms to 15 arc ms. The reconstruction can be obtained with complex inverse filtering of two HST filmings. An optical digital simulation shows the dependence of the signal to noise ratio on the structure of the point image and the photon noise. ESA

90 ASTROPHYSICS

Includes cosmology; celestial mechanics; space plasmas; and interstellar and interplanetary gases and dust.
For related information see also *75 Plasma Physics*.

N90-19940*# National Aeronautics and Space Administration, Washington, DC.
RELATIVISTIC GRAVITATIONAL EXPERIMENTS IN SPACE
Ronald W. Hellings, ed. Aug. 1989 242 p Workshop held in Annapolis, MD, 28-30 Jun. 1988
(NASA-CP-3046; NAS 1.55:3046) Avail: NTIS HC A11/MF A02 CSCL 03B

The results are summarized of a workshop on future gravitational physics space missions. The purpose of the workshop was to define generic technological requirements for such missions. NASA will use the results to direct its program of advanced technology development. For individual titles, see N90-19941 through N90-19977.

N90-19941*# Washington Univ., Saint Louis, MO. Dept. of Physics.
GRAVITATIONAL RADIATION AS A TEST OF RELATIVISTIC GRAVITY
Clifford M. Will *In* NASA, Relativistic Gravitational Experiments in Space Aug. 1989 p 1-6 (For primary document see N90-19940 12-90)
Avail: NTIS HC A11/MF A02 CSCL 03B

Gravitational radiation can be used to test theories of gravitation. When the waves are ultimately detected directly, their speed and polarization properties can be measured and compared with predictions of alternative theories. The multipole nature of gravitational radiation was already tested in the binary pulsar, where observations of the decay of the orbit verify the quadrupole formula for gravitational radiation damping of general relativity and put strong constraints on dipole gravitational radiation predicted by many alternative theories. Author

N90-19942*# University Coll., Cardiff (Wales). Dept. of Applied Mathematics and Astronomy.
SOURCES OF GRAVITATIONAL WAVES
Bernard F. Schutz *In* NASA, Relativistic Gravitational Experiments in Space Aug. 1989 p 7-13 (For primary document see N90-19940 12-90)
Avail: NTIS HC A11/MF A02 CSCL 03B

Sources of low frequency gravitational radiation are reviewed from an astrophysical point of view. Cosmological sources include the formation of massive black holes in galactic nuclei, the capture by such holes of neutron stars, the coalescence of orbiting pairs of giant black holes, and various means of producing a stochastic background of gravitational waves in the early universe. Sources local to our Galaxy include various kinds of close binaries and coalescing binaries. Gravitational wave astronomy can provide information that no other form of observing can supply; in particular, the positive identification of a cosmological background originating in the early universe would be an event as significant as was the detection of the cosmic microwave background. Author

N90-19943*# Jet Propulsion Lab., California Inst. of Tech., Pasadena.
DETECTING GRAVITY WAVES FROM BINARY BLACK HOLES
Hugo D. Wahlquist *In* NASA, Relativistic Gravitational Experiments in Space Aug. 1989 p 14-17 (For primary document see N90-19940 12-90)
Avail: NTIS HC A11/MF A02 CSCL 03B

One of the most attractive possible sources of strong gravitational waves would be a binary system comprising massive black holes (BH). The gravitational radiation from a binary is an elliptically polarized, periodic wave which could be observed continuously - or at intervals whenever a detector was available. This continuity of the signal is certainly appealing compared to waiting for individual pulses from infrequent random events. It also has the advantage over pulses that continued observation can increase the signal-to-noise ratio almost indefinitely. Furthermore, this system is dynamically simple; the theory of the generation of the radiation is unambiguous; all characteristics of the signal can be precisely related to the dynamical parameters of the source. The current situation is that while there is no observational evidence as yet for the existence of massive binary BH, their formation is theoretically plausible, and within certain coupled constraints of mass and location, their existence cannot be observationally excluded. Detecting gravitational waves from these objects might be the first observational proof of their existence. Author

N90-19944*# California Univ., Santa Barbara. Inst. for Theoretical Physics.
GRAVITATIONAL RADIATION FROM ROTATING GRAVITATIONAL COLLAPSE
Richard F. Stark *In* NASA, Relativistic Gravitational Experiments in Space Aug. 1989 p 18-24 (For primary document see N90-19940 12-90)
Avail: NTIS HC A11/MF A02 CSCL 03B

The efficiency of gravitational wave emission from axisymmetric rotating collapse to a black hole was found to be very low: Delta E/Mc sq. less than 7 x 10(exp -4). The main waveform shape is well defined and nearly independent of the details of the collapse. Such a signature will allow pattern recognition techniques to be used when searching experimental data. These results (which can be scaled in mass) were obtained using a fully general relativistic computer code that evolves rotating axisymmetric configurations and directly computes their gravitational radiation emission.
Author

N90-19945*# Texas Univ., Austin. Dept. of Physics.
THE PREGALACTIC COSMIC GRAVITATIONAL WAVE BACKGROUND
Richard A. Matzner *In* NASA, Relativistic Gravitational Experiments in Space Aug. 1989 p 25-37 (For primary document see N90-19940 12-90)
Avail: NTIS HC A11/MF A02 CSCL 03B

An outline is given that estimates the expected gravitational wave background, based on plausible pregalactic sources. Some cosmologically significant limits can be put on incoherent gravitational wave background arising from pregalactic cosmic evolution. The spectral region of cosmically generated and cosmically limited radiation is, at long periods, P greater than 1 year, in contrast to more recent cosmological sources, which have P approx. 10 to 10(exp -3). Author

N90-19946*# Washington Univ., Saint Louis, MO. Dept. of Physics.
EXPERIMENTAL CONSTRAINTS ON METRIC AND NON-METRIC THEORIES OF GRAVITY
Clifford M. Will *In* NASA, Relativistic Gravitational Experiments in Space Aug. 1989 p 38-47 (For primary document see N90-19940 12-90)
(Grant NSF PHY-85-13953)
Avail: NTIS HC A11/MF A02 CSCL 03B

Experimental constraints on metric and non-metric theories of gravitation are reviewed. Tests of the Einstein Equivalence Principle indicate that only metric theories of gravity are likely to be viable. Solar system experiments constrain the parameters of the weak field, post-Newtonian limit to be close to the values predicted by general relativity. Future space experiments will provide further constraints on post-Newtonian gravity. Author

N90-19947*# California Univ., Santa Barbara. Dept. of Physics.
GRAVITATIONAL CONSEQUENCES OF MODERN FIELD THEORIES
Gary T. Horowitz *In* NASA, Relativistic Gravitational Experiments in Space Aug. 1989 p 48-50 (For primary document see N90-19940 12-90)
Avail: NTIS HC A11/MF A02 CSCL 03B

Some gravitational consequences of certain extensions of Einstein's general theory of relativity are discussed. These theories are not alternative theories of gravity in the usual sense. It is

assumed that general relativity is the appropriate description of all gravitational phenomena which were observed to date. Author

N90-19948*# Montana State Univ., Bozeman.
TOWARD HIGHER ORDER TESTS OF THE GRAVITATIONAL INTERACTION
Ken Nordtvedt *In* NASA, Relativistic Gravitational Experiments in Space Aug. 1989 p 51-54 (For primary document see N90-19940 12-90)
Avail: NTIS HC A11/MF A02 CSCL 03B

Analyses and interpretations of experiments which test post-Newtonian gravity are usually done under the assumption that gravity is a metric field phenomenon - a manifestation of space-time geometry. This, however, is unnecessary and one can start at a more primitive level - that there simply exists a phenomenological, gravitational, many-body equation of motion which must be determined by a package of observations. In fact, over the last couple decades, a diverse collection of solar system interbody tracking observations, supplemented by data from the binary pulsar system PSR 1913 + 16, has completely mapped out the first post-Newtonian order. After the fact, using empirically determined equations of motion, along with some observed properties of nongravitational clocks and rulers and conservation laws for energy, momentum and angular momentum, a post-Newtonian Lagrangian can be constructed, a geometrical space-time metric field conceptual interpretation can be developed, Lorentz invariance of the equations of motion can be shown, and the equations of motion are found to agree with the predictions of Einstein's gravitational theory, General Relativity, within experimental accuracy. Author

N90-19949*# Los Alamos National Lab., NM. Theoretical Div.
THE INVERSE-SQUARE LAW AND QUANTUM GRAVITY
Michael Martin Nieto, T. Goldman, and Richard J. Hughes *In* NASA, Relativistic Gravitational Experiments in Space Aug. 1989 p 55-58 (For primary document see N90-19940 12-90)
Avail: NTIS HC A11/MF A02 CSCL 03B

A program is described which measures the gravitational acceleration of antiprotons. This idea was approached from a particle physics point of view. That point of view is examined starting with some history of physics over the last 200 years. Author

N90-19950*# Colorado Univ., Boulder. Dept. of Physics.
APPLIED GENERAL RELATIVITY
Neil Ashby *In* NASA, Relativistic Gravitational Experiments in Space Aug. 1989 p 59-69 (For primary document see N90-19940 12-90)
Avail: NTIS HC A11/MF A02 CSCL 03B

Important relativistic effects and issues are discussed which must be considered in the interpretation of current measurements such as ranging measurements to LAGEOS and to the moon, in the implementation of the Global Positioning System, in the synchronization of clocks near the earth's surface, and in the adoption of appropriate scales of time and length for the communication of scientific results. Author

N90-19951*# Jet Propulsion Lab., California Inst. of Tech., Pasadena.
ADVANCED DOPPLER TRACKING EXPERIMENTS
J. W. Armstrong *In* NASA, Relativistic Gravitational Experiments in Space Aug. 1989 p 70-74 (For primary document see N90-19940 12-90)
Avail: NTIS HC A11/MF A02 CSCL 03B

The Doppler tracking method is currently the only technique available for broadband gravitational wave searches in the approx. 10(exp -4) to 10(exp -1) Hz low frequency band. A brief review is given of the Doppler method, a discussion of the main noise sources, and a review of experience with current spacecraft and the prospects for sensitivity improvements in an advanced Doppler tracking experiment. Author

N90-19952*# Uppsala Univ. (Sweden). Planetary Geodesy and Geophysics.
THE SPACE MICROWAVE INTERFEROMETER AND THE SEARCH FOR COSMIC BACKGROUND GRAVITATIONAL WAVE RADIATION
Allen Joel Anderson *In* NASA, Relativistic Gravitational Experiments in Space Aug. 1989 p 75-79 (For primary document see N90-19940 12-90)
Avail: NTIS HC A11/MF A02 CSCL 03B

Present and planned investigations which use interplanetary spacecraft for gravitational wave searches are severely limited in their detection capability. This limitation has to do both with the Earth-based tracking procedures used and with the configuration of the experiments themselves. It is suggested that a much improved experiment can now be made using a multiarm interferometer designed with current operating elements. An important source of gravitational wave radiation, the cosmic background, may well be within reach of detection with these procedures. It is proposed to make a number of experimental steps that can now be carried out using TDRSS spacecraft and would conclude in the establishment of an operating multiarm microwave interferometer. This interferometer is projected to have a sensitivity to cosmic background gravitational wave radiation with an energy of less than 10(exp -4) cosmic closure density and to periodic waves generating spatial strain approaching 10(exp -19) in the range 0.1 to 0.001 Hz. Author

N90-19953*# Joint Inst. for Lab. Astrophysics, Boulder, CO. Quantum Physics Div.
OPTICAL INTERFEROMETER IN SPACE
Peter L. Bender, J. E. Faller, J. L. Hall, D. Hils, R. T. Stebbins, and Mark A. Vincent *In* NASA, Relativistic Gravitational Experiments in Space Aug. 1989 p 80-88 Sponsored in part by National Inst. of Standards and Technology (For primary document see N90-19940 12-90)
(Grant NAGw-822)
Avail: NTIS HC A11/MF A02 CSCL 03B

The present design concepts for a Laser Gravitational Wave Observatory in Space are described. Laser heterodyne distance measurements are made between test masses located in three spacecraft separated by roughly 10(exp 6) km. The major technology issues are: the reduction of spurious acceleration noise for the test masses to below 2 x 10(exp -15) cm/sq sec/Hz(0.5) from 10(exp -5) to 10(exp -3) Hz; and the measurement of changes in the difference of the antenna arm lengths to 5 x 10(exp -11) cm/Hz(0.5) from 10(exp -3) to 1 Hz with high reliability. The science objectives are: to measure discrete sinusoidal gravitational wave signals from individual sources with periods of 1 second to 1 day; to measure the stochastic background due to unresolved binaries; and to search for gravitational wave pulses with periods longer than 1 sec from possible exotic sources such as gravitational collapse of very massive objects. Author

N90-19954*# Maryland Univ., College Park. Dept. of Physics and Astronomy.
EARTH-ORBITING RESONANT-MASS GRAVITATIONAL WAVE DETECTORS
Ho Jung Paik *In* NASA, Relativistic Gravitational Experiments in Space Aug. 1989 p 89-92 (For primary document see N90-19940 12-90)
Avail: NTIS HC A11/MF A02 CSCL 03B

Earth-based gravitational wave detectors suffer from the need to support the large antenna masses against the earth's gravity without transmitting a significant amount of seismic noise. Passive vibration isolation is difficult to achieve below 1 Hz on the earth. Vibration-free space environment thus gives an opportunity to extend the frequency window of gravitational wave detection to ultralow frequencies. The weightless condition of a space laboratory also enables construction of a highly symmetric multimode antenna which is capable of resolving the direction of the source and the polarization of the incoming wave without resorting to multiantenna coincidence. Two types of earth-orbiting resonant-mass gravitational wave detectors are considered. One is a skyhook

gravitational wave detector, proposed by Braginsky and Thorne (1985). The other is a spherical detector, proposed by Forward (1971) and analyzed by Wagoner and Paik (1976). Author

N90-19955*# Jet Propulsion Lab., California Inst. of Tech., Pasadena.
PULSAR TIMING AND GRAVITATIONAL WAVES
Ronald W. Hellings *In* NASA, Relativistic Gravitational Experiments in Space Aug. 1989 p 93-97 (For primary document see N90-19940 12-90)
Avail: NTIS HC A11/MF A02 CSCL 03B

In the last few years, several researchers have used timing data from pulsars to search for ultra-low frequency (ULF) gravitational waves (waves at periods from a few days to a few years), especially for the waves making up the stochastic cosmic background such waves. How these limits are obtained are discussed and several precautions are pointed out that must be taken in the analysis of these data. Author

N90-19956*# Stanford Univ., CA. Dept. of Physics.
X RAY TIMING OBSERVATIONS AND GRAVITATIONAL PHYSICS
Peter F. Michelson and Kent S. Wood (Naval Research Lab., Washington, DC.) *In* NASA, Relativistic Gravitational Experiments in Space Aug. 1989 p 98-103 (For primary document see N90-19940 12-90)
Avail: NTIS HC A11/MF A02 CSCL 03B

Photon-rich x ray observations on bright compact galactic sources will make it possible to detect many fast processes that may occur in these systems on millisecond and submillisecond timescales. Many of these processes are of direct relevance to gravitational physics because they arise in regions of strong gravity near neutron stars and black holes where the dynamical timescales for compact objects of stellar mass are milliseconds. To date, such observations have been limited by the detector area and telemetry rates available. However, instruments such as the proposed X ray Large Array (XLA) would achieve collecting areas of about 100 sq m. This instrument has been described elsewhere (Wood and Michelson 1988) and was the subject of a recent prephase A feasibility study at Marshall Space Flight Center. Observations with an XLA class instrument will directly impact five primary areas of astrophysics research: the attempt to detect gravitational radiation, the study of black holes, the physics of mass accretion onto compact objects, the structure of neutron stars and nuclear matter, and the characterization of dark matter in the universe. Those observations are discussed that are most directly relevant to gravitational physics: the search for millisecond x ray pulsars that are potential sources of continuous gravitational radiation; and the use of x ray timing observations to probe the physical conditions in extreme relativistic regions of space near black holes, both stellar-sized and supermassive. Author

N90-19957*# California Univ., Santa Barbara. Inst. for Theoretical Physics.
GENERAL RELATIVISTIC X RAY (UV) POLARIZATION ROTATIONS AS A QUANTITATIVE TEST FOR BLACK HOLES
Richard F. Stark *In* NASA, Relativistic Gravitational Experiments in Space Aug. 1989 p 104-109 (For primary document see N90-19940 12-90)
Avail: NTIS HC A11/MF A02 CSCL 03B

It is now 11 years since a potentially easily observable and quantitative test for black holes using general relativistic polarization rotations was proposed (Stark and Connors 1977, and Connors and Stark 1977). General relativistic rotations of the x ray polarization plane of 10 to 100 degrees with x ray energy (between 1 and 100 keV) are predicted for black hole x ray binaries. (Classically, by symmetry, there is no rotation.) Unfortunately, x ray polarimetry has not been taken sufficiently seriously during this period, and this test has not yet been performed. A similar (though probably less clean) effect is expected in the UV for supermassive black holes in some quasars active galactic nuclei. Summarizing: (1) a quantitative test (proposed in 1977) for black holes exists; (2) x ray polarimetry of galactic x ray binaries sensitive to at least 1/2 percent between 1 keV and 100 keV is needed (polarimetry in the UV of quasars and AGN will also be of interest); and (3) proportional counters using timerise discrimination were shown in laboratory experiments able to perform x ray polarimetry and this and other methods need to be developed. Author

N90-19958*# National Aeronautics and Space Administration, Washington, DC.
SPACE TELESCOPE SEARCHES FOR BLACK HOLES IN GALACTIC NUCLEI
Richard J. Harms *In its* Relativistic Gravitational Experiments in Space Aug. 1989 p 110-113 (For primary document see N90-19940 12-90)
Avail: NTIS HC A11/MF A02 CSCL 03B

The Hubble Space Telescope (HST) will allow astronomers to obtain luminosity profiles, rotation curves, and velocity dispersions at angular scales that are an order of magnitude superior to those obtained previously. This enhanced spatial resolution will greatly improve the sensitivity for detecting centrally condensed matter in nearby galactic nuclei including, possibly, black holes. Author

N90-19959*# National Aeronautics and Space Administration. Goddard Space Flight Center, Greenbelt, MD.
THE COBE COSMIC 3 K ANISOTROPY EXPERIMENT: A GRAVITY WAVE AND COSMIC STRING PROBE
Charles L. Bennett and George F. Smoot (California Univ., Berkeley. Lawrence Berkeley Lab.) *In* NASA, Relativistic Gravitational Experiments in Space Aug. 1989 p 114-117 (For primary document see N90-19940 12-90)
Avail: NTIS HC A11/MF A02 CSCL 03B

Among the experiments to be carried into orbit next year, by the COBE satellite, are differential microwave radiometers. They will make sensitive all-sky maps of the temperature of the cosmic microwave background radiation at three frequencies, giving dipole, quadrupole, and higher order multipole measurements of the background radiation. The experiment will either detect, or place significant constraints on, the existence of cosmic strings and long wavelength gravity waves. Author

N90-19960*# Stanford Univ., CA. Lab. of Physics.
THE GRAVITY PROBE B RELATIVITY GYROSCOPE PROGRAM
C. W. Francis Everitt, B. W. Parkinson, and J. P. Turneaure *In* NASA, Relativistic Gravitational Experiments in Space Aug. 1989 p 118-125 (For primary document see N90-19940 12-90)
Avail: NTIS HC A11/MF A02 CSCL 03B

The idea of testing general relativity through observations on Earth orbiting gyroscopes was suggested in 1959 to 1960. The direction, it was noted, of spin of a suitably oriented gyroscope should change with respect to the line of sight to a guide star for two reasons: a geodetic effect from the motion of the gyroscope through the curved space-time around the Earth, and a frame-dragging effect from the Earth's rotation. NASA began supporting laboratory research on the experiment, now called Gravity Probe B, in 1964. Technologies for it were progressively established, and an error analysis demonstrated the potential of measuring frame-dragging to 1 to 2 percent and the geodetic effect to 1 part in 10(exp 4). Later analyses, discussed herein, suggest possibilities for further improving those precisions each by a further factor of 10. In 1984, after technical and scientific reviews by the Space Science Board and other bodies, and completion by NASA Marshall Center of a Phase B Study, the NASA Administrator approved the start of a program known as STORE (Shuttle Test Of the Relativity Experiment). The purpose of STORE is to verify the final Gravity Probe B science payload, perform on the Shuttle a 7-day experiment rehearsal (including sophisticated gyro tests in low gravity), and then return the payload to Earth for refurbishment and integration into the Science Mission spacecraft. The payload comprises four gyroscopes, a telescope, and a drag-free proof mass, all mounted in a quartz block assembly within an evacuated magnetically shielded probe, which in turn is inserted into a 10-ft long, 6-ft diameter liquid helium dewar,

operating at 1.8 K and maintaining low temperature for 2 years. STORE is manifested on Shuttle OV-105, for launch MSSN 69 in February 1993. The Science Mission is set tentatively for June 1995. Author

N90-19961*# Texas Univ., Austin. Center for Space Research.
LAGEOS 3 AND THE GRAVITOMAGNETIC FIELD
Ignazio Ciufolini *In* NASA, Relativistic Gravitational Experiments in Space Aug. 1989 p 126-131 (For primary document see N90-19940 12-90)
Avail: NTIS HC A11/MF A02 CSCL 03B

The importance of the gravitomagnetic field is discussed. A never-measured field of nature, the foundations of inertia in Einstein General Relativity, and a key role in theories of quasars and active galactic nuclei are important aspects of this field and are discussed. In high energy astrophysics, some theories of energy storage, power generation, jet formation and jet alignment of quasars and active galactic nuclei are based on the existence of the gravitomagnetic field of a supermassive black hole (Thorne et al. 1986). LAGEOS 3 is discussed in terms of laser ranged satellites to detect the gravitomagnetic field and supplementary inclination satellites to avoid gravity field uncertainties. Many experiments have been proposed to measure the gravitomagnetic field. The GPB experiment intends to measure the Lense-Thirring-Schiff precession of gyroscopes orbiting the earth. Polar satellites have been proposed to measure the Lense-Thirring precession of the orbital plane (an enormous gyroscope and two guided, drag-free, counter-rotating, polar satellites have been suggested to avoid orbital inclination errors.) The new idea to measure the gravitomagnetic drag of the nodes of two nonpolar, supplementary inclination, satellites is summarized. Author

N90-19962*# Missouri Univ., Columbia. Dept. of Physics and Astronomy.
GRADIOMETRY AND GRAVITOMAGNETIC FIELD DETECTION
Bahram Mashhoon *In* NASA, Relativistic Gravitational Experiments in Space Aug. 1989 p 132-136 (For primary document see N90-19940 12-90)
Avail: NTIS HC A11/MF A02 CSCL 03B

Gravitomagnetism was apparently first introduced into physics about 120 years ago when major developments in electrodynamics and the strong similarity between Coulomb's law of electricity and Newton's law of gravity led to the hypothesis that mass current generates a fundamental force of gravitational origin analogous to the magnetic force caused by charge current. According to general relativity, the rotation of a body leads to the dragging of the local inertial frames. In the weak-field approximation, the dragging frequency can be interpreted, up to a constant proportionality factor, as a gravitational magnetic field. There is, as yet, no direct evidence regarding the existence of such a field. The possibility is examined of detecting the gravitomagnetic field of the Earth by gravity gradiometry. Author

N90-19963*# Stanford Univ., CA. Dept. of Physics.
THE STANFORD EQUIVALENCE PRINCIPLE PROGRAM
Paul W. Worden, Jr., C. W. Francis Everitt, and M. Bye *In* NASA, Relativistic Gravitational Experiments in Space Aug. 1989 p 137-140 (For primary document see N90-19940 12-90)
Avail: NTIS HC A11/MF A02 CSCL 03B

The Stanford Equivalence Principle Program (Worden, Jr. 1983) is intended to test the uniqueness of free fall to the ultimate possible accuracy. The program is being conducted in two phases: first, a ground-based version of the experiment, which should have a sensitivity to differences in rate of fall of one part in 10(exp 12); followed by an orbital experiment with a sensitivity of one part in 10(exp 17) or better. The ground-based experiment, although a sensitive equivalence principle test in its own right, is being used for technology development for the orbital experiment. A secondary goal of the experiment is a search for exotic forces. The instrument is very well suited for this search, which would be conducted mostly with the ground-based apparatus. The short range predicted for these forces means that forces originating in the Earth would not be detectable in orbit. But detection of Yukawa-type exotic forces from a nearby large satellite (such as Space Station) is feasible, and gives a very sensitive and controllable test for little more effort than the orbiting equivalence principle test itself. Author

N90-19964*# Jet Propulsion Lab., California Inst. of Tech., Pasadena.
ICARUS LANDER
Ronald W. Hellings *In* NASA, Relativistic Gravitational Experiments in Space Aug. 1989 p 141-143 (For primary document see N90-19940 12-90)
Avail: NTIS HC A11/MF A02 CSCL 03B

Icarus is one of the earth-crossing asteroids. It has a semi-major axis of 1.078 AU, giving it a period of 1.12 years, and an eccentricity of 0.827. The perihelion distance is thus 0.187 AU. The inclination of Icarus's orbit is 23 deg. Although it is a small body, it is still massive enough to be essentially immune to non-gravitational forces. These orbital and physical qualities make it an attractive target for testing General Relativity. The close passage to the sun means that it will be subject to a large relativistic perihelion precession; the high eccentricity makes the precession easy to measure; the high inclination allows the solar quadrupole moment (J sub 2) to be simultaneously determined via the nodal precession it predicts. The degeneracy between the relativistic effect and the effect of J sub 2 in the perihelion precession may thus be broken. Results are presented from a preliminary study of a possible trajectory design for an Icarus lander and from a covariance study of the scientific return to be expected from such a mission. Author

N90-19965*# Joint Inst. for Lab. Astrophysics, Boulder, CO.
SMALL MERCURY RELATIVITY ORBITER
Peter L. Bender and Mark A. Vincent *In* NASA, Relativistic Gravitational Experiments in Space Aug. 1989 p 144-147 (For primary document see N90-19940 12-90)
(Grant NAGw-822)
Avail: NTIS HC A11/MF A02 CSCL 03B

The accuracy of solar system tests of gravitational theory could be very much improved by range and Doppler measurements to a Small Mercury Relativity Orbiter. A nearly circular orbit at roughly 2400 km altitude is assumed in order to minimize problems with orbit determination and thermal radiation from the surface. The spacecraft is spin-stabilized and has a 30 cm diameter de-spun antenna. With K-band and X-band ranging systems using a 50 MHz offset sidetone at K-band, a range accuracy of 3 cm appears to be realistically achievable. The estimated spacecraft mass is 50 kg. A consider-covariance analysis was performed to determine how well the Earth-Mercury distance as a function of time could be determined with such a Relativity Orbiter. The minimum data set is assumed to be 40 independent 8-hour arcs of tracking data at selected times during a two year period. The gravity field of Mercury up through degree and order 10 is solved for, along with the initial conditions for each arc and the Earth-Mercury distance at the center of each arc. The considered parameters include the gravity field parameters of degree 11 and 12 plus the tracking station coordinates, the tropospheric delay, and two parameters in a crude radiation pressure model. The conclusion is that the Earth-Mercury distance can be determined to 6 cm accuracy or better. From a modified worst-case analysis, this would lead to roughly 2 orders of magnitude improvement in the knowledge of the precession of perihelion, the relativistic time delay, and the possible change in the gravitational constant with time. Author

N90-19966*# Jet Propulsion Lab., California Inst. of Tech., Pasadena.
GRAVITATIONAL EXPERIMENTS ON A SOLAR PROBE MISSION: SCIENTIFIC OBJECTIVES AND TECHNOLOGY CONSIDERATIONS
John D. Anderson *In* NASA, Relativistic Gravitational Experiments in Space Aug. 1989 p 148-154 (For primary document see N90-19940 12-90)
Avail: NTIS HC A11/MF A02 CSCL 03B

The concept of a solar impact probe (either solar plunger or sun grazer) led to the initiation of a NASA study at JPL in 1978 on the engineering and scientific feasibility of a Solar Probe Mission, named Starprobe, in which a spacecraft is placed in a high eccentricity orbit with a perihelion near 4 solar radii. The Starprobe study showed that the concept was feasible and in fact preliminary mission and spacecraft designs were developed. In the early stages of the Solar Probe studies the emphasis was placed on gravitational science, but by the time of a workshop at Caltech in May 1978 (Neugebauer and Davies, 1978) there was about an equal division of interest between heliospheric physics and gravitation. The last of the gravitational studies for Solar Probe was conducted at JPL in 1983. Since that time, the Committee on Solar and Space Physics (CSSP) of the National Academy of Sciences has recommended the pursuit of a focused mission, featuring fields and particles instrumentation and emphasizing studies of the solar wind source region. Such a solar probe mission is currently listed as the 1994 Major New Star candidate. In the remainder of this review, the unique gravitational science that can be accomplished with a solar probe mission is reviewed. In addition the technology issues that were identified in 1980 by the ad hoc working group for Gravity and Relativity Science are addressed. Author

N90-19967*# Smithsonian Astrophysical Observatory, Cambridge, MA.

OPTICAL INTERFEROMETERS FOR TESTS OF RELATIVISTIC GRAVITY IN SPACE

R. D. Reasenberg *In* NASA, Relativistic Gravitational Experiments in Space Aug. 1989 p 155-162 (For primary document see N90-19940 12-90)

Avail: NTIS HC A11/MF A02 CSCL 03B

A space-based astrometric interferometer with a large optical bandwidth is considered. POINTS (Precision Optical INTerferometry in Space) would measure the angular separation of two stars separated by about 90 deg on the sky with a nominal measurement error of 5 microarcseconds (mas). For a pair of mag 10 stars, the observation would require about 10 minutes. It is estimated that the instrument would measure daily the separation of two stars for each of about 60 pairs of stars; a random sequence of such measurements, if suitably redundant, contains the closure information necessary to detect and correct time dependent measurement biases to well below the nominal measurement accuracy. The 90 deg target separation permits absolute parallax measurements in all directions. A redundant observing schedule for 300 stars and 5 quasars would provide extra redundancy to compensate for the quasars' higher magnitude. If a nominal 30-day observation sequence were repeated 4 times per year for 10 years, stellar parameter uncertainties would be obtained of: 0.6 mas, position; 0.4 mas/y, proper motion; and 0.4 mas, parallax. This set of well-observed stars and quasars would form a rigid frame and the stars would serve as reference objects for measurements of all additional targets, as well as being targets of direct scientific interest. The instrument global data analysis since objectives are considered including a relativity test and technology. Author

N90-19968*# Harvard-Smithsonian Center for Astrophysics, Cambridge, MA.

NEW TESTS WITH OLD DATA

John F. Chandler *In* NASA, Relativistic Gravitational Experiments in Space Aug. 1989 p 163-165 (For primary document see N90-19940 12-90)

Avail: NTIS HC A11/MF A02 CSCL 03B

The discussion of new tests of relativity must begin with a definition of the word new. Included, under that rubric, not only tests that have never been attempted before or never produced a useful result, but also those that may be repeated with significantly improved results. Thus, the classical tests insofar as they have been recently refined are discussed and the results are given obtained at the Center for Astrophysics (CFA). A new test of relativity is described via the detection of the de Sitter precession of the Moon's orbit. These tests, when considered in the parameterized post-Newtonian (PPN) framework, have all involved determining combinations of beta and gamma. A further topic of consideration is that of old data. In attempting to improve a test of relativity, particularly when the effect to be discerned is a secular one, such as the relativistic perihelion advance of Mercury, it is important to maintain the original set of data, so that the experiment need not start all over. Author

N90-19969*# Stanford Univ., CA. Dept. of Applied Physics.

FREQUENCY STABLE HIGH POWER LASERS IN SPACE c36

Robert L. Byer *In* NASA, Relativistic Gravitational Experiments in Space Aug. 1989 p 166-170 (For primary document see N90-19940 12-90)

Avail: NTIS HC A11/MF A02 CSCL 20E

The concept of a laser heterodyne gravity wave antenna that would operate in solar orbit with a one million kilometer path length is discussed. Laser technology that would be appropriate for operation of this space-based gravity wave detector is also discussed. The rapid progress in diode laser coupled with the energy storage and potentially sub-Hertz linewidths of solid state lasers, and the possibility of efficient frequency conversion by nonlinear optical techniques defines a technology that is appropriate for laser interferometry in space. The present status of diode-laser-pumped, solid state lasers is summarized and future progress is projected in areas of linewidth control, high average power, operating efficiency, and operational lifetimes that are essential for space-based applications. Author

N90-19970*# Jet Propulsion Lab., California Inst. of Tech., Pasadena.

HIGH STABILITY RADIO LINKS c32

E. Robert Kursinski *In* NASA, Relativistic Gravitational Experiments in Space Aug. 1989 p 171-178 (For primary document see N90-19940 12-90)

Avail: NTIS HC A11/MF A02 CSCL 17B

Radio telecommunication links are used for communication with deep space probes. These links consist of sinusoidal carrier signals at radio frequencies (RF) modulated with information sent between the spacecraft and the earth. This carrier signal is a very pure and stable sinusoid, typically derived from an atomic frequency standard whose frequency and phase are used to measure the radial velocity of the probe and from this and other data types derive its trajectory. This same observable can be used to search for space-time distortions cased by low frequency (0.1 to 100 MHz) gravitation radiation. How such a system works, what its sensitivity limitations are, and what potential future improvements can be made are discussed. Author

N90-19971*# Jet Propulsion Lab., California Inst. of Tech., Pasadena.

TROPOSPHERIC MONITORING TECHNOLOGY FOR GRAVITY WAVE EXPERIMENTS

R. N. Treuhaft and G. M. Resch *In* NASA, Relativistic Gravitational Experiments in Space Aug. 1989 p 179-185 (For primary document see N90-19940 12-90)

Avail: NTIS HC A11/MF A02 CSCL 03B

Tropospheric refractivity fluctuations are an important error source for gravity wave detection by Doppler tracking in that they alter the phase and phase rate of electromagnetic signals. Estimates are presented of the effect of tropospheric fluctuations on the Doppler signal and some examples are suggested of methods which minimize the effect. A model of the fluctuations is utilized to achieve those goals. Four possible methods for reducing the fluctuation effect are suggested: (1) observation and analysis strategies, which separate the atmospheric and gravity wave signatures; (2) water vapor radiometry for the wet component; (3) calibration using Global Positioning System (GPS) satellites; and (4) Doppler observations from multiple antennas to average fluctuation effects. The last two techniques could be used to calibrate both wet and dry fluctuations, or could be used in conjunction with water vapor radiometry to calibrate only the dry component. Author

N90-19972*# Smithsonian Astrophysical Observatory, Cambridge, MA.
A REVIEW OF ATOMIC CLOCK TECHNOLOGY, THE PERFORMANCE CAPABILITY OF PRESENT SPACEBORNE AND TERRESTRIAL ATOMIC CLOCKS, AND A LOOK TOWARD THE FUTURE **c35**
Robert F. C. Vessot *In* NASA, Relativistic Gravitational Experiments in Space Aug. 1989 p 186-201 (For primary document see N90-19940 12-90)
Avail: NTIS HC A11/MF A02 CSCL 14B

Clocks have played a strong role in the development of general relativity. The concept of the proper clock is presently best realized by atomic clocks, whose development as precision instruments has evolved very rapidly in the last decades. To put a historical prospective on this progress since the year AD 1000, the time stability of various clocks expressed in terms of seconds of time error over one day of operation is shown. This stability of operation must not be confused with accuracy. Stability refers to the constancy of a clock operation as compared to that of some other clocks that serve as time references. Accuracy, on the other hand, is the ability to reproduce a previously defined frequency. The issues are outlined that must be considered when accuracy and stability of clocks and oscillators are studied. In general, the most widely used resonances result from the hyperfine interaction of the nuclear magnetic dipole moment and that of the outermost electron, which is characteristic of hydrogen and the alkali atoms. During the past decade hyperfine resonances of ions have also been used. The principal reason for both the accuracy and the stability of atomic clocks is the ability of obtaining very narrow hyperfine transition resonances by isolating the atom in some way so that only the applied stimulating microwave magnetic field is a significant source of perturbation. It is also important to make resonance transitions among hyperfine magnetic sublevels where separation is independent, at least to first order, of the magnetic field. In the case of ions stored in traps operating at high magnetic fields, one selects the trapping field to be consistent with a field-independent transition of the trapped atoms. Author

N90-19973*# Jet Propulsion Lab., California Inst. of Tech., Pasadena.
IMPROVED RANGING SYSTEMS **c35**
Larry E. Young *In* NASA, Relativistic Gravitational Experiments in Space Aug. 1989 p 203-205 (For primary document see N90-19940 12-90)
Avail: NTIS HC A11/MF A02 CSCL 14B

Spacecraft range measurements have provided the most accurate tests, to date, of some relativistic gravitational parameters, even though the measurements were made with ranging systems having error budgets of about 10 meters. Technology is now available to allow an improvement of two orders of magnitude in the accuracy of spacecraft ranging. The largest gains in accuracy result from the replacement of unstable analog components with high speed digital circuits having precisely known delays and phase shifts. Author

N90-19974*# Stanford Univ., CA.
DRAG-FREE SATELLITE CONTROL **c18**
Daniel B. DeBra *In* NASA, Relativistic Gravitational Experiments in Space Aug. 1989 p 206-210 (For primary document see N90-19940 12-90)
Avail: NTIS HC A11/MF A02 CSCL 22B

A drag-free satellite cancels the effect of external disturbances. Although the forces may be small, a satellite is disturbed by residual air drag, radiation pressure, micrometeorite impact, and other small forces that act on its surface disturbing its orbit, which is principally determined by the gravity field. In some missions, these small perturbations that make the satellite deviate from its purely gravitational orbit are limiting. An internal unsupported proof mass is shielded by the satellite from the external disturbances. The position of the shield (or the main part of the satellite) is measured with respect to the internal proof mass, and this information is used to actuate a propulsion system which moves the satellite to follow the proof mass. A drag-free control system is illustrated. Since the proof mass is shielded it follows a purely gravitational orbit - as does the satellite following it - hence the name drag-free satellite. The idea was conceived by Lange (1964) and has been applied to many mission studies since. In some cases, it is not necessary to cancel the disturbances, only to measure them so they may be taken into account. In such cases, an accelerometer may be a more suitable solution (for example, using the ONERA Cactus or the Bell Aerosystems MESA). Author

N90-19975*# Maryland Univ., College Park. Dept. of Physics and Astronomy.
SUPERCONDUCTING GRAVITY GRADIOMETER AND A TEST OF INVERSE SQUARE LAW **c35**
M. V. Moody and Ho Jung Paik *In* NASA, Relativistic Gravitational Experiments in Space Aug. 1989 p 211-212 (For primary document see N90-19940 12-90)
Avail: NTIS HC A11/MF A02 CSCL 14B

The equivalence principle prohibits the distinction of gravity from acceleration by a local measurement. However, by making a differential measurement of acceleration over a baseline, platform accelerations can be cancelled and gravity gradients detected. In an in-line superconducting gravity gradiometer, this differencing is accomplished with two spring-mass accelerometers in which the proof masses are confined to motion in a single degree of freedom and are coupled together by superconducting circuits. Platform motions appear as common mode accelerations and are cancelled by adjusting the ratio of two persistent currents in the sensing circuit. The sensing circuit is connected to a commercial SQUID amplifier to sense changes in the persistent currents generated by differential accelerations, i.e., gravity gradients. A three-axis gravity gradiometer is formed by mounting six accelerometers on the faces of a precision cube, with the accelerometers on opposite faces of the cube forming one of three in-line gradiometers. A dedicated satellite mission for mapping the earth's gravity field is an important one. Additional scientific goals are a test of the inverse square law to a part in 10(exp 10) at 100 km, and a test of the Lense-Thirring effect by detecting the relativistic gravity magnetic terms in the gravity gradient tensor for the earth. Author

N90-19976*# Jet Propulsion Lab., California Inst. of Tech., Pasadena.
INERTIAL CORRECTIONS BY DYNAMIC ESTIMATION **c35**
David Sonnabend *In* NASA, Relativistic Gravitational Experiments in Space Aug. 1989 p 213-214 (For primary document see N90-19940 12-90)
Avail: NTIS HC A11/MF A02 CSCL 14B

The highlights are presented of an Engineering Memorandum, Dynamic Estimation for Floated Gradiometers. The original impetus for the work was that gradiometers, in principle, measure components of the gravity gradient tensor, plus rotation effects, similar to centrifugal and Coriolis effects in accelerometers. The problem is that the rotation effects are often quite large, compared to the gradient, and that available inertial instruments can't measure them to adequate accuracy. The paper advances the idea that, if the instruments can be floated in a package subject to very low disturbances, a dynamic estimation, based on the Euler and translational equations of motion, plus models of all the instruments, can be used to greatly strengthen the estimates of the gradient and the rotation parameters. Moreover, symmetry constraints can be imposed directly in the filter, further strengthening the solution. Author

N90-19977*# Clauser (J. F.) and Associates, Livermore, CA. Custom Sensor Development.
ULTRA-SENSITIVE INERTIAL SENSORS VIA NEUTRAL-ATOM INTERFEROMETRY **c35**
John F. Clauser *In* NASA, Relativistic Gravitational Experiments in Space Aug. 1989 p 215-221 (For primary document see N90-19940 12-90)
Avail: NTIS HC A11/MF A02 CSCL 14B

Upon looking at the various colossal interferometers, etc., discussed at this conference to test gravitational theory, one cannot

avoid feeling that easier approaches exist. The use of low velocity, neutral atom matter waves in place of electromagnetic waves in sensitive inertial interferometer configurations is proposed. For applications, spacecraft experiments to sense a drag-free condition, to measure the Lense-Thirring precession, to measure the gravitomagnetic effect and/or the earth's geopotential (depending on altitude), and to detect long period gravitational waves are considered. Also, a terrestrial precision test of the equivalence principle on spin polarized atoms, capable of detecting effects of the 5th force is considered. While the ideas described herein are preliminary, the orders of magnitude are sufficiently tantalizing to warrant further study. Although existing proposed designs may be adequate for some of these experiments, the use of matter-wave interferometry offers reduced complexity and cost, and an absence of cryogenics. Author

N90-19978 Yale Univ., New Haven, CT.
PHOTOMETRIC ANALYSES OF ABUNDANCES IN DWARF SPHEROIDAL GALAXIES AND GLOBULAR CLUSTERS Ph.D. Thesis
Robert Miles Light 1988 230 p
Avail: Univ. Microfilms Order No. DA8917703

The abundance characteristics of several dwarf spheriodal galaxies are studied. The chemical properties of stars in these galaxies are tracers of the origin and evolution of their stellar populations, and thus can provide constraints on the theories of their formation. To derive this abundance information, photometric observations of stars in a sample of globular clusters, covering a large range in metallicity, were analyzed. Parameters describing the position of the red giant branch were found to correlate very well with cluster metallicity over a large range in abundance. These measurements, made in the Thuan-Gunn photometry system, provide ranking schemes which are, with accurate photometry, more sensitive to changes in metallicity than similar broadband BV parameters. The relations were used to derive an improved estimate of the metallicity of cluster NGC 5053. These metallicity relations were used to analyze the Thuan-Gunn system photometry produced for the Sculptor, Ursa Minor, and Carina galaxies. The excellent agreement between their metallicities and those from other previous studies indicates that globular cluster red giant branch parameters are very useful in ranking dwarf spheriodal populations by metallicity. The large dispersion in metallicity found in the Sculptor system is consistent with other data. Large errors associated with the Carina data made the determination of a metallicity dispersion highly uncertain. Additionally, a large set of BV photometry taken of the Fornax dwarf speriodal was analyzed in a similar manner, producing estimates of the mean metallicity and metallicity dispersion that are consistent with previous results. Dissert. Abstr.

N90-19979 Johns Hopkins Univ., Baltimore, MD.
FAR-ULTRAVIOLET SPECTROSCOPY OF COMET HALLEY Ph.D. Thesis
Kenneth Floyd Dymond 1989 199 p
Avail: Univ. Microfilms Order No. DA8923673

Far ultraviolet spectra were obtained of Comet Halley (1986 III) on 26 February 1986 and on 13 March 1986 using an imaging spectrograph launched aboard a sounding rocket. The spectral resolution is approx. 13A over the bandpass of 1200 to 1750A. The imaging capability of the long slit spectrograph permitted the determination of the spatial distribution of the coma emissions. Most of the far ultraviolet emissions are excited by fluorescence with solar line emission; therefore, the fluorescence excitation rates were reevaluated as functions of heliocentric velocity using high resolution solar fluxes and the latest values for the oscillator strengths. The spectra are analyzed with particular emphasis placed on identifying the weak features present. The upper limits on the production rate of OCS and CS2 determined from upper limits placed on sulfur emissions are found to be consistent with production rates inferred by other observers. The spatial distribution of the CO Fourth Positive Band emissions and the CI lambda 1561 and CI lambda 1657 emissions are examined. The shapes of the C emission profiles cannot be adequately described by models which assume that C is produced by photodissociation of CO and other carbon bearing species. Dissert. Abstr.

N90-19980 California Univ., Berkeley.
INFRARED HETERODYNE SPECTROSCOPY OF POLYATOMIC MOLECULES IN CIRCUMSTELLAR ENVELOPES Ph.D. Thesis
David Moses Goldhaber 1988 200 p
Avail: Univ. Microfilms Order No. DA8916674

A heterodyne spectrometer operating a wavelengths near 10 microns was constructed for use at the Cassegrain foci of three-meter-class optical and infrared telescopes. The instrument was used for observations of vibrational-rotational transitions of SiH4, C2H4, and NH3 in the envelope surrounding the carbon star IRC +10216, and of NH3 in the envelopes of the OH/IR supergiants VY CMa and NML Cyg. A calculation of the excitation of the molecular level populations by the Sobolev method predicts that pumping in infrared transitions is the dominant excitation mechanism and that the populations are nearly equilibrated and characterized by a temperature equal to the temperature of the ambient dust. A modified spherical cloud model, in which the excitation is treated as a free parameter, provides good fits to the observed line profiles of silane and ammonia in IRC +10216. The abundances of SiH4 and NH3 are much higher than are predicted to be produced in chemical equilibrium in cool (1500 K) stellar atmospheres and suggest that some other processes are responsible for forming these species. The observed profiles provide high precision estimates of the expansion velocity of the gas relative to the star, for the region between approximately 10 r* and 100 r*. The measured line widths provide a measure of the combined effects of local velocity turbulence and radial velocity gradients. In VY CMa and NML Cyg we observe velocity dispersions much greater than that of IRC +10216. These are attributed to large velocity gradients in the OH/IR sources. Dissert. Abstr.

N90-19981 Maryland Univ., College Park.
COMET HALLEY: AN OPTICAL CONTINUUM STUDY Ph.D. Thesis
Susan Mary Hoban 1989 147 p
Avail: Univ. Microfilms Order No. DA8924166

From an analysis of narrowband CCD images of Comet Halley from 1986 January, March and April, certain dust structures which are redder than the remainder of the dust coma have become apparent. Mie calculations suggest that this reddening is due to an enhancement of particles with sizes comparable to the observing wavelengths. The location of the sunward extension of the red envelopes which are evident in the color maps is consistent with the measurements by Vega 1 and 2 of a depletion of intermediate mass particles. This dip in the mass distribution occurs at the region where particles are most sensitive to solar radiation pressure. Although the mass range derived from the calculations presented is somewhat uncertain as a result of the limitations of Mie theory, these values are in the expected range of particle sizes which would be both sensitive to radiation pressure and significantly reddened with respect to the solar spectrum at the observing wavelengths. Thus, the red envelopes are plausibly the result of size sorting by solar radiation pressure. The red jets observed on 1986 January 10, March 1 and March 9 can then be explained by the enhanced dust flux at the jet sources, and the subsequent trapping of a relative excess of intermediate mass (i.e., red) particles into the jets which are visible in the continuum images.
Dissert. Abstr.

N90-19982 Colorado Univ., Boulder.
O-STAR PARAMETERS FROM LINE PROFILES OF WIND-BLANKETED MODEL ATMOSPHERES Ph.D. Thesis
Stephen Arthur Voels 1989 184 p
Avail: Univ. Microfilms Order No. DA8923541

The basic stellar parameters (i.e., effective temperature, gravity, helium content, bolometric correction, etc...) of several O-stars are determined by matching high signal-to-noise observed line profiles of optical hydrogen and helium line transitions with theoretical line profiles from a core hallo model of the stellar

atmosphere. The core halo atmosphere includes the effect of radiation backscattered from a stellar wind (i.e., wind-blanketing) by incorporating the stellar wind model of Abbott and Lucy (1985) as a reflective upper boundary condition in the Mihalas (1972) atmosphere model. The wind-blanketing introduces systematic shifts in the effective temperatures; lowering the values at spectral class O4 and increasing the difference between supergiants and dwarfs at spectral class O9.5. This shift is reflected in other stellar parameters i.e., bolometric correction and number of ionizing photons emitted. Thus, some stellar parameters determined are significantly different from those assumed from spectral type calibrations. Three of the four supergiants analyzed showed an enhanced surface abundance of helium. Using a large sample of equivalent width data from Conti (1973) a simple argument is made that surface enhancement of helium may be a common property of the most luminous supergiants. The stellar atmosphere theory is sufficient to determine the stellar parameters only if careful attention is paid to the detection and exclusion of lines which are not accurately modeled by the physical processes included.
Dissert. Abstr.

N90-19983# Iowa State Univ. of Science and Technology, Ames.
VERY HIGH ENERGY GAMMA RAY ASTROPHYSICS Progress Report, 1 May 1989 - 1 Feb. 1990
R. C. Lamb and D. A. Lewis Feb. 1990 20 p
(Contract DE-AC02-80ER-10774)
(DE90-006645; DOE/ER-10774/10) Avail: NTIS HC A03/MF A01

Our scientific goal is to discover and study by means of gamma-ray astronomy those regions of the universe where particles are accelerated to extreme energies. The atmospheric Cherenkov technique provides a unique and potentially sensitive window in the region of 10(11) to approximately 10(14) eV for this purpose. The Whipple Observatory Collaboration is currently engaged in the development of a Cherenkov camera which has the ultimate capability of distinguishing gamma-ray showers from the numerous cosmic-ray background showers by imaging the Cherenkov light from each shower. We have recently demonstrated the potential of the imaging technique with our 18 sigma detection of TeV photons from the Crab Nebula using a camera of 10 elements, pixel spacing 0.25 degrees. This detection represents a factor of 10 improvement in sensitivity compared to a non-imaging detector. The next step in the development of the detector is to obtain a second large reflector, similar to the present 10 meter instrument, for stereoscopic viewing of showers. This project, named GRANITE, is now approved by DOE. With GRANITE it should be possible to probe more deeply in space by a factor of 7, and to fully investigate the possibility of new physics which has been suggested by reports of anomalous radiation from Hercules X-1. DOE

N90-19984# Louisiana State Univ., Baton Rouge. Dept. of Physics and Astronomy.
NUCLEAR INTERACTIONS OF HIGH ENERGY HEAVY IONS AND APPLICATIONS IN ASTROPHYSICS Technical Progress Report, 1 Apr. 1989 - 31 Mar. 1990
John P. Wefel 22 Dec. 1989 20 p
(Contract DE-FG05-84ER-40147)
(DE90-006691; DOE/ER-40147/8) Avail: NTIS HC A03/MF A01

The calibration and performance evaluation are mostly completed for the drift chamber trajectory subsystem, the calibration was finished of the detector PSD's, and preliminary mass resolution was obtained for the fragments of Silicon in the solid state detector telescope. New processing software was written for the Oxygen and the Silicon datasets, and reprocessing (Oxygen)/initial processing (Silicon) is to be undertaken in the next few months. The analysis of the energy dependence of the widths of the longitudinal momentum distributions was re-done with a different analysis technique, confirming the previous results and adding confidence to the conclusions. The total charge changing cross sections for silicon have also undergone a reanalysis and detailed comparison to different models. The drift tube calibrations were finalized and significant progress was made in understanding the HISS drift chamber calibration and operation during the run. New drift chamber analysis software is nearly complete and will be checked in an initial data processing pass in the next several months. Preliminary time-of-flight wall beam calibrations show charge resolution below 0.1 units and time resolution of 90 pico-seconds (Neon) and 127 pico-seconds (Helium). These will improve when the full time-of-flight subsystem calibration is performed, the next task following the completion of the drift chamber calibration/software development. DOE

N90-19985# Lawrence Livermore National Lab., CA.
TIME-DEPENDENT TWO-DIMENSIONAL RADIATION HYDRODYNAMICS OF ACCRETING MATTER ONTO HIGHLY MAGNETIZED NEUTRON STARS
Richard I. Klein and Jonathan Arons 24 Nov. 1989 12 p Presented at the 23rd ESLAB Symposium on X Ray Astronomy, Bologna, Italy, 13-20 Sep. 1989 Submitted for publication
(Contract W-7405-eng-48)
(DE90-006927; UCRL-102499; CONF-8909275-3) Avail: NTIS HC A03/MF A01

We present for the first time, the self-consistent solution of the two-dimensional, time-dependent equations of radiation-hydrodynamics governing the accretion of matter onto the highly magnetized polar caps of luminous x ray pulsars. The calculations show a structure in the accretion column very different from previous one-zone uniform models. We have included all the relevant magnetic field corrections to both the hydrodynamics and the radiative transport. We include a new theory for the diffusion and advection of both radiation energy density and photon number density. For initially uniformly accreting models with super-Eddington flows, we have uncovered evidence of strong radiation-driven outflowing optically thin radiation filled regions of the accretion column embedded in optically-thick inflowing plasma. The development of these photon bubbles have growth times on the order of a millisecond and show fluctuations on sub-millisecond timescales. The photon bubbles are likely to be a consequence of convective over-stability and may result in observable fluctuations in the emitted luminosity leading to luminosity dependent changes in the pulse profile. This may provide important new diagnostics for conditions in accreting x ray pulsars. DOE

N90-19986# International Centre for Theoretical Physics, Trieste (Italy).
DISTURBANCE STRUCTURES AND ITS MAGNETIC FIELD FEATURES IN PLASMA COMET TAIL
Zhongyuan Li Aug. 1989 10 p Submitted for publication
(DE90-610636; IC-89/198) Avail: NTIS (US Sales Only) HC A02/MF A01

The solar wind disturbances result in the emergence of condensation structures in plasma comet tails. Most of them are correlated with plasma vortex flow. In this paper, we analyze the features of condensations based on the theories of MHD and force-free field. Specifically, we discuss the construction and the distribution of magnetic field and its energy in condensations. We also analyze in detail the coupling process between an unsteady plasma motion and a magnetic field. The coupling effect will let the energy in comet tail change into the force-free field in condensations, so that the magnetic field energy in the condensations increases constantly. Many phenomena observed in comet tails can be explained with the model. DOE

N90-19987# Los Alamos National Lab., NM.
THE ADVANCED COMPOSITION EXPLORER
E. C. Stone, L. F. Burlaga, A. C. Cummings, W. C. Feldman, W. E. Frain, J. Geiss, G. Gloeckler, R. E. Gold, D. Hovestadt, and S. M. Krimigis (Johns Hopkins Univ., Laurel, MD.) et al 1989 11 p Presented at the Particle Astrophysics: NASA Cosmic Ray Program for the 1990's and Beyond, Greenbelt, MD, 6-8 Nov. 1989 Prepared in cooperation with Chicago Univ., IL
(Contract W-7405-eng-36)
(DE90-006522; LA-UR-90-42; CONF-8911161-2) Avail: NTIS HC A03/MF A01

The Advanced Composition Explorer (ACE) was recently selected as one of two new Explorer-class missions to be developed for launch during the mid-1990's. ACE will observe particles of solar, interplanetary, interstellar, and galactic origins, spanning the energy range from that of the solar wind (approx. 1 keV/nucleon) to galactic cosmic ray energies (several hundred MeV/nucleon). Definitive studies will be made of the abundance of nearly all isotopes from H to Zn (1 less than or = Z less than or = 30), with exploratory isotope studies extending to Zr (Z = 40). To accomplish this, the ACE payload includes six high-resolution spectrometers, each designed to provide the optimum charge, mass, or charge-state resolution in its particular energy range, and each having a geometry factor optimized for the expected flux levels, so as to provide a collecting power a factor of 10 to 1000 times greater than previous or planned experiments. The payload also includes several instruments of standard design that will monitor solar wind and magnetic field conditions and energetic H, He, and electron fluxes. The scientific objectives, instrumentation, spacecraft, and mission approach that were defined for ACE during the Phase-A study period are summarized. DOE

N90-19988# Tokyo Metropolitan Univ. (Japan). Inst. for Nuclear Study.
COSMIC STRING IN COMPACTIFIED GAUGE THEORY
A. Nakamuru, S. Hirenjaki, and K. Shiraishi (Tokyo Univ., Tanashi, Japan) Aug. 1989 28 p Sponsored in part by Japanese Ministry of Education, Science and Culture; Japan Society for the Promotion of Science; and Iwanami Fujukai
(DE90-741463; INS-759) Avail: NTIS (US Sales Only) HC A03/MF A01

A solution of the vortex type is given in a six-dimensional SU(2)xU(1) pure gauge theory coupled to Einstein gravity in a compactified background geometry.The solution of an effective Abelian-Higgs model was constructed in terms of dimensional reduction. The solution, however, has a peculiarity in its physically relevant quantity, a deficit angle, which is given as a function of the ratio of the gauge couplings of SU(2) and U(1). The size of the extra space (sphere) is shown to vary with the distance from the axis of the string. DOE

N90-19989# European Space Agency, Paris (France).
PHYSICS AND MECHANICS OF COMETARY MATERIALS
J. Hunt, ed. and T. D. Guyenne, ed. Dec. 1989 223 p Workshop held in Muenster, Fed. Republic of Germany, 9-11 Oct. 1989; sponsored by Westfaelische Wilhelms-Univ. and ESA/ESTEC
(ESA-SP-302; ISBN-92-9092-050-5; ISSN-0379-6566; ETN-90-96299) Copyright Avail: NTIS HC A10/MF A02; ESA Publications Div., ESTEC, Noordwijk, Netherlands, 60 Dutch guilders

The proceedings of an international workshop on the physics and mechanics of cometary materials are presented. Comet missions and models were reported including the future ESA Rosetta comet nucleus sample return mission. A review of physical and compositional comet nucleus models were given. Physical, chemical, and mechanical properties of ices and ice-dust mixtures were examined. Experimental techniques such as the characterization of snow structures and the Rosetta altimeter and sounding radar were described. References to the KOSI (comet simulation) project appeared. A poster session included items such as gas diffusion in a cometary crust and cohesive forces in Sun-grazing comets. Observations of comets Halley and Churyumov-Gerasimenko were used. Recommendations for studies pertaining to the Rosetta mission and drilling requirements are to be found. For individual titles, see N90-19990 through N90-20023.

N90-19990# European Space Agency. European Space Research and Technology Center, ESTEC, Noordwijk (Netherlands).
ROSETTA/CNSR, ESA'S PLANETARY CORNERSTONE MISSION
G. Schwehm *In its* Physics and Mechanics of Cometary Materials Dec. 1989 p 11-15 (For primary document see N90-19989 12-90)
Copyright Avail: NTIS HC A10/MF A02; ESA Publications Div., ESTEC, Noordwijk, Netherlands, 60 Dutch guilders

The Rosetta/Comet Nucleus Sample Return (CNSR) mission is described in terms of scenario, spacecraft concept, comet approach, sampling, return to Earth and Earth approach and re-entry phase. The preparatory program of ESA and NASA to provide new technologies is discussed. The prime scientific objective is to return a comet nucleus sample to Earth while preserving such fundamental properties as: the chemical and isotopic composition of the individual molecular species of remaining volatile compounds; the chemical, isotopic and structural state of the individual phases and crystals constituting higher temperature condensates and aggregates; and the preservation of complex hydrocarbon compounds and their aggregates. The sample will allow the study of the most primitive material in the solar system and the physical and chemical processes that marked the system's beginning, and hopefully will establish correspondence between interstellar matter, cometary material and primitive meteorites already, collected. ESA

N90-19991# Cassino Univ. (Italy).
PHYSICAL MODELS OF COMETARY NUCLEI: A REVIEW
L. Colangeli, E. Bussoletti, and G. Schwehm (European Space Agency. European Space Research and Technology Center, ESTEC, Noordwijk, Netherlands) *In* ESA, Physics and Mechanics of Cometary Materials Dec. 1989 p 17-22 (For primary document see N90-19989 12-90)
(Contracts PSN-88-RB-020; ASI-88-RB-060)
Copyright Avail: NTIS HC A10/MF A02; ESA Publications Div., ESTEC, Noordwijk, Netherlands, 60 Dutch guilders

The physical structure of comets is studied and theoretical models are reviewed to describe the status and evolution of a comet nucleus. Critical and uncertain aspects are focused on, for example, the unclear crust formation mechanisms and undetermined stratigraphic composition. For a meaningful theoretical work, a continuous comparison between starting hypotheses and outcoming results with both astronomical observations and laboratory data is suggested. ESA

N90-19992# Westfaelische Wilhelms Univ., Muenster (Germany, F.R.). Inst. fuer Planetologie.
PETROGRAPHIC WORKING MODEL OF THE ROSETTA SAMPLING AND MODELLING SUBGROUP FOR A COMET NUCLEUS
D. Stoeffler *In* ESA, Physics and Mechanics of Cometary Materials Dec. 1989 p 23-29 (For primary document see N90-19989 12-90)
Copyright Avail: NTIS HC A10/MF A02; ESA Publications Div., ESTEC, Noordwijk, Netherlands, 60 Dutch guilders

Based on the most probable ranges of the interior and surface properties of a comet nucleus as far as they are relevant for the planning of a comet nucleus sample return mission (Rosetta), documented according to the present status of discussion within the joint Rosetta science working group of ESA and NASA, a comet nucleus regolith was developed which describes the properties of the near surface layer of a model comet nucleus at the macro and microscale with respect to textural, compositional, and geological properties. It consists of a multi-component system of fine-grained constituents forming a porous matrix (frozen volatiles and dust) and coarser grained, coherent inclusions of solid polycrystalline ice(s) and rock-like aggregates. A list of most probable phases is given. For simulation experiments and tests of spacecraft systems cometary analog materials are proposed which contain H2O, CO2, NH2, C, hydrocarbons such as asphalt or kerogen, and inorganic minerals like olivine, pyroxene, montmorillonite and kaolinite. ESA

N90-19993# Tecnospazio S.p.A., Milan (Italy).
DESIGN AND DEVELOPMENT ACTIVITIES ON THE CANDIDATE SAMPLE ACQUISITION SYSTEM FOR THE ROSETTA MISSION

C. Gerli and P. Vielmo (Tecnomare S.p.A., Italy) *In* ESA, Physics and Mechanics of Cometary Materials Dec. 1989 p 31-36 (For primary document see N90-19989 12-90)
Copyright Avail: NTIS HC A10/MF A02; ESA Publications Div., ESTEC, Noordwijk, Netherlands, 60 Dutch guilders

The main results obtained in the assessment and design of a flexible concept of Sample Acquisition System (SAS) to cope with demanding mission targets of Rosetta are illustrated. In particular, the main design features of the proposed SAS and sampling tool concepts are described and impact of mission requirements on system dealt with. The guidelines for a development activity are identified. A development effort (integrated and supported by extensive simulation and development testing) is foreseen in the critical areas of robotic structure elements for handling tools, corer tool and relevant drive devices, and anchoring system. The program of future activities is described. ESA

N90-19994# Max-Planck-Inst. fuer Aeronomie, Katlenburg-Lindau (Germany, F.R.).
COMETS: DIRTY SNOWBALLS OR ICY DIRTBALLS
H. U. Keller *In* ESA, Physics and Mechanics of Cometary Materials Dec. 1989 p 39-45 (For primary document see N90-19989 12-90)
Copyright Avail: NTIS HC A10/MF A02; ESA Publications Div., ESTEC, Noordwijk, Netherlands, 60 Dutch guilders

The observations of comet Halley show that the non-volatile (dust) component of the cometary nucleus has become more dominant if compared to the perception based on the icy conglomerate nucleus. The in-situ observations on the Giotto spacecraft revealed an excess of large dust particles that dominate the mass distribution. Even larger particles were derived from the attitude changes of the spacecraft bridging the gap to the cloud of particles observed by radar techniques. A dust to gas ratio larger than one was derived for comet Halley. The importance of dust for the structure of the nucleus is corroborated by the amount of particles and their lifetime in meteor streams. Fireballs show that large (meter size) objects separate from the nucleus and are stable enough to survive hundreds of orbital periods. From the various lines of evidence it is concluded that the structure of cometary nuclei is determined by the non-volatile component rather than by ice or snow. Laboratory models based on icy agglomerations do not seem realistic as nucleus analogs. ESA

N90-19995*# Leiden Univ. (Netherlands). Astrophysics Lab.
A TEST OF THE INTERSTELLAR DUST MODEL OF COMETS
J. M. Greenberg and J. I. Hage *In* ESA, Physics and Mechanics of Cometary Materials Dec. 1989 p 47-52 (For primary document see N90-19989 12-90)
(Grant NGR-33018148)
Copyright Avail: NTIS HC A10/MF A02; ESA Publications Div., ESTEC, Noordwijk, Netherlands, 60 Dutch guilders CSCL 03B

The interstellar dust model of comets is used as a basis to simultaneously satisfy various observational constraints and to derive the porosity of comet dust. The observational constraints are: the strengths of the 3.4 and 9.7 micron emission bands; the shape of the 9.7 micron band; the relative amount of silicates to organic materials; the mass distribution of the dust. The method used involves precise calculation of the temperatures and emission characteristics of porous aggregates of interstellar dust as a function of their mass, porosity and distance to the Sun and the wavelength. The results indicate a high porosity of comet dust. ESA

N90-19996# Centre National de la Recherche Scientifique, Saint Martin d'Heres (France). Lab de Glaciologie et de Geophysique de l'Environnement.
PHYSICAL PROCESSES IN COMETARY ICES INFERRED FROM LABORATORY STUDIES
J. Klinger *In* ESA, Physics and Mechanics of Cometary Materials Dec. 1989 p 55-63 Sponsored by the French Institut National des Sciences de l'Univers (For primary document see N90-19989 12-90)
Copyright Avail: NTIS HC A10/MF A02; ESA Publications Div., ESTEC, Noordwijk, Netherlands, 60 Dutch guilders

Based on recent laboratory studies, an overview is given of the properties of various ices and ice mixtures condensed at low temperatures, and on their evolution during heating up to temperatures typical of the perihelion temperatures of short period comets. The kinetics of formation and of decomposition of clathrate hydrates and molecular hydrates is outlined and the possibility of their occurrence in comet nuclei is discussed. Special attention is given to the thermal behavior of amorphous and fluffy icy material. ESA

N90-19997# Centre National de la Recherche Scientifique, Saint Martin d'Heres (France). Lab. de Glaciologie et de Geophysique de l'Environnement.
LABORATORY STUDIES OF COMETARY ICE ANALOGUES
B. Schmitt, S. Espinasse, R. J. A. Grim, J. M. Greenberg (Leiden Univ., Netherlands), and J. Klinger *In* ESA, Physics and Mechanics of Cometary Materials Dec. 1989 p 65-69 Sponsored by ESA and the French Institut National des Sciences de l'Univers (For primary document see N90-19989 12-90)
Copyright Avail: NTIS HC A10/MF A02; ESA Publications Div., ESTEC, Noordwijk, Netherlands, 60 Dutch guilders

Laboratory studies were performed in order to simulate the physico-chemical processes that are likely to occur in the near surface layers of short and intermediate period comets. Pure H2O ice as well as CO:H2O, CO2:H2O, CH4:H2O, CO:CO2:H2O, and NH3:H2O ice mixtures were studied in the temperature range between 10 and 180 K. The evolution of the composition of ice mixtures, the crystallization of H2O ice as well as the formation and decompostion of clathrate hydrate by different processes were studied as a function of temperature and time. Using the results together with numerical modeling, predictions are made about the survival of amorphous ice, CO, CO2, CH4, and NH3 in the near surface layers of short period comets. The likeliness of finding clathrate and molecular hydrates is discussed. It is proposed that the analytical methods developed here could be fruitfully adapted to the analysis of returned comet samples. ESA

N90-19998# Istituto Elettrotecnico Nazionale (Galileo Ferraris), Turin (Itlay).
EVOLUTION OF ICES AND CARBONACEOUS MATERIALS IN THE LABORATORY AND IN COMETS
E. Bussoletti, L. Colangeli, and G. Strazzulla (Catania Univ., Italy) *In* ESA, Physics and Mechanics of Cometary Materials Dec. 1989 p 71-76 Sponsored in part by the Italian Ministry of Public Education (For primary document see N90-19989 12-90)
(Contracts PSN-88-RB-020; ASI-88-RB-060; ASI-88-RB-047)
Copyright Avail: NTIS HC A10/MF A02; ESA Publications Div., ESTEC, Noordwijk, Netherlands, 60 Dutch guilders

Some of the main laboratory results concerning amorphous carbon production and organic ice irradiation are described. The experimental data are used to reproduce P/Halley's and other cometary IR spectra. The results indicate that the above mentioned materials appear to be among the best candidates to simulate the actual carbonaceous and organic components in comets. ESA

N90-19999# Westfaelische Wilhelms Univ., Muenster (Germany, F.R.). Inst. fuer Planetologie.
THERMAL CONDUCTIVITIES AND DIFFUSIVITIES OF POROUS ICE SAMPLES AT LOW PRESSURES AND TEMPERATURES AND POSSIBLE MODES OF HEAT TRANSFER IN NEAR SURFACE LAYERS OF COMETS
T. Spohn, K. Seiferlin, and J. Benkhoff *In* ESA, Physics and Mechanics of Cometary Materials Dec. 1989 p 77-81 Sponsored by Deutsche Forschungsgemeinschaft (For primary document see N90-19989 12-90)
Copyright Avail: NTIS HC A10/MF A02; ESA Publications Div., ESTEC, Noordwijk, Netherlands, 60 Dutch guilders

Thermal conductivities of solid water ice, porous water ice and porous water ice/dust samples with porosities between 0.5 and

0.6 have been measured at a pressure of 1 Pa and at temperatures between 80 K and 170 K. The thermal conductivity was found to be 0.25 + or - 0.05 W/mK and to depend little on temperature and composition in the range of values considered. Thermal diffusivities and ratios between rates of matrix conductive heat transfer and heat transfer due to vapor flow have been estimated from the results of recent KOSI (comet simulation) experiments. The thermal diffusivities were between 10(exp -7) and 10(exp -8) powers sq m/sec and the ratio between vapor and matrix conductive heat ransfer was 10. Water vapor heat transfer is most likely less important if the near surface temperature of the Rosetta target comet is below 150 K. It is still possible, however, that vapors of more volatile phases contribute significantly to heat transfer. ESA

N90-20000# Southwest Research Inst., San Antonio, TX.
PHYSICO-CHEMICAL PROPERTIES OF FORMALDEHYDE-ICE-DUST MIXTURES
D. C. Boice, D. W. Naegeli, and W. F. Huebner *In* ESA, Physics and Mechanics of Cometary Materials Dec. 1989 p 83-88 (For primary document see N90-19989 12-90)
Copyright Avail: NTIS HC A10/MF A02; ESA Publications Div., ESTEC, Noordwijk, Netherlands, 60 Dutch guilders

One of the spectacular surprises of the recent spacecraft encounters with the comet Halley was the discovery of complex organic molecules associated with dust grains in the coma, namely the CHON particles. Formaldehyde oligomers were identified as a constituent of the complex mixture that constitutes the organic componept of the dust. These oligomers when end-capped with water are observed in the laboratory to be stable in the gas phase up to 5 monomeric units in length and at temperatures characteristic of dust grains in the coma and higher. An overview of further experiments concerning the physico-chemical nature of formaldehyde-ice-dust mixtures relevant to the comet nucleus and dust is given. ESA

N90-20001# Open Univ., Milton (England). Dept. of Earth Sciences.
STABLE ISOTOPE STUDIES OF COMETARY ANALOGUE MATERIALS
I. A. Franchi, C. M. O. Alexander, C. T. Pillinger, C. X. Mendoza-Gomez, and J. M. Greenberg (Leiden Univ., Netherlands) *In* ESA, Physics and Mechanics of Cometary Materials Dec. 1989 p 89-92 Sponsored by the United Kingdom Science and Engineering Research Council (For primary document see N90-19989 12-90)
Copyright Avail: NTIS HC A10/MF A02; ESA Publications Div., ESTEC, Noordwijk, Netherlands, 60 Dutch guilders

Some preliminary experiments exploring the isotopic exchange of water and CO2 at low temperature are reported. The results indicate that isotopic signatures of these components may be lost even at sub-ambient temperatures and thus have implications for the storage of cometary nucleus samples during return to Earth. Photochemically produced organics are made up of species with different stability to combustion including some of high volatility and others which are quite refractory. These materials are worthy of consideration as cometary analogs for use in preparing for the return of cometary nucleus samples. Their study could also help in the interpretation of the data which will eventually be gathered from the comet samples themselves. ESA

N90-20002# Army Cold Regions Research and Engineering Lab., Hanover, NH.
INTRODUCTION TO DRILLING TECHNOLOGY **c31**
Malcom Mellor *In* ESA, Physics and Mechanics of Cometary Materials Dec. 1989 p 95-114 (For primary document see N90-19989 12-90)
Copyright Avail: NTIS HC A10/MF A02; ESA Publications Div., ESTEC, Noordwijk, Netherlands, 60 Dutch guilders

Terrestrial drilling technology is reviewed. The general requirements for a drilling system are given and conventional drilling techniques (rotary drag-bit, rotary roller-bit, percussive, rotary percussive) are described. Unconventional techniques for penetrating solids are outlined, including thermal drilling (spalling or melting), projectile penetration, high pressure liquid jets, explosive jets, erosion by projectile streams, and chemical penetration. Special attention is given to drilling in ice and frozen soils, performance data are given, including values for penetration rate and specific energy consumption. The principles, theory and equipment relating to each drilling technique are indicated by means of diagrams. ESA

N90-20003# Deutsche Forschungsanstalt fuer Luft- und Raumfahrt, Cologne (Germany, F.R.).
CRUSTAL STRENGTH OF DIFFERENT MODEL COMET MATERIALS
H. Kochan, K. Roessler, L. Ratke, M. Heyl, H. Hellman, and G. Schwehm (European Space Agency. European Space Research and Technology Center, ESTEC, Noordwijk, Netherlands) *In* ESA, Physics and Mechanics of Cometary Materials Dec. 1989 p 115-119 (For primary document see N90-19989 12-90)
Copyright Avail: NTIS HC A10/MF A02; ESA Publications Div., ESTEC, Noordwijk, Netherlands, 60 Dutch guilders

In the context of comet simulation experiments the physical differentation of icy analogs is investigated. During and after the artificial insolation the hardness of the samples is measured as a function of depth. The simple experimental set-up elucidates for the first time the effect of insolation on the mechanical properties of fluffy ice-dust mixtures. Starting from a fluffy ice-mineral mixture of low density, a remarkable hardening of the sample is observed within distinct layers. These layers are inhomogeneous in thickness and hardness. The variation of hardness with depth is attributed to the crustal formation by sintering. It can be explained qualitatively by models of crust formation via sublimation, diffusion and condensation of volatiles. During typical experiments the hardness increases by a factor of 5 to 10. ESA

N90-20004# Deutsche Forschungsanstalt fuer Luft- und Raumfahrt, Cologne (Germany, F.R.).
FRACTURE MECHANICAL ASPECTS OF DUST EMISSION PROCESSES FROM A MODEL COMET SURFACE
L. Ratke and H. Kochan *In* ESA, Physics and Mechanics of Cometary Materials Dec. 1989 p 121-128 (For primary document see N90-19989 12-90)
Copyright Avail: NTIS HC A10/MF A02; ESA Publications Div., ESTEC, Noordwijk, Netherlands, 60 Dutch guilders

Laboratory space simulation experiments are reported. High resolution video records taken from the virgin surface of a model comet in the small simulation chamber at the DLR showed a highly structure, rough surface during irradiation with artificial sunlight. The observations demonstrated that the surface itself is not calm, but partially in motion. Particles vibrate within the gas jet originating from sublimation of ice. After a certain time they lift off. Particles which are obviously bonded to the surface loose after a certain time the bonds to their neighbors until they are free and accelerated by the gas jet. The observations show that the commonly considered view of dust emission processes by gravity force dominated particles has to be revised as well as the supposition of loosely deposited particles at fresh surfaces without any bonding. Model calculations of bond strength based on material parameters of ice show that these can be orders of magnitude higher than the gravity force. The mechanisms observed are analyzed with fracture mechanical models, which are also applicable to the fracture of a cometary crust. ESA

N90-20005# Ruhr Univ., Bochum (Germany, F.R.). Inst. fuer Hoch- und Hoechstfrequenztechnik.
SIMULATION OF RADAR AND RADIOMETER SIGNALS REMOTE SENSING COMETARY SURFACE AND SUBSURFACE STRUCTURES
P. Edenhofer and J. Noll *In* ESA, Physics and Mechanics of Cometary Materials Dec. 1989 p 129-138 (For primary document see N90-19989 12-90)
Copyright Avail: NTIS HC A10/MF A02; ESA Publications Div., ESTEC, Noordwijk, Netherlands, 60 Dutch guilders

Results of numerical calculations in the microwave range are

presented concerned with the reflection, backscattering, and emission coefficient of simulated cometary surfaces as a function of signal frequency, angle of incidence, polarization, and surface roughness. The variations of the dielectric permittivity and loss tangent are estimated as to be expected for typical cometary surface conditions. The spatial resolution of potential Rosetta radar measurements is discussed. The subsurface penetration depth is given and a one layer model is introduced. Preliminary results from experimental investigations are presented simulating radar measurements probing a cometary surface in the frequency range 8 to 12.5 GHz. A special calibration technique using time domain transformation is applied to resolve the cometary reflection coefficient against background noise as to be expected in a simulation chamber. The results are discussed for different surface conditions and the determination of specific surface and subsurface parameters is demonstrated. ESA

N90-20006# Ruhr Univ., Bochum (Germany, F.R.).
COMPRESSIVE STRENGTH OF SYNTHETIC COMET NUCLEUS SAMPLES
H. L. Jessberger and M. Kotthaus *In* ESA, Physics and Mechanics of Cometary Materials Dec. 1989 p 141-146 (For primary document see N90-19989 12-90)
Copyright Avail: NTIS HC A10/MF A02; ESA Publications Div., ESTEC, Noordwijk, Netherlands, 60 Dutch guilders

Material properties such as uniaxial compressive strength and Young's modulus of elasticity of the comet nucleus material are investigated for the design of drills, shovels and other instruments for acquisition systems of comet nucleus samples to be used in the ESA Rosetta comet nucleus sample return mission. Different ice-dust mixtures with contents of solid material between 1 and 20 percent by weight as synthetic comet nucleus materials were prepared. Cylindrical samples of these materials with average densities in the range of 0.5 to 0.8 g/cu cm were produced by densification. These samples were used for uniaxial compression tests at temperatures of 253, 233, and 123 K, to determine the compressive strength and the Young's modulus. The stress-strain curves showed a difference in behavior depending on test temperature and material. Further tests and investigation of the effects of age hardening are advised. ESA

N90-20007# Eidgenoessisches Inst. fuer Schnee- und Lawinenforschung, Weissfluhjoch/Davos (Switzerland).
LABORATORY TECHNIQUES FOR THE CHARACTERISATION OF SNOW STRUCTURES **c46**
W. Good *In* ESA, Physics and Mechanics of Cometary Materials Dec. 1989 p 147-151 (For primary document see N90-19989 12-90)
Copyright Avail: NTIS HC A10/MF A02; ESA Publications Div., ESTEC, Noordwijk, Netherlands, 60 Dutch guilders

The methods of collecting, preparing and analyzing samples of seasonal snow are summarized. To investigate the geometric structure and the texture, the skeleton of the snow is fixed and random sections are prepared. Image analysis is performed using filtering, segmentation and morphological operations to emphasize the relevant structures. Quantitative geometric analysis, as used in material sciences, is illustrated with nivological examples. Simple geometric features can be represented with sampling parameters whereas complex ones often need pattern recognition techniques for a more accurate description. A few parameters which were processed on different systems are compared. If the assumptions of stereology, namely regular shapes of the particles, are not fulfilled, a 3-D study of the geometry is necessary. ESA

N90-20008# Rome Univ. (Italy). Dipt. Aerospaziale.
THERMAL PERTURBATION OF COMET SAMPLES DURING THEIR ACQUISITION
S. Sgubini and A. Buratti (Space Systems Studies, Rome, Italy) *In* ESA, Physics and Mechanics of Cometary Materials Dec. 1989 p 153-158 (For primary document see N90-19989 12-90)
Copyright Avail: NTIS HC A10/MF A02; ESA Publications Div., ESTEC, Noordwijk, Netherlands, 60 Dutch guilders

Comet sample temperature rises due to the adduction of mechanical energy connected with sample acquisition operations should be kept as small as possible, in order to minimize the probability of modifications of the samples chemical-physical properties. In addressing this problem, mathematical models are developed for determining the time evolution of the temperature field in the sample acquisition, together with the results obtained for different sampling techniques, comet material characteristics, drill power and penetration rate or harpoon speed of impact. Temperature rises are shown to be very significant. ESA

N90-20009# Rome Univ. (Italy). Info-Com Dept.
ROSETTA/CNSR ALTIMETER AND SOUNDING RADAR
G. Picardi, R. Seu, and P. T. Melacci (Perugia Univ., Italy) *In* ESA, Physics and Mechanics of Cometary Materials Dec. 1989 p 159-163 (For primary document see N90-19989 12-90)
Copyright Avail: NTIS HC A10/MF A02; ESA Publications Div., ESTEC, Noordwijk, Netherlands, 60 Dutch guilders

The altimeter and sounding radar, one of the planned instruments on board the spacecraft in the Comet Nucleus Sampling Return (CNSR) mission, is addressed. This mission involves the study and design of a complete spacecraft system capable of landing on the comet nucleus and performing subsurface analysis. The requirements are recalled and the performance of a conventional beam-limited and pulse-limited radar altimeter are considered. In order to improve the horizontal resolution the synthetic aperture approach is proposed to be integrated to the radar altimeter. ESA

N90-20010# Institut d'Astrophysique, Paris (France).
COMETARY BODIES IN THE CIRCUMSTELLAR DISK AROUND BETA PICTORIS
H. Beust, A. M. Lagrange-Henri, A. Vidal-Madjar, and R. Ferlet *In* ESA, Physics and Mechanics of Cometary Materials Dec. 1989 p 167-172 (For primary document see N90-19989 12-90)
Copyright Avail: NTIS HC A10/MF A02; ESA Publications Div., ESTEC, Noordwijk, Netherlands, 60 Dutch guilders

The IRAS (Infrared Astronomy Satellite) star beta Pictoris, as the only one in which a disk made of both dust and gas has been detected, is studied. Spectroscopic observations of beta Pic revealed that some metallic absorption lines present redshifted additional components which strongly variate with time. This is interpreted as the result of the infall of small evaporating cometary-like bodies toward the star. To improve this model, a theoretical description of such an event is taken. Numerical simulations of such infalling bodies are able to reproduce quite faithfully the observed behavior of some metallic ions, and the observed difference between these behaviors is explained by means of radiation pressure. Some constraints on the orbits of the bodies are deduced through the simulations which should be related to a possible interpretation concerning beta Pic's disk. ESA

N90-20011# Max-Planck-Inst. fuer Kernphysik, Heidelberg (Germany, F.R.).
LOW VELOCITY DUST-DUST COLLISIONS
J. Blum and H. Fechtig *In* ESA, Physics and Mechanics of Cometary Materials Dec. 1989 p 173-175 (For primary document see N90-19989 12-90)
(Grants DFG-Ig-3/13-1; DFG-Ig-3/13-2; DFG-Ig-3/13-3)
Copyright Avail: NTIS HC A10/MF A02; ESA Publications Div., ESTEC, Noordwijk, Netherlands, 60 Dutch guilders

An experimental setup was developed to investigate collisional processes between protoplanetary and/or protocometary particles. The relative velocities of the order-of-mm-sized particles can be varied from approx. 10 cm/s to approximately 10 m/s. The first experiments were performed with fluffy agglomerates of particles each consisting of a glass core and an organic mantle (n-pentacosane) at relative velocities around 1.2 m/s. No sticking of the collided agglomerates was observed for relative amounts of n-pentacosane lower than or equal to 17 weight percent, whereas sticking was observed for relative amounts of organic material

greater than or equal to 22 weight percent. The coagulation probability increases with increasing proportion of n-pentacosane. ESA

N90-20012# Observatoire de Besancon (France).
HOT OH AND CN: EVIDENCE FOR ORGANIC MOLECULES CLOSE TO THE NUCLEUS OF COMET HALLEY
J. Clairemidi and G. Moreels *In* ESA, Physics and Mechanics of Cometary Materials Dec. 1989 p 177-184 Sponsored by CNES; Univerite de Franche-Comte, France; and Region de Franche-Comte, France (For primary document see N90-19989 12-90)
Copyright Avail: NTIS HC A10/MF A02; ESA Publications Div., ESTEC, Noordwijk, Netherlands, 60 Dutch guilders

During the encounter session of Vega 2 with comet Halley on 6 Mar. 1986, advantage was taken of the approach motion and of the resulting zoom effect to assemble the monochromatic charts produced by a three channel spectrometer in composite images at selected wavelengths. Two jets are clearly apparent in most of the monochromatic images. The OH and CN emission originating from the jets exhibit a pronounced peculiarity. The bands located at 309 and 388 nm show an excess of emission at 305 and 383 nm. The proposed mechanism, specific to the jets, is the photodissociation of one or several organic molecules of the type A-OH or B-CN which would release hot OH and CN when submitted to the solar UV flux. These organic molecules would be a component of the envelope of the CHON submicronic grains dragged by the gaseous jets. They provide an additional argument in favor of the similarity between cometary and interstellar matter. ESA

N90-20013# Centre National de la Recherche Scientifique, Saint Martin d'Heres (France). Lab. de Glaciologie et de Geophysique de l'Environnement.
A METHOD OF ESTIMATING TEMPERATURE PROFILES AND CHEMICAL DIFFERENTIATION IN THE NEAR SURFACE LAYERS OF POROUS COMET NUCLEI: FIRST RESULTS FOR COMET P/CHURYUMOV-GERASIMENKO
S. Espinasse, J. Klinger, C. Ritz, and B. Schmidt *In* ESA, Physics and Mechanics of Cometary Materials Dec. 1989 p 185-190 (For primary document see N90-19989 12-90)
(Contract INSU-883719)
Copyright Avail: NTIS HC A10/MF A02; ESA Publications Div., ESTEC, Noordwijk, Netherlands, 60 Dutch guilders

A method for a quantitative estimation of thermal gradients and chemical differentiation in porous icy mixtures is presented. This method was applied to comet nuclei containing different volatile species with special attention given to subsurface layers. Heat conduction by the solid and heat and mass transport by the gas phase in the pore system are included. Based on recent laboratory studies, the influence of the crystallization of amorphous ice on the thermal behavior and the gas release is considered. First results are presented for comet P/Churyumov-Gerasimenko. ESA

N90-20014# Kernforschungsanlage, Juelich (Germany, F.R.). Inst. fuer Chemie 1.
CO2 DEPTH PROFILES IN COMETARY MODEL SUBSTANCES OF KOSI
P. Hsiung and K. Roessler *In* ESA, Physics and Mechanics of Cometary Materials Dec. 1989 p 191-196 Sponsored by Deutsche Forschungsgemeinschaft (For primary document see N90-19989 12-90)
Copyright Avail: NTIS HC A10/MF A02; ESA Publications Div., ESTEC, Noordwijk, Netherlands, 60 Dutch guilders

The CO2 content of cometary analogs used in the KOSI 3 and 4 (comet simulation) experiments was measured by gaschromatography. CO2 depth profiles were determined after insolation in cm layers taken from the samples which originally contained 14 to 15 percent frozen CO2 which show an upper layer completely depleted of the volatile component, while the deeper layers are not affected. A transition layer where the CO2 content ranges from 0 percent to a value which is higher than that of the starting (greater than 20 percent) is interpreted as inward diffusion of CO2 which can recondense in colder zones. Correlation with the temperature profiles was observed. The upper and lower layers show a rather constant but different temperature, while a very steep temperature gradient is found in the transition layer. The water-ice profile showed no significant change with respect to the starting material. Inward diffusion and correlated thermal effects are concluded to be governed by the lighter volatiles (here CO2) and less by water. Sharp enrichment zones may be found in comets for various substances at different depths, depending on their volatility (thermochromatography). ESA

N90-20015# Centre National de la Recherche Scientifique, Saint Martin d'Heres (France). Lab. de Glaciologie et de Geophysique de l'Environnement.
SOME CONSIDERATIONS ON COHESIVE FORCES IN SUN-GRAZING COMETS
J. Klinger, S. Espinasse, and B. Schmidt *In* ESA, Physics and Mechanics of Cometary Materials Dec. 1989 p 197-200 (For primary document see N90-19989 12-90)
(Contract INSU-893709)
Copyright Avail: NTIS HC A10/MF A02; ESA Publications Div., ESTEC, Noordwijk, Netherlands, 60 Dutch guilders

Using a theory developed by Aggarwal and Oberbeck (1974) on tidal disruption of rigid bodies, an estimate is given for the internal cohesion of prominent Sun-grazers. Considering the comet as a fluffy body, requirements are set on the tensile strength of the matrix material. The resistance against tidal disruption of Sun-grazing cometary bodies is compatible with a fluffy texture of the nucleus considered as an aggregate of small particles glued together by cold ices or cold hydrocarbons. If the material properties of the surface layers of short period comets are similar to the properties of the deep layers of Sun-grazers, then achoring and sampling procedures for the Rosetta mission are predicted to have good chances of success. ESA

N90-20016# Max-Planck-Inst. fuer Kernphysik, Heidelberg (Germany, F.R.).
POSSIBLE TARGETING OF PARTICLE EMISSION BY MECHANICAL STRESS AND PENETRATION OF SUBLIMATING ICE-DUST-SURFACES
H. Kohl, E. Gruen, M. Baghul, G. Koelzer, K. Thiel, and H. Kochan (Deutsche Forschungsanstalt fuer Luft- und Raumfahrt, Cologne, Germany, F.R.) *In* ESA, Physics and Mechanics of Cometary Materials Dec. 1989 p 201-203 (For primary document see N90-19989 12-90)
Copyright Avail: NTIS HC A10/MF A02; ESA Publications Div., ESTEC, Noordwijk, Netherlands, 60 Dutch guilders

Laboratory simulation experiments showed that sublimating surfaces of ice-dust mixtures are unstable against mechanical stress. This instability may be caused by a pressure gradient within the uppermost layers of the simulated cometary surface. Different kinds of stress, such as penetration, pressure change and low velocity particle impact were examined. In every case sudden increase of dust emission activity was observed. Evidence for real comets and possible consequences for the Rosetta mission are discussed. ESA

N90-20017# Academy of Sciences, Graz (Austria). Space Research Inst.
GAS DIFFUSION IN A COMETARY CRUST
N. I. Koemle, M. Banaszewskiewicz (Polish Academy of Sciences, Warsaw.), and G. Steiner *In* ESA, Physics and Mechanics of Cometary Materials Dec. 1989 p 205-209 (For primary document see N90-19989 12-90)
(Grant P7246-GEO)
Copyright Avail: NTIS HC A10/MF A02; ESA Publications Div., ESTEC, Noordwijk, Netherlands, 60 Dutch guilders

An investigation into the outflow of vapor sublimated from the underlaying ice of a cometary nucleus through the pores of the nonvolatile dust mantle is presented. Some critical comments regarding the validity of the Knudsen diffusion formula, which is generally used for the gas outflow through a cometary dust mantle

at low densities, are made. An alternative model for the gas flow through straight capillaries based on a Monte Carlo calculation is presented. The results are compared with those given by the simple Knudsen diffusion formula, and the differences between these two approaches are discussed. The relevance of the Monte Carlo model for the interpretation of recent KOSI (comet simulation) experiments is pointed out. ESA

N90-20018# Paris VI Univ. (France). Service d'Aeronomie.
POROSITY AND ICE-DUST MIXTURES IN COMETARY PARTICLES
A. C. Levasseur-Regourd *In* ESA, Physics and Mechanics of Cometary Materials Dec. 1989 p 209-213 Sponsored by French Institut National des Sciences de l'Univers (For primary document see N90-19989 12-90)
Copyright Avail: NTIS HC A10/MF A02; ESA Publications Div., ESTEC, Noordwijk, Netherlands, 60 Dutch guilders

From numerous and consistent observations of light scattered by cometary dust, the degree of linear polarization as a function of the phase angle, and the bulk geometric albedo are accurately derived. The derived values are typical of rough pitted or aggregated textures. The decay with decreasing solar distance of interplanetary grains spiralling towards the Sun may be a clue to the thermal evolution of the coating which aggregates the cometary grains. The results indicate some break off of the clumps of grains, some loss of organic mantles by heating and the existence of various populations of dust particles. ESA

N90-20019# Max-Planck-Inst. fuer Kernphysik, Heidelberg (Germany, F.R.).
MECHANICAL PROPERTIES OF FLUFFY AGGLOMERATES CONSISTING OF CORE-MANTLE-PARTICLES
S. Pinter, J. Blum, and E. Gruen *In* ESA, Physics and Mechanics of Cometary Materials Dec. 1989 p 215-219 (For primary document see N90-19989 12-90)
Copyright Avail: NTIS HC A10/MF A02; ESA Publications Div., ESTEC, Noordwijk, Netherlands, 60 Dutch guilders

In order to simulate the coagulation of protoplanetary dust particles and the electrostatic fragmentation of interplanetary dust, a technique for producing fluffy agglomerates consisting of core-mantle-particles was developed. Spherical glass with different size distributions (less than or equal to 30 microns and 40 to 80 microns) is used as core material. N-pentacosane is chosen as mantle material. The densities of the fluffy agglomerates vary from 0.6 to 0.9 g/cu cm and their porosity is ranging from 50 to 70 percent. The compaction behavior of the samples is investigated by measuring the pressure needed for a given compaction. Measurements of the tensile strength of the particles are carried out by means of electrostatic fragmentation. The derived values for the tensile strength range from approximately 10 to the 5th power to approximately 10 to the 7th power Pa. ESA

N90-20020# Cologne Univ. (Germany, F.R.). Abt. Nuklearchemie.
DYNAMICS OF CRUST FORMATION AND DUST EMISSION OF COMET NUCLEUS ANALOGUES UNDER ISOLATION
K. Thiel, G. Koelzer, H. Kochan, L. Ratke, E. Gruen, and H. Koehl (Max-Planck-Inst. fuer Kernphysik, Heidelberg, Germany, F.R.) *In* ESA, Physics and Mechanics of Cometary Materials Dec. 1989 p 221-225 (For primary document see N90-19989 12-90)
Copyright Avail: NTIS HC A10/MF A02; ESA Publications Div., ESTEC, Noordwijk, Netherlands, 60 Dutch guilders

The lack of direct observations of near surface phenomena on cometary nuclei is one of the reasons of performing simulation experiments with various ice/dust mixtures under artificial insolation in the course of the KOSI (comet simulation) project. The objective of this project is a controlled simulation of processes that occur during the penetration of comets into the inner solar system (approximlately 1 AU). The experiments confirm that ice sublimation under insolation leads to the formation of an upper volatile free dust mantle covering a solidified dust/ice crust, both overlaying essentially unaltered material. The formation of a crust is explained by the inward diffusion and recondensation of gases. The outward gas flow gives rise to the emission of mantle particles in a size range of approximately 1 micron to approximately 1 cm. The emission process is ruled mainly by two different regimes: predominantly cohesion controlled and predominantly gravity controlled. Particle emission shows steep forward characteristics towards the light source and is consistent with the observation of dust jets of real comets. ESA

N90-20021# Army Cold Regions Research and Engineering Lab., Hanover, NH.
FIRST IMPRESSIONS OF THE COMET DRILLING PROBLEM
Malcom Mellor *In* ESA, Physics and Mechanics of Cometary Materials Dec. 1989 p 229-232 (For primary document see N90-19989 12-90)
Copyright Avail: NTIS HC A10/MF A02; ESA Publications Div., ESTEC, Noordwijk, Netherlands, 60 Dutch guilders

Preliminary impressions gained from the workshop by someone with no prior knowledge of comets or space technology are presented. Ideas on the composition and density of comet material are suggested as needing refinement in order to give the drill designer a fair chance of success. Comments on the subsurface sampling, power allocation, static force and torque for drilling, design limits for drilling rate, materials for cutting tools clearing drill cuttings, anchoring the lander, positioning the core drill, inertial drilling systems and testing are given. The influence of the drilling and sampling needs on the basic design of the lander and return capsule are called into question. A warning of possible flaws in the comments due to insufficient understanding of the problem is given. ESA

N90-20022# Washington Univ., Seattle. Dept. of Astronomy.
THE COMPOSITION OF COMETARY NUCLEI
D. E. Brownlee *In* ESA, Physics and Mechanics of Cometary Materials Dec. 1989 p 233-236 (For primary document see N90-19989 12-90)
Copyright Avail: NTIS HC A10/MF A02; ESA Publications Div., ESTEC, Noordwijk, Netherlands, 60 Dutch guilders

The most detailed information on the elemental and molecular composition of comets was obtained during the 1986 apparition of comet Halley. Although there are uncertainties in the dust/gas ratio and the abundances of several gaseous species, there is a reasonably good understanding of the major composition of the comet. The ice component is dominated by water, and the abundances of CO, H2CO, NH3 and other carbon and nitrogen bearing species are sufficiently low that the carbon and nitrogen are underabundant in the ice relative to solar proportions. These elements are abundant in the dust and it is likely that the cumulative composition of dust plus ice is a reasonably close match to solar abundances for those elements that are carried in compounds that condense at temperatures above 30K. ESA

N90-20023# Tel-Aviv Univ. (Israel). Dept. of Geophysics and Planetary Sciences.
RELEVANCE OF LABORATORY STUDIES TO COMETS
Akiva Bar-Nun *In* ESA, Physics and Mechanics of Cometary Materials Dec. 1989 p 237-239 (For primary document see N90-19989 12-90)
Copyright Avail: NTIS HC A10/MF A02; ESA Publications Div., ESTEC, Noordwijk, Netherlands, 60 Dutch guilders

The past and anticipated contributions of laboratory studies are described and evaluated. The extreme complexity of cometary phenomena and the existence of only very vague ideas on the microscopic and macroscopic structures of the nucleus make a firmer knowledge of the structure essential for the forthcoming Craf and Rosetta mission. A probable cometary material could be quite easy to drill through with the exception of the possible (rare) meteoritic debris, but very large scale laboratory drilling tests performed on all extreme cases are advised, to ensure that Rosetta returns to Earth with a deep core of cometary materials and not just a scooped surface sample. ESA

N90-20024# Technische Hochschule, Darmstadt (Germany, F.R.). Mathematisch-Naturwissenschaftlichen Fachbereiche.
NUCLEAR ACTIVITY, MORPHOLOGY, AND FAR INFRARED PROPERTIES OF SPIRAL GALAXIES Ph.D. Thesis [NUKLEARE AKTIVITAET, MORPHOLOGIE UND FERNINFRAROT-EIGENSCHAFTEN VON SPIRAL GALAXIEN]
Juergen Hellwig 1988 255 p In GERMAN
(Contracts DFG-FR-325/21-1; DFG-FR-325/21-4)
(ETN-90-95373) Avail: NTIS HC A12/MF A02

Work based on the greatest, so far obtained, sample of galaxies whose nuclear spectrum is in visible light, with the intention of getting information about stardust properties from satellite data, is presented. It is noticed that barred galaxies are more rarely spectroscopically inactive than normal spiral galaxies, and a spectrum of type starburst is presented twice as often; it is asked if starburst is the cause of Seyfert activity. Far infrared properties of spiral galaxies are well approximated by a two components model for dust temperature which allows separation of nuclear dust from others. It can be assumed that far infrared data and activity classifications from optical spectra give criteria for the identification of Seyfert galaxies and quasars. ESA

N90-20025# Tuebingen Univ. (Germany, F.R.). Astronomisches Inst.
MODEL CALCULATIONS FOR DYNAMIC DEVELOPMENT OF PLANETARY NEBULAE Thesis [MODELLRECHNUNGEN ZUR DYNAMISCHEN ENTWICKLUNG PLANETARISCHER NEBEL]
Bernd Goetting Sep. 1988 137 p In GERMAN
(ETN-90-95734) Avail: NTIS HC A07/MF A01

Several models for the description of the development of planetary nebulae are discussed from the theory of the ionization of rarefied gases and the gas dynamics. Some three-wind-models are calculated by means of a program that can simulate the dynamic development of such a nebula by unidimensional geometry with spheric symmetry. It is shown that the development of such nebulae has four phases: early ionization, recombination, and late phase. With reference to the ionized part of the nebula, the mean expansion velocity, the mean electron density and the luminous power are compared with the observed values. The assumption of the spherical symmetry is too superficial to reproduce the complex appearance forms of the planetary nebulae which may need two or three dimensional models, that allow instabilities and mass condensation to be taken into account. ESA

N90-20026# Tuebingen Univ. (Germany, F.R.).
STRUCTURAL EXPERIMENTS OF PLANETARY NEBULAE: CHARGE-COUPLED DEVICES, IMAGE REDUCTION UNDER MIDAS, INFORMATION REPRESENTATION, AND DEVELOPMENT OF AN EVOLUTION CLASSIFICATION FOR PN'S Thesis [STRUKTURUNTERSUCHUNGEN PLANETARISCHER NEBEL. CHARGE-COUPLED DEVICES, BILDREDUKTION UNTER MIDAS, INFORMATIONSDARSTELLUNG UND ENTWICKLUNG EINER EVOLUTIONSKLASSIFIKATION FUER PN'S]
Michael Bremer 1989 162 p In GERMAN Original contains color illustrations
(ETN-90-95736) Avail: NTIS HC A08/MF A01

A hydrodynamic model to explain the development of the main known Planetary Nebulae (PN) is studied. Local variations due to the wind in the chemical composition can be responsible for the formation of the ansae. Two dimensional must be included in development calculations. The properties of the wind ions must be included in two dimensional development calculations. A resonance mechanism could account for the multiaxis nebulae. To test the veracity of the model calculations, three dimensional distribution of density, temperature and velocity must be studied. ESA

N90-20027# Lawrence Livermore National Lab., CA. Inst. of Geophysics and Planetary Physics.
ACCRETION FLOWS IN HIGH MASS STAR FORMATION
Eric Keto 12 May 1989 7 p Presented at the I.A.U. Colloquium on Structure and Dynamics of the Interstellar Medium Conference, Granada, Spain, 17-26 Apr. 1989
(Contract W-7405-eng-48)
(DE90-007251; UCRL-101123; CONF-8904318-1) Avail: NTIS HC A02/MF A01

Observed and simulated images are compared of the accretion flows associated with high mass star formation in the regions G10.6 to 0.4 and DR21. As a result of the comparison, the temperature, density, and velocity fields are described. The results indicate that the G10.6 to 0.4 cloud core is strongly condensed and has approximately equal velocities in rotation and infall at its current evolutionary state. The rapid collapse and lack of rotational support suggests that significant angular momentum transfer is occurring over scales at least as large as those observed (0.5 pc). A milligauss magnetic field would have sufficient energy to supply the required braking torque of 10(exp 47) ergs. The DR21 core shows approximately spherically symmetric radial accretion with no detectable rotation. Unlike the G10.6 to 0.4 core, the DR21 core does not contain an embedded HII region. Thus this core may represent a molecular cloud condensation undergoing gravitational collapse and accretion just prior to the formation of massive stars. DOE

91 LUNAR AND PLANETARY EXPLORATION

Includes planetology; and manned and unmanned flights. For spacecraft design or space stations see *18 Spacecraft Design, Testing and Performance.*

N90-20028 Arizona Univ., Tucson.
LARGE IMPACT EVENTS AND ATMOSPHERIC EVOLUTION ON THE TERRESTRIAL PLANETS Ph.D. Thesis
David Harry Grinspoon 1989 210 p
Avail: Univ. Microfilms Order No. DA8915959

An examination is given of the effects of the collision of large asteriods and comets on the atmosphere of the Earth and Earth-like planets. The first task undertaken is the characterization of the impact rates in the inner solar system during the present time, and during the first billion years of Solar System history when the flux was changing rapidly. Once defined, these fluxes are used to model the long term cumulative effect of multiple impacts on planetary atmospheres. The implications of cometary impacts on evolution of the water and deuterium abundances on Venus are examined. The short lifetime of water on Venus suggests that the water abundance is in a quasi-steady-state balance between loss by escape and replenishment by infall. In addition, the observed deuterium-to-hydrogen ratio on Venus is consistent with a steady state and does not necessarily imply a past water excess. Results are presented of a model incorporating a stochastic cometary source and nonthermal escape of hydrogen that produces the observed water abundance and D/H ratio. A study of the effects of impact-generated dust clouds on the primitive Earth leads to the conclusion that such clouds were significant perturbers of the early climate. The Earth was shrouded by an optically-thick dust cloud for approximately equals 150 to 250 m.y. During this time the surface temperature was equal to the planetary equilibrium temperature unless significant heating by impacts or surface heat flow existed beneath the dust cloud. An admixture of a few percent of organic materials in the cloud may have significantly lowered the planetary bond albedo, thereby raising the equilibrium temperature. The epoch of continuous dust shrouding was followed by a period of stochastically intermittent dust clouds occurring at greater intervals as the early intense bombardment subsided towards the present day flux. Dissert. Abstr.

N90-20029*# Los Alamos National Lab., NM.
GETTING LUNAR ILMENITE: FROM SOILS OR ROCKS
D. T. Vaniman and G. H. Heiken 1989 15 p Presented at the Engineering, Construction and Operations for Space, Albuquerque, NM, Apr. 1990
(Contract W-7405-eng-36)

(NASA-CR-186498; NAS 1.26:186498; DE90-000538; LA-UR-89-3013; CONF-900442-2) Avail: NTIS HC A03/MF A01 CSCL 03B

Lunar soils or rocks can be mined as sources of ilmenite for producing oxygen. However, separable crystals of loose ilmenite in lunar soils are rare (less than 2 percent) and small (less than 200 microns); most ilmenite in the regolith is locked together with silicate minerals as rock fragments. Since fragmentation of rock sources must be attempted to win appreciable amounts of ilmenite (approximately 10 percent or more), selective collection of high-Ti basalt fragments larger than 1 cm for fragmentation and ilmenite beneficiation may be advantageous over extensive processing of fine lunar soil. Many alternative processing schemes for fragmenting rocks on the Moon have been proposed; one process which was tested early in the Apollo program successfully disaggregated lunar and terrestrial basalts by passive exposure to low-pressure alkali (K) vapor. This process is worthy of reinvestigation. DOE

92 SOLAR PHYSICS

Includes solar activity, solar flares, solar radiation and sunspots.

For related information see *93 Space Radiation.*

N90-20030*# Air Force Geophysics Lab., Hanscom AFB, MA.
MAX 1991. THE ACTIVE SUN: A PLAN FOR PURSUING THE STUDY OF THE ACTIVE SUN AT THE TIME OF THE NEXT MAXIMUM IN SOLAR ACTIVITY, JANUARY 1985
L. Acton 17 Aug. 1989 28 p Sponsored by NASA and the American Astronomical Society
(AF Proj. 2311)
(NASA-CR-186125; NAS 1.26:186125; AD-A211700; GL-TR-89-0218) Avail: NTIS HC A03/MF A01 CSCL 03/2

The results of the discusions of a working group for the definition of a program for the forthcoming crest of solar activity, 1990 to 1993 are presented. The MAX '91 program described are intended to achieve important scientific goals within the context of the natural solar variability. The heart of the MAX '91 program is a series of campaigns oriented towards specific scientific problems, and taking place in the solar maximum period 1990 to 1993. These campaigns will take advantage of the load-carrying capability of the Space Shuttle to fly instruments with observational capabilities very different from those of the Solar Maximum Mission. Various combinations of instruments appropriate to the specific scientific problem of a given campaign would be flown on a Shuttle sortie mission. Author

N90-20031# National Geophysical Data Center, Boulder, CO.
SOLAR-GEOPHYSICAL DATA NUMBER 541, SEPTEMBER 1989. PART 2: (COMPREHENSIVE REPORTS). DATA FOR MARCH 1989 AND MISCELLANEOUS
Helen E. Coffey, ed. Sep. 1989 185 p
(PB90-122755; SGD-541-Pt-2; ISSN-0038-0911; LC-79-640375)
Avail: NTIS HC A09/MF A01 CSCL 03B

A detailed index for 1989 is presented. Data for March 1989 includes solar flares, solar radio bursts at fixed frequencies, interplanetary solar particles and plasma, solar x ray radiation from GOES satellite, mass ejections from the sun, and active prominences and filaments. Miscellaneous data includes Meudon carte synoptique Carrington rotation 1810 December 1988, and solar ultraviolet radiation NOAA-9 May 1986 to December 1987. GRA

N90-20032# National Geophysical Data Center, Boulder, CO.
SOLAR-GEOPHYSICAL DATA NUMBER 541, SEPTEMBER 1989. PART 1: (PROMPT REPORTS). DATA FOR AUGUST, JULY 1989, AND LATE DATA
Helen E. Coffey, ed. Sep. 1989 166 p
(PB90-122763; SGD-541-Pt-1; ISSN-0038-0911; LC-79-640375)
Avail: NTIS HC A08/MF A01 CSCL 03B

A detailed index for 1989 is presented. Data for August 1989 includes IUWDS alert periods (Advance and Worldwide), solar activity indices, solar flare, solar radio emission, and Stanford mean solar magnetic field. Data for July 1989 includes solar active regions, sudden ionospheric disturbances, solar radio spectral observations, cosmic ray measurements by neutron monitor, and geomagnetic indices. Other data includes geomagnetic indices-(sudden commencements/solar flare effects May to June, 1989, and provisional values of hourly Dst March to April 1988), August 1989 special event data-plots of GOES x rays, protons, and magnetometer. GRA

N90-20033# Midwest Research Inst., Golden, CO. Solar Energy Research Inst.
SPECTRAL SOLAR RADIATION DATA BASE DOCUMENTATION
Carol J. Riordan, Daryl R. Myers, and Roland L. Hulstrom Jan. 1990 401 p
(Contract DE-AC02-83CH-10093)
(DE89-009448; SERI/TR-215-3513B) Avail: NTIS HC A18/MF A03

The Solar Energy Research Institute (SERI), Electric Power Research Institute, Florida Solar Energy Center, and Pacific Gas and Electric Company cooperated to produce a spectral solar radiation data base representing a range of atmospheric conditions. These data will help to characterize the neutral variability in the spectral (color) content to outdoor solar radiation so that the sensitivity of spectrally selective solar devices (such as photovoltaics) to these variations can be studied quantitatively. Volume 1 documents the history, approach, content, and format of the data base; Volume 2 contains graphs and field notes for each of the spectral data sets. The data reside on magnetic tape at SERI. DOE

93 SPACE RADIATION

Includes cosmic radiation; and inner and outer earth's radiation belts.

For biological effects of radiation see *52 Aerospace Medicine.* For theory see *73 Nuclear and High-Energy Physics.*

N90-20034 Pennsylvania Univ., Philadelphia.
SEARCH FOR ANISOTROPIES IN THE UNDERGROUND COSMIC RAY MUON FLUX Ph.D. Thesis
Steven Clifford Corbato 1989 184 p
Avail: Univ. Microfilms Order No. DA8922483

Over the last decade, several very and ultra high energy gamma ray detectors have reported observations of air showers exhibiting hadronic characteristics from the direction of two binary systems, Cygnus X-3 and Hercules X-1. In addition, two underground detectors, NUSEX and Soudan, observed muon signals correlated with the 4.8 hour x ray period of Cygnus X-3. Either effect, if substantiated, would imply the existence of either a previously undetected light, neutral hadron or an enhanced photon-nucleon interaction above center-of-mass energies of 100 GeV. From January, 1985 until May, 1987, enhancements were sought in the underground muon flux with a liquid scintillation detector in the Homestake Gold Mine, Lead, South Dakota. A survey of the Northern sky yielded no evidence for a time independent point source. Two other potential sources were examined. PSR 1957+20, a recently discovered radio binary composed of a millisecond pulsar and an ablated companion, is thought to represent an advanced stage in the evolution of accreting binary systems. A 2.4 standard deviation excess was observed during the orbital phase interval phi = 0.7 to 0.8. Dissert. Abstr.

N90-20035 Pennsylvania State Univ., University Park.
COSMIC RAY COMPOSITION AND MUON DECOHERENCE AT THE KNEE OF THE ALL-PARTICLE COSMIC RAY SPECTRUM Ph.D. Thesis
David Basil Kieda 1989 311 p
Avail: Univ. Microfilms Order No. DA8922532

The charge resolved cosmic ray energy spectrum provides important clues for determining the origin of these particles. High energy muons, created by primary nuclei in extensive air showers, exhibit sensitivity to the atomic mass of the progenitor nucleus. Using the Homestake Liquid Scintillation Hodoscope, the rates and multiplicity distribution of high energy muons was examined for sensitivity to primary composition in the 10(exp 14) to 10(exp 16) eV energy range. The primary composition is determined from a comparison of the measured muon multiplicity spectrum with the spectrum predicted by various primary composition models. Muon pair separation rates are examined to measure the secondary pions created in high energy nucleus-nucleus collisions. The muon pair decoherence is measured over several zenith angle ranges corresponding to various mean interaction energies. A detailed description is given of the Homestake surface array. This extensive air shower detector is used for directional calibration of the underground hodoscope as well as for simultaneously measuring the electron shower sizes associated with underground muon events. Dissert. Abstr.

N90-20036*# National Aeronautics and Space Administration. Langley Research Center, Hampton, VA.
RELIABILITY OF EQUIVALENT SPHERE MODEL IN BLOOD-FORMING ORGAN DOSE ESTIMATION
Judy L. Shinn, John W. Wilson, and John E. Nealy Washington Apr. 1990 11 p
(NASA-TM-4178; L-16733; NAS 1.15:4178) Avail: NTIS HC A03/MF A01 CSCL 03B

The radiation dose equivalents to blood-forming organs (BFO's) of the astronauts at the Martian surface due to major solar flare events are calculated using the detailed body geometry of Langley and Billings. The solar flare spectra of February 1956, November 1960, and August 1972 events are employed instead of the idealized Webber form. The detailed geometry results are compared with those based on the 5-cm sphere model which was used often in the past to approximate BFO dose or dose equivalent. Larger discrepancies are found for the later two events possibly due to the lower numbers of highly penetrating protons. It is concluded that the 5-cm sphere model is not suitable for quantitative use in connection with future NASA deep-space, long-duration mission shield design studies. Author

N90-20037# Argonne National Lab., IL.
COSMIC RAY EVENTS IN SOUDAN 2
W. W. M. Allison, G. J. Alner, I. Ambats, D. S. Ayres, L. Balka, G. D. Barr, W. L. Barrett, D. Benjamin, P. Border, and C. B. Brooks (Oxford Univ., England) et al 23 Aug. 1989 4 p Presented at the 21st International Cosmic Ray Conference, Adelaide (Australia), 6-19 Jan. 1990
(Contract W-31-109-eng-38)
(DE90-005657; ANL-HEP-CP-89-94; CONF-900129-6) Avail: NTIS HC A01/MF A01

The Soudan 2 detector is located at a depth of 2090 meters-water equivalent (mwe). About 2 million muon events have been recorded. Here we report on our plans to analyze them for comparison with expectations from atmospheric cosmic ray models. Plans and capabilities to analyze multiple muons and monopoles are also discussed. DOE

N90-20038# Argonne National Lab., IL. High Energy Physics Div.
UNDERGROUND MUONS FROM THE DIRECTION OF CYGNUS X-3
K. Johns, M. L. Marshak, E. A. Peterson, M. Shupe (Minnesota Univ., Minneapolis.), D. S. Ayres, T. H. Fields, E. N. May, and L. E. Price 11 Sep. 1989 4 p Presented at the 21st International Cosmic Ray Conference, Adelaide, Australia, 6-19 Jan. 1990
(Contract W-31-109-eng-38)
(DE90-005646; ANL-HEP-CP-89-99; CONF-900122-6) Avail: NTIS HC A01/MF A01

We report on 3.2 years live time of underground muon observations taken between 1981 and 1989 using the Soudan 1 proportional tube detector, located at a depth of 1800 m water equivalent. The post-1984 observations are consistent with our earlier data on an excess signal apparently correlated with the Cygnus X-3 orbital period. The signal-to-background ratio in the entire data sample is 1 to 3 percent, depending on phase width. DOE

N90-20039# Washington Univ., Seattle.
JACEE LONG DURATION BALLOON FLIGHTS
T. Burnett, S. Dake, J. Derrickson, W. Fountain, M. Fuki, J. Gregory, T. Hayashi, R. Holynski, J. Iwai, and W. V. Jones (Louisiana State Univ., Baton Rouge.) 1989 4 p Presented at the Workshop on Astrophysics in Antarctica, Newark, DE, 8-10 Jun. 1989
(Contract DE-AS06-88ER-40423)
(DE90-006008; CONF-8906234-1) Avail: NTIS HC A01/MF A01

JACEE balloon-borne emulsion chamber detectors are used to observe the spectra and interactions of cosmic ray protons and nuclei in the energy range 1 to 100A TeV. Experience with long duration mid-latitude balloon flights and characteristics of the detector system that make it ideal for planned Antarctic balloon flights are discussed. DOE

N90-20040*# Louisiana State Univ., Baton Rouge.
A DRIFT CHAMBER TELESCOPE FOR HIGH-Z PARTICLES
J. Isbert, H. J. Crawford, T. J. Gusick, M. Hof, K. D. Mathis, J. W. Mitchell, J. Neuhaus, M. Simon (Siegen Univ.,, Germany, F.R.), and John P. Wefel 1990 4 p Presented at the 21st International Cosmic Ray Conference, Adelaide (Australia), 6-14 Jan. 1990 Sponsored in part by NASA, DFG and BMFT Submitted for publication
(Contract DE-FG05-84ER-40147)
(NASA-CR-186497; NAS 1.26:186497; DE90-006668; CONF-900129-10) Avail: NTIS HC A01/MF A01 CSCL 03B

Drift chambers are one of the position sensing technologies used in cosmic ray balloon and satellite experiments with potential application to the next generation of detectors for space flight. A low mass TPC type drift chamber, employing 8 distinct drift regions within a single gas volume has been built, tested and used at the LBL Bevalac. From the drift time X-coordinate, spatial resolutions below 100 micron are obtained for a variety of heavy ions with selected trigger modes. The Y-coordinate is determined by pickup pads located behind the anode wire, thereby providing both X and Y coordinates from the same avalanche. Results from different timing schemes, delta-ray effects and the pickup pad resolution are presented. DOE

N90-20041# Tuebingen Univ. (Germany, F.R.). Astronomisches Inst.
EXAMINATION OF THE BACKGROUND BY HIGH ENERGY X RAY EXPERIMENT (HEXE) ON THE SPACE STATION MIR Thesis [UNTERSUCHUNG DES HINTERGRUNDES BEIM HOCHENERGIE-ROENTGENEXPERIMENT HEXE AUF DER RAUMSTATION MIR]
Bruno Mony Aug. 1988 95 p In GERMAN
(ETN-90-95735) Avail: NTIS HC A05/MF A01

The last results of the HEXE mission showed considerable declinations between the known x ray source positions and the view direction of the HEXE, which reduces the photon flux from the source, significantly in some cases. For this experiment many programs were written and tested for the reduction of data. Quick-look programs are presented that allow the data acquisition. A program was developed that can give the measurement results of the housekeeping counter by way of the catalog system and gathering in plot files. An orbit program is proposed to carry out the center correction for the arrival time of the photons and to study the influences of the geomagnetic field on the background observed by HEXE. ESA

N90-20042# Tuebingen Univ. (Germany, F.R.).
ANALYSIS OF AN OBSERVATION OF THE X RAY ASTRONOMY SATELLITE EXOSAT AT THE LOW MASS X RAY BINARY STAR SYSTEM GX5-1 Ph.D. Thesis [ANALYSE EINER BEOBACHTUNG DES ROENTGENASTRONOMIE-SATELLITEN EXOSAT AM MASSEARMEN ROENTGENDOPPELSTERNSYSTEM GX5-1]
Werner Collmar 1988 135 p In GERMAN
(ETN-90-95828) Avail: NTIS HC A07/MF A01

The first spectral analaysis of GX5-1 is presented, with the source located on the horizontal coordinate axis in the hardness-intensity diagram. It is clear that on all intensity levels two spectral components are necessary to describe the x ray spectra. The first component is always a black body spectrum with a temperature of RT = 1keV approximately. The second component is well depicted by different spectral functions. Intensity variations are caused by intensity changes of black body components, while temperature variations are few. An examination of possible optic candidates for GX5-1 showed that none of them represent a good optic picture of x ray source. EXOSAT data collected by observation of a Gamma-ray burst-source were analyzed; EXOSAT did not discover a burst, perhaps because optic flashes and Gamma-ray bursts are different pictures of a phenomenon. ESA

N90-19403*# Mankato State Coll., MN. Dept. of Mathematics, Astronomy, and Statistics.
MONTE CARLO MODELS AND ANALYSIS OF GALACTIC DISK GAMMA-RAY BURST DISTRIBUTIONS
Jon Hakkila *In* Alabama Univ., Research Reports: 1989 NASA/ASEE Summer Faculty Fellowship Program Dec. 1989 22 p (For primary document see N90-19390 12-31)
(Grant NGT-01-008-021)
Avail: NTIS HC A99/MF E06 CSCL 03B

N90-19408*# Mississippi State Univ., Mississippi State. Dept. of Physics and Astronomy.
RADIAL RESPONSE OF THE BURST AND TRANSIENT SOURCE EXPERIMENT
John Patrick Lestrade *In* Alabama Univ., Research Reports: 1989 NASA/ASEE Summer Faculty Fellowship Program Dec. 1989 29 p (For primary document see N90-19390 12-31)
(Grant NGT-01-008-021)
Avail: NTIS HC A99/MF E06 CSCL 03B

99 GENERAL

N90-20043# Technische Univ., Brunswick (Germany, F.R.). Inst. fuer Nachrichtentechnik.
[ACTIVITIES REPORT OF THE INSTITUTE FOR COMMUNICATION TECHNOLOGY] Annual Report, 1988
E.-A. Erichsen-Rua, ed. 1988 68 p In GERMAN
(ETN-90-95383) Avail: NTIS HC A04/MF A01

News relating to the institute is presented, with particular reference to the professional lives of its members, public relations with other universities, and the latest results of research activities. Articles about the work of the institute which have been published in newspapers are presented. ESA

Typical Subject Index Listing

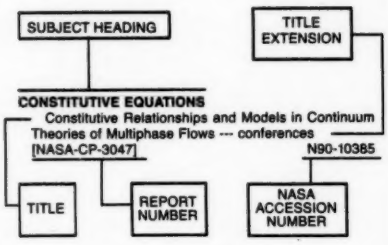

The subject heading is a key to the subject content of the document. Titles, report numbers, and accession numbers of pertinent documents are provided under each subject heading. When the title is insufficiently descriptive of the document content, a title extension has been added, separated from the title by three hyphens. The report number helps to indicate the type of document cited (e.g., NASA report, NASA translation, NASA contractor report). The NASA accession number is the number by which the document abstracts are arranged in this journal and by which the document is sold or requested. The titles, with title extensions if present, are arranged under each subject heading in ascending accession number order. The subject headings have been selected from the latest revision of the *NASA Thesaurus* (NASA SP-7064).

A

ABLATION
Laser mass spectrometric studies of high temperature superconductor ablation
[DE90-006518] N90-19585
Laser-matter interaction at intensities of 10(sup 12) W/cm(sup 2) and below
[DE90-007536] N90-19590
Characterization of ground state neutral and ion transport during laser ablation of 1:2:3 superconductors by transient optical absorption spectroscopy
[DE90-006623] N90-19878

ABNORMALITIES
Techniques for studying the effects of microgravity on model particle/cell systems N90-19424

ABSORPTION COOLING
Numerical and experimental analysis of a thin liquid film on a rotating disk related to development of a spacecraft absorption cooling system
[NASA-CR-183457] N90-19523

ABSORPTION CROSS SECTIONS
A ground state depleted laser in neodymium doped yttrium orthosilicate
[DE90-006773] N90-19586
Measurement of cross sections: New needs and possibilities
[DE90-007248] N90-19829

ABSORPTION SPECTROSCOPY
Characterization of ground state neutral and ion transport during laser ablation of 1:2:3 superconductors by transient optical absorption spectroscopy
[DE90-006623] N90-19878

ABSORPTIVITY
Background studies in gas ionizing x ray detectors N90-19399

ABSTRACTS
Proceedings of a contractors meeting on Combustion Rocket Propulsion Diagnostics of Reacting Flow
[AD-A216445] N90-19297

ABUNDANCE
Photometric analyses of abundances in dwarf spheroidal galaxies and globular clusters N90-19978

ACCELERATION (PHYSICS)
Nonlinear system vibration: The appearance of chaos
[DE90-007546] N90-19810

ACCELEROMETERS
Test component attachment effects on resonant plate pyrotechnic shock simulation
[DE90-006478] N90-19551

ACCIDENT PREVENTION
Security calculations of rip reached construction elements by means of probabilistic breaking mechanics and a Markov process
[ETN-90-95890] N90-19624

ACCIDENTS
Safety Status Report for the Ulysses mission. Book 1: Risk analysis. General purpose heat source radiosotope thermoelectric generator program
[DE90-006826] N90-19282
Safety status report for the Ulysses mission. Book 2: Risk analysis. General purpose heat source radiosotope thermoelectric generator program
[DE90-006827] N90-19283
Safety Status Report for the Ulysses mission: Summary. General purpose heat source radiosotope thermoelectric generator program
[DE90-006828] N90-19284
Safety Status Report for the Ulysses mission. Book 2: Accident analysis-appendices. General purpose heat source radioisotope thermoelectric generator program
[DE90-006830] N90-19286

ACCRETION DISKS
Nearly simultaneous optical, ultraviolet, and x ray observations of three PG quasars
[NASA-CR-186355] N90-19932

ACCUMULATIONS
Mechanical properties of fluffy agglomerates consisting of core-mantle-particles N90-20019

ACETATES
An evaluation of ethylene-vinyl acetate copolymers as desensitizers for RDX in insensitive booster compositions prepared by slurry coating technology
[MRL-TR-89-33] N90-19385

ACID RAIN
NAPAP (National Acid Precipitation Assessment Program) emissions inventory: Overview of allocation factors, 1985
[PB90-126012] N90-19679
The EURAD Model: Structure and First Results
[REPT-61] N90-19680
Development and status of the EURAD project N90-19681
Cloud parameterization in EURAD and its future development N90-19692
Initialization of EURAD. Part 1: Utilization of ECMWF analysis data N90-19695
Initialization of EURAD, part 2 N90-19696
Modelization of dry deposition in the Chemical Transport Model (CTM) of EURAD N90-19698
Estimation of the distribution of SO2 and NOX emission in Europe N90-19699
Emission data for the EURAD project N90-19700
The EURAD model in EUROTRAC N90-19701

ACOUSTIC ATTENUATION
Comparison between design and installed acoustic characteristics of NASA Lewis 9- by 15-foot low-speed wind tunnel acoustic treatment
[NASA-TP-2996] N90-19242

ACOUSTIC MEASUREMENT
Comparison between design and installed acoustic characteristics of NASA Lewis 9- by 15-foot low-speed wind tunnel acoustic treatment
[NASA-TP-2996] N90-19242
Sandia National Laboratories' new high level acoustic test facility
[DE90-006610] N90-19820

ACOUSTIC MICROSCOPES
Foundations of millimeter-wave frequency acoustic microscopy N90-19816

ACOUSTIC PROPERTIES
A note on an acoustic response during an engine nacelle flight experiment
[NASA-TM-102585] N90-19821

ACOUSTIC SCATTERING
Numerical simulation of acoustic scatter from subsurface bubble clouds
[AD-A217068] N90-19822

ACOUSTIC VELOCITY
Elastic properties of silica xerogels
[AD-A216528] N90-19366

ACOUSTICAL HOLOGRAPHY
Improved processes for ultrasonic object recognition in robotics
[ETN-90-95362] N90-19604

ACOUSTICS
A linear systems theory approach to the range-independent acoustic channel
[AD-A216551] N90-19817

ACOUSTO-OPTICS
Modeling and realization of plane acousto-optic unilateral band modulators
[ETN-90-95824] N90-19818

ACQUISITION
Rosetta/CNSR, ESA's planetary cornerstone mission N90-19990
Design and development activities on the candidate sample acquisition system for the Rosetta mission N90-19993

ACTIVE CONTROL
Modified independent modal space control of flexible structures N90-19597

ACTIVE GALAXIES
Nuclear activity, morphology, and far infrared properties of spiral galaxies
[ETN-90-95373] N90-20024

ACTUATORS
Advanced topics in structural dynamics: The maneuver of flexible spacecraft, and on-off decentralized control of flexible structures N90-19274
Dynamics and control of robot manipulators with closed-kinematic chain mechanism N90-19598

ADA (PROGRAMMING LANGUAGE)
Development of an Ada programming support environment database SEAD (Software Engineering and Ada Database) administration manual
[NASA-CR-186064] N90-19757
Object Oriented Programming Systems (OOPS) and frame representations: An investigation of programming paradigms
[NASA-CR-186084] N90-19758
Lessons learned in the transition to ADA from FORTRAN at NASA/Goddard
[NASA-CR-186458] N90-19765

ADAPTATION
Active phase and amplitude modulator
[AD-D014318] N90-19480

ADAPTIVE CONTROL
A rule-based paradigm for intelligent adaptive flight control N90-19238

ADAPTIVE FILTERS
General multidimensional scanning ratio transformation and its utilization for norm transformation of television signals
[ETN-90-96058] N90-19470

ADDITIVES
Crystallization behavior and properties of BaO-Al2O3-2SiO2 glass matrices
[NASA-CR-185209] N90-19374
Annealing group III-V compound doped silicon-germanium alloy for improved thermo-electric conversion efficiency
[NASA-CASE-NPO-17259-1-CU] N90-19884
The preparation and properties of iron doped II-VI chalcogenides
[AD-A217569] N90-19903

ADHESIVE BONDING
Viscoelastic adherend effects in adhesively bonded composite-to-composite joints N90-19594

ADHESIVES
Viscoelastic adherend effects in adhesively bonded composite-to-composite joints N90-19594

ADIABATIC FLOW
Experimental and analytical investigation of adiabatic critical water air two phase flow in small diameter tubes
[TB-88/1] N90-19540

ADSORPTION
Direct absorption receiver
[DE90-000311] N90-19667
Tunneling microscopy of submonolayer adsorbates on Si3
[AD-A216985] N90-19676

ADVANCED LAUNCH SYSTEM (STS)
Low-energy impact resistance of graphite-epoxy plates and ALS honeycomb sandwich panels N90-19405

AERIAL PHOTOGRAPHY
Possible applications of remote sensing in the preparatory phase of a land management project
[BCRS-88-19] N90-19642
Technical and administrative feasibility of microlight remote sensing applications for river boards
[BCRS-89-01] N90-19643

AERODYNAMIC CHARACTERISTICS
Computation of hypersonic unsteady viscous flow over a cylinder N90-19194
Performance of an optimized rotor blade at off-design flight conditions
[NASA-CR-4288] N90-19226
Low-speed wind-tunnel investigation of the flight dynamic characteristics of an advanced turboprop business/commuter aircraft configuration
[NASA-TP-2982] N90-19239
Output model-following control synthesis for an oblique-wing aircraft
[NASA-TM-100454] N90-19241

AERODYNAMIC COEFFICIENTS
On the evaluation of aerodynamic influence coefficients
[NLR-MP-87019-U] N90-19191

AERODYNAMIC CONFIGURATIONS
Implementation of a finite element process for the Euler equations of the gas dynamics
[PREPRINT-500] N90-19545

AERODYNAMIC HEAT TRANSFER
Heat transfer measurements from a NACA 0012 airfoil in flight and in the NASA Lewis icing research tunnel
[NASA-CR-4278] N90-19203

AERODYNAMIC HEATING
Heat transfer definitions and equations
[ESDU-89022] N90-19522
Information on the use of data items on hot structures
[ESDU-89021] N90-19611
Temperatures in plates subjected to a sudden increase in recovery temperature
[ESDU-89026] N90-19904

AERODYNAMIC LOADS
X-29A aircraft structural loads flight testing
[NASA-TM-101715] N90-19225

AERODYNAMICS
Aeronautical engineering: A continuing bibliography with indexes (supplement 249)
[NASA-SP-7037(249)] N90-19190
Three-dimensional structural analyses of reentry vehicles
[DE90-006278] N90-19291
Nonlinear mechanics of unstable plasmas as related to high altitude aerodynamics
[AD-A215126] N90-19852

AEROELASTICITY
Aeroservoelasticity
[NASA-TM-102620] N90-19227
An experimental study of the aeroelastic behaviour of two parallel interfering circular cylinders N90-19609

AERONAUTICAL ENGINEERING
Aeronautical engineering: A continuing bibliography with indexes (supplement 249)
[NASA-SP-7037(249)] N90-19190

AERONAUTICS
FY 1989 scientific and technical reports, articles, papers, and presentations
[NASA-TM-100384] N90-19916

AEROSOLS
Transport of atmospheric aerosols above the Sierra Nevada slopes
[PB90-120288] N90-19675
Atmospheric thermal blooming and beam clearing by aerosol vaporization
[DE90-006271] N90-19711
Numerical modeling of atmospheric growth processes
[REPT-70] N90-19726

AEROSPACE ENGINEERING
Remote Attitude Measurement Sensor (RAMS) N90-19271
Research Reports: 1989 NASA/ASEE Summer Faculty Fellowship Program
[NASA-CR-183837] N90-19390
FY 1989 scientific and technical reports, articles, papers, and presentations
[NASA-TM-100384] N90-19916

AEROSPACE ENVIRONMENTS
Large antenna measurement and compensation techniques N90-19263
Reflector surface distortion analysis techniques (thermal distortion analysis of antennas in space) N90-19267

AEROSPACE MEDICINE
Activities in aerospace medicine
[ETN-90-95468] N90-19739

AEROSPACE PLANES
Rapid near-optimal trajectory generation and guidance law development for single-stage-to-orbit airbreathing vehicles
[NASA-CR-186299] N90-19275

AEROSPACE SAFETY
Safety Status Report for the Ulysses mission. Book 1: Accident analysis. General purpose heat source radioisotope thermoelectric generator program
[DE90-006829] N90-19285
Aerospace Safety Advisory Panel
[NASA-TM-101748] N90-19389

AEROSPACE SCIENCES
FY 1989 scientific and technical reports, articles, papers, and presentations
[NASA-TM-100384] N90-19916
Science and technology report and outlook, 1985-1988
[PB90-115270] N90-19926

AEROSPACE SYSTEMS
Orbital servicing: Issue or answer
[AD-A217284] N90-19295

AEROTHERMODYNAMICS
Heat transfer measurements from a NACA 0012 airfoil in flight and in the NASA Lewis icing research tunnel
[NASA-CR-4278] N90-19203

AFTERBODIES
Study of the turbulent boundary layer on an afterbody
[TM-EA-8901] N90-19212

AFTERGLOWS
Ion and electron interactions at thermal and suprathermal energies
[AD-A216905] N90-19323

AGGLOMERATION
Mechanical properties of fluffy agglomerates consisting of core-mantle-particles N90-20019

AGING (MATERIALS)
Experimental results of aging and thermal effects in high-power laser diodes
[DE90-005955] N90-19573

AGING (METALLURGY)
Heat treatment study of the SiC/Ti-15-3 composite system
[NASA-TP-2970] N90-19302

AGRICULTURE
Mechanics of aeolian processes: Soil erosion and dust production N90-19410

AIR
Two-dimensional, long-pulse computer calculation of microwave-induced electron layer formation in low-pressure air
[DE90-005994] N90-19459
Sparse breakdown and statistical sneakthrough effects in low-altitude microwave propagation
[DE90-007252] N90-19473

AIR BREATHING ENGINES
Flight and driving optimization of air breathing aerodynamic space vehicle
[ETN-90-95379] N90-19246
Proceedings of a contractors meeting on Combustion Rocket Propulsion Diagnostics of Reacting Flow
[AD-A216445] N90-19297

AIR CONDUCTIVITY
Conductive polymers of transition-metal complexes coordinated by a Diamino-Dichalcogen-Benzene compound
[AD-D014326] N90-19360

AIR COOLING
The utilization of an infrared imaging system as a cooling slot blockage detector in the inspection of a transpiration cooled nozzle
[NASA-TM-102608] N90-19555

AIR CURRENTS
Characterization of thunderstorm induced Maxwell current densities in the middle atmosphere N90-19391

AIR DEFENSE
Limitations of the conventional role of the B-1B in the European theater
[AD-A217285] N90-19230

AIR LAND INTERACTIONS
A PBL-radiation model for application to regional numerical weather prediction N90-19394

AIR NAVIGATION
Interoperability issues in the use of satellite-based navigation systems for civil aviation purposes
[AD-A217279] N90-19223

AIR POLLUTION
Transport of atmospheric aerosols above the Sierra Nevada slopes
[PB90-120288] N90-19675
Development of an atmospheric diffusion model in fog (1). Literature review of scavenging process by precipitation
[DE89-782318] N90-19676
Chemical composition of precipitation and wet/dry deposition of sulfur compounds around the coastal area
[DE89-782324] N90-19677
Proceedings of the 2nd United States/USSR Symposium on Air Pollution Effects on Vegetation Including Forest Ecosystems
[PB90-127119] N90-19678
The RADM 2 gas-phase chemical mechanism N90-19684
Simulation of the propagation of radiactive substances from the example of Chernobyl (USSR) N90-19685
Implementation of the RADM/EURAD models on the great calculation system of the Juelich KFA N90-19687
GeoNet 88: Calculation connection system concept for the EURAD project N90-19688
Validation of the EURAD cloud modules N90-19693
Estimation of the distribution of SO2 and NOX emission in Europe N90-19699
Emission data for the EURAD project N90-19700
The EURAD model in EUROTRAC N90-19701
Predicting effects of global climate change on reservoir water quality and fish habitat
[DE90-003674] N90-19704

AIR TRAFFIC CONTROL
Symposium on air traffic control training for tomorrow's technology
[PB90-127325] N90-19216
Interoperability issues in the use of satellite-based navigation systems for civil aviation purposes
[AD-A217279] N90-19223
Operational evaluation of initial data link air traffic control services, volume 1
[DOT/FAA/CT-90/1-VOL-1] N90-19472

AIR TRAFFIC CONTROLLERS (PERSONNEL)
Symposium on air traffic control training for tomorrow's technology
[PB90-127325] N90-19216

AIR WATER INTERACTIONS
Drifting buoy data from Western Tropical Pacific for the period February 1, 1986 through February 28, 1989
[PB90-113978] N90-19732

AIRCRAFT CONSTRUCTION MATERIALS
Evaluation and choice algorithms of cost optimal prepreg-application processes: Production of strongly charged plane parts made of fiber reinforced plastics
[ETN-90-95895] N90-19313

AIRCRAFT CONTROL
Unsteady aerodynamics of delta wings performing maneuvers to high angle of attack N90-19196

AIRCRAFT DESIGN
Analysis and design of symmetrical airfoils
[PD-CF-8943] N90-19213
Flow simulation for aircraft
[NLR-MP-87082-U] N90-19543
A note on an acoustic response during an engine nacelle flight experiment
[NASA-TM-102585] N90-19821

AIRCRAFT ENGINES
In-flight evaluations of turbine fuel extenders
[DOT/FAA/CT-89/33] N90-19387

AIRCRAFT MANEUVERS
Unsteady aerodynamics of delta wings performing maneuvers to high angle of attack N90-19196
A study of flows over highly-swept wings designed for maneuver at supersonic speeds
[AD-A216837] N90-19202

AIRCRAFT NOISE
Comparison between design and installed acoustic characteristics of NASA Lewis 9- by 15-foot low-speed wind tunnel acoustic treatment
[NASA-TP-2996] N90-19242

AIRCRAFT PERFORMANCE
Development of a preliminary high-angle-of-attack nose-down pitch control requirement for high-performance aircraft
[NASA-TM-101684] N90-19206

AIRCRAFT PILOTS
Pilot candidate selection
[AD-A217296] N90-19742

AIRCRAFT STRUCTURES
X-29A aircraft structural loads flight testing
[NASA-TM-101715] N90-19225

A new method for measuring the transmissivity of aircraft transparencies
[AD-A216953] N90-19842

AIRCRAFT TIRES
Modeling and analysis of the space shuttle nose-gear tire with semianalytic finite elements
[NASA-TP-2977] N90-19595

AIRFOILS
Calculation of excrescence drag magnification due to pressure gradient at high subsonic speeds
[ESDU-87004] N90-19195
Heat transfer measurements from a NACA 0012 airfoil in flight and in the NASA Lewis icing research tunnel
[NASA-CR-4278] N90-19203
Analysis and design of symmetrical airfoils
[PD-CF-8943] N90-19213

AIRFRAMES
Static strength and damage tolerance tests on the Fokker 100 airframe
[NLR-MP-88023-U] N90-19228

ALGEBRA
Uniqueness of closure of the constraint algebra for quantum gravity
[DE90-610476] N90-19712
Superconformal algebra on meromorphic vector fields with three poles on super-Riemann sphere
[DE90-610423] N90-19796
Banach C*-algebras not containing a subspace isomorphic to C(sub 0)
[DE90-610428] N90-19798

ALGORITHMS
A streamwise upwind algorithm applied to vortical flow over a delta wing
[NASA-TM-102225] N90-19201
Heli/SITAN: A terrain referenced navigation algorithm for helicopters
[DE90-005193] N90-19217
Remote Attitude Measurement Sensor (RAMS) N90-19271
Evaluation and choice algorithms of cost optimal prepreg-application processes: Production of strongly charged plane parts made of fiber reinforced plastics
[ETN-90-95895] N90-19313
Hydrogen assay foil counting system
[DE90-007415] N90-19332
Investigations into a new algorithm for calculating H infinity optimal controllers N90-19406
A vectorized algorithm for 3D dynamics of a tethered satellite N90-19423
Costas loop lock detection in the advanced receiver N90-19441
Memory management in traceback Viterbi decoders N90-19443
Some easily analyzable convolutional codes N90-19444
Fast transform decoding of nonsystematic Reed-Solomon codes N90-19447
Application of adaptive least-squares algorithm to multi-element array signal reconstruction N90-19448
Signal processing
[DE90-006904] N90-19464
Parallel distributed networks for image smoothing and segmentation in analog VSLI
[AD-A216780] N90-19491
A high resolution automatic image measuring system
[WISS-ARB-VERMESSUNGSWESEN-154] N90-19559
Selection of optimal textural features for maximum likelihood image classification
[DE90-006901] N90-19638
Automated visibility and cloud cover measurements with a solid-state imaging system
[AD-A216906] N90-19724
Random access transmission algorithms for data local area networks
[AD-A216443] N90-19761
An optimized algorithm for solving the nodal diffusion method on shared memory multiprocessors
[DE90-002703] N90-19762
Object detection and amplitude estimation based on maximum a posteriori reconstructions
[DE90-007511] N90-19770
Theory and applications of belief functions
[AD-A217092] N90-19774
Adaptive, asynchronous stochastic global optimization algorithms for sequential and parallel computation
[AD-A217093] N90-19775
Parallel algorithms for boundary value problems
[NASA-TM-102498] N90-19783
On the parallel efficiency of the Frederickson-McBryan multigrid
[NASA-CR-181999] N90-19791
A tensor product B-spline method for numerical grid generation
[DE90-005979] N90-19792
Hierarchical basis preconditioners for second order elliptic problems in three dimensions
[DE90-005980] N90-19793
Convergence properties of iterative algorithms for solving the nodal diffusion equations
[DE89-016859] N90-19804
Algorithms for calorimeter simulation with parameterized showers by example of H1 detectors
[MPI-PAE/EXP.EL-200] N90-19828
Thermal infrared scene simulation
[DE90-006900] N90-19845
Visibility problems in numerical models of terrain
[INPE-4921-TDL/382] N90-19919

ALIGNMENT
Drag reduction by longitudinal riblets on the surface of a streamwise aligned body of revolution
[MPIS-MITT-92] N90-19210
Development and testing of a universally implementable recording aligning system
[SER-C-349] N90-19716

ALKALINITY
Conductive polymers of transition-metal complexes coordinated by a Diamino-Dichalcogen-Benzene compound
[AD-D014326] N90-19360

ALLOCATIONS
Science requirements for passive microwave sensors on earth science geostationary platforms N90-19251

ALLUVIUM
Geochemical survey on faults overland with alluvial deposits, part 1. Application for the Neodani and the Atera faults survey
[DE89-782326] N90-19707

ALPHA PARTICLES
Marginal test and analysis of DRAM with masked alpha radiation
[RB-4180] N90-19754

ALPINE METEOROLOGY
Simulation of a weather situation with high ozone concentrations during ALPEX N90-19686

ALTERNATING CURRENT
Ac loss measurements of two multifilamentary NbTi composite strands
[DE90-005388] N90-19304
Critical current density and transition temperature measurements of Y-Ba-Cu-O rods
[AD-A216695] N90-19875

ALUMINUM
Nanolayer reactions in aluminum-metal interfaces
[DE90-004955] N90-19342
Glancing angle XAFS (X ray Absorption Fine Structure) and x ray reflectivity studies of transition-metal/aluminum interfaces
[DE90-005575] N90-19353
Creep behavior of alloys based on TiAl containing TiB2 and TiN particulates
[DE90-006489] N90-19355
Origin and effect of pores in aluminum welded joints
[REPT-87M/43/05720/SCP/GRF] N90-19620

ALUMINUM ALLOYS
Optimizing superplastic response in navalite, a lithium containing aluminum-magnesium alloy
[AD-A216552] N90-19346
Deformation and fracture of TiAl + W at elevated temperatures
[DE90-006490] N90-19356
Liquid oxygen LOX compatibility evaluations of aluminum lithium (Al-Li) alloys: Investigation of the Alcoa 2090 and MMC weldalite 049 alloys N90-19398
Evaluation of the response of aluminum alloys to single and multiple particle impacts
[DE90-003689] N90-19626

ALUMINUM CARBIDES
Fabrication, phase transformation studies, and characterization of SiC-AlN-Al2OC ceramics
[DE90-006591] N90-19371

ALUMINUM COMPOUNDS
Activation of methane by transition metal-substituted aluminophosphate molecular sieves
[DE90-005663] N90-19331

ALUMINUM GALLIUM ARSENIDES
Low threshold current implanted-planar-buried-heterostructure, graded-index, separate-confinement-heterostructure GaAs-AlGaAs laser
[DE90-002579] N90-19572

ALUMINUM NITRIDES
Fabrication, phase transformation studies, and characterization of SiC-AlN-Al2OC ceramics
[DE90-006591] N90-19371

ALUMINUM OXIDES
Preparation and characterization of alumina films prepared by a novel spray pyrolysis method
[AD-A217570] N90-19339

AMAZON REGION (SOUTH AMERICA)
Availability of multitemporal LANDSAT data accompanying the variation of water surfaces in the program area of Careiro PDRI/AM
[INPE-4896-PRE/1496] N90-19634
An observational study of squall lines in the Amazon
[INPE-4865-TDL/376] N90-19723

AMMUNITION
Jam resistant fluid power actuator for ballistic-damage tolerant redundant cylinder assemblies
[AD-D014360] N90-19600

AMORPHOUS MATERIALS
International conference on Surface Modification of Metals by Ion Beams
[AD-A215872] N90-19345
Optical studies of dynamical processes in disordered materials
[DE90-007080] N90-19372
Evolution of ices and carbonaceous materials in the laboratory and in comets N90-19998

AMPLIFIERS
Results of the PALADIN experiment
[DE90-006776] N90-19578

AMPLITUDE MODULATION
Active phase and amplitude modulator
[AD-D014318] N90-19480

AMPLITUDES
Effects of amplitude distortions and IF equalization on satellite communication system bit-error rate performance
[NASA-TM-102415] N90-19454

ANALOG TO DIGITAL CONVERTERS
A digitally controlled system for effecting and presenting a selected electrical resistance
[NASA-CASE-MFS-29149-1] N90-19492

ANALOGS
Laboratory studies of cometary ice analogues N90-19997
Stable isotope studies of cometary analogue materials N90-20001
Crustal strength of different model comet materials N90-20003
CO2 depth profiles in cometary model substances of KOSI N90-20014
Dynamics of crust formation and dust emission of comet nucleus analogues under isolation N90-20020

ANALYSIS (MATHEMATICS)
Rule matrices, degree vectors, and preimages for cellular automata
[DE90-007492] N90-19805

ANALYZERS
FOMA: A Fast Optical Multichannel Analyzer
[DE90-004093] N90-19839

ANCHORS (FASTENERS)
Design and development activities on the candidate sample acquisition system for the Rosetta mission N90-19993

ANGLE OF ATTACK
Unsteady aerodynamics of delta wings performing maneuvers to high angle of attack N90-19196
Development of a preliminary high-angle-of-attack nose-down pitch control requirement for high-performance aircraft
[NASA-TM-101684] N90-19206

ANGULAR MOMENTUM
Accretion flows in high mass star formation
[DE90-007251] N90-20027

ANISOTROPIC SHELLS
Modeling and analysis of the space shuttle nose-gear tire with semianalytic finite elements
[NASA-TP-2977] N90-19595

ANISOTROPY
Integrated optics anisotropic waveguides and devices
[AD-A217064] N90-19849
The COBE cosmic 3 K anisotropy experiment: A gravity wave and cosmic string probe N90-19959
Search for anisotropies in the underground cosmic ray muon flux N90-20034

ANNEALING
Effect of electron-excitation on radiation damage in ion-irradiated FCC metals
[DE90-719537] N90-19344
Silicon carbide semiconductor device fabrication and characterization
[NASA-CR-186354] N90-19873

ANNIHILATION REACTIONS
Dislocation annihilation mechanism for the formation of dislocation free zone at a crack tip
[DE90-610552] N90-19615
The effects of cold dark matter on Big Bang nucleosynthesis N90-19749

ANODES
Anode plasma formation as a possible mechanism for an electrical stress limit in cold cathode diodes
[DE90-007503] N90-19516

ANTENNA ARRAYS
An investigation of the transfer of monopulse tracking between two coherent point sources
[AD-A217007] N90-19457
ANTENNA DESIGN
Earth Science Geostationary Platform Technology
[NASA-CP-3040] N90-19249
Large space antenna concepts for ESGP N90-19253
Large-diameter geostationary millimeter wavelength antenna concept N90-19254
Design of a low-frequency (5-20 GHz), 15-meter-diameter passive radiometer for geostationary earth science platforms N90-19255
Structures for remotely deployable precision antennas N90-19256
Unfurlable, continuous-surface reflector concept N90-19257
Advances in large inflatable reflectors N90-19258
Millimeter radiometer system technology N90-19260
Synthetic Aperture Interferometric Radiometer (SAIR) N90-19261
Rain radars for earth science geostationary platforms: Some possibilities N90-19262
Large antenna measurement and compensation techniques N90-19263
A comparison of reflector antenna designs for wide-angle scanning N90-19264
Arrays for space applications N90-19265
Conjugate field approaches for active array compensation N90-19266
Reflector surface distortion analysis techniques (thermal distortion analysis of antennas in space) N90-19267
Antennas for 20/30 GHz and beyond N90-19269
The 32-GHz performance of the DSS-14 70-meter antenna: 1989 configuration N90-19452
ANTENNA FEEDS
A comparison of reflector antenna designs for wide-angle scanning N90-19264
Dual frequency launcher for circularly polarized antenna
[AD-D014361] N90-19456
ANTENNA RADIATION PATTERNS
Conjugate field approaches for active array compensation N90-19266
Mesh surfaces for reflector applications N90-19268
An investigation of the transfer of monopulse tracking between two coherent point sources
[AD-A217007] N90-19457
ANTENNAS
Disturbance torque rejection properties of the NASA/JPL 70-meter antenna axis servos N90-19450
An investigation of the transfer of monopulse tracking between two coherent point sources
[AD-A217007] N90-19457
Single antenna interferometry
[DE90-008120] N90-19474
Lightning protection apparatus for RF equipment and the like
[AD-D014336] N90-19483
ANTIPARTICLES
The effects of cold dark matter on Big Bang nucleosynthesis N90-19749
ANTIPROTONS
The inverse-square law and quantum gravity N90-19949
ANTISHIP MISSILES
Suboptimal period design for a maneuvering missile to evade tracking filters N90-19479
APERTURES
Radar transponder antenna pattern analysis for the space shuttle N90-19414
Green's functions for a theoretical model of an aperture fed stacked-patch microstrip antenna
[AD-A216280] N90-19455
APPLICATION SPECIFIC INTEGRATED CIRCUITS
VLSI implementation of moment invariants for automated inspection
[DE90-005318] N90-19493
APPROACH
Rosetta/CNSR, ESA's planetary cornerstone mission N90-19990
APPROACH INDICATORS
Tracking performance of the AN/GPN-22 precision approach radar
[FEL-1988-34] N90-19467
APPROXIMATION
Iterative procedures for space shuttle main engine performance models N90-19416
Networks and the best approximation property
[AD-A216712] N90-19778
The 0-1 multiknapsack problem: Heuristic and reduction methods
[INPE-4894-PRE/1495] N90-19782
On the approximative normal values of multivalued operators in topological vector space
[DE90-610430] N90-19800
ARC DISCHARGES
Plasma centrifuge with vacuum arc discharge applied to the separation of stable isotopes
[INPE-4925-TDL/385] N90-19854
ARC WELDING
A new model for hydrogen absorption in welds
[AD-A216951] N90-19347
Trailer shield assembly for a welding torch
[NASA-CASE-MFS-29260-1] N90-19602
ARCHITECTURE (COMPUTERS)
Flight crew aiding for recovery from subsystem failures
[NASA-CR-181905] N90-19741
An approach to elemental task learning
[DE90-006614] N90-19745
Design and architecture of fourth and fifth generation software engineering environments
[ETN-90-95365] N90-19752
A virtual zero-time, monolithic systolic sorting array
[DE90-001000] N90-19753
Flosolver Mk1B: An eight processor parallel machine
[PD-CF-8941] N90-19755
Random access transmission algorithms for data local area networks
[AD-A216443] N90-19761
Image manipulation in the SIGGRAPH Interactive Proceedings
[DE90-007542] N90-19771
ARTIFICIAL INTELLIGENCE
Artificial intelligence issues related to automated computing operations N90-19404
Flight crew aiding for recovery from subsystem failures
[NASA-CR-181905] N90-19741
An approach to elemental task learning
[DE90-006614] N90-19745
High-level connectionist models
[AD-A216581] N90-19751
Parallel neural net path-planner on hypercube and transputer
[DE90-006324] N90-19777
Hybrid neural network and rule-based pattern recognition system capable of self-modification
[DE90-007482] N90-19779
ARTIFICIAL SATELLITES
Present and future risk of satellite and manned platforms collisions with other space objects and particles on earth orbits
[R-8841] N90-19287
Present and future risk of collision of satellites and manned platforms with other space objects and particles in terrestrial orbit
[R-8840] N90-19288
Low-cost small satellites for astrophysical missions
[DE90-007625] N90-19293
ASSEMBLY LANGUAGE
Yaw rate control of an air bearing vehicle N90-19420
ASTROMETRY
Photon statistical limitations for daytime optical tracking N90-19442
Optical interferometers for tests of relativistic gravity in space N90-19967
ASTRONAUT TRAINING
Working on the moon: The Apollo experience
[DE90-003662] N90-19744
ASTRONAUTICS
FY 1989 scientific and technical reports, articles, papers, and presentations
[NASA-TM-100384] N90-19916
ASTRONAUTS
Reliability of equivalent sphere model in blood-forming organ dose estimation
[NASA-TM-4178] N90-20036
ASTRONOMICAL MODELS
The Moon has set
[REPT-89-07] N90-19933
Cosmic string in compactified gauge theory
[DE90-741463] N90-19988
Physics and Mechanics of Cometary Materials
[ESA-SP-302] N90-19989
Physical models of cometary nuclei: A review N90-19991
ASTRONOMICAL OBSERVATORIES
Optical interferometer in space N90-19953
ASTRONOMICAL PHOTOGRAPHY
Information reconstruction from speckle interferograms
[ETN-90-95918] N90-19939
ASTRONOMICAL SPECTROSCOPY
Infrared heterodyne spectroscopy of polyatomic molecules in circumstellar envelopes N90-19980
O-star parameters from line profiles of wind-blanketed model atmospheres N90-19982
ASTRONOMY
Speckle interferometry for high resolution pictures of astronomical objects
[ETN-90-95827] N90-19936
MAX 1991. The active sun: A plan for pursuing the study of the active sun at the time of the next maximum in solar activity, January 1985
[NASA-CR-186125] N90-20030
ASTROPHYSICS
Low-cost small satellites for astrophysical missions
[DE90-007625] N90-19293
Measurement of cross sections: New needs and possibilities
[DE90-007248] N90-19829
Experimental and theoretical high energy physics
[DE90-005974] N90-19834
Astronomy and astrophysics
[REPT-33/89] N90-19938
Pulsar timing and gravitational waves N90-19955
LAGEOS 3 and the gravitomagnetic field N90-19961
Very high energy gamma ray astrophysics
[DE90-006645] N90-19983
Nuclear interactions of high energy heavy ions and applications in astrophysics
[DE90-006691] N90-19984
The Advanced Composition Explorer
[DE90-006522] N90-19987
ATMOSPHERIC BOUNDARY LAYER
Wind tunnel design of heat island turbulent boundary layer
[IHW-ET/50] N90-19542
Transport of atmospheric aerosols above the Sierra Nevada slopes
[PB90-120288] N90-19675
Modelization of dry deposition in the Chemical Transport Model (CTM) of EURAD N90-19698
ATMOSPHERIC CHEMISTRY
The EURAD Model: Structure and First Results
[REPT-61] N90-19680
ATMOSPHERIC CIRCULATION
NAPAP (National Acid Precipitation Assessment Program) emissions inventory: Overview of allocation factors, 1985
[PB90-126012] N90-19679
An observational study of squall lines in the Amazon
[INPE-4865-TDL/376] N90-19723
Wind conditions near the ground in Federal Republic of Germany
[ISBN-3-88148-248-2] N90-19727
ATMOSPHERIC COMPOSITION
The role of clouds in the photochemistry of the background troposphere N90-19694
Emission data for the EURAD project N90-19700
Ultraviolet observations of the atmosphere of Io and the plasma torus N90-19929
ATMOSPHERIC DIFFUSION
Development of an atmospheric diffusion model in fog (1). Literature review of scavenging process by precipitation
[DE89-782318] N90-19676
Modelization of dry deposition in the Chemical Transport Model (CTM) of EURAD N90-19698
ATMOSPHERIC GENERAL CIRCULATION MODELS
Regional climate change predictions from the Goddard Institute for Space Studies high resolution GCM
[NASA-CR-186375] N90-19725
ATMOSPHERIC MODELS
The mesoscale meteorological model MM4 and its modifications for EURAD N90-19682
The Chemical Transfer Model (CTM) of EURAD: Development status N90-19683
The RADM 2 gas-phase chemical mechanism N90-19684
Simulation of the propagation of radiactive substances from the example of Chernobyl (USSR) N90-19685
Simulation of a weather situation with high ozone concentrations during ALPEX N90-19686
Implementation of the RADM/EURAD models on the great calculation system of the Juelich KFA N90-19687
GeoNet 88: Calculation connection system concept for the EURAD project N90-19688
Comparison of a 6-layer and a 15-layer version of the Chemical Transfer Model (CTM) N90-19689
Control of the RADM chemistry mechanism of the gas phase N90-19690
On the question of spray effects N90-19691
Cloud parameterization in EURAD and its future development N90-19692
Validation of the EURAD cloud modules N90-19693
Initialization of EURAD. Part 1: Utilization of ECMWF analysis data N90-19695
Initialization of EURAD, part 2 N90-19696
Boundary layer parameterization in CTM and MM4 N90-19697
Modelization of dry deposition in the Chemical Transport Model (CTM) of EURAD N90-19698
Estimation of the distribution of SO2 and NOX emission in Europe N90-19699
Emission data for the EURAD project N90-19700
The EURAD model in EUROTRAC N90-19701

Simulation of global Kr-85 and (14)CO2 distribution by means of a time-dependent, two dimensional model of the atmosphere
[ETN-90-95376] N90-19702
Synoptic-scale forcing of the low-level jet in developing baroclinic waves N90-19717
Exploiting surface observations of cloudiness for globalscale nephanalyses N90-19719
The atmospheric energy cycle of stationary and transient waves
[ISSN-0069-5882] N90-19728

ATMOSPHERIC PHYSICS
Active probing of space plasmas
[AD-A216867] N90-19855

ATMOSPHERIC RADIATION
On the question of spray effects N90-19691
Atmospheric Radiation Measurement Program plan
[DE90-006349] N90-19705

ATMOSPHERIC REFRACTION
Visibility problems in numerical models of terrain
[INPE-4921-TDL/382] N90-19919
Information reconstruction from speckle interferograms
[ETN-90-95918] N90-19939
Tropospheric monitoring technology for gravity wave experiments N90-19971

ATMOSPHERIC TEMPERATURE
Ionospheric heating with oblique waves. Volume 1: Electron density perturbations
[AD-A216260] N90-19709

ATOMIC CLOCKS
A review of atomic clock technology, the performance capability of present spaceborne and terrestrial atomic clocks, and a look toward the future N90-19972

ATOMIC STRUCTURE
Exchange and correlation effects in the Visscher-Falicov model for metal intercalated graphite
[DE90-610553] N90-19349
Supercomputer applications for materials science: Ordering effects of hydrogen in palladium
[DE90-004664] N90-19870
Band electronic structures and crystal packing forces
[DE90-007669] N90-19898

ATOMIC THEORY
A review of atomic clock technology, the performance capability of present spaceborne and terrestrial atomic clocks, and a look toward the future N90-19972

ATOMIZING
Simulation of thermal dynamics of a vaporizing coal-water droplet in a combustor
[DE90-005356] N90-19317
Assessment of research needs for laser technologies applied to advanced spectroscopic methods
[DE90-007402] N90-19588

ATTITUDE (INCLINATION)
Remote Attitude Measurement Sensor (RAMS)
N90-19271
Determination of the implementation of the 3-axis attitude motion simulator digital position controller
N90-19409

AUDIO SIGNALS
A waveform capture and storage unit and its use for investigating disturbances on digital transmission links
[BBC-RD-1989/17] N90-19478

AUGMENTATION
Muzzle shunt augmentation of conventional railguns
[DE90-007505] N90-19248
Multibody modeling and verification N90-19422

AURORAS
Active probing of space plasmas
[AD-A216867] N90-19855

AUSFORMING
Austempered ductile iron data base: A cooperative program between industry and the Trade Adjustment Assistance Program of the Department of Commerce
[PB90-115569] N90-19343

AUSTENITE
Austempered ductile iron data base: A cooperative program between industry and the Trade Adjustment Assistance Program of the Department of Commerce
[PB90-115569] N90-19343

AUSTENITIC STAINLESS STEELS
Evaluation of radiation-induced sensitization using electrochemical potentiokinetic reactivation technique for austenitic stainless steels
[DE90-002708] N90-19352

AUTOCORRELATION
Spanwise measurements of vertical components of atmospheric turbulence
[NASA-TP-2963] N90-19718

AUTOMATA THEORY
Rule matrices, degree vectors, and preimages for cellular automata
[DE90-007492] N90-19805

AUTOMATIC CONTROL
A high resolution automatic image measuring system
[WISS-ARB-VERMESSUNGSWESEN-154] N90-19559

AUTONOMIC NERVOUS SYSTEM
Neurocontrol systems and wing-fluid interactions underlying dragonfly flight N90-19240

AVIONICS
Marshall Avionics Testbed System (MAST)
N90-19417

AXIAL COMPRESSION LOADS
Compressive strength of synthetic comet nucleus samples N90-20006

AXIAL STRESS
Steady state temperatures and thermal stresses in a spherical or cylindrical laminated shell
[ESDU-89027] N90-19612

AXISYMMETRIC FLOW
Separation bubbles at high Reynolds number: Measurement and computation
[CUED/A-AERO/15] N90-19525

AZOLES
Second-generation ordered polymers
[AD-A216126] N90-19365

B

BACKGROUND RADIATION
Sources of gravitational waves N90-19942
The pregalactic cosmic gravitational wave background
N90-19945
The space microwave interferometer and the search for cosmic background gravitational wave radiation
N90-19952
The COBE cosmic 3 K anisotropy experiment: A gravity wave and cosmic string probe N90-19959
Examination of the background by High Energy X ray Experiment (HEXE) on the space station MIR
[ETN-90-95735] N90-20041

BACKWARD FACING STEPS
Separation bubbles at high Reynolds number: Measurement and computation
[CUED/A-AERO/15] N90-19525

BALL BEARINGS
A parametric heat transfer study for cryogenic ball bearings in SSME HPOTP N90-19397

BALLISTICS
External flow computations for a finned 60mm ramjet in steady supersonic flight
[AD-A216998] N90-19233
Computational fluid dynamics method for low Reynolds number flow in a precessing/spinning, liquid filled cylinder with rounded endcaps
[AD-A216997] N90-19531

BALLOON FLIGHT
JACEE long duration balloon flights
[DE90-006008] N90-20039

BANACH SPACE
Banach C*-algebras not containing a subspace isomorphic to C(sub 0)
[DE90-610428] N90-19798
Projection-iteration methods for solving nonlinear operator equations
[DE90-610433] N90-19801
Classical mechanics on superspace
[DE90-608907] N90-19906

BANDPASS FILTERS
Transmission and reflection studies of thin films in the vacuum ultraviolet N90-19412
The effects of sinusoidal interference on the second-order carrier tracking loop preceded by a bandpass limiter in the Block 4 receiver N90-19449

BANDWIDTH
The influence of gamma-radiation on the bandwidth of optical fibres and the reduction of the induced attenuation by bleaching and hardening the fibre
[FEL-1988-62] N90-19846

BARIUM
Low temperature elastic and dielectric properties of incommensurate barium sodium niobate
[AD-A216969] N90-19815

BARIUM OXIDES
Laser surface interactions of high-(Tc) superconductors
[DE90-006894] N90-19587
Superconductivity in Ba(1-x)BiO3
[DE90-003781] N90-19869

BAROCLINIC INSTABILITY
Cyclogeneses and extratropical cyclones in the south-southeast region of Brazil and its influence in time
[INPE-4812-TDL/359] N90-19722
Evolution of finite amplitude baroclinic waves in the atmosphere and ocean
[INPE-4752-TDL/346] N90-19733

BAROCLINIC WAVES
Synoptic-scale forcing of the low-level jet in developing baroclinic waves N90-19717
The atmospheric energy cycle of stationary and transient waves
[ISSN-0069-5882] N90-19728
Evolution of finite amplitude baroclinic waves in the atmosphere and ocean
[INPE-4752-TDL/346] N90-19733

BAROCLINITY
Cyclogeneses and extratropical cyclones in the south-southeast region of Brazil and its influence in time
[INPE-4812-TDL/359] N90-19722
Evolution of finite amplitude baroclinic waves in the atmosphere and ocean
[INPE-4752-TDL/346] N90-19733

BARRED GALAXIES
Nuclear activity, morphology, and far infrared properties of spiral galaxies
[ETN-90-95373] N90-20024

BARRIER LAYERS
Influence of heat treating on the mechanical values and the stability of heat barrier coatings
[ETN-90-95902] N90-19375
Field effect transistor structures based on strain induced polarization charges
[DE90-007247] N90-19515
Effect of barrier layers in burn-through experiments with 351-nm laser illumination
[DE90-006806] N90-19577

BARYONS
The effects of cold dark matter on Big Bang nucleosynthesis N90-19749

BASALT
Stored mafic/ultramafic crust and early Archean mantle depletion
[NASA-CR-186460] N90-19715

BCS THEORY
BCS (Bardeen-Cooper-Schrieffer) primer: A guide to computational methods in superconductivity theory
[AD-A216393] N90-19874

BEADS
Heat sink effects on weld bead: VPPA process
N90-19418

BEAM INJECTION
Negative ion surface plasma source development for plasma trap injectors in Novosibirsk
[DE90-006082] N90-19856

BEAM SPLITTERS
Narrow-bandwidth unstable laser resonator
[AD-D014362] N90-19568
Literature file on fast kickers and SEPTA: Components for deflection and separation of particle beams
[LINO-162] N90-19924

BEAM SWITCHING
The 32-GHz performance of the DSS-14 70-meter antenna: 1989 configuration N90-19452
Dynamics of plasma injection along magnetic field lines in the PBFA 2 (Particle Beam Fusion Accelerator 2) plasma opening switch
[DE90-006751] N90-19862

BEAMS (RADIATION)
Optically tunable gratings for optical interconnects
[AD-A216978] N90-19844

BEAMS (SUPPORTS)
Plastic bending tests of cold-formed rectangular hollow sections
[PB90-124611] N90-19613
Modal analysis of nonprismatic beams: Uniform segment method
[AD-A216952] N90-19614
Development of finished beam and shell elements from engineering models for structures under high inelastic deformations
[ETN-90-95377] N90-19619

BENDING
Plastic bending tests of cold-formed rectangular hollow sections
[PB90-124611] N90-19613

BERYLLIUM
High-purity beryllium foils
[DE90-006408] N90-19348
The optical properties of beryllium
[DE90-006372] N90-19848

BIBLIOGRAPHIES
Aeronautical engineering: A continuing bibliography with indexes (supplement 249)
[NASA-SP-7037(249)] N90-19190
FY 1989 scientific and technical reports, articles, papers, and presentations
[NASA-TM-100384] N90-19916

BIG BANG COSMOLOGY
The effects of cold dark matter on Big Bang nucleosynthesis N90-19749

BINARY CODES
On linear structure and phase rotation invariant properties of block 2(sup l)-PSK modulation codes
[NASA-CR-186308] N90-19429
BINOMIALS
Priority arbitration with busses
[AD-A216392] N90-19784
BIOCHEMISTRY
Assessment of research needs for laser technologies applied to advanced spectroscopic methods
[DE90-007402] N90-19588
BIOMEDICAL DATA
Potential biomedical application of the Los Alamos infrared free-electron laser: DNA spectroscopy
[DE90-006505] N90-19575
BIOSYNTHESIS
Metabolism, seizures, and blood flow in brain following organophosphate exposure: Mechanisms of action and possible therapeutic agents
[AD-A217098] N90-19740
BIREFRINGENCE
Integrated optics anisotropic waveguides and devices
[AD-A217064] N90-19849
BISMALEIMIDE
Utilization of thermometric methods for the testing of carbon reinforced plastics
[ETN-90-96076] N90-19314
BISMUTH OXIDES
Superconductivity in Ba(1-x)BiO3
[DE90-003781] N90-19869
BISTABLE CIRCUITS
Optically tunable gratings for optical interconnects
[AD-A216978] N90-19844
BIT ERROR RATE
Effects of amplitude distortions and IF equalization on satellite communication system bit-error rate performance
[NASA-TM-102415] N90-19454
BIVARIATE ANALYSIS
Use of Coxian-type distributions in a general model of the maximum of bivariate random variables
[PB90-121229] N90-19780
BLACK BODY RADIATION
Development of the blackbody probe type pyrometer, part 1. Experimental study on the fundamental characteristics
[DE89-782288] N90-19553
BLACK HOLES (ASTRONOMY)
Nearly simultaneous optical, ultraviolet, and x ray observations of three PG quasars
[NASA-CR-186355] N90-19932
Relativistic Gravitational Experiments in Space
[NASA-CP-3046] N90-19940
Sources of gravitational waves N90-19942
Detecting gravity waves from binary black holes N90-19943
Gravitational radiation from rotating gravitational collapse N90-19944
General relativistic x ray (UV) polarization rotations as a quantitative test for black holes N90-19957
Space telescope searches for black holes in galactic nuclei N90-19958
LAGEOS 3 and the gravitomagnetic field N90-19961
BLAZARS
An optical and infrared study of blazars N90-19930
BLOCKING
The utilization of an infrared imaging system as a cooling slot blockage detector in the inspection of a transpiration cooled nozzle
[NASA-TM-102608] N90-19555
BLUNT BODIES
Interaction of an oblique shock wave with supersonic flow over a blunt body N90-19197
BLUNT TRAILING EDGES
A study on upstream moving pressure waves induced by vortex separation
[ISL-CO-203/88] N90-19192
BODIES OF REVOLUTION
Drag reduction by longitudinal riblets on the surface of a streamwise aligned body of revolution
[MPIS-MITT-92] N90-19210
BOILERS
Test results from a full-scale sodium reflux pool-boiler solar receiver
[DE90-003577] N90-19671
BOMBER AIRCRAFT
Limitations of the conventional role of the B-1B in the European theater
[AD-A217285] N90-19230
BOMBS (ORDNANCE)
Limitations of the conventional role of the B-1B in the European theater
[AD-A217285] N90-19230
BONDING
Method for maintaining precise suction strip porosities
[NASA-CASE-LAR-13638-1] N90-19427
BOOLEAN ALGEBRA
Error detection in data processing devices by means of residue codes
[ETN-90-95370] N90-19767
BOOLEAN FUNCTIONS
Optimal layout via Boolean satisfiability
[AD-A216777] N90-19787
BOOSTERS (EXPLOSIVES)
An evaluation of ethylene-vinyl acetate copolymers as desensitizers for RDX in insensitive booster compositions prepared by slurry coating technology
[MRL-TR-89-33] N90-19385
BORON NITRIDES
The effect of fiber coatings on interfacial shear strength and the mechanical behavior of ceramic composites
[DE90-007574] N90-19380
BOSONS
Distributed bosonic states and condensed matter fusion
[AD-A217605] N90-19868
BOUNDARIES
Causal boundary construction for space-times of the general relativity theory
[ETN-90-95357] N90-19915
BOUNDARY ELEMENT METHOD
A combined finite element-boundary element formulation for solution of two-dimensional problems via CGFFT
[NASA-CR-186464] N90-19309
BOUNDARY INTEGRAL METHOD
Effects of nonuniform potential and current distributions in electrochemical systems
[DE90-007349] N90-19325
BOUNDARY LAYER SEPARATION
Influence of friction and separation phenomena on the dynamic blade loading of transonic turbine cascades
[MITT-88-04] N90-19235
Separation bubbles at high Reynolds number: Measurement and computation
[CUED/A-AERO/15] N90-19525
BOUNDARY LAYERS
Swept shock/boundary layer interaction experiments in support of CFD code validation
[NASA-CR-186397] N90-19535
BOUNDARY VALUE PROBLEMS
Initialization of EURAD. Part 1: Utilization of ECMWF analysis data N90-19695
Parallel algorithms for boundary value problems
[NASA-TM-102498] N90-19783
On the parallel efficiency of the Frederickson-McBryan multigrid
[NASA-CR-181999] N90-19791
Hierarchical basis preconditioners for second order elliptic problems in three dimensions
[DE90-005980] N90-19793
BRAIN CIRCULATION
Metabolism, seizures, and blood flow in brain following organophosphate exposure: Mechanisms of action and possible therapeutic agents
[AD-A217098] N90-19740
BRAYTON CYCLE
Low cost Brayton engine for gas-fired cogeneration system, phase 1
[PB90-127457] N90-19655
BRAZIL
Areas of aquatic macrophytes classified through vegetative indexes extracted from LANDSAT/TM imagery
[INPE-4880-PRE/1489] N90-19633
Analysis of tectonic movements utilizing remote sensor products in the Southern Espinhaco (SE) region
[INPE-4830-PRE/1451] N90-19708
BREAKING
Security calculations of rip reached construction elements by means of probabilistic breaking mechanics and a Markov process
[ETN-90-95890] N90-19624
BREATHING APPARATUS
Evaluation of the Scott aviation portable protective breathing device for contaminant leakage as prescribed by FAA Action Notice A-8150.2. Phase 1: Original tests of the portable protective breathing device. Phase 2: Tests of the redesigned portable protective breathing device
[AD-A216799] N90-19214
BRIGHTNESS
A new method for measuring the transmissivity of aircraft transparencies
[AD-A216953] N90-19842
BROADBAND
Field theoretical analysis and synthesis of broadband waveguide: Height, plane shunt circulators with multiple layer material insertions
[ETN-90-95360] N90-19469
BROADBAND AMPLIFIERS
Compton amplifier
[DIGEL-1985-5] N90-19506
BROADCASTING
Accuracy of global positioning system broadcast orbits for relative surveys
[PB90-125428] N90-19218
BROKEN SYMMETRY
Goldstone excitation and symmetry breaking mechanism in superfluid He-4
[DE90-610676] N90-19881
BUBBLES
Numerical simulation of acoustic scatter from subsurface bubble clouds
[AD-A217068] N90-19822
BUCKLING
PATRAN-STAGS translator (PATSTAGS)
[NASA-TM-100388] N90-19616
Interlaminar shear stress effects on the postbuckling response of graphite-epoxy panels
[NASA-TM-102626] N90-19630
BULK MODULUS
Elastic properties of silica xerogels
[AD-A216528] N90-19366
BUOYANCY
Siphon flows in isolated magnetic flux tubes. 3: The equilibrium path of the flux tube arch
[NASA-CR-186297] N90-19813
BUOYS
Drifting buoy data from Western Tropical Pacific for the period February 1, 1986 through February 28, 1989
[PB90-113978] N90-19732
BURNERS
Investigation of the processes controlling the flame generation of refractory materials
[DE90-007564] N90-19333
BUTADIENE
Synthesis and chemistry of unsaturated metal nitrogen compounds
[AD-A216550] N90-19321

C

C (PROGRAMMING LANGUAGE)
Yaw rate control of an air bearing vehicle N90-19420
CABLES (ROPES)
An experimental investigation of the flow field around yawed stranded cables
[AD-A215782] N90-19529
CADMIUM TELLURIDES
CdTe buffered GaAs thin-slab IR waveguide modulators and T/R filter
[AD-A215999] N90-19488
CALCULUS
Monostable electrovalve
[INPE-4928-RPE/595] N90-19487
CALIBRATING
Radial response of the burst and transient source experiment N90-19408
Transmission and reflection studies of thin films in the vacuum ultraviolet N90-19412
The 32-GHz performance of the DSS-14 70-meter antenna: 1989 configuration N90-19452
Calibration of the sonic measuring and control cross section in the gas feed installation of the solid fuel combustion chamber
[LR-552] N90-19548
Development of the blackbody probe type pyrometer, part 1. Experimental study on the fundamental characteristics
[DE89-782288] N90-19553
ARGUS/LLNL IR camera calibration and characterization
[AD-A217076] N90-19563
Recalibrating software reliability models
[NASA-CR-186407] N90-19763
Cosmic ray composition and muon decoherence at the knee of the all-particle cosmic ray spectrum N90-20035
CALORIMETERS
Algorithms for calorimeter simulation with parameterized showers by example of H1 detectors
[MPI-PAE/EXP.EL-200] N90-19828
CAMBER
A study of flows over highly-swept wings designed for maneuver at supersonic speeds
[AD-A216837] N90-19202
CAMERAS
The microchannel plate camera as a detector at high resolution spectrographs: Experiments for velocity distribution in planetary nebulae
[ETN-90-95733] N90-19560
ARGUS/LLNL IR camera calibration and characterization
[AD-A217076] N90-19563
Very high energy gamma ray astrophysics
[DE90-006645] N90-19983

CAMS
Phase control mechanism for wave energy conversion
[AD-D014354] N90-19657
CANARD CONFIGURATIONS
X-29A aircraft structural loads flight testing
[NASA-TM-101715] N90-19225
CANOPIES
A new method for measuring the transmissivity of aircraft transparencies
[AD-A216953] N90-19842
CAPACITANCE
Temperature compensated crystal oscillator (TCXO) with improved temperature compensation
[AD-D014334] N90-19482
Lightning protection apparatus for RF equipment and the like
[AD-D014336] N90-19483
Development and utilization of new diagnostics for dense-phase pneumatic transport
[DE90-006787] N90-19536
CAPACITORS
Alternate film dielectric materials
[DE90-007213] N90-19378
Advanced double layer capacitor
[AD-A217110] N90-19518
CARBON
Carbon black/polyethylene composites for PTC (Positive Temperature Coefficient) thermistor applications
[AD-A215988] N90-19307
The effect of fiber coatings on interfacial shear strength and the mechanical behavior of ceramic composites
[DE90-007574] N90-19380
CARBON DIOXIDE
A preliminary analysis of US CO2 emissions reduction potential from energy conservation and the substitution of natural gas for coal in the period to 2010
[DOE/NBB-0085] N90-19673
Simulation of global Kr-85 and (14)CO2 distribution by means of a time-dependent, two dimensional model of the atmosphere
[ETN-90-95376] N90-19702
CARBON DIOXIDE CONCENTRATION
CO2 depth profiles in cometary model substances of KOSI N90-20014
CARBON DIOXIDE LASERS
CdTe buffered GaAs thin-slab IR waveguide modulators and T/R filter
[AD-A215999] N90-19488
CO2 laser plus optimization for harmonic generation
[AD-D014341] N90-19565
Results of the PALADIN experiment
[DE90-006776] N90-19578
CARBON FIBER REINFORCED PLASTICS
Practical calculation of the liveload of carbon fiber reinforced plastics by the finite element method
[ETN-90-95867] N90-19311
Evaluation and choice algorithms of cost optimal prepreg-application processes: Production of strongly charged plane parts made of fiber reinforced plastics
[ETN-90-95895] N90-19313
Utilization of thermometric methods for the testing of carbon reinforced plastics
[ETN-90-96076] N90-19314
CARBON FIBERS
Fluorinated graphite fibers as a new engineering material: Promises and challenges
[NASA-TM-102511] N90-19301
CARBON ISOTOPES
Stable isotope studies of cometary analogue materials N90-20001
CARBON 13
Plasma centrifuge with vacuum arc discharge applied to the separation of stable isotopes
[INPE-4925-TDL/385] N90-19854
CARBON 14
Simulation of global Kr-85 and (14)CO2 distribution by means of a time-dependent, two dimensional model of the atmosphere
[ETN-90-95376] N90-19702
CARBONACEOUS MATERIALS
Spatially high-resolution flame diagnosis by means of spontaneous Raman spectroscopy
[ETN-90-95870] N90-19328
Evolution of ices and carbonaceous materials in the laboratory and in comets N90-19998
CARRIER LIFETIME
A simple model for the determination of L(sub 0), D and tau in a semiconductor and their temperature dependence
[DE90-610564] N90-19879
CARRIER TRANSPORT (SOLID STATE)
Costas loop lock detection in the advanced receiver N90-19441
CASCADE FLOW
Influence of friction and separation phenomena on the dynamic blade loading of transonic turbine cascades
[MITT-88-04] N90-19235
Digital determination of the three dimensional flow in turbomachines with the S1-S2 current function process
[ITSM-MITT-30] N90-19236
CASSEGRAIN OPTICS
A comparison of reflector antenna designs for wide-angle scanning N90-19264
CASTING
High density tape casting system
[NASA-CASE-NPO-16901-1-CU] N90-19425
CATALYSTS
Synthesis and properties of a novel catalyst for the combustion of methane
[PB90-127499] N90-19320
Enhancement of processes for solar photocatalytic detoxification of water
[DE90-003949] N90-19330
CATALYTIC ACTIVITY
Hydrous metal oxide-supported catalysts. Part 2: Catalytic properties and applications
[DE90-008098] N90-19336
CAVITIES
Fast optical switch and limiter using quantum size effect in metal grain composites
[AD-D014332] N90-19305
Elastomeric electrical isolation membrane
[AD-D014365] N90-19490
Analysis of unsteady heat transfer by natural convection in a two-dimensional square cavity using a high order finite-volume method N90-19521
CAVITY RESONATORS
A simple method using MAFIA to calculate external Q values of waveguide-loaded cavities
[DE90-741487] N90-19465
Field theoretical analysis and synthesis of broadband waveguide: Height, plane shunt circulators with multiple layer material insertions
[ETN-90-95360] N90-19469
Narrow-bandwidth unstable laser resonator
[AD-D014362] N90-19568
CELLS (BIOLOGY)
Study of hydrazine metabolism and toxicity
[AD-A217103] N90-19736
CENTRAL AMERICA
Evolution of finite amplitude baroclinic waves in the atmosphere and ocean
[INPE-4752-TDL/346] N90-19733
CENTRAL PROCESSING UNITS
The mesoscale meteorological model MM4 and its modifications for EURAD N90-19682
Parallel algorithms for boundary value problems
[NASA-TM-102498] N90-19783
CENTRIFUGES
Plasma centrifuge with vacuum arc discharge applied to the separation of stable isotopes
[INPE-4925-TDL/385] N90-19854
CERAMIC COATINGS
Influence of heat treating on the mechanical values and the stability of heat barrier coatings
[ETN-90-95902] N90-19375
CERAMICS
Processing of advanced ceramics using microwaves thermal treatments
[DE90-606349] N90-19362
Development of ceramic combustor for low BTU gases. Design and basic combustion characteristics
[DE89-782287] N90-19363
Fracture strength analysis of silicon nitride and silicon carbide ceramics from an international cooperative research program
[DE90-005319] N90-19368
Advanced ceramics
[DE90-608004] N90-19370
Optical studies of dynamical processes in disordered materials
[DE90-007080] N90-19372
The effect of fiber coatings on interfacial shear strength and the mechanical behavior of ceramic composites
[DE90-007574] N90-19380
Proposal of arc driving type fault current limiter
[DE89-782290] N90-19485
FWP executive summaries: Basic energy sciences materials sciences programs
[DE90-006373] N90-19893
CEREBRUM
Metabolism, seizures, and blood flow in brain following organophosphate exposure: Mechanisms of action and possible therapeutic agents
[AD-A217098] N90-19740
CERENKOV RADIATION
Radiation of electromagnetic waves by an accelerated charged particle in medium
[DE90-610458] N90-19461
Very high energy gamma ray astrophysics
[DE90-006645] N90-19983
CERTIFICATION
Assessment of crew workload measurement methods, techniques and procedures. Volume 2: Guidelines for the use of workload assessment techniques in aircraft certification
[AD-A217067] N90-19748
CH-47 HELICOPTER
A rule-based paradigm for intelligent adaptive flight control N90-19238
CHALCOGENIDES
The preparation and properties of iron doped II-VI chalcogenides
[AD-A217569] N90-19903
CHANNEL CAPACITY
Quantization effects in Viterbi decoding rate 1/n convolutional codes N90-19445
CHANNEL FLOW
Carrier wing profile in nonstationary current
[ETN-90-95368] N90-19208
CHANNELS (DATA TRANSMISSION)
A linear systems theory approach to the range-independent acoustic channel
[AD-A216551] N90-19817
CHAOS
Chaotic transients, higher dimensional phenomena, and coupled ordinary differential equations
[DE90-006641] N90-19794
Nonlinear system vibration: The appearance of chaos
[DE90-007546] N90-19810
Computation at the edge of chaos: Phase transition and emergent computation
[DE90-007488] N90-19811
CHARACTERIZATION
Characterization of thunderstorm induced Maxwell current densities in the middle atmosphere N90-19391
Liquid oxygen LOX compatibility evaluations of aluminum lithium (Al-Li) alloys: Investigation of the Alcoa 2090 and MMC weldalite 049 alloys N90-19398
Mechanics of aeolian processes: Soil erosion and dust production N90-19410
Construction and characterization of a valve for rapid gas injection
[INPE-4789-RPE/583] N90-19486
CHARGE COUPLED DEVICES
Investigations of x ray sensitive PN-CCD's
[MPE-213] N90-19499
Structural experiments of planetary nebulae: Charge-coupled devices, image reduction under MIDAS, information representation, and development of an evolution classification for PN's
[ETN-90-95736] N90-20026
CHARGED PARTICLES
Identification and solution of a charging problem in a high-altitude detector
[DE90-008637] N90-19296
Radiation of electromagnetic waves by an accelerated charged particle in medium
[DE90-610458] N90-19461
Fifth-order aberrations in magnetic quadrupole-octupole systems
[DE90-007489] N90-19831
The 41st Annual Gaseous Electronics Conference
[AD-A214540] N90-19851
Electrical resistivity of strongly coupled plasmas in intense fields
[DE90-002236] N90-19861
CHEBYSHEV APPROXIMATION
Conforming Chebyshev spectral collocation methods for the solution of laminar flow in a constricted channel
[NASA-CR-182011] N90-19539
CHEMICAL ANALYSIS
Liquid oxygen LOX compatibility evaluations of aluminum lithium (Al-Li) alloys: Investigation of the Alcoa 2090 and MMC weldalite 049 alloys N90-19398
CHEMICAL CLOUDS
The EURAD Model: Structure and First Results
[REPT-61] N90-19680
CHEMICAL COMPOSITION
High-purity beryllium foils
[DE90-006408] N90-19348
Chemical composition of precipitation and wet/dry deposition of sulfur compounds around the coastal area
[DE89-782324] N90-19677
Geochemical survey on faults overland with alluvial deposits, part 1. Application for the Neodani and the Atera faults survey
[DE89-782326] N90-19707
Tunneling microscopy of submonolayer adsorbates on Si3
[AD-A216985] N90-19876
The composition of cometary nuclei N90-20022

CHEMICAL PROPERTIES
The preparation and properties of iron doped II-VI chalcogenides
[AD-A217569] N90-19903
Physics and Mechanics of Cometary Materials
[ESA-SP-302] N90-19989
CHEMICAL REACTIONS
Nanolayer reactions in aluminum-metal interfaces
[DE90-004955] N90-19342
Determination of the mechanism of decomposition of energetic molecules
[AD-A217061] N90-19388
Laboratory studies of free radical reactions in cloudwater
[DE90-003961] N90-19730
Ion mixing and surface modification in metal-semiconductor systems
[DE90-007557] N90-19897
CHEMICAL REACTORS
Radiative transport models for solar thermal receiver/reactors
[DE90-000303] N90-19665
CHIPS (ELECTRONICS)
A gate array structure for the efficient project of digital circuits: The unit cell array
[ETN-90-95364] N90-19502
A virtual zero-time, monolithic systolic sorting array
[DE90-001000] N90-19753
Flosolver Mk1B: An eight processor parallel machine
[PD-CF-8941] N90-19755
CHROMIUM STEELS
Oscillation and damping behavior of fine steel test tubes, with particular consideration to destruction free proofs from hydrogen fragilization
[ETN-90-95371] N90-19351
Modification of surface mechanical properties of high-chromium tool steel by carbon-implanted codeposited Fe-Ti films
[DE90-007502] N90-19358
CIRCUIT DIAGRAMS
Optimal layout via Boolean satisfiability
[AD-A216777] N90-19787
CIRCUIT PROTECTION
Power diode switching behavior
[ETN-90-95363] N90-19501
CIRCUITS
Muzzle shunt augmentation of conventional railguns
[DE90-007505] N90-19248
Modeling A circuit switched multiprocessor interconnect
[AD-A217122] N90-19519
CIRCULAR CYLINDERS
Computation of hypersonic unsteady viscous flow over a cylinder N90-19194
Dual frequency launcher for circularly polarized antenna
[AD-D014361] N90-19456
An experimental study of the aeroelastic behaviour of two parallel interfering circular cylinders N90-19609
CIRCULAR POLARIZATION
Dual frequency launcher for circularly polarized antenna
[AD-D014361] N90-19456
CIRCULATORS (PHASE SHIFT CIRCUITS)
Field theoretical analysis and synthesis of broadband waveguide: Height, plane shunt circulators with multiple layer material insertions
[ETN-90-95360] N90-19469
CIRRUS CLOUDS
Exploiting surface observations of cloudiness for globalscale nephanalyses N90-19719
CIVIL AVIATION
Interoperability issues in the use of satellite-based navigation systems for civil aviation purposes
[AD-A217279] N90-19223
CLASSICAL MECHANICS
Classical mechanics on superspace
[DE90-606907] N90-19906
CLASSIFICATIONS
Areas of aquatic macrophytes classified through vegetative indexes extracted from LANDSAT/TM imagery
[INPE-4880-PRE/1489] N90-19633
CLASSIFYING
A virtual zero-time, monolithic systolic sorting array
[DE90-001000] N90-19753
CLIMATE
Exploiting surface observations of cloudiness for globalscale nephanalyses N90-19719
Large impact events and atmospheric evolution on the terrestrial planets N90-20028
CLIMATE CHANGE
Sensitivity of ecological landscapes and regions to global climatic change
[PB90-120072] N90-19674
Predicting effects of global climate change on reservoir water quality and fish habitat
[DE90-003674] N90-19704
Regional climate change predictions from the Goddard Institute for Space Studies high resolution GCM
[NASA-CR-186375] N90-19725
CLIMATOLOGY
Predicting effects of global climate change on reservoir water quality and fish habitat
[DE90-003674] N90-19704
Exploiting surface observations of cloudiness for globalscale nephanalyses N90-19719
Colloquium on Synoptic Meteorology
[PB90-121112] N90-19720
Cyclogeneses and extratropical cyclones in the south-southeast region of Brazil and its influence in time
[INPE-4812-TDL/359] N90-19722
Regional climate change predictions from the Goddard Institute for Space Studies high resolution GCM
[NASA-CR-186375] N90-19725
CLOSURE LAW
Uniqueness of closure of the constraint algebra for quantum gravity
[DE90-610476] N90-19712
CLOSURES
Analytical methods for the development of Reynolds stress closures in turbulence
[NASA-CR-182017] N90-19538
CLOUD COVER
Exploiting surface observations of cloudiness for globalscale nephanalyses N90-19719
Automated visibility and cloud cover measurements with a solid-state imaging system
[AD-A216906] N90-19724
CLOUD SEEDING
Numerical modeling of atmospheric growth processes
[REPT-70] N90-19726
CLOUDS
Numerical simulation of acoustic scatter from subsurface bubble clouds
[AD-A217068] N90-19822
Large impact events and atmospheric evolution on the terrestrial planets N90-20028
CLOUDS (METEOROLOGY)
Validation of the EURAD cloud modules N90-19693
The role of clouds in the photochemistry of the background troposphere N90-19694
Exploiting surface observations of cloudiness for globalscale nephanalyses N90-19719
Digital simulation of a Boerline
[ISSN-0069-5882] N90-19729
Laboratory studies of free radical reactions in cloudwater
[DE90-003961] N90-19730
COAGULATION
Low velocity dust-dust collisions N90-20011
Mechanical properties of fluffy agglomerates consisting of core-mantle-particles N90-20019
COAL
Simulation of thermal dynamics of a vaporizing coal-water droplet in a combustor
[DE90-005356] N90-19317
Analysis of competition among kinds of energy at the era of complexed energy. (Report on overseas study)
[DE89-910213] N90-19650
COAL DERIVED GASES
Development of ceramic combustor for low BTU gases. Design and basic combustion characteristics
[DE89-782287] N90-19363
COAL DERIVED LIQUIDS
Development and use of an advanced coal-fueled diesel engine cycle simulation with group effects
[DE90-000450] N90-19607
COAL GASIFICATION
Development of ceramic combustor for low BTU gases. Design and basic combustion characteristics
[DE89-782287] N90-19363
COAL LIQUEFACTION
Hydrous metal oxide-supported catalysts. Part 2: Catalytic properties and applications
[DE90-008098] N90-19336
COASTS
Satellite imagery for water quality assessment in coastal regions
[INPE-4891-PRE/1492] N90-19636
Cyclogeneses and extratropical cyclones in the south-southeast region of Brazil and its influence in time
[INPE-4812-TDL/359] N90-19722
An observational study of squall lines in the Amazon
[INPE-4865-TDL/376] N90-19723
COATING
An evaluation of ethylene-vinyl acetate copolymers as desensitizers for RDX in insensitive booster compositions prepared by slurry coating technology
[MRL-TR-89-33] N90-19385
Electromagnetic properties of material coated surfaces
[NASA-CR-186466] N90-19466
COATINGS
Modification of surface mechanical properties of high-chromium tool steel by carbon-implanted codeposited Fe-Ti films
[DE90-007502] N90-19358
Microstructural characterization of multiphase coatings produced by chemical vapor deposition
[DE90-007573] N90-19379
The effect of fiber coatings on interfacial shear strength and the mechanical behavior of ceramic composites
[DE90-007574] N90-19380
Electromagnetic properties of material coated surfaces
[NASA-CR-186466] N90-19466
COAXIAL CABLES
Thermal coefficient of delay for various coaxial and fiber-optic cables N90-19439
COCKPITS
Human factors engineering testing of aircraft cockpit lighting systems
[AD-A216853] N90-19743
A new method for measuring the transmissivity of aircraft transparencies
[AD-A216953] N90-19842
CODING
Dynamic reconfiguration and link fault tolerance in a transputer network
[AD-A215105] N90-19433
Some easily analyzable convolutional codes N90-19444
Quantization effects in Viterbi decoding rate 1/n convolutional codes N90-19445
Big Viterbi Decoder (BVD) results for (7,1/2) convolutional code N90-19446
Fast transform decoding of nonsystematic Reed-Solomon codes N90-19447
Digital video: Studio signal processing
[BBC-RD-1989/14] N90-19478
COGENERATION
Solid oxide fuel cell cogeneration system conceptual design, program 2
[PB90-114968] N90-19653
Survey on the possibility of introducing new energy to regional development plans
[DE89-782627] N90-19654
Low cost Brayton engine for gas-fired cogeneration system, phase 1
[PB90-127457] N90-19655
COGNITIVE PSYCHOLOGY
Symposium on air traffic control training for tomorrow's technology
[PB90-127325] N90-19216
COHERENT RADAR
Coherent radar measurement of ocean currents from geostationary orbit N90-19259
COHESION
Some considerations on cohesive forces in sun-grazing comets N90-20015
COLD NEUTRONS
The effects of cold dark matter on Big Bang nucleosynthesis N90-19749
COLD PRESSING
Crystallization behavior and properties of BaO-Al2O3-2SiO2 glass matrices
[NASA-CR-185209] N90-19374
COLD ROLLING
Novel processing of HTS based conductors
[DE90-005956] N90-19892
COLD WORKING
Plastic bending tests of cold-formed rectangular hollow sections
[PB90-124611] N90-19613
COLLISIONAL PLASMAS
The 41st Annual Gaseous Electronics Conference
[AD-A214540] N90-19851
COLLISIONLESS PLASMAS
Longitudinal traveling waves bifurcating from Vlasov plasma equilibria N90-19850
COLLISIONS
Present and future risk of satellite and manned platforms collisions with other space objects and particles on earth orbits
[R-8841] N90-19287
Present and future risk of collision of satellites and manned platforms with other space objects and particles in terrestrial orbit
[R-8840] N90-19288
Satellites and debris in earth revolution orbits and first estimation of the collision probability
[R-8709] N90-19289
Project for the Eurcpean space organization in the area of space debris
[REPT-29/89] N90-19290

Large impact events and atmospheric evolution on the terrestrial planets N90-20028

COLLOCATION

A panel process for the calculation of the flow around a wing with front angle damping
[ETN-90-95367] N90-19207

Conforming Chebyshev spectral collocation methods for the solution of laminar flow in a constricted channel
[NASA-CR-182011] N90-19539

COLOR

Comet Halley: An optical continuum study N90-19981

COLOR VISION

A new method for measuring the transmissivity of aircraft transparencies
[AD-A216953] N90-19642

COMBUSTION

Proceedings of a contractors meeting on Combustion Rocket Propulsion Diagnostics of Reacting Flow
[AD-A216445] N90-19297

Simulation of thermal dynamics of a vaporizing coal-water droplet in a combustor
[DE90-005356] N90-19317

Synthesis and properties of a novel catalyst for the combustion of methane
[PB90-127499] N90-19320

Effect of barrier layers in burn-through experiments with 351-nm laser illumination
[DE90-006806] N90-19577

COMBUSTION CHAMBERS

Simulation of thermal dynamics of a vaporizing coal-water droplet in a combustor
[DE90-005356] N90-19317

The use of the gas feed system and the vitiator for the solid fuel combustion chamber
[LR-528] N90-19329

Development of ceramic combustor for low BTU gases. Design and basic combustion characteristics
[DE89-782287] N90-19363

Calibration of the sonic measuring and control cross section in the gas feed installation of the solid fuel combustion chamber
[LR-552] N90-19548

Design of a pyrometer for temperature measurements on the solid fuel combustion chamber
[LR-530] N90-19561

COMET NUCLEI

Physics and Mechanics of Cometary Materials
[ESA-SP-302] N90-19989

Rosetta/CNSR, ESA's planetary cornerstone mission N90-19990

Physical models of cometary nuclei: A review N90-19991

Petrographic working model of the Rosetta sampling and modelling subgroup for a comet nucleus N90-19992

Design and development activities on the candidate sample acquisition system for the Rosetta mission N90-19993

Comets: Dirty snowballs or icy dirtballs N90-19994

A test of the interstellar dust model of comets N90-19995

Physical processes in cometary ices inferred from laboratory studies N90-19996

Laboratory studies of cometary ice analogues N90-19997

Evolution of ices and carbonaceous materials in the laboratory and in comets N90-19998

Thermal conductivities and diffusivities of porous ice samples at low pressures and temperatures and possible modes of heat transfer in near surface layers of comets N90-19999

Physico-chemical properties of formaldehyde-ice-dust mixtures N90-20000

Stable isotope studies of cometary analogue materials N90-20001

Compressive strength of synthetic comet nucleus samples N90-20006

Thermal perturbation of comet samples during their acquisition N90-20008

Rosetta/CNSR altimeter and sounding radar N90-20009

Hot OH and CN: Evidence for organic molecules close to the nucleus of comet Halley N90-20012

Some considerations on cohesive forces in sun-grazing comets N90-20015

Gas diffusion in a cometary crust N90-20017

Porosity and ice-dust mixtures in cometary particles N90-20018

Dynamics of crust formation and dust emission of comet nucleus analogues under isolation N90-20020

Relevance of laboratory studies to comets N90-20023

COMET RENDEZVOUS ASTEROID FLYBY MISSION

Relevance of laboratory studies to comets N90-20023

COMET TAILS

Disturbance structures and its magnetic field features in plasma comet tail
[DE90-610636] N90-19986

COMETARY ATMOSPHERES

Comet Halley: An optical continuum study N90-19981

A test of the interstellar dust model of comets N90-19995

Thermal conductivities and diffusivities of porous ice samples at low pressures and temperatures and possible modes of heat transfer in near surface layers of comets N90-19999

Physico-chemical properties of formaldehyde-ice-dust mixtures N90-20000

Gas diffusion in a cometary crust N90-20017

Porosity and ice-dust mixtures in cometary particles N90-20018

The composition of cometary nuclei N90-20022

COMETS

Disturbance structures and its magnetic field features in plasma comet tail
[DE90-610636] N90-19986

Physics and Mechanics of Cometary Materials
[ESA-SP-302] N90-19989

A test of the interstellar dust model of comets N90-19995

Laboratory studies of cometary ice analogues N90-19997

Evolution of ices and carbonaceous materials in the laboratory and in comets N90-19998

Thermal conductivities and diffusivities of porous ice samples at low pressures and temperatures and possible modes of heat transfer in near surface layers of comets N90-19999

Crustal strength of different model comet materials N90-20003

Fracture mechanical aspects of dust emission processes from a model comet surface N90-20004

Simulation of radar and radiometer signals remote sensing cometary surface and subsurface structures N90-20005

Rosetta/CNSR altimeter and sounding radar N90-20009

Cometary bodies in the circumstellar disk around beta Pictoris N90-20010

A method of estimating temperature profiles and chemical differentiation in the near surface layers of porous comet nuclei: First results for comet P/Churyumov-Gerasimenko N90-20013

CO2 depth profiles in cometary model substances of KOSI N90-20014

Some considerations on cohesive forces in sun-grazing comets N90-20015

Possible targeting of particle emission by mechanical stress and penetration of sublimating ice-dust-surfaces N90-20016

Gas diffusion in a cometary crust N90-20017

Porosity and ice-dust mixtures in cometary particles N90-20018

Dynamics of crust formation and dust emission of comet nucleus analogues under isolation N90-20020

First impressions of the comet drilling problem N90-20021

Large impact events and atmospheric evolution on the terrestrial planets N90-20028

COMMERCE

From invention to innovation: Commercialization of new technology by independent and small business inventors
[DE90-006944] N90-19927

COMMUNICATION

Activities report of the Institute for Communication Technology
[ETN-90-95383] N90-20043

COMMUNICATION NETWORKS

Low earth orbiting satellite for international information exchange system
[DE90-007186] N90-19292

Packet radio networks under dynamic jamming
[AD-A217094] N90-19475

COMMUTER AIRCRAFT

Low-speed wind-tunnel investigation of the flight dynamic characteristics of an advanced turboprop business/commuter aircraft configuration
[NASA-TP-2982] N90-19239

COMPATIBILITY

Liquid oxygen LOX compatibility evaluations of aluminum lithium (Al-Li) alloys: Investigation of the Alcoa 2090 and MMC weldalite 049 alloys N90-19398

COMPETITION

Analysis of competition among kinds of energy at the era of complexed energy. (Report on overseas study)
[DE89-910213] N90-19650

COMPLEX COMPOUNDS

Synthesis and chemistry of unsaturated metal nitrogen compounds
[AD-A216550] N90-19321

Conductive polymers of transition-metal complexes coordinated by a Diamino-Dichalcogen-Benzene compound
[AD-D014326] N90-19360

COMPOSITE MATERIALS

Three-dimensional structural analyses of reentry vehicles
[DE90-006278] N90-19291

Ac loss measurements of two multifilamentary NbTi composite strands
[DE90-005388] N90-19304

Fast optical switch and limiter using quantum size effect in metal grain composites
[AD-D014332] N90-19305

Heterogeneous composite and method of making
[AD-D014337] N90-19306

Carbon black/polyethylene composites for PTC (Positive Temperature Coefficient) thermistor applications
[AD-A215988] N90-19307

The effect of fiber coatings on interfacial shear strength and the mechanical behavior of ceramic composites
[DE90-007574] N90-19380

Viscoelastic adherend effects in adhesively bonded composite-to-composite joints N90-19594

COMPOSITE STRUCTURES

Evaluation of repeated impact damage in composite structures N90-19303

Carbon black/polyethylene composites for PTC (Positive Temperature Coefficient) thermistor applications
[AD-A215988] N90-19307

Innovative design of composite structures: The use of curvilinear fiber format in structural design of composites
[NASA-CR-186406] N90-19308

Demonstration of capabilities of high temperature composites analyzer code HITCAN
[NASA-TM-102560] N90-19629

COCOMAT: A Computer Aided Engineering (CAE) system for composite structures design
[NLR-MP-87078-U] N90-19756

COMPRESSIBILITY EFFECTS

Application of a Reynolds stress turbulence model to the compressible shear layer
[NASA-CR-182002] N90-19537

COMPRESSIVE STRENGTH

Compressive strength of synthetic comet nucleus samples N90-20006

COMPTON EFFECT

Background studies in gas ionizing x ray detectors N90-19399

Compton amplifier
[DIGEL-1985-5] N90-19506

COMPUTATION

Visual processing in texture segregation
[AD-A216539] N90-19737

Adaptive, asynchronous stochastic global optimization algorithms for sequential and parallel computation
[AD-A217093] N90-19775

Computation at the edge of chaos: Phase transition and emergent computation
[DE90-007488] N90-19811

BCS (Bardeen-Cooper-Schrieffer) primer: A guide to computational methods in superconductivity theory
[AD-A216393] N90-19874

COMPUTATIONAL FLUID DYNAMICS

On the evaluation of aerodynamic influence coefficients
[NLR-MP-87019-U] N90-19191

Computation of hypersonic unsteady viscous flow over a cylinder N90-19194

A streamwise upwind algorithm applied to vortical flow over a delta wing
[NASA-TM-102225] N90-19201

External flow computations for a finned 60mm ramjet in steady supersonic flight
[AD-A216998] N90-19233

Experimental and theoretical investigations of flowfields and heat transfer in modern gas turbines
[AD-A217663] N90-19237

Numerical study of diffusion jet flames N90-19316

Potential theory of radiation N90-19395

The influence of a wall function on turbine blade heat transfer prediction N90-19421

Numerical and experimental analysis of a thin liquid film on a rotating disk related to development of a spacecraft absorption cooling system
[NASA-CR-183457] N90-19523

Computational fluid dynamics method for low Reynolds number flow in a precessing/spinning, liquid filled cylinder with rounded endcaps
[AD-A216997] N90-19531

Swept shock/boundary layer interaction experiments in support of CFD code validation [NASA-CR-186397] N90-19535
Flow simulation for aircraft [NLR-MP-87082-U] N90-19543

COMPUTATIONAL GRIDS
Comparison of a 6-layer and a 15-layer version of the Chemical Transfer Model (CTM) N90-19689
The p- and h-p versions of the finite element method: An overview [AD-A216902] N90-19789
On the parallel efficiency of the Frederickson-McBryan multigrid [NASA-CR-181999] N90-19791
A tensor product B-spline method for numerical grid generation [DE90-005979] N90-19792
Finite element mesh generation starting from general geometric models [REPT-88-93] N90-19803

COMPUTER AIDED DESIGN
Kinematic control of robotic manipulators with multiple interchangeable wrists N90-19592
COCOMAT: A Computer Aided Engineering (CAE) system for composite structures design [NLR-MP-87078-U] N90-19756
User-friendly software for the design of digital line-of-sight radio links [PB90-118472] N90-19760

COMPUTER AIDED MANUFACTURING
COCOMAT: A Computer Aided Engineering (CAE) system for composite structures design [NLR-MP-87078-U] N90-19756

COMPUTER AIDED MAPPING
Thematic coupling between digital images and geographic information systems [ETN-90-95723] N90-19646

COMPUTER AIDED TOMOGRAPHY
Object detection and amplitude estimation based on maximum a posteriori reconstructions [DE90-007511] N90-19770

COMPUTER GRAPHICS
Image manipulation in the SIGGRAPH Interactive Proceedings [DE90-007542] N90-19771

COMPUTER NETWORKS
Report of the First Annual Airborne Weapons Training Technology Review [DE90-007189] N90-19747
Networks and the best approximation property [AD-A216712] N90-19778

COMPUTER PROGRAMMING
ROCOPT: A user friendly interactive code to optimize rocket structural components N90-19415
Implementation of the RADM/EURAD models on the great calculation system of the Juelich KFA N90-19687
Software development: A paradigm for the future [NASA-CR-186456] N90-19766
Deceit: A flexible distributed file system [NASA-CR-186412] N90-19923

COMPUTER PROGRAMS
Heat transfer measurements from a NACA 0012 airfoil in flight and in the NASA Lewis icing research tunnel [NASA-CR-4278] N90-19203
Conjugate field approaches for active array compensation N90-19266
Reflector surface distortion analysis techniques (thermal distortion analysis of antennas in space) N90-19267
Mesh surfaces for reflector applications N90-19268
The measurement, modeling, and prediction of traction for rocket propellant 1 [NASA-CR-185186] N90-19386
Augmenting and updating NASA spacelink electronic information system N90-19392
Potential theory of radiation N90-19395
Artificial intelligence issues related to automated computing operations N90-19404
Evaluation of the heat transfer module (FAHT) of Failure Analysis Nonlinear Thermal And Structural integrated Code (FANTASTIC) N90-19407
ROCOPT: A user friendly interactive code to optimize rocket structural components N90-19415
Marshall Avionics Testbed System (MAST) N90-19417
Yaw rate control of an air bearing vehicle N90-19420
The influence of a wall function on turbine blade heat transfer prediction N90-19421
Multibody modeling and verification N90-19422
Determination of Earth orientation using the Global Positioning System N90-19435
Memory management in traceback Viterbi decoders N90-19443
Quantization effects in Viterbi decoding rate 1/n convolutional codes N90-19445
Big Viterbi Decoder (BVD) results for (7,1/2) convolutional code N90-19446
Fast transform decoding of nonsystematic Reed-Solomon codes N90-19447
A simple method using MAFIA to calculate external Q values of waveguide-loaded cavities [DE90-741487] N90-19465
Tracking performance of the AN/GPN-22 precision approach radar [FEL-1988-34] N90-19467
PATRAN-STAGS translator (PATSTAGS) [NASA-TM-100388] N90-19616
Demonstration of capabilities of high temperature composites analyzer code HITCAN [NASA-TM-102560] N90-19629
Development of software routines for remote sensing digital image processing [ETN-90-95452] N90-19640
User-friendly software for the design of digital line-of-sight radio links [PB90-118472] N90-19760
Recalibrating software reliability models [NASA-CR-186407] N90-19763
A nonparametric software reliability growth model [NASA-CR-186438] N90-19764
Software development: A paradigm for the future [NASA-CR-186456] N90-19766
Generic distributed systems model [AD-A217078] N90-19773
Local area network with fault-checking, priorities, and redundant backup [NASA-CASE-NPO-16949-1-CU] N90-19776
The 0-1 multiknapsack problem: Heuristic and reduction methods [INPE-4894-PRE/1495] N90-19782
Executive information systems for providing next generation strategic information: An evaluation of EIS (Executive Information System) software and recommended applicability within the FAA computing environment [AD-A216672] N90-19920
Conception of an automatic measurement installation for spatial resolution detectors [ETN-90-95732] N90-19935
Nuclear interactions of high energy heavy ions and applications in astrophysics [DE90-006691] N90-19984

COMPUTER STORAGE DEVICES
Modeling A circuit switched multiprocessor interconnect [AD-A217122] N90-19519

COMPUTER SYSTEMS DESIGN
Local area network with fault-checking, priorities, and redundant backup [NASA-CASE-NPO-16949-1-CU] N90-19776

COMPUTER SYSTEMS PERFORMANCE
Using Rexx to coordinate relational commands [DE90-007569] N90-19772

COMPUTER SYSTEMS PROGRAMS
Development of software routines for remote sensing digital image processing [ETN-90-95452] N90-19640

COMPUTER TECHNIQUES
Multibody modeling and verification N90-19422
CRISP (Computer Retrieval of Information on Scientific Projects) thesauras, fiscal year 1990 [PB90-138652] N90-19922

COMPUTERIZED SIMULATION
Aeroservoelasticity [NASA-TM-102620] N90-19227
Antennas for 20/30 GHz and beyond N90-19269
Evaluation and choice algorithms of cost optimal prepreg-application processes: Production of strongly charged plane parts made of fiber reinforced plastics [ETN-90-95895] N90-19313
Numerical study of diffusion jet flames N90-19316
Analytical optical scattering in clouds N90-19413
Costas loop lock detection in the advanced receiver N90-19441
Two-dimensional, long-pulse computer calculation of microwave-induced electron layer formation in low-pressure air [DE90-005994] N90-19459
Numerical simulation of cross field amplifiers [DE90-006459] N90-19496
Laser-matter interaction at intensities of 10(sup 12) W/cm(sup 2) and below [DE90-007536] N90-19590
Advanced control schemes and kinematic analysis for a kinematically redundant 7 DOF manipulator [NASA-CR-186175] N90-19599
Development and use of an advanced coal-fueled diesel engine cycle simulation with group effects [DE90-000450] N90-19607
Comparison of a 6-layer and a 15-layer version of the Chemical Transfer Model (CTM) N90-19689
Flight crew aiding for recovery from subsystem failures [NASA-CR-181905] N90-19741
Theory and applications of belief functions [AD-A217092] N90-19774
Parallel neural net path-planner on hypercube and transputer [DE90-006324] N90-19777
Electron energy distributions and vibrational population distributions [DE90-005550] N90-19825
Molecular theory and computer simulation studies of natural and synthetic gas mixtures [PB90-130329] N90-19826
Thermal infrared scene simulation [DE90-006900] N90-19845
Supercomputer applications for materials science: Ordering effects of hydrogen in palladium [DE90-004664] N90-19870
Computer simulation of recrystallization in the presence of second phase particles [DE90-007531] N90-19896
Time-dependent two-dimensional radiation hydrodynamics of accreting matter onto highly magnetized neutron stars [DE90-006927] N90-19985

CONCRETES
Development of finished beam and shell elements from engineering models for structures under high inelastic deformations [ETN-90-95377] N90-19619

CONDENSATES
Bose condensate in superfluid (sup 4)He and momentum distributions by deep inelastic scattering [DE90-007541] N90-19832
Physical processes in cometary ices inferred from laboratory studies N90-19996

CONDENSATION NUCLEI
Disturbance structures and its magnetic field features in plasma comet tail [DE90-610636] N90-19986

CONDENSED MATTER PHYSICS
Distributed bosonic states and condensed matter fusion [AD-A217605] N90-19868

CONDUCTIVE HEAT TRANSFER
Numerical modelling of shocks in gases and metals [MRL-RR-8-89] N90-19528
Evolution of midplate hotspot swells: Numerical solutions [NASA-CR-186482] N90-19713

CONFERENCES
Symposium on air traffic control training for tomorrow's technology [PB90-127325] N90-19216
Earth Science Geostationary Platform Technology [NASA-CP-3040] N90-19249
Proceedings of a contractors meeting on Combustion Rocket Propulsion Diagnostics of Reacting Flow [AD-A216445] N90-19297
International conference on Surface Modification of Metals by Ion Beams [AD-A215872] N90-19345
Proceedings of the 2nd United States/USSR Symposium on Air Pollution Effects on Vegetation Including Forest Ecosystems [PB90-127119] N90-19678
The EURAD Model: Structure and First Results [REPT-61] N90-19680
Colloquium on Synoptic Meteorology [PB90-121112] N90-19720
The 41st Annual Gaseous Electronics Conference [AD-A214540] N90-19851
National Technical Information Service 1989 Users Conference proceedings [PB90-142563] N90-19921
Physics and Mechanics of Cometary Materials [ESA-SP-302] N90-19989

CONGRESSIONAL REPORTS
Advancing automation and robotics technology for the Space Station Freedom and for the US economy: Submitted to the United States Congress [NASA-TM-101647] N90-19279

CONICAL BODIES
External flow computations for a finned 60mm ramjet in steady supersonic flight [AD-A216998] N90-19233
Series reversion/inversion of Lambert's time function [AD-A216243] N90-19245

CONJUGATE GRADIENT METHOD
A combined finite element-boundary element formulation for solution of two-dimensional problems via CGFFT [NASA-CR-186464] N90-19309

CONJUGATES
Conjugate field approaches for active array compensation N90-19266

CONSTRAINTS
Uniqueness of closure of the constraint algebra for quantum gravity
[DE90-610476] N90-19712
CONSTRUCTION
Construction and characterization of a valve for rapid gas injection
[INPE-4789-RPE/583] N90-19486
CONTAMINANTS
Evaluation of the Scott aviation portable protective breathing device for contaminant leakage as prescribed by FAA Action Notice A-8150.2. Phase 1: Original tests of the portable protective breathing device. Phase 2: Tests of the redesigned portable protective breathing device
[AD-A216799] N90-19214
Development of inspection techniques for quantitatively measuring surface contamination on SRM hardware
[NASA-CR-183902] N90-19608
The Chemical Transfer Model (CTM) of EURAD: Development status N90-19683
The pollution hazard assessment system: Documentation and users manual
[AD-A217108] N90-19706
CONTAMINATION
Development of inspection techniques for quantitatively measuring surface contamination on SRM hardware
[NASA-CR-183902] N90-19608
The pollution hazard assessment system: Documentation and users manual
[AD-A217108] N90-19706
CONTINUITY EQUATION
The Chemical Transfer Model (CTM) of EURAD: Development status N90-19683
CONTINUOUS RADIATION
Progress in the CW operation of a 140 GHz gyrotron
[DE90-007382] N90-19558
CONTINUOUS WAVE LASERS
Applications of FM-CW laser radar to antenna contour mapping N90-19270
Proceedings of Air Force Office of Scientific Research workshop on Laser Propulsion
[AD-A216563] N90-19569
CONTINUUM MECHANICS
Nonlinear continuum mechanics and applied analysis
[AD-A213629] N90-19812
CONTINUUM MODELING
Characterization of reaction kinetics in a porous electrode
[NASA-CR-186504] N90-19340
CONTINUUMS
Comet Halley: An optical continuum study N90-19981
CONTOUR SENSORS
Improved processes for ultrasonic object recognition in robotics
[ETN-90-95362] N90-19604
CONTOURS
Dynamics of a class of vortex rings
[NASA-TM-102257] N90-19524
CONTROL EQUIPMENT
Multibody modeling and verification N90-19422
CONTROL SYSTEMS DESIGN
Induction motor control
[NASA-TM-102533] N90-19234
Self-tuning control techniques, implicit and explicit, with parameter estimation in Kalman filters, applied to artificial satellite attitude
[INPE-4857-TDL/368] N90-19276
Application of attachment modes in the control of large space structures
[NASA-CR-185604] N90-19280
Integrated control/structure optimization by multilevel decomposition
[NASA-TM-102619] N90-19281
A computer control system for the alternating gradient magnetometer N90-19402
Experiments in end-point control of a flexible robot with a mini-manipulator N90-19596
Dynamics and control of robot manipulators with closed-kinematic chain mechanism N90-19598
CONTROL THEORY
Aeroservoelasticity
[NASA-TM-102620] N90-19227
Output model-following control synthesis for an oblique-wing aircraft
[NASA-TM-100454] N90-19241
A complete description of robot manipulator dynamics based on Lagrangian mechanics
[DE90-741467] N90-19603
Drag-free satellite control N90-19974
CONTROLLERS
A rule-based paradigm for intelligent adaptive flight control N90-19238
Output model-following control synthesis for an oblique-wing aircraft
[NASA-TM-100454] N90-19241
Investigations into a new algorithm for calculating H infinity optimal controllers N90-19406
Determination of the implementation of the 3-axis attitude motion simulator digital position controller N90-19409
Disturbance torque rejection properties of the NASA/JPL 70-meter antenna axis servos N90-19450
Deceit: A flexible distributed file system
[NASA-CR-186412] N90-19923
CONVECTION
A PBL-radiation model for application to regional numerical weather prediction N90-19394
Analysis of unsteady heat transfer by natural convection in a two-dimensional square cavity using a high order finite-volume method N90-19521
Application of a Reynolds stress turbulence model to the compressible shear layer
[NASA-CR-182002] N90-19537
An observational study of squall lines in the Amazon
[INPE-4865-TDL/376] N90-19723
CONVECTION CLOUDS
Cloud parameterization in EURAD and its future development N90-19692
CONVECTION CURRENTS
An optical white light speckle process in forward dispersion for measurement of the velocity field in free convective currents
[ETN-90-95913] N90-19546
CONVECTIVE HEAT TRANSFER
A parametric heat transfer study for cryogenic ball bearings in SSME HPOTP N90-19397
A method of estimating temperature profiles and chemical differentiation in the near surface layers of porous comet nuclei: First results for comet P/Churyumov-Gerasimenko N90-20013
CONVERGENCE
Techniques for studying the effects of microgravity on model particle/cell systems N90-19424
Banach C*-algebras not containing a subspace isomorphic to C(sub 0)
[DE90-610428] N90-19798
Convergence properties of iterative algorithms for solving the nodal diffusion equations
[DE89-016859] N90-19804
CONVERGENT-DIVERGENT NOZZLES
Static investigation of a two-dimensional convergent-divergent exhaust nozzle with multiaxis thrust-vectoring capability
[NASA-TP-2973] N90-19193
Computation of hypersonic unsteady viscous flow over a cylinder N90-19194
Internal performance of two nozzles utilizing gimbal concepts for thrust vectoring
[NASA-TP-2991] N90-19200
CONVULSIONS
Metabolism, seizures, and blood flow in brain following organophosphate exposure: Mechanisms of action and possible therapeutic agents
[AD-A217098] N90-19740
COORDINATES
Analysis and design of symmetrical airfoils
[PD-CF-8943] N90-19213
Development of a standardized three axis sensor for inertial data achievement for future flight rule systems
[ETN-90-96075] N90-19231
COPOLYMERS
Synthesis of poly(dimethylsiloxane) - nylon 6 diblock copolymers
[AD-A216850] N90-19367
An evaluation of ethylene-vinyl acetate copolymers as desensitizers for RDX in insensitive booster compositions prepared by slurry coating technology
[MRL-TR-89-33] N90-19385
COPPER
Nanolayer reactions in aluminum-metal interfaces
[DE90-004955] N90-19342
Defect structures in copper and gold irradiated with fast neutrons, 14 MeV neutrons and 600 to 800 MeV protons
[DE90-007529] N90-19359
COPPER OXIDES
Band electronic structures and crystal packing forces
[DE90-007669] N90-19898
Preparation and properties of the system Cu(x)Pd(1-x)O (0 less than or equal to x less than or equal to 0.175)
[AD-A217567] N90-19901
COPPER SELENIDES
Investigations of CuInSe2 thin films and contacts
[DE90-000301] N90-19886
CORE SAMPLING
Rosetta/CNSR, ESA's planetary cornerstone mission N90-19990
Design and development activities on the candidate sample acquisition system for the Rosetta mission N90-19993
Introduction to drilling technology N90-20002
Compressive strength of synthetic comet nucleus samples N90-20006
Rosetta/CNSR altimeter and sounding radar N90-20009
First impressions of the comet drilling problem N90-20021
Relevance of laboratory studies to comets N90-20023
CORIOLIS EFFECT
Finite element analysis of a quartz rotation sensor
[DE90-006959] N90-19562
CORRELATION
Correlation-induced changes of spectra
[AD-A217087] N90-19591
CORROSION PREVENTION
Mitigation of stress corrosion cracking of AISI 304 stainless steel in oxygenated water at 289 C by organic species at low concentration
[DE90-005631] N90-19354
CORROSION RESISTANCE
An attempt of improving high-temperature fatigue properties of Ni-Cr-W superalloys in HTGR helium
[DE90-741482] N90-19350
Heat-resistant and anticorrosive paint
[DE90-006077] N90-19369
COSMIC BACKGROUND EXPLORER SATELLITE
The COBE cosmic 3 K anisotropy experiment: A gravity wave and cosmic string probe N90-19959
COSMIC RAY SHOWERS
Search for anisotropies in the underground cosmic ray muon flux N90-20034
Cosmic ray composition and muon decoherence at the knee of the all-particle cosmic ray spectrum N90-20035
COSMIC RAYS
Measurement of cross sections: New needs and possibilities
[DE90-007248] N90-19829
The pregalactic cosmic gravitational wave background N90-19945
The space microwave interferometer and the search for cosmic background gravitational wave radiation N90-19952
Cosmic ray events in Soudan 2
[DE90-005657] N90-20037
JACEE long duration balloon flights
[DE90-006008] N90-20039
COSMIC X RAYS
Underground muons from the direction of Cygnus X-3
[DE90-005646] N90-20038
COSMOLOGY
Propagation of electromagnetic waves in multidimensional homogeneous cosmologies
[DE90-610474] N90-19462
The ultimate structure of matter: The high energy physics program from the 1950s through the 1980s
[DE90-005682] N90-19836
Dimensional transition of the universe
[DE90-741461] N90-19910
Cosmic string in compactified gauge theory
[DE90-741463] N90-19988
COULOMB POTENTIAL
Exchange and correlation effects in the Visscher-Falicov model for metal intercalated graphite
[DE90-610553] N90-19349
COUNTER-ROTATING WHEELS
Theory of gearing
[NASA-RP-1212] N90-19593
COUPLED MODES
Positioning control of highest accuracy for very dynamic coupled system
[ETN-90-95893] N90-19769
COUPLERS
Discontinuous-taper directional coupler
[AD-D014324] N90-19481
Optically tunable gratings for optical interconnects
[AD-A216978] N90-19844
COUPLING
Optically tunable gratings for optical interconnects
[AD-A216978] N90-19844
COUPLING COEFFICIENTS
Discontinuous-taper directional coupler
[AD-D014324] N90-19481
COVARIANCE
Comparison of artificial matrices and covariance functions
[ETN-90-95722] N90-19645
COVERINGS
Hatch cover
[NASA-CASE-MSC-21356-1] N90-19278
CRAB NEBULA
High energy x ray observations on the Crab nebula and the double star source GX 1+4
[ETN-90-95829] N90-19937

CRACK TIPS
Dislocation annihilation mechanism for the formation of dislocation free zone at a crack tip
[DE90-610552] N90-19615
CRACKS
Technology evaluation for space station atmospheric leakage
[DE90-007844] N90-19294
CREEP PROPERTIES
The creep behavior of an aramide fiber reinforced wound tow-strap
[LR-546] N90-19312
Radiation-induced density changes and creep in surface layers of glass
[DE90-008112] N90-19383
Evaluation of thermal cycling creep-fatigue damage for a molten salt receiver
[DE90-002907] N90-19670
CRITERIA
First impressions of the comet drilling problem N90-20021
CRITICAL EXPERIMENTS
Analysis and evaluation of ZPPR (Zero Power Physics Reactor) critical experiments for a 100 kilowatt-electric space reactor
[DE90-005634] N90-19835
CRITICAL FLOW
Experimental and analytical investigation of adiabatic critical water air two phase flow in small diameter tubes
[TB-88/1] N90-19540
CRITICAL MASS
Neon novae, recurrent novae, and type I supernovae
[DE90-003188] N90-19931
CRITICAL POINT
Vapor-liquid equilibria for complex mixtures with special emphasis on the critical region
[PB90-130345] N90-19324
CROP IDENTIFICATION
Segmentation of Side-Looking Airborne Radar (SLAR) images using a priori knowledge
[BCRS-89-03] N90-19644
CROSS CORRELATION
Spanwise measurements of vertical components of atmospheric turbulence
[NASA-TP-2963] N90-19718
CROSS FLOW
A streamwise upwind algorithm applied to vortical flow over a delta wing
[NASA-TM-102225] N90-19201
CROSSLINKING
Carbon black/polyethylene composites for PTC (Positive Temperature Coefficient) thermistor applications
[AD-A215988] N90-19307
CRUSTAL FRACTURES
Fracture mechanical aspects of dust emission processes from a model comet surface N90-20004
CRUSTS
Physical models of cometary nuclei: A review N90-19991
Crustal strength of different model comet materials N90-20003
CRYOGENIC COOLING
Reliability testing of the Hughes temperature controlled 1/4 watt split cycle cryogenic cooler (HD-1045 (V)/UA)
[AD-A216696] N90-19426
Mechano-caloric cooling device
[NASA-CR-186316] N90-19552
CRYOPUMPING
Mechano-caloric cooling device
[NASA-CR-186316] N90-19552
CRYSTAL DEFECTS
Search for far infrared radiation from optically pumped defect modes
[AD-A216976] N90-19643
Digital capacity transient spectroscopy of deep structure defects in III-V-Semiconductor structures
[ETN-90-96057] N90-19890
NMR (Nuclear Magnetic Resonance) imaging development for the study of solids
[AD-A217073] N90-19899
CRYSTAL DISLOCATIONS
Microstructural simulations of dynamic recrystallization
[DE90-007504] N90-19895
CRYSTAL GROWTH
Solid State Photovoltaic Research Branch
[DE89-009463] N90-19660
Opto-Em and devices investigation
[AD-A215033] N90-19814
Computer simulation of recrystallization in the presence of second phase particles
[DE90-007531] N90-19896
CRYSTAL LATTICES
The renormalization group and lattice QCD
[DE90-004860] N90-19905
CRYSTAL OSCILLATORS
Temperature compensated crystal oscillator (TCXO) with improved temperature compensation
[AD-D014334] N90-19482
CRYSTAL STRUCTURE
Creep behavior of alloys based on TiAl containing TiB2 and TiN particulates
[DE90-006489] N90-19355
Diffraction studies of the structure of glasses and liquids
[DE90-007862] N90-19381
Laser surface interactions of high-(Tc) superconductors
[DE90-006894] N90-19587
Supercomputer applications for materials science: Ordering effects of hydrogen in palladium
[DE90-004664] N90-19870
Neutron scattering measurements of the magnetic excitations of high-temperature superconducting materials
[DE90-006567] N90-19885
The effects of gradients on boundary stability
[DE90-007428] N90-19894
Band electronic structures and crystal packing forces
[DE90-007669] N90-19898
CRYSTAL SURFACES
An evaluation of ethylene-vinyl acetate copolymers as desensitizers for RDX in insensitive booster compositions prepared by slurry coating technology
[MRL-TR-89-33] N90-19385
CRYSTALLIZATION
Crystallization behavior and properties of BaO-Al2O3-2SiO2 glass matrices
[NASA-CR-185209] N90-19374
CRYSTALS
Synthesis and properties of a novel catalyst for the combustion of methane
[PB90-127499] N90-19320
CURRENT DENSITY
Ac loss measurements of two multifilamentary NbTi composite strands
[DE90-005388] N90-19304
Effects of nonuniform potential and current distributions in electrochemical systems
[DE90-007349] N90-19325
Characterization of thunderstorm induced Maxwell current densities in the middle atmosphere N90-19391
An electrical model for plasma armature voltage
[DE90-007530] N90-19866
Critical current density and transition temperature measurements of Y-Ba-Cu-O rods
[AD-A216695] N90-19875
CURRENT DISTRIBUTION
Effects of nonuniform potential and current distributions in electrochemical systems
[DE90-007349] N90-19325
CURVATURE
Theory of gearing
[NASA-RP-1212] N90-19593
CURVES
Theory of gearing
[NASA-RP-1212] N90-19593
CYCLOGENESIS
Simulation of a weather situation with high ozone concentrations during ALPEX N90-19686
Colloquium on Synoptic Meteorology
[PB90-121112] N90-19720
CYCLONES
Cyclogeneses and extratropical cyclones in the south-southeast region of Brazil and its influence in time
[INPE-4812-TDL/359] N90-19722
CYCLOTRON RESONANCE DEVICES
Design considerations in achieving 1 MW CW operation with a whispering-gallery-mode gyrotron
[DE90-007283] N90-19557
Progress in the CW operation of a 140 GHz gyrotron
[DE90-007382] N90-19558
CYGNUS CONSTELLATION
Search for anisotropies in the underground cosmic ray muon flux N90-20034
Underground muons from the direction of Cygnus X-3
[DE90-005646] N90-20038
CYLINDRICAL BODIES
Computational fluid dynamics method for low Reynolds number flow in a precessing/spinning, liquid filled cylinder with rounded endcaps
[AD-A216997] N90-19531
Jam resistant fluid power actuator for ballistic-damage tolerant redundant cylinder assemblies
[AD-D014360] N90-19600
CYLINDRICAL SHELLS
Steady state temperatures and thermal stresses in a spherical or cylindrical laminated shell
[ESDU-89027] N90-19612

D

DAMAGE
Jam resistant fluid power actuator for ballistic-damage tolerant redundant cylinder assemblies
[AD-D014360] N90-19600
Simulation fidelity in lightning penetration studies
[DE90-006367] N90-19731
Ion mixing and surface modification in metal-semiconductor systems
[DE90-007557] N90-19897
DAMPING
Oscillation and damping behavior of fine steel test tubes, with particular consideration to destruction free proofs from hydrogen fragilization
[ETN-90-95371] N90-19351
An experimental study of the aeroelastic behaviour of two parallel interfering circular cylinders N90-19609
DAMS
Technical and administrative feasibility of microlight remote sensing applications for river boards
[BCRS-89-01] N90-19643
DARK MATTER
The effects of cold dark matter on Big Bang nucleosynthesis N90-19749
DATA ACQUISITION
The Telecommunications and Data Acquisition Report
[NASA-CR-185033] N90-19434
Data reduction of GOES (Geostationary Operational Environmental Satellite) information from DCP (Data Collection Platform) networks
[AD-A215844] N90-19637
FOMA: A Fast Optical Multichannel Analyzer
[DE90-004093] N90-19839
Physical models of cometary nuclei: A review N90-19991
DATA BASE MANAGEMENT SYSTEMS
Data reduction of GOES (Geostationary Operational Environmental Satellite) information from DCP (Data Collection Platform) networks
[AD-A215844] N90-19637
Using Rexx to coordinate relational commands
[DE90-007589] N90-19772
Searching for existing nuclear data
[DE90-007535] N90-19925
Spectral solar radiation data base documentation
[DE89-009448] N90-20033
DATA BASES
Austempered ductile iron data base: A cooperative program between industry and the Trade Adjustment Assistance Program of the Department of Commerce
[PB90-115569] N90-19343
High throughput data communication system
[AD-D014342] N90-19432
Development of an Ada programming support environment database SEAD (Software Engineering and Ada Database) administration manual
[NASA-CR-186064] N90-19757
An equational language for specifying, querying, and updating database domains
[PB90-124694] N90-19918
Executive information systems for providing next generation strategic information: An evaluation of EIS (Executive Information System) software and recommended applicability within the FAA computing environment
[AD-A216672] N90-19920
CRISP (Computer Retrieval of Information on Scientific Projects) thesauras, fiscal year 1990
[PB90-138652] N90-19922
Spectral solar radiation data base documentation
[DE89-009448] N90-20033
DATA COLLECTION PLATFORMS
Data reduction of GOES (Geostationary Operational Environmental Satellite) information from DCP (Data Collection Platform) networks
[AD-A215844] N90-19637
DATA COMPRESSION
Evaluation and analysis of the orbital maneuvering vehicle video system N90-19411
DATA LINKS
Dynamic reconfiguration and link fault tolerance in a transputer network
[AD-A215105] N90-19433
Operational evaluation of initial data link air traffic control services, volume 1
[DOT/FAA/CT-90/1-VOL-1] N90-19472
User-friendly software for the design of digital line-of-sight radio links
[PB90-118472] N90-19760
High stability radio links N90-19970
DATA PROCESSING
GeoNet 88: Calculation connection system concept for the EURAD project N90-19688

Error detection in data processing devices by means of residue codes
[ETN-90-95370] N90-19767
Electron energy distributions and vibrational population distributions
[DE90-005550] N90-19825

DATA REDUCTION
PC-based PCM (Pulse Code Modulation) telemetry data reduction system hardware
[DE90-000316] N90-19273
Data reduction of GOES (Geostationary Operational Environmental Satellite) information from DCP (Data Collection Platform) networks
[AD-A215844] N90-19637

DATA STORAGE
A waveform capture and storage unit and its use for investigating disturbances on digital transmission links
[BBC-RD-1989/17] N90-19478

DATA TRANSMISSION
Performance of the all-digital data-transition tracking loop in the advanced receiver N90-19440
Operational evaluation of initial data link air traffic control services, volume 1
[DOT/FAA/CT-90/1-VOL-1] N90-19472

DAYTIME
Photon statistical limitations for daytime optical tracking N90-19442

DEAD RECKONING
Carin and GPS: The combination of dead reckoning, map matching and satellite navigation in a hybrid automobile navigation system
[ETN-90-95451] N90-19220

DECISION MAKING
Artificial intelligence issues related to automated computing operations N90-19404
Distributed detection by a large team of sensors in tandem
[AD-A216607] N90-19807
Executive information systems for providing next generation strategic information: An evaluation of EIS (Executive Information System) software and recommended applicability within the FAA computing environment
[AD-A216672] N90-19920

DECISION THEORY
Distributed detection by a large team of sensors in tandem
[AD-A216607] N90-19807

DECODERS
Memory management in traceback Viterbi decoders N90-19443
Quantization effects in Viterbi decoding rate 1/n convolutional codes N90-19445
Big Viterbi Decoder (BVD) results for (7,1/2) convolutional code N90-19446
Fast transform decoding of nonsystematic Reed-Solomon codes N90-19447

DECOMPOSITION
Determination of the mechanism of decomposition of energetic molecules
[AD-A217061] N90-19388
A comparison between the propagators method and the decomposition method for nonlinear equations
[DE90-005783] N90-19781

DEEP SPACE
High stability radio links N90-19970

DEEP SPACE NETWORK
The Telecommunications and Data Acquisition Report
[NASA-CR-185033] N90-19434
Determination of Earth orientation using the Global Positioning System N90-19435

DEFECTS
Defect structures in copper and gold irradiated with fast neutrons, 14 MeV neutrons and 600 to 800 MeV protons
[DE90-007529] N90-19359

DEFLECTION
Application of attachment modes in the control of large space structures
[NASA-CR-185604] N90-19280

DEFLECTORS
Literature file on fast kickers and SEPTA: Components for deflection and separation of particle beams
[LINO-162] N90-19924

DEFORMATION
Irradiation-induced amorphization and elastic shear instability in intermetallic compounds
[DE90-004845] N90-19341
Analysis of tectonic movements utilizing remote sensor products in the Southern Espinhaco (SE) region
[INPE-4830-PRE/1451] N90-19708
P-T condition fo deformation from fluid inclusions in mylonites
[NASA-CR-186377] N90-19710

DELTA WINGS
Unsteady aerodynamics of delta wings performing maneuvers to high angle of attack N90-19196
Leading edge vortex dynamics on a pitching delta wing
[NASA-CR-186327] N90-19198
A streamwise upwind algorithm applied to vortical flow over a delta wing
[NASA-TM-102225] N90-19201
Conical Euler solution for a highly-swept delta wing undergoing wing-rock motion
[NASA-TM-102609] N90-19211

DENSITY MEASUREMENT
Critical current density and transition temperature measurements of Y-Ba-Cu-O rods
[AD-A216695] N90-19875

DEOXYRIBONUCLEIC ACID
Potential biomedical application of the Los Alamos infrared free-electron laser: DNA spectroscopy
[DE90-006505] N90-19575

DEPLOYMENT
Structures for remotely deployable precision antennas N90-19256
Advances in large inflatable reflectors N90-19258
Kalman estimation for SEDS measurements N90-19393

DEPOSITION
The effect of fiber coatings on interfacial shear strength and the mechanical behavior of ceramic composites
[DE90-007574] N90-19380
NAPAP (National Acid Precipitation Assessment Program) emissions inventory: Overview of allocation factors, 1985
[PB90-126012] N90-19679
Analysis of tectonic movements utilizing remote sensor products in the Southern Espinhaco (SE) region
[INPE-4830-PRE/1451] N90-19708

DEPOSITS
Geochemical survey on faults overland with alluvial deposits, part 1. Application for the Neodani and the Atera faults survey
[DE89-782326] N90-19707

DEPTH MEASUREMENT
CO2 depth profiles in cometary model substances of KOSI N90-20014

DESIGN ANALYSIS
Solid oxide fuel cell cogeneration system conceptual design, program 2
[PB90-114968] N90-19653

DESORPTION
Electron stimulated O(-) desorption from O2 condensed on a rare-gas film: Evidence for an indirect Bounce trajectory
[AD-A216725] N90-19322
Experiments on oxygen desorption from surface warm seawater under Open-Cycle Ocean Thermal Energy Conversion (OC-OTEC) conditions
[DE90-000308] N90-19666

DEUTERONS
Distributed bosonic states and condensed matter fusion
[AD-A217605] N90-19868

DIAGNOSIS
Development and utilization of new diagnostics for dense-phase pneumatic transport
[DE90-006787] N90-19536

DIAMAGNETISM
Optical paramagnetic/diamagnetic gas sensor
[AD-D014368] N90-19554

DIAMETERS
Precision segmented reflector, figure verification sensor N90-19272

DIELECTRIC PROPERTIES
Discontinuous-taper directional coupler
[AD-D014324] N90-19481
Low temperature elastic and dielectric properties of incommensurate barium sodium niobate
[AD-A216969] N90-19815

DIELECTRICS
Fast optical switch and limiter using quantum size effect in metal grain composites
[AD-D014332] N90-19305
Heterogeneous composite and method of making
[AD-D014337] N90-19306
Alternate film dielectric materials
[DE90-007213] N90-19378
Thermal coefficient of delay for various coaxial and fiber-optic cables N90-19439
Electromagnetic properties of material coated surfaces
[NASA-CR-186466] N90-19486
Elastomeric electrical isolation membrane
[AD-D014365] N90-19490

DIESEL ENGINES
Development and use of an advanced coal-fueled diesel engine cycle simulation with group effects
[DE90-000450] N90-19607

DIFFERENTIAL EQUATIONS
A vectorized algorithm for 3D dynamics of a tethered satellite N90-19423
Chaotic transients, higher dimensional phenomena, and coupled ordinary differential equations
[DE90-006641] N90-19794
Differential operators associated with Gegenbauer polynomials. 3: The regular case
[DE90-610422] N90-19795
Longitudinal traveling waves bifurcating from Vlasov plasma equilibria N90-19850

DIFFUSE RADIATION
Spatially high-resolution flame diagnosis by means of spontaneous Raman spectroscopy
[ETN-90-95870] N90-19328

DIFFUSION
A new model for hydrogen absorption in welds
[AD-A216951] N90-19347
Frequency response of electrochemical cells N90-19419
Convergence properties of iterative algorithms for solving the nodal diffusion equations
[DE89-016859] N90-19804

DIFFUSION FLAMES
Numerical study of diffusion jet flames N90-19316
Investigation of the processes controlling the flame generation of refractory materials
[DE90-007564] N90-19333

DIFFUSION LENGTH
A simple model for the determination of L(sub 0), D and tau in a semiconductor and their temperature dependence
[DE90-610564] N90-19879

DIFFUSION WELDING
Time-dependent failure of silver-interlayer diffusion bonds between non-deforming base-metals
[DE90-006925] N90-19357

DIGITAL COMPUTERS
High throughput data communication system
[AD-D014342] N90-19432
High speed modem
[AD-D014319] N90-19750

DIGITAL DATA
A waveform capture and storage unit and its use for investigating disturbances on digital transmission links
[BBC-RD-1989/17] N90-19478
Thematic coupling between digital images and geographic information systems
[ETN-90-95723] N90-19646

DIGITAL ELECTRONICS
A gate array structure for the efficient project of digital circuits: The unit cell array
[ETN-90-95364] N90-19502

DIGITAL INTEGRATORS
Digital integrator
[DIGEL-1989-2] N90-19508

DIGITAL RADAR SYSTEMS
Automatic thresholding multichannel digital radar early warning system
[AD-D014323] N90-19431

DIGITAL SIMULATION
Flow simulation for aircraft
[NLR-MP-87082-U] N90-19543
Feasibility of using Extreme Ultraviolet Explorer (EUVE) reaction wheels to satisfy Space Infrared Telescope Facility (SIRTF) maneuver requirements
[NASA-TM-100389] N90-19556
Noise behavior of semiconductor lasers by optic feedback
[ETN-90-95726] N90-19583
Digital treatment of elastic-plastic structures by means of quadratic optimization processes from the finite element method
[ETN-90-95823] N90-19621
Initialization of EURAD. Part 1: Utilization of ECMWF analysis data N90-19695
Numerical modeling of atmospheric growth processes
[REPT-70] N90-19726
Digital simulation of a Boerline
[ISSN-0069-5882] N90-19729
Digital production of perspective images
[SER-C-347] N90-19768
Positioning control of highest accuracy for very dynamic coupled system
[ETN-90-95893] N90-19769
Numerical simulation of acoustic scatter from subsurface bubble clouds
[AD-A217068] N90-19822

DIGITAL SYSTEMS
High throughput data communication system
[AD-D014342] N90-19432
Performance of the all-digital data-transition tracking loop in the advanced receiver N90-19440
Costas loop lock detection in the advanced receiver N90-19441

High speed modem
[AD-D014319] N90-19750
User-friendly software for the design of digital line-of-sight radio links
[PB90-118472] N90-19760
Priority arbitration with busses
[AD-A216392] N90-19784

DIGITAL TECHNIQUES
Digital to position converter
[DIGEL-1984-4] N90-19509
Development of software routines for remote sensing digital image processing
[ETN-90-95452] N90-19640
User-friendly software for the design of digital line-of-sight radio links
[PB90-118472] N90-19760

DIGITAL TELEVISION
Digital video: Studio signal processing
[BBC-RD-1989/14] N90-19476
A digital HDTV recorder using a cluster of four D1 DVTRs
[BBC-RD-1989/13] N90-19477

DIODES
Power diode switching behavior
[ETN-90-95363] N90-19501
Experimental results of aging and thermal effects in high-power laser diodes
[DE90-005955] N90-19573

DIPOLE ANTENNAS
Dual frequency launcher for circularly polarized antenna
[AD-D014361] N90-19456

DIRECT CURRENT
Design of a high power density, permanent magnet, axial gap dc motor
[DE90-005449] N90-19514

DIRECTIONAL STABILITY
Yaw rate control of an air bearing vehicle N90-19420

DISK GALAXIES
Cometary bodies in the circumstellar disk around beta Pictoris N90-20010

DISK OPERATING SYSTEM (DOS)
PC-based PCM (Pulse Code Modulation) telemetry data reduction system hardware
[DE90-000316] N90-19273

DISPLAY DEVICES
Visual processing in texture segregation
[AD-A216539] N90-19737

DISSIPATION
Heterogeneous composite and method of making
[AD-D014337] N90-19306
On dissipative states in narrow current-carrying superconducting filaments
[ETN-90-95915] N90-19889

DISSOCIATION
Electron stimulated O(-) desorption from O2 condensed on a rare-gas film: Evidence for an indirect Bounce trajectory
[AD-A216725] N90-19322
Ion and electron interactions at thermal and suprathermal energies
[AD-A216905] N90-19323

DISTRIBUTED FEEDBACK LASERS
Noise behavior of semiconductor lasers by optic feedback
[ETN-90-95728] N90-19583

DISTRIBUTED PROCESSING
High-level connectionist models
[AD-A216581] N90-19751
Generic distributed systems model
[AD-A217078] N90-19773
Deceit: A flexible distributed file system
[NASA-CR-186412] N90-19923

DISTRIBUTION FUNCTIONS
Use of Coxian-type distributions in a general model of the maximum of bivariate random variables
[PB90-121229] N90-19780
Bose condensate in superfluid (sup 4)He and momentum distributions by deep inelastic scattering
[DE90-007541] N90-19832

DISTURBANCES
Disturbance torque rejection properties of the NASA/JPL 70-meter antenna axis servos N90-19450

DOCUMENTS
Augmenting and updating NASA spacelink electronic information system N90-19392
Topics in HPM (High-Power Microwave) generation, coupling, and interaction
[AD-A216682] N90-19658

DOPED CRYSTALS
Power diode switching behavior
[ETN-90-95363] N90-19501
Digital capacity transient spectroscopy of deep structure defects in III-V-Semiconductor structures
[ETN-90-96057] N90-19890

DOPPLER EFFECT
Coherent radar measurement of ocean currents from geostationary orbit N90-19259
Correlation-induced changes of spectra
[AD-A217087] N90-19591

DOPPLER RADAR
Advanced Doppler tracking experiments N90-19951
Tropospheric monitoring technology for gravity wave experiments N90-19971

DOSAGE
Study of hydrazine metabolism and toxicity
[AD-A217103] N90-19736

DOUBLE STARS
Speckle interferometry for high resolution pictures of astronomical objects
[ETN-90-95827] N90-19936
High energy x ray observations on the Crab nebula and the double star source GX 1+4
[ETN-90-95829] N90-19937

DRAG
Calculation of excrescence drag magnification due to pressure gradient at high subsonic speeds
[ESDU-87004] N90-19195

DRAG REDUCTION
Drag reduction by longitudinal riblets on the surface of a streamwise aligned body of revolution
[MPIS-MITT-92] N90-19210
Drag-free satellite control N90-19974

DRILL BITS
Design and development activities on the candidate sample acquisition system for the Rosetta mission N90-19993
Introduction to drilling technology N90-20002

DRILLING
Introduction to drilling technology N90-20002

DRILLS
Design and development activities on the candidate sample acquisition system for the Rosetta mission N90-19993
Compressive strength of synthetic comet nucleus samples N90-20006

DROP SIZE
On the question of spray effects N90-19691

DROPS (LIQUIDS)
Simulation of thermal dynamics of a vaporizing coal-water droplet in a combustor
[DE90-005356] N90-19317
Effects of turbulence mixing, variable properties, and vaporization on spray droplet combustion
[NASA-CR-186463] N90-19326

DUCTILITY
Austempered ductile iron data base: A cooperative program between industry and the Trade Adjustment Assistance Program of the Department of Commerce
[PB90-115569] N90-19343
Optimizing superplastic response in navalite, a lithium containing aluminum-magnesium alloy
[AD-A216552] N90-19346

DUST
Aeolian removal of dust from photovoltaic surfaces on Mars
[NASA-TM-102507] N90-19299
Mechanics of aeolian processes: Soil erosion and dust production N90-19410
Comet Halley: An optical continuum study N90-19981
Petrographic working model of the Rosetta sampling and modelling subgroup for a comet nucleus N90-19992
Comets: Dirty snowballs or icy dirtballs N90-19994
A test of the interstellar dust model of comets N90-19995
Physico-chemical properties of formaldehyde-ice-dust mixtures N90-20000
Cometary bodies in the circumstellar disk around beta Pictoris N90-20010
Low velocity dust-dust collisions N90-20011
Possible targeting of particle emission by mechanical stress and penetration of sublimating ice-dust-surfaces N90-20016
Gas diffusion in a cometary crust N90-20017
The composition of cometary nuclei N90-20022
Large impact events and atmospheric evolution on the terrestrial planets N90-20028

DUST STORMS
Aeolian removal of dust from photovoltaic surfaces on Mars
[NASA-TM-102507] N90-19299

DWARF GALAXIES
Photometric analyses of abundances in dwarf spheroidal galaxies and globular clusters N90-19978

DWARF STARS
Magnetic fields in late-type dwarfs: Preliminary results from a multiline approach
[SER-C-PREPUB-FASC-31] N90-19928

DYE LASERS
Investigation of a simulated tritium plasma using Coherent Anti-Stokes Raman Spectroscopy (CARS)
[DE90-005696] N90-19319
Blue upconversion thulium laser
[DE90-006517] N90-19584

DYNAMIC CHARACTERISTICS
Leading edge vortex dynamics on a pitching delta wing
[NASA-CR-186327] N90-19198
Compensating for pneumatic distortion in pressure sensing devices
[NASA-TM-101716] N90-19224
Performance of an optimized rotor blade at off-design flight conditions
[NASA-CR-4288] N90-19226
Low-speed wind-tunnel investigation of the flight dynamic characteristics of an advanced turboprop business/commuter aircraft configuration
[NASA-TP-2982] N90-19239

DYNAMIC CONTROL
Advanced topics in structural dynamics: The maneuver of flexible spacecraft, and on-off decentralized control of flexible structures N90-19274
Kinematic control of robotic manipulators with multiple interchangeable wrists N90-19592

DYNAMIC LOADS
Influence of friction and separation phenomena on the dynamic blade loading of transonic turbine cascades
[MITT-88-04] N90-19235

DYNAMIC MODELS
Feasibility of using Extreme Ultraviolet Explorer (EUVE) reaction wheels to satisfy Space Infrared Telescope Facility (SIRTF) maneuver requirements
[NASA-TM-100389] N90-19556

DYNAMIC RESPONSE
Advanced topics in structural dynamics: The maneuver of flexible spacecraft, and on-off decentralized control of flexible structures N90-19274
Application of attachment modes in the control of large space structures
[NASA-CR-185604] N90-19280
Applications of frequency and wavenumber nonlinear digital signal processing to nonlinear hydrodynamics research
[AD-A216259] N90-19530
Study of the optimization of reference parameters to the dynamic constraints of solar panels
[INPE-4793-TDL/355] N90-19656

DYNAMIC STABILITY
The effects of gradients on boundary stability
[DE90-007428] N90-19894

DYNAMIC STRUCTURAL ANALYSIS
Remote Attitude Measurement Sensor (RAMS) N90-19271
Advanced topics in structural dynamics: The maneuver of flexible spacecraft, and on-off decentralized control of flexible structures N90-19274
Investigation of SSME alternate high pressure fuel turbopump lift-off seal fluid and structural dynamic interaction N90-19400
An experimental study of the aeroelastic behaviour of two parallel interfering circular cylinders N90-19609
Modal analysis of nonprismatic beams: Uniform segment method
[AD-A216952] N90-19614

DYNAMICAL SYSTEMS
A PBL-radiation model for application to regional numerical weather prediction N90-19394
Development of dynamic equivalent network structures with a universal identification and optimization process
[ETN-90-95822] N90-19507

E

EARLY WARNING SYSTEMS
Automatic thresholding multichannel digital radar early warning system
[AD-D014323] N90-19431

EARTH ATMOSPHERE
Large impact events and atmospheric evolution on the terrestrial planets N90-20028

EARTH CRUST
Stored mafic/ultramafic crust and early Archean mantle depletion
[NASA-CR-186460] N90-19715

EARTH IONOSPHERE
Incoherent retrodiffusion of radiowaves in plasma with particle impulse
[ETN-90-95375] N90-19864

EARTH MAGNETOSPHERE
Active probing of space plasmas
[AD-A216867] N90-19855

EARTH OBSERVATIONS (FROM SPACE)
ESRIN
[ESA-BR-58] N90-19631
Visibility problems in numerical models of terrain
[INPE-4921-TDL/382] N90-19919
EARTH ORBITS
Series reversion/inversion of Lambert's time function
[AD-A216243] N90-19245
Low earth orbiting satellite for international information exchange system
[DE90-007186] N90-19292
EARTH RESOURCES
Sensitivity of ecological landscapes and regions to global climatic change
[PB90-120072] N90-19674
EARTH ROTATION
Determination of Earth orientation using the Global Positioning System N90-19435
EARTH SURFACE
Mechanics of aeolian processes: Soil erosion and dust production N90-19410
EARTH TIDES
Earth tidal analysis based on gravimeter observations and the influence of ocean tides
[ETN-90-95721] N90-19734
ECOLOGY
Sensitivity of ecological landscapes and regions to global climatic change
[PB90-120072] N90-19674
ECONOMIC ANALYSIS
Solid oxide fuel cell cogeneration system conceptual design, program 2
[PB90-114968] N90-19653
ECONOMICS
Survey on the social and economic influences of wide-spreading heat-pump technology
[DE89-782294] N90-19526
ECONOMY
Advancing automation and robotics technology for the Space Station Freedom and for the US economy: Submitted to the United States Congress
[NASA-TM-101647] N90-19279
ECOSYSTEMS
Sensitivity of ecological landscapes and regions to global climatic change
[PB90-120072] N90-19674
Proceedings of the 2nd United States/USSR Symposium on Air Pollution Effects on Vegetation Including Forest Ecosystems
[PB90-127119] N90-19678
EDGE DISLOCATIONS
Dislocation annihilation mechanism for the formation of dislocation free zone at a crack tip
[DE90-610552] N90-19615
EIGENVALUES
Initialization of EURAD. Part 1: Utilization of ECMWF analysis data N90-19695
EINSTEIN EQUATIONS
On Einsteinization of background curved space in the induced quantum gravity
[DE90-610477] N90-19907
Dimensional transition of the universe
[DE90-741461] N90-19910
Linearized analysis of (2+1)-dimensional Einstein-Maxwell theory
[DE90-741470] N90-19913
Experimental constraints on metric and non-metric theories of gravity N90-19946
Gravitational consequences of modern field theories N90-19947
Applied general relativity N90-19950
ELASTIC DEFORMATION
Three-dimensional Fe analysis of the surface distribution in notched compact samples of 20 MnMoNi 55
[W-1/89] N90-19625
ELASTIC PROPERTIES
Elastic solutions in a semi-infinite solid with an ellipsoidal inclusion
[AD-A217063] N90-19338
Elastic properties of silica xerogels
[AD-A216528] N90-19366
A transient plasticity study and low cycle fatigue analysis of the Space Station Freedom photovoltaic solar array blanket
[NASA-TM-102516] N90-19617
Error analysis of some Galerkin least squares methods for the elasticity equations
[DE90-608611] N90-19790
Low temperature elastic and dielectric properties of incommensurate barium sodium niobate
[AD-A216969] N90-19815
ELASTIC SCATTERING
Background studies in gas ionizing x ray detectors N90-19399
The electron momentum-transfer cross sections of tungsten, silicon, and silicon dioxide at energies from 0.1 to 10,000 eV
[DE90-009041] N90-19833
ELASTIC SHELLS
Development of finished beam and shell elements from engineering models for structures under high inelastic deformations
[ETN-90-95377] N90-19619
ELASTIC WAVES
A study on upstream moving pressure waves induced by vortex separation
[ISL-CO-203/88] N90-19192
ELASTOMERS
Elastic recovery and polymer-polymer interactions
[AD-A217085] N90-19384
Elastomeric electrical isolation membrane
[AD-D014365] N90-19490
ELASTOPLASTICITY
Development of finished beam and shell elements from engineering models for structures under high inelastic deformations
[ETN-90-95377] N90-19619
Digital treatment of elastic-plastic structures by means of quadratic optimization processes from the finite element method
[ETN-90-95823] N90-19621
Development of finite beam and shell elements for structures under great inelastic deformations
[ETN-90-95869] N90-19623
ELECTRIC ARCS
Proposal of arc driving type fault current limiter
[DE89-782290] N90-19485
ELECTRIC CONNECTORS
Elastomeric electrical isolation membrane
[AD-D014365] N90-19490
Modeling A circuit switched multiprocessor interconnect
[AD-A217122] N90-19519
Random access transmission algorithms for data local area networks
[AD-A216443] N90-19761
ELECTRIC CONTACTS
Contact formation on (Hg,Cd) Te
[AD-A217088] N90-19900
ELECTRIC FIELDS
Causality of plasma permittivity with loss and restoring terms
[NASA-TM-101671] N90-19453
Two-dimensional, long-pulse computer calculation of microwave-induced electron layer formation in low-pressure air
[DE90-005994] N90-19459
Numerical simulation of cross field amplifiers
[DE90-006459] N90-19496
Field effect transistor structures based on strain induced polarization charges
[DE90-007247] N90-19515
Energy transfer and photochemistry in biomimetic solar conversion
[PB90-114562] N90-19652
Ionospheric heating with oblique waves. Volume 1: Electron density perturbations
[AD-A216260] N90-19709
ELECTRIC MOTORS
Design of a high power density, permanent magnet, axial gap dc motor
[DE90-005449] N90-19514
ELECTRIC NETWORKS
Development of dynamic equivalent network structures with a universal identification and optimization process
[ETN-90-95822] N90-19507
Modeling A circuit switched multiprocessor interconnect
[AD-A217122] N90-19519
Parallel methods for solving nonlinear block bordered systems of equations
[AD-A217062] N90-19806
ELECTRIC POTENTIAL
Simple analytic potentials for linear ion traps N90-19436
Lightning surge characteristics of transmission towers. Lightning surge characteristics of 15-meter-high scale model tower
[DE89-782322] N90-19721
An electrical model for plasma armature voltage
[DE90-007530] N90-19866
Tunneling microscopy of submonolayer adsorbates on Si3
[AD-A216985] N90-19876
ELECTRIC POWER PLANTS
Vision for the introduction of the wind power generation system. Survey on the prospective market, part 2
[DE89-910386] N90-19651
ELECTRIC POWER SUPPLIES
Development of dynamic equivalent network structures with a universal identification and optimization process
[ETN-90-95822] N90-19507
ELECTRIC POWER TRANSMISSION
Proposal of arc driving type fault current limiter
[DE89-782290] N90-19485
Lightning surge characteristics of transmission towers. Lightning surge characteristics of 15-meter-high scale model tower
[DE89-782322] N90-19721
ELECTRICAL FAULTS
Proposal of arc driving type fault current limiter
[DE89-782290] N90-19485
ELECTRICAL IMPEDANCE
Impedance characteristics of terawatt ion diodes
[DE90-006276] N90-19494
A contribution to the theory of transient conductor simulations
[ETN-90-95891] N90-19511
ELECTRICAL INSULATION
Elastomeric electrical isolation membrane
[AD-D014365] N90-19490
ELECTRICAL MEASUREMENT
High voltage pickup plate
[LINO-1989-3] N90-19510
ELECTRICAL PROPERTIES
Zirconia-based electrodes for solid oxide fuel cells
[DE90-000462] N90-19513
ELECTRICAL RESISTANCE
A digitally controlled system for effecting and presenting a selected electrical resistance
[NASA-CASE-MFS-29149-1] N90-19492
ELECTRICAL RESISTIVITY
Fast optical switch and limiter using quantum size effect in metal grain composites
[AD-D014332] N90-19305
Heterogeneous composite and method of making
[AD-D014337] N90-19306
Electrical resistivity of strongly coupled plasmas in intense fields
[DE90-002236] N90-19861
ELECTRICITY
Conductive polymers of transition-metal complexes coordinated by a Diamino-Dichalcogen-Benzene compound
[AD-D014326] N90-19360
ELECTRO-OPTICS
The III-V semiconductor quantum well lasers and related optoelectronic devices on silicon
[AD-A216980] N90-19570
Opto-Em and devices investigation
[AD-A215033] N90-19814
ELECTROACOUSTIC TRANSDUCERS
Foundations of millimeter-wave frequency acoustic microscopy N90-19816
ELECTROCATALYSTS
Gas cooled fuel cell systems technology development program
[DE90-000446] N90-19668
ELECTROCHEMICAL CELLS
Effects of nonuniform potential and current distributions in electrochemical systems
[DE90-007349] N90-19325
Frequency response of electrochemical cells N90-19419
Advanced double layer capacitor
[AD-A217110] N90-19518
ELECTROCHEMICAL OXIDATION
International conference on Surface Modification of Metals by Ion Beams
[AD-A215872] N90-19345
ELECTROCHEMISTRY
Evaluation of radiation-induced sensitization using electrochemical potentiokinetic reactivation technique for austenitic stainless steels
[DE90-002708] N90-19352
Linear free energy relations for multielectron transfer kinetics: A brief look at the Bronsted/Tafel analogy
[AD-A215078] N90-19823
ELECTRODES
Studies of photochemically and electrochemically driven electron transport in zeolites
[DE90-007659] N90-19335
Characterization of reaction kinetics in a porous electrode
[NASA-CR-186504] N90-19340
Frequency response of electrochemical cells N90-19419
Zirconia-based electrodes for solid oxide fuel cells
[DE90-000462] N90-19513
Advanced double layer capacitor
[AD-A217110] N90-19518

ELECTROLYSIS
IEA (International Energy Agency) implementing agreement for a program of research and development on the production of hydrogen from water. Task 9: Hydrogen production
[DE90-007354] N90-19337
ELECTROMAGNETIC FIELDS
Muzzle shunt augmentation of conventional railguns
[DE90-007505] N90-19248
Radiation of electromagnetic waves by an accelerated charged particle in medium
[DE90-610458] N90-19461
Finite element analysis of a quartz rotation sensor
[DE90-006959] N90-19582
ELECTROMAGNETIC PROPERTIES
Electromagnetic properties of material coated surfaces
[NASA-CR-186466] N90-19466
ELECTROMAGNETIC PROPULSION
Proceedings of a contractors meeting on Combustion Rocket Propulsion Diagnostics of Reacting Flow
[AD-A216445] N90-19297
ELECTROMAGNETIC RADIATION
Apparatus and method for minimizing polarization-induced signal fading in an interferometric fiber-optic sensor using input-polarization modulation
[AD-D014315] N90-19430
Propagation of electromagnetic waves in multidimensional homogeneous cosmologies
[DE90-610474] N90-19462
ELECTROMAGNETIC SCATTERING
A combined finite element-boundary element formulation for solution of two-dimensional problems via CGFFT
[NASA-CR-186464] N90-19309
ELECTROMAGNETIC WAVE FILTERS
Internal transmission line filter element
[AD-D014353] N90-19489
ELECTROMAGNETIC WAVE TRANSMISSION
Propagation of electromagnetic waves in multidimensional homogeneous cosmologies
[DE90-610474] N90-19462
Vector circuit theory for multilayered isotropic and chiral structures: Reflection and transmission
[PB90-122474] N90-19495
Active probing of space plasmas
[AD-A216867] N90-19855
ELECTROMAGNETISM
Earth Science Geostationary Platform Technology
[NASA-CP-3040] N90-19249
Large space antenna concepts for ESGP N90-19253
Potential theory of radiation N90-19395
Radar transponder antenna pattern analysis for the space shuttle N90-19414
ELECTROMECHANICAL DEVICES
Induction motor control
[NASA-TM-102533] N90-19234
ELECTRON ATTACHMENT
Ion and electron interactions at thermal and suprathermal energies
[AD-A216905] N90-19323
ELECTRON BEAMS
Anode plasma formation as a possible mechanism for an electrical stress limit in cold cathode diodes
[DE90-007503] N90-19516
Time resolved gain/loss studies under low and high power loading for the XeF C-A transition
[DE90-007506] N90-19517
On 140 GHz microwave FEL experiments using ELF-2
[DE90-006764] N90-19576
First direct observation of FEL (Free-Electron Laser) from lambda=20 to 45 microns
[DE90-007508] N90-19589
The EGS4 Code System: Solution of gamma-ray and electron transport problems
[DE90-008100] N90-19838
ELECTRON CAPTURE
The electron momentum-transfer cross sections of tungsten, silicon, and silicon dioxide at energies from 0.1 to 10,000 eV
[DE90-009041] N90-19833
ELECTRON CYCLOTRON HEATING
Design considerations in achieving 1 MW CW operation with a whispering-gallery-mode gyrotron
[DE90-007283] N90-19557
ELECTRON DENSITY (CONCENTRATION)
Two-dimensional, long-pulse computer calculation of microwave-induced electron layer formation in low-pressure air
[DE90-005994] N90-19459
Ionospheric heating with oblique waves. Volume 1: Electron density perturbations
[AD-A216260] N90-19709
ELECTRON EMISSION
Particle emission by oblique ion bombardment of gold
[ETN-90-95625] N90-19827
ELECTRON ENERGY
Electron stimulated O(-) desorption from O2 condensed on a rare-gas film: Evidence for an indirect Bounce trajectory
[AD-A216725] N90-19322
Electron energy distributions and vibrational population distributions
[DE90-005550] N90-19825
The electron momentum-transfer cross sections of tungsten, silicon, and silicon dioxide at energies from 0.1 to 10,000 eV
[DE90-009041] N90-19833
ELECTRON GAS
Exchange and correlation effects in the Visscher-Falicov model for metal intercalated graphite
[DE90-610553] N90-19349
ELECTRON GUNS
High voltage pickup plate
[LINO-1989-3] N90-19510
ELECTRON MOBILITY
Anomalous transport in toroidal plasmas
[DE90-006549] N90-19859
ELECTRON PHONON INTERACTIONS
Superconductivity in Ba(1-x)BiO3
[DE90-003781] N90-19869
ELECTRON PUMPING
Charge pumping as a measurement method for the characterization of short channel MOSFETS: Review, development, and comparison of measurement process
[ETN-90-95726] N90-19504
ELECTRON RECOMBINATION
Charge pumping as a measurement method for the characterization of short channel MOSFETS: Review, development, and comparison of measurement process
[ETN-90-95726] N90-19504
ELECTRON SCATTERING
Background studies in gas ionizing x ray detectors N90-19399
The 41st Annual Gaseous Electronics Conference
[AD-A214540] N90-19851
ELECTRON TRAJECTORIES
Electron stimulated O(-) desorption from O2 condensed on a rare-gas film: Evidence for an indirect Bounce trajectory
[AD-A216725] N90-19322
ELECTRON TRANSFER
Studies of photochemically and electrochemically driven electron transport in zeolites
[DE90-007659] N90-19335
Energy transfer and photochemistry in biomimetic solar conversion
[PB90-114562] N90-19652
Linear free energy relations for multielectron transfer kinetics: A brief look at the Bronsted/Tafel analogy
[AD-A215078] N90-19823
ELECTRON TUNNELING
Tunneling microscopy of submonolayer adsorbates on Si9
[AD-A216985] N90-19876
ELECTRON-ION RECOMBINATION
Ion and electron interactions at thermal and suprathermal energies
[AD-A216905] N90-19323
ELECTRONIC EQUIPMENT
Preparation and characterization of alumina films prepared by a novel spray pyrolysis method
[AD-A217570] N90-19339
Influence of the parameters: Charge order, sequence classification, partial sequential circuit, and process regularity of a working charge (Gaussian process) on the lifetime of a component made of 3.1354 T3 and 3.4377 T76
[ETN-90-95378] N90-19503
Passivating layer for III-V semiconductor materials
[AD-D014321] N90-19872
ELECTRONIC EQUIPMENT TESTS
SINA: A test system for proximity fuses
[FEL-1989-101] N90-19498
ELECTRONS
Identification and solution of a charging problem in a high-altitude detector
[DE90-008637] N90-19296
Effect of electron-excitation on radiation damage in ion-irradiated FCC metals
[DE90-719537] N90-19344
Causality of plasma permittivity with loss and restoring terms
[NASA-TM-101671] N90-19453
Preparation and properties of the system Cu(x)Pd(1-x)O (0 less than or equal to x less than or equal to 0.175)
[AD-A217567] N90-19901
ELECTROPHYSICS
The 41st Annual Gaseous Electronics Conference
[AD-A214540] N90-19851
ELECTROSTATIC PROBES
Ion and electron interactions at thermal and suprathermal energies
[AD-A216905] N90-19323
ELECTROSTATIC WAVES
Nonlinear interaction of electrostatic waves at a narrow inhomogeneous layer of a warm magnetoactive plasma
[DE90-610624] N90-19857
ELECTROSTATICS
Large-diameter geostationary millimeter wavelength antenna concept N90-19254
ELLIPTIC FUNCTIONS
The p- and h-p versions of the finite element method: An overview
[AD-A216902] N90-19789
ELLIPTICAL POLARIZATION
Integrated optics anisotropic waveguides and devices
[AD-A217064] N90-19849
ELONGATION
Elastic recovery and polymer-polymer interactions
[AD-A217085] N90-19384
EMISSION
Effect of barrier layers in burn-through experiments with 351-nm laser illumination
[DE90-006806] N90-19577
EMISSION SPECTRA
Noise behavior of semiconductor lasers by optic feedback
[ETN-90-95728] N90-19583
Far-ultraviolet spectroscopy of Comet Halley N90-19979
ENCAPSULATING
Object Oriented Programming Systems (OOPS) and frame representations: An investigation of programming paradigms
[NASA-CR-186084] N90-19758
END EFFECTORS
Kinematic control of robotic manipulators with multiple interchangeable wrists N90-19592
Advanced control schemes and kinematic analysis for a kinematically redundant 7 DOF manipulator
[NASA-CR-186175] N90-19599
ENERGY CONSERVATION
Operational fact-finding report on heat pump systems for industrial use
[DE89-782295] N90-19527
A preliminary analysis of US CO2 emissions reduction potential from energy conservation and the substitution of natural gas for coal in the period to 2010
[DOE/NBB-0085] N90-19673
ENERGY CONSUMPTION
Advanced absorption technology development in the United States
[DE90-001336] N90-19428
Survey on the possibility of introducing new energy to regional development plans
[DE89-782627] N90-19654
ENERGY CONVERSION
Phase control mechanism for wave energy conversion
[AD-D014354] N90-19657
ENERGY CONVERSION EFFICIENCY
Advanced absorption technology development in the United States
[DE90-001336] N90-19428
ENERGY DISSIPATION
Muzzle shunt augmentation of conventional railguns
[DE90-007505] N90-19248
ENERGY DISTRIBUTION
Electron energy distributions and vibrational population distributions
[DE90-005550] N90-19825
ENERGY LEVELS
Coherent state in the roton region of superfluid helium-4
[DE90-610677] N90-19882
ENERGY POLICY
Analysis of competition among kinds of energy at the era of complexed energy. (Report on overseas study)
[DE89-910213] N90-19650
Pyranometry
[DWD-14] N90-19661
ENERGY SPECTRA
Background studies in gas ionizing x ray detectors N90-19399
Cosmic ray composition and muon decoherence at the knee of the all-particle cosmic ray spectrum N90-20035
ENERGY TECHNOLOGY
Operational fact-finding report on heat pump systems for industrial use
[DE89-782295] N90-19527
Solid oxide fuel cell cogeneration system conceptual design, program 2
[PB90-114968] N90-19653

A preliminary analysis of US CO2 emissions reduction potential from energy conservation and the substitution of natural gas for coal in the period to 2010
[DOE/NBB-0085] N90-19673

ENERGY TRANSFER
Energy transfer and photochemistry in biomimetic solar conversion
[PB90-114562] N90-19652

ENGINE DESIGN
Investigation of SSME alternate high pressure fuel turbopump lift-off seal fluid and structural dynamic interaction N90-19400
Monostable electrovalve
[INPE-4928-RPE/595] N90-19487
Low cost Brayton engine for gas-fired cogeneration system, phase 1
[PB90-127457] N90-19655

ENGINE PARTS
Development of inspection techniques for quantitatively measuring surface contamination on SRM hardware
[NASA-CR-183902] N90-19608

ENGINE TESTS
The Uniform Engine Test Programme
[AGARD-AR-248] N90-19232
Iterative procedures for space shuttle main engine performance models N90-19416

ENTHALPY
Vapor-liquid equilibria for complex mixtures with special emphasis on the critical region
[PB90-130345] N90-19324

ENTRAINMENT
Leading edge vortex dynamics on a pitching delta wing
[NASA-CR-186327] N90-19198
A review of models for the analysis of the injection of densely loaded flows into entrained flow gasifiers
[DE90-000453] N90-19550

ENUMERATION
The 0-1 multiknapsack problem: Heuristic and reduction methods
[INPE-4894-PRE/1495] N90-19782

ENVIRONMENT EFFECTS
Sensitivity of ecological landscapes and regions to global climatic change
[PB90-120072] N90-19674

ENVIRONMENT PROTECTION
Proceedings of the 2nd United States/USSR Symposium on Air Pollution Effects on Vegetation Including Forest Ecosystems
[PB90-127119] N90-19678

ENVIRONMENT SIMULATION
The EURAD Model: Structure and First Results
[REPT-61] N90-19680
Simulation of the propagation of radiactive substances from the example of Chernobyl (USSR) N90-19685
Fracture mechanical aspects of dust emission processes from a model comet surface N90-20004

ENVIRONMENTAL MONITORING
Real time environment monitoring using data from METEOSAT and NOAA imaging satellites
[NLR-MP-87070-U] N90-19672

EPITAXY
Passivating layer for III-V semiconductor materials
[AD-D014321] N90-19872
Heteroepitaxial growth of germanium films by supersonic free jet chemical beam epitaxy
[DE90-006621] N90-19877

EQUATIONS OF MOTION
A vectorized algorithm for 3D dynamics of a tethered satellite N90-19423
Causality of plasma permittivity with loss and restoring terms
[NASA-TM-101671] N90-19453
Nonlinear continuum mechanics and applied analysis
[AD-A213629] N90-19812

EQUATIONS OF STATE
Vapor-liquid equilibria for complex mixtures with special emphasis on the critical region
[PB90-130345] N90-19324
Numerical modelling of shocks in gases and metals
[MRL-RR-8-89] N90-19528

EQUILIBRIUM FLOW
Siphon flows in isolated magnetic flux tubes. 3: The equilibrium path of the flux tube arch
[NASA-CR-186297] N90-19813

EQUIPMENT SPECIFICATIONS
Design of a pyrometer for temperature measurements on the solid fuel combustion chamber
[LR-530] N90-19561

EQUIVALENCE
Experimental constraints on metric and non-metric theories of gravity N90-19946
The Stanford equivalence principle program N90-19963
Superconducting gravity gradiometer and a test of inverse square law N90-19975

EQUIVALENT CIRCUITS
Vector circuit theory for multilayered isotropic and chiral structures: Reflection and transmission
[PB90-122474] N90-19495

ERBIUM ISOTOPES
Optogalvanic laser spectroscopic and interference spectroscopic experiments of isotope gap and hyperfine structure for spectrum of Europium 1 and Erbium 2
[ETN-90-95358] N90-19327

EROSION
Evaluation of the response of aluminum alloys to single and multiple particle impacts
[DE90-003689] N90-19626

ERROR ANALYSIS
Error analysis of some Galerkin least squares methods for the elasticity equations
[DE90-608611] N90-19790

ERROR CORRECTING CODES
Fast transform decoding of nonsystematic Reed-Solomon codes N90-19447
Local area network with fault-checking, priorities, and redundant backup
[NASA-CASE-NPO-16949-1-CU] N90-19776

ERROR DETECTION CODES
Error detection in data processing devices by means of residue codes
[ETN-90-95370] N90-19767
Local area network with fault-checking, priorities, and redundant backup
[NASA-CASE-NPO-16949-1-CU] N90-19776

ERRORS
Determination of Earth orientation using the Global Positioning System N90-19435
Disturbance torque rejection properties of the NASA/JPL 70-meter antenna axis servos N90-19450
Marginal test and analysis of DRAM with masked alpha radiation
[RB-4180] N90-19754

ESA SATELLITES
Compendium of meteorological space programs, satellites, and experiments
[NASA-TM-102924] N90-19243

ESA SPACECRAFT
Rosetta/CNSR, ESA's planetary cornerstone mission N90-19990

ESTIMATING
Methods for trend analysis: Examples with problem/failure data N90-19396
Survey on the social and economic influences of wide-spreading heat-pump technology
[DE89-782294] N90-19526

ETCHING
Oxygenation and possible etching of high T(sub c) superconducting films by oxygen plasma
[DE90-004956] N90-19871

ETHYL ALCOHOL
In-flight evaluations of turbine fuel extenders
[DOT/FAA/CT-89/33] N90-19387

EULER EQUATIONS OF MOTION
Implementation of a finite element process for the Euler equations of the gas dynamics
[PREPRINT-500] N90-19545

EUROPE
The EURAD Model: Structure and First Results
[REPT-61] N90-19680
Development and status of the EURAD project N90-19681

EUROPEAN SPACE AGENCY
ESRIN
[ESA-BR-58] N90-19631

EUROPEAN SPACE PROGRAMS
TOPAS preparation study: Summary representation of the study results
[OHB-TN-TOP-011/87] N90-19244
Project for the European space organization in the area of space debris
[REPT-29/89] N90-19290
Physics and Mechanics of Cometary Materials
[ESA-SP-302] N90-19989
Rosetta/CNSR altimeter and sounding radar N90-20009
First impressions of the comet drilling problem N90-20021

EUROPIUM ISOTOPES
Optogalvanic laser spectroscopic and interference spectroscopic experiments of isotope gap and hyperfine structure for spectrum of Europium 1 and Erbium 2
[ETN-90-95358] N90-19327

EVALUATION
First impressions of the comet drilling problem N90-20021

EVOLUTION (DEVELOPMENT)
Physical models of cometary nuclei: A review N90-19991
Physical processes in cometary ices inferred from laboratory studies N90-19996
Laboratory studies of cometary ice analogues N90-19997
Evolution of ices and carbonaceous materials in the laboratory and in comets N90-19998

EXCITATION
Time resolved gain/loss studies under low and high power loading for the XeF C-A transition
[DE90-007506] N90-19517
Goldstone excitation and symmetry breaking mechanism in superfluid He-4
[DE90-610676] N90-19881

EXHAUST EMISSION
A preliminary analysis of US CO2 emissions reduction potential from energy conservation and the substitution of natural gas for coal in the period to 2010
[DOE/NBB-0085] N90-19673

EXHAUST GASES
Estimation of the distribution of SO2 and NOX emission in Europe N90-19699
Emission data for the EURAD project N90-19700

EXHAUST NOZZLES
Static investigation of a two-dimensional convergent-divergent exhaust nozzle with multiaxis thrust-vectoring capability
[NASA-TP-2973] N90-19193

EXOSAT SATELLITE
Analysis of an observation of the x ray astronomy satellite EXOSAT at the low mass x ray binary star system GX5-1
[ETN-90-95828] N90-20042

EXOTHERMIC REACTIONS
Numerical study of diffusion jet flames N90-19316

EXPERIMENT DESIGN
The Advanced Composition Explorer
[DE90-006522] N90-19987

EXPERIMENTATION
Low velocity dust-dust collisions N90-20011

EXPERT SYSTEMS
A rule-based paradigm for intelligent adaptive flight control N90-19238
Artificial intelligence issues related to automated computing operations N90-19404
Flight crew aiding for recovery from subsystem failures
[NASA-CR-181905] N90-19741

EXPLORER SATELLITES
The Advanced Composition Explorer
[DE90-006522] N90-19987

EXPLOSIONS
Safety Status Report for the Ulysses mission. Book 2: Accident analysis-appendices. General purpose heat source radioisotope thermoelectric generator program
[DE90-006830] N90-19286
Present and future risk of collision of satellites and manned platforms with other space objects and particles in terrestrial orbit
[R-8840] N90-19288

EXTERNAL STORES
Water-tunnel investigation of concepts for alleviation of adverse inlet spillage interactions with external stores
[NASA-TM-4181] N90-19199

EXTRAVEHICULAR ACTIVITY
Working on the moon: The Apollo experience
[DE90-003662] N90-19744

EXTREME ULTRAVIOLET EXPLORER SATELLITE
Feasibility of using Extreme Ultraviolet Explorer (EUVE) reaction wheels to satisfy Space Infrared Telescope Facility (SIRTF) maneuver requirements
[NASA-TM-100389] N90-19556

EXTRUDING
Deformation and fracture of TiAl + W at elevated temperatures
[DE90-006490] N90-19358
Novel processing of HTS based conductors
[DE90-005956] N90-19892

F

FABRICATION
Unfurlable, continuous-surface reflector concept N90-19257
Silicon carbide semiconductor device fabrication and characterization
[NASA-CR-186354] N90-19873

FAILURE
Effect of temperature on the storage life of polysulfide aircraft sealants
[MRL-TR-89-31] N90-19364

FAILURE ANALYSIS
Innovative design of composite structures: The use of curvilinear fiber format in structural design of composites
[NASA-CR-186406] N90-19308
Time-dependent failure of silver-interlayer diffusion bonds between non-deforming base-metals
[DE90-006925] N90-19357

Methods for trend analysis: Examples with problem/failure data N90-19396
Evaluation of the heat transfer module (FAHT) of Failure Analysis Nonlinear Thermal And Structural Integrated Code (FANTASTIC) N90-19407

FAR FIELDS
Near-field bistatic RCS (Radar Cross-Section) measurements
[AD-A217011] N90-19458

FAR INFRARED RADIATION
Search for far infrared radiation from optically pumped defect modes
[AD-A216976] N90-19843
Nuclear activity, morphology, and far infrared properties of spiral galaxies
[ETN-90-95373] N90-20024

FAR ULTRAVIOLET RADIATION
Transmission and reflection studies of thin films in the vacuum ultraviolet N90-19412
Quantum yield of photocathodes in far and extreme ultraviolet wavelength area
[ETN-90-95731] N90-19505

FARMLANDS
Availability of multitemporal LANDSAT data accompanying the variation of water surfaces in the program area of Careiro PDRI/AM
[INPE-4896-PRE/1496] N90-19634

FAST FOURIER TRANSFORMATIONS
A combined finite element-boundary element formulation for solution of two-dimensional problems via CGFFT
[NASA-CR-186464] N90-19309
Fast transform decoding of nonsystematic Reed-Solomon codes N90-19447

FAST NEUTRONS
Defect structures in copper and gold irradiated with fast neutrons, 14 MeV neutrons and 600 to 800 MeV protons
[DE90-007529] N90-19359

FATIGUE (MATERIALS)
Security calculations of rip reached construction elements by means of probabilistic breaking mechanics and a Markov process
[ETN-90-95890] N90-19624
Evaluation of thermal cycling creep-fatigue damage for a molten salt receiver
[DE90-002907] N90-19670
Fracture mechanical aspects of dust emission processes from a model comet surface N90-20004

FATIGUE LIFE
A transient plasticity study and low cycle fatigue analysis of the Space Station Freedom photovoltaic solar array blanket
[NASA-TM-102516] N90-19617

FATIGUE TESTS
Static strength and damage tolerance tests on the Fokker 100 airframe
[NLR-MP-88023-U] N90-19228

FAULT TOLERANCE
Dynamic reconfiguration and link fault tolerance in a transputer network
[AD-A215105] N90-19433

FAULT TREES
Safety Status Report for the Ulysses mission. Book 2: Accident analysis-appendices. General purpose heat source radioisotope thermoelectric generator program
[DE90-006830] N90-19286

FEASIBILITY
Feasibility of using Extreme Ultraviolet Explorer (EUVE) reaction wheels to satisfy Space Infrared Telescope Facility (SIRTF) maneuver requirements
[NASA-TM-100389] N90-19556

FEASIBILITY ANALYSIS
Technical and administrative feasibility of microlight remote sensing applications for river boards
[BCRS-89-01] N90-19643

FEDERAL BUDGETS
National Action Plan on Superconductivity Research and Development
[PB89-136512] N90-19883

FEED SYSTEMS
The use of the gas feed system and the vitiator for the solid fuel combustion chamber
[LR-528] N90-19329

FEEDBACK
Microwave oscillator with reduced phase noise by negative feedback incorporating microwave signals with suppressed carrier N90-19437

FEEDBACK CONTROL
Output model-following control synthesis for an oblique-wing aircraft
[NASA-TM-100454] N90-19241
Advanced topics in structural dynamics: The maneuver of flexible spacecraft, and on-off decentralized control of flexible structures N90-19274

FERRITES
Field theoretical analysis and synthesis of broadband waveguide: Height, plane shunt circulators with multiple layer material insertions
[ETN-90-95360] N90-19469
Dual-mode latching reciprocal ferrite phase shifter
[FEL-1988-55] N90-19497

FERRITIC STAINLESS STEELS
Three-dimensional Fe analysis of the surface distribution in notched compact samples of 20 MnMoNi 55
[W-1/89] N90-19625

FIBER COMPOSITES
Heat treatment study of the SiC/Ti-15-3 composite system
[NASA-TP-2970] N90-19302
Innovative design of composite structures: The use of curvilinear fiber format in structural design of composites
[NASA-CR-186406] N90-19308
Thermo-oxidative stability studies of PMR-15 polymer matrix composites reinforced with various fibers
[NASA-TM-102439] N90-19310
The creep behavior of an aramide fiber reinforced wound tow-strap
[LR-546] N90-19312
Tensile behavior of cylindrical pressure tanks in fiber assembling + metal hybrid structure
[ILR-MITT-213] N90-19618

FIBER OPTICS
Applications of FM-CW laser radar to antenna contour mapping N90-19270
Apparatus and method for minimizing polarization-induced signal fading in an interferometric fiber-optic sensor using input-polarization modulation
[AD-D014315] N90-19430
Effect of laser frequency noise on fiber-optic frequency reference distribution N90-19438
Thermal coefficient of delay for various coaxial and fiber-optic cables N90-19439
Opto-Em and devices investigation
[AD-A215033] N90-19614

FIBER ORIENTATION
Innovative design of composite structures: The use of curvilinear fiber format in structural design of composites
[NASA-CR-186406] N90-19308

FIBER STRENGTH
The effect of fiber coatings on interfacial shear strength and the mechanical behavior of ceramic composites
[DE90-007574] N90-19380

FIBERS
Optical studies of dynamical processes in disordered materials
[DE90-007080] N90-19372
The effect of fiber coatings on interfacial shear strength and the mechanical behavior of ceramic composites
[DE90-007574] N90-19380
All-fiber SFPM (Stimulated Four Photon Mixing) amplifier
[AD-D014358] N90-19841

FIELD EFFECT TRANSISTORS
Charge pumping as a measurement method for the characterization of short channel MOSFETS: Review, development, and comparison of measurement process
[ETN-90-95726] N90-19504
Field effect transistor structures based on strain induced polarization charges
[DE90-007247] N90-19515
Silicon carbide semiconductor device fabrication and characterization
[NASA-CR-186354] N90-19873

FIELD INTENSITY METERS
Gradiometry and gravitomagnetic field detection N90-19962

FIELD OF VIEW
Arrays for space applications N90-19265

FIELD THEORY (PHYSICS)
Goldstone excitation and symmetry breaking mechanism in superfluid He-4
[DE90-610676] N90-19881
Dimensional transition of the universe
[DE90-741461] N90-19910
Quantum field theory on higher-genus Riemann surfaces
[DE90-741469] N90-19912

FILM COOLING
Numerical and experimental analysis of a thin liquid film on a rotating disk related to development of a spacecraft absorption cooling system
[NASA-CR-183457] N90-19523

FINE STRUCTURE
Glancing angle XAFS (X ray Absorption Fine Structure) and x ray reflectivity studies of transition-metal/aluminum interfaces
[DE90-005575] N90-19353

FINITE DIFFERENCE THEORY
Computation of hypersonic unsteady viscous flow over a cylinder N90-19194
Three-dimensional viscous rotor flow calculations using a viscous-inviscid interaction approach
[NASA-TM-102235] N90-19204
Digital determination of the three dimensional flow in turbomachines with the S1-S2 current function process
[ITSM-MITT-30] N90-19236
A parametric heat transfer study for cryogenic ball bearings in SSME HPOTP N90-19397
Computational fluid dynamics method for low Reynolds number flow in a precessing/spinning, liquid filled cylinder with rounded endcaps
[AD-A216997] N90-19531

FINITE ELEMENT METHOD
Three-dimensional structural analyses of reentry vehicles
[DE90-006278] N90-19291
A combined finite element-boundary element formulation for solution of two-dimensional problems via CGFFT
[NASA-CR-186464] N90-19309
Practical calculation of the liveload of carbon fiber reinforced plastics by the finite element method
[ETN-90-95867] N90-19311
Effects of turbulence mixing, variable properties, and vaporization on spray droplet combustion
[NASA-CR-186463] N90-19326
Finite element approximations of the stokes flow problem based upon various variational principles
[DE90-608612] N90-19533
Finite element analysis of a quartz rotation sensor
[DE90-006959] N90-19562
Viscoelastic adherend effects in adhesively bonded composite-to-composite joints N90-19594
Modeling and analysis of the space shuttle nose-gear tire with semianalytic finite elements
[NASA-TP-2977] N90-19595
Computational aspects of sensitivity calculations in linear transient structural analysis
[NASA-TM-4156] N90-19610
Modal analysis of nonprismatic beams: Uniform segment method
[AD-A216952] N90-19614
PATRAN-STAGS translator (PATSTAGS)
[NASA-TM-100388] N90-19616
Development of finished beam and shell elements from engineering models for structures under high inelastic deformations
[ETN-90-95377] N90-19619
Digital treatment of elastic-plastic structures by means of quadratic optimization processes from the finite element method
[ETN-90-95823] N90-19621
Development of finite beam and shell elements for structures under great inelastic deformations
[ETN-90-95869] N90-19623
Interlaminar shear stress effects on the postbuckling response of graphite-epoxy panels
[NASA-TM-102626] N90-19630
Study of the optimization of reference parameters to the dynamic constraints of solar panels
[INPE-4793-TDL/355] N90-19656
The p- and h-p versions of the finite element method: An overview
[AD-A216902] N90-19789
Hierarchical basis preconditioners for second order elliptic problems in three dimensions
[DE90-005980] N90-19793
Finite element mesh generation starting from general geometric models
[REPT-88-93] N90-19803

FINITE VOLUME METHOD
Analysis of unsteady heat transfer by natural convection in a two-dimensional square cavity using a high order finite-volume method N90-19521

FINNED BODIES
External flow computations for a finned 60mm ramjet in steady supersonic flight
[AD-A216998] N90-19233

FIRING (IGNITING)
An evaluation of ethylene-vinyl acetate copolymers as desensitizers for RDX in insensitive booster compositions prepared by slurry coating technology
[MRL-TR-89-33] N90-19385

FISHES
Predicting effects of global climate change on reservoir water quality and fish habitat
[DE90-003674] N90-19704

FIXED POINTS (MATHEMATICS)
A method for computing the stationary points of a function subject to linear equality constraints
[DE90-610427] N90-19797

FLAME TEMPERATURE
Design of a pyrometer for temperature measurements on the solid fuel combustion chamber
[LR-530] N90-19561

FLAMES
Spatially high-resolution flame diagnosis by means of spontaneous Raman spectroscopy
[ETN-90-95870] N90-19328
FLAT PLATES
Calculation of excrescence drag magnification due to pressure gradient at high subsonic speeds
[ESDU-87004] N90-19195
Leading edge vortex dynamics on a pitching delta wing
[NASA-CR-186327] N90-19198
FLEXIBILITY
A study of the effects of disk flexibility on the rotordynamics of the space shuttle main engine turbo-pumps N90-19401
Design and implementation of a flexible robot
[AD-A216453] N90-19601
FLEXIBLE BODIES
Experiments in end-point control of a flexible robot with a mini-manipulator N90-19596
Modified independent modal space control of flexible structures N90-19597
FLEXIBLE SPACECRAFT
Advanced topics in structural dynamics: The maneuver of flexible spacecraft, and on-off decentralized control of flexible structures N90-19274
FLIGHT CHARACTERISTICS
Low-speed wind-tunnel investigation of the flight dynamic characteristics of an advanced turboprop business/commuter aircraft configuration
[NASA-TP-2982] N90-19239
FLIGHT CONTROL
Compensating for pneumatic distortion in pressure sensing devices
[NASA-TM-101716] N90-19224
A rule-based paradigm for intelligent adaptive flight control N90-19238
Neurocontrol systems and wing-fluid interactions underlying dragonfly flight N90-19240
FLIGHT CREWS
Flight crew aiding for recovery from subsystem failures
[NASA-CR-181905] N90-19741
Assessment of crew workload measurement methods, techniques and procedures. Volume 2: Guidelines for the use of workload assessment techniques in aircraft certification
[AD-A217067] N90-19748
FLIGHT OPTIMIZATION
Flight and driving optimization of air breathing aerodynamic space vehicle
[ETN-90-95379] N90-19246
FLIGHT PATHS
Series reversion/inversion of Lambert's time function
[AD-A216243] N90-19245
FLIGHT RULES
Development of a standardized three axis sensor for inertial data achievement for future flight rule systems
[ETN-90-96075] N90-19231
FLIGHT SIMULATION
Calculation and optimization of rotor start process
[ETN-90-95894] N90-19229
Yaw rate control of an air bearing vehicle N90-19420
FLIGHT TESTS
Heat transfer measurements from a NACA 0012 airfoil in flight and in the NASA Lewis icing research tunnel
[NASA-CR-4278] N90-19203
Helicopter flight vibration of large transportation containers: A case for testing tailoring
[DE90-007429] N90-19215
X-29A aircraft structural loads flight testing
[NASA-TM-101715] N90-19225
Low-speed wind-tunnel investigation of the flight dynamic characteristics of an advanced turboprop business/commuter aircraft configuration
[NASA-TP-2982] N90-19239
In-flight evaluations of turbine fuel extenders
[DOT/FAA/CT-89/33] N90-19387
Sandia National Laboratories' new high level acoustic test facility
[DE90-006810] N90-19820
A note on an acoustic response during an engine nacelle flight experiment
[NASA-TM-102585] N90-19821
FLIGHT TIME
Series reversion/inversion of Lambert's time function
[AD-A216243] N90-19245
FLIR DETECTORS
Reliability testing of the Hughes temperature controlled 1/4 watt split cycle cryogenic cooler (HD-1045 (V)/UA)
[AD-A216696] N90-19426
FLOODS
Availability of multitemporal LANDSAT data accompanying the variation of water surfaces in the program area of Careiro PDRI/AM
[INPE-4896-PRE/1496] N90-19634
FLOW CHARACTERISTICS
Calculation of excrescence drag magnification due to pressure gradient at high subsonic speeds
[ESDU-87004] N90-19195
Measuring flow properties of wicks for heat pipe solar receivers
[DE89-016537] N90-19664
FLOW DISTORTION
Compensating for pneumatic distortion in pressure sensing devices
[NASA-TM-101716] N90-19224
FLOW DISTRIBUTION
On the evaluation of aerodynamic influence coefficients
[NLR-MP-87019-U] N90-19191
Unsteady aerodynamics of delta wings performing maneuvers to high angle of attack N90-19196
Interaction of an oblique shock wave with supersonic flow over a blunt body N90-19197
A study of flows over highly-swept wings designed for maneuver at supersonic speeds
[AD-A216837] N90-19202
A panel process for the calculation of the flow around a wing with front angle damping
[ETN-90-95367] N90-19207
External flow computations for a finned 60mm ramjet in steady supersonic flight
[AD-A216998] N90-19233
Experimental and theoretical investigations of flowfields and heat transfer in modern gas turbines
[AD-A217663] N90-19237
Elastic recovery and polymer-polymer interactions
[AD-A217085] N90-19384
Separation bubbles at high Reynolds number: Measurement and computation
[CUED/A-AERO/15] N90-19525
An experimental investigation of the flow field around yawed stranded cables
[AD-A215782] N90-19529
Flow simulation for aircraft
[NLR-MP-87082-U] N90-19543
Constructibility limits of multiflow wind turbines with pivots
[ILR-MITT-215] N90-19662
Spanwise measurements of vertical components of atmospheric turbulence
[NASA-TP-2963] N90-19718
Siphon flows in isolated magnetic flux tubes. 3: The equilibrium path of the flux tube arch
[NASA-CR-186297] N90-19813
A storage process of the magnetic energy results from the unsteady plasma flow field in the space active regions and stellar atmosphere
[DE90-610638] N90-19858
FLOW EQUATIONS
Conical Euler solution for a highly-swept delta wing undergoing wing-rock motion
[NASA-TM-102609] N90-19211
FLOW GEOMETRY
An experimental investigation of the flow field around yawed stranded cables
[AD-A215782] N90-19529
FLOW STABILITY
Turbulent mixing effects in models of thermal blooming
[DE90-007245] N90-19580
FLOW VELOCITY
Study of interfacial behavior in cocurrent gas-liquid flows
[DE90-005988] N90-19532
Development and utilization of new diagnostics for dense-phase pneumatic transport
[DE90-006787] N90-19536
Accretion flows in high mass star formation
[DE90-007251] N90-20027
FLOW VISUALIZATION
Water-tunnel investigation of concepts for alleviation of adverse inlet spillage interactions with external stores
[NASA-TM-4181] N90-19199
Dynamics of a class of vortex rings
[NASA-TM-102257] N90-19524
An experimental investigation of the flow field around yawed stranded cables
[AD-A215782] N90-19529
FLUID DYNAMICS
Proceedings of a contractors meeting on Combustion Rocket Propulsion Diagnostics of Reacting Flow
[AD-A216445] N90-19297
An experimental investigation of the flow field around yawed stranded cables
[AD-A215782] N90-19529
FLUID FILMS
Numerical and experimental analysis of a thin liquid film on a rotating disk related to development of a spacecraft absorption cooling system
[NASA-CR-183457] N90-19523
FLUID FLOW
Numerical and experimental analysis of a thin liquid film on a rotating disk related to development of a spacecraft absorption cooling system
[NASA-CR-183457] N90-19523
An experimental study of the aeroelastic behaviour of two parallel interfering circular cylinders N90-19609
Application of natural isotopes in groundwater for solving environmental problems
[DE90-000223] N90-19703
FLUID POWER
Jam resistant fluid power actuator for ballistic-damage tolerant redundant cylinder assemblies
[AD-D014360] N90-19600
FLUORINATION
Fluorinated graphite fibers as a new engineering material: Promises and challenges
[NASA-TM-102511] N90-19301
FLUOROHYDROCARBONS
New Condensation polyimides containing 1,1,1-triaryl-2,2,2-trifluoroethane structures
[NASA-CASE-LEW-14346-1] N90-19300
FLUOROPOLYMERS
New Condensation polyimides containing 1,1,1-triaryl-2,2,2-trifluoroethane structures
[NASA-CASE-LEW-14346-1] N90-19300
FOG
Development of an atmospheric diffusion model in fog (1). Literature review of scavenging process by precipitation
[DE89-782318] N90-19678
FOKKER AIRCRAFT
Static strength and damage tolerance tests on the Fokker 100 airframe
[NLR-MP-88023-U] N90-19228
FOLDING
Analysis of photogeologic lineaments in the Ithacare (BA) region: A proposed methodology
[INPE-4855-PRE/1478] N90-19635
FORECASTING
Atmospheric Radiation Measurement Program plan
[DE90-006349] N90-19705
FORMALDEHYDE
The role of clouds in the photochemistry of the background troposphere N90-19694
Physico-chemical properties of formaldehyde-ice-dust mixtures N90-20000
FORTRAN
Lessons learned in the transition to ADA from FORTRAN at NASA/Goddard
[NASA-CR-186458] N90-19765
FORWARD SCATTERING
An optical white light speckle process in forward dispersion for measurement of the velocity field in free convective currents
[ETN-90-95913] N90-19546
FOSSIL FUELS
A preliminary analysis of US CO2 emissions reduction potential from energy conservation and the substitution of natural gas for coal in the period to 2010
[DOE/NBB-0085] N90-19673
FOURIER TRANSFORMATION
Signal processing
[DE90-006904] N90-19464
A technique for convolving unequally spaced samples using fast Fourier transforms
[DE90-006466] N90-19802
FRACTALS
Chaotic transients, higher dimensional phenomena, and coupled ordinary differential equations
[DE90-006641] N90-19794
FRACTURE MECHANICS
Fracture mechanical aspects of dust emission processes from a model comet surface N90-20004
FRACTURE STRENGTH
Identification and development of optimum SiC whiskers for silicon nitride matrix composites
[DE90-006888] N90-19315
Fracture strength analysis of silicon nitride and silicon carbide ceramics from an international cooperative research program
[DE90-005319] N90-19368
FRAGMENTATION
Getting lunar ilmenite: From soils or rocks
[NASA-CR-186498] N90-20029
FRAMES (DATA PROCESSING)
Object Oriented Programming Systems (OOPS) and frame representations: An investigation of programming paradigms
[NASA-CR-186084] N90-19758
FREE CONVECTION
Experiments of thermoconvection in a cubic cell
[MPIS-6/1989] N90-19544

FREE ELECTRON LASERS
Transient and sustained resonance in very slowly varying oscillatory Hamiltonian systems with application to free-electron lasers
[DE90-005984] N90-19574
Potential biomedical application of the Los Alamos infrared free-electron laser: DNA spectroscopy
[DE90-006505] N90-19575
On 140 GHz microwave FEL experiments using ELF-2
[DE90-006764] N90-19576
Results of the PALADIN experiment
[DE90-006776] N90-19578
First direct observation of FEL (Free-Electron Laser) from lambda = 20 to 45 microns
[DE90-007506] N90-19589
FREE ENERGY
Linear free energy relations for multielectron transfer kinetics: A brief look at the Bronsted/Tafel analogy
[AD-A215078] N90-19823
FREE FALL
The Stanford equivalence principle program N90-19963
FREE FLOW
A study of flows over highly-swept wings designed for maneuver at supersonic speeds
[AD-A216837] N90-19202
An experimental investigation of the flow field around yawed stranded cables
[AD-A215782] N90-19529
FREE JETS
Tomographic investigations of weakly perturbed supersonic free jets
[MPIS-MITT-91] N90-19208
Heteroepitaxial growth of germanium films by supersonic free jet chemical beam epitaxy
[DE90-006621] N90-19877
FREE RADICALS
Laboratory studies of free radical reactions in cloudwater
[DE90-003961] N90-19730
FRENCH SATELLITES
Compendium of meteorological space programs, satellites, and experiments
[NASA-TM-102924] N90-19243
FREQUENCIES
Antennas for 20/30 GHz and beyond N90-19269
FREQUENCY DISTRIBUTION
Induction motor control
[NASA-TM-102533] N90-19234
FREQUENCY SCANNING
General multidimensional scanning ratio transformation and its utilization for norm transformation of television signals
[ETN-90-96058] N90-19470
FREQUENCY SHIFT
Coherent radar measurement of ocean currents from geostationary orbit N90-19259
Correlation-induced changes of spectra
[AD-A217087] N90-19591
FREQUENCY SHIFT KEYING
Power spectral densities for selected digital phase-continuous MFSK (M-ary Frequency Shift Keying) emissions
[PB90-129990] N90-19463
FREQUENCY STABILITY
Effect of laser frequency noise on fiber-optic frequency reference distribution N90-19438
Frequency stable high power lasers in space N90-19969
A review of atomic clock technology, the performance capability of present spaceborne and terrestrial atomic clocks, and a look toward the future N90-19972
FREQUENCY STANDARDS
Thermal coefficient of delay for various coaxial and fiber-optic cables N90-19439
A review of atomic clock technology, the performance capability of present spaceborne and terrestrial atomic clocks, and a look toward the future N90-19972
FUEL CELLS
Zirconia-based electrodes for solid oxide fuel cells
[DE90-000462] N90-19513
Solid oxide fuel cell cogeneration system conceptual design, program 2
[PB90-114968] N90-19653
FUEL COMBUSTION
Effects of turbulence mixing, variable properties, and vaporization on spray droplet combustion
[NASA-CR-186463] N90-19326
Development and use of an advanced coal-fueled diesel engine cycle simulation with group effects
[DE90-000450] N90-19607
FUEL CONSUMPTION
In-flight evaluations of turbine fuel extenders
[DOT/FAA/CT-89/33] N90-19387
FUEL FLOW
Numerical study of diffusion jet flames N90-19316
FUEL TESTS
In-flight evaluations of turbine fuel extenders
[DOT/FAA/CT-89/33] N90-19387
FUNCTIONAL ANALYSIS
Theory and applications of belief functions
[AD-A217092] N90-19774
Classical mechanics on superspace
[DE90-608907] N90-19906
FUNCTIONS (MATHEMATICS)
A method for computing the stationary points of a function subject to linear equality constraints
[DE90-610427] N90-19797
FUSES (ORDNANCE)
SINA: A test system for proximity fuses
[FEL-1989-101] N90-19498

G

GALACTIC CLUSTERS
Photometric analyses of abundances in dwarf spheroidal galaxies and globular clusters N90-19978
GALACTIC COSMIC RAYS
The Advanced Composition Explorer
[DE90-006522] N90-19987
GALACTIC NUCLEI
Space telescope searches for black holes in galactic nuclei N90-19958
GALACTIC STRUCTURE
Monte Carlo models and analysis of galactic disk gamma-ray burst distributions N90-19403
GALERKIN METHOD
Implementation of a finite element process for the Euler equations of the gas dynamics
[PREPRINT-500] N90-19545
Error analysis of some Galerkin least squares methods for the elasticity equations
[DE90-608611] N90-19790
GALLIUM ARSENIDE LASERS
The III-V semiconductor quantum well lasers and related optoelectronic devices on silicon
[AD-A216980] N90-19570
GALLIUM ARSENIDES
CdTe buffered GaAs thin-slab IR waveguide modulators and T/R filter
[AD-A215999] N90-19488
Heteroepitaxial growth of germanium films by supersonic free jet chemical beam epitaxy
[DE90-006621] N90-19877
Digital capacity transient spectroscopy of deep structure defects in III-V-Semiconductor structures
[ETN-90-96057] N90-19890
GALLIUM OXIDES
Growth and characterization of gallium (III) oxide films
[AD-A217568] N90-19902
GALLIUM PHOSPHIDES
Annealing group III-V compound doped silicon-germanium alloy for improved thermo-electric conversion efficiency
[NASA-CASE-NPO-17259-1-CU] N90-19884
GAMMA RAY ASTRONOMY
Radial response of the burst and transient source experiment N90-19408
Astronomy and astrophysics
[REPT-33/89] N90-19938
Very high energy gamma ray astrophysics
[DE90-006545] N90-19983
GAMMA RAY BURSTS
Monte Carlo models and analysis of galactic disk gamma-ray burst distributions N90-19403
Radial response of the burst and transient source experiment N90-19408
GAMMA RAYS
Monte Carlo models and analysis of galactic disk gamma-ray burst distributions N90-19403
Radial response of the burst and transient source experiment N90-19408
The influence of gamma-radiation on the bandwidth of optical fibres and the reduction of the induced attenuation by bleaching and hardening the fibre
[FEL-1988-62] N90-19846
Very high energy gamma ray astrophysics
[DE90-006545] N90-19983
GANGLIA
Neurocontrol systems and wing-fluid interactions underlying dragonfly flight N90-19240
GAS BEARINGS
Yaw rate control of an air bearing vehicle N90-19420
GAS COOLING
Gas cooled fuel cell systems technology development program
[DE90-000446] N90-19668
GAS DETECTORS
Background studies in gas ionizing x ray detectors N90-19399
Optical paramagnetic/diamagnetic gas sensor
[AD-D014368] N90-19554
GAS DYNAMICS
Model calculations for dynamic development of planetary nebulae
[ETN-90-95734] N90-20025
GAS FLOW
Three-dimensional structural analyses of reentry vehicles
[DE90-006278] N90-19291
Development and utilization of new diagnostics for dense-phase pneumatic transport
[DE90-006787] N90-19536
GAS INJECTION
The use of the gas feed system and the vitiator for the solid fuel combustion chamber
[LR-528] N90-19329
Construction and characterization of a valve for rapid gas injection
[INPE-4789-RPE/583] N90-19486
Calibration of the sonic measuring and control cross section in the gas feed installation of the solid fuel combustion chamber
[LR-552] N90-19548
GAS MIXTURES
Molecular theory and computer simulation studies of natural and synthetic gas mixtures
[PB90-130329] N90-19826
Comets: Dirty snowballs or icy dirtballs N90-19994
Cometary bodies in the circumstellar disk around beta Pictoris N90-20010
GAS PIPES
Trailer shield assembly for a welding torch
[NASA-CASE-MFS-29260-1] N90-19602
GAS TURBINE ENGINES
Experimental and theoretical investigations of flowfields and heat transfer in modern gas turbines
[AD-A217663] N90-19237
In-flight evaluations of turbine fuel extenders
[DOT/FAA/CT-89/33] N90-19387
GAS TURBINES
Development of ceramic combustor for low BTU gases. Design and basic combustion characteristics
[DE89-782287] N90-19363
Low cost Brayton engine for gas-fired cogeneration system, phase 1
[PB90-127457] N90-19655
GAS-GAS INTERACTIONS
A new model for hydrogen absorption in welds
[AD-A216951] N90-19347
The 41st Annual Gaseous Electronics Conference
[AD-A214540] N90-19851
GAS-SOLID INTERACTIONS
Development and utilization of new diagnostics for dense-phase pneumatic transport
[DE90-006787] N90-19536
GASEOUS DIFFUSION
Experimental examination of the development behavior of a gaseous body in a steady state and neutral layer turbulent sheet boundary layer with ground asperity
[ETN-90-96067] N90-19549
Solar and thermic utilization in high temperature area: Research and development
[ETN-90-96062] N90-19663
Gas diffusion in a cometary crust N90-20017
GATES (CIRCUITS)
A gate array structure for the efficient project of digital circuits: The unit cell array
[ETN-90-95364] N90-19502
GAUGE THEORY
Research accomplishments and future goals in particle physics
[DE90-007296] N90-19830
Cosmic string in compactified gauge theory
[DE90-741463] N90-19988
GEAR TEETH
Theory of gearing
[NASA-RP-1212] N90-19593
GEARS
Theory of gearing
[NASA-RP-1212] N90-19593
GENERATORS
A digitally controlled system for effecting and presenting a selected electrical resistance
[NASA-CASE-MFS-29149-1] N90-19492
GEOCHEMISTRY
Application of natural isotopes in groundwater for solving environmental problems
[DE90-000223] N90-19703
Geochemical survey on faults overland with alluvial deposits, part 1. Application for the Neodani and the Atera faults survey
[DE89-782326] N90-19707

GEODESY
Highly accurate navigation: Integration of navigation and geodesic methods
[SFB-226] N90-19221
GEODETIC COORDINATES
Applications of the GPS in photogrammetry
[ETN-90-96004] N90-19648
GEOGRAPHIC INFORMATION SYSTEMS
Thematic coupling between digital images and geographic information systems
[ETN-90-95723] N90-19646
The mesoscale meteorological model MM4 and its modifications for EURAD N90-19682
Visibility problems in numerical models of terrain
[INPE-4921-TDL/382] N90-19919
GEOIDS
Evolution of midplate hotspot swells: Numerical solutions
[NASA-CR-186462] N90-19713
GEOLOGY
Working on the moon: The Apollo experience
[DE90-003662] N90-19744
GEOMAGNETISM
Attitude and spin rate control of a spinning satellite using geomagnetic field
[INPE-4818-NTE/289] N90-19277
Solar-geophysical data number 541, September 1989. Part 1: (Prompt reports). Data for August, July 1989, and late data
[PB90-122763] N90-20032
Examination of the background by High Energy X ray Experiment (HEXE) on the space station MIR
[ETN-90-95735] N90-20041
GEOMETRICAL THEORY OF DIFFRACTION
Radar transponder antenna pattern analysis for the space shuttle N90-19414
GEOPHYSICS
An analytic model of axisymmetric mantle plume due to thermal and chemical diffusion
[NASA-CR-186461] N90-19714
Solar-geophysical data number 541, September 1989. Part 2: (Comprehensive reports). Data for March 1989 and miscellaneous
[PB90-122755] N90-20031
Solar-geophysical data number 541, September 1989. Part 1: (Prompt reports). Data for August, July 1989, and late data
[PB90-122763] N90-20032
GEOSTROPHIC WIND
Synoptic-scale forcing of the low-level jet in developing baroclinic waves N90-19717
GEOSYNCHRONOUS ORBITS
Geostationary earth science platform concepts N90-19252
Large space antenna concepts for ESGP N90-19253
Large-diameter geostationary millimeter wavelength antenna concept N90-19254
Design of a low-frequency (5-20 GHz), 15-meter-diameter passive radiometer for geostationary earth science platforms N90-19255
Structures for remotely deployable precision antennas N90-19256
Coherent radar measurement of ocean currents from geostationary orbit N90-19259
Synthetic Aperture Interferometric Radiometer (SAIR) N90-19261
Rain radars for earth science geostationary platforms: Some possibilities N90-19262
GERMANIUM
Heteroepitaxial growth of germanium films by supersonic free jet chemical beam epitaxy
[DE90-006621] N90-19877
GERMANIUM ALLOYS
Annealing group III-V compound doped silicon-germanium alloy for improved thermo-electric conversion efficiency
[NASA-CASE-NPO-17259-1-CU] N90-19884
GIMBALS
Internal performance of two nozzles utilizing gimbal concepts for thrust vectoring
[NASA-TP-2991] N90-19200
GLASS
Elimination of platinum inclusions in phosphate laser glasses
[DE90-004470] N90-19361
Optical studies of dynamical processes in disordered materials
[DE90-007080] N90-19372
Crystallization behavior and properties of BaO-Al2O3-2SiO2 glass matrices
[NASA-CR-185209] N90-19374
Radiation-induced density changes and creep in surface layers of glass
[DE90-008112] N90-19383
GLOBAL AIR POLLUTION
A preliminary analysis of US CO2 emissions reduction potential from energy conservation and the substitution of natural gas for coal in the period to 2010
[DOE/NBB-0085] N90-19673
GLOBAL POSITIONING SYSTEM
Accuracy of global positioning system broadcast orbits for relative surveys
[PB90-125428] N90-19218
Calculation of ionospheric corrections for single frequency GPS observations: Investigation of two models
[ETN-90-95450] N90-19219
Carin and GPS: The combination of dead reckoning, map matching and satellite navigation in a hybrid automobile navigation system
[ETN-90-95451] N90-19220
The global positioning system
[AD-A217266] N90-19222
Interoperability issues in the use of satellite-based navigation systems for civil aviation purposes
[AD-A217279] N90-19223
Determination of Earth orientation using the Global Positioning System N90-19435
Applications of the GPS in photogrammetry
[ETN-90-96004] N90-19648
GLOBULAR CLUSTERS
Photometric analyses of abundances in dwarf spheroidal galaxies and globular clusters N90-19978
GLOW DISCHARGES
The 41st Annual Gaseous Electronics Conference
[AD-A214540] N90-19851
GNEISS
Stored mafic/ultramafic crust and early Archean mantle depletion
[NASA-CR-186460] N90-19715
GOES SATELLITES
Data reduction of GOES (Geostationary Operational Environmental Satellite) information from DCP (Data Collection Platform) networks
[AD-A215844] N90-19637
GOGGLES
Human factors engineering testing of aircraft cockpit lighting systems
[AD-A216853] N90-19743
GOLD
Defect structures in copper and gold irradiated with fast neutrons, 14 MeV neutrons and 600 to 800 MeV protons
[DE90-007529] N90-19359
Particle emission by oblique ion bombardment of gold
[ETN-90-95825] N90-19827
GRADIENTS
Optimal iteration steps by stochastic approximation processes for the solution of optimization problems with twice differentiable functions
[ETN-90-95887] N90-19809
GRAIN BOUNDARIES
Evaluation of radiation-induced sensitization using electrochemical potentiokinetic reactivation technique for austenitic stainless steels
[DE90-002708] N90-19352
Glancing angle XAFS (X ray Absorption Fine Structure) and x ray reflectivity studies of transition-metal/aluminum interfaces
[DE90-005575] N90-19353
The effects of gradients on boundary stability
[DE90-007428] N90-19894
GRAPH THEORY
Minimum cycle covering and integer flows
[AD-A216546] N90-19785
Panconnectivity of locally connected K(1,3)-free graphs
[AD-A216548] N90-19786
GRAPHITE
Fluorinated graphite fibers as a new engineering material: Promises and challenges
[NASA-TM-102511] N90-19301
Exchange and correlation effects in the Visscher-Falicov model for metal intercalated graphite
[DE90-610553] N90-19349
GRAPHITE-EPOXY COMPOSITES
Low-energy impact resistance of graphite-epoxy plates and ALS honeycomb sandwich panels N90-19405
Viscoelastic adherend effects in adhesively bonded composite-to-composite joints N90-19594
Interlaminar shear stress effects on the postbuckling response of graphite-epoxy panels
[NASA-TM-102626] N90-19630
GRAPHITIZATION
Fluorinated graphite fibers as a new engineering material: Promises and challenges
[NASA-TM-102511] N90-19301
GRATINGS (SPECTRA)
Optically tunable gratings for optical interconnects
[AD-A216978] N90-19844
GRAVIMETERS
Earth tidal analysis based on gravimeter observations and the influence of ocean tides
[ETN-90-95721] N90-19734
GRAVITATION
TOPAS preparation study: Summary representation of the study results
[OHB-TN-TOP-011/87] N90-19244
Uniqueness of closure of the constraint algebra for quantum gravity
[DE90-610476] N90-19712
On Einsteinization of background curved space in the induced quantum gravity
[DE90-610477] N90-19907
Dimensional transition of the universe
[DE90-741461] N90-19910
Reparametrization BRS cohomology in two-dimensional gravity and non-critical string theories
[DE90-741468] N90-19911
High stability radio links N90-19970
GRAVITATION THEORY
Experimental constraints on metric and non-metric theories of gravity N90-19946
Ultra-sensitive inertial sensors via neutral-atom interferometry N90-19977
GRAVITATIONAL COLLAPSE
Sources of gravitational waves N90-19942
Gravitational radiation from rotating gravitational collapse N90-19944
Optical interferometer in space N90-19953
Accretion flows in high mass star formation
[DE90-007251] N90-20027
GRAVITATIONAL CONSTANT
Small Mercury Relativity Orbiter N90-19965
GRAVITATIONAL EFFECTS
Techniques for studying the effects of microgravity on model particle/cell systems N90-19424
Design and implementation of a flexible robot
[AD-A216453] N90-19601
Earth tidal analysis based on gravimeter observations and the influence of ocean tides
[ETN-90-95721] N90-19734
Gravitational radiation as a test of relativistic gravity N90-19941
Toward higher order tests of the gravitational interaction N90-19948
The inverse-square law and quantum gravity N90-19949
Earth-orbiting resonant-mass gravitational wave detectors N90-19954
Gradiometry and gravitomagnetic field detection N90-19962
GRAVITATIONAL FIELDS
On Einsteinization of background curved space in the induced quantum gravity
[DE90-610477] N90-19907
Linearized analysis of (2+1)-dimensional Einstein-Maxwell theory
[DE90-741470] N90-19913
On the Langevin equation for stochastic quantization of gravity
[DE90-750024] N90-19914
Gravitational radiation as a test of relativistic gravity N90-19941
Gravitational consequences of modern field theories N90-19947
LAGEOS 3 and the gravitomagnetic field N90-19961
Gradiometry and gravitomagnetic field detection N90-19962
The Stanford equivalence principle program N90-19963
Icarus lander N90-19964
Small Mercury Relativity Orbiter N90-19965
Drag-free satellite control N90-19974
Superconducting gravity gradiometer and a test of inverse square law N90-19975
GRAVITATIONAL WAVE ANTENNAS
Earth-orbiting resonant-mass gravitational wave detectors N90-19954
Frequency stable high power lasers in space N90-19969
GRAVITATIONAL WAVES
Relativistic Gravitational Experiments in Space
[NASA-CP-3046] N90-19940
Gravitational radiation as a test of relativistic gravity N90-19941
Sources of gravitational waves N90-19942
Detecting gravity waves from binary black holes N90-19943
Gravitational radiation from rotating gravitational collapse N90-19944
The pregalactic cosmic gravitational wave background N90-19945
Gravitational consequences of modern field theories N90-19947

Toward higher order tests of the gravitational interaction N90-19948
The inverse-square law and quantum gravity N90-19949
Advanced Doppler tracking experiments N90-19951
The space microwave interferometer and the search for cosmic background gravitational wave radiation N90-19952
Optical interferometer in space N90-19953
Pulsar timing and gravitational waves N90-19955
X ray timing observations and gravitational physics N90-19956
Gravitational experiments on a solar probe mission: Scientific objectives and technology considerations N90-19966
New tests with old data N90-19968
Improved ranging systems N90-19973
Superconducting gravity gradiometer and a test of inverse square law N90-19975
Ultra-sensitive inertial sensors via neutral-atom interferometry N90-19977

GRAVITY GRADIOMETERS
Gradiometry and gravitomagnetic field detection N90-19962
Superconducting gravity gradiometer and a test of inverse square law N90-19975
Inertial corrections by dynamic estimation N90-19976

GRAVITY PROBE B
The gravity probe B relativity gyroscope program N90-19960

GRAVITY WAVES
The COBE cosmic 3 K anisotropy experiment: A gravity wave and cosmic string probe N90-19959
Tropospheric monitoring technology for gravity wave experiments N90-19971

GRAZING INCIDENCE
Some considerations on cohesive forces in sun-grazing comets N90-20015

GREEN'S FUNCTIONS
Green's functions for a theoretical model of an aperture fed stacked-patch microstrip antenna [AD-A216280] N90-19455
A comparison between the propagators method and the decomposition method for nonlinear equations [DE90-005783] N90-19781
Self-consistant calculation of point and pair structure defects in silicium [ETN-90-96059] N90-19891

GREENHOUSE EFFECT
Atmospheric Radiation Measurement Program plan [DE90-006349] N90-19705

GRID GENERATION (MATHEMATICS)
Evaluation of the heat transfer module (FAHT) of Failure Analysis Nonlinear Thermal And Structural Integrated Code (FANTASTIC) N90-19407
A tensor product B-spline method for numerical grid generation [DE90-005979] N90-19792

GROUND BASED CONTROL
A method for determination of control pixels for LANSAT using a reflector [INPE-4884-PRE/1491] N90-19632

GROUND EFFECT (AERODYNAMICS)
Calculation and optimization of rotor start process [ETN-90-95894] N90-19229

GROUND STATE
A ground state depleted laser in neodymium doped yttrium orthosilicate [DE90-006773] N90-19586
Characterization of ground state neutral and ion transport during laser ablation of 1:2:3 superconductors by transient optical absorption spectroscopy [DE90-006623] N90-19878

GROUND STATIONS
The Telecommunications and Data Acquisition Report [NASA-CR-185033] N90-19434
ESRIN [ESA-BR-58] N90-19631

GROUND WATER
Application of natural isotopes in groundwater for solving environmental problems [DE90-000223] N90-19703

GUARDS (SHIELDS)
Trailer shield assembly for a welding torch [NASA-CASE-MFS-29260-1] N90-19602

GUIDANCE (MOTION)
Suboptimal period design for a maneuvering missile to evade tracking filters N90-19479

GUSTS
Spanwise measurements of vertical components of atmospheric turbulence [NASA-TP-2963] N90-19718

GYROSCOPES
The gravity probe B relativity gyroscope program N90-19960

H

HABITATS
Predicting effects of global climate change on reservoir water quality and fish habitat [DE90-003674] N90-19704

HADRONS
Digital integrator [DIGEL-1989-2] N90-19508
Algorithms for calorimeter simulation with parameterized showers by example of H1 detectors [MPI-PAE/EXP.EL-200] N90-19828

HALF LIFE
Measurement of cross sections: New needs and possibilities [DE90-007248] N90-19829

HALLEY'S COMET
Far-ultraviolet spectroscopy of Comet Halley N90-19979
Comet Halley: An optical continuum study N90-19981
Comets: Dirty snowballs or icy dirtballs N90-19994
Hot OH and CN: Evidence for organic molecules close to the nucleus of comet Halley N90-20012
The composition of cometary nuclei N90-20022

HAMILTONIAN FUNCTIONS
Transient and sustained resonance in very slowly varying oscillatory Hamiltonian systems with application to free-electron lasers [DE90-005984] N90-19574
Panconnectivity of locally connected K(1,3)-free graphs [AD-A216548] N90-19786

HANDBOOKS
Methods for trend analysis: Examples with problem/failure data N90-19396

HANKEL FUNCTIONS
Elastic solutions in a semi-infinite solid with an ellipsoidal inclusion [AD-A217063] N90-19338

HARDNESS
Evaluation of the response of aluminum alloys to single and multiple particle impacts [DE90-003689] N90-19626
Crustal strength of different model comet materials N90-20003

HARMONIC ANALYSIS
Earth tidal analysis based on gravimeter observations and the influence of ocean tides [ETN-90-95721] N90-19734

HARMONIC GENERATORS
CO2 laser plus optimization for harmonic generation [AD-D014341] N90-19565
The nonlinear interaction of intense laser pulses in plasmas [AD-A217604] N90-19867

HARMONIC RADIATION
The nonlinear interaction of intense laser pulses in plasmas [AD-A217604] N90-19867

HATCHES
Hatch cover [NASA-CASE-MSC-21356-1] N90-19278

HAZARDS
Safety status report for the Ulysses mission. Book 2: Risk analysis. General purpose heat source radioisotope thermoelectric generator program [DE90-006827] N90-19283
The pollution hazard assessment system: Documentation and users manual [AD-A217106] N90-19706

HEAT EXCHANGERS
Experimental investigation of condensation of steam in the presence of noncondensable gases using plate heat exchangers [DE90-002251] N90-19659

HEAT FLUX
Radiative transport models for solar thermal receiver/reactors [DE90-000303] N90-19665
Evolution of midplate hotspot swells: Numerical solutions [NASA-CR-186462] N90-19713

HEAT ISLANDS
Wind tunnel design of heat island turbulent boundary layer [IHW-ET/50] N90-19542

HEAT MEASUREMENT
Thermodynamic properties of supercritical mixtures [DE90-006720] N90-19909

HEAT PIPES
Measuring flow properties of wicks for heat pipe solar receivers [DE89-016537] N90-19664

HEAT PUMPS
Advanced absorption technology development in the United States [DE90-001336] N90-19428
Survey on the social and economic influences of wide-spreading heat-pump technology [DE89-782294] N90-19526
Operational fact-finding report on heat pump systems for industrial use [DE89-782295] N90-19527

HEAT RESISTANT ALLOYS
An attempt of improving high-temperature fatigue properties of Ni-Cr-W superalloys in HTGR helium [DE90-741482] N90-19350

HEAT SHIELDING
Three-dimensional structural analyses of reentry vehicles [DE90-006278] N90-19291

HEAT SINKS
Heat sink effects on weld bead: VPPA process N90-19418

HEAT SOURCES
Operational fact-finding report on heat pump systems for industrial use [DE89-782295] N90-19527

HEAT TRANSFER
Experimental and theoretical investigations of flowfields and heat transfer in modern gas turbines [AD-A217663] N90-19237
Evaluation of the heat transfer module (FAHT) of Failure Analysis Nonlinear Thermal And Structural Integrated Code (FANTASTIC) N90-19407
The influence of a wall function on turbine blade heat transfer prediction N90-19421
Heat transfer definitions and equations [ESDU-89022] N90-19522
Numerical and experimental analysis of a thin liquid film on a rotating disk related to development of a spacecraft absorption cooling system [NASA-CR-183457] N90-19523
Swept shock/boundary layer interaction experiments in support of CFD code validation [NASA-CR-186397] N90-19535
Theoretical and experimental examination of the beginning of turbulence in a heated laminar conduit flow [ETN-90-95369] N90-19541
Experimental investigation of condensation of steam in the presence of noncondensable gases using plate heat exchangers [DE90-002251] N90-19659
Radiative transport models for solar thermal receiver/reactors [DE90-000303] N90-19665
Thermal conductivities and diffusivities of porous ice samples at low pressures and temperatures and possible modes of heat transfer in near surface layers of comets N90-19999

HEAT TRANSFER COEFFICIENTS
Heat transfer definitions and equations [ESDU-89022] N90-19522

HEAT TREATMENT
Processing of advanced ceramics using microwaves thermal treatments [DE90-606349] N90-19362
Crystallization behavior and properties of BaO-Al2O3-2SiO2 glass matrices [NASA-CR-185209] N90-19374
Influence of heat treating on the mechanical values and the stability of heat barrier coatings [ETN-90-95902] N90-19375

HEATING EQUIPMENT
The use of the gas feed system and the vitiator for the solid fuel combustion chamber [LR-528] N90-19329

HEAVY IONS
Searching for existing nuclear data [DE90-007535] N90-19925
Nuclear interactions of high energy heavy ions and applications in astrophysics [DE90-006691] N90-19984
A drift chamber telescope for high-Z particles [NASA-CR-186497] N90-20040

HELICOPTER PERFORMANCE
Helicopter flight vibration of large transportation containers: A case for testing tailoring [DE90-007429] N90-19215

HELICOPTERS
Heli/SITAN: A terrain referenced navigation algorithm for helicopters [DE90-005193] N90-19217

HELIOSTATS
Status of stretched-membrane heliostats [DE90-000801] N90-19669

HELIUM
An attempt of improving high-temperature fatigue properties of Ni-Cr-W superalloys in HTGR helium
[DE90-741482] N90-19350
HELIUM ISOTOPES
Nucleation of vortices in superfluid helium-4
[DE90-610675] N90-19880
Goldstone excitation and symmetry breaking mechanism in superfluid He-4
[DE90-610676] N90-19881
Coherent state in the roton region of superfluid helium-4
[DE90-610677] N90-19882
HETEROGENEITY
Heterogeneous composite and method of making
[AD-D014337] N90-19306
HETEROJUNCTIONS
The III-V semiconductor quantum well lasers and related optoelectronic devices on silicon
[AD-A216980] N90-19570
HEURISTIC METHODS
Iterative procedures for space shuttle main engine performance models N90-19416
The 0-1 multiknapsack problem: Heuristic and reduction methods
[INPE-4894-PRE/1495] N90-19782
HIERARCHIES
Object Oriented Programming Systems (OOPS) and frame representations: An investigation of programming paradigms
[NASA-CR-186084] N90-19758
HIGH ALTITUDE
Nonlinear mechanics of unstable plasmas as related to high altitude aerodynamics
[AD-A215126] N90-19852
HIGH ELECTRON MOBILITY TRANSISTORS
The 32-GHz performance of the DSS-14 70-meter antenna: 1989 configuration N90-19452
HIGH ENERGY ELECTRONS
Algorithms for calorimeter simulation with parameterized showers by example of H1 detectors
[MPI-PAE/EXP.EL-200] N90-19828
HIGH ENERGY INTERACTIONS
Research accomplishments and future goals in particle physics
[DE90-007296] N90-19830
Experimental and theoretical high energy physics
[DE90-005974] N90-19834
HIGH FREQUENCIES
High power, high frequency component test facility
[NASA-TM-102500] N90-19484
Use of chaotic and random vibrations to generate high frequency test inputs. Part 2: Chaotic vibrations
[DE90-007153] N90-19627
Use of chaotic and random vibrations to generate high frequency test inputs
[DE90-007412] N90-19628
HIGH POWER LASERS
Experimental results of aging and thermal effects in high-power laser diodes
[DE90-005955] N90-19573
HIGH PRESSURE
A parametric heat transfer study for cryogenic ball bearings in SSME HPOTP N90-19397
Investigation of SSME alternate high pressure fuel turbopump lift-off seal fluid and structural dynamic interaction N90-19400
A study of the effects of disk flexibility on the rotordynamics of the space shuttle main engine turbo-pumps N90-19401
HIGH RESOLUTION
Spatially high-resolution flame diagnosis by means of spontaneous Raman spectroscopy
[ETN-90-95870] N90-19328
A high resolution automatic image measuring system
[WISS-ARB-VERMESSUNGSWESEN-154] N90-19559
Regional climate change predictions from the Goddard Institute for Space Studies high resolution GCM
[NASA-CR-186375] N90-19725
HIGH REYNOLDS NUMBER
Separation bubbles at high Reynolds number: Measurement and computation
[CUED/A-AERO/15] N90-19525
HIGH SPEED
High speed modem
[AD-D014319] N90-19750
HIGH TEMPERATURE
Deformation and fracture of TiAl + W at elevated temperatures
[DE90-006490] N90-19356
Demonstration of capabilities of high temperature composites analyzer code HITCAN
[NASA-TM-102560] N90-19629
Solar and thermic utilization in high temperature area: Research and development
[ETN-90-96062] N90-19663
HIGH TEMPERATURE GAS COOLED REACTORS
An attempt of improving high-temperature fatigue properties of Ni-Cr-W superalloys in HTGR helium
[DE90-741482] N90-19350
HIGH TEMPERATURE GASES
Proceedings of Air Force Office of Scientific Research workshop on Laser Propulsion
[AD-A216563] N90-19569
HIGH TEMPERATURE SUPERCONDUCTORS
Laser mass spectrometric studies of high temperature superconductor ablation
[DE90-006518] N90-19585
Characterization of ground state neutral and ion transport during laser ablation of 1:2:3 superconductors by transient optical absorption spectroscopy
[DE90-006623] N90-19878
Neutron scattering measurements of the magnetic excitations of high-temperature superconducting materials
[DE90-006567] N90-19885
Novel processing of HTS based conductors
[DE90-005956] N90-19892
Band electronic structures and crystal packing forces
[DE90-007669] N90-19898
HIGH VOLTAGES
Lightning protection apparatus for RF equipment and the like
[AD-D014336] N90-19483
High voltage pickup plate
[LINO-1989-3] N90-19510
HILBERT SPACE
Iteration methods for solving nonlinear equations in Frechet spaces
[DE90-610429] N90-19799
Linearized analysis of (2+1)-dimensional Einstein-Maxwell theory
[DE90-741470] N90-19913
HIPPARCOS SATELLITE
Signature objects: Preliminaries for the satellite project HIPPARCOS/TYCHO
[ETN-90-95730] N90-19934
HMX
Ignition of HMX (cyclotetramethylenetetranitramine) using low energy laser diodes
[DE90-007637] N90-19334
HOLES (ELECTRON DEFICIENCIES)
Self-consistant calculation of point and pair structure defects in silicium
[ETN-90-96059] N90-19891
HOMING
Suboptimal period design for a maneuvering missile to evade tracking filters N90-19479
HOMOGENEOUS TURBULENCE
Analytical methods for the development of Reynolds stress closures in turbulence
[NASA-CR-182017] N90-19538
HOMOLOGY
Reparametrization BRS cohomology in two-dimensional gravity and non-critical string theories
[DE90-741468] N90-19911
HONEYCOMB STRUCTURES
Low-energy impact resistance of graphite-epoxy plates and ALS honeycomb sandwich panels N90-19405
HORIZONTAL FLIGHT
Three-dimensional viscous rotor flow calculations using a viscous-inviscid interaction approach
[NASA-TM-102235] N90-19204
HOT PRESSING
Crystallization behavior and properties of BaO-Al2O3-2SiO2 glass matrices
[NASA-CR-185209] N90-19374
HOVERING
Three-dimensional viscous rotor flow calculations using a viscous-inviscid interaction approach
[NASA-TM-102235] N90-19204
HUBBLE SPACE TELESCOPE
Information reconstruction from speckle interferograms
[ETN-90-95918] N90-19939
Space telescope searches for black holes in galactic nuclei N90-19958
HUMAN BEINGS
The pollution hazard assessment system: Documentation and users manual
[AD-A217108] N90-19706
HUMAN BODY
Reliability of equivalent sphere model in blood-forming organ dose estimation
[NASA-TM-4178] N90-20036
HUMAN FACTORS ENGINEERING
Human factors engineering testing of aircraft cockpit lighting systems
[AD-A216853] N90-19743
A human factors testbed for ground-vehicle telerobotics research
[DE90-006618] N90-19746
HYBRID NAVIGATION SYSTEMS
Carin and GPS: The combination of dead reckoning, map matching and satellite navigation in a hybrid automobile navigation system
[ETN-90-95451] N90-19220
HYBRID STRUCTURES
Tensile behavior of cylindrical pressure tanks in fiber assembling + metal hybrid structure
[ILR-MITT-213] N90-19618
HYDRAZINES
Study of hydrazine metabolism and toxicity
[AD-A217103] N90-19736
HYDROCARBON FUELS
Dual-fuel, dual-mode rocket engine
[NASA-CASE-LAR-13773-1] N90-19298
HYDRODYNAMIC EQUATIONS
Turbulent mixing effects in models of thermal blooming
[DE90-007245] N90-19580
Boundary layer parameterization in CTM and MM4 N90-19697
HYDRODYNAMICS
Applications of frequency and wavenumber nonlinear digital signal processing to nonlinear hydrodynamics research
[AD-A216259] N90-19530
Laser-matter interaction at intensities of 10(sup 12) W/cm(sup 2) and below
[DE90-007536] N90-19590
Direct absorption receiver
[DE90-000311] N90-19667
Application of natural isotopes in groundwater for solving environmental problems
[DE90-000223] N90-19703
Time-dependent two-dimensional radiation hydrodynamics of accreting matter onto highly magnetized neutron stars
[DE90-006927] N90-19985
HYDROGEN
A new model for hydrogen absorption in welds
[AD-A216951] N90-19347
Electron energy distributions and vibrational population distributions
[DE90-005550] N90-19825
Supercomputer applications for materials science: Ordering effects of hydrogen in palladium
[DE90-004664] N90-19870
HYDROGEN ATOMS
Hydrogen assay foil counting system
[DE90-007415] N90-19332
HYDROGEN FUELS
Dual-fuel, dual-mode rocket engine
[NASA-CASE-LAR-13773-1] N90-19298
HYDROGEN PRODUCTION
IEA (International Energy Agency) implementing agreement for a program of research and development on the production of hydrogen from water. Task 9: Hydrogen production
[DE90-007354] N90-19337
HYDROGENATION
Hydrous metal oxide-supported catalysts. Part 2: Catalytic properties and applications
[DE90-008098] N90-19336
HYDROMETEOROLOGY
Data reduction of GOES (Geostationary Operational Environmental Satellite) information from DCP (Data Collection Platform) networks
[AD-A215844] N90-19637
HYDROXYL RADICALS
Control of the RADM chemistry mechanism of the gas phase N90-19690
The role of clouds in the photochemistry of the background troposphere N90-19694
HYPERBOLIC DIFFERENTIAL EQUATIONS
Implementation of a finite element process for the Euler equations of the gas dynamics
[PREPRINT-500] N90-19545
HYPERCUBE MULTIPROCESSORS
An optimized algorithm for solving the nodal diffusion method on shared memory multiprocessors
[DE90-002703] N90-19762
Parallel neural net path-planner on hypercube and transputer
[DE90-006324] N90-19777
HYPERSONIC FLOW
Computation of hypersonic unsteady viscous flow over a cylinder N90-19194
HYPERSONIC VEHICLES
Aeroservoelasticity
[NASA-TM-102620] N90-19227
Rapid near-optimal trajectory generation and guidance law development for single-stage-to-orbit airbreathing vehicles
[NASA-CR-186299] N90-19275

HYPERSONICS
Computation of hypersonic unsteady viscous flow over a cylinder N90-19194
HYSTERESIS
Ac loss measurements of two multifilamentary NbTi composite strands
[DE90-005388] N90-19304

I

ICE
Petrographic working model of the Rosetta sampling and modelling subgroup for a comet nucleus N90-19992
Physical processes in cometary ices inferred from laboratory studies N90-19996
Laboratory studies of cometary ice analogues N90-19997
Evolution of ices and carbonaceous materials in the laboratory and in comets N90-19998
Physico-chemical properties of formaldehyde-ice-dust mixtures N90-20000
Introduction to drilling technology N90-20002
Possible targeting of particle emission by mechanical stress and penetration of sublimating ice-dust-surfaces N90-20016
ICE FORMATION
Heat transfer measurements from a NACA 0012 airfoil in flight and in the NASA Lewis icing research tunnel
[NASA-CR-4278] N90-19203
IDEAL GAS
Numerical modelling of shocks in gases and metals
[MRL-RR-8-89] N90-19528
IGNITION
Ignition of HMX (cyclotetramethylenetetranitramine) using low energy laser diodes
[DE90-007637] N90-19334
ILLUMINATING
Human factors engineering testing of aircraft cockpit lighting systems
[AD-A216853] N90-19743
ILMENITE
Getting lunar ilmenite: From soils or rocks
[NASA-CR-186498] N90-20029
IMAGE ANALYSIS
A high resolution automatic image measuring system
[WISS-ARB-VERMESSUNGSWESEN-154] N90-19559
Possible applications of remote sensing satellite pictures for the water quality management of the Frisian lakes, Netherlands
[BCRS-88-17] N90-19641
Thematic coupling between digital images and geographic information systems
[ETN-90-95723] N90-19646
Using image analysis to determine petrophysical properties of reservoir rocks
[DE90-000222] N90-19649
Thermal infrared scene simulation
[DE90-006900] N90-19845
Laboratory techniques for the characterisation of snow structures N90-20007
IMAGE PROCESSING
Highly accurate navigation: Integration of navigation and geodesic methods
[SFB-228] N90-19221
Signal processing
[DE90-006904] N90-19464
Single antenna interferometry
[DE90-008120] N90-19474
The microchannel plate camera as a detector at high resolution spectrographs: Experiments for velocity distribution in planetary nebulae
[ETN-90-95733] N90-19560
Selection of optimal textural features for maximum likelihood image classification
[DE90-006901] N90-19638
Development of software routines for remote sensing digital image processing
[ETN-90-95452] N90-19640
Segmentation of Side-Looking Airborne Radar (SLAR) images using a priori knowledge
[BCRS-89-03] N90-19644
Visual processing in texture segregation
[AD-A216539] N90-19737
Digital production of perspective images
[SER-C-347] N90-19768
Image manipulation in the SIGGRAPH Interactive Proceedings
[DE90-007542] N90-19771
Hybrid neural network and rule-based pattern recognition system capable of self-modification
[DE90-007482] N90-19779
Processing infrared images for target detection: A literature study
[IZF-1988-12] N90-19847
Structural experiments of planetary nebulae: Charge-coupled devices, image reduction under MIDAS, information representation, and development of an evolution classification for PN's
[ETN-90-95736] N90-20026
IMAGE RECONSTRUCTION
Object detection and amplitude estimation based on maximum a posteriori reconstructions
[DE90-007511] N90-19770
IMAGE RESOLUTION
Precision segmented reflector, figure verification sensor N90-19272
A high resolution automatic image measuring system
[WISS-ARB-VERMESSUNGSWESEN-154] N90-19559
IMAGE TUBES
Reliability testing of the Hughes temperature controlled 1/4 watt split cycle cryogenic cooler (HD-1045 (V)/UA)
[AD-A216696] N90-19426
IMAGES
Using image analysis to determine petrophysical properties of reservoir rocks
[DE90-000222] N90-19649
A technique for convolving unequally spaced samples using fast Fourier transforms
[DE90-006466] N90-19802
IMAGING TECHNIQUES
Operational requirements and the geostationary platform N90-19250
Synthetic Aperture Interferometric Radiometer (SAIR) N90-19261
General multidimensional scanning ratio transformation and its utilization for norm transformation of television signals
[ETN-90-96058] N90-19470
Parallel distributed networks for image smoothing and segmentation in analog VSLI
[AD-A216780] N90-19491
A method for determination of control pixels for LANSAT using a reflector
[INPE-4884-PRE/1491] N90-19632
Availability of multitemporal LANDSAT data accompanying the variation of water surfaces in the program area of Careiro PDRI/AM
[INPE-4896-PRE/1496] N90-19634
Automated visibility and cloud cover measurements with a solid-state imaging system
[AD-A216906] N90-19724
NMR (Nuclear Magnetic Resonance) imaging development for the study of solids
[AD-A217073] N90-19899
Very high energy gamma ray astrophysics
[DE90-006645] N90-19983
IMPACT DAMAGE
Evaluation of repeated impact damage in composite structures N90-19303
Evaluation of the response of aluminum alloys to single and multiple particle impacts
[DE90-003689] N90-19526
IMPACT LOADS
Test component attachment effects on resonant plate pyrotechnic shock simulation
[DE90-006478] N90-19551
IMPACT RESISTANCE
Low-energy impact resistance of graphite-epoxy plates and ALS honeycomb sandwich panels N90-19405
IMPACT TESTS
Liquid oxygen LOX compatibility evaluations of aluminum lithium (Al-Li) alloys: Investigation of the Alcoa 2090 and MMC weldalite 049 alloys N90-19398
Use of chaotic and random vibrations to generate high frequency test inputs. Part 2: Chaotic vibrations
[DE90-007153] N90-19627
IMPROVEMENT
Blue upconversion thulium laser
[DE90-006517] N90-19584
INCLUSIONS
Elastic solutions in a semi-infinite solid with an ellipsoidal inclusion
[AD-A217063] N90-19338
Elimination of platinum inclusions in phosphate laser glasses
[DE90-004479] N90-19361
P-T condition fo deformation from fluid inclusions in mylonites
[NASA-CR-186377] N90-19710
INCOMPRESSIBLE FLOW
Computational fluid dynamics method for low Reynolds number flow in a precessing/spinning, liquid filled cylinder with rounded endcaps
[AD-A216997] N90-19531
INDEXES (DOCUMENTATION)
Aeronautical engineering: A continuing bibliography with indexes (supplement 249)
[NASA-SP-7037(249)] N90-19190
INDIAN SPACECRAFT
Compendium of meteorological space programs, satellites, and experiments
[NASA-TM-102924] N90-19243
INDIUM
Digital capacity transient spectroscopy of deep structure defects in III-V-Semiconductor structures
[ETN-90-96057] N90-19890
INDIUM COMPOUNDS
Investigations of CuInSe2 thin films and contacts
[DE90-000301] N90-19886
INDIUM PHOSPHIDES
Opto-Em and devices investigation
[AD-A215033] N90-19814
INDUCTION MOTORS
Induction motor control
[NASA-TM-102533] N90-19234
INDUSTRIAL MANAGEMENT
Operational fact-finding report on heat pump systems for industrial use
[DE89-782295] N90-19527
INELASTIC SCATTERING
Background studies in gas ionizing x ray detectors N90-19399
Transverse spin observables in chromodynamics
[DE90-005638] N90-19824
Bose condensate in superfluid (sup 4)He and momentum distributions by deep inelastic scattering
[DE90-007541] N90-19832
The electron momentum-transfer cross sections of tungsten, silicon, and silicon dioxide at energies from 0.1 to 10,000 eV
[DE90-009041] N90-19833
INERTIA PRINCIPLE
Inertial corrections by dynamic estimation N90-19976
Ultra-sensitive inertial sensors via neutral-atom interferometry N90-19977
INFERENCE
Theory and applications of belief functions
[AD-A217092] N90-19774
INFLATABLE STRUCTURES
Advances in large inflatable reflectors N90-19258
INFLUENCE COEFFICIENT
On the evaluation of aerodynamic influence coefficients
[NLR-MP-87019-U] N90-19191
INFORMATION DISSEMINATION
Research Reports: 1989 NASA/ASEE Summer Faculty Fellowship Program
[NASA-CR-183837] N90-19390
INFORMATION RETRIEVAL
The expression of syntagmatic relationships in frame-based indexing N90-19917
CRISP (Computer Retrieval of Information on Scientific Projects) thesaurus, fiscal year 1990
[PB90-138652] N90-19922
INFORMATION SYSTEMS
Low earth orbiting satellite for international information exchange system
[DE90-007186] N90-19292
Augmenting and updating NASA spacelink electronic information system N90-19392
ESRIN
[ESA-BR-58] N90-19631
Executive information systems for providing next generation strategic information: An evaluation of EIS (Executive Information System) software and recommended applicability within the FAA computing environment
[AD-A216672] N90-19920
National Technical Information Service 1989 Users Conference proceedings
[PB90-142563] N90-19921
INFORMATION THEORY
Computation at the edge of chaos: Phase transition and emergent computation
[DE90-007488] N90-19811
INFORMATION TRANSFER
Low earth orbiting satellite for international information exchange system
[DE90-007186] N90-19292
High throughput data communication system
[AD-D014342] N90-19432
High speed modem
[AD-D014319] N90-19750
INFRARED DETECTORS
Contact formation on (Hg,Cd) Te
[AD-A217088] N90-19900
INFRARED FILTERS
CdTe buffered GaAs thin-slab IR waveguide modulators and T/R filter
[AD-A215999] N90-19488
INFRARED IMAGERY
Reliability testing of the Hughes temperature controlled 1/4 watt split cycle cryogenic cooler (HD-1045 (V)/UA)
[AD-A216696] N90-19426

The utilization of an infrared imaging system as a cooling slot blockage detector in the inspection of a transpiration cooled nozzle
[NASA-TM-102608] N90-19555
ARGUS/LLNL IR camera calibration and characterization
[AD-A217076] N90-19563
Processing infrared images for target detection: A literature study
[IZF-1988-12] N90-19847

INFRARED LASERS
Potential biomedical application of the Los Alamos infrared free-electron laser: DNA spectroscopy
[DE90-006505] N90-19575

INFRARED PHOTOGRAPHY
ARGUS/LLNL IR camera calibration and characterization
[AD-A217076] N90-19563

INFRARED PHOTOMETRY
An optical and infrared study of blazars N90-19930

INFRARED RADIATION
Development of the blackbody probe type pyrometer, part 1. Experimental study on the fundamental characteristics
[DE89-782288] N90-19553
Atmospheric Radiation Measurement Program plan
[DE90-006349] N90-19705
Thermal infrared scene simulation
[DE90-006900] N90-19845

INFRARED RADIOMETERS
The utilization of an infrared imaging system as a cooling slot blockage detector in the inspection of a transpiration cooled nozzle
[NASA-TM-102608] N90-19555
ARGUS/LLNL IR camera calibration and characterization
[AD-A217076] N90-19563

INFRARED SPECTRA
The optical properties of beryllium
[DE90-006372] N90-19848
Evolution of ices and carbonaceous materials in the laboratory and in comets N90-19998

INFRARED SPECTROMETERS
Infrared heterodyne spectroscopy of polyatomic molecules in circumstellar envelopes N90-19980

INFRARED SPECTROSCOPY
Infrared heterodyne spectroscopy of polyatomic molecules in circumstellar envelopes N90-19980

INFRARED STARS
Cometary bodies in the circumstellar disk around beta Pictoris N90-20010

INFRARED TELESCOPES
Feasibility of using Extreme Ultraviolet Explorer (EUVE) reaction wheels to satisfy Space Infrared Telescope Facility (SIRTF) maneuver requirements
[NASA-TM-100389] N90-19556

INGESTION (BIOLOGY)
The pollution hazard assessment system: Documentation and users manual
[AD-A217108] N90-19706

INJECTION
A review of models for the analysis of the injection of densely loaded flows into entrained flow gasifiers
[DE90-000453] N90-19550

INLET FLOW
Water-tunnel investigation of concepts for alleviation of adverse inlet spillage interactions with external stores
[NASA-TM-4181] N90-19199

INSPECTION
VLSI implementation of moment invariants for automated inspection
[DE90-005318] N90-19493
Development of inspection techniques for quantitatively measuring surface contamination on SRM hardware
[NASA-CR-183902] N90-19608

INSTITUTIONS
Activities report of the Institute for Communication Technology
[ETN-90-95383] N90-20043

INSTRUCTORS
Research Reports: 1989 NASA/ASEE Summer Faculty Fellowship Program
[NASA-CR-183837] N90-19390

INSTRUMENT ERRORS
Identification and solution of a charging problem in a high-altitude detector
[DE90-008637] N90-19296

INSULATION
Heterogeneous composite and method of making
[AD-D014337] N90-19306

INTEGERS
Minimum cycle covering and integer flows
[AD-A216546] N90-19785

INTEGRAL EQUATIONS
A comparison between the propagators method and the decomposition method for nonlinear equations
[DE90-005783] N90-19781

INTEGRATED CIRCUITS
A virtual zero-time, monolithic systolic sorting array
[DE90-001000] N90-19753
CCST (Center for Compound Semiconductor Technology) research briefs
[DE90-006446] N90-19887

INTEGRATED OPTICS
All-fiber SFPM (Stimulated Four Photon Mixing) amplifier
[AD-D014358] N90-19841
Integrated optics anisotropic waveguides and devices
[AD-A217064] N90-19849

INTERCALATION
Exchange and correlation effects in the Visscher-Falicov model for metal intercalated graphite
[DE90-610553] N90-19349

INTERFACE STABILITY
Study of interfacial behavior in cocurrent gas-liquid flows
[DE90-005988] N90-19532

INTERFACES
Nanolayer reactions in aluminum-metal interfaces
[DE90-004955] N90-19342

INTERFEROMETRY
Synthetic Aperture Interferometric Radiometer (SAIR) N90-19261
Apparatus and method for minimizing polarization-induced signal fading in an interferometric fiber-optic sensor using input-polarization modulation
[AD-D014315] N90-19430
Single antenna interferometry
[DE90-008120] N90-19474

INTERMETALLICS
Irradiation-induced amorphization and elastic shear instability in intermetallic compounds
[DE90-004845] N90-19341
Creep behavior of alloys based on TiAl containing TiB2 and TiN particulates
[DE90-006489] N90-19355

INTERPLANETARY DUST
Porosity and ice-dust mixtures in cometary particles N90-20018
Mechanical properties of fluffy agglomerates consisting of core-mantle-particles N90-20019

INTERPOLATION
Analysis and design of symmetrical airfoils
[PD-CF-8943] N90-19213
Analysis of unsteady heat transfer by natural convection in a two-dimensional square cavity using a high order finite-volume method N90-19521
Calculation of nonlinear viscoelastic processes for plastic layer textile membranes
[ETN-90-95868] N90-19622
Initialization of EURAD, part 2 N90-19696
A technique for convolving unequally spaced samples using fast Fourier transforms
[DE90-006466] N90-19802

INTERPROCESSOR COMMUNICATION
Flosolver Mk1B: An eight processor parallel machine
[PD-CF-8941] N90-19755

INTERSTELLAR EXTINCTION
Comet Halley: An optical continuum study N90-19981

INTERSTELLAR MATTER
A test of the interstellar dust model of comets N90-19995

INVENTIONS
From invention to innovation: Commercialization of new technology by independent and small business inventors
[DE90-006944] N90-19927

INVENTORIES
NAPAP (National Acid Precipitation Assessment Program) emissions inventory: Overview of allocation factors, 1985
[PB90-126012] N90-19679

INVERTERS
Utilization criteria for transistors of diverse technology in pulse inverters with high switching frequency
[ETN-90-95359] N90-19500

INVISCID FLOW
Numerical modelling of shocks in gases and metals
[MRL-RR-8-89] N90-19528

IO
Ultraviolet observations of the atmosphere of Io and the plasma torus N90-19929

ION BEAMS
International conference on Surface Modification of Metals by Ion Beams
[AD-A215872] N90-19345
The TISOL facility at TRIUMF
[DE90-006882] N90-19837
Ion mixing and surface modification in metal-semiconductor systems
[DE90-007557] N90-19897

ION DENSITY (CONCENTRATION)
Characterization of ground state neutral and ion transport during laser ablation of 1:2:3 superconductors by transient optical absorption spectroscopy
[DE90-006623] N90-19878

ION EXCHANGING
Hydrous metal oxide-supported catalysts. Part 2: Catalytic properties and applications
[DE90-008098] N90-19336

ION IMPLANTATION
International conference on Surface Modification of Metals by Ion Beams
[AD-A215872] N90-19345
Modification of surface mechanical properties of high-chromium tool steel by carbon-implanted codeposited Fe-Ti films
[DE90-007502] N90-19358
Particle emission by oblique ion bombardment of gold
[ETN-90-95825] N90-19827
Silicon carbide semiconductor device fabrication and characterization
[NASA-CR-186354] N90-19873

ION SOURCES
The TISOL facility at TRIUMF
[DE90-006882] N90-19837

ION TRAPS (INSTRUMENTATION)
Simple analytic potentials for linear ion traps N90-19436

IONIC REACTIONS
Searching for existing nuclear data
[DE90-007535] N90-19925

IONIZATION
Two-dimensional, long-pulse computer calculation of microwave-induced electron layer formation in low-pressure air
[DE90-005994] N90-19459
Radiation of electromagnetic waves by an accelerated charged particle in medium
[DE90-610458] N90-19461
Electron energy distributions and vibrational population distributions
[DE90-005550] N90-19825
Model calculations for dynamic development of planetary nebulae
[ETN-90-95734] N90-20025

IONOSPHERIC DISTURBANCES
Calculation of ionospheric corrections for single frequency GPS observations: Investigation of two models
[ETN-90-95450] N90-19219
Ionospheric heating with oblique waves. Volume 1: Electron density perturbations
[AD-A216260] N90-19709

IONOSPHERIC HEATING
Ionospheric heating with oblique waves. Volume 1: Electron density perturbations
[AD-A216260] N90-19709

IONOSPHERIC PROPAGATION
Calculation of ionospheric corrections for single frequency GPS observations: Investigation of two models
[ETN-90-95450] N90-19219

IRON
The preparation and properties of iron doped II-VI chalcogenides
[AD-A217569] N90-19903

IRRADIATION
Irradiation-induced amorphization and elastic shear instability in intermetallic compounds
[DE90-004845] N90-19341
Effect of electron-excitation on radiation damage in ion-irradiated FCC metals
[DE90-719537] N90-19344
Defect structures in copper and gold irradiated with fast neutrons, 14 MeV neutrons and 600 to 800 MeV protons
[DE90-007529] N90-19359

ISING MODEL
The renormalization group and lattice QCD
[DE90-004860] N90-19905

ISLANDS
Evolution of midplate hotspot swells: Numerical solutions
[NASA-CR-186462] N90-19713

ISOLATION
Elastomeric electrical isolation membrane
[AD-D014365] N90-19490

ISOMORPHISM
Banach C*-algebras not containing a subspace isomorphic to C(sub 0)
[DE90-610428] N90-19798

ISOTOPE EFFECT
Superconductivity in Ba(1-x)BiO3
[DE90-003781] N90-19889

Stable isotope studies of cometary analogue materials N90-20001
ISOTOPE SEPARATION
The TISOL facility at TRIUMF
[DE90-006882] N90-19837
ISOTOPES
Application of natural isotopes in groundwater for solving environmental problems
[DE90-000223] N90-19703
ISOTROPIC TURBULENCE
Application of a Reynolds stress turbulence model to the compressible shear layer
[NASA-CR-182002] N90-19537
ISOTROPY
Background studies in gas ionizing x ray detectors N90-19399
ITERATION
Iterative procedures for space shuttle main engine performance models N90-19416
Convergence properties of iterative algorithms for solving the nodal diffusion equations
[DE89-016859] N90-19804
Optimal iteration steps by stochastic approximation processes for the solution of optimization problems with twice differentiable functions
[ETN-90-95887] N90-19809
Integrated optics anisotropic waveguides and devices
[AD-A217064] N90-19849
ITERATIVE SOLUTION
Hierarchical basis preconditioners for second order elliptic problems in three dimensions
[DE90-005980] N90-19793
Iteration methods for solving nonlinear equations in Frechet spaces
[DE90-610429] N90-19799
Projection-iteration methods for solving nonlinear operator equations
[DE90-610433] N90-19801

J

JACOBI MATRIX METHOD
Integrated optics anisotropic waveguides and devices
[AD-A217064] N90-19849
JAMMING
Packet radio networks under dynamic jamming
[AD-A217094] N90-19475
JAPAN
Survey on the possibility of introducing new energy to regional development plans
[DE89-782627] N90-19654
JET FLOW
Numerical study of diffusion jet flames N90-19316
JET STREAMS (METEOROLOGY)
Synoptic-scale forcing of the low-level jet in developing baroclinic waves N90-19717
JOINTS (JUNCTIONS)
Thermo-oxidative stability studies of PMR-15 polymer matrix composites reinforced with various fibers
[NASA-TM-102439] N90-19310
Viscoelastic adherend effects in adhesively bonded composite-to-composite joints N90-19594
JOSEPHSON JUNCTIONS
Novel processing of HTS based conductors
[DE90-005956] N90-19892
JP-4 JET FUEL
In-flight evaluations of turbine fuel extenders
[DOT/FAA/CT-89/33] N90-19387
JUNCTION DIODES
Contact formation on (Hg,Cd) Te
[AD-A217088] N90-19900

K

KALMAN FILTERS
Self-tuning control techniques, implicit and explicit, with parameter estimation in Kalman filters, applied to artificial satellite attitude
[INPE-4857-TDL/368] N90-19276
Suboptimal period design for a maneuvering missile to evade tracking filters N90-19479
KEROSENE
The measurement, modeling, and prediction of traction for rocket propellant 1
[NASA-CR-185186] N90-19386
KINEMATIC EQUATIONS
Dynamics and control of robot manipulators with closed-kinematic chain mechanism N90-19598
KINEMATICS
Kinematic control of robotic manipulators with multiple interchangeable wrists N90-19592
Theory of gearing
[NASA-RP-1212] N90-19593
Advanced control schemes and kinematic analysis for a kinematically redundant 7 DOF manipulator
[NASA-CR-186175] N90-19599
KINETIC ENERGY
Two-meter laser material response impulse measurements
[AD-A215834] N90-19567
The atmospheric energy cycle of stationary and transient waves
[ISSN-0069-5882] N90-19728
KINETIC EQUATIONS
Longitudinal traveling waves bifurcating from Vlasov plasma equilibria N90-19850
KINETICS
Evaluation of radiation-induced sensitization using electrochemical potentiokinetic reactivation technique for austenitic stainless steels
[DE90-002708] N90-19352
Nonlinear continuum mechanics and applied analysis
[AD-A213629] N90-19812
Linear free energy relations for multielectron transfer kinetics: A brief look at the Bronsted/Tafel analogy
[AD-A215078] N90-19823
KLYSTRONS
Digital to position converter
[DIGEL-1984-4] N90-19509
KNUDSEN FLOW
Gas diffusion in a cometary crust N90-20017
KRYPTON FLUORIDE LASERS
Anode plasma formation as a possible mechanism for an electrical stress limit in cold cathode diodes
[DE90-007503] N90-19516
KRYPTON 85
Simulation of global Kr-85 and (14)CO2 distribution by means of a time-dependent, two dimensional model of the atmosphere
[ETN-90-95376] N90-19702
KUTTA-JOUKOWSKI CONDITION
Experimental study of validity of the unstationary Kutta condition, with high Strouhal numbers
[ETN-90-95914] N90-19547

L

LAGEOS (SATELLITE)
LAGEOS 3 and the gravitomagnetic field N90-19961
LAGRANGE COORDINATES
A complete description of robot manipulator dynamics based on Lagrangian mechanics
[DE90-741467] N90-19603
LAKES
Possible applications of remote sensing satellite pictures for the water quality management of the Frisian lakes, Netherlands
[BCRS-88-17] N90-19641
LAMINAR FLOW
Computation of hypersonic unsteady viscous flow over a cylinder N90-19194
Spatially high-resolution flame diagnosis by means of spontaneous Raman spectroscopy
[ETN-90-95870] N90-19328
Method and apparatus for detecting laminar flow separation and reattachment
[NASA-CASE-LAR-13952-1-SB] N90-19534
Conforming Chebyshev spectral collocation methods for the solution of laminar flow in a constricted channel
[NASA-CR-182011] N90-19539
Theoretical and experimental examination of the beginning of turbulence in a heated laminar conduit flow
[ETN-90-95369] N90-19541
A note on an acoustic response during an engine nacelle flight experiment
[NASA-TM-102585] N90-19821
LAMINATES
Evaluation of repeated impact damage in composite structures N90-19303
Steady state temperatures and thermal stresses in a spherical or cylindrical laminated shell
[ESDU-89027] N90-19612
LAND MANAGEMENT
Possible applications of remote sensing in the preparatory phase of a land management project
[BCRS-88-19] N90-19642
LAND USE
The potential of combined use of satellite data with topographic TM information for manual/visual and digital updating of land use
[NLR-MP-88021-U] N90-19639
LANDING GEAR
Modeling and analysis of the space shuttle nose-gear tire with semianalytic finite elements
[NASA-TP-2977] N90-19595
LANGEVIN FORMULA
On the Langevin equation for stochastic quantization of gravity
[DE90-750024] N90-19914
LARGE DEPLOYABLE REFLECTOR
Unfurlable, continuous-surface reflector concept N90-19257
Millimeter radiometer system technology N90-19260
LARGE SPACE STRUCTURES
Earth Science Geostationary Platform Technology
[NASA-CP-3040] N90-19249
Science requirements for passive microwave sensors on earth science geostationary platforms N90-19251
Structures for remotely deployable precision antennas N90-19256
Advances in large inflatable reflectors N90-19258
Large antenna measurement and compensation techniques N90-19263
Application of attachment modes in the control of large space structures
[NASA-CR-185604] N90-19280
Modified independent modal space control of flexible structures N90-19597
LASER APPLICATIONS
Laser Technology Center
[PB90-115387] N90-19564
Potential biomedical application of the Los Alamos infrared free-electron laser: DNA spectroscopy
[DE90-006505] N90-19575
FWP executive summaries: Basic energy sciences materials sciences programs
[DE90-006373] N90-19893
LASER BEAMS
Linear theory of thermal blooming in turbulence
[DE90-007243] N90-19579
Correlation-induced changes of spectra
[AD-A217087] N90-19591
Atmospheric thermal blooming and beam clearing by aerosol vaporization
[DE90-006271] N90-19711
The nonlinear interaction of intense laser pulses in plasmas
[AD-A217604] N90-19867
LASER CAVITIES
CO2 laser plus optimization for harmonic generation
[AD-D014341] N90-19565
Narrow-bandwidth unstable laser resonator
[AD-D014362] N90-19568
LASER DAMAGE
Effect of barrier layers in burn-through experiments with 351-nm laser illumination
[DE90-006806] N90-19577
LASER INDUCED FLUORESCENCE
Time resolved gain/loss studies under low and high power loading for the XeF C-A transition
[DE90-007506] N90-19517
Development and utilization of new diagnostics for dense-phase pneumatic transport
[DE90-006787] N90-19536
Development of a receiver for a space-based laser radar system
[AD-A215079] N90-19566
Definition study of Laser Experimental Active Fluorsensor (LEAF)
[BCRS-88-18] N90-19582
LASER INTERFEROMETRY
Optical interferometer in space N90-19953
Optical interferometers for tests of relativistic gravity in space N90-19967
Frequency stable high power lasers in space N90-19969
LASER MATERIALS
Elimination of platinum inclusions in phosphate laser glasses
[DE90-004479] N90-19361
LASER OUTPUTS
Narrow-bandwidth unstable laser resonator
[AD-D014362] N90-19568
LASER PLASMA INTERACTIONS
Laser-matter interaction at intensities of 10(sup 12) W/cm(sup 2) and below
[DE90-007536] N90-19590
The 41st Annual Gaseous Electronics Conference
[AD-A214540] N90-19851
LASER PLASMAS
Proceedings of a contractors meeting on Combustion Rocket Propulsion Diagnostics of Reacting Flow
[AD-A216445] N90-19297
Two-meter laser material response impulse measurements
[AD-A215834] N90-19567
The 41st Annual Gaseous Electronics Conference
[AD-A214540] N90-19851

Characterization of ground state neutral and ion transport during laser ablation of 1:2:3 superconductors by transient optical absorption spectroscopy
[DE90-006623] N90-19878

LASER PROPULSION
Proceedings of Air Force Office of Scientific Research workshop on Laser Propulsion
[AD-A216563] N90-19569

LASER SPECTROSCOPY
Generation of intensive UV laser radiation and utilization in high resolution spectroscopy of SO2
[ETN-90-95361] N90-19581
Definition study of Laser Experimental Active Fluorsensor (LEAF)
[BCRS-88-18] N90-19582
A ground state depleted laser in neodymium doped yttrium orthosilicate
[DE90-006773] N90-19586
Assessment of research needs for laser technologies applied to advanced spectroscopic methods
[DE90-007402] N90-19588
Characterization of ground state neutral and ion transport during laser ablation of 1:2:3 superconductors by transient optical absorption spectroscopy
[DE90-006623] N90-19878

LASER STABILITY
Noise behavior of semiconductor lasers by optic feedback
[ETN-90-95728] N90-19583

LASER TARGET INTERACTIONS
Two-meter laser material response impulse measurements
[AD-A215834] N90-19567

LASER TARGETS
Effect of barrier layers in burn-through experiments with 351-nm laser illumination
[DE90-006806] N90-19577

LASERS
A high optical density measuring spectrometer
[AD-D014331] N90-19318
Effect of barrier layers in burn-through experiments with 351-nm laser illumination
[DE90-006806] N90-19577
Atmospheric thermal blooming and beam clearing by aerosol vaporization
[DE90-006271] N90-19711

LASING
Two-meter laser material response impulse measurements
[AD-A215834] N90-19567
Generation of intensive UV laser radiation and utilization in high resolution spectroscopy of SO2
[ETN-90-95361] N90-19581
First direct observation of FEL (Free-Electron Laser) from lambda=20 to 45 microns
[DE90-007508] N90-19589

LATCH-UP
Dual-mode latching reciprocal ferrite phase shifter
[FEL-1988-55] N90-19497
A gate array structure for the efficient project of digital circuits: The unit cell array
[ETN-90-95364] N90-19502

LATE STARS
Magnetic fields in late-type dwarfs: Preliminary results from a multiline approach
[SER-C-PREPUB-FASC-31] N90-19926

LATENT HEAT
Cloud parameterization in EURAD and its future development N90-19692

LAUNCHERS
Dual frequency launcher for circularly polarized antenna
[AD-D014361] N90-19456

LAUNCHING PADS
TOPAS preparation study: Summary representation of the study results
[OHB-TN-TOP-011/87] N90-19244

LAYOUTS
Optimal layout via Boolean satisfiability
[AD-A216777] N90-19787

LEADING EDGES
Leading edge vortex dynamics on a pitching delta wing
[NASA-CR-186327] N90-19198

LEAKAGE
Evaluation of the Scott aviation portable protective breathing device for contaminant leakage as prescribed by FAA Action Notice A-8150.2. Phase 1: Original tests of the portable protective breathing device. Phase 2: Tests of the redesigned portable protective breathing device
[AD-A216799] N90-19214
Technology evaluation for space station atmospheric leakage
[DE90-007844] N90-19294

LEARNING
An approach to elemental task learning
[DE90-006614] N90-19745

LEARNING THEORY
Symposium on air traffic control training for tomorrow's technology
[PB90-127325] N90-19216

LEAST SQUARES METHOD
Self-tuning control techniques, implicit and explicit, with parameter estimation in Kalman filters, applied to artificial satellite attitude
[INPE-4857-TDL/368] N90-19276
Application of adaptive least-squares algorithm to multi-element array signal reconstruction N90-19448
Error analysis of some Galerkin least squares methods for the elasticity equations
[DE90-608611] N90-19790

LENSES
Narrow-bandwidth unstable laser resonator
[AD-D014362] N90-19568

LIFE (DURABILITY)
Effect of temperature on the storage life of polysulfide aircraft sealants
[MRL-TR-89-31] N90-19364
Influence of the parameters: Charge order, sequence classification, partial sequential circuit, and process regularity of a working charge (Gaussian process) on the lifetime of a component made of 3.1354 T3 and 3.4377 T761
[ETN-90-95378] N90-19503

LIFTING ROTORS
Performance of an optimized rotor blade at off-design flight conditions
[NASA-CR-4288] N90-19226

LIGHT (VISIBLE RADIATION)
Correlation-induced changes of spectra
[AD-A217087] N90-19591
Speckle interferometry for high resolution pictures of astronomical objects
[ETN-90-95827] N90-19936

LIGHT AMPLIFIERS
All-fiber SFPM (Stimulated Four Photon Mixing) amplifier
[AD-D014358] N90-19841

LIGHT BEAMS
Thermal modulation of light beams
[AD-D014322] N90-19840

LIGHT IONS
Impedance characteristics of terawatt ion diodes
[DE90-006276] N90-19494

LIGHT MODULATION
Apparatus and method for minimizing polarization-induced signal fading in an interferometric fiber-optic sensor using input-polarization modulation
[AD-D014315] N90-19430

LIGHT SCATTERING
Light-scattering measurements of CVD (Chemical Vapor Deposition) silicon carbide
[DE90-007885] N90-19382

LIGHTING EQUIPMENT
Human factors engineering testing of aircraft cockpit lighting systems
[AD-A216853] N90-19743

LIGHTNING
Lightning surge characteristics of transmission towers. Lightning surge characteristics of 15-meter-high scale model tower
[DE89-782322] N90-19721
Simulation fidelity in lightning penetration studies
[DE90-006367] N90-19731
The 41st Annual Gaseous Electronics Conference
[AD-A214540] N90-19851

LIGHTNING SUPPRESSION
Lightning protection apparatus for RF equipment and the like
[AD-D014336] N90-19483

LIMITER CIRCUITS
Proposal of arc driving type fault current limiter
[DE89-782290] N90-19485

LINE OF SIGHT
User-friendly software for the design of digital line-of-sight radio links
[PB90-118472] N90-19760

LINE SPECTRA
Power spectral densities for selected digital phase-continuous MFSK (M-ary Frequency Shift Keying) emissions
[PB90-129990] N90-19463
Definition study of Laser Experimental Active Fluorsensor (LEAF)
[BCRS-88-18] N90-19582
Correlation-induced changes of spectra
[AD-A217087] N90-19591
Far-ultraviolet spectroscopy of Comet Halley N90-19979
O-star parameters from line profiles of wind-blanketed model atmospheres N90-19982

LINEAR ACCELERATORS
On 140 GHz microwave FEL experiments using ELF-2
[DE90-006764] N90-19576
Fifth-order aberrations in magnetic quadrupole-octupole systems
[DE90-007489] N90-19831

LINEAR ENERGY TRANSFER (LET)
Linear free energy relations for multielectron transfer kinetics: A brief look at the Bronsted/Tafel analogy
[AD-A215078] N90-19823

LINEAR EQUATIONS
A method for computing the stationary points of a function subject to linear equality constraints
[DE90-610427] N90-19797

LINEAR QUADRATIC GAUSSIAN CONTROL
Experiments in end-point control of a flexible robot with a mini-manipulator N90-19596

LINEAR QUADRATIC REGULATOR
Integrated control/structure optimization by multilevel decomposition
[NASA-TM-102619] N90-19281

LINEAR SYSTEMS
Simple analytic potentials for linear ion traps N90-19436
Computational aspects of sensitivity calculations in linear transient structural analysis
[NASA-TM-4156] N90-19610
Parallel algorithms for boundary value problems
[NASA-TM-102498] N90-19783
A linear systems theory approach to the range-independent acoustic channel
[AD-A216551] N90-19817

LIQUID CRYSTALS
Structures instabilities in filament liquid crystals
[ETN-90-95916] N90-19888

LIQUID FILLED SHELLS
Computational fluid dynamics method for low Reynolds number flow in a precessing/spinning, liquid filled cylinder with rounded endcaps
[AD-A216997] N90-19531

LIQUID HELIUM 2
Mechano-caloric cooling device
[NASA-CR-186316] N90-19552

LIQUID METALS
Particle emission by oblique ion bombardment of gold
[ETN-90-95825] N90-19827

LIQUID OXYGEN
Liquid oxygen LOX compatibility evaluations of aluminum lithium (Al-Li) alloys: Investigation of the Alcoa 2090 and MMC weldalite 049 alloys N90-19398

LIQUID-GAS MIXTURES
Study of interfacial behavior in cocurrent gas-liquid flows
[DE90-005988] N90-19532

LIQUID-VAPOR EQUILIBRIUM
Vapor-liquid equilibria for complex mixtures with special emphasis on the critical region
[PB90-130345] N90-19324

LIQUID-VAPOR INTERFACES
Study of interfacial behavior in cocurrent gas-liquid flows
[DE90-005988] N90-19532
Molecular theory and computer simulation studies of natural and synthetic gas mixtures
[PB90-130329] N90-19826

LIQUIDS
Diffraction studies of the structure of glasses and liquids
[DE90-007662] N90-19381

LITERATURE
Origin and effect of pores in aluminum welded joints
[REPT-87M/43/05720/SCP/GRF] N90-19620
Processing infrared images for target detection: A literature study
[IZF-1988-12] N90-19847
Literature file on fast kickers and SEPTA: Components for deflection and separation of particle beams
[LINO-162] N90-19924
The Moon has set
[REPT-89-07] N90-19933

LITHIUM
Optimizing superplastic response in navalite, a lithium containing aluminum-magnesium alloy
[AD-A216552] N90-19346

LITHIUM ALLOYS
Optimizing superplastic response in navalite, a lithium containing aluminum-magnesium alloy
[AD-A216552] N90-19346
Liquid oxygen LOX compatibility evaluations of aluminum lithium (Al-Li) alloys: Investigation of the Alcoa 2090 and MMC weldalite 049 alloys N90-19398

LITHIUM FLUORIDES
Hot filament technique for measuring the thermal conductivity of molten lithium fluoride
[NASA-TM-102506] N90-19373
LITHIUM NIOBATES
Modeling and realization of plane acousto-optic unilateral band modulators
[ETN-90-95824] N90-19818
LITHOSPHERE
Evolution of midplate hotspot swells: Numerical solutions
[NASA-CR-186462] N90-19713
An analytic model of axisymmetric mantle plume due to thermal and chemical diffusion
[NASA-CR-186461] N90-19714
Stored mafic/ultramafic crust and early Archean mantle depletion
[NASA-CR-186460] N90-19715
LIVER
Study of hydrazine metabolism and toxicity
[AD-A217103] N90-19736
LOAD DISTRIBUTION (FORCES)
Application of attachment modes in the control of large space structures
[NASA-CR-185604] N90-19280
LOADS (FORCES)
Temperature compensated crystal oscillator (TCXO) with improved temperature compensation
[AD-D014334] N90-19482
LOCAL AREA NETWORKS
Random access transmission algorithms for data local area networks
[AD-A216443] N90-19781
Local area network with fault-checking, priorities, and redundant backup
[NASA-CASE-NPO-18949-1-CU] N90-19776
LOCKING
Phase control mechanism for wave energy conversion
[AD-D014354] N90-19657
LONGITUDINAL CONTROL
Development of a preliminary high-angle-of-attack nose-down pitch control requirement for high-performance aircraft
[NASA-TM-101684] N90-19206
LONGITUDINAL WAVES
Longitudinal traveling waves bifurcating from Vlasov plasma equilibria N90-19850
LOSSES
Ac loss measurements of two multifilamentary NbTi composite strands
[DE90-005388] N90-19304
Quantization effects in Viterbi decoding rate 1/n convolutional codes N90-19445
LOW ALTITUDE
Sparse breakdown and statistical sneakthrough effects in low-altitude microwave propagation
[DE90-007252] N90-19473
LOW COST
Low-cost small satellites for astrophysical missions
[DE90-007625] N90-19293
LOW FREQUENCIES
Design of a low-frequency (5-20 GHz), 15-meter-diameter passive radiometer for geostationary earth science platforms N90-19255
LOW PRESSURE
Two-dimensional, long-pulse computer calculation of microwave-induced electron layer formation in low-pressure air
[DE90-005994] N90-19459
LOW REYNOLDS NUMBER
Computational fluid dynamics method for low Reynolds number flow in a precessing/spinning, liquid filled cylinder with rounded endcaps
[AD-A216997] N90-19531
LOW SPEED WIND TUNNELS
Comparison between design and installed acoustic characteristics of NASA Lewis 9- by 15-foot low-speed wind tunnel acoustic treatment
[NASA-TP-2996] N90-19242
LOW TEMPERATURE
Low temperature elastic and dielectric properties of incommensurate barium sodium niobate
[AD-A216969] N90-19815
Physical processes in cometary ices inferred from laboratory studies N90-19996
LOW TEMPERATURE PHYSICS
Record of forum on cold fusion
[DE90-749883] N90-19663
LUMINOSITY
Nearly simultaneous optical, ultraviolet, and x ray observations of three PG quasars
[NASA-CR-186355] N90-19932
LUMPED PARAMETER SYSTEMS
Nonlinear mechanics of unstable plasmas as related to high altitude aerodynamics
[AD-A215126] N90-19852
LUNAR BASES
Extending terrestrial mobile robotics to a proposed lunar base
[DE89-016179] N90-19606
LUNAR SOIL
Getting lunar ilmenite: From soils or rocks
[NASA-CR-186496] N90-20029
LUNAR SURFACE VEHICLES
Extending terrestrial mobile robotics to a proposed lunar base
[DE89-016179] N90-19606
LUNAR TOPOGRAPHY
Analysis of alternative concepts for transport systems on the Moon surface
[ETN-90-95727] N90-19605

M

MAGMA
Stored mafic/ultramafic crust and early Archean mantle depletion
[NASA-CR-186460] N90-19715
MAGNESIUM ALLOYS
Optimizing superplastic response in navalite, a lithium containing aluminum-magnesium alloy
[AD-A216552] N90-19346
MAGNESIUM ISOTOPES
Plasma centrifuge with vacuum arc discharge applied to the separation of stable isotopes
[INPE-4925-TDL/385] N90-19654
MAGNETIC FIELDS
Green's functions for a theoretical model of an aperture fed stacked-patch microstrip antenna
[AD-A216280] N90-19455
Impedance characteristics of terawatt ion diodes
[DE90-006276] N90-19494
Numerical simulation of cross field amplifiers
[DE90-006459] N90-19496
Theoretical and experimental studies of a brushless disk rotor motor with permanent magnetic excitation and gap windings
[ETN-90-96056] N90-19512
Overview of recent results from the Advanced Toroidal Facility
[DE90-005673] N90-19853
Nonlinear interaction of electrostatic waves at a narrow inhomogeneous layer of a warm magnetoactive plasma
[DE90-610624] N90-19857
Critical current density and transition temperature measurements of Y-Ba-Cu-O rods
[AD-A216695] N90-19875
High energy x ray observations on the Crab nebula and the double star source GX 1+4
[ETN-90-95829] N90-19937
LAGEOS 3 and the gravitomagnetic field N90-19961
Gradiometry and gravitomagnetic field detection N90-19962
Time-dependent two-dimensional radiation hydrodynamics of accreting matter onto highly magnetized neutron stars
[DE90-006927] N90-19985
Disturbance structures and its magnetic field features in plasma comet tail
[DE90-610636] N90-19986
MAGNETIC FLUX
Siphon flows in isolated magnetic flux tubes. 3: The equilibrium path of the flux tube arch
[NASA-CR-186297] N90-19813
Overview of recent results from the Advanced Toroidal Facility
[DE90-005673] N90-19853
MAGNETIC MATERIALS
Neutron scattering measurements of the magnetic excitations of high-temperature superconducting materials
[DE90-006567] N90-19885
MAGNETIC MOMENTS
Attitude and spin rate control of a spinning satellite using geomagnetic field
[INPE-4818-NTE/289] N90-19277
Anomalous transport in toroidal plasmas
[DE90-006549] N90-19859
MAGNETIC PERMEABILITY
Theoretical and experimental studies of a brushless disk rotor motor with permanent magnetic excitation and gap windings
[ETN-90-96056] N90-19512
MAGNETIC PROPERTIES
Neutron scattering measurements of the magnetic excitations of high-temperature superconducting materials
[DE90-006567] N90-19885
Preparation and properties of the system Cu(x)Pd(1-x)O (0 less than or equal to x less than or equal to 0.175)
[AD-A217567] N90-19901
The preparation and properties of iron doped II-VI chalcogenides
[AD-A217569] N90-19903
MAGNETIC STORMS
Active probing of space plasmas
[AD-A216867] N90-19855
MAGNETIZATION
A computer control system for the alternating gradient magnetometer N90-19402
MAGNETOHYDRODYNAMIC FLOW
A storage process of the magnetic energy results from the unsteady plasma flow field in the space active regions and stellar atmosphere
[DE90-610638] N90-19858
MAGNETOHYDRODYNAMIC STABILITY
Nonlinear mechanics of unstable plasmas as related to high altitude aerodynamics
[AD-A215126] N90-19852
Overview of recent results from the Advanced Toroidal Facility
[DE90-005673] N90-19853
Theory of field reversed configurations
[DE90-006702] N90-19860
Plasma simulation on magnetohydrodynamic time scales
[DE90-007490] N90-19865
MAGNETOHYDRODYNAMICS
A storage process of the magnetic energy results from the unsteady plasma flow field in the space active regions and stellar atmosphere
[DE90-610638] N90-19858
Plasma simulation on magnetohydrodynamic time scales
[DE90-007490] N90-19865
MAGNETOMETERS
A computer control system for the alternating gradient magnetometer N90-19402
MAGNETRON SPUTTERING
Negative ion surface plasma source development for plasma trap injectors in Novosibirsk
[DE90-006082] N90-19856
MAGNETRONS
Numerical simulation of cross field amplifiers
[DE90-006459] N90-19496
MAGNIFICATION
Calculation of excrescence drag magnification due to pressure gradient at high subsonic speeds
[ESDU-87004] N90-19195
MAINTENANCE TRAINING
Report of the First Annual Airborne Weapons Training Technology Review
[DE90-007189] N90-19747
MAN MACHINE SYSTEMS
Assessment of crew workload measurement methods, techniques and procedures. Volume 2: Guidelines for the use of workload assessment techniques in aircraft certification
[AD-A217067] N90-19748
MAN-COMPUTER INTERFACE
Design and architecture of fourth and fifth generation software engineering environments
[ETN-90-95365] N90-19752
Queuing theory approach to modelling the dynamics of the human-computer interface
[AD-A216870] N90-19788
MANEUVERABILITY
Nonlinear continuum mechanics and applied analysis
[AD-A213629] N90-19812
MANEUVERS
Suboptimal period design for a maneuvering missile to evade tracking filters N90-19479
MANIFOLDS (MATHEMATICS)
Dynamics of a class of vortex rings
[NASA-TM-102257] N90-19524
MANIPULATORS
Kinematic control of robotic manipulators with multiple interchangeable wrists N90-19592
Experiments in end-point control of a flexible robot with a mini-manipulator N90-19596
Dynamics and control of robot manipulators with closed-kinematic chain mechanism N90-19598
Advanced control schemes and kinematic analysis for a kinematically redundant 7 DOF manipulator
[NASA-CR-186175] N90-19599
A complete description of robot manipulator dynamics based on Lagrangian mechanics
[DE90-741467] N90-19603
MANNED SPACE FLIGHT
Present and future risk of satellite and manned platforms collisions with other space objects and particles on earth orbits
[R-8841] N90-19287
Augmenting and updating NASA spacelink electronic information system N90-19392

MANNED SPACECRAFT
Hatch cover
[NASA-CASE-MSC-21356-1] N90-19278
MANUFACTURING
Operational fact-finding report on heat pump systems for industrial use
[DE89-782295] N90-19527
MANY BODY PROBLEM
Multibody modeling and verification N90-19422
MAP MATCHING GUIDANCE
Carin and GPS: The combination of dead reckoning, map matching and satellite navigation in a hybrid automobile navigation system
[ETN-90-95451] N90-19220
MAPPING
A method for determination of control pixels for LANSAT using a reflector
[INPE-4884-PRE/1491] N90-19632
MARKETING
From invention to innovation: Commercialization of new technology by independent and small business inventors
[DE90-006944] N90-19927
MARKOV PROCESSES
Influence of the parameters: Charge order, sequence classification, partial sequential circuit, and process regularity of a working charge (Gaussian process) on the lifetime of a component made of 3.1354 T3 and 3.4377 T761
[ETN-90-95378] N90-19503
Security calculations of rip reached construction elements by means of probabilistic breaking mechanics and a Markov process
[ETN-90-95890] N90-19624
MARS ENVIRONMENT
Aeolian removal of dust from photovoltaic surfaces on Mars
[NASA-TM-102507] N90-19299
MARS SURFACE
Aeolian removal of dust from photovoltaic surfaces on Mars
[NASA-TM-102507] N90-19299
MASKING
Method for maintaining precise suction strip porosities
[NASA-CASE-LAR-13638-1] N90-19427
MASS SPECTROSCOPY
Laser mass spectrometric studies of high temperature superconductor ablation
[DE90-006518] N90-19585
CCST (Center for Compound Semiconductor Technology) research briefs
[DE90-006446] N90-19887
MATCHING
Conjugate field approaches for active array compensation N90-19266
On the verification of hypothesized matches in model-based recognition
[AD-A214718] N90-19759
MATHEMATICAL MODELS
Calculation of ionospheric corrections for single frequency GPS observations: Investigation of two models
[ETN-90-95450] N90-19219
Calculation and optimization of rotor start process
[ETN-90-95894] N90-19229
Muzzle shunt augmentation of conventional railguns
[DE90-007505] N90-19248
Self-tuning control techniques, implicit and explicit, with parameter estimation in Kalman filters, applied to artificial satellite attitude
[INPE-4857-TDL/368] N90-19276
Application of attachment modes in the control of large space structures
[NASA-CR-185604] N90-19280
Safety Status Report for the Ulysses mission. Book 1: Accident analysis. General purpose heat source radioisotope thermoelectric generator program
[DE90-006829] N90-19285
Numerical study of diffusion jet flames N90-19316
Effects of nonuniform potential and current distributions in electrochemical systems
[DE90-007349] N90-19325
The measurement, modeling, and prediction of traction for rocket propellant 1
[NASA-CR-185186] N90-19386
A PBL-radiation model for application to regional numerical weather prediction N90-19394
A parametric heat transfer study for cryogenic ball bearings in SSME HPOTP N90-19397
A study of the effects of disk flexibility on the rotordynamics of the space shuttle main engine turbo-pumps N90-19401
Monte Carlo models and analysis of galactic disk gamma-ray burst distributions N90-19403
Analytical optical scattering in clouds N90-19413
Multibody modeling and verification N90-19422
A vectorized algorithm for 3D dynamics of a tethered satellite N90-19423
Simple analytic potentials for linear ion traps N90-19436
Performance of the all-digital data-transition tracking loop in the advanced receiver N90-19440
Costas loop lock detection in the advanced receiver N90-19441
Green's functions for a theoretical model of an aperture fed stacked-patch microstrip antenna
[AD-A216280] N90-19455
Signal processing
[DE90-006904] N90-19484
Numerical modelling of shocks in gases and metals
[MRL-RR-8-89] N90-19528
Conforming Chebyshev spectral collocation methods for the solution of laminar flow in a constricted channel
[NASA-CR-182011] N90-19539
Flow simulation for aircraft
[NLR-MP-87082-U] N90-19543
A review of models for the analysis of the injection of densely loaded flows into entrained flow gasifiers
[DE90-000453] N90-19550
Turbulent mixing effects in models of thermal blooming
[DE90-007245] N90-19580
Modeling and analysis of the space shuttle nose-gear tire with semianalytic finite elements
[NASA-TP-2977] N90-19595
A complete description of robot manipulator dynamics based on Lagrangian mechanics
[DE90-741467] N90-19603
PATRAN-STAGS translator (PATSTAGS)
[NASA-TM-100388] N90-19616
Development of finished beam and shell elements from engineering models for structures under high inelastic deformations
[ETN-90-95377] N90-19619
Use of chaotic and random vibrations to generate high frequency test inputs. Part 2: Chaotic vibrations
[DE90-007153] N90-19627
Use of chaotic and random vibrations to generate high frequency test inputs
[DE90-007412] N90-19628
Selection of optimal textural features for maximum likelihood image classification
[DE90-006901] N90-19638
Study of the optimization of reference parameters to the dynamic constraints of solar panels
[INPE-4793-TDL/355] N90-19656
An analytic model of axisymmetric mantle plume due to thermal and chemical diffusion
[NASA-CR-186461] N90-19714
Status of a nonlinear water surge model in February 1988
[KNMI-WR-88-03] N90-19735
Positioning control of highest accuracy for very dynamic coupled system
[ETN-90-95893] N90-19769
Finite element mesh generation starting from general geometric models
[REPT-88-93] N90-19803
Numerical simulation of acoustic scatter from subsurface bubble clouds
[AD-A217068] N90-19822
A simple model for the determination of L(sub 0), D and tau in a semiconductor and their temperature dependence
[DE90-610564] N90-19879
Construction of four-dimensional open superstrings
[DE90-006484] N90-19908
Visibility problems in numerical models of terrain
[INPE-4921-TDL/382] N90-19919
Reliability of equivalent sphere model in blood-forming organ dose estimation
[NASA-TM-4178] N90-20036
MATRICES (MATHEMATICS)
Comparison of artificial matrices and covariance functions
[ETN-90-95722] N90-19645
MATRIX MATERIALS
Identification and development of optimum SiC whiskers for silicon nitride matrix composites
[DE90-006888] N90-19315
MATTER (PHYSICS)
The ultimate structure of matter: The high energy physics program from the 1950s through the 1980s
[DE90-005682] N90-19836
MAXIMUM LIKELIHOOD ESTIMATES
Selection of optimal textural features for maximum likelihood image classification
[DE90-006901] N90-19638
MAXWELL EQUATION
Characterization of thunderstorm induced Maxwell current densities in the middle atmosphere N90-19391
Linearized analysis of (2+1)-dimensional Einstein-Maxwell theory
[DE90-741470] N90-19913
MEASURING INSTRUMENTS
Photon statistical limitations for daytime optical tracking N90-19442
MECHANICAL OSCILLATORS
The drum: Mechanical oscillators and acoustic rad iators
[REPT-FB-01/88] N90-19819
MECHANICAL PROPERTIES
Thermo-oxidative stability studies of PMR-15 polymer matrix composites reinforced with various fibers
[NASA-TM-102439] N90-19310
Modification of surface mechanical properties of high-chromium tool steel by carbon-implanted codeposited Fe-Ti films
[DE90-007502] N90-19358
Liquid oxygen LOX compatibility evaluations of aluminum lithium (Al-Li) alloys: Investigation of the Alcoa 2090 and MMC weldalite 049 alloys N90-19398
ROCOPT: A user friendly interactive code to optimize rocket structural components N90-19415
A transient plasticity study and low cycle fatigue analysis of the Space Station Freedom photovoltaic solar array blanket
[NASA-TM-102516] N90-19617
Physics and Mechanics of Cometary Materials
[ESA-SP-302] N90-19989
Mechanical properties of fluffy agglomerates consisting of core-mantle-particles N90-20019
MEDICAL SERVICES
Activities in aerospace medicine
[ETN-90-95468] N90-19739
MELANIN
Diffraction studies of the structure of glasses and liquids
[DE90-007662] N90-19381
MELT SPINNING
Novel processing of HTS based conductors
[DE90-005956] N90-19892
MELTING
Elimination of platinum inclusions in phosphate laser glasses
[DE90-004479] N90-19361
MEMBRANES
Elastomeric electrical isolation membrane
[AD-D014365] N90-19490
Advanced double layer capacitor
[AD-A217110] N90-19518
Calculation of nonlinear viscoelastic processes for plastic layer textile membranes
[ETN-90-95868] N90-19622
Status of stretched-membrane heliostats
[DE90-000801] N90-19669
The drum: Mechanical oscillators and acoustic rad iators
[REPT-FB-01/88] N90-19819
MEMORY (COMPUTERS)
Memory management in traceback Viterbi decoders N90-19443
GeoNet 88: Calculation connection system concept for the EURAD project N90-19688
MERCURY (PLANET)
Small Mercury Relativity Orbiter N90-19965
MESOMETEOROLOGY
A PBL-radiation model for application to regional numerical weather prediction N90-19394
Synoptic-scale forcing of the low-level jet in developing baroclinic waves N90-19717
Colloquium on Synoptic Meteorology
[PB90-121112] N90-19720
MESOSCALE PHENOMENA
A PBL-radiation model for application to regional numerical weather prediction N90-19394
Transport of atmospheric aerosols above the Sierra Nevada slopes
[PB90-120288] N90-19675
Initialization of EURAD, part 2 N90-19696
Boundary layer parameterization in CTM and MM4 N90-19697
Synoptic-scale forcing of the low-level jet in developing baroclinic waves N90-19717
Colloquium on Synoptic Meteorology
[PB90-121112] N90-19720
Digital simulation of a Boenline
[ISSN-0069-5882] N90-19729
Evolution of finite amplitude baroclinic waves in the atmosphere and ocean
[INPE-4752-TDL/346] N90-19733
MESSAGE PROCESSING
Dynamic reconfiguration and link fault tolerance in a transputer network
[AD-A215105] N90-19433

Queuing theory approach to modelling the dynamics of the human-computer interface
[AD-A216870] N90-19788

METABOLISM
Study of hydrazine metabolism and toxicity
[AD-A217103] N90-19736
Metabolism, seizures, and blood flow in brain following organophosphate exposure: Mechanisms of action and possible therapeutic agents
[AD-A217098] N90-19740

METAL DRAWING
Novel processing of HTS based conductors
[DE90-005956] N90-19892

METAL FATIGUE
An attempt of improving high-temperature fatigue properties of Ni-Cr-W superalloys in HTGR helium
[DE90-741482] N90-19350

METAL FOILS
High-purity beryllium foils
[DE90-006408] N90-19348

METAL MATRIX COMPOSITES
Demonstration of capabilities of high temperature composites analyzer code HITCAN
[NASA-TM-102560] N90-19629

METAL OXIDE SEMICONDUCTORS
Charge pumping as a measurement method for the characterization of short channel MOSFETS: Review, development, and comparison of measurement process
[ETN-90-95726] N90-19504

METAL PLATES
Experimental investigation of condensation of steam in the presence of noncondensable gases using plate heat exchangers
[DE90-002251] N90-19659

METAL SPRAYING
Preparation and characterization of alumina films prepared by a novel spray pyrolysis method
[AD-A217570] N90-19339

METAL STRIPS
Method for maintaining precise suction strip porosities
[NASA-CASE-LAR-13638-1] N90-19427

METAL SURFACES
International conference on Surface Modification of Metals by Ion Beams
[AD-A215872] N90-19345

METAL-WATER REACTIONS
Mitigation of stress corrosion cracking of AISI 304 stainless steel in oxygenated water at 289 C by organic species at low concentration
[DE90-005631] N90-19354

METALLIC GLASSES
Diffraction studies of the structure of glasses and liquids
[DE90-007662] N90-19381

METALS
Fast optical switch and limiter using quantum size effect in metal grain composites
[AD-D014332] N90-19305
Exchange and correlation effects in the Visscher-Falicov model for metal intercalated graphite
[DE90-610553] N90-19349
Numerical modelling of shocks in gases and metals
[MRL-RR-8-89] N90-19528

METEORITIC DAMAGE
Technology evaluation for space station atmospheric leakage
[DE90-007844] N90-19294

METEOROLOGICAL PARAMETERS
Transport of atmospheric aerosols above the Sierra Nevada slopes
[PB90-120288] N90-19675
Validation of the EURAD cloud modules N90-19693

METEOROLOGICAL RADAR
Rain radars for earth science geostationary platforms: Some possibilities N90-19262

METEOROLOGICAL SATELLITES
Compendium of meteorological space programs, satellites, and experiments
[NASA-TM-102924] N90-19243

METEOROLOGY
Compendium of meteorological space programs, satellites, and experiments
[NASA-TM-102924] N90-19243
Science requirements for passive microwave sensors on earth science geostationary platforms N90-19251
Rain radars for earth science geostationary platforms: Some possibilities N90-19262
The EURAD Model: Structure and First Results
[REPT-61] N90-19680
The mesoscale meteorological model MM4 and its modifications for EURAD N90-19682
An observational study of squall lines in the Amazon
[INPE-4865-TDL/376] N90-19723

METEOSAT SATELLITE
Real time environment monitoring using data from METEOSAT and NOAA imaging satellites
[NLR-MP-87070-U] N90-19672

METHANE
Synthesis and properties of a novel catalyst for the combustion of methane
[PB90-127499] N90-19320
Activation of methane by transition metal-substituted aluminophosphate molecular sieves
[DE90-005663] N90-19331

METROLOGY
Earth Science Geostationary Platform Technology
[NASA-CP-3040] N90-19249

MICHELSON INTERFEROMETERS
Ultra-sensitive inertial sensors via neutral-atom interferometry N90-19977

MICROSTRIP ANTENNAS
Green's functions for a theoretical model of an aperture fed stacked-patch microstrip antenna
[AD-A216280] N90-19455

MICROSTRIP TRANSMISSION LINES
Planar integrated circuits for microwave transmission and reception
[AD-A217676] N90-19520

MICROSTRUCTURE
High-purity beryllium foils
[DE90-006408] N90-19348
Creep behavior of alloys based on TiAl containing TiB2 and TiN particulates
[DE90-006489] N90-19355
Modification of surface mechanical properties of high-chromium tool steel by carbon-implanted codeposited Fe-Ti films
[DE90-007502] N90-19358
Fabrication, phase transformation studies, and characterization of SiC-AlN-Al2OC ceramics
[DE90-006591] N90-19371
Microstructural characterization of multiphase coatings produced by chemical vapor deposition
[DE90-007573] N90-19379
Liquid oxygen LOX compatibility evaluations of aluminum lithium (Al-Li) alloys: Investigation of the Alcoa 2090 and MMC weldalite 049 alloys N90-19398
Microstructural simulations of dynamic recrystallization
[DE90-007504] N90-19895

MICROWAVE AMPLIFIERS
Numerical simulation of cross field amplifiers
[DE90-006459] N90-19496

MICROWAVE COUPLING
Topics in HPM (High-Power Microwave) generation, coupling, and interaction
[AD-A216882] N90-19658

MICROWAVE EQUIPMENT
On 140 GHz microwave FEL experiments using ELF-2
[DE90-006764] N90-19576

MICROWAVE IMAGERY
Coherent radar measurement of ocean currents from geostationary orbit N90-19259

MICROWAVE INTERFEROMETERS
The space microwave interferometer and the search for cosmic background gravitational wave radiation N90-19952

MICROWAVE OSCILLATORS
Microwave oscillator with reduced phase noise by negative feedback incorporating microwave signals with suppressed carrier N90-19437

MICROWAVE RADIOMETERS
Synthetic Aperture Interferometric Radiometer (SAIR) N90-19261

MICROWAVE SENSORS
Earth Science Geostationary Platform Technology
[NASA-CP-3040] N90-19249
Science requirements for passive microwave sensors on earth science geostationary platforms N90-19251

MICROWAVE TRANSMISSION
Planar integrated circuits for microwave transmission and reception
[AD-A217676] N90-19520

MICROWAVES
Processing of advanced ceramics using microwaves thermal treatments
[DE90-606349] N90-19362
Sparse breakdown and statistical sneakthrough effects in low-altitude microwave propagation
[DE90-007252] N90-19473
Planar integrated circuits for microwave transmission and reception
[AD-A217676] N90-19520
On 140 GHz microwave FEL experiments using ELF-2
[DE90-006764] N90-19576

MIDDLE ATMOSPHERE
Characterization of thunderstorm induced Maxwell current densities in the middle atmosphere N90-19391

MILITARY HELICOPTERS
Reliability testing of the Hughes temperature controlled 1/4 watt split cycle cryogenic cooler (HD-1045 (V)/UA)
[AD-A216696] N90-19426

MILITARY OPERATIONS
The global positioning system
[AD-A217268] N90-19222
Limitations of the conventional role of the B-1B in the European theater
[AD-A217285] N90-19230

MILLIMETER WAVES
Large-diameter geostationary millimeter wavelength antenna concept N90-19254
Structures for remotely deployable precision antennas N90-19256
Millimeter radiometer system technology N90-19260
Foundations of millimeter-wave frequency acoustic microscopy N90-19816
Search for far infrared radiation from optically pumped defect modes
[AD-A216976] N90-19843

MINERALOGY
Analysis of tectonic movements utilizing remote sensor products in the Southern Espinhaco (SE) region
[INPE-4830-PRE/1451] N90-19708
Stored mafic/ultramafic crust and early Archean mantle depletion
[NASA-CR-186460] N90-19715

MINES (ORDNANCE)
Limitations of the conventional role of the B-1B in the European theater
[AD-A217285] N90-19230

MINIATURIZATION
Low-cost small satellites for astrophysical missions
[DE90-007625] N90-19293

MIR SPACE STATION
Examination of the background by High Energy X ray Experiment (HEXE) on the space station MIR
[ETN-90-95735] N90-20041

MISSILE CONFIGURATIONS
External flow computations for a finned 60mm ramjet in steady supersonic flight
[AD-A216998] N90-19233

MISSILE DEFENSE
Suboptimal period design for a maneuvering missile to evade tracking filters N90-19479

MISSILE TRACKING
Suboptimal period design for a maneuvering missile to evade tracking filters N90-19479

MISSION PLANNING
Physics and Mechanics of Cometary Materials
[ESA-SP-302] N90-19989
Rosetta/CNSR, ESA's planetary cornerstone mission N90-19990
MAX 1991. The active sun: A plan for pursuing the study of the active sun at the time of the next maximum in solar activity, January 1985
[NASA-CR-186125] N90-20030

MIXERS
Dual-fuel, dual-mode rocket engine
[NASA-CASE-LAR-13773-1] N90-19298

MIXING
Effects of turbulence mixing, variable properties, and vaporization on spray droplet combustion
[NASA-CR-186463] N90-19326
All-fiber SFPM (Stimulated Four Photon Mixing) amplifier
[AD-D014358] N90-19841
Ion mixing and surface modification in metal-semiconductor systems
[DE90-007557] N90-19897

MIXTURES
Thermodynamic properties of supercritical mixtures
[DE90-006720] N90-19909

MOBILITY
Nonlinear continuum mechanics and applied analysis
[AD-A213629] N90-19812

MODELS
Kalman estimation for SEDS measurements N90-19393
Monostable electrovalve
[INPE-4928-RPE/595] N90-19487
Recalibrating software reliability models
[NASA-CR-186407] N90-19763
Modeling and realization of plane acousto-optic unilateral band modulators
[ETN-90-95824] N90-19818
An equational language for specifying, querying, and updating database domains
[PB90-124694] N90-19918
Petrographic working model of the Rosetta sampling and modelling subgroup for a comet nucleus N90-19992

MODEMS
High throughput data communication system
[AD-D014342] N90-19432

High speed modem
[AD-D014319] N90-19750

MODULATION
Thermal modulation of light beams
[AD-D014322] N90-19840

MODULATORS
Active phase and amplitude modulator
[AD-D014318] N90-19480
CdTe buffered GaAs thin-slab IR waveguide modulators and T/R filter
[AD-A215999] N90-19488
Modeling and realization of plane acousto-optic unilateral band modulators
[ETN-90-95824] N90-19818

MODULUS OF ELASTICITY
Fluorinated graphite fibers as a new engineering material: Promises and challenges
[NASA-TM-102511] N90-19301
Compressive strength of synthetic comet nucleus samples N90-20006

MOLECULAR ABSORPTION
Activation of methane by transition metal-substituted aluminophosphate molecular sieves
[DE90-005663] N90-19331

MOLECULAR BEAM EPITAXY
Digital capacity transient spectroscopy of deep structure defects in III-V-Semiconductor structures
[ETN-90-96057] N90-19890

MOLECULAR CHAINS
Second-generation ordered polymers
[AD-A216126] N90-19365
Theory of polymer blends
[DE90-002532] N90-19377

MOLECULAR DIFFUSION
Modelization of dry deposition in the Chemical Transport Model (CTM) of EURAD N90-19698

MOLECULAR EXCITATION
Infrared heterodyne spectroscopy of polyatomic molecules in circumstellar envelopes N90-19980

MOLECULAR INTERACTIONS
Elastic recovery and polymer-polymer interactions
[AD-A217085] N90-19384
Superconductivity in Ba(1-x)BiO3
[DE90-003781] N90-19869

MOLECULAR ORBITALS
Preparation and properties of the system Cu(x)Pd(1-x)O (0 less than or equal to x less than or equal to 0.175)
[AD-A217567] N90-19901

MOLECULAR STRUCTURE
Theory of polymer blends
[DE90-002532] N90-19377
Preparation and properties of the system Cu(x)Pd(1-x)O (0 less than or equal to x less than or equal to 0.175)
[AD-A217567] N90-19901

MOLECULAR THEORY
Molecular theory and computer simulation studies of natural and synthetic gas mixtures
[PB90-130329] N90-19826

MOLECULES
Determination of the mechanism of decomposition of energetic molecules
[AD-A217061] N90-19388
Laser surface interactions of high-(Tc) superconductors
[DE90-006894] N90-19587

MOLTEN SALTS
Hot filament technique for measuring the thermal conductivity of molten lithium fluoride
[NASA-TM-102506] N90-19373
Direct absorption receiver
[DE90-000311] N90-19667
Evaluation of thermal cycling creep-fatigue damage for a molten salt receiver
[DE90-002907] N90-19670

MOMENTUM TRANSFER
Bose condensate in superfluid (sup 4)He and momentum distributions by deep inelastic scattering
[DE90-007541] N90-19832
The electron momentum-transfer cross sections of tungsten, silicon, and silicon dioxide at energies from 0.1 to 10,000 eV
[DE90-009041] N90-19833

MONOMERS
New Condensation polyimides containing 1,1,1-triaryl-2,2,2-trifluoroethane structures
[NASA-CASE-LEW-14346-1] N90-19300

MONOPULSE RADAR
An investigation of the transfer of monopulse tracking between two coherent point sources
[AD-A217007] N90-19457

MONOTONE FUNCTIONS
A nonparametric software reliability growth model
[NASA-CR-186438] N90-19764

MONTE CARLO METHOD
Three-dimensional structural analyses of reentry vehicles
[DE90-006278] N90-19291
Monte Carlo models and analysis of galactic disk gamma-ray burst distributions N90-19403
Analytical optical scattering in clouds N90-19413
A nonparametric software reliability growth model
[NASA-CR-186438] N90-19764
Numerical solution to the problem of criticality by Monte Carlo method
[DE90-608886] N90-19808
Microstructural simulations of dynamic recrystallization
[DE90-007504] N90-19895
Computer simulation of recrystallization in the presence of second phase particles
[DE90-007531] N90-19896
Gas diffusion in a cometary crust N90-20017

MOON
Analysis of alternative concepts for transport systems on the Moon surface
[ETN-90-95727] N90-19605
Extending terrestrial mobile robotics to a proposed lunar base
[DE89-016179] N90-19606
Working on the moon: The Apollo experience
[DE90-003662] N90-19744

MORPHOLOGY
Light-scattering measurements of CVD (Chemical Vapor Deposition) silicon carbide
[DE90-007885] N90-19382
Investigations of CuInSe2 thin films and contacts
[DE90-000301] N90-19886
Novel processing of HTS based conductors
[DE90-005956] N90-19892

MOTION SICKNESS
Vestibular examination of motion sick student pilots
[IZF-1988-22] N90-19738

MOTION SIMULATORS
Determination of the implementation of the 3-axis attitude motion simulator digital position controller N90-19409

MULTIBEAM ANTENNAS
Large antenna measurement and compensation techniques N90-19263

MULTILAYER INSULATION
Preparation and characterization of alumina films prepared by a novel spray pyrolysis method
[AD-A217570] N90-19339

MULTIPATH TRANSMISSION
Effects of amplitude distortions and IF equalization on satellite communication system bit-error rate performance
[NASA-TM-102415] N90-19454

MULTIPLEXING
Automatic thresholding multichannel digital radar early warning system
[AD-D014323] N90-19431
Digital video: Studio signal processing
[BBC-RD-1989/14] N90-19476
A digital HDTV recorder using a cluster of four D1 DVTRs
[BBC-RD-1989/13] N90-19477
A waveform capture and storage unit and its use for investigating disturbances on digital transmission links
[BBC-RD-1989/17] N90-19478

MULTIPROCESSING (COMPUTERS)
Modeling A circuit switched multiprocessor interconnect
[AD-A217122] N90-19519
Generic distributed systems model
[AD-A217078] N90-19773

MULTISPECTRAL PHOTOGRAPHY
The potential of combined use of satellite data with topographic TM information for manual/visual and digital updating of land use
[NLR-MP-88021-U] N90-19639

MULTISTATIC RADAR
Near-field bistatic RCS (Radar Cross-Section) measurements
[AD-A217011] N90-19458

MUONS
Search for anisotropies in the underground cosmic ray muon flux N90-20034
Cosmic ray composition and muon decoherence at the knee of the all-particle cosmic ray spectrum N90-20035
Cosmic ray events in Soudan 2
[DE90-005657] N90-20037
Underground muons from the direction of Cygnus X-3
[DE90-005646] N90-20038

MUSCLES
Techniques for studying the effects of microgravity on model particle/cell systems N90-19424

MUSCULOSKELETAL SYSTEM
Techniques for studying the effects of microgravity on model particle/cell systems N90-19424

N

NACELLES
A note on an acoustic response during an engine nacelle flight experiment
[NASA-TM-102585] N90-19821

NARROWBAND
Narrow-bandwidth unstable laser resonator
[AD-D014362] N90-19568

NASA PROGRAMS
Research Reports: 1989 NASA/ASEE Summer Faculty Fellowship Program
[NASA-CR-183837] N90-19390
Development of an Ada programming support environment database SEAD (Software Engineering and Ada Database) administration manual
[NASA-CR-186064] N90-19757
MAX 1991. The active sun: A plan for pursuing the study of the active sun at the time of the next maximum in solar activity, January 1985
[NASA-CR-186125] N90-20030

NASA SPACE PROGRAMS
Aerospace Safety Advisory Panel
[NASA-TM-101748] N90-19389

NATIONAL PARKS
Transport of atmospheric aerosols above the Sierra Nevada slopes
[PB90-120288] N90-19675

NATURAL LANGUAGE (COMPUTERS)
High-level connectionist models
[AD-A216581] N90-19751

NAVIER-STOKES EQUATION
Numerical solution of 3D Navier-Stokes equations with upwind implicit schemes
[NASA-TM-101656] N90-19205
LAGEOS 3 and the gravitomagnetic field N90-19961

NAVIGATION
Heli/SITAN: A terrain referenced navigation algorithm for helicopters
[DE90-005193] N90-19217
Highly accurate navigation: Integration of navigation and geodesic methods
[SFB-228] N90-19221
Suboptimal period design for a maneuvering missile to evade tracking filters N90-19479
Extending terrestrial mobile robotics to a proposed lunar base
[DE89-016179] N90-19606
A human factors testbed for ground-vehicle telerobotics research
[DE90-006618] N90-19746
Parallel neural net path-planner on hypercube and transputer
[DE90-006324] N90-19777

NAVIGATION SATELLITES
Interoperability issues in the use of satellite-based navigation systems for civil aviation purposes
[AD-A217279] N90-19223

NEAR FIELDS
Green's functions for a theoretical model of an aperture fed stacked-patch microstrip antenna
[AD-A216280] N90-19455
Near-field bistatic RCS (Radar Cross-Section) measurements
[AD-A217011] N90-19458

NEGATIVE IONS
Negative ion surface plasma source development for plasma trap injectors in Novosibirsk
[DE90-006082] N90-19856

NEPHANALYSIS
Exploiting surface observations of cloudiness for globalscale nephanalyses N90-19719

NEPTUNE (PLANET)
Parkes radio science system design and testing for Voyager Neptune encounter N90-19451

NETWORK ANALYSIS
Modeling A circuit switched multiprocessor interconnect
[AD-A217122] N90-19519
Parallel methods for solving nonlinear block bordered systems of equations
[AD-A217062] N90-19806

NEURAL NETS
Parallel neural net path-planner on hypercube and transputer
[DE90-006324] N90-19777
Hybrid neural network and rule-based pattern recognition system capable of self-modification
[DE90-007482] N90-19779
Opto-Em and devices investigation
[AD-A215033] N90-19814

NEUROPHYSIOLOGY
Neurocontrol systems and wing-fluid interactions underlying dragonfly flight N90-19240
NEUTRAL ATOMS
The 41st Annual Gaseous Electronics Conference [AD-A214540] N90-19851
Ultra-sensitive inertial sensors via neutral-atom interferometry N90-19977
NEUTRINOS
Cosmic ray events in Soudan 2 [DE90-005657] N90-20037
NEUTRON BEAMS
Hydrogen assay foil counting system [DE90-007415] N90-19332
NEUTRON DIFFRACTION
Bose condensate in superfluid (sup 4)He and momentum distributions by deep inelastic scattering [DE90-007541] N90-19832
NEUTRON SCATTERING
Neutron scattering measurements of the magnetic excitations of high-temperature superconducting materials [DE90-006567] N90-19885
NEUTRON SPECTRA
Hydrogen assay foil counting system [DE90-007415] N90-19332
NEUTRON STARS
Sources of gravitational waves N90-19942
Time-dependent two-dimensional radiation hydrodynamics of accreting matter onto highly magnetized neutron stars [DE90-006927] N90-19985
NEWTON THEORY
Toward higher order tests of the gravitational interaction N90-19948
NEWTON-RAPHSON METHOD
Iterative procedures for space shuttle main engine performance models N90-19416
NICKEL
Nanolayer reactions in aluminum-metal interfaces [DE90-004955] N90-19342
NIGHT VISION
Reliability testing of the Hughes temperature controlled 1/4 watt split cycle cryogenic cooler (HD-1045 (V)/UA) [AD-A216696] N90-19426
Human factors engineering testing of aircraft cockpit lighting systems [AD-A216853] N90-19743
NIOBATES
Low temperature elastic and dielectric properties of incommensurate barium sodium niobate [AD-A216969] N90-19815
NIOBIUM ALLOYS
Ac loss measurements of two multifilamentary NbTi composite strands [DE90-005388] N90-19304
NITRAMINE PROPELLANTS
Determination of the mechanism of decomposition of energetic molecules [AD-A217061] N90-19388
NITRIC OXIDE
Estimation of the distribution of SO2 and NOX emission in Europe N90-19699
NITROGEN COMPOUNDS
Synthesis and chemistry of unsaturated metal nitrogen compounds [AD-A216550] N90-19321
NITROGEN OXIDES
The RADM 2 gas-phase chemical mechanism N90-19684
NOAA SATELLITES
Operational requirements and the geostationary platform N90-19250
Real time environment monitoring using data from METEOSAT and NOAA imaging satellites [NLR-MP-87070-U] N90-19672
NOISE INTENSITY
Self-tuning control techniques, implicit and explicit, with parameter estimation in Kalman filters, applied to artificial satellite attitude [INPE-4857-TDL/368] N90-19276
Noise floors of subnanosecond transient recording systems [DE90-002339] N90-19571
NOISE REDUCTION
Microwave oscillator with reduced phase noise by negative feedback incorporating microwave signals with suppressed carrier N90-19437
NOISE SPECTRA
Advanced Doppler tracking experiments N90-19951
NOISE THRESHOLD
Noise floors of subnanosecond transient recording systems [DE90-002339] N90-19571
NONCONDENSABLE GASES
Experimental investigation of condensation of steam in the presence of noncondensable gases using plate heat exchangers [DE90-002251] N90-19659
NONDESTRUCTIVE TESTS
Hydrogen assay foil counting system [DE90-007415] N90-19332
Frequency response of electrochemical cells N90-19419
NONEQUILIBRIUM PLASMAS
The 41st Annual Gaseous Electronics Conference [AD-A214540] N90-19851
NONLINEAR EQUATIONS
A vectorized algorithm for 3D dynamics of a tethered satellite N90-19423
A comparison between the propagators method and the decomposition method for nonlinear equations [DE90-005783] N90-19781
Iteration methods for solving nonlinear equations in Frechet spaces [DE90-610429] N90-19799
Projection-iteration methods for solving nonlinear operator equations [DE90-610433] N90-19801
Parallel methods for solving nonlinear block bordered systems of equations [AD-A217062] N90-19806
NONLINEAR OPTICS
Optically tunable gratings for optical interconnects [AD-A216978] N90-19844
NONLINEAR SYSTEMS
Applications of frequency and wavenumber nonlinear digital signal processing to nonlinear hydrodynamics research [AD-A216259] N90-19530
Parallel methods for solving nonlinear block bordered systems of equations [AD-A217062] N90-19806
Nonlinear system vibration: The appearance of chaos [DE90-007546] N90-19810
Nonlinear continuum mechanics and applied analysis [AD-A213629] N90-19812
Nonlinear mechanics of unstable plasmas as related to high altitude aerodynamics [AD-A215126] N90-19852
NONLINEARITY
Numerical solution of 3D Navier-Stokes equations with upwind implicit schemes [NASA-TM-101656] N90-19205
Evaluation of the heat transfer module (FAHT) of Failure Analysis Nonlinear Thermal And Structural Integrated Code (FANTASTIC) N90-19407
Calculation of nonlinear viscoelastic processes for plastic layer textile membranes [ETN-90-95868] N90-19622
Status of a nonlinear water surge model in February 1988 [KNMI-WR-88-03] N90-19735
NOSE WHEELS
Modeling and analysis of the space shuttle nose-gear tire with semianalytic finite elements [NASA-TP-2977] N90-19595
NOSES (FOREBODIES)
Development of a preliminary high-angle-of-attack nose-down pitch control requirement for high-performance aircraft [NASA-TM-101684] N90-19206
NOTCH TESTS
Three-dimensional Fe analysis of the surface distribution in notched compact samples of 20 MnMoNi 55 [W-1/89] N90-19625
NOZZLE DESIGN
Static investigation of a two-dimensional convergent-divergent exhaust nozzle with multiaxis thrust-vectoring capability [NASA-TP-2973] N90-19193
NOZZLE EFFICIENCY
Static investigation of a two-dimensional convergent-divergent exhaust nozzle with multiaxis thrust-vectoring capability [NASA-TP-2973] N90-19193
Internal performance of two nozzles utilizing gimbal concepts for thrust vectoring [NASA-TP-2991] N90-19200
NOZZLE FLOW
Computation of hypersonic unsteady viscous flow over a cylinder N90-19194
NOZZLE GEOMETRY
Internal performance of two nozzles utilizing gimbal concepts for thrust vectoring [NASA-TP-2991] N90-19200
NUCLEAR ELECTRIC POWER GENERATION
Analysis of competition among kinds of energy at the era of complexed energy. (Report on overseas study) [DE89-910213] N90-19650
NUCLEAR FUSION
The effects of cold dark matter on Big Bang nucleosynthesis N90-19749
Measurement of cross sections: New needs and possibilities [DE90-007248] N90-19829
Record of forum on cold fusion [DE90-749883] N90-19863
Distributed bosonic states and condensed matter fusion [AD-A217605] N90-19868
NUCLEAR INTERACTIONS
Nuclear interactions of high energy heavy ions and applications in astrophysics [DE90-006691] N90-19984
Cosmic ray composition and muon decoherence at the knee of the all-particle cosmic ray spectrum N90-20035
NUCLEAR MAGNETIC RESONANCE
NMR (Nuclear Magnetic Resonance) imaging development for the study of solids [AD-A217073] N90-19899
NUCLEAR MEDICINE
Assessment of research needs for laser technologies applied to advanced spectroscopic methods [DE90-007402] N90-19588
NUCLEAR REACTIONS
Nuclear activity, morphology, and far infrared properties of spiral galaxies [ETN-90-95373] N90-20024
NUCLEAR REACTOR CONTROL
Analysis and evaluation of ZPPR (Zero Power Physics Reactor) critical experiments for a 100 kilowatt-electric space reactor [DE90-005634] N90-19835
NUCLEAR STRUCTURE
Searching for existing nuclear data [DE90-007535] N90-19925
NUCLEATION
Investigation of the processes controlling the flame generation of refractory materials [DE90-007564] N90-19333
Nucleation of vortices in superfluid helium-4 [DE90-610675] N90-19880
NUMERICAL ANALYSIS
Numerical and experimental analysis of a thin liquid film on a rotating disk related to development of a spacecraft absorption cooling system [NASA-CR-183457] N90-19523
Evolution of midplate hotspot swells: Numerical solutions [NASA-CR-186462] N90-19713
NUMERICAL CONTROL
A computer control system for the alternating gradient magnetometer N90-19402
Determination of the implementation of the 3-axis attitude motion simulator digital position controller N90-19409
Disturbance torque rejection properties of the NASA/JPL 70-meter antenna axis servos N90-19450
A digitally controlled system for effecting and presenting a selected electrical resistance [NASA-CASE-MFS-29149-1] N90-19492
NUMERICAL STABILITY
Finite element approximations of the stokes flow problem based upon various variational principles [DE90-608612] N90-19533
NUMERICAL WEATHER FORECASTING
A PBL-radiation model for application to regional numerical weather prediction N90-19394
NYLON (TRADEMARK)
The creep behavior of an aramide fiber reinforced wound tow-strap [LR-546] N90-19312
Synthesis of poly(dimethylsiloxane) - nylon 6 diblock copolymers [AD-A216850] N90-19367

O

O STARS
O-star parameters from line profiles of wind-blanketed model atmospheres N90-19982
OBJECT PROGRAMS
Object Oriented Programming Systems (OOPS) and frame representations: An investigation of programming paradigms [NASA-CR-186084] N90-19758
OBLIQUE SHOCK WAVES
Interaction of an oblique shock wave with supersonic flow over a blunt body N90-19197
OBLIQUE WINGS
Output model-following control synthesis for an oblique-wing aircraft [NASA-TM-100454] N90-19241

OBSERVATION
Comets: Dirty snowballs or icy dirtballs N90-19994
OCEAN BOTTOM
Stored mafic/ultramafic crust and early Archean mantle depletion
[NASA-CR-186460] N90-19715
OCEAN CURRENTS
Coherent radar measurement of ocean currents from geostationary orbit N90-19259
OCEAN MODELS
Evolution of finite amplitude baroclinic waves in the atmosphere and ocean
[INPE-4752-TDL/346] N90-19733
A linear systems theory approach to the range-independent acoustic channel
[AD-A216551] N90-19817
OCEAN SURFACE
Earth tidal analysis based on gravimeter observations and the influence of ocean tides
[ETN-90-95721] N90-19734
OCEAN THERMAL ENERGY CONVERSION
Experimental investigation of condensation of steam in the presence of noncondensable gases using plate heat exchangers
[DE90-002251] N90-19659
Experiments on oxygen desorption from surface warm seawater under Open-Cycle Ocean Thermal Energy Conversion (OC-OTEC) conditions
[DE90-000308] N90-19666
OCEANOGRAPHY
Single antenna interferometry
[DE90-008120] N90-19474
OCEANS
A linear systems theory approach to the range-independent acoustic channel
[AD-A216551] N90-19817
ON-LINE SYSTEMS
ESRIN
[ESA-BR-58] N90-19631
OPERATORS (MATHEMATICS)
Differential operators associated with Gegenbauer polynomials. 3: The regular case
[DE90-610422] N90-19795
OPERATORS (PERSONNEL)
An approach to elemental task learning
[DE90-006614] N90-19745
OPTICAL COMMUNICATION
Direct detection optical intersatellite link at 220 Mbps using AlGaAs laser diode and silicon APD with 4-ary PPM signaling
[NASA-CR-186380] N90-19480
Development of a receiver for a space-based laser radar system
[AD-A215079] N90-19566
OPTICAL DENSITY
A high optical density measuring spectrometer
[AD-D014331] N90-19318
OPTICAL EQUIPMENT
Highly accurate navigation: Integration of navigation and geodesic methods
[SFB-228] N90-19221
Precision segmented reflector, figure verification sensor N90-19272
A high optical density measuring spectrometer
[AD-D014331] N90-19318
FOMA: A Fast Optical Multichannel Analyzer
[DE90-004093] N90-19839
OPTICAL FIBERS
The influence of gamma-radiation on the bandwidth of optical fibres and the reduction of the induced attenuation by bleaching and hardening the fibre
[FEL-1988-62] N90-19846
OPTICAL FILTERS
Development of a receiver for a space-based laser radar system
[AD-A215079] N90-19566
Visual processing in texture segregation
[AD-A216539] N90-19737
OPTICAL HETERODYNING
Optical interferometer in space N90-19953
OPTICAL MEASUREMENT
Development and testing of a universally implementable recording aligning system
[SER-C-349] N90-19716
OPTICAL POLARIZATION
An optical and infrared study of blazars N90-19930
OPTICAL PROPERTIES
A high optical density measuring spectrometer
[AD-D014331] N90-19318
Analytical optical scattering in clouds N90-19413
All-fiber SFPM (Stimulated Four Photon Mixing) amplifier
[AD-D014358] N90-19841
The optical properties of beryllium
[DE90-006372] N90-19848
OPTICAL PUMPING
Anode plasma formation as a possible mechanism for an electrical stress limit in cold cathode diodes
[DE90-007503] N90-19516
Time resolved gain/loss studies under low and high power loading for the XeF C-A transition
[DE90-007506] N90-19517
Blue upconversion thulium laser
[DE90-006517] N90-19584
OPTICAL RADAR
Applications of FM-CW laser radar to antenna contour mapping N90-19270
Remote Attitude Measurement Sensor (RAMS) N90-19271
Development of a receiver for a space-based laser radar system
[AD-A215079] N90-19566
OPTICAL RESONATORS
Narrow-bandwidth unstable laser resonator
[AD-D014362] N90-19568
OPTICAL SCANNERS
Optically tunable gratings for optical interconnects
[AD-A216978] N90-19844
OPTICAL TRACKING
Photon statistical limitations for daytime optical tracking N90-19442
OPTICAL WAVEGUIDES
CdTe buffered GaAs thin-slab IR waveguide modulators and T/R filter
[AD-A215999] N90-19488
Modeling and realization of plane acousto-optic unilateral band modulators
[ETN-90-95824] N90-19818
Thermal modulation of light beams
[AD-D014322] N90-19840
Optically tunable gratings for optical interconnects
[AD-A216978] N90-19844
OPTIMAL CONTROL
Output model-following control synthesis for an oblique-wing aircraft
[NASA-TM-100454] N90-19241
Investigations into a new algorithm for calculating H infinity optimal controllers N90-19406
OPTIMIZATION
Near-field bistatic RCS (Radar Cross-Section) measurements
[AD-A217011] N90-19458
Development of dynamic equivalent network structures with a universal identification and optimization process
[ETN-90-95822] N90-19507
CO2 laser plus optimization for harmonic generation
[AD-D014341] N90-19565
Digital treatment of elastic-plastic structures by means of quadratic optimization processes from the finite element method
[ETN-90-95823] N90-19621
Selection of optimal textural features for maximum likelihood image classification
[DE90-006901] N90-19638
Study of the optimization of reference parameters to the dynamic constraints of solar panels
[INPE-4793-TDL/355] N90-19656
An optimized algorithm for solving the nodal diffusion method on shared memory multiprocessors
[DE90-002703] N90-19762
Adaptive, asynchronous stochastic global optimization algorithms for sequential and parallel computation
[AD-A217093] N90-19775
Minimum cycle covering and integer flows
[AD-A216546] N90-19785
Optimal layout via Boolean satisfiability
[AD-A216777] N90-19787
Optimal iteration steps by stochastic approximation processes for the solution of optimization problems with twice differentiable functions
[ETN-90-95887] N90-19809
Nonlinear continuum mechanics and applied analysis
[AD-A213629] N90-19812
OPTOELECTRONIC DEVICES
The III-V semiconductor quantum well lasers and related optoelectronic devices on silicon
[AD-A216980] N90-19570
OPTOGALVANIC SPECTROSCOPY
Optogalvanic laser spectroscopic and interference spectroscopic experiments of isotope gap and hyperfine structure for spectrum of Europium 1 and Erbium 2
[ETN-90-95358] N90-19327
ORBIT CALCULATION
Small Mercury Relativity Orbiter N90-19965
ORBIT TRANSFER VEHICLES
Flight and driving optimization of air breathing aerodynamic space vehicle
[ETN-90-95379] N90-19246
ORBITAL MANEUVERING VEHICLES
Evaluation and analysis of the orbital maneuvering vehicle video system N90-19411
ORBITAL MECHANICS
Accuracy of global positioning system broadcast orbits for relative surveys
[PB90-125428] N90-19218
ORBITAL SERVICING
Orbital servicing: Issue or answer
[AD-A217284] N90-19295
ORDER-DISORDER TRANSFORMATIONS
Second-generation ordered polymers
[AD-A216126] N90-19365
Optical studies of dynamical processes in disordered materials
[DE90-007080] N90-19372
ORGANIC PHOSPHORUS COMPOUNDS
Metabolism, seizures, and blood flow in brain following organophosphate exposure: Mechanisms of action and possible therapeutic agents
[AD-A217098] N90-19740
ORGANS
Reliability of equivalent sphere model in blood-forming organ dose estimation
[NASA-TM-4178] N90-20036
ORIENTATION
Development of a preliminary high-angle-of-attack nose-down pitch control requirement for high-performance aircraft
[NASA-TM-101684] N90-19206
Determination of Earth orientation using the Global Positioning System N90-19435
ORTHOPHOTOGRAPHY
Digital production of perspective images
[SER-C-347] N90-19768
ORTHOTROPIC SHELLS
ROCOPT: A user friendly interactive code to optimize rocket structural components N90-19415
OSCILLATIONS
Oscillation and damping behavior of fine steel test tubes, with particular consideration to destruction free proofs from hydrogen fragilization
[ETN-90-95371] N90-19351
Microwave oscillator with reduced phase noise by negative feedback incorporating microwave signals with suppressed carrier N90-19437
Transient and sustained resonance in very slowly varying oscillatory Hamiltonian systems with application to free-electron lasers
[DE90-005984] N90-19574
An experimental study of the aeroelastic behaviour of two parallel interfering circular cylinders N90-19609
Initialization of EURAD. Part 1: Utilization of ECMWF analysis data N90-19695
OSCILLATORS
Planar integrated circuits for microwave transmission and reception
[AD-A217676] N90-19520
OXIDATION
Heat treatment study of the SiC/Ti-15-3 composite system
[NASA-TP-2970] N90-19302
Synthesis and properties of a novel catalyst for the combustion of methane
[PB90-127499] N90-19320
Effect of temperature on the storage life of polysulfide aircraft sealants
[MRL-TR-89-31] N90-19364
Control of the RADM chemistry mechanism of the gas phase N90-19690
OXIDATION-REDUCTION REACTIONS
Linear free energy relations for multielectron transfer kinetics: A brief look at the Bronsted/Tafel analogy
[AD-A215078] N90-19823
OXIDE FILMS
Growth and characterization of gallium (III) oxide films
[AD-A217568] N90-19902
OXIDES
Solid oxide fuel cell cogeneration system conceptual design, program 2
[PB90-114968] N90-19653
OXIDIZERS
A parametric heat transfer study for cryogenic ball bearings in SSME HPOTP N90-19397
OXYGEN
Electron stimulated O(-) desorption from O2 condensed on a rare-gas film: Evidence for an indirect Bounce trajectory
[AD-A216725] N90-19322
High-purity beryllium foils
[DE90-006408] N90-19348
Laser surface interactions of high-(Tc) superconductors
[DE90-006894] N90-19587
Experiments on oxygen desorption from surface warm seawater under Open-Cycle Ocean Thermal Energy Conversion (OC-OTEC) conditions
[DE90-000308] N90-19666

Predicting effects of global climate change on reservoir water quality and fish habitat
[DE90-003674] N90-19704

OXYGEN BREATHING
Evaluation of the Scott aviation portable protective breathing device for contaminant leakage as prescribed by FAA Action Notice A-8150.2. Phase 1: Original tests of the portable protective breathing device. Phase 2: Tests of the redesigned portable protective breathing device
[AD-A216799] N90-19214

OXYGEN ISOTOPES
Stable isotope studies of cometary analogue materials
N90-20001

OXYGEN PLASMA
Oxygenation and possible etching of high T(sub c) superconducting films by oxygen plasma
[DE90-004956] N90-19871

OXYGEN PRODUCTION
Getting lunar ilmenite: From soils or rocks
[NASA-CR-186498] N90-20029

OXYGENATION
Oxygenation and possible etching of high T(sub c) superconducting films by oxygen plasma
[DE90-004956] N90-19871

OZONE
Simulation of a weather situation with high ozone concentrations during ALPEX N90-19686
The EURAD model in EUROTRAC N90-19701

P

P-N JUNCTIONS
Investigations of x ray sensitive PN-CCD's
[MPE-213] N90-19499

PACIFIC OCEAN
Drifting buoy data from Western Tropical Pacific for the period February 1, 1986 through February 28, 1989
[PB90-113978] N90-19732

PACKET SWITCHING
Packet radio networks under dynamic jamming
[AD-A217094] N90-19475

PACKING DENSITY
High density tape casting system
[NASA-CASE-NPO-16901-1-CU] N90-19425

PAINTS
Heat-resistant and anticorrosive paint
[DE90-006077] N90-19389

PALEONTOLOGY
Analysis of tectonic movements utilizing remote sensor products in the Southern Espinhaco (SE) region
[INPE-4830-PRE/1451] N90-19706

PALLADIUM
Supercomputer applications for materials science: Ordering effects of hydrogen in palladium
[DE90-004564] N90-19670

PALLADIUM COMPOUNDS
Preparation and properties of the system Cu(x)Pd(1-x)O (0 less than or equal to x less than or equal to 0.175)
[AD-A217567] N90-19901

PANEL METHOD (FLUID DYNAMICS)
On the evaluation of aerodynamic influence coefficients
[NLR-MP-87019-U] N90-19191
A panel process for the calculation of the flow around a wing with front angle damping
[ETN-90-95367] N90-19207

PANELS
Comparison between design and installed acoustic characteristics of NASA Lewis 9- by 15-foot low-speed wind tunnel acoustic treatment
[NASA-TP-2996] N90-19242
Precision segmented reflector, figure verification sensor N90-19272
Interlaminar shear stress effects on the postbuckling response of graphite-epoxy panels
[NASA-TM-102626] N90-19630
Study of the optimization of reference parameters to the dynamic constraints of solar panels
[INPE-4793-TDL/355] N90-19656

PARABOLIC FLIGHT
External flow computations for a finned 60mm ramjet in steady supersonic flight
[AD-A216998] N90-19233

PARABOLIC REFLECTORS
Test results from a full-scale sodium reflux pool-boiler solar receiver
[DE90-003577] N90-19671

PARALLEL COMPUTERS
Flosolver Mk1B: An eight processor parallel machine
[PD-CF-8941] N90-19755

PARALLEL PROCESSING (COMPUTERS)
Memory management in traceback Viterbi decoders
N90-19443
High-level connectionist models
[AD-A216581] N90-19751
Flosolver Mk1B: An eight processor parallel machine
[PD-CF-8941] N90-19755
Adaptive, asynchronous stochastic global optimization algorithms for sequential and parallel computation
[AD-A217093] N90-19775
Parallel neural net path-planner on hypercube and transputer
[DE90-006324] N90-19777
Parallel algorithms for boundary value problems
[NASA-TM-102498] N90-19783
On the parallel efficiency of the Frederickson-McBryan multigrid
[NASA-CR-181999] N90-19791

PARAMAGNETISM
Optical paramagnetic/diamagnetic gas sensor
[AD-D014368] N90-19554

PARAMETER IDENTIFICATION
Satellite imagery for water quality assessment in coastal regions
[INPE-4891-PRE/1492] N90-19636
Wind conditions near the ground in Federal Republic of Germany
[ISBN-3-88148-248-2] N90-19727

PARAMETERIZATION
The Uniform Engine Test Programme
[AGARD-AR-248] N90-19232
Study of the optimization of reference parameters to the dynamic constraints of solar panels
[INPE-4793-TDL/355] N90-19656
Boundary layer parameterization in CTM and MM4
N90-19697
Reparametrization BRS cohomology in two-dimensional gravity and non-critical string theories
[DE90-741468] N90-19911
Laboratory techniques for the characterisation of snow structures N90-20007

PARTIAL DIFFERENTIAL EQUATIONS
Convergence properties of iterative algorithms for solving the nodal diffusion equations
[DE89-016859] N90-19804

PARTICLE ACCELERATION
Radiation of electromagnetic waves by an accelerated charged particle in medium
[DE90-610458] N90-19461
Research accomplishments and future goals in particle physics
[DE90-007296] N90-19830
The inverse-square law and quantum gravity
N90-19949

PARTICLE ACCELERATORS
Dynamics of plasma injection along magnetic field lines in the PBFA 2 (Particle Beam Fusion Accelerator 2) plasma opening switch
[DE90-006751] N90-19862

PARTICLE BEAMS
Fifth-order aberrations in magnetic quadrupole-octupole systems
[DE90-007489] N90-19831
Dynamics of plasma injection along magnetic field lines in the PBFA 2 (Particle Beam Fusion Accelerator 2) plasma opening switch
[DE90-006751] N90-19862
Literature file on fast kickers and SEPTA: Components for deflection and separation of particle beams
[LINO-162] N90-19924

PARTICLE COLLISIONS
The electron momentum-transfer cross sections of tungsten, silicon, and silicon dioxide at energies from 0.1 to 10,000 eV
[DE90-009041] N90-19833
Electrical resistivity of strongly coupled plasmas in intense fields
[DE90-002236] N90-19861
Incoherent retrodiffusion of radiowaves in plasma with particle impulse
[ETN-90-95375] N90-19864
Low velocity dust-dust collisions N90-20011
Possible targeting of particle emission by mechanical stress and penetration of sublimating ice-dust-surfaces
N90-20016

PARTICLE DENSITY (CONCENTRATION)
Development and utilization of new diagnostics for dense-phase pneumatic transport
[DE90-006787] N90-19536

PARTICLE DIFFUSION
An optimized algorithm for solving the nodal diffusion method on shared memory multiprocessors
[DE90-002703] N90-19762

PARTICLE EMISSION
Possible targeting of particle emission by mechanical stress and penetration of sublimating ice-dust-surfaces
N90-20016

PARTICLE FLUX DENSITY
Search for anisotropies in the underground cosmic ray muon flux N90-20034

PARTICLE SIZE DISTRIBUTION
Satellites and debris in earth revolution orbits and first estimation of the collision probability
[R-8709] N90-19289

PARTICLE SPIN
Transverse spin observables in chromodynamics
[DE90-005638] N90-19824

PARTICLE TELESCOPES
A drift chamber telescope for high-Z particles
[NASA-CR-186497] N90-20040

PARTICLE THEORY
The inverse-square law and quantum gravity
N90-19949

PARTICLES
A review of models for the analysis of the injection of densely loaded flows into entrained flow gasifiers
[DE90-000453] N90-19550
Evaluation of the response of aluminum alloys to single and multiple particle impacts
[DE90-003689] N90-19626

PARTICULATES
Creep behavior of alloys based on TiAl containing TiB2 and TiN particulates
[DE90-006489] N90-19355
Chemical composition of precipitation and wet/dry deposition of sulfur compounds around the coastal area
[DE89-782324] N90-19677

PASTES
Effect of temperature on the storage life of polysulfide aircraft sealants
[MRL-TR-89-31] N90-19364

PATTERN RECOGNITION
VLSI implementation of moment invariants for automated inspection
[DE90-005318] N90-19493
Selection of optimal textural features for maximum likelihood image classification
[DE90-006901] N90-19638
An approach to elemental task learning
[DE90-006614] N90-19745
On the verification of hypothesized matches in model-based recognition
[AD-A214718] N90-19759
Object detection and amplitude estimation based on maximum a posteriori reconstructions
[DE90-007511] N90-19770
Hybrid neural network and rule-based pattern recognition system capable of self-modification
[DE90-007482] N90-19779

PATTERNS
Radar transponder antenna pattern analysis for the space shuttle N90-19414

PAYLOADS
Geostationary earth science platform concepts
N90-19252

PENETRATION
Simulation fidelity in lightning penetration studies
[DE90-006367] N90-19731
Possible targeting of particle emission by mechanical stress and penetration of sublimating ice-dust-surfaces
N90-20016

PERFORATED PLATES
Comparison between design and installed acoustic characteristics of NASA Lewis 9- by 15-foot low-speed wind tunnel acoustic treatment
[NASA-TP-2996] N90-19242

PERFORMANCE PREDICTION
Three-dimensional viscous rotor flow calculations using a viscous-inviscid interaction approach
[NASA-TM-102235] N90-19204
Aeroservoelasticity
[NASA-TM-102620] N90-19227
Flight and driving optimization of air breathing aerodynamic space vehicle
[ETN-90-95379] N90-19246
Effects of turbulence mixing, variable properties, and vaporization on spray droplet combustion
[NASA-CR-186463] N90-19326
Iterative procedures for space shuttle main engine performance models N90-19416
Recalibrating software reliability models
[NASA-CR-186407] N90-19763

PERFORMANCE TESTS
A comparison of reflector antenna designs for wide-angle scanning N90-19264
Radial response of the burst and transient source experiment N90-19408
Reliability testing of the Hughes temperature controlled 1/4 watt split cycle cryogenic cooler (HD-1045 (V)/UA)
[AD-A216696] N90-19426
Big Viterbi Decoder (BVD) results for (7,1/2) convolutional code N90-19446
The 32-GHz performance of the DSS-14 70-meter antenna: 1989 configuration N90-19452

Operational evaluation of initial data link air traffic control services, volume 1
[DOT/FAA/CT-90/1-VOL-1] N90-19472
High power, high frequency component test facility
[NASA-TM-102500] N90-19484
Progress in the CW operation of a 140 GHz gyrotron
[DE90-007382] N90-19556
Solid State Photovoltaic Research Branch
[DE89-009463] N90-19660
Marginal test and analysis of DRAM with masked alpha radiation
[RB-4180] N90-19754

PERMAFROST
Introduction to drilling technology N90-20002

PERMANENT MAGNETS
Induction motor control
[NASA-TM-102533] N90-19234
Theoretical and experimental studies of a brushless disk rotor motor with permanent magnetic excitation and gap windings
[ETN-90-96056] N90-19512
Design of a high power density, permanent magnet, axial gap dc motor
[DE90-005449] N90-19514

PERMEABILITY
A contribution to the theory of transient conductor simulations
[ETN-90-95891] N90-19511
Using image analysis to determine petrophysical properties of reservoir rocks
[DE90-000222] N90-19649

PERMITTIVITY
Heterogeneous composite and method of making
[AD-D014337] N90-19306
Alternate film dielectric materials
[DE90-007213] N90-19378
Causality of plasma permittivity with loss and restoring terms
[NASA-TM-101671] N90-19453

PERTURBATION
Tomographic investigations of weakly perturbed supersonic free jets
[MPIS-MITT-91] N90-19209
Ionospheric heating with oblique waves. Volume 1: Electron density perturbations
[AD-A216260] N90-19709
Evolution of finite amplitude baroclinic waves in the atmosphere and ocean
[INPE-4752-TDL/346] N90-19733

PERTURBATION THEORY
Nonlinear system vibration: The appearance of chaos
[DE90-007546] N90-19810
Drag-free satellite control N90-19974

PETROGRAPHY
Using image analysis to determine petrophysical properties of reservoir rocks
[DE90-000222] N90-19649
Analysis of tectonic movements utilizing remote sensor products in the Southern Espinhaco (SE) region
[INPE-4830-PRE/1451] N90-19708

PETROLOGY
P-T condition fo deformation from fluid inclusions in mylonites
[NASA-CR-186377] N90-19710
Stored mafic/ultramafic crust and early Archean mantle depletion
[NASA-CR-186460] N90-19715
Petrographic working model of the Rosetta sampling and modelling subgroup for a comet nucleus N90-19992

PHASE CONTROL
Phase control mechanism for wave energy conversion
[AD-D014354] N90-19657

PHASE DEVIATION
On linear structure and phase rotation invariant properties of block 2(sup I)-PSK modulation codes
[NASA-CR-186308] N90-19429

PHASE DIAGRAMS
Fabrication, phase transformation studies, and characterization of SiC-AlN-Al2OC ceramics
[DE90-006591] N90-19371
Molecular theory and computer simulation studies of natural and synthetic gas mixtures
[PB90-130329] N90-19826

PHASE ERROR
On linear structure and phase rotation invariant properties of block 2(sup I)-PSK modulation codes
[NASA-CR-186308] N90-19429

PHASE LOCKED SYSTEMS
The effects of sinusoidal interference on the second-order carrier tracking loop preceded by a bandpass limiter in the Block 4 receiver N90-19449

PHASE MODULATION
Active phase and amplitude modulator
[AD-D014316] N90-19480
Thermal modulation of light beams
[AD-D014322] N90-19640

PHASE SEPARATION (MATERIALS)
Mechano-caloric cooling device
[NASA-CR-186316] N90-19552

PHASE SHIFT
On linear structure and phase rotation invariant properties of block 2(sup I)-PSK modulation codes
[NASA-CR-186308] N90-19429
Dual-mode latching reciprocal ferrite phase shifter
[FEL-1988-55] N90-19497

PHASE SHIFT KEYING
On linear structure and phase rotation invariant properties of block 2(sup I)-PSK modulation codes
[NASA-CR-186308] N90-19429
Costas loop lock detection in the advanced receiver N90-19441

PHASE TRANSFORMATIONS
Advanced ceramics
[DE90-608004] N90-19370
Fabrication, phase transformation studies, and characterization of SiC-AlN-Al2OC ceramics
[DE90-006591] N90-19371
Computation at the edge of chaos: Phase transition and emergent computation
[DE90-007488] N90-19811
Low temperature elastic and dielectric properties of incommensurate barium sodium niobate
[AD-A216969] N90-19815
The effects of gradients on boundary stability
[DE90-007428] N90-19894

PHASED ARRAYS
Science requirements for passive microwave sensors on earth science geostationary platforms N90-19251

PHENANTHRENE
Synthesis and chemistry of unsaturated metal nitrogen compounds
[AD-A216550] N90-19321

PHOSPHATES
Activation of methane by transition metal-substituted aluminophosphate molecular sieves
[DE90-005663] N90-19331
Elimination of platinum inclusions in phosphate laser glasses
[DE90-004479] N90-19361

PHOSPHORIC ACID FUEL CELLS
Gas cooled fuel cell systems technology development program
[DE90-000446] N90-19668

PHOTOCATHODES
Quantum yield of photocathodes in far and extreme ultraviolet wavelength area
[ETN-90-95731] N90-19505

PHOTOCHEMICAL REACTIONS
The role of clouds in the photochemistry of the background troposphere N90-19694

PHOTOCONDUCTIVITY
Transient photoconduction in doped polymers: Spatial and energetic disorder
[ETN-90-95917] N90-19376

PHOTODIODES
Contact formation on (Hg,Cd) Te
[AD-A217088] N90-19900

PHOTOELECTROCHEMISTRY
Studies of photochemically and electrochemically driven electron transport in zeolites
[DE90-007659] N90-19335

PHOTOGEOLOGY
Analysis of photogeologic lineaments in the Ithacare (BA) region: A proposed methodology
[INPE-4855-PRE/1478] N90-19635

PHOTOGRAMMETRY
Applications of the GPS in photogrammetry
[ETN-90-96004] N90-19648

PHOTOLYSIS
Studies of photochemically and electrochemically driven electron transport in zeolites
[DE90-007659] N90-19335

PHOTOMETERS
Optical paramagnetic/diamagnetic gas sensor
[AD-D014368] N90-19554

PHOTOMETRY
Photometric analyses of abundances in dwarf spheroidal galaxies and globular clusters N90-19978

PHOTONS
Photon statistical limitations for daytime optical tracking N90-19442
The EGS4 Code System: Solution of gamma-ray and electron transport problems
[DE90-008100] N90-19838
All-fiber SFPM (Stimulated Four Photon Mixing) amplifier
[AD-D014358] N90-19841
Toward higher order tests of the gravitational interaction N90-19948

PHOTOOXIDATION
The RADM 2 gas-phase chemical mechanism N90-19684

PHOTOSYNTHESIS
Energy transfer and photochemistry in biomimetic solar conversion
[PB90-114562] N90-19652

PHOTOVOLTAIC CELLS
Aeolian removal of dust from photovoltaic surfaces on Mars
[NASA-TM-102507] N90-19299
A transient plasticity study and low cycle fatigue analysis of the Space Station Freedom photovoltaic solar array blanket
[NASA-TM-102516] N90-19617
Solid State Photovoltaic Research Branch
[DE89-009463] N90-19660

PHYSICAL CHEMISTRY
Laboratory studies of cometary ice analogues N90-19997
Physico-chemical properties of formaldehyde-ice-dust mixtures N90-20000
Crustal strength of different model comet materials N90-20003

PHYSICAL EXAMINATIONS
Activities in aerospace medicine
[ETN-90-95468] N90-19739

PHYSICAL OPTICS
Analytical optical scattering in clouds N90-19413

PI-ELECTRONS
Algorithms for calorimeter simulation with parameterized showers by example of H1 detectors
[MPI-PAE/EXP.EL-200] N90-19828

PIEZOELECTRICITY
Temperature compensated crystal oscillator (TCXO) with improved temperature compensation
[AD-D014334] N90-19482
Field effect transistor structures based on strain induced polarization charges
[DE90-007247] N90-19515

PILOT SELECTION
Pilot candidate selection
[AD-A217296] N90-19742

PILOT TRAINING
Pilot candidate selection
[AD-A217296] N90-19742

PILOTS
Vestibular examination of motion sick student pilots
[IZF-1988-22] N90-19738

PIPE FLOW
Separation bubbles at high Reynolds number: Measurement and computation
[CUED/A-AERO/15] N90-19525
Experimental and analytical investigation of adiabatic critical water air two phase flow in small diameter tubes
[TB-88/1] N90-19540

PIPES (TUBES)
Oscillation and damping behavior of fine steel test tubes, with particular consideration to destruction free proofs from hydrogen fragilization
[ETN-90-95371] N90-19351

PIVOTS
Constructibility limits of multiflow wind turbines with pivots
[ILR-MITT-215] N90-19662

PIXELS
A method for determination of control pixels for LANSAT using a reflector
[INPE-4884-PRE/1491] N90-19632

PLANAR STRUCTURES
Internal transmission line filter element
[AD-D014353] N90-19489

PLANETARY BOUNDARY LAYER
A PBL-radiation model for application to regional numerical weather prediction N90-19394

PLANETARY GEOLOGY
Aeolian removal of dust from photovoltaic surfaces on Mars
[NASA-TM-102507] N90-19299

PLANETARY NEBULAE
The microchannel plate camera as a detector at high resolution spectrographs: Experiments for velocity distribution in planetary nebulae
[ETN-90-95733] N90-19560
Signature objects: Preliminaries for the satellite project HIPPARCOS/TYCHO
[ETN-90-95730] N90-19934
Model calculations for dynamic development of planetary nebulae
[ETN-90-95734] N90-20025
Structural experiments of planetary nebulae: Charge-coupled devices, image reduction under MIDAS, information representation, and development of an evolution classification for PN's
[ETN-90-95736] N90-20026

PLANETARY TEMPERATURE
Large impact events and atmospheric evolution on the terrestrial planets N90-20026
PLANETS
Large impact events and atmospheric evolution on the terrestrial planets N90-20026
PLANNING
Working on the moon: The Apollo experience [DE90-003662] N90-19744
PLASMA ARC WELDING
Heat sink effects on weld bead: VPPA process N90-19418
PLASMA CLOUDS
Two-meter laser material response impulse measurements [AD-A215834] N90-19567
PLASMA CONTROL
Overview of recent results from the Advanced Toroidal Facility [DE90-005673] N90-19853
Anomalous transport in toroidal plasmas [DE90-006549] N90-19859
Theory of field reversed configurations [DE90-006702] N90-19860
PLASMA DIAGNOSTICS
FOMA: A Fast Optical Multichannel Analyzer [DE90-004093] N90-19639
PLASMA DIFFUSION
Incoherent retrodiffusion of radiowaves in plasma with particle impulse [ETN-90-95375] N90-19864
PLASMA DIODES
Anode plasma formation as a possible mechanism for an electrical stress limit in cold cathode diodes [DE90-007503] N90-19516
PLASMA DYNAMICS
Active probing of space plasmas [AD-A216867] N90-19855
PLASMA HEATING
Nonlinear mechanics of unstable plasmas as related to high altitude aerodynamics [AD-A215126] N90-19852
Overview of recent results from the Advanced Toroidal Facility [DE90-005673] N90-19853
Negative ion surface plasma source development for plasma trap injectors in Novosibirsk [DE90-006082] N90-19856
PLASMA INTERACTIONS
Active probing of space plasmas [AD-A216867] N90-19855
The nonlinear interaction of intense laser pulses in plasmas [AD-A217604] N90-19867
PLASMA RADIATION
The nonlinear interaction of intense laser pulses in plasmas [AD-A217604] N90-19867
PLASMA TURBULENCE
Proceedings of a contractors meeting on Combustion Rocket Propulsion Diagnostics of Reacting Flow [AD-A216445] N90-19297
Nonlinear mechanics of unstable plasmas as related to high altitude aerodynamics [AD-A215126] N90-19852
PLASMA WAVES
Nonlinear interaction of electrostatic waves at a narrow inhomogeneous layer of a warm magnetoactive plasma [DE90-610624] N90-19857
PLASMAS (PHYSICS)
Investigation of a simulated tritium plasma using Coherent Anti-Stokes Raman Spectroscopy (CARS) [DE90-005696] N90-19319
Causality of plasma permittivity with loss and restoring terms [NASA-TM-101671] N90-19453
Longitudinal traveling waves bifurcating from Vlasov plasma equilibria N90-19850
Nonlinear mechanics of unstable plasmas as related to high altitude aerodynamics [AD-A215126] N90-19852
Negative ion surface plasma source development for plasma trap injectors in Novosibirsk [DE90-006082] N90-19856
Plasma simulation on magnetohydrodynamic time scales [DE90-007490] N90-19865
An electrical model for plasma armature voltage [DE90-007530] N90-19866
PLASTIC DEFORMATION
Three-dimensional Fe analysis of the surface distribution in notched compact samples of 20 MnMoNi 55 [W-1/89] N90-19625
PLASTIC PROPERTIES
A transient plasticity study and low cycle fatigue analysis of the Space Station Freedom photovoltaic solar array blanket [NASA-TM-102516] N90-19617
PLATES (STRUCTURAL MEMBERS)
Test component attachment effects on resonant plate pyrotechnic shock simulation [DE90-006478] N90-19551
Development of finite beam and shell elements for structures under great inelastic deformations [ETN-90-95869] N90-19623
Interlaminar shear stress effects on the postbuckling response of graphite-epoxy panels [NASA-TM-102626] N90-19630
PLATINUM
Elimination of platinum inclusions in phosphate laser glasses [DE90-004479] N90-19361
PLEIADES CLUSTER
The Moon has set [REPT-89-07] N90-19933
PLUMES
Evolution of midplate hotspot swells: Numerical solutions [NASA-CR-186462] N90-19713
An analytic model of axisymmetric mantle plume due to thermal and chemical diffusion [NASA-CR-186461] N90-19714
PNEUMATIC PROBES
Compensating for pneumatic distortion in pressure sensing devices [NASA-TM-101716] N90-19224
PNEUMATICS
Development and utilization of new diagnostics for dense-phase pneumatic transport [DE90-006787] N90-19536
POINT DEFECTS
Self-consistant calculation of point and pair structure defects in silicium [ETN-90-96059] N90-19891
POINT SOURCES
An investigation of the transfer of monopulse tracking between two coherent point sources [AD-A217007] N90-19457
Emission data for the EURAD project N90-19700
An analytic model of axisymmetric mantle plume due to thermal and chemical diffusion [NASA-CR-186461] N90-19714
Research accomplishments and future goals in particle physics [DE90-007296] N90-19830
Search for anisotropies in the underground cosmic ray muon flux N90-20034
POINTING CONTROL SYSTEMS
Disturbance torque rejection properties of the NASA/JPL 70-meter antenna axis servos N90-19450
POLARITY
Heat sink effects on weld bead: VPPA process N90-19418
POLARIZATION (CHARGE SEPARATION)
Field effect transistor structures based on strain induced polarization charges [DE90-007247] N90-19515
POLARIZATION (WAVES)
Vector circuit theory for multilayered isotropic and chiral structures: Reflection and transmission [PB90-122474] N90-19495
Earth-orbiting resonant-mass gravitational wave detectors N90-19954
Pulsar timing and gravitational waves N90-19955
General relativistic x ray (UV) polarization rotations as a quantitative test for black holes N90-19957
POLARIZED LIGHT
Porosity and ice-dust mixtures in cometary particles N90-20018
POLICIES
Survey on the social and economic influences of wide-spreading heat-pump technology [DE89-782294] N90-19526
POLLUTION CONTROL
A preliminary analysis of US CO2 emissions reduction potential from energy conservation and the substitution of natural gas for coal in the period to 2010 [DOE/NBB-0085] N90-19673
POLLUTION TRANSPORT
Transport of atmospheric aerosols above the Sierra Nevada slopes [PB90-120288] N90-19675
On the question of spray effects N90-19691
Boundary layer parameterization in CTM and MM4 N90-19697
Modelization of dry deposition in the Chemical Transport Model (CTM) of EURAD N90-19698
POLYATOMIC MOLECULES
Infrared heterodyne spectroscopy of polyatomic molecules in circumstellar envelopes N90-19980
POLYETHYLENES
Carbon black/polyethylene composites for PTC (Positive Temperature Coefficient) thermistor applications [AD-A215988] N90-19307
POLYIMIDES
New Condensation polyimides containing 1,1,1-triaryl-2,2,2-trifluoroethane structures [NASA-CASE-LEW-14346-1] N90-19300
POLYMER BLENDS
Theory of polymer blends [DE90-002532] N90-19377
POLYMER CHEMISTRY
New Condensation polyimides containing 1,1,1-triaryl-2,2,2-trifluoroethane structures [NASA-CASE-LEW-14346-1] N90-19300
POLYMER MATRIX COMPOSITES
Thermo-oxidative stability studies of PMR-15 polymer matrix composites reinforced with various fibers [NASA-TM-102439] N90-19310
Transient photoconduction in doped polymers: Spatial and energetic disorder [ETN-90-95917] N90-19376
POLYMERIC FILMS
Heterogeneous composite and method of making [AD-D014337] N90-19306
Alternate film dielectric materials [DE90-007213] N90-19378
POLYMERIZATION
New Condensation polyimides containing 1,1,1-triaryl-2,2,2-trifluoroethane structures [NASA-CASE-LEW-14346-1] N90-19300
Second-generation ordered polymers [AD-A216126] N90-19365
Synthesis of poly(dimethylsiloxane) - nylon 6 diblock copolymers [AD-A216850] N90-19367
POLYMORPHISM
Object Oriented Programming Systems (OOPS) and frame representations: An investigation of programming paradigms [NASA-CR-186084] N90-19758
POLYNOMIALS
Some easily analyzable convolutional codes N90-19444
Differential operators associated with Gegenbauer polynomials. 3: The regular case [DE90-610422] N90-19795
POLYSULFIDES
Effect of temperature on the storage life of polysulfide aircraft sealants [MRL-TR-89-31] N90-19364
PONDEROMOTIVE FORCES
Simple analytic potentials for linear ion traps N90-19438
POPULATIONS
Electron energy distributions and vibrational population distributions [DE90-005550] N90-19825
POROSITY
Characterization of reaction kinetics in a porous electrode [NASA-CR-186504] N90-19340
Method for maintaining precise suction strip porosities [NASA-CASE-LAR-13638-1] N90-19427
Origin and effect of pores in aluminum welded joints [REPT-87M/43/05720/SCP/GRF] N90-19620
Using image analysis to determine petrophysical properties of reservoir rocks [DE90-000222] N90-19649
A test of the interstellar dust model of comets N90-19995
Porosity and ice-dust mixtures in cometary particles N90-20018
PORTABLE EQUIPMENT
Evaluation of the Scott aviation portable protective breathing device for contaminant leakage as prescribed by FAA Action Notice A-8150.2. Phase 1: Original tests of the portable protective breathing device. Phase 2: Tests of the redesigned portable protective breathing device [AD-A216799] N90-19214
POSITION (LOCATION)
Thermal coefficient of delay for various coaxial and fiber-optic cables N90-19439
Drifting buoy data from Western Tropical Pacific for the period February 1, 1986 through February 28, 1989 [PB90-113978] N90-19732
POSITION SENSING
Heli/SITAN: A terrain referenced navigation algorithm for helicopters [DE90-005193] N90-19217
Development and testing of a universally implementable recording aligning system [SER-C-349] N90-19716

POSITIONING
Positioning control of highest accuracy for very dynamic coupled system
[ETN-90-95893] N90-19769
POSTFLIGHT ANALYSIS
Kalman estimation for SEDS measurements N90-19393
POTENTIAL FIELDS
Potential theory of radiation N90-19395
POTENTIAL THEORY
Potential theory of radiation N90-19395
POWDER (PARTICLES)
Investigation of the processes controlling the flame generation of refractory materials
[DE90-007564] N90-19333
POWER SERIES
Series reversion/inversion of Lambert's time function
[AD-A216243] N90-19245
POWER SPECTRA
Power spectral densities for selected digital phase-continuous MFSK (M-ary Frequency Shift Keying) emissions
[PB90-129990] N90-19463
PREAMPLIFIERS
Direct detection optical intersatellite link at 220 Mbps using AlGaAs laser diode and silicon APD with 4-ary PPM signaling
[NASA-CR-186380] N90-19460
PRECIPITATION (METEOROLOGY)
Validation of the EURAD cloud modules N90-19693
PRECISION
Comparison of artificial matrices and covariance functions
[ETN-90-95722] N90-19645
PREDICTION ANALYSIS TECHNIQUES
A PBL-radiation model for application to regional numerical weather prediction N90-19394
Potential theory of radiation N90-19395
The influence of a wall function on turbine blade heat transfer prediction N90-19421
Simple analytic potentials for linear ion traps N90-19436
The effects of sinusoidal interference on the second-order carrier tracking loop preceded by a bandpass limiter in the Block 4 receiver N90-19449
Synoptic-scale forcing of the low-level jet in developing baroclinic waves N90-19717
PREDICTOR-CORRECTOR METHODS
Computation of hypersonic unsteady viscous flow over a cylinder N90-19194
PREPREGS
Evaluation and choice algorithms of cost optimal prepreg-application processes: Production of strongly charged plane parts made of fiber reinforced plastics
[ETN-90-95895] N90-19313
PRESSURE DISTRIBUTION
Calculation of excrescence drag magnification due to pressure gradient at high subsonic speeds
[ESDU-87004] N90-19195
A panel process for the calculation of the flow around a wing with front angle damping
[ETN-90-95367] N90-19207
PRESSURE EFFECTS
Possible targeting of particle emission by mechanical stress and penetration of sublimating ice-dust-surfaces N90-20016
PRESSURE GRADIENTS
Calculation of excrescence drag magnification due to pressure gradient at high subsonic speeds
[ESDU-87004] N90-19195
PRESSURE MEASUREMENT
Study of the turbulent boundary layer on an afterbody
[TM-EA-8901] N90-19212
Compensating for pneumatic distortion in pressure sensing devices
[NASA-TM-101716] N90-19224
PRESSURE OSCILLATIONS
Investigation of SSME alternate high pressure fuel turbopump lift-off seal fluid and structural dynamic interaction N90-19400
PRESSURE SENSORS
Compensating for pneumatic distortion in pressure sensing devices
[NASA-TM-101716] N90-19224
PRESSURIZING
Tensile behavior of cylindrical pressure tanks in fiber assembling + metal hybrid structure
[ILR-MITT-213] N90-19618
PRIORITIES
Priority arbitration with busses
[AD-A216392] N90-19784
PROBABILITY THEORY
Security calculations of rip reached construction elements by means of probabilistic breaking mechanics and a Markov process
[ETN-90-95890] N90-19624
Theory and applications of belief functions
[AD-A217092] N90-19774
Use of Coxian-type distributions in a general model of the maximum of bivariate random variables
[PB90-121229] N90-19780
Distributed detection by a large team of sensors in tandem
[AD-A216607] N90-19607
PROBLEM SOLVING
Elastic solutions in a semi-infinite solid with an ellipsoidal inclusion
[AD-A217063] N90-19338
The 0-1 multiknapsack problem: Heuristic and reduction methods
[INPE-4894-PRE/1495] N90-19782
PRODUCT DEVELOPMENT
Compton amplifier
[DIGEL-1985-5] N90-19506
Design of a pyrometer for temperature measurements on the solid fuel combustion chamber
[LR-530] N90-19561
PROGRAMMED INSTRUCTION
TOPAS preparation study: Summary representation of the study results
[OHB-TN-TOP-011/87] N90-19244
PROGRAMMING LANGUAGES
Design and architecture of fourth and fifth generation software engineering environments
[ETN-90-95365] N90-19752
Using Rexx to coordinate relational commands
[DE90-007569] N90-19772
An equational language for specifying, querying, and updating database domains
[PB90-124694] N90-19918
PROJECT MANAGEMENT
Operational evaluation of initial data link air traffic control services, volume 1
[DOT/FAA/CT-90/1-VOL-1] N90-19472
Development of an Ada programming support environment database SEAD (Software Engineering and Ada Database) administration manual
[NASA-CR-186064] N90-19757
PROJECT PLANNING
Atmospheric Radiation Measurement Program plan
[DE90-006349] N90-19705
National Action Plan on Superconductivity Research and Development
[PB89-138512] N90-19883
PROJECTILES
External flow computations for a finned 60mm ramjet in steady supersonic flight
[AD-A216996] N90-19233
Computational fluid dynamics method for low Reynolds number flow in a precessing/spinning, liquid filled cylinder with rounded endcaps
[AD-A216997] N90-19531
PROPELLANT TESTS
The measurement, modeling, and prediction of traction for rocket propellant 1
[NASA-CR-185186] N90-19386
PROPULSION
Proceedings of a contractors meeting on Combustion Rocket Propulsion Diagnostics of Reacting Flow
[AD-A216445] N90-19297
PROPULSION SYSTEM PERFORMANCE
Rapid near-optimal trajectory generation and guidance law development for single-stage-to-orbit airbreathing vehicles
[NASA-CR-186299] N90-19275
PROTECTION
Lightning protection apparatus for RF equipment and the like
[AD-D014336] N90-19483
PROTECTIVE COATINGS
Aeolian removal of dust from photovoltaic surfaces on Mars
[NASA-TM-102507] N90-19299
Effect of barrier layers in burn-through experiments with 351-nm laser illumination
[DE90-006806] N90-19577
PROTONS
Defect structures in copper and gold irradiated with fast neutrons, 14 MeV neutrons and 600 to 800 MeV protons
[DE90-007529] N90-19359
PROTOPLANETS
Low velocity dust-dust collisions N90-20011
Mechanical properties of fluffy agglomerates consisting of core-mantle-particles N90-20019
PROTOTYPES
Digital integrator
[DIGEL-1989-2] N90-19508
Deceit: A flexible distributed file system
[NASA-CR-186412] N90-19923
PUBLIC HEALTH
Safety Status Report for the Ulysses mission. Book 1: Risk analysis. General purpose heat source radiosotope thermoelectric generator program
[DE90-006826] N90-19282
Safety status report for the Ulysses mission. Book 2: Risk analysis. General purpose heat source radiosotope thermoelectric generator program
[DE90-006827] N90-19283
The pollution hazard assessment system: Documentation and users manual
[AD-A217108] N90-19706
PULSARS
Pulsar timing and gravitational waves N90-19955
Time-dependent two-dimensional radiation hydrodynamics of accreting matter onto highly magnetized neutron stars
[DE90-006927] N90-19985
PULSE CODE MODULATION
PC-based PCM (Pulse Code Modulation) telemetry data reduction system hardware
[DE90-000316] N90-19273
A waveform capture and storage unit and its use for investigating disturbances on digital transmission links
[BBC-RD-1989/17] N90-19478
PULSE GENERATORS
Blue upconversion thulium laser
[DE90-006517] N90-19584
PULSE POSITION MODULATION
Direct detection optical intersatellite link at 220 Mbps using AlGaAs laser diode and silicon APD with 4-ary PPM signaling
[NASA-CR-186380] N90-19480
PULSED LASERS
The nonlinear interaction of intense laser pulses in plasmas
[AD-A217604] N90-19867
PULSED RADIATION
Topics in HPM (High-Power Microwave) generation, coupling, and interaction
[AD-A216882] N90-19658
PULSES
Laser-matter interaction at intensities of 10(sup 12) W/cm(sup 2) and below
[DE90-007536] N90-19590
PURITY
High-purity beryllium foils
[DE90-006408] N90-19348
PYRANOMETERS
Pyranometry
[DWD-14] N90-19661
PYROHELIOMETERS
Pyranometry
[DWD-14] N90-19661
PYROLYSIS
Preparation and characterization of alumina films prepared by a novel spray pyrolysis method
[AD-A217570] N90-19339
Determination of the mechanism of decomposition of energetic molecules
[AD-A217061] N90-19388
Growth and characterization of gallium (III) oxide films
[AD-A217568] N90-19902
PYROMETERS
Development of the blackbody probe type pyrometer, part 1. Experimental study on the fundamental characteristics
[DE89-782288] N90-19553
Design of a pyrometer for temperature measurements on the solid fuel combustion chamber
[LR-530] N90-19561
PYROTECHNICS
Test component attachment effects on resonant plate pyrotechnic shock simulation
[DE90-006478] N90-19551

Q

Q VALUES
A simple method using MAFIA to calculate external Q values of waveguide-loaded cavities
[DE90-741487] N90-19465
QUADRATIC PROGRAMMING
Digital treatment of elastic-plastic structures by means of quadratic optimization processes from the finite element method
[ETN-90-95823] N90-19621
QUADRUPOLES
Fifth-order aberrations in magnetic quadrupole-octupole systems
[DE90-007489] N90-19831
Icarus lander N90-19964
QUALIFICATIONS
Monostable electrovalve
[INPE-4928-RPE/595] N90-19487

QUALITY CONTROL
Methode for trend analysis: Examples with problem/failure data N90-19396
QUANTITATIVE ANALYSIS
A method of estimating temperature profiles and chemical differentiation in the near surface layers of porous comet nuclei: First results for comet P/Churyumov-Gerasimenko N90-20013
QUANTUM CHROMODYNAMICS
Transverse spin observables in chromodynamics [DE90-005638] N90-19824
The renormalization group and lattice QCD [DE90-004860] N90-19905
QUANTUM EFFICIENCY
Quantum yield of photocathodes in far and extreme ultraviolet wavelength area [ETN-90-95731] N90-19505
QUANTUM ELECTRONICS
Fast optical switch and limiter using quantum size effect in metal grain composites [AD-D014332] N90-19305
QUANTUM THEORY
Goldstone excitation and symmetry breaking mechanism in superfluid He-4 [DE90-610676] N90-19881
Quantum field theory on higher-genus Riemann surfaces [DE90-741469] N90-19912
Gravitational consequences of modern field theories N90-19947
The inverse-square law and quantum gravity N90-19949
QUANTUM WELLS
The III-V semiconductor quantum well lasers and related optoelectronic devices on silicon [AD-A216980] N90-19570
QUARKS
Transverse spin observables in chromodynamics [DE90-005638] N90-19824
QUARTZ
Finite element analysis of a quartz rotation sensor [DE90-006959] N90-19562
QUASARS
Nearly simultaneous optical, ultraviolet, and x ray observations of three PG quasars [NASA-CR-186355] N90-19932
QUEUEING THEORY
Queuing theory approach to modelling the dynamics of the human-computer interface [AD-A216870] N90-19788

R

RADAR
Automatic thresholding multichannel digital radar early warning system [AD-D014323] N90-19431
RADAR ANTENNAS
Applications of FM-CW laser radar to antenna contour mapping N90-19270
Radar transponder antenna pattern analysis for the space shuttle N90-19414
An investigation of the transfer of monopulse tracking between two coherent point sources [AD-A217007] N90-19457
RADAR APPROACH CONTROL
Tracking performance of the AN/GPN-22 precision approach radar [FEL-1988-34] N90-19467
RADAR CROSS SECTIONS
Near-field bistatic RCS (Radar Cross-Section) measurements [AD-A217011] N90-19458
Electromagnetic properties of material coated surfaces [NASA-CR-186466] N90-19466
RADAR DETECTION
Aspects of VHF radars illustrated by the example of an experimental system [REPT-1-89] N90-19468
RADAR EQUIPMENT
Heli/SITAN: A terrain referenced navigation algorithm for helicopters [DE90-005193] N90-19217
Development of a receiver for a space-based laser radar system [AD-A215079] N90-19566
RADAR IMAGERY
Analysis of photogeologic lineaments in the Ithacare (BA) region: A proposed methodology [INPE-4855-PRE/1478] N90-19535
Analysis of tectonic movements utilizing remote sensor products in the Southern Espinhaco (SE) region [INPE-4830-PRE/1451] N90-19708
RADAR MEASUREMENT
Coherent radar measurement of ocean currents from geostationary orbit N90-19259
Near-field bistatic RCS (Radar Cross-Section) measurements [AD-A217011] N90-19458
Simulation of radar and radiometer signals remote sensing cometary surface and subsurface structures N90-20005
RADAR RANGE
An investigation of the transfer of monopulse tracking between two coherent point sources [AD-A217007] N90-19457
RADAR SCATTERING
Electromagnetic properties of material coated surfaces [NASA-CR-186466] N90-19466
RADAR TRACKING
Tracking performance of the AN/GPN-22 precision approach radar [FEL-1988-34] N90-19467
Advanced Doppler tracking experiments N90-19951
RADIANT HEATING
Heat transfer definitions and equations [ESDU-89022] N90-19522
RADIATION ABSORPTION
CO2 laser plus optimization for harmonic generation [AD-D014341] N90-19565
RADIATION COUNTERS
Radial response of the burst and transient source experiment N90-19408
RADIATION DAMAGE
Identification and solution of a charging problem in a high-altitude detector [DE90-008637] N90-19296
Irradiation-induced amorphization and elastic shear instability in intermetallic compounds [DE90-004845] N90-19341
Effect of electron-excitation on radiation damage in ion-irradiated FCC metals [DE90-719537] N90-19344
Evaluation of radiation-induced sensitization using electrochemical potentiokinetic reactivation technique for austenitic stainless steels [DE90-002708] N90-19352
RADIATION DETECTORS
Background studies in gas ionizing x ray detectors N90-19399
Digital integrator [DIGEL-1989-2] N90-19508
The space microwave interferometer and the search for cosmic background gravitational wave radiation N90-19952
Earth-orbiting resonant-mass gravitational wave detectors N90-19954
Space telescope searches for black holes in galactic nuclei N90-19958
Frequency stable high power lasers in space N90-19969
Cosmic ray events in Soudan 2 [DE90-005657] N90-20037
RADIATION DISTRIBUTION
Potential theory of radiation N90-19395
RADIATION DOSAGE
Reliability of equivalent sphere model in blood-forming organ dose estimation [NASA-TM-4178] N90-20036
RADIATION EFFECTS
Radiation-induced density changes and creep in surface layers of glass [DE90-008112] N90-19383
Transmission and reflection studies of thin films in the vacuum ultraviolet N90-19412
The influence of gamma-radiation on the bandwidth of optical fibres and the reduction of the induced attenuation by bleaching and hardening the fibre [FEL-1988-62] N90-19846
RADIATION HAZARDS
Safety Status Report for the Ulysses mission. Book 1: Risk analysis. General purpose heat source radioisotope thermoelectric generator program [DE90-006826] N90-19282
Safety Status Report for the Ulysses mission: Summary. General purpose heat source radioisotope thermoelectric generator program [DE90-006828] N90-19284
Safety Status Report for the Ulysses mission. Book 2: Accident analysis-appendices. General purpose heat source radioisotope thermoelectric generator program [DE90-006830] N90-19286
RADIATION MEASUREMENT
Atmospheric Radiation Measurement Program plan [DE90-006349] N90-19705
Detecting gravity waves from binary black holes N90-19943
RADIATION PROTECTION
Safety Status Report for the Ulysses mission. Book 1: Risk analysis. General purpose heat source radioisotope thermoelectric generator program [DE90-006826] N90-19282
Safety status report for the Ulysses mission. Book 2: Risk analysis. General purpose heat source radioisotope thermoelectric generator program [DE90-006827] N90-19283
Safety Status Report for the Ulysses mission: Summary. General purpose heat source radioisotope thermoelectric generator program [DE90-006828] N90-19284
RADIATION SOURCES
An investigation of the transfer of monopulse tracking between two coherent point sources [AD-A217007] N90-19457
Sources of gravitational waves N90-19942
Detecting gravity waves from binary black holes N90-19943
The pregalactic cosmic gravitational wave background N90-19945
The space microwave interferometer and the search for cosmic background gravitational wave radiation N90-19952
X ray timing observations and gravitational physics N90-19956
A drift chamber telescope for high-Z particles [NASA-CR-186497] N90-20040
RADIATION SPECTRA
JACEE long duration balloon flights [DE90-006008] N90-20039
RADIO ALTIMETERS
Heli/SITAN: A terrain referenced navigation algorithm for helicopters [DE90-005193] N90-19217
Rosetta/CNSR altimeter and sounding radar N90-20009
RADIO ANTENNAS
Large antenna measurement and compensation techniques N90-19263
RADIO ASTRONOMY
The Telecommunications and Data Acquisition Report [NASA-CR-185033] N90-19434
Parkes radio science system design and testing for Voyager Neptune encounter N90-19451
RADIO EQUIPMENT
Parkes radio science system design and testing for Voyager Neptune encounter N90-19451
Packet radio networks under dynamic jamming [AD-A217094] N90-19475
RADIO FILTERS
Lightning protection apparatus for RF equipment and the like [AD-D014336] N90-19483
RADIO FREQUENCIES
Lightning protection apparatus for RF equipment and the like [AD-D014336] N90-19483
RADIO FREQUENCY INTERFERENCE
The effects of sinusoidal interference on the second-order carrier tracking loop preceded by a bandpass limiter in the Block 4 receiver N90-19449
RADIO RELAY SYSTEMS
User-friendly software for the design of digital line-of-sight radio links [PB90-118472] N90-19760
Random access transmission algorithms for data local area networks [AD-A216443] N90-19761
High stability radio links N90-19970
RADIO SOURCES (ASTRONOMY)
The 32-GHz performance of the DSS-14 70-meter antenna: 1989 configuration N90-19452
RADIO TRANSMISSION
Experimental measurements in secondary radar field: Conception and first results [ETN-90-96074] N90-19471
RADIO WAVES
Incoherent retrodiffusion of radiowaves in plasma with particle impulse [ETN-90-95375] N90-19864
RADIOACTIVE CONTAMINANTS
Simulation of the propagation of radiactive substances from the example of Chernobyl (USSR) N90-19685
Boundary layer parameterization in CTM and MM4 N90-19697
RADIOACTIVE ISOTOPES
The TISOL facility at TRIUMF [DE90-006882] N90-19837
RADIOACTIVITY
Application of natural isotopes in groundwater for solving environmental problems [DE90-000223] N90-19703

RADIOISOTOPE BATTERIES
Safety Status Report for the Ulysses mission. Book 1: Accident analysis. General purpose heat source radioisotope thermoelectric generator program
[DE90-006829] N90-19285
RADIOMETERS
Design of a low-frequency (5-20 GHz), 15-meter-diameter passive radiometer for geostationary earth science platforms N90-19255
Millimeter radiometer system technology N90-19260
Synthetic Aperture Interferometric Radiometer (SAIR) N90-19261
RAILGUN ACCELERATORS
Computational and experimental of railgun structural performance
[DE90-006418] N90-19247
Muzzle shunt augmentation of conventional railguns
[DE90-007505] N90-19248
An electrical model for plasma armature voltage
[DE90-007530] N90-19866
RAIN
Rain radars for earth science geostationary platforms: Some possibilities N90-19262
RAMAN SPECTROSCOPY
Investigation of a simulated tritium plasma using Coherent Anti-Stokes Raman Spectroscopy (CARS)
[DE90-005696] N90-19319
Spatially high-resolution flame diagnosis by means of spontaneous Raman spectroscopy
[ETN-90-95870] N90-19328
RAMJET ENGINES
External flow computations for a finned 60mm ramjet in steady supersonic flight
[AD-A216998] N90-19233
RANDOM ACCESS MEMORY
Marginal test and analysis of DRAM with masked alpha radiation
[RB-4180] N90-19754
Random access transmission algorithms for data local area networks
[AD-A216443] N90-19761
RANDOM PROCESSES
Numerical solution to the problem of criticality by Monte Carlo method
[DE90-608886] N90-19808
RANDOM SAMPLING
Laboratory techniques for the characterisation of snow structures N90-20007
RANDOM VARIABLES
Use of Coxian-type distributions in a general model of the maximum of bivariate random variables
[PB90-121229] N90-19780
RANDOM VIBRATION
Use of chaotic and random vibrations to generate high frequency test inputs. Part 2: Chaotic vibrations
[DE90-007153] N90-19627
Use of chaotic and random vibrations to generate high frequency test inputs
[DE90-007412] N90-19628
RANGEFINDING
Improved ranging systems N90-19973
RARE EARTH ALLOYS
Fifth-order aberrations in magnetic quadrupole-octupole systems
[DE90-007489] N90-19831
RARE GASES
Electron stimulated O(-) desorption from O2 condensed on a rare-gas film: Evidence for an indirect Bounce trajectory
[AD-A216725] N90-19322
RATIOS
Comets: Dirty snowballs or icy dirtballs N90-19994
RAYLEIGH NUMBER
Experiments of thermoconvection in a cubic cell
[MPIS-6/1989] N90-19544
RAYLEIGH-BENARD CONVECTION
Structures instabilities in filament liquid crystals
[ETN-90-95916] N90-19888
RDX
An evaluation of ethylene-vinyl acetate copolymers as desensitizers for RDX in insensitive booster compositions prepared by slurry coating technology
[MRL-TR-89-33] N90-19385
REACTION KINETICS
Proceedings of a contractors meeting on Combustion Rocket Propulsion Diagnostics of Reacting Flow
[AD-A216445] N90-19297
Characterization of reaction kinetics in a porous electrode
[NASA-CR-186504] N90-19340
Second-generation ordered polymers
[AD-A216126] N90-19365
Determination of the mechanism of decomposition of energetic molecules
[AD-A217061] N90-19388
Laboratory studies of free radical reactions in cloudwater
[DE90-003961] N90-19730
REACTION WHEELS
Feasibility of using Extreme Ultraviolet Explorer (EUVE) reaction wheels to satisfy Space Infrared Telescope Facility (SIRTF) maneuver requirements
[NASA-TM-100389] N90-19556
REACTIVITY
Synthesis and chemistry of unsaturated metal nitrogen compounds
[AD-A216550] N90-19321
REACTOR DESIGN
Analysis and evaluation of ZPPR (Zero Power Physics Reactor) critical experiments for a 100 kilowatt-electric space reactor
[DE90-005634] N90-19835
REACTOR TECHNOLOGY
Theory of field reversed configurations
[DE90-006702] N90-19860
READ-ONLY MEMORY DEVICES
National Technical Information Service 1989 Users Conference proceedings
[PB90-142563] N90-19921
REAL TIME OPERATION
A rule-based paradigm for intelligent adaptive flight control N90-19238
A computer control system for the alternating gradient magnetometer N90-19402
Advanced control schemes and kinematic analysis for a kinematically redundant 7 DOF manipulator
[NASA-CR-186175] N90-19599
REATTACHED FLOW
Separation bubbles at high Reynolds number: Measurement and computation
[CUED/A-AERO/15] N90-19525
Method and apparatus for detecting laminar flow separation and reattachment
[NASA-CASE-LAR-13952-1-SB] N90-19534
RECEIVERS
Development of a receiver for a space-based laser radar system
[AD-A215079] N90-19566
Solar and thermic utilization in high temperature area: Research and development
[ETN-90-96062] N90-19663
Direct absorption receiver
[DE90-000311] N90-19667
RECOGNITION
Improved processes for ultrasonic object recognition in robotics
[ETN-90-95362] N90-19604
On the verification of hypothesized matches in model-based recognition
[AD-A214718] N90-19759
RECONSTRUCTION
Application of adaptive least-squares algorithm to multi-element array signal reconstruction N90-19448
RECORDING
Noise floors of subnanosecond transient recording systems
[DE90-002339] N90-19571
RECOVERABILITY
Flight crew aiding for recovery from subsystem failures
[NASA-CR-181905] N90-19741
RECRYSTALLIZATION
Microstructural simulations of dynamic recrystallization
[DE90-007504] N90-19895
Computer simulation of recrystallization in the presence of second phase particles
[DE90-007531] N90-19896
RED GIANT STARS
Structural experiments of planetary nebulae: Charge-coupled devices, image reduction under MIDAS, information representation, and development of an evolution classification for PN's
[ETN-90-95736] N90-20026
REDUCED GRAVITY
Techniques for studying the effects of microgravity on model particle/cell systems N90-19424
REDUNDANT COMPONENTS
Jam resistant fluid power actuator for ballistic-damage tolerant redundant cylinder assemblies
[AD-D014360] N90-19600
REENTRY VEHICLES
Three-dimensional structural analyses of reentry vehicles
[DE90-006278] N90-19291
REFLECTANCE
Unfurlable, continuous-surface reflector concept N90-19257
Glancing angle XAFS (X ray Absorption Fine Structure) and x ray reflectivity studies of transition-metal/aluminum interfaces
[DE90-005575] N90-19353
REFLECTOR ANTENNAS
A comparison of reflector antenna designs for wide-angle scanning N90-19264
Reflector surface distortion analysis techniques (thermal distortion analysis of antennas in space) N90-19267
Mesh surfaces for reflector applications N90-19268
REFLECTORS
Advances in large inflatable reflectors N90-19258
Reflector surface distortion analysis techniques (thermal distortion analysis of antennas in space) N90-19267
Mesh surfaces for reflector applications N90-19268
Precision segmented reflector, figure verification sensor N90-19272
A method for determination of control pixels for LANSAT using a reflector
[INPE-4884-PRE/1491] N90-19632
REFRACTIVITY
Thermal modulation of light beams
[AD-D014322] N90-19840
Information reconstruction from speckle interferograms
[ETN-90-95918] N90-19939
REFRACTORY MATERIALS
Investigation of the processes controlling the flame generation of refractory materials
[DE90-007564] N90-19333
Heat-resistant and anticorrosive paint
[DE90-006077] N90-19369
REGIONS
Sensitivity of ecological landscapes and regions to global climatic change
[PB90-120072] N90-19674
REGOLITH
Petrographic working model of the Rosetta sampling and modelling subgroup for a comet nucleus N90-19992
REGRESSION ANALYSIS
Satellite imagery for water quality assessment in coastal regions
[INPE-4891-PRE/1492] N90-19636
REGULATORY MECHANISMS (BIOLOGY)
Neurocontrol systems and wing-fluid interactions underlying dragonfly flight N90-19240
REINFORCED PLASTICS
The creep behavior of an aramide fiber reinforced wound tow-strap
[LR-546] N90-19312
REINFORCED PLATES
Innovative design of composite structures: The use of curviinear fiber format in structural design of composites
[NASA-CR-186406] N90-19308
REINFORCING MATERIALS
Jam resistant fluid power actuator for ballistic-damage tolerant redundant cylinder assemblies
[AD-D014360] N90-19600
RELATIVISTIC EFFECTS
Gravitational radiation as a test of relativistic gravity N90-19941
Applied general relativity N90-19950
The gravity probe B relativity gyroscope program N90-19960
Icarus lander N90-19964
Small Mercury Relativity Orbiter N90-19965
RELATIVITY
Dimensional transition of the universe
[DE90-741461] N90-19910
Causal boundary construction for space-times of the general relativity theory
[ETN-90-95357] N90-19915
Relativistic Gravitational Experiments in Space
[NASA-CP-3046] N90-19940
Gravitational radiation as a test of relativistic gravity N90-19941
Gravitational radiation from rotating gravitational collapse N90-19944
Experimental constraints on metric and non-metric theories of gravity N90-19946
Gravitational consequences of modern field theories N90-19947
Toward higher order tests of the gravitational interaction N90-19948
Applied general relativity N90-19950
General relativistic x ray (UV) polarization rotations as a quantitative test for black holes N90-19957
The gravity probe B relativity gyroscope program N90-19960
LAGEOS 3 and the gravitomagnetic field N90-19961
The Stanford equivalence principle program N90-19963
Icarus lander N90-19964
Small Mercury Relativity Orbiter N90-19965
Gravitational experiments on a solar probe mission: Scientific objectives and technology considerations N90-19966
Optical interferometers for tests of relativistic gravity in space N90-19967

New tests with old data N90-19968
A review of atomic clock technology, the performance capability of present spaceborne and terrestrial atomic clocks, and a look toward the future N90-19972
Improved ranging systems N90-19973
Inertial corrections by dynamic estimation N90-19976

RELIABILITY
A nonparametric software reliability growth model [NASA-CR-186438] N90-19764
Theory and applications of belief functions [AD-A217092] N90-19774

RELIABILITY ANALYSIS
Recalibrating software reliability models [NASA-CR-186407] N90-19763
A nonparametric software reliability growth model [NASA-CR-186438] N90-19764

RELIABILITY ENGINEERING
Reliability testing of the Hughes temperature controlled 1/4 watt split cycle cryogenic cooler (HD-1045 (V)/UA) [AD-A216696] N90-19426

REMOTE CONTROL
A human factors testbed for ground-vehicle telerobotics research [DE90-006618] N90-19746

REMOTE MANIPULATOR SYSTEM
A complete description of robot manipulator dynamics based on Lagrangian mechanics [DE90-741467] N90-19603

REMOTE SENSING
Earth Science Geostationary Platform Technology [NASA-CP-3040] N90-19249
Large space antenna concepts for ESGP N90-19253
Remote Attitude Measurement Sensor (RAMS) N90-19271
Definition study of Laser Experimental Active Fluorsensor (LEAF) [BCRS-88-18] N90-19582
Areas of aquatic macrophytes classified through vegetative indexes extracted from LANDSAT/TM imagery [INPE-4880-PRE/1489] N90-19633
Development of software routines for remote sensing digital image processing [ETN-90-95452] N90-19640
Possible applications of remote sensing satellite pictures for the water quality management of the Frisian lakes, Netherlands [BCRS-88-17] N90-19641
Possible applications of remote sensing in the preparatory phase of a land management project [BCRS-88-19] N90-19642
Technical and administrative feasibility of microlight remote sensing applications for river boards [BCRS-89-01] N90-19643
Segmentation of Side-Looking Airborne Radar (SLAR) images using a priori knowledge [BCRS-89-03] N90-19644
Activities report in remote sensing [ETN-90-95472] N90-19647

REMOTE SENSORS
Analysis of tectonic movements utilizing remote sensor products in the Southern Espinhaco (SE) region [INPE-4830-PRE/1451] N90-19708

REPORTS
Activities report in remote sensing [ETN-90-95472] N90-19647

REQUIREMENTS
Parkes radio science system design and testing for Voyager Neptune encounter N90-19451

RESEARCH AND DEVELOPMENT
Research Reports: 1989 NASA/ASEE Summer Faculty Fellowship Program [NASA-CR-183837] N90-19390
The Telecommunications and Data Acquisition Report [NASA-CR-185033] N90-19434
National Action Plan on Superconductivity Research and Development [PB89-138512] N90-19883
Science and technology report and outlook, 1985-1988 [PB90-115270] N90-19926
Design and development activities on the candidate sample acquisition system for the Rosetta mission N90-19993
Activities report of the Institute for Communication Technology [ETN-90-95383] N90-20043

RESEARCH FACILITIES
High power, high frequency component test facility [NASA-TM-102500] N90-19484
Relevance of laboratory studies to comets N90-20023

RESEARCH PROJECTS
Science and technology report and outlook, 1985-1988 [PB90-115270] N90-19926

RESERVOIRS
Areas of aquatic macrophytes classified through vegetative indexes extracted from LANDSAT/TM imagery [INPE-4880-PRE/1489] N90-19633
Predicting effects of global climate change on reservoir water quality and fish habitat [DE90-003674] N90-19704

RESIDUAL STRENGTH
Evaluation of repeated impact damage in composite structures N90-19303

RESIN MATRIX COMPOSITES
Utilization of thermometric methods for the testing of carbon reinforced plastics [ETN-90-96076] N90-19314

RESONANCE
Transient and sustained resonance in very slowly varying oscillatory Hamiltonian systems with application to free-electron lasers [DE90-005984] N90-19574

RESONANT FREQUENCIES
Investigation of SSME alternate high pressure fuel turbopump lift-off seal fluid and structural dynamic interaction N90-19400
Design and implementation of a flexible robot [AD-A216453] N90-19601

RESONATORS
Temperature compensated crystal oscillator (TCXO) with improved temperature compensation [AD-D014334] N90-19482
Finite element analysis of a quartz rotation sensor [DE90-006959] N90-19562
Generation of intensive UV laser radiation and utilization in high resolution spectroscopy of SO2 [ETN-90-95361] N90-19581

RESOURCE ALLOCATION
The 0-1 multiknapsack problem: Heuristic and reduction methods [INPE-4894-PRE/1495] N90-19782

RESOURCES MANAGEMENT
Development of an Ada programming support environment database SEAD (Software Engineering and Ada Database) administration manual [NASA-CR-186064] N90-19757

RESPIRATION
Evaluation of the Scott aviation portable protective breathing device for contaminant leakage as prescribed by FAA Action Notice A-8150.2. Phase 1: Original tests of the portable protective breathing device. Phase 2: Tests of the redesigned portable protective breathing device [AD-A216799] N90-19214

RETROREFLECTORS
Remote Attitude Measurement Sensor (RAMS) N90-19271

RETURN TO EARTH SPACE FLIGHT
Rosetta/CNSR altimeter and sounding radar N90-20009
First impressions of the comet drilling problem N90-20021
Relevance of laboratory studies to comets N90-20023

REVERBERATION
Numerical simulation of acoustic scatter from subsurface bubble clouds [AD-A217068] N90-19822

REYNOLDS NUMBER
Carrier wing profile in nonstationary current [ETN-90-95368] N90-19208
Theoretical and experimental examination of the beginning of turbulence in a heated laminar conduit flow [ETN-90-95369] N90-19541
Wind tunnel design of heat island turbulent boundary layer [IHW-ET/50] N90-19542

REYNOLDS STRESS
Application of a Reynolds stress turbulence model to the compressible shear layer [NASA-CR-182002] N90-19537
Analytical methods for the development of Reynolds stress closures in turbulence [NASA-CR-182017] N90-19538

RHEOLOGY
Elastic recovery and polymer-polymer interactions [AD-A217085] N90-19384
Calculation of nonlinear viscoelastic processes for plastic layer textile membranes [ETN-90-95868] N90-19622

RIBLETS
Drag reduction by longitudinal riblets on the surface of a streamwise aligned body of revolution [MPIS-MITT-92] N90-19210

RIBS (SUPPORTS)
Large-diameter geostationary millimeter wavelength antenna concept N90-19254
Design of a low-frequency (5-20 GHz), 15-meter-diameter passive radiometer for geostationary earth science platforms N90-19255

RICCATI EQUATION
A comparison between the propagators method and the decomposition method for nonlinear equations [DE90-005783] N90-19781

RIEMANN MANIFOLD
Superconformal algebra on meromorphic vector fields with three poles on super-Riemann sphere [DE90-610423] N90-19796
Quantum field theory on higher-genus Riemann surfaces [DE90-741469] N90-19912

RIGID WINGS
COCOMAT: A Computer Aided Engineering (CAE) system for composite structures design [NLR-MP-87078-U] N90-19756

RISK
Safety Status Report for the Ulysses mission. Book 1: Risk analysis. General purpose heat source radioisotope thermoelectric generator program [DE90-006826] N90-19282
The pollution hazard assessment system: Documentation and users manual [AD-A217108] N90-19706

ROBOT ARMS
Kinematic control of robotic manipulators with multiple interchangeable wrists N90-19592
Dynamics and control of robot manipulators with closed-kinematic chain mechanism N90-19598
A complete description of robot manipulator dynamics based on Lagrangian mechanics [DE90-741467] N90-19603

ROBOT DYNAMICS
Kinematic control of robotic manipulators with multiple interchangeable wrists N90-19592

ROBOTICS
Advancing automation and robotics technology for the Space Station Freedom and for the US economy: Submitted to the United States Congress [NASA-TM-101647] N90-19279
Kinematic control of robotic manipulators with multiple interchangeable wrists N90-19592
Advanced control schemes and kinematic analysis for a kinematically redundant 7 DOF manipulator [NASA-CR-186175] N90-19599
Improved processes for ultrasonic object recognition in robotics [ETN-90-95362] N90-19604
Extending terrestrial mobile robotics to a proposed lunar base [DE89-016179] N90-19606
A human factors testbed for ground-vehicle telerobotics research [DE90-006618] N90-19746

ROBOTS
Multibody modeling and verification N90-19422
Experiments in end-point control of a flexible robot with a mini-manipulator N90-19596
Advanced control schemes and kinematic analysis for a kinematically redundant 7 DOF manipulator [NASA-CR-186175] N90-19599
Design and implementation of a flexible robot [AD-A216453] N90-19601
A complete description of robot manipulator dynamics based on Lagrangian mechanics [DE90-741467] N90-19603
Extending terrestrial mobile robotics to a proposed lunar base [DE89-016179] N90-19606
An approach to elemental task learning [DE90-006614] N90-19745
A human factors testbed for ground-vehicle telerobotics research [DE90-006618] N90-19746
Parallel neural net path-planner on hypercube and transputer [DE90-006324] N90-19777
Nonlinear continuum mechanics and applied analysis [AD-A213629] N90-19812

ROCKET ENGINE DESIGN
Dual-fuel, dual-mode rocket engine [NASA-CASE-LAR-13773-1] N90-19298

ROCKET ENGINES
Proceedings of a contractors meeting on Combustion Rocket Propulsion Diagnostics of Reacting Flow [AD-A216445] N90-19297

ROCKET PROPELLANTS
The measurement, modeling, and prediction of traction for rocket propellant 1 [NASA-CR-185186] N90-19386

ROCKS
Using image analysis to determine petrophysical properties of reservoir rocks [DE90-000222] N90-19649

P-T condition fo deformation from fluid inclusions in mylonites
[NASA-CR-186377] N90-19710

RODS
Critical current density and transition temperature measurements of Y-Ba-Cu-O rods
[AD-A216695] N90-19875

ROLL FORMING
Optimizing superplastic response in navalite, a lithium containing aluminum-magnesium alloy
[AD-A216552] N90-19346
Structures instabilities in filament liquid crystals
[ETN-90-95916] N90-19888

ROLLING
Unfurlable, continuous-surface reflector concept N90-19257

ROTARY WINGS
Performance of an optimized rotor blade at off-design flight conditions
[NASA-CR-4288] N90-19226

ROTATING DISKS
Numerical and experimental analysis of a thin liquid film on a rotating disk related to development of a spacecraft absorption cooling system
[NASA-CR-183457] N90-19523

ROTATING SHAFTS
Analysis of unsteady heat transfer by natural convection in a two-dimensional square cavity using a high order finite-volume method N90-19521

ROTATION
Techniques for studying the effects of microgravity on model particle/cell systems N90-19424
Finite element analysis of a quartz rotation sensor
[DE90-006959] N90-19562

ROTONS
Coherent state in the roton region of superfluid helium-4
[DE90-610677] N90-19882

ROTOR BLADES (TURBOMACHINERY)
Digital determination of the three dimensional flow in turbomachines with the S1-S2 current function process
[ITSM-MITT-30] N90-19236

ROTOR DYNAMICS
A study of the effects of disk flexibility on the rotordynamics of the space shuttle main engine turbo-pumps N90-19401

ROTORS
Three-dimensional viscous rotor flow calculations using a viscous-inviscid interaction approach
[NASA-TM-102235] N90-19204
Calculation and optimization of rotor start process
[ETN-90-95894] N90-19229
A study of the effects of disk flexibility on the rotordynamics of the space shuttle main engine turbo-pumps N90-19401
Theoretical and experimental studies of a brushless disk rotor motor with permanent magnetic excitation and gap windings
[ETN-90-96056] N90-19512

RUNGE-KUTTA METHOD
Conical Euler solution for a highly-swept delta wing undergoing wing-rock motion
[NASA-TM-102609] N90-19211

S

SAFETY
Safety Status Report for the Ulysses mission. Book 1: Risk analysis. General purpose heat source radioisotope thermoelectric generator program
[DE90-006826] N90-19282
Safety status report for the Ulysses mission. Book 2: Risk analysis. General purpose heat source radioisotope thermoelectric generator program
[DE90-003827] N90-19283
Safety Status Report for the Ulysses mission. Book 2: Accident analysis-appendices. General purpose heat source radioisotope thermoelectric generator program
[DE90-006830] N90-19286

SAFETY DEVICES
Error detection in data processing devices by means of residue codes
[ETN-90-95370] N90-19767

SAFETY FACTORS
Safety Status Report for the Ulysses mission. Book 1: Accident analysis. General purpose heat source radiosotope thermoelectric generator program
[DE90-006829] N90-19285

SAMPLES
Thermal perturbation of comet samples during their acquisition N90-20008

SAMPLING
Exploiting surface observations of cloudiness for globalscale nephanalyses N90-19719
A technique for convolving unequally spaced samples using fast Fourier transforms
[DE90-006466] N90-19802

SANDWICH STRUCTURES
Low-energy impact resistance of graphite-epoxy plates and ALS honeycomb sandwich panels N90-19405

SATELLITE ANTENNAS
Mesh surfaces for reflector applications N90-19268
Antennas for 20/30 GHz and beyond N90-19269

SATELLITE ATTITUDE CONTROL
Self-tuning control techniques, implicit and explicit, with parameter estimation in Kalman filters, applied to artificial satellite attitude
[INPE-4857-TDL/368] N90-19276
Attitude and spin rate control of a spinning satellite using geomagnetic field
[INPE-4818-NTE/289] N90-19277

SATELLITE COMMUNICATION
Large antenna measurement and compensation techniques N90-19263

SATELLITE CONTROL
Drag-free satellite control N90-19974

SATELLITE IMAGERY
Areas of aquatic macrophytes classified through vegetative indexes extracted from LANDSAT/TM imagery
[INPE-4880-PRE/1489] N90-19633
Availability of multitemporal LANDSAT data accompanying the variation of water surfaces in the program area of Careiro PDRI/AM
[INPE-4896-PRE/1496] N90-19634
Satellite imagery for water quality assessment in coastal regions
[INPE-4891-PRE/1492] N90-19636
The potential of combined use of satellite data with topographic TM information for manual/visual and digital updating of land use
[NLR-MP-88021-U] N90-19639
Possible applications of remote sensing satellite pictures for the water quality management of the Frisian lakes, Netherlands
[BCRS-88-17] N90-19641
Activities report in remote sensing
[ETN-90-95472] N90-19647
Real time environment monitoring using data from METEOSAT and NOAA imaging satellites
[NLR-MP-87070-U] N90-19672
Cyclogeneses and extratropical cyclones in the south-southeast region of Brazil and its influence in time
[INPE-4812-TDL/359] N90-19722
An observational study of squall lines in the Amazon
[INPE-4865-TDL/376] N90-19723

SATELLITE NAVIGATION SYSTEMS
Carin and GPS: The combination of dead reckoning, map matching and satellite navigation in a hybrid automobile navigation system
[ETN-90-95451] N90-19220

SATELLITE OBSERVATION
Coherent radar measurement of ocean currents from geostationary orbit N90-19259
Self-tuning control techniques, implicit and explicit, with parameter estimation in Kalman filters, applied to artificial satellite attitude
[INPE-4857-TDL/368] N90-19276
Exploiting surface observations of cloudiness for globalscale nephanalyses N90-19719
Analysis of an observation of the x ray astronomy satellite EXOSAT at the low mass x ray binary star system GX5-1
[ETN-90-95828] N90-20042

SATELLITE ORBITS
Accuracy of global positioning system broadcast orbits for relative surveys
[PB90-125428] N90-19218

SATELLITE ROTATION
Attitude and spin rate control of a spinning satellite using geomagnetic field
[INPE-4818-NTE/289] N90-19277

SATELLITE TRANSMISSION
Effects of amplitude distortions and IF equalization on satellite communication system bit-error rate performance
[NASA-TM-102415] N90-19454

SCALARS
Potential theory of radiation N90-19395

SCALE EFFECT
An electrical model for plasma armature voltage
[DE90-007530] N90-19866

SCALE MODELS
Lightning surge characteristics of transmission towers. Lightning surge characteristics of 15-meter-high scale model tower
[DE89-782322] N90-19721

SCATTERING
Correlation-induced changes of spectra
[AD-A217087] N90-19591

SCATTERING CROSS SECTIONS
The electron momentum-transfer cross sections of tungsten, silicon, and silicon dioxide at energies from 0.1 to 10,000 eV
[DE90-009041] N90-19833

SCAVENGING
Development of an atmospheric diffusion model in fog (1). Literature review of scavenging process by precipitation
[DE89-782318] N90-19678
Numerical modeling of atmospheric growth processes
[REPT-70] N90-19726

SCHEDULES
Marshall Avionics Testbed System (MAST) N90-19417
Priority arbitration with busses
[AD-A216392] N90-19784

SCHOOLS
Laser Technology Center
[PB90-115387] N90-19564

SCINTILLATION COUNTERS
Conception of an automatic measurement installation for spatial resolution detectors
[ETN-90-95732] N90-19935

SCOUT PROJECT
TOPAS preparation study: Summary representation of the study results
[OHB-TN-TOP-011/87] N90-19244

SEA LEVEL
Status of a nonlinear water surge model in February 1988
[KNMI-WR-88-03] N90-19735

SEA WATER
Experiments on oxygen desorption from surface warm seawater under Open-Cycle Ocean Thermal Energy Conversion (OC-OTEC) conditions
[DE90-000308] N90-19866

SEALERS
Effect of temperature on the storage life of polysulfide aircraft sealants
[MRL-TR-89-31] N90-19364

SEALS (STOPPERS)
Investigation of SSME alternate high pressure fuel turbopump lift-off seal fluid and structural dynamic interaction N90-19400

SECONDARY RADAR
Experimental measurements in secondary radar field: Conception and first results
[ETN-90-96074] N90-19471

SEDIMENTS
Analysis of tectonic movements utilizing remote sensor products in the Southern Espinhaco (SE) region
[INPE-4830-PRE/1451] N90-19708

SEGMENTS
Precision segmented reflector, figure verification sensor N90-19272
Parallel distributed networks for image smoothing and segmentation in analog VSLI
[AD-A216780] N90-19491
Segmentation of Side-Looking Airborne Radar (SLAR) images using a priori knowledge
[BCRS-89-03] N90-19644

SEMANTICS
The expression of syntagmatic relationships in frame-based indexing N90-19917
Deceit: A flexible distributed file system
[NASA-CR-186412] N90-19923

SEMICONDUCTOR DEVICES
Utilization criteria for transistors of diverse technology in pulse inverters with high switching frequency
[ETN-90-95359] N90-19500
Silicon carbide semiconductor device fabrication and characterization
[NASA-CR-186354] N90-19873
Digital capacity transient spectroscopy of deep structure defects in III-V-Semiconductor structures
[ETN-90-96057] N90-19890
Self-consistant calculation of point and pair structure defects in silicium
[ETN-90-96059] N90-19891
Contact formation on (Hg,Cd) Te
[AD-A217088] N90-19900

SEMICONDUCTOR DIODES
Ignition of HMX (cyclotetramethylenetetranitramine) using low energy laser diodes
[DE90-007637] N90-19334
Noise floors of subnanosecond transient recording systems
[DE90-002339] N90-19571

SEMICONDUCTOR LASERS
Direct detection optical intersatellite link at 220 Mbps using AlGaAs laser diode and silicon APD with 4-ary PPM signaling
[NASA-CR-186380] N90-19460

Time resolved gain/loss studies under low and high power loading for the XeF C-A transition
[DE90-007506] N90-19517
The III-V semiconductor quantum well lasers and related optoelectronic devices on silicon
[AD-A216980] N90-19570
Experimental results of aging and thermal effects in high-power laser diodes
[DE90-005955] N90-19573
Noise behavior of semiconductor lasers by optic feedback
[ETN-90-95728] N90-19583

SEMICONDUCTORS (MATERIALS)
Low threshold current implanted-planar-buried-heterostructure, graded-index, separate-confinement-heterostructure GaAs-AlGaAs laser
[DE90-002579] N90-19572
Solid State Photovoltaic Research Branch
[DE89-009463] N90-19660
Passivating layer for III-V semiconductor materials
[AD-D014321] N90-19872
A simple model for the determination of L(sub 0), D and tau in a semiconductor and their temperature dependence
[DE90-610564] N90-19879
CCST (Center for Compound Semiconductor Technology) research briefs
[DE90-006446] N90-19887
Ion mixing and surface modification in metal-semiconductor systems
[DE90-007557] N90-19897
Contact formation on (Hg,Cd) Te
[AD-A217068] N90-19900

SENSITIVITY
Computational aspects of sensitivity calculations in linear transient structural analysis
[NASA-TM-4156] N90-19610
Sensitivity of ecological landscapes and regions to global climatic change
[PB90-120072] N90-19674

SEPARATED FLOW
Numerical solution of 3D Navier-Stokes equations with upwind implicit schemes
[NASA-TM-101656] N90-19205
Method and apparatus for detecting laminar flow separation and reattachment
[NASA-CASE-LAR-13952-1-SB] N90-19534

SEQUENCING
Influence of the parameters: Charge order, sequence classification, partial sequential circuit, and process regularity of a working charge (Gaussian process) on the lifetime of a component made of 3.1354 T3 and 3.4377 T761
[ETN-90-95378] N90-19503
Adaptive, asynchronous stochastic global optimization algorithms for sequential and parallel computation
[AD-A217093] N90-19775

SERVOCONTROL
Digital to position converter
[DIGEL-1984-4] N90-19509

SERVOMECHANISMS
Disturbance torque rejection properties of the NASA/JPL 70-meter antenna axis servos N90-19450
Digital to position converter
[DIGEL-1984-4] N90-19509

SEYFERT GALAXIES
Nearly simultaneous optical, ultraviolet, and x ray observations of three PG quasars
[NASA-CR-186355] N90-19932
Nuclear activity, morphology, and far infrared properties of spiral galaxies
[ETN-90-95373] N90-20024

SHAFTS (MACHINE ELEMENTS)
Phase control mechanism for wave energy conversion
[AD-D014354] N90-19657

SHEAR LAYERS
Separation bubbles at high Reynolds number: Measurement and computation
[CUED/A-AERO/15] N90-19525
Application of a Reynolds stress turbulence model to the compressible shear layer
[NASA-CR-182002] N90-19537
Experimental study of validity of the unstationary Kutta condition, with high Strouhal numbers
[ETN-90-95914] N90-19547

SHEAR PROPERTIES
Irradiation-induced amorphization and elastic shear instability in intermetallic compounds
[DE90-004845] N90-19341

SHEAR STRENGTH
The effect of fiber coatings on interfacial shear strength and the mechanical behavior of ceramic composites
[DE90-007574] N90-19380

SHEAR STRESS
Method and apparatus for detecting laminar flow separation and reattachment
[NASA-CASE-LAR-13952-1-SB] N90-19534
Application of a Reynolds stress turbulence model to the compressible shear layer
[NASA-CR-182002] N90-19537
Interlaminar shear stress effects on the postbuckling response of graphite-epoxy panels
[NASA-TM-102626] N90-19630

SHELL THEORY
Modeling and analysis of the space shuttle nose-gear tire with semianalytic finite elements
[NASA-TP-2977] N90-19595

SHELLS (STRUCTURAL FORMS)
Development of finite beam and shell elements for structures under great inelastic deformations
[ETN-90-95869] N90-19623

SHIELDING
Technology evaluation for space station atmospheric leakage
[DE90-007844] N90-19294
Trailer shield assembly for a welding torch
[NASA-CASE-MFS-29260-1] N90-19602

SHIPS
Suboptimal period design for a maneuvering missile to evade tracking filters N90-19479

SHOCK FRONTS
Numerical modelling of shocks in gases and metals
[MRL-RR-8-89] N90-19528

SHOCK TESTS
Test component attachment effects on resonant plate pyrotechnic shock simulation
[DE90-006478] N90-19551

SHOCK TUBES
A study on upstream moving pressure waves induced by vortex separation
[ISL-CO-203/88] N90-19192
Numerical modelling of shocks in gases and metals
[MRL-RR-8-89] N90-19528

SHOCK WAVE INTERACTION
Interaction of an oblique shock wave with supersonic flow over a blunt body N90-19197
Swept shock/boundary layer interaction experiments in support of CFD code validation
[NASA-CR-186397] N90-19535

SHOCK WAVE PROPAGATION
A study on upstream moving pressure waves induced by vortex separation
[ISL-CO-203/88] N90-19192

SHOCK WAVES
Calculation of excrescence drag magnification due to pressure gradient at high subsonic speeds
[ESDU-87004] N90-19195
Numerical modelling of shocks in gases and metals
[MRL-RR-8-89] N90-19528

SIDE-LOOKING RADAR
Segmentation of Side-Looking Airborne Radar (SLAR) images using a priori knowledge
[BCRS-89-03] N90-19644

SIERRA NEVADA MOUNTAINS (CA)
Transport of atmospheric aerosols above the Sierra Nevada slopes
[PB90-120288] N90-19675

SIEVES
Activation of methane by transition metal-substituted aluminophosphate molecular sieves
[DE90-005663] N90-19331

SIGNAL ANALYSIS
Simulation of radar and radiometer signals remote sensing cometary surface and subsurface structures N90-20005

SIGNAL DETECTION
Costas loop lock detection in the advanced receiver N90-19441

SIGNAL DETECTORS
Method and apparatus for detecting laminar flow separation and reattachment
[NASA-CASE-LAR-13952-1-SB] N90-19534

SIGNAL DISTORTION
Effects of amplitude distortions and IF equalization on satellite communication system bit-error rate performance
[NASA-TM-102415] N90-19454
Active phase and amplitude modulator
[AD-D014318] N90-19480

SIGNAL ENCODING
On linear structure and phase rotation invariant properties of block 2(sup l)-PSK modulation codes
[NASA-CR-186308] N90-19429

SIGNAL FADING
Apparatus and method for minimizing polarization-induced signal fading in an interferometric fiber-optic sensor using input-polarization modulation
[AD-D014315] N90-19430
Effects of amplitude distortions and IF equalization on satellite communication system bit-error rate performance
[NASA-TM-102415] N90-19454

SIGNAL GENERATORS
SINA: A test system for proximity fuses
[FEL-1989-101] N90-19498

SIGNAL PROCESSING
The Telecommunications and Data Acquisition Report
[NASA-CR-185033] N90-19434
Microwave oscillator with reduced phase noise by negative feedback incorporating microwave signals with suppressed carrier N90-19437
Effect of laser frequency noise on fiber-optic frequency reference distribution N90-19438
Thermal coefficient of delay for various coaxial and fiber-optic cables N90-19439
Performance of the all-digital data-transition tracking loop in the advanced receiver N90-19440
Costas loop lock detection in the advanced receiver N90-19441
Memory management in traceback Viterbi decoders N90-19443
Application of adaptive least-squares algorithm to multi-element array signal reconstruction N90-19448
The effects of sinusoidal interference on the second-order carrier tracking loop preceded by a bandpass limiter in the Block 4 receiver N90-19449
Parkes radio science system design and testing for Voyager Neptune encounter N90-19451
Signal processing
[DE90-006904] N90-19464
General multidimensional scanning ratio transformation and its utilization for norm transformation of television signals
[ETN-90-96058] N90-19470
Digital video: Studio signal processing
[BBC-RD-1989/14] N90-19476
Applications of frequency and wavenumber nonlinear digital signal processing to nonlinear hydrodynamics research
[AD-A216259] N90-19530
All-fiber SFPM (Stimulated Four Photon Mixing) amplifier
[AD-D014358] N90-19841

SIGNAL RECEPTION
The effects of sinusoidal interference on the second-order carrier tracking loop preceded by a bandpass limiter in the Block 4 receiver N90-19449
Planar integrated circuits for microwave transmission and reception
[AD-A217676] N90-19520

SIGNAL REFLECTION
A linear systems theory approach to the range-independent acoustic channel
[AD-A216551] N90-19817

SIGNAL TO NOISE RATIOS
Hydrogen assay foil counting system
[DE90-007415] N90-19332

SIGNAL TRANSMISSION
Effect of laser frequency noise on fiber-optic frequency reference distribution N90-19438

SILICA GEL
Elastic properties of silica xerogels
[AD-A216528] N90-19366

SILICON
The III-V semiconductor quantum well lasers and related optoelectronic devices on silicon
[AD-A216980] N90-19570

SILICON ALLOYS
Annealing group III-V compound doped silicon-germanium alloy for improved thermo-electric conversion efficiency
[NASA-CASE-NPO-17259-1-CU] N90-19884

SILICON CARBIDES
Heat treatment study of the SiC/Ti-15-3 composite system
[NASA-TP-2970] N90-19302
Identification and development of optimum SiC whiskers for silicon nitride matrix composites
[DE90-006888] N90-19315
Fracture strength analysis of silicon nitride and silicon carbide ceramics from an international cooperative research program
[DE90-005319] N90-19368
Fabrication, phase transformation studies, and characterization of SiC-AlN-Al2OC ceramics
[DE90-006591] N90-19371
The effect of fiber coatings on interfacial shear strength and the mechanical behavior of ceramic composites
[DE90-007574] N90-19380
Light-scattering measurements of CVD (Chemical Vapor Deposition) silicon carbide
[DE90-007885] N90-19382

Silicon carbide semiconductor device fabrication and characterization
[NASA-CR-186354] N90-19873

SILICON DIOXIDE
Elastic properties of silica xerogels
[AD-A216528] N90-19366
Radiation-induced density changes and creep in surface layers of glass
[DE90-008112] N90-19383
Growth and characterization of gallium (III) oxide films
[AD-A217568] N90-19902

SILICON FILMS
Preparation and characterization of alumina films prepared by a novel spray pyrolysis method
[AD-A217570] N90-19339

SILICON JUNCTIONS
Preparation and characterization of alumina films prepared by a novel spray pyrolysis method
[AD-A217570] N90-19339
Tunneling microscopy of submonolayer adsorbates on Si3
[AD-A216985] N90-19876

SILICON NITRIDES
Identification and development of optimum SiC whiskers for silicon nitride matrix composites
[DE90-006888] N90-19315
Fracture strength analysis of silicon nitride and silicon carbide ceramics from an international cooperative research program
[DE90-005319] N90-19368

SILICON TRANSISTORS
A gate array structure for the efficient project of digital circuits: The unit cell array
[ETN-90-95364] N90-19502

SILOXANES
Synthesis of poly(dimethylsiloxane) - nylon 6 diblock copolymers
[AD-A216850] N90-19367

SIMULATION
Simulation of thermal dynamics of a vaporizing coal-water droplet in a combustor
[DE90-005356] N90-19317
Kalman estimation for SEDS measurements N90-19393
Parallel distributed networks for image smoothing and segmentation in analog VSLI
[AD-A216780] N90-19491
Test component attachment effects on resonant plate pyrotechnic shock simulation
[DE90-006478] N90-19551
Regional climate change predictions from the Goddard Institute for Space Studies high resolution GCM
[NASA-CR-186375] N90-19725
Simulation fidelity in lightning penetration studies
[DE90-006367] N90-19731
Recalibrating software reliability models
[NASA-CR-186407] N90-19763
Plasma simulation on magnetohydrodynamic time scales
[DE90-007490] N90-19865
Microstructural simulations of dynamic recrystallization
[DE90-007504] N90-19895
Physics and Mechanics of Cometary Materials
[ESA-SP-302] N90-19989
Thermal conductivities and diffusivities of porous ice samples at low pressures and temperatures and possible modes of heat transfer in near surface layers of comets N90-19999
Simulation of radar and radiometer signals remote sensing cometary surface and subsurface structures N90-20005
CO2 depth profiles in cometary model substances of KOSI N90-20014
Possible targeting of particle emission by mechanical stress and penetration of sublimating ice-dust-surfaces N90-20016
Mechanical properties of fluffy agglomerates consisting of core-mantle-particles N90-20019
Dynamics of crust formation and dust emission of comet nucleus analogues under isolation N90-20020

SIMULATORS
SINA: A test system for proximity fuses
[FEL-1989-101] N90-19498
Lessons learned in the transition to ADA from FORTRAN at NASA/Goddard
[NASA-CR-186458] N90-19765

SINGLE CRYSTALS
Opto-Em and devices investigation
[AD-A215033] N90-19814
Search for far infrared radiation from optically pumped defect modes
[AD-A216976] N90-19843
The preparation and properties of iron doped II-VI chalcogenides
[AD-A217569] N90-19903

SINGLE STAGE TO ORBIT VEHICLES
Rapid near-optimal trajectory generation and guidance law development for single-stage-to-orbit airbreathing vehicles
[NASA-CR-186299] N90-19275

SINTERING
Crystallization behavior and properties of BaO-Al2O3-2SiO2 glass matrices
[NASA-CR-185209] N90-19374

SIPHONING
Siphon flows in isolated magnetic flux tubes. 3: The equilibrium path of the flux tube arch
[NASA-CR-186297] N90-19813

SISO (CONTROL SYSTEMS)
Experiments in end-point control of a flexible robot with a mini-manipulator N90-19596

SITE SELECTION
Vision for the introduction of the wind power generation system. Survey on the prospective market, part 2
[DE89-910386] N90-19651

SKIN (STRUCTURAL MEMBER)
The drum: Mechanical oscillators and acoustic radiators
[REPT-FB-01/88] N90-19819

SKY SURVEYS (ASTRONOMY)
The COBE cosmic 3 K anisotropy experiment: A gravity wave and cosmic string probe N90-19959

SLURRIES
An evaluation of ethylene-vinyl acetate copolymers as desensitizers for RDX in insensitive booster compositions prepared by slurry coating technology
[MRL-TR-89-33] N90-19385

SMOOTHING
Parallel distributed networks for image smoothing and segmentation in analog VSLI
[AD-A216780] N90-19491

SNOW
Laboratory techniques for the characterisation of snow structures N90-20007

SOCIAL FACTORS
Survey on the social and economic influences of wide-spreading heat-pump technology
[DE89-782294] N90-19526

SODIUM
Test results from a full-scale sodium reflux pool-boiler solar receiver
[DE90-003577] N90-19671
Low temperature elastic and dielectric properties of incommensurate barium sodium niobate
[AD-A216969] N90-19815

SODIUM CHLORIDES
NMR (Nuclear Magnetic Resonance) imaging development for the study of solids
[AD-A217073] N90-19899

SOFTWARE ENGINEERING
Marshall Avionics Testbed System (MAST) N90-19417
Design and architecture of fourth and fifth generation software engineering environments
[ETN-90-95365] N90-19752
Development of an Ada programming support environment database SEAD (Software Engineering and Ada Database) administration manual
[NASA-CR-186064] N90-19757
Recalibrating software reliability models
[NASA-CR-186407] N90-19763
A nonparametric software reliability growth model
[NASA-CR-186438] N90-19764
Software development: A paradigm for the future
[NASA-CR-186456] N90-19766
Deceit: A flexible distributed file system
[NASA-CR-186412] N90-19923

SOFTWARE TOOLS
Design and architecture of fourth and fifth generation software engineering environments
[ETN-90-95365] N90-19752

SOIL EROSION
Mechanics of aeolian processes: Soil erosion and dust production N90-19410

SOILS
The pollution hazard assessment system: Documentation and users manual
[AD-A217108] N90-19706

SOL-GEL PROCESSES
Advanced ceramics
[DE90-608004] N90-19370

SOLAR ACTIVITY
Solar-geophysical data number 541, September 1989. Part 1: (Prompt reports). Data for August, July 1989, and late data
[PB90-122763] N90-20032

SOLAR ARRAYS
A transient plasticity study and low cycle fatigue analysis of the Space Station Freedom photovoltaic solar array blanket
[NASA-TM-102516] N90-19617

SOLAR CELLS
Study of the optimization of reference parameters to the dynamic constraints of solar panels
[INPE-4793-TDL/355] N90-19656
Investigations of CuInSe2 thin films and contacts
[DE90-000301] N90-19886

SOLAR COLLECTORS
Measuring flow properties of wicks for heat pipe solar receivers
[DE89-016537] N90-19664
Radiative transport models for solar thermal receiver/reactors
[DE90-000303] N90-19665
Status of stretched-membrane heliostats
[DE90-000801] N90-19669
Evaluation of thermal cycling creep-fatigue damage for a molten salt receiver
[DE90-002907] N90-19670
Test results from a full-scale sodium reflux pool-boiler solar receiver
[DE90-003577] N90-19671

SOLAR DYNAMIC POWER SYSTEMS
Hot filament technique for measuring the thermal conductivity of molten lithium fluoride
[NASA-TM-102506] N90-19373

SOLAR ENERGY
Enhancement of processes for solar photocatalytic detoxification of water
[DE90-003949] N90-19330
Solar and thermic utilization in high temperature area: Research and development
[ETN-90-98062] N90-19663
Radiative transport models for solar thermal receiver/reactors
[DE90-000303] N90-19665
Spectral solar radiation data base documentation
[DE89-009448] N90-20033

SOLAR ENERGY CONVERSION
Energy transfer and photochemistry in biomimetic solar conversion
[PB90-114562] N90-19652
Direct absorption receiver
[DE90-000311] N90-19667
Status of stretched-membrane heliostats
[DE90-000801] N90-19669

SOLAR FLARES
Solar-geophysical data number 541, September 1989. Part 2: (Comprehensive reports). Data for March 1989 and miscellaneous
[PB90-122755] N90-20031
Solar-geophysical data number 541, September 1989. Part 1: (Prompt reports). Data for August, July 1989, and late data
[PB90-122763] N90-20032
Reliability of equivalent sphere model in blood-forming organ dose estimation
[NASA-TM-4178] N90-20036

SOLAR GRAVITATION
Gravitational experiments on a solar probe mission: Scientific objectives and technology considerations N90-19666

SOLAR HEATING
Pyranometry
[DWD-14] N90-19661

SOLAR MAGNETIC FIELD
Solar-geophysical data number 541, September 1989. Part 1: (Prompt reports). Data for August, July 1989, and late data
[PB90-122763] N90-20032

SOLAR MAXIMUM MISSION
MAX 1991. The active sun: A plan for pursuing the study of the active sun at the time of the next maximum in solar activity, January 1985
[NASA-CR-186125] N90-20030

SOLAR PHYSICS
MAX 1991. The active sun: A plan for pursuing the study of the active sun at the time of the next maximum in solar activity, January 1985
[NASA-CR-186125] N90-20030
Solar-geophysical data number 541, September 1989. Part 2: (Comprehensive reports). Data for March 1989 and miscellaneous
[PB90-122755] N90-20031
Solar-geophysical data number 541, September 1989. Part 1: (Prompt reports). Data for August, July 1989, and late data
[PB90-122763] N90-20032

SOLAR PROBES
Gravitational experiments on a solar probe mission: Scientific objectives and technology considerations N90-19666

SOLAR PROMINENCES
Solar-geophysical data number 541, September 1989. Part 2: (Comprehensive reports). Data for March 1989 and miscellaneous
[PB90-122755] N90-20031

SOLAR RADIATION
Solar and thermic utilization in high temperature area: Research and development
[ETN-90-96062] N90-19663
Solar-geophysical data number 541, September 1989. Part 2: (Comprehensive reports). Data for March 1989 and miscellaneous
[PB90-122755] N90-20031
Spectral solar radiation data base documentation
[DE89-009448] N90-20033
SOLAR RADIATION SHIELDING
Reliability of equivalent sphere model in blood-forming organ dose estimation
[NASA-TM-4178] N90-20036
SOLAR RADIO BURSTS
Solar-geophysical data number 541, September 1989. Part 2: (Comprehensive reports). Data for March 1989 and miscellaneous
[PB90-122755] N90-20031
SOLAR RADIO EMISSION
Solar-geophysical data number 541, September 1989. Part 1: (Prompt reports). Data for August, July 1989, and late data
[PB90-122763] N90-20032
SOLAR REFLECTORS
Enhancement of processes for solar photocatalytic detoxification of water
[DE90-003949] N90-19330
SOLAR SPECTRA
Far-ultraviolet spectroscopy of Comet Halley N90-19979
Comet Halley: An optical continuum study N90-19981
SOLAR WIND
Gravitational experiments on a solar probe mission: Scientific objectives and technology considerations N90-19966
Disturbance structures and its magnetic field features in plasma comet tail
[DE90-610636] N90-19986
The Advanced Composition Explorer
[DE90-006522] N90-19987
SOLAR X-RAYS
Solar-geophysical data number 541, September 1989. Part 2: (Comprehensive reports). Data for March 1989 and miscellaneous
[PB90-122755] N90-20031
SOLID ELECTROLYTES
Advanced double layer capacitor
[AD-A217110] N90-19518
SOLID STATE
Solid State Photovoltaic Research Branch
[DE89-009463] N90-19660
SOLID STATE DEVICES
Automated visibility and cloud cover measurements with a solid-state imaging system
[AD-A216906] N90-19724
SOLID STATE LASERS
Low threshold current implanted-planar-buried-heterostructure, graded-index, separate-confinement-heterostructure GaAs-AlGaAs laser
[DE90-002579] N90-19572
Assessment of research needs for laser technologies applied to advanced spectroscopic methods
[DE90-007402] N90-19588
CCST (Center for Compound Semiconductor Technology) research briefs
[DE90-006446] N90-19687
SOLID-SOLID INTERFACES
Glancing angle XAFS (X ray Absorption Fine Structure) and x ray reflectivity studies of transition-metal/aluminum interfaces
[DE90-005575] N90-19353
SOLIDS
Elastic solutions in a semi-infinite solid with an ellipsoidal inclusion
[AD-A217063] N90-19338
NMR (Nuclear Magnetic Resonance) imaging development for the study of solids
[AD-A217073] N90-19699
SOLUTIONS
Minimum cycle covering and integer flows
[AD-A216546] N90-19785
SOUND FIELDS
A linear systems theory approach to the range-independent acoustic channel
[AD-A216551] N90-19817
SOUND TRANSMISSION
A linear systems theory approach to the range-independent acoustic channel
[AD-A216551] N90-19817
SOUND WAVES
Dynamics of a class of vortex rings
[NASA-TM-102257] N90-19524
The drum: Mechanical oscillators and acoustic radiators
[REPT-FB-01/88] N90-19819
Sandia National Laboratories' new high level acoustic test facility
[DE90-006810] N90-19820
SOUTH AMERICA
Cyclogeneses and extratropical cyclones in the south-southeast region of Brazil and its influence in time
[INPE-4812-TDL/359] N90-19722
Evolution of finite amplitude baroclinic waves in the atmosphere and ocean
[INPE-4752-TDL/346] N90-19733
SOVIET SATELLITES
Compendium of meteorological space programs, satellites, and experiments
[NASA-TM-102924] N90-19243
SPACE BASED RADAR
Arrays for space applications N90-19265
Development of a receiver for a space-based laser radar system
[AD-A215079] N90-19566
SPACE CHARGE
identification and solution of a charging problem in a high-altitude detector
[DE90-006837] N90-19296
Impedance characteristics of terawatt ion diodes
[DE90-006276] N90-19494
SPACE COOLING (BUILDINGS)
Advanced absorption technology development in the United States
[DE90-001336] N90-19428
SPACE DEBRIS
Present and future risk of satellite and manned platforms collisions with other space objects and particles on earth orbits
[R-8841] N90-19287
Present and future risk of collision of satellites and manned platforms with other space objects and particles in terrestrial orbit
[R-8840] N90-19288
Satellites and debris in earth revolution orbits and first estimation of the collision probability
[R-8709] N90-19289
Project for the European space organization in the area of space debris
[REPT-29/89] N90-19290
SPACE ENVIRONMENT SIMULATION
Analysis of alternative concepts for transport systems on the Moon surface
[ETN-90-95727] N90-19605
SPACE FLIGHT
Safety Status Report for the Ulysses mission: Summary. General purpose heat source radioisotope thermoelectric generator program
[DE90-006828] N90-19284
Working on the moon: The Apollo experience
[DE90-003662] N90-19744
SPACE MAINTENANCE
Orbital servicing: Issue or answer
[AD-A217284] N90-19295
SPACE MISSIONS
Structures for remotely deployable precision antennas N90-19256
SPACE PLASMAS
Active probing of space plasmas
[AD-A216867] N90-19855
SPACE POWER REACTORS
Analysis and evaluation of ZPPR (Zero Power Physics Reactor) critical experiments for a 100 kilowatt-electric space reactor
[DE90-005634] N90-19835
SPACE PROBES
Active probing of space plasmas
[AD-A216867] N90-19855
High stability radio links N90-19970
SPACE PROGRAMS
Compendium of meteorological space programs, satellites, and experiments
[NASA-TM-102924] N90-19243
Antennas for 20/30 GHz and beyond N90-19269
SPACE SHUTTLE BOOSTERS
Aerospace Safety Advisory Panel
[NASA-TM-101748] N90-19389
Development of inspection techniques for quantitatively measuring surface contamination on SRM hardware
[NASA-CR-183902] N90-19608
SPACE SHUTTLE MAIN ENGINE
Aerospace Safety Advisory Panel
[NASA-TM-101748] N90-19389
A parametric heat transfer study for cryogenic ball bearings in SSME HPOTP N90-19397
Investigation of SSME alternate high pressure fuel turbopump lift-off seal fluid and structural dynamic interaction N90-19400
A study of the effects of disk flexibility on the rotordynamics of the space shuttle main engine turbo-pumps N90-19401
Iterative procedures for space shuttle main engine performance models N90-19416
SPACE SHUTTLE MISSIONS
Aerospace Safety Advisory Panel
[NASA-TM-101748] N90-19389
SPACE SHUTTLE ORBITERS
Aerospace Safety Advisory Panel
[NASA-TM-101748] N90-19389
Modeling and analysis of the space shuttle nose-gear tire with semianalytic finite elements
[NASA-TP-2977] N90-19595
SPACE SHUTTLE PAYLOADS
Large antenna measurement and compensation techniques N90-19263
SPACE SHUTTLES
Safety Status Report for the Ulysses mission. Book 2: Accident analysis-appendices. General purpose heat source radioisotope thermoelectric generator program
[DE90-006830] N90-19286
Radar transponder antenna pattern analysis for the space shuttle N90-19414
SPACE STATIONS
Advancing automation and robotics technology for the Space Station Freedom and for the US economy: Submitted to the United States Congress
[NASA-TM-101647] N90-19279
Technology evaluation for space station atmospheric leakage
[DE90-007844] N90-19294
Aerospace Safety Advisory Panel
[NASA-TM-101748] N90-19389
A transient plasticity study and low cycle fatigue analysis of the Space Station Freedom photovoltaic solar array blanket
[NASA-TM-102516] N90-19617
SPACE TRANSPORTATION SYSTEM
Aerospace Safety Advisory Panel
[NASA-TM-101748] N90-19389
SPACE TRANSPORTATION SYSTEM FLIGHTS
Aerospace Safety Advisory Panel
[NASA-TM-101748] N90-19389
SPACE-TIME FUNCTIONS
Propagation of electromagnetic waves in multidimensional homogeneous cosmologies
[DE90-610474] N90-19462
Causal boundary construction for space-times of the general relativity theory
[ETN-90-95357] N90-19915
Toward higher order tests of the gravitational interaction N90-19948
Applied general relativity N90-19950
High stability radio links N90-19970
SPACEBORNE EXPERIMENTS
Compendium of meteorological space programs, satellites, and experiments
[NASA-TM-102924] N90-19243
Relativistic Gravitational Experiments in Space
[NASA-CP-3046] N90-19940
Optical interferometers for tests of relativistic gravity in space N90-19967
SPACEBORNE LASERS
Development of a receiver for a space-based laser radar system
[AD-A215079] N90-19566
Frequency stable high power lasers in space N90-19969
SPACECRAFT ANTENNAS
Large space antenna concepts for ESGP N90-19253
Mesh surfaces for reflector applications N90-19268
Antennas for 20/30 GHz and beyond N90-19269
SPACECRAFT COMMUNICATION
The Telecommunications and Data Acquisition Report
[NASA-CR-185033] N90-19434
Effects of amplitude distortions and IF equalization on satellite communication system bit-error rate performance
[NASA-TM-102415] N90-19454
SPACECRAFT CONTROL
Advanced topics in structural dynamics: The maneuver of flexible spacecraft, and on-off decentralized control of flexible structures N90-19274
SPACECRAFT DESIGN
Operational requirements and the geostationary platform N90-19250
SPACECRAFT DOCKING
Yaw rate control of an air bearing vehicle N90-19420
SPACECRAFT GUIDANCE
Rapid near-optimal trajectory generation and guidance law development for single-stage-to-orbit airbreathing vehicles
[NASA-CR-186299] N90-19275

SPACECRAFT INSTRUMENTS
Identification and solution of a charging problem in a high-altitude detector
[DE90-008637] N90-19296
SPACECRAFT LAUNCHING
Geostationary earth science platform concepts N90-19252
SPACECRAFT MOTION
Advanced topics in structural dynamics: The maneuver of flexible spacecraft, and on-off decentralized control of flexible structures N90-19274
SPACECRAFT POWER SUPPLIES
Safety Status Report for the Ulysses mission. Book 1: Accident analysis. General purpose heat source radioisotope thermoelectric generator program
[DE90-006829] N90-19285
Hot filament technique for measuring the thermal conductivity of molten lithium fluoride
[NASA-TM-102506] N90-19373
High power, high frequency component test facility
[NASA-TM-102500] N90-19484
SPACECRAFT PROPULSION
Rapid near-optimal trajectory generation and guidance law development for single-stage-to-orbit airbreathing vehicles
[NASA-CR-186299] N90-19275
Monostable electrovalve
[INPE-4928-RPE/595] N90-19487
SPACECRAFT TRAJECTORIES
Rapid near-optimal trajectory generation and guidance law development for single-stage-to-orbit airbreathing vehicles
[NASA-CR-186299] N90-19275
Icarus lander N90-19964
SPATIAL DISTRIBUTION
Monte Carlo models and analysis of galactic disk gamma-ray burst distributions N90-19403
SPATIAL RESOLUTION
Spatially high-resolution flame diagnosis by means of spontaneous Raman spectroscopy
[ETN-90-95870] N90-19328
Conception of an automatic measurement installation for spatial resolution detectors
[ETN-90-95732] N90-19935
Space telescope searches for black holes in galactic nuclei N90-19958
Simulation of radar and radiometer signals remote sensing cometary surface and subsurface structures N90-20005
SPECIFICATIONS
A digital HDTV recorder using a cluster of four D1 DVTRs
[BBC-RD-1989/13] N90-19477
Design considerations in achieving 1 MW CW operation with a whispering-gallery-mode gyrotron
[DE90-007283] N90-19557
Progress in the CW operation of a 140 GHz gyrotron
[DE90-007382] N90-19558
An equational language for specifying, querying, and updating database domains
[PB90-124694] N90-19918
SPECIMEN GEOMETRY
Thermo-oxidative stability studies of PMR-15 polymer matrix composites reinforced with various fibers
[NASA-TM-102439] N90-19310
SPECKLE INTERFEROMETRY
Speckle interferometry for high resolution pictures of astronomical objects
[ETN-90-95827] N90-19936
Information reconstruction from speckle interferograms
[ETN-90-95918] N90-19939
SPECKLE PATTERNS
An optical white light speckle process in forward dispersion for measurement of the velocity field in free convective currents
[ETN-90-95913] N90-19546
SPECTRAL EMISSION
Power spectral densities for selected digital phase-continuous MFSK (M-ary Frequency Shift Keying) emissions
[PB90-129990] N90-19463
SPECTRAL METHODS
Conforming Chebyshev spectral collocation methods for the solution of laminar flow in a constricted channel
[NASA-CR-182011] N90-19539
SPECTRAL THEORY
Correlation-induced changes of spectra
[AD-A217087] N90-19591
SPECTROGRAPHS
Quantum yield of photocathodes in far and extreme ultraviolet wavelength area
[ETN-90-95731] N90-19505
The microchannel plate camera as a detector at high resolution spectrographs: Experiments for velocity distribution in planetary nebulae
[ETN-90-95733] N90-19560
SPECTROPHOTOMETRY
Hot OH and CN: Evidence for organic molecules close to the nucleus of comet Halley N90-20012
SPECTROSCOPY
Correlation-induced changes of spectra
[AD-A217087] N90-19591
FOMA: A Fast Optical Multichannel Analyzer
[DE90-004093] N90-19839
Digital capacity transient spectroscopy of deep structure defects in III-V-Semiconductor structures
[ETN-90-96057] N90-19890
SPECTRUM ANALYSIS
Far-ultraviolet spectroscopy of Comet Halley N90-19979
SPHERICAL SHELLS
Steady state temperatures and thermal stresses in a spherical or cylindrical laminated shell
[ESDU-89027] N90-19612
SPILLING
Water-tunnel investigation of concepts for alleviation of adverse inlet spillage interactions with external stores
[NASA-TM-4181] N90-19199
SPIN DYNAMICS
Computational fluid dynamics method for low Reynolds number flow in a precessing/spinning, liquid filled cylinder with rounded endcaps
[AD-A216997] N90-19531
SPIN STABILIZATION
Attitude and spin rate control of a spinning satellite using geomagnetic field
[INPE-4818-NTE/289] N90-19277
Computational fluid dynamics method for low Reynolds number flow in a precessing/spinning, liquid filled cylinder with rounded endcaps
[AD-A216997] N90-19531
SPIRAL GALAXIES
Nuclear activity, morphology, and far infrared properties of spiral galaxies
[ETN-90-95373] N90-20024
SPLINE FUNCTIONS
A tensor product B-spline method for numerical grid generation
[DE90-005979] N90-19792
SPRAYERS
Effects of turbulence mixing, variable properties, and vaporization on spray droplet combustion
[NASA-CR-186463] N90-19326
Preparation and characterization of alumina films prepared by a novel spray pyrolysis method
[AD-A217570] N90-19339
Growth and characterization of gallium (III) oxide films
[AD-A217568] N90-19902
SPRAYING
On the question of spray effects N90-19691
SPREAD SPECTRUM TRANSMISSION
Packet radio networks under dynamic jamming
[AD-A217094] N90-19475
SPUTTERING
Particle emission by oblique ion bombardment of gold
[ETN-90-95825] N90-19827
Silicon carbide semiconductor device fabrication and characterization
[NASA-CR-186354] N90-19873
SQUALLS
An observational study of squall lines in the Amazon
[INPE-4865-TDL/376] N90-19723
SQUID (DETECTORS)
Superconducting gravity gradiometer and a test of inverse square law N90-19975
STABILITY
Thermo-oxidative stability studies of PMR-15 polymer matrix composites reinforced with various fibers
[NASA-TM-102439] N90-19310
Contact formation on (Hg,Cd) Te
[AD-A217088] N90-19900
STABILITY AUGMENTATION
Output model-following control synthesis for an oblique-wing aircraft
[NASA-TM-100454] N90-19241
STABILITY DERIVATIVES
Computational fluid dynamics method for low Reynolds number flow in a precessing/spinning, liquid filled cylinder with rounded endcaps
[AD-A216997] N90-19531
STAINLESS STEELS
Mitigation of stress corrosion cracking of AISI 304 stainless steel in oxygenated water at 289 C by organic species at low concentration
[DE90-005631] N90-19354
STANDARDS
The Uniform Engine Test Programme
[AGARD-AR-248] N90-19232
STAR FORMATION
Accretion flows in high mass star formation
[DE90-007251] N90-20027
STAR TRACKERS
Remote Attitude Measurement Sensor (RAMS) N90-19271
STARS
Signature objects: Preliminaries for the satellite project HIPPARCOS/TYCHO
[ETN-90-95730] N90-19934
STARTING
Calculation and optimization of rotor start process
[ETN-90-95894] N90-19229
STATE ESTIMATION
Physical models of cometary nuclei: A review N90-19991
STATIC ELECTRICITY
Passivating layer for III-V semiconductor materials
[AD-D014321] N90-19872
STATIC PRESSURE
Study of the turbulent boundary layer on an afterbody
[TM-EA-8901] N90-19212
STATIC TESTS
Static investigation of a two-dimensional convergent-divergent exhaust nozzle with multiaxis thrust-vectoring capability
[NASA-TP-2973] N90-19193
Static strength and damage tolerance tests on the Fokker 100 airframe
[NLR-MP-88023-U] N90-19228
STATISTICAL ANALYSIS
Kalman estimation for SEDS measurements N90-19393
Photon statistical limitations for daytime optical tracking N90-19442
STATISTICAL DISTRIBUTIONS
Automated visibility and cloud cover measurements with a solid-state imaging system
[AD-A216906] N90-19724
STEADY FLOW
Carrier wing profile in nonstationary current
[ETN-90-95368] N90-19208
STEADY STATE
Steady state temperatures and thermal stresses in a spherical or cylindrical laminated shell
[ESDU-89027] N90-19612
Plasma centrifuge with vacuum arc discharge applied to the separation of stable isotopes
[INPE-4925-TDL/385] N90-19854
STEEL STRUCTURES
Plastic bending tests of cold-formed rectangular hollow sections
[PB90-124811] N90-19613
STEERING
Structures for remotely deployable precision antennas N90-19256
STELLAR ATMOSPHERES
A storage process of the magnetic energy results from the unsteady plasma flow field in the space active regions and stellar atmosphere
[DE90-610638] N90-19858
O-star parameters from line profiles of wind-blanketed model atmospheres N90-19982
STELLAR COMPOSITION
O-star parameters from line profiles of wind-blanketed model atmospheres N90-19982
STELLAR ENVELOPES
Infrared heterodyne spectroscopy of polyatomic molecules in circumstellar envelopes N90-19980
Cometary bodies in the circumstellar disk around beta Pictoris N90-20010
STELLAR GRAVITATION
O-star parameters from line profiles of wind-blanketed model atmospheres N90-19982
STELLAR LUMINOSITY
Signature objects: Preliminaries for the satellite project HIPPARCOS/TYCHO
[ETN-90-95730] N90-19934
STELLAR MAGNETIC FIELDS
Magnetic fields in late-type dwarfs: Preliminary results from a multiline approach
[SER-C-PREPUB-FASC-31] N90-19928
Accretion flows in high mass star formation
[DE90-007251] N90-20027
STELLAR MASS
Nearly simultaneous optical, ultraviolet, and x ray observations of three PG quasars
[NASA-CR-186355] N90-19932
STELLAR MASS ACCRETION
Accretion flows in high mass star formation
[DE90-007251] N90-20027
STELLAR MASS EJECTION
Neon novae, recurrent novae, and type I supernovae
[DE90-003188] N90-19931

STELLAR MODELS
O-star parameters from line profiles of wind-blanketed model atmospheres N90-19982
Model calculations for dynamic development of planetary nebulae
[ETN-90-95734] N90-20025
STELLAR PARALLAX
Signature objects: Preliminaries for the satellite project HIPPARCOS/TYCHO
[ETN-90-95730] N90-19934
STELLAR SPECTRA
Magnetic fields in late-type dwarfs: Preliminary results from a multiline approach
[SER-C-PREPUB-FASC-31] N90-19928
Infrared heterodyne spectroscopy of polyatomic molecules in circumstellar envelopes N90-19980
O-star parameters from line profiles of wind-blanketed model atmospheres N90-19982
STELLAR TEMPERATURE
O-star parameters from line profiles of wind-blanketed model atmospheres N90-19982
STELLAR WINDS
O-star parameters from line profiles of wind-blanketed model atmospheres N90-19982
STEREOPHOTOGRAPHY
Technical and administrative feasibility of microlight remote sensing applications for river boards
[BCRS-89-01] N90-19643
STIFFNESS
Evaluation of repeated impact damage in composite structures N90-19303
STOCHASTIC PROCESSES
Parallel distributed networks for image smoothing and segmentation in analog VSLI
[AD-A216780] N90-19491
Implementation of a finite element process for the Euler equations of the gas dynamics
[PREPRINT-500] N90-19545
Adaptive, asynchronous stochastic global optimization algorithms for sequential and parallel computation
[AD-A217093] N90-19775
Optimal iteration steps by stochastic approximation processes for the solution of optimization problems with twice differentiable functions
[ETN-90-95867] N90-19809
On the Langevin equation for stochastic quantization of gravity
[DE90-750024] N90-19914
STOKES FLOW
Finite element approximations of the stokes flow problem based upon various variational principles
[DE90-606612] N90-19533
STORAGE STABILITY
Effect of temperature on the storage life of polysulfide aircraft sealants
[MRL-TR-89-31] N90-19364
STRANGE ATTRACTORS
Chaotic transients, higher dimensional phenomena, and coupled ordinary differential equations
[DE90-006641] N90-19794
STRAPDOWN INERTIAL GUIDANCE
Development of a standardized three axis sensor for inertial data achievement for future flight rule systems
[ETN-90-96075] N90-19231
STRAPS
The creep behavior of an aramide fiber reinforced wound low-strap
[LR-546] N90-19312
STRATEGY
Investigations into a new algorithm for calculating H infinity optimal controllers N90-19406
STRATIGRAPHY
Physical models of cometary nuclei: A review N90-19991
Petrographic working model of the Rosetta sampling and modelling subgroup for a comet nucleus N90-19992
Dynamics of crust formation and dust emission of comet nucleus analogues under isolation N90-20020
STREAK CAMERAS
Noise floors of subnanosecond transient recording systems
[DE90-002339] N90-19571
STRESS ANALYSIS
Computational and experimental of railgun structural performance
[DE90-006418] N90-19247
Three-dimensional structural analyses of reentry vehicles
[DE90-006278] N90-19291
Fracture strength analysis of silicon nitride and silicon carbide ceramics from an international cooperative research program
[DE90-005319] N90-19368
Radiation-induced density changes and creep in surface layers of glass
[DE90-008112] N90-19383
Anode plasma formation as a possible mechanism for an electrical stress limit in cold cathode diodes
[DE90-007503] N90-19516
Application of a Reynolds stress turbulence model to the compressible shear layer
[NASA-CR-182002] N90-19537
Analytical methods for the development of Reynolds stress closures in turbulence
[NASA-CR-182017] N90-19538
Use of chaotic and random vibrations to generate high frequency test inputs. Part 2: Chaotic vibrations
[DE90-007153] N90-19627
Use of chaotic and random vibrations to generate high frequency test inputs
[DE90-007412] N90-19628
Tunneling microscopy of submonolayer adsorbates on Si3
[AD-A216985] N90-19876
STRESS CORROSION
Mitigation of stress corrosion cracking of AISI 304 stainless steel in oxygenated water at 289 C by organic species at low concentration
[DE90-005631] N90-19354
STRESS CORROSION CRACKING
Evaluation of radiation-induced sensitization using electrochemical potentiokinetic reactivation technique for austenitic stainless steels
[DE90-002708] N90-19352
Mitigation of stress corrosion cracking of AISI 304 stainless steel in oxygenated water at 289 C by organic species at low concentration
[DE90-005631] N90-19354
STRESS DISTRIBUTION
Innovative design of composite structures: The use of curvilinear fiber format in structural design of composites
[NASA-CR-186406] N90-19308
Interlaminar shear stress effects on the postbuckling response of graphite-epoxy panels
[NASA-TM-102626] N90-19630
STRESS-STRAIN RELATIONSHIPS
Demonstration of capabilities of high temperature composites analyzer code HITCAN
[NASA-TM-102560] N90-19629
STRING THEORY
Superconformal algebra on meromorphic vector fields with three poles on super-Riemann sphere
[DE90-610423] N90-19796
Research accomplishments and future goals in particle physics
[DE90-007296] N90-19830
Construction of four-dimensional open superstrings
[DE90-006484] N90-19908
Reparametrization BRS cohomology in two-dimensional gravity and non-critical string theories
[DE90-741468] N90-19911
Gravitational consequences of modern field theories N90-19947
The COBE cosmic 3 K anisotropy experiment: A gravity wave and cosmic string probe N90-19959
Cosmic string in compactified gauge theory
[DE90-741463] N90-19988
STRIP TRANSMISSION LINES
Discontinuous-taper directional coupler
[AD-D014324] N90-19481
Internal transmission line filter element
[AD-D014353] N90-19489
STRONG INTERACTIONS (FIELD THEORY)
The ultimate structure of matter: The high energy physics program from the 1950s through the 1980s
[DE90-005682] N90-19836
STRONGLY COUPLED PLASMAS
Electrical resistivity of strongly coupled plasmas in intense fields
[DE90-002236] N90-19861
STROUHAL NUMBER
Experimental study of validity of the unstationary Kutta condition, with high Strouhal numbers
[ETN-90-95914] N90-19547
STRUCTURAL ANALYSIS
Computational and experimental of railgun structural performance
[DE90-006418] N90-19247
Integrated control/structure optimization by multilevel decomposition
[NASA-TM-102619] N90-19281
Three-dimensional structural analyses of reentry vehicles
[DE90-006278] N90-19291
An experimental study of the aeroelastic behaviour of two parallel interfering circular cylinders N90-19609
Computational aspects of sensitivity calculations in linear transient structural analysis
[NASA-TM-4156] N90-19610
PATRAN-STAGS translator (PATSTAGS)
[NASA-TM-100388] N90-19616
A transient plasticity study and low cycle fatigue analysis of the Space Station Freedom photovoltaic solar array blanket
[NASA-TM-102516] N90-19617
Digital treatment of elastic-plastic structures by means of quadratic optimization processes from the finite element method
[ETN-90-95823] N90-19621
COCOMAT: A Computer Aided Engineering (CAE) system for composite structures design
[NLR-MP-87078-U] N90-19756
STRUCTURAL DESIGN
X-29A aircraft structural loads flight testing
[NASA-TM-101715] N90-19225
Aeroservoelasticity
[NASA-TM-102620] N90-19227
Unfurlable, continuous-surface reflector concept N90-19257
ROCOPT: A user friendly interactive code to optimize rocket structural components N90-19415
Frequency response of electrochemical cells N90-19419
Design considerations in achieving 1 MW CW operation with a whispering-gallery-mode gyrotron
[DE90-007283] N90-19557
Computational aspects of sensitivity calculations in linear transient structural analysis
[NASA-TM-4156] N90-19610
STRUCTURAL ENGINEERING
COCOMAT: A Computer Aided Engineering (CAE) system for composite structures design
[NLR-MP-87078-U] N90-19756
Parallel methods for solving nonlinear block bordered systems of equations
[AD-A217062] N90-19806
STRUCTURAL PROPERTIES (GEOLOGY)
Analysis of photogeologic lineaments in the Ithacare (BA) region: A proposed methodology
[INPE-4855-PRE/1478] N90-19635
Analysis of tectonic movements utilizing remote sensor products in the Southern Espinhaco (SE) region
[INPE-4830-PRE/1451] N90-19708
Comets: Dirty snowballs or icy dirtballs N90-19994
Laboratory techniques for the characterisation of snow structures N90-20007
STRUCTURAL STABILITY
Structures instabilities in filament liquid crystals
[ETN-90-95916] N90-19888
STRUCTURAL VIBRATION
Helicopter flight vibration of large transportation containers: A case for testing tailoring
[DE90-007429] N90-19215
Modified independent modal space control of flexible structures N90-19597
STRUCTURAL WEIGHT
ROCOPT: A user friendly interactive code to optimize rocket structural components N90-19415
Earth-orbiting resonant-mass gravitational wave detectors N90-19954
STUDENTS
Vestibular examination of motion sick student pilots
[IZF-1988-22] N90-19738
SUBDUCTION (GEOLOGY)
Stored mafic/ultramafic crust and early Archean mantle depletion
[NASA-CR-186460] N90-19715
SUBMARINES
Design of a high power density, permanent magnet, axial gap dc motor
[DE90-005449] N90-19514
SUBSONIC FLOW
A study on upstream moving pressure waves induced by vortex separation
[ISL-CO-203/88] N90-19192
Digital determination of the three dimensional flow in turbomachines with the S1-S2 current function process
[ITSM-MITT-30] N90-19236
SUBSTRATES
The III-V semiconductor quantum well lasers and related optoelectronic devices on silicon
[AD-A216980] N90-19570
A method of estimating temperature profiles and chemical differentiation in the near surface layers of porous comet nuclei: First results for comet P/Churyumov-Gerasimenko N90-20013
SUCTION
Method for maintaining precise suction strip porosities
[NASA-CASE-LAR-13638-1] N90-19427
SULFATES
Chemical composition of precipitation and wet/dry deposition of sulfur compounds around the coastal area
[DE89-762324] N90-19677

SULFUR DIOXIDES
Generation of intensive UV laser radiation and utilization in high resolution spectroscopy of SO2
[ETN-90-95361] N90-19581
Estimation of the distribution of SO2 and NOX emission in Europe N90-19699
Ultraviolet observations of the atmosphere of Io and the plasma torus N90-19929

SUN
Some considerations on cohesive forces in sun-grazing comets N90-20015

SUPERCHARGERS
Low cost Brayton engine for gas-fired cogeneration system, phase 1
[PB90-127457] N90-19655

SUPERCOMPUTERS
Dynamic reconfiguration and link fault tolerance in a transputer network
[AD-A215105] N90-19433
Supercomputer applications for materials science: Ordering effects of hydrogen in palladium
[DE90-004664] N90-19870

SUPERCONDUCTING FILMS
Laser mass spectrometric studies of high temperature superconductor ablation
[DE90-006518] N90-19585
Oxygenation and possible etching of high T(sub c) superconducting films by oxygen plasma
[DE90-004956] N90-19871
Characterization of ground state neutral and ion transport during laser ablation of 1:2:3 superconductors by transient optical absorption spectroscopy
[DE90-006623] N90-19878

SUPERCONDUCTIVITY
Superconductivity in Ba(1-x)BiO3
[DE90-003781] N90-19869
BCS (Bardeen-Cooper-Schrieffer) primer: A guide to computational methods in superconductivity theory
[AD-A216393] N90-19874
Critical current density and transition temperature measurements of Y-Ba-Cu-O rods
[AD-A216695] N90-19875
National Action Plan on Superconductivity Research and Development
[PB89-138512] N90-19883
Neutron scattering measurements of the magnetic excitations of high-temperature superconducting materials
[DE90-006567] N90-19885

SUPERCONDUCTORS
Laser surface interactions of high-(Tc) superconductors
[DE90-006894] N90-19587
BCS (Bardeen-Cooper-Schrieffer) primer: A guide to computational methods in superconductivity theory
[AD-A216393] N90-19874
Critical current density and transition temperature measurements of Y-Ba-Cu-O rods
[AD-A216695] N90-19875
On dissipative states in narrow current-carrying superconducting filaments
[ETN-90-95915] N90-19889
FWP executive summaries: Basic energy sciences materials sciences programs
[DE90-006373] N90-19893

SUPERCRITICAL FLUIDS
Thermodynamic properties of supercritical mixtures
[DE90-006720] N90-19909

SUPERFLUIDITY
Bose condensate in superfluid (sup 4)He and momentum distributions by deep inelastic scattering
[DE90-007541] N90-19832
Nucleation of vortices in superfluid helium-4
[DE90-610675] N90-19880
Goldstone excitation and symmetry breaking mechanism in superfluid He-4
[DE90-610676] N90-19881
Coherent state in the roton region of superfluid helium-4
[DE90-610677] N90-19882

SUPERNOVAE
Neon novae, recurrent novae, and type I supernovae
[DE90-003188] N90-19931

SUPERPLASTICITY
Optimizing superplastic response in navalite, a lithium containing aluminum-magnesium alloy
[AD-A216552] N90-19346

SUPERSONIC DRAG
Influence of friction and separation phenomena on the dynamic blade loading of transonic turbine cascades
[MITT-88-04] N90-19235

SUPERSONIC FLIGHT
External flow computations for a finned 60mm ramjet in steady supersonic flight
[AD-A216998] N90-19233

SUPERSONIC FLOW
Interaction of an oblique shock wave with supersonic flow over a blunt body N90-19197

SUPERSONIC JET FLOW
Tomographic investigations of weakly perturbed supersonic free jets
[MPIS-MITT-91] N90-19209

SUPERSONIC SPEED
A study of flows over highly-swept wings designed for maneuver at supersonic speeds
[AD-A216837] N90-19202

SUPERSONIC TURBINES
Influence of friction and separation phenomena on the dynamic blade loading of transonic turbine cascades
[MITT-88-04] N90-19235

SUPERSYMMETRY
Superconformal algebra on meromorphic vector fields with three poles on super-Riemann sphere
[DE90-610423] N90-19796
Construction of four-dimensional open superstrings
[DE90-006484] N90-19908

SURFACE DISTORTION
Reflector surface distortion analysis techniques (thermal distortion analysis of antennas in space) N90-19267

SURFACE LAYERS
Preparation and characterization of alumina films prepared by a novel spray pyrolysis method
[AD-A217570] N90-19339
Radiation-induced density changes and creep in surface layers of glass
[DE90-008112] N90-19383
A method of estimating temperature profiles and chemical differentiation in the near surface layers of porous comet nuclei: First results for comet P/Churyumov-Gerasimenko N90-20013

SURFACE NAVIGATION
Carin and GPS: The combination of dead reckoning, map matching and satellite navigation in a hybrid automobile navigation system
[ETN-90-95451] N90-19220

SURFACE PROPERTIES
Coherent radar measurement of ocean currents from geostationary orbit N90-19259
International conference on Surface Modification of Metals by Ion Beams
[AD-A215872] N90-19345
Modification of surface mechanical properties of high-chromium tool steel by carbon-implanted codeposited Fe-Ti films
[DE90-007502] N90-19358
Light-scattering measurements of CVD (Chemical Vapor Deposition) silicon carbide
[DE90-007885] N90-19382
Single antenna interferometry
[DE90-008120] N90-19474
Three-dimensional Fe analysis of the surface distribution in notched compact samples of 20 MnMoNi 55
[W-1/89] N90-19625
Passivating layer for III-V semiconductor materials
[AD-D014321] N90-19872
Investigations of CuInSe2 thin films and contacts
[DE90-000301] N90-19886
The effects of gradients on boundary stability
[DE90-007428] N90-19894
Petrographic working model of the Rosetta sampling and modelling subgroup for a comet nucleus N90-19992
Laboratory studies of cometary ice analogues N90-19997
Simulation of radar and radiometer signals remote sensing cometary surface and subsurface structures N90-20005
Dynamics of crust formation and dust emission of comet nucleus analogues under isolation N90-20020

SURFACE REACTIONS
Aeolian removal of dust from photovoltaic surfaces on Mars
[NASA-TM-102507] N90-19299
Development of inspection techniques for quantitatively measuring surface contamination on SRM hardware
[NASA-CR-183902] N90-19608

SURFACE ROUGHNESS
Heat transfer measurements from a NACA 0012 airfoil in flight and in the NASA Lewis icing research tunnel
[NASA-CR-4278] N90-19203
Numerical simulation of acoustic scatter from subsurface bubble clouds
[AD-A217068] N90-19822

SURFACE VEHICLES
A human factors testbed for ground-vehicle telerobotics research
[DE90-006618] N90-19746

SURFACE WAVES
Green's functions for a theoretical model of an aperture fed stacked-patch microstrip antenna
[AD-A216280] N90-19455

SURFACES
Theory of gearing
[NASA-RP-1212] N90-19583

SURFACTANTS
An evaluation of ethylene-vinyl acetate copolymers as desensitizers for RDX in insensitive booster compositions prepared by slurry coating technology
[MRL-TR-89-33] N90-19385

SURGES
Lightning surge characteristics of transmission towers. Lightning surge characteristics of 15-meter-high scale model tower
[DE89-782322] N90-19721

SURVEILLANCE RADAR
Experimental measurements in secondary radar field: Conception and first results
[ETN-90-98074] N90-19471

SURVEYS
Survey on the social and economic influences of wide-spreading heat-pump technology
[DE89-782294] N90-19526
Survey on the possibility of introducing new energy to regional development plans
[DE89-782627] N90-19654

SWEPT FORWARD WINGS
X-29A aircraft structural loads flight testing
[NASA-TM-101715] N90-19225

SWEPT WINGS
A study of flows over highly-swept wings designed for maneuver at supersonic speeds
[AD-A216837] N90-19202
Output model-following control synthesis for an oblique-wing aircraft
[NASA-TM-100454] N90-19241

SWITCHES
Fast optical switch and limiter using quantum size effect in metal grain composites
[AD-D014332] N90-19305
Modeling A circuit switched multiprocessor interconnect
[AD-A217122] N90-19519
Dynamics of plasma injection along magnetic field lines in the PBFA 2 (Particle Beam Fusion Accelerator 2) plasma opening switch
[DE90-006751] N90-19862

SWITCHING
Induction motor control
[NASA-TM-102533] N90-19234
Fast optical switch and limiter using quantum size effect in metal grain composites
[AD-D014332] N90-19305
Modeling A circuit switched multiprocessor interconnect
[AD-A217122] N90-19519

SWITCHING CIRCUITS
Power diode switching behavior
[ETN-90-95363] N90-19501

SYMMETRY
Dynamics of a class of vortex rings
[NASA-TM-102257] N90-19524

SYNCHRONISM
Priority arbitration with busses
[AD-A216392] N90-19784

SYNCHRONOUS MOTORS
Induction motor control
[NASA-TM-102533] N90-19234

SYNCHRONOUS PLATFORMS
Earth Science Geostationary Platform Technology
[NASA-CP-3040] N90-19249
Operational requirements and the geostationary platform N90-19250
Science requirements for passive microwave sensors on earth science geostationary platforms N90-19251
Geostationary earth science platform concepts N90-19252
Large space antenna concepts for ESGP N90-19253
Design of a low-frequency (5-20 GHz), 15-meter-diameter passive radiometer for geostationary earth science platforms N90-19255
Structures for remotely deployable precision antennas N90-19256
Coherent radar measurement of ocean currents from geostationary orbit N90-19259
Rain radars for earth science geostationary platforms: Some possibilities N90-19262

SYNOPTIC METEOROLOGY
Colloquium on Synoptic Meteorology
[PB90-121112] N90-19720

SYNTHESIS (CHEMISTRY)
New Condensation polyimides containing 1,1,1-triaryl-2,2,2-trifluoroethane structures
[NASA-CASE-LEW-14346-1] N90-19300
Synthesis and chemistry of unsaturated metal nitrogen compounds
[AD-A216550] N90-19321

FWP executive summaries: Basic energy sciences materials sciences programs
[DE90-006373] N90-19893
Preparation and properties of the system Cu(x)Pd(1-x)O (0 less than or equal to x less than or equal to 0.175)
[AD-A217567] N90-19901

SYNTHETIC APERTURE RADAR
Rosetta/CNSR altimeter and sounding radar N90-20009

SYNTHETIC APERTURES
Science requirements for passive microwave sensors on earth science geostationary platforms N90-19251
Synthetic Aperture Interferometric Radiometer (SAIR) N90-19261

SYSTEM FAILURES
Flight crew aiding for recovery from subsystem failures
[NASA-CR-181905] N90-19741

SYSTEMS ANALYSIS
A linear systems theory approach to the range-independent acoustic channel
[AD-A216551] N90-19817

SYSTEMS ENGINEERING
Augmenting and updating NASA spacelink electronic information system N90-19392
Parkes radio science system design and testing for Voyager Neptune encounter N90-19451
Aspects of VHF radars illustrated by the example of an experimental system
[REPT-1-89] N90-19488
Flight crew aiding for recovery from subsystem failures
[NASA-CR-181905] N90-19741
Generic distributed systems model
[AD-A217078] N90-19773

SYSTEMS INTEGRATION
Highly accurate navigation: Integration of navigation and geodesic methods
[SFB-228] N90-19221
Big Viterbi Decoder (BVD) results for (7,1/2) convolutional code N90-19446

SYSTEMS MANAGEMENT
The global positioning system
[AD-A217266] N90-19222

SYSTOLIC ARRAYS
A virtual zero-time, monolithic systolic sorting array
[DE90-001000] N90-19753

T

TANKS (CONTAINERS)
Tensile behavior of cylindrical pressure tanks in fiber assembling + metal hybrid structure
[ILR-MITT-213] N90-19618

TAPERING
Discontinuous-taper directional coupler
[AD-D014324] N90-19481

TAPES
High density tape casting system
[NASA-CASE-NPO-16901-1-CU] N90-19425

TARGET RECOGNITION
ARGUS/LLNL IR camera calibration and characterization
[AD-A217076] N90-19563
Processing infrared images for target detection: A literature study
[IZF-1988-12] N90-19847

TASKS
An approach to elemental task learning
[DE90-006614] N90-19745

TECHNOLOGY ASSESSMENT
Advanced ceramics
[DE90-608004] N90-19370
High throughput data communication system
[AD-D014342] N90-19432
Assessment of research needs for laser technologies applied to advanced spectroscopic methods
[DE90-007402] N90-19588
Solid State Photovoltaic Research Branch
[DE89-009463] N90-19660
A preliminary analysis of US CO2 emissions reduction potential from energy conservation and the substitution of natural gas for coal in the period to 2010
[DOE/NBB-0085] N90-19673
High speed modem
[AD-D014319] N90-19750
Science and technology report and outlook, 1985-1988
[PB90-115270] N90-19926
First impressions of the comet drilling problem N90-20021

TECHNOLOGY TRANSFER
Report of the First Annual Airborne Weapons Training Technology Review
[DE90-007189] N90-19747

TECHNOLOGY UTILIZATION
Large-diameter geostationary millimeter wavelength antenna concept N90-19254
Arrays for space applications N90-19265
Antennas for 20/30 GHz and beyond N90-19269
Multibody modeling and verification N90-19422
First direct observation of FEL (Free-Electron Laser) from lambda=20 to 45 microns
[DE90-007508] N90-19589
Possible applications of remote sensing in the preparatory phase of a land management project
[BCRS-88-19] N90-19642

TECTONICS
Analysis of tectonic movements utilizing remote sensor products in the Southern Espinhaco (SE) region
[INPE-4830-PRE/1451] N90-19708
P-T condition fo deformation from fluid inclusions in mylonites
[NASA-CR-186377] N90-19710
Development and testing of a universally implementable recording aligning system
[SER-C-349] N90-19716

TELECOMMUNICATION
High throughput data communication system
[AD-D014342] N90-19432

TELEMETRY
PC-based PCM (Pulse Code Modulation) telemetry data reduction system hardware
[DE90-000316] N90-19273
Kalman estimation for SEDS measurements N90-19383

TELEOPERATORS
Design and implementation of a flexible robot
[AD-A216453] N90-19601
Extending terrestrial mobile robotics to a proposed lunar base
[DE89-016179] N90-19606

TELEVISION RECEPTION
General multidimensional scanning ratio transformation and its utilization for norm transformation of television signals
[ETN-90-96058] N90-19470

TEMPERATURE COMPENSATION
Temperature compensated crystal oscillator (TCXO) with improved temperature compensation
[AD-D014334] N90-19482

TEMPERATURE CONTROL
Temperature compensated crystal oscillator (TCXO) with improved temperature compensation
[AD-D014334] N90-19482
Development of the blackbody probe type pyrometer, part 1. Experimental study on the fundamental characteristics
[DE89-782288] N90-19553

TEMPERATURE DEPENDENCE
A simple model for the determination of L(sub 0), D and tau in a semiconductor and their temperature dependence
[DE90-610564] N90-19879

TEMPERATURE DISTRIBUTION
Heat transfer definitions and equations
[ESDU-89022] N90-19522
Information on the use of data items on hot structures
[ESDU-89021] N90-19611
An analytic model of axisymmetric mantle plume due to thermal and chemical diffusion
[NASA-CR-186461] N90-19714
Temperatures in plates subjected to a sudden increase in recovery temperature
[ESDU-89026] N90-19904
Thermal perturbation of comet samples during their acquisition N90-20008

TEMPERATURE EFFECTS
Effect of temperature on the storage life of polysulfide aircraft sealants
[MRL-TR-89-31] N90-19364
Alternate film dielectric materials
[DE90-007213] N90-19378
A parametric heat transfer study for cryogenic ball bearings in SSME HPOTP N90-19397
Thermal coefficient of delay for various coaxial and fiber-optic cables N90-19439
Experimental results of aging and thermal effects in high-power laser diodes
[DE90-005955] N90-19573
Ion mixing and surface modification in metal-semiconductor systems
[DE90-007557] N90-19897
Physical processes in cometary ices inferred from laboratory studies N90-19996
Laboratory studies of cometary ice analogues N90-19997
Thermal perturbation of comet samples during their acquisition N90-20008

TEMPERATURE GRADIENTS
Carbon black/polyethylene composites for PTC (Positive Temperature Coefficient) thermistor applications
[AD-A215988] N90-19307
Heat transfer definitions and equations
[ESDU-89022] N90-19522
A method of estimating temperature profiles and chemical differentiation in the near surface layers of porous comet nuclei: First results for comet P/Churyumov-Gerasimenko N90-20013

TEMPERATURE MEASUREMENT
Utilization of thermometric methods for the testing of carbon reinforced plastics
[ETN-90-96076] N90-19314
Drifting buoy data from Western Tropical Pacific for the period February 1, 1986 through February 28, 1989
[PB90-113978] N90-19732
Critical current density and transition temperature measurements of Y-Ba-Cu-O rods
[AD-A216695] N90-19875

TEMPERING
Austempered ductile iron data base: A cooperative program between industry and the Trade Adjustment Assistance Program of the Department of Commerce
[PB90-115569] N90-19343

TEMPORAL RESOLUTION
Time resolved gain/loss studies under low and high power loading for the XeF C-A transition
[DE90-007506] N90-19517

TENSILE CREEP
Creep behavior of alloys based on TiAl containing TiB2 and TiN particulates
[DE90-006489] N90-19355
Deformation and fracture of TiAl + W at elevated temperatures
[DE90-006490] N90-19356
Time-dependent failure of silver-interlayer diffusion bonds between non-deforming base-metals
[DE90-006925] N90-19357

TENSILE DEFORMATION
Deformation and fracture of TiAl + W at elevated temperatures
[DE90-006490] N90-19356
Time-dependent failure of silver-interlayer diffusion bonds between non-deforming base-metals
[DE90-006925] N90-19357

TENSILE STRENGTH
Fluorinated graphite fibers as a new engineering material: Promises and challenges
[NASA-TM-102511] N90-19301
Heat treatment study of the SiC/Ti-15-3 composite system
[NASA-TP-2970] N90-19302
Evaluation of repeated impact damage in composite structures N90-19303
Time-dependent failure of silver-interlayer diffusion bonds between non-deforming base-metals
[DE90-006925] N90-19357
Tensile behavior of cylindrical pressure tanks in fiber assembling + metal hybrid structure
[ILR-MITT-213] N90-19618
Some considerations on cohesive forces in sun-grazing comets N90-20015

TENSILE STRESS
Practical calculation of the liveload of carbon fiber reinforced plastics by the finite element method
[ETN-90-95867] N90-19311

TENSORS
A tensor product B-spline method for numerical grid generation
[DE90-005979] N90-19792

TERMINAL BALLISTICS
Jam resistant fluid power actuator for ballistic-damage tolerant redundant cylinder assemblies
[AD-D014360] N90-19600

TERMS
CRISP (Computer Retrieval of Information on Scientific Projects) thesauras, fiscal year 1990
[PB90-138652] N90-19922

TERRAIN
Heli/SITAN: A terrain referenced navigation algorithm for helicopters
[DE90-005193] N90-19217
A method for determination of control pixels for LANSAT using a reflector
[INPE-4884-PRE/1491] N90-19632
Visibility problems in numerical models of terrain
[INPE-4921-TDL/382] N90-19919

TERRESTRIAL PLANETS
Large impact events and atmospheric evolution on the terrestrial planets N90-20028

TEST FACILITIES
The Uniform Engine Test Programme
[AGARD-AR-248] N90-19232
Marshall Avionics Testbed System (MAST) N90-19417

Sandia National Laboratories' new high level acoustic test facility
[DE90-006810] N90-19820
Relevance of laboratory studies to comets N90-20023

TETHERED SATELLITES
Kalman estimation for SEDS measurements N90-19393
A vectorized algorithm for 3D dynamics of a tethered satellite N90-19423

TETHERING
Kalman estimation for SEDS measurements N90-19393

TEXTILES
Calculation of nonlinear viscoelastic processes for plastic layer textile membranes
[ETN-90-95868] N90-19622

TEXTURES
Visual processing in texture segregation
[AD-A216539] N90-19737

THEMATIC MAPPERS (LANDSAT)
The potential of combined use of satellite data with topographic TM information for manual/visual and digital updating of land use
[NLR-MP-88021-U] N90-19639

THEMATIC MAPPING
Areas of aquatic macrophytes classified through vegetative indexes extracted from LANDSAT/TM imagery
[INPE-4880-PRE/1489] N90-19633
Thematic coupling between digital images and geographic information systems
[ETN-90-95723] N90-19648

THEOREM PROVING
Panconnectivity of locally connected K(1,3)-free graphs
[AD-A216548] N90-19786

THEORETICAL PHYSICS
Research accomplishments and future goals in particle physics
[DE90-007296] N90-19830
Experimental and theoretical high energy physics
[DE90-005974] N90-19834

THERMAL ANALYSIS
Reflector surface distortion analysis techniques (thermal distortion analysis of antennas in space) N90-19267

THERMAL BLOOMING
Narrow-bandwidth unstable laser resonator
[AD-D014362] N90-19568
Linear theory of thermal blooming in turbulence
[DE90-007243] N90-19579
Turbulent mixing effects in models of thermal blooming
[DE90-007245] N90-19580
Atmospheric thermal blooming and beam clearing by aerosol vaporization
[DE90-006271] N90-19711

THERMAL CONDUCTIVITY
Hot filament technique for measuring the thermal conductivity of molten lithium fluoride
[NASA-TM-102506] N90-19373
Heat transfer definitions and equations
[ESDU-89022] N90-19522
Experiments of thermoconvection in a cubic cell
[MPIS-6/1989] N90-19544
Thermal conductivities and diffusivities of porous ice samples at low pressures and temperatures and possible modes of heat transfer in near surface layers of comets N90-19999

THERMAL CYCLING TESTS
Evaluation of thermal cycling creep-fatigue damage for a molten salt receiver
[DE90-002907] N90-19670

THERMAL DEGRADATION
Experimental results of aging and thermal effects in high-power laser diodes
[DE90-005955] N90-19573

THERMAL DIFFUSION
Numerical study of diffusion jet flames N90-19316
An analytic model of axisymmetric mantle plume due to thermal and chemical diffusion
[NASA-CR-186461] N90-19714

THERMAL DIFFUSIVITY
Heat transfer definitions and equations
[ESDU-89022] N90-19522
Thermal conductivities and diffusivities of porous ice samples at low pressures and temperatures and possible modes of heat transfer in near surface layers of comets N90-19999

THERMAL ENERGY
Ion and electron interactions at thermal and suprathermal energies
[AD-A216905] N90-19323
Direct absorption receiver
[DE90-000311] N90-19667
An analytic model of axisymmetric mantle plume due to thermal and chemical diffusion
[NASA-CR-186461] N90-19714

THERMAL EXPANSION
Fluorinated graphite fibers as a new engineering material: Promises and challenges
[NASA-TM-102511] N90-19301
Crystallization behavior and properties of BaO-Al2O3-2SiO2 glass matrices
[NASA-CR-185209] N90-19374

THERMAL FATIGUE
An attempt of improving high-temperature fatigue properties of Ni-Cr-W superalloys in HTGR helium
[DE90-741482] N90-19350

THERMAL INSULATION
Information on the use of data items on hot structures
[ESDU-89021] N90-19611
Temperatures in plates subjected to a sudden increase in recovery temperature
[ESDU-89026] N90-19904

THERMAL MAPPING
ARGUS/LLNL IR camera calibration and characterization
[AD-A217076] N90-19563

THERMAL NOISE
Advanced Doppler tracking experiments N90-19951

THERMAL PLASMAS
The 41st Annual Gaseous Electronics Conference
[AD-A214540] N90-19851

THERMAL RESISTANCE
Steady state temperatures and thermal stresses in a spherical or cylindrical laminated shell
[ESDU-89027] N90-19612

THERMAL STABILITY
Thermo-oxidative stability studies of PMR-15 polymer matrix composites reinforced with various fibers
[NASA-TM-102439] N90-19310
An evaluation of ethylene-vinyl acetate copolymers as desensitizers for RDX in insensitive booster compositions prepared by slurry coating technology
[MRL-TR-89-33] N90-19385
Stable isotope studies of cometary analogue materials N90-20001

THERMAL STRESSES
Steady state temperatures and thermal stresses in a spherical or cylindrical laminated shell
[ESDU-89027] N90-19612

THERMIONIC DIODES
Impedance characteristics of terawatt ion diodes
[DE90-006276] N90-19494

THERMISTORS
Carbon black/polyethylene composites for PTC (Positive Temperature Coefficient) thermistor applications
[AD-A215988] N90-19307

THERMOCHROMATIC MATERIALS
CO2 depth profiles in cometary model substances of KOSI N90-20014

THERMODYNAMIC CYCLES
Mechano-caloric cooling device
[NASA-CR-186316] N90-19552

THERMODYNAMIC EQUILIBRIUM
Vapor-liquid equilibria for complex mixtures with special emphasis on the critical region
[PB90-130345] N90-19324
Longitudinal traveling waves bifurcating from Vlasov plasma equilibria N90-19850

THERMODYNAMIC PROPERTIES
A transient plasticity study and low cycle fatigue analysis of the Space Station Freedom photovoltaic solar array blanket
[NASA-TM-102516] N90-19617
An observational study of squall lines in the Amazon
[INPE-4865-TDL/376] N90-19723
Thermal modulation of light beams
[AD-D014322] N90-19840
Thermodynamic properties of supercritical mixtures
[DE90-006720] N90-19909

THERMODYNAMICS
Demonstration of capabilities of high temperature composites analyzer code HITCAN
[NASA-TM-102560] N90-19629
Linear free energy relations for multielectron transfer kinetics: A brief look at the Bronsted/Tafel analogy
[AD-A215078] N90-19823
Thermal infrared scene simulation
[DE90-006900] N90-19845
Theory of field reversed configurations
[DE90-006702] N90-19860
The renormalization group and lattice QCD
[DE90-004860] N90-19905

THERMOELECTRIC GENERATORS
Safety Status Report for the Ulysses mission. Book 1: Risk analysis. General purpose heat source radioisotope thermoelectric generator program
[DE90-006826] N90-19282
Safety status report for the Ulysses mission. Book 2: Risk analysis. General purpose heat source radioisotope thermoelectric generator program
[DE90-006827] N90-19283
Safety Status Report for the Ulysses mission: Summary. General purpose heat source radioisotope thermoelectric generator program
[DE90-006828] N90-19284

THERMOELECTRICITY
Annealing group III-V compound doped silicon-germanium alloy for improved thermo-electric conversion efficiency
[NASA-CASE-NPO-17259-1-CU] N90-19884

THERMONUCLEAR REACTIONS
Neon novae, recurrent novae, and type I supernovae
[DE90-003188] N90-19931

THESAURI
CRISP (Computer Retrieval of Information on Scientific Projects) thesauras, fiscal year 1990
[PB90-138652] N90-19922

THICK PLATES
Information on the use of data items on hot structures
[ESDU-89021] N90-19611
Temperatures in plates subjected to a sudden increase in recovery temperature
[ESDU-89026] N90-19904

THIN FILMS
Preparation and characterization of alumina films prepared by a novel spray pyrolysis method
[AD-A217570] N90-19339
Nanolayer reactions in aluminum-metal interfaces
[DE90-004955] N90-19342
Glancing angle XAFS (X ray Absorption Fine Structure) and x ray reflectivity studies of transition-metal/aluminum interfaces
[DE90-005575] N90-19353
Transmission and reflection studies of thin films in the vacuum ultraviolet N90-19412
High density tape casting system
[NASA-CASE-NPO-16901-1-CU] N90-19425
Numerical and experimental analysis of a thin liquid film on a rotating disk related to development of a spacecraft absorption cooling system
[NASA-CR-183457] N90-19523
Laser mass spectrometric studies of high temperature superconductor ablation
[DE90-006518] N90-19585
Heteroepitaxial growth of germanium films by supersonic free jet chemical beam epitaxy
[DE90-006621] N90-19677
Characterization of ground state neutral and ion transport during laser ablation of 1:2:3 superconductors by transient optical absorption spectroscopy
[DE90-006623] N90-19678
Investigations of CuInSe2 thin films and contacts
[DE90-000301] N90-19886
Growth and characterization of gallium (III) oxide films
[AD-A217568] N90-19902

THORIUM COMPOUNDS
Dynamics of plasma injection along magnetic field lines in the PBFA 2 (Particle Beam Fusion Accelerator 2) plasma opening switch
[DE90-006751] N90-19862

THREE AXIS STABILIZATION
Operational requirements and the geostationary platform N90-19250
Determination of the implementation of the 3-axis attitude motion simulator digital position controller N90-19409

THREE DIMENSIONAL FLOW
Three-dimensional viscous rotor flow calculations using a viscous-inviscid interaction approach
[NASA-TM-102235] N90-19204
Tomographic investigations of weakly perturbed supersonic free jets
[MPIS-MITT-91] N90-19209
Digital determination of the three dimensional flow in turbomachines with the S1-S2 current function process
[ITSM-MITT-30] N90-19236

THREE DIMENSIONAL MOTION
A vectorized algorithm for 3D dynamics of a tethered satellite N90-19423

THRESHOLD CURRENTS
Low threshold current implanted-planar-buried-heterostructure, graded-index, separate-confinement-heterostructure GaAs-AiGaAs laser
[DE90-002579] N90-19572

THRUST CONTROL
Performance of an optimized rotor blade at off-design flight conditions
[NASA-CR-4288] N90-19226

THRUST VECTOR CONTROL
Static investigation of a two-dimensional convergent-divergent exhaust nozzle with multiaxis thrust-vectoring capability
[NASA-TP-2973] N90-19193
Internal performance of two nozzles utilizing gimbal concepts for thrust vectoring
[NASA-TP-2991] N90-19200
THUNDERSTORMS
Characterization of thunderstorm induced Maxwell current densities in the middle atmosphere N90-19391
TIDES
Status of a nonlinear water surge model in February 1988
[KNMI-WR-88-03] N90-19735
TIME
Pulsar timing and gravitational waves N90-19955
TIME DEPENDENCE
Time-dependent failure of silver-interlayer diffusion bonds between non-deforming base-metals
[DE90-006925] N90-19357
Simulation of global Kr-85 and (14)CO2 distribution by means of a time-dependent, two dimensional model of the atmosphere
[ETN-90-95376] N90-19702
TIME FUNCTIONS
Series reversion/inversion of Lambert's time function
[AD-A216243] N90-19245
TIME MEASUREMENT
Thermal coefficient of delay for various coaxial and fiber-optic cables N90-19439
X ray timing observations and gravitational physics N90-19956
A review of atomic clock technology, the performance capability of present spaceborne and terrestrial atomic clocks, and a look toward the future N90-19972
TIME OF FLIGHT SPECTROMETERS
Nuclear interactions of high energy heavy ions and applications in astrophysics
[DE90-006691] N90-19984
TITANATES
Heat treatment study of the SiC/Ti-15-3 composite system
[NASA-TP-2970] N90-19302
TITANIUM ALLOYS
Ac loss measurements of two multifilamentary NbTi composite strands
[DE90-005388] N90-19304
Deformation and fracture of TiAl + W at elevated temperatures
[DE90-006490] N90-19356
TITANIUM COMPOUNDS
Creep behavior of alloys based on TiAl containing TiB2 and TiN particulates
[DE90-006489] N90-19355
TITANIUM OXIDES
Studies of photochemically and electrochemically driven electron transport in zeolites
[DE90-007659] N90-19335
Hydrous metal oxide-supported catalysts. Part 2: Catalytic properties and applications
[DE90-008098] N90-19336
Diffraction studies of the structure of glasses and liquids
[DE90-007662] N90-19361
Zirconia-based electrodes for solid oxide fuel cells
[DE90-000462] N90-19513
TOKAMAK DEVICES
On 140 GHz microwave FEL experiments using ELF-2
[DE90-006784] N90-19576
FOMA: A Fast Optical Multichannel Analyzer
[DE90-004093] N90-19839
TOLERANCES (MECHANICS)
Static strength and damage tolerance tests on the Fokker 100 airframe
[NLR-MP-88023-U] N90-19228
TOLERANCES (PHYSIOLOGY)
The pollution hazard assessment system: Documentation and users manual
[AD-A217108] N90-19706
Metabolism, seizures, and blood flow in brain following organophosphate exposure: Mechanisms of action and possible therapeutic agents
[AD-A217098] N90-19740
TOMOGRAPHY
Tomographic investigations of weakly perturbed supersonic free jets
[MPIS-MITT-91] N90-19209
TOPOGRAPHY
Applications of FM-CW laser radar to antenna contour mapping N90-19270
Analysis of photogeologic lineaments in the Ithacare (BA) region: A proposed methodology
[INPE-4855-PRE/1478] N90-19635
The potential of combined use of satellite data with topographic TM information for manual/visual and digital updating of land use
[NLR-MP-88021-U] N90-19639
Evolution of midplate hotspot swells: Numerical solutions
[NASA-CR-186462] N90-19713
Digital production of perspective images
[SER-C-347] N90-19768
TOPOLOGY
On the approximative normal values of multivalued operators in topological vector space
[DE90-610430] N90-19800
Linearized analysis of (2+1)-dimensional Einstein-Maxwell theory
[DE90-741470] N90-19913
TOROIDAL PLASMAS
Overview of recent results from the Advanced Toroidal Facility
[DE90-005673] N90-19853
Anomalous transport in toroidal plasmas
[DE90-006549] N90-19859
Ultraviolet observations of the atmosphere of Io and the plasma torus N90-19929
TORQUE
Disturbance torque rejection properties of the NASA/JPL 70-meter antenna axis servos N90-19450
TORSION
Positioning control of highest accuracy for very dynamic coupled system
[ETN-90-95893] N90-19769
TOXICITY
Study of hydrazine metabolism and toxicity
[AD-A217103] N90-19736
TRACE ELEMENTS
Geochemical survey on faults overland with alluvial deposits, part 1. Application for the Neodani and the Atera faults survey
[DE89-782326] N90-19707
TRACKING (POSITION)
The Telecommunications and Data Acquisition Report
[NASA-CR-185033] N90-19434
Performance of the all-digital data-transition tracking loop in the advanced receiver N90-19440
An investigation of the transfer of monopulse tracking between two coherent point sources
[AD-A217007] N90-19457
TRACKING FILTERS
Suboptimal period design for a maneuvering missile to evade tracking filters N90-19479
TRACKING PROBLEM
Investigations into a new algorithm for calculating H infinity optimal controllers N90-19406
TRACTION
The measurement, modeling, and prediction of traction for rocket propellant 1
[NASA-CR-185186] N90-19386
TRADEOFFS
Applications of FM-CW laser radar to antenna contour mapping N90-19270
TRAILING EDGES
Calculation of excrescence drag magnification due to pressure gradient at high subsonic speeds
[ESDU-87004] N90-19195
TRAINING ANALYSIS
Symposium on air traffic control training for tomorrow's technology
[PB90-127325] N90-19216
Laser Technology Center
[PB90-115387] N90-19564
Pilot candidate selection
[AD-A217296] N90-19742
TRAINING EVALUATION
Report of the First Annual Airborne Weapons Training Technology Review
[DE90-007189] N90-19747
TRAJECTORIES
The EGS4 Code System: Solution of gamma-ray and electron transport problems
[DE90-008100] N90-19838
TRAJECTORY OPTIMIZATION
Rapid near-optimal trajectory generation and guidance law development for single-stage-to-orbit airbreathing vehicles
[NASA-CR-186299] N90-19275
Icarus lander N90-19964
TRANSFER FUNCTIONS
Some easily analyzable convolutional codes N90-19444
TRANSFER ORBITS
Series reversion/inversion of Lambert's time function
[AD-A216243] N90-19245
TRANSFERRING
An investigation of the transfer of monopulse tracking between two coherent point sources
[AD-A217007] N90-19457
TRANSFORMATIONS (MATHEMATICS)
Optimal layout via Boolean satisfiability
[AD-A216777] N90-19787
TRANSIENT OSCILLATIONS
A contribution to the theory of transient conductor simulations
[ETN-90-95891] N90-19511
TRANSIENT RESPONSE
Computational aspects of sensitivity calculations in linear transient structural analysis
[NASA-TM-4156] N90-19610
TRANSISTOR CIRCUITS
Planar integrated circuits for microwave transmission and reception
[AD-A217676] N90-19520
TRANSISTORS
Utilization criteria for transistors of diverse technology in pulse inverters with high switching frequency
[ETN-90-95359] N90-19500
TRANSIT TIME
Transient photoconduction in doped polymers: Spatial and energetic disorder
[ETN-90-95917] N90-19376
TRANSITION METALS
Conductive polymers of transition-metal complexes coordinated by a Diamino-Dichalcogen-Benzene compound
[AD-D014326] N90-19360
TRANSMISSION
Conjugate field approaches for active array compensation N90-19266
TRANSMISSION LINES
A contribution to the theory of transient conductor simulations
[ETN-90-95891] N90-19511
Lightning surge characteristics of transmission towers. Lightning surge characteristics of 15-meter-high scale model tower
[DE89-782322] N90-19721
All-fiber SFPM (Stimulated Four Photon Mixing) amplifier
[AD-D014358] N90-19841
TRANSMISSIVITY
A new method for measuring the transmissivity of aircraft transparencies
[AD-A216953] N90-19842
TRANSMITTER RECEIVERS
Planar integrated circuits for microwave transmission and reception
[AD-A217676] N90-19520
TRANSONIC FLOW
Calibration of the sonic measuring and control cross section in the gas feed installation of the solid fuel combustion chamber
[LR-552] N90-19548
TRANSPARENCE
A new method for measuring the transmissivity of aircraft transparencies
[AD-A216953] N90-19842
TRANSPIRATION
The utilization of an infrared imaging system as a cooling slot blockage detector in the inspection of a transpiration cooled nozzle
[NASA-TM-102608] N90-19555
TRANSPONDERS
Radar transponder antenna pattern analysis for the space shuttle N90-19414
TRANSPORT PROPERTIES
The EGS4 Code System: Solution of gamma-ray and electron transport problems
[DE90-008100] N90-19838
Characterization of ground state neutral and ion transport during laser ablation of 1:2:3 superconductors by transient optical absorption spectroscopy
[DE90-006623] N90-19878
TRANSPORT THEORY
Anomalous transport in toroidal plasmas
[DE90-006549] N90-19859
TRANSPORTATION
Analysis of alternative concepts for transport systems on the Moon surface
[ETN-90-95727] N90-19605
TRANSPUTERS
Dynamic reconfiguration and link fault tolerance in a transputer network
[AD-A215105] N90-19433
Parallel neural net path-planner on hypercube and transputer
[DE90-006324] N90-19777
TRANSVERSE WAVES
Elastic properties of silica xerogels
[AD-A216528] N90-19366
TRAPPING
Laser surface interactions of high-(Tc) superconductors
[DE90-006894] N90-19587

TRAVELING WAVES
Longitudinal traveling waves bifurcating from Vlasov plasma equilibria N90-19850
TREND ANALYSIS
Methods for trend analysis: Examples with problem/failure data N90-19396
TRENDS
Heat sink effects on weld bead: VPPA process N90-19418
Survey on the social and economic influences of wide-spreading heat-pump technology [DE89-782294] N90-19526
Analysis of photogeologic lineaments in the Ithacare (BA) region: A proposed methodology [INPE-4855-PRE/1478] N90-19635
TRIGGER CIRCUITS
CCST (Center for Compound Semiconductor Technology) research briefs [DE90-006446] N90-19887
TRITIUM
Investigation of a simulated tritium plasma using Coherent Anti-Stokes Raman Spectroscopy (CARS) [DE90-005696] N90-19319
TROPICAL REGIONS
Drifting buoy data from Western Tropical Pacific for the period February 1, 1986 through February 28, 1989 [PB90-113978] N90-19732
TROPOSPHERE
Development and status of the EURAD project N90-19681
The Chemical Transfer Model (CTM) of EURAD: Development status N90-19683
The EURAD model in EUROTRAC N90-19701
TROPOSPHERIC RADIATION
Tropospheric monitoring technology for gravity wave experiments N90-19971
TUNGSTEN ALLOYS
Deformation and fracture of TiAl + W at elevated temperatures [DE90-006490] N90-19356
TURBINE BLADES
Influence of friction and separation phenomena on the dynamic blade loading of transonic turbine cascades [MITT-88-04] N90-19235
The influence of a wall function on turbine blade heat transfer prediction N90-19421
TURBINE PUMPS
A parametric heat transfer study for cryogenic ball bearings in SSME HPOTP N90-19397
Investigation of SSME alternate high pressure fuel turbopump lift-off seal fluid and structural dynamic interaction N90-19400
TURBOCOMPRESSORS
Low cost Brayton engine for gas-fired cogeneration system, phase 1 [PB90-127457] N90-19655
TURBOPROP AIRCRAFT
Low-speed wind-tunnel investigation of the flight dynamic characteristics of an advanced turboprop business/commuter aircraft configuration [NASA-TP-2982] N90-19239
TURBULENCE
Carrier wing profile in nonstationary current [ETN-90-95368] N90-19208
Overview of recent results from the Advanced Toroidal Facility [DE90-005673] N90-19853
TURBULENCE EFFECTS
Effects of turbulence mixing, variable properties, and vaporization on spray droplet combustion [NASA-CR-186463] N90-19326
Separation bubbles at high Reynolds number: Measurement and computation [CUED/A-AERO/15] N90-19525
TURBULENCE MODELS
Numerical solution of 3D Navier-Stokes equations with upwind implicit schemes [NASA-TM-101656] N90-19205
The influence of a wall function on turbine blade heat transfer prediction N90-19421
Application of a Reynolds stress turbulence model to the compressible shear layer [NASA-CR-182002] N90-19537
TURBULENT BOUNDARY LAYER
Study of the turbulent boundary layer on an afterbody [TM-EA-8901] N90-19212
Swept shock/boundary layer interaction experiments in support of CFD code validation [NASA-CR-186397] N90-19535
Wind tunnel design of heat island turbulent boundary layer [IHW-ET/50] N90-19542
Experimental examination of the development behavior of a gaseous body in a steady state and neutral layer turbulent sheet boundary layer with ground asperity [ETN-90-96067] N90-19549
TURBULENT FLOW
Separation bubbles at high Reynolds number: Measurement and computation [CUED/A-AERO/15] N90-19525
Theoretical and experimental examination of the beginning of turbulence in a heated laminar conduit flow [ETN-90-95369] N90-19541
A review of models for the analysis of the injection of densely loaded flows into entrained flow gasifiers [DE90-000453] N90-19550
Linear theory of thermal blooming in turbulence [DE90-007243] N90-19579
TURBULENT HEAT TRANSFER
Analysis of unsteady heat transfer by natural convection in a two-dimensional square cavity using a high order finite-volume method N90-19521
Turbulent mixing effects in models of thermal blooming [DE90-007245] N90-19580
TURBULENT MIXING
Turbulent mixing effects in models of thermal blooming [DE90-007245] N90-19580
TWO BODY PROBLEM
Series reversion/inversion of Lambert's time function [AD-A216243] N90-19245
TWO DIMENSIONAL MODELS
Heat sink effects on weld bead: VPPA process N90-19418
Reparametrization BRS cohomology in two-dimensional gravity and non-critical string theories [DE90-741468] N90-19911
TWO PHASE FLOW
Study of interfacial behavior in cocurrent gas-liquid flows [DE90-005988] N90-19532
Experimental and analytical investigation of adiabatic critical water air two phase flow in small diameter tubes [TB-88/1] N90-19540

U

ULTRASONIC WAVE TRANSDUCERS
Foundations of millimeter-wave frequency acoustic microscopy N90-19816
ULTRASONICS
Improved processes for ultrasonic object recognition in robotics [ETN-90-95362] N90-19604
ULTRAVIOLET ASTRONOMY
Ultraviolet observations of the atmosphere of Io and the plasma torus N90-19929
ULTRAVIOLET LASERS
Generation of intensive UV laser radiation and utilization in high resolution spectroscopy of SO2 [ETN-90-95361] N90-19581
ULTRAVIOLET RADIATION
Enhancement of processes for solar photocatalytic detoxification of water [DE90-003949] N90-19330
Search for far infrared radiation from optically pumped defect modes [AD-A216976] N90-19843
ULTRAVIOLET SPECTRA
Ultraviolet observations of the atmosphere of Io and the plasma torus N90-19929
Nearly simultaneous optical, ultraviolet, and x ray observations of three PG quasars [NASA-CR-186355] N90-19932
ULTRAVIOLET SPECTROSCOPY
Far-ultraviolet spectroscopy of Comet Halley N90-19979
ULYSSES MISSION
Safety Status Report for the Ulysses mission. Book 1: Risk analysis. General purpose heat source radiosotope thermoelectric generator program [DE90-006826] N90-19282
Safety status report for the Ulysses mission. Book 2: Risk analysis. General purpose heat source radiosotope thermoelectric generator program [DE90-006827] N90-19283
Safety Status Report for the Ulysses mission: Summary. General purpose heat source radiosotope thermoelectric generator program [DE90-006828] N90-19284
Safety Status Report for the Ulysses mission. Book 1: Accident analysis. General purpose heat source radiosotope thermoelectric generator program [DE90-006829] N90-19285
Safety Status Report for the Ulysses mission. Book 2: Accident analysis-appendices. General purpose heat source radioisotope thermoelectric generator program [DE90-006830] N90-19286
UNDERWATER OPTICS
All-fiber SFPM (Stimulated Four Photon Mixing) amplifier [AD-D014358] N90-19641
UNIQUENESS
Uniqueness of closure of the constraint algebra for quantum gravity [DE90-610476] N90-19712
UNITED STATES
Advancing automation and robotics technology for the Space Station Freedom and for the US economy: Submitted to the United States Congress [NASA-TM-101647] N90-19279
UNIVERSE
Dimensional transition of the universe [DE90-741461] N90-19910
Cosmic string in compactified gauge theory [DE90-741463] N90-19988
UNIVERSITIES
Research Reports: 1989 NASA/ASEE Summer Faculty Fellowship Program [NASA-CR-183837] N90-19390
UNSTEADY AERODYNAMICS
Unsteady aerodynamics of delta wings performing maneuvers to high angle of attack N90-19196
Conical Euler solution for a highly-swept delta wing undergoing wing-rock motion [NASA-TM-102609] N90-19211
Aeroservoelasticity [NASA-TM-102620] N90-19227
UNSTEADY FLOW
Computation of hypersonic unsteady viscous flow over a cylinder N90-19194
UPLINKING
Experimental measurements in secondary radar field: Conception and first results [ETN-90-96074] N90-19471
USER MANUALS (COMPUTER PROGRAMS)
The pollution hazard assessment system: Documentation and users manual [AD-A217108] N90-19706
USER REQUIREMENTS
The global positioning system [AD-A217266] N90-19222
National Technical Information Service 1989 Users Conference proceedings [PB90-142563] N90-19921

V

VACUUM
Quantum yield of photocathodes in far and extreme ultraviolet wavelength area [ETN-90-95731] N90-19505
Plasma centrifuge with vacuum arc discharge applied to the separation of stable isotopes [INPE-4925-TDL/385] N90-19854
VALVES
Construction and characterization of a valve for rapid gas injection [INPE-4789-RPE/583] N90-19486
Monostable electrovalve [INPE-4928-RPE/595] N90-19487
VAPOR DEPOSITION
Preparation and characterization of alumina films prepared by a novel spray pyrolysis method [AD-A217570] N90-19339
Microstructural characterization of multiphase coatings produced by chemical vapor deposition [DE90-007573] N90-19379
Light-scattering measurements of CVD (Chemical Vapor Deposition) silicon carbide [DE90-007885] N90-19382
Comparison of a 6-layer and a 15-layer version of the Chemical Transfer Model (CTM) N90-19689
Control of the RADM chemistry mechanism of the gas phase N90-19690
FWP executive summaries: Basic energy sciences materials sciences programs [DE90-006373] N90-19883
VAPOR PHASES
Control of the RADM chemistry mechanism of the gas phase N90-19690
VAPORIZING
Simulation of thermal dynamics of a vaporizing coal-water droplet in a combustor [DE90-005356] N90-19317
Effects of turbulence mixing, variable properties, and vaporization on spray droplet combustion [NASA-CR-186463] N90-19326
Atmospheric thermal blooming and beam clearing by aerosol vaporization [DE90-006271] N90-19711

VAPORS
Laser-matter interaction at intensities of 10(sup 12) W/cm(sup 2) and below
[DE90-007536] N90-19590
VARIATIONAL PRINCIPLES
Finite element approximations of the stokes flow problem based upon various variational principles
[DE90-608612] N90-19533
The p- and h-p versions of the finite element method: An overview
[AD-A216902] N90-19789
VARIATIONS
Finite element analysis of a quartz rotation sensor
[DE90-006959] N90-19562
VECTOR SPACES
On the approximative normal values of multivalued operators in topological vector space
[DE90-610430] N90-19800
Classical mechanics on superspace
[DE90-608907] N90-19906
VECTORS (MATHEMATICS)
A vectorized algorithm for 3D dynamics of a tethered satellite N90-19423
Vector circuit theory for multilayered isotropic and chiral structures: Reflection and transmission
[PB90-122474] N90-19495
VEGETATION
Definition study of Laser Experimental Active Fluorsensor (LEAF)
[BCRS-88-18] N90-19582
Proceedings of the 2nd United States/USSR Symposium on Air Pollution Effects on Vegetation Including Forest Ecosystems
[PB90-127119] N90-19678
Visibility problems in numerical models of terrain
[INPE-4921-TDL/382] N90-19919
VEGETATIVE INDEX
Areas of aquatic macrophytes classified through vegetative indexes extracted from LANDSAT/TM imagery
[INPE-4880-PRE/1489] N90-19633
VELOCITY DISTRIBUTION
Study of the turbulent boundary layer on an afterbody
[TM-EA-8901] N90-19212
Analysis of unsteady heat transfer by natural convection in a two-dimensional square cavity using a high order finite-volume method N90-19521
VELOCITY MEASUREMENT
An optical white light speckle process in forward dispersion for measurement of the velocity field in free convective currents
[ETN-90-95913] N90-19546
VENUS ATMOSPHERE
Large impact events and atmospheric evolution on the terrestrial planets N90-20028
VERTICAL AIR CURRENTS
Spanwise measurements of vertical components of atmospheric turbulence
[NASA-TP-2963] N90-19718
VERTICAL ORIENTATION
Techniques for studying the effects of microgravity on model particle/cell systems N90-19424
VERY HIGH FREQUENCIES
Aspects of VHF radars illustrated by the example of an experimental system
[REPT-1-89] N90-19468
VERY LARGE SCALE INTEGRATION
Parallel distributed networks for image smoothing and segmentation in analog VSLI
[AD-A216780] N90-19491
VLSI implementation of moment invariants for automated inspection
[DE90-005316] N90-19493
VESTIBULAR TESTS
Vestibular examination of motion sick student pilots
[IZF-1988-22] N90-19738
VHSIC (CIRCUITS)
Direct detection optical intersatellite link at 220 Mbps using AlGaAs laser diode and silicon APD with 4-ary PPM signaling
[NASA-CR-185380] N90-19460
VIBRATION
Nonlinear system vibration: The appearance of chaos
[DE90-007546] N90-19810
VIBRATION DAMPING
Modified independent modal space control of flexible structures N90-19597
Design and implementation of a flexible robot
[AD-A216453] N90-19601
An experimental study of the aeroelastic behaviour of two parallel interfering circular cylinders N90-19609
Constructibility limits of multiflow wind turbines with pivots
[ILR-MITT-215] N90-19662
VIBRATION TESTS
Helicopter flight vibration of large transportation containers: A case for testing tailoring
[DE90-007429] N90-19215
VIBRATIONAL SPECTRA
Modal analysis of nonprismatic beams: Uniform segment method
[AD-A216952] N90-19614
VIDEO DATA
Evaluation and analysis of the orbital maneuvering vehicle video system N90-19411
VIDEO EQUIPMENT
Evaluation and analysis of the orbital maneuvering vehicle video system N90-19411
Contact formation on (Hg,Cd) Te
[AD-A217088] N90-19900
VIDEO TAPE RECORDERS
A digital HDTV recorder using a cluster of four D1 DVTRs
[BBC-RD-1989/13] N90-19477
VISCOELASTICITY
Elastic recovery and polymer-polymer interactions
[AD-A217085] N90-19384
Viscoelastic adherend effects in adhesively bonded composite-to-composite joints N90-19594
Calculation of nonlinear viscoelastic processes for plastic layer textile membranes
[ETN-90-95868] N90-19622
VISCOUS FLOW
Computation of hypersonic unsteady viscous flow over a cylinder N90-19194
Three-dimensional viscous rotor flow calculations using a viscous-inviscid interaction approach
[NASA-TM-102235] N90-19204
Analysis of unsteady heat transfer by natural convection in a two-dimensional square cavity using a high order finite-volume method N90-19521
VISIBILITY
Automated visibility and cloud cover measurements with a solid-state imaging system
[AD-A216906] N90-19724
Visibility problems in numerical models of terrain
[INPE-4921-TDL/382] N90-19919
VISION
Parallel distributed networks for image smoothing and segmentation in analog VSLI
[AD-A216780] N90-19491
VISUAL ACUITY
A new method for measuring the transmissivity of aircraft transparencies
[AD-A216953] N90-19842
VISUAL PERCEPTION
Visual processing in texture segregation
[AD-A216539] N90-19737
VOLCANOES
Evolution of midplate hotspot swells: Numerical solutions
[NASA-CR-186462] N90-19713
VORTEX BREAKDOWN
Leading edge vortex dynamics on a pitching delta wing
[NASA-CR-186327] N90-19198
VORTEX RINGS
Dynamics of a class of vortex rings
[NASA-TM-102257] N90-19524
VORTEX SHEDDING
A study on upstream moving pressure waves induced by vortex separation
[ISL-CO-203/88] N90-19192
VORTICES
Leading edge vortex dynamics on a pitching delta wing
[NASA-CR-186327] N90-19198
Water-tunnel investigation of concepts for alleviation of adverse inlet spillage interactions with external stores
[NASA-TM-4181] N90-19199
A streamwise upwind algorithm applied to vortical flow over a delta wing
[NASA-TM-102225] N90-19201
Conforming Chebyshev spectral collocation methods for the solution of laminar flow in a constricted channel
[NASA-CR-182011] N90-19539
Experiments of thermoconvection in a cubic cell
[MPIS-6/1989] N90-19544
Nucleation of vortices in superfluid helium-4
[DE90-610675] N90-19880
VORTICITY
Analysis of unsteady heat transfer by natural convection in a two-dimensional square cavity using a high order finite-volume method N90-19521
Dynamics of a class of vortex rings
[NASA-TM-102257] N90-19524
VOYAGER PROJECT
Parkes radio science system design and testing for Voyager Neptune encounter N90-19451

W

WAFERS
Preparation and characterization of alumina films prepared by a novel spray pyrolysis method
[AD-A217570] N90-19339
WAKES
Study of the turbulent boundary layer on an afterbody
[TM-EA-8901] N90-19212
WALLS
The influence of a wall function on turbine blade heat transfer prediction N90-19421
WATER
Simulation of thermal dynamics of a vaporizing coal-water droplet in a combustor
[DE90-005356] N90-19317
Enhancement of processes for solar photocatalytic detoxification of water
[DE90-003949] N90-19330
Advanced double layer capacitor
[AD-A217110] N90-19518
Laboratory studies of free radical reactions in cloudwater
[DE90-003961] N90-19730
Large impact events and atmospheric evolution on the terrestrial planets N90-20028
WATER CURRENTS
Status of a nonlinear water surge model in February 1988
[KNMI-WR-88-03] N90-19735
WATER HEATING
Operational fact-finding report on heat pump systems for industrial use
[DE89-782295] N90-19527
WATER POLLUTION
Enhancement of processes for solar photocatalytic detoxification of water
[DE90-003949] N90-19330
The pollution hazard assessment system: Documentation and users manual
[AD-A217108] N90-19706
WATER QUALITY
Enhancement of processes for solar photocatalytic detoxification of water
[DE90-003949] N90-19330
Satellite imagery for water quality assessment in coastal regions
[INPE-4891-PRE/1492] N90-19636
Possible applications of remote sensing satellite pictures for the water quality management of the Frisian lakes, Netherlands
[BCRS-88-17] N90-19641
Predicting effects of global climate change on reservoir water quality and fish habitat
[DE90-003674] N90-19704
WATER SPLITTING
IEA (International Energy Agency) implementing agreement for a program of research and development on the production of hydrogen from water. Task 9: Hydrogen production
[DE90-007354] N90-19337
WATER TREATMENT
Enhancement of processes for solar photocatalytic detoxification of water
[DE90-003949] N90-19330
WATER TUNNEL TESTS
Water-tunnel investigation of concepts for alleviation of adverse inlet spillage interactions with external stores
[NASA-TM-4181] N90-19199
WATER VAPOR
Cloud parameterization in EURAD and its future development N90-19692
WATER WAVES
Phase control mechanism for wave energy conversion
[AD-D014354] N90-19657
WAVE AMPLIFICATION
All-fiber SFPM (Stimulated Four Photon Mixing) amplifier
[AD-D014358] N90-19841
WAVE ATTENUATION
The influence of gamma-radiation on the bandwidth of optical fibres and the reduction of the induced attenuation by bleaching and hardening the fibre
[FEL-1988-62] N90-19846
WAVE DISPERSION
Longitudinal traveling waves bifurcating from Vlasov plasma equilibria N90-19650
Tropospheric monitoring technology for gravity wave experiments N90-19971
WAVE EQUATIONS
Linear theory of thermal blooming in turbulence
[DE90-007243] N90-19579
A linear systems theory approach to the range-independent acoustic channel
[AD-A216551] N90-19817

WAVE EXCITATION
Applications of frequency and wavenumber nonlinear digital signal processing to nonlinear hydrodynamics research
[AD-A216259] N90-19530
WAVE FUNCTIONS
Study of interfacial behavior in cocurrent gas-liquid flows
[DE90-005988] N90-19532
WAVE INTERACTION
Nonlinear interaction of electrostatic waves at a narrow inhomogeneous layer of a warm magnetoactive plasma
[DE90-610624] N90-19857
WAVE PROPAGATION
Two-dimensional, long-pulse computer calculation of microwave-induced electron layer formation in low-pressure air
[DE90-005994] N90-19459
Propagation of electromagnetic waves in multidimensional homogeneous cosmologies
[DE90-610474] N90-19462
Sparse breakdown and statistical sneakthrough effects in low-altitude microwave propagation
[DE90-007252] N90-19473
Linear theory of thermal blooming in turbulence
[DE90-007243] N90-19579
Atmospheric thermal blooming and beam clearing by aerosol vaporization
[DE90-006271] N90-19711
Nonlinear interaction of electrostatic waves at a narrow inhomogeneous layer of a warm magnetoactive plasma
[DE90-610624] N90-19857
WAVE REFLECTION
Vector circuit theory for multilayered isotropic and chiral structures: Reflection and transmission
[PB90-122474] N90-19495
WAVEFORMS
A waveform capture and storage unit and its use for investigating disturbances on digital transmission links
[BBC-RD-1989/17] N90-19478
A linear systems theory approach to the range-independent acoustic channel
[AD-A216551] N90-19817
WAVEGUIDE FILTERS
CdTe buffered GaAs thin-slab IR waveguide modulators and T/R filter
[AD-A215999] N90-19488
WAVEGUIDES
A simple method using MAFIA to calculate external Q values of waveguide-loaded cavities
[DE90-741487] N90-19465
Field theoretical analysis and synthesis of broadband waveguide: Height, plane shunt circulators with multiple layer material insertions
[ETN-90-95360] N90-19469
Discontinuous-taper directional coupler
[AD-D014324] N90-19481
Low threshold current implanted-planar-buried-heterostructure, graded-index, separate-confinement-heterostructure GaAs-AlGaAs laser
[DE90-002579] N90-19572
A linear systems theory approach to the range-independent acoustic channel
[AD-A216551] N90-19817
WEAK INTERACTIONS (FIELD THEORY)
The ultimate structure of matter: The high energy physics program from the 1950s through the 1980s
[DE90-005682] N90-19836
Experimental constraints on metric and non-metric theories of gravity N90-19946
WEAPON SYSTEMS
Limitations of the conventional role of the B-1B in the European theater
[AD-A217285] N90-19230
Reliability testing of the Hughes temperature controlled 1/4 watt split cycle cryogenic cooler (HD-1045 (V)/UA)
[AD-A216696] N90-19426
WEAPONS
Report of the First Annual Airborne Weapons Training Technology Review
[DE90-007189] N90-19747
WEATHER
Colloquium on Synoptic Meteorology
[PB90-121112] N90-19720
WEATHER FORECASTING
Validation of the EURAD cloud modules N90-19693
Synoptic-scale forcing of the low-level jet in developing baroclinic waves N90-19717
Colloquium on Synoptic Meteorology
[PB90-121112] N90-19720
WEIGHTING FUNCTIONS
Initialization of EURAD, part 2 N90-19696
WEIGHTLESSNESS
Earth-orbiting resonant-mass gravitational wave detectors N90-19954
WELDED JOINTS
A new model for hydrogen absorption in welds
[AD-A216951] N90-19347
Heat sink effects on weld bead: VPPA process N90-19418
Origin and effect of pores in aluminum welded joints
[REPT-87M/43/05720/SCP/GRF] N90-19620
WEST GERMANY
Wind conditions near the ground in Federal Republic of Germany
[ISBN-3-88148-248-2] N90-19727
WHISKER COMPOSITES
Identification and development of optimum SiC whiskers for silicon nitride matrix composites
[DE90-006888] N90-19315
WHISPERING GALLERY MODES
Design considerations in achieving 1 MW CW operation with a whispering-gallery-mode gyrotron
[DE90-007283] N90-19557
Progress in the CW operation of a 140 GHz gyrotron
[DE90-007382] N90-19558
WHITE DWARF STARS
Neon novae, recurrent novae, and type I supernovae
[DE90-003188] N90-19931
WICKS
Measuring flow properties of wicks for heat pipe solar receivers
[DE89-016537] N90-19664
WIGGLER MAGNETS
Results of the PALADIN experiment
[DE90-006776] N90-19578
First direct observation of FEL (Free-Electron Laser) from lambda=20 to 45 microns
[DE90-007508] N90-19589
WIND (METEOROLOGY)
Transport of atmospheric aerosols above the Sierra Nevada slopes
[PB90-120288] N90-19675
WIND EFFECTS
Aeolian removal of dust from photovoltaic surfaces on Mars
[NASA-TM-102507] N90-19299
Mechanics of aeolian processes: Soil erosion and dust production N90-19410
Chemical composition of precipitation and wet/dry deposition of sulfur compounds around the coastal area
[DE89-782324] N90-19677
WIND EROSION
Mechanics of aeolian processes: Soil erosion and dust production N90-19410
WIND TUNNEL NOZZLES
The utilization of an infrared imaging system as a cooling slot blockage detector in the inspection of a transpiration cooled nozzle
[NASA-TM-102608] N90-19555
WIND TUNNEL TESTS
Heat transfer measurements from a NACA 0012 airfoil in flight and in the NASA Lewis icing research tunnel
[NASA-CR-4278] N90-19203
Conical Euler solution for a highly-swept delta wing undergoing wing-rock motion
[NASA-TM-102609] N90-19211
Aeroservoelasticity
[NASA-TM-102620] N90-19227
Low-speed wind-tunnel investigation of the flight dynamic characteristics of an advanced turboprop business/commuter aircraft configuration
[NASA-TP-2982] N90-19239
Separation bubbles at high Reynolds number: Measurement and computation
[CUED/A-AERO/15] N90-19525
An experimental investigation of the flow field around yawed stranded cables
[AD-A215782] N90-19529
WIND TUNNELS
Wind tunnel design of heat island turbulent boundary layer
[IHW-ET/50] N90-19542
Experimental examination of the development behavior of a gaseous body in a steady state and neutral layer turbulent sheet boundary layer with ground asperity
[ETN-90-96067] N90-19549
WIND TURBINES
PC-based PCM (Pulse Code Modulation) telemetry data reduction system hardware
[DE90-000316] N90-19273
Constructibility limits of multiflow wind turbines with pivots
[ILR-MITT-215] N90-19662
WIND VELOCITY
The microchannel plate camera as a detector at high resolution spectrographs: Experiments for velocity distribution in planetary nebulae
[ETN-90-95733] N90-19560
Spanwise measurements of vertical components of atmospheric turbulence
[NASA-TP-2963] N90-19718
Wind conditions near the ground in Federal Republic of Germany
[ISBN-3-88148-248-2] N90-19727
WINDMILLS (WINDPOWERED MACHINES)
Constructibility limits of multiflow wind turbines with pivots
[ILR-MITT-215] N90-19662
WINDPOWER UTILIZATION
Vision for the introduction of the wind power generation system. Survey on the prospective market, part 2
[DE89-910386] N90-19651
WINDPOWERED GENERATORS
Vision for the introduction of the wind power generation system. Survey on the prospective market, part 2
[DE89-910386] N90-19651
WINDSHIELDS
A new method for measuring the transmissivity of aircraft transparencies
[AD-A216953] N90-19842
WING OSCILLATIONS
Constructibility limits of multiflow wind turbines with pivots
[ILR-MITT-215] N90-19662
WING PROFILES
A panel process for the calculation of the flow around a wing with front angle damping
[ETN-90-95367] N90-19207
WINGS
Carrier wing profile in nonstationary current
[ETN-90-95368] N90-19208
WORDS (LANGUAGE)
The expression of syntagmatic relationships in frame-based indexing N90-19917
WORKLOADS (PSYCHOPHYSIOLOGY)
Assessment of crew workload measurement methods, techniques and procedures. Volume 2: Guidelines for the use of workload assessment techniques in aircraft certification
[AD-A217067] N90-19748

X

X RAY ABSORPTION
Nanolayer reactions in aluminum-metal interfaces
[DE90-004955] N90-19342
X RAY ASTRONOMY
High energy x ray observations on the Crab nebula and the double star source GX 1+4
[ETN-90-95829] N90-19937
Astronomy and astrophysics
[REPT-33/89] N90-19938
X ray timing observations and gravitational physics N90-19956
X RAY BINARIES
Detecting gravity waves from binary black holes N90-19943
General relativistic x ray (UV) polarization rotations as a quantitative test for black holes N90-19957
Underground muons from the direction of Cygnus X-3
[DE90-005646] N90-20038
Analysis of an observation of the x ray astronomy satellite EXOSAT at the low mass x ray binary star system GX5-1
[ETN-90-95828] N90-20042
X RAY DIFFRACTION
Diffraction studies of the structure of glasses and liquids
[DE90-007662] N90-19381
X RAY SOURCES
Conception of an automatic measurement installation for spatial resolution detectors
[ETN-90-95732] N90-19935
Examination of the background by High Energy X ray Experiment (HEXE) on the space station MIR
[ETN-90-95735] N90-20041
X RAY SPECTRA
Investigations of x ray sensitive PN-CCD's
[MPE-213] N90-19499
X RAY TELESCOPES
X ray timing observations and gravitational physics N90-19956
X RAYS
Background studies in gas ionizing x ray detectors N90-19399
Effect of barrier layers in burn-through experiments with 351-nm laser illumination
[DE90-006806] N90-19577
Nearly simultaneous optical, ultraviolet, and x ray observations of three PG quasars
[NASA-CR-186355] N90-19932

X-29 AIRCRAFT
X-29A aircraft structural loads flight testing
[NASA-TM-101715] N90-19225

Y

YAW
Yaw rate control of an air bearing vehicle N90-19420
YTTRIUM
Influence of heat treating on the mechanical values and the stability of heat barrier coatings
[ETN-90-95902] N90-19375
YTTRIUM COMPOUNDS
A ground state depleted laser in neodymium doped yttrium orthosilicate
[DE90-006773] N90-19586
YTTRIUM OXIDES
Optical studies of dynamical processes in disordered materials
[DE90-007080] N90-19372
Zirconia-based electrodes for solid oxide fuel cells
[DE90-000462] N90-19513
Laser surface interactions of high-(Tc) superconductors
[DE90-006894] N90-19587

Z

ZERO POWER REACTORS
Analysis and evaluation of ZPPR (Zero Power Physics Reactor) critical experiments for a 100 kilowatt-electric space reactor
[DE90-005634] N90-19835
ZINC SELENIDES
Passivating layer for III-V semiconductor materials
[AD-D014321] N90-19872
ZIRCONIUM OXIDES
Influence of heat treating on the mechanical values and the stability of heat barrier coatings
[ETN-90-95902] N90-19375
Zirconia-based electrodes for solid oxide fuel cells
[DE90-000462] N90-19513

Typical Personal Author Index Listing

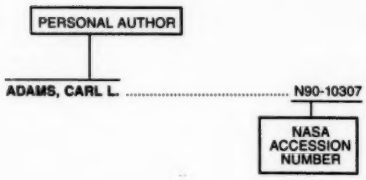

Listings in this index are arranged alphabetically by personal author. The NASA accession number denotes the number by which the citation is identified.

A

AARTS, W. J. A. M. N90-19561
ABBASSI, P. N90-19552
ABE, TOSHIO N90-19363
N90-19553
ABRAMOFF, BENNET N90-19366
ACOSTA, R. J. N90-19264
N90-19266
ACTON, L. N90-20030
ADAMS, NIGEL G. N90-19323
ADAMSKI, JOSEPH A. N90-19814
ADKINS, DOUGLAS R. N90-19664
AEPPLI, G. N90-19885
AGARWAL, ANANT N90-19519
AGRAWAL, DHARMA P. N90-19773
AHMAD, MUBARAK N90-19680
N90-19881
N90-19882
AHMED, FEROZ N90-19879
AIKIN, ROBERT M., JR. N90-19355
AIKIN, ROBERT M., SR. N90-19355
AIROLDI, VLADIMIR JESUS TRAVA N90-19487
ALBERT, M. N90-19903
ALBLAS, B. P. N90-19847
ALBRECHT, G. N90-19586
ALDERFER, DAVID W. N90-19555
ALEXANDER, C. M. O. N90-20001
ALLARD, L. F. N90-19315
ALLEN, S. L. N90-19576
ALLISON, W. W. M. N90-20037
ALLTON, CHARLES S. N90-19278
ALNER, G. J. N90-20037
ALPERT, D. J. N90-19689
ALSTON, WILLIAM B. N90-19300
ALVAREZ, R. A. N90-19459
N90-19473
AMBATS, I. N90-20037
ANABITARTE, E. N90-19853
ANDERSON, ALLEN JOEL N90-19952
ANDERSON, F. S. B. N90-19853
ANDERSON, JOHN D. N90-19966
ANDERSON, M. P. N90-19896
ANDRAKA, C. E. N90-19671
ANDRE, SANDRA N90-19835
ANG, MARCELO HUIBONHOA, JR. N90-19592
ANH, TRAN THI LAN N90-19801
ANNAMALAI, K. N90-19607
ANTOLAK, A. J. N90-19383
ANTONIAK, Z. I. N90-19294
ANTONIK, PAUL N90-19265
AOSHIMA, YOSHIHIDE N90-19721
APEL, UWE N90-19605
ARAKAWA, E. T. N90-19848
ARMAND, SASAN C. N90-19617
ARMSTRONG, G. A. N90-19493
ARMSTRONG, J. W. N90-19951
ARONS, JONATHAN N90-19985
ASHBY, NEIL N90-19950
ASHILL, P. R. N90-19202
ASHTON, W. B. N90-19673
ASHWOOD, PETER F. N90-19232
ASO, Y. N90-19486
ATHANS, MICHAEL N90-19807
ATKINSON, D. P. N90-19576
AUTY, DAVID N90-19758
AYRES, D. S. N90-20037
N90-20038
AZMY, YOUSRY Y. N90-19762
N90-19781
N90-19804

B

BABUSKA, IVO N90-19789
BACKHUIJS, A. J. W. M. N90-19846
BAGHUL, M. N90-20016
BAGINSKI, MICHAEL EDWARD N90-19391
BAILEY, J. M. N90-19514
BALAKRISHNAN, L. N90-19537
BALKA, L. N90-20037
BALLESTER, GILDA E. N90-19929
BANASZEWSKIEWICZ, M. N90-20017
BANSAL, NAROTTAM P. N90-19374
BAR-NUN, AKIVA N90-20023
BARBER, JOHN W. N90-19364
BARON, SHELDON N90-19741
BARR, G. D. N90-20037
BARRERA, ENRIQUE V. N90-19342
N90-19353
BARRETT, W. L. N90-20037
BASILI, VICTOR R. N90-19766
BASIT, BOLIS N90-19798
BATILL, STEPHEN M. N90-19529
BATINA, JOHN T. N90-19211
BAUBERGER, ALFRED N90-19351
BAUGHMAN, R. J. N90-19892
BAUMHEFNER, DAVID P. N90-19720
BAYER, D. N90-19726
BAYER, MARKUS N90-19767
BEACH, R. N90-19586
BEACH, RICHARD J. N90-19771
BEARD, L. N90-19466
BECHER, P. F. N90-19315
BECK, JACOB N90-19737
BECK, W. A. N90-19900
BECKMAN, T. M. N90-19334
BEDROSSIAN, PETER JOHN N90-19876
BEHENG, K. D. N90-19726
BEIGHTOL, D. B. N90-19215
BELCHENKO, YU. I. N90-19856
BELL, G. E. C. N90-19352
BELL, G. L. N90-19853
BELL, J. D. N90-19853
BELL, R. GLENN N90-19551
BELMANS, PHILIPPE N90-19745
BENDER, PETER L. N90-19953
N90-19965
BENJAMIN, D. N90-20037
BENKHOFF, J. N90-19999
BENNETT, CHARLES L. N90-19959
BERKSTRESSER, G. N90-19586
BERN, ZVI N90-19908
BERNSTEIN, E. R. N90-19815
BERRIE, J. N90-19466
BERRIER, BOBBY L. N90-19200
BERZINS, GEORGE J. N90-19296
BESMANN, T. M. N90-19379
N90-19382
BEUST, H. N90-20010
BHADRA, R. N90-19341
BHASAVANICH, D. N90-19566
BIFERNO, MICHAEL A. N90-19748
BIGELOW, T. S. N90-19853
BINDER, MICHAEL N90-19306
BINH, TRAN QUOC N90-19801
BIRKAN, M. A. N90-19297
BIRKAN, MITAT A. N90-19569
BIRKELAND, JOEL N90-19520
BIRMAN, KENNETH N90-19923
BITLER, STEVEN P. N90-19365
BLAKE, JEAN A. N90-19392
BLES, W. N90-19738
BLOECHL, BERNHARD N90-19542
BLOOM, JEROME H. N90-19814
BLOOM, R. M. N90-19709
BLUM, J. N90-20011
N90-20019
BOBB, LLOYD C. N90-19840
BOENDER, E. N90-19803
BOESCHE, GERALD V. N90-19742
BOHN, MARK S. N90-19665
N90-19667
BOICE, D. C. N90-20000
BOLTON, P. R. N90-19473
BONATTI, JOSE PAULO N90-19733
BORDER, P. N90-20037
BORG, STEPHEN E. N90-19555
BOSLEY, DAVID LEE N90-19574
BOSMAN, A. M. N90-19846
BOUCEK, GEORGE P., JR. N90-19748
BOULDIN, D. W. N90-19493
N90-19753
BOULWARE, DAVID N90-19834
BOURCIER, R. J. N90-19892
BOWLES, KENNETH J. N90-19310
BOXER, STEVEN G. N90-19652
BRACKBILL, J. U. N90-19865
BRADLEY, D. K. N90-19577
BRAMSON, G. N90-19839
BRANDLE, C. N90-19586
BREEN, DALE H. N90-19343
BREMER, MICHAEL N90-20026
BRENNAN, T. M. N90-19572
BRIDGEMAN, JOHN O. N90-19204
BRINKMEYER, ALAN N90-19649
BRITTON, C. L., JR. N90-19753
BROCKLEHURST, SARAH N90-19763
BROOKS, C. B. N90-20037
BROOKS, N. H. N90-19839
BROPHY, CAROLYN ELIZABETH N90-19765
BROWN, R. T. N90-19488
BROWNLEE, D. E. N90-20022
BRUCKDEANDRADE, GLENIO N90-19634
BUCHMANN, L. N90-19837
BUDHANI, R. C. N90-19871
BURATTI, A. N90-20008
BURFIELD, P. R. N90-19477
BURKHOLDER, R. N90-19466
BURLAGA, L. F. N90-19987
BURNETT, T. N90-20039
BUSSOLETTI, E. N90-19991
N90-19998
BYE, M. N90-19963
BYER, ROBERT L. N90-19969
BYRD, RICHARD H. N90-19806
BYUN, YUNGHWAN N90-19194

C

CACUCI, D. G. N90-19781
CALISE, A. J. N90-19275
CALLCOTT, T. A. N90-19848
CAMPBELL, BILL N90-19674
CAMPBELL, J. H. N90-19361
CAMPBELL, THOMAS G. N90-19249
CANDELA, G. A. N90-19875
CAPONE, D. W. N90-19892
CARANDANG, R. M. N90-19552
CARASSO, MEIR N90-19667
CARLI, RAFFAELLO N90-19937
CARPENTER, STUART G. N90-19835
CARR, FREDERICK H. N90-19720
CARRERAS, B. A. N90-19853
CARRIER, G. N90-19488
CARRINGTON, CONNIE K. N90-19393
CARTER, DAVID H. N90-19355
CASEY, KENDALL F. N90-19658
CATES, MICHAEL C. N90-19567
CATON, J. A. N90-19607
CAULFIELD, H. J. N90-19814
CERBE, THOMAS N90-19229
CHALLENGER, K. D. N90-19357
CHAMBERS, D. H. N90-19579
N90-19580
CHAMBERS, F. N90-19578

CHAMIS, CHRISTOS C. N90-19629
CHAN, CHANG N90-19955
CHAN, P. Y. N90-19763
CHANDLER, JOHN F. N90-19968
CHANG, CHIA-BO N90-19394
CHANG, JULIUS S. N90-19884
CHANG, LISA H. N90-19704
CHANG, YUN-CHING N90-19848
CHANTRY, P. J. N90-19566
CHARETTE, R. F. N90-19308
CHARLAND, SHAWN N90-19457
CHARLTON, L. A. N90-19853
CHASE, CLEMENT G. N90-19713
N90-19714
N90-19715
CHATTOPADHYAY, ADITI N90-19226
CHEN, C. H. N90-19587
CHEN, C. HARRY N90-19269
CHEN, CHING S. N90-19204
CHEN, HUAIYU N90-19353
CHEN, MING H. N90-19456
CHENG, H. C. N90-19673
CHENG, U. N90-19440
CHEO, P. K. N90-19488
CHESTER, ALDEN P., III N90-19346
CHEUNG, K.-M. N90-19445
N90-19447
CHIU, HUEI-HUANG N90-19395
CHONG, Y. P. N90-19578
CHOU, G. F. N90-19324
CHOW, ANDREA W. N90-19365
CHRISTIAN, ANDREW D. N90-19601
CHRISTODOULAKIS, T. N90-19712
CHRISTODOULOU, LEO N90-19355
CHRISTOFFER, JUERGEN N90-19727
CHUBB, S. R. N90-19668
CHUBB, T. A. N90-19668
CHUNG, T. J. N90-19326
CHUONG, NGUYEN MINH N90-19799
N90-19600
N90-19801
CHURCH, CURTIS K. N90-19396
CHYU, MINGKING K. N90-19397
CICARLO, J. N90-19903
CIUFOLINI, IGNAZIO N90-19981
CLAIREMIDI, J. N90-20012
CLARK, J. C. N90-19576
CLARK, T. L. N90-19853
CLARKE, C. K. P. N90-19476
CLAUSER, JOHN F. N90-19977
COCKRELL, C. R. N90-19453
COE, PAUL L., JR. N90-19239
COFFEY, HELEN E. N90-20031
N90-20032
COHEN, JULIA CLARINDA PAIVA N90-19723
COHEN, R. E. N90-19367
COKAL, H. N90-19925
COLANGELI, L. N90-19991
N90-19998
COLCHIN, R. J. N90-19853
COLLINGS, E. W. N90-19304
COLLINS, EARL R., JR. N90-19425
COLLINS, JEFFREY D. N90-19309
COLLINS, O. N90-19443
N90-19445
COLLINS, PETER J. N90-19835
COLLINS, R. T. N90-19515
COLLMAR, WERNER N90-20042
COLUCCI, STEPHEN J. N90-19720
COMASKEY, B. N90-19586
COMER, JOSEPH J. N90-19814
COOPER, DAVID G. N90-19568
CORAT, EVALDO JOSE N90-19487
CORBAN, J. E. N90-19275
CORBATO, STEVEN CLIFFORD N90-20034
CORBETT, G. K. N90-19746
CORKER, K. N90-19741
CORWIN, WILLIAM H. N90-19748
COSTILLA, MARCOS N90-19223
COWAN, CHARLES L. N90-19635
CRAIG, ROY R., JR. N90-19280
CRAMER, P. N90-19579
CRANE, ROBERT G. N90-19725
CRAWFORD, H. J. N90-20040
CUMMINGS, A. C. N90-19987
CURRO, JOHN G. N90-19377

D

DACONCEICAOFERREIRA, CELESTE N90-19722
DACRUZ, JOSE JAIME N90-19277
DAGLEY, I. J. N90-19385
DAHL, MILO D. N90-19242
DAKE, S. N90-20039
DALY, STEVEN F. N90-19637
DAMASCENOFERREIRA, LUIZ DANILO N90-19277
N90-19632
DANIEL, D. S. N90-19514
DAS, K. N90-19873
DAURIA, J. N90-19837
DAVID, VALERIE N90-19631
DAVIDSON, FREDERIC M. N90-19480
DAVIS, G. D. N90-19900
DAVIS, H. W. N90-19271
DAVIS, JON P. N90-19840
DAVIS, R. F. N90-19873
DEBRA, DANIEL B. N90-19974
DECKER, NAOMI H. N90-19791
DECOFF, GARY W. N90-19637
DEGANI, MARCOS H. N90-19869
DEHNE, KLAUS N90-19661
DEICHSEL, MICHAEL N90-19540
DEIS, G. A. N90-19578
DEKRIJGER, A. J. T. N90-19846
DELBOSCO, EDSON N90-19654
DELETTREZ, J. N90-19577
DEMABDON, MYRIAN N90-19633
DEMPSTER, ARTHUR P. N90-19774
DEOLIVEIRA, ISMAEL EMILIO, JR. N90-19487
DERRICKSON, J. N90-20039
DESISTO, W. J. N90-19339
DESJARLAIS, M. P. N90-19494
DEVADAS, SRINIVAS N90-19787
DEVANEY, JOSEPH J. N90-19833
DEVAULT, R. C. N90-19428
DEVELICE, ROBERT L. N90-19674
DEVENPORT, WILLIAM JOHN N90-19525
DEVRIES, W. T. N90-19734
DIASDASILVA, VITOR N90-19622
DICK, G. J. N90-19437
DIENER, W. N90-19439
DIESCH, CHRISTOPH N90-19560
DIMOV, G. I. N90-19858
DINGUS, RONALD S. N90-19590
DIVER, R. B. N90-19671
DIWAN, RAVINDER M. N90-19398
DOANE, DOUGLAS V. N90-19343
DOBBE, NILS N90-19510
DOGGETT, J. W. N90-19215
DOHERTY, R. D. N90-19896
DOLINAR, S. N90-19444
DOLPH, JAYNE N90-19674
DOMBSKY, M. N90-19837
DOMES, HELMUT N90-19376
DOMINEK, A. N90-19466
DONCALS, RICHARD A. N90-19835
DOSANJOSFERREIRAPINTO, SERGIO N90-19634
DOSCH, R. G. N90-19336
DOSSER, LARRY R. N90-19319
DRAKE, FRANCES N90-19719
DRAPER, SUSAN L. N90-19884
DREES, H. N90-19688
DREWES, LESTER R. N90-19740
DROESEN, WIM J. N90-19642
DRUDE, MARTIN N90-19716
DRUDEDELACERDA, LUIZ N90-19636
DRUMMOND, CHARLES H., III N90-19374
DUAILIBIFILHO, JAMIL N90-19370
DUBACH, LELAND L. N90-19243
DUDLEY, V. N90-19671
DUDNIKOV, V. G. N90-19856
DULICK, MICHAEL N90-19584
DUNBAR, DAVID C. N90-19908
DUNMIRE, HOWARD N90-19426
DWIGHT, K. N90-19339
N90-19901
N90-19902
N90-19903
DYER, GERALD E. N90-19602
DYMOND, KENNETH FLOYD N90-19979

E

EASTON, ROGER L., JR. N90-19464
EBEL, A. N90-19680
N90-19681
N90-19701
EDELMAN, R. N90-19550
EDENHOFER, P. N90-20005
EDMONDS, J. A. N90-19673
EDWARDS, J. O. N90-19339
EGAR, THOMAS W. N90-19347
EICHLER, P. N90-19287
N90-19288
N90-19289
ELDRIDGE, HUDSON B. N90-19399
ELFADEL, I. N90-19491
ELLIS, R. F. N90-19852
ELROD, DAVID A. N90-19400
ENGELSTAD, S. P. N90-19630
EPPLEY, KENNETH N90-19496
EPSTEIN, A. H. N90-19237
ERES, DJULA N90-19877
ERICHSEN-RUA, E.-A. N90-20043
ERICSON, M. N. N90-19753
ERNIE, DOUGLAS W. N90-19851
ERTELT, HANS-JUERGEN N90-19503
ESAREY, E. N90-19867
ESKOW, ELIZABETH N90-19775
ESPINASSE, S. N90-19997
N90-20013
N90-20015
ESTLER, RON C. N90-19585
EVERETT, GLYNN N90-19231
EVERITT, C. W. FRANCIS N90-19960
N90-19963
EVESSON, DONNA N90-19757
EWELL, DIANE N90-19675
EWICK, D. W. N90-19334

F

FAGHRI, AMIR N90-19523
FALLER, J. E. N90-19953
FARR, EVERETT G. N90-19458
FARROW, J. E. N90-19760
FAULKNER, GEORGE E. N90-19584
FECHTIG, H. N90-20011
FEDKIW, PETER S. N90-19340
FELCH, K. N90-19557
N90-19558
FELDMAN, BARRY J. N90-19565
FELDMAN, D. W. N90-19589
FELDMAN, NATHAN W. N90-19483
FELDMAN, W. C. N90-19987
FELKER, B. N90-19576
FELTHAUSER, HARRY E. N90-19296
FERBER, M. F. N90-19315
FERBER, M. K. N90-19368
FERET, J. M. N90-19668
FERGUSON, S. W. N90-19576
FERLET, R. N90-20010
FERRARA, AUGUSTO M. N90-19387
FERZIGER, JOEL H. N90-19524
FIELD, E. C., JR. N90-19709
FIELDS, T. H. N90-20038
FIGUEIREDO, DIVINO C. N90-19633
FINGER, M. H. N90-19442
FISCHER, MARK J. N90-19222
FISHER, R. J. N90-19731
FISK, Z. N90-19885
FITCH, J. P. N90-19474
FITTINGHOFF, D. N. N90-19473
FLANDRO, G. A. N90-19275
FLEISCHER, HELMUT N90-19819
FLETCHER, JAMES C. N90-19492
FLEURY, CASSIA DEASSIS N90-19656
FLOCCHINI, R. G. N90-19675
FLOWERS, GEORGE T. N90-19401
FOLKNER, W. M. N90-19442
FOSTER, JAMES C. N90-19378
FOSTER, JOHN V. N90-19206
FOSTER, LESTER ANDERSON N90-19274
FOUNTAIN, W. N90-20039
FOX, GEOFFREY C. N90-19777
FRAIN, W. E. N90-19987
FRANCA, LEOPOLDO P. N90-19533
N90-19790
FRANCAVILLA, T. L. N90-19875
FRANCHI, I. A. N90-20001
FRATT, DAVID B. N90-19679
FREDERKING, T. H. K. N90-19552
FREEDMAN, A. P. N90-19435
FREEMAN, L. MICHAEL N90-19390
FRESE, MICHAEL H. N90-19862
FRICHTL, PAUL J. N90-19230
FRIEDMAN, GARY L. N90-19776
FRIESEL, M. A. N90-19294
FUJIKAWA, GENE N90-19454
FUJIKAWA, KAZUO N90-19911
FUJITA, SHINICHI N90-19676
N90-19677
FUKI, M. N90-20039
FULKER, J. L. N90-19202
FUNKHOUSER, GORDON E. N90-19214

G

GABB, TIMOTHY P. N90-19302
GAIER, JAMES R. N90-19299
GALLIMORE, FRANK H. N90-19427
GALLUS, H. E. N90-19235
GAO, Y-M. N90-19902
GARCIA, A. E. N90-19575

GARLAND, MICHAEL M. N90-19402
GARRIOTT, GARY L. N90-19292
GASIEWSKI, A. J. N90-19251
GAST, RONALD G. N90-19614
GATTI, M. S. N90-19452
GAUGGEL, ROLAND N90-19789
GAUTESEN, A. K. N90-19579
GAYLORD, THOMAS K. N90-19849
GEDEON, STEVEN A. N90-19347
GEISLER, OLAF N90-19502
GEISS, H. N90-19685
N90-19687
N90-19689
GEISS, J. N90-19987
GEOHEGAN, DAVID B. N90-19878
GEORGE, THOMAS F. N90-19874
GERLI, C. N90-19993
GIALLORENZI, THOMAS G. N90-19554
GILBERT, MICHAEL G. N90-19281
GILDEN, M. N90-19488
GILES, M. B. N90-19237
GINLEY, D. S. N90-19892
GINN, W. C. N90-19671
GIORGIO, PAUL J. N90-19432
N90-19750
GIRIUNAS, J. N90-19267
GIROSI, FEDERICO N90-19778
GLEIS, DIETER N90-19754
GLICK, GAIL N90-19674
GLOECKLER, G. N90-19987
GLOVER, CHARLES W. N90-19779
GLUECK, W. N90-19488
GOETTING, BERND N90-20025
GOGINENI, S. P. N90-19262
GOLD, R. E. N90-19987
GOLDEN, DAVID M. N90-19388
GOLDFARB, R. B. N90-19304
GOLDHABER, DAVID MOSES N90-19980
GOLDMAN, S. ROBERT N90-19590
GOLDMAN, T. N90-19949
GOLDSTEIN, J. C. N90-19589
GOOD, W. N90-20007
GOORJIAN, PETER M. N90-19201
GRASSMANN, VOLKER N90-19864
GRATZ, ROY F. N90-19300
GREBOGI, CELSO N90-19794
GREEN, REBECCA JOYCE N90-19917
GREENBERG, J. M. N90-19995
N90-19997
N90-20001
GREENE, WILLIAM H. N90-19610
GREGORWICH, W. S. N90-19254
GREGORY, DAN L. N90-19627
N90-19628
GREGORY, J. N90-20039
GREST, G. S. N90-19896
GRIFFIN, J. W. N90-19294
GRIM, R. J. A. N90-19997
GRIMSDITCH, M. H. N90-19341
GRIMSON, W. ERIC L. N90-19759
GRINSPOON, DAVID HARRY N90-20028
GROBEL, MICHAEL N90-19546
GROSSMAN, JAMES W. N90-19670
GRUEN, E. N90-20016
N90-20019
N90-20020
GUBBINS, KEITH E. N90-19826
GUENETTE, G. R. N90-19237
GUIDOS, BERNARD J. N90-19233
GUPTA, RAJAN N90-19905
GURGELDEALBUQUERQUE, PAUL CESAR N90-19632
GUSICK, T. J. N90-20040
GUYENNE, T. D. N90-19989
GWINN, KENNETH W. N90-19291

H

HAAG, KARLHEINZ N90-19207
HAAS, CHRISTOPH N90-19505
HABIB, FADHIL A. N90-19303
HACKNEY, S. A. N90-19894
HAGANS, KARLA G. N90-19571
HAGE, J. I. N90-19995
HAHN, DIETRICH N90-19469
HAKKILA, JON N90-19403
HALBACH, K. N90-19578
HALL, J. L. N90-19953
HALLORAN, J. W. N90-19892
HAMADA, S. JIM N90-19269
HAMAMATSU, TERUHIDE N90-19553
HAMMONS, B. E. N90-19572
HAN, C. S. N90-19646
HANAFEE, J. E. N90-19348
HANCOCK, G. J. N90-19613
HANDELMAN, DAVID ANDREW N90-19238
HANHELA, PETER J. N90-19364
HANNA, MIKHAEIL H. N90-19881
N90-19882
HANNIGAN, C. N90-19339
HANSEN, IRVING G. N90-19234
HANSON, K. M. N90-19770
HARMS, RICHARD J. N90-19958
HARRIS, JAMES O. N90-19378
HASAN, S. W. N90-19613
HASEGAWA, TOSHIAKI N90-19363
HASKOVEC, J. S. N90-19839
HASS, HEINZ N90-19683
N90-19685
N90-19687
N90-19689
N90-19698
HAUS, JOSEPH W. N90-19305
HAWSEY, R. A. N90-19514
HAYASHI, T. N90-20039
HAYDEN, J. S. N90-19361
HAYDEN, S. M. N90-19685
HEALD, S. M. N90-19342
HEALD, STEVE M. N90-19353
HECKES, A. A. N90-19669
HEDGEPETH, J. M. N90-19256
HEIDORN, DIETER N90-19511
HEIGHWAY, J. N90-19267
HEIKEN, G. H. N90-20029
HEIKES, K. E. N90-19709
HEINISCH, H. L. N90-19359
HELLINGS, RONALD W. N90-19940
N90-19955
N90-19964
HELLMAN, H. N90-20003
HELLWIG, JUERGEN N90-20024
HENDRICK, DAVID M. N90-19820
HENNE, J. N90-19235
HENSHALL, G. A. N90-19357
HEPPE, G. N90-19548
HERARDIAN, M. M. N90-19252
HERBERT, F. N90-19726
HERING, WAYNE S. N90-19724
HERMAN, M. N90-19746
HERS, CHARLES R. N90-19323
HERSCHBERG, I. S. N90-19933
HESS, C. N90-19557
N90-19558
HEWITSON, BRUCE N90-19725
HEYL, M. N90-20003
HICKS, ROBERT F. N90-19320
HIGGINS, E. A. N90-19214
HILL, R. E. N90-19450
HILS, D. N90-19953
HINCKEL, JOSE NIVALDO N90-19487
HINDENLANG, ULRICH GERHARD WILHELM N90-19619
N90-19623
HINEDI, S. N90-19440
N90-19441
HINRICHS, HANS-JUERGEN N90-19507
HIRENJAKI, S. N90-19988
HIRVONEN, J.-P. N90-19358
HISAMATSU, TORU N90-19363
N90-19553
HISHINUMA, A. N90-19352
HISKES, J. R. N90-19825
HISLOP, ALFRED R. N90-19489
HO, ALEX W. N90-19777
HOBAN, SUSAN MARY N90-19981
HOF, M. N90-20040
HOFMANN-WELLENHOF, B. N90-19218
HOLLOWAY, JAMES PAUL N90-19850
HOLLOWELL, JEFF N90-19217
HOLONYAK, N., JR. N90-19570
HOLTROP, JOHN W. N90-19600
HOLY, J. A. N90-19334
HOLYNSKI, R. N90-20039
HOLZAPFEL, CHRISTIAN N90-19699
HORDIJK, J. N90-19467
HORNFECK, WILLIAM A. N90-19404
HOROWITZ, GARY T. N90-19947
HORSEWELL, A. N90-19359
HOTARD, DOUGLAS P. N90-19295
HOUSER, R. M. N90-19689
HOUSHMAND, B. N90-19264
HOVESTADT, D. N90-19987
HSIEH, K. C. N90-19570
HSIUNG, P. N90-20014
HUANG, ROBERT H. E. N90-19364
HUDLICKA, E. N90-19741
HUEBNER, W. F. N90-20000
HUEY, H. N90-19557
N90-19558
HUGHES, RICHARD J. N90-19949
HUGHES, THOMAS J. R. N90-19533
HUI, DAVID N90-19405
HULSTROM, ROLAND L. N90-20033
HUNG, CHING-CHEH N90-19301
HUNT, J. N90-19989
HUNTER, NORMAN F. N90-19810
HUNTLEY, WILLIAM P. N90-19491
HUPP, JOSEPH T. N90-19823
HUSSEIN, A. M. N90-19857
HUTTENLOCHER, DANIEL P. N90-19759
HYER, M. W. N90-19308

I

ICKERT, KLAUS N90-19311
INABA, TSUGINORI N90-19485
INAZUMI, T. N90-19352
INGUVA, RAMARAO N90-19305
INMAN, R. M. N90-19478
INOUE, ATSUYUKI N90-19721
IRWIN, R. DENNIS N90-19406
ISBERT, J. N90-20040
ITOH, TATSUO N90-19520
ITON, L. E. N90-19331
IWAI, J. N90-20039
IWASE, AKIHIRO N90-19344
IZATT, R. M. N90-19909
IZUMITANI, T. N90-19361

J

JAANIMAGI, P. A. N90-19577
JAENICHEN, PAUL N., SR. N90-19657
JAKOBS, HERMANN J. N90-19682
N90-19685
N90-19686
JAMES, R. D. N90-19379
JANIK, G. R. N90-19436
JANKIEWITZ, HARALD N90-19934
JARRAH, MOHAMMAD-AMEEN MAHMOUD N90-19196
JAWORSKE, DONALD A. N90-19373
JEFFRIES, JAY B. N90-19388
JEN, ERICA N90-19805
JENKINS, JAMES T. N90-19536
JENSEN, KEITH F. N90-19678
JERVIS, T. R. N90-19358
JESSBERGER, H. L. N90-20006
JIN, JIAN-MING N90-19309
JOHNS, K. N90-20038
JOHNSON, RICHARD W. N90-19724
JOHNSON, W. J. N90-19589
JONES, ERIC M. N90-19744
JONES, L. T. N90-19463
JONES, W. V. N90-20039
JONES, WENDELL B. N90-19670
JONG, R. A. N90-19576
JONGEWAARD, E. N90-19557
N90-19558
JONKER, BERNED T. N90-19872
JORY, H. N90-19557
N90-19558

K

KAGEYAMA, TATSUYA N90-19465
KALIA, RAJIV K. N90-19869
KALKUNTE, M. V. N90-19780
KALYANIWALLA, NAUSER N90-19305
KAMIGAWA, JUN N90-19527
KANAORI, YUJI N90-19707
KARAGEORGHIS, ANDREAS N90-19539
KARR, GERALD R. N90-19390
KARR, T. J. N90-19579
N90-19580
KASAL, PETER N90-19328
KASSNER, F. N90-19354
KASSNER, M. E. N90-19357
KATAYAMA, KOZO N90-19526
KATO, HISAYUKI N90-19676
KATSUMA, KUNION N90-19369
KATZ, JOSEPH L. N90-19333
KAUFFMAN, FRANK N90-19268
KEISER, JAMES R. N90-19626
KELLER, H. U. N90-19994
KELLER, KURT N90-19231
KENNEDY, ROBERT S. N90-19814
KERCZEWSKI, ROBERT J. N90-19454
KERRUTH, MICHAEL N90-19549
KERSEY, ALAN A. N90-19430
KERSHAW, R. N90-19339
N90-19902
KESSELI, JAMES N90-19655
KETO, ERIC N90-20027
KEYHANI, MAJID N90-19407
KIEDA, DAVID BASIL N90-20035
KIERSTEAD, JOHN D. N90-19814

KIHO, KENZO N90-19707
KILLOUGH, S. M. N90-19746
KIM, KYUN O. N90-19595
KIM, OH-KIL N90-19360
KIM, Y. M. N90-19326
KING, GEORGE A. N90-19674
KIPNIS, SHLOMO N90-19784
KIRCHHOFF, UWE N90-19231
KIRK, BERNADETTE L. N90-19762
N90-19804
KIRKPATRICK, RONALD C. N90-19590
KLARER, PAUL R. N90-19606
KLEIJWEG, JAN C. M. N90-19644
KLEIN, LISA C. N90-19366
KLEIN, M. J. N90-19452
KLEIN, RICHARD I. N90-19985
KLEINSCHMIDT, MICHAEL N90-19231
KLENNER, JUERGEN N90-19313
KLINGER, J. N90-19996
N90-19997
N90-20013
N90-20015
KLISS, MARK HOLCOMBE N90-19240
KNIGHT, N. F., JR. N90-19630
KNOLL, ALOIS N90-19604
KOCH, STEFAN N90-19544
KOCHAN, H. N90-20003
N90-20004
N90-20016
N90-20020
KOEHL, H. N90-20020
KOEHNE, RAINER N90-19663
KOELMAN, H. J. W. M. N90-19756
KOELZER, G. N90-20016
N90-20020
KOEMLE, N. I. N90-20017
KOETZ, ANDREAS N90-19691
KOHL, H. N90-20018
KOIKE, J. N90-19341
KOK, C. J. N90-19735
KOOMEN, P. J. N90-19497
KOPP, ROGER A. N90-19590
KORB, WOLFGANG N90-19890
KORFIATIS, E. N90-19712
KORTING, P. A. O. G. N90-19329
KOSINSKI, JOHN A. N90-19482
KOST, BERND N90-19621
KOTTHAUS, M. N90-20006
KOTTNIK, WOLFGANG N90-19541
KRAFT, RAYMOND H. N90-19596
KRAPCHEV, VLADIMIR B. N90-19711
KRAWCZONEK, WALTER N90-19484
KREBS, JAMES J. N90-19872
KRIMIGIS, S. M. N90-19987
KRISHNAN, V. N90-19212
KRISS, GERARD A. N90-19932
KRUIJER, A. H. N90-19509
KRUPKE, W. N90-19586
KUBO, REIJIRO N90-19912
KUECH, T. F. N90-19515
KUHN, HELMUT N90-19768
KUIPER, T. B. H. N90-19452
KULICK, S. N90-19257
KUMAR, R. N90-19448
KUPRIYANOV, A. S. N90-19856
KURSINSKI, E. ROBERT N90-19970
KURTZ, R. J. N90-19294
KUSCHEL, H. N90-19468
KWAK, J. F. N90-19892
KYNCL, J. N90-19808

L

LACKNEY, JOSEPH J. N90-19629
LACOMB, LLOYD JOHN, JR. N90-19816
LACONTI, ANTHONY B. N90-19518
LAGIN, A. N90-19267
LAGRANGE-HENRI, A. M. N90-20010
LAI, LIN-YING N90-19479
LAMB, R. C. N90-19983
LANDRY, M. J. N90-19573
LANGNER, ANDREAS N90-19874
LANGTON, CHRIS N90-19811
LASHINSKY, H. N90-19852
LASKEY, KENNETH JERRY N90-19316
LAU, S. S. N90-19897
LAUBE, MANFRED N90-19685
N90-19692
LAW, R. D. N90-19608
LEE, ELIZABETH M. N90-19211
LEE, J. K. N90-19694
LEE, S. W. N90-19264
LEE, Y. N90-19535
LEKOUDIS, S. G. N90-19297
LELIEVELD, J. N90-19894
LEMAY, SCOTT P. N90-19198
LEMMENS, ROB L. G. N90-19220
LEMON, D. K. N90-19294
LENIHAN, JAMES N90-19674
LEONARD, ANTHONY N90-19524
LEONDES, CORNELIUS T. N90-19224
LERCH, BRADLEY A. N90-19302
LESSNER, PHILIP N90-19518
LESTRADE, JOHN PATRICK N90-19408
LEVASSEUR-REGOURD, A. C. N90-20018
LEWIS, D. A. N90-19983
LI, ZHONGYUAN N90-19858
N90-19986
LIAO, M. N90-19267
LIAO, MEI-HWA N90-19617
LIAW, MORRIS N90-19757
LIBERMAN, I. N90-19566
LIEBCHEN, M. N90-19688
N90-19700
LIGHT, ROBERT MILES N90-19978
LIGHTSEY, W. D. N90-19556
LILLO, T. M. N90-19894
LIN, AVI N90-19783
LIN, SHU N90-19429
LING, K. M. N90-19831
LIPSITT, HARRY A. N90-19356
LITTERIO, MARCO N90-19462
LITTLEWOOD, BEV N90-19763
LITVIN, FAYDOR L. N90-19593
LIU, CHAN CHIANG N90-19635
LIU, MIAN N90-19713
N90-19714
LIZANICH, PAUL J. N90-19454
LOBITZ, D. W. N90-19562
LODGE, ARTHUR S. N90-19384
LOEVE, W. N90-19543
LOGAN, R. T., JR. N90-19438
LONG, MARTIN N90-19301
LONGDON, NORMAN N90-19631
LOPESDESOUZA, LUIZ ALBERTO N90-19817
LOUEY, C. N. N90-19385
LOUGE, MICHEL Y. N90-19536
LOUGHRAN, R. J. N90-19304
LOVE, ALLAN W. N90-19253
LOWDEN, RICHARD A. N90-19379
N90-19380
LOWNDES, D. H. N90-19877
LUHMANN, THOMAS N90-19559
LUMPKIN, A. H. N90-19575
N90-19589
LUMSDAINE, A. N90-19491
LUNA, JACK N90-19552
LUNDBERG, W. L. N90-19653
LUNG, C. W. N90-19615
LUTES, G. F. N90-19438
N90-19439
LUTON, M. J. N90-19895
LYNE, PEGGY J. N90-19214

M

MACENKA, STEVE A. N90-19272
MACKAY, REBECCA A. N90-19302
MADDOCKS, J. H. N90-19812
MAGANA, MARIO E. N90-19409
MAGGIORE, C. J. N90-19925
MAHDI, HASHIM SALMAN N90-19521
MAILHIOT, C. N90-19515
MAKOWSKI, M. A. N90-19576
MALAGISI, CARMEN N90-19265
MALEKI, L. N90-19436
N90-19438
MALLIOT, H. A. N90-19254
MALLOUK, THOMAS E. N90-19335
MALLWITZ, ROLAND N90-19471
MAMMONE, ROBERT J. N90-19306
MANGALAM, SIVARAMAKRISHNAN M. N90-19534
MANGUEIRA, L. S. N90-19486
MANHART, PAUL K. N90-19272
MANKE, JOSEPH W. N90-19792
MARABITO, MARK N90-19299
MAREK, E. L. N90-19562
MARKEN, K. R. N90-19304
MARKER, A. J., JR. N90-19361
MARKS, DANNY N90-19674
MAROLDA, VICTOR J., JR. N90-19490
MARONI, V. A. N90-19331
MARRONE, MICHAEL J. N90-19430
MARSHAK, M. L. N90-20038
MARTIN, JAMES A. N90-19298
MARTIN, JURI L. N90-19678
MARTIN, PATRICK L. N90-19355
N90-19356
MARTINEZ, JESUS I. N90-19378
MARTINI, PAULO ROBERTO N90-19634
MARX, YVES P. N90-19205
MARZULLO, KEITH N90-19923
MASHBURN, DOUGLAS N. N90-19878
MASHHOON, BAHRAM N90-19962
MATHIS, K. D. N90-20040
MATHYS, G. N90-19928
MATSUDA, EIKO N90-19651
MATZNER, RICHARD A. N90-19945
MAURER, JOERG N90-19662
MAY, E. N. N90-20038
MAYER, J. W. N90-19897
MAYHALL, D. J. N90-19459
MCCANN, M. P. N90-19587
MCCREADY, MARK J. N90-19532
MCCROSSON, PAUL N90-19225
MCELIECE, R. N90-19444
MCEWEN, ALAN B. N90-19388
MCFARLANE, HAROLD F. N90-19835
MCINTOSH, R. E. N90-19259
MCLEAN, GARNET A. N90-19214
MCLELLAN, EILEEN N90-19710
MCMILLIEN, DONALD F. N90-19388
MEAD, ANDREW ROBERT GRAHAM N90-19930
MEBIUS, J. E. N90-19933
MEDEIROS, EDUARDO BAUZER N90-19609
MEHOS, MARK S. N90-19665
MEHRABADI, M. M. N90-19410
MEIER, MARTIN N90-19499
MEIJERS, L. G. N90-19312
MEIJERS, P. J. M. N90-19640
MEISSNER, H. N90-19361
MELACCI, P. T. N90-20009
MELGERS, J. J. N90-19219
MELLOR, MALCOM N90-20002
N90-20021
MEMMESHEIMER, M. N90-19685
N90-19700
MENDEL, C. W., JR. N90-19494
MENDOZA-GOMEZ, C. X. N90-20001
MERKEL, HAROLD S. N90-19842
MESHII, M. N90-19341
MEZZINA, ALESSIO N90-19337
MICHELSON, PETER F. N90-19958
MIESENBOECK, H. M. N90-19349
MIGNERY, LEZZA ANN N90-19594
MIKSAD, RICHARD W. N90-19530
MILEANT, A. N90-19441
MILLER, DOUGLAS R. N90-19764
MILLER, J. L. N90-19578
MILLICAN, GEORGE L. N90-19481
MITCHELL, J. W. N90-20040
MITCHELL, JAMES J. N90-19232
MITCHELL, M. A. N90-19892
MITCHELL, S. N90-19586
MITTAS, A. N90-19573
MIYACHIKA, HIDETO N90-19651
MODICA, LYSA G. N90-19679
MOELDERS, NICOLE N90-19693
MONTESINIS, BENJAMIN N90-19813
MONY, BRUNO N90-20041
MOODY, M. V. N90-19975
MOOK, H. A. N90-19885
MOON, YOUNG JUNE N90-19197
MOORE, R. K. N90-19262
MOORHEAD, ROBERT J., II N90-19411
MORALES, SERGIO N90-19778
MORE, KARREN L. N90-19379
N90-19380
MOREELS, G. N90-20012
MORENO, J. B. N90-19671
MORI, NORIYUKI N90-19363
N90-19553
MOROSIN, B. N90-19892
MORRIS, J. R. N90-19579
MORRIS, RONALD W. N90-19617
MOSKO, JOSEPH A. N90-19481
MOSS, S. C. N90-19381
MOSS, TIMOTHY N90-19664
MOTOYAMA, HIDEKI N90-19721
MOURICK, PAUL CHRISTIAAN N90-19501
MUELLER, MANFRED N90-19939
MUENZENBERG, ANNETTE N90-19697
MURAKAMI, M. N90-19853
MURTHY, PAPPU L. N. N90-19629
MUSKET, R. G. N90-19348
MYERS, D. R. N90-19572
MYERS, DARYL R. N90-20033
MYRUP, L. O. N90-19675

N

NAEGELI, D. W. N90-20000
NAGATA, KOICHI N90-19651
NAKAJIMA, HAJIME N90-19350
NAKAJIMA, S. N90-19361

NAKAMURU, A. N90-19988
NAKAZAWA, NACHITO N90-19914
NAKAZAWA, YASUHARU N90-19651
NAMITO, YOSHIHITO N90-19838
NANEVICZ, JOSEPH E. N90-19296
NASTASI, M. N90-19358
NAZAR, JAMES B. N90-19455
NEAL, N. J. N90-19892
NEALY, JOHN E. N90-20036
NEBRES, JOSE Y. N90-19529
NEGLEY, ROBERT M., JR. N90-19742
NEILSON, J. N90-19557
N90-19558
NEILSON, RONALD P. N90-19674
NELSON, ROBERT C. N90-19529
NELSON, W. R. N90-19838
NERI, ROBERTO N90-19936
NESENBERGS, M. N90-19463
NEUBAUER, F. M. N90-19680
NEUBERT, HARALD N90-19314
NEUHART, DAN H. N90-19199
NEUHAUS, J. N90-20040
NEUMANN, DIETER N90-19210
NEVESMONTEIRO, SERGIO N90-19370
NEWNAM, B. E. N90-19589
NEXSEN, W. E. N90-19576
NG, CAROLYN N90-19243
NGO, HOC D. N90-19822
NGUYEN, CHARLES C. N90-19599
NGUYEN, DINH C. N90-19584
NGUYEN, HIEPHOA N90-19331
NGUYEN, LUAT T. N90-19206
NIEROPEREIRA, MADALENE N90-19634
NIETO, MICHAEL MARTIN N90-19949
NISHINOMIYA, SAKAE N90-19676
NIU, C-M. N90-19901
NOBLE, REGINALD D. N90-19678
NOGAR, NICHOLAS S. N90-19585
NOGUEIRALORENA, LUIZ ANTONIO N90-19782
NOLL, J. N90-20005
NOLL, THOMAS E. N90-19227
NOOR, AHMED K. N90-19595
NORDTVEDT, KEN N90-19948
NOVOZHILOV, YURI V. N90-19907
NOWAK, R. N90-19815
NUSCA, MICHAEL J. N90-19531
NUSSBAUM, DANIEL N90-19519

O

OBAYASHI, SHIGERU N90-19201
OBERREUTER, A. N90-19688
OCCHIONERO, FRANCO N90-19462
OHARA, TOMOYUKI N90-19708
OJIMA, SHUICHI N90-19912
OKAMOTO, P. R. N90-19341
OKANE, JAMES H. N90-19278
OKAZAKI, MASAYUKI N90-19485
OKSANEN, MARKKU I. N90-19495
OLIPHANT, A. N90-19478
OLIVER, W. F. N90-19815
OLSEN, DAVID N. N90-19835
OLVER, TERENCE E. N90-19480
ONG, MARIA ELIZABETH GO N90-19793
ONYANGO-OTIENO, V. P. N90-19795
ONYSZCHUK, I. M. N90-19445
ORZECHOWSKI, T. J. N90-19578
OTTE, NEIL N90-19616
OWENS, D. BRUCE N90-19239
OZDES, DEMIR N90-19231

P

PACHECO, JAMES E. N90-19330
PAEZ, THOMAS L. N90-19627
N90-19628
PAHLE, JOSEPH W. N90-19241
PAIK, HO JUNG N90-19954
N90-19975
PANCHAL, C. B. N90-19659
PANGBURN, TIMOTHY N90-19637
PAPANTONI-KAZAKOS, P. N90-19761
PAPASTAVROU, JASON D. N90-19807
PARKER, JERALD V. N90-19248
N90-19866
PARKER, R. P. N90-19385
PARKER, RONALD JOHN DAVID N90-19749
PARKINSON, B. W. N90-19960
PARKS, JAMES E. N90-19564
PATCHETT, P. J. N90-19715
PAUL, C. N90-19578
PAUL, D. BRENTON N90-19364
PAUL, SAMIR K. N90-19912
PAYNE, GAIL B. N90-19747
PAZOS, MAYRA C. N90-19732
PENDLETON, R. N90-19557
N90-19558
PEREIRA, C. A. N90-19486
PEREIRADACUNHA, ROBERTO N90-19632
PEREZ-DAVIS, MARLA E. N90-19299
PERRY, M. N90-19839
PERRY, WILLIAM D. N90-19373
PESARAN, AHMAD A. N90-19666
PETERSON, E. A. N90-20038
PETERSON, LENNART R. N90-19412
PETRY, HERIBERT N90-19696
PHANORD, DIEUDONNE D. N90-19413
PHILLIPS, R. C. N90-19587
PHILLIPS, RICHARD L. N90-19771
PHILLIPS, TIMOTHY N. N90-19539
PICARDI, G. N90-20009
PIKELIS, WINFRED PRESCOTT N90-19433
PILLINGER, C. T. N90-20001
PINTER, S. N90-20019
PIRKLE, D. N90-19557
N90-19558
PIRROELONGO, WALDIMIR N90-19370
PLICHTA, M. R. N90-19894
PLOECHINGER, ERNST N90-19809
POGGIO, TOMASO N90-19778
POH, SOON-NEO N90-19597
POINSATTE, PHILIP E. N90-19203
POINTON, T. D. N90-19494
POLLACK, JORDAN B. N90-19751
POLLARA, F. N90-19443
N90-19444
POLYDOROS, ANDREAS N90-19475
POORAN, FARHAD JABBARI N90-19598
POPPE, DIRK N90-19690
PORTER, CHARLES A. N90-19835
POSNER, E. C. N90-19434
POWERS, EDWARD J. N90-19530
PRASAD, S. K. N90-19213
PRAUSNITZ, J. M. N90-19324
PRESTAGE, J. D. N90-19436
PRICE, L. E. N90-20038
PRIEDHORSKY, WILLIAM C. N90-19293
PRINZ, GARY A. N90-19872
PROENNECKE, S. N90-19359
PROSNITZ, D. N90-19578
PROTOPOPESCU, V. N90-19781
PRZYREMBEL, GEORGES N90-19504
PUNJABI, ALKESH N90-19859
PYATOV, P. N. N90-19906

Q

QIAN, Y.-T. N90-19339
QIU, S. L. N90-19871
QIYU, LIAO N90-19732
QUINTENZ, J. P. N90-19494

R

RABKIN, J. N90-19446
RADCLIFF, ROGER N90-19414
RAHMATSAMII, Y. N90-19263
N90-19264
RAILSBACK, STEVEN F. N90-19704
RAINA, T. K. N90-19881
N90-19882
RAM, M. S. N90-19823
RAMAKER, DAVID E. N90-19322
RAMAMOORTHY, P. N90-19213
RANGELCARDENAS, RAFAEL ERNESTO N90-19689
RAO, MUKUND N90-19626
RAO, NAGESWARA S. V. N90-19779
RASCHKE, E. N90-19680
RATH, HANS-KARL N90-19702
RATKE, L. N90-20003
N90-20004
N90-20020
RAWLINSON, K. S. N90-19671
RAZUMOV, A. V. N90-19906
REA, CAROL N90-19387
REASENBERG, R. D. N90-19967
REBOLD, T. A. N90-19451
REDDY, J. N. N90-19630
REDDY, PADALA V. N90-19740
REED, I. S. N90-19447
REESE, G. M. N90-19562
REHN, L. E. N90-19341
REINTJES, JOHN F. N90-19568
REMONDI, B. W. N90-19218
RESCH, G. M. N90-19971
REUTER, THOMAS N90-19470
REX, D. N90-19287
N90-19288
N90-19289
REYNOLDS, MICHAEL N90-19472
RHODE, MATTHEW N. N90-19199
RICE, B. W. N90-19576
RICHARDSON, B. S. N90-19746
RICHTER, JOERG N90-19752
RIEGER, P. H. N90-19901
RINO, CHARLES L. N90-19822
RIORDAN, CAROL J. N90-20033
RISBUD, A. A. N90-19481
RITZ, C. N90-20013
RIVERA, JOE N90-19225
RIZK, M. A. N90-19550
ROBERTSON, KARIN N90-19567
RODRIGUES, JOSE EDUARDO N90-19635
ROESSLER, K. N90-20003
N90-20014
ROGERS, J. D. N90-19215
ROGERS, J. W. N90-19332
ROGERS, JONATHAN D. N90-19820
ROGERS, ROBERT B. N90-19458
ROHLFING, LORI LOUISE N90-19307
ROLLETT, A. D. N90-19895
N90-19896
ROSEN, R. S. N90-19357
ROSENBLUM, WENDY I. N90-19638
ROSENTHAL, S. E. N90-19494
ROSOCHA, LOUIS A. N90-19516
ROSS, WALTER L. N90-19492
ROSSI, J. O. N90-19486
ROTH, MARY ELLEN N90-19484
ROTHACKER, FRANK N90-19772
ROTHSCHILD, S. L. N90-19760
ROWDEN, CHARLES M. N90-19305
ROY, G. S. N90-19297
RUCKMAN, M. W. N90-19342
N90-19871
RUDOWICZ, MATTHIAS N90-19828
RUEBE, PETRA N90-19915
RUF, C. S. N90-19261
RUGGIER, C. J. N90-19449
RUIZENAAR, M. G. A. N90-19498
RULE, WILLIAM K. N90-19415
RUPERT, J. N90-19573
RUSSELL, STEPHEN D. N90-19841
RUTHER, W. E. N90-19354
RYAN, ROBERT N90-19225
RYBKIN, G. N. N90-19906
RYTZ, D. N90-19885

S

SACHIVALAYA, MARG N90-19912
SAHU, DEVARAJ N90-19874
SALO, GLEN R. N90-19458
SALOUR, MICHAEL N90-19814
SALVAGGIO, CARL N90-19638
SAMARA, G. A. N90-19893
SAMBE, H. N90-19322
SAMUELS, RAEMON N90-19426
SANCHESPADILHA, ORLANDO N90-19276
SANDAY, S. C. N90-19338
SANDRY-GARZA, DIANE L. N90-19748
SANTI, L. MICHAEL N90-19416
SANTOSSILVA, EWERTON N90-19919
SAPAK, D. L. N90-19361
SARANGAPANI, S. N90-19518
SARASAMMA, V. R. N90-19755
SARKAR, S. N90-19537
SASAKI, SHINOBU N90-19603
SAUNDERS, J. N90-19437
SAUNDERS, ROGER N90-19655
SCHAAF, KLAUS N90-19547
SCHAEFER, ROBERT W. N90-19835
SCHAEFFER, CHRISTIAN N90-19818
SCHARLEMANN, E. T. N90-19578
SCHEEPENS, C. P. N90-19620
SCHEIDGEN, PETER N90-19729
SCHIPPERS, H. N90-19191
SCHMIDT, B. N90-20013
N90-20015
SCHMIDT, THOMAS N90-19624
SCHMITT-THOMAS, KH. G. N90-19375
SCHMITT, B. N90-19997
SCHNABEL, ROBERT B. N90-19775
N90-19806
SCHOENSTER, JAMES A. N90-19821
SCHOETTLE, ULRICH MICHAEL N90-19246
SCHOTT, JOHN R. N90-19638
N90-19845
SCHROEDER, HELMUT N90-19500
SCHROEDER, HERBERT N90-19935
SCHUDY, R. N90-19741
SCHUMAN, HARVEY K. N90-19265
SCHUNK, NIKOLAUS N90-19583
SCHUTZ, BERNARD F. N90-19942

SCHWARTZ, STEPHAN E. N90-19730
SCHWEHM, G. N90-19990
N90-19991
N90-20003
SCHWEITZER, WILLI-BERT N90-19208
SCHWEIZER, KENNETH S. N90-19377
SCOTT, J. F. N90-19815
SEIDEL, D. B. N90-19494
SEIFERLIN, K. N90-19999
SEIFERT, PEDRO N90-19327
SEILER, F. N90-19192
SENDA, TOSHIAKI N90-19651
SENTIS, MARC N90-19517
SETTLES, G. S. N90-19535
SEU, R. N90-20009
SGUBINI, S. N90-20008
SHAFFER, JAMES N90-19426
SHAR, MALVIN L. N90-19483
SHARIFF, KARIM N90-19524
SHARP, J. W. N90-19877
SHARP, R. N90-19267
SHAVIV, GIORA N90-19931
SHELDON, B. W. N90-19382
SHEPARD, C. L. N90-19294
SHIELDS, JANET E. N90-19724
SHIKAZONO, NAOMOTO N90-19863
SHINGLEDECKER, CLARK N90-19472
SHINN, JUDY L. N90-20036
SHIOZAKI, A. N90-19447
SHIRAISHI, K. N90-19968
SHOR, ERIC N90-19845
SHUPE, M. N90-20038
SIEGEL, ALEX N90-19923
SIEGER, G. E. N90-19459
N90-19473
SIEV, B. N90-19446
SIEVERS, A. J. N90-19843
SILEVITCH, MICHAEL B. N90-19855
SILLIMAN, MIKE N90-19779
SILVER, RICHARD N. N90-19832
SILVERMAN, J. N90-19852
SIMMONS, M. J. N90-19202
SIMON, M. N90-20040
SIMPSON, M. L. N90-19493
SIMS, ROBERT N90-19225
SINGH, B. N. N90-19359
SINGHAL, SURENDRA N. N90-19629
SINHA, A. K. N90-19254
N90-19255
SITARSKI, MAREK A. N90-19317
SIVARAMAKRISHNAN, RAJALAKSHMY N90-19755
SIVERS, DENNIS N90-19824
SIWECKI, STEPHEN A. N90-19319
SIX, FRANK N90-19390
SKORPIK, J. R. N90-19294
SLEEPER, ROBERT K. N90-19718
SLOTWINSKI, A. R. N90-19270
SLUIJK, TOM N90-19510
SLUTZ, S. A. N90-19494
SMALL, MITCHELL J. N90-19706
SMITH, D. L. N90-19463
N90-19515
SMITH, DALE M. N90-19835
SMITH, DAVID N90-19323
SMITH, SHARON N90-19775
SMITH, WAYNE D. N90-19417
SMOOT, GEORGE F. N90-19959
SMORENBURG, C. N90-19582
SNECK, H. J. N90-19614
SNELL, JOHN N90-19763
SNYDER, CATHRINE E. N90-19747
SODA, JIRO N90-19913
SOFER, ARIELA N90-19764
SOKOL, PAUL E. N90-19832
SOKOLOWSKI, LESZEK M. N90-19462
SOLANKI, S. K. N90-19928
SOLARZ, R. N90-19586
SOLLID, J. E. N90-19589
SOLLINGER, MICHAEL N90-19236
SOMMER, W. F. N90-19359
SONNABEND, DAVID N90-19976
SOPPET, W. K. N90-19354
SOULEN, R. J., JR. N90-19675
SPARKMAN, JAMES K., JR. N90-19250
SPARKS, WARREN M. N90-19931
SPENCER, H. J. N90-19365
SPETH, P. N90-19680
SPEZIALE, CHARLES G. N90-19538
SPOHN, T. N90-19999
SPRANGLE, P. N90-19867
SPRENGER, H. N90-19837
SREENIVASAN, C. R. N90-19755
SROLOVITZ, D. J. N90-19895
N90-19896
SRULIJES, J. N90-19192
STACK, JOHN P. N90-19534
STAELIN, D. H. N90-19251
STAMNITZ, TIMOTHY C. N90-19841
STARK, RICHARD F. N90-19944
N90-19957
STARRFIELD, SUMNER N90-19931
STATMAN, J. N90-19446
STEBBINS, R. T. N90-19953
STEGEMAN, G. I. N90-19844
STEIN, W. E. N90-19589
STEINBACH, R. N90-19267
STEINBERG, M. N90-19673
STEINER, G. N90-20017
STEINHAUER, LOREN C. N90-19860
STENBERG, ROLF N90-19533
N90-19790
STENDEL, M. N90-19695
STEPHENS, H. P. N90-19336
STERANKA, PAUL O., JR. N90-19418
STERNBERG, MARTIN N90-19827
STEWART, PAUL H. N90-19388
STILLMAN, G. E. N90-19570
STOCKWELL, WILLIAM R. N90-19684
STOECKL, H. N90-19625
STOEFFLER, D. N90-19992
STOHL, F. V. N90-19336
STONE, E. C. N90-19987
STOVER, ELMER K. N90-19590
STRATMAN, M. S. N90-19348
STRAZZULLA, G. N90-19998
STRUCK, BERND DIETER N90-19337
STUMM, J. E. N90-19257
SUITS, B. H. N90-19899
SULLIVAN, THOMAS D. N90-19802
SUMPTION, M. D. N90-19304
SUN, XIAOLI N90-19460
SURI, MANIL N90-19789
SVOBODA, JAMES S. N90-19454
SWANSON, P. N. N90-19260
SWANSON, THEODORE D. N90-19523
SZE, ROBERT C. N90-19517
SZPAKIEWICZ, MICHAEL N90-19703

T

TACHIKAWA, ENZO N90-19863
TAKEDA, TATSUCKI N90-19863
TALOTTA, NICHOLAS J. N90-19472
TANG, XIAO-YAN N90-19684
TANNER, JOHN A. N90-19595
TASK, HARRY L. N90-19842
TAVARESDEMATTOS, JUERCIO N90-19708
TAYLOR, JOHN G. N90-19193
N90-19200
TENNERY, V. J. N90-19368
TERAZAWA, HIDEZUMI N90-19910
TESMER, J. R. N90-19925
TEVAARWERK, J. L. N90-19386
THAYER, JEFFREY S. N90-19296
THIEL, K. N90-20016
N90-20020
THOMAS, DANIEL L. N90-19419
THOMAS, JOHN H. N90-19813
THOMAS, M. N90-19258
THOMAS, R. J. N90-19514
THOMPKINS, W. T., JR. N90-19237
THOMSON, CLAY N90-19637
THORNE, JAMES DANA N90-19245
THORPE, R. N90-19334
THROOP, A. L. N90-19576
TIEGS, T. N90-19315
TIKOO, S. K. N90-19881
N90-19882
TIMBRELL, J. A. N90-19736
TING, A. N90-19867
TISHKOFF, J. M. N90-19297
TOMUTSA, LIVIN N90-19649
TORATANI, H. N90-19361
TOSI, M. P. N90-19349
TRAPP, REINHARD N90-19661
TREITLER, INGA E. N90-19747
TRENCH, CLAUER DEFREITAS N90-19362
TRETYAKOV, SERGEI A. N90-19495
TREUHAFT, R. N. N90-19971
TREWHELLA, J. N90-19575
TRICE, J. L. N90-19894
TRIVELY, MARTIN N90-19426
TROGLER, WILLIAM C. N90-19321
TRUONG, T. K. N90-19447
TRURAN, JAMES W. N90-19931
TRUSKE, THEODORE N. N90-19458
TSINTSADZE, N. L. N90-19481
TSUJI, HIROKAZU N90-19350
TURNEAURE, J. P. N90-19960
TURNER, JOYCE E. N90-19916
TURNER, STEVEN G. N90-19239
TYNDALL, M. B. N90-19528
TYNER, CRAIG E. N90-19330

U

UEDO, M. N90-19486
UKO, U. L. N90-19797
ULBRICH, UWE N90-19728
ULBRICHT-EISSING, MONIKA N90-19727
UMAN, M. A. N90-19731

V

VALENCIA, JOHN E. N90-19296
VANBEUZEKOM, M. N90-19508
VANDENBERG, R. P. N90-19548
VANDERLAAN, F. B. N90-19639
VANDERLINDEN, AD N90-19924
VANDERSANDE, JAN W. N90-19884
VANDERSCHOOT, R. C. P. N90-19645
VANDERVOOREN, J. N90-19543
VANDEVEGTE, J. M. E. N90-19788
VANES, J. T. N90-19506
N90-19509
VANIMAN, D. T. N90-20029
VANINGENSCHENAU, H. A. N90-19672
VANLIESHOUT, ARNO M. N90-19642
VANNINH, KHUAT N90-19799
N90-19800
VANNINI, MATTEO N90-19517
VANTILBORG, H. N90-19444
VASHISHTA, PRIYA N90-19869
VASSILEVICH, D. V. N90-19907
VAWTER, G. A. N90-19572
VEERBEEK, H. W. N90-19756
VEERS, PAUL S. N90-19670
VEITH, C. A. N90-19367
VENEMA, J. C. N90-19672
VENEZIANI, PAULO N90-19708
VENTURINI, E. L. N90-19892
VERDON, C. P. N90-19577
VERKOOIJEN, J. C. N90-19506
VESSOT, ROBERT F. C. N90-19972
VIALLS, R. E. N90-19478
VIDAL-MADJAR, A. N90-20010
VIECELLI, J. A. N90-19579
N90-19580
VIELMO, P. N90-19993
VILLALON, ELENA N90-19855
VINCENT, J. N90-19837
VINCENT, MARK A. N90-19953
N90-19965
VIRKAR, ANIL V. N90-19371
VLIEGER, H. N90-19228
VOELS, STEPHEN ARTHUR N90-19982
VOELZKE, HOLGER N90-19618
VOLAKIS, JOHN L. N90-19309
VONMOERS, FALK N90-19581
VOOK, F. L. N90-19893
VUONG-ADLERBERG, INGMAR N90-19519

W

WADE, WILLIAM L., JR. N90-19306
WAGNER, R. N90-19488
WAHLQUIST, HUGO D. N90-19943
WALCOTT, BRUCE L. N90-19420
WALKER, MARK N90-19779
WALKHOFF, LUTZ-RUEDIGER N90-19512
WALLERSTEIN, E. P. N90-19361
WALTER, A. N90-19545
WALTERS, MICHAEL KENT N90-19717
WALTERS, ROBERT A. N90-19879
WALTON, E. N90-19466
WANG, N. N90-19466
WANG, SHIKUN N90-19796
WARNICK, JAMES S. N90-19845
WARREN, R. W. N90-19589
WARRINGTON, D. E. N90-19361
WATSON, J. M. N90-19589
WATT, ROBERT G. N90-19590
WEBER, MICHAEL E. N90-19584
WEESE, J. F. N90-19451
WEFEL, JOHN P. N90-19984
N90-20040
WEIDER, DIETMAR N90-19891
WEINSTEIN-LLOYD, JUDITH N90-19730
WEIR, J. T. N90-19578
WELCH, JEANNE A. N90-19318
WELLMAN, G. W. N90-19247
WENSKUS, RUPERT N90-19209
WEST, A. C. N90-19325
WHANGBO, M.-H. N90-19898
WHIPPLE, JANET C. N90-19555

WHITAKER, KEVIN W. N90-19421
WHITE, J. N90-19840
WHITMORE, STEPHEN A. N90-19224
WIENS, GLORIA J. N90-19422
WIERINGA, ROEL N90-19918
WIJCHERS, T. N90-19561
WILHELM, W. E. N90-19780
WILL, CLIFFORD M. N90-19941
N90-19946
WILLIAMS, G. N90-19258
WILLMS, K. A. N90-19331
WILSON, HOWARD B. N90-19423
WILSON, JOHN W. N90-20036
WILSON, W. J. N90-19260
WINTER, EDGAR R. F. N90-19540
WITMER, RICHARD N90-19648
WITTE, DAVID J. N90-19563
WOLD, A. N90-19339
N90-19901
N90-19902
N90-19903
WOLF, EMIL N90-19591
WOLFE, JAMES F. N90-19365
WOLFER, W. G. N90-19383
WONG, WILLIAM C. N90-19269
WOOD, CHARLES N90-19884
WOOD, KENT S. N90-19956
WOODWARD, RICHARD P. N90-19242
WOOLSTON, T. L. N90-19573
WORDEN, PAUL W., JR. N90-19963
WORRELL, WAYNE L. N90-19513
WRIGHT, ROBERT E., JR. N90-19555
WRIGHT, ROBERT L. N90-19249
WU, P. N90-19902
WYATT, J. N90-19491

X

XU, KAIWEN N90-19796

Y

YEE, J. H. N90-19459
YEN, WILLIAM N. N90-19372
YORKE, JAMES A. N90-19794
YOSHU, HISAHIRO N90-19912
YOUNG, JOSEPH W. N90-19214
YOUNG, LARRY E. N90-19973
YOUNG, RONALD B. N90-19424
YU, H. Y. N90-19338
YU, S. H. N90-19894

Z

ZEILER, THOMAS A. N90-19281
ZELLWEGER, JEAN-MICHEL N90-19388
ZHANG, CUN-QUAN N90-19785
N90-19786
ZHANG, XIAODONG N90-19806
ZHOU, ZHEN-LEI N90-19599
ZIMMERMAN, M. N90-19264
ZIMMERMAN, ROGER M. N90-19551
ZIMMERMANN, WALTER N90-19888
ZOCCO, T. N90-19358
ZUCCARIFERNANDESBRAGA, CLAUDIA N90-19636

Typical Corporate Source Index Listing

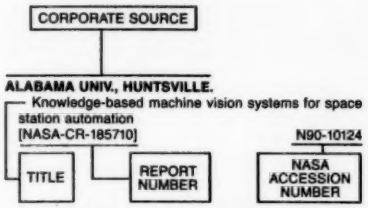

Listings in this index are arranged alphabetically by corporate source. The title of the document provides the user with a brief description of the subject matter. The report number helps to indicate the type of document cited (e.g., NASA report, translation, NASA contractor report). The NASA accession number denotes the number by which the citation is identified. The titles are arranged under each corporate source in ascending accession number order.

A

ACADEMY OF SCIENCES, GRAZ (AUSTRIA).
Gas diffusion in a cometary crust N90-20017

ACADEMY OF SCIENCES (USSR), NOVOSIBIRSK.
Negative ion surface plasma source development for plasma trap injectors in Novosibirsk
[DE90-006082] N90-19856

ADVISORY GROUP FOR AEROSPACE RESEARCH AND DEVELOPMENT, NEUILLY-SUR-SEINE (FRANCE).
The Uniform Engine Test Programme
[AGARD-AR-248] N90-19232

AEROSPACE MEDICAL RESEARCH LABS., WRIGHT-PATTERSON AFB, OH.
A new method for measuring the transmissivity of aircraft transparencies
[AD-A216953] N90-19842

AIR FORCE GEOPHYSICS LAB., HANSCOM AFB, MA.
MAX 1991. The active sun: A plan for pursuing the study of the active sun at the time of the next maximum in solar activity, January 1985
[NASA-CR-186125] N90-20030

AIR FORCE INST. OF TECH., WRIGHT-PATTERSON AFB, OH.
Series reversion/inversion of Lambert's time function
[AD-A216243] N90-19245
Green's functions for a theoretical model of an aperture fed stacked-patch microstrip antenna
[AD-A216280] N90-19455

AIR FORCE OFFICE OF SCIENTIFIC RESEARCH, BOLLING AFB, WASHINGTON, DC.
Proceedings of Air Force Office of Scientific Research workshop on Laser Propulsion
[AD-A216563] N90-19569

AIR FORCE WEAPONS LAB., KIRTLAND AFB, NM.
ARGUS/LLNL IR camera calibration and characterization
[AD-A217076] N90-19563

AIR WAR COLL., MAXWELL AFB, AL.
The global positioning system
[AD-A217266] N90-19222
Interoperability issues in the use of satellite-based navigation systems for civil aviation purposes
[AD-A217279] N90-19223
Limitations of the conventional role of the B-1B in the European theater
[AD-A217285] N90-19230
Orbital servicing: Issue or answer
[AD-A217284] N90-19295
Pilot candidate selection
[AD-A217296] N90-19742

ALABAMA A & M UNIV., HUNTSVILLE.
Augmenting and updating NASA spacelink electronic information system N90-19392

ALABAMA UNIV., HUNTSVILLE.
Effects of turbulence mixing, variable properties, and vaporization on spray droplet combustion
[NASA-CR-186463] N90-19326
Research Reports: 1989 NASA/ASEE Summer Faculty Fellowship Program
[NASA-CR-183837] N90-19390
Analytical optical scattering in clouds N90-19413
Frequency response of electrochemical cells N90-19419
The influence of a wall function on turbine blade heat transfer prediction N90-19421
Techniques for studying the effects of microgravity on model particle/cell systems N90-19424

ALABAMA UNIV., TUSCALOOSA.
Research Reports: 1989 NASA/ASEE Summer Faculty Fellowship Program
[NASA-CR-183837] N90-19390
Determination of the implementation of the 3-axis attitude motion simulator digital position controller N90-19409
ROCOPT: A user friendly interactive code to optimize rocket structural components N90-19415
A vectorized algorithm for 3D dynamics of a tethered satellite N90-19423

ALLIANCE TECHNOLOGIES CORP., BEDFORD, MA.
NAPAP (National Acid Precipitation Assessment Program) emissions inventory: Overview of allocation factors, 1985
[PB90-126012] N90-19679

AMERICAN SOCIETY OF MECHANICAL ENGINEERS, NAPERVILLE, IL.
Austempered ductile iron data base: A cooperative program between industry and the Trade Adjustment Assistance Program of the Department of Commerce
[PB90-115569] N90-19343

ANALYTICAL SERVICES AND MATERIALS, INC., HAMPTON, VA.
Performance of an optimized rotor blade at off-design flight conditions
[NASA-CR-4288] N90-19226

ARGONNE NATIONAL LAB., IL.
Activation of methane by transition metal-substituted aluminophosphate molecular sieves
[DE90-005663] N90-19331
Irradiation-induced amorphization and elastic shear instability in intermetallic compounds
[DE90-004845] N90-19341
Mitigation of stress corrosion cracking of AISI 304 stainless steel in oxygenated water at 289 C by organic species at low concentration
[DE90-005631] N90-19354
Experimental investigation of condensation of steam in the presence of noncondensable gases using plate heat exchangers
[DE90-002251] N90-19659
Transverse spin observables in chromodynamics
[DE90-005638] N90-19824
Analysis and evaluation of ZPPR (Zero Power Physics Reactor) critical experiments for a 100 kilowatt-electric space reactor
[DE90-005634] N90-19835
Superconductivity in Ba(1-x)BiO3
[DE90-003781] N90-19869
From invention to innovation: Commercialization of new technology by independent and small business inventors
[DE90-006944] N90-19927
Cosmic ray events in Soudan 2
[DE90-005657] N90-20037
Underground muons from the direction of Cygnus X-3
[DE90-005646] N90-20038

ARIZONA UNIV., TUCSON.
Analysis of unsteady heat transfer by natural convection in a two-dimensional square cavity using a high order finite-volume method N90-19521
Evolution of midplate hotspot swells: Numerical solutions
[NASA-CR-186462] N90-19713
An analytic model of axisymmetric mantle plume due to thermal and chemical diffusion
[NASA-CR-186461] N90-19714
Stored mafic/ultramafic crust and early Archean mantle depletion
[NASA-CR-186460] N90-19715
Optically tunable gratings for optical interconnects
[AD-A216978] N90-19844
Large impact events and atmospheric evolution on the terrestrial planets N90-20028

ARMY ARMAMENT RESEARCH, DEVELOPMENT AND ENGINEERING CENTER, WATERVLIET, NY.
Modal analysis of nonprismatic beams: Uniform segment method
[AD-A216952] N90-19614

ARMY AVIATION SYSTEMS COMMAND, CLEVELAND, OH.
Theory of gearing
[NASA-RP-1212] N90-19593

ARMY BIOMEDICAL RESEARCH AND DEVELOPMENT LAB., FORT DETRICK, MD.
The pollution hazard assessment system: Documentation and users manual
[AD-A217108] N90-19706

ARMY COLD REGIONS RESEARCH AND ENGINEERING LAB., HANOVER, NH.
Data reduction of GOES (Geostationary Operational Environmental Satellite) information from DCP (Data Collection Platform) networks
[AD-A215844] N90-19637
Introduction to drilling technology N90-20002
First impressions of the comet drilling problem N90-20021

ARMY INST. FOR RESEARCH IN MANAGEMENT INFORMATION AND COMPUTER SCIENCES, ATLANTA, GA.
Generic distributed systems model
[AD-A217078] N90-19773

ARMY MATERIALS TECHNOLOGY LAB., WATERTOWN, MA.
A new model for hydrogen absorption in welds
[AD-A216951] N90-19347

ARMY TEST AND EVALUATION COMMAND, ABERDEEN PROVING GROUND, MD.
Human factors engineering testing of aircraft cockpit lighting systems
[AD-A216853] N90-19743

ASTRO AEROSPACE CORP., CARPINTERIA, CA.
Structures for remotely deployable precision antennas N90-19256

ATLANTIC RESEARCH CORP., ROME, NY.
Arrays for space applications N90-19265

AUBURN UNIV., AL.
Characterization of thunderstorm induced Maxwell current densities in the middle atmosphere N90-19391
Multibody modeling and verification N90-19422

AXIOMATIX, LOS ANGELES, CA.
Packet radio networks under dynamic jamming
[AD-A217094] N90-19475

B

BALL AEROSPACE SYSTEMS DIV., BOULDER, CO.
Remote Attitude Measurement Sensor (RAMS) N90-19271

BALLISTIC RESEARCH LABS., ABERDEEN PROVING GROUND, MD.
External flow computations for a finned 60mm ramjet in steady supersonic flight
[AD-A216998] N90-19233
Computational fluid dynamics method for low Reynolds number flow in a precessing/spinning, liquid filled cylinder with rounded endcaps
[AD-A216997] N90-19531

BATTELLE COLUMBUS LABS., OH.
The measurement, modeling, and prediction of traction for rocket propellant 1
[NASA-CR-185186] N90-19386

BATTELLE MEMORIAL INST., COLUMBUS, OH.
Ac loss measurements of two multifilamentary NbTi composite strands
[DE90-005388] N90-19304

BAYREUTH UNIV. (GERMANY, F.R.).
Transient photoconduction in doped polymers: Spatial and energetic disorder
[ETN-90-95917] N90-19376
Structures instabilities in filament liquid crystals
[ETN-90-95916] N90-19888
On dissipative states in narrow current-carrying superconducting filaments
[ETN-90-95915] N90-19889
BBN SYSTEMS AND TECHNOLOGIES CORP., CAMBRIDGE, MA.
Flight crew aiding for recovery from subsystem failures
[NASA-CR-181905] N90-19741
BDM CORP., ALBUQUERQUE, NM.
Near-field bistatic RCS (Radar Cross-Section) measurements
[AD-A217011] N90-19458
BELEIDSCOMMISSIE REMOTE SENSING, DELFT (NETHERLANDS).
Definition study of Laser Experimental Active Fluorsensor (LEAF)
[BCRS-88-18] N90-19582
Possible applications of remote sensing satellite pictures for the water quality management of the Frisian lakes, Netherlands
[BCRS-88-17] N90-19641
Possible applications of remote sensing in the preparatory phase of a land management project
[BCRS-88-19] N90-19642
Technical and administrative feasibility of microlight remote sensing applications for river boards
[BCRS-89-01] N90-19643
Segmentation of Side-Looking Airborne Radar (SLAR) images using a priori knowledge
[BCRS-89-03] N90-19644
Activities report in remote sensing
[ETN-90-95472] N90-19647
BIRMINGHAM UNIV. (ENGLAND).
Ion and electron interactions at thermal and suprathermal energies
[AD-A216905] N90-19323
BOEING COMMERCIAL AIRPLANE CO., SEATTLE, WA.
Assessment of crew workload measurement methods, techniques and procedures. Volume 2: Guidelines for the use of workload assessment techniques in aircraft certification
[AD-A217067] N90-19748
BOSTON UNIV., MA.
Research accomplishments and future goals in particle physics
[DE90-007296] N90-19830
BRIGHAM YOUNG UNIV., PROVO, UT.
Thermodynamic properties of supercritical mixtures
[DE90-006720] N90-19909
BRITISH BROADCASTING CORP., KINGSWOOD (ENGLAND).
Digital video: Studio signal processing
[BBC-RD-1989/14] N90-19476
A digital HDTV recorder using a cluster of four D1 DVTRs
[BBC-RD-1989/13] N90-19477
A waveform capture and storage unit and its use for investigating disturbances on digital transmission links
[BBC-RD-1989/17] N90-19478
BRITISH COLUMBIA UNIV., VANCOUVER.
The TISOL facility at TRIUMF
[DE90-006682] N90-19837
BROOKHAVEN NATIONAL LAB., UPTON, NY.
IEA (International Energy Agency) implementing agreement for a program of research and development on the production of hydrogen from water. Task 9: Hydrogen production
[DE90-007354] N90-19337
Nanolayer reactions in aluminum-metal interfaces
[DE90-004955] N90-19342
Glancing angle XAFS (X ray Absorption Fine Structure) and x ray reflectivity studies of transition-metal/aluminum interfaces
[DE90-005575] N90-19353
Laboratory studies of free radical reactions in cloudwater
[DE90-003961] N90-19730
Oxygenation and possible etching of high T(sub c) superconducting films by oxygen plasma
[DE90-004956] N90-19871
BROWN UNIV., PROVIDENCE, RI.
Preparation and characterization of alumina films prepared by a novel spray pyrolysis method
[AD-A217570] N90-19339
Preparation and properties of the system Cu(x)Pd(1-x)O (0 less than or equal to x less than or equal to 0.175)
[AD-A217567] N90-19901
Growth and characterization of gallium (III) oxide films
[AD-A217568] N90-19902
The preparation and properties of iron doped II-VI chalcogenides
[AD-A217569] N90-19903
BUNDESMINISTERIUM FUER FORSCHUNG UND TECHNOLOGIE, BONN (GERMANY, F.R.).
Project for the European space organization in the area of space debris
[REPT-29/89] N90-19290
Astronomy and astrophysics
[REPT-33/89] N90-19938

C

CALIFORNIA INST. OF TECH., PASADENA.
Proceedings of a contractors meeting on Combustion Rocket Propulsion Diagnostics of Reacting Flow
[AD-A216445] N90-19297
Parallel neural net path-planner on hypercube and transputer
[DE90-006324] N90-19777
Investigations of CuInSe2 thin films and contacts
[DE90-000301] N90-19886
CALIFORNIA UNIV., BERKELEY.
Interaction of an oblique shock wave with supersonic flow over a blunt body N90-19197
Vapor-liquid equilibria for complex mixtures with special emphasis on the critical region
[PB90-130345] N90-19324
Effects of nonuniform potential and current distributions in electrochemical systems
[DE90-007349] N90-19325
Infrared heterodyne spectroscopy of polyatomic molecules in circumstellar envelopes N90-19960
CALIFORNIA UNIV., BERKELEY. LAWRENCE BERKELEY LAB.
Effects of nonuniform potential and current distributions in electrochemical systems
[DE90-007349] N90-19325
CALIFORNIA UNIV., DAVIS.
Transport of atmospheric aerosols above the Sierra Nevada slopes
[PB90-120288] N90-19675
CALIFORNIA UNIV., LOS ANGELES.
Synthesis and properties of a novel catalyst for the combustion of methane
[PB90-127499] N90-19320
Mechano-caloric cooling device
[NASA-CR-186316] N90-19552
CALIFORNIA UNIV., SAN DIEGO.
Ion mixing and surface modification in metal-semiconductor systems
[DE90-007557] N90-19897
CALIFORNIA UNIV., SAN DIEGO, LA JOLLA.
Synthesis and chemistry of unsaturated metal nitrogen compounds
[AD-A216550] N90-19321
CALIFORNIA UNIV., SANTA BARBARA.
Gravitational radiation from rotating gravitational collapse N90-19944
Gravitational consequences of modern field theories N90-19947
General relativistic x ray (UV) polarization rotations as a quantitative test for black holes N90-19957
CAMBRIDGE UNIV. (ENGLAND).
Separation bubbles at high Reynolds number: Measurement and computation
[CUED/A-AERO/15] N90-19525
CARNEGIE-MELLON UNIV., PITTSBURGH, PA.
Numerical study of diffusion jet flames N90-19316
A parametric heat transfer study for cryogenic ball bearings in SSME HPOTP N90-19397
CASSINO UNIV. (ITALY).
Physical models of cometary nuclei: A review N90-19991
CATHOLIC UNIV. OF AMERICA, WASHINGTON, DC.
Modified independent modal space control of flexible structures N90-19597
Dynamics and control of robot manipulators with closed-kinematic chain mechanism N90-19598
Advanced control schemes and kinematic analysis for a kinematically redundant 7 DOF manipulator
[NASA-CR-186175] N90-19599
CENTER FOR NIGHT VISION AND ELECTRO-OPTICS, FORT BELVOIR, VA.
Reliability testing of the Hughes temperature controlled 1/4 watt split cycle cryogenic cooler (HD-1045 (V)/UA)
[AD-A216696] N90-19426
CENTRAL RESEARCH INST. OF ELECTRIC POWER INDUSTRY, TOKYO (JAPAN).
Development of ceramic combustor for low BTU gases. Design and basic combustion characteristics
[DE89-782287] N90-19363
Proposal of arc driving type fault current limiter
[DE89-782290] N90-19485
Development of the blackbody probe type pyrometer, part 1. Experimental study on the fundamental characteristics
[DE89-782288] N90-19553
Development of an atmospheric diffusion model in fog (1). Literature review of scavenging process by precipitation
[DE89-782318] N90-19676
Chemical composition of precipitation and wet/dry deposition of sulfur compounds around the coastal area
[DE89-782324] N90-19677
Geochemical survey on faults overland with alluvial deposits, part 1. Application for the Neodani and the Atera faults survey
[DE89-782326] N90-19707
Lightning surge characteristics of transmission towers. Lightning surge characteristics of 15-meter-high scale model tower
[DE89-782322] N90-19721
CENTRE NATIONAL DE LA RECHERCHE SCIENTIFIQUE, SAINT MARTIN D'HERES (FRANCE).
Physical processes in cometary ices inferred from laboratory studies N90-19996
Laboratory studies of cometary ice analogues N90-19997
A method of estimating temperature profiles and chemical differentiation in the near surface layers of porous comet nuclei: First results for comet P/Churyumov-Gerasimenko N90-20013
Some considerations on cohesive forces in sun-grazing comets N90-20015
CHICAGO UNIV., IL.
The Advanced Composition Explorer
[DE90-006522] N90-19987
CITY UNIV., LONDON (ENGLAND).
Recalibrating software reliability models
[NASA-CR-186407] N90-19763
CLARKSON UNIV., POTSDAM, NY.
Simulation of thermal dynamics of a vaporizing coal-water droplet in a combustor
[DE90-005356] N90-19317
CLAUSER (J. F.) AND ASSOCIATES, LIVERMORE, CA.
Ultra-sensitive inertial sensors via neutral-atom interferometry N90-19977
COLOGNE UNIV. (GERMANY, F.R.).
The EURAD Model: Structure and First Results
[REPT-61] N90-19680
Development and status of the EURAD project N90-19681
The mesoscale meteorological model MM4 and its modifications for EURAD N90-19682
The Chemical Transfer Model (CTM) of EURAD: Development status N90-19683
Simulation of the propagation of radiactive substances from the example of Chernobyl (USSR) N90-19685
Simulation of a weather situation with high ozone concentrations during ALPEX N90-19686
GeoNet 88: Calculation connection system concept for the EURAD project N90-19688
Control of the RADM chemistry mechanism of the gas phase N90-19690
On the question of spray effects N90-19691
Cloud parameterization in EURAD and its future development N90-19692
Validation of the EURAD cloud modules N90-19693
Initialization of EURAD. Part 1: Utilization of ECMWF analysis data N90-19695
Initialization of EURAD, part 2 N90-19696
Boundary layer parameterization in CTM and MM4 N90-19697
Modelization of dry deposition in the Chemical Transport Model (CTM) of EURAD N90-19698
Emission data for the EURAD project N90-19700
The EURAD model in EUROTRAC N90-19701
The atmospheric energy cycle of stationary and transient waves
[ISSN-0069-5882] N90-19728
Digital simulation of a Boenline
[ISSN-0069-5882] N90-19729
Dynamics of crust formation and dust emission of comet nucleus analogues under isolation N90-20020
COLORADO STATE UNIV., FORT COLLINS.
Low temperature elastic and dielectric properties of incommensurate barium sodium niobate
[AD-A216969] N90-19815
COLORADO UNIV., BOULDER.
Neurocontrol systems and wing-fluid interactions underlying dragonfly flight N90-19240
Adaptive, asynchronous stochastic global optimization algorithms for sequential and parallel computation
[AD-A217093] N90-19775
Applied general relativity N90-19950
O-star parameters from line profiles of wind-blanketed model atmospheres N90-19982

COMPOSITE OPTICS, INC., SAN DIEGO, CA.
Unfurlable, continuous-surface reflector concept N90-19257
CONSULTEC SCIENTIFIC, INC., KNOXVILLE, TN.
Assessment of research needs for laser technologies applied to advanced spectroscopic methods
[DE90-007402] N90-19588
CORNELL UNIV., ITHACA, NY.
Development and utilization of new diagnostics for dense-phase pneumatic transport
[DE90-006787] N90-19536
Molecular theory and computer simulation studies of natural and synthetic gas mixtures
[PB90-130329] N90-19826
Search for far infrared radiation from optically pumped defect modes
[AD-A216976] N90-19843
Deceit: A flexible distributed file system
[NASA-CR-186412] N90-19923
COUNCIL FOR NATIONAL ACADEMIC AWARDS (ENGLAND).
Evaluation of repeated impact damage in composite structures N90-19303

D

DEFENCE AND CIVIL INST. OF ENVIRONMENTAL MEDICINE, DOWNSVIEW (ONTARIO).
Queuing theory approach to modelling the dynamics of the human-computer interface
[AD-A216870] N90-19788
DEFENCE RESEARCH ESTABLISHMENT, OTTAWA (ONTARIO).
An investigation of the transfer of monopulse tracking between two coherent point sources
[AD-A217007] N90-19457
DEPARTMENT OF ENERGY, WASHINGTON, DC.
Atmospheric Radiation Measurement Program plan
[DE90-006349] N90-19705
The ultimate structure of matter: The high energy physics program from the 1950s through the 1980s
[DE90-005682] N90-19836
DEPARTMENT OF THE ARMY, WASHINGTON, DC.
Fast optical switch and limiter using quantum size effect in metal grain composites
[AD-D014332] N90-19305
Heterogeneous composite and method of making
[AD-D014337] N90-19306
Temperature compensated crystal oscillator (TCXO) with improved temperature compensation
[AD-D014334] N90-19482
Lightning protection apparatus for RF equipment and the like
[AD-D014336] N90-19483
DEPARTMENT OF THE NAVY, WASHINGTON, DC.
A high optical density measuring spectrometer
[AD-D014331] N90-19318
Conductive polymers of transition-metal complexes coordinated by a Diamino-Dichalcogen-Benzene compound
[AD-D014326] N90-19360
Apparatus and method for minimizing polarization-induced signal fading in an interferometric fiber-optic sensor using input-polarization modulation
[AD-D014315] N90-19430
Automatic thresholding multichannel digital radar early warning system
[AD-D014323] N90-19431
High throughput data communication system
[AD-D014342] N90-19432
Dual frequency launcher for circularly polarized antenna
[AD-D014361] N90-19456
Active phase and amplitude modulator
[AD-D014318] N90-19480
Discontinuous-taper directional coupler
[AD-D014324] N90-19481
Internal transmission line filter element
[AD-D014353] N90-19489
Elastomeric electrical isolation membrane
[AD-D014365] N90-19490
Optical paramagnetic/diamagnetic gas sensor
[AD-D014368] N90-19554
CO2 laser plus optimization for harmonic generation
[AD-D014341] N90-19565
Narrow-bandwidth unstable laser resonator
[AD-D014362] N90-19568
Jam resistant fluid power actuator for ballistic-damage tolerant redundant cylinder assemblies
[AD-D014360] N90-19600
Phase control mechanism for wave energy conversion
[AD-D014354] N90-19657
High speed modem
[AD-D014319] N90-19750
Thermal modulation of light beams
[AD-D014322] N90-19840
All-fiber SFPM (Stimulated Four Photon Mixing) amplifier
[AD-D014358] N90-19841
Passivating layer for III-V semiconductor materials
[AD-D014321] N90-19872
DEUTSCHE FORSCHUNGS- UND VERSUCHSANSTALT FUER LUFT- UND RAUMFAHRT, STUTTGART (GERMANY, F.R.).
Solar and thermic utilization in high temperature area: Research and development
[ETN-90-96062] N90-19683
DEUTSCHE FORSCHUNGSANSTALT FUER LUFT- UND RAUMFAHRT, COLOGNE (GERMANY, F.R.).
Crustal strength of different model comet materials N90-20003
Fracture mechanical aspects of dust emission processes from a model comet surface N90-20004
DEUTSCHE GEODAETISCHE KOMMISSION, MUNICH (GERMANY, F.R.).
Development and testing of a universally implementable recording aligning system
[SER-C-349] N90-19716
Digital production of perspective images
[SER-C-347] N90-19768
DEUTSCHE GESELLSCHAFT FUER CHEMISCHES APPARATEWESEN (DECHEMA), FRANKFURT AM MAIN (GERMANY, F.R.).
Influence of heat treating on the mechanical values and the stability of heat barrier coatings
[ETN-90-95902] N90-19375
DEUTSCHER WETTERDIENST, OFFENBACH AM MAIN (GERMANY, F.R.).
Pyranometry
[DWD-14] N90-19661
Wind conditions near the ground in Federal Republic of Germany
[ISBN-3-88148-248-2] N90-19727
DHV RAADGEVEND INGENIEURSBUREAU B.V., AMERSFOORT (NETHERLANDS).
Possible applications of remote sensing satellite pictures for the water quality management of the Frisian lakes, Netherlands
[BCRS-88-17] N90-19641
DIGITAL SIGNAL CORP., SPRINGFIELD, VA.
Applications of FM-CW laser radar to antenna contour mapping N90-19270
DOUGLAS AIRCRAFT CO., INC., LONG BEACH, CA.
Assessment of crew workload measurement methods, techniques and procedures. Volume 2: Guidelines for the use of workload assessment techniques in aircraft certification
[AD-A217067] N90-19748

E

EDINBURGH UNIV. (SCOTLAND).
An optical and infrared study of blazars N90-19930
EG AND G MOUND APPLIED TECHNOLOGIES, MIAMISBURG, OH.
Ignition of HMX (cyclotetramethylenetetranitramine) using low energy laser diodes
[DE90-007637] N90-19334
EIDGENOESSISCHES INST. FUER SCHNEE- UND LAWINENFORSCHUNG, WEISSFLUHJOCH/DAVOS (SWITZERLAND).
Laboratory techniques for the characterisation of snow structures N90-20007
ENVIRONMENTAL ANALYSIS AND REMOTE SENSING, DELFT (NETHERLANDS).
Technical and administrative feasibility of microlight remote sensing applications for river boards
[BCRS-89-01] N90-19643
ENVIRONMENTAL RESEARCH INST. OF MICHIGAN, ANN ARBOR.
ARGUS/LLNL IR camera calibration and characterization
[AD-A217076] N90-19563
ERLANGEN-NUREMBERG UNIV. (GERMANY, F.R.).
Information reconstruction from speckle interferograms
[ETN-90-95918] N90-19939
ESDU INTERNATIONAL LTD., LONDON (ENGLAND).
Calculation of excrescence drag magnification due to pressure gradient at high subsonic speeds
[ESDU-87004] N90-19195
Heat transfer definitions and equations
[ESDU-89022] N90-19522
Information on the use of data items on hot structures
[ESDU-89021] N90-19611
Steady state temperatures and thermal stresses in a spherical or cylindrical laminated shell
[ESDU-89027] N90-19612
Temperatures in plates subjected to a sudden increase in recovery temperature
[ESDU-89026] N90-19904
ESSEN UNIV. (GERMANY, F.R.).
Utilization of thermometric methods for the testing of carbon reinforced plastics
[ETN-90-96076] N90-19314
An optical white light speckle process in forward dispersion for measurement of the velocity field in free convective currents
[ETN-90-95913] N90-19548
EUROPEAN SPACE AGENCY, PARIS (FRANCE).
Physics and Mechanics of Cometary Materials
[ESA-SP-302] N90-19989
EUROPEAN SPACE AGENCY. EUROPEAN SPACE RESEARCH AND TECHNOLOGY CENTER, ESTEC, NOORDWIJK (NETHERLANDS).
ESRIN
[ESA-BR-58] N90-19631
Rosetta/CNSR, ESA's planetary cornerstone mission N90-19990
EXECUTIVE OFFICE OF THE PRESIDENT, WASHINGTON, DC.
National Action Plan on Superconductivity Research and Development
[PB89-138512] N90-19883

F

FEDERAL AVIATION ADMINISTRATION, ATLANTIC CITY, NJ.
In-flight evaluations of turbine fuel extenders
[DOT/FAA/CT-89/33] N90-19387
Operational evaluation of initial data link air traffic control services, volume 1
[DOT/FAA/CT-90/1-VOL-1] N90-19472
FEDERAL AVIATION ADMINISTRATION, WASHINGTON, DC.
Evaluation of the Scott aviation portable protective breathing device for contaminant leakage as prescribed by FAA Action Notice A-8150.2. Phase 1: Original tests of the portable protective breathing device. Phase 2: Tests of the redesigned portable protective breathing device
[AD-A216799] N90-19214
Symposium on air traffic control training for tomorrow's technology
[PB90-127325] N90-19216
FLORIDA UNIV., GAINESVILLE.
Transmission and reflection studies of thin films in the vacuum ultraviolet N90-19412
FORSCHUNGSINSTITUT FUER HOCHFREQUENZPHYSIK, WERTHHOVEN (GERMANY, F.R.).
Aspects of VHF radars illustrated by the example of an experimental system
[REPT-1-89] N90-19468
FRAUNHOFER INST. FUER WERKSTOFFMECHANIK, FREIBURG (GERMANY, F.R.).
Three-dimensional Fe analysis of the surface distribution in notched compact samples of 20 MnMoNi 55
[W-1/89] N90-19625

G

GENERAL ATOMIC CO., SAN DIEGO, CA.
FOMA: A Fast Optical Multichannel Analyzer
[DE90-004093] N90-19839
GENERAL ELECTRIC CO., PHILADELPHIA, PA.
Safety Status Report for the Ulysses mission. Book 1: Accident analysis. General purpose heat source radioisotope thermoelectric generator program
[DE90-006829] N90-19285
Safety Status Report for the Ulysses mission. Book 2: Accident analysis-appendices. General purpose heat source radioisotope thermoelectric generator program
[DE90-006830] N90-19286
GENEVA OBSERVATORY (SWITZERLAND).
Magnetic fields in late-type dwarfs: Preliminary results from a multiline approach
[SER-C-PREPUB-FASC-31] N90-19928
GEORGE WASHINGTON UNIV., WASHINGTON, DC.
Electron stimulated O(-) desorption from O2 condensed on a rare-gas film: Evidence for an indirect Bounce trajectory
[AD-A216725] N90-19322
A nonparametric software reliability growth model
[NASA-CR-186438] N90-19764
GEORGIA INST. OF TECH., ATLANTA.
Rapid near-optimal trajectory generation and guidance law development for single-stage-to-orbit airbreathing vehicles
[NASA-CR-186299] N90-19275
Integrated optics anisotropic waveguides and devices
[AD-A217064] N90-19849

Overview of recent results from the Advanced Toroidal Facility
[DE90-005673] N90-19853

GEORGIA UNIV., ATHENS.
Optical studies of dynamical processes in disordered materials
[DE90-007080] N90-19372

GINER, INC., WALTHAM, MA.
Advanced double layer capacitor
[AD-A217110] N90-19518

GOETTINGEN UNIV. (GERMANY, F.R.).
Experimental study of validity of the unstationary Kutta condition, with high Strouhal numbers
[ETN-90-95914] N90-19547

GOSUDARSTVENNYI KOMITET PO ISPOLZOVANIYU ATOMNOI ENERGII, SERPUKHOV (USSR).
Classical mechanics on superspace
[DE90-606907] N90-19906

H

HAMPTON UNIV., VA.
Anomalous transport in toroidal plasmas
[DE90-006549] N90-19859

HARVARD-SMITHSONIAN CENTER FOR ASTROPHYSICS, CAMBRIDGE, MA.
New tests with old data N90-19968

HARVARD UNIV., CAMBRIDGE, MA.
Theory and applications of belief functions
[AD-A217092] N90-19774
Tunneling microscopy of submonolayer adsorbates on Si3
[AD-A216885] N90-19876

HAWAII UNIV., HONOLULU.
On linear structure and phase rotation invariant properties of block 2(sup l)-PSK modulation codes
[NASA-CR-186308] N90-19429

HEAT PUMP TECHNOLOGY CENTER OF JAPAN, TOKYO.
Survey on the social and economic influences of wide-spreading heat-pump technology
[DE89-782294] N90-19526
Operational fact-finding report on heat pump systems for industrial use
[DE89-782295] N90-19527

HEIDELBERG UNIV. (GERMANY, F.R.).
Implementation of a finite element process for the Euler equations of the gas dynamics
[PREPRINT-500] N90-19545
Simulation of global Kr-85 and (14)CO2 distribution by means of a time-dependent, two dimensional model of the atmosphere
[ETN-90-95376] N90-19702

HELSINKI UNIV. OF TECHNOLOGY, ESPOO (FINLAND).
Vector circuit theory for multilayered isotropic and chiral structures: Reflection and transmission
[PB90-122474] N90-19495

HIROSHIMA UNIV., TAKEHARA (JAPAN).
Reparametrization BRS cohomology in two-dimensional gravity and non-critical string theories
[DE90-741468] N90-19911
Quantum field theory on higher-genus Riemann surfaces
[DE90-741469] N90-19912
Linearized analysis of (2+1)-dimensional Einstein-Maxwell theory
[DE90-741470] N90-19913

HOCHSCHULE DER BUNDESWEHR, HAMBURG (GERMANY, F.R.).
A contribution to the theory of transient conductor simulations
[ETN-90-95891] N90-19511
Security calculations of rip reached construction elements by means of probabilistic breaking mechanics and a Markov process
[ETN-90-95890] N90-19624

HOUSTON UNIV., CLEAR LAKE, TX.
Development of an Ada programming support environment database SEAD (Software Engineering and Ada Database) administration manual
[NASA-CR-186064] N90-19757
Object Oriented Programming Systems (OOPS) and frame representations: An investigation of programming paradigms
[NASA-CR-186084] N90-19758

HOUSTON UNIV., TX.
Diffraction studies of the structure of glasses and liquids
[DE90-007662] N90-19381

I

IDAHO NATIONAL ENGINEERING LAB., IDAHO FALLS.
Hydrogen assay foil counting system
[DE90-007415] N90-19332

IIT RESEARCH INST., BARTLESVILLE, OK.
Using image analysis to determine petrophysical properties of reservoir rocks
[DE90-000222] N90-19649
Application of natural isotopes in groundwater for solving environmental problems
[DE90-000223] N90-19703

ILLINOIS UNIV., CHICAGO.
Potential theory of radiation N90-19395
Theory of gearing
[NASA-RP-1212] N90-19593

ILLINOIS UNIV., URBANA.
The III-V semiconductor quantum well lasers and related optoelectronic devices on silicon
[AD-A216960] N90-19570

INSTITUT D'ASTROPHYSIQUE, PARIS (FRANCE).
Cometary bodies in the circumstellar disk around beta Pictoris N90-20010

INSTITUT FRANCO-ALLEMAND DE RECHERCHES, SAINT-LOUIS (FRANCE).
A study on upstream moving pressure waves induced by vortex separation
[ISL-CO-203/88] N90-19192

INSTITUTE FOR COMPUTER APPLICATIONS IN SCIENCE AND ENGINEERING, HAMPTON, VA.
Application of a Reynolds stress turbulence model to the compressible shear layer
[NASA-CR-182002] N90-19537
Analytical methods for the development of Reynolds stress closures in turbulence
[NASA-CR-182017] N90-19538
Conforming Chebyshev spectral collocation methods for the solution of laminar flow in a constricted channel
[NASA-CR-182011] N90-19539
On the parallel efficiency of the Frederickson-McBryan multigrid
[NASA-CR-181999] N90-19791

INSTITUTE FOR PERCEPTION RVO-TNO, SOESTERBERG (NETHERLANDS).
Vestibular examination of motion sick student pilots
[IZF-1988-22] N90-19738
Processing infrared images for target detection: A literature study
[IZF-1988-12] N90-19847

INSTITUTE OF ENERGY ECONOMICS OF JAPAN.
Analysis of competition among kinds of energy at the era of complexed energy. (Report on overseas study)
[DE89-910213] N90-19650
Vision for the introduction of the wind power generation system. Survey on the prospective market, part 2
[DE89-910386] N90-19651

INSTITUTO DE PESQUISAS ENERGETICAS E NUCLEARES, SAO PAULO (BRAZIL).
Processing of advanced ceramics using microwaves thermal treatments
[DE90-606349] N90-19362

INSTITUTO DE PESQUISAS ESPACIAIS, SAO JOSE DOS CAMPOS (BRAZIL).
Self-tuning control techniques, implicit and explicit, with parameter estimation in Kalman filters, applied to artificial satellite attitude
[INPE-4857-TDL/368] N90-19276
Attitude and spin rate control of a spinning satellite using geomagnetic field
[INPE-4818-NTE/289] N90-19277
Construction and characterization of a valve for rapid gas injection
[INPE-4789-RPE/583] N90-19486
Monostable electrovalve
[INPE-4928-RPE/595] N90-19487
A method for determination of control pixels for LANSAT using a reflector
[INPE-4884-PRE/1491] N90-19632
Areas of aquatic macrophytes classified through vegetative indexes extracted from LANDSAT/TM imagery
[INPE-4880-PRE/1489] N90-19633
Availability of multitemporal LANDSAT data accompanying the variation of water surfaces in the program area of Careiro PDRI/AM
[INPE-4898-PRE/1496] N90-19634
Analysis of photogeologic lineaments in the Ithacare (BA) region: A proposed methodology
[INPE-4855-PRE/1478] N90-19635
Satellite imagery for water quality assessment in coastal regions
[INPE-4891-PRE/1492] N90-19636
Study of the optimization of reference parameters to the dynamic constraints of solar panels
[INPE-4793-TDL/355] N90-19656
Analysis of tectonic movements utilizing remote sensor products in the Southern Espinhaco (SE) region
[INPE-4830-PRE/1451] N90-19708
Cyclogeneses and extratropical cyclones in the south-southeast region of Brazil and its influence in time
[INPE-4812-TDL/359] N90-19722
An observational study of squall lines in the Amazon
[INPE-4865-TDL/376] N90-19723
Evolution of finite amplitude baroclinic waves in the atmosphere and ocean
[INPE-4752-TDL/346] N90-19733
The 0-1 multiknapsack problem: Heuristic and reduction methods
[INPE-4894-PRE/1495] N90-19782
Plasma centrifuge with vacuum arc discharge applied to the separation of stable isotopes
[INPE-4925-TDL/385] N90-19854
Visibility problems in numerical models of terrain
[INPE-4921-TDL/382] N90-19919

INTERNATIONAL CENTRE FOR THEORETICAL PHYSICS, TRIESTE (ITALY).
Exchange and correlation effects in the Visscher-Falicov model for metal intercalated graphite
[DE90-610553] N90-19349
Radiation of electromagnetic waves by an accelerated charged particle in medium
[DE90-610458] N90-19461
Propagation of electromagnetic waves in multidimensional homogeneous cosmologies
[DE90-610474] N90-19462
Dislocation annihilation mechanism for the formation of dislocation free zone at a crack tip
[DE90-610552] N90-19615
Uniqueness of closure of the constraint algebra for quantum gravity
[DE90-610476] N90-19712
Differential operators associated with Gegenbauer polynomials. 3: The regular case
[DE90-610422] N90-19795
Superconformal algebra on meromorphic vector fields with three poles on super-Riemann sphere
[DE90-610423] N90-19796
A method for computing the stationary points of a function subject to linear equality constraints
[DE90-610427] N90-19797
Banach C*-algebras not containing a subspace isomorphic to C(sub 0)
[DE90-610428] N90-19798
Iteration methods for solving nonlinear equations in Frechet spaces
[DE90-610429] N90-19799
On the approximative normal values of multivalued operators in topological vector space
[DE90-610430] N90-19800
Projection-iteration methods for solving nonlinear operator equations
[DE90-610433] N90-19801
Nonlinear interaction of electrostatic waves at a narrow inhomogeneous layer of a warm magnetoactive plasma
[DE90-610624] N90-19857
A storage process of the magnetic energy results from the unsteady plasma flow field in the space active regions and stellar atmosphere
[DE90-610638] N90-19858
A simple model for the determination of L(sub 0), D and tau in a semiconductor and their temperature dependence
[DE90-610564] N90-19879
Nucleation of vortices in superfluid helium-4
[DE90-610675] N90-19880
Goldstone excitation and symmetry breaking mechanism in superfluid He-4
[DE90-610676] N90-19881
Coherent state in the roton region of superfluid helium-4
[DE90-610677] N90-19882
On Einsteinization of background curved space in the induced quantum gravity
[DE90-610477] N90-19907
Disturbance structures and its magnetic field features in plasma comet tail
[DE90-610636] N90-19986

IOWA STATE UNIV. OF SCIENCE AND TECHNOLOGY, AMES.
Very high energy gamma ray astrophysics
[DE90-006545] N90-19983

ISTITUTO ELETTROTECNICO NAZIONALE (GALILEO FERRARIS), TURIN (ITLAY).
Evolution of ices and carbonaceous materials in the laboratory and in comets N90-19998

J

JAPAN ATOMIC ENERGY RESEARCH INST., TOKAI.
An attempt of improving high-temperature fatigue properties of Ni-Cr-W superalloys in HTGR helium
[DE90-741482] N90-19350
Record of forum on cold fusion
[DE90-749883] N90-19863
JAPAN ATOMIC ENERGY RESEARCH INST., TOKYO.
Effect of electron-excitation on radiation damage in ion-irradiated FCC metals
[DE90-719537] N90-19344
A complete description of robot manipulator dynamics based on Lagrangian mechanics
[DE90-741467] N90-19603
JAYCOR, FREMONT, CA.
Topics in HPM (High-Power Microwave) generation, coupling, and interaction
[AD-A216882] N90-19658
JET PROPULSION LAB., CALIFORNIA INST. OF TECH., PASADENA.
Millimeter radiometer system technology N90-19260
Synthetic Aperture Interferometric Radiometer (SAIR) N90-19261
Large antenna measurement and compensation techniques N90-19263
Precision segmented reflector, figure verification sensor N90-19272
The Telecommunications and Data Acquisition Report
[NASA-CR-185033] N90-19434
Determination of Earth orientation using the Global Positioning System N90-19435
Simple analytic potentials for linear ion traps N90-19436
Microwave oscillator with reduced phase noise by negative feedback incorporating microwave signals with suppressed carrier N90-19437
Effect of laser frequency noise on fiber-optic frequency reference distribution N90-19438
Thermal coefficient of delay for various coaxial and fiber-optic cables N90-19439
Performance of the all-digital data-transition tracking loop in the advanced receiver N90-19440
Costas loop lock detection in the advanced receiver N90-19441
Photon statistical limitations for daytime optical tracking N90-19442
Memory management in traceback Viterbi decoders N90-19443
Some easily analyzable convolutional codes N90-19444
Quantization effects in Viterbi decoding rate 1/n convolutional codes N90-19445
Big Viterbi Decoder (BVD) results for (7,1/2) convolutional code N90-19446
Fast transform decoding of nonsystematic Reed-Solomon codes N90-19447
Application of adaptive least-squares algorithm to multi-element array signal reconstruction N90-19448
The effects of sinusoidal interference on the second-order carrier tracking loop preceded by a bandpass limiter in the Block 4 receiver N90-19449
Disturbance torque rejection properties of the NASA/JPL 70-meter antenna axis servos N90-19450
Parkes radio science system design and testing for Voyager Neptune encounter N90-19451
The 32-GHz performance of the DSS-14 70-meter antenna: 1989 configuration N90-19452
Detecting gravity waves from binary black holes N90-19943
Advanced Doppler tracking experiments N90-19951
Pulsar timing and gravitational waves N90-19955
Icarus lander N90-19964
Gravitational experiments on a solar probe mission: Scientific objectives and technology considerations N90-19966
High stability radio links N90-19970
Tropospheric monitoring technology for gravity wave experiments N90-19971
Improved ranging systems N90-19973
Inertial corrections by dynamic estimation N90-19976
JOHANN-WOLFGANG-GOETHE-UNIV., FRANKFURT AM MAIN (GERMANY, F.R.).
Numerical modeling of atmospheric growth processes
[REPT-70] N90-19726
JOHNS HOPKINS UNIV., BALTIMORE, MD.
Investigation of the processes controlling the flame generation of refractory materials
[DE90-007564] N90-19333
Direct detection optical intersatellite link at 220 Mbps using AlGaAs laser diode and silicon APD with 4-ary PPM signaling
[NASA-CR-186380] N90-19460
Ultraviolet observations of the atmosphere of Io and the plasma torus N90-19929
Nearly simultaneous optical, ultraviolet, and x ray observations of three PG quasars
[NASA-CR-186355] N90-19932
Far-ultraviolet spectroscopy of Comet Halley N90-19979
JOINT INST. FOR LAB. ASTROPHYSICS, BOULDER, CO.
Optical interferometer in space N90-19953
Small Mercury Relativity Orbiter N90-19965

K

KANSAS UNIV. CENTER FOR RESEARCH, INC., LAWRENCE.
Rain radars for earth science geostationary platforms: Some possibilities N90-19262
KARLSRUHE UNIV. (GERMANY, F.R.).
Wind tunnel design of heat island turbulent boundary layer
[IHW-ET/50] N90-19542
KENTUCKY UNIV., LEXINGTON.
Yaw rate control of an air bearing vehicle N90-19420
KERNFORSCHUNGSANLAGE, JUELICH (GERMANY, F.R.).
Implementation of the RADM/EURAD models on the great calculation system of the Juelich KFA N90-19687
Comparison of a 6-layer and a 15-layer version of the Chemical Transfer Model (CTM) N90-19689
Estimation of the distribution of SO2 and NOX emission in Europe N90-19699
CO2 depth profiles in cometary model substances of KOSI N90-20014
KYOTO UNIV. (JAPAN).
Overview of recent results from the Advanced Toroidal Facility
[DE90-005673] N90-19853

L

L'GARDE, INC., TUSTIN, CA.
Advances in large inflatable reflectors N90-19258
LABORATORIO DE COMPUTACAO CIENTIFICA, RIO DE JANEIRO (BRAZIL).
Finite element approximations of the stokes flow problem based upon various variational principles
[DE90-608612] N90-19533
Error analysis of some Galerkin least squares methods for the elasticity equations
[DE90-608611] N90-19790
LAFAYETTE COLL., EASTON, PA.
Artificial intelligence issues related to automated computing operations N90-19404
LANGUAGE SERVICES, KNOXVILLE, TN.
Heat-resistant and anticorrosive paint
[DE90-006077] N90-19369
LASER TECHNOLOGY CENTER, KNOXVILLE, TN.
Laser Technology Center
[PB90-115387] N90-19564
LAWRENCE LIVERMORE NATIONAL LAB., CA.
High-purity beryllium foils
[DE90-006408] N90-19348
Time-dependent failure of silver-interlayer diffusion bonds between non-deforming base-metals
[DE90-006925] N90-19357
Elimination of platinum inclusions in phosphate laser glasses
[DE90-004479] N90-19361
Two-dimensional, long-pulse computer calculation of microwave-induced electron layer formation in low-pressure air
[DE90-005994] N90-19459
Sparse breakdown and statistical sneakthrough effects in low-altitude microwave propagation
[DE90-007252] N90-19473
Single antenna interferometry
[DE90-008120] N90-19474
Field effect transistor structures based on strain induced polarization charges
[DE90-007247] N90-19515
Design considerations in achieving 1 MW CW operation with a whispering-gallery-mode gyrotron
[DE90-007283] N90-19557
Progress in the CW operation of a 140 GHz gyrotron
[DE90-007382] N90-19558
Noise floors of subnanosecond transient recording systems
[DE90-002339] N90-19571
On 140 GHz microwave FEL experiments using ELF-2
[DE90-006764] N90-19576
Results of the PALADIN experiment
[DE90-006776] N90-19578
Linear theory of thermal blooming in turbulence
[DE90-007243] N90-19579
Turbulent mixing effects in models of thermal blooming
[DE90-007245] N90-19580
A ground state depleted laser in neodymium doped yttrium orthosilicate
[DE90-006773] N90-19586
Atmospheric thermal blooming and beam clearing by aerosol vaporization
[DE90-006271] N90-19711
Electron energy distributions and vibrational population distributions
[DE90-005550] N90-19825
Measurement of cross sections: New needs and possibilities
[DE90-007248] N90-19829
Electrical resistivity of strongly coupled plasmas in intense fields
[DE90-002236] N90-19861
Time-dependent two-dimensional radiation hydrodynamics of accreting matter onto highly magnetized neutron stars
[DE90-006927] N90-19985
Accretion flows in high mass star formation
[DE90-007251] N90-20027
LEIDEN UNIV. (NETHERLANDS).
A test of the interstellar dust model of comets N90-19995
LITEF, FREIBURG (GERMANY, F.R.).
Development of a standardized three axis sensor for inertial data achievement for future flight rule systems
[ETN-90-96075] N90-19231
LIVERPOOL UNIV. (ENGLAND).
Exploiting surface observations of cloudiness for globalscale nephanalyses N90-19719
LOCKHEED MISSILES AND SPACE CO., SUNNYVALE, CA.
Geostationary earth science platform concepts N90-19252
Large-diameter geostationary millimeter wavelength antenna concept N90-19254
Design of a low-frequency (5-20 GHz), 15-meter-diameter passive radiometer for geostationary earth science platforms N90-19255
LONDON UNIV. (ENGLAND).
Study of hydrazine metabolism and toxicity
[AD-A217103] N90-19736
LOS ALAMOS NATIONAL LAB., NM.
Muzzle shunt augmentation of conventional railguns
[DE90-007505] N90-19248
Low-cost small satellites for astrophysical missions
[DE90-007625] N90-19293
Identification and solution of a charging problem in a high-altitude detector
[DE90-008637] N90-19296
Creep behavior of alloys based on TiAl containing TiB2 and TiN particulates
[DE90-006489] N90-19355
Deformation and fracture of TiAl + W at elevated temperatures
[DE90-006490] N90-19356
Modification of surface mechanical properties of high-chromium tool steel by carbon-implanted codeposited Fe-Ti films
[DE90-007502] N90-19358
Defect structures in copper and gold irradiated with fast neutrons, 14 MeV neutrons and 600 to 800 MeV protons
[DE90-007529] N90-19359
Anode plasma formation as a possible mechanism for an electrical stress limit in cold cathode diodes
[DE90-007503] N90-19516
Time resolved gain/loss studies under low and high power loading for the XeF C-A transition
[DE90-007506] N90-19517
Potential biomedical application of the Los Alamos infrared free-electron laser: DNA spectroscopy
[DE90-006505] N90-19575
Blue upconversion thulium laser
[DE90-006517] N90-19584
Laser mass spectrometric studies of high temperature superconductor ablation
[DE90-006518] N90-19585
First direct observation of FEL (Free-Electron Laser) from lambda=20 to 45 microns
[DE90-007508] N90-19589
Laser-matter interaction at intensities of 10(sup 12) W/cm(sup 2) and below
[DE90-007536] N90-19590
Working on the moon: The Apollo experience
[DE90-003662] N90-19744
Object detection and amplitude estimation based on maximum a posteriori reconstructions
[DE90-007511] N90-19770
Image manipulation in the SIGGRAPH Interactive Proceedings
[DE90-007542] N90-19771

Rule matrices, degree vectors, and preimages for cellular automata
[DE90-007492] N90-19805
Nonlinear system vibration: The appearance of chaos
[DE90-007546] N90-19810
Computation at the edge of chaos: Phase transition and emergent computation
[DE90-007488] N90-19811
Fifth-order aberrations in magnetic quadrupole-octupole systems
[DE90-007489] N90-19831
Bose condensate in superfluid (sup 4)He and momentum distributions by deep inelastic scattering
[DE90-007541] N90-19832
The electron momentum-transfer cross sections of tungsten, silicon, and silicon dioxide at energies from 0.1 to 10,000 eV
[DE90-009041] N90-19833
Plasma simulation on magnetohydrodynamic time scales
[DE90-007490] N90-19865
An electrical model for plasma armature voltage
[DE90-007530] N90-19866
Microstructural simulations of dynamic recrystallization
[DE90-007504] N90-19895
Computer simulation of recrystallization in the presence of second phase particles
[DE90-007531] N90-19896
The renormalization group and lattice QCD
[DE90-004860] N90-19905
Construction of four-dimensional open superstrings
[DE90-006484] N90-19908
Searching for existing nuclear data
[DE90-007535] N90-19925
Neon novae, recurrent novae, and type I supernovae
[DE90-003188] N90-19931
The inverse-square law and quantum gravity N90-19949
The Advanced Composition Explorer
[DE90-006522] N90-19987
Getting lunar ilmenite: From soils or rocks
[NASA-CR-186496] N90-20029

LOUISIANA STATE UNIV., BATON ROUGE.
Nuclear interactions of high energy heavy ions and applications in astrophysics
[DE90-006691] N90-19984
A drift chamber telescope for high-Z particles
[NASA-CR-186497] N90-20040

M

MAHARISHI INTERNATIONAL UNIV., FAIRFIELD, IA.
The effects of cold dark matter on Big Bang nucleosynthesis N90-19749

MANKATO STATE COLL., MN.
Monte Carlo models and analysis of galactic disk gamma-ray burst distributions N90-19403

MARTIN MARIETTA LABS., BALTIMORE, MD.
Contact formation on (Hg,Cd) Te
[AD-A217088] N90-19900

MARYLAND UNIV., COLLEGE PARK.
Computation of hypersonic unsteady viscous flow over a cylinder N90-19194
Innovative design of composite structures: The use of curvilinear fiber format in structural design of composites
[NASA-CR-186406] N90-19308
P-T condition to deformation from fluid inclusions in mylonites
[NASA-CR-186377] N90-19710
Lessons learned in the transition to ADA from FORTRAN at NASA/Goddard
[NASA-CR-186458] N90-19765
Software development: A paradigm for the future
[NASA-CR-186456] N90-19766
The p- and h-p versions of the finite element method: An overview
[AD-A216902] N90-19789
Chaotic transients, higher dimensional phenomena, and coupled ordinary differential equations
[DE90-006641] N90-19794
Nonlinear continuum mechanics and applied analysis
[AD-A213629] N90-19812
Nonlinear mechanics of unstable plasmas as related to high altitude aerodynamics
[AD-A215126] N90-19852
The expression of syntagmatic relationships in frame-based indexing N90-19917
Earth-orbiting resonant-mass gravitational wave detectors N90-19954
Superconducting gravity gradiometer and a test of inverse square law N90-19975
Comet Halley: An optical continuum study N90-19981

MASSACHUSETTS INST. OF TECH., CAMBRIDGE.
Experimental and theoretical investigations of flowfields and heat transfer in modern gas turbines
[AD-A217663] N90-19237
Science requirements for passive microwave sensors on earth science geostationary platforms N90-19251
Synthesis of poly(dimethylsiloxane) - nylon 6 diblock copolymers
[AD-A216850] N90-19367
Parallel distributed networks for image smoothing and segmentation in analog VSLI
[AD-A216780] N90-19491
Modeling A circuit switched multiprocessor interconnect
[AD-A217122] N90-19519
Design and implementation of a flexible robot
[AD-A216453] N90-19601
On the verification of hypothesized matches in model-based recognition
[AD-A214718] N90-19759
Networks and the best approximation property
[AD-A216712] N90-19778
Priority arbitration with busses
[AD-A216392] N90-19784
Optimal layout via Boolean satisfiability
[AD-A216777] N90-19787
Distributed detection by a large team of sensors in tandem
[AD-A216607] N90-19807

MASSACHUSETTS INST. OF TECH., LEXINGTON.
CdTe buffered GaAs thin-slab IR waveguide modulators and T/R filter
[AD-A215999] N90-19488

MASSACHUSETTS UNIV., AMHERST.
Coherent radar measurement of ocean currents from geostationary orbit N90-19259

MATERIALS RESEARCH LABS., ASCOT VALE (AUSTRALIA).
Effect of temperature on the storage life of polysulfide aircraft sealants
[MRL-TR-89-31] N90-19364
An evaluation of ethylene-vinyl acetate copolymers as desensitizers for RDX in insensitive booster compositions prepared by slurry coating technology
[MRL-TR-89-33] N90-19385
Numerical modelling of shocks in gases and metals
[MRL-RR-8-89] N90-19528

MAX-PLANCK-INST. FUER AERONOMIE, KATLENBURG-LINDAU (GERMANY, F.R.).
Comets: Dirty snowballs or icy dirtballs N90-19994

MAX-PLANCK-INST. FUER CHEMIE, MAINZ (GERMANY, F.R.).
The role of clouds in the photochemistry of the background troposphere N90-19694

MAX-PLANCK-INST. FUER KERNPHYSIK, HEIDELBERG (GERMANY, F.R.).
Low velocity dust-dust collisions N90-20011
Possible targeting of particle emission by mechanical stress and penetration of sublimating ice-dust-surfaces N90-20016
Mechanical properties of fluffy agglomerates consisting of core-mantle-particles N90-20019

MAX-PLANCK-INST. FUER PHYSIK UND ASTROPHYSIK, GARCHING (GERMANY, F.R.).
Investigations of x ray sensitive PN-CCD's
[MPE-213] N90-19499

MAX-PLANCK-INST. FUER PHYSIK UND ASTROPHYSIK, MUNICH (GERMANY, F.R.).
Algorithms for calorimeter simulation with parameterized showers by example of H1 detectors
[MPI-PAE/EXP.EL-200] N90-19828

MAX-PLANCK-INST. FUER STROEMUNGSFORSCHUNG, GOETTINGEN (GERMANY, F.R.).
Tomographic investigations of weakly perturbed supersonic free jets
[MPIS-MITT-91] N90-19209
Drag reduction by longitudinal riblets on the surface of a streamwise aligned body of revolution
[MPIS-MITT-92] N90-19210
Experiments of thermoconvection in a cubic cell
[MPIS-6/1989] N90-19544

MEMPHIS STATE UNIV., TN.
A computer control system for the alternating gradient magnetometer N90-19402
Iterative procedures for space shuttle main engine performance models N90-19416

METAALINSTITUT TNO, APELDOORN (NETHERLANDS).
Origin and effect of pores in aluminum welded joints
[REPT-87M/43/05720/SCP/GRF] N90-19620

MICHIGAN TECHNOLOGICAL UNIV., HOUGHTON.
The effects of gradients on boundary stability
[DE90-007428] N90-19894
NMR (Nuclear Magnetic Resonance) imaging development for the study of solids
[AD-A217073] N90-19899

MICHIGAN UNIV., ANN ARBOR.
A combined finite element-boundary element formulation for solution of two-dimensional problems via CGFFT
[NASA-CR-186464] N90-19309

MIDDLE TENNESSEE STATE UNIV., MURFREESBORO.
Methods for trend analysis: Examples with problem/failure data N90-19396

MIDWEST RESEARCH INST., GOLDEN, CO.
PC-based PCM (Pulse Code Modulation) telemetry data reduction system hardware
[DE90-000316] N90-19273
Solid State Photovoltaic Research Branch
[DE89-009463] N90-19660
Radiative transport models for solar thermal receiver/reactors
[DE90-000303] N90-19665
Experiments on oxygen desorption from surface warm seawater under Open-Cycle Ocean Thermal Energy Conversion (OC-OTEC) conditions
[DE90-000308] N90-19666
Direct absorption receiver
[DE90-000311] N90-19667
Spectral solar radiation data base documentation
[DE89-009448] N90-20033

MINNESOTA UNIV., DULUTH.
Metabolism, seizures, and blood flow in brain following organophosphate exposure: Mechanisms of action and possible therapeutic agents
[AD-A217098] N90-19740

MINNESOTA UNIV., MINNEAPOLIS.
The 41st Annual Gaseous Electronics Conference
[AD-A214540] N90-19851

MISSISSIPPI STATE UNIV., MISSISSIPPI STATE.
Radial response of the burst and transient source experiment N90-19408
Evaluation and analysis of the orbital maneuvering vehicle video system N90-19411
Marshall Avionics Testbed System (MAST) N90-19417

MISSOURI UNIV., COLUMBIA.
Gradiometry and gravitomagnetic field detection N90-19962

MITECH, INC., WASHINGTON, DC.
Executive information systems for providing next generation strategic information: An evaluation of EIS (Executive Information System) software and recommended applicability within the FAA computing environment
[AD-A216672] N90-19920

MOHAWK RESEARCH CORP., ROCKVILLE, MD.
From invention to innovation: Commercialization of new technology by independent and small business inventors
[DE90-006944] N90-19927

MONTANA STATE UNIV., BOZEMAN.
Toward higher order tests of the gravitational interaction N90-19948

MORTON THIOKOL, BRIGHAM CITY, UT.
Development of inspection techniques for quantitatively measuring surface contamination on SRM hardware
[NASA-CR-183902] N90-19608

MOUND LAB., MIAMISBURG, OH.
Investigation of a simulated tritium plasma using Coherent Anti-Stokes Raman Spectroscopy (CARS)
[DE90-005696] N90-19319

N

NATIONAAL INST. VOOR KERNFYSICA EN HOGE ENERGIEFYSICA, AMSTERDAM (NETHERLANDS).
Compton amplifier
[DIGEL-1985-5] N90-19506
Digital integrator
[DIGEL-1989-2] N90-19508
Digital to position converter
[DIGEL-1984-4] N90-19509
High voltage pickup plate
[LINO-1989-3] N90-19510
Literature file on fast kickers and SEPTA: Components for deflection and separation of particle beams
[LINO-162] N90-19924

NATIONAL AERONAUTICAL LAB., BANGALORE (INDIA).
Study of the turbulent boundary layer on an afterbody
[TM-EA-8901] N90-19212
Analysis and design of symmetrical airfoils
[PD-CF-8943] N90-19213
Flosolver Mk1B: An eight processor parallel machine
[PD-CF-8941] N90-19755

NATIONAL AERONAUTICS AND SPACE ADMINISTRATION, WASHINGTON, DC.
Aeronautical engineering: A continuing bibliography with indexes (supplement 249)
[NASA-SP-7037(249)] N90-19190

Aerospace Safety Advisory Panel
[NASA-TM-101748] N90-19389
Relativistic Gravitational Experiments in Space
[NASA-CP-3046] N90-19940
Space telescope searches for black holes in galactic nuclei N90-19958

NATIONAL AERONAUTICS AND SPACE ADMINISTRATION. AMES RESEARCH CENTER, MOFFETT FIELD, CA.

A streamwise upwind algorithm applied to vortical flow over a delta wing
[NASA-TM-102225] N90-19201
Three-dimensional viscous rotor flow calculations using a viscous-inviscid interaction approach
[NASA-TM-102235] N90-19204
Dynamics of a class of vortex rings
[NASA-TM-102257] N90-19524

NATIONAL AERONAUTICS AND SPACE ADMINISTRATION. GODDARD SPACE FLIGHT CENTER, GREENBELT, MD.

Compendium of meteorological space programs, satellites, and experiments
[NASA-TM-102924] N90-19243
Numerical and experimental analysis of a thin liquid film on a rotating disk related to development of a spacecraft absorption cooling system
[NASA-CR-183457] N90-19523
The COBE cosmic 3 K anisotropy experiment: A gravity wave and cosmic string probe N90-19959

NATIONAL AERONAUTICS AND SPACE ADMINISTRATION. HUGH L. DRYDEN FLIGHT RESEARCH CENTER, EDWARDS, CA.

Output model-following control synthesis for an oblique-wing aircraft
[NASA-TM-100454] N90-19241

NATIONAL AERONAUTICS AND SPACE ADMINISTRATION. HUGH L. DRYDEN FLIGHT RESEARCH FACILITY, EDWARDS, CA.

Compensating for pneumatic distortion in pressure sensing devices
[NASA-TM-101716] N90-19224
X-29A aircraft structural loads flight testing
[NASA-TM-101715] N90-19225

NATIONAL AERONAUTICS AND SPACE ADMINISTRATION. LYNDON B. JOHNSON SPACE CENTER, HOUSTON, TX.

Hatch cover
[NASA-CASE-MSC-21356-1] N90-19278

NATIONAL AERONAUTICS AND SPACE ADMINISTRATION. LANGLEY RESEARCH CENTER, HAMPTON, VA.

Static investigation of a two-dimensional convergent-divergent exhaust nozzle with multiaxis thrust-vectoring capability
[NASA-TP-2973] N90-19193
Water-tunnel investigation of concepts for alleviation of adverse inlet spillage interactions with external stores
[NASA-TM-4181] N90-19199
Internal performance of two nozzles utilizing gimbal concepts for thrust vectoring
[NASA-TP-2991] N90-19200
Numerical solution of 3D Navier-Stokes equations with upwind implicit schemes
[NASA-TM-101656] N90-19205
Development of a preliminary high-angle-of-attack nose-down pitch control requirement for high-performance aircraft
[NASA-TM-101684] N90-19206
Conical Euler solution for a highly-swept delta wing undergoing wing-rock motion
[NASA-TM-102609] N90-19211
Aeroservoelasticity
[NASA-TM-102620] N90-19227
Low-speed wind-tunnel investigation of the flight dynamic characteristics of an advanced turboprop business/commuter aircraft configuration
[NASA-TP-2982] N90-19239
Earth Science Geostationary Platform Technology
[NASA-CP-3040] N90-19249
Advancing automation and robotics technology for the Space Station Freedom and for the US economy: Submitted to the United States Congress
[NASA-TM-101647] N90-19279
Integrated control/structure optimization by multilevel decomposition
[NASA-TM-102619] N90-19281
Dual-fuel, dual-mode rocket engine
[NASA-CASE-LAR-13773-1] N90-19298
Method for maintaining precise suction strip porosities
[NASA-CASE-LAR-13638-1] N90-19427
Causality of plasma permittivity with loss and restoring terms
[NASA-TM-101671] N90-19453
Method and apparatus for detecting laminar flow separation and reattachment
[NASA-CASE-LAR-13952-1-SB] N90-19534
The utilization of an infrared imaging system as a cooling slot blockage detector in the inspection of a transpiration cooled nozzle
[NASA-TM-102608] N90-19555
Modeling and analysis of the space shuttle nose-gear tire with semianalytic finite elements
[NASA-TP-2977] N90-19595
Computational aspects of sensitivity calculations in linear transient structural analysis
[NASA-TM-4156] N90-19610
Interlaminar shear stress effects on the postbuckling response of graphite-epoxy panels
[NASA-TM-102626] N90-19630
Spanwise measurements of vertical components of atmospheric turbulence
[NASA-TP-2963] N90-19718
A note on an acoustic response during an engine nacelle flight experiment
[NASA-TM-102585] N90-19821
Reliability of equivalent sphere model in blood-forming organ dose estimation
[NASA-TM-4178] N90-20036

NATIONAL AERONAUTICS AND SPACE ADMINISTRATION. LEWIS RESEARCH CENTER, CLEVELAND, OH.

Induction motor control
[NASA-TM-102533] N90-19234
Comparison between design and installed acoustic characteristics of NASA Lewis 9- by 15-foot low-speed wind tunnel acoustic treatment
[NASA-TP-2996] N90-19242
A comparison of reflector antenna designs for wide-angle scanning N90-19264
Conjugate field approaches for active array compensation N90-19266
Reflector surface distortion analysis techniques (thermal distortion analysis of antennas in space) N90-19267
Aeolian removal of dust from photovoltaic surfaces on Mars
[NASA-TM-102507] N90-19299
New Condensation polyimides containing 1,1,1-triaryl-2,2,2-trifluoroethane structures
[NASA-CASE-LEW-14346-1] N90-19300
Fluorinated graphite fibers as a new engineering material: Promises and challenges
[NASA-TM-102511] N90-19301
Heat treatment study of the SiC/Ti-15-3 composite system
[NASA-TP-2970] N90-19302
Thermo-oxidative stability studies of PMR-15 polymer matrix composites reinforced with various fibers
[NASA-TM-102439] N90-19310
Hot filament technique for measuring the thermal conductivity of molten lithium fluoride
[NASA-TM-102506] N90-19373
Effects of amplitude distortions and IF equalization on satellite communication system bit-error rate performance
[NASA-TM-102415] N90-19454
High power, high frequency component test facility
[NASA-TM-102500] N90-19484
A transient plasticity study and low cycle fatigue analysis of the Space Station Freedom photovoltaic solar array blanket
[NASA-TM-102516] N90-19617
Demonstration of capabilities of high temperature composites analyzer code HITCAN
[NASA-TM-102560] N90-19629
Parallel algorithms for boundary value problems
[NASA-TM-102498] N90-19783

NATIONAL AERONAUTICS AND SPACE ADMINISTRATION. MARSHALL SPACE FLIGHT CENTER, HUNTSVILLE, AL.

A digitally controlled system for effecting and presenting a selected electrical resistance
[NASA-CASE-MFS-29149-1] N90-19492
Feasibility of using Extreme Ultraviolet Explorer (EUVE) reaction wheels to satisfy Space Infrared Telescope Facility (SIRTF) maneuver requirements
[NASA-TM-100389] N90-19556
Trailer shield assembly for a welding torch
[NASA-CASE-MFS-29260-1] N90-19602
PATRAN-STAGS translator (PATSTAGS)
[NASA-TM-100388] N90-19616
FY 1989 scientific and technical reports, articles, papers, and presentations
[NASA-TM-100384] N90-19916

NATIONAL AERONAUTICS AND SPACE ADMINISTRATION. PASADENA OFFICE, CA.

High density tape casting system
[NASA-CASE-NPO-16901-1-CU] N90-19425
Local area network with fault-checking, priorities, and redundant backup
[NASA-CASE-NPO-16949-1-CU] N90-19776
Annealing group III-V compound doped silicon-germanium alloy for improved thermo-electric conversion efficiency
[NASA-CASE-NPO-17259-1-CU] N90-19884

NATIONAL AEROSPACE LAB., AMSTERDAM (NETHERLANDS).

On the evaluation of aerodynamic influence coefficients
[NLR-MP-87019-U] N90-19191
Static strength and damage tolerance tests on the Fokker 100 airframe
[NLR-MP-88023-U] N90-19228
Flow simulation for aircraft
[NLR-MP-87082-U] N90-19543
The potential of combined use of satellite data with topographic TM information for manual/visual and digital updating of land use
[NLR-MP-88021-U] N90-19639
Real time environment monitoring using data from METEOSAT and NOAA imaging satellites
[NLR-MP-87070-U] N90-19672
COCOMAT: A Computer Aided Engineering (CAE) system for composite structures design
[NLR-MP-87078-U] N90-19756

NATIONAL AEROSPACE MEDICAL CENTRE, SOESTERBERG (NETHERLANDS).

Activities in aerospace medicine
[ETN-90-95468] N90-19739

NATIONAL CENTER FOR ATMOSPHERIC RESEARCH, BOULDER, CO.

Colloquium on Synoptic Meteorology
[PB90-121112] N90-19720

NATIONAL GEODETIC SURVEY, ROCKVILLE, MD.

Accuracy of global positioning system broadcast orbits for relative surveys
[PB90-125428] N90-19218

NATIONAL GEOPHYSICAL DATA CENTER, BOULDER, CO.

Solar-geophysical data number 541, September 1989. Part 2: (Comprehensive reports). Data for March 1989 and miscellaneous
[PB90-122755] N90-20031
Solar-geophysical data number 541, September 1989. Part 1: (Prompt reports). Data for August, July 1989, and late data
[PB90-122763] N90-20032

NATIONAL INST. FOR FUSION SCIENCE, NAGOYA (JAPAN).

Overview of recent results from the Advanced Toroidal Facility
[DE90-005673] N90-19853

NATIONAL INST. OF HEALTH, BETHESDA, MD.

CRISP (Computer Retrieval of Information on Scientific Projects) thesauras, fiscal year 1990
[PB90-138652] N90-19922

NATIONAL LAB. FOR HIGH ENERGY PHYSICS, TSUKUBA (JAPAN).

A simple method using MAFIA to calculate external Q values of waveguide-loaded cavities
[DE90-741487] N90-19465

NATIONAL OCEANIC AND ATMOSPHERIC ADMINISTRATION, MIAMI, FL.

Drifting buoy data from Western Tropical Pacific for the period February 1, 1986 through February 28, 1989
[PB90-113978] N90-19732

NATIONAL OCEANIC AND ATMOSPHERIC ADMINISTRATION, WASHINGTON, DC.

Operational requirements and the geostationary platform N90-19250

NATIONAL SCIENCE FOUNDATION, WASHINGTON, DC.

Science and technology report and outlook, 1985-1988
[PB90-115270] N90-19926

NATIONAL TECHNICAL INFORMATION SERVICE, SPRINGFIELD, VA.

National Technical Information Service 1989 Users Conference proceedings
[PB90-142563] N90-19921

NATIONAL TELECOMMUNICATIONS AND INFORMATION ADMINISTRATION, BOULDER, CO.

Power spectral densities for selected digital phase-continuous MFSK (M-ary Frequency Shift Keying) emissions
[PB90-129990] N90-19483
User-friendly software for the design of digital line-of-sight radio links
[PB90-118472] N90-19760

NAVAL POSTGRADUATE SCHOOL, MONTEREY, CA.

Optimizing superplastic response in navalite, a lithium containing aluminum-magnesium alloy
[AD-A216552] N90-19348
Dynamic reconfiguration and link fault tolerance in a transputer network
[AD-A215105] N90-19433

A linear systems theory approach to the range-independent acoustic channel
[AD-A216551] N90-19817

NAVAL RESEARCH LAB., WASHINGTON, DC.
Elastic solutions in a semi-infinite solid with an ellipsoidal inclusion
[AD-A217063] N90-19338
The nonlinear interaction of intense laser pulses in plasmas
[AD-A217604] N90-19667
Distributed bosonic states and condensed matter fusion
[AD-A217605] N90-19668
Critical current density and transition temperature measurements of Y-Ba-Cu-O rods
[AD-A216695] N90-19675

NEW ENERGY DEVELOPMENT ORGANIZATION, TOKYO (JAPAN).
Survey on the possibility of introducing new energy to regional development plans
[DE89-782627] N90-19654

NEW ORLEANS UNIV., LA.
Low-energy impact resistance of graphite-epoxy plates and ALS honeycomb sandwich panels N90-19405

NON-LINEAR SYSTEMS, INC., CAMBRIDGE, MA.
Atmospheric thermal blooming and beam clearing by aerosol vaporization
[DE90-006271] N90-19711

NORTH CAROLINA STATE UNIV., RALEIGH.
Mesh surfaces for reflector applications N90-19268
Advanced topics in structural dynamics: The maneuver of flexible spacecraft, and on-off decentralized control of flexible structures N90-19274
Characterization of reaction kinetics in a porous electrode
[NASA-CR-186504] N90-19340
Silicon carbide semiconductor device fabrication and characterization
[NASA-CR-186354] N90-19673
Band electronic structures and crystal packing forces
[DE90-007669] N90-19698

NORTHEASTERN FOREST EXPERIMENT STATION, BROOMALL, PA.
Proceedings of the 2nd United States/USSR Symposium on Air Pollution Effects on Vegetation Including Forest Ecosystems
[PB90-127119] N90-19678

NORTHEASTERN UNIV., BOSTON, MA.
Active probing of space plasmas
[AD-A216867] N90-19655

NORTHWESTERN UNIV., EVANSTON, IL.
Linear free energy relations for multielectron transfer kinetics: A brief look at the Bronsted/Tafel analogy
[AD-A215078] N90-19823

NOTRE DAME UNIV., IN.
Leading edge vortex dynamics on a pitching delta wing
[NASA-CR-186327] N90-19198
An experimental investigation of the flow field around yawed stranded cables
[AD-A215782] N90-19529
Study of interfacial behavior in cocurrent gas-liquid flows
[DE90-005988] N90-19532

NUCLEAR UTILITY SERVICES, INC., GAITHERSBURG, MD.
Safety Status Report for the Ulysses mission. Book 1: Risk analysis. General purpose heat source radioisotope thermoelectric generator program
[DE90-006826] N90-19282
Safety status report for the Ulysses mission. Book 2: Risk analysis. General purpose heat source radioisotope thermoelectric generator program
[DE90-006827] N90-19283
Safety Status Report for the Ulysses mission: Summary. General purpose heat source radioisotope thermoelectric generator program
[DE90-006828] N90-19284

O

OAK RIDGE GASEOUS DIFFUSION PLANT, TN.
Heat-resistant and anticorrosive paint
[DE90-006077] N90-19369
Report of the First Annual Airborne Weapons Training Technology Review
[DE90-007189] N90-19747

OAK RIDGE NATIONAL LAB., TN.
Identification and development of optimum SiC whiskers for silicon nitride matrix composites
[DE90-006888] N90-19315
Evaluation of radiation-induced sensitization using electrochemical potentiokinetic reactivation technique for austenitic stainless steels
[DE90-002708] N90-19352
Fracture strength analysis of silicon nitride and silicon carbide ceramics from an international cooperative research program
[DE90-005319] N90-19368
Microstructural characterization of multiphase coatings produced by chemical vapor deposition
[DE90-007573] N90-19379
The effect of fiber coatings on interfacial shear strength and the mechanical behavior of ceramic composites
[DE90-007574] N90-19380
Light-scattering measurements of CVD (Chemical Vapor Deposition) silicon carbide
[DE90-007685] N90-19382
Advanced absorption technology development in the United States
[DE90-001336] N90-19428
VLSI implementation of moment invariants for automated inspection
[DE90-005318] N90-19493
Design of a high power density, permanent magnet, axial gap dc motor
[DE90-005449] N90-19514
Laser surface interactions of high-(Tc) superconductors
[DE90-006894] N90-19587
Evaluation of the response of aluminum alloys to single and multiple particle impacts
[DE90-003689] N90-19626
Predicting effects of global climate change on reservoir water quality and fish habitat
[DE90-003674] N90-19704
An approach to elemental task learning
[DE90-006614] N90-19745
A human factors testbed for ground-vehicle telerobotics research
[DE90-006618] N90-19746
A virtual zero-time, monolithic systolic sorting array
[DE90-001000] N90-19753
An optimized algorithm for solving the nodal diffusion method on shared memory multiprocessors
[DE90-002703] N90-19762
Hybrid neural network and rule-based pattern recognition system capable of self-modification
[DE90-007482] N90-19779
A comparison between the propagators method and the decomposition method for nonlinear equations
[DE90-005783] N90-19781
Convergence properties of iterative algorithms for solving the nodal diffusion equations
[DE89-016859] N90-19804
The optical properties of beryllium
[DE90-006372] N90-19848
Overview of recent results from the Advanced Toroidal Facility
[DE90-005873] N90-19853
Negative ion surface plasma source development for plasma trap injectors in Novosibirsk
[DE90-006062] N90-19858
Heteroepitaxial growth of germanium films by supersonic free jet chemical beam epitaxy
[DE90-006821] N90-19877
Characterization of ground state neutral and ion transport during laser ablation of 1:2:3 superconductors by transient optical absorption spectroscopy
[DE90-006823] N90-19878
Neutron scattering measurements of the magnetic excitations of high-temperature superconducting materials
[DE90-006567] N90-19885

OBSERVATOIRE DE BESANCON (FRANCE).
Hot OH and CN: Evidence for organic molecules close to the nucleus of comet Halley N90-20012

OFFICE OF SCIENCE AND TECHNOLOGY, WASHINGTON, DC.
Science and technology report and outlook, 1985-1988
[PB90-115270] N90-19926

OHB-SYSTEM G.M.B.H., BREMEN (GERMANY, F.R.).
TOPAS preparation study: Summary representation of the study results
[OHB-TN-TOP-011/87] N90-19244

OHIO STATE UNIV., COLUMBUS.
Crystallization behavior and properties of BaO-Al2O3-2SiO2 glass matrices
[NASA-CR-185209] N90-19374
Electromagnetic properties of material coated surfaces
[NASA-CR-186466] N90-19466
High-level connectionist models
[AD-A216581] N90-19751
Use of Coxian-type distributions in a general model of the maximum of bivariate random variables
[PB90-121229] N90-19780
Measurement of cross sections: New needs and possibilities
[DE90-007248] N90-19829

OHIO UNIV., ATHENS.
Investigations into a new algorithm for calculating H infinity optimal controllers N90-19406
Radar transponder antenna pattern analysis for the space shuttle N90-19414

OPEN UNIV., MILTON (ENGLAND).
Stable isotope studies of cometary analogue materials N90-20001

OREGON STATE UNIV., CORVALLIS.
Sensitivity of ecological landscapes and regions to global climatic change
[PB90-120072] N90-19674

OREGON UNIV., EUGENE.
Visual processing in texture segregation
[AD-A216539] N90-19737

P

PACIFIC NORTHWEST LAB., RICHLAND, WA.
Technology evaluation for space station atmospheric leakage
[DE90-007844] N90-19294
A preliminary analysis of US CO2 emissions reduction potential from energy conservation and the substitution of natural gas for coal in the period to 2010
[DOE/NBB-0085] N90-19673

PACIFIC-SIERRA RESEARCH CORP., LOS ANGELES, CA.
Ionospheric heating with oblique waves. Volume 1: Electron density perturbations
[AD-A216260] N90-19709

PARIS VI UNIV. (FRANCE).
Porosity and ice-dust mixtures in cometary particles N90-20018

PARKE MATHEMATICAL LABS., INC., CARLISLE, MA.
Opto-Em and devices investigation
[AD-A215033] N90-19814

PENNSYLVANIA STATE UNIV., UNIVERSITY PARK.
Carbon black/polyethylene composites for PTC (Positive Temperature Coefficient) thermistor applications
[AD-A215988] N90-19307
Swept shock/boundary layer interaction experiments in support of CFD code validation
[NASA-CR-186397] N90-19535
Regional climate change predictions from the Goddard Institute for Space Studies high resolution GCM
[NASA-CR-186375] N90-19725
Cosmic ray composition and muon decoherence at the knee of the all-particle cosmic ray spectrum N90-20035

PENNSYLVANIA UNIV., PHILADELPHIA.
Zirconia-based electrodes for solid oxide fuel cells
[DE90-000462] N90-19513
Search for anisotropies in the underground cosmic ray muon flux N90-20034

PHYSICS AND ELECTRONICS LAB. TNO, THE HAGUE (NETHERLANDS).
Tracking performance of the AN/GPN-22 precision approach radar
[FEL-1988-34] N90-19467
Dual-mode latching reciprocal ferrite phase shifter
[FEL-1988-55] N90-19497
SINA: A test system for proximity fuses
[FEL-1989-101] N90-19498
The influence of gamma-radiation on the bandwidth of optical fibres and the reduction of the induced attenuation by bleaching and hardening the fibre
[FEL-1988-62] N90-19846

PK CORP., STORRS, CT.
Random access transmission algorithms for data local area networks
[AD-A216443] N90-19761

PRINCETON UNIV., NJ.
A rule-based paradigm for intelligent adaptive flight control N90-19238

PRINS MAURITS LAB. TNO, RIJSWIJK (NETHERLANDS).
The use of the gas feed system and the vitiator for the solid fuel combustion chamber
[LR-528] N90-19329
Calibration of the sonic measuring and control cross section in the gas feed installation of the solid fuel combustion chamber
[LR-552] N90-19548
Design of a pyrometer for temperature measurements on the solid fuel combustion chamber
[LR-530] N90-19561

R

ROCHESTER INST. OF TECH., NY.
Signal processing
[DE90-006904] N90-19484

Selection of optimal textural features for maximum likelihood image classification
[DE90-006901] N90-19638
Thermal infrared scene simulation
[DE90-006900] N90-19645

ROCHESTER UNIV., NY.
Effect of barrier layers in burn-through experiments with 351-nm laser illumination
[DE90-006806] N90-19577
Correlation-induced changes of spectra
[AD-A217087] N90-19591
Kinematic control of robotic manipulators with multiple interchangeable wrists N90-19592
Siphon flows in isolated magnetic flux tubes. 3: The equilibrium path of the flux tube arch
[NASA-CR-186297] N90-19813

ROCKWELL INTERNATIONAL CORP., SEAL BEACH, CA.
Large space antenna concepts for ESGP N90-19253

ROME UNIV. (ITALY).
Thermal perturbation of comet samples during their acquisition N90-20008
Rosetta/CNSR altimeter and sounding radar N90-20009

ROYAL AEROSPACE ESTABLISHMENT, FARNBOROUGH (ENGLAND).
A study of flows over highly-swept wings designed for maneuver at supersonic speeds
[AD-A216837] N90-19202

ROYAL NETHERLANDS METEOROLOGICAL INST., DE BILT.
Status of a nonlinear water surge model in February 1988
[KNMI-WR-88-03] N90-19735

RUHR UNIV., BOCHUM (GERMANY, F.R.).
Simulation of radar and radiometer signals remote sensing cometary surface and subsurface structures N90-20005
Compressive strength of synthetic comet nucleus samples N90-20006

RUTGERS - THE STATE UNIV., NEW BRUNSWICK, NJ.
Elastic properties of silica xerogels
[AD-A216528] N90-19366

S

SALFORD UNIV. (ENGLAND).
An experimental study of the aeroelastic behaviour of two parallel interfering circular cylinders N90-19609

SANDERS NUCLEAR CORP., NASHUA, NH.
Low cost Brayton engine for gas-fired cogeneration system, phase 1
[PB90-127457] N90-19655

SANDIA NATIONAL LABS., ALBUQUERQUE, NM.
Helicopter flight vibration of large transportation containers: A case for testing tailoring
[DE90-007429] N90-19215
Heli/SITAN: A terrain referenced navigation algorithm for helicopters
[DE90-005193] N90-19217
Computational and experimental of railgun structural performance
[DE90-006418] N90-19247
Three-dimensional structural analyses of reentry vehicles
[DE90-006278] N90-19291
Enhancement of processes for solar photocatalytic detoxification of water
[DE90-003949] N90-19330
Hydrous metal oxide-supported catalysts. Part 2: Catalytic properties and applications
[DE90-006098] N90-19336
Theory of polymer blends
[DE90-002532] N90-19377
Alternate film dielectric materials
[DE90-007213] N90-19378
Radiation-induced density changes and creep in surface layers of glass
[DE90-008112] N90-19383
Impedance characteristics of terawatt ion diodes
[DE90-006276] N90-19484
Test component attachment effects on resonant plate pyrotechnic shock simulation
[DE90-006478] N90-19551
Finite element analysis of a quartz rotation sensor
[DE90-006959] N90-19562
Low threshold current implanted-planar-buried-heterostructure, graded-index, separate-confinement-heterostructure GaAs-AlGaAs laser
[DE90-002579] N90-19572
Experimental results of aging and thermal effects in high-power laser diodes
[DE90-005955] N90-19573
Extending terrestrial mobile robotics to a proposed lunar base
[DE89-016179] N90-19606
Use of chaotic and random vibrations to generate high frequency test inputs. Part 2: Chaotic vibrations
[DE90-007153] N90-19627
Use of chaotic and random vibrations to generate high frequency test inputs
[DE90-007412] N90-19628
Measuring flow properties of wicks for heat pipe solar receivers
[DE89-016537] N90-19664
Status of stretched-membrane heliostats
[DE90-000801] N90-19669
Evaluation of thermal cycling creep-fatigue damage for a molten salt receiver
[DE90-002907] N90-19670
Test results from a full-scale sodium reflux pool-boiler solar receiver
[DE90-003577] N90-19671
Simulation fidelity in lightning penetration studies
[DE90-006367] N90-19731
A technique for convolving unequally spaced samples using fast Fourier transforms
[DE90-006466] N90-19802
Sandia National Laboratories' new high level acoustic test facility
[DE90-006810] N90-19820
Dynamics of plasma injection along magnetic field lines in the PBFA 2 (Particle Beam Fusion Accelerator 2) plasma opening switch
[DE90-006751] N90-19862
CCST (Center for Compound Semiconductor Technology) research briefs
[DE90-006446] N90-19887
Novel processing of HTS based conductors
[DE90-005958] N90-19892
FWP executive summaries: Basic energy sciences materials sciences programs
[DE90-006373] N90-19893

SCIENCE APPLICATIONS INTERNATIONAL CORP., TORRANCE, CA.
A review of models for the analysis of the injection of densely loaded flows into entrained flow gasifiers
[DE90-000453] N90-19550

SCRIPPS INSTITUTION OF OCEANOGRAPHY, LA JOLLA, CA.
Automated visibility and cloud cover measurements with a solid-state imaging system
[AD-A216906] N90-19724

SECRETARIA ESTADUAL DE CIENCIA E TECNOLOGIA, RIO DE JANEIRO (BRAZIL).
Advanced ceramics
[DE90-608004] N90-19370

SMITHSONIAN ASTROPHYSICAL OBSERVATORY, CAMBRIDGE, MA.
Optical interferometers for tests of relativistic gravity in space N90-19967
A review of atomic clock technology, the performance capability of present spaceborne and terrestrial atomic clocks, and a look toward the future N90-19972

SOUTH CAROLINA UNIV., COLUMBIA.
Kalman estimation for SEDS measurements N90-19393

SOUTHERN UNIV., BATON ROUGE, LA.
Liquid oxygen LOX compatibility evaluations of aluminum lithium (Al-Li) alloys: Investigation of the Alcoa 2090 and MMC weldalite 049 alloys N90-19398

SOUTHWEST RESEARCH INST., SAN ANTONIO, TX.
Physico-chemical properties of formaldehyde-ice-dust mixtures N90-20000

SPECTRA TECHNOLOGY, INC., BELLEVUE, WA.
Theory of field reversed configurations
[DE90-006702] N90-19860

SRI INTERNATIONAL CORP., MENLO PARK, CA.
Second-generation ordered polymers
[AD-A216126] N90-19365
Determination of the mechanism of decomposition of energetic molecules
[AD-A217061] N90-19388

STANFORD LINEAR ACCELERATOR CENTER, CA.
Numerical simulation of cross field amplifiers
[DE90-006459] N90-19496
Using Rexx to coordinate relational commands
[DE90-007569] N90-19772
The EGS4 Code System: Solution of gamma-ray and electron transport problems
[DE90-008100] N90-19838

STANFORD UNIV., CA.
Unsteady aerodynamics of delta wings performing maneuvers to high angle of attack N90-19196
Experiments in end-point control of a flexible robot with a mini-manipulator N90-19596
Energy transfer and photochemistry in biomimetic solar conversion
[PB90-114562] N90-19652
Foundations of millimeter-wave frequency acoustic microscopy N90-19816
X ray timing observations and gravitational physics N90-19956
The gravity probe B relativity gyroscope program N90-19960
The Stanford equivalence principle program N90-19963
Frequency stable high power lasers in space N90-19969
Drag-free satellite control N90-19974

STATE UNIV. OF NEW YORK, ALBANY.
The RADM 2 gas-phase chemical mechanism N90-19684

STATE UNIV. OF NEW YORK, BUFFALO.
BCS (Bardeen-Cooper-Schrieffer) primer: A guide to computational methods in superconductivity theory
[AD-A216393] N90-19874

STUTTGART UNIV. (GERMANY, F.R.).
Highly accurate navigation: Integration of navigation and geodesic methods
[SFB-228] N90-19221
Digital determination of the three dimensional flow in turbomachines with the S1-S2 current function process
[ITSM-MITT-30] N90-19236
Flight and driving optimization of air breathing aerodynamic space vehicle
[ETN-90-95379] N90-19246
Practical calculation of the liveload of carbon fiber reinforced plastics by the finite element method
[ETN-90-95867] N90-19311
Spatially high-resolution flame diagnosis by means of spontaneous Raman spectroscopy
[ETN-90-95870] N90-19328
Influence of the parameters: Charge order, sequence classification, partial sequential circuit, and process regularity of a working charge (Gaussian process) on the lifetime of a component made of 3.1354 T3 and 3.4377 T761
[ETN-90-95378] N90-19503
Development of finished beam and shell elements from engineering models for structures under high inelastic deformations
[ETN-90-95377] N90-19619
Calculation of nonlinear viscoelastic processes for plastic layer textile membranes
[ETN-90-95868] N90-19622
Development of finite beam and shell elements for structures under great inelastic deformations
[ETN-90-95869] N90-19623

SYDNEY UNIV. (AUSTRALIA).
Plastic bending tests of cold-formed rectangular hollow sections
[PB90-124611] N90-19613

SYSTEMS SCIENCE AND SOFTWARE, LA JOLLA, CA.
Two-meter laser material response impulse measurements
[AD-A215834] N90-19567

T

TECHNISCHE HOCHSCHULE, AACHEN (GERMANY, F.R.).
A panel process for the calculation of the flow around a wing with front angle damping
[ETN-90-95367] N90-19207
Carrier wing profile in nonstationary current
[ETN-90-95368] N90-19208
Influence of friction and separation phenomena on the dynamic blade loading of transonic turbine cascades
[MITT-88-04] N90-19235

TECHNISCHE HOCHSCHULE, DARMSTADT (GERMANY, F.R.).
Theoretical and experimental examination of the beginning of turbulence in a heated laminar conduit flow
[ETN-90-95369] N90-19541
Incoherent retrodiffusion of radiowaves in plasma with particle impulse
[ETN-90-95375] N90-19864
Nuclear activity, morphology, and far infrared properties of spiral galaxies
[ETN-90-95373] N90-20024

TECHNISCHE UNIV., BERLIN (GERMANY, F.R.).
Optogalvanic laser spectroscopic and interference spectroscopic experiments of isotope gap and hyperfine structure for spectrum of Europium 1 and Erbium 2
[ETN-90-95358] N90-19327
Field theoretical analysis and synthesis of broadband waveguide: Height, plane shunt circulators with multiple layer material insertions
[ETN-90-95360] N90-19489
General multidimensional scanning ratio transformation and its utilization for norm transformation of television signals
[ETN-90-96058] N90-19470

Utilization criteria for transistors of diverse technology in pulse inverters with high switching frequency
[ETN-90-95359] N90-19500
Power diode switching behavior
[ETN-90-95363] N90-19501
A gate array structure for the efficient project of digital circuits: The unit cell array
[ETN-90-95364] N90-19502
Charge pumping as a measurement method for the characterization of short channel MOSFETS: Review, development, and comparison of measurement process
[ETN-90-95726] N90-19504
Development of dynamic equivalent network structures with a universal identification and optimization process
[ETN-90-95822] N90-19507
Theoretical and experimental studies of a brushless disk rotor motor with permanent magnetic excitation and gap windings
[ETN-90-96056] N90-19512
Generation of intenelve UV laser radiation and utilization in high resolution spectroscopy of SO2
[ETN-90-95361] N90-19581
Noise behavior of semiconductor lasers by optic feedback
[ETN-90-95728] N90-19583
Improved processes for ultrasonic object recognition in robotics
[ETN-90-95362] N90-19604
Analysis of alternative concepts for transport systems on the Moon surface
[ETN-90-95727] N90-19605
Tensile behavior of cylindrical pressure tanks in fiber assembling + metal hybrid structure
[ILR-MITT-213] N90-19618
Digital treatment of elastic-plastic structures by means of quadratic optimization processes from the finite element method
[ETN-90-95823] N90-19621
Constructibility limits of multiflow wind turbines with pivots
[ILR-MITT-215] N90-19662
Design and architecture of fourth and fifth generation software engineering environments
[ETN-90-95365] N90-19752
Modeling and realization of plane acousto-optic unilateral band modulators
[ETN-90-95824] N90-19818
Particle emission by oblique ion bombardment of gold
[ETN-90-95825] N90-19827
Digital capacity transient spectroscopy of deep structure defects in III-V-Semiconductor structures
[ETN-90-96057] N90-19890
Self-consistant calculation of point and pair structure defects in silicium
[ETN-90-96059] N90-19891
Causal boundary construction for space-times of the general relativity theory
[ETN-90-95357] N90-19915

TECHNISCHE UNIV., BRUNSWICK (GERMANY, F.R.).
Calculation and optimization of rotor start process
[ETN-90-95894] N90-19229
Present and future risk of satellite and manned platforms collisions with other space objects and particles on earth orbits
[R-8841] N90-19287
Present and future risk of collision of satellites and manned platforms with other space objects and particles in terrestrial orbit
[R-8840] N90-19288
Satellites and debris in earth revolution orbits and first estimation of the collision probability
[R-8709] N90-19289
Evaluation and choice algorithms of cost optimal prepreg-application processes: Production of strongly charged plane parts made of fiber reinforced plastics
[ETN-90-95895] N90-19313
Experimental measurements in secondary radar field: Conception and first results
[ETN-90-96074] N90-19471
Positioning control of highest accuracy for very dynamic coupled system
[ETN-90-95893] N90-19789
Activities report of the Institute for Communication Technology
[ETN-90-95383] N90-20043

TECHNISCHE UNIV., DELFT (NETHERLANDS).
Calculation of ionospheric corrections for single frequency GPS observations: Investigation of two models
[ETN-90-95450] N90-19219
Carin and GPS: The combination of dead reckoning, map matching and satellite navigation in a hybrid automobile navigation system
[ETN-90-95451] N90-19220
The creep behavior of an aramide fiber reinforced wound tow-strap
[LR-546] N90-19312
The use of the gas feed system and the vitiator for the solid fuel combustion chamber
[LR-528] N90-19329
Calibration of the sonic measuring and control cross section in the gas feed installation of the solid fuel combustion chamber
[LR-552] N90-19548
Design of a pyrometer for temperature measurements on the solid fuel combustion chamber
[LR-530] N90-19561
Development of software routines for remote sensing digital image processing
[ETN-90-95452] N90-19640
Comparison of artificial matrices and covariance functions
[ETN-90-95722] N90-19645
Thematic coupling between digital images and geographic information systems
[ETN-90-95723] N90-19646
Applications of the GPS in photogrammetry
[ETN-90-96004] N90-19648
Earth tidal analysis based on gravimeter observations and the influence of ocean tides
[ETN-90-95721] N90-19734
Finite element mesh generation starting from general geometric models
[REPT-88-93] N90-19803
The Moon has set
[REPT-89-07] N90-19933

TECHNISCHE UNIV., HANOVER (GERMANY, F.R.).
A high resolution automatic image measuring system
[WISS-ARB-VERMESSUNGSWESEN-154] N90-19559

TECHNISCHE UNIV., MUNICH (GERMANY, F.R.).
Oscillation and damping behavior of fine steel test tubes, with particular consideration to destruction free proofs from hydrogen fragilization
[ETN-90-95371] N90-19351
Experimental and analytical investigation of adiabatic critical water air two phase flow in small diameter tubes
[TB-88/1] N90-19540
Error detection in data processing devices by means of residue codes
[ETN-90-95370] N90-19767

TECNOSPAZIO S.P.A., MILAN (ITALY).
Design and development activities on the candidate sample acquisition system for the Rosetta mission N90-19993

TEL-AVIV UNIV. (ISRAEL).
Relevance of laboratory studies to comets N90-20023

TENNESSEE UNIV., KNOXVILLE.
Evaluation of the heat transfer module (FAHT) of Failure Analysis Nonlinear Thermal And Structural Integrated Code (FANTASTIC) N90-19407
The optical properties of beryllium
[DE90-006372] N90-19848

TEXAS A&M UNIV., COLLEGE STATION.
Viscoelastic adherend effects in adhesively bonded composite-to-composite joints N90-19594
Development and use of an advanced coal-fueled diesel engine cycle simulation with group effects
[DE90-000450] N90-19607
Synoptic-scale forcing of the low-level jet in developing baroclinic waves N90-19717

TEXAS TECHNOLOGICAL UNIV., LUBBOCK.
A PBL-radiation model for application to regional numerical weather prediction N90-19394

TEXAS UNIV., AUSTIN.
Application of attachment modes in the control of large space structures
[NASA-CR-185604] N90-19280
Studies of photochemically and electrochemically driven electron transport in zeolites
[DE90-007659] N90-19335
Planar integrated circuits for microwave transmission and reception
[AD-A217676] N90-19520
Applications of frequency and wavenumber nonlinear digital signal processing to nonlinear hydrodynamics research
[AD-A216259] N90-19530
Overview of recent results from the Advanced Toroidal Facility
[DE90-005673] N90-19853
The pregalactic cosmic gravitational wave background N90-19945
LAGEOS 3 and the gravitomagnetic field N90-19961

TEXAS UNIV., SAN ANTONIO.
Parallel methods for solving nonlinear block bordered systems of equations
[AD-A217062] N90-19806

TOKYO METROPOLITAN UNIV. (JAPAN).
Cosmic string in compactified gauge theory
[DE90-741463] N90-19988

TOKYO UNIV., TANASHI (JAPAN).
Dimensional transition of the universe
[DE90-741461] N90-19910
On the Langevin equation for stochastic quantization of gravity
[DE90-750024] N90-19914

TOLEDO UNIV., OH.
Heat transfer measurements from a NACA 0012 airfoil in flight and in the NASA Lewis icing research tunnel
[NASA-CR-4278] N90-19203

TRENTO UNIV. (ITALY).
International conference on Surface Modification of Metals by Ion Beams
[AD-A215872] N90-19345

TRW, INC., LIVERMORE, CA.
Results of the PALADIN experiment
[DE90-006776] N90-19578

TRW ELECTRONIC SYSTEMS GROUP, REDONDO BEACH, CA.
Antennas for 20/30 GHz and beyond N90-19289

TUEBINGEN UNIV. (GERMANY, F.R.).
Quantum yield of photocathodes in far and extreme ultraviolet wavelength area
[ETN-90-95731] N90-19505
The microchannel plate camera as a detector at high resolution spectrographs: Experiments for velocity distribution in planetary nebulae
[ETN-90-95733] N90-19560
Signature objects: Preliminaries for the satellite project HIPPARCOS/TYCHO
[ETN-90-95730] N90-19934
Conception of an automatic measurement installation for spatial resolution detectors
[ETN-90-95732] N90-19935
Speckle interferometry for high resolution pictures of astronomical objects
[ETN-90-95827] N90-19936
High energy x ray observations on the Crab nebula and the double star source GX 1+4
[ETN-90-95829] N90-19937
Model calculations for dynamic development of planetary nebulae
[ETN-90-95734] N90-20025
Structural experiments of planetary nebulae: Charge-coupled devices, image reduction under MIDAS, information representation, and development of an evolution classification for PN's
[ETN-90-95736] N90-20026
Examination of the background by High Energy X ray Experiment (HEXE) on the space station MIR
[ETN-90-95735] N90-20041
Analysis of an observation of the x ray astronomy satellite EXOSAT at the low mass x ray binary star system GX5-1
[ETN-90-95828] N90-20042

TULANE UNIV., NEW ORLEANS, LA.
Mechanics of aeolian processes: Soil erosion and dust production N90-19410

U

UNITED TECHNOLOGIES RESEARCH CENTER, EAST HARTFORD, CT.
CdTe buffered GaAs thin-slab IR waveguide modulators and T/R filter
[AD-A215999] N90-19488

UNIVERSITAET DER BUNDESWEHR MUENCHEN, NEUBIBERG (GERMANY, F.R.).
Experimental examination of the development behavior of a gaseous body in a steady state and neutral layer turbulent sheet boundary layer with ground asperity
[ETN-90-96067] N90-19549
Marginal test and analysis of DRAM with masked alpha radiation
[RB-4180] N90-19754
Optimal iteration steps by stochastic approximation processes for the solution of optimization problems with twice differentiable functions
[ETN-90-95887] N90-19809
The drum: Mechanical oscillators and acoustic rad iators
[REPT-FB-01/88] N90-19819

UNIVERSITY COLL., CARDIFF (WALES).
Sources of gravitational waves N90-19942

UNIVERSITY OF CENTRAL ARKANSAS, CONWAY.
Background studies in gas ionizing x ray detectors N90-19399

UNIVERSITY OF CENTRAL FLORIDA, ORLANDO.
A study of the effects of disk flexibility on the rotordynamics of the space shuttle main engine turbo-pumps N90-19401

UPPSALA UNIV. (SWEDEN).
The space microwave interferometer and the search for cosmic background gravitational wave radiation N90-19952
USTAV JADERNEHO VYZUMU, REZ (CZECHOSLOVAKIA).
Numerical solution to the problem of criticality by Monte Carlo method
[DE90-606886] N90-19808
UTAH UNIV., SALT LAKE CITY.
Fabrication, phase transformation studies, and characterization of SiC-AlN-Al2OC ceramics
[DE90-006591] N90-19371

V

VARIAN ASSOCIATES, PALO ALTO, CA.
Design considerations in achieving 1 MW CW operation with a whispering-gallery-mode gyrotron
[DE90-007283] N90-19557
Progress in the CW operation of a 140 GHz gyrotron
[DE90-007382] N90-19558
VIRGINIA POLYTECHNIC INST. AND STATE UNIV., BLACKSBURG.
Investigation of SSME alternate high pressure fuel turbopump lift-off seal fluid and structural dynamic interaction N90-19400
Suboptimal period design for a maneuvering missile to evade tracking filters N90-19479
VIRGINIA UNIV., CHARLOTTESVILLE.
Longitudinal traveling waves bifurcating from Vlasov plasma equilibria N90-19850
VISTA RESEARCH CORP., MOUNTAIN VIEW, CA.
Numerical simulation of acoustic scatter from subsurface bubble clouds
[AD-A217068] N90-19822
VOLUNTEERS IN TECHNICAL ASSISTANCE, INC., ARLINGTON, VA.
Low earth orbiting satellite for international information exchange system
[DE90-007186] N90-19292
VRIJE UNIV., AMSTERDAM (NETHERLANDS).
An equational language for specifying, querying, and updating database domains
[PB90-124694] N90-19918

W

WASHINGTON UNIV., SAINT LOUIS, MO.
Gravitational radiation as a test of relativistic gravity N90-19941
Experimental constraints on metric and non-metric theories of gravity N90-19946
WASHINGTON UNIV., SEATTLE.
Transient and sustained resonance in very slowly varying oscillatory Hamiltonian systems with application to free-electron lasers
[DE90-005984] N90-19574
A tensor product B-spline method for numerical grid generation
[DE90-005979] N90-19792
Hierarchical basis preconditioners for second order elliptic problems in three dimensions
[DE90-005980] N90-19793
Experimental and theoretical high energy physics
[DE90-005974] N90-19834
The composition of cometary nuclei N90-20022
JACEE long duration balloon flights
[DE90-006008] N90-20039
WEST VIRGINIA UNIV., MORGANTOWN.
Minimum cycle covering and integer flows
[AD-A216546] N90-19785
Panconnectivity of locally connected K(1,3)-free graphs
[AD-A216548] N90-19786
WESTFAELISCHE WILHELMS UNIV., MUENSTER (GERMANY, F.R.).
Petrographic working model of the Rosetta sampling and modelling subgroup for a comet nucleus N90-19992
Thermal conductivities and diffusivities of porous ice samples at low pressures and temperatures and possible modes of heat transfer in near surface layers of comets N90-19999
WESTINGHOUSE ELECTRIC CORP., PITTSBURGH, PA.
Development of a receiver for a space-based laser radar system
[AD-A215079] N90-19566
Solid oxide fuel cell cogeneration system conceptual design, program 2
[PB90-114968] N90-19653
Gas cooled fuel cell systems technology development program
[DE90-000446] N90-19668
WESTINGHOUSE SAVANNAH RIVER CO., AIKEN, SC.
Supercomputer applications for materials science: Ordering effects of hydrogen in palladium
[DE90-004664] N90-19870
WICHITA STATE UNIV., KS.
Heat sink effects on weld bead: VPPA process N90-19416
WISCONSIN UNIV., MADISON.
Elastic recovery and polymer-polymer interactions
[AD-A217085] N90-19384

Y

YALE UNIV., NEW HAVEN, CT.
Photometric analyses of abundances in dwarf spheroidal galaxies and globular clusters N90-19978

Typical Contract Number Index Listing

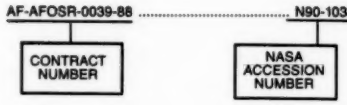

Listings in this index are arranged alphanumerically by contract number. Under each contract number the NASA accession numbers denoting documents that have been produced as a result of research done under that contract are arranged in ascending order. The NASA accession number denotes the number by which the citation is identified.

AF PROJ. D822 ..... N90-19761
AF PROJ. 317J N90-19724
AF PROJ. 2301 ..... N90-19736
N90-19851
AF PROJ. 2303 ..... N90-19321
N90-19323
AF PROJ. 2304 ..... N90-19785
N90-19786
N90-19812
AF PROJ. 2305 ..... N90-19458
AF PROJ. 2307 ..... N90-19365
N90-19852
AF PROJ. 2308 ..... N90-19297
N90-19569
AF PROJ. 2310 ..... N90-19709
AF PROJ. 2311 ..... N90-20030
AF PROJ. 2313 ..... N90-19737
AF PROJ. 2403 ..... N90-19748
AF PROJ. 4600 ..... N90-19814
AF PROJ. 7184 ..... N90-19842
AF-AFOSR-0027-86 ..... N90-19321
AF-AFOSR-0068-89 ..... N90-19785
N90-19786
AF-AFOSR-0097-86 ..... N90-19812
AF-AFOSR-0130-87 ..... N90-19766
AF-AFOSR-0207-88 ..... N90-19851
AF-AFOSR-0251-85 ..... N90-19775
N90-19806
AF-AFOSR-0252-89 ..... N90-19789
AF-AFOSR-0313-88 ..... N90-19736
AF-AFOSR-0323-88 ..... N90-19737
AF-AFOSR-0337-86 ..... N90-19297
AF-AFOSR-0355-87 ..... N90-19323
AF-AFOSR-3129-76 ..... N90-19852
ARB-A4-127-32 ..... N90-19675
ARC-87-154/CO-9901 ..... N90-19564
ARPA ORDER 4462 ..... N90-19822
ARPA ORDER 6037 ..... N90-19923
ARPA ORDER 9526 ..... N90-19518
ASI-88-RB-047 ..... N90-19998
ASI-88-RB-060 ..... N90-19991
N90-19998
AVRADA PROJ. 5620112DA N90-19217
A82/KL/040 ..... N90-19846
A83/KLU/055 ..... N90-19497
A83/KLU/115 ..... N90-19738
A83/KM/017 ..... N90-19620
A85/KLU/113 ..... N90-19467
A85/KM/119 ..... N90-19498
BCRS-PROJ-4551/TE-1.14 ..... N90-19582
BF-07KF212 ..... N90-19728
BMFT-LFL-7974 ..... N90-19231
BMFT-01-OO-8604 ..... N90-19289
BMFT-01QV86810 ..... N90-19287
N90-19288
BMFT-03E8543A/4 ..... N90-19661
BMVG-T/RF31/I0003/I1303 ..... N90-19468
DA PROJ. 1L1-62105-AH-84 ..... N90-19347
DA PROJ. 1L1-62209-AH-76 ..... N90-19593
DA PROJ. 1L1-62618-AH-80 ..... N90-19233
N90-19531
DA PROJ. 3M1-61102-BS-10 ..... N90-19740
DAAG29-85-C-0023 ..... N90-19900
DAAL03-86-D-0001 ..... N90-19773
DAAL03-86-G-0065 ..... N90-19899
DAAL03-86-K-0030 ..... N90-19388
DAAL03-86-K-0042 ..... N90-19774
DAAL03-86-K-0103 ..... N90-19843
DAAL03-86-K-0143 ..... N90-19844
DAAL03-86-K-0157 ..... N90-19849
DAAL03-86-K-0173 ..... N90-19591
DAAL03-86-K-0174 ..... N90-19384
DAAL03-87-C-0007 ..... N90-19475
DAAL03-88-K-0005 ..... N90-19520
DAAL03-88-K-0086 ..... N90-19775
N90-19806
DAAL03-89-K-0008 ..... N90-19570
DACA76-85-C-0010 ..... N90-19778
DAJA45-88-M-0134 ..... N90-19345
DAMD17-86-C-6036 ..... N90-19740
DE-AC01-79ET-32043 ..... N90-19285
N90-19286
DE-AC01-87NE-32134 ..... N90-19282
N90-19283
N90-19284
DE-AC01-88ER-30131 ..... N90-19588
DE-AC02-76CH-00016 ..... N90-19337
N90-19342
N90-19353
N90-19730
N90-19871
DE-AC02-80ER-10774 ..... N90-19983
DE-AC02-83CH-10093 ..... N90-19273
N90-19660
N90-19665
N90-19666
N90-19667
N90-19886
N90-20033
DE-AC02-86ER-40296 ..... N90-19304
DE-AC02-89ER-40509 ..... N90-19830
DE-AC03-76SF-00098 ..... N90-19325
N90-19578
DE-AC03-76SF-00515 ..... N90-19496
N90-19772
N90-19838
DE-AC03-89ER-51114 ..... N90-19839
DE-AC03-868S-16006 ..... N90-19835
DE-AC04-76DP-00789 ..... N90-19215
N90-19217
N90-19247
N90-19291
N90-19330
N90-19336
N90-19377
N90-19378
N90-19383
N90-19494
N90-19551
N90-19562
N90-19572
N90-19573
N90-19606
N90-19627
N90-19628
N90-19664
N90-19669
N90-19670
N90-19671
N90-19731
N90-19802
N90-19820
N90-19862
N90-19887
N90-19892
N90-19893
DE-AC04-88DP-43495 ..... N90-19319
N90-19334
DE-AC05-84OR-21400 ..... N90-19315
N90-19352
N90-19368
N90-19369
N90-19379
N90-19380
N90-19382
N90-19428
N90-19493
N90-19514
N90-19587
N90-19626
N90-19704
N90-19745
N90-19746
N90-19753
N90-19762
N90-19779
N90-19781
N90-19804
N90-19848
N90-19853
N90-19856
N90-19877
N90-19878
N90-19885
DE-AC05-84OT-21400 ..... N90-19747
DE-AC06-76RL-01830 ..... N90-19294
N90-19673
DE-AC06-80ER-53096 ..... N90-19860
DE-AC07-76ID-01570 ..... N90-19332
DE-AC09-76SR-00001 ..... N90-19870
DE-AC09-88SR-18035 ..... N90-19870
DE-AC21-82MC-24223 ..... N90-19668
DE-AC21-85MC-22064 ..... N90-19550
DE-AC21-85MC-22073 ..... N90-19317
DE-AC21-86MC-23256 ..... N90-19607
DE-AC22-88PC-88947 ..... N90-19536
DE-AS05-80ER-10742 ..... N90-19342
N90-19353
N90-19871
DE-AS06-88ER-40423 ..... N90-19834
N90-20039
DE-FC03-85DP-40200 ..... N90-19577
DE-FC22-83FE-60149 ..... N90-19649
N90-19703
DE-FG01-87CE-33007 ..... N90-19292
DE-FG01-88DP-20153 ..... N90-19464
N90-19638
N90-19845
DE-FG02-85ER-13443 ..... N90-19909
DE-FG02-87ER-45286 ..... N90-19371
DE-FG02-87ER-45315 ..... N90-19894
DE-FG02-88ER-13913 ..... N90-19532
DE-FG02-88ER-45356 ..... N90-19333
DE-FG03-84ER-45156 ..... N90-19897
DE-FG03-85ER-25009 ..... N90-19777
DE-FG05-84ER-40147 ..... N90-19984
N90-20040
DE-FG05-86ER-45259 ..... N90-19898
DE-FG05-87ER-13789 ..... N90-19335
DE-FG05-87ER-25036 ..... N90-19794
DE-FG05-87ER-45325 ..... N90-19381
DE-FG05-88ER-53265 ..... N90-19859
DE-FG06-86ER-25019 ..... N90-19574
DE-FG06-88ER-25061 ..... N90-19792
N90-19793
DE-FG09-87ER-45291 ..... N90-19372
DE-FG21-86MC-23139 ..... N90-19513
DFG-AZ-SCHM-522/6-1 ..... N90-19625
DFG-FR-325/21-1 ..... N90-20024
DFG-FR-325/21-4 ..... N90-20024
DFG-IG-3/13-1 ..... N90-20011
DFG-IG-3/13-2 ..... N90-20011
DFG-IG-3/13-3 ..... N90-20011
DFG-WI-32/35-1 ..... N90-19618
DFG-WI-364/26 ..... N90-19540
DFVLR-FV-0328617-A N90-19683
DLA900-83-C-1744 ..... N90-19386
DLR-15.0120 ..... N90-19329
DNA001-85-C-0186 ..... N90-19567
DNA001-86-C-0003 ..... N90-19658
DTFA03-88-C-00064 ..... N90-19920
EPA-68-C8-0006 ..... N90-19674
EPA-68-02-4274 ..... N90-19679
EPA-68-02-4396 ..... N90-19679
ERP-2565 ..... N90-19662
F19628-84-K-0047 ..... N90-19724
F19628-85-C-0002 ..... N90-19488

F19628-85-K-0053 ..... N90-19855
F19628-86-C-0206 ..... N90-19458
F19628-87-C-0026 ..... N90-19709
F19628-87-C-0155 ..... N90-19814
F33615-86-C-3600 ..... N90-19748
F49620-85-K-0015 ..... N90-19365
F49620-87-C-0107 ..... N90-19761
F49620-88-K-0001 ..... N90-19365
GA PROJ. 3466 ..... N90-19839
GRI-5083-260-0824 ..... N90-19652
GRI-5083-260-0953 ..... N90-19324
GRI-5086-260-1247 ..... N90-19320
GRI-5088-294-1273 ..... N90-19653
GRI-5087-260-1452 ..... N90-19826
GRI-5087-293-1514 ..... N90-19655
INSU-883719 ..... N90-20013
INSU-893709 ..... N90-20015
ITA-99-26-07220-30 ..... N90-19343
MIPR-W31-RPD-7-D4041 ..... N90-19579
N90-19580
MIPR-W43-GBL-0-5007 ..... N90-19711
NAGW-822 ..... N90-19953
N90-19965
NAG1-665 ..... N90-19308
NAG1-727 ..... N90-19198
NAG1-771 ..... N90-19763
N90-19764
NAG1-922 ..... N90-19275
NAG2-516 ..... N90-19552
NAG2-541 ..... N90-19309
NAG2-592 ..... N90-19535
NAG2-593 ..... N90-19923
NAG3-72 ..... N90-19203
NAG3-649 ..... N90-19340
NAG3-655 ..... N90-19593
NAG3-782 ..... N90-19873
NAG3-783 ..... N90-19593
NAG3-913 ..... N90-19466
NAG5-356 ..... N90-19460
NAG5-444 ..... N90-19713
N90-19714
N90-19715
NAG5-931 ..... N90-19429
NAG5-934 ..... N90-19813
NAG5-956 ..... N90-19523
NAG5-968 ..... N90-19710
NAG5-1124 ..... N90-19599
NAG5-1133 ..... N90-19725
NAG8-095 ..... N90-19326
NAG8-562 ..... N90-19932
NASA ORDER C-30012-M N90-19386
NASA ORDER C-99066-G N90-19783
NAS1-17335 ..... N90-19741
NAS1-18599 ..... N90-19226
NAS1-18605 ..... N90-19537
N90-19538
N90-19539
N90-19791
NAS3-24564 ..... N90-19454
NAS3-25266 ..... N90-19454
NAS8-30490 ..... N90-19608
NAS9-17254 ..... N90-19280
NCC3-133 ..... N90-19374
NCC9-16 ..... N90-19757
N90-19758
NGR-33018148 ..... N90-19965
NGT-01-008-021 ..... N90-19390
N90-19391
N90-19392
N90-19393
N90-19394
N90-19395
N90-19396
N90-19397
N90-19398
N90-19399
N90-19400
N90-19401
N90-19402
N90-19403
N90-19404
N90-19405
N90-19406
N90-19407
N90-19408
N90-19409
N90-19410
N90-19411
N90-19412
N90-19413
N90-19415
N90-19416
N90-19417
N90-19418
N90-19419
N90-19420
N90-19421
N90-19422
N90-19423
N90-19424
NIVR-03506N N90-19756
NIVR-06501N N90-19228
NSF ASC-85-19353 ..... N90-19793
NSF ATM-87-09659 ..... N90-19720
NSF CDA-84-20944 ..... N90-19606
NSF DMC-85-00698 ..... N90-19780
NSF DMR-86-0666 ..... N90-19815
NSF EAR-86-15844 ..... N90-19715
NSF IRI-89-02755 ..... N90-19807
NSF MIP-88-14612 ..... N90-19491
NSF PHY-85-13953 ..... N90-19946
NSG-5123 ..... N90-19765
N90-19766
NSG-5172 ..... N90-19765
NSG-7562 ..... N90-19813
N00014-79-C-0647 ..... N90-19815
N00014-81-K-0024 ..... N90-19237
N00014-83-K-0239 ..... N90-19529
N00014-84-K-0519 ..... N90-19807
N00014-85-K-0124 ..... N90-19759
N90-19778
N00014-85-K-0169 ..... N90-19789
N00014-85-K-0182 ..... N90-19873
N00014-86-C-2028 ..... N90-19307
N00014-86-K-0685 ..... N90-19601
N90-19759
N00014-87-C-0473 ..... N90-19822
N00014-87-C-8904 ..... N90-19923
N00014-87-K-0307 ..... N90-19766
N00014-87-K-0511 ..... N90-19876
N00014-87-K-0517 ..... N90-19367
N00014-87-K-0529 ..... N90-19366
N00014-87-K-0825 ..... N90-19491
N90-19519
N90-19784
N90-19787
N00014-88-C-0391 ..... N90-19518
N00014-88-C-0600 ..... N90-19566
N00014-88-K-0369 ..... N90-19823
N00014-89-J-1103 ..... N90-19322
N00014-89-J-1200 ..... N90-19751
N00014-89-J-1849 ..... N90-19339
N90-19901
N90-19902
N90-19903
N00014-90-J-1193 ..... N90-19874
N00167-88-K-0049 ..... N90-19530
PSN-88-RIB-020 ..... N90-19991
N90-19998
P7245-GEO N90-20017
R87/KL/094 ..... N90-19847
SRI PROJ. PYU-4621 ..... N90-19365
W-31-109-ENG-38 ..... N90-19331
N90-19341
N90-19354
N90-19659
N90-19824
N90-19835
N90-19869
N90-19927
N90-20037
N90-20038
W-7405-ENG-36 ..... N90-19248
N90-19293
N90-19296
N90-19341
N90-19355
N90-19356
N90-19358
N90-19359
N90-19516
N90-19517
N90-19575
N90-19584
N90-19585
N90-19589
N90-19590
N90-19744
N90-19770
N90-19771
N90-19805
N90-19810
N90-19811
N90-19831
N90-19832
N90-19833
N90-19865
N90-19866
N90-19895
N90-19896
N90-19905
N90-19908
N90-19925
N90-19931
N90-19987
N90-20029
W-7405-ENG-48 ..... N90-19348
N90-19357
N90-19361
N90-19459
N90-19473
N90-19474
N90-19515
N90-19557
N90-19558
N90-19571
N90-19576
N90-19578
N90-19579
N90-19580
N90-19588
N90-19711
N90-19825
N90-19829
N90-19861
N90-19985
N90-20027
199-04-16-11 ..... N90-20036
310-10-61-87-02 ..... N90-19435
310-10-62-15 ..... N90-19436
310-10-62-16 ..... N90-19438
N90-19439
310-10-62-34 ..... N90-19437
310-20-64-89 ..... N90-19452
310-20-67-89-02 ..... N90-19442
310-30-70-04-02 ..... N90-19440
N90-19441
310-30-70-87-02 ..... N90-19447
310-30-70-89-01 ..... N90-19448
310-30-71-83-02 ..... N90-19443
N90-19444
310-30-72-88-01 ..... N90-19445
N90-19446
314-30-42-01-44 ..... N90-19450
314-40-41-81-11 ..... N90-19451
315-20-50-00-05 ..... N90-19449
474-46-10 ..... N90-19617
505-42-94 ..... N90-19593
505-60-00 ..... N90-19201
N90-19524
505-60-01-01 ..... N90-19205
505-61-01-05 ..... N90-19555
505-61-51 ..... N90-19204
505-61-71-07 ..... N90-19206
505-62-21 ..... N90-19242
N90-19783
505-62-41-07 ..... N90-19239
505-62-71-01 ..... N90-19193
N90-19199
505-63-01-10 ..... N90-19630
505-63-21-01 ..... N90-19211
505-63-21-04 ..... N90-19227
N90-19281
N90-19718
505-63-41-02 ..... N90-19595
505-63-51-10 ..... N90-19226
505-67-21 ..... N90-19741
505-68-71 ..... N90-19224
505-68-91-06 ..... N90-19200
505-90-21-01 ..... N90-19537
N90-19538
N90-19539
N90-19791
506-41-31 ..... N90-19373
506-41-41 ..... N90-19301
N90-19484
506-43-41-02 ..... N90-19810
506-44-21-03 ..... N90-19249
506-68-11 ..... N90-19203
506-80-31-06 ..... N90-19821
510-01-0A N90-19310
N90-19374
510-01-01 ..... N90-19302
533-02-51 ..... N90-19225
533-06-01 ..... N90-19241
582-01-11 ..... N90-19386
583-01-11-12 ..... N90-19453
591-14-41 ..... N90-19299
650-60-23 ..... N90-19454
763-01-4B N90-19629
946-02-20 ..... N90-19234

Typical Report Number Index Listing

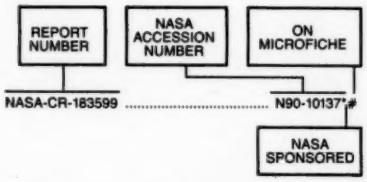

Listings in this index are arranged alphanumerically by report number. The NASA accession number denotes the number by which the citation is identified. An asterisk (*) indicates that the item is a NASA report. A pound sign (#) indicates that the item is available on microfiche.

A-89230 ..... N90-19201* #
A-89246 ..... N90-19204* #
A-90016 ..... N90-19524* #

AAMRL-TR-89-044 ..... N90-19842 #

AD-A211700 ..... N90-20030* #
AD-A213629 ..... N90-19812 #
AD-A214540 ..... N90-19851 #
AD-A214718 ..... N90-19759 #
AD-A215033 ..... N90-19814 #
AD-A215078 ..... N90-19823 #
AD-A215079 ..... N90-19566 #
AD-A215105 ..... N90-19433 #
AD-A215126 ..... N90-19852 #
AD-A215782 ..... N90-19529 #
AD-A215834 ..... N90-19567 #
AD-A215844 ..... N90-19637 #
AD-A215872 ..... N90-19345 #
AD-A215988 ..... N90-19307 #
AD-A215999 ..... N90-19488 #
AD-A216126 ..... N90-19365 #
AD-A216243 ..... N90-19245 #
AD-A216259 ..... N90-19530 #
AD-A216260 ..... N90-19709 #
AD-A216280 ..... N90-19455 #
AD-A216392 ..... N90-19784 #
AD-A216393 ..... N90-19874 #
AD-A216443 ..... N90-19761 #
AD-A216445 ..... N90-19297 #
AD-A216453 ..... N90-19601 #
AD-A216528 ..... N90-19366 #
AD-A216539 ..... N90-19737 #
AD-A216546 ..... N90-19785 #
AD-A216548 ..... N90-19786 #
AD-A216550 ..... N90-19321 #
AD-A216551 ..... N90-19817 #
AD-A216552 ..... N90-19346 #
AD-A216563 ..... N90-19569 #
AD-A216581 ..... N90-19751 #
AD-A216607 ..... N90-19807 #
AD-A216672 ..... N90-19920 #
AD-A216695 ..... N90-19875 #
AD-A216696 ..... N90-19426 #
AD-A216712 ..... N90-19778 #
AD-A216725 ..... N90-19322 #
AD-A216777 ..... N90-19787 #
AD-A216780 ..... N90-19491 #
AD-A216799 ..... N90-19214 #
AD-A216837 ..... N90-19202 #
AD-A216850 ..... N90-19367 #
AD-A216853 ..... N90-19743 #
AD-A216867 ..... N90-19855 #
AD-A216870 ..... N90-19788 #
AD-A216882 ..... N90-19658 #
AD-A216902 ..... N90-19789 #
AD-A216905 ..... N90-19323 #
AD-A216906 ..... N90-19724 #
AD-A216951 ..... N90-19347 #
AD-A216952 ..... N90-19614 #
AD-A216953 ..... N90-19842 #
AD-A216969 ..... N90-19815 #
AD-A216976 ..... N90-19843 #
AD-A216978 ..... N90-19844 #
AD-A216980 ..... N90-19570 #
AD-A216985 ..... N90-19876 #
AD-A216997 ..... N90-19531 #
AD-A216998 ..... N90-19233 #
AD-A217007 ..... N90-19457 #
AD-A217011 ..... N90-19458 #
AD-A217061 ..... N90-19388 #
AD-A217062 ..... N90-19806 #
AD-A217063 ..... N90-19336 #
AD-A217064 ..... N90-19849 #
AD-A217067 ..... N90-19748 #
AD-A217068 ..... N90-19822 #
AD-A217073 ..... N90-19899 #
AD-A217076 ..... N90-19563 #
AD-A217078 ..... N90-19773 #
AD-A217085 ..... N90-19384 #
AD-A217087 ..... N90-19591 #
AD-A217088 ..... N90-19900 #
AD-A217092 ..... N90-19774 #
AD-A217093 ..... N90-19775 #
AD-A217094 ..... N90-19475 #
AD-A217098 ..... N90-19740 #
AD-A217103 ..... N90-19736 #
AD-A217108 ..... N90-19706 #
AD-A217110 ..... N90-19518 #
AD-A217122 ..... N90-19519 #
AD-A217266 ..... N90-19222 #
AD-A217279 ..... N90-19223 #
AD-A217284 ..... N90-19295 #
AD-A217285 ..... N90-19230 #
AD-A217296 ..... N90-19742 #
AD-A217567 ..... N90-19901 #
AD-A217568 ..... N90-19902 #
AD-A217569 ..... N90-19903 #
AD-A217570 ..... N90-19339 #
AD-A217604 ..... N90-19867 #
AD-A217605 ..... N90-19868 #
AD-A217663 ..... N90-19237 #
AD-A217676 ..... N90-19520 #

AD-D014315 ..... N90-19430 #
AD-D014318 ..... N90-19480
AD-D014319 ..... N90-19750
AD-D014321 ..... N90-19872
AD-D014322 ..... N90-19840
AD-D014323 ..... N90-19431
AD-D014324 ..... N90-19481
AD-D014326 ..... N90-19360
AD-D014331 ..... N90-19318 #
AD-D014332 ..... N90-19305 #
AD-D014334 ..... N90-19482 #
AD-D014336 ..... N90-19483 #
AD-D014337 ..... N90-19306 #
AD-D014341 ..... N90-19565
AD-D014342 ..... N90-19432
AD-D014353 ..... N90-19489
AD-D014354 ..... N90-19657 #
AD-D014358 ..... N90-19841
AD-D014360 ..... N90-19600 #
AD-D014361 ..... N90-19456 #
AD-D014362 ..... N90-19568
AD-D014365 ..... N90-19490
AD-D014368 ..... N90-19554

AFGL-TR-88-0336-VOL-1 ..... N90-19709 #

AFIT/GA/ENY/89D-6 ..... N90-19245 #

AFIT/GE/ENG/89D-37 ..... N90-19455 #

AFOSR-88-1340TR ..... N90-19569 #
AFOSR-89-0397TR ..... N90-19385 #
AFOSR-89-1278TR ..... N90-19812 #
AFOSR-89-1333TR ..... N90-19851 #
AFOSR-89-1710TR ..... N90-19297 #
AFOSR-89-1718TR ..... N90-19761 #
AFOSR-89-1780TR ..... N90-19737 #
AFOSR-89-1865TR ..... N90-19785 #
AFOSR-89-1866TR ..... N90-19786 #
AFOSR-89-1867TR ..... N90-19321 #

AGARD-AR-248 ..... N90-19232 #

AI-M-1110 ..... N90-19759 #
AI-M-1164 ..... N90-19778 #

AI-TR-1153 ..... N90-19601 #

AIAA-90-0878 ..... N90-19454* #

AMSEL-NV-TR-0089 ..... N90-19426 #

ANL-HEP-CP-89-94 ..... N90-20037 #
ANL-HEP-CP-89-99 ..... N90-20038 #
ANL-HEP-CP-89-132 ..... N90-19824 #

AR-005-730 ..... N90-19364 #
AR-005-735 ..... N90-19385 #
AR-005-742 ..... N90-19528 #

ARB-R-89/417 ..... N90-19675 #

ARCCB-TR-89033 ..... N90-19614 #

ARO-TCN-88-048 ..... N90-19773 #

ARO-21077.8-MS ..... N90-19900 #
ARO-22964.14-MA ..... N90-19774 #
ARO-23336.5-CH ..... N90-19388 #
ARO-23602.2-EL ..... N90-19849 #
ARO-23654.28-PH ..... N90-19843 #
ARO-23808.3-MS-F ..... N90-19899 #
ARO-23845.1-PH ..... N90-19844 #
ARO-24623.44-EG-UIR ..... N90-19384 #
ARO-24626.119-PH-UIR ..... N90-19591 #
ARO-24649.8-EL-S ..... N90-19475 #
ARO-24923.6-MA ..... N90-19775 #
ARO-24923.7-MA ..... N90-19806 #
ARO-25045.31-EL ..... N90-19520 #
ARO-26434.2-EL ..... N90-19570 #

ASQBG-C-89-024 ..... N90-19773 #

AVSCOM-TR-88-C-035 ..... N90-19593* #

BBC-RD-1989/13 ..... N90-19477
BBC-RD-1989/14 ..... N90-19476
BBC-RD-1989/17 ..... N90-19478

BCRS-88-17 ..... N90-19641 #
BCRS-88-18 ..... N90-19582 #
BCRS-88-19 ..... N90-19642 #
BCRS-89-01 ..... N90-19643 #
BCRS-89-03 ..... N90-19644 #

BDM/ABQ-88-0996-TR ..... N90-19458 #

BN-1101 ..... N90-19789 #

BNL-43119 ..... N90-19871 #
BNL-43235 ..... N90-19342 #
BNL-43428 ..... N90-19337 #
BNL-43551 ..... N90-19730 #
BNL-43662 ..... N90-19353 #

BRL-MR-3792 ..... N90-19531 #
BRL-MR-3801 ..... N90-19233 #

CAR-89-3 ..... N90-19280* #

CONF-880418-2 ..... N90-19317 #
CONF-890701-23 ..... N90-19304 #
CONF-891007-112 ..... N90-19839 #
CONF-891044-5 ..... N90-19837 #
CONF-891055-2 ..... N90-19825 #
CONF-891093-20 ..... N90-19871 #
CONF-891097-4 ..... N90-19473 #
CONF-891119-47 ..... N90-19341 #
CONF-891119-58 ..... N90-19342 #
CONF-891119-86 ..... N90-19878 #
CONF-891119-87 ..... N90-19877 #
CONF-891119-96 ..... N90-19515 #
CONF-891119-99 ..... N90-19379 #
CONF-891119-100 ..... N90-19380 #

CONF-891119-101 ..... N90-19382 #
CONF-891124-2 ..... N90-19869 #
CONF-891192-26 ..... N90-19870 #
CONF-891204-20 ..... N90-19359 #
CONF-891205-3 ..... N90-19557 #
CONF-891240-5 ..... N90-19853 #
CONF-891261-3 ..... N90-19573 #
CONF-891276-4 ..... N90-19293 #
CONF-900122-6 ..... N90-20038 #
CONF-900129-6 ..... N90-20037 #
CONF-900129-10 ..... N90-20040* #
CONF-900140-6 ..... N90-19580 #
CONF-900140-9 ..... N90-19579 #
CONF-900140-10 ..... N90-19585 #
CONF-900140-11 ..... N90-19586 #
CONF-900162-2 ..... N90-19584 #
CONF-900163-2 ..... N90-19496 #
CONF-900163-3 ..... N90-19831 #
CONF-900164-1 ..... N90-19711 #
CONF-900230-1 ..... N90-19771 #
CONF-900236-1 ..... N90-19770 #
CONF-900254-2 ..... N90-19334 #
CONF-900264-1 ..... N90-19494 #
CONF-900328-1 ..... N90-19572 #
CONF-900333-2 ..... N90-19571 #
CONF-900334-1 ..... N90-19428 #
CONF-900339-1 ..... N90-19659 #
CONF-900343-1 ..... N90-19762 #
CONF-900343-3 ..... N90-19836 #
CONF-900343-4 ..... N90-19865 #
CONF-900368-1 ..... N90-19590 #
CONF-900368-2 ..... N90-19517 #
CONF-900371-2 ..... N90-19378 #
CONF-900372-1 ..... N90-19217 #
CONF-900378-1 ..... N90-19493 #
CONF-900392-1 ..... N90-19777 #
CONF-900402-1 ..... N90-19377 #
CONF-900402-2 ..... N90-19730 #
CONF-900402-4 ..... N90-19331 #
CONF-900403-1 ..... N90-19352 #
CONF-900403-2 ..... N90-19626 #
CONF-900403-7 ..... N90-19354 #
CONF-900414-1 ..... N90-19587 #
CONF-900418-1 ..... N90-19804 #
CONF-900418-4 ..... N90-19835 #
CONF-900419-1 ..... N90-19358 #
CONF-900425-1 ..... N90-19356 #
CONF-900425-3 ..... N90-19355 #
CONF-900425-4 ..... N90-19357 #
CONF-900442-1 ..... N90-19606 #
CONF-900442-2 ..... N90-20029* #
CONF-900442-3 ..... N90-19744 #
CONF-900449-1 ..... N90-19664 #
CONF-900449-2 ..... N90-19669 #
CONF-900449-3 ..... N90-19670 #
CONF-900449-4 ..... N90-19671 #
CONF-900449-5 ..... N90-19330 #
CONF-900449-7 ..... N90-19665 #
CONF-900449-8 ..... N90-19666 #
CONF-900464-1 ..... N90-19753 #
CONF-900464-2 ..... N90-19514 #
CONF-900464-4 ..... N90-19746 #
CONF-900466-1 ..... N90-19892 #
CONF-900479-1 ..... N90-19820 #
CONF-900479-2 ..... N90-19627 #
CONF-900479-3 ..... N90-19551 #
CONF-900479-4 ..... N90-19215 #
CONF-900479-5 ..... N90-19628 #
CONF-900479-6 ..... N90-19810 #
CONF-900483-1 ..... N90-19704 #
CONF-900497-1 ..... N90-19353 #
CONF-8904242-4 ..... N90-19578 #
CONF-8904318-1 ..... N90-20027 #
CONF-8905201-5 ..... N90-19811 #
CONF-8906186-7 ..... N90-19925 #
CONF-8906200-4 ..... N90-19516 #
CONF-8906234-1 ..... N90-20039 #
CONF-8906239-3 ..... N90-19805 #
CONF-8906267-3 ..... N90-19905 #
CONF-8907176-1 ..... N90-19931 #
CONF-8908133-9 ..... N90-19861 #
CONF-8908134-26 ..... N90-19575 #
CONF-8908134-28 ..... N90-19576 #
CONF-8908134-30 ..... N90-19589 #
CONF-8908187 ..... N90-19370 #
CONF-8909275-3 ..... N90-19985 #
CONF-8910121-2 ..... N90-19824 #
CONF-8910248-2 ..... N90-19315 #
CONF-8910248-3 ..... N90-19368 #
CONF-8910304-2 ..... N90-19696 #
CONF-8910304-3 ..... N90-19895 #
CONF-8910320-3 ..... N90-19829 #
CONF-8910342-1 ..... N90-19459 #
CONF-8910350-1 ..... N90-19885 #
CONF-8910353-2 ..... N90-19558 #
CONF-8910358-2 ..... N90-19296 #
CONF-8911150-2 ..... N90-19832 #
CONF-8911161-2 ..... N90-19987 #
CONF-8911164-1 ..... N90-19908 #
CONF-9004116-1 ..... N90-19291 #
CONF-9004116-2 ..... N90-19562 #
CONF-9004125-1 ..... N90-19745 #
CONF-9004125-2 ..... N90-19779 #
CONF-9004136-2 ..... N90-19866 #
CONF-9004136-3 ..... N90-19248 #
CRIE-T-87088 ..... N90-19721 #
CRIE-T-87103 ..... N90-19677 #
CRIE-T-87104 ..... N90-19676 #
CRIE-U-88004 ..... N90-19707 #
CRIE-W-87040 ..... N90-19485 #
CRIE-W-87046 ..... N90-19553 #
CRIE-W-87047 ..... N90-19363 #
CRREL-SR-89-29 ..... N90-19637 #
CS-TR-2263 ..... N90-19766* #
CS-TR-2305 ..... N90-19765* #
CU-CS-449-89 ..... N90-19775 #
CU-CS-454-89 ..... N90-19806 #
CUED/A-AERO/15 ..... N90-19525 #
C87A-25 ..... N90-19518 #
DCIEM-89-RR-45 ..... N90-19788 #
DE89-009448 ..... N90-20033 #
DE89-009463 ..... N90-19560 #
DE89-016179 ..... N90-19606 #
DE89-016537 ..... N90-19664 #
DE89-016659 ..... N90-19804 #
DE89-782287 ..... N90-19363 #
DE89-782288 ..... N90-19553 #
DE89-782290 ..... N90-19485 #
DE89-782294 ..... N90-19526 #
DE89-782295 ..... N90-19527 #
DE89-782318 ..... N90-19676 #
DE89-782322 ..... N90-19721 #
DE89-782324 ..... N90-19677 #
DE89-782326 ..... N90-19707 #
DE89-782627 ..... N90-19654 #
DE89-910213 ..... N90-19650 #
DE89-910386 ..... N90-19651 #
DE90-000222 ..... N90-19649 #
DE90-000223 ..... N90-19703 #
DE90-000301 ..... N90-19886 #
DE90-000303 ..... N90-19665 #
DE90-000308 ..... N90-19666 #
DE90-000311 ..... N90-19667 #
DE90-000316 ..... N90-19273 #
DE90-000446 ..... N90-19668 #
DE90-000450 ..... N90-19607 #
DE90-000453 ..... N90-19550 #
DE90-000462 ..... N90-19513 #
DE90-000538 ..... N90-20029* #
DE90-000801 ..... N90-19669 #
DE90-001000 ..... N90-19753 #
DE90-001336 ..... N90-19428 #
DE90-002236 ..... N90-19861 #
DE90-002251 ..... N90-19659 #
DE90-002339 ..... N90-19571 #
DE90-002532 ..... N90-19377 #
DE90-002579 ..... N90-19572 #
DE90-002703 ..... N90-19762 #
DE90-002708 ..... N90-19352 #
DE90-002907 ..... N90-19670 #
DE90-003188 ..... N90-19931 #
DE90-003577 ..... N90-19671 #
DE90-003662 ..... N90-19744 #
DE90-003674 ..... N90-19704 #
DE90-003689 ..... N90-19626 #
DE90-003781 ..... N90-19669 #
DE90-003949 ..... N90-19330 #
DE90-003961 ..... N90-19730 #
DE90-004093 ..... N90-19839 #
DE90-004479 ..... N90-19361 #
DE90-004664 ..... N90-19870 #
DE90-004845 ..... N90-19341 #
DE90-004860 ..... N90-19905 #
DE90-004955 ..... N90-19342 #
DE90-004956 ..... N90-19871 #
DE90-005193 ..... N90-19217 #
DE90-005318 ..... N90-19493 #
DE90-005319 ..... N90-19368 #
DE90-005356 ..... N90-19317 #
DE90-005388 ..... N90-19304 #
DE90-005449 ..... N90-19514 #
DE90-005550 ..... N90-19825 #
DE90-005575 ..... N90-19353 #
DE90-005631 ..... N90-19354 #
DE90-005634 ..... N90-19835 #
DE90-005638 ..... N90-19824 #
DE90-005648 ..... N90-20038 #
DE90-005657 ..... N90-20037 #
DE90-005663 ..... N90-19331 #
DE90-005673 ..... N90-19853 #
DE90-005682 ..... N90-19836 #
DE90-005696 ..... N90-19319 #
DE90-005783 ..... N90-19781 #
DE90-005955 ..... N90-19573 #
DE90-005958 ..... N90-19892 #
DE90-005974 ..... N90-19834 #
DE90-005979 ..... N90-19792 #
DE90-005980 ..... N90-19793 #
DE90-005984 ..... N90-19574 #
DE90-005988 ..... N90-19532 #
DE90-005994 ..... N90-19459 #
DE90-006008 ..... N90-20039 #
DE90-006077 ..... N90-19369 #
DE90-006082 ..... N90-19856 #
DE90-006271 ..... N90-19711 #
DE90-006276 ..... N90-19494 #
DE90-006278 ..... N90-19291 #
DE90-006324 ..... N90-19777 #
DE90-006349 ..... N90-19705 #
DE90-006367 ..... N90-19731 #
DE90-006372 ..... N90-19848 #
DE90-006373 ..... N90-19893 #
DE90-006408 ..... N90-19348 #
DE90-006418 ..... N90-19247 #
DE90-006446 ..... N90-19887 #
DE90-006459 ..... N90-19496 #
DE90-006466 ..... N90-19802 #
DE90-006478 ..... N90-19551 #
DE90-006484 ..... N90-19908 #
DE90-006489 ..... N90-19355 #
DE90-006490 ..... N90-19356 #
DE90-006505 ..... N90-19575 #
DE90-006517 ..... N90-19584 #
DE90-006518 ..... N90-19585 #
DE90-006522 ..... N90-19987 #
DE90-006549 ..... N90-19859 #
DE90-006567 ..... N90-19885 #
DE90-006591 ..... N90-19371 #
DE90-006614 ..... N90-19745 #
DE90-006618 ..... N90-19746 #
DE90-006621 ..... N90-19877 #
DE90-006623 ..... N90-19878 #
DE90-006641 ..... N90-19794 #
DE90-006645 ..... N90-19983 #
DE90-006668 ..... N90-20040* #
DE90-006691 ..... N90-19984 #
DE90-006702 ..... N90-19860 #
DE90-006720 ..... N90-19909 #
DE90-006751 ..... N90-19862 #
DE90-006764 ..... N90-19576 #
DE90-006773 ..... N90-19586 #
DE90-006776 ..... N90-19578 #
DE90-006787 ..... N90-19536 #
DE90-006806 ..... N90-19577 #
DE90-006810 ..... N90-19820 #
DE90-006826 ..... N90-19282 #
DE90-006827 ..... N90-19283 #
DE90-006828 ..... N90-19284 #
DE90-006829 ..... N90-19285 #
DE90-006830 ..... N90-19286 #
DE90-006882 ..... N90-19837 #
DE90-006888 ..... N90-19315 #
DE90-006894 ..... N90-19587 #
DE90-006900 ..... N90-19845 #
DE90-006901 ..... N90-19638 #
DE90-006904 ..... N90-19484 #
DE90-006925 ..... N90-19357 #
DE90-006927 ..... N90-19985 #
DE90-006944 ..... N90-19927 #
DE90-006959 ..... N90-19582 #
DE90-007080 ..... N90-19372 #
DE90-007153 ..... N90-19627 #
DE90-007186 ..... N90-19892 #
DE90-007189 ..... N90-19847 #
DE90-007213 ..... N90-19878 #
DE90-007243 ..... N90-19579 #
DE90-007245 ..... N90-19580 #
DE90-007247 ..... N90-19515 #
DE90-007248 ..... N90-19829 #
DE90-007251 ..... N90-20027 #
DE90-007252 ..... N90-19473 #
DE90-007283 ..... N90-19557 #
DE90-007296 ..... N90-19830 #
DE90-007349 ..... N90-19325 #
DE90-007354 ..... N90-19337 #
DE90-007382 ..... N90-19558 #
DE90-007402 ..... N90-19588 #
DE90-007412 ..... N90-19628 #

DE90-007415 ..... N90-19332 #
DE90-007428 ..... N90-19694 #
DE90-007429 ..... N90-19215 #
DE90-007482 ..... N90-19779 #
DE90-007488 ..... N90-19811 #
DE90-007489 ..... N90-19831 #
DE90-007490 ..... N90-19665 #
DE90-007492 ..... N90-19805 #
DE90-007502 ..... N90-19358 #
DE90-007503 ..... N90-19516 #
DE90-007504 ..... N90-19895 #
DE90-007505 ..... N90-19248 #
DE90-007506 ..... N90-19517 #
DE90-007508 ..... N90-19589 #
DE90-007511 ..... N90-19770 #
DE90-007529 ..... N90-19359 #
DE90-007530 ..... N90-19866 #
DE90-007531 ..... N90-19896 #
DE90-007535 ..... N90-19925 #
DE90-007536 ..... N90-19590 #
DE90-007541 ..... N90-19832 #
DE90-007542 ..... N90-19771 #
DE90-007546 ..... N90-19810 #
DE90-007557 ..... N90-19897 #
DE90-007564 ..... N90-19333 #
DE90-007569 ..... N90-19772 #
DE90-007573 ..... N90-19379 #
DE90-007574 ..... N90-19380 #
DE90-007625 ..... N90-19293 #
DE90-007637 ..... N90-19334 #
DE90-007659 ..... N90-19335 #
DE90-007662 ..... N90-19381 #
DE90-007669 ..... N90-19898 #
DE90-007844 ..... N90-19294 #
DE90-007885 ..... N90-19382 #
DE90-008098 ..... N90-19336 #
DE90-008100 ..... N90-19838 #
DE90-008112 ..... N90-19383 #
DE90-008120 ..... N90-19474 #
DE90-008637 ..... N90-19296 #
DE90-009041 ..... N90-19833 #
DE90-606349 ..... N90-19362 #
DE90-608004 ..... N90-19370 #
DE90-608611 ..... N90-19790 #
DE90-608612 ..... N90-19533 #
DE90-608886 ..... N90-19808 #
DE90-608907 ..... N90-19906 #
DE90-610422 ..... N90-19795 #
DE90-610423 ..... N90-19796 #
DE90-610427 ..... N90-19797 #
DE90-610428 ..... N90-19798 #
DE90-610429 ..... N90-19799 #
DE90-610430 ..... N90-19800 #
DE90-610433 ..... N90-19801 #
DE90-610458 ..... N90-19461 #
DE90-610474 ..... N90-19462 #
DE90-610476 ..... N90-19712 #
DE90-610477 ..... N90-19907 #
DE90-610552 ..... N90-19615 #
DE90-610553 ..... N90-19349 #
DE90-610564 ..... N90-19879 #
DE90-610624 ..... N90-19857 #
DE90-610636 ..... N90-19986 #
DE90-610638 ..... N90-19858 #
DE90-610675 ..... N90-19880 #
DE90-610676 ..... N90-19801 #
DE90-610677 ..... N90-19882 #
DE90-719537 ..... N90-19344 #
DE90-741461 ..... N90-19910 #
DE90-741463 ..... N90-19988 #
DE90-741467 ..... N90-19803 #
DE90-741468 ..... N90-19911 #
DE90-741469 ..... N90-19912 #
DE90-741470 ..... N90-19913 #
DE90-741482 ..... N90-19350 #
DE90-741487 ..... N90-19465 #
DE90-749883 ..... N90-19863 #
DE90-750024 ..... N90-19914 #

DIGEL-1984-4 ..... N90-19509 #
DIGEL-1985-5 ..... N90-19506 #
DIGEL-1989-2 ..... N90-19508 #

DNA-TR-87-144 ..... N90-19567 #
DNA-TR-89-108 ..... N90-19658 #

DOE/CE-33007/T2 ..... N90-19292 #

DOE/DP-20153/T4 ..... N90-19464 #
DOE/DP-20153/T7 ..... N90-19638 #
DOE/DP-20153/T8 ..... N90-19845 #
DOE/DP-40200/113 ..... N90-19577 #

DOE/ER-0435 ..... N90-19836 #
DOE/ER-0442 ..... N90-19705 #
DOE/ER-10774/10 ..... N90-19983 #

DOE/ER-13443/3 ..... N90-19909 #
DOE/ER-13789/3 ..... N90-19335 #
DOE/ER-13913/2 ..... N90-19532 #
DOE/ER-25009/648 ..... N90-19777 #
DOE/ER-25019/14 ..... N90-19574 #
DOE/ER-25036/3 ..... N90-19794 #
DOE/ER-25061/4 ..... N90-19792 #
DOE/ER-25061/5 ..... N90-19793 #
DOE/ER-30131/T9 ..... N90-19588 #
DOE/ER-40147/8 ..... N90-19984 #
DOE/ER-40423/26 ..... N90-19834 #
DOE/ER-40509/1 ..... N90-19830 #
DOE/ER-45156/T3 ..... N90-19897 #
DOE/ER-45259/8 ..... N90-19898 #
DOE/ER-45286/3 ..... N90-19371 #
DOE/ER-45291/3 ..... N90-19372 #
DOE/ER-45315/3 ..... N90-19894 #
DOE/ER-45325/3 ..... N90-19381 #
DOE/ER-45356/3 ..... N90-19333 #
DOE/ER-53098/T1 ..... N90-19860 #
DOE/ER-53265/1 ..... N90-19859 #

DOE/ET-32043/T29-BK-1 ..... N90-19285 #
DOE/ET-32043/T29-BK-2 ..... N90-19286 #

DOE/MC-22064/2796 ..... N90-19550 #
DOE/MC-23139/2794 ..... N90-19513 #
DOE/MC-23256/2787-VOL-2 ..... N90-19607 #
DOE/MC-24223/2792 ..... N90-19668 #

DOE/NBB-0085 ..... N90-19673 #
DOE/NBB-0087 ..... N90-19927 #

DOE/PC-88947/T5 ..... N90-19536 #

DOT/FAA/AM-89/11 ..... N90-19214 #

DOT/FAA/CT-89/8 ..... N90-19920 #
DOT/FAA/CT-89/33 ..... N90-19387 #
DOT/FAA/CT-90/1-VOL-1 ..... N90-19472 #

DREO-TN-89-15 ..... N90-19457 #

DRIC-BR-112012 ..... N90-19202 #

DWD-14 ..... N90-19661

E-2641 ..... N90-19593* #
E-4981 ..... N90-19242* #
E-4985 ..... N90-19302* #
E-5180 ..... N90-19454* #
E-5208 ..... N90-19310* #
E-5228 ..... N90-19203* #
E-5292 ..... N90-19783* #
E-5297 ..... N90-19484* #
E-5308 ..... N90-19373* #
E-5309 ..... N90-19299* #
E-5313 ..... N90-19301* #
E-5314 ..... N90-19374* #
E-5321 ..... N90-19617* #
E-5342 ..... N90-19234* #
E-5380 ..... N90-19629* #

EGG-M-89447 ..... N90-19332 #

EOARD-TR-90-013 ..... N90-19736 #

EPA/600/3-89/073 ..... N90-19674 #
EPA/600/7-89/010A ..... N90-19679 #

ERIM-222300-1-F ..... N90-19583 #

ESA-BR-58 ..... N90-19631 #

ESA-SP-302 ..... N90-19989 #

ESD-TR-89-222 ..... N90-19488 #

ESDU-STRUCT-H.00.00.02 ..... N90-19522
ESDU-STRUCT-H.02.00.00 ..... N90-19611
ESDU-STRUCT-H.02.00.05 ..... N90-19904
ESDU-STRUCT-H.04.00.01 ..... N90-19612

ESDU-87004 ..... N90-19195
ESDU-89021 ..... N90-19611
ESDU-89022 ..... N90-19522
ESDU-89026 ..... N90-19904
ESDU-89027 ..... N90-19612

ETN-89-93747 ..... N90-19928 #
ETN-89-94032 ..... N90-19191 #
ETN-89-94044 ..... N90-19672 #
ETN-89-94047 ..... N90-19758 #
ETN-89-94113 ..... N90-19192 #
ETN-90-94422 ..... N90-19661
ETN-90-95076 ..... N90-19467

ETN-90-95078 ..... N90-19497
ETN-90-95080 ..... N90-19848
ETN-90-95088 ..... N90-19498
ETN-90-95089 ..... N90-19847
ETN-90-95091 ..... N90-19738
ETN-90-95318 ..... N90-19540 #
ETN-90-95324 ..... N90-19235 #
ETN-90-95335 ..... N90-19680 #
ETN-90-95336 ..... N90-19726 #
ETN-90-95338 ..... N90-19499
ETN-90-95347 ..... N90-19466
ETN-90-95351 ..... N90-19559 #
ETN-90-95353 ..... N90-19618 #
ETN-90-95354 ..... N90-19662 #
ETN-90-95357 ..... N90-19915 #
ETN-90-95358 ..... N90-19327 #
ETN-90-95359 ..... N90-19500 #
ETN-90-95360 ..... N90-19489 #
ETN-90-95361 ..... N90-19581 #
ETN-90-95362 ..... N90-19604 #
ETN-90-95363 ..... N90-19501 #
ETN-90-95364 ..... N90-19502 #
ETN-90-95365 ..... N90-19752 #
ETN-90-95367 ..... N90-19207 #
ETN-90-95368 ..... N90-19208 #
ETN-90-95369 ..... N90-19541 #
ETN-90-95370 ..... N90-19767 #
ETN-90-95371 ..... N90-19351 #
ETN-90-95372 ..... N90-19542 #
ETN-90-95373 ..... N90-20024 #
ETN-90-95375 ..... N90-19864 #
ETN-90-95376 ..... N90-19702 #
ETN-90-95377 ..... N90-19619 #
ETN-90-95378 ..... N90-19503 #
ETN-90-95379 ..... N90-19246 #
ETN-90-95383 ..... N90-20043 #
ETN-90-95406 ..... N90-19510 #
ETN-90-95408 ..... N90-19924 #
ETN-90-95413 ..... N90-19543 #
ETN-90-95418 ..... N90-19639 #
ETN-90-95419 ..... N90-19228 #
ETN-90-95435 ..... N90-19803 #
ETN-90-95441 ..... N90-19933 #
ETN-90-95450 ..... N90-19219 #
ETN-90-95451 ..... N90-19220 #
ETN-90-95452 ..... N90-19640 #
ETN-90-95468 ..... N90-19739 #
ETN-90-95470 ..... N90-19620 #
ETN-90-95472 ..... N90-19647 #
ETN-90-95478 ..... N90-19641 #
ETN-90-95479 ..... N90-19582 #
ETN-90-95480 ..... N90-19642 #
ETN-90-95483 ..... N90-19643 #
ETN-90-95485 ..... N90-19644 #
ETN-90-95599 ..... N90-19735
ETN-90-95721 ..... N90-19734 #
ETN-90-95722 ..... N90-19845 #
ETN-90-95723 ..... N90-19846 #
ETN-90-95726 ..... N90-19504 #
ETN-90-95727 ..... N90-19605 #
ETN-90-95728 ..... N90-19583 #
ETN-90-95729 ..... N90-19727
ETN-90-95730 ..... N90-19934 #
ETN-90-95731 ..... N90-19505 #
ETN-90-95732 ..... N90-19935 #
ETN-90-95733 ..... N90-19560 #
ETN-90-95734 ..... N90-20025 #
ETN-90-95735 ..... N90-20041 #
ETN-90-95736 ..... N90-20026 #
ETN-90-95756 ..... N90-19329 #
ETN-90-95802 ..... N90-19506 #
ETN-90-95822 ..... N90-19507 #
ETN-90-95823 ..... N90-19621 #
ETN-90-95824 ..... N90-19818 #
ETN-90-95825 ..... N90-19827 #
ETN-90-95827 ..... N90-19936 #
ETN-90-95828 ..... N90-20042 #
ETN-90-95829 ..... N90-19937 #
ETN-90-95851 ..... N90-19209 #
ETN-90-95852 ..... N90-19210 #
ETN-90-95853 ..... N90-19544 #
ETN-90-95859 ..... N90-19828 #
ETN-90-95865 ..... N90-19236 #
ETN-90-95866 ..... N90-19221 #
ETN-90-95867 ..... N90-19311 #
ETN-90-95868 ..... N90-19622 #
ETN-90-95869 ..... N90-19623 #
ETN-90-95870 ..... N90-19328 #
ETN-90-95874 ..... N90-19244 #
ETN-90-95880 ..... N90-19545 #
ETN-90-95884 ..... N90-19768
ETN-90-95885 ..... N90-19716
ETN-90-95887 ..... N90-19809 #
ETN-90-95889 ..... N90-19819 #
ETN-90-95890 ..... N90-19624 #
ETN-90-95891 ..... N90-19511 #

ETN-90-95893 N90-19769 #
ETN-90-95894 N90-19229 #
ETN-90-95895 N90-19313 #
ETN-90-95896 N90-19287 #
ETN-90-95897 N90-19288 #
ETN-90-95898 N90-19289 #
ETN-90-95902 N90-19375 #
ETN-90-95903 N90-19290 #
ETN-90-95904 N90-19938 #
ETN-90-95913 N90-19546 #
ETN-90-95914 N90-19547 #
ETN-90-95915 N90-19889 #
ETN-90-95916 N90-19888 #
ETN-90-95917 N90-19376 #
ETN-90-95918 N90-19939 #
ETN-90-95977 N90-19508 #
ETN-90-95978 N90-19509 #
ETN-90-95989 N90-19312 #
ETN-90-95997 N90-19561 #
ETN-90-95999 N90-19548 #
ETN-90-96004 N90-19648 #
ETN-90-96056 N90-19512 #
ETN-90-96057 N90-19890 #
ETN-90-96058 N90-19470 #
ETN-90-96059 N90-19891 #
ETN-90-96062 N90-19663 #
ETN-90-96067 N90-19549 #
ETN-90-96068 N90-19754 #
ETN-90-96069 N90-19728 #
ETN-90-96070 N90-19729 #
ETN-90-96072 N90-19625 #
ETN-90-96074 N90-19471 #
ETN-90-96075 N90-19231 #
ETN-90-96076 N90-19314 #
ETN-90-96299 N90-19989 #

FEL-1988-34 N90-19467
FEL-1988-55 N90-19497
FEL-1988-62 N90-19846
FEL-1989-101 N90-19498

GA-A-19753 N90-19839 #

GL-TR-89-0061 N90-19724 #
GL-TR-89-0218 N90-20030* #
GL-TR-89-0266 N90-19323 #
GL-TR-89-0272 N90-19655 #

GRI-88/0301 N90-19324 #
GRI-89/0134-PHASE-1 N90-19655 #
GRI-89/0162 N90-19653 #
GRI-89/0175 N90-19826 #
GRI-89/0209 N90-19320 #
GRI-89/0223 N90-19652 #

G8558-8701 N90-19386* #

H-1522 N90-19241* #
H-1574 N90-19225* #
H-1586 N90-19224* #

HPTC-05 N90-19526 #
HPTC-8801 N90-19527 #

HUF-2 N90-18337 #

IC-88/400 N90-19880 #
IC-88/401 N90-19881 #
IC-88/402 N90-19882 #
IC-89/151 N90-19461 #
IC-89/165 N90-19857 #
IC-89/175 N90-19879 #
IC-89/193-3 N90-19795 #
IC-89/198 N90-19986 #
IC-89/199 N90-19462 #
IC-89/200 N90-19858 #
IC-89/207 N90-19796 #
IC-89/240 N90-19615 #
IC-89/241 N90-19349 #
IC-89/248 N90-19712 #
IC-89/269 N90-19797 #
IC-89/280 N90-19907 #
IC-89/285 N90-19798 #
IC-89/300 N90-19799 #
IC-89/301 N90-19800 #
IC-89/305 N90-19801 #

ICASE-90-17 N90-19791* #
ICASE-90-18 N90-19537* #
ICASE-90-22 N90-19539* #
ICASE-90-26 N90-19538* #

ICOMP-90-03 N90-19783* #

ICW-1832 N90-19642 #

IEE-SR-207 N90-19850 #

IFVE-OTF-88-212 N90-19906 #

IHW-ET/50 N90-19542 #

ILR-MITT-213 N90-19618 #
ILR-MITT-215 N90-19662 #

INIS-BR-1640 N90-19362 #
INIS-BR-1752 N90-19370 #

INPE-4752-TDL/346 N90-19733 #
INPE-4789-RPE/583 N90-19486 #
INPE-4793-TDL/355 N90-19656 #
INPE-4812-TDL/359 N90-19722 #
INPE-4818-NTE/289 N90-19277 #
INPE-4830-PRE/1451 N90-19708 #
INPE-4855-PRE/1478 N90-19635 #
INPE-4857-TDL/368 N90-19276 #
INPE-4865-TDL/376 N90-19723 #
INPE-4880-PRE/1489 N90-19633 #
INPE-4884-PRE/1491 N90-19632 #
INPE-4891-PRE/1492 N90-19636 #
INPE-4894-PRE/1495 N90-19782 #
INPE-4896-PRE/1496 N90-19634 #
INPE-4921-TDL/382 N90-19919 #
INPE-4925-TDL/385 N90-19654 #
INPE-4928-RPE/595 N90-19487 #

INS-759 N90-19988 #
INS-762 N90-19910 #
INS-778 N90-19914 #

IR-192 N90-19918 #

ISBN-0-85679-597-6 N90-19195
ISBN-0-85679-693-X N90-19522
ISBN-0-85679-694-8 N90-19611
ISBN-0-85679-698-0 N90-19904
ISBN-0-85679-699-9 N90-19612
ISBN-3-7686-9395-7 N90-19768
ISBN-3-7686-9397-3 N90-19716
ISBN-3-88148-248-2 N90-19727
ISBN-92-835-0501-8 N90-19232 #
ISBN-92-9092-050-5 N90-19989 #
ISBN-951-754-981-4 N90-19495 #

ISL-CO-203/88 N90-19192 #

ISSN-0038-0911 N90-20031 #
ISSN-0038-0911 N90-20032 #
ISSN-0065-5325 N90-19716
ISSN-0065-5325 N90-19768
ISSN-0069-5882 N90-19680 #
ISSN-0069-5882 N90-19728 #
ISSN-0069-5882 N90-19729 #
ISSN-0072-4130 N90-19727
ISSN-0141-4097 N90-19522
ISSN-0141-4097 N90-19611
ISSN-0141-4097 N90-19612
ISSN-0141-4097 N90-19904
ISSN-0141-4356 N90-19195
ISSN-0169-1651 N90-19735
ISSN-0174-1454 N90-19559 #
ISSN-0178-0719 N90-19499
ISSN-0250-1589 N90-19631 #
ISSN-0309-7293 N90-19525 #
ISSN-0374-1257 N90-19209 #
ISSN-0374-1257 N90-19210 #
ISSN-0379-6566 N90-19969 #
ISSN-0436-1199 N90-19544 #
ISSN-0920-2358 N90-19803 #

ITA-90-26-001 N90-19343 #

ITSM-MITT-30 N90-19236 #

IZF-1988-12 N90-19847
IZF-1988-22 N90-19738

JAERI-M-89-071 N90-19344 #
JAERI-M-89-106 N90-19350 #
JAERI-M-89-121 N90-19603 #
JAERI-M-89-132 N90-19863 #

JPL-TDA-PR-42-99 N90-19434* #

K/DSRD-119 N90-19747 #

K/TR-89/7 N90-19369 #

KEK-89-4 N90-19485 #

KNMI-WR-88-03 N90-19735

L-89-600204 N90-19593* #
L-16550 N90-19718* #
L-16612 N90-19249* #
L-16632 N90-19193* #
L-16639 N90-19595* #
L-16643 N90-19610* #
L-16664 N90-19239* #
L-16710 N90-19199* #
L-16722 N90-19200* #
L-16733 N90-20036* #

LA-UR-89-669 N90-19517 #
LA-UR-89-3013 N90-20029* #
LA-UR-89-3737 N90-19931 #
LA-UR-89-3858 N90-19744 #
LA-UR-89-4160 N90-19341 #
LA-UR-89-4210 N90-19905 #
LA-UR-90-3 N90-19908 #
LA-UR-90-24 N90-19355 #
LA-UR-90-25 N90-19356 #
LA-UR-90-42 N90-19987 #
LA-UR-90-161 N90-19584 #
LA-UR-90-165 N90-19585 #
LA-UR-90-170 N90-19296 #
LA-UR-90-223 N90-19575 #
LA-UR-90-356 N90-19810 #
LA-UR-90-379 N90-19811 #
LA-UR-90-383 N90-19831 #
LA-UR-90-443 N90-19293 #
LA-UR-90-452 N90-19359 #
LA-UR-90-456 N90-19866 #
LA-UR-90-459 N90-19896 #
LA-UR-90-493 N90-19925 #
LA-UR-90-496 N90-19590 #
LA-UR-90-539 N90-19832 #
LA-UR-90-540 N90-19771 #
LA-UR-90-608 N90-19865 #
LA-UR-90-627 N90-19805 #
LA-UR-90-654 N90-19358 #
LA-UR-90-655 N90-19516 #
LA-UR-90-660 N90-19895 #
LA-UR-90-668 N90-19248 #
LA-UR-90-696 N90-19589 #
LA-UR-90-714 N90-19770 #

LA-11725-MS N90-19833 #

LBL-28078 N90-19325 #

LC-79-640375 N90-20031 #
LC-79-640375 N90-20032 #

LFD-282 N90-19488

LIDS-P-1929 N90-19807 #

LINO-162 N90-19924 #
LINO-1988-3 N90-19510 #

LNCC-009/89 N90-19790 #
LNCC-010/89 N90-19533 #

LR-528 N90-19329 #
LR-530 N90-19561 #
LR-548 N90-19312 #
LR-552 N90-19548 #

LSDI-90-06 N90-19608* #

MIT/LCS/TM-406 N90-19784 #

MITT-88-04 N90-19235 #

MLM-3613 N90-19319 #
MLM-3628-OP N90-19334 #

MML-TR-89-117C N90-19900 #

MPE-213 N90-19499

MPI-PAE/EXP.EL-200 N90-19828 #

MPIS-MITT-91 N90-19209 #
MPIS-MITT-92 N90-19210 #

MPIS-6/1989 N90-19544 #

MPL-U-26/89 N90-19724 #

MRL-RR-8-89 N90-19528 #

MRL-TR-89-31 N90-19364 #
MRL-TR-89-33 N90-19385 #

MT/01-89.A1 N90-19920 #

MTL-TR-89-46 N90-19347 #

MW-89-P-4 N90-19520 #

NAS 1.15:4156 N90-19610* #
NAS 1.15:4178 N90-20036* #
NAS 1.15:4181 N90-19199* #
NAS 1.15:100384 N90-19916* #
NAS 1.15:100388 N90-19616* #
NAS 1.15:100389 N90-19556* #
NAS 1.15:100454 N90-19241* #
NAS 1.15:101647 N90-19279* #
NAS 1.15:101656 N90-19205* #
NAS 1.15:101671 N90-19453* #
NAS 1.15:101684 N90-19206* #
NAS 1.15:101715 N90-19225* #
NAS 1.15:101716 N90-19224* #
NAS 1.15:101748 N90-19389* #
NAS 1.15:102225 N90-19201* #
NAS 1.15:102235 N90-19204* #
NAS 1.15:102257 N90-19524* #
NAS 1.15:102415 N90-19454* #
NAS 1.15:102439 N90-19310* #
NAS 1.15:102498 N90-19783* #
NAS 1.15:102500 N90-19484* #
NAS 1.15:102506 N90-19373* #
NAS 1.15:102507 N90-19299* #
NAS 1.15:102511 N90-19301* #
NAS 1.15:102516 N90-19617* #
NAS 1.15:102533 N90-19234* #
NAS 1.15:102560 N90-19629* #
NAS 1.15:102585 N90-19821* #
NAS 1.15:102608 N90-19555* #
NAS 1.15:102609 N90-19211* #
NAS 1.15:102619 N90-19281* #
NAS 1.15:102620 N90-19227* #
NAS 1.15:102626 N90-19630* #
NAS 1.15:102924 N90-19243* #
NAS 1.21:7037(249) N90-19190*
NAS 1.26:4278 N90-19203* #
NAS 1.26:4288 N90-19226* #
NAS 1.26:181905 N90-19741* #
NAS 1.26:181999 N90-19791* #
NAS 1.26:182002 N90-19537* #
NAS 1.26:182011 N90-19539* #
NAS 1.26:182017 N90-19538* #
NAS 1.26:183457 N90-19523* #
NAS 1.26:183837 N90-19390* #
NAS 1.26:183902 N90-19608* #
NAS 1.26:185033 N90-19434* #
NAS 1.26:185186 N90-19386* #
NAS 1.26:185209 N90-19374* #
NAS 1.26:185604 N90-19280* #
NAS 1.26:186064 N90-19757* #
NAS 1.26:186084 N90-19758* #
NAS 1.26:186125 N90-20030* #
NAS 1.26:186175 N90-19599* #
NAS 1.26:186297 N90-19613* #
NAS 1.26:186299 N90-19275* #
NAS 1.26:186308 N90-19429* #
NAS 1.26:186316 N90-19552* #
NAS 1.26:186327 N90-19198* #
NAS 1.26:186354 N90-19873* #
NAS 1.26:186355 N90-19932* #
NAS 1.26:186375 N90-19725* #
NAS 1.26:186377 N90-19710* #
NAS 1.26:186380 N90-19460* #
NAS 1.26:186397 N90-19535* #
NAS 1.26:186406 N90-19308* #
NAS 1.26:186407 N90-19763* #
NAS 1.26:186412 N90-19923* #
NAS 1.26:186438 N90-19764* #
NAS 1.26:186456 N90-19766* #
NAS 1.26:186458 N90-19765* #
NAS 1.26:186460 N90-19715* #
NAS 1.26:186461 N90-19714* #
NAS 1.26:186462 N90-19713* #
NAS 1.26:186463 N90-19326* #
NAS 1.26:186464 N90-19309* #
NAS 1.26:186466 N90-19466* #
NAS 1.26:186497 N90-20040* #
NAS 1.26:186498 N90-20029* #
NAS 1.26:186504 N90-19340* #
NAS 1.55:3040 N90-19249* #
NAS 1.55:3046 N90-19940* #
NAS 1.60:2963 N90-19718* #
NAS 1.60:2970 N90-19302* #
NAS 1.60:2973 N90-19193* #
NAS 1.60:2977 N90-19595* #
NAS 1.60:2982 N90-19239* #
NAS 1.60:2991 N90-19200* #
NAS 1.60:2996 N90-19242* #
NAS 1.61:1212 N90-19593* #

NASA-CASE-LAR-13638-1 N90-19427*
NASA-CASE-LAR-13773-1 N90-19298*
NASA-CASE-LAR-13952-1-SB N90-19534*

NASA-CASE-LEW-14346-1 N90-19300*

NASA-CASE-MFS-29149-1 N90-19492*
NASA-CASE-MFS-29260-1 N90-19602*

NASA-CASE-MSC-21356-1 N90-19278*

NASA-CASE-NPO-16901-1-CU N90-19425*
NASA-CASE-NPO-16949-1-CU N90-19776*
NASA-CASE-NPO-17259-1-CU N90-19884*

NASA-CP-3040 N90-19249* #
NASA-CP-3046 N90-19940* #

NASA-CR-4278 N90-19203* #
NASA-CR-4288 N90-19226* #
NASA-CR-181905 N90-19741* #
NASA-CR-181999 N90-19791* #
NASA-CR-182002 N90-19537* #
NASA-CR-182011 N90-19539* #
NASA-CR-182017 N90-19538* #
NASA-CR-183457 N90-19523* #
NASA-CR-183837 N90-19390* #
NASA-CR-183902 N90-19608* #
NASA-CR-185033 N90-19434* #
NASA-CR-185186 N90-19386* #
NASA-CR-185209 N90-19374* #
NASA-CR-185604 N90-19280* #
NASA-CR-186064 N90-19757* #
NASA-CR-186084 N90-19758* #
NASA-CR-186125 N90-20030* #
NASA-CR-186175 N90-19599* #
NASA-CR-186297 N90-19813* #
NASA-CR-186299 N90-19275* #
NASA-CR-186308 N90-19429* #
NASA-CR-186316 N90-19552* #
NASA-CR-186327 N90-19198* #
NASA-CR-186354 N90-19873* #
NASA-CR-186355 N90-19932* #
NASA-CR-186375 N90-19725* #
NASA-CR-186377 N90-19710* #
NASA-CR-186380 N90-19460* #
NASA-CR-186397 N90-19535* #
NASA-CR-186406 N90-19308* #
NASA-CR-186407 N90-19763* #
NASA-CR-186412 N90-19923* #
NASA-CR-186438 N90-19764* #
NASA-CR-186456 N90-19766* #
NASA-CR-186458 N90-19765* #
NASA-CR-186460 N90-19715* #
NASA-CR-186461 N90-19714* #
NASA-CR-186462 N90-19713* #
NASA-CR-186463 N90-19326* #
NASA-CR-186464 N90-19309* #
NASA-CR-186466 N90-19466* #
NASA-CR-186497 N90-20040* #
NASA-CR-186498 N90-20029* #
NASA-CR-186504 N90-19340* #

NASA-RP-1212 N90-19593* #

NASA-SP-7037(249) N90-19190*

NASA-TM-4156 N90-19610* #
NASA-TM-4178 N90-20036* #
NASA-TM-4181 N90-19199* #
NASA-TM-100384 N90-19916* #
NASA-TM-100388 N90-19616* #
NASA-TM-100389 N90-19556* #
NASA-TM-100454 N90-19241* #
NASA-TM-101647 N90-19279* #
NASA-TM-101656 N90-19205* #
NASA-TM-101671 N90-19453* #
NASA-TM-101684 N90-19206* #
NASA-TM-101715 N90-19225* #
NASA-TM-101716 N90-19224* #
NASA-TM-101748 N90-19389* #
NASA-TM-102225 N90-19201* #
NASA-TM-102235 N90-19204* #
NASA-TM-102257 N90-19524* #
NASA-TM-102415 N90-19454* #
NASA-TM-102439 N90-19310* #
NASA-TM-102498 N90-19783* #
NASA-TM-102500 N90-19484* #
NASA-TM-102506 N90-19373* #
NASA-TM-102507 N90-19299* #
NASA-TM-102511 N90-19301* #
NASA-TM-102516 N90-19617* #
NASA-TM-102533 N90-19234* #
NASA-TM-102560 N90-19629* #
NASA-TM-102585 N90-19821* #
NASA-TM-102608 N90-19555* #
NASA-TM-102609 N90-19211* #
NASA-TM-102619 N90-19281* #
NASA-TM-102620 N90-19227* #
NASA-TM-102626 N90-19630* #
NASA-TM-102924 N90-19243* #

NASA-TP-2963 N90-19718* #
NASA-TP-2970 N90-19302* #
NASA-TP-2973 N90-19193* #
NASA-TP-2977 N90-19595* #
NASA-TP-2982 N90-19239* #
NASA-TP-2991 N90-19200* #
NASA-TP-2996 N90-19242* #

NCSC-CR-2210-89-1 N90-19529 #

NEDOJ-P-8717 N90-19654 #
NEDOJ-P-8731 N90-19651 #

NEFES/89-18 N90-19678 #

NGS-45 N90-19218 #

NIPER-444 N90-19649 #
NIPER-450 N90-19703 #

NLR-MP-87019-U N90-19191 #
NLR-MP-87070-U N90-19672 #
NLR-MP-87078-U N90-19756 #
NLR-MP-87082-U N90-19543 #
NLR-MP-88021-U N90-19639 #
NLR-MP-88023-U N90-19228 #

NOAA-DR-ERL-AOML-14 N90-19732 #

NOAA-TR-NOS-132 N90-19218 #

NRL-MR-6534 N90-19875 #
NRL-MR-6545 N90-19867 #
NRL-MR-6583 N90-19338 #
NRL-MR-6600 N90-19868 #

NSF/ENG-89052 N90-19780 #

NSSDC/WDC-A-R/S-88-03 N90-19243* #

NTIA-89-248 N90-19760 #
NTIA-89-250 N90-19463 #

NUS-5235-BK-1 N90-19282 #
NUS-5235-BK-2 N90-19283 #
NUS-5238 N90-19284 #

OHB-TN-TOP-011/87 N90-19244 #

ORNL/OMIS-89/9 N90-19848 #

ORNL/TM-11316 N90-19781 #

ORNL/TR-89/54 N90-19856 #

OSU-TR-720964-5 N90-19466* #

PB89-138512 N90-19883 #
PB90-113978 N90-19732 #
PB90-114562 N90-19652 #
PB90-114968 N90-19653 #
PB90-115270 N90-19926 #
PB90-115387 N90-19564 #
PB90-115569 N90-19343 #
PB90-118472 N90-19760 #
PB90-120072 N90-19674 #
PB90-120288 N90-19675 #
PB90-121112 N90-19720 #
PB90-121229 N90-19780 #
PB90-122474 N90-19495 #
PB90-122755 N90-20031 #
PB90-122763 N90-20032 #
PB90-124611 N90-19613 #
PB90-124694 N90-19918 #
PB90-125428 N90-19218 #
PB90-126012 N90-19679 #
PB90-127119 N90-19678 #
PB90-127325 N90-19216 #
PB90-127457 N90-19655 #
PB90-127499 N90-19320 #
PB90-129990 N90-19483 #
PB90-130329 N90-19826 #
PB90-130345 N90-19324 #
PB90-138652 N90-19922 #
PB90-142563 N90-19921 #

PD-CF-8941 N90-19755 #
PD-CF-8943 N90-19213 #

PKC-TR-89-3 N90-19761 #

PML-1987-C103 N90-19329 #

PML-1987-C123 N90-19561 #
PML-1988-C27 N90-19548 #

PNL-7269 N90-19294 #

PREPRINT-88-14 N90-19656 #
PREPRINT-500 N90-19545 #

PSR-1864-VOL-1 N90-19709 #

PSU-ME-R-89/90-0011 N90-19535* #

R-586 N90-19613 #
R-8709 N90-19289 #
R-8840 N90-19288 #
R-8841 N90-19287 #

R/D-6003-EE-02 N90-19345 #

RADC-TR-89-67 N90-19614 #
RADC-TR-89-198 N90-19458 #

RAE-TM-AERO-2147 N90-19202 #

RB-4180 N90-19754 #

REPT-FB-01/88 N90-19619 #

REPT-1-89 N90-19468
REPT-29/89 N90-19290 #
REPT-33/89 N90-19938 #
REPT-50 N90-19495 #
REPT-61 N90-19680 #
REPT-70 N90-19726 #
REPT-87M/43/05720/SCP/GRF N90-19620 #
REPT-88-93 N90-19803 #
REPT-89-07 N90-19933 #
REPT-1273-15 N90-19653 #
REPT-8990 N90-19741* #

RIT/DIRS-89/90-50-135 N90-19464 #
RIT/DIRS-89/90-51-133 N90-19645 #
RIT/DIRS-89/90-66-131 N90-19638 #

RRK-89-24 N90-19911 #
RRK-89-25 N90-19912 #
RRK-89-27 N90-19913 #

R8912-1 N90-19475 #

SAND-89-0077 N90-19602 #
SAND-89-0753C N90-19606 #
SAND-89-1500C N90-19669 #
SAND-89-1506C N90-19330 #
SAND-89-1582C N90-19664 #
SAND-89-1658C N90-19551 #
SAND-89-1972C N90-19217 #
SAND-89-1980C N90-19562 #
SAND-89-2140C N90-19215 #
SAND-89-2360C N90-19670 #
SAND-89-2400-PT-2 N90-19336 #
SAND-89-2512C N90-19377 #
SAND-89-2535 N90-19247 #
SAND-89-2631C N90-19572 #
SAND-89-2772C N90-19671 #
SAND-89-2784 N90-19887 #
SAND-89-2867C N90-19820 #
SAND-89-2959C N90-19892 #
SAND-89-3051 N90-19731 #
SAND-89-3135C N90-19378 #
SAND-89-7154 N90-19862 #
SAND-90-0092C N90-19291 #
SAND-90-0258C N90-19494 #
SAND-90-0334C N90-19628 #
SAND-90-0335C-PT-2 N90-19627 #
SAND-90-0395 N90-19893 #
SAND-90-8200 N90-19383 #
SAND-1350C N90-19573 #

SER-C-PREPUB-FASC-31 N90-19928 #

SER-C-347 N90-19768
SER-C-349 N90-19716

SERI/PR-212-3494 N90-19660 #

SERI/STR-211-3612 N90-19656 #

SERI/TP-253-3614 N90-19665 #
SERI/TP-254-3619 N90-19666 #
SERI/TP-257-3662 N90-19273 #

SERI/TR-215-3513B N90-20033 #
SERI/TR-253-3438 N90-19667 #

SFB-228 N90-19221 #

SFCC-47 N90-19329 #
SFCC-48 N90-19561 #
SFCC-51 N90-19548 #

SGD-541-PT-1 N90-20032 #
SGD-541-PT-2 N90-20031 #

SIO-REF-89-7 N90-19724 #

SR-1-VOL-1 N90-19709 #
SR-2 N90-19323 #

SU-SLAC-PUB-5183 N90-19496 #
SU-SLAC-PUB-5193 N90-19838 #

SU-SLAC-TN-90-2 N90-19772 #

TB-88/1 N90-19540 #

TD-88-3861 N90-19467
TD-88-3881 N90-19497
TD-88-4124 N90-19847
TD-88-4127 N90-19846
TD-89-0531 N90-19738
TD-89-1656 N90-19458

TM-EA-8901 N90-19212 #

TOP-7-2-513 N90-19743 #

TPD-733.806 N90-19582 #

TR-1 N90-19876 #
TR-2 N90-19366 #
TR-2 N90-19570 #
TR-3 N90-19339 #
TR-3 N90-19823 #
TR-5 N90-19902 #
TR-6 N90-19901 #
TR-7 N90-19903 #
TR-8 N90-19367 #
TR-54 N90-19322 #
TR-64 N90-19815 #
TR-89-3 N90-19793 #
TR-89-4 N90-19792 #
TR-89-7 N90-19574 #
TR-89-1042 N90-19923* #
TR-1988 N90-19337 #

TRI-PP-89-92 N90-19837 #

TR045 N90-19673 #

TWR-50087 N90-19608* #

UBUFFALO/DC/89/TR-4 N90-19874 #

UCID-21835 N90-19474 #
UCID-21847 N90-19348 #

UCLA-ENG-90-05 N90-19552* #

UCRL-21231 N90-19558 #
UCRL-21272 N90-19711 #
UCRL-53932 N90-19361 #
UCRL-100367 N90-19578 #
UCRL-101123 N90-20027 #
UCRL-101650 N90-19586 #
UCRL-101784 N90-19557 #
UCRL-101807 N90-19473 #
UCRL-101946 N90-19576 #
UCRL-101952 N90-19459 #
UCRL-102037 N90-19861 #
UCRL-102151 N90-19571 #
UCRL-102284 N90-19357 #
UCRL-102293 N90-19829 #
UCRL-102454 N90-19825 #
UCRL-102499 N90-19985 #
UCRL-102673 N90-19579 #
UCRL-102674 N90-19580 #
UCRL-102757 N90-19515 #

UJV-8727-R N90-19608 #

UM-025921-11-T N90-19309* #

UMIACS-TR-89-57 N90-19766* #
UMIACS-TR-89-84 N90-19765* #

US-PATENT-APPL-SN-024202 N90-19565
US-PATENT-APPL-SN-073541 N90-19492*
US-PATENT-APPL-SN-145020 N90-19840
US-PATENT-APPL-SN-154565 N90-19554
US-PATENT-APPL-SN-156059 N90-19602*
US-PATENT-APPL-SN-165946 N90-19298*
US-PATENT-APPL-SN-165956 N90-19278*

US-PATENT-APPL-SN-174261 N90-19360
US-PATENT-APPL-SN-176115 N90-19872
US-PATENT-APPL-SN-176958 N90-19431
US-PATENT-APPL-SN-184234 N90-19884*
US-PATENT-APPL-SN-195991 N90-19750
US-PATENT-APPL-SN-195992 N90-19432
US-PATENT-APPL-SN-203178 N90-19534*
US-PATENT-APPL-SN-223124 N90-19427*
US-PATENT-APPL-SN-239156 N90-19841
US-PATENT-APPL-SN-242001 N90-19456 #
US-PATENT-APPL-SN-246703 N90-19490
US-PATENT-APPL-SN-260847 N90-19568
US-PATENT-APPL-SN-262380 N90-19480
US-PATENT-APPL-SN-280869 N90-19657 #
US-PATENT-APPL-SN-392866 N90-19305 #
US-PATENT-APPL-SN-415740 N90-19318 #
US-PATENT-APPL-SN-417132 N90-19482 #
US-PATENT-APPL-SN-428792 N90-19483 #
US-PATENT-APPL-SN-431277 N90-19306 #
US-PATENT-APPL-SN-498338 N90-19481
US-PATENT-APPL-SN-674901 N90-19600 #
US-PATENT-APPL-SN-838390 N90-19430 #
US-PATENT-APPL-SN-881419 N90-19489
US-PATENT-APPL-SN-921574 N90-19425*
US-PATENT-APPL-SN-924470 N90-19300*
US-PATENT-APPL-SN-927987 N90-19776*

US-PATENT-CLASS-49-253 N90-19278*
US-PATENT-CLASS-60-204 N90-19298*
US-PATENT-CLASS-60-259 N90-19298*
US-PATENT-CLASS-60-260 N90-19298*
US-PATENT-CLASS-60-497 N90-19657 #
US-PATENT-CLASS-73-432.1 N90-19534*
US-PATENT-CLASS-92-169.1 N90-19600 #
US-PATENT-CLASS-114-112 N90-19278*
US-PATENT-CLASS-114-201R N90-19278*
US-PATENT-CLASS-148-13 N90-19884*
US-PATENT-CLASS-148-13.1 N90-19884*
US-PATENT-CLASS-156-344 N90-19427*
US-PATENT-CLASS-219-72 N90-19602*
US-PATENT-CLASS-219-74 N90-19602*
US-PATENT-CLASS-244-129.5 N90-19278*
US-PATENT-CLASS-244-133 N90-19427*
US-PATENT-CLASS-244-158R N90-19278*
US-PATENT-CLASS-264-114 N90-19425*
US-PATENT-CLASS-264-311 N90-19425*
US-PATENT-CLASS-323-354 N90-19492*
US-PATENT-CLASS-324-62 N90-19492*
US-PATENT-CLASS-330-4.3 N90-19568
US-PATENT-CLASS-333-116 N90-19481
US-PATENT-CLASS-333-204 N90-19489
US-PATENT-CLASS-343-778 N90-19456 #
US-PATENT-CLASS-350-96.15 N90-19841
US-PATENT-CLASS-356-345 N90-19840
US-PATENT-CLASS-364-481 N90-19492*
US-PATENT-CLASS-364-482 N90-19492*
US-PATENT-CLASS-370-16 N90-19776*
US-PATENT-CLASS-371-8 N90-19776*
US-PATENT-CLASS-372-25 N90-19565
US-PATENT-CLASS-425-73 N90-19425*
US-PATENT-CLASS-425-75 N90-19425*
US-PATENT-CLASS-425-425 N90-19425*
US-PATENT-CLASS-425-435 N90-19425*
US-PATENT-CLASS-427-272 N90-19427*
US-PATENT-CLASS-428-641 N90-19884*
US-PATENT-CLASS-437-903 N90-19884*
US-PATENT-CLASS-439-273 N90-19490
US-PATENT-CLASS-528-188 N90-19300*
US-PATENT-CLASS-528-210 N90-19360
US-PATENT-CLASS-528-229 N90-19300*
US-PATENT-CLASS-528-352 N90-19300*
US-PATENT-CLASS-528-353 N90-19300*

US-PATENT-4,737,740 N90-19481
US-PATENT-4,828,935 N90-19872
US-PATENT-4,831,818 N90-19298*
US-PATENT-4,839,121 N90-19425*
US-PATENT-4,839,489 N90-19602*
US-PATENT-4,842,223 N90-19278*
US-PATENT-4,845,167 N90-19300*
US-PATENT-4,847,837 N90-19776*
US-PATENT-4,848,153 N90-19534*
US-PATENT-4,849,033 N90-19884*
US-PATENT-4,849,903 N90-19492*
US-PATENT-4,851,071 N90-19427*
US-PATENT-4,859,059 N90-19840
US-PATENT-4,860,013 N90-19431
US-PATENT-4,861,859 N90-19360
US-PATENT-4,862,116 N90-19480
US-PATENT-4,862,456 N90-19750
US-PATENT-4,864,567 N90-19432
US-PATENT-4,864,580 N90-19565
US-PATENT-4,867,044 N90-19600 #
US-PATENT-4,867,518 N90-19841
US-PATENT-4,868,515 N90-19568
US-PATENT-4,872,211 N90-19456 #

US-PATENT-4,872,309 ..... N90-19657 #
US-PATENT-4,873,501 ..... N90-19489
US-PATENT-4,874,326 ..... N90-19490
US-PATENT-4,875,357 ..... N90-19554

USABRDL-TR-9003 ..... N90-19706 #

VLSI-MEMO-89-556 ..... N90-19787 #
VLSI-MEMO-89-562 ..... N90-19491 #
VLSI-MEMO-89-567 ..... N90-19519 #

W-1/89 ..... N90-19625 #

WISS-ARB-VERMESSUNGSWESEN-154 N90-19559 #

WRDC-TR-89-7006-VOL-2 ..... N90-19748 #

WSRC-RP-89-475 ..... N90-19870 #

Appendix—About STAR

Scientific and Technical Aerospace Reports (STAR) is a major component of a comprehensive National Aeronautics and Space Administration information system covering aeronautics, space, and supporting disciplines. *STAR* is issued on the 8th and 23rd of each month and announces current publications of the following types:

- NASA, NASA contractor, and NASA grantee reports
- Reports issued by other U.S. Government agencies, domestic and foreign institutions, universities, and private firms
- Translations in report form
- NASA-owned patents and patent applications
- Other U.S. Government agency and foreign patents and patent applications
- Domestic and foreign dissertations and theses

Journal, book, and conference literature, cover-to-cover journal translations, and certain foreign dissertations are announced in a companion journal, *International Aerospace Abstracts (IAA),* available on subscription from the American Institute of Aeronautics and Astronautics, Technical Information Service, 555 West 57th Street, 12th Floor, New York, NY 10019.

SUBJECT SCOPE

The subject scope of *STAR* and *IAA* includes all aspects of aeronautics and space research and development, supporting basic and applied research, and applications. Aerospace aspects of earth resources, energy development, conservation, oceanography, environmental protection, urban transportation, and other topics of high national priority are also covered.

OTHER NASA PUBLICATIONS

Other NASA publications and information services are described in the publication, *The NASA Scientific and Technical Information System ... and How to Use It,* available without charge from the NASA Scientific and Technical Information Facility, P.O. Box 8757, BWI Airport, MD 21240.

HOW TO USE *STAR* SUBJECT CATEGORIES

STAR is categorized by 10 major subject divisions broken down further into 76 specific subject categories and one general division/category. The major subject divisions are listed on page ii in the Table of Contents, together with a note for each that defines its scope and provides any cross-references. For example:

AERONAUTICS

Includes aeronautics (general); aerodynamics; air transportation and safety; aircraft communications and navigation; aircraft design, testing and performance; aircraft instrumentation; aircraft propulsion and power; aircraft stability and control; and research and support facilities (air).

For related information see also *Astronautics.*

Each major division is further divided into as many as nine specific categories, which are identified by category numbers.

Abstracts in *STAR* are grouped by subject category, the categories appearing in sequential order. Category breaks in the abstract section are identified by the category number and title, and a scope note. Cross-references to other categories are provided as appropriate. For example:

02 AERODYNAMICS

Includes aerodynamics of bodies, combinations, wings, rotors, and control surfaces; and internal flow in ducts and turbomachinery.

For related information see also *34 Fluid Mechanics and Heat Transfer.*

CROSS-REFERENCES

Individual *STAR* abstracts are not ordinarily cross-referenced, except for certain conference reports or book translations that have had separate abstracts written for their component papers or chapters. Citations and abstracts of the components follow immediately after those of the parent document. When the subject content of a component differs sufficiently from the general content of the parent, a cross-reference citation also is printed at the end of the category to which it normally would have been assigned if it were independent.

DOCUMENTS ON MICROFICHE

Documents on microfiche[1] are designated by a pound sign (#) following the accession number. The pound sign is used without regard to the source or quality of the microfiche.

LIMITED REPRODUCIBILITY

A Note of Limited Reproducibility appears in the citation, if one or a combination of the following factors affect the reproducibility of more than 20% of the document. These factors include: faint or broken type, color photographs, black and white photographs, foldouts, dot matrix print, charts/graphs with script notation, non-Roman alphabet, or some other factor that limits the reproducibility of that document. This notation also appears on the microfiche header, with the specific causing factor checked off on a list visible in the second frame.

COLOR COPIES

An increasing number of NASA scientific and technical reports are being produced with color graphs, charts, illustrations, and photographs. A message indicating that a document has color pages follows the Sales and Pricing (SAP) information in the *STAR* citation.

Registered users of the NASA Scientific and Technical Information System will receive ordered documents with color at no *additional* cost, as long as stock copies of that document are available. Otherwise, an additional fee of $2.00 per color page, over and above the standard document price will be charged. The NASA STI Facility staff will work with registered users over the telephone to inform and meet each individual's ordering needs.

AVAILABILITIES

One or more sources from which a document announced in *STAR* is available to the public is given in each citation. The most commonly indicated sources and their acronyms or abbreviations are listed below. If the publication is available from a source other than those listed, the publisher and his address will be displayed on the availability line or in combination with the corporate source line.

Avail: NTIS. Sold by the National Technical Information Service. Prices for hard copy (HC) and microfiche (MF) are indicated by a price code following the letters HC or MF in the *STAR* citation. Current values for the price codes are given in the tables on page A-7.

(1) A microfiche is a transparent sheet of film, 105 by 148 mm in size, containing as many as 60 to 98 pages of information reduced to micro images (not to exceed 26:1 reduction).

Initially distributed microfiche under the NTIS SRIM (Selected Research in Microfiche) is available at greatly reduced unit prices. For this service and for information concerning subscription to NASA printed reports, consult the NTIS Subscription Section, Springfield, VA 22161.

NOTE ON ORDERING DOCUMENTS: When ordering NASA publications (those followed by the * symbol), use the N accession number. NASA patent applications (only the specifications are offered) should be ordered by the US-Patent-Appl-SN number. Non-NASA publications (no asterisk) should be ordered by the AD, PB, or other *report number* shown on the last line of the citation, not by the N accession number. It is also advisable to cite the title and other bibliographic identification.

Avail: SOD (or GPO). Sold by the Superintendent of Documents, U.S. Government Printing Office, in hard copy. The current price and order number are given following the availability line. (NTIS will fill microfiche requests, as indicated above, for those documents identified by a # symbol.)

Avail: BLL (formerly NLL): British Library Lending Division, Boston Spa, Wetherby, Yorkshire, England. Photocopies available from this organization at the price shown. (If none is given, address inquiry to the BLL.)

Avail: DOE Depository Libraries. Organizations in U.S. cities and abroad that maintain collections of Department of Energy reports, usually in microfiche form, are listed in *Energy Research Abstracts*. Services available from the DOE and its depositories are described in a booklet, *DOE Technical Information Center - Its Functions and Services* (TID-4660), which may be obtained without charge from the DOE Technical Information Center.

Avail: ESDU. Pricing information on specific data, computer programs, and details on Engineering Sciences Data Unit (ESDU) topic categories can be obtained from ESDU International Ltd. Requesters in North America should use the Virginia address while all other requesters should use the London address, both of which are on page A-6.

Avail: Fachinformationszentrum, Karlsruhe. Sold by the Fachinformationszentrum Energie, Physik, Mathematik GMBH, Eggenstein Leopoldshafen, Federal Republic of Germany, at the price shown in deutschmarks (DM).

Avail: HMSO. Publications of Her Majesty's Stationery Office are sold in the U.S. by Pendragon House, Inc. (PHI), Redwood City, CA. The U.S. price (including a service and mailing charge) is given, or a conversion table may be obtained from PHI.

Avail: NASA Public Document Rooms. Documents so indicated may be examined at or purchased from the National Aeronautics and Space Administration, Public Documents Room (Room 126), 600 Independence Ave., S.W., Washington, DC 20546, or public document rooms located at NASA installations, and the NASA Pasadena Office at the Jet Propulsion Laboratory.

Avail: Univ. Microfilms. Documents so indicated are dissertations selected from *Dissertation Abstracts* and are sold by University Microfilms as xerographic copy (HC) and microfilm. All requests should cite the author and the Order Number as they appear in the citation.

Avail: US Patent and Trademark Office. Sold by Commissioner of Patents and Trademarks, U.S. Patent and Trademark Office, at the standard price of

$1.50 each, postage free. (See discussion of NASA patents and patent applications below.)

Avail: (US Sales Only). These foreign documents are available to users within the United States from the National Technical Information Service (NTIS). They are available to users outside the United States through the International Nuclear Information Service (INIS) representative in their country, or by applying directly to the issuing organization.

Avail: USGS. Originals of many reports from the U.S. Geological Survey, which may contain color illustrations, or otherwise may not have the quality of illustrations preserved in the microfiche or facsimile reproduction, may be examined by the public at the libraries of the USGS field offices whose addresses are listed in this Introduction. The libraries may be queried concerning the availability of specific documents and the possible utilization of local copying services, such as color reproduction.

Avail: Issuing Activity, or Corporate Author, or no indication of availability. Inquiries as to the availability of these documents should be addressed to the organization shown in the citation as the corporate author of the document.

NASA PATENTS AND PATENT APPLICATIONS

Patents and patent applications owned by NASA are announced in *STAR* under appropriate subject categories and are referenced in the *STAR* indexes. In the Report/Accession Number Index, patents are indexed by the NASA Case Number (which appears in lieu of the report number in other indexes), the U.S. Patent Number, the U.S. Patent Application Serial Number, and the U.S. Patent Class. Patent applications for which patents have not yet been issued are indexed by the NASA Case Number and the U.S. Patent Application Serial Number.

NASA *patent application specifications* are sold in paper copy and microfiche by the National Technical Information Service (NTIS). The US-Patent-Appl-SN- number should be used in ordering either paper copy or microfiche from NTIS. Printed copies of *patents* (which are not microfiched) are available for purchase from:

Commissioner of Patents and Trademarks
U.S. Patent and Trademark Office
Washington, DC 20231

When ordering patents, the U.S. Patent Number should be used, and payment must be remitted in advance, by money order or check payable to the Commissioner of Patents and Trademarks. Prepaid purchase coupons for ordering are also available from the Patent and Trademark Office. The patents and patent applications announced in *STAR* are owned by NASA and are available for royalty-free licensing. Requests for licensing terms and further information should be addressed to:

Associate General Counsel for Intellectual Property/Code GP
National Aeronautics and Space Administration
Washington, DC 20546

ELIGIBILITY AND REGISTRATION FOR NASA INFORMATION PRODUCTS AND SERVICES

A variety of services is available to organizations of the following types that have registered with NASA to receive specific services or products:

1. NASA offices and installations, contractors, subcontractors, grantees, and consultants;
2. Other U.S. Government agencies and their contractors;
3. Libraries in the United States that have arrangements with NASA to maintain collections of NASA documents for public reference;
4. Other organizations in the United States having a need for NASA documents in work related to aeronautics and space research;
5. Organizations abroad that have established reciprocal document exchange arrangements with NASA.

Only the central service points or central points of document acquisition and control within qualified organizations are eligible to register for NASA products and services. Domestic organizations that may be eligible to receive various classes of NASA publications and services should address their requests for registration or for further information to:

NASA Scientific and Technical Information Facility
ATTN: Registration Services
P.O. Box 8757
BWI Airport, MD 21240
301-621-0153

Organizations abroad should direct requests to Manager, International STI Activities, NTT, NASA Headquarters, Washington, DC 20546.

AVAILABILITY OF *STAR* ABSTRACTS ON MICROFICHE

Microfiche of the abstract sections of this issue and other issues of *STAR* are available on annual subscription from NTIS as PB90-911300, Attn: Subscriptions, 5285 Port Royal Road, Springfield, VA 22161. Annual subscription rates are $75.50 North America; $151.00 foreign. Abstract sections for previous years retroactive to 1964 are available at the current rates. Microfiche for individual *STAR* issue abstract sections are not available.

PUBLIC COLLECTIONS OF NASA DOCUMENTS

DOMESTIC: NASA and NASA-sponsored documents and a large number of aerospace publications are available to the public for reference purposes at the library maintained by the American Institute of Aeronautics and Astronautics, Technical Information Service, 555 West 57th Street, 12th Floor, New York, NY 10019

EUROPEAN: An extensive collection of NASA and NASA-sponsored publications is maintained by the British Library Lending Division, Boston Spa, Wetherby, Yorkshire, England, for public access. The British Library Lending Division also has available many of the non-NASA publications cited in *STAR*. European requesters may purchase facsimile copy or microfiche of NASA and NASA-sponsored documents, those identified by both the symbols # and * from ESA - Information Retrieval Service, European Space Agency, 8-10 rue Mario-Nikis, 75738 Paris CEDEX 15, France.

FEDERAL DEPOSITORY LIBRARY PROGRAM

In order to provide the general public with greater access to U.S. Government publications, Congress established the Federal Depository Library Program under the Government Printing Office (GPO), with 51 regional depositories responsible for permanent retention of material, inter-library loan, and reference services. At least one copy of nearly every NASA and NASA-sponsored publication, either in printed or microfiche format, is received and retained by the 51 regional depositories. A list of the regional GPO libraries, arranged alphabetically by state, appears on the inside back cover. These libraries are *not* sales outlets. A local library can contact a Regional Depository to help locate specific reports, or direct contact may be made by an individual.

ADDRESSES OF ORGANIZATIONS

American Institute of Aeronautics and Astronautics
Technical Information Service
555 West 57th Street, 12th Floor
New York, New York 10019

British Library Lending Division,
Boston Spa, Wetherby, Yorkshire,
England

Commissioner of Patents and Trademarks
U.S. Patent and Trademark Office
Washington, DC 20231

Department of Energy
Technical Information Center
P.O. Box 62
Oak Ridge, Tennessee 37830

European Space Agency-Information Retrieval Service
ESRIN
Via Galileo Galilei
00044 Frascati (Rome) Italy

Engineering Sciences Data Unit International
P.O. Box 1633
Manassas, Virginia 22110

Engineering Sciences Data Unit International, Ltd.
251-259 Regent Street
London, W1R 7AD, England

Fachinformationszentrum Energie, Physik, Mathematik
GMBH
7514 Eggenstein Leopoldshafen
Federal Republic of Germany

Her Majesty's Stationery Office
P.O. Box 569, S.E. 1
London, England

NASA Scientific and Technical Information Facility
P.O. Box 8757
BWI Airport, Maryland 21240

National Aeronautics and Space Administration
Scientific and Technical Information Division (NTT)
Washington, DC 20546

National Technical Information Service
5285 Port Royal Road
Springfield, Virginia 22161

Pendragon House, Inc.
899 Broadway Avenue
Redwood City, California 94063

Superintendent of Documents
U.S. Government Printing Office
Washington, DC 20402

University Microfilms
A Xerox Company
300 North Zeeb Road
Ann Arbor, Michigan 48106

University Microfilms, Ltd.
Tylers Green
London, England

U.S. Geological Survey Library National Center
MS 950
12201 Sunrise Valley Drive
Reston, Virginia 22092

U.S. Geological Survey Library
2255 North Gemini Drive
Flagstaff, Arizona 86001

U.S. Geological Survey
345 Middlefield Road
Menlo Park, California 94025

U.S. Geological Survey Library
Box 25046
Denver Federal Center, MS914
Denver, Colorado 80225

NTIS PRICE SCHEDULES

(Effective January 1, 1990)

Schedule A
STANDARD PRICE DOCUMENTS AND MICROFICHE

PRICE CODE	NORTH AMERICAN PRICE	FOREIGN PRICE
A01	$ 8.00	$ 16.00
A02	11.00	22.00
A03	15.00	30.00
A04-A05	17.00	34.00
A06-A09	23.00	46.00
A10-A13	31.00	62.00
A14-A17	39.00	78.00
A18-A21	45.00	90.00
A22-A25	53.00	106.00
A99	*	*
N01	60.00	120.00
N02	59.00	118.00
N03	20.00	40.00

Schedule E
EXCEPTION PRICE DOCUMENTS AND MICROFICHE

PRICE CODE	NORTH AMERICAN PRICE	FOREIGN PRICE
E01	$10.00	$ 20.00
E02	12.00	24.00
E03	14.00	28.00
E04	16.50	33.00
E05	18.50	37.00
E06	21.50	43.00
E07	24.00	48.00
E08	27.00	54.00
E09	29.50	59.00
E10	32.50	65.00
E11	35.00	70.00
E12	38.50	77.00
E13	41.00	82.00
E14	45.00	90.00
E15	48.50	97.00
E16	53.00	106.00
E17	57.50	115.00
E18	62.00	124.00
E19	69.00	138.00
E20	80.00	160.00
E99	*	*

* Contact NTIS for price quote.

IMPORTANT NOTICE

NTIS Shipping and Handling Charges

U.S., Canada, Mexico — ADD $3.00 per TOTAL ORDER

All Other Countries — ADD $4.00 per TOTAL ORDER

Exceptions — Does NOT apply to:

ORDERS REQUESTING NTIS RUSH HANDLING
ORDERS FOR SUBSCRIPTION OR STANDING ORDER PRODUCTS *ONLY*

NOTE: Each additional delivery address on an order requires a separate shipping and handling charge.

FEDERAL REGIONAL DEPOSITORY LIBRARIES

ALABAMA

AUBURN UNIV. AT MONTGOMERY LIBRARY
Documents Department
Montgomery, AL 36193
(205) 279-9110 ext.253

UNIV. OF ALABAMA LIBRARY
Reference Department/Documents
Box S
Tuscaloosa, AL 35486
(205) 348-6046

ARIZONA

DEPT. OF LIBRARY, ARCHIVES, AND PUBLIC RECORDS
Third Floor State Capitol
1700 West Washington
Phoenix, AZ 85007
(602) 255-4121

ARKANSAS

ARKANSAS STATE LIBRARY
Documents Service Section
One Capitol Mall
Little Rock, AR 72201
(501) 371-2090

CALIFORNIA

CALIFORNIA STATE LIBRARY
Govt. Publications Section
914 Capitol Mall
Sacramento, CA 95814
(916) 322-4572

COLORADO

UNIV. OF COLORADO
Norlin Library
Government Publications Division
Campus Box 184
Boulder, CO 80309
(303) 492-8834

DENVER PUBLIC LIBRARY
Govt. Pub. Department
1357 Broadway
Denver, CO 80203
(303) 571-2346

CONNECTICUT

CONNECTICUT STATE LIBRARY
231 Capitol Avenue
Hartford, CT 06106
(203) 566-4971

FLORIDA

UNIV. OF FLORIDA LIBRARIES
Documents Department
Library West
Gainesville, FL 32611
(904) 392-0367

GEORGIA

UNIV. OF GEORGIA LIBRARIES
Government Documents Dept.
Athens, GA 30602
(404) 542-8949

HAWAII

UNIV. OF HAWAII
Hamilton Library
Government Documents Collection
2550 The Mall
Honolulu, HI 96822
(808) 948-8230

IDAHO

UNIV. OF IDAHO LIBRARY
Documents Section
Moscow, ID 83843
(208) 885-6344

ILLINOIS

ILLINOIS STATE LIBRARY
Federal Documents
Centennial Building
Springfield, IL 62756
(217) 782-5012

INDIANA

INDIANA STATE LIBRARY
Serials Section
140 North Senate Avenue
Indianapolis, IN 46204
(317) 232-3686

IOWA

UNIV. OF IOWA LIBRARIES
Government Publications Dept.
Iowa City, IA 52242
(319) 335-5926

KANSAS

UNIVERSITY OF KANSAS
Spencer Research Library
Government Documents
Lawrence, KS 66045
(913) 864-4662

KENTUCKY

UNIV. OF KENTUCKY LIBRARIES
Government Publications/Maps Dept.
Lexington, KY 40506
(606) 257-8400

LOUISIANA

LOUISIANA STATE UNIVERSITY
Middleton Library
Government Documents Dept.
Baton Rouge, LA 70803
(504) 388-2570

LOUISIANA TECHNICAL UNIV.
Prescott Memorial Library
Government Documents Dept.
Ruston, LA 71272
(318) 257-4962

MAINE

UNIVERSITY OF MAINE
Raymond H. Fogler Library
Govt. Documents & Microforms Dept.
Orono, ME 04469
(207) 581-1680

MARYLAND

UNIVERSITY OF MARYLAND
McKeldin Library
Documents/Maps Room
College Park, MD 20742
(301) 454-3034

MASSACHUSETTS

BOSTON PUBLIC LIBRARY
Government Documents Dept.
666 Boylston Street
Boston, MA 02117
(617) 536-5400 ext.226

MICHIGAN

DETROIT PUBLIC LIBRARY
5201 Woodward Avenue
Detroit, MI 48202
(313) 833-1409

LIBRARY OF MICHIGAN
Government Documents
P.O. Box 30007
735 E. Michigan Avenue
Lansing, MI 48909
(517) 373-1593

MINNESOTA

UNIVERSITY OF MINNESOTA
Wilson Library
Government Publications
309 Nineteenth Avenue South
Minneapolis, MN 55455
(612) 373-7813

MISSISSIPPI

UNIV. OF MISSISSIPPI LIB.
Government Documents Dept.
106 Old Gym Bldg.
University, MS 38677
(601) 232-5857

MISSOURI

University of Missouri at Columbia Library
Government Documents
Columbia, MO 65201
(314) 882-6733

MONTANA

UNIV. OF MONTANA
Mansfield Library
Documents Division
Missoula, MT 59812
(406) 243-6700

NEBRASKA

UNIVERSITY OF NEBRASKA - LINCOLN
Love Memorial Library
Documents Department
Lincoln, NE 68588
(402) 472-2562

NEVADA

UNIV. OF NEVADA-RENO LIB.
Govt. Pub. Department
Reno, NV 89557
(702) 784-6579

NEW JERSEY

NEWARK PUBLIC LIBRARY
U.S. Documents Division
5 Washington Street
P.O. Box 630
Newark, NJ 07101
(201) 733-7812

NEW MEXICO

UNIVERSITY OF NEW MEXICO
General Library
Government Publications/Maps Dept.
Albuquerque, NM 87131
(505) 277-5441

NEW MEXICO STATE LIBRARY
325 Don Gaspar Avenue
Santa Fe, NM 87501
(505) 827-3826

NEW YORK

NEW YORK STATE LIBRARY
Documents Sect. Cultural Educ. Ctr.
Empire State Plaza
Albany, NY 12230
(518) 474-5563

NORTH CAROLINA

UNIVERSITY OF NORTH CAROLINA AT CHAPEL HILL
Davis Library 080A
BA/SS Department Documents
Chapel Hill, NC 27514
(919) 962-1151

NORTH DAKOTA

NORTH DAKOTA STATE UNIVERSITY LIBRARY
Government Documents Dept.
Fargo, ND 58105
(701) 237-8352
In cooperation with Univ. of North Dakota, Chester Fritz Library
Grand Forks

OHIO

STATE LIBRARY OF OHIO
Documents Section
65 South Front Street
Columbus, OH 43266
(614) 644-7051

OKLAHOMA

OKLAHOMA DEPT. OF LIBRARIES
Government Documents
200 NE 18th Street
Oklahoma City, OK 73105
(405) 521-2502, ext. 252

OKLAHOMA STATE UNIV. LIB.
Documents Department
Stillwater, OK 74078
(405) 624-0489

OREGON

PORTLAND STATE UNIV.
Millar Library
934 SW Harrison - P.O. Box 1151
Portland, OR 97207
(503) 229-3673

PENNSYLVANIA

STATE LIBRARY OF PENN.
Government Publications Section
Box 1601
Walnut St. & Commonwealth Ave.
Harrisburg, PA 17105
(717) 787-3752

SOUTH CAROLINA

CLEMSON UNIV. COOPER LIB.
Documents Department
Clemson, SC 29634
(803) 656-5174
In cooperation with Univ. of South Carolina, Thomas Cooper Library, Columbia

TEXAS

TEXAS STATE LIBRARY
Public Services Department
P.O. Box 12927 - 1201 Brazos
Austin, TX 78711
(512) 463-5455

TEXAS TECH. UNIV. LIBRARY
Documents Department
Lubbock, TX 79409
(806) 742-2268

UTAH

UTAH STATE UNIVERSITY
Merrill Library & Learning Resources Center, UMC-30
Documents Department
Logan, UT 84322
(801) 750-2682

VIRGINIA

UNIVERSITY OF VIRGINIA
Alderman Library
Government Documents
Charlottesville, VA 22903
(804) 924-3133

WASHINGTON

WASHINGTON STATE LIBRARY
Document Section
Olympia, WA 98504
(206) 753-4027

WEST VIRGINIA

WEST VIRGINIA UNIV. LIB.
Government Documents Section
P.O. Box 6069
Morgantown, WV 26506
(304) 293-3640

WISCONSIN

ST. HIST SOC. OF WISCONSIN LIB.
Government Pub. Section
816 State Street
Madison, WI 53706
(608) 262-2781
In cooperation with Univ. of Wisconsin-Madison, Memorial Library

MILWAUKEE PUBLIC LIBRARY
Documents Division
814 West Wisconsin Avenue
Milwaukee, WI 53233
(414) 278-3065

WYOMING

WYOMING STATE LIBRARY
Supreme Court & Library Bldg.
Cheyenne, WY 82002
(307) 777-5919

National Aeronautics and
Space Administration
Code NTT
Washington, D.C.
20546
Official Business
Penalty for Private Use, $300

SPECIAL FOURTH-CLASS RATE
POSTAGE & FEES PAID
NASA
PERMIT No. G27

NASA

POSTMASTER: If Undeliverable (Section 158 Postal Manual) Do Not Return